

DIRECTORIO DE PROFESORES DEL CURSO: DISEÑO DE ESTRUCTURAS DE ACERO

1.           ING. FERNANDO FRIAS BELTRAN  
FESA  
ANTONIO SUVIETA NO. 10.  
LOS REYES IZTACALA  
TLALNEPANTLA, EDO. DE MEXICO  
565 68 00
  
2.           ING. MANUEL LINS LUJAN  
GERENTE GENERAL  
INGENIERIA DEL ACERO  
DIV. DEL NORTE 525 DESPACHO 303  
COL. DEL VALLE  
687 57 45 Y 687 57 64
  
3.           ING. ENRIQUE MARTINEZ ROMERO  
DIRECTOR GENERAL  
CIA. ENRIQUE MARTINEZ ROMERO  
AV. NUEVO LEON 54-2° PISO  
COL. CONDESA  
MEXICO, D.F.  
553 55 96
  
4.           ING. RAUL GRANADOS GRANADOS  
GERENTE  
PROYECTISTAS ESTRUCTURALES, ASOCIADOS, S.C.  
DARWIN 18 A 2° PISO  
COL. ANZURES  
MEXICO, D.F.  
528 52 80
  
5.           ING. OSCAR DE BUEN LOPEZ DE HEREDIA (COORDINADOR)  
DIRECTOR GENERAL  
COLINAS DE BUEN, S.A.  
V. M. ALEMAN NO. 190  
03010 MEXICO, D.F.  
519 72 40
  
6.           ING. JOSE LUIS SANCHEZ MARTINEZ  
GERENTE GENERAL  
COLINAS DE BUEN, S.A.  
VIADUCTO MIGUEL ALEMAN 190  
03010 MEXICO, D.F.  
538 05 44
  
7.           ING. OSCAR DE LA TORRE  
GERENTE GENERAL  
PROYECTISTAS ESTRUCTURALES ASOCIADOS, S.C.  
DARWIN 18A 2° PISO  
COL. ANZURES  
MEXICO, d. f.  
528 52 80
  
8.           DR. PORFIRIO BALLESTEROS BAROCIO (COORDINADOR)  
PROFESOR  
DEPFI  
UNAM  
MEXICO, D.F.  
550 52 15 EXT. 4498

1941

MC

1941

1941

1941

1941

1941

1941

1941

1941

1941

1941

1941

U.N.A.M. FACULTAD DE INGENIERIA  
 DIVISION DE EDUCACION CONTINUA

PROGRAMA DEL CURSO : DISEÑO DE ESTRUCTURAS DE ACERO  
 QUE SE IMPARTIRA DEL 26 AL 30 DE NOVIEMBRE

DE 1984

FECHA	HORARIO	T E M A	P R O F E S O R
26 Nov.	10-11.30	INTRODUCCION	ING. OSCAR DE BUEN LOPEZ DE HEREDIA
	12-13.30	PROPIEDADES MECANICAS DEL ACERO	ING. OSCAR DE BUEN LOPEZ DE HEREDIA
	15-16.30	MIEMBROS A TENSION	ING. MANUEL LINS LUJAN
	17-18.30	CONEXIONES CON PERNOS	ING. JOSE LUIS SANCHEZ MARTINEZ
27 NOV.	10-11.30	SOLDADURA	ING. ENRIQUE MARTINEZ ROMERO
	12-13.30	VIGAS	ING. RAUL GRANADOS GRANADOS
	15-16.30	VIGAS	ING. RAUL GRANADOS GRANADOS
	17-18.30	EJEMPLOS DE TORRES	ING. FERNANDO FRIAS BELTRAN
28 NOV.	10-11.30	ACCION COMPUESTA	DR. PORFIRIO BALLESTEROS BAROCIO
	12-13.30	FLEXION BI-AXIAL	DR. PORFIRIO BALLESTEROS BAROCIO
	15-16.30	EJEMPLO-PEMEX	ING. JOSE LUIS SANCHEZ MARTINEZ
	17-18.30	EJEMPLO-TORRE DE MEXICANA	ING. JOSE LUIS SANCHEZ MARTINEZ
29 NOV.	10-13.30	COLUMNAS	ING. OSCAR DE BUEN LOPEZ DE HEREDIA
	15-18.30	EDIFICIO CONVENCIONAL	ING. MANUEL LINS - DR. PORFIRIO BALLESTEROS
30 NOV.	10-11.30	ESTRUCTURA IND. DE MARCO RIGIDO	ING. OSCAR DE LA TORRE
	12-13.30	FALLAS EN TORRES	ING. FERNANDO FRIAS BELTRAN
	15-18.30	MESA REDONDA CLAUSURA	



**DIVISION DE EDUCACION CONTINUA  
FACULTAD DE INGENIERIA U.N.A.M.**

DISEÑO DE ESTRUCTURAS DE ACERO

APUNTES

ING. MANÚEL LINSS LUJAN

NOV. 84



En este curso llamaremos estructura a un conjunto de elementos conectados entre sí, que tienen por objeto transmitir un sistema de fuerzas en el espacio a una base de apoyo ó sustentación. Por ejemplo, si tuviésemos el problema de colocar un tanque de agua a cierta altura, lo podríamos resolver poniéndolo en la parte superior de una torre. Esta torre tendría como función transmitir las fuerzas que se originen por estar el tanque en esa posición, a la base de sustentación ( Fig. 1 a ). En la Fig. 1 b tenemos un marco de un edificio -- donde marcamos unas trayectorias que siguen las fuerzas desde los puntos de aplicación de las cargas a los apoyos.

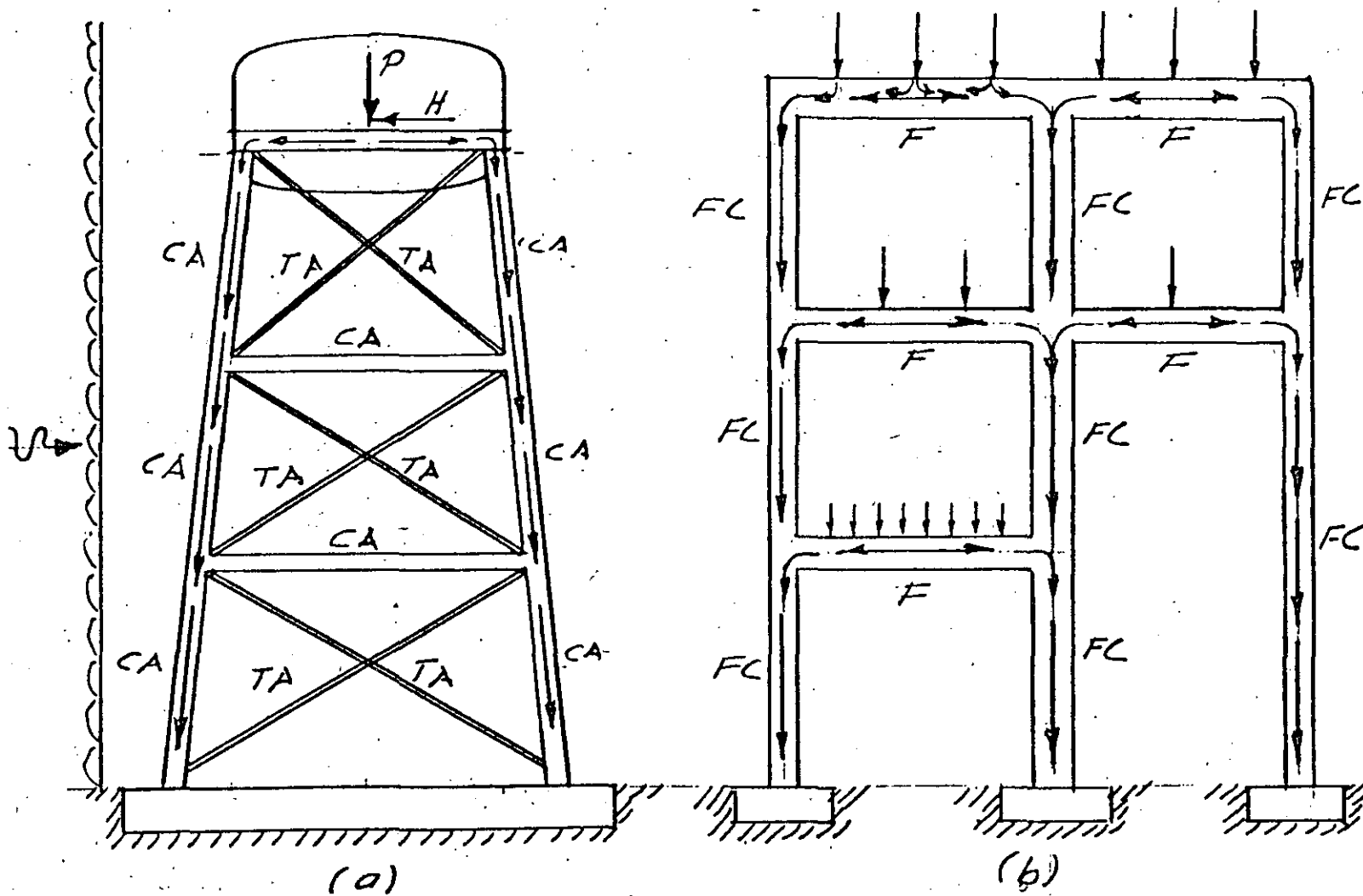


Fig 1

Como estos tenemos multitudes de ejemplos, como son torres para soportar líneas de transmisión de energía eléctrica, puentes para vehículos, edificios industriales, auditorios, estadios, edificios para oficinas, -- etc.

En cada caso existirá una estructura con características especiales para transmitir las diferentes acciones que se presenten.

En este curso estudiaremos el diseño de estructuras formadas con barras primáticas, entendiéndose por barra al elemento que tiene una dimensión mucho mayor que las otras dos. Las estructuras de la figura 1 están formadas por barras prismáticas que transmiten distintas -- acciones. Para el estudio de las barras conviene clasificarlas de acuerdo con el tipo de acción que transmiten (Fig. 2 ), ya que su comportamiento depende de esta.

Por ejemplo, en una barra sujeta a una fuerza axial de compresión se puede presentar el fenómeno de pandeo. en cambio la misma barra sujeta a una fuerza axial de tensión, este fenómeno no existe. Así pues, el estudio de la barra comprimida y el de la barra sujeta a tensión axial son completamente distintos.

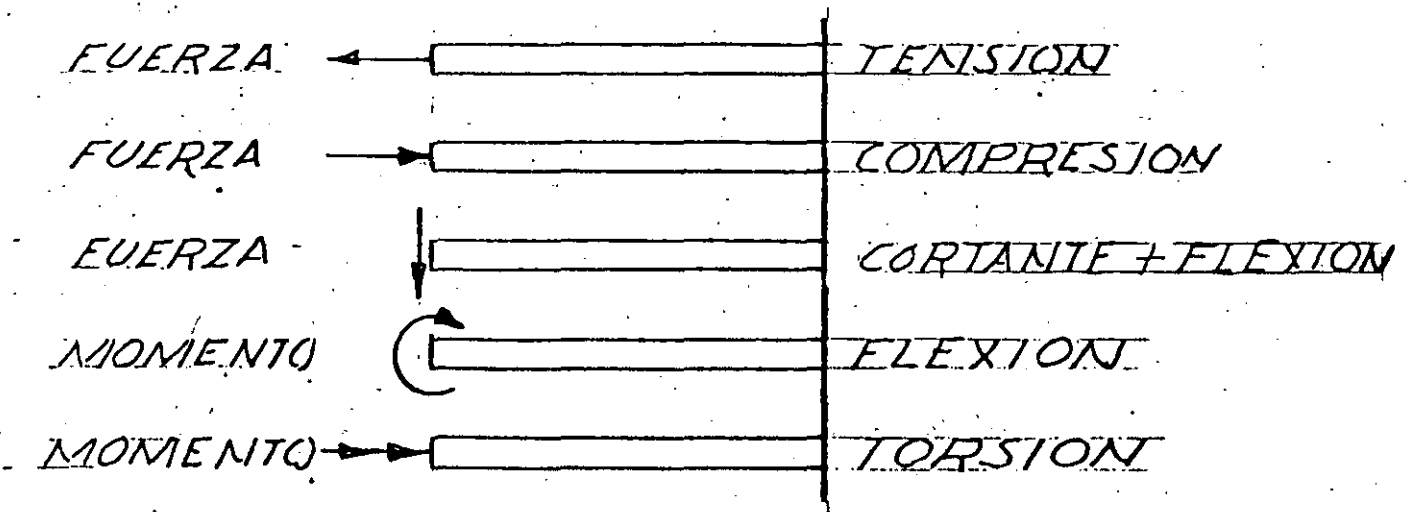


FIG 2

También se presentan casos donde actúan dos o más acciones simultáneamente. La combinación más frecuente en estructuras, es la flexión con carga axial: flexotensión y flexocompresión, las cuales se estudian por separado.

**MIEMBROS EN TENSION.** - Se considera que trabajan en tensión ó compresión axial los elementos estructurales siguientes:

- Las barras de armaduras trianguladas sobre las que no obran directamente fuerzas exteriores, excepto cuando en sus conexiones haya excentricidades que produzcan flexiones que no puedan ignorarse en el diseño.
- Las celosías de columnas compuestas que formen una triangulación completa tal que cualquier plano perpendicular al eje de la columna corte cuando menos una diagonal o coincida con un montante.

c) Los puntales y tirantes colocados para el contraventeo lateral de la estructura principal.

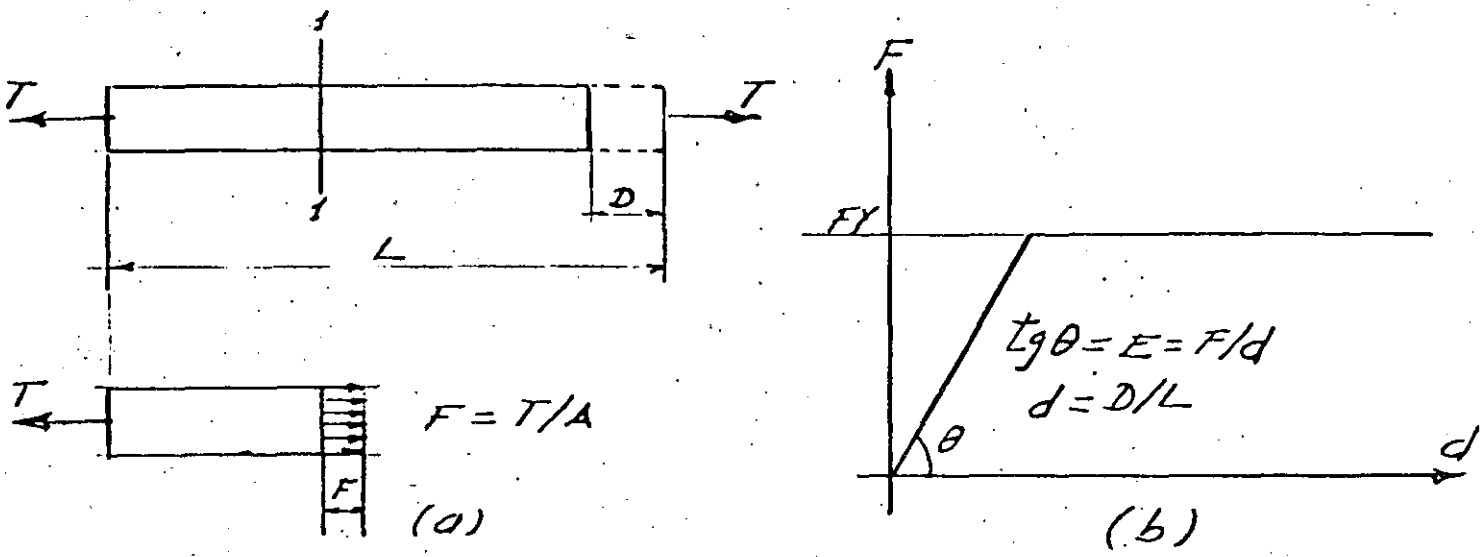
d) Tirantes.

Al aplicar una fuerza de tensión axial a una barra prismática todos los puntos de una sección transversal cualesquiera, quedan sujetos al mismo esfuerzo  $T/A$  ( Fig. 4 a ). Al incrementar la fuerza  $T$ , el esfuerzo se incrementará uniformemente en la sección hasta alcanzar el valor del esfuerzo de fluencia  $FY$ , momento a partir del cual las deformaciones quedan sin restricción (Punto 1 Fig. 4 b). La capacidad de la barra será :

$$T_{max} = A \cdot FY$$

$A =$  Area de sección transversal.

El alargamiento elástico vendrá dado por la fórmula :  $D = \frac{T \cdot X \cdot L}{A \cdot X \cdot E}$



$$T_{max} = A \cdot FY \quad D = T \cdot L / (A \cdot E)$$

FIG. 4

Si la barra tiene un agujero o algún otro tipo de discontinuidad - el comportamiento varía con relación al descrito anteriormente. Estas discontinuidades causarán una concentración de esfuerzos en la sección en que se encuentran (Fig. 5 a ), motivo por el cual el comportamiento en este caso será diferente al de la barra sin discontinuidades.

Veamos como se comporta una barra con un agujero susjeta a una fuerza de tensión axial. El esfuerzo máximo se presenta en la orilla del agujero, alcanzando un valor de aproximadamente 3 veces el valor del esfuerzo promedio en la sección neta.

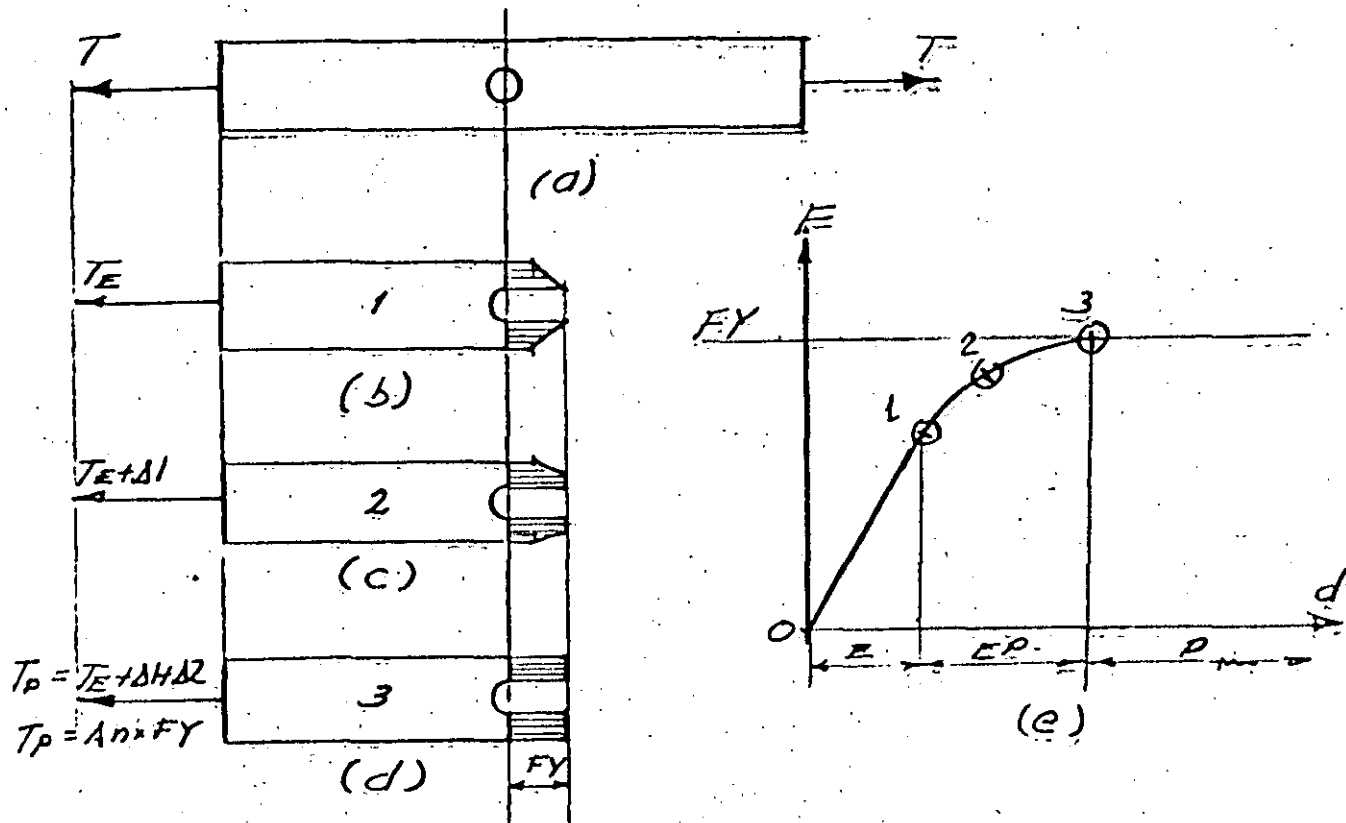


FIG 5

Aplicamos una fuerza \$T\$ que vamos incrementando hasta que el esfuerzo máximo alcance el valor \$F\_Y\$. La gráfica esfuerzo deformación que dará representada por la recta \$O-1\$ ( Fig. 5 e ); al seguir incrementando la fuerza \$T\$, se alcanzará el esfuerzo de fluencia en otros puntos de la sección transversal ( Fig. 5 c ), y la gráfica esfuerzo deformación seguirá la curva \$1-2\$ ( Fig. 5 e ) y las deformaciones estarán restringidas por la zona elástica de la sección. Continuamos incrementando la fuerza \$T\$ hasta alcanzar el esfuerzo \$F\_Y\$ en toda la sección, la curva esfuerzo deformación sigue hasta el punto 3; a partir de este punto la pieza se deforma sin restricción. En este caso la capacidad máxima será de :

$$T_{max} = A_n \cdot F_Y$$

$$A_n = \text{Area neta.}$$

La eficiencia con que trabaja una barra sujeta a un sistema de cargas, depende de la distribución de esfuerzos en ella; la eficiencia máxima se alcanza cuando todas las secciones transversales están trabajando al esfuerzo máximo permisible. Esta situación solo se presenta en las barras primáticas sujetas a tensión axial.

## DISEÑO DE PIEZAS A TENSION.

5

Las barras primáticas sujetas a fuerzas axiales de tensión se pueden diseñar usando el criterio elástico ó el plástico.

En el primer caso la sección seleccionada debe tener una área A tal que multiplicada por el esfuerzo permisible FP nos dé una fuerza -- igual o mayor que la fuerza actuante T, esto es :

$$T \leq A \times FP$$

$$A \geq T / FP \quad (I)$$

En el diseño plástico se debe cumplir la condición de que el área de la sección transversal de la barra multiplicada por el esfuerzo de fluencia FY, sea igual o mayor que la fuerza axial multiplicada por el factor de carga fc, o sea :

$$fc \times T \leq A \times FY$$

$$A \geq fc \times T / FY \quad (II)$$

El esfuerzo permisible generalmente se fija como un porcentaje del es fuerzo de fluencia.

Los dos métodos de diseño darán el mismo resultado si se cumple la siguiente condición :

$$fc \times T / FY = T / FP$$

$$fc = FY / FP$$

EJEMPLO 1.- seleccionar, usando el criterio elástico y el plástico, una barra plana de acero con límite de fluencia de 2500 Kg/cm<sup>2</sup> que -- sea capaz de soportar una carga de 50000 Kg. El esfuerzo permisible es de 0.6 FY y el factor de carga es igual a 1.67.

Diseño elástico :

$$A = 50000 \text{ Kg.} / (0.6 \times 2500) = 33.3 \text{ cm}^2$$

Diseño plástico :

$$A = 1.67 \times 50000 / 2500 = 33.4 \text{ cm}^2$$

Utilizando una barra de 25 mm de espesor necesitamos un ancho de :

$$a = 33.4 \text{ cm}^2 / 2.5 = 13.36 \text{ cm.}$$

## 6

Si bien los dos criterios coinciden al diseñar una barra a tensión axial, en el caso de una estructura no se presenta esta misma situación como lo veremos en el siguiente ejemplo.

EJEMPLO 2.- Vamos a estudiar a continuación el comportamiento de la estructura de la Fig. 6a, formada por tres barras sujetas a una carga vertical P. el área de la sección transversal de las barras diagonales es A1 y la de la barra central es A2; el límite de fluencia para las tres barras es Fy.

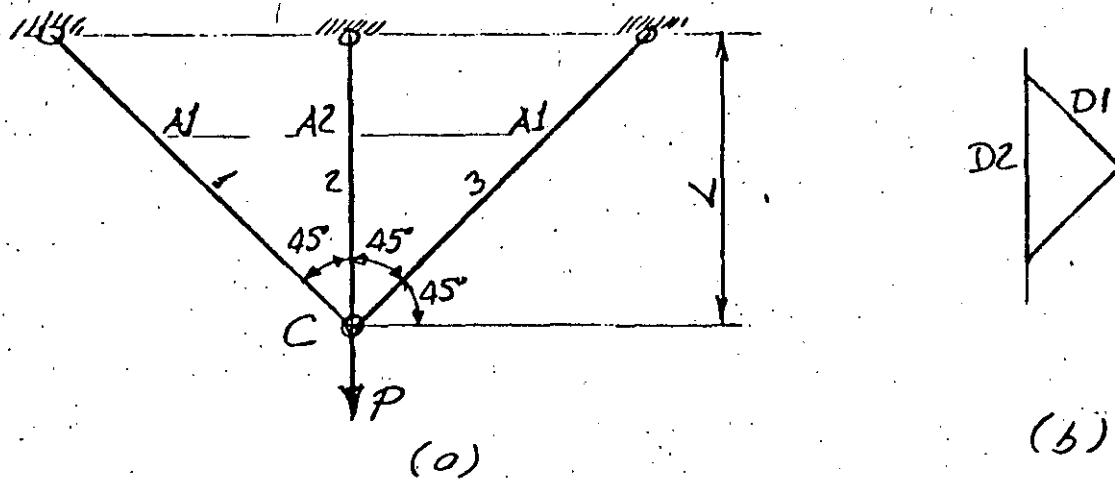


FIG 6

Del diagrama de desplazamiento (Fig. 6 b) tenemos :

$$D2 \times \cos 45^\circ = D1 \quad (1)$$

Sustituyendo a D1 y D2 en función de T1 y T2 :

$$(T2 \times L)/(A2 \times E) \times \cos 45^\circ = (T1 \times L/\cos 45^\circ)/(A1 \times E) \quad (2)$$

Simplificando obtenemos :

$$T1/A1 = \frac{1}{2} \times T2/A2 \quad (3)$$

$$F1 = T_1/A1 \text{ Esfuerzo en las barras 1 y 3}$$

$$F2 = T_2/A2 \text{ Esfuerzo en la barra 2}$$

De la ecuación (3) concluimos que en esta estructura, en el intervalo elástico, el esfuerzo en las barras 1 y 3 vale la mitad del esfuerzo en la barra 2. La capacidad elástica de la estructura se alcanza cuando el esfuerzo en la barra 2 vale  $F_Y$ . El valor máximo de la carga  $P$  con el criterio elástico lo obtenemos del equilibrio del nudo C (Fig. 6 a) :

$$P = 2 \times T_1 \times \cos 45^\circ + T_2 \quad (4)$$

Sustituyendo los valores de  $T_1$  y  $T_2$  en función de las áreas  $A_1$  y  $A_2$ , y del esfuerzo de fluencia  $F_Y$ , tendremos en el momento en que la barra central alcanza el esfuerzo  $F_Y$ , la carga máxima ( $P_E$ ) valdrá:

$$P_E = (2 \times A_1 \times F_Y \times \cos 45^\circ) / 2 + A_2 \times F_Y$$

$$P_E = (A_1 \times \cos 45^\circ + A_2) \times F_Y \quad (5)$$

Sin embargo, la estructura aún tiene capacidad de carga, debido a -- que el esfuerzo en las barras diagonales no ha alcanzado el límite de fluencia. Podemos incrementar la carga  $P$  hasta que el esfuerzo en estas barras valga  $F_Y$ . A partir de este momento la estructura sufre desplazamientos sin restricción, señal de que se ha alcanzado su capacidad máxima de carga ( $P_P$ ). Su valor lo obtendremos sustituyendo en la ecuación (4). Los valores de  $T_1$  y  $T_3$  en función de  $F_Y$  :

$$P_P = (2A_1 \times F_Y \times \cos 45^\circ) + A_2 \times F_Y$$

$$P_P = (2 \times A_1 \times \cos 45^\circ + A_2) \times F_Y \quad (6)$$

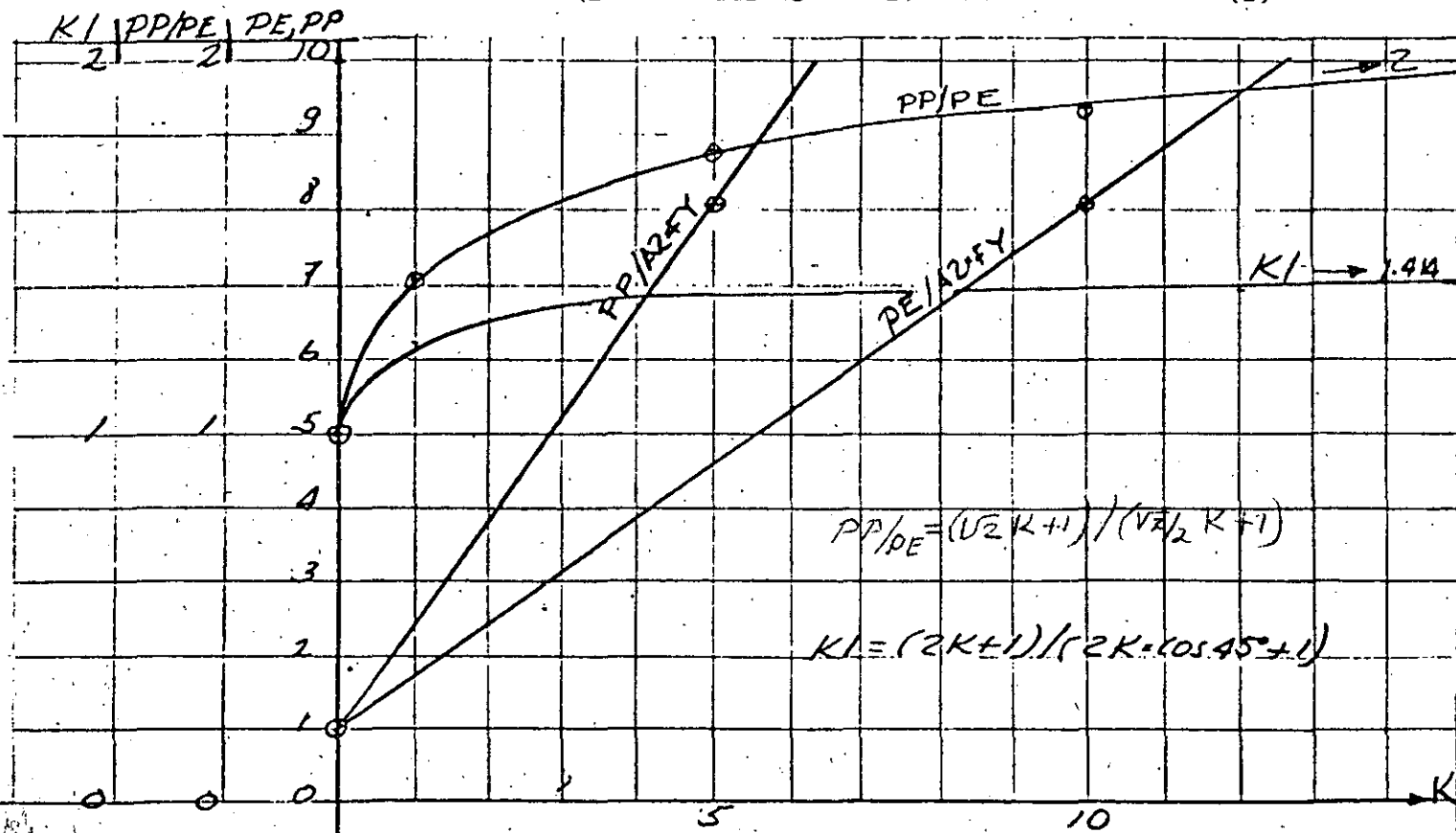


FIG 3

La capacidad de carga de la estructura es función de las áreas y los esfuerzos de fluencia de las tres barras. Vamos a estudiar la variación de las capacidades elástica (PE) y plástica (PP) con la variación de las áreas A1 y A2.

$$PE = (A1 \times \cos 45^\circ + A2) \times FY$$

$$K = A1/A2$$

$$PE = (K \times \cos 45^\circ + 1) \times A2 \times FY$$

$$PP = (2 K \times \cos 45^\circ + 1) \times A2 \times FY$$

Vamos a calcular la suma de las áreas de las secciones transversales (AT) de las tres barras en función de A2 y K para la máxima resistencia plástica :

$$A1 = K \times A2$$

$$A2 = PP / ((2 K \times \cos 45^\circ + 1) \times FY)$$

$$AT = 2 \times A1 + A2$$

$$AT = (2 K + 1) \times A2$$

$$AT = PP \times (2K + 1) / (2K \times \cos 45^\circ + 1) \times FY$$

$$AT = (PP/FY) \times (2k + 1) / (2K \times \cos 45^\circ + 1)$$

$$AT = K1 \times PP/FY$$

Cuando A1 tiende a 0, K tiende a infinito tendremos :

$$AT = (PP/FY) (1/\cos 45^\circ)$$

$$AT = 1.414 (PP/FY)$$

$$K1 = 1.414$$

En la fig. 7 veremos gráficamente los resultados anteriores.

Los valores de PE y PP coinciden cuando A1 y A3 valen 0, como era de esperarse, pues existirá solamente una barra a tensión. Conforme aumentan los valores de A1 y A3, aumentan PE y PP; siendo más rápido el aumento de PP.



La relación entre PP y PE tiende a 1.0 cuando K tiende 0, y tiende a 2.0 cuando K tiende a infinito.

El volumen total de acero para los casos extremos será :

$$A = PP/FY$$

Para  $A_1 = 0 :$

$$V_1 = A \times L$$

Para  $A_2 = 0 :$

$$V_2 = 1.414 \times L \times 1.414 \times A = 2 \times A \times L$$

$$V_2/V_1 = A \times A \times L / (A \times L) = 2$$

A continuación vamos a estudiar el comportamiento de la estructura cuando el límite de fluencia de las barras 1 y 3 (FY1) es diferente del límite de fluencia de la barra 2 (FY2). Se pueden presentar los siguientes casos :

- 1)  $FY1 < FY2/2$
- 2)  $FY1 = FY2/2$
- 3)  $FY1 > FY2/2$

En la figura 8 tenemos las gráficas que describen el comportamiento de los 3 casos.

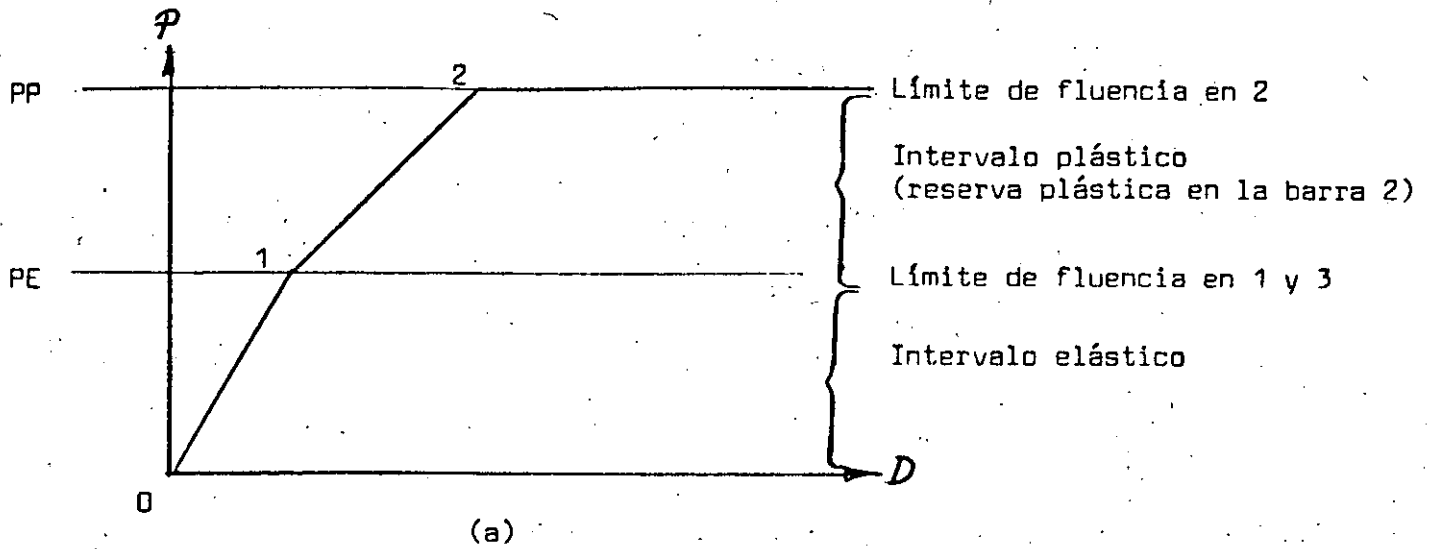
Del estudio que hemos realizado de esta estructura podemos concluir lo siguiente :

Las capacidades máximas PE y PP serán iguales sólo en el caso de que el esfuerzo de fluencia de la barra 2 sea el doble del esfuerzo de fluencia en las barras 1 y 3. En los demás casos será mayor PP. La reserva plástica puede estar en las barras 1 y 3 en la barra 2 dependiendo de los valores relativos de los límites de fluencia FY1 y FY2.

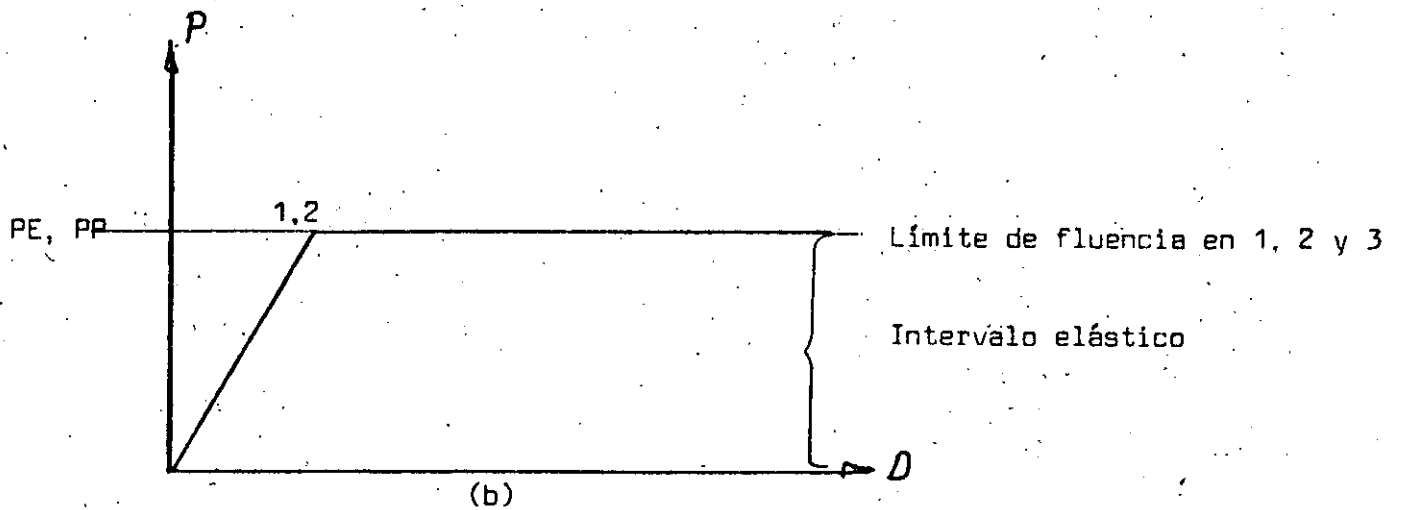
El valor de la reserva plástica dependerá de la diferencia entre -- FY1 y FY2/2 : mientras mayor sea la diferencia, mayor será la reserva plástica.

1)  $F_{Y1} < F_{Y2}/2$

10



2)  $F_{Y1} = F_{Y2}/2$



3)  $F_{Y1} > F_{Y2}/2$

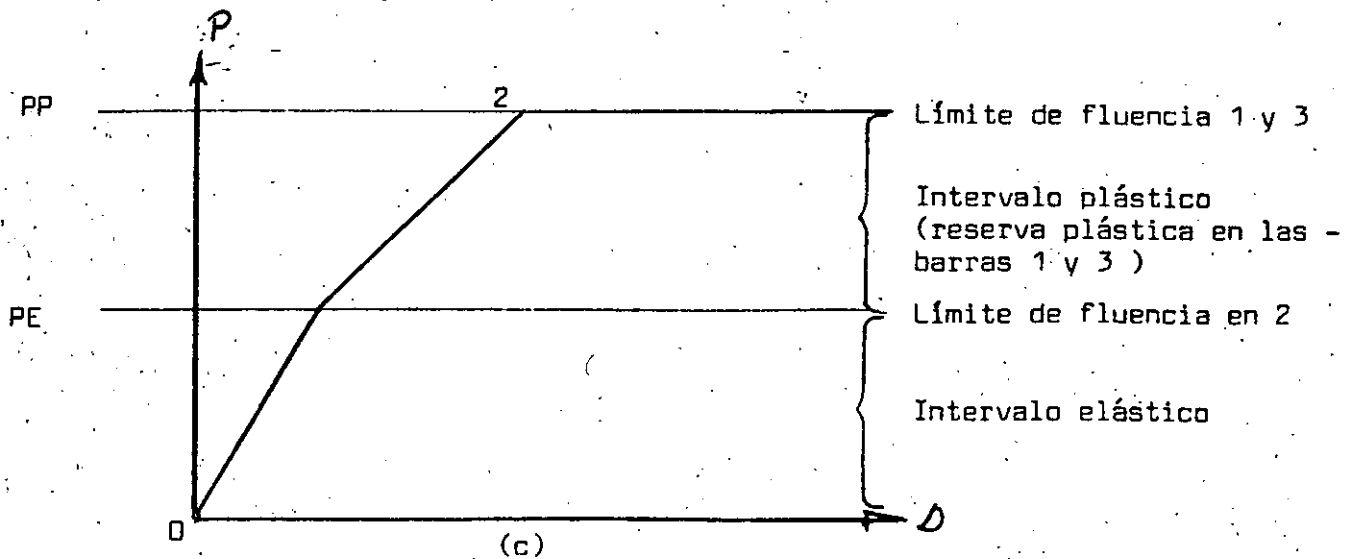


Fig. 8

Los distintos tipos de elementos que se utilizan para trabajar en tensión los podemos clasificar en los siguientes grupos :

- 1) Cables : elementos flexibles.
- 2) Barras redondas cuadradas y planas : elementos poco rígidos.
- 3) Secciones de perfiles simples : elementos rígidos
- 4) Secciones armadas : elementos rígidos.

En la Fig. 9 mostramos algunos de estos tipos de secciones.

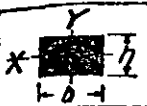
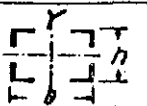
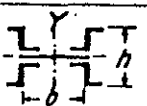
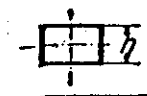

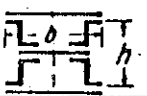

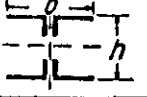
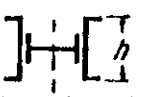

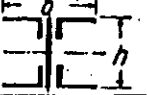
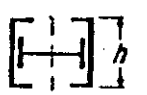
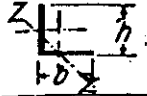
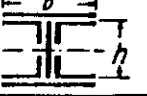

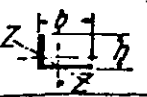
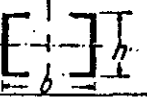
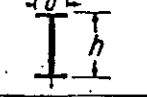
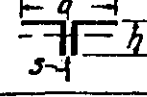


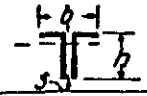


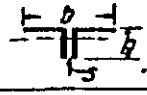

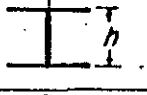

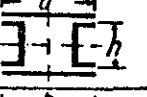
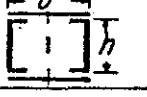
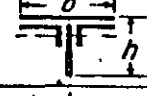
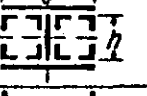

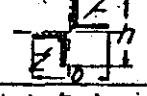
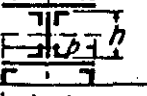
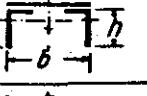
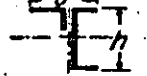
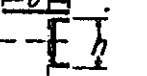

 $r_x = 0.29h$ $r_y = 0.29b$	 $r_x = 0.42h$ $r_y = 0.42b$	 $r_x = 0.31h$ $r_y = 0.48b$
 $r_x = 0.40h$ $h = \text{mean } h$	 $r_y = \text{same as for 2 L's}$	 $r_x = 0.37h$ $r_y = 0.28b$
 $r_x = 0.25h$	 $r_x = 0.42h$ $r_y = \text{same as for 2 L's}$	 $r_x = 0.31h$
 $r = \sqrt{\frac{h^2 + b^2}{16}}$ $r = 0.35 M_m$	 $r_x = 0.39h$ $r_y = 0.21b$	 $r_x = 0.31h$
 $r_x = 0.31h$ $r_y = 0.31b$ $r_z = 0.197h$	 $r_x = 0.45h$ $r_y = 0.235b$	 $r_x = 0.40h$ $r_y = 0.21b$
 $r_x = 0.29h$ $r_y = 0.32b$ $r_z = 0.18 \frac{h \cdot b}{2}$	 $r_x = 0.36h$ $r_y = 0.45b$	 $r_x = 0.38h$ $r_y = 0.22b$
 $r_x = 0.31h$ $r_y = 0.215b$ $b(0.21 + 0.002s)$	 $r_x = 0.36h$ $r_y = 0.60b$	 $r_x = 0.39h$
 $r_x = 0.32h$ $r_y = 0.21b$ $b(0.19 + 0.002s)$	 $r_x = 0.36h$ $r_y = 0.53b$	 $r_x = 0.35h$
 $r_x = 0.29h$ $r_y = 0.24b$ $b(0.23 + 0.002s)$	 $r_x = 0.39h$ $r_y = 0.55b$	 $r_x = 0.435h$ $r_y = 0.25b$
 $r_x = 0.30h$ $r_y = 0.17b$	 $r_x = 0.42h$ $r_y = 0.32b$	 $r_x = 0.42h$
 $r_x = 0.25h$ $r_y = 0.21b$	 $r_x = 0.44h$ $r_y = 0.28b$	 $r_x = 0.42h$
 $r_x = 0.21h$ $r_y = 0.21b$ $r_z = 0.19h$	 $r_x = 0.50h$ $r_y = 0.28b$	 $r_x = 0.285h$ $r_y = 0.37b$
 $r_x = 0.38h$ $r_y = 0.19b$	 $r_x = 0.39h$ $r_y = 0.21b$	 $r_x = 0.42h$ $r_y = 0.23b$

Fig. 9

Los cables se definen como miembros flexibles a tensión formados por uno o más grupos de alambres, torones o cuerdas. Un torón es un arreglo de alambres colocados helicoidalmente alrededor de un alambre central para obtener una sección simétrica; y un cable es un conjunto de torones colocados también helicoidalmente alrededor de un núcleo formado, a su vez, ya sea por un torón, por otro cable de alambres, o por un cable de fibras. Los cables de alambres con núcleo de fibras se emplean casi totalmente para propósitos de izaje; los torones y cables (Fig. 9) con núcleos de torones o núcleos independientes de cables de alambre son los que se usan para aplicaciones estructurales, y sus propiedades las estudiaremos a continuación. Consideraremos primero las propiedades mecánicas de los alambres, ya que son los elementos con los que están formados torones y cables.

Un alambre se define como una extensión simple y continua de metal, obtenida por estirado en frío a partir de varillas de acero de alto contenido de carbono laminadas en caliente y cuya composición química es estrictamente controlada. Los alambres se recubren de cinc, ya sea por el proceso de inmersión en caliente o por el proceso electrolítico. Aunque pueden usarse varios tipos de acero, el más común para aplicaciones estructurales es el alambre galvanizado para puentes, el cual también se usa para hacer torones y cables para puentes.

En la tabla 1 se muestran las resistencias de fluencia y de tensión, así como la elongación, del alambre galvanizado para puentes.

TABLA 1

Recubrimiento, Clase	Diámetro pgs.	Resistencia min. a la tensión, Kg./cm. <sup>2</sup>	Resistencia min. de fluencia a 0.7 % de extensión bajo carga	Elongación total min. en 10 pgs. por ciento
A	0.041 y mayores	15 470	11 250	4.0
B	Todos los diámetros	14 770	10 550	4.0
C	Todos los diámetros	14 060	9 840	4.0

La resistencia mínima de fluencia se mide al 0.7% de elongamiento bajo carga y el módulo de elasticidad del alambre varía de  $1.97 \times 10^6$  hasta  $2.11 \times 10^6$  Kg./cm<sup>2</sup>. Frecuentemente se especifica el tamaño del alambre por un número de calibre, en vez del diámetro; el estándar más común es el U.S. Steel Wire Gage. El alambre para puentes usado en torones y cables está galvanizado con un recubrimiento mínimo requerido, que depende del diámetro. El recubrimiento mínimo es el del grupo A, el grupo B tienen un recubrimiento del doble de espesor que el grupo A y el grupo C lo tiene del triple.

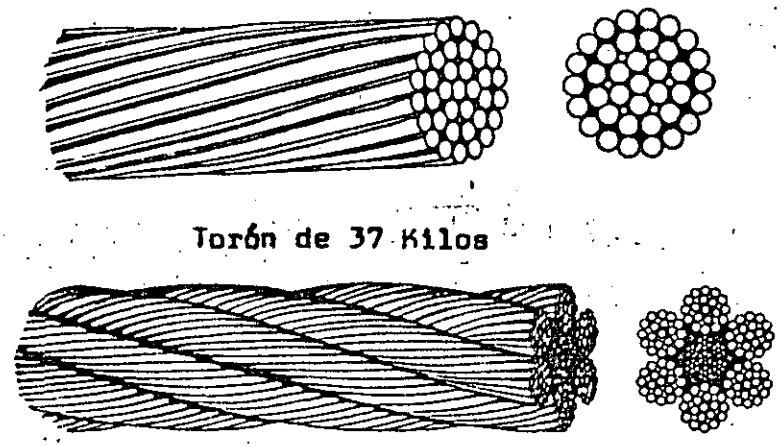
Los torones y cables que se usan para propósitos estructurales se fabrican a partir de componentes formados helicoidalmente, por lo que su comportamiento es algo distinto del de las varillas, barras de ojo, y del de los alambres individuales de que están hechos. - Cuando se aplica una carga de tensión a un torón o a un cable, la elongación resultante consistirá de (a) un alargamiento estructural ocasionado por los ajustes radiales y axiales de los alambres y torones bajo las cargas, y (b) el alargamiento elástico de los alambres.

El alargamiento estructural varía con el número de alambres por torón, el número de torones por cable y la longitud del tendido (paso de la Hélice) de los alambres y torones. El alargamiento varía también con la magnitud de la carga impuesta y con la cantidad de flexión a que pueda estar sujeto el cable; consecuentemente, puede observarse que el alargamiento estructural es eliminado gradualmente incrementándose el módulo de elasticidad del cable o torón completo.

Para aplicaciones estructurales en las cuales es permisible una elongación limitada bajo carga y donde se requiere un módulo de elasticidad estable, se logra eliminar el alargamiento estructural preestirando el cable o torón. Esto se lleva a cabo sometiendo dichos elementos a una carga predeterminada, durante un lapso suficiente para permitir el reacomodo de las partes componentes individuales.

A continuación se indican los módulos de elasticidad necesarios para determinar la deformación elástica de los torones y cables preestirados para puentes.

Torones de 1/2" a 2.9/16" de diámetro	:	1.69 X 10 <sup>6</sup>	Kg/cm <sup>2</sup>
Torones de 2.5/8" y mayores de diámetro	:	1.62 X 10 <sup>6</sup>	Kg/cm <sup>2</sup>
Cable de 3/8" a 4" de diámetro	:	1.46 X 10 <sup>6</sup>	Kg/cm <sup>2</sup>



Torón de 37 Kilos

Cable

FIG. 9

Los torones y cables para puentes no tienen un punto de fluencia -- definido porque se manufacturan con alambre estirado en frío; por tanto, de manera distinta a otros tipos de miembros en tensión, la carga de trabajo o el esfuerzo permisible de diseño se basa en la resistencia mínima de ruptura o resistencia última del cable o torón. Sus propiedades mecánicas se indican en las Tablas 2 y 3.

Los cables de acero se utilizan para cubrir grandes claros como -- son los puentes colgantes y cubiertas para gimnasios, auditorios, estadios, etc. ( Fig. 10 ).

Debido a que en estas estructuras se puede presentar el fenómeno de inestabilidad aerodinámica ó vibraciones excesivas se deberán -- utilizar cables de pretensado ó traveses de rigidez.

Es interesante hacer notar que las estructuras colgantes tienen -- cualidades excepcionales por lo que respecta al factor de seguridad nominal: en las estructuras tradicionales tales como armaduras, ácos y cascarones la seguridad se disminuye conforme aumenta su de formación, mientras que en las estructuras colgantes ocurre lo o-- puesto, debido a que al aumentar la deformación de los cables las fuerzas internas disminuyen.

TABLA 2

Propiedades mecánicas de los cables recubiertos de cinc

Normas establecidas por la "Wire Rope Technical Board"

Diámetro nominal en pulgs.	Resistencia mínima de ruptura en toneladas métricas. Recubri- miento Clase A	Peso aproximado. Kg./m.	Área metálica aproxi- mada en cm. <sup>2</sup>
3/8	5.9	0.36	0.419
1/2	10.4	0.62	0.768
5/8	16.3	0.97	1.174
3/4	23.6	1.41	1.729
7/8	31.7	1.90	2.328
1	41.4	2.48	3.038
1 1/8	52.4	3.14	3.844
1 1/4	65.5	3.93	4.805
1 3/8	79.6	4.78	5.844
1 1/2	94.3	5.68	6.940
1 5/8	111.5	6.71	8.192
1 3/4	129.5	7.80	9.482
1 7/8	148.7	8.97	10.901
2	168.7	10.19	12.384
2 1/8	190.5	11.50	13.997
2 1/4	213.1	12.89	15.609
2 3/8	236.7	14.30	17.351
2 1/2	261.2	15.77	19.157
2 5/8	287.5	17.29	21.092
2 3/4	314.7	18.96	23.091
2 7/8	343.8	20.68	25.219
3	373.7	22.48	27.413
3 1/4	430.8	26.78	32.508
3 1/2	503.4	31.25	37.604
3 3/4	580.5	35.71	43.022
4	662.1	40.18	48.956

TABLA 3

Propiedades mecánicas de los torones para puentes recubiertos de zinc

Normas establecidas por la "Wire Rope Technical Board"

Diámetro nominal p/ags.	Resistencia mínima de ruptura en toneladas métricas			Área metálica aproximada en cm. <sup>2</sup>	Peso aproximado en Kg./m
	Clase "A" recubrimiento completo	Clase "A" recubrimiento en los alambres interiores, Clase "B" recubrimiento en los alambres exteriores,	Clase "A" recubrimiento en los alambres interiores, Clase "C" recubrimiento en los alambres exteriores.		
1/2	13.6	13.2	12.9	0.97	0.77
9/16	17.2	16.7	16.4	1.23	0.98
5/8	21.8	21.1	20.7	1.51	1.22
11/16	26.3	25.5	24.9	1.83	1.47
3/4	30.8	29.9	29.3	2.18	1.76
13/16	36.3	35.2	34.5	2.55	2.07
7/8	41.7	40.5	39.6	2.96	2.40
15/16	50.0	47.5	46.5	3.40	2.75
1	55.3	53.7	52.5	3.87	3.13
1 1/16	62.6	60.7	59.4	4.37	3.53
1 1/8	70.8	68.7	67.2	4.90	3.96
1 3/16	78.0	75.7	74.1	5.46	4.40
1 1/4	87.1	85.4	83.6	6.05	4.88
1 5/16	96.2	94.3	92.5	6.65	5.59
1 3/8	105.2	103.4	100.7	7.29	5.91
1 7/16	114.3	111.6	109.8	8.00	6.46
1 1/2	125.2	122.5	119.8	8.71	7.04
1 9/16	136.0	133.4	130.6	9.48	7.63
1 5/8	147.0	144.2	140.6	10.28	8.26
1 11/16	159.7	156.0	153.3	11.03	8.90
1 3/4	170.6	166.9	163.3	11.87	9.57
1 13/16	183.3	179.6	176.0	12.71	10.27
1 7/8	196.0	192.3	187.8	13.61	11.00
1 15/16	208.7	205.0	200.5	14.52	11.74
2	222.3	218.6	215.9	15.48	12.50
2 1/16	236.8	233.2	229.5	16.45	13.30
2 1/8	251.3	247.7	244.0	17.48	14.52
2 3/16	265.8	262.2	257.6	18.52	14.95
2 1/4	281.2	276.7	273.1	19.61	15.83
2 3/8	312.1	322.1	303.0	21.81	17.63
2 5/16	296.7	292.1	287.6	20.71	16.73
2 7/16	326.6	322.1	316.6	23.03	18.57
2 1/2	341.1	335.7	331.1	24.20	19.54
2 9/16	355.6	350.2	344.7	25.41	20.53
2 5/8	378.3	372.9	366.4	26.65	21.53
2 11/16	391.9	385.6	380.0	27.94	22.56
2 3/4	410.1	403.7	397.3	29.29	23.63
2 7/8	448.2	440.9	434.5	32.00	25.83
3	488.1	480.8	473.5	34.84	28.12
3 1/8	529.8	521.6	513.4	37.81	30.52
3 1/4	567.0	558.8	549.6	40.91	33.00
3 3/8	610.5	601.5	592.3	44.07	35.59
3 1/2	656.8	648.2	636.7	47.92	38.29
3 5/8	696.7	686.8	675.7	50.84	41.07
3 3/4	745.7	734.8	722.9	54.45	43.94
3 7/8	796.5	784.7	772.8	58.13	46.92
4	839.2	826.5	813.6	61.94	50.00

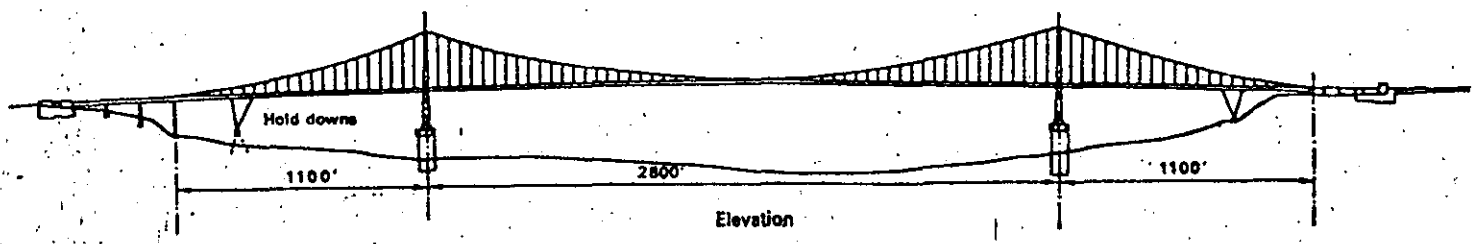
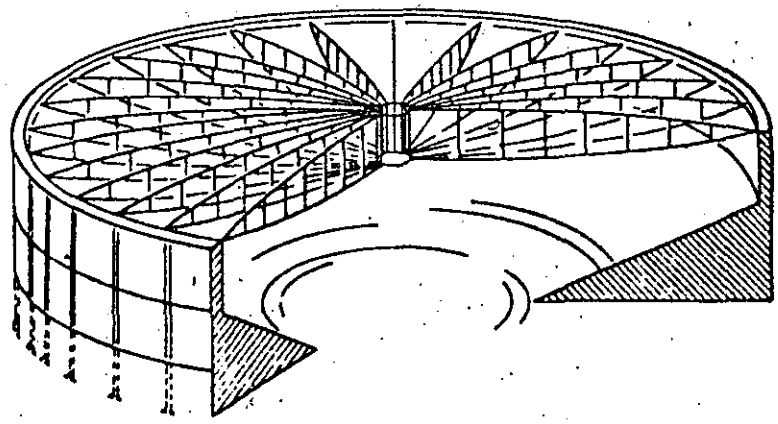
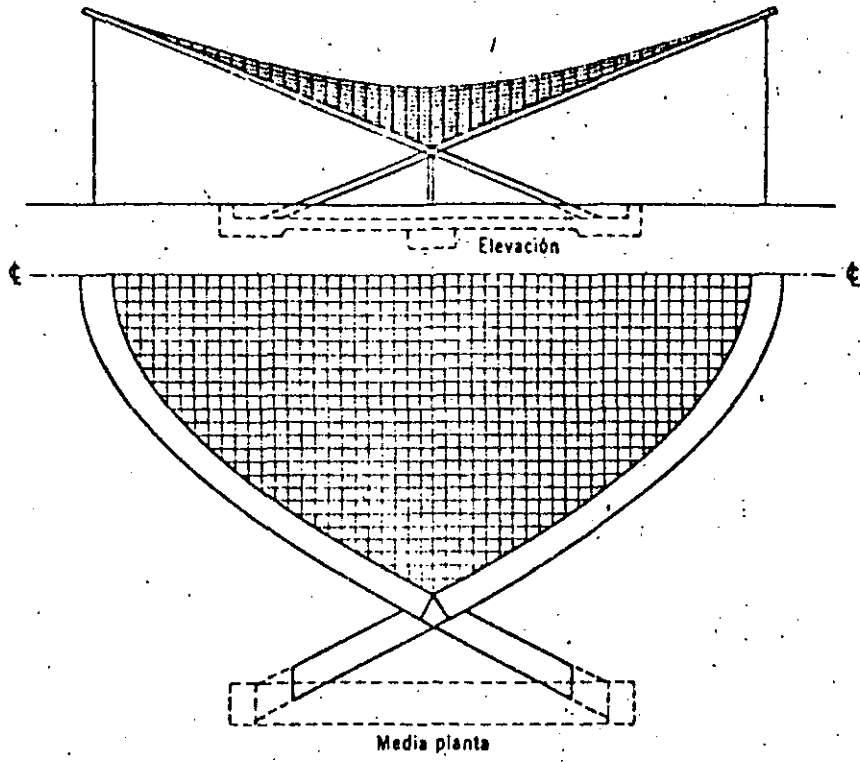


FIG. 10



Existen varios tipos de elementos para conectar los cables a los apoyos o a otros elementos de la estructura. En la fig. 11 se muestran dos tipos de casquillos y las mordazas ó perros cuando se usan abrazaderas, con las recomendaciones para el uso de las mordazas.

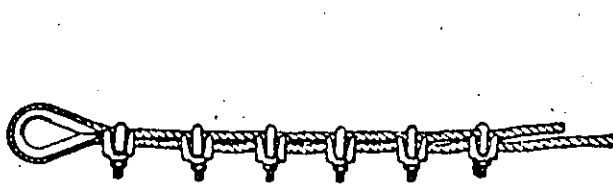
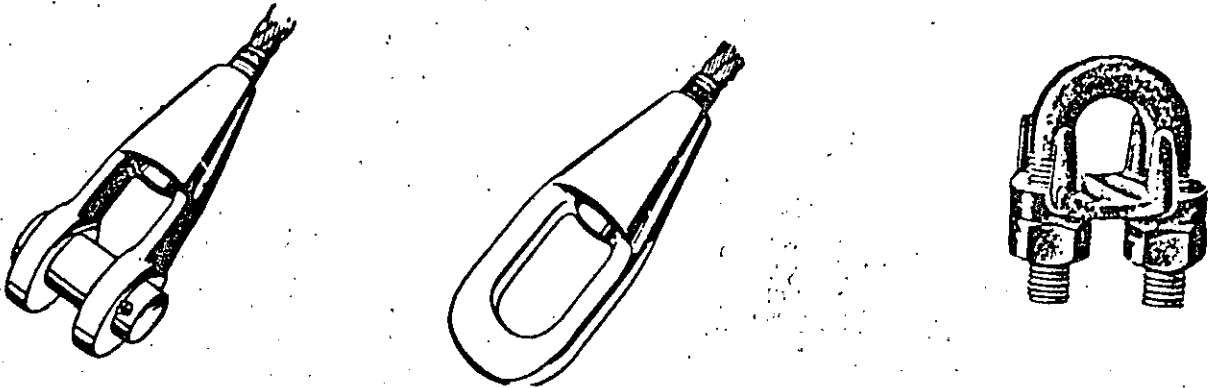


Figura 100 a

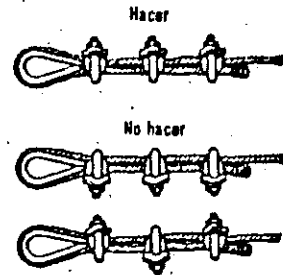


Figura 100 b

TABLA 81  
Número de ajustes y características dimensionales

Diámetro del cable		Número de ajustes		Espaciado de las mordazas	Longitud muerta del cable	Observaciones
En pulgadas	En mm	Cables ordinarios de alma vegetal	Cable de alta resistencia sobre alma metálica y antigiratoria			
	5 a					En caso de duda sobre la longitud entre ajustes tomar diámetro del cable por 8
	12	3	4			
1/2	12,7	4	5	0,089	0,305	
5/8	15,9	4	5	0,108	0,305	
3/4	19	4	5	0,127	0,457	
7/8	22,2	5	6	0,146	0,457	
1	25,4	5	6	0,165	0,609	
4 1/8	28,6	6	7	0,180	0,609	
1 1/4	31,2	6	7	0,200	0,609	
1 3/8	35,4	6	7	0,220	0,609	
1 1/2	38,1	7	8	0,240	0,609	
	38 a					
	50	7	8			

El diseño de cables trabajando como miembros a tensión es directo, se basa en la resistencia máxima a la tensión del cable utilizado, de acuerdo con los datos proporcionados por el fabricante; conocida la carga total que debe soportar el cable se busca en la tabla de resistencias del cable que se va a emplear uno cuya resistencia sea igual ó mayor que la carga multiplicada por el factor de seguridad, cuyo valor se toma entre 3 y 4 para estructuras.

Es importante verificar el alargamiento máximo que tendrá el cable y que éste dentro de los límites admisibles. Este alargamiento se calcula con la fórmula :

$$D = PL/AE$$

P = Carga sobre el cable

L = Longitud del cable

A = Area de la sección metálica del cable

E = Módulo de elasticidad del cable

EJEMPLO 3.- Determine el diámetro necesario de un cable de acero galvanizado para puente que debe soportar una carga de 50000 Kg. Calcule el alargamiento máximo del tirante considerando que tiene una longitud de 22.00 m y un módulo de elasticidad de  $1.5 \times 10^6$  Kg/cm<sup>2</sup>. Use un factor de seguridad de 4.

Resistencia necesaria del cable

$$R = 4 \times 50000 = 200000 \text{ Kg.}$$

De la tabla 2 seleccionamos un cable de 2.1/4" de diámetro que tiene una resistencia de 213000 Kg. El área metálica es de 15.61 cm<sup>2</sup>.

El alargamiento del cable sera :

$$D = (5000 \times 2200)/(15.61 \times 1.5 \times 10^6) = 4.7 \text{ cm.}$$

Las barras redondas y cuadradas son los elementos más sencillos - utilizados para trabajar en tensión axial. Las barras redondas se suelen utilizar con los extremos roscados con objeto de poder ajustar su longitud en el montaje. En ocasiones se suele aumentar el diámetro de los extremos, ya sea forjándolos ó soldando una barra redonda de mayor diámetro, con objeto de que el área neta en la -- sección de la rosca sea igual o un poco mayor que el área de la -- sección transversal donde no hay rosca.

Si los extremos de estas barras se conectan con soldadura es conveniente utilizar un templador intermedio para evitar que quede floja la barra. Las barras redondas se utilizan para diagonales de torres, para el arriostreimiento de naves industriales no muy grandes, para tirantes de arcos etc. No deben usarse donde haya equipo o maquinaría que transmita algún movimiento a la estructura, ya que fáci--mente pueden vibrar y, aparte de la molestia que esto ocasiona por el ruido, pueden fallar por fatiga.

Las barras planas generalmente se conectan con un pasador (Fig. 12). Se utilizan principalmente para transmitir la carga de un cable de acero a alguna parte de la estructura o a la cimentación.

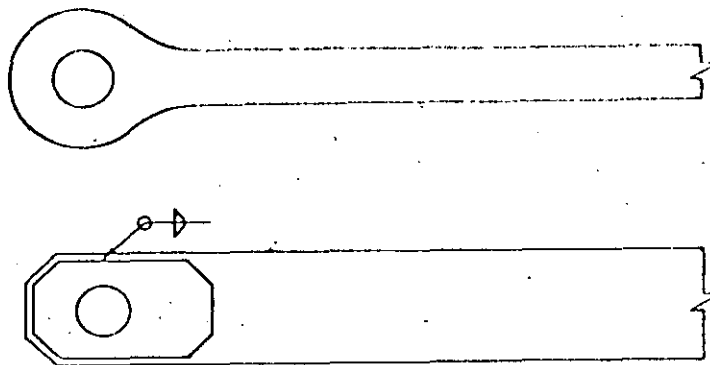


FIG. 12

En pruebas de laboratorio se ha visto que el tipo de falla que se -- puede presentar en la conexión con pasador es alguno de los siguientes :

- 1) Fractura de la placa en la dirección paralela al eje, en la parte posterior del perno. Esta falla se presenta cuando el agujero -- queda muy cerca de la orilla (Fig. 13 a ).
- 2) Falla en la sección neta en donde se encuentra el agujero, en la dirección perpendicular al eje de la barra. Este tipo de falla si el área de la sección neta es igual o menor al área de la sección bruta de la barra. (Fig. 13 b).

- 3) Falla por pandeo local debido a que, en la parte posterior del perno, la relación ancho a espesor de la placa es muy grande. -- (Fig. 13 c).

Para lograr que la falla se produzca en la parte principal de la barra y no en los extremos, las normas y especificaciones definen -- los criterios para dimensionar estos.

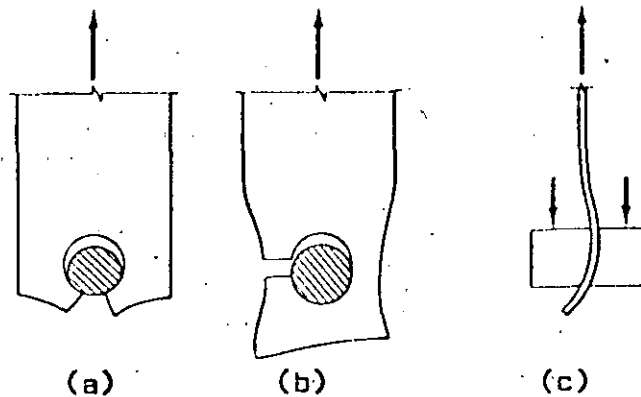


FIG. 13

#### Secciones de perfiles simples y secciones armadas.

Estos elementos se utilizan cuando se requiere un cierto grado de rigidez ó cuando se puede presentar una inversión de carga que cause que la pieza trabaje compresión bajo ciertas condiciones de carga, por ejemplo, en diagonales y montantes de armaduras. Las secciones compuestas se utilizan, cuando las cargas son de mayor intensidad y las secciones simples no tienen la resistencia necesaria. También se puede requerir una sección armada para aumentar la rigidez de la barra. Las secciones armadas se construyen con perfiles simples conectados entre si por medio de celosias, placas interrumpidas ó placas continuas.

Para diseñar los elementos de una estructura es necesario basarnos en normas ó especificaciones que siempre están apoyadas en la experiencia pasada y en una gran cantidad de pruebas de laboratorio. En esta forma se evita, en gran parte, que el proyectista use criterios erróneos que conduzcan a estructuras antieconómicas por usar factores de seguridad muy grandes, ó por el contrario, que buscando economías mal entendidas, se usen factores de seguridad tan bajos que hagan peligrar la seguridad de la estructura.

Los ejemplos que veremos están resueltos usando las especificaciones del AMERICAN INSTITUTE OF STEEL CONSTRUCTION y las normas complementarias del REGLAMENTO PARA LAS CONSTRUCCIONES DEL D.F. usando el -- criterio de esfuerzos permisibles.

Los miembros a tensión se deben dimensionar de tal manera que el -- esfuerzo promedio en la sección no exceda al esfuerzo permisible que fija la especificación ó norma, como una fracción del esfuerzo de -- fluencia ó del de ruptura. El esfuerzo en la barra se determina dividiendo la fuerza actuante entre el área total ó el área neta efectiva, según proceda :

$$f_t = P/A$$

Es conveniente procurar reducir al mínimo las causas que originan -- concentración de esfuerzos, especialmente en los casos de cargas variables con gran número de repeticiones. Los esfuerzos provenientes de las concentraciones mencionadas no se suman a los esfuerzos promedios. Se ha comprobado experimentalmente en pruebas llevadas hasta -- la falla, que las zonas donde se presenta una fluencia localizada -- del material en piezas bien diseñadas y bien fabricadas, no impidan que la sección total alcance el límite de fluencia y que lo sobrepase, alcanzando a desarrollar la resistencia completa de la barra antes de fallas.

Cuando una estructura está sujeta a cargas variables que se repitan miles y a veces millones de veces, pueden aparecer grietas en el acero que se van extendiendo en la sección hasta ocasionar la ruptura -- de la pieza. A esta falla se llama falla por fatiga. La falla por fatiga se presenta principalmente cuando existen esfuerzos de tensión. Las concentraciones de esfuerzos aumentan la susceptibilidad a fallar por fatiga. Los aceros de altas resistencias presentan una resistencia a la fatiga similar al acero A 36.

Las especificaciones AISC han introducido un enfoque que simplifica considerablemente el diseño de las barras sujetas a cargas repetidas. Se basa en el valor del intervalo de esfuerzo comprendido entre el -- valor máximo y el valor mínimo del esfuerzo en la sección. El intervalo de esfuerzo es igual a la diferencia algebraica entre los valores máximo y mínimo del esfuerzo que se presenta en un ciclo completo de carga.

El intervalo de esfuerzo permitido depende del número de ciclos y de las características locales de la sección que se revisa. En las especificaciones establecen cuatro condiciones de carga de acuerdo con -- el número de repeticiones, y seis categorías de esfuerzo de acuerdo con las características de la sección.

EXTRACTO DE LAS "ESPECIFICACIONES -  
PARA EL DISEÑO, FABRICACION Y MONTA  
JE DE ACERO ESTRUCTURAL PARA EDIFI-  
CIOS" DEL AMERICAN INSTITUTE OF - -  
STEEL CONSTRUCTION REQUERIDAS PARA  
EL DISEÑO DE MIEMBROS EN TENSIÓN.

**1.4.1 Acero Estructural**

1.4.1.1 El material que se ajuste a una de las siguientes especificaciones (última fecha de edición) está aprobado para el uso bajo esta Especificación:

*Structural Steel, ASTM A36*

*Welded and Seamless Steel Pipe, ASTM A53, Grade B*

*High-Strength Low-Alloy Structural Steel, ASTM A242*

*High-Strength Low-Alloy Structural Manganese Vanadium Steel, ASTM A441*

*Cold-Formed Welded and Seamless Carbon Steel Structural Tubing in Rounds and Shapes, ASTM A500*

*Hot-Formed Welded and Seamless Carbon Steel Structural Tubing, ASTM A501*

*High-Yield Strength Quenched and Tempered Alloy Steel Plate, Suitable for Welding, ASTM A514*

*Structural Steel with 42,000 psi Minimum Yield Point, ASTM A529*

*Hot-Rolled Carbon Steel Sheets and Strip, Structural Quality, ASTM A570, Grades D and E*

*High-Strength Low-Alloy Columbium-Vanadium Steels of Structural Quality, ASTM A572*

*High-Strength Low-Alloy Structural Steel with 50,000 psi Minimum Yield Point to 4 in. Thick, ASTM A588*

*Steel Sheet and Strip, Hot-Rolled and Cold-Rolled, High-Strength, Alloy, with Improved Corrosion Resistance, ASTM A656*

*Steel Sheet and Strip, Hot-Rolled and Cold-Rolled, High-Strength, Low-Alloy, Columbium and/or Vanadium, ASTM A607*

*Hot-Formed Welded and Seamless High-Strength Low-Alloy Structural Tubing, ASTM A618*

Los informes certificados de ensayos de fabricación de aceros, o los informes certificados de ensayos ejecutados por el fabricante, o un laboratorio de ensayo de acuerdo con ASTM A6 o A568, según sea aplicable, y con la especificación correspondiente, constituirán evidencia suficiente de conformidad con una de las normas ASTM indicadas. Adicionalmente, el fabricante, si se le solicita, suplirá una certificación de que el acero estructural suministrado cumple con los requisitos del grado especificado.

1.4.1.2 Podrán ser usados aceros no identificados, si están libres de imperfecciones superficiales, en partes de menor importancia o en detalles sin importancia, donde las propiedades físicas estrictas del acero y su soldabilidad, no afectan la resistencia de la estructura.

**SECCION 1.5 ESFUERZOS ADMISIBLES****1.5.1 Acero Estructural****1.5.1.1 Tracción**

Excepto para miembros con unión de pasador,  $F_t$  no excederá  $0,60 F_y$  en el área total, ni  $0,50 F_u$  en el área neta efectiva.\*

Para miembros con unión de pasador:  $F_t = 0,45 F_y$  en el área neta\*.

Para tracción en partes roscadas: Ver Tabla 1.5.2.1.

TABLA 1.5.2.1  
Tensión Admisible de Conectores, kg/cm<sup>2</sup> (MPa)

Descripción de los Conectores	Tracción Admisible <sup>a</sup> (F <sub>t</sub> )	Corte Admisible <sup>a</sup> (F <sub>v</sub> )			
		Uniones Tipo Fricción <sup>c,1</sup>			Uniones Tipo Aplastamiento <sup>i</sup>
		Perforaciones Normales	Perforaciones Mayores y Ovaladas Cortas	Perforaciones Ovaladas Largas	
Remaches A502, Grado 1, colocados en caliente	1620 <sup>a</sup> (159)				1230 <sup>f</sup> (121)
Remaches A502, Grados 2 y 3, colocados en caliente	2040 <sup>a</sup> (200)				1550 <sup>f</sup> (152)
Pernos A307	1410 <sup>a</sup> (138)				703 <sup>b, f</sup> (69)
Partes roscadas que cumplen los requisitos de las Secciones 1.4.1 y 1.4.4, y pernos A449 que cumplen los requisitos de la Sección 1.4.4, cuando las roscas están incluidas en los planos de corte	0,33 F <sub>u</sub> <sup>a, c, h</sup>				0,17 F <sub>u</sub> <sup>h</sup>
Partes roscadas que cumplen los requisitos de las Secciones 1.4.1 y 1.4.4, y pernos A449 que cumplen los requisitos de la Sección 1.4.4, cuando las roscas están excluidas de los planos de corte	0,33 F <sub>u</sub> <sup>a, h</sup>				0,22 F <sub>u</sub> <sup>h</sup>
Pernos A325, cuando las roscas están incluidas en los planos de corte	3090 <sup>d</sup> (303)	1230 (121)	1050 (103)	879 (86)	1480 <sup>f</sup> (145)
Pernos A325, cuando las roscas están excluidas de los planos de corte	3090 <sup>d</sup> (303)	1230 (121)	1050 (103)	879 (86)	2110 <sup>f</sup> (207)
Pernos A490, cuando las roscas están incluidas en los planos de corte	3800 <sup>d</sup> (372)	1550 (152)	1340 (131)	1120 (110)	1970 <sup>f</sup> (193)
Pernos A490, cuando las roscas están excluidas de los planos de corte	3800 <sup>d</sup> (372)	1550 (152)	1340 (131)	1120 (110)	2810 <sup>f</sup> (276)

<sup>a</sup> Solamente para carga estática.

<sup>b</sup> Roscas permitidas en los planos de corte.

<sup>c</sup> La capacidad de tracción de la parte roscada de una barra de rosca sobrepuesta, basada en el área de la sección transversal, A<sub>b</sub>, en su diámetro mayor de rosca, será mayor que el área del cuerpo nominal de la barra, antes de sobreponerle la rosca multiplicada por 0,60 F<sub>y</sub>.

<sup>d</sup> Para pernos A325 y A490 sometidos a fatiga por carga de tracción, ver Apéndice B, Sección B3.

<sup>e</sup> Cuando lo especifique el ingeniero, la tensión admisible de corte para uniones tipo fricción, que tengan condiciones de superficie de empalme especial, podrán incrementarse el valor aplicable dado en el Apéndice E.

<sup>f</sup> Cuando las uniones tipo aplastamiento, usadas para empalmar miembros a tracción, tienen una disposición de conectores cuya longitud, medida paralelamente a la línea de la fuerza, excede 127 cm (50 in), los valores tabulados serán reducidos en un 20%.

<sup>g</sup> Ver Sección 1.5.6.

<sup>h</sup> Ver Apéndice A, Tabla 2, para valores específicos de especificaciones de acero ASTM.

<sup>i</sup> Para limitaciones en el uso de perforaciones mayores y ovaladas, ver Sección 1.23.4.

### 1.5.6 Tensiones Causadas por Viento y Sismo

Las tensiones admisibles podrán ser incrementadas en un tercio por encima de los valores anteriores previstos, cuando son producidas por cargas de viento o sismo, actuando solas o en combinación con las cargas muertas y vivas de diseño, siempre que la sección requerida, calculada sobre esta base, no sea menor que la requerida para el diseño por cargas muertas, vivas e impacto (si lo hay), calculada sin el tercio de incremento de la tensión, y siempre que las tensiones no requieran ser calculadas de otra forma\*, en base a factores de reducción aplicados a las cargas de diseño combinadas. El aumento de tensión anterior no se aplica a los rangos de variación de tensión admisible previstos en el Apéndice B.



**SECCION 1.7 MIEMBROS Y UNIONES SOMETIDOS A VARIACION REPETIDA DE TENSION (FATIGA)**

**1.7.1 Generalidades**

La fatiga, como se usa en esta Especificación, se define como el daño que puede resultar en una fractura después de un número suficiente de fluctuaciones de tensión. El rango de variación de tensión es definido como la magnitud de esas fluctuaciones. En el caso de inversión de tensión, el rango de variación de tensión será calculado como la suma numérica de las máximas tensiones repetitivas de tracción y compresión, o la suma de las máximas tensiones de corte de dirección opuesta en un punto dado, que resultan de las diferentes disposiciones de la carga viva.

Pocos miembros o uniones en edificios convencionales necesitan ser diseñados para fatiga, puesto que la mayoría de los cambios de carga en tales estructuras ocurren sólo un pequeño número de veces o producen sólo fluctuaciones menores de tensión. La situación de que exista la ocurrencia de la totalidad de las cargas de diseño por viento o sismo es demasiado improbable como para justificar consideraciones de diseño por fatiga. Sin embargo, las vigas porta-grúas y las estructuras de soporte para maquinaria y equipo a menudo están sometidas a condiciones de carga que producen fatiga.

**1.7.2 Diseño por Fatiga**

Los miembros y sus uniones sometidos a cargas que producen fatiga, serán dimensiones estipuladas en el Apéndice B.

**SECCION 1.8 ESTABILIDAD Y RELACIONES DE ESBELTEZ**

**1.8.4 Relaciones Máximas de Esbeltez**

La relación de esbeltez,  $KL/r$ , de miembros comprimidos no excederá de 200. La relación de esbeltez,  $L/r$ , de miembros traccionados, que no sean barras, preferiblemente no excederá:

Para miembros principales .....	240
Para miembros de arriostamiento lateral y otros miembros secundarios .....	300

**SECCION 1.14 AREA NETA Y AREA TOTAL**

**1.14.1 Definiciones**

El área total de un miembro en cualquier punto se determinará sumando los productos del espesor y el ancho total de cada elemento medido en sentido normal al eje del miembro. El área neta se determinará sustituyendo el ancho total por el ancho neto calculado de acuerdo con las Secciones 1.14.2 a 1.14.5, inclusive.

### 1.14.2 Area Neta y Area Neta Efectiva

1.14.2.1 En el caso de una cadena de perforaciones prolongadas a través de una parte en cualquier línea diagonal o zig-zag, el ancho neto de la parte se obtendrá restando del ancho total la suma de los diámetros de todas las perforaciones en la cadena, y sumando, para cada espacio entre perforaciones en la cadena, la cantidad  $s^2/4g$

donde

$s$  = separación longitudinal centro a centro ("paso") entre dos perforaciones consecutivas cualesquiera, mm

$g$  = separación transversal centro ("gramil") de las mismas dos perforaciones, mm

El área neta crítica,  $A_n$ , de la parte considerada se obtiene a partir de la cadena que dé el menor ancho neto.

En la determinación del área neta a través de soldaduras de tapón o canal, el metal de soldadura no se considerará como contribuyente al área neta.

1.14.2.2 El área neta efectiva,  $A_e$ , de miembros traccionados cargados axialmente, donde la carga es transmitida por pernos o remaches a través de algunos,

pero no por todos los elementos de la sección transversal del miembro\*, deberá calcularse por la fórmula

$$A_e = C_1 A_n$$

donde

$A_n$  = área neta del miembro

$C_1$  = un coeficiente de reducción

A menos que un coeficiente mayor pueda ser justificado por ensayos o por otros criterios reconocidos\*, en los cálculos se deberán utilizar los siguientes valores de  $C_1$ :

1. Para perfiles W, M o S con anchos de ala no menores que 2/3 de la altura, y T estructurales cortadas de estos perfiles, siempre que la unión sea a las alas y no tenga menos de tres conectores por línea en la dirección de la tensión .....  $C_1 = 0,90$
2. Para perfiles W, M o S que no cumplan las condiciones del subpárrafo 1, T estructurales cortadas de estos perfiles, y cualquier otro perfil, incluyendo las secciones armadas, siempre que la unión no tenga menos de 3 conectores por fila en la dirección de la tensión .....  $C_1 = 0,85$
3. Para todos los miembros cuyas uniones tengan solamente 2 conectores por línea en la dirección de la tensión .....  $C_1 = 0,75$

1.14.2.3 Los empalmes, cartelas y otros accesorios de uniones remachados y empernados, sometidos a fuerzas de tracción serán diseñados en conformidad con las disposiciones de la Sección 1.5.1.1, donde el área neta efectiva será tomada como el área neta real, excepto que, para el propósito de cálculos de diseño, ésta no se considerará mayor que el 85 por ciento del área total.

### 1.14.3 Angulos

Para ángulos, el ancho total será la suma de los anchos de las alas menos el espesor. El gramil para perforaciones en alas opuestas será la suma de los gramiles desde la parte posterior de los ángulos menos el espesor.

### 1.14.4 Tamaño de las Perforaciones

En el cálculo del área neta, se considerará el ancho de una perforación para remache o perno como 1,6 mm (1/16 in) mayor que la dimensión nominal de la perforación normal a la dirección de la tensión aplicada.

Las barras de ojo serán de espesor uniforme, sin refuerzo en las perforaciones de pasadores. Deberán tener cabezas "circulares" en las cuales la periferia de la cabeza, más allá de la perforación del pasador, sea concéntrica con la perforación del pasador. El radio de transición, entre la cabeza circular y el cuerpo de la barra de ojo, será igual o mayor que el diámetro de la cabeza.

El ancho del cuerpo de la barra de ojo no excederá 8 veces su espesor, y el espesor no será menor de 12,7 mm (1/2 in). El área neta de la cabeza a través de la perforación del pasador, transversal al eje de la barra de ojo, no será menor de 1,33 ni mayor de 1,5 veces el área de la sección transversal del cuerpo de la barra de ojo. El diámetro del pasador no será menor que 7/8 veces el ancho del cuerpo de la barra de ojo. El diámetro de la perforación del pasador no podrá exceder más de 0,8 mm (1/32 in) el diámetro del pasador. Para aceros que tengan una tensión de fluencia mayor que 4920 kgf/cm<sup>2</sup> (483 MPa), el diámetro de la perforación del pasador no excederá 5 veces el espesor de la plancha.

En planchas unidas con pasadores, que no sean barras de ojo, la tensión de tracción en el área neta, transversal al eje del miembro, no excederá la tensión admisible estipulada en la Sección 1.5.1.1, y la tensión de aplastamiento en el área proyectada del pasador no excederá la tensión admisible estipulada en la Sección 1.5.1.5.1. El área neta mínima más allá de la perforación del pasador, paralela al eje del miembro, no será menor que 2/3 veces el área neta a través de la perforación del pasador.

La distancia transversal al eje de una plancha unida con pasador o cualquier elemento individual de un miembro armado, desde el borde de una perforación para pasador al borde del miembro o elemento, no excederá 4 veces al espesor en la perforación del pasador. El diámetro de la perforación del pasador no será menor de 1,25 veces la menor de las distancias unida el borde de la perforación del pasador al borde de una plancha unida con pasador, o de un elemento separado de un miembro armado en la perforación del pasador. Para miembros unidos con pasadores, en los cuales se cuente con el pasador para permitir movimiento relativo entre las partes unidas, cuando se está bajo la carga total, el diámetro de la perforación del pasador no será mayor de 0,8 mm (1/32 in) que el diámetro del pasador.

Las esquinas más allá de la perforación del pasador podrán ser cortadas a 45° del eje del miembro; siempre que el área neta más allá de la perforación del pasador, en un plano perpendicular al de corte, no sea menor que la requerida más allá de la perforación del pasador paralelo al eje del miembro.

Se podrán obviar las limitaciones de espesor, tanto en barras de ojo como en planchas unidas con pasadores, siempre que se coloquen tuercas exteriores a fin de apretar las placas con pasadores y planchas de relleno con un contacto ajustado. Cuando las planchas estén dispuestas de este modo, la tensión admisible de aplastamiento no será mayor que la especificada en la Sección 1.5.1.5.1.

## SECCION 1.15 UNIONES

### 1.15.1 Uniones Mínimas

Las uniones que transmitan tensiones calculadas, excepto para las barras de celosías de enlace, tirantes y correas de pared, se diseñarán para soportar no menos de 2720 kgf (26,7 kN).

### 1.15.2 Uniones Excéntricas

Siempre que sea posible, los ejes de gravedad de los miembros que concurren en un punto y estén sometidos a tensión axial deberán intersectarse; de no ser así, se deberá tomar en cuenta las tensiones de flexión originadas por la excentricidad.

### 1.15.3 Colocación de Remaches, Pernos y Soldaduras

Excepto para los casos que se describirán más adelante, los grupos de remaches, pernos o soldaduras en los extremos de cualquier miembro que transmitan tensión axial en esos miembros, tendrán sus centros de gravedad en el eje de gravedad del miembro, a menos que se considere debidamente el efecto de la excentricidad resultante. Excepto en los miembros sometidos a variación repetida de tensión, tal como se definió en la Sección 1.7, no se requiere la disposición de filetes de soldadura para balancear las fuerzas alrededor del eje o ejes neutros en uniones extremas de ángulos simples, ángulos dobles y miembros de tipo similar. La excentricidad entre los ejes de gravedad de tales miembros y las líneas de gramiles para sus uniones extremas remachadas o empalmadas, podrá ser despreciada en miembros cargados estáticamente, pero deberá ser considerada en miembros sometidos a cargas de fatiga.

### 1.15.7 Uniones de Miembros a Tracción y Compresión en Armaduras

Las uniones en los extremos de miembros a tracción o compresión en armaduras, deberán desarrollar la fuerza requerida por la carga de diseño, pero no menos del 50 por ciento de la resistencia efectiva del miembro, basada en el tipo de tensión que controle la selección del miembro.

## SECCION 1.18 MIEMBROS ARMADOS

### 1.18.3 Miembros a Tracción

**1.18.3.1** La separación longitudinal de conectores y soldaduras en filete intermitente, que unan una plancha y un perfil laminado en un miembro armado traccionado, o dos planchas componentes en contacto entre sí, no excederá 24 veces el espesor de la plancha más delgada ni 305 mm (12 in). La separación longitudinal de conectores y soldaduras intermitentes que unan dos o más perfiles en contacto entre sí en un miembro traccionado no excederá 610 mm (24 in). Los miembros traccionados constituidos por dos o más perfiles o planchas separados unos de otros por planchas de relleno intermitentes, serán unidos entre sí en estas planchas de relleno a intervalos tales que la relación de esbeltez de cada uno de los componentes entre conectores no exceda 240.

**1.18.3.2** Se podrán usar tanto platabandas como planchas de unión sin celosías en los lados abiertos de miembros armados a tracción. Las planchas de unión tendrán una longitud no menor que dos tercios la distancia entre las líneas de conectores o soldaduras que las unan a los componentes del miembro. El espesor de tales planchas de unión no será menor que 1/50 de la distancia entre estas líneas. La separación longitudinal de conectores o soldaduras intermitentes en las planchas de unión no excederá 152 mm (6 in). La separación de las planchas de unión será tal que la relación de esbeltez de cualquier componente en la longitud entre las planchas de unión no excederá 240.

**SECCION B. CONDICIONES DE CARGA; TIPO Y UBICACION DEL MATERIAL**

En el diseño de los miembros y uniones sometidos a variación repetitiva de tensión por carga viva, se considerará el número de ciclos de tensión, amplitud del rango de tensión esperado y el tipo y ubicación de miembros o detalles.

Las condiciones de carga serán clasificadas como se muestra en la Tabla B1.

El tipo y la ubicación del material serán clasificados de acuerdo a la Tabla B2.

**TABLA B1**  
Número de Ciclos de Carga

Condición de Carga	Desde	Hasta
1	20000 <sup>a</sup>	100000 <sup>b</sup>
2	100000	500000 <sup>c</sup>
3	500000	2000000 <sup>d</sup>
4	Sobre 2000000	

<sup>a</sup> Aproximadamente equivalente a dos aplicaciones diarias durante 25 años.  
<sup>b</sup> Aproximadamente equivalente a diez aplicaciones diarias durante 25 años.  
<sup>c</sup> Aproximadamente equivalente a cincuenta aplicaciones diarias durante 25 años.  
<sup>d</sup> Aproximadamente equivalente a doscientas aplicaciones diarias durante 25 años.

**SECCION B2 TENSIONES ADMISIBLES**

La tensión máxima no excederá la tensión básica admisible estipulada en las Secciones 1.5 y 1.6 de esta Especificación, y el rango máximo de variación de tensión no excederá al dado en la Tabla B3.

**SECCION B3 DISPOSICIONES PARA CONECTORES MECANICOS**

B3.1 El rango de variación de la tensión de tracción en pernos A325 o A490 apretados correctamente no necesita ser considerado, pero la tensión máxima calculada, incluyendo la acción de palanca, no excederá los valores dados en la Tabla 1.5.2.1, sometida a las siguientes disposiciones:

1. Las uniones sometidas a más de 20000 ciclos, pero no más de 500000 ciclos, de tracción directa podrán ser diseñadas para la tensión producida por la suma de las cargas aplicadas y la carga de palanca, si la carga de palanca no excede 10 por ciento de la carga aplicada externamente. Si la fuerza de palanca excede de 10 por ciento, la tensión admisible de tracción dada en la Tabla 1.5.2.1 se reducirá en un 40%, aplicable sólo a la carga externa.
2. Las uniones sometidas a más de 500000 ciclos de tracción directa podrán ser diseñadas para la tensión producida por la suma de las cargas aplicadas y la carga de palanca, si la carga de palanca no excede 5 por ciento de la carga aplicada externamente. Si la fuerza de palanca excede del 5 por ciento, la tensión admisible de tracción dada en la Tabla 1.5.2.1 se reducirá en un 50 por ciento, aplicable sólo a la carga externa.

B3.2 No se recomienda el uso de otros pernos y partes roscadas sometidos a cargas de fatiga de tracción.

B3.3 Los remaches, pernos y partes roscadas sometidos a cargas cíclicas de corte podrán ser diseñados para las tensiones de corte tipo aplastamiento dadas en la Tabla 1.5.2.1, en cuanto concierne a la resistencia a la fatiga de los conectores en sí mismos.

**TABLA B2**

Condición General	Situación	Clase de Tensión <sup>a</sup>	Categoría de Tensión (Ver Tabla B3)	Número de los ejemplos ilustrativos (Ver Fig. B1) <sup>b</sup>
Material Plano	Metal base con superficies laminadas o limpias	To Rev.	A	1,2
Miembros Armados	Metal base y metal de soldadura en miembros sin apéndices, armados con planchas o perfiles unidos por soldaduras continuas en ranura de penetración completa o parcial, o soldaduras continuas en filete paralelas a la dirección de la tensión aplicada.	To Rev.	B	3,4,5,6
	Tensión de flexión calculada, $f_b$ , en el metal base al pie de las soldaduras en almas o alas de viga adyacentes a atiesadores transversales soldados.	To Rev.	C	7
	Metal base en el extremo de platabandas soldadas de longitud parcial que tengan extremos a escuadra o de sección variable, con o sin soldaduras a través de los extremos.	To Rev.	E	5
Uniones Fijadas Mecánicamente	Metal base en la sección total de uniones tipo fricción empernadas con pernos de alta resistencia, excepto uniones sometidas a inversión de tensión y juntas cargadas axialmente, las cuales inducen flexión fuera del plano en el material unido.	To Rev.	B	8
	Metal base en la sección neta de otras uniones fijadas mecánicamente	To Rev.	D	8,9
	Metal en la sección neta de uniones tipo aplastamiento empernadas con pernos de alta resistencia.	To Rev.	B	8,9
Uniones soldadas con soldaduras en Filete	Metal base en soldaduras intermitentes en filete.	To Rev.	E	
	Metal base en el empalme de miembros cargados axialmente con uniones extremas soldadas con soldadura en filete. Las soldaduras se deberán colocar alrededor del eje del miembro de manera de balancear las tensiones de las soldaduras.	To Rev.	E	17,18,20
	Metal de soldadura en soldaduras en filete continuas o intermitentes, longitudinales o transversales.	S	F	5,17,18,21
Soldaduras en Ranura	Metal base y metal de soldadura en empalmes soldados con soldaduras en ranura de penetración completa de partes de sección transversal similar esmeriladas al ras, con esmerilado en la dirección de la tensión aplicada, y con pureza de soldadura establecida por inspección radiográfica o ultrasónica en conformidad con los requerimientos de la Tabla 9.25.3 de AWS D1.1-77.	To Rev.	B	10
	Metal base y metal de soldadura en empalmes soldados con soldaduras en ranura de penetración completa en transiciones de ancho o espesor, con soldaduras esmeriladas para proveer inclinaciones con pendiente no mayor de 40%, con esmerilado en la dirección de la tensión aplicada, y con pureza de soldadura establecida por inspección radiográfica o ultrasónica en conformidad con los requerimientos de la Tabla 9.25.3 de AWS D1.1-77.	To Rev.	B	12,13

<sup>a</sup> "T" significa rango de variación de tensión de tracción solamente; "Rev." significa un rango de variación que involucra inversión de tensión de tracción ó compresión; "S" significa rango de variación en corte incluyendo la inversión de tensión de corte.  
<sup>b</sup> Se proporcionan estos ejemplos como guías y no intentan excluir otras situaciones razonablemente similares. B

TABLA B 2 (CONTINUACION)

Condición General	Situación	Clase de Tensión <sup>a</sup>	Categoría de Tensión (Ver Tabla B3)	Número de los Ejemplos Ilustrativos (Ver (Fig. B1) <sup>b</sup> )
Soldaduras en Ranura	Metal base y metal de soldadura en empalmes soldados con soldadura en ranura de penetración completa, con o sin transiciones que tengan inclinaciones no mayores de 40%, cuando no se remueve el refuerzo y/o la pureza de soldadura no sea establecida por inspección radiográfica o ultrasónica en conformidad con los requerimientos de la Tabla 9.25.3 de AWS D1.1-77.	To Rev.	C	10,11,12,13
	Metal de soldadura de soldaduras en ranura transversal de penetración parcial, basado en el área efectiva de la garganta de la soldadura o soldaduras.	To Rev.	F	16
Soldaduras en Tapón o Muecas	Metal base en soldaduras en tapón o en muesca.	To Rev.	E	27
	Corte en soldaduras en tapón o en muesca.	S	F	27
Accesorios	Metal base en detalle de cualquier longitud unido por soldaduras en ranura sometidas a carga transversal y/o longitudinal, cuando el detalle incorpora un radio de transición, R, de 51 mm o mayor, con terminación de la soldadura esmerilada lisa: R ≥ 610 mm 610 mm > R ≥ 152 mm 152 mm > R ≥ 51 mm	To Rev. To Rev. To Rev.	B C D	14 14 14
	Metal base en un detalle unido por soldadura en ranura o en filete sometidas a carga longitudinal, con radio de transición, si lo hay, menor de 51 mm: 51 mm ≤ a ≤ 12 b o 102 mm a > 12 b o 102 mm donde a = dimensión del detalle paralela a la dirección de la tensión b = dimensión del detalle normal a la dirección de la tensión y a la superficie del metal base	To Rev. To Rev.	D E	15 15,23,24, 25,26
	Metal base en un detalle de cualquier longitud unido por soldaduras en filete o en ranura de penetración parcial en la dirección paralela a la tensión, cuando el detalle incorpora un radio de transición, R, de 51 mm o mayor, con terminación de la soldadura esmerilada lisa: R ≥ 610 mm 610 mm > R ≥ 152 mm 152 mm > R ≥ 51 mm	To Rev. To Rev. To Rev.	B C D	19 19 19
	Metal base en un detalle unido por soldaduras en ranura o en filete, donde la dimensión del detalle paralelo a la dirección de la tensión, a, es menor de 51 mm	To Rev.	C	23,24,25
	Metal base de un conector de corte unido por soldadura en filete.	T ó Rev.	C	22
	Tensión de corte en el área nominal de conectores.	S	F	22

TABLA B3  
Rango de Tensiones Admisibles F<sub>sr</sub>, kgf/cm<sup>2</sup> (MPa)

Categoría (De la Tabla B2)	Condición de Carga 1 F <sub>sr1</sub>	Condición de Carga 2 F <sub>sr2</sub>	Condición de Carga 3 F <sub>sr3</sub>	Condición de Carga 4 F <sub>sr4</sub>
A	4220	2530	1690	1690
B	3160	1930	1270	1120
C	2250	1340	914	703 <sup>a</sup>
D	1900	1120	703	492
E	1480	879	562	352
F	1050	844	633	562

<sup>a</sup> Se permite un rango de tensión de flexión de 844 kgf/cm<sup>2</sup> (MPa) al pie de las soldaduras de atisadores so almas o alas.

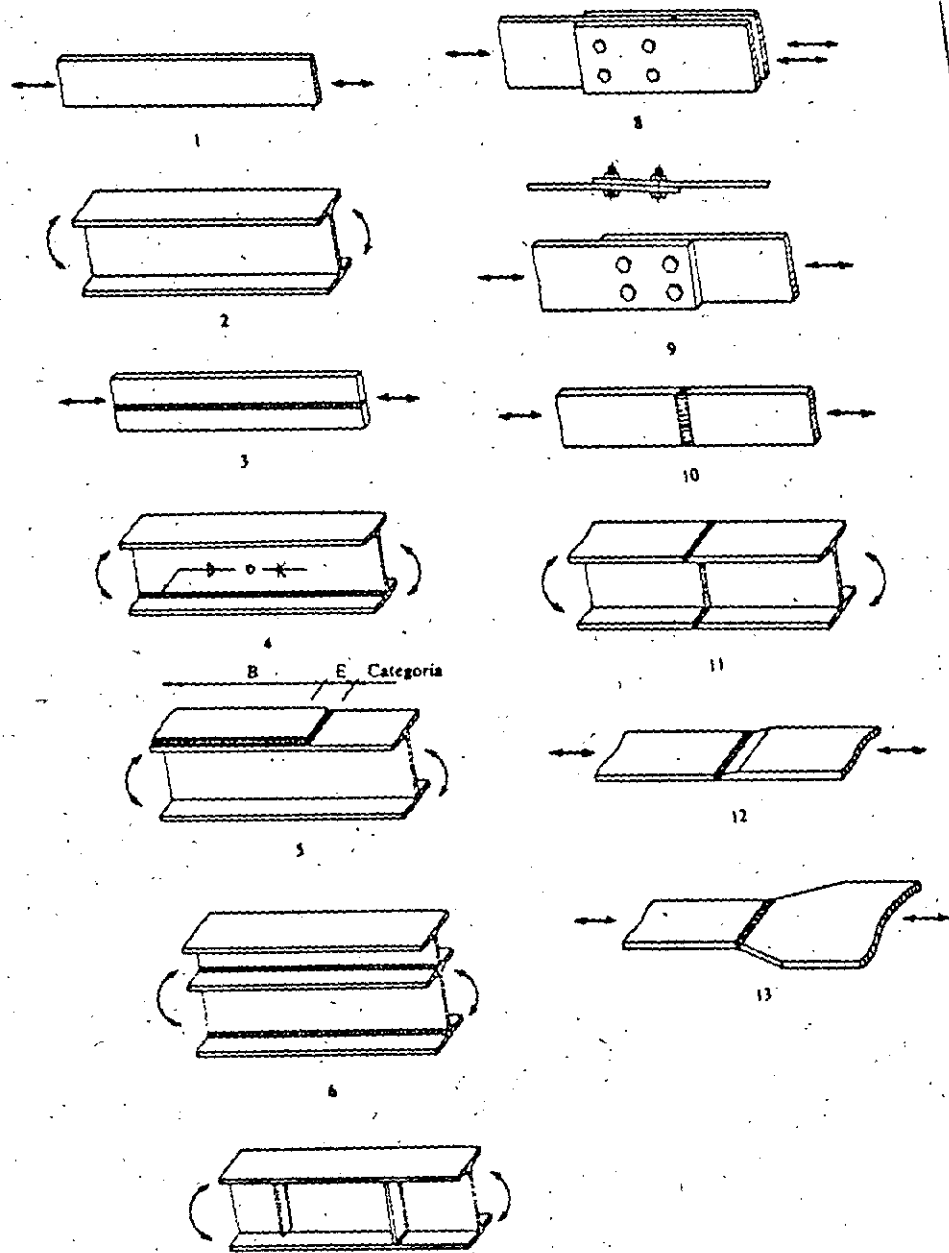


Figura B.1  
Ejemplos Ilustrativos

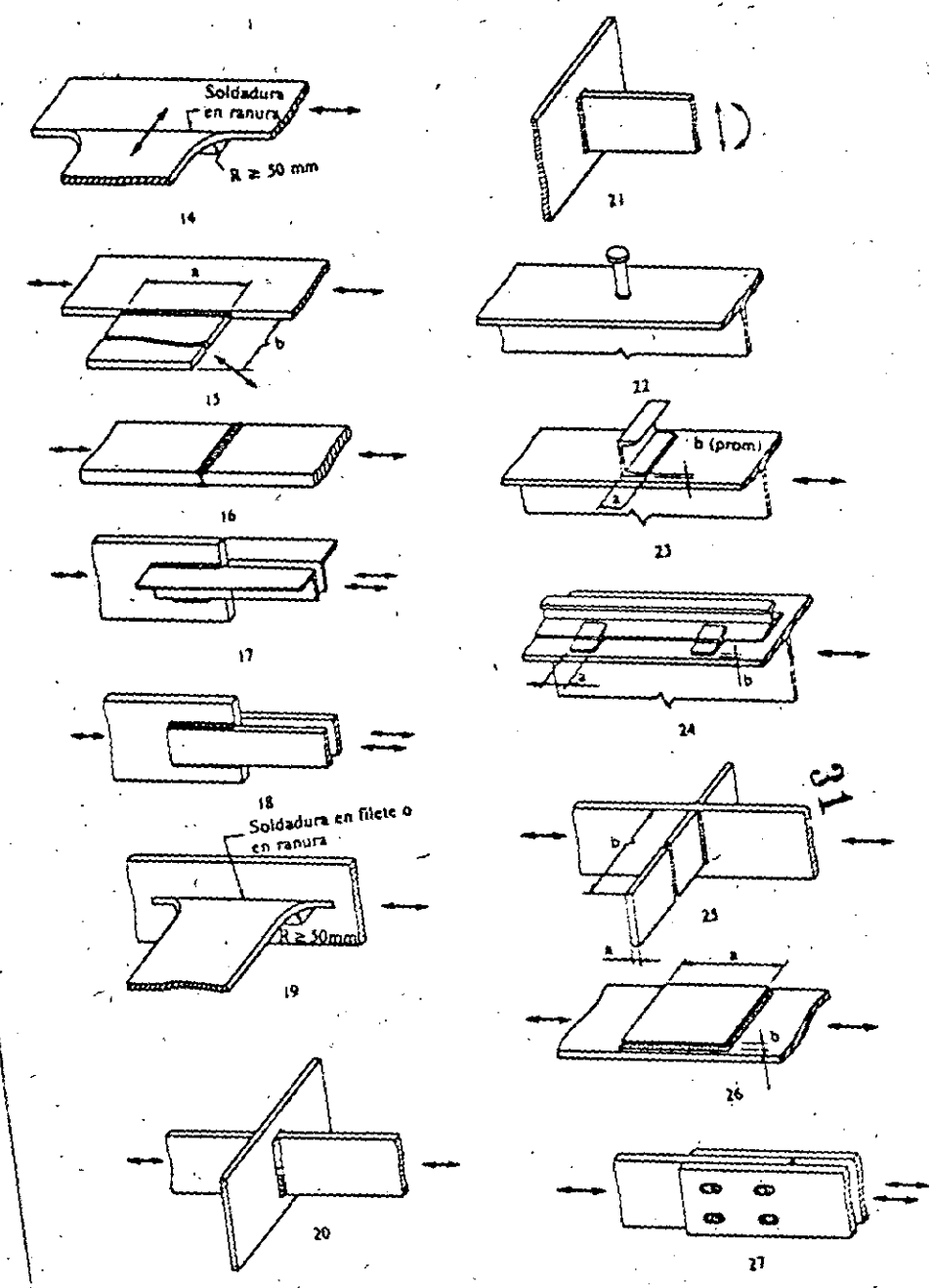
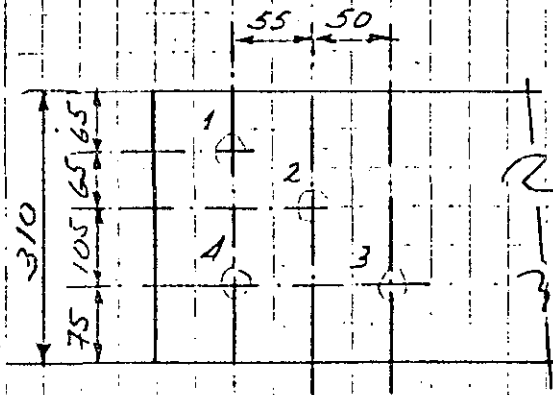


Figura B.1  
Ejemplos Ilustrativos

## Ejemplo 4

Calcule el área neta del miembro que se muestra en la siguiente figura, considerando que se usarán tornillos de 22 mm ( $7/8"$ ) de diámetro. La placa es de 8 mm ( $5/16"$ ) de espesor.



Revisaremos el ancho neta en cada una de las trayectorias de falla posibles.

Los diámetros de los agujeros se consideran 3 mm mayores que el diámetro de los tornillos.

Trayectoria 1-4

$$a_n = 310 - 2(22+3) = 260 \text{ mm}$$

Trayectoria 1-2-4

$$a_n = 310 - 3(22+3) + 55^2/(4 \times 65) + 55^2/(4 \times 105) = 254 \text{ mm}$$

Trayectoria 1-2-3

$$a_n = 310 - 3(22+3) + 55^2/(4 \times 65) + 50^2/(4 \times 105) = 253 \text{ mm}$$

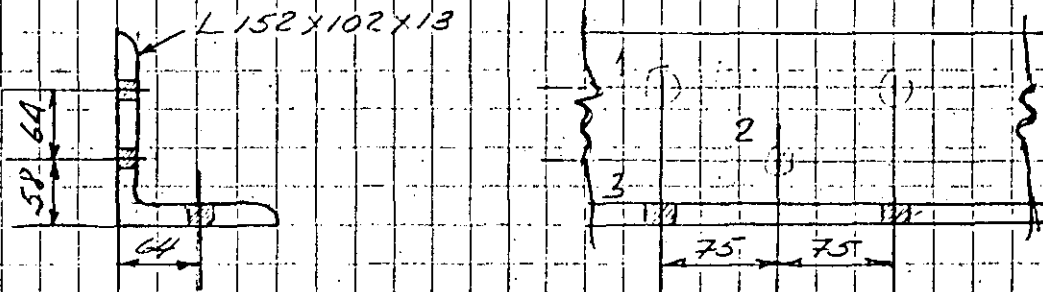
El ancho mínimo corresponde a la trayectoria 1-2-3, por lo tanto, el área neta será:

$$A_n = 8 \times 253 = 2024 \text{ mm}^2$$



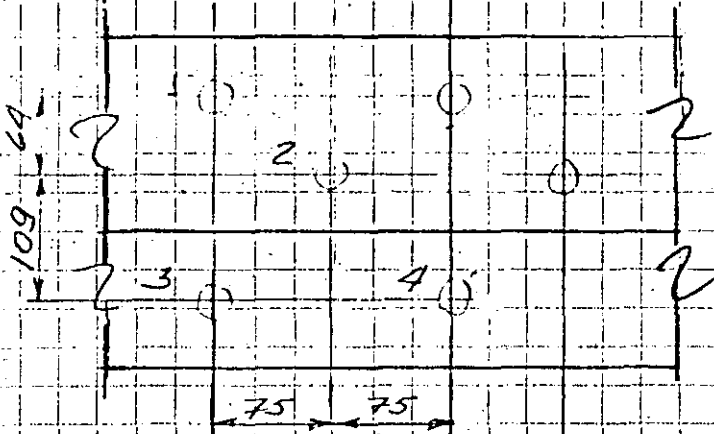
## Ejemplo 5

Calcule el área neta y la resistencia del ángulo mostrado en la figura. El acero utilizado será NOM B-254 (ASTM A36) y los tornillos tendrán un diámetro de 22mm (7/8")



El ancho total del ángulo es:

$$a_t = 152 + 102 - 13 = 241 \text{ mm}$$



El valor máximo para el área neta es el 85% del área total

$$A_n \leq 0.85 A_t = 0.85 \times 31.3 = 26.6 \text{ cm}^2$$

Trojectoria 1-3

$$a_n = 241 - 2(22 + 3) = 191 \text{ mm}$$

Trojectoria 1-2-3 o 1-2-4

$$a_n = 241 - 3(22 + 3) + 75^2 / (4 \times 64) + 75^2 / (4 \times 109) = 201 \text{ mm}$$

El ancho mínimo corresponde a 1-3

$$A_n = 191 \times 13 = 2483 \text{ mm}^2 = 24.83 \text{ cm}^2 < 26.6 \text{ cm}^2 \text{ ok}$$

$$R = 0.6 F_Y \times A_n = 0.6 \times 2500 \text{ kg/cm}^2 \times 24.83 \text{ cm}^2 = 37245 \text{ kg}$$

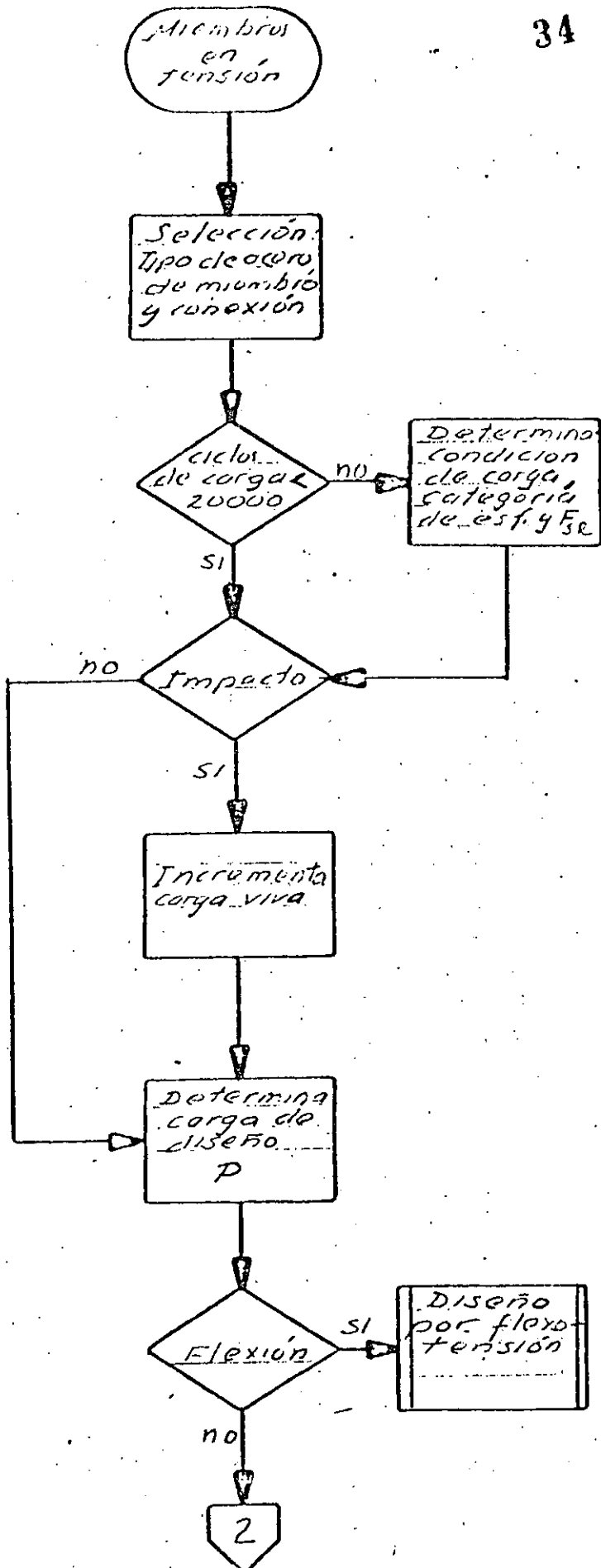
ESJEMPLO 7.

Diseñar un tirante para soportar un sistema de piso sujeto a una fuerza de tensión de 10000, debido a carga permanente y a una 15000 kg debido a carga viva.

Tipo de acero: NOM B251 (ASTM A36)

Tipo de miembro: barra redonda

Conexión: Cuerdos en los extremos.



ciclos de carga < 20000 (SI)

Impacto (SI)

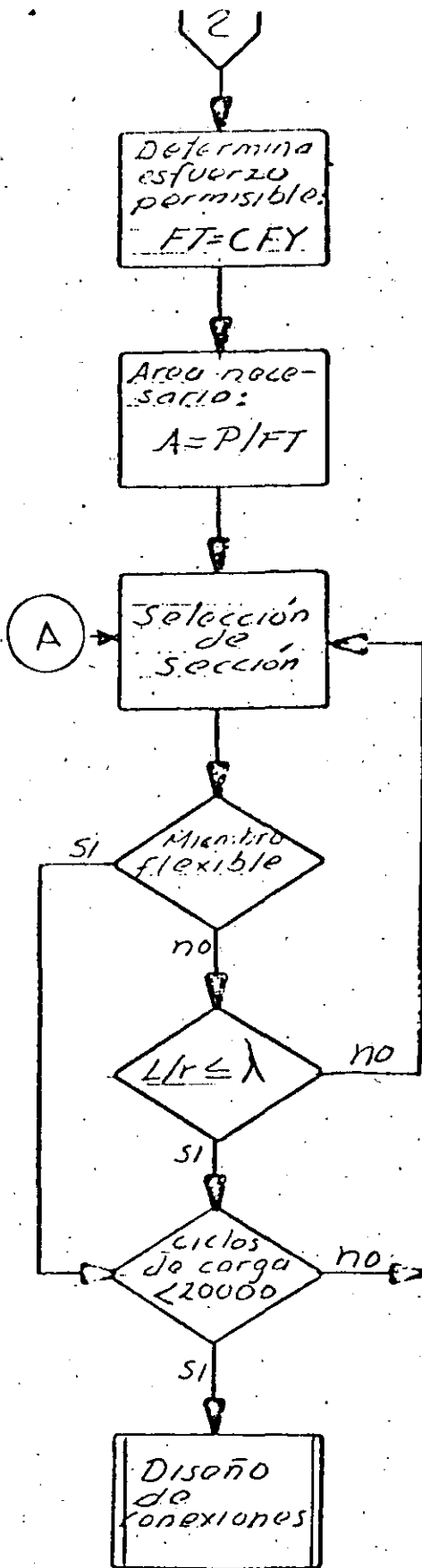
$$T_v = 1.33 \times 15000 = 20000 \text{ kg}$$

$$T = 10000 + 20000 = 30000 \text{ kg}$$

Flexión (NO)

# Ejemplo 7 (continúo)

35



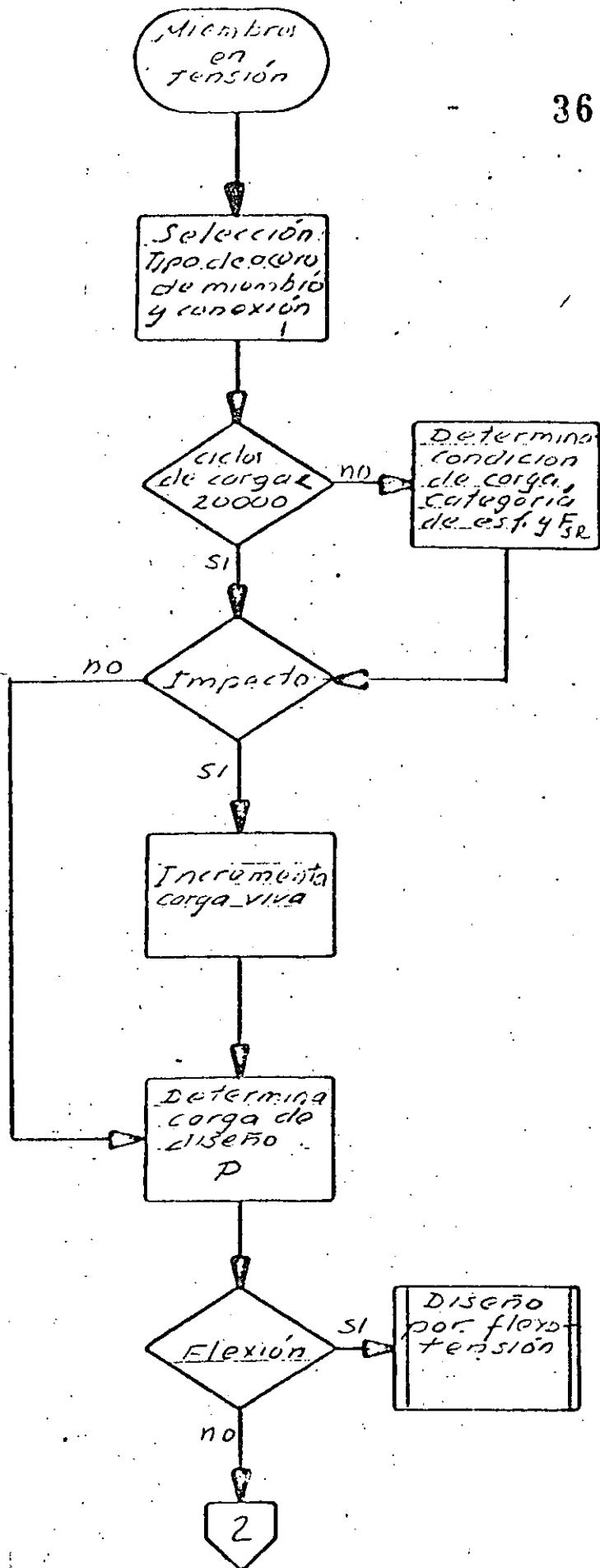
En la sección sin rosca:  
 $F_T = 0.6 \times 2500 = 1500 \text{ kg/cm}^2$   
 En la sección con rosca:  
 $F_T = 0.33 \times 4100 = 1353 \text{ kg/cm}^2$

$$A = 30000 / 1353 = 22.2 \text{ cm}^2$$

$$d = \sqrt{4A/\pi} = 5.3 \text{ cm}$$

flexible SI

ciclos de carga < 20000 SI



Ejemplo 2. Diseñar la cuerda inferior de una armadura. Su longitud entre nudos es de, 500cm y está sujeto a las siguientes cargas:

- Carga permanente + 10000 kg
- Carga viva + 12.000 kg
- Carga de viento + 8000 kg
- Acero A242 (ASTM A36)
- Sección T estructural
- Conexión atornillada en el patín (2 líneas de tornillos)

ciclos de carga < 20000

SI

Impacto

NO

Condición I:  $T = 10000 + 12000 = 30000 \text{ kg}$

Condición II:  $T = 10000 + 12000 + 8000 = 30000 \text{ kg}$

flexión

NO

Ejemplo 8 (continúa)

	Condición I $F_T$ (kg/cm <sup>2</sup> )	Condición II $F_T$ (kg/cm <sup>2</sup> )
$A_T$	$0.6 \times 2500 = 1500$	$1/3 \times 1500 = 2000$
$A_n$	$0.5 \times 2100 = 2050$	$1/3 \times 2050 = 2733$

	Condición I	Condición II
$A_T$	$38000/1500 = 20 \text{ cm}^2$	$38000/2000 = 19 \text{ cm}^2$
$A_n$	$38000/2050 = 14.6 \text{ cm}^2$	$38000/2733 = 13.9 \text{ cm}^2$

La condición I controla el diseño

TPR  $6 \times 4$  (16.4 kN)

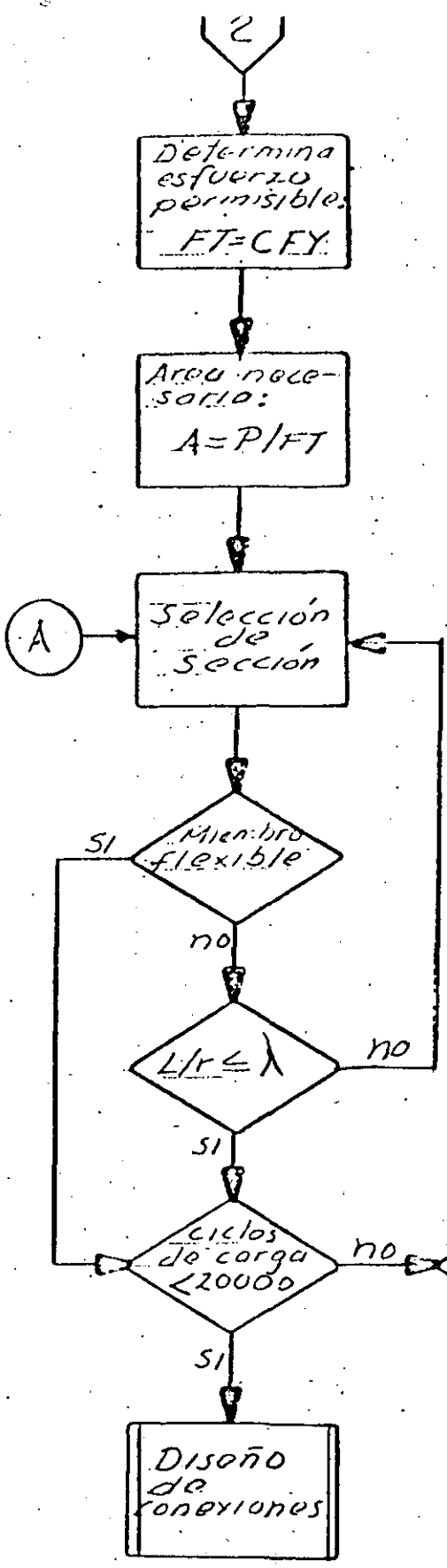
$A = 20.67 \text{ cm}^2$ ;  $r_x = 4.82 \text{ cm}$ ,  $r_y = 2.13$   
 $t_f = 1.08 \text{ cm}$ ; Tornillos de 16mm (3/8)  
 $A_n = 20.67 - 2 \times (1.6 + 0.32) = 16.83 \text{ cm} > 14.6 \text{ cm}$   
 $A_{ne} = 0.85 \times 16.83 = 14.3 \text{ cm}^2$

flexible

no

$500/2.13 = 235 < 250$

ciclos de carga  $< 20000$  SI





**DIVISION DE EDUCACION CONTINUA  
FACULTAD DE INGENIERIA U.N.A.M.**

DISEÑO DE ESTRUCTURAS DE ACERO

CONEXIONES ATORNILLADAS  
DISEÑO  
DESCRIPCION Y COMPORTAMIENTO

ING. JOSE LUIS SANCHEZ MARTINEZ

NOV. 1984

C O N E X I O N E S   A T O R N I L L A D A S

D I S E Ñ O

## DISEÑO DE JUNTAS ATORNILLADAS.

### 1.- Partes Roscadas y tornillos sometidos a tensión.-

Los tirantes de varilla roscada en sus extremos y las anclas también roscadas son elementos a tensión utilizadas muy comunmente. Para diseñarlos se requiere tener presente la reducción de área que implica la presencia de la zona rosca. Las normas del AISC establecen, sin embargo, esfuerzos permisibles basados en el área nominal de la zona no rosca.

**TABLE I-A. BOLTS AND RIVETS**  
Tension on gross (nominal) area

ASTM Designation	F <sub>t</sub> Ksi	Nominal Diameter, d, in.							
		5/8	3/4	7/8	1	1 1/8	1 1/4	1 3/8	1 1/2
		Area (Based on Nominal Diameter), in. <sup>2</sup>							
		0.3068	0.4418	0.6013	0.7854	0.9940	1.227	1.485	1.767
A307 bolts	20.0	6.1	8.8	12.0	15.7	19.9	24.5	29.7	35.3
A325 bolts	44.0	13.5	19.4	26.5	34.6	43.7	54.0	65.3	77.7
A490 bolts	54.0	16.6	23.9	32.5	42.4	53.7	66.3	80.2	95.4
A502-1 rivets	23.0	7.1	10.2	13.8	18.1	22.9	28.2	34.2	40.6
A502-2,3 rivets	29.0	8.9	12.8	17.4	22.8	28.8	35.6	43.1	51.2

The above table lists ASTM specified materials that are generally intended for use as structural fasteners.

For dynamic and fatigue loading, only A325 or A490 high-strength bolts should be specified. See AISC Specification, Appendix B, Sect. B3.

For allowable combined shear and tension loads, see AISC Specification Sect. 1.6.3.

**TABLE I-B. THREADED FASTENERS**  
Tension on gross (nominal) area

ASTM Designation	F <sub>y</sub> Ksi	F <sub>u</sub> Ksi	F <sub>t</sub> Ksi	Nominal Diameter, d, in.							
				5/8	3/4	7/8	1	1 1/8	1 1/4	1 3/8	1 1/2
				Area (Based on Nominal Diameter), in. <sup>2</sup>							
				0.3068	0.4418	0.6013	0.7854	0.9940	1.227	1.485	1.767
A36	36	58	19.1	5.9	8.4	11.5	15.0	19.0	23.4	28.4	33.7
A572, Gr. 50	50	65	21.5	6.6	9.5	12.9	16.9	21.4	26.4	31.9	38.0
A588	50	70	23.1	7.1	10.2	13.9	18.1	23.0	28.3	34.3	40.8
A449											
d ≤ 1	92	120	39.6	12.1	17.5	23.8	31.1	—	—	—	—
1 < d ≤ 1 1/2	81	105	34.7	—	—	—	—	34.5	42.6	51.5	61.3

The above table lists ASTM specified materials available in round bar stock that are generally intended for use in threaded applications such as tie rods, cross bracing and similar uses.

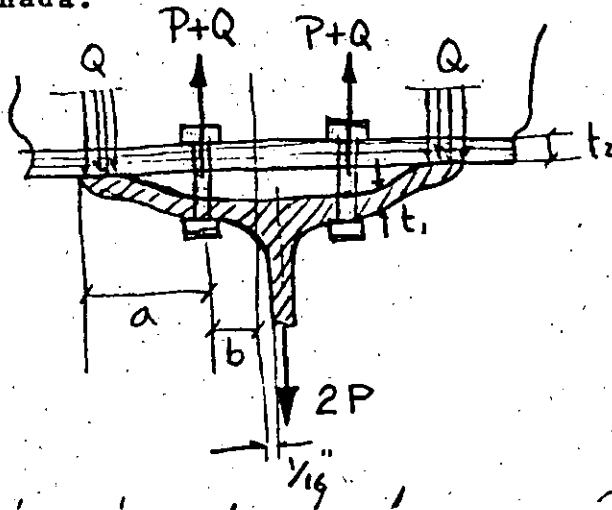
The tensile capacity of the threaded portion of an upset rod shall be larger than the body area times 0.6F<sub>y</sub>.

F<sub>u</sub> = specified minimum tensile strength of the fastener material.

F<sub>t</sub> = 0.33F<sub>u</sub> = allowable tensile stress in threaded fastener.



En el dimensionamiento de tornillos a tensión es importante tener en cuenta la carga adicional a la fuerza exterior aplicada y que es debida a la flexibilidad de las piezas que transmiten la carga a los tornillos. En la siguiente figura se puede observar la naturaleza de la fuerza adicional mencionada.



Q = Fuerza adicional debida a la flexibilidad de la junta

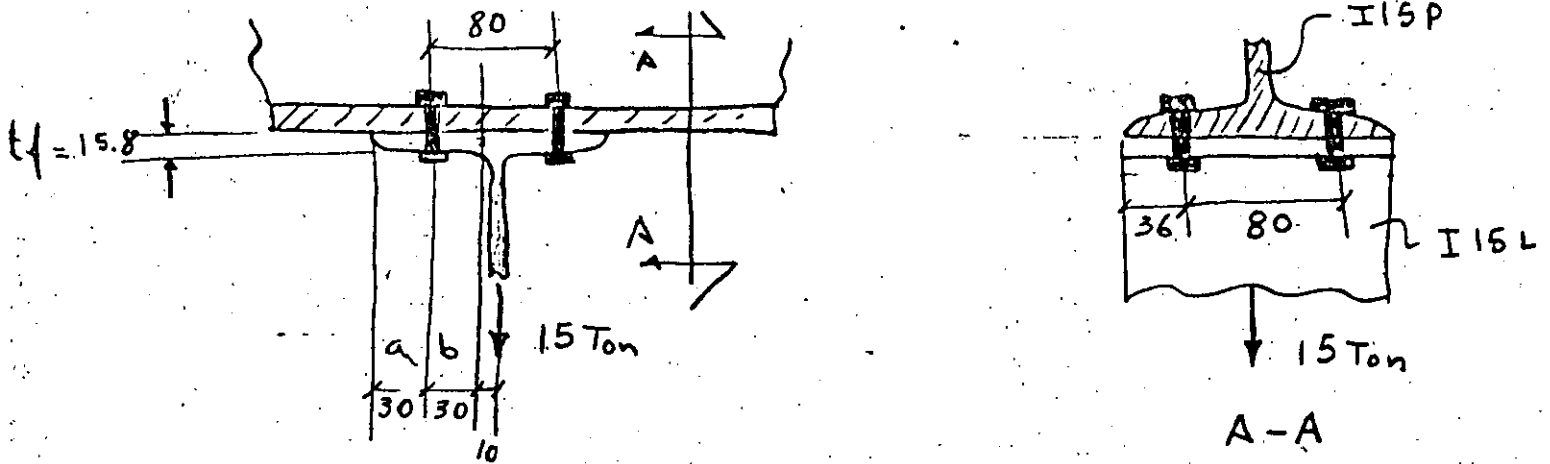
El valor de la fuerza Q puede estimarse usando la siguiente fórmula semiempírica para tornillos comunes:

$$Q = \left[ \frac{\frac{1}{2} - \frac{wt^4}{30ab^2Ab}}{\frac{3a}{4b} \left( \frac{a}{4b} + 1 \right) + \frac{wt^4}{30ab^2Ab}} \right] P$$

Ab = área nominal del tornillo  
 t = espesor del elemento más delgado en la unión  
 w = dimensión tributaria al tornillo (normal al papel)

Ejemplo.-

Diseñar la unión de la figura:



Si se usan tornillos de alta resistencia A325 se recomienda la expresión siguiente (1) para el cálculo de Q en vez de la presentada antes:

$$Q = P \left[ \frac{100 b (db)^2 - 18 w (t_f)^2}{70 a (db)^2 + 21 w (t_f)^2} \right]$$

Suponiendo tornillos de 3/4";  $db = 1.9 \text{ cm}; db^2 = 3.61$   
 $b = 3.0; a = 3.0 < 2 t_f$   
 $w = 7.6 \text{ cm}; t_f = 1.58 \text{ cm}$

$$\begin{array}{r} 100 b (db)^2 = 1083.0 \\ - 18 w (t_f)^2 = \underline{341.5} \\ \hline 741.5 \end{array}$$

$$Q = 3.75 \times 0.64 = 2.4 \text{ ton.}$$

$$\begin{array}{r} 70 a (db)^2 = 758.1 \\ + 21 w (t_f)^2 = \underline{398.4} \\ \hline 1156.5 \end{array}$$

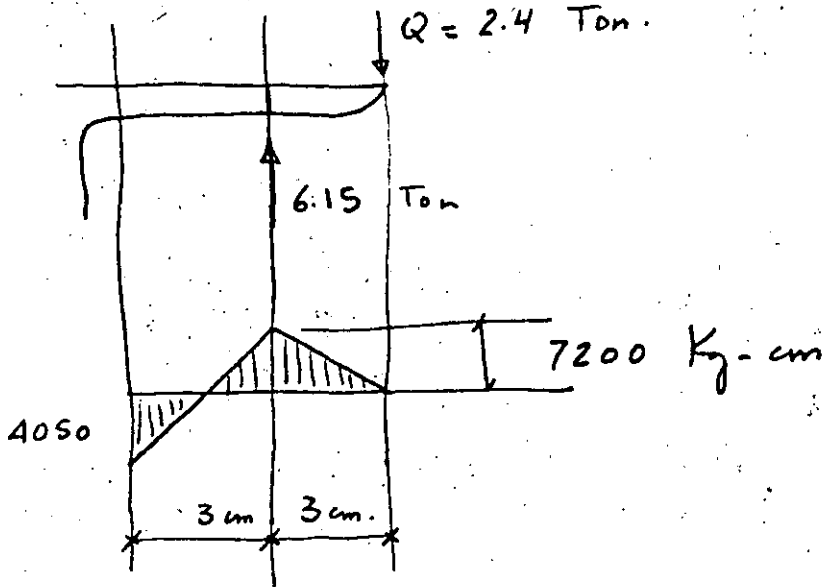
Tensión de cada tornillo =  $3.75 + 2.4 = 6.15 \text{ ton.}$

Capacidad del tornillo =  $2.84 \times 3080 = 8.75 \text{ ton.}$

---

(1) Behavior of bolts in tee Connections  
 Research series # 325, University of Illinois, 1969

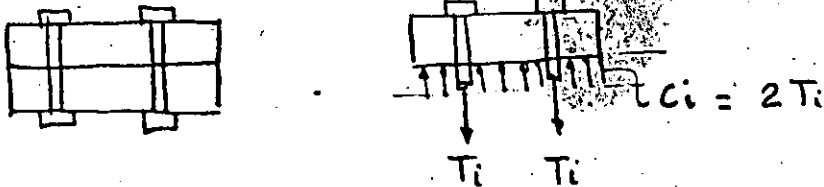
Revisión del patín.-



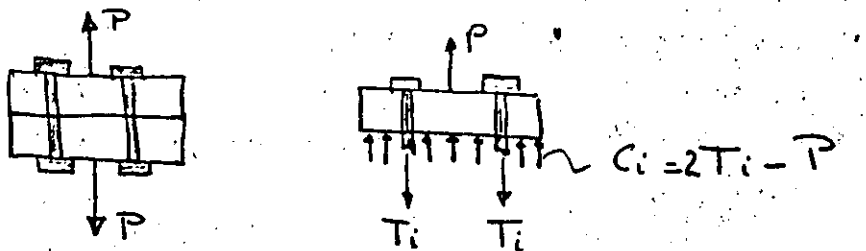
$$f_1 = \frac{7200 \times 6}{1.58^2 \times 15.2} = 1138.5 \text{ Kg/cm}^2 < 1900 \text{ Kg/cm}^2$$

Los tornillos de alta resistencia se someten a una tensión inicial considerable al colocarse. Conviene hacer notar que la mencionada tensión no tiene influencia práctica - notable en la resistencia de la junta; esto puede ilustrarse con las figuras que siguen en que se muestran, la tensión -- inicial y diversos valores de la carga exterior:

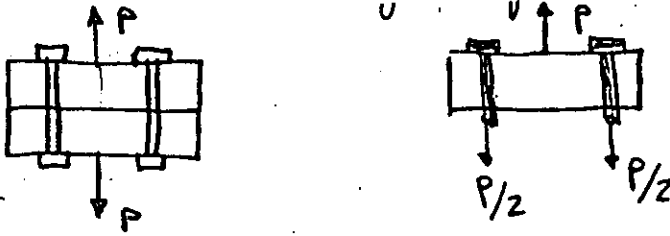
a) Tensión inicial y carga 0:



b) Tensión inicial y carga menor que ella:

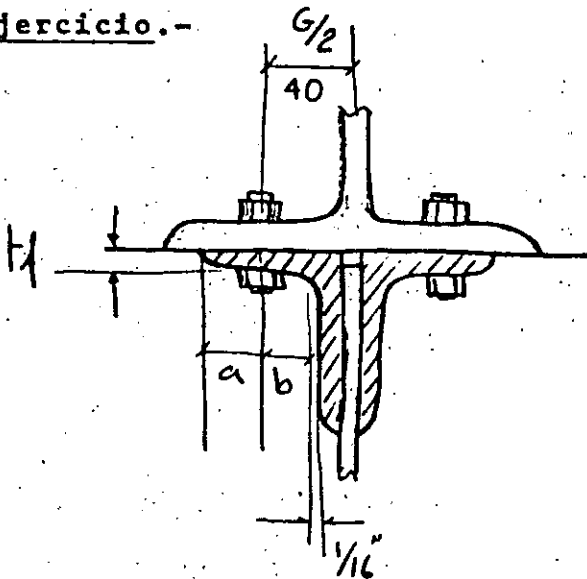


c) Tensión inicial y carga mayor que ella:



Luego los tornillos trabajarán con una carga igual a la tensión inicial o a la carga que se le transmite al trabajar la junta (la mayor de las dos).

Ejercicio.-

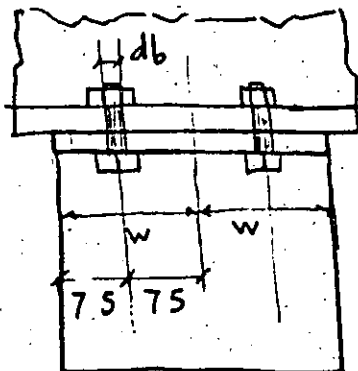


Del patín inferior de una vigueta I15P se colgarán dos ángulos de  $2 \frac{1}{2}'' \times 2 \frac{1}{2}'' \times \frac{3}{8}''$  para transmitirle una carga de 10 Ton.

Diseñar los cuatro tornillos de alta resistencia A325 que se utilizan en la conexión.

Se utilizará la siguiente expresión empírica:

$$Q = F \left[ \frac{100 b (d_b)^2 - 18 w (t_f)^2}{70 a (d_b)^2 + 21 w (t_f)^2} \right]$$



F = 10 Ton

b = (35 - 10 + 1.5) = 23 mm. Manual

a = (64 - 35) = 29 mm. pag. 200

db = 19 mm. (supuesto)

tf = 10 mm.

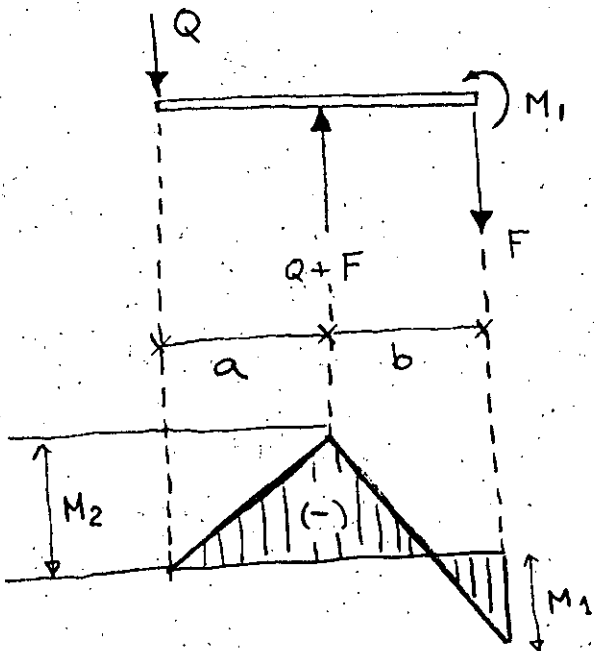
w = 150 mm.

En cada tornillo:

$$F' = \frac{F}{4} + Q = 2.5 + 1.3 = 3.8 \text{ Ton.}$$

1 tornillo de  $\frac{5}{8}$ " tiene una capacidad de 6.1 Ton.

Revisión del ángulo:-



$$Q = 1.3 \text{ Ton.}$$

$$F = 2.5 \text{ Ton.}$$

$$a = 2.9 \text{ cm.}$$

$$b = 2.3 \text{ cm.}$$

Cálculo de momentos:

$$M_2 = Qa = -1.3 \times 2.9 = -3.8 \text{ T - cm.}$$

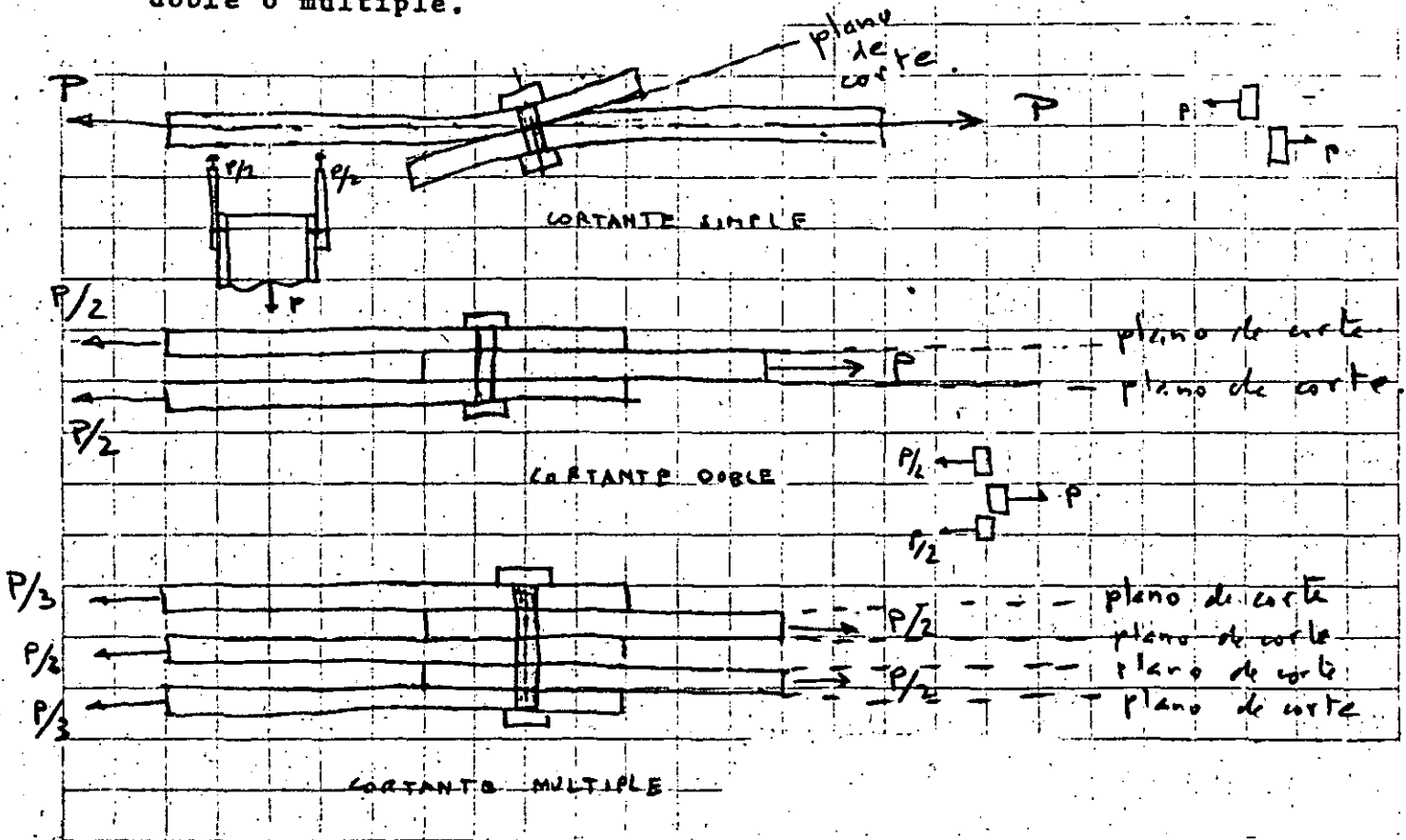
$$M_1 = (Q + F)b - Q(a + b) = 3.8 \times 2.3 - 1.3 \times 5.2 = +1.98 \text{ T - cm.}$$

Revisión de esfuerzos:

$$\sigma = \frac{3800 \times 0.5}{\frac{1}{2} \times 15 \times 1^3} = 1520 \text{ kg/cm}^2 < 0.75 F_y = 1897.5 \text{ Kg/cm}^2$$

### JUNTAS DE APLASTAMIENTO

Las fuerzas se transmiten por aplastamiento de los tornillos contra los elementos que aplican dichas fuerzas. Los tornillos trabajan además a cortante que puede ser simple, -doble o múltiple.



La falla puede presentarse por cortante, por aplastamiento o por distancia insuficiente entre centro de agujeros o al borde. El diseño se basa en la hipótesis de que las fuerzas actuantes se distribuyen por igual entre todos los tornillos que componen la junta lo que, en conexiones usuales, coincide bien con los resultados obtenidos a la falla. Se recomienda utilizar juntas lo más compactas posible y las normas del AISC recomiendan reducir los esfuerzos permisibles especificados en un 20% si la longitud de la zona atornillada

excede 50".

El esfuerzo cortante permisible es de 2109 kg/cm<sup>2</sup> en tornillos A325 cuando la zona roscada esta fuera de los planos de corte y un 70% de este valor en caso contrario, lo -- que aproximadamente tiene en cuenta la reduccion en área que provoca la rosca.

Al aplastamiento se acepta un esfuerzo permisible igual a una vez y media la resistencia mínima a la tensión del material conectado, valor para el cual la conexión presenta un -- comportamiento inadecuado si bien el fenómeno de aplastamiento entre tornillo y material tal como normalmente se concibe no se ha observado en casos reales.

Es práctico obtener el espesor de las placas necesario para que no se presente el aplastamiento; para cortante simple se tendría:

$$\text{Resistencia al aplastamiento} = Dt (1.5 Fu)$$

$$\text{Resistencia a cortante simple} = \frac{\pi D^2}{4} Fv$$

$$\frac{\pi D^2}{4} Fv = Dt (1.5 Fu)$$

$$t = \frac{\pi D Fv}{4 \times 1.5 Fu}$$

$$\text{Si } Fv = 30 \text{ ksi y } Fu = 58 \text{ ksi}$$

A325

A36

$$t = \frac{30 \pi}{6 \times 58} D = 0.27 D$$

Si el grueso de la placa es igual o mayor que 0.27 -- veces el diámetro del tornillo el aplastamiento no resulta -- crítico.

En igual forma, en el caso de cortante doble, la placa central deberá tener un espesor no menor a 0.54 veces el diámetro del tornillo.

Para evitar la falla por distancia entre agujeros el AISC recomienda una distancia mínima a lo largo de una línea de transmisión de fuerzas dada por:

$$\text{dist.} = 2 \frac{2}{3} D \leq \frac{2 P}{F_u t} + \frac{D}{2} = \frac{2 \times 15 \pi D^2}{58 t} + \frac{D}{2} = 1.63 \frac{D^2}{t} + \frac{D}{2}$$

en que :

D ; es el diámetro del perno y

t ; el espesor de la placa crítica en la conexión, en cortante doble suele ser la central.

Para que rija la separación de  $2 \frac{2}{3} D$  el espesor de la placa debería tener como mínimo el valor siguiente:

$$2 \frac{2}{3} D = 1.63 \frac{D^2}{t} + \frac{D}{2}$$

$$2 \frac{2}{3} = 1.63 \frac{D}{t} + \frac{1}{2}$$

$$\frac{2.17 t}{1.63} = D \quad \therefore \quad t = \frac{1.63 t}{2.17} = 0.75 D$$

La mínima distancia al borde está dada por la tabla -- 1.16.5.1 pero no menos de la dada por la expresión:

$$\frac{2 P}{F_u t}$$

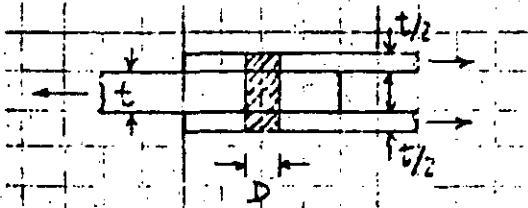


Resistencia de pernos A325 en conexiones por aplastamiento. (Las roscas estan fuera de los planos de corte).

Diámetro Pulg. (cm)	Area (cm <sup>2</sup> )	FUERZA CORTANTE ADMISIBLE (TON)				t mín. de la placa central para aplast. no crítico	t mín. de la placa central para aplast. S = 2 <sup>2</sup> / <sub>3</sub> d	
		Esf. Perm. (Kg/cm <sup>2</sup> )	Cortante Simple	x 1.33	Cortante Doble			x 1.33
3/4 (1.90)	2.85	2109	6,0	8,0	12,0	16,0	1.03 (7/16")	1.43 (9/16")
7/8 (2.22)	3.88	2109	8,2	10,9	16,4	21,8	1.20 (1/2")	1.67 (11/16")
1 (2.54)	5.06	2109	10,7	14,2	21,4	28,4	1.38 (9/16")	1.90 (3/4")
1 <sup>1</sup> / <sub>8</sub> (2.86)	6.41	2109	13,5	18,0	27,0	35,9	1.55 (5/8")	2.15 (7/8")
1 <sup>1</sup> / <sub>4</sub> (3.17)	7.91	2109	16,7	22,2	33,4	44,9	1.72 (3/4")	2.38 (5/16")

Aplastamiento. Resistencia al aplastamiento =

$$\frac{A}{Dt} (1,5 Fu) = 87 Dt \text{ (Kips, pulg)}$$



$$\text{Resistencia al cortante doble} = 2 \times \frac{\pi D^2}{4} \times 30 = 15\pi D^2$$

$$87 Dt = 15 D^2, \quad t = \frac{15\pi}{87} D = 0.542 D$$

Si el grueso de la placa central es igual o mayor que 0.542 veces el diámetro del perno, el aplastamiento no es crítico.

Comprobación. Resistencia al aplastamiento de un perno Ø 1" en placa de 9/16" =

$$2.54 \times 1.43 \times 6116 = 22215 \text{ kg} = 22.2 \text{ ton} > 21.4$$

TABLE 1.16.5.1  
MINIMUM EDGE DISTANCE, INCHES  
(CENTER OF STANDARD HOLE<sup>a</sup> TO EDGE OF CONNECTED PART)

Nominal Rivet or Bolt Diameter (Inches)	At Sheared Edges	At Rolled Edges of Plates, Shapes or Bars or Gas Cut Edges <sup>b</sup>
1/2	7/8	3/4
5/8	1 1/8	7/8
3/4	1 1/4	1
7/8	1 1/2 <sup>c</sup>	1 1/8
1	1 3/4 <sup>c</sup>	1 1/4
1 1/8	2	1 1/2
1 1/4	2 1/4	1 5/8
Over 1 1/4	1 3/4 × Diameter	1 1/4 × Diameter

<sup>a</sup> For oversized or slotted holes, see Sect. 1.16.5.4.  
<sup>b</sup> All edge distances in this column may be reduced 1/8-in. when the hole is at a point where stress does not exceed 25% of the maximum allowed stress in the element.  
<sup>c</sup> These may be 1 1/4-in. at the ends of beam connection angles.

TABLE 1.16.5.4  
VALUES OF EDGE DISTANCE INCREMENT C<sub>2</sub> IN SECT. 1.16.5.4, INCHES

Nominal Diameter of Fastener (Inches)	Oversized Holes	Slotted Holes		Parallel to Edge
		Perpendicular to Edge		
		Short Slots	Long Slots <sup>a</sup>	
≤ 7/8	1/16	1/8	3/4d	0
1	1/8	1/8		
≥ 1 1/8	1/8	3/16		

<sup>a</sup> When length of slot is less than maximum allowable (see Table 1.23.4), C<sub>2</sub> may be reduced by one-half the difference between the maximum and actual slot lengths.

Ejemplo:

Conexión de una diagonal de contraventeo (ver figuras )  
a una columna.

Fuerza en la diagonal 1250 Ton. (CV + S)

Cortante doble

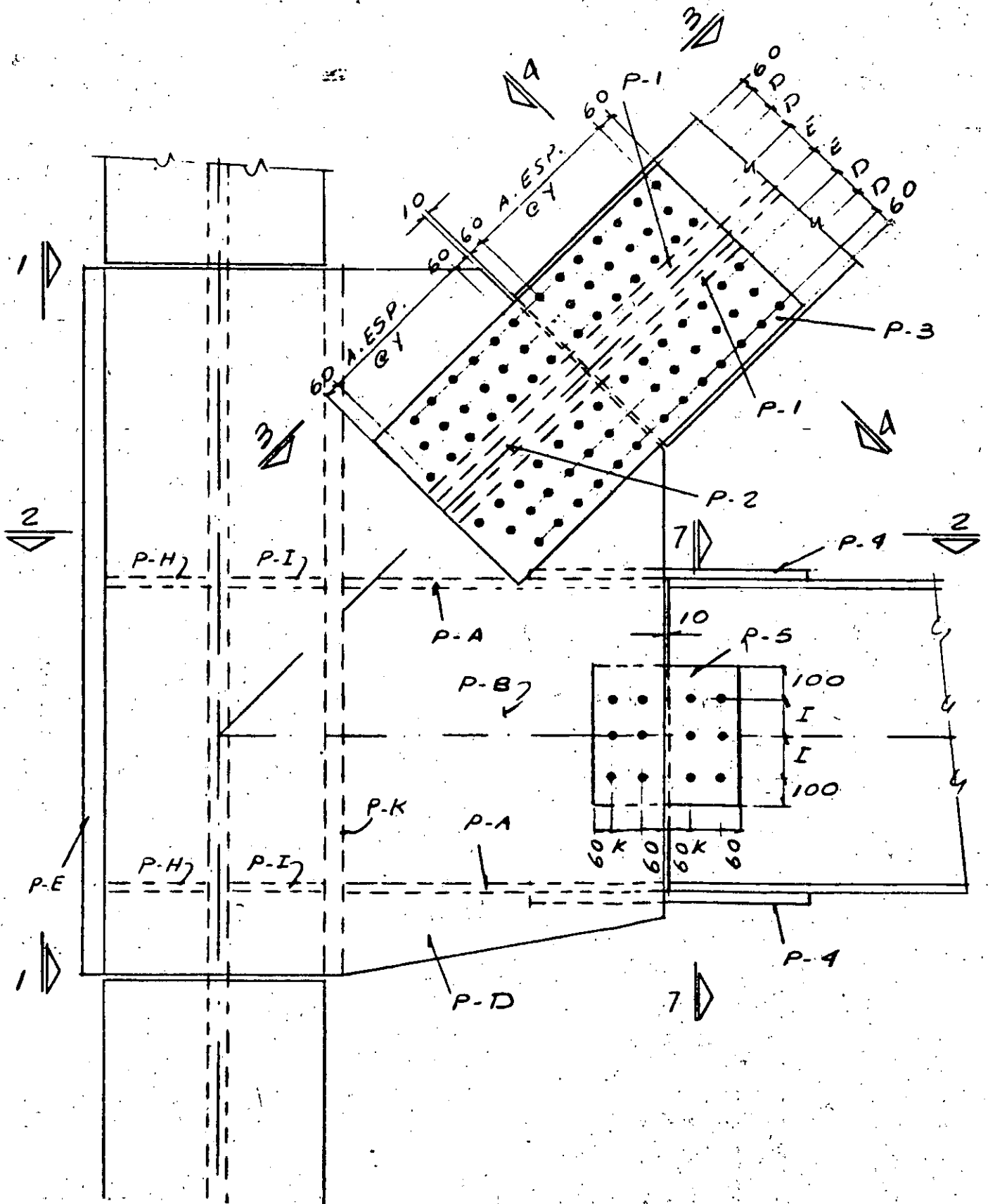
Con tornillos de 1"

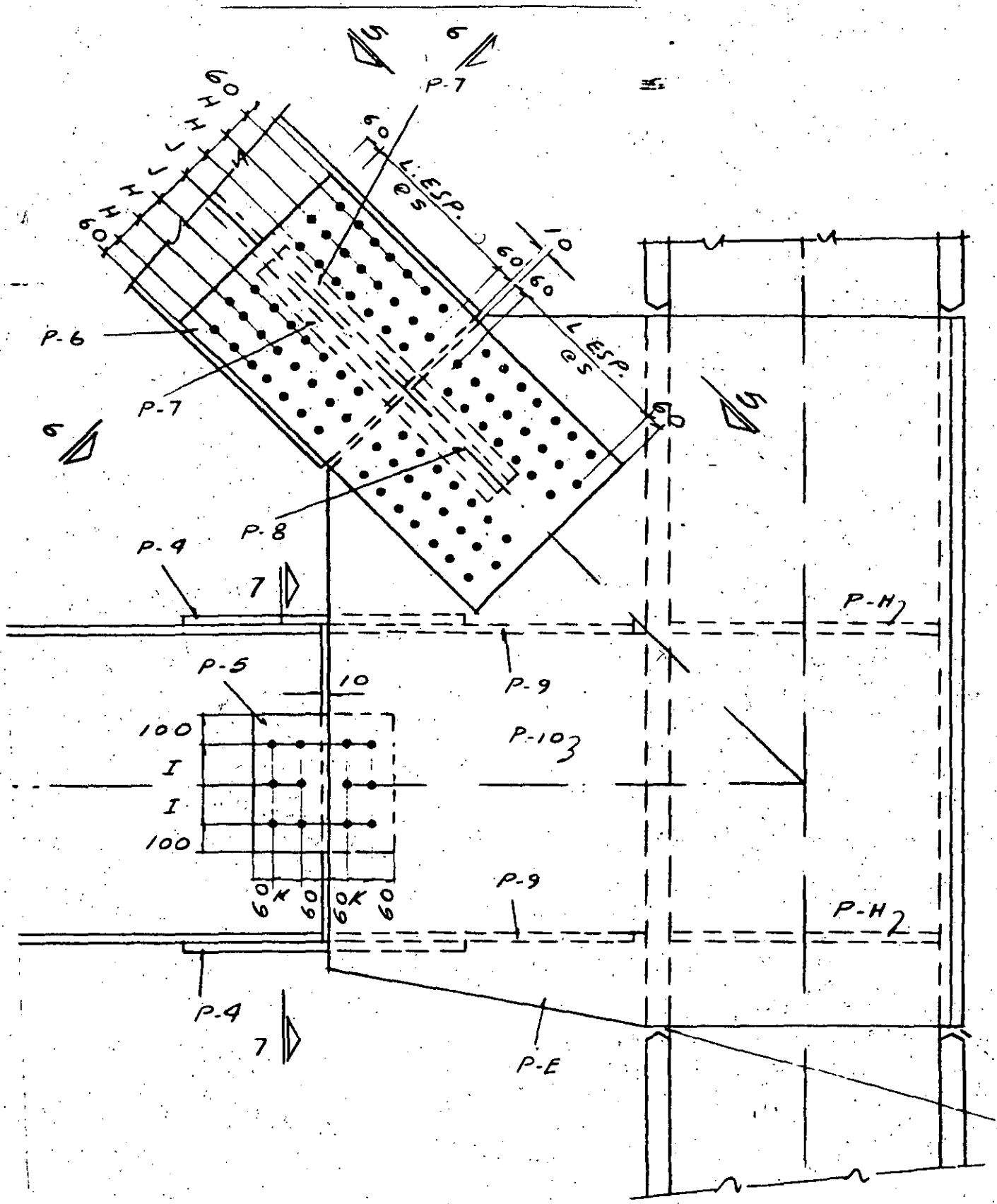
No. de tornillos  $\frac{1250}{28.4} = 44$  tornillos

Se repartiran entre dos patines y el alma proporcional  
mente al área de cada elemento:

patines 16 pernos

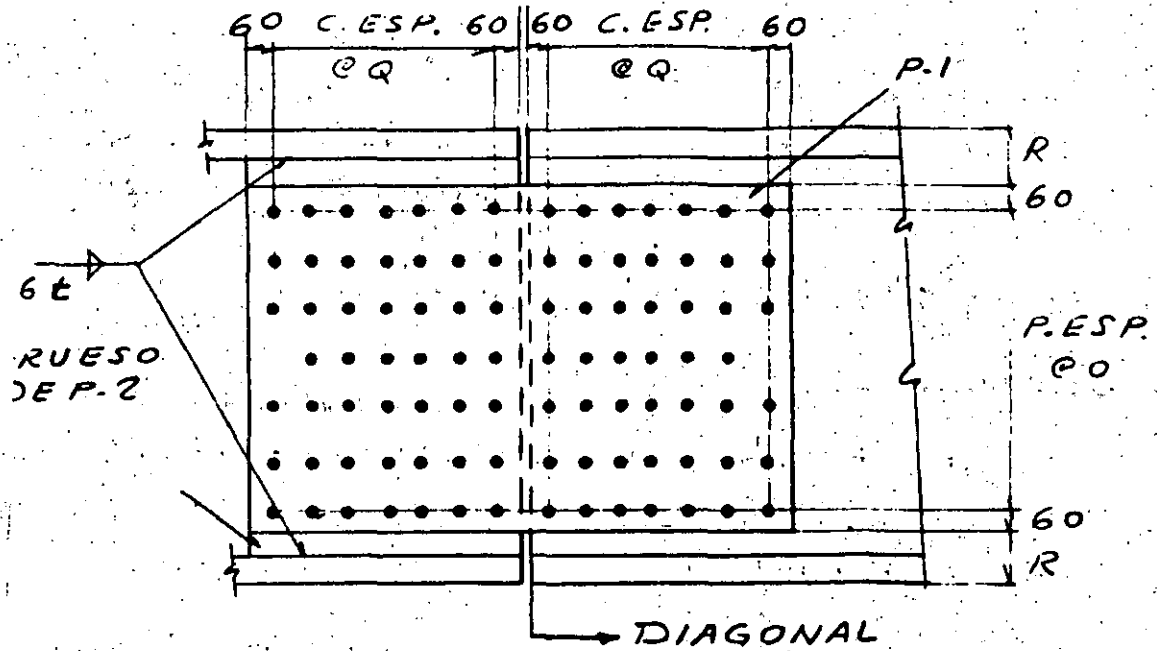
alma 12 pernos





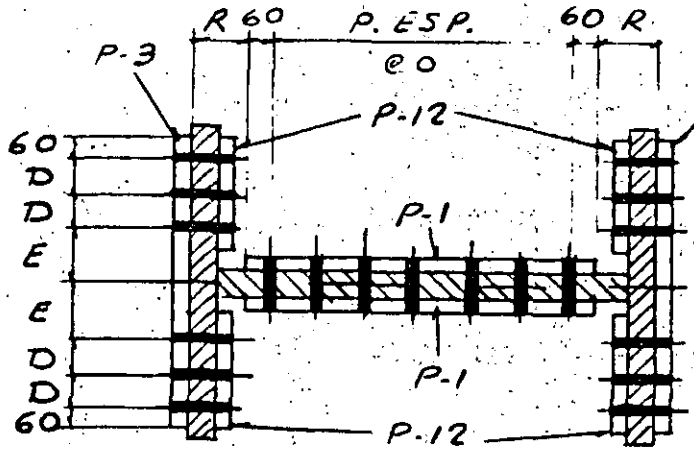
VISTA 1-1



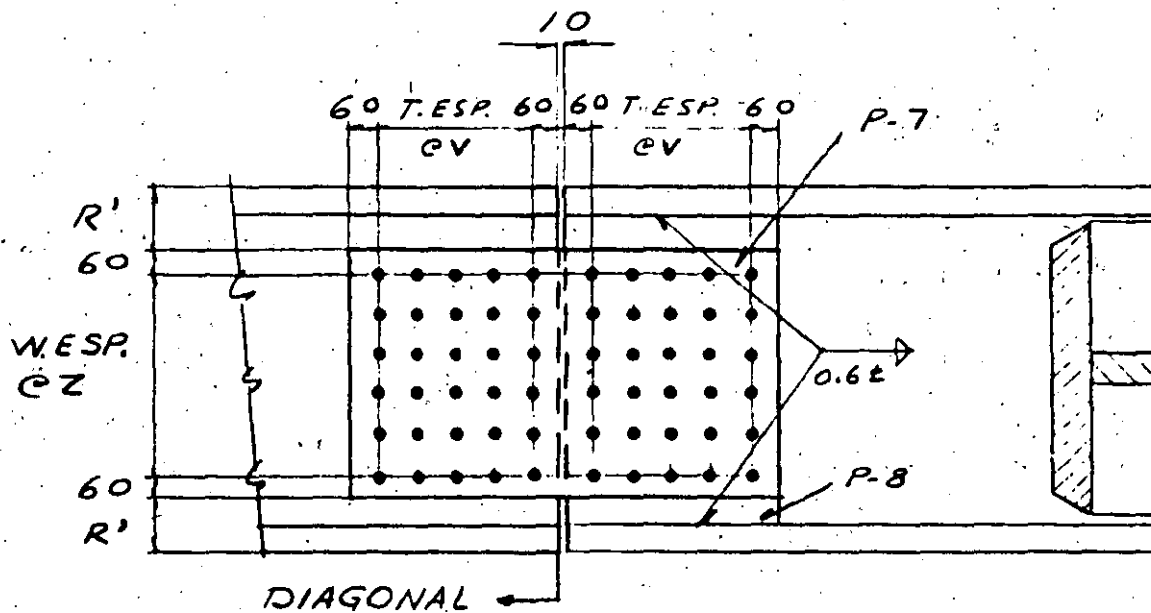


VISTA 3-3

(NO SE MUESTRA P-12 NI P. 3)

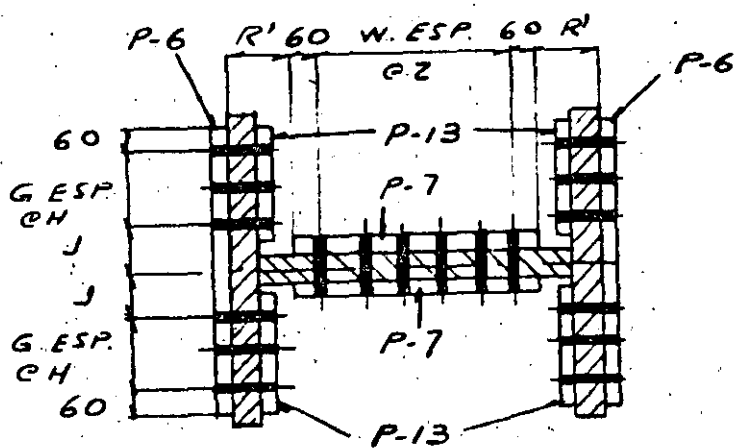


CORTE 4-4

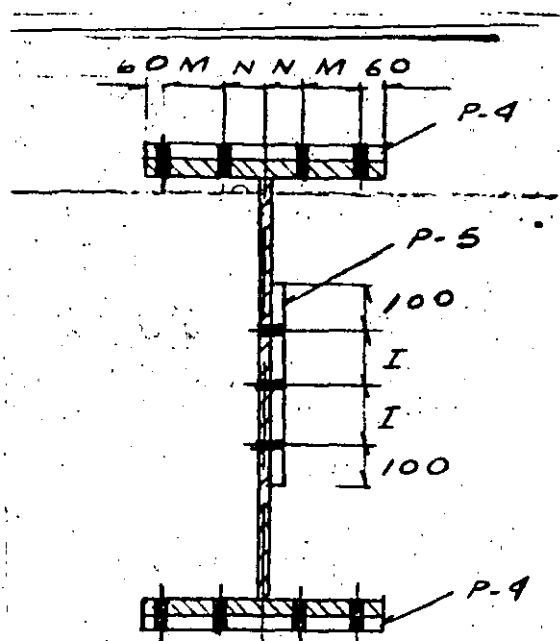


VISTA 5-5

(NO SE MUESTRA P-6 NI P-13)



CORTE 6-6



CORTE 7-7



Separaciones

Distancia mínima entre centros de agujeros a lo largo de una línea de transmisión de fuerza:

$$2 \frac{2}{3} D \text{ sin exceder de } \frac{2P}{F_{ut}} + \frac{D}{2} = \frac{2 \times 15\pi D^2}{58t} + \frac{D}{2} = 1.63 \frac{D^2}{t} + \frac{D}{2}$$

D; es el diámetro del perno y

t; el grueso de la placa central, ambos en cm.

Ejemplo:  $D = 1"$ ,  $t = 9/16"$ ,  $P = \frac{2 \pi D^2}{4} \times 30 = 15\pi D^2$  (cortante doble)

S. Inglés  $\frac{2P}{F_{ut}} + \frac{d}{2} = \frac{2 \times 15\pi \times 1^2}{58 \times 9/16} + \frac{1}{2} = 3.39" > 2 \frac{2}{3} D$

S.M.D.  $1.63 \frac{D^2}{t} + \frac{D}{2} = 1.63 \times \frac{2.54^2}{1.43} + \frac{2.54}{2} = 8.62 \text{ cm}^2 = 3.39"$

VALUES OF SPACING INCREMENT  $C_1$  IN SECT. 1.16.4.2, INCHES

Nominal Diameter of Fastener (Inches)	Oversized Holes	Slotted Holes		
		Perpendicular to Line of Force	Parallel to Line of Force	
			Short Slots	Long Slots*
$\leq \frac{7}{8}$	$\frac{1}{8}$	0	$\frac{3}{16}$	$1\frac{1}{2}d - \frac{1}{16}$
1	$\frac{3}{16}$	0	$\frac{1}{4}$	$1\frac{7}{8}$
$\geq 1\frac{1}{8}$	$\frac{1}{4}$	0	$\frac{5}{16}$	$1\frac{1}{2}d - \frac{1}{16}$

\* When length of slot is less than maximum allowable (see Table 1.23.4),  $C_1$  may be reduced by the difference between the maximum and actual slot lengths.

JUNTAS SOMETIDAS A CARGA EXCENTRICA

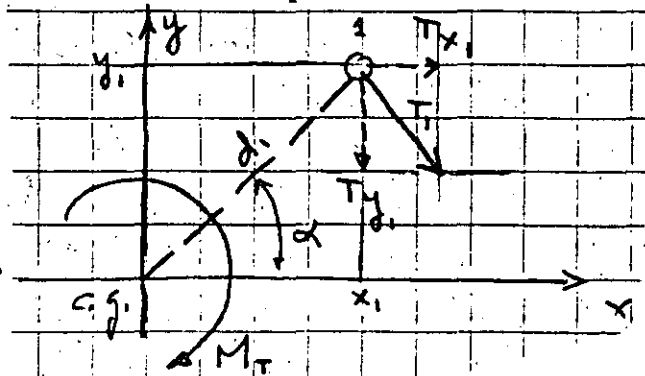
El centro de gravedad de una junta puede definirse como el centro de gravedad de las capacidades de los tornillos.

Si una junta está sometida a una fuerza que pasa por su centro de gravedad dicha fuerza se distribuye entre los tornillos proporcionalmente a la capacidad de cada uno de ellos.

En caso contrario se debe calcular el efecto de la excentricidad, para ello la fuerza excéntrica se traslada mediante un par de transporte al centro de gravedad de la junta, al efecto que se produce en los tornillos por la fuerza centrada se le añade el que produce el par.

El efecto del par suele establecerse como sigue:

En cualquier tornillo de la junta se tiene:



Area del tornillo 1 =  $A_1$

$$T_1 = k d_1 A_1$$

$$T_{x_1} = T_1 \text{ sen } \alpha = T_1 \frac{y_1}{d_1} = k y_1 A_1$$

$$T_{y_1} = T_1 \text{ cos } \alpha = T_1 \frac{x_1}{d_1} = k x_1 A_1$$

Considerando todos los tornillos de la conexión.

y estableciendo las ecuaciones de equilibrio de fuerzas y de momentos.

$$\Sigma T_x = k \quad \Sigma A_y = 0$$

$$\Sigma T_y = k \quad \Sigma A_x = 0$$

$$\Sigma M = k \quad \Sigma Ad^2 = M$$

$$k = \frac{M}{\Sigma Ad^2}$$

Sustituyendo el valor de k se tiene:

$$T = \frac{M Ad}{\Sigma Ad^2}$$

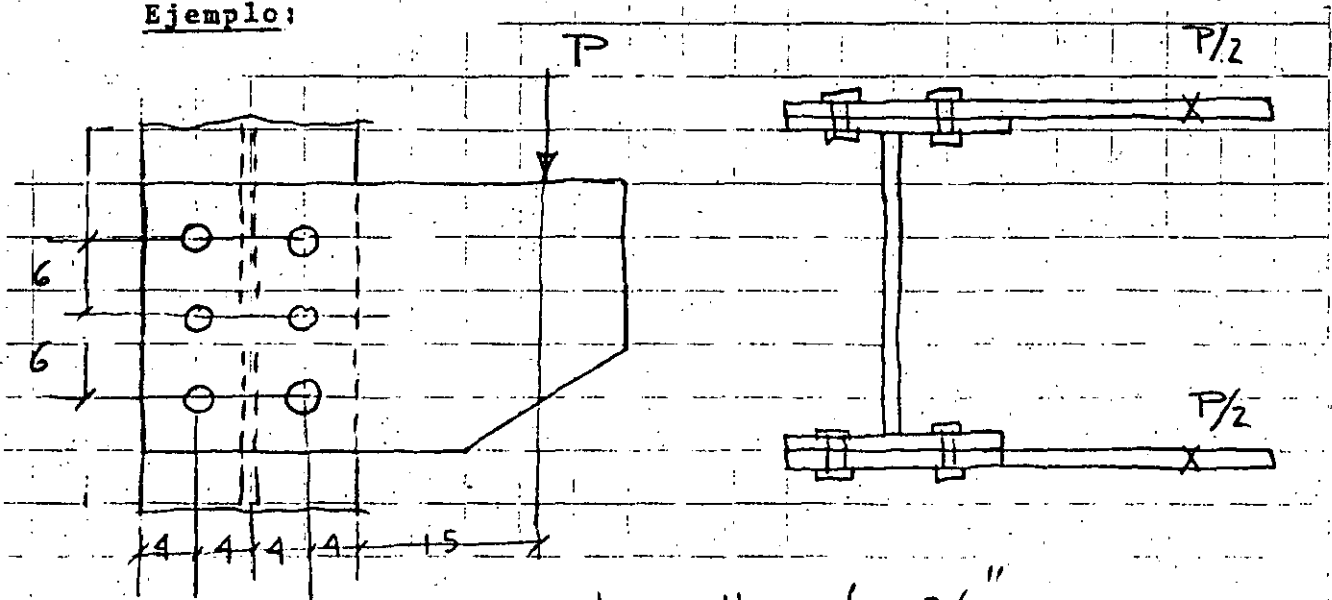
si A = cte.

$$T = \frac{Md}{\Sigma d^2}$$

$$T_x = \frac{My}{\Sigma d^2}$$

$$T_y = \frac{Mx}{\Sigma d^2}$$

Ejemplo:



tuornillos de 3/4"

$$\text{Momento} = 23 \frac{P}{2}$$

Capacidad de tornillos;

A cortante simple: 6 ton.

Espesor de las placas para aplastamiento no crítico en cortante simple:

$$t_{\min.} = 0.27 \times 1.9 = 0.51 \text{ cm.}$$

Espesor de las placas para una separación entre agujeros de  $2 \frac{2}{3} D$

$$t_{\min.} = 1.43 \text{ cm.}$$

Fuerza debida a la carga

$$\frac{P}{2 \times 6}$$

Fuerza debida al momento:

$$\Sigma x^2 = 4^2 \times 6 = 96$$

$$\Sigma y^2 = 6^2 \times 4 = 144$$

$$\Sigma d^2 = 240$$

$$T_x = \frac{23}{2} P \frac{4}{240} = 0.19 P$$

$$T_y = \frac{23}{2} P \frac{6}{240} = 0.29 P$$

$$T = \sqrt{(0.19 P)^2 + (0.29 P + 0.08 P)^2} = \sqrt{0.036 P^2 + 0.14 P^2} = \sqrt{0.17 P^2} = 0.42 P$$

$$6000 = 0.42 P \quad \therefore P = 14285 \text{ Kg.}$$

Cuando los tornillos estan sometidos a tensión y cortante en forma simultanea se utiliza una fórmula de interacción que proporciona la tensión máxima que puede aplicarse a la junta - dado el cortante actuante.

La expresión es de la forma:

$$F_t = 55 - 1.4 f_v \leq 44$$

En que  $F_t$  es el esfuerzo de tensión admisible en Kips por pulgada cuadrada y  $f_v$  el esfuerzo cortante calculado.

Para la combinación de acciones permanentes y accidentales las constantes en la fórmula se incrementan en un 33% pero  $f_v$  no se incrementa.

TABLE 1.6.3  
ALLOWABLE TENSION STRESS ( $F_t$ ) FOR FASTENERS  
IN BEARING-TYPE CONNECTIONS

Description of Fastener	Threads Not Excluded from Shear Planes	Threads Excluded from Shear Planes
Threaded parts	$0.43F_u - 1.8f_u \leq 0.33F_u$	$0.43F_u - 1.4f_u \leq 0.33F_u$
A449 bolts over 1½-in. diameter		
A325 bolts	$55 - 1.8f_u \leq 44$	$55 - 1.4f_u \leq 44$
A490 bolts	$68 - 1.8f_u \leq 54$	$68 - 1.4f_u \leq 54$
A502 Grade 1 rivets	$30 - 1.3f_u \leq 23$	
A502 Grades 2 and 3 rivets	$38 - 1.3f_u \leq 29$	
A307 bolts	$26 - 1.8f_u \leq 20$	

JUNTAS DE FRICCIÓN

Aunque en estas juntas los tornillos no trabajan a cortante ni a aplastamiento, las especificaciones dan esfuerzos permisibles a cortante de modo que su diseño se pueda tratar en la misma forma que en tornillos de aplastamiento.

Cuando las superficies de contacto llenen los requisitos indicados en la tabla E-1 pueden tomarse los esfuerzos permisibles que en ella se especifican, teniendo como límite el que correspondería al mismo perno en una junta de aplastamiento.

TABLE E1  
ALLOWABLE SHEAR STRESSES, KSI,\* BASED UPON SURFACE  
CONDITION OF BOLTED PARTS IN FRICTION-TYPE CONNECTIONS

Class	Surface Condition of Bolted Parts	Standard Holes		Oversized Holes and Short-slotted Holes		Long-slotted Holes	
		A325	A490	A325	A490	A325	A490
A	Clean mill scale	17.5	22.0	15.0	19.0	12.5	16.0
B	Blast-cleaned carbon and low alloy steel	27.5	34.5	23.5	29.5	19.5	24.0
C	Blast-cleaned quenched and tempered steel	19.0	23.5	16.0	20.0	13.5	16.5
D	Hot-dip galvanized and roughened <sup>b</sup>	21.5	27.0	18.5	23.0	15.0	19.0
E	Blast-cleaned, organic zinc rich paint	21.0	26.0	18.0	22.0	14.5	18.0
F	Blast-cleaned, inorganic zinc rich paint	29.5	37.0	25.0	31.5	20.5	26.0
G	Blast-cleaned, metallized with zinc	29.5	37.0	25.0	31.5	20.5	26.0
H	Blast-cleaned, metallized with aluminum	30.0	37.5	25.5	32.0	21.0	26.5
I	Vinyl wash	16.5	20.5	14.0	17.5	11.5	14.5

\* Values from this table are applicable only when they do not exceed the lowest appropriate allowable working stresses for bearing-type connections, taking into account the position of threads relative to shear planes and, if required, the 20% reduction due to joint length. (See Table 1.5.2.1.)

<sup>b</sup> If loads causing actual stresses in excess of one-half the tabulated allowable stresses are sustained over a long period of time (e.g., gravity), slip into bearing may occur. If such slip would be severely detrimental, these increased working stresses are not recommended.

5-102 • AISC Specification (Effective 11/1/78)

### SECTION E1 DEFINITIONS

This Specification recognizes nine classes of commercially practical surface conditions (Classes A to I) in friction-type connections, each having distinctive slip-resistant characteristics. These nine classifications, together with corresponding recommended working values,  $F_v$ , for friction-type connections assembled with A325 or A490 bolts in standard size holes, are briefly identified in Table E1. The several classes shall conform to the following provisions:

1. Class A, B, and C surfaces shall be free of oil, paint, lacquer, or other coatings. Contact surfaces for coated joints shall conform to the appropriate conditions as listed below.
2. Class D, Hot-dip Galvanized and Roughened, shall have the contact surfaces scored by wire brushing or blasting after galvanizing and prior to assembly.
3. Classes E and F, Blast Cleaned Zinc Rich Paint, shall have blast cleaned contact surfaces coated with organic or inorganic zinc rich paint, as defined in the Steel Structures Painting Council's Paint System Specification SSPC-PS 12.00, *Guide to Zinc-Rich Coating Systems*.
4. Classes G and H, Blast Cleaned Metallized Zinc or Aluminum, shall have metal applied to the contact surfaces in accordance with the American Welding Society's *Recommended Practice for Metallizing with Aluminum and Zinc for Protection of Iron and Steel*, C2.2, except that subsequent sealing treatments, described in Section IV therein, shall not be used.
5. Class I, Vinyl Wash, shall have the contact surfaces coated in accordance with the provisions of the Steel Structures Painting Council's Pretreatment Specification SSPC-PT 3, *Basic Zinc Chromate—Vinyl Butyral Washcoat*.

### SECTION E2 USE OF HIGHER WORKING STRESSES

Subject to the approval of the responsible engineer, when the contact surfaces of friction-type connections assembled with A325 or A490 bolts in standard size holes meet the provisions of Sect. E1, the allowable working values given in Table E1 may be substituted in lieu of those given in Table 1.5.2.1. However, the value thus obtained shall not exceed that specified in Table 1.5.2.1 for a bearing-type connection having bolts of the same size and thread length.

Los tornillos en juntas de fricción pueden utilizarse en combinación con remaches y soldadura, cosa que no se admite en juntas de aplastamiento.

Cuando exista tensión además de cortante los esfuerzos permisibles se multiplicarán por el factor de reducción  $(1 - f_t A_b / T_b)$  en que  $f_v$  es el esfuerzo debido a tensión y  $T_b$  a la pretensión especificada (Tabla 1.23.5)

TABLE 1.23.5  
MINIMUM BOLT TENSION, KIPS\*

Bolt Size, Inches	A325 Bolts	A490 Bolts
1/2	12	15
5/8	19	24
3/4	28	35
7/8	39	49
1	51	64
1 1/8	56	80
1 1/4	71	102
1 3/8	85	121
1 1/2	103	148

\* Equal to 0.70 of specified minimum tensile strengths of bolts, rounded off to nearest kip.



Como ejemplo se puede plantear nuevamente el de la conexión entre una diagonal de contraventeo y una columna, utilizando en este caso una junta de fricción y agujeros agrandados.

Diámetro pulg (cm)	Area (cm <sup>2</sup> )	Esf. perm. (kg/cm <sup>2</sup> )	Cortante Simple	x 1.33	Cortante Doble	x 1.33	Separación car. (cm)	Dist. mín al borde (cm)
1" (2.54)	5.07	1055	5.3	7.1	10.7	14.2	7.62	
1 1/8" (2.86)	6.42	1055	6.8	9.0	13.5	18.0	8.58	
1 1/4" (3.18)	7.92	1055	8.4	11.1	16.7	22.2	9.54	
1 3/8" (3.49)	9.57	1055	10.1	13.4	20.2	26.9	10.47	
1 1/2" (3.81)	11.40	1055	12.0	16.0	24.1	32.0	11.43	

Número de pernos necesario en cada diagonal

Fuerza total = 1276 ton. (incluye sismo)

Diám.	No. total	En cada patín	En el alma
1"	90	32	27
1 1/8"	71	25	21
1 1/4"	58	21	17
1 3/8"	48	17	14
1 1/2"	40	14	12

El número de pernos se ha calculado suponiendo que trabajan en cortante doble; se han distribuido -- entre patines y almas proporcionalmente a sus áreas.

nd

CONEXIONES A TORNILLADAS

DESCRIPCION Y COMPORTAMIENTO

## CONEXIONES ATORNILLADAS EN ESTRUCTURAS DE ACERO

La mayor parte de las especificaciones relativas a estructuras de acero reconocen como medios de unión entre sus elementos, a los remaches, los tornillos y la soldadura.

Desde hace años, los primeros han caído en desuso y se puede decir que actualmente han desaparecido ya en la práctica.

Esto se ha debido al uso creciente de la soldadura y a la aparición de los tornillos de alta resistencia que sustituyen con ventaja a los remaches.

Se utilizan dos tipos de tornillos, los llamados comunes y los de alta resistencia.

Se designan, con el nombre que les dan las normas del ASTM para especificar sus características químicas y mecánicas, los primeros como tornillos A307 y los de alta resistencia como tornillos A325 ó A490.

### TORNILLOS COMUNES (A 307)

Son históricamente, el primer medio de unión utilizado en estructuras de acero; en la actualidad tienen una aplicación estructural muy limitada ya que su resistencia es reducida y no se recomiendan cuando pueden esperarse cambios de signo en los esfuerzos de las piezas que conectan o cuando sean de esperarse cargas dinámicas.

En este sentido, las especificaciones del AISC fijan una serie de casos concretos en que los tornillos A-307 no

deben usarse.

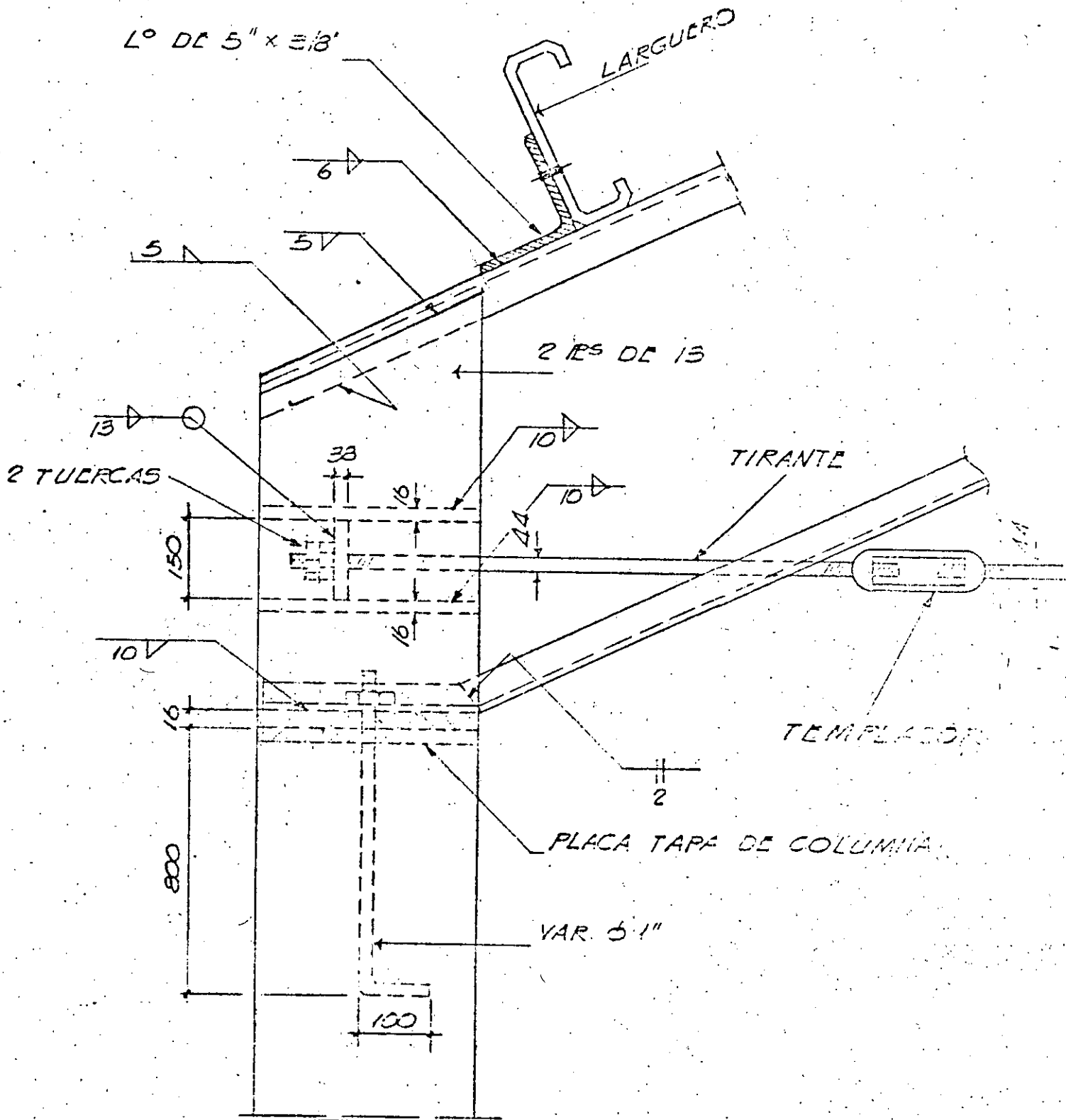
No se usarán para uniones entre tramos de columnas en estructuras esbeltas:

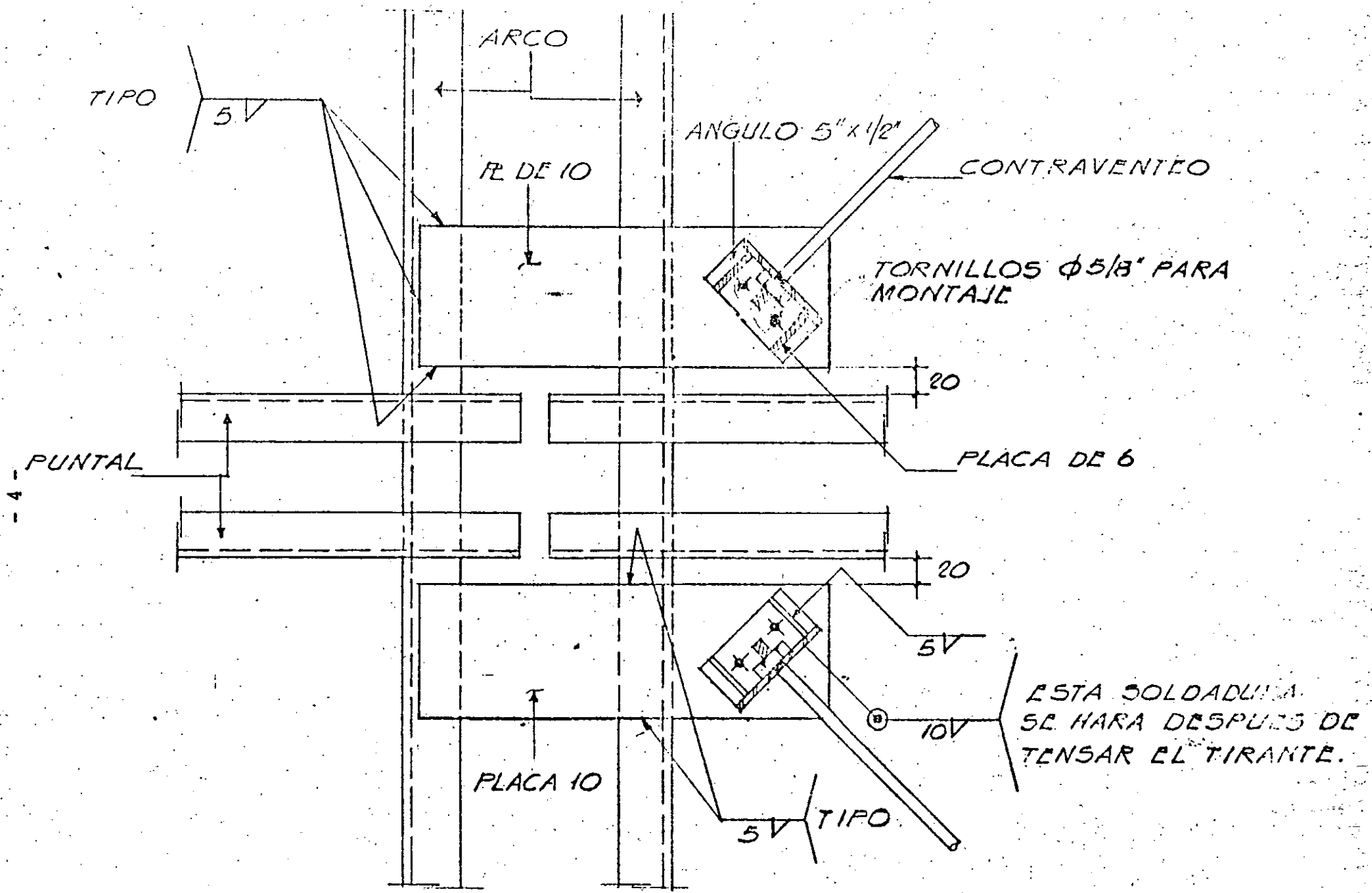
- a) Que tengan una altura de más de 60 m.
- b) Que tengan una altura entre 30 y 60 m. cuando la base es menor del 40% de la altura.
- c) Que tengan una altura cualquiera si la base mide menos del 25% de la altura.

No se usará en estructuras que deban soportar travesaños -- grua.

No se usarán donde halla máquinas o alguna carga viva que produzca impacto o reversión de esfuerzos.

Sin embargo, en estructuras ligeras en que los problemas mencionados no aparecen, así como en conexiones de elementos secundarios tales como largueros de techo, constituyen una -- buena solución pues son económicos y su manejo y colocación -- es muy simple.





CONEXIÓN DE CONTRAVENTEO A LA CUERDA SUPERIOR DEL ARCO.

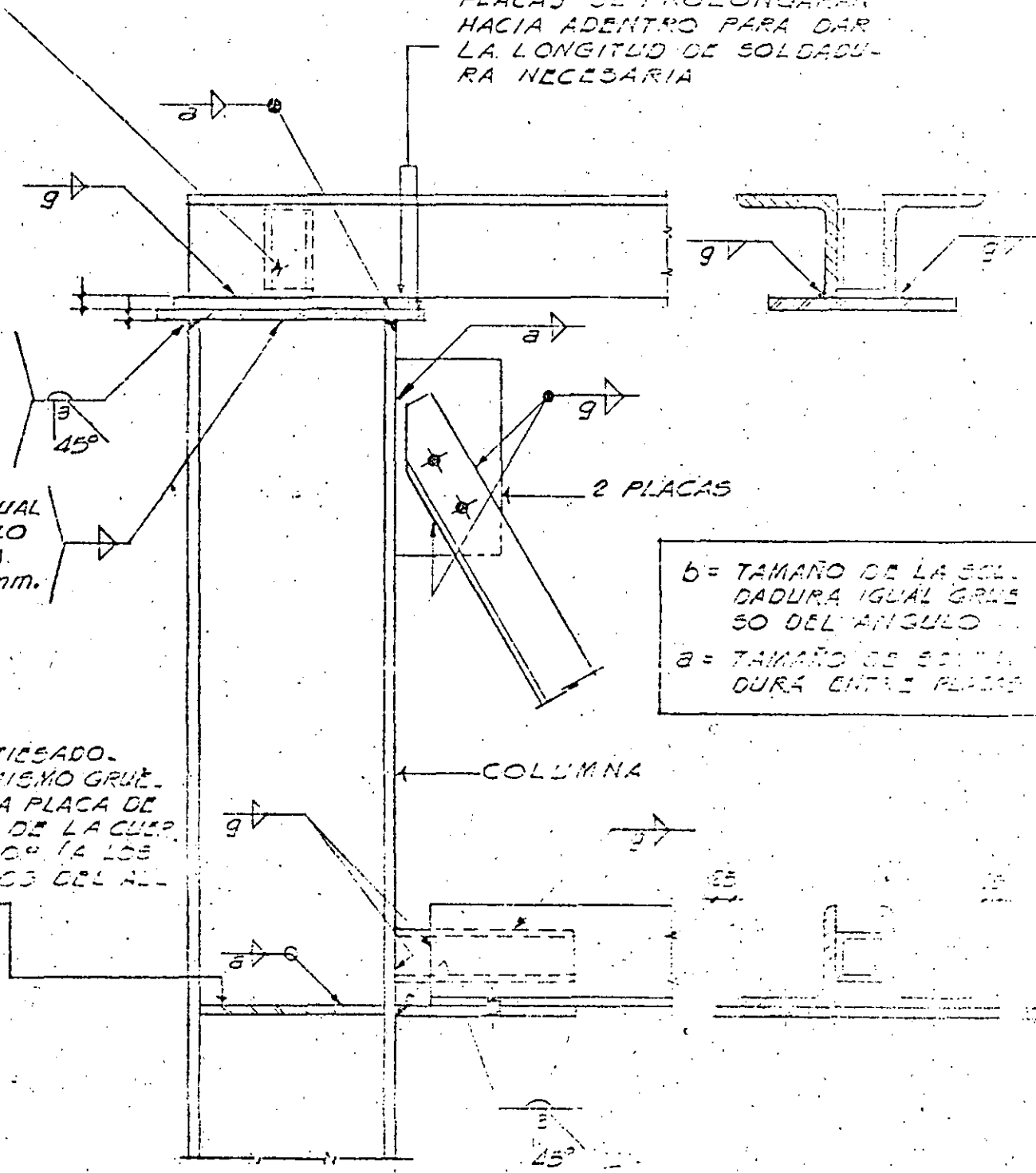
CAJON FORMADO POR DOS ANGULOS

SI ES NECESARIO ESTAS DOS PLACAS SE PROLONGARAN HACIA ADETRON PARA DAR LA LONGITUD DE SOLDADURA NECESARIA

EN LOS DOS PANTINES

TAMAÑO IGUAL AL GRUEZO DEL ALMA. MENOS 3mm.

PLACAS ATIBESADO. RAS DEL MISMO GRUESO QUE LA PLACA DE CONEXION DE LA CUBETA INFERIOR (A LOS DOS LADOS DEL ALMA.)



b = TAMAÑO DE LA SOLDADURA IGUAL GRUESO DEL ANGULO  
 a = TAMAÑO DE SOLDADURA ENTRE PLACAS

CONEXION DE ARMADURAS A COLUMNA EXTRINIAS

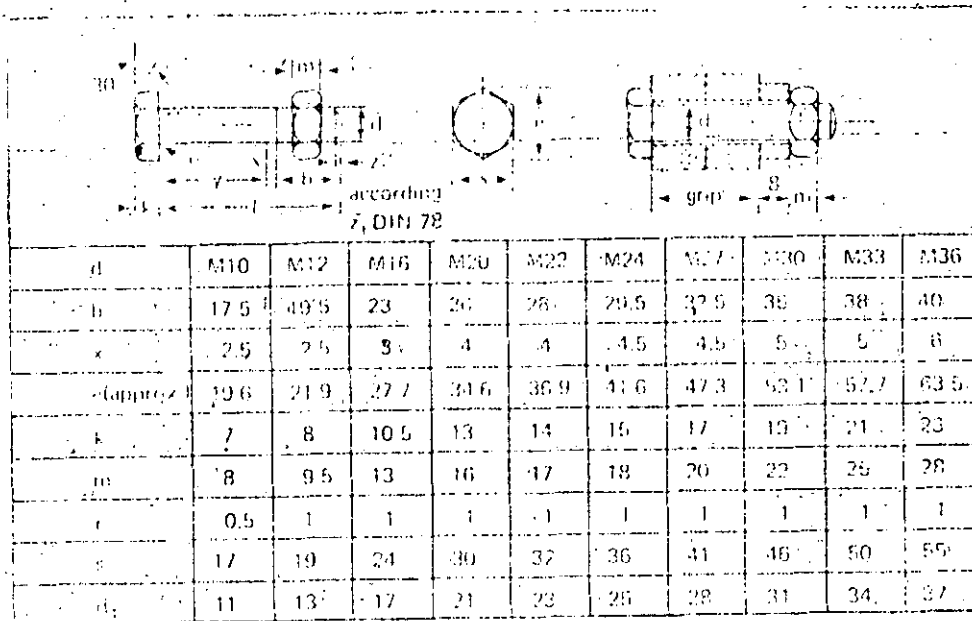


Figure 3.1 Unfinished Hexagonal Bolts A307, DIN 7990 (Dimensions in mm). (From *Stahlbau*, Deutsches Stahlbau-Verband, Cologne, 1957, p. 15).

### TORNILLOS DE ALTA RESISTENCIA

A 325

A 490

Basan su capacidad en el hecho de que pueden ser sometidos a una gran fuerza de tensión controlada que aprieta firmemente los elementos de la conexión.

Las ventajas de este apriete firme se conocen desde hace tiempo, pero su aplicación práctica en estructuras proviene de 1951 en que se publicaron las primeras normas para regir su utilización. Desde entonces los tornillos de alta resistencia se han venido utilizando en forma creciente en EE.UU. y en la última década, también en México.



A partir de 1951, las normas relativas a estos tornillos se han modificado varias veces para poder incluir los resultados de las investigaciones que, en forma casi continua, se -- han venido realizando en torno a ellos.

Los primeros tornillos de alta resistencia que se desarrollaron y aún los más comunmente usados son los A-325; posteriormente y con objeto de contar con capacidades aún mayores, se desarrollaron los A-490, ambos se obtienen de aceros al carbón tratados térmicamente.

Los tornillos A-325 se marcan, para distinguirlos, con la leyenda: A-325 y a veces con tres líneas radiales en su cabeza; la tuerca tiene tres marcas espaciadas 120°.

Los tornillos A-490 se marcan con su nombre en la cabeza y con la leyenda 2H ó DH en la tuerca.

Las últimas normas reconocen 3 tipos distintos de tornillos A325; los tornillos tipo 1 son los originales y cuando se solicitan simplemente tornillos A325 son los que se suministran. Son los más utilizados.

Los tornillos tipo 2 (A325) se fabrican con acero martensítico de bajo carbono, para distinguirlos se marcan con líneas radiales a 60° en vez de 120° como los tipo 1.

Los tornillos A325 tipo 3 se caracterizan por tener una alta resistencia a la corrosión, suelen usarse con aceros -- de características similares a ellos. Se marcan con la leyenda A325 subrayada, la tuerca se marca con el número 3.

En México los únicos usados en forma extensa han sido los tipo 1.

Inicialmente los tornillos de alta resistencia consistían en un tornillo, una tuerca, y dos rondanas; actualmente las dimensiones de la cabeza y de la tuerca se han diseñado de tal forma que se puede, en muchos casos, prescindir totalmente de las rondanas y usar en los demás, una sola.

CARACTERISTICAS QUIMICAS Y MECANICAS

La composición química de los tornillos de alta resistencia, junto con el tratamiento térmico a que son sometidos, -- les proporciona sus características de resistencia; el contenido de carbono y de manganeso es la variable más significativa en los tornillos A325. En los A490 el contenido de carbono se fija y el elemento de aleación se deja abierto para poder proporcionar por distintos caminos las propiedades mecánicas requeridas.

Aunque, cuando es posible, los tornillos deben someterse a una prueba de tensión para probar su resistencia; a menudo son demasiado cortos para que la prueba directa de tensión se pueda realizar, se recurre entonces a controlar la resistencia, indirectamente a través de una prueba de dureza.

Se realizan con ese fin las pruebas Brinell ó Rockwell.

Table 5

Nominal Bolt Size, Inches <i>D</i>	Bolt Dimensions, Inches Heavy Hex Structural Bolts			Nut Dimensions, Inches Heavy Hex Nuts	
	Width across flats <i>F</i>	Height <i>H</i>	Thread length	Width across flats <i>W</i>	Height <i>H</i>
1/2	3/8	5/16	1	3/8	3/4
5/8	11/16	23/32	1 1/4	11/16	3/4
3/4	1 1/4	1 1/8	1 3/8	1 1/4	4 3/4
7/8	1 3/4	3 3/32	1 3/2	1 3/4	5 3/4
1	1 7/8	3 3/16	1 3/4	1 7/8	6 3/4
1 1/8	1 11/16	1 1/4	2	1 11/16	1 3/4
1 1/4	2	2 7/16	2	2	1 7/8
1 3/8	2 1/16	2 1/2	2 1/4	2 1/16	1 9/8
1 1/2	2 1/2	1 5/8	2 3/4	2 1/2	1 7/8

TABLE 2 Chemical Requirements for Type 3 Bolts, Nuts, and Washers

Element	Composition, percent						
	Type 3 Bolts <sup>a</sup>					Type 3 Nuts <sup>a</sup>	Type 3 Washers <sup>a</sup>
	A	B	C	D	E		
Carbon:							
Heat analysis	0.33-0.40	0.38-0.48	0.15-0.25	0.15-0.25	0.20-0.25	....	....
Product analysis	0.31-0.42	0.36-0.50	0.14-0.26	0.14-0.26	0.18-0.27	....	....
Manganese:							
Heat analysis	0.90-1.20	0.70-0.90	0.80-1.35	0.40-1.20	0.60-1.00	....	....
Product analysis	0.86-1.24	0.67-0.83	0.76-1.39	0.36-1.24	0.56-1.04	....	....
Phosphorus:							
Heat analysis	0.040 max	0.06-0.12	0.035 max	0.040 max	0.040 max	0.07-0.15	0.040 max
Product analysis	0.045 max	0.06-0.125	0.040 max	0.045 max	0.045 max	0.07-0.155	0.045 max
Sulfur:							
Heat analysis	0.050 max	0.050 max	0.040 max	0.050 max	0.040 max	0.050 max	0.050 max
Product analysis	0.055 max	0.055 max	0.045 max	0.055 max	0.045 max	0.055 max	0.055 max
Silicon:							
Heat analysis	0.15-0.30	0.30-0.50	0.15-0.30	0.25-0.50	0.15-0.30	0.20-0.50	0.15-0.30
Product analysis	0.13-0.32	0.25-0.55	0.13-0.32	0.20-0.55	0.13-0.32	0.15-0.55	0.13-0.32
Copper:							
Heat analysis	0.25-0.45	0.20-0.40	0.20-0.50	0.30-0.50	0.30-0.60	0.25-0.55	0.25-0.45
Product analysis	0.22-0.48	0.17-0.43	0.17-0.53	0.27-0.53	0.27-0.63	0.22-0.53	0.22-0.43
Nickel:							
Heat analysis	0.25-0.45	0.50-0.80	0.25-0.50	0.50-0.80	0.30-0.60	1.00 max	0.25-0.45
Product analysis	0.22-0.48	0.47-0.83	0.22-0.53	0.47-0.83	0.27-0.63	1.03 max	0.22-0.43
Chromium:							
Heat analysis	0.45-0.65	0.50-0.75	0.30-0.50	0.50-0.75	0.60-0.90	0.30-1.25	0.45-0.65
Product analysis	0.42-0.68	0.47-0.83	0.27-0.53	0.45-1.05	0.50-0.95	0.25-1.30	0.42-0.65
Vanadium:							
Heat analysis	....	....	0.020 min	....	....	....	....
Product analysis	....	....	0.010 min	....	....	....	....
Molybdenum:							
Heat analysis	....	0.06 max	....	0.10 max	....	....	....
Product analysis	....	0.07 max	....	0.11 max	....	....	....
Titanium:							
Heat analysis	....	....	....	0.05 max	....	....	....
Product analysis	....	....	....	....	....	....	....

A, B, C, D, and E are classes of material used for Type 3 bolts. Selection of a class shall be at the option of the bolt manufacturer. Nuts or washers may also be made of any of the above listed bolt material classes. Selection of the class shall be at the option of the manufacturer.

TABLE 3 Hardness Requirements for Bolts

Bolt Size, in.	Hardness Number			
	Brinell		Rockwell C	
	Min	Max	Min	Max
1/2 to 1 inch	211	331	23	35
1 1/8 to 1 1/2 inch	223	293	19	31

TABLE 1 Chemical Requirements for Types 1 and 2 Bolts, Nuts, and Washers

Element	Composition, percent				
	Type 1 Bolts	Type 2 Bolts <sup>a</sup>	Nuts	Washers	
				Quenched and Tempered	Carburized
Carbon:					
Heat analysis	0.30 min	0.15 to 0.23	...	...	•
Product analysis	0.27 min	0.13 to 0.25	...	...	...
Manganese, min:					
Heat analysis	0.50	0.70	...	...	1.00 max
Product analysis	0.47	0.67	...	...	1.00 max
Phosphorus, max:					
Heat analysis	0.040	0.040	0.120	0.040	0.040
Product analysis	0.048	0.048	0.128	0.050	0.050
Sulfur, max:					
Heat analysis	0.050	0.050	0.23	0.050	0.050
Product analysis	0.058	0.058	...	0.060	0.060
Boron, min:					
Heat analysis	...	0.0005	...	...	...
Product analysis	...	0.0005	...	...	...

<sup>a</sup>Type 2 bolts shall be fully killed, fine grain steel.  
<sup>b</sup>The stock used for manufacture of carburized washers shall not contain over 0.25 percent carbon.

ESPECIFICACIONES

ASTM

5. (3) • Specification for Structural Bolts (ASTM)

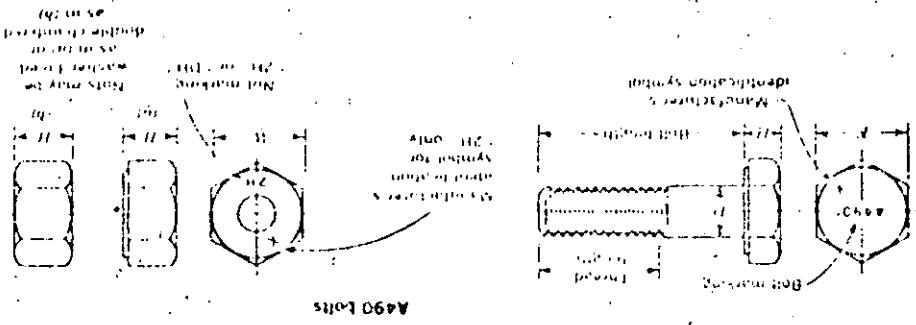
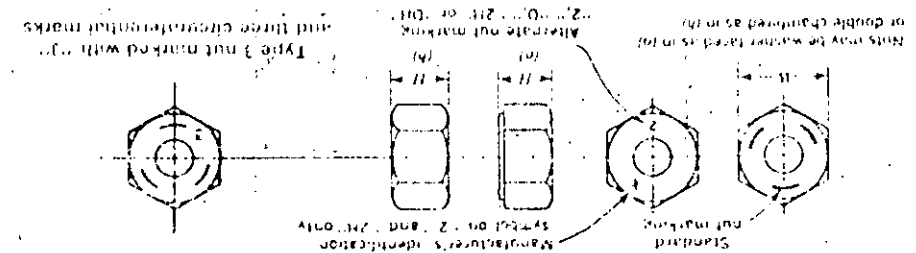
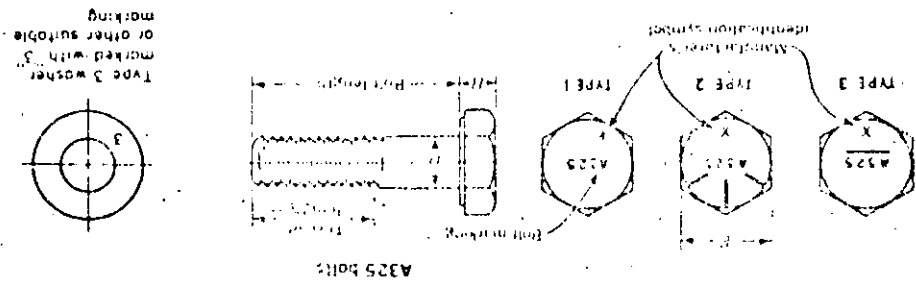


Table 1 Washer Dimensions, <sup>1</sup>Inches

Nominal Bolt Size	Nominal Outside Diameter	Nominal Diameter of Hole	Thickness		Minimum Hole Dimension	Minimum Thickness	Slope or Topper Thickness
			Min.	Max.			
1/2"	1 1/16"	1 1/16"	0.097	0.177	1 1/8"	3/16"	1:6
3/8"	1 1/8"	1 1/8"	0.122	0.177	1 1/8"	3/16"	1:6
1/2"	1 3/8"	1 3/8"	0.136	0.177	1 1/2"	3/16"	1:6
5/8"	1 7/8"	1 7/8"	0.136	0.177	1 1/2"	3/16"	1:6
3/4"	2 1/8"	2 1/8"	0.136	0.177	1 3/4"	3/16"	1:6
7/8"	2 3/8"	2 3/8"	0.136	0.177	2 1/8"	3/16"	1:6
1"	2 7/8"	2 7/8"	0.136	0.177	2 1/4"	3/16"	1:6
1 1/8"	3 1/8"	3 1/8"	0.136	0.177	2 3/8"	3/16"	1:6
1 1/4"	3 3/8"	3 3/8"	0.136	0.177	2 3/8"	3/16"	1:6

<sup>1</sup>Table notes:  
 The most outside dimension shown here is from the flat surface on the outer side and not from the top surface immediately adjacent to the flat surface more than 1/8" beyond.

TORNILLOS A490

Element	Ladle Analysis, percent	Check Analysis, percent
Carbon		
For sizes through 1½ in.	0.30 to 0.48	0.28 to 0.50
For size 1½ in.	0.35 to 0.53	0.33 to 0.55
Phosphorus, max	0.040	0.045
Sulfur, max	0.040	0.045

Bolt Size, in.	Hardness Number.			
	Brinell		Rockwell C	
	min	max	min	max
¾ to 1½ in., incl	302	341	32	38

## COMPORTAMIENTO DE JUNTAS CON TORNILLOS DE ALTA RESISTENCIA

El comportamiento de una junta con tornillos de alta resistencia se puede visualizar mediante la observación de los resultados de una prueba carga-deformación en un espécimen típico.

Se define una zona de comportamiento lineal (zona I) que termina en el instante en que se produce un deslizamiento de los tornillos con carga prácticamente constante (zona II) y que está controlado por el diámetro del agujero, al hacer contacto con sus bordes, el tornillo toma nuevamente carga y se reinicia un comportamiento nuevamente lineal (zona III); esta zona termina al iniciarse el comportamiento inelástico (zona IV) que termina con la falla de la junta.

Teniendo en cuenta el comportamiento mencionado se distinguen dos tipos de juntas con tornillos de alta resistencia: las juntas de fricción y las juntas de aplastamiento.

Las primeras se caracterizan por que la transmisión de las fuerzas que actúan en la conexión se logra únicamente por la fricción que se desarrolla entre los elementos que la constituyen.

En estas juntas el deslizamiento entre las piezas que se unen no es aceptable; se considera que el deslizamiento equivaldría a la falla, si bien, los coeficientes de seguridad contra el deslizamiento se aceptan pequeños pues las consecuencias de su ocurrencia no son graves.

La magnitud de la fricción depende de la fuerza de tensión en el tornillo y de las características de la superfi-

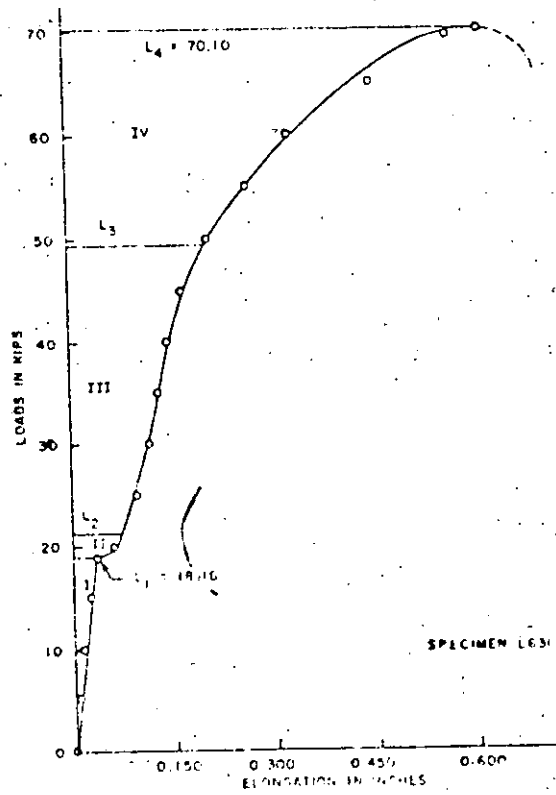


FIG. 6.—TYPICAL LOAD-JOINT ELONGATION RELATIONSHIP FOR SPECIMENS



cie de los elementos que se conectan.

Bresler p 160

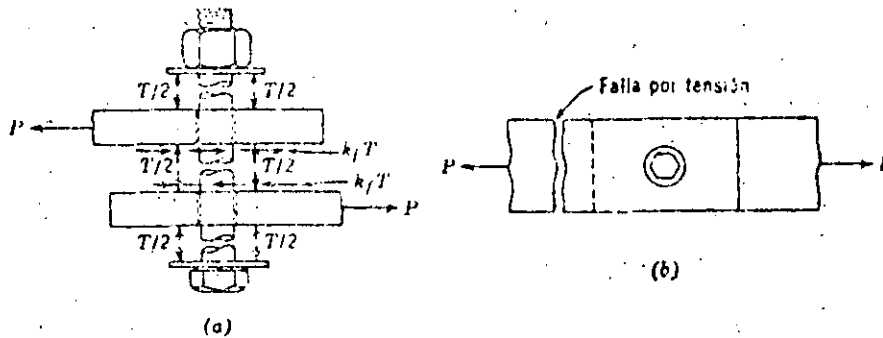


Fig. 5-15 Tornillo de alta resistencia. (a) Transmisión de carga por fricción, y (b) Falla fuera de la sección neta.

Aunque es claro que en juntas de fricción los tornillos no trabajan a esfuerzo cortante, tradicionalmente se ha venido estableciendo un esfuerzo cortante permisible ficticio, - para la determinación del número de tornillos que se requieren en una junta, esto ha permitido tratar el diseño de juntas con tornillos de fricción con los mismos criterios con - que durante mucho tiempo, se han proporcionado las juntas re - machadas.

Las conexiones de fricción, se especifican como necesarias en todos aquellos casos en que se esperan inversiones - de esfuerzos y en los que en condiciones de trabajo, el deslizamiento se considera indeseable.

Hay ocasiones en que la inversión de esfuerzos no ocurre y en que, al colocar los tornillos, la carga muerta los presiona contra los lados del agujero, entonces el trabajo de la junta puede ser por aplastamiento y por cortante y se presen-

tan entonces las conexiones llamadas de aplastamiento.

Si bien, también en estas juntas, la tensión en el tornillo, que es la misma que en juntas de fricción, produce -- una fricción que probablemente podría tomar las cargas de -- trabajo, esta en realidad no se requiere. En estas juntas - se puede sacar ventaja de la resistencia de los tornillos, sobre todo si se logra que la rosca se encuentre fuera de los planos de corte. Con el fin de lograr ésto en lo posible, -- los tornillos de alta resistencia tienen una rosca bastante - corta.

En estructuras para puentes los tornillos en juntas de aplastamiento se limitan a piezas que sólo trabajan a compresión y a miembros secundarios, se exige además que en todos los casos la rosca se excluya de los planos de corte.

5.7.2 • Specification for Structural Joints (226778)

Table 2 Allowable Working Stresses for Fasteners,<sup>a</sup> ksi

Load Condition	Hole Type	ASTM A325 Bolts	ASTM A490 Bolts
Applied Tension <sup>b</sup>	Standard, oversize, or slotted	44.0	54.0
Shear; Friction-Type Connection	Standard	17.5 <sup>c</sup>	22.0 <sup>c</sup>
	Oversize	15.0 <sup>c</sup>	19.0 <sup>c</sup>
	Short slotted	15.0 <sup>c</sup>	19.0 <sup>c</sup>
	Long slotted	12.5 <sup>c</sup>	16.0 <sup>c</sup>
Shear; Bearing-Type Connection: Threads in any shear plane No threads in shear plane	Standard or slotted	21.0 <sup>d</sup>	28.0 <sup>d</sup>
	Standard or slotted	30.0 <sup>d</sup>	40.0 <sup>d</sup>
Bearing <sup>e</sup>	Standard, oversize, or slotted	$\frac{1.7F_u}{2d}$ or $1.5F_u$ (whichever is smaller)	

- <sup>a</sup> The tabulated stresses, except for bearing stress, apply to the nominal area of bolts used in any grade of steel.
- <sup>b</sup> For allowable working stresses when bolts are subjected to fatigue loading in tension, see subsection 4(b).
- <sup>c</sup> Applicable for contact surfaces with clean mill scale (Class A surface, subsection 3(c)). When the designer has specified special treatment of the contact surfaces in a friction-type connection, values in Table 2a may be substituted.
- <sup>d</sup> In bearing-type connections whose length between extreme fasteners measured parallel to the line of an axial force exceeds 50 inches, tabulated values shall be reduced by 20%.
- <sup>e</sup>  $L$  is the distance in inches measured in the line of force from the center line of a bolt to the nearest edge of an adjacent bolt or to the end of the connected part toward which the force is directed;  $d$  is the diameter of the bolt; and  $F_u$  is the lowest specified minimum tensile strength of the connected parts.

Para mantener la fricción es necesario que las superficies estén libres de todo elemento que la disminuya, se prohíbe por ello, que haya aceite, pintura, óxido suelto, etc. Dada la importancia de este hecho, las últimas normas reconocen nueve condiciones distintas en que se pueden encontrar las superficies de la junta y asocian a cada una de ellas un esfuerzo permisible diferente, reconociendo las diferencias existentes en el coeficiente de fricción.

ASTM A325 or A490 Bolts • 5 213

Table 2a. Allowable Working Stresses,\* ksi, Based Upon Surface Condition of Bolted Parts, for Lock-washer-Type Shear Connections.

Class	Surface Condition of Bolted Part	Standard Bolts		Over-sized Holes and Short Slotted Holes		Long Slotted Holes	
		A325	A490	A325	A490	A325	A490
A	Clean mill scale	17.5	22.0	15.0	19.0	12.5	16.0
B	Blast cleaned carbon and low alloy steel	27.5	31.5	23.5	29.5	19.5	24.0
C	Blast cleaned quenched and tempered steel	19.0	23.5	16.0	20.0	13.5	16.5
D	Hot dip galvanized and roughened <sup>b</sup>	21.5	27.0	18.5	22.0	15.0	19.0
E	Blast cleaned, organic zinc rich paint	21.0	26.0	18.0	22.0	14.5	18.0
F	Blast cleaned, inorganic zinc rich paint	29.5	37.0	25.0	31.5	20.5	26.0
G	Blast cleaned, metallized with zinc	29.5	37.0	25.0	31.5	20.5	26.0
H	Blast cleaned, metallized with aluminum	39.0	37.5	25.5	37.0	21.0	26.5
I	Vinyl wash	16.5	20.5	14.0	17.5	11.5	14.5

\* Values from this table are applicable only when they do not exceed the lowest appropriate allowable working stresses for bearing type connections, taking into account the position of threads relative to shear planes and, if required, the 20% reduction due to joint length. (See Table 2.)

<sup>b</sup> Due to values not recommended if the actual stresses due to sustained loading (e.g., gravity) exceed 1/2 the allowable working stresses, and slip into bearing, would be generally detrimental, occurrence of creep deformation may occur at holes/sustained stresses.

## INSTALACION

Sea en juntas de fricción o en juntas de aplastamiento, los tornillos de alta resistencia deben colocarse de modo que queden sometidos a una fuerza mínima de tensión especificada.

Esta fuerza es de aproximadamente el 70% de la resistencia a tensión del tornillo, se denomina carga de prueba y es normalmente algo menor al límite de proporcionalidad del tornillo.

La tensión especificada se puede dar haciendo uso de un indicador directo de tensión o usando cualquiera de otros -- dos métodos que también se especifican en las normas y que -- se basan en el hecho de que la tensión en el tornillo se puede relacionar con dos cantidades observables, el alargamiento del tornillo y el giro de la tuerca.

El primero de estos métodos consigue la tensión usando llaves calibradas, el segundo dando un giro especificado a -- la tuerca.

### METODO DE LLAVES CALIBRADAS

Implica el ajuste frecuente de la llave con un dispositivo capaz de medir la tensión en tornillos típicos de la -- conexión, ya que el ajuste pierde precisión con facilidad -- porque las condiciones de distintas juntas son muy diferentes entre sí; se especifica que la calibración se realice -- una vez por cada día de trabajo y por cada diámetro o lote de tornillo que se utilice, aún en el caso de que se aprieten juntas similares.

Se exige también, cuando se usa este método, que se coloque una rondana bajo la parte del tornillo que se accione con la llave, con objeto de minimizar las irregularidades -- en la tensión producida que inevitablemente existen al utilizar este procedimiento.

TABLE 12.5  
MINIMUM BOLT TENSION, KIPS\*

Bolt Size, Inches	A325 Bolts	A490 Bolts
$\frac{1}{2}$	12	15
$\frac{3}{8}$	19	24
$\frac{1}{2}$	28	35
$\frac{3}{4}$	39	48
1	51	64
$1\frac{1}{8}$	56	80
$1\frac{1}{4}$	71	102
$1\frac{3}{8}$	85	121
$1\frac{1}{2}$	101	118

\* Equal to 0.70 of specified minimum tensile strengths of bolts, rounded off to nearest kip.

# RIVETS AND THREADED FASTENERS

## Erection Clearances

### BOLT IMPACT WRENCHES

Diagram showing dimensions A, B, C, and D for a bolt impact wrench.

EXTENSION BAR  
2 1/4  
\*

\*Available in lengths 6 1/2' to 1'-3.

MINIMUM CLEARANCES  
E  
F

UNIVERSAL JOINT  
(for bolts up to 1")  
2 1/4  
3  
2

±20° for 3/4"  
15° for 7/8", 1"

	Size	C	D	Sockets		Min. Clear.	
				A	B	E	F
Light Wrenches	3/8	2 3/8	1 1/4	1 1/4	1 1/4	1 1/4	1 1/4
	3/4	3	2 1/4	1 1/4	1 1/4	1 1/4	1 1/4
	7/8	3 1/4	2 1/2	1 1/4	1 1/4	1 1/4	1 1/4
Heavy Wrenches	1	3 1/2	2 3/4	1 1/2	1 1/2	1 1/2	1 1/2
	1 1/8	3 3/4	2 7/8	1 1/2	1 1/2	1 1/2	1 1/2
	1 1/4	4	3 1/8	1 1/2	1 1/2	1 1/2	1 1/2
	1 1/2	4 1/4	3 3/8	1 1/2	1 1/2	1 1/2	1 1/2
	1 3/4	4 3/4	4 1/4	2 1/4	2 1/4	2 1/4	2 1/4

### RIVET GUNS

STANDARD OPEN HANDLE  
C  
D

INVERTED HANDLE  
L

	Rivet Size	D	Standard		Inverted	
			L	C	L	C
Light Hammer	3/8, 3/4, 7/8	2 1/2	1-5 1/2 to 1-9 1/2	1-9 to 2-2	1-2 to 1-3 3/4	1-5 to 1-7
Medium Hammer	3/4 to 1 1/8	2 1/2	1-10 1/4 to 1-11 1/2	2-2 to 2-4	1-5 1/2 to 1-6 1/4	1-9 to 1-10 1/2
Heavy Hammer	1 1/2	2 1/2	2-2 1/2	2-7	...	...

### METODO DEL GIRO DE LA TUERCA

Este procedimiento requiere un control de la colocación de los tornillos más simples que el anterior y es por ello, más utilizado.

Consiste en términos generales, en apretar, en una primera etapa, todos los tornillos con una llave normal de tuercas hasta el esfuerzo máximo de un hombre y enseguida, dar a la tuerca 1/2 vuelta adicional; excepcionalmente, el giro debe ser mayor (ver tabla 4).

Ha sido posible determinar experimentalmente la relación que existe entre la rotación de la tuerca y el alargamiento y la tensión en el tornillo, con ese fin se han realizado -- una cantidad importante de pruebas, en ellas se ha observado que la resistencia a tensión en un tornillo es menor cuando esta tensión se da girando la tuerca que cuando se da en forma directa, esta es la razón de que la carga de prueba se -- fije sólo en un 70% de la resistencia a tensión directa.

Se observa que una vez dado el primer tercio de vuelta hay una reserva importante de deformación posible adicional hasta la falla, esto hace que el método no sea muy sensible a errores relativos al apriete que debe tener el tornillo -- en la primera etapa, al iniciarse la media vuelta pedida. -- Debido a esto, cuando se utiliza este método, no se requiere la colocación de ninguna rondana, excepto cuando se usan tornillos A490 en aceros con esfuerzo de fluencia inferior a -- 2800 kg/cm<sup>2</sup>, caso en que se necesita una rondana, cualquiera que sea el método de apriete.

Con objeto de garantizar el buen comportamiento de cone

xiones apretadas con este método se ha estudiado el efecto de una serie de variables que intervienen en su ejecución. Se ha estudiado, por ejemplo, el efecto de girar la tuerca en -- pequeños incrementos en vez de en forma continua, el efecto de la longitud del agarre y la posición relativa de tuerca y rosca. Se ha investigado, así mismo, la posibilidad del -- reuso del tornillo colocados con este método.

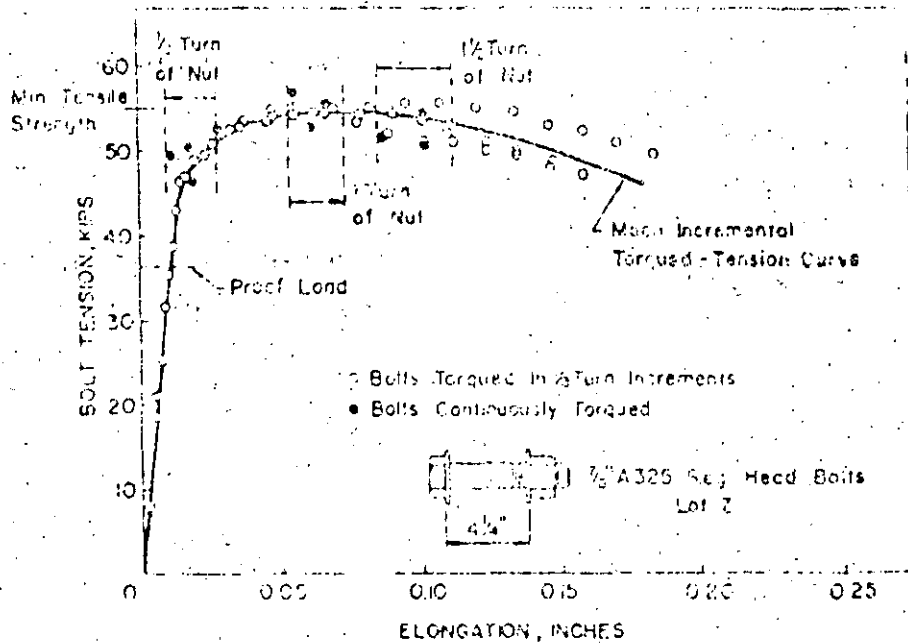


FIG. 2. COMPARISON OF CONTINUOUSLY AND INCREMENTALLY TORQUED BOLTS



5-196 • Specification for Structural Joints

Table 4. Nut Rotation<sup>a</sup> from Snug Tight Condition

Disposition of Outer Faces of Bolted Parts		
Both faces normal to bolt axis, or one face normal to axis and other face sloped not more than 1:20 (bevel washer not used)		Both faces sloped not more than 1:20 from normal to bolt axis (bevel washers not used)
Bolt length <sup>b</sup> not exceeding 8 diameters or 8 inches	Bolt length <sup>b</sup> exceeding 8 diameters or 8 inches	For all length of bolts
½ turn	¾ turn	¾ turn

<sup>a</sup> Nut rotation is rotation relative to bolt regardless of the element (nut or bolt) being turned. Tolerance on rotation: 30° over or under.  
For coarse thread heavy hex structural bolts of all sizes and length and heavy hex semi-finished nuts.

<sup>b</sup> Bolt length is measured from underside of head to extreme end of point.

Una recomendación práctica para lograr un buen apriete general de la junta consiste en iniciarlo en los tornillos - localizados en la parte más rígida de la unión y avanzar - - hacia los extremos libres. Durante el apriete la parte que no se gira, cabeza o tuerca se sostendrá con la llave.

OTROS TOPICOS RELATIVOS A TORNILLOS DE ALTA RESISTENCIA

AGUJEROS.-

Durante bastante tiempo sólo se aceptaron agujeros exactamente 1/16" mayores que el diámetro del tornillo, sin embargo, la necesidad de facilitar las condiciones de montaje de las estructuras atornilladas indujo a que se realizaran una extensa serie de pruebas para demostrar la posibilidad de utilizar agujeros con diámetros algo mayores sin detrimento de la resistencia.

El resultado de esas investigaciones ha conducido a que se acepten agujeros mayores aunque en este caso se requiere colocar una rondana en el lado exterior de la junta.

En juntas de aplastamiento sólo se permiten agujeros ovalados, el lado alargado normal a la dirección de los esfuerzos.

Table 7 Oversize and Slotted Holes

Nominal Bolt Size, Inches	Maximum Hole Size (Nominal), Inches		
	Oversize Holes	Short Slotted Holes	Long Slotted Holes
3/16	1/8	1/16 x 3/16	1/16 x 1/16
1/4	1/16	1/16 x 1/2	1/16 x 1/8
5/16	1/16	1/16 x 1/4	1/16 x 2 1/16
3/8	1/8	1/16 x 1/16	1/16 x 2 1/2
1/2	1/16	1/16 x 1/2	1/16 x 2 1/16
5/8	1/16	1/16 x 1/2	1/16 x 3/16
3/4	1/16	1/16 x 1/2	1/16 x 3/16
1	1/16	1/16 x 1/2	1/16 x 3/4

DETERMINACION DE LA LONGITUD DE LOS TORNILLOS

Debe añadirse al agarre (espesor de todo el material -- conectado) ciertas distancias especificadas con objeto de -- garantizar la colocación correcta de los tornillos teniendo en cuenta las tolerancias de fabricación. Estas distancias estan dadas en la tabla 6.

Adicionalmente, por cada rondana plana se debe considerar una longitud adicional de 5/32" y por cada una tipo cuña 5/16". La longitud así obtenida se cierra al cuarto de pulgada superior más próximo.

Por lo que se refiere a la ejecución de los agujeros las normas recomiendan que cuando el espesor del material no es mayor que el diámetro del tornillo más 1/8" se pueden punzonar, en caso contrario deben ser taladrados o subpunzonados y rimados.

Table 6

Normal Bolt Size, inches	The Distance Between the End of the Thread and the End of the Bolt
1/8	1/16
3/8	3/16
1/4	1
5/8	1 1/8
1	1 1/2
1 1/8	1 7/8
1 1/4	2
1 3/8	2 1/8
1 1/2	2 1/2

GALVANIZADO

Otro avance importante respecto a criterios anteriores -- lo marca el hecho de que se permita ahora galvanizarlos tor-

nillos A325; tras una amplia serie de pruebas que han demostrado un comportamiento adecuado aún teniendo en cuenta posibles efectos de fatiga.

No ha ocurrido lo mismo con los tornillos A490 cuyo galvanizado no se permite.

En juntas de fricción, se permite también el galvanizado de la estructura siempre que se trate la zona de la conexión con cepillo de alambre o chorro de arena para garantizar la fricción adecuada. Debe cuidarse por supuesto, no dañar el galvanizado.

REFERENCIAS

1. Specification for the Design, Fabrication and Erection of Structural steel for Buildings, AISC, 1978
2. Specifications for structural joints using ASTM A325 or A490 bolts, AISC, 1978
3. Standard Specifications for high-strength bolts, ASTM 1971
4. Structural Steel Design, Tall, 1974
5. Diseño de Estructuras de Acero, Bresler, 1978
6. Steel Design for Structural Engineers, Bogdan O. Kujhanovic, Nicholas Willems, 1977
7. Calibration of A325 Bolts, John L. Rumpf: John W. Fisher, ASCE, 1963
8. Bolted Connectios with vaned holes diameters; Shoukry, ASCE, 1970.



**DIVISION DE EDUCACION CONTINUA  
FACULTAD DE INGENIERIA U.N.A.M.**

DISEÑO DE ESTRUCTURAS DE ACERO

MÉTODOS DE DISEÑO

ING. OSCAR DE BUEN L.

NOV. 1984

EL DISEÑO ESTRUCTURAL ES UN ARTE EN EL QUE SE UTILIZAN LA EXPERIENCIA OBTENIDA EN CONSTRUCCIONES ANTERIORES, REALIZADAS CON O SIN ÉXITO, LAS LEYES DE LA FÍSICA Y LAS MATEMÁTICAS Y LOS RESULTADOS DE INVESTIGACIONES DE LABORATORIO, PARA OBTENER LA GEOMETRÍA Y LAS DIMENSIONES DE ESTRUCTURAS QUE SE COMPORTEM DE UNA MANERA SEGURA Y EFICIENTE, QUE SEAN ECONÓMICAS EN CONSTRUCCIÓN Y MANTENIMIENTO Y QUE SEAN ESTÉTICAMENTE AGRADABLES.

EN ESTE CURSO NOS REFERIREMOS A UNO SOLO DE LOS MUCHOS ASPECTOS DEL PROCESO DE DISEÑO, EL ESTUDIO DEL COMPORTAMIENTO BAJO CARGA DE ESTRUCTURAS RETICULARES DE ACERO Y DE LOS ELEMENTOS QUE LAS COMPONEN, PARA DETERMINAR SI ESTÁ SUFICIENTEMENTE CERCA DEL COMPORTAMIENTO DESEADO.

EL DISEÑO DE UNA ESTRUCTURA SIGUE UN PROCESO ITERATIVO:

1. SE SUPONEN LAS DIMENSIONES DE LAS SECCIONES TRANSVERSALES DE LOS MIEMBROS, PARA LO QUE SE UTILIZA LA EXPERIENCIA DE DISEÑOS ANTERIORES O LA INFORMACIÓN OBTENIDA CON MÉTODOS APROXIMADOS DE ANÁLISIS Y DISEÑO.

2. SE DETERMINAN LOS EFECTOS OCASIONADOS POR LAS SOLICITACIONES EN UNA ESTRUCTURA CON LAS CARACTERÍSTICAS ESCOGIDAS EN 1.

3. SE REVISIA EL COMPORTAMIENTO DE LOS MIEMBROS Y CONEXIONES SUPUESTOS, ASÍ COMO EL DE LA ESTRUCTURA COMPLETA, SOMETIDOS A LOS EFECTOS CALCULADOS EN 2. SI EL COMPORTAMIENTO ES SATISFACTORIO, EL PROBLEMA HA SIDO RESUELTO; EN CASO CONTRARIO SE REPITE EL CICLO, PARTIENDO DE UN CONJUNTO MODIFICADO DE DIMENSIONES.

PARA CONOCER ADECUADAMENTE EL COMPORTAMIENTO DE UN ELEMENTO ESTRUCTURAL DEBE ESTUDIARSE SU RESPUESTA BAJO SOLICITACIONES DE MAGNITUD CRECIENTE, DESDE QUE SE INICIA EL PROCESO DE CARGA HASTA QUE SE LLEGA A LA FALLA. BAJO SOLICITACIONES DE PEQUEÑA INTENSIDAD LA RESPUESTA DE LAS ESTRUCTURAS DE ACERO ES APROXIMADAMENTE ELÁSTICA Y LINEAL, EL ESTUDIO DE SU COMPORTAMIENTO SE BASA EN LA LEY DE HOOKE Y SE REALIZA MEDIANTE LOS MÉTODOS CONVENCIONALES DE ANÁLISIS ELÁSTICO

Y POR MEDIO DE LAS FÓRMULAS DE LA RESISTENCIA DE MATERIALES, APLICADAS EN ESE INTERVALO. SIN EMBARGO, COMO LOS MÉTODOS ELÁSTICOS NO SON VÁLIDOS CUANDO LOS ESFUERZOS SOBREPASAN EL LÍMITE DE PROPORCIONALIDAD DEL MATERIAL, SON INSERVIBLES PARA DESCRIBIR EL COLAPSO CUANDO, COMO SUCEDE CON FRECUENCIA, SE PRESENTA ALCIBIA DE ESE LÍMITE, Y ES NECESARIO EMPLEAR OTROS PROCEDIMIENTOS DE ANÁLISIS Y DISEÑO.

EL CONCEPTO DE SEGURIDAD. EL INGENIERO CIVIL EN GENERAL, Y EL ESTRUCTURISTA EN PARTICULAR, SE HA PREOCUPADO SIEMPRE POR LA SEGURIDAD DE LAS ESTRUCTURAS QUE CREA.

EN UN PRINCIPIO EL CONCEPTO DE SEGURIDAD ESTABA INCLUIDO IMPLÍCITAMENTE EN LA EXPERIENCIA E INTUICIÓN DEL DISEÑADOR, SIN QUE EXISTIESE NINGUNA DEFINICIÓN EXPLÍCITA. EL ESTUDIO DE LAS ESTRUCTURAS CONSTRUIDAS CON ÉXITO Y DE LAS NUMEROSAS FALLAS QUE HUBO EN ESA ETAPA FUE LLEVANDO A UNA MEJOR COMPRENSIÓN DEL COMPORTAMIENTO ESTRUCTURAL, QUE SE TRADUJO EN UNA SEGURIDAD CADA VEZ MAYOR EN PROYECTOS SUBSECUENT

AL INCORPORARSE LA TEORÍA DE LA ELASTICIDAD EN EL DISEÑO EL CONCEPTO DE SEGURIDAD EMPEZO A SER EXPRESADO DE UNA MANERA FORMAL EN EL LLAMADO COEFICIENTE DE SEGURIDAD Y EN LOS ESFUERZOS PERMISIBLES ASOCIADOS CON ÉL. EN ESTE PERÍODO, UN CONOCIMIENTO LIMITADO DE LAS PROPIEDADES DE LOS MATERIALES SE ASOCIÓ CON UNA MEJORA SUPUESTA EN LA COMPRENSIÓN DEL COMPORTAMIENTO DE LAS ESTRUCTURAS. APARENTEMENTE, DE ACUERDO CON LOS RESULTADOS OBTENIDOS EL MÉTODO SEGUIDO PROPORCIONA UNA SEGURIDAD SATISFACTORIA, PERO TIENE LA GRAVE LIMITACIÓN DE QUE NO PERMITE CONOCER EL GRADO DE SEGURIDAD REAL, CONTRA LA FALLA, DE LAS ESTRUCTURAS QUE SE OBTIENEN AL APLICARLO.

EN LA ACTUALIDAD EL DIMENSIONAMIENTO DE LAS ESTRUCTURAS DE METAL SE SIGUE BASANDO, EN LA MAYORÍA DE LOS CASOS, EN EL CONCEPTO TRADICIONAL DEL COEFICIENTE DE SEGURIDAD: SE SUPONE QUE UNA CONSTRUCCIÓN TIENE UNA SEGURIDAD ADECUADA RESPECTO A LA FALLA SI LOS ESFUERZOS MÁXIMOS PRODUCIDOS POR LAS CARGAS DE SERVICIO



Y CALCULADOS CON LAS FÓRMULAS DE LA RESISTENCIA DE MATERIALES,<sup>3</sup> EN RÉGIMEN ELÁSTICO, NO SOBREPASAN EN NINGÚN PUNTO EL ESFUERZO ADMISIBLE  $\sigma_a = \sigma_y / C_s$  (ó  $\sigma_a = \sigma_u / C_s$ , SI LA FALLA SE PRODUCE POR INESTABILIDAD), DONDE  $\sigma_y$  ES EL ESFUERZO DE FLUENCIA DEL ACERO Y  $C_s$ , QUE ES SIEMPRE MAYOR QUE UNO, EL COEFICIENTE DE SEGURIDAD ESCOGIDO PARA LA SOLICITACIÓN QUE SE ESTÉ CONSIDERANDO.

LA NOCIÓN DEL COEFICIENTE DE SEGURIDAD ESTÁ BASADA EN LAS DOS HIPÓTESIS IMPLÍCITAS SIGUIENTES:

1. LA DISTRIBUCIÓN DE ESFUERZOS EN LA ESTRUCTURA EN EL INSTANTE DEL COLAPSO ES SEMEJANTE A LA EXISTENTE EN EL INTERVALO ELÁSTICO; ES DECIR, SE SUPONE QUE LAS RELACIONES ENTRE LAS MAGNITUDES DE LOS ESFUERZOS EN LOS DIVERSOS PUNTOS DE LA ESTRUCTURA SE MANTIENEN FIJAS DURANTE TODO EL PROCESO DE CARGA, HASTA LLEGAR AL COLAPSO.

2. LA FALLA DE LA ESTRUCTURA ES PRODUCCADA POR UN INCREMENTO PROPORCIONAL DE TODAS LAS SOLICITACIONES.

LA PRIMERA HIPÓTESIS ES CON FRECUENCIA FALSA PORQUE IGNORA LA REDISTRIBUCIÓN DE ESFUERZOS, OCASIONADA POR LA PLASTIFICACIÓN DEL MATERIAL, QUE SUELE PRECEDER A LA FALLA, Y LA SEGUNDA NO ES REALISTA PORQUE MIENTRAS LAS CARGAS MUERTAS SE PUEDEN CONSIDERAR FIJAS A TRAVÉS DEL TIEMPO LAS VIVAS Y LAS ACCIDENTALES VARIAN EN POSICIÓN Y MAGNITUD DENTRO DE LÍMITES MUY SEPARADOS.

SE OBTIENE UN CONCEPTO DE SEGURIDAD ALGO DISTINTO DEL TRADICIONAL UTILIZANDO FACTORES DE CARGA Y LA RESISTENCIA ÚLTIMA DE MIEMBROS Y ESTRUCTURAS (EL FACTOR DE CARGA SE DEFINE COMO EL COCIENTE DE LA CARGA DE COLAPSO DIVIDIDA ENTRE LA DE TRABAJO) PERO, AUNQUE REPRESENTA UNA MEJORA IMPORTANTE SOBRE EL TRATAMIENTO ORIGINAL, TAMPOCO ESTE PROCEDIMIENTO PERMITE RESOLVER EL PROBLEMA CENTRAL DE DEFINIR Y EXPRESAR EL CONCEPTO DE SEGURIDAD DE UNA MANERA RACIONAL.

LA ECUACIÓN BÁSICA DE ESTE MÉTODO ES  $\lambda P_T \leq P_u$ , DONDE  $P_T$  Y  $P_u$  SON LA CARGA DE TRABAJO Y LA MÁXIMA QUE RESISTE LA ESTRUCTURA

Y  $\lambda$  ES EL FACTOR DE CARGA, SIEMPRE MAYOR QUE LA UNIDAD.

4

PARA RESOLVER EL PROBLEMA DE LA SEGURIDAD ESTRUCTURAL DEBE TENERSE EN CUENTA QUE LAS CARGAS QUE OBRAN SOBRE LAS ESTRUCTURAS, LAS PROPIEDADES MECÁNICAS Y GEOMÉTRICAS DE LOS MATERIALES UTILIZADOS EN ELLAS Y LA CALIDAD DE LA MANO DE OBRERA SON CANTIDADES VARIABLES; ADEMÁS, DEBE RECORDARSE QUE LA IMPORTANCIA DE LOS ERRORES INTRODUCIDOS POR LAS SUPOSICIONES Y LA FALTA DE EXACTITUD DE LOS MÉTODOS DE ANÁLISIS Y DISEÑO ES SIEMPRE INCERTEZA, EN MAYOR O MENOR GRADO.

COMO UN RESULTADO DE ESTOS FENÓMENOS SE CONCLUYE QUE EL DISEÑO ESTRUCTURAL DEBE BASARSE, NECESARIAMENTE, EN UN CONCEPTO DE SEGURIDAD QUE INCLUYA LA PROBABILIDAD DE FALLA. ESTO HA SIDO EXPRESADO POR FREUDENTHAL AL AFIRMAR QUE "LA DIFERENCIA ENTRE UN DISEÑO SEGURO Y OTRO INSEGURO ESTÁ EN EL GRADO DE RIESGO CONSIDERADO ACEPTABLE, NO EN LA FALSA ILUSIÓN DE QUE ESE RIESGO PUEDE SER ELIMINADO POR COMPLETO.\*"

SIN EMBARGO, LOS FENÓMENOS MENCIONADOS ANTERIOR, AUNQUE VARIABLES, NO SON NECESARIAMENTE ALEATORIOS,\*\* DE MANERA QUE EN LA ACTUALIDAD NO ES POSIBLE TRATAR LA SEGURIDAD DE LAS ESTRUCTURAS DE UNA MANERA COMPLETAMENTE PROBABILÍSTICA; ESTA SITUACIÓN SEGUIRÁ PREVALECIENDO CUANDO MENOS EN EL FUTURO INMEDIATO.

PUEDE AFIRMARSE QUE EL OBJETIVO DEL DISEÑO ESTRUCTURAL ES OBTENER ESTRUCTURAS QUE TENGAN UNA PROBABILIDAD ACEPTABLE, QUE DEBE SER UNIFORME PARA TODAS LAS CONSTRUCCIONES DE UN MISMO TIPO, DE NO VOLVERSE INSERVIBLES DURANTE CIERTO PERÍODO ESPECIFICADO DE TIEMPO, LLAMADO VIDA ÚTIL DE LA ESTRUCTURA, TENIENDO EN CUENTA AL MISMO TIEMPO LA ESTÉTICA Y LA ECONOMÍA DE LA CONSTRUCCIÓN, RELACIONADA CON SU COSTO TOTAL, QUE INCLUYE COSTOS DE DISEÑO, CONSTRUCCIÓN, MANTENIMIENTO Y REPARACIÓN.

CON LOS CONOCIMIENTOS ACTUALES ES DIFÍCIL, SI NO IMPOSIBLE,

(\*), (\*\*), VER EL REVERSO

\* LA INCERTIDUMBRE APARECE EN LOS PROBLEMAS DE INGENIERIA POR LAS VARIACIONES PROPIAS DE LOS FENOMENOS NATURALES, LA FALTA DE COMPRESION DE TODAS LAS CAUSAS Y EFECTOS EN LOS SISTEMAS FISICOS Y LA FALTA DE DATOS SUFICIENTES.

COMO UN RESULTADO DE ESA INCERTIDUMBRE, EL INGENIERO NO PUEDE NUNCA PREDECIR EL FUTURO CON EXACTITUD, SINO DEBE CONSIDERAR LA POSIBILIDAD DE QUE OCURRAN EVENTOS PARTICULARES Y DETERMINAR LA PROBABILIDAD DE SU OCURRENCIA.

\*\* UNA VARIABLE ALEATORIA ES UNA VARIABLE NUMERICA CUYO VALOR ESPECIFICO NO PUEDE PREDECIRSE CON CERTEZA ANTES DE UN EXPERIMENTO.

DETERMINAR QUÉ CONSTITUYE UN RIESGO<sup>6</sup> ACEPTABLE, EN TÉRMINOS DE PROBABILIDADES, Y TAMPOCO ES FÁCIL FIJAR LAS VIDAS ÚTILES DE ESTRUCTURAS DE DIVERSOS TIPOS; ADEMÁS, HAY FENÓMENOS NO ALEATORIOS QUE INFLUYEN EN EL PROCESO DE DISEÑO Y QUE NO PUEDEN INCLUIRSE EN UN ENFOQUE PROBABILÍSTICO, Y ES MUY DIFÍCIL OBTENER LA INFORMACIÓN RELEVANTE DE LOS FENÓMENOS ALEATORIOS; POR ÚLTIMO, NO ES FÁCIL INCLUIR CONCEPTOS PROBABILÍSTICOS DE UNA MANERA SUFICIENTEMENTE SENCILLA PARA SER UTILIZADOS EN DISEÑOS RUTINARIOS.

POR EJEMPLO, NO SE CUENTA TODAVÍA CON INFORMACIÓN COMPLETA SOBRE FENÓMENOS TAN FUNDAMENTALES COMO SON LA VARIACIÓN DEL ESFUERZO DE FLUENCIA DEL ACERO, LA DE LAS CARGAS VIVAS Y LA DE LAS PROPIEDADES GEOMÉTRICAS DE LOS PERFILES ESTRUCTURALES, Y HAY OTROS TIPOS DE INFORMACIÓN, COMO LA RELATIVA A LAS INCERTIDUMBRES PRODUCIDAS POR LAS IDEALIZACIONES ANALÍTICAS, LAS IMPERFECCIONES EN LA CONSTRUCCIÓN, O LOS ESFUERZOS INTRODUCIDOS DURANTE LA FABRICACIÓN O POR HUNDIMIENTOS DIFERENCIALES IMPREVISIBLES DE LOS APOYOS, QUE NO SE CONOCERÁN NUNCA POR COMPLETO.

ACEPTANDO LA IMPOSIBILIDAD ACTUAL DE UTILIZAR MÉTODOS QUE SEAN COMPLETAMENTE PROBABILÍSTICOS, PERO CON LA INTENCIÓN DE MEJORAR LA METODOLOGÍA DEL DISEÑO Y DE OBTENER ESTRUCTURAS CON UNA CONFIABILIDAD MÁS UNIFORME, SE HAN BUSCADO PROCEDIMIENTOS QUE CONSERVANDO LAS FORMAS TRADICIONALES PERMITAN INCORPORAR EN EL DISEÑO CONSIDERACIONES ESTADÍSTICAS RELATIVAS A LAS CARGAS, RESISTENCIAS, PROPIEDADES GEOMÉTRICAS, ETC, UTILIZANDO LA TEORÍA DE PROBABILIDADES COMO LA HERRAMIENTA PARA MANEJAR ESA INFORMACIÓN.

MÉTODOS DE ANÁLISIS Y DISEÑO. LAS ESTRUCTURAS SE ANALIZAN Y DISEÑAN UTILIZANDO ALGUNO DE LOS CUATRO MÉTODOS SIGUIENTES (EL DISEÑO PUEDE EFECTUARSE TAMBIÉN POR MEDIO DE MODELOS, PERO ESE PROCEDIMIENTO SE SALE DE LOS OBJETIVOS DE ESTE CURSO)

MÉTODO ELÁSTICO (O DE ESFUERZOS PERMISIBLES). ESTE PROCEDIMIENTO, QUE SE HA USADO DESDE PRINCIPIOS DEL

SIGLO XIX, SIGUE SIENDO EL MÁS EMPLEADO EN LA ACTUALIDAD. CONSISTE EN CALCULAR, POR MEDIO DE UN ANÁLISIS ELÁSTICO, LAS ACCIONES INTERNAS QUE PRODUCEN LAS SOLICITACIONES DE SERVICIO (O DE TRABAJO) EN LOS DIVERSOS ELEMENTOS ESTRUCTURALES, Y EN COMPARAR LOS ESFUERZOS OCASIONADOS POR ESAS ACCIONES, DETERMINADOS TAMBIÉN POR MÉTODOS ELÁSTICOS, CON LOS PERMISIBLES O DE TRABAJO, QUE SE OBTIENEN DIVIDIENDO CIERTOS ESFUERZOS CARACTERÍSTICOS (DE FLUENCIA, DE FALLA POR INESTABILIDAD, ETC) ENTRE UN COEFICIENTE DE SEGURIDAD.

ESTE MÉTODO ES ÚTIL PARA PREDECIR EL COMPORTAMIENTO DE LAS ESTRUCTURAS EN CONDICIONES DE SERVICIO, PERO EN MUCHOS CASOS NO PERMITE ESTUDIARLAS EN LAS CERCANÍAS DEL COLAPSO, YA QUE ÉSTE SE PRESENTA CON FRECUENCIA FUERA DEL INTERVALO ELÁSTICO, CUANDO LA LEY DE HOOKE YA NO RIGE LAS RELACIONES ENTRE ESFUERZOS Y DEFORMACIONES. CUANDO ESTO SUCEDE NO PUEDE DETERMINARSE EL COEFICIENTE DE SEGURIDAD REAL DE LA ESTRUCTURA, RESPECTO A LA FALLA.

MÉTODO PLÁSTICO (O DE DISEÑO AL LÍMITE). CUANDO LAS SOLICITACIONES QUE ACTÚAN EN UNA SECCIÓN TRANSVERSAL PRODUCEN LA PLASTIFICACIÓN COMPLETA DEL MATERIAL DE QUE ESTÁ COMPUESTA SE FORMA EN ELLA UNA ARTICULACIÓN PLÁSTICA, CAPAZ DE ADMITIR ROTACIONES IMPORTANTES BAJO MOMENTO CONSTANTE. ESTO OCASIONA UNA REDISTRIBUCIÓN DE MOMENTOS, CUANDO AUMENTA LA CARGA, Y HACE QUE LA FALLA SE PRESENTE CUANDO APARECEN ARTICULACIONES PLÁSTICAS SUFICIENTES PARA QUE LA ESTRUCTURA EN CONJUNTO, O UNA PARTE DE ELLA, SE CONVIERTA EN UN MECANISMO.

AL DISEÑAR UNA ESTRUCTURA PLÁSTICAMENTE, LOS ELEMENTOS QUE LA COMPONEN SE DIMENSIONAN DE MANERA QUE FALLE CUANDO OBRAN SOBRE ELLA LAS SOLICITACIONES DE TRABAJO MULTIPLICADAS POR UN NÚMERO MAYOR QUE LA UNIDAD, AL QUE SE LLAMA FACTOR DE CARGA.

ESTE MÉTODO PERMITE DETERMINAR EL COEFICIENTE DE SEGURIDAD REAL CONTRA EL COLAPSO, PERO NO PROPORCIONA INFORMACIÓN SOBRE EL COMPORTAMIENTO DE LA ESTRUCTURA EN CONDICIONES DE SERVICIO.

8

NO ES APLICABLE CUANDO LA FALLA SE PRESENTA SIN LAS DEFORMACIONES PLÁSTICAS NECESARIAS PARA QUE SE FORME EL MECANISMO DE COLAPSO LO QUE PUEDE SUCEDER, POR EJEMPLO, EN ESTRUCTURAS SOMETIDAS A UN NÚMERO MUY ELEVADO DE CICLOS DE CARGA O CUANDO EL LÍMITE DE UTILIDAD ESTRUCTURAL CORRESPONDE A ALGUNA FORMA DE INESTABILIDAD.

DISEÑO BASADO EN LA RESISTENCIA ÚLTIMA. CUANDO SE EMPLEA ESTE MÉTODO LAS ACCIONES INTERNAS SE DETERMINAN POR MEDIO DE UN ANÁLISIS ELÁSTICO Y LOS ELEMENTOS ESTRUCTURALES SE DIMENSIONAN DE MANERA QUE SU RESISTENCIA SEA IGUAL A ESAS ACCIONES MULTIPLICADAS POR UN FACTOR DE CARGA.

EL NOMBRE DEL MÉTODO ES INCORRECTO PUES EL DISEÑO NO SE BASA EN LA RESISTENCIA ÚLTIMA DE LA ESTRUCTURA, YA QUE EN EL ANÁLISIS NO SE TIENEN EN CUENTA LAS REDISTRIBUCIONES DE EFECTOS INTERNOS QUE SE PRESENTAN DESPUÉS DE QUE TERMINA EL COMPORTAMIENTO ELÁSTICO Y ANTES DE LA FALLA. ADEMÁS, TIENE UNA CONTRADICCIÓN, PUES LA DETERMINACIÓN DE LA RESISTENCIA DE LAS SECCIONES ESTÁ BASADA EN EL COMPORTAMIENTO INELÁSTICO DE LOS MATERIALES PREVIO A LA FALLA MIENTRAS QUE LAS ACCIONES INTERNAS SE CALCULAN CON PROCEDIMIENTOS ELÁSTICOS.

DISEÑO BASADO EN ESTADOS LÍMITE. (O DISEÑO POR MEDIO DE FACTORES DE CARGA Y RESISTENCIA) (EN INGLÉS, "LIMIT STATES DESIGN" O "LOAD AND RESISTANCE FACTOR DESIGN", LRFD). PARA UTILIZAR MÉTODOS PROBABILÍSTICOS DE DISEÑO ESTRUCTURAL DEBE OBTENERSE LA SOLUCIÓN DE LOS PROBLEMAS SIGUIENTES:

1. ESTABLECIMIENTO DE UNA DEFINICIÓN CLARA DE LOS ESTADOS DE LA ESTRUCTURA QUE VAN A SERVIR COMO REFERENCIAS PARA EL DISEÑO, CON RESPECTO A LOS QUE SE DESEA UN CIERTO MARGEN DE SEGURIDAD. ESOS ESTADOS DE REFERENCIA O ESTADOS LÍMITE, QUE SON DIFERENTES PARA DISTINTOS MATERIALES Y TIPOS DE ESTRUCTURAS, DEBEN DEFINIRSE DE UNA MANERA INEQUÍVOCASÍ SE QUIERE TENER UNA EVALUACIÓN CORRECTA DE LOS RESULTADOS DE LOS CÁLCULOS CON RELACIÓN A LA SEGURIDAD DE LA ESTRUCTURA.

2. ANÁLISIS DEL CARÁCTER ALEATORIO DE TODAS LAS MAGNITUDES

QUE INTERVIENEN EN LOS CÁLCULOS, PARA ESTABLECER BASES ESTADÍSTICAS QUE PERMITAN EVALUAR LA PROBABILIDAD DE QUE SE ALCANCE UN CIERTO ESTADO LÍMITE.

3. ESTABLECIMIENTO DE CRITERIOS QUE PERMITAN DEFINIR CUAL DEBE SER LA PROBABILIDAD ADMISIBLE DE QUE SE PRESENTE CADA UNO DE LOS ESTADOS LÍMITE PERTINENTES.

4. DESARROLLO DE UN PROCEDIMIENTO OPERATIVO PRÁCTICO QUE, INTRODUCIENDO COEFICIENTES EN LOS CÁLCULOS, PROPORCIONE SEGURIDAD DE QUE LA PROBABILIDAD DE QUE SE ALCANCE UN ESTADO LÍMITE NO ES MAYOR QUE EL VALOR PERMISIBLE.

(SE DICE QUE SE HA ALCANZADO UN ESTADO LÍMITE, O LÍMITE DE UTILIDAD ESTRUCTURAL, CUANDO LA ESTRUCTURA COMPLETA, O UNA PARTE DE ELLA, DEJA DE CUMPLIR SATISFACTORIAMENTE ALGUNA DE LAS FUNCIONES PARA LAS QUE FUE DISEÑADA Y CONSTRUIDA).

EN VISTA DE LAS DIFICULTADES QUE SE PRESENTAN CUANDO SE TRATA DE RESOLVER EL PROBLEMA EN SUS ASPECTOS ESTADÍSTICOS Y PROBABILÍSTICOS EL ENFOQUE QUE PARECE MÁS CONVENIENTE EN LA PRÁCTICA ES EL DISEÑO BASADO EN ESTADOS LÍMITE (O DISEÑO POR MEDIO DE FACTORES DE CARGA Y RESISTENCIA). ESTE MÉTODO SE BASA EN LOS DOS ASPECTOS SIGUIENTES :

1. HAY "CARGAS" EXTERNAS APLICADAS A LA ESTRUCTURA QUE CORRESPONDEN A CADA UNO DE LOS ESTADOS LÍMITE QUE DEBEN ESTUDIARSE. SI LAS MAGNITUDES DE ESAS CARGAS CRECEN, LA ESTRUCTURA ALCANZARÁ EVENTUALMENTE EL ESTADO LÍMITE CONSIDERADO.

2. PUEDE DEFINIRSE COMO FUNCIÓN DE CARGA  $S$  EL EFECTO PRODUCIDO POR LAS ACCIONES EXTERNAS QUE CORRESPONDE AL ESTADO LÍMITE EN ESTUDIO (PUEDEN SER FUERZAS GENERALIZADAS, DEFORMACIONES O VIBRACIONES, POR EJEMPLO); Y COMO FUNCIÓN DE RESISTENCIA  $R$  LA RESPUESTA DE LA ESTRUCTURA A LA FUNCIÓN DE CARGA.

EN LA ACTUALIDAD EXISTEN VARIAS FORMAS DE DISEÑO BASADAS EN ESTADOS LÍMITE, Y HAY OTRAS EN PROCESO. ESTE MÉTODO DE DISEÑO TIENE LA VENTAJA DE QUE SE PUEDE UTILIZAR CON UN FORMATO SEMEJANTE AL QUE SE EMPLEA EN EL DISEÑO ELÁSTICO CONVENCIONAL.

EL CRITERIO DE DISEÑO SE EXPRESA POR MEDIO DE LA FÓRMULA GENERAL

$$\phi R_n \geq \gamma_A \sum_{i=1}^j \gamma_i S_i \dots 10 \quad (1)$$

EL LADO IZQUIERDO DE LA FÓRMULA CORRESPONDE A LA RESISTENCIA DE LA ESTRUCTURA; ESTÁ FORMADO POR EL PRODUCTO DE LA RESISTENCIA NOMINAL  $R_n$  MULTIPLICADA POR EL FACTOR DE RESISTENCIA  $\phi$ . LA RESISTENCIA NOMINAL ES LA CALCULADA CON UNA FÓRMULA (POR EJEMPLO,  $R_n = M_p = Z \sigma_y$ ), Y ESTÁ BASADA EN LAS PROPIEDADES FÍSICAS Y GEOMÉTRICAS NOMINALES DEL MATERIAL Y DEL ELEMENTO ESTRUCTURAL. EL FACTOR DE RESISTENCIA, QUE ES SIEMPRE MENOR QUE LA UNIDAD, TIENE EN CUENTA LAS INCERTIDUMBRES ASOCIADAS CON LA DETERMINACIÓN DE LA RESISTENCIA.  $R_n$  ES UNA FUERZA GENERALIZADA (MOMENTO FLEXIONANTE, FUERZA AXIAL, FUERZA CORTANTE, ETC) ASOCIADA CON UN ESTADO LÍMITE, Y  $\phi$  ES UN FACTOR SIN DIMENSIONES. EN CIERTOS ESTADOS LÍMITE  $R_n$  SE DEFINE POR MEDIO DE ECUACIONES DE INTERACCIÓN.

EL LADO DERECHO CORRESPONDE A LAS ACCIONES QUE ACTÚAN SOBRE LA ESTRUCTURA.  $\gamma_A$  ES UN FACTOR DE ANÁLISIS, QUE TIENE EN CUENTA LAS INCERTIDUMBRES DEL ANÁLISIS ESTRUCTURAL, QUE MULTIPLICA LA SUMA DE PRODUCTOS  $\gamma_i S_i$ , DONDE  $S_i$  ES EL EFEECTO MEDIO PRODUCIDO POR LA CARGA  $i$  Y  $\gamma_i$  ES EL FACTOR DE CARGA CORRESPONDIENTE, QUE REFLEJA SOBRECARGAS POTENCIALES Y LAS INCERTIDUMBRES INHERENTES A LA DETERMINACIÓN DE LOS EFECTOS DE LAS CARGAS;  $\gamma_A$  Y  $\gamma_i$  SON CANTIDADES SIN DIMENSIONES Y  $S_i$  SON FUERZAS GENERALIZADAS. EL SIGNO  $\Sigma$  INDICA LA COMBINACIÓN DE EFECTOS QUE PROVIENEN DE CAUSAS DIFERENTES, POR EJEMPLO, SI SOLO SE CONSIDERAN LOS EFECTOS PRODUCIDOS POR CARGAS MUERTAS Y VIVAS,

$$\gamma_A \sum_{i=1}^j \gamma_i S_i = \gamma_A (\gamma_M S_{Mm} + \gamma_V S_{Vm})$$

$S_{Mm}$  Y  $S_{Vm}$  SON LOS EFECTOS MEDIOS PRODUCIDOS POR LAS CARGAS MUERTAS Y VIVAS, RESPECTIVAMENTE, Y  $\gamma_M$  Y  $\gamma_V$  SON LOS FACTORES DE CARGA CORRESPONDIENTES.

EN EL DISEÑO BASADO EN ESTADOS LÍMITE SE UTILIZA UNA EXPRESIÓN DEL TIPO DADO POR LA EC. 1 PARA CADA COMBINACIÓN DE CARGAS QUE DEBA CONSIDERARSE.



11

LOS FACTORES DE CARGA  $\gamma$  SUELEN SER MAYORES QUE LA UNIDAD; SON MENORES QUE ELLA CUANDO EL EFECTO DE LA ACCIÓN CORRESPONDIENTE ES FAVORABLE PARA LA ESTABILIDAD DE LA ESTRUCTURA (POR EJEMPLO, LA CARGA VIVA EN PROBLEMAS DE VOLTEO O FLOTACIÓN).

EN EL TÍTULO IV "REQUISITOS DE SEGURIDAD Y SERVICIO PARA LAS ESTRUCTURAS" DEL REGLAMENTO DE LAS CONSTRUCCIONES PARA EL DISTRITO FEDERAL, DE DICIEMBRE DE 1976, SE ESPECIFICA UN MÉTODO DE DISEÑO, BASADO EN ESTADO LÍMITE, SEMEJANTE AL QUE SE ESTÁ DISCUTIENDO AQUÍ. DE ACUERDO CON ÉL, SE UTILIZAN VALORES CARACTERÍSTICOS (O NOMINALES) DE LAS RESISTENCIAS Y DE LAS CARGAS (O ACCIONES), BASADOS EN UNA PROBABILIDAD FIJA DE QUE LOS VALORES REALES SEAN MENORES O MAYORES, SEGÚN EL CASO, QUE LOS ESCOGIDOS, Y SE CUBREN LOS FACTORES DE INCERTIDUMBRE RESTANTES TRANSFORMÁNDOLOS EN VALORES DE DISEÑO POR MEDIO DE COEFICIENTES QUE DEPENDEN DEL TIPO DE FALLA QUE SE DESEE EVITAR, DE LA CLASE DE MATERIAL Y ESTRUCTURA, DE LAS CONSECUENCIAS DE LA FALLA, ETC.

LA RESISTENCIA DE LOS MATERIALES, DETERMINADA POR MEDIO DE ENSAYES ADECUADOS, Y LA DE LOS ELEMENTOS ESTRUCTURALES, OBTENIDA ANALÍTICA O EXPERIMENTALMENTE, SE UTILIZA PARA DEFINIR LA RESISTENCIA NOMINAL  $R_k$ :

$$R_k = R_m - K\bar{S}$$

$R_m$  ES EL VALOR MEDIO DE LOS RESULTADOS DE LOS ENSAYES (O EL CALCULADO ANALÍTICAMENTE),  $\bar{S}$  LA DESVIACIÓN ESTÁNDAR DE ESOS RESULTADOS Y  $K$  UN COEFICIENTE QUE DEPENDE DE LA PROBABILIDAD, ACEPTADA A PRIORI, DE QUE EN LA ESTRUCTURA SE OBTENGAN RESISTENCIAS MENORES QUE  $R_k$  (EL RDF FIJA ESA PROBABILIDAD EN DOS POR CIENTO).

LAS SOLICITACIONES NOMINALES SE DETERMINAN UTILIZANDO UN TRATAMIENTO ANÁLOGO:

$$S_k = S_m + K\bar{S}$$

NOMINALES

EN EL RDF SE ESPECIFICAN LOS VALORES  $\sqrt{\quad}$  DE LAS SOLICITACIONES (O ACCIONES) MÁS COMUNES (CARGAS MUERTAS Y VIVAS, SISMO Y VIENTO) Y SE INDICA QUE EN CASOS NO INCLUIDOS EXPRESAMENTE EN EL REGLAMENTO LA INTENSIDAD NOMINAL SE DETERMINARÁ DE MANERA

QUE LA PROBABILIDAD DE QUE SEA EXCEDIDA EN EL LAPSO DE INTERÉS SEA DE DOS POR CIENTO, EXCEPTO CUANDO EL EFECTO DE LA ACCIÓN SEA FAVORABLE PARA LA ESTABILIDAD DE LA ESTRUCTURA, EN CUYO CASO SE TOMARÁ COMO VALOR NOMINAL AQUEL QUE TENGA UNA PROBABILIDAD DE DOS POR CIENTO DE NO SER EXCEDIDO.

LA RESISTENCIA Y LA SOLICITACIÓN (O ACCIÓN) DE DISEÑO ESTÁN DADAS POR

$$R_D = \phi R_k, \quad S_D = \gamma S_k$$

$\phi$  ES UN COEFICIENTE DE DISMINUCIÓN DE LA RESISTENCIA Y  $\gamma$  UN FACTOR DE CARGA.

PARA LAS DISTINTAS COMBINACIONES DE ACCIONES ESPECIFICADAS EN EL REGLAMENTO, Y ANTE LA APARICIÓN DE CUALQUIER ESTADO LÍMITE DE FALLA, DEBE COMPROBARSE QUE LA RESISTENCIA DE DISEÑO ES MAYOR O IGUAL QUE EL EFECTO DE LAS ACCIONES NOMINALES QUE INTERVIENEN EN LA COMBINACIÓN DE CARGAS EN ESTUDIO, MULTIPLICADO POR EL FACTOR DE CARGA CORRESPONDIENTE.

EL CRITERIO DE DISEÑO ES, PUES,

$$R_D \geq \sum_{i=1}^j S_{Di}, \quad \text{o} \quad \phi R_k = \sum_{i=1}^j \gamma_i S_{ki}$$

SEMEJANTE AL EXPRESADO EN LA EC. 4.

ESTADOS LÍMITE, SE DEFINEN ESTADOS LÍMITE DE DOS TIPOS:

- a) DE RESISTENCIA O DE FALLA
- b) DE SERVICIO

LOS PRIMEROS CORRESPONDEN AL AGOTAMIENTO DEFINITIVO DE LA CAPACIDAD DE CARGA DE LA ESTRUCTURA O DE ALGUNO DE SUS MIEMBROS, ASOCIADO CON UN COLAPSO TOTAL O PARCIAL, O AL HECHO DE QUE LA ESTRUCTURA, SIN AGOTAR SU CAPACIDAD DE CARGA, SUFRA DAÑOS IRREVERSIBLES QUE AFECTEN SU RESISTENCIA ANTE NUEVAS APLICACIONES DE CARGA O EXPERIMENTE DEFORMACIONES INELÁSTICAS DE MAGNITUD INACEPTABLE. LOS SEGUNDOS ESTÁN RELACIONADOS CON

LOS CRITERIOS QUE GOBIERNAN EL USO<sup>13</sup> NORMAL DE LAS CONSTRUCCIONES CON RESPECTO A DEFORMACIONES INACEPTABLES, DESPLAZAMIENTOS, VIBRACIONES ETC, O DAÑOS QUE AFECTEN SU FUNCIONAMIENTO CORRECTO, PERO NO SU CAPACIDAD PARA SOPORTAR CARGAS.

### ESTADOS LIMITE DE SERVICIO.

ESTADOS LIMITE DE DEFORMACIONES. LA IMPORTANCIA DE LAS DEFORMACIONES DE LAS ESTRUCTURAS NO PROVIENE DE ELLAS EN SI, SINO DE SUS CONSECUENCIAS, POR LO QUE PUEDEN CONSIDERARSE CUATRO GRUPOS DE ESTADOS LIMITE:

- a) APARIENCIA
- b) RIESGO DE DAÑOS EN OTRAS PARTES DE LA CONSTRUCCION, O EN EQUIPOS QUE HAYA EN ELLA
- c) SENSACION DE INSEGURIDAD Y FALTA DE COMFORT EN LAS PERSONAS QUE VIVEN O TRABAJAN EN EL EDIFICIO
- d) POSIBLES CAMBIOS EN LAS CARGAS COMO CONSECUENCIA DE LAS DEFORMACIONES (POR EJEMPLO, ACUMULACION DE AGUA DE LUVIA EN UN TECHO HORIZONTAL MUY FLEXIBLE).

DESDE EL PUNTO DE VISTA DEL ASPECTO DE UNA CONSTRUCCION NO ES POSIBLE DAR VALORES GENERALES DE LAS MAGNITUDES PERMISIBLES DE LAS DEFORMACIONES LAS QUE, ADENAS, DEPENDEN DE SU DURACION, YA QUE PUEDEN ACEPTARSE DEFORMACIONES MUCHO MAYORES CUANDO SON DE PEQUEÑA DURACION QUE CUANDO SON PERMANENTES.

ALGO SEHEJANTE SUCEDE CON RESPECTO A LA SENSACION DE INSEGURIDAD O FALTA DE CONFIANZA DE LOS USUARIOS, AUNQUE EN LOS ULTIMOS TIEMPOS SE HAN REALIZADO INVESTIGACIONES SOBRE ESTE PROBLEMA QUE HAN SEÑALADO QUE LOS FACTORES DETERMINANTES NO SON, EN GENERAL, LAS MAGNITUDES DE LAS DEFORMACIONES, SINO LAS CARACTERISTICAS DE LAS VIBRACIONES DEL EDIFICIO, SOBRE TODO LAS ACELERACIONES O CAMBIOS DE ACELERACION.

LAS DEFORMACIONES PERMISIBLES DE LAS ESTRUCTURAS SE RELACIONAN EN LA MAYORIA DE LOS CASOS CON EL RIESGO DE QUE SI SE EXCEDEN SE PRODUCAN DAÑOS EN OTRAS PARTES DEL EDIFICIO, COMO MUROS DE

DELLENDO, CANCELES Y VENTANAS. COMO <sup>14</sup>UNA CONSECUENCIA, LOS VALORES MÁXIMOS PERMISIBLES DEPENDEN DE LOS ELEMENTOS QUE PUEDEN SER DATADOS, Y NO DE LA ESTRUCTURA EN SÍ. NO HAY, POR TANTO, NINGUNA RAZÓN PARA FIJAR UNOS VALORES PARA ESTRUCTURAS DE ACERO Y OTE PARA LAS DE CONCRETO, SINO DEBEN SER INDEPENDIENTES DEL MATERIAL CON EL QUE ESTÉ HECHA LA ESTRUCTURA.

ESTADO LÍMITE DE DURABILIDAD. LA CORROSIÓN CONSTITUYE EL PROBLEMA PRINCIPAL REFERENTE A LA DURABILIDAD DE LAS ESTRUCTURAS DE ACERO. LOS ASPECTOS DEL DISEÑO RELATIVOS A LA DURABILIDAD NO ENCAJAN EN EL MÉTODO DE DISEÑO POR ESTADOS LÍMITE, SI SE LÍMITE A LOS EFECTOS DE LAS CARGAS, O FACTORES SIMILARES. SIN EMBARGO, ES TEÓRICAMENTE POSIBLE EXTENDER LOS PRINCIPIOS DEL MÉTODO PARA QUE INCLUYA ESTE ESTADO LÍMITE, SUSTITUYENDO LAS CARGAS POR CONDICIONES CLIMÁTICAS Y LA RESISTENCIA MECÁNICA POR RESISTENCIA A LA CORROSIÓN.

LA FATIGA PUEDE TRATARSE TAMBIÉN COMO UN ESTADO LÍMITE DE DURABILIDAD, PERO EN GENERAL SE CONSIDERA UNO DE LOS ESTADOS LÍMITE DE RESISTENCIA.

LAS CARACTERÍSTICAS DE LOS ESTADOS LÍMITE DE SERVICIO HACEN QUE EL MÉTODO MÁS APROPIADO PARA INVESTIGARLOS SEA, CASI SIEMPRE, LA TEORÍA DE LA ELASTICIDAD.

ESTADOS LÍMITE DE RESISTENCIA. SE ALCANZA UN ESTADO LÍMITE DE RESISTENCIA CUANDO SE PRESENTA UN COLAPSO TOTAL DE LA ESTRUCTURA O DE UNA PARTE DE ELLA, O CUANDO SUFRE DAÑOS TAN GRANDES QUE TODA O PARTE PUEDE CONSIDERARSE DESTRUÍDA. (EN ESTE ÚLTIMO CASO PUEDE HABER DIFICULTADES PARA DEFINIR EL ESTADO LÍMITE, SEMEJANTES A LAS MENCIONADAS PREVIAMENTE RESPECTO A LOS ESTADOS LÍMITE DE SERVICIO).

SE DISTINGUEN LOS SIGUIENTES ESTADOS LÍMITE DE RESISTENCIA:

ESTADO LÍMITE DE COLAPSO. SE ALCANZA CUANDO LAS RESISTENCIAS MÁXIMAS SE UTILIZAN SIMULTÁNEAMENTE EN UN NÚMERO DE SECCIONES TRANSVERSALES SUFICIENTE PARA QUE LA ESTRUCTURA, O PARTE DE ELLA, SE CONVIERTA EN UN MECANISMO, INCAPAZ DE SATISFACER LAS CONDICIONES DE

EQUILIBRIO SI SE AUMENTAN LAS CARGAS. 15

EN ESTRUCTURAS ISOSTÁTICAS ESTE ESTADO LÍMITE QUEDA DETERMINADO EN GENERAL POR UNA SOLA SECCIÓN, MIENTRAS QUE EN LAS HIPERESTÁTICAS LO DETERMINA EL COMPORTAMIENTO DE VARIAS SECCIONES, LAS NECESARIAS PARA QUE SE FORME EL MECANISMO.

CUANDO LAS RESISTENCIAS MÁXIMAS SE ALCANZAN AL MISMO TIEMPO EN TODAS LAS SECCIONES QUE DEFINEN EL MECANISMO LOS MOMENTOS Y FUERZAS EN LA ESTRUCTURA SE CALCULAN APLICANDO LA TEORÍA DE LA PLASTICIDAD (SUELE HABLARSE ENTONCES DE UN ESTADO LÍMITE DE MECANISMO), PERO HAY CASOS EN QUE LAS CARACTERÍSTICAS DE DEFORMACIÓN DE LA ESTRUCTURA HACEN IMPOSIBLE QUE SE LLEGUE A LA CARGA QUE CORRESPONDE AL MECANISMO DE COLAPSO, Y EL PAUSEO LOCAL DE ALGUNOS PARTES PUEDE TAMBIÉN REDUCIR LA RESISTENCIA MÁXIMA POR DEBAJO DE LA PREVISTA POR EL ANÁLISIS PLÁSTICO.

POR ESTAS RAZONES, SI BIEN EN MUCHOS CASOS SE JUSTIFICA SUPONER UN COMPORTAMIENTO PLÁSTICO COMPLETO Y UTILIZAR EL ANÁLISIS PLÁSTICO PARA DEFINIR ESTE ESTADO LÍMITE, EN OTROS DEBEN EMPLEARSE TEORÍAS PLÁSTICAS MODIFICADAS, O LA TEORÍA ELÁSTICA.

ESTADO LÍMITE DE INESTABILIDAD. LA CAPACIDAD DE CARGA DE UNA ESTRUCTURA, CON RESPECTO A FENÓMENOS DE INESTABILIDAD, DEPENDE BÁSICAMENTE DE LA RIGIDEZ DE LOS ELEMENTOS QUE LA COMPONEN Y DE IMPERFECCIONES EN SU GEOMETRÍA (EXCENTRICIDADES, CURVATURAS INICIALES DE MIEMBROS SUPUESTAMENTE RECTOS, ETC; ESTAS IMPERFECCIONES DEBEN TRATARSE COMO VARIABLES ALEATORIAS, COMO SE HACE CON CARGAS, RESISTENCIA Y DIMENSIONES). EL ESTADO LÍMITE SE ALCANZA CUANDO LA ESTRUCTURA EN CONJUNTO, O UNA PARTE DE ELLA, PIERDE POR CURETO SU RIGIDEZ, LO QUE LLEVA CON FRECUENCIA A UN COLAPSO REPENTINO.

LOS CÁLCULOS PUEDEN HACERSE MEDIANTE LA TEORÍA DE LA ELASTICIDAD O DE LA PLASTICIDAD, CUALQUIERA DE ELLAS DE SEGUNDO ORDEN. (SI SE UTILIZA LA TEORÍA DE LA PLASTICIDAD DE SEGUNDO ORDEN NO HAY DIFERENCIAS FUNDAMENTALES ENTRE LOS ESTADOS LÍMITE DE INESTABILIDAD Y DE COLAPSO).

EN OCASIONES DEBE PRESTARSE CONSIDERACIÓN ESPECIAL A MÉTODOS DE ANÁLISIS Y DISEÑO QUE PERMITAN DETERMINAR EL COMPORTAMIENTO EN EL INTERVALO POSTERIOR A LA INICIACIÓN DEL PAUSEO, SOBRE TODO EN ELEMENTOS DE PAREDES DELGADAS.

ESTADO LÍMITE DE FRACTURA FRÁGIL. LA POSIBILIDAD DE UNA FRACTURA FRÁGIL EN UN ELEMENTO ESTRUCTURAL DEPENDE FUNDAMENTALMENTE DE LAS PROPIEDADES DEL MATERIAL CON QUE ESTÁ HECHO, DE LA FORMA Y CARACTERÍSTICAS DE LOS DETALLES DE LA ESTRUCTURA, DE LA TEMPERATURA Y DE LA VELOCIDAD DE APLICACIÓN DE LAS CARGAS.

LAS CONDICIONES DESFAVORABLES COMO, POR EJEMPLO, UNA TEMPERATURA DE TRABAJO MUY BAJA, PUEDEN COMPENSARSE EN GENERAL UTILIZANDO MATERIALES DE DUCTILIDAD ADECUADA A ESA TEMPERATURA Y DISEÑANDO LOS DETALLES (ENFALMES, CONEXIONES ENTRE MIEMBROS, ETC) DE MANERA QUE NO HAYA HUESCAS QUE PRODUZCAN CONCENTRACIONES DE ESFUERZOS, POR LO QUE LAS FRACTURAS DE TIPO FRÁGIL PUEDEN EVITARSE CASI SIEMPRE EN ESTRUCTURAS DE ACERO. CUANDO SE PRESENTAN, SON INICIADAS CON FRECUENCIA POR ALGÚN TIPO DE ESFUERZO RESIDUAL, QUE PUEDE SER INDEPENDIENTE DE LAS CARGAS Y DE LA RESISTENCIA DEL MATERIAL, POR LO QUE EL DISEÑO REFERENTE AL RIESGO DE FALLA FRÁGIL NO PUEDE HACERSE NORMALMENTE UTILIZANDO LA FILOSOFÍA DE ESTADOS LÍMITE, AUNQUE EN CASOS ESPECIALES LA POSIBILIDAD DE UNA FRACTURA DE ESTE TIPO SÍ ES DETERMINADA POR LA RESISTENCIA DE LA ESTRUCTURA Y SUS CONDICIONES DE CARGA.

ESTADO LÍMITE DE FATIGA. SE DEFINE POR LA AMPLITUD DE LOS ESFUERZOS QUE CAUSA LA RUPTURA DE UNA CONEXIÓN, BARRA O ESTRUCTURA, DESPUÉS DE UN NÚMERO DETERMINADO DE CICLOS DE CARGA. DEBE INVESTIGARSE CON MÉTODOS ELÁSTICOS, PUES LAS FALLAS POR FATIGA SUELEN PRESENTARSE CON DEFORMACIONES PLÁSTICAS CASI NUNCA.

LOS CÁLCULOS RELATIVOS A LOS ESTADOS LÍMITE DE RESISTENCIA SE HACEN, COMO ACABA DE VERSE, UTILIZANDO LA TEORÍA PLÁSTICA O LA ELÁSTICA, DEPENDIENDO DEL COMPORTAMIENTO DE LA ESTRUCTURA RELACIONADO CON CADA ESTADO LÍMITE PARTICULAR.

UNA VEZ DETERMINADOS LOS ESTADOS LÍMITE DE INTERÉS EN UN PROBLEMA DADO EL DISEÑO ESTRUCTURAL CONSISTE EN ASEGURARSE DE QUE HAY UNA PROBABILIDAD SUFICIENTEMENTE PEQUEÑA DE QUE LA RESISTENCIA DE DISEÑO CORRESPONDIENTE A CADA UNO DE ELLOS SEA MENOR QUE LA SOLICITACIÓN DE DISEÑO ASOCIADA A ÉL (O, LO QUE ES LO MISMO, HAY UNA PROBABILIDAD SUFICIENTEMENTE GRANDE DE QUE LA RESISTENCIA

SEA MAYOR QUE LA SOLICITACIÓN); ES DECIR, DEBE SATISFACERSE LA ECUACIÓN (1), QUE SE REPRODUCE AQUÍ:

17

$$\phi R_n \geq \gamma_A \sum_{i=1}^j \gamma_i S_i \quad (1)$$

ESCOGIENDO VALORES CONVENIENTES DE  $\phi$ ,  $\gamma_A$  Y  $\gamma_i$  PUEDE LOGRARSE QUE LA PROBABILIDAD DE FALLA SE MANTENGA DENTRO DE LOS LÍMITES DESEADOS,

POR EJEMPLO, SI UNA VIGA DE SECCIÓN TRANSVERSAL CONSTANTE, EMPOTRADA EN LOS DOS EXTREMOS Y CON CARGA UNIFORME, TIENE CARACTERÍSTICAS DE DUCTILIDAD ADECUADAS (LO QUE SUPONE QUE EL MATERIAL SEA DÚCTIL, QUE LOS ELEMENTOS PLANOS QUE LA COMPONEN NO TENGAN RELACIONES ANCHO/GROSO EXCESIVAS, Y QUE ESTE PROVISTA DE CONTRAVIENTO), EL ESTADO LÍMITE DE RESISTENCIA SE ALCANZA CUANDO SE FORMA UN MECANISMO DE COLAPSO, CON ARTICULACIONES PLÁSTICAS EN LOS EXTREMOS Y EN EL CENTRO DEL CLARO. ESTO SUCEDE CUANDO LOS MOMENTOS EXTERIOR E INTERIOR EN LAS SECCIONES MENCIONADAS ALCANZAN VALORES NOMINALES IGUALES RESPECTIVAMENTE A  $wL^2/16$  Y  $Z\sigma_y$ , DONDE  $w$  ES LA CARGA DE TRABAJO NOMINAL POR UNIDAD DE LONGITUD,  $L$  EL CLARO DE LA VIGA Y  $Z$  Y  $\sigma_y$  EL MÓDULO DE SECCIÓN PLÁSTICO DE LA SECCIÓN TRANSVERSAL DE LA VIGA Y EL ESFUERZO DE FLUENCIA DEL ACERO, AMBOS NOMINALES.

LA RESISTENCIA DE DISEÑO ES  $\phi R_n = \phi Z\sigma_y$  Y LA ACCIÓN DE DISEÑO,  $\gamma S = \gamma wL^2/16$ .

EL ESTADO LÍMITE DE RESISTENCIA POR FORMACIÓN DEL MECANISMO DE COLAPSO QUEDA DEFINIDO POR

$$\phi Z\sigma_y = \gamma wL^2/16$$

SI SE HACE  $\phi = 1$ , ESTA ECUACIÓN COINCIDE CON LA QUE SE OBTIENE AL APLICAR EL MÉTODO DEL FACTOR DE CARGA,  $Z\sigma_y = (\gamma w)L^2/16$ .

CUANDO  $w$  ESTÁ FORMADA POR CARGAS DE VARIOS TIPOS CONVIENE DESCOMPONER EL FACTOR  $\gamma$ ; POR EJEMPLO,

$$\phi Z\sigma_y = \gamma_m w_m L^2/16 + \gamma_v w_v L^2/16$$

LOS ÍNDICES  $m$  Y  $v$  CORRESPONDEN A CARGA MUERTA Y VIVA.

LA DISCUSIÓN QUE SIGUE ESTÁ BASADA EN EL DISEÑO POR MEDIO DE FACTORES DE CARGA Y RESISTENCIA (LOAD AND RESISTANCE FACTOR DESIGN, LRFD) EN LA FORMA EN QUE APARECERÁ, SEGURAMENTE, EN LA PRÓXIMA VERSIÓN DE LAS ESPECIFICACIONES DEL AISC.

18

### CARGAS Y COMBINACIONES DE CARGAS.

EL LADO DE LA EC. 1 CORRESPONDIENTE A LAS CARGAS (O ACCIONES) INTRODUCE EN EL DISEÑO ESTRUCTURAL ALGUNOS CONCEPTOS NUEVOS.

PRIMERO, TODAS LAS CARGAS SON VALORES MEDIOS, ES DECIR, SE UTILIZAN LOS VALORES MÁS PROBABLES DE LAS CARGAS, EN VEZ DE VALORES EXTREMOS. LOS FACTORES DE CARGA DEL LRFD TIENEN EN CUENTA LA VARIABILIDAD.

SE OBTIENE UNA BUENA ESTIMACIÓN DE LA CARGA MUERTA MEDIA MULTIPLICANDO EL VOLUMEN INICIAL DE MATERIAL POR SU DENSIDAD NOMINAL. SI SE QUIERE, SE PUEDEN TENER EN CUENTA CARGAS MUERTAS FUTURAS.

LAS CARGAS DE LARGA DURACIÓN, COMO LAS MUERTAS, TIENDEN A SER MENOS VARIABLES QUE LAS QUE SE APLICAN DURANTE PERÍODOS CORTOS, COMO LAS DE VIENTO O LAS SÍSMICAS. DE ACUERDO CON ESTO, LAS ACCIONES SE SUBDIVIDEN DE ACUERDO CON SU DURACIÓN Y FRECUENCIA, ASPECTOS QUE GOBIERNAN LA PROBABILIDAD DE QUE SE PRESENTEN EN COMBINACIÓN.

LAS CARGAS VIVAS DEPENDEN DEL DESTINO DEL EDIFICIO. DE ACUERDO CON LA COMBINACIÓN DE ACCIONES PARA LA QUE SE ESTÉ DISEÑANDO, SE UTILIZARÁ EL VALOR MEDIO DE ALGUNA DE LAS TRES INTENSIDADES POSIBLES SIGUIENTES:

INTENSIDAD MEDIA, QUE SE SUMARÁ AL VALOR MEDIO DE LAS ACCIONES PERMANENTES, PARA ESTIMAR EFECTOS A LARGO PLAZO.

INTENSIDAD INSTANTÁNEA (O CARGA VIVA SOSTENIDA), QUE SE EMPLEA PARA COMBINACIONES QUE INCLUYAN ACCIONES PERMANENTES Y ACCIDENTALES.

INTENSIDAD MÁXIMA, QUE SE UTILIZA EN COMBINACIONES QUE INCLUYAN TAN SOLO ACCIONES PERMANENTES.

LA CARGA VIVA INSTANTÁNEA ES LA QUE ESTÁ PRESENTE NORMALMENTE, MIENTRAS QUE LA MÁXIMA CORRESPONDE A LA SUMA DE CARGAS SOSTENIDAS Y EXTRAORDINARIAS, DE INTENSIDAD ELEVADA PERO CORTA DURACIÓN Y APLICACIÓN POCO FRECUENTE (POR EJEMPLO, MUEBLES CONCENTRADOS EN UN



ÁREA PEQUEÑA DURANTE UNA MUDANZA<sup>19</sup> O UNA REDISTRIBUCIÓN DE ESPACIOS).

LCFD PERMITE LA ELECCIÓN DE COMBINACIONES DE CARGAS ESCALAS EN POSIBILIDADES CONSERVADORAS, PERO REALISTAS. POR EJEMPLO, LA PROBABILIDAD DE UN EVENTO QUE COMBINE CARGAS MÁXIMAS DE DOS TIPOS DIFERENTES ES MUY PEQUEÑA, POR LO QUE TENERLO EN CUENTA PUEDE NO SER REALISTA.

COMO LA CARGA MUERTA ESTÁ PRESENTE SIEMPRE, SE COMBINA CON LA CARGA VIVA MÁXIMA, PERO SI HAY UNA TERCERA ACCIÓN SIMULTÁNEA, SE TOMA LA INTENSIDAD INSTANTÁNEA. POR EJEMPLO, SE TENDRÁ EN CUENTA EN EL DISEÑO LA COMBINACIÓN FORMADA POR CARGA MUERTA, VIENTO O SISMO, Y CARGA VIVA INSTANTÁNEA.

ESTUDIOS PROBABILÍSTICOS DE LA CARGA VIVA EN OFICINAS, REALIZADOS EN LOS EUA, HAN LLEVADO A LOS VALORES SIGUIENTES:

VALOR MEDIO DE LA CARGA VIVA INSTANTÁNEA  $\approx 12 \text{ lb/pie}^2 (\approx 60 \text{ kg/m}^2)$ , QUE ES APROXIMADAMENTE LA CUARTA PARTE DE LA CARGA ESPECIFICADA PARA DISEÑO BASADO EN ESFUERZOS PERMISIBLES.

VALOR MEDIO DE LA CARGA VIVA MÁXIMA:

$$15 + 760/\sqrt{A_1} \leq 60 \text{ lb/pie}^2 \quad (72.7 + 1135/\sqrt{A_1} \leq 293 \text{ kg/m}^2)$$

EL ÁREA DE INFLUENCIA  $A_1$  ( $\text{pies}^2, \text{m}^2$ ) SE TOMA IGUAL AL DOBLE DEL ÁREA TRIBUTARIA PARA VIGAS Y A CUATRO VECES ESA ÁREA PARA COLUMNAS.

CONFIABILIDAD ESTRUCTURAL. EL ESTUDIO DE LA CONFIABILIDAD ESTRUCTURAL SE INICIA RECONOCIENDO QUE LAS PRINCIPALES VARIABLES QUE INTERVIENEN EN EL DISEÑO, RESISTENCIA,  $R$ , Y EFECTO DE LAS CARGAS,  $S$ , NO PUEDEN DETERMINARSE CON EXACTITUD. SUS MAGNITUDES SE ENCUENTRAN ARRIBA O ABAJO DE CIERTOS VALORES MEDIOS, Y LA MEDIDA ESTADÍSTICA DE SU VARIACIÓN ES LA DESVIACIÓN ESTANDAR.

62

LOS CRITERIOS GENERALES DE DISEÑO SE ILUSTRAN EN LA FIG. 1, EN LA QUE  $R$  REPRESENTA LA RESISTENCIA DE UN ELEMENTO

ESTRUCTURAL Y  $S$  EL EFECTO DE LA CARGA (FUERZA GENÉRICA CALCULADA DEBIDA A LAS CARGAS MÁXIMAS ESPERADAS DURANTE LA VIDA ÚTIL DE LA ESTRUCTURA).  $S_s$  Y  $R_s$  REPRESENTAN EL EFECTO DE LAS CARGAS DE TRABAJO ESPECIFICADAS Y LA RESISTENCIA ESPECIFICADA MÍNIMA.

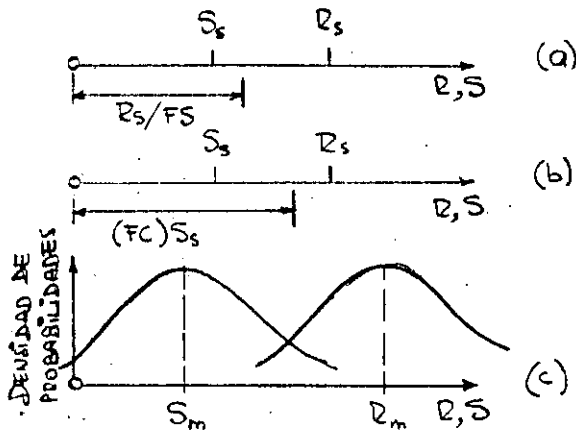


Fig. 1

LA FIG. 1A REPRESENTA EL DEP\* LA RESISTENCIA DIVIDIDA ENTRE  $FS$  DEBE SER MAYOR QUE LA SOLICITACIÓN. 1B CORRESPONDE A DP\*\* LA SOLICITACIÓN MULTIPLICADA POR  $FC$  DEBE SER MENOR QUE LA RESISTENCIA.

TANTO  $FS$  COMO  $FC$  TIENEN EL OBJETO DE PROPORCIONAR UN MARGEN DE SEGURIDAD

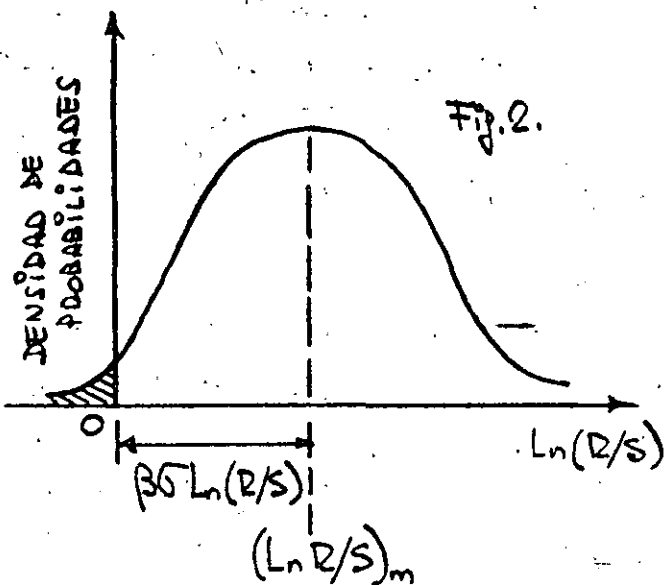
ENTRE  $R_s$  Y  $S_s$ , PARA TENER EN CUENTA LA POSIBILIDAD DE QUE LA CARGA REAL SEA MAYOR QUE LA ESPECIFICADA Y/O QUE LA RESISTENCIA REAL SEA MENOR QUE LA ESPECIFICADA.

DE HECHO, TANTO LOS EFECTOS DE LAS CARGAS COMO LAS RESISTENCIAS TIENEN DISTRIBUCIONES PROBABILÍSTICAS, CARACTERIZADAS POR CURVAS EN FORMA DE CAMPANA (FIG. 1C) CON UN VALOR MEDIO ( $R_m$  O  $S_m$ ) Y UNA DESVIACIÓN ESTÁNDAR.

UN ESTADO LÍMITE SE EXCEDE CUANDO  $R < S$ , LO QUE ES SIEMPRE POSIBLE. LA SEGURIDAD ESTRUCTURAL SE DEFINE COMO LA PROBABILIDAD ACEPTABLEMENTE PEQUEÑA DE QUE  $S$  EXCEDA A  $R$ , Y EL PAPEL REAL DE  $FS$  O  $FC$  ES ASEGURAR QUE ESA PROBABILIDAD ES SUFICIENTEMENTE PEQUEÑA.

\* DEP - DISEÑO POR ESPECIOS PERMISIBLES. \*\* DP - DISEÑO PLÁSTICO

PARA OBTENER UN MARGEN DE SEGURIDAD ADECUADO DESDE UN PUNTO DE VISTA PROBABILÍSTICO SE PROCEDE COMO SIGUE: UNA ESTRUCTURA ES SEGURA (ES DECIR, NO SE VIOLA UN ESTADO LÍMITE) SI  $R - S \geq 0$ , O  $R/S \geq 1$ , O  $\ln(R/S) \geq 0$ . EN LA FIG. 2 SE MUESTRA LA DISTRIBUCIÓN DE  $\ln(R/S)$ ; EL ESTADO LÍMITE SE VIOLA SI  $\ln(R/S)$  ES NEGATIVO, Y LA PROBABILIDAD DE QUE ÉSTO SUCEDA ESTÁ REPRESENTADA POR EL ÁREA SOMBRADA; CUANTO MENOR ES, MÁS CONFIABLE ES EL ELEMENTO ESTRUCTURAL.



EL ÁREA SOMBRADA DISMINUYE CUANDO CRECE LA DISTANCIA DEL VALOR MEDIO DE  $\ln(R/S)$  AL ORIGEN, LA QUE DEPENDE DE DOS FACTORES: EL ANCHO DE LA CUBA DE DISTRIBUCIÓN DE PROBABILIDADES, CARACTERIZADA POR SU DESVIACIÓN ESTÁNDAR  $\sigma \ln(R/S)$  (ES DECIR,

LA DISPERSIÓN DE LOS DATOS) Y UN FACTOR  $\beta$ , LLAMADO ÍNDICE DE SEGURIDAD. PARA UNA DISTRIBUCIÓN  $\ln(R/S)$  DADA, LA PROBABILIDAD DE QUE UN ESTADO LÍMITE SEA EXCEDIDO DISMINUYE CUANDO  $\beta$  AUMENTA.

DESGRACIADAMENTE, LAS DISTRIBUCIONES PROBABILÍSTICAS DE  $R$  Y  $S$  SE CONOCEN SÓLO PARA POCOS CASOS DE CARGAS Y RESISTENCIAS. PERO SI SE CONOCEN LOS VALORES MEDIOS Y LAS DESVIACIONES ESTÁNDAR, OBTENIDOS DEL ANÁLISIS DE DATOS SOBRE CARGAS Y PROPIEDADES DE LOS MATERIALES. PARTIENDO DE ESTE CONOCIMIENTO Y HACIENDO ALGUNAS SIMPLIFICACIONES SE LLEGA A LA FÓRMULA

SIGUIENTE PARA CALCULAR EL INDICE DE SEGURIDAD  $\beta$  :

$$\beta = \frac{\ln(R_m/S_m)}{\sqrt{V_R^2 + V_S^2}} \quad (2)$$

$R_m$  y  $S_m$  SON LOS VALORES MEDIOS DE RESISTENCIA Y SOLICITACIÓN (EFECTO DE LA CARGA) Y  $V_R$  Y  $V_S$  SON LOS COEFICIENTES DE VARIACIÓN CORRESPONDIENTES (DESVIACIÓN ESTANDAR/VALOR MEDIO).

LA ALEATORIEDAD EN LA RESISTENCIA  $R$  DE UN ELEMENTO ESTRUCTURAL PROVIENE DE LA VARIABILIDAD INHERENTE EN LAS PROPIEDADES MECÁNICAS DE LOS MATERIALES, DE LAS VARIACIONES EN DIMENSIONES (TOLERANCIAS) Y DE LAS INCERTIDUMBRES EN LA TEORÍA QUE SIRVE COMO BASE PARA DEFINIR LA RESISTENCIA DEL MIEMBRO.

LA RESISTENCIA  $R$  TOMA CON FRECUENCIA LA FORMA

$$R = R_n M F P \quad (3)$$

DONDE  $R_n$  ES LA RESISTENCIA NOMINAL ESPECIFICADA EN LOS CÓDIGOS Y  $R$ ,  $M$ ,  $F$  Y  $P$  SON VARIABLES ALEATORIAS.  $R_n$  ES UN MOMENTO, FUERZA AXIAL O CORTANTE, ETC, CORRESPONDIENTE AL ESTADO LÍMITE QUE SE ESTÉ INVESTIGANDO Y  $M$ ,  $F$  Y  $P$  SON FACTORES SIN DIMENSIONES

SE SUPONE QUE LAS VARIABLES ALEATORIAS  $M$ ,  $F$  Y  $P$  NO ESTÁN CORRELACIONADAS.

EL COEFICIENTE DE VARIACIÓN DE LA RESISTENCIA,  $V_R$ , ES APROXIMADAMENTE IGUAL A :

$$V_R \approx \sqrt{V_M^2 + V_F^2 + V_P^2} \quad (4)$$

$V_M$ ,  $V_F$  Y  $V_P$  SON LOS COEFICIENTES DE VARIACIÓN DE  $M$ ,  $F$  Y  $P$ .

$M$  REPRESENTA LA VARIACIÓN EN RESISTENCIA O RIGIDEZ DEL MATERIAL; SE OBTIENE, LO MISMO QUE  $V_M$ , DE ENSAYES RUTINARIOS.

$F$  CARACTERIZA LAS INCERTIDUMBRES EN LA FABRICACIÓN. SE

23

INCLUYEN AQUI LAS VARIACIONES EN PROPIEDADES GEOMÉTRICAS PRODUCIDAS POR EL LAMINADO, LAS TOLERANCIAS DE FABRICACIÓN (CORTE, SOLDADURA, ETC), DISTORSIONES INICIALES, TOLERANCIAS DE MONTAJE, ETC, QUE HACEN QUE EL MIEMBRO EN LA ESTRUCTURA MONTADA DIFIERA DEL MIEMBRO IDEAL DISEÑADO.

A LA VARIABLE  $P$  SE LE DA EL NOMBRE DE "FACTOR PROFESIONAL" REFLEJA LA INCERTIDUMBRE QUE PROVIENE DE LAS SUPOSICIONES QUE SE HACEN PARA DETERMINAR LA RESISTENCIA POR MEDIO DE MODELOS ANALÍTICOS, Y QUE RESULTA DE UTILIZAR APROXIMACIONES EN VEZ DE MÉTODOS DE ANÁLISIS Y DISEÑO EXACTOS EN TEORÍA, DE SUPONER QUE EL MATERIAL ES PERFECTAMENTE ELÁSTICO O PERFECTAMENTE PLÁSTICO, ETC. NO HAY EN LA ACTUALIDAD INFORMACIÓN SUFICIENTE PARA EVALUAR LOS PARÁMETROS  $P_m$  Y  $V_p$  EN TODOS LOS CASOS POSIBLES, PERO SÍ SE HAN ESTIMADO EN ALGUNAS SITUACIONES COMPARANDO PREDICCIONES DE DISEÑO CON RESULTADOS EXPERIMENTALES O LOS RESULTADOS DE FÓRMULAS "EXACTAS" Y APROXIMADAS.

SE SUPONE QUE EL EFECTO DE CARGA  $S$  QUE CORRESPONDE A CARGAS MUERTAS Y VIVAS COMBINADAS TIENE LA FORMA (OTRAS COMBINACIONES SE PUEDEN TRATAR DE UNA MANERA SEMEJANTE):

$$S = E (C_M AM + C_V BV) \quad (5)$$

LOS TÉRMINOS EN LA EC. 5 TIENEN LOS SIGNIFICADOS SIGUIENTES:  $M$  Y  $V$ , VARIABLES ALEATORIAS QUE REPRESENTAN LAS INTENSIDADES DE LAS CARGAS MUERTA Y VIVA, RESPECTIVAMENTE;  $C_M$  Y  $C_V$ , COEFICIENTES DE INFLUENCIA DETERMINÍSTICOS QUE TRANSFORMAN LAS INTENSIDADES DE LAS CARGAS EN EFECTOS DE LAS MISMAS (POR EJEMPLO, MOMENTOS Y FUERZAS CORTANTES Y NORMALES);  $A$  Y  $B$ , VARIABLES ALEATORIAS QUE REFLEJAN LAS INCERTIDUMBRES DE LA TRANSFORMACIÓN DE LAS CARGAS EN LOS EFECTOS QUE PRODUCEN;  $E$ , UNA VARIABLE ALEATORIA QUE REPRESENTA LAS INCERTIDUMBRES EN EL ANÁLISIS ESTRUCTURAL. LOS VALORES MEDIOS CORRESPONDIENTES SON  $M_m$ ,  $V_m$ ,  $A_m$ ,  $B_m$  Y  $E_m$ , Y LOS COEFICIENTES DE VARIACIÓN,  $V_M$ ,  $V_V$ ,  $V_A$ ,  $V_B$  Y  $V_E$ .

SE SUPONE QUE LA CARGA MUERTA ES CONSTANTE DURANTE TODA

LA VIDA DE UNA ESTRUCTURA, PERO QUE VARÍA ALGO DE UNA ESTRUCTURA A OTRA EN UNA POBLACIÓN DE ESTRUCTURAS TEÓRICAMENTE IGUALES. LA CARGA VIVA VARÍA ALEATORIAAMENTE DE UNA A OTRA EN UNA CLASE DE ESTRUCTURAS IDENTICAS, Y CAMBIA TAMBIÉN ALEATORIAAMENTE, CON EL TIEMPO, EN UNA ESTRUCTURA PARTICULAR. LAS VARIABLES ALEATORIAS  $M$  Y  $V$  INCLUYEN LAS INCERTIDUMBRES INHERENTES EN LA IDEALIZACIÓN DE LAS CARGAS, AL SUSTITUIRLAS POR CARGAS DE DISEÑO UNIFORMES O CONCENTRADAS.

LA VARIABLE  $E$  INCLUYE LAS INCERTIDUMBRES PRODUCIDAS AL MODELAR UNA ESTRUCTURA REAL, DE TRES DIMENSIONES Y GEOMETRÍA Y COMPORTAMIENTO COMPLEJOS, POR MEDIO DE UN CONJUNTO DE MIEMBROS Y CONEXIONES DE GEOMETRÍA FIJA Y COMPORTAMIENTO ESTIPULADO. TIENE TAMBIÉN EN CUENTA LAS INCERTIDUMBRES DEBIDAS AL USO DE MÉTODOS DE ANÁLISIS SIMPLIFICADOS EN LUGAR DE TEORÍAS COMPLICADAS Y DEFINIDAS (POR EJEMPLO, SUPOSICIÓN DE PUNTOS DE INFLEXIÓN, EMPLEO DE SISTEMAS FORJADOS POR MASAS Y RESORTES EN ANÁLISIS DINÁMICOS, ETC).

EL VALOR MEDIO Y EL COEFICIENTE DE VARIACIÓN DE  $S$  SE OBTIENEN CON LAS ECUACIONES SIGUIENTES, EN LAS QUE SE HA TOMADO  $E_m = 1.0$ :

$$S_m = C_M A_m M_m + C_V B_m V_m \quad (6)$$

$$V_S \cong \sqrt{V_E^2 + \frac{C_M^2 A_m^2 M_m^2 (V_A^2 + V_H^2) + C_V^2 B_m^2 V_m^2 (V_B^2 + V_V^2)}{(C_M A_m M_m + C_V B_m V_m)^2}} \quad (6A)$$

CALIBRACIÓN. EL ÍNDICE DE SEGURIDAD  $\beta$  ES UNA MEDIDA RELATIVA DE LA SEGURIDAD ESTRUCTURAL, QUE DEBE ESPECIFICARSE PARA DESARROLLAR UN CONJUNTO CONSISTENTE DE CRITERIOS DE DISEÑO.

PUEDE DARSELE UN VALOR ACORDADO POR LA PROFESIÓN PARA OBTENER EL GRADO DE CONFIABILIDAD DESEADO, O PUEDE ASIGNARSELE UN VALOR TAL QUE CON EL NUEVO CRITERIO SE OBTENGA EL MISMO GRADO DE CONFIABILIDAD QUE CON LOS MÉTODOS DE DISEÑO EXISTENTES EN VARIOS ELEMENTOS ESTRUCTURALES COMUNES, COMO SON VIGAS LIBREMENTE APOYADAS, COLUMNAS CON CARGA AXIAL, MIEMBROS EN TENSIÓN, PERNO DE ALTA RESISTENCIA, SOLDADURAS DE FILETE, ETC. ESTE SEGUNDO PROCEDIMIENTO, QUE DECIBE EL NOMBRE DE CALIBRACIÓN, TIENE LA VENTAJA DE QUE UTILIZA LA EXPERIENCIA DE MUCHOS AÑOS. CON EL MÉTODO PROBABILÍSTICO DE PRIMER ORDEN PROPUESTO NO SE NECESITA CONOCER LA DISTRIBUCIÓN DE PROBABILIDADES DE R/S, Y SE EVITA LA NECESIDAD DE EXPRESAR LA SEGURIDAD EN TÉRMINOS DE PROBABILIDADES ABSOLUTAS.

EL LRED SE "CALIBRÓ" EN VARIOS CASOS ESTANDAR, EL PROCEDIMIENTO SE ILUSTRÁ AQUÍ TOMANDO COMO BASE UNA VIGA DISEÑADA DE ACUERDO CON LA PARTE 2 DE LAS ESPECIFICACIONES AISC.

UNA VIGA LIBREMENTE APOYADA CON CARGAS MUERTA Y VIVA DISTRIBUIDA UNIFORMEMENTE, COMPACTA Y CON CONTRAVIENTOS LATERAL ADECUADO, REQUIERE UN MÓDULO DE SECCIÓN PLÁSTICO  $Z$  DADO POR

$$Z = \frac{1.7 [C_m M_c + C_v V_c (1 - \rho)]}{\sigma_y} \quad (7)$$

$\sigma_y$  ES EL ESFUERZO DE FLUENCIA MÍNIMO ESPECIFICADO DEL ACERO EMPLEADO,  $C_m$  Y  $C_v$  SON COEFICIENTES DE INFLUENCIA, IGUALES A  $Sl^2/B$ , DONDE  $S$  ES LA SEPARACIÓN ENTRE VIGAS Y  $L$  EL CLARO,  $M_c$  Y  $V_c$  SON LAS CARGAS MUERTA Y VIVA ESPECIFICADAS EN EL CÓDIGO Y  $\rho$  ES LA REDUCCIÓN POR CARGA VIVA, DADA POR

$$\rho = 0 \quad \text{PARA} \quad A_T \leq 150 \text{ ft}^2 \quad (14 \text{ m}^2);$$

26

$\rho = 0.0008 A_T$  PARA  $150 \text{ ft}^2 (14 \text{ m}^2) \leq A_T \leq 750 \text{ ft}^2 (70 \text{ m}^2)$ ;  
 PARA  $A_T > 750 \text{ ft}^2 (70 \text{ m}^2)$ , EL MENOR DE LOS VALORES SIGUIENTES:

$$\rho = 0.60, \text{ ó } \rho = 0.23 \left(1 + \frac{M_c}{V_c}\right) \quad (B)$$

$A_T$  ES EL ÁREA TRIBUTARIA.

SE PUEDE OBTENER UN VALOR DE  $\beta$  ESCOGIENDO UNA SITUACIÓN DE DISEÑO "ESTANDAR" Y OBLIGANDO A QUE EL LRFD PRODUZCA EL MISMO DISEÑO QUE LA ESPECIFICACIÓN AISC (ES DECIR, QUE SE REQUIERA EL MISMO MÓDULO DE SECCIÓN PLÁSTICO  $Z$  CON LOS DOS MÉTODOS). PARA OBTENER UN VALOR REPRESENTATIVO DEL ÍNDICE DE SEGURIDAD LA CALIBRACIÓN NO SE LIMITA A UN SOLO CASO, SINO SE ESTUDIA UN ESPECTRO COMPLETO DE SITUACIONES DE DISEÑO, CARACTERIZADAS POR ÁREAS TRIBUTARIAS Y CARGAS MUERTAS VARIABLES.

EL ÍNDICE DE SEGURIDAD  $\beta$  SE CALCULA CON LA EC. 2 PARA EL VALOR DE  $Z$  QUE SE REQUIERE SEGÚN LA NORMA AISC. PARA ELLO, SE DETERMINAN PRIMERO LAS DIVERSAS CANTIDADES QUE APARECEN EN ESA EC.

LA RESISTENCIA MEDIA  $R_m$  ES IGUAL A

$$R_m = Z_m (\sigma_y)_m \left( \frac{\text{ENSAYE}}{\text{PREDICCIÓN}} \right)_m \quad (9)$$

SE SUPONE QUE EL VALOR MEDIO DEL MÓDULO DE SECCIÓN PLÁSTICO,  $Z_m$ , ES IGUAL A SU VALOR NOMINAL, Y LA CALIBRACIÓN SE LOGRA UTILIZANDO  $Z$  CALCULADO CON LA EC. 7, QUE ES EL VALOR AISC. LA VARIABILIDAD DEL MÓDULO DE SECCIÓN SE TIENE EN CUENTA ESTIMANDO EL COEFICIENTE DE VARIACIÓN DE "FABRICACIÓN"  $V_F$ , QUE SE SUPONE IGUAL A 0.05, LO QUE CORRESPONDE A UN BUEN CONTROL DE TOLERANCIAS.  $(\sigma_y)_m$  ES EL ESFUERZO DE FLUENCIA MEDIO DEL ACERO BAJO CARGA ESTÁTICA, DEL ESTUDIO DEL GRAN NÚMERO



DE ENSAYES DE LABORATORIO CON QUE SE CUENTA SE HA LLEGADO A LOS SIGUIENTES VALORES APROXIMADOS PARA ESE ESFUERZO MEDIO Y SU COEFICIENTE DE VARIACIÓN:  $(\sigma_y)_m = 1.05 \sigma_y$ ,  $V_{\sigma_y} = V_M = 0.10$ .

EL TÉRMINO (ENSAYE/PREDICCIÓN)<sub>m</sub> CORRESPONDE AL FACTOR PROFESIONAL P DE LA EC. 3; SU VALOR SE HA ESTIMADO TOMANDO COMO BASE RESULTADOS EXPERIMENTALES OBTENIDOS CON VIGAS COMPACTAS CONTRAVENTADAS, SOMETIDAS A FLEXIÓN UNIFORME: (ENSAYE/PREDIC.)<sub>m</sub> = 1.02,  $V_p = 0.06$ .

SUSTITUYENDO LOS VALORES MEDIOS ESTIMADOS EN LA EC. 9, Y TOMANDO PARA Z EL VALOR NECESARIO DE ACUERDO CON AISC, EC. 7, SE LLEGA A:

$$R_m = Z_m (\sigma_y)_m \left( \frac{\text{ENSAYE}}{\text{PREDIC.}} \right)_m = Z (1.05 \sigma_y) (1.02) = \frac{1.7 (1.05 \sigma_y) (1.02)}{\sigma_y} [C_u M_c + C_v V_c (1-p)]$$

$$\text{FINALMENTE, } R_m = 1.82 [C_u M_c + C_v V_c (1-p)] \quad (10)$$

EL COEFICIENTE DE VARIACIÓN DE LA RESISTENCIA,  $V_R$ , SE CALCULA CON LA EC. 4:

$$V_R = \sqrt{V_M^2 + V_F^2 + V_p^2} = \sqrt{(0.10)^2 + (0.05)^2 + (0.06)^2} = 0.13$$

PARA CALCULAR  $Q_m$  Y  $V_Q$  SE HAN ESTUDIADO LAS CANTIDADES QUE APARECEN EN LAS ECS. 6 Y 6A Y SE HAN PROPUESTO LOS VALORES SIGUIENTES, QUE REPRESENTAN ESTIMACIONES RAZONABLES DE ACUERDO CON LOS DATOS QUE SE POSEEN Y EL JUICIO DE LAS PERSONAS QUE HAN EFECTUADO LOS ESTUDIOS:  $E_m = 1.0$ ;  $V_E = 0.05$ ;  $A_m = 1.0$ ;  $V_A = 0.04$ ;  $B_m = 1.0$ ;  $V_B = 0.20$ ;  $M_m = M_c$ ;  $V_M = 0.04$ .

EL VALOR MEDIO  $V_m$  Y LA DESVIACIÓN ESTÁNDAR  $\sigma_V$  DE LA CARGA VIVA MÁXIMA EN OFICINAS SE CALCULAN CON LAS EXPRESIONES

$$V_m = 15 + 760/\sqrt{A_2} \quad (\text{lb/ft}^2), \quad 73 + 1135/\sqrt{A_2} \quad (\text{kg/m}^2)$$

$$\sigma_V = \sqrt{11.3 + 15000/A_2} \quad (A_2 \text{ en ft}^2), \quad \sqrt{11.3 + 1394/A_2} \quad (A_2 \text{ en m}^2)$$

COMO SE HA MENCIONADO CON ANTERIORIDAD,  $A_I$  ES EL "AREA DE INFLUENCIA", QUE PARA VIGAS DE PISO SE TOMA IGUAL AL DOBLE DEL AREA TRIBUTARIA  $A_T$ .

EL COEFICIENTE DE VARIACION DE LA CARGA VIVA  $V_v = \bar{G}_v / V_m$  SE DETERMINA CON LOS RESULTADOS DE LAS ECUACIONES ANTERIORES.

CONOCIDOS  $R_m$ ,  $S_m$ ,  $V_R$  Y  $V_S$ , EL INDICE DE SEGURIDAD  $\beta$  SE CALCULA CON LA EC. 2.

CONSIDEREMOS EL CASO PARTICULAR CONSISTENTE EN UNA SERIE DE VIGAS, DE 40' DE CLARO Y SEPARADAS 12.5' C.A.C., QUE SOPORTAN UN PISO DE OFICINAS.

$$A_T = 40 \times 12.5 = 500 \text{ FT}^2$$

$$V_m = 15 + 760 / \sqrt{2 \times 500} = 39.0 \text{ LB/FT}^2; \bar{G}_v = \sqrt{11.3 + 15000 / 1000} = 5.13$$

DE ACUERDO CON LAS NORMAS ANSI, EN OFICINAS DEBE CONSIDERARSE UNA CARGA VIVA UNIFORME MINIMA DE 50 LB/FT<sup>2</sup> ∴

$V_c = 50 \text{ LB/FT}^2$  SUPONGASE, ADEMAS, QUE LA CARGA MUERTA NOMINAL  $M_c$  ES DE 100 LB/FT<sup>2</sup>, O SEA  $M_c = M_m = 100 \text{ LB/FT}^2$ .

$R_m$  SE CALCULA CON LA EC. 10; COMO  $A_T = 500 \text{ FT}^2$  ESTÁ COMPRENDIDA ENTRE 150 Y 750 FT<sup>2</sup>,  $\rho = 0.0008 A_T = 0.4$ .  $C_H = C_V = 5L^2 / B = 12.5 \times 40^2 / B = 2500 \text{ FT}^3$ .

SUSTITUYENDO VALORES, SE LLEGA A 8

$$R_m = 1.82 [2500 \times 100 + 2500 \times 50 (1 - 0.4)] = 591500 \text{ LB.FT.}$$

$V_R$  YA SE HA CALCULADO; VALE 0.13.

$S_m$  Y  $V_S$  SE DETERMINAN CON LAS ECS. 6 Y 6A.

$$S_m = C_H A_m M_m + C_V B_m V_m = 2500 \times 1.0 \times 100 + 2500 \times 1.0 \times 39 = 347500 \text{ LB.FT}$$

$$V_S = \sqrt{(0.05)^2 + \frac{(2500)^2 (1.0)^2 (100)^2 (0.04^2 + 0.04^2) + (2500)^2 (1.0)^2 (39.0)^2 (0.20^2 + 0.13^2)}{(2500 \times 1.0 \times 100 + 2500 \times 1.0 \times 39)^2}} = 0.09$$

FINALMENTE, DE LA EC. 2: 29

$$\beta = \frac{\ln(R_m/S_m)}{\sqrt{V_R^2 + V_S^2}} = \frac{\ln(591500/347500)}{\sqrt{(0.13)^2 + (0.09)^2}} = 3.36$$

OBSÉRVESE QUE EN UN PROBLEMA DADO  $\beta$  PUEDE EXPRESARSE EN FUNCIÓN DE SOLO DOS VARIABLES, LA CARGA MUERTA ESPECIFICADA  $M_c$  Y EL ÁREA TRIBUTARIA  $A_T$ . (ES INDEPENDIENTE DE  $C_v$  Y  $C_m$ , QUE SE ANULAN AL DIVIDIR  $R_m$  ENTRE  $S_m$ , ASÍ COMO AL CALCULAR  $V_s$ ).

EN LA FIG. 3 SE MUESTRA CÓMO VARIA  $\beta$  EN FUNCIÓN DEL ÁREA TRIBUTARIA, PARA DOS VALORES DE  $M_c$ .  $\beta = 3.36$ , CALCULADO ARRIBA, CORRESPONDE A LA CURVA SUPERIOR.

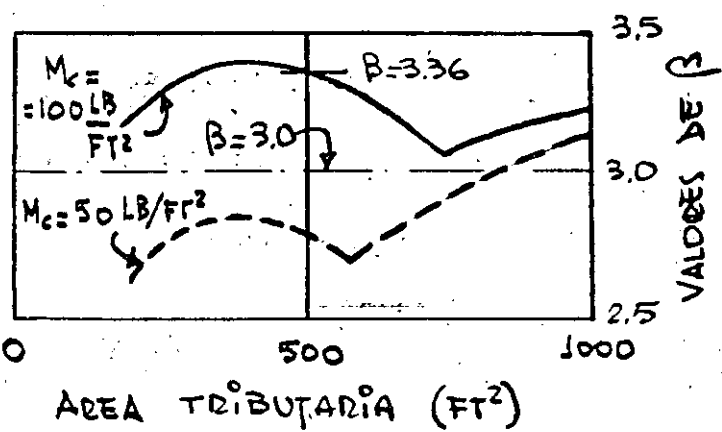


FIG. 3

SE LLEGÓ A LA CONCLUSIÓN DE QUE  $\beta = 3.0$  ES UN VALOR REPRESENTATIVO DEL ÍNDICE DE SEGURIDAD IMPLÍCITO EN LAS VIGAS LIBREMENTE APOYADAS DISEÑADAS DE ACUERDO CON LA PARTE 2 DE LAS NORMAS AISC

DE 1978. UTILIZANDO LA PARTE 1 SE OBTUVIERON RESULTADOS SEMEJANTES.

SE HAN EFECTUADO TAMBIÉN CALIBRACIONES CON COLUMNAS CARGADAS AXIALMENTE, PERNOS DE ALTA RESISTENCIA Y SOLDADURAS DE FILETE. COMO UN RESULTADO DE ESTOS TRABAJOS SE HA PROPUESTO QUE SE TOME  $\beta = 3.0$  Y  $4.5$ , RESPECTIVAMENTE, PARA MIEMBROS Y ELEMENTOS DE CONEXIÓN, COMO BASE PARA

OBTENER LOS FACTORES DE CARGA Y RESISTENCIA. EL VALOR MÁS ALTO DE  $\beta$  PARA COLECTORES REFLEJA EL HECHO DE QUE LAS CONEXIONES SE HAN DISEÑADO TRADICIONALMENTE CON MAYOR RESISTENCIA QUE LOS MIEMBROS QUE UNEN.

LOS VALORES ESCOGIDOS PARA  $\beta$  REPRESENTAN LA RELACIÓN ENTRE EL CÓDIGO ACTUAL Y EL PROPUESTO. AL SER CONSTANTES, PROPORCIONAN UNA CONFIABILIDAD MÁS UNIFORME QUE LA QUE SE OBTIENE CON LAS NORMAS DE DISEÑO EN VIGOR.

FACTORES DE CARGA Y RESISTENCIA. DE ACUERDO CON LRFD, LA CONDICIÓN QUE DEBE SATISFACERSE EN EL DISEÑO DE UN MIEMBRO BAJO CARGAS MUERTAS Y VIVAS COMBINADAS ES:

$$\phi R_n \geq \gamma_E (\gamma_M C_M M_m + \gamma_V C_V V_m) \quad (11)$$

LOS FACTORES  $\phi$  Y  $\gamma$  SE DETERMINAN CON LAS EXPRESIONES 12 A 15, EN LAS QUE SE INTRODUCEN EL ÍNDICE DE SEGURIDAD  $\beta$  ESPECIFICADO Y LOS DATOS ESTADÍSTICOS APROPIADOS:

$$\phi = \frac{R_m}{R_n} e^{-\alpha\beta V_R} \quad (12) \quad \gamma_E = e^{\alpha\beta V_E} \quad (13)$$

$$\gamma_M = 1 + \alpha\beta \sqrt{V_A^2 + V_M^2} \quad (14) \quad \gamma_V = 1 + \alpha\beta \sqrt{V_B^2 + V_V^2} \quad (15)$$

$\alpha$  ES UN FACTOR DE SEPARACIÓN DE VARIABLES IGUAL A 0.55. CON LOS VALORES MEDIOS Y DE LOS COEFICIENTES DE VARIACIÓN QUE SE ACABAN DE PRESENTAR, Y TOMANDO  $\beta = 3.0$ , SE OBTIENE  $R_m/R_n = 1.07$ ,  $\phi = 0.86$ ,  $\gamma_E = 1.09$ ,  $\gamma_M = 1.09$ ,  $\gamma_V = 1.39$ .

REDONDEANDO ALGUNOS FACTORES, EL CRITERIO DEL LRFD PARA EL DISEÑO PLÁSTICO DE UNA VIGA DE ACERO LIBREMENTE APOYADA Y CON CARGA UNIFORME ES

$$0.86 Z \sigma_y \geq 1.1 (1.1 C_m M_m + 1.4 C_v V_m) \quad (16)$$

$C_m = C_v = S L^2 / 8$ ,  $M_m = M_c$  (CARGA MUERTA ESPECIFICADA EN EL CÓDIGO)

Y  $V_m$  SE CALCULA CON LA EC. DE LA PÁG. 18.

LOS RESULTADOS DE LA EC. 16 CONCUERDAN RAZONABLEMENTE CON LOS QUE SE OBTIENEN AL APLICAR LA PARTE 2 DE LAS NORMAS AISC. EL LRFD REQUIERE EN GENERAL MÓDULOS PLÁSTICOS DE 0 A 10% MENORES PARA LA MAYOR PARTE DE LAS ÁREAS TRIANGULARES E INTENSIDADES DE CARGA QUE SE HAN ESTUDIADO; SÓLO CUANDO ÁREAS Y CARGAS MUERTAS SON PEQUEÑAS REQUIERE MÓDULOS PLÁSTICOS HASTA 10% MAYORES QUE LOS NECESARIOS SEGÚN LAS NORMAS EN VIGOR.

FACTORES DE CARGA Y RESISTENCIA PARA DIFERENTES ELEMENTOS ESTRUCTURALES. EL CÁLCULO DEL FACTOR DE RESISTENCIA PARA UN ELEMENTO ESTRUCTURAL DADO SE HACE COMO SIGUE:

1. SE ESCOGE UNA FÓRMULA O ALGORITMO QUE PROPORCIONE LA RESISTENCIA NOMINAL DEL ELEMENTO.

2. SE CALCULA EL VALOR MEDIO Y EL COEFICIENTE DE VARIACIÓN DE LA RESISTENCIA DEL ELEMENTO UTILIZANDO LA RELACIÓN DEL PASO 1 Y LA INFORMACIÓN CON QUE SE CUENTE SOBRE LAS PROPIEDADES MECÁNICAS DEL MATERIAL Y EL COMPORTAMIENTO EXPERIMENTAL DEL ELEMENTO.

3. SE CALCULA EL FACTOR DE RESISTENCIA  $\phi = \frac{R_m}{R_n} e^{-\alpha \beta V^2}$ .

4. EN LA MAYOR PARTE DE LOS CASOS LA RESISTENCIA DE UN ELEMENTO ESTRUCTURAL SE EXPRESA EN FUNCIÓN DE UNA VARIABLE CARACTERÍSTICA (POR EJEMPLO, LA RELACIÓN DE ESBELTEZ EN COLUMNAS). EL FACTOR DE RESISTENCIA  $\phi$  PUEDE DEPENDER TAMBIÉN DE ESA VARIABLE.

SE HA EFECTUADO UN ESFUERZO CONSIDERABLE PARA DETERMINAR EL VALOR DEL TÉRMINO  $\phi R_n$  CORRESPONDIENTE A LOS DISTINTOS ELEMENTOS ESTRUCTURALES QUE SE INCLUYEN EN UNAS NORMAS PARA DISEÑO DE ESTRUCTURAS DE ACERO: MIEMBROS EN TENSIÓN Y EN COMPRESIÓN, VIGAS Y TRABES ARMADAS (INCLUYENDO LOS ESTADOS LÍMITE DE MOMENTO PLÁSTICO, PANDEO LATERAL O LOCAL Y CORTANTE), BARRAS FLEXOCOMPRESIDAS Y VARIOS TIPOS DE CONEXIONES Y CONECTORES. A CONTINUACIÓN SE PRESENTAN ALGUNOS EJEMPLOS DE LOS RESULTADOS.

### MIEMBROS EN TENSIÓN (EXCEPTUANDO LAS BARRAS DE OJO).

ESTADO LÍMITE DE FLUJO PLÁSTICO:

$$R_n = A_n \sigma_y ; \phi = 0.88 \quad (17)$$

ESTADO LÍMITE DE FRACTURA:

$$R_n = A_n \sigma_u ; \phi = 0.74 \quad (18)$$

$A_n$  ES EL ÁREA NETA Y  $\sigma_y$  Y  $\sigma_u$  SON LOS ESFUERZOS MÍNIMOS ESPECIFICADOS DE FLUENCIA Y FRACTURA EN TENSIÓN.

### COLUMNAS EN COMPRESIÓN AXIAL.

$$R_n = A_T \sigma_{cr} \quad (19)$$

$$\left. \begin{aligned} \phi &= 0.86 \text{ PARA } \lambda \leq 0.16 \quad (KL/r \leq 0.11 C_c) \\ \phi &= 0.90 - 0.25 \lambda \text{ PARA } 0.16 \leq \lambda \leq 1.0 \quad (0.11 C_c \leq KL/r \leq 0.71 C_c) \\ \phi &= 0.65 \text{ PARA } \lambda \geq 1.0 \quad (KL/r \geq 0.71 C_c) \end{aligned} \right\} (20)$$

$A_T$  ES EL ÁREA TOTAL DE LA SECCIÓN TRANSVERSAL, Y

$$\left. \begin{aligned} \sigma_{cr} &= \sigma_y (1 - 0.25 \lambda^2) \text{ PARA } \lambda \leq \sqrt{2} \quad \left( \sigma_{cr} = \sigma_y \left[ 1 - \frac{(KL/r)^2}{2 C_c^2} \right] \text{ PARA } \frac{KL}{r} \leq C_c \right) \\ \sigma_{cr} &= \sigma_y / \lambda^2 \text{ PARA } \lambda \geq \sqrt{2} \quad \left( \sigma_{cr} = \pi^2 E / (KL/r)^2 \text{ PARA } KL/r \geq C_c \right) \end{aligned} \right\} (21)$$

$$\lambda = \frac{KL}{r} \frac{1}{\pi} \sqrt{\frac{\sigma_y}{E}} \quad (22)$$

$KL/r$  Y  $E$  SON LA RELACIÓN DE ESBELTEZ EFECTIVA Y EL M. DE YOUNG.

COMBINACIONES DE CARGAS. LAS CONSIDERACIONES ANTERIORES SE REFIEREN A LOS EFECTOS DE CARGAS MUERTAS Y VIVAS, PERO PUEDEN COMBINARSE OTRAS SOLICITACIONES SIGUIENDO UN RAZONAMIENTO SEMEJANTE. POR EJEMPLO, LOS EFECTOS DEL VIENTO PUEDEN INCLUIRSE EN EL CRITERIO DE DISEÑO SUMÁNDOLOS A LOS DE CARGAS MUERTA Y VIVA:

$$\phi R_n \geq \gamma_E (\gamma_M C_M M_m + \gamma_V C_V V_m + \gamma_W C_W W_m) \quad (23)$$

$\gamma_W$  ES EL FACTOR DE CARGA PARA VIENTO Y  $W_m$  LA CARGA DE VIENTO MEDIA. PUEDE DEMOSTRARSE QUE

$$\gamma_W = 1 + \alpha \beta \sqrt{V_E^2 + V_W^2} \quad (24)$$

$W$  ES UNA VARIABLE ALEATORIA QUE REPRESENTA LA CARGA DE VIENTO ( $W_m$  ES LA INTENSIDAD MEDIA Y  $V_W$  SU COEFICIENTE DE VARIACIÓN) Y  $C_W$  UN FACTOR QUE REFLEJA LAS INCERTIDUMBRES QUE HAY EN EL PROCESO DE CONVERTIR LA INTENSIDAD DEL VIENTO EN EFECTOS DE CARGA.

LOS EFECTOS DE LAS DISTINTAS CARGAS DEBEN COMBINARSE DE MANERA QUE SE OBTENGA UN NIVEL CONSISTENTE DE CONFIABILIDAD. LA MAYOR PARTE DE LOS EFECTOS DE LAS CARGAS SON FUNCIONES ALEATORIAS DEL TIEMPO. UNA POSIBLE COMBINACIÓN ES, COMO YA SE HA VISTO, LA FORMADA POR LA CARGA MUERTA, QUE SE CONSIDERA CONSTANTE CON EL TIEMPO, Y LA CARGA VIVA MÁXIMA DURANTE LA VIDA ÚTIL DE LA ESTRUCTURA. AL INCLUIR LOS EFECTOS DEL VIENTO DEBE TENERSE EN CUENTA QUE ES IMPROBABLE QUE LAS CARGAS MÁXIMAS VIVA Y DE VIENTO SE PRESENTEN SIMULTÁNEAMENTE, MÁS AÚN, ESAS DOS FUNCIONES ALEATORIAS VARIAN CON EL TIEMPO DE MANERA MUY DIFERENTE, LENTAMENTE LA PRIMERA Y EN FORMA RÁPIDA LA SEGUNDA. POR CONSIGUIENTE, ALGUNAS DE LAS COMBINACIONES QUE DEBEN

ESTUDIARSE, Y LOS FACTORES DE CARGA CORRESPONDIENTES, SON:

CARGA MUERTA + CARGA VIVA MÁXIMA

$$\phi R_n \geq 1.1 (1.4 C_M M_m + 1.4 C_v V_m) \quad (25)$$

CARGA MUERTA + CARGA VIVA SOSTENIDA + VIENTO MÁXIMO

$$\phi R_n \geq 1.1 (1.1 C_M M_m + 2.0 C_v V_m + 1.6 C_w W_m) \quad (26)$$

VIENTO MÁXIMO - CARGA MUERTA

$$\phi R_n \geq 1.1 (1.6 C_w W_m - 0.9 C_M M_m) \quad (27)$$

LOS COEFICIENTES DE VARIACIÓN Y LOS ÍNDICES DE SEGURIDAD PUEDEN VARIARSE PARA REFLEJAR CONDICIONES PARTICULARES DEFERENTES A INCERTIDUMBRES EN LAS PROPIEDADES MECÁNICAS DE LOS MATERIALES, CALIDAD DE LA MANO DE OBRA, ETC.

EL VALOR DEL ÍNDICE DE SEGURIDAD PUEDE HACERSE VARIAR TAMBIÉN DE ACUERDO CON LA IMPORTANCIA DE LA ESTRUCTURA Y EL TIPO DE FALLA QUE PUEDA PRESENTARSE; EN ALGUNAS ESTRUCTURAS LA FALLA DE UNO O DE POCOS ELEMENTOS CRÍTICOS OCASIONA LA PÉRDIDA TOTAL, EN CONTRASTE CON LO QUE SUCEDE EN ESTRUCTURAS CONTINUAS DÚCTILES. SE HA PROPUESTO  $\beta = 3.0$  EN EDIFICIOS ORDINARIOS,  $\beta = 4.5$  EN EDIFICIOS MUY IMPORTANTES Y  $\beta = 2.5$  EN ESTRUCTURAS PROVISIONALES.

HASTA AHORA EL CRITERIO DEL LRFD SE HA OBTENIDO POR MEDIO DE CALIBRACIONES EN LAS QUE SE HA CONSIDERADO TAN SOLO LA CONFIABILIDAD DE SECCIONES TRANSVERSALES, PERO SE PUEDE INCORPORAR LA CORRELACIÓN ESTADÍSTICA ENTRE SECCIONES TRANSVERSALES Y ENTRE MIEMBROS Y NODOS DE FALLA, VARIANDO ADECUADAMENTE EL ÍNDICE DE SEGURIDAD  $\beta$ .



CLASIFICACIÓN DE LAS ACCIONES. SE CONSIDERARÁN TRES CATEGORÍAS DE ACCIONES, DE ACUERDO CON EL TIEMPO EN QUE OBRAN SOBRE LA ESTRUCTURA CON SU INTENSIDAD MÁXIMA:

ACCIONES PERMANENTES. SON LAS QUE OBRAN EN FORMA CONTINUA SOBRE LA ESTRUCTURA, Y CUYA INTENSIDAD PUEDE CONSIDERARSE QUE NO VARIA CON EL TIEMPO (CARGAS MUERTAS, EMPUJE ESTÁTICO PERMANENTE DE TIERRAS Y LÍQUIDOS, EFECTOS DEBIDOS A PRESFUERZO O MOVIMIENTOS DIFERENCIALES PERMANENTES DE LOS APOYOS).

ACCIONES VARIABLES. SON LAS QUE OBRAN SOBRE LA ESTRUCTURA CON UNA INTENSIDAD VARIABLE EN EL TIEMPO (CARGAS VIVAS, CAMBIOS DE TEMPERATURA Y CONTRACCIONES, HUNDIMIENTOS DIFERENCIALES QUE VARTEN CON EL TIEMPO, EFECTOS DE MAQUINARIA Y EQUIPO INCLUYENDO, CUANDO SEAN SIGNIFICATIVAS, ACCIONES DINÁMICAS PRODUCIDAS POR VIBRACIONES, IMPACTO Y FRENADO).

SEGÚN LA COMBINACIÓN DE ACCIONES PARA LA QUE SE ESTÉ DISEÑANDO CADA ACCIÓN VARIABLE SE TOMARÁ CON ALGUNA DE LAS INTENSIDADES SIGUIENTES:

INTENSIDAD MEDIA, CUYO VALOR NOMINAL SE SUMARÁ AL DE LAS ACCIONES PERMANENTES PARA ESTIMAR EFECTOS A LARGO PLAZO.

INTENSIDAD INSTANTÁNEA, QUE SE EMPLEARÁ PARA CONDICIONES QUE INCLUYAN ACCIONES PERMANENTES Y ACCIDENTALES.

INTENSIDAD MÁXIMA, PARA COMBINACIONES QUE INCLUYAN SOLO ACCIONES PERMANENTES.

ACCIONES ACCIDENTALES. SON LAS QUE NO SE DEBEN AL FUNCIONAMIENTO PROPIO DE LA CONSTRUCCIÓN Y QUE PUEDEN ALCANZAR VALORES SIGNIFICATIVOS SOLO DURANTE LAPROS BREVES (SISMO, VIENTO, OTRAS (EXPLOSIONES, INCENDIOS)).

COMBINACIONES DE ACCIONES. LA SEGURIDAD DE LAS ESTRUCTURAS, SE VERIFICADA PARA EL EFECTO COMBINADO DE TODAS LAS ACCIONES QUE TENGAN UNA PROBABILIDAD NO DESPRECIABLE DE OCURRIR SIMULTANEAMENTE. SE CONSIDERARÁN DOS CATEGORÍAS DE COMBINACIONES:

1. COMBINACIONES QUE INCLUYAN ACCIONES PERMANENTES Y VARIABLES. SE CONSIDERARÁN TODAS LAS ACCIONES PERMANENTES QUE ACTÚEN SOBRE LA ESTRUCTURA Y LAS DISTINTAS ACCIONES VARIABLES, LA MÁS DESFAVORABLE CON LA INTENSIDAD MÁXIMA Y EL RESTO CON LA INSTANTÁNEA, O TODAS CON LA INTENSIDAD MEDIA CUANDO SE EVALÚEN EFECTOS A LARGO PLAZO. DEBEN REVISARSE TODOS LOS EDOS. LÍMITE POSIBLES, DE FALLA Y DE SERVICIO.

2. COMBINACIONES QUE INCLUYAN ACCIONES PERMANENTES, VARIABLES Y ACCIDENTALES. SE CONSIDERARÁN TODAS LAS ACCIONES PERMANENTES, LAS VARIABLES CON SUS VALORES INSTANTÁNEOS Y UNA SOLA ACCIÓN ACCIDENTAL EN CADA COMBINACIÓN.

EVALUACIÓN DE LA SEGURIDAD. SE REVISARÁ QUE PARA LAS DISTINTAS COMBINACIONES DE ACCIONES ESPECIFICADAS, Y ANTE LA APARICIÓN DE CUALQUIER EDO. LÍMITE DE FALLA QUE PUEDA PRESENTARSE, LA RESISTENCIA DE DISEÑO SEA MAYOR O IGUAL QUE EL EFECTO DE LAS ACCIONES NOMINALES QUE INTERVENGAN EN LA COMBINACIÓN DE CARGAS EN ESTUDIO, MULTIPLICADO POR EL FACTOR DE CARGA CORRESPONDIENTE.

$$F_d R \geq \sum F_c S$$

TAMBIÉN SE REVISARÁ QUE NO SE DEBASE NINGÚN EDO LÍMITE DE SERVICIO.

FACTORES DE CARGA. EL FACTOR DE CARGA  $F_c$  SE DETERMINARÁ COMO SIGUE:

1.  $F_c = 1.4$  PARA COMBINACIONES QUE INCLUYAN SOLO ACCIONES PERMANENTES O VARIABLES, EN ESTRUCTURAS EN LAS QUE HAYA CON

FRECUENCIA ASLOMEACIÓN DE PERSONAS (CENTROS DE REUNIÓN, ESCUELAS, TEATROS, CINES, LOCALES PARA ESPECTÁCULOS DEPORTIVOS, TEMPLOS), Y EN ESTRUCTURAS QUE CONTENGAN EQUIPO MUY VALIOSO U OBRAS DE ARTE, SE TOMARÁ  $F_c = 1.5$ .

2.  $F_c = 1.1$  PARA COMBINACIONES QUE INCLUYAN UNA ACCIÓN ACCIDENTAL, ADEÑÁS DE LAS PERMANENTES Y VARIABLES. (HAY ALGUNAS SALVEDADEZ QUE SE INCLUYEN EN LOS CAPÍTULOS DE DISEÑO POR SISMO Y POR VIENTO).

3.  $F_c = 0.9$  PARA ACCIONES O FUERZAS INTERNAS CUYO EFECTO SEA FAVORABLE A LA RESISTENCIA O ESTABILIDAD DE LA ESTRUCTURA. ADEÑÁS, SE TOMARÁ COMO VALOR NOMINAL DE LA INTENSIDAD DE LA ACCIÓN EL MÍNIMO PROBABLE.

4.  $F_c = 1.0$  PARA LA REVISIÓN DE TODOS LOS EDOS. LÍMITE DE SERVICIO.

EJEMPLOS. CARGAS MUERTA Y VIVA:  $\sum F_c S = 1.4 (C_u + C_v)$  (O  $1.5 (C_u + C_v)$ ).

CARGAS MUERTA Y VIVA, + SISMO O VIENTO:  $\sum F_c S = 1.1 (C_u + C_v + S (O V))$

FACTORES DE RESISTENCIA (PARA ESTRUCTURAS DE ACERO)

TENSIÓN -  $F_R = 0.9$

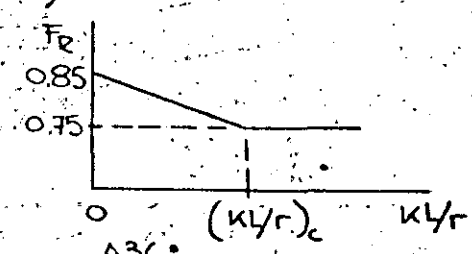
COMPRESIÓN -  $F_R = 0.85$  PARA  $KL/r = 0$ , DECEDE LINEALMENTE HASTA 0.75 CUANDO  $KL/r = (KL/r)_c$ ,

Y CONSERVA ESTE VALOR PARA  $KL/r > (KL/r)_c$

FLEXIÓN -  $F_R = 0.9$  (EL PANDEO LATERAL NO ES CRÍTICO)

$F_R = 0.85$  (EL PANDEO LATERAL ES CRÍTICO)

FLEXOCOMPRESIÓN - SE EMPLEAN FÓRMULAS DE INTERACCIÓN EN LAS QUE SE INCLUYEN LOS FACTORES DE RESISTENCIA PARA COMPRESIÓN Y FLEXIÓN.

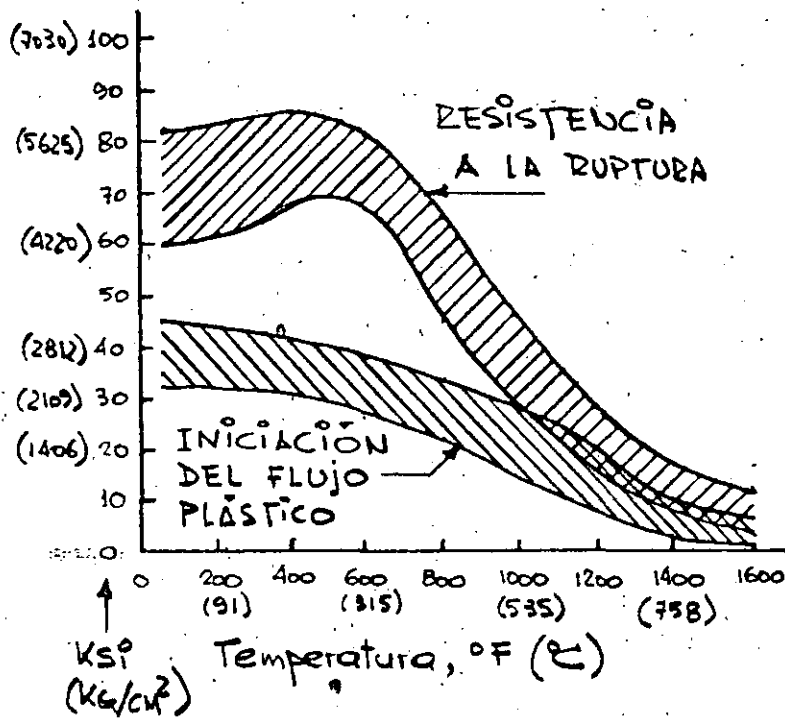


A36:

KL/r	20	40	60	80	100	120	126
$F_R$	.83	.82	.80	.79	.77	.75	0.75

TEMPERATURAS ALTAS. LAS PROPIEDADES FÍSICAS Y QUÍMICAS DE LA MAYOR PARTE DE LOS ACEROS ESTRUCTURALES USUALES SE CONSERVAN SIN CAMBIO SÓLO EN UN INTERVALO DE TEMPERATURAS RELATIVAMENTE PEQUEÑO. ESAS PROPIEDADES Y, POR CONSIGUIENTE, EL COMPORTAMIENTO DEL ACERO, CAMBIAN SUSTANCIALMENTE CUANDO ESTÁ EXPUERTO A TEMPERATURAS ELEVADAS DURANTE UN TIEMPO LARGO LO QUE PUEDE SUCEDER, POR EJEMPLO, DURANTE UN INCENDIO.

EN LA FIG. SE MUESTRAN LOS EFECTOS DE LAS TEMPERATURAS ELEVADAS EN LA RESISTENCIA A LA TENSION Y EN EL ESFUERZO CORRESPONDIENTE



A LA INICIACIÓN DEL FLUJO PLÁSTICO EN EL ACERO A36.

LAS ALTAS TEMPERATURAS QUE SE ALCANZAN DURANTE UN INCENDIO SUELEN SER DE CORTA DURACIÓN, CON FRECUENCIA NO AFECTAN EL COMPORTAMIENTO DE LA ESTRUCTURA. SIN EMBARGO, SUELE SER NECESARIO PROTEGER LAS ESTRUCTURAS DE ACERO CONTRA EL FUEGO, LO QUE SE

LOGRA RECUBRIÉNDOLAS CON MATERIALES AISLANTES DE DIVERSOS TIPOS.

BAJAS TEMPERATURAS Y FALLA FRÁGIL. LA FALLA FRÁGIL, QUE CONSISTE ESENCIALMENTE EN LA RUPTURA SIN DEFORMACIONES PLÁSTICAS PREVIAS, SUELE ESTAR ASOCIADA CON TEMPERATURAS BAJAS. TAMBIÉN INFLUYEN EN ELLA EL ESTADO DE ESFUERZOS A QUE ESTÉ SOMETIDA LA PIEZA, LA EXISTENCIA DE MUESCAS Y LA VELOCIDAD DE APLICACIÓN DE LA CARGA. EN LA FIG. SE INDICA LA INFLUENCIA DE LA TEMPERATURA SOBRE VARIAS PROPIEDADES IMPORTANTES DE UN ACERO.

FRECUENCIA AGLOMERACIÓN DE PERSONAS (CENTROS DE REUNIÓN, ESCUELAS, TEATROS, CINES, LOCALES PARA ESPECTÁCULOS DEPORTIVOS, TEMPLOS), Y EN ESTRUCTURAS QUE CONTENGAN EQUIPO MUY VALIOSO U OBRAS DE ARTE, SE TOUARÁ  $F_c = 1.5$ .

2.  $F_c = 1.1$  PARA COMBINACIONES QUE INCLUYAN UNA ACCIÓN ACCIDENTAL, ADEMÁS DE LAS PERMANENTES Y VARIABLES. (HAY ALGUNAS SALVEDADE QUE SE INCLUYEN EN LOS CAPÍTULOS DE DISEÑO POR SISMO Y POR VIENTO).

3.  $F_c = 0.9$  PARA ACCIONES O FUERZAS INTERNAS CUYO EFECTO SEA FAVORABLE A LA RESISTENCIA O ESTABILIDAD DE LA ESTRUCTURA. ADEMÁS, SE TOUARÁ COMO VALOR NOMINAL DE LA INTENSIDAD DE LA ACCIÓN EL MÍNIMO PROBABLE.

4.  $F_c = 1.0$  PARA LA REVISIÓN DE TODOS LOS EDOS LÍMITE DE SERVICIO.

EJEMPLOS. CARGAS MUERTA Y VIVA:  $\sum F_c S = 1.4 (C_u + C_v)$  (O  $1.5 (C_u + C_v)$ )

CARGAS MUERTA Y VIVA, + SISMO O VIENTO:  $\sum F_c S = 1.1 (C_u + C_v + S (O V))$

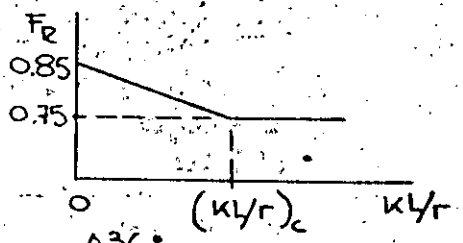
FACTORES DE RESISTENCIA (PARA ESTRUCTURAS DE ACERO)

TENSIÓN -  $F_R = 0.9$

COMPRESIÓN -  $F_R = 0.85$  PARA  $KL/r = 0$ , DECRECE

LÍNEALMENTE HASTA 0.75 CUANDO  $KL/r = (KL/r)_c$ ,

Y CONSERVA ESTE VALOR PARA  $KL/r > (KL/r)_c$



A36:

KL/r	20	40	60	80	100	120	126
$F_R$	.83	.82	.80	.79	.77	.75	.75

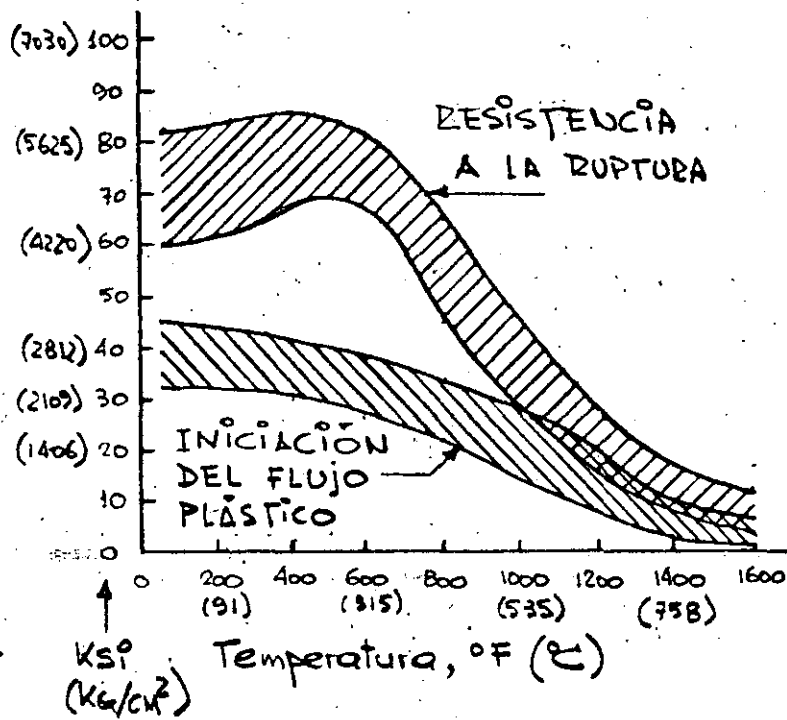
FLEXIÓN -  $F_R = 0.9$  (EL PANDEO LATERAL NO ES CRÍTICO)

$F_R = 0.85$  (EL PANDEO LATERAL ES CRÍTICO)

FLEXOCOMPRESIÓN - SE EMPLEAN FÓRMULAS DE INTERACCIÓN EN LAS QUE SE INCLUYEN LOS FACTORES DE RESISTENCIA PARA COMPRESIÓN Y FLEXIÓN.

TEMPERATURAS ALTAS. LAS PROPIEDADES FÍSICAS Y QUÍMICAS DE LA MAYOR PARTE DE LOS ACEROS ESTRUCTURALES USUALES SE CONSERVAN SIN CAMBIO SÓLO EN UN INTERVALO DE TEMPERATURAS RELATIVAMENTE PEQUEÑO. ESAS PROPIEDADES Y, POR CONSIGUIENTE, EL COMPORTAMIENTO DEL ACERO, CAMBIAN SUSTANCIALMENTE CUANDO ESTÁ EXPOSTO A TEMPERATURAS ELEVADAS DURANTE UN TIEMPO LARGO LO QUE PUEDE SUCEDER, POR EJEMPLO, DURANTE UN INCENDIO.

EN LA FIG. SE MUESTRAN LOS EFECTOS DE LAS TEMPERATURAS ELEVADAS EN LA RESISTENCIA A LA TENSION Y EN EL ESFUERZO CORRESPONDIENTE

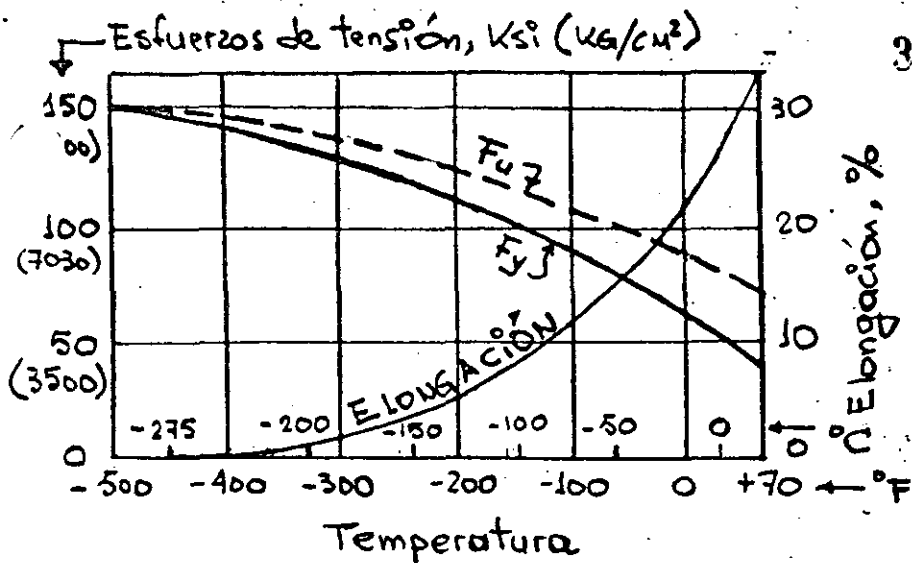


A LA INICIACIÓN DEL FLUJO PLÁSTICO EN EL ACERO A 36.

LAS ALTAS TEMPERATURAS QUE SE ALCANZAN DURANTE UN INCENDIO SUELEN SER DE CORTA DURACIÓN, CON FRECUENCIA NO AFECTAN EL COMPORTAMIENTO DE LA ESTRUCTURA. SIN EMBARGO, SUELE SER NECESARIO PROTEGER LAS ESTRUCTURAS DE ACERO CONTRA EL FUEGO, LO QUE SE

LOGRA DECUBIÉNDOLAS CON MATERIALES AISLANTES DE DIVERSOS TIPOS.

BAJAS TEMPERATURAS Y FALLA FRÁGIL. LA FALLA FRÁGIL, QUE CONSISTE ESENCIALMENTE EN LA RUPTURA SIN DEFORMACIONES PLÁSTICAS PREVIAS, SUELE ESTAR ASOCIADA CON TEMPERATURAS BAJAS. TAMBIÉN INFLUYEN EN ELLA EL ESTADO DE ESFUERZOS A QUE ESTÉ SOMETIDA LA PIERA, LA EXISTENCIA DE MUESCAS Y LA VELOCIDAD DE APLICACIÓN DE LA CARGA. EN LA FIG. SE INDICA LA INFLUENCIA DE LA TEMPERATURA SOBRE VARIAS PROPIEDADES IMPORTANTES DE UN ACERO.



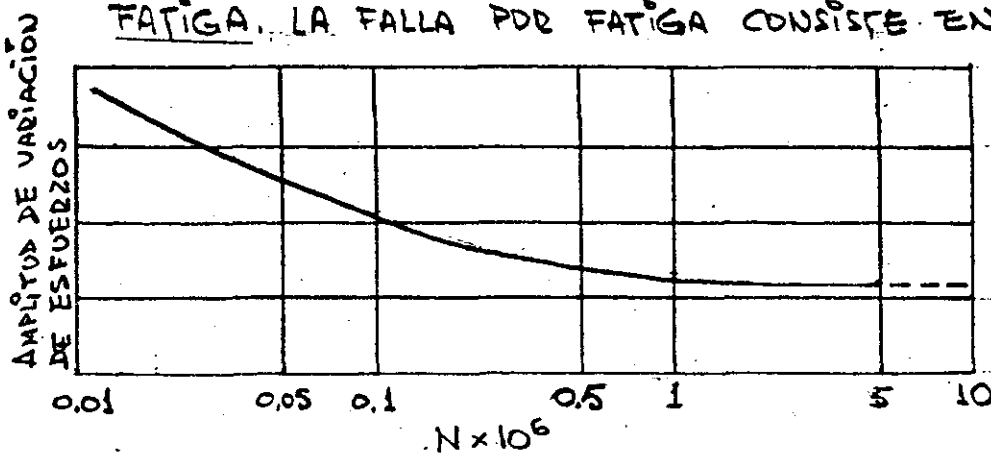
39 LAS FALLAS DE TIPO FRÁGIL SUELEN INICIARSE A TEMPERAT. BAJAS CUANDO, ADEMÁS, SE PRODUCE UN EFECTO DE MUESCA (CAMBIO DE SECCIÓN, DEFECTO), BAJO ESFUERZOS DE TENSIÓN.

PUEBEN EVITARSE DE

ALGUNA DE LAS MANERAS SIGUIENTES (O POR COMBINACIÓN DE VARIAS):

1. DETALLANDO LOS MIEMBROS Y SUS CONEXIONES Y UTILIZANDO PROCESOS DE FABRICACIÓN Y SECUENCIAL DE ARRUADO QUE MINIMICEN LOS ESFUERZOS RESIDUALES DE TENSIÓN.
2. EMPLEANDO ACEROS DE ALIACIÓN DISEÑADOS PARA TRABAJAR A BAJAS TEMPERATURAS.
3. REDUCIENDO LA VELOCIDAD DE APLICACIÓN DE LAS CARGAS.

FATIGA. LA FALLA POR FATIGA CONSISTE EN LA FRACTURA DEL MATERIAL,



BAJO ESF. RELATIVAMENTE REDUCIDOS, DESPUÉS DE UN NÚMERO SUFICIENTEMENTE GRANDE DE APLICACIONES DE LA CARGA, QUE PUEBEN O NO INCLUIR CAMBIOS DE SIGNO EN LOS ESFUERZOS.

LA FRACTURA SE INICIA EN UN LUGAR DONDE HAY UNA PEQUEÑA IMPERFECCIÓN, QUE PUEDE SER DE TAMAÑO

MICROSCÓPICO, Y SE PROPAGA EN FORMA DE UNA GRIETA, QUE SUELE CRECER LENTAMENTE, HASTA QUE LA PIEZA SE ROMPE.

LA CURVA DE LA FIGURA DESCRIBE, DE MANERA CUALITATIVA, EL COMPORTAMIENTO DE LA MAYOR PARTE DE LOS METALES, ENSAYADOS EN LABORATORIO BAJO CARGAS CÍCLICAS O REPETIDAS.

LA AMPLITUD DE VARIACIÓN DE LOS ESF. SE DEFINE  $F_{SR} = F_{MAX} - F_{MIN}$ .



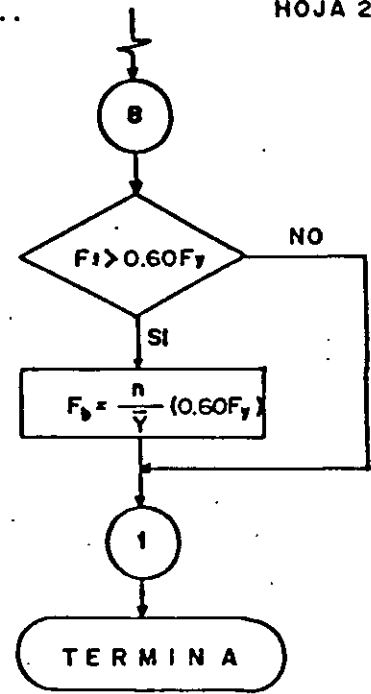
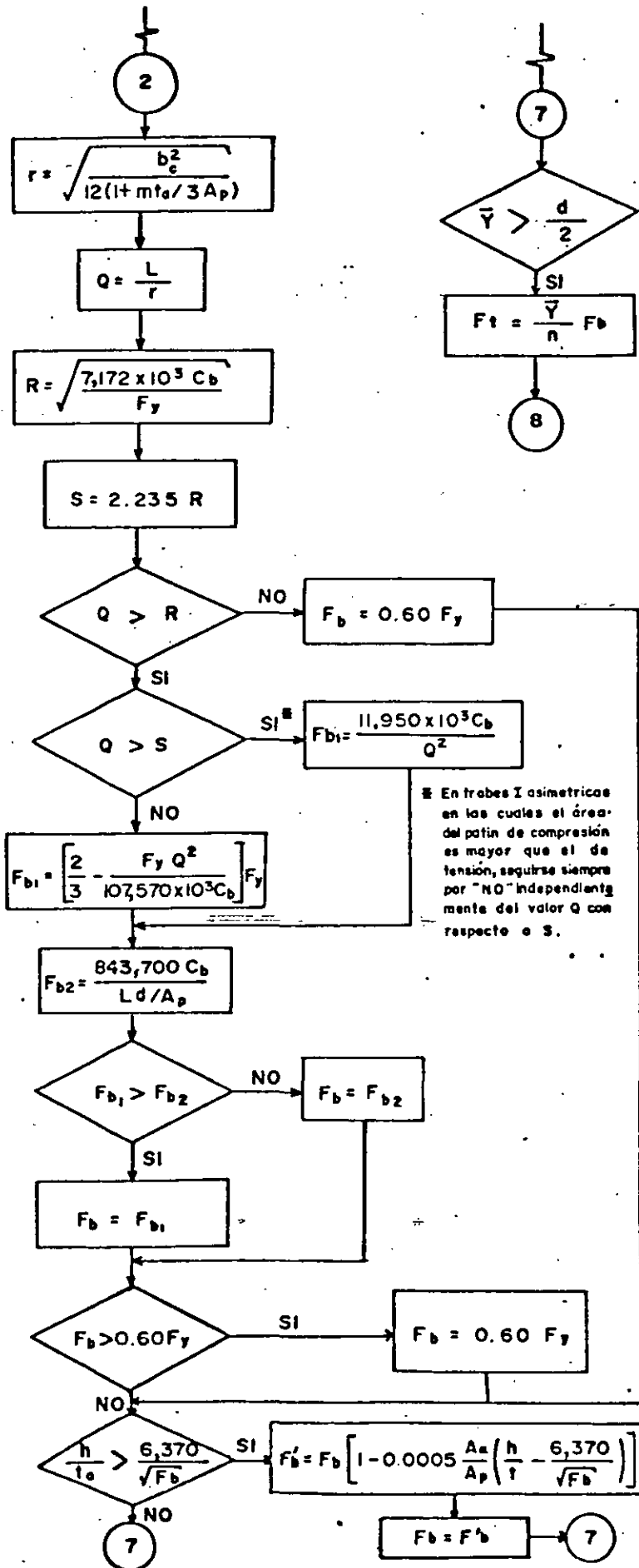
**DIVISION DE EDUCACION CONTINUA  
FACULTAD DE INGENIERIA U.N.A.M.**

DISEÑO DE ESTRUCTURAS DE ACERO

DIAGRAMA DE FLUJO PARA CALCULAR EL ESFUERZO  
PERMISIBLE  $F_b$  POR PANDEO LATERAL EN VIGAS  
COLUMNA

NOV. 1984





NOTAS :

1.- La relación  $h/t$  puede aumentarse hasta  $\frac{16,700}{\sqrt{F_y}}$  siempre y cuando se coloquen atiesadores intermedios espaciados a no más de 1.5h.

2.-  $A_p$  es el área del patín de compresión de la viga-columna, y  $A_a$  el área de su alma.

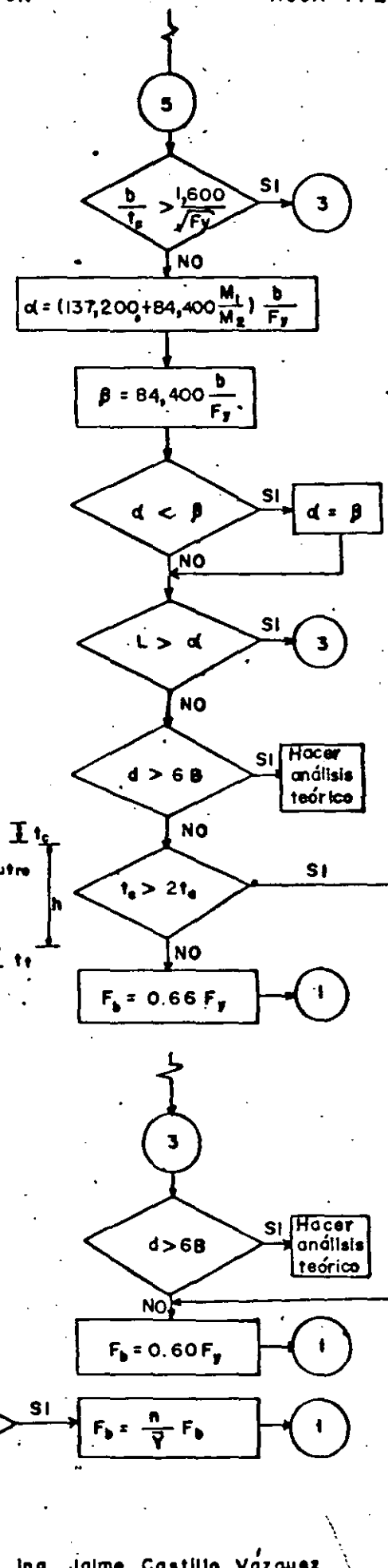
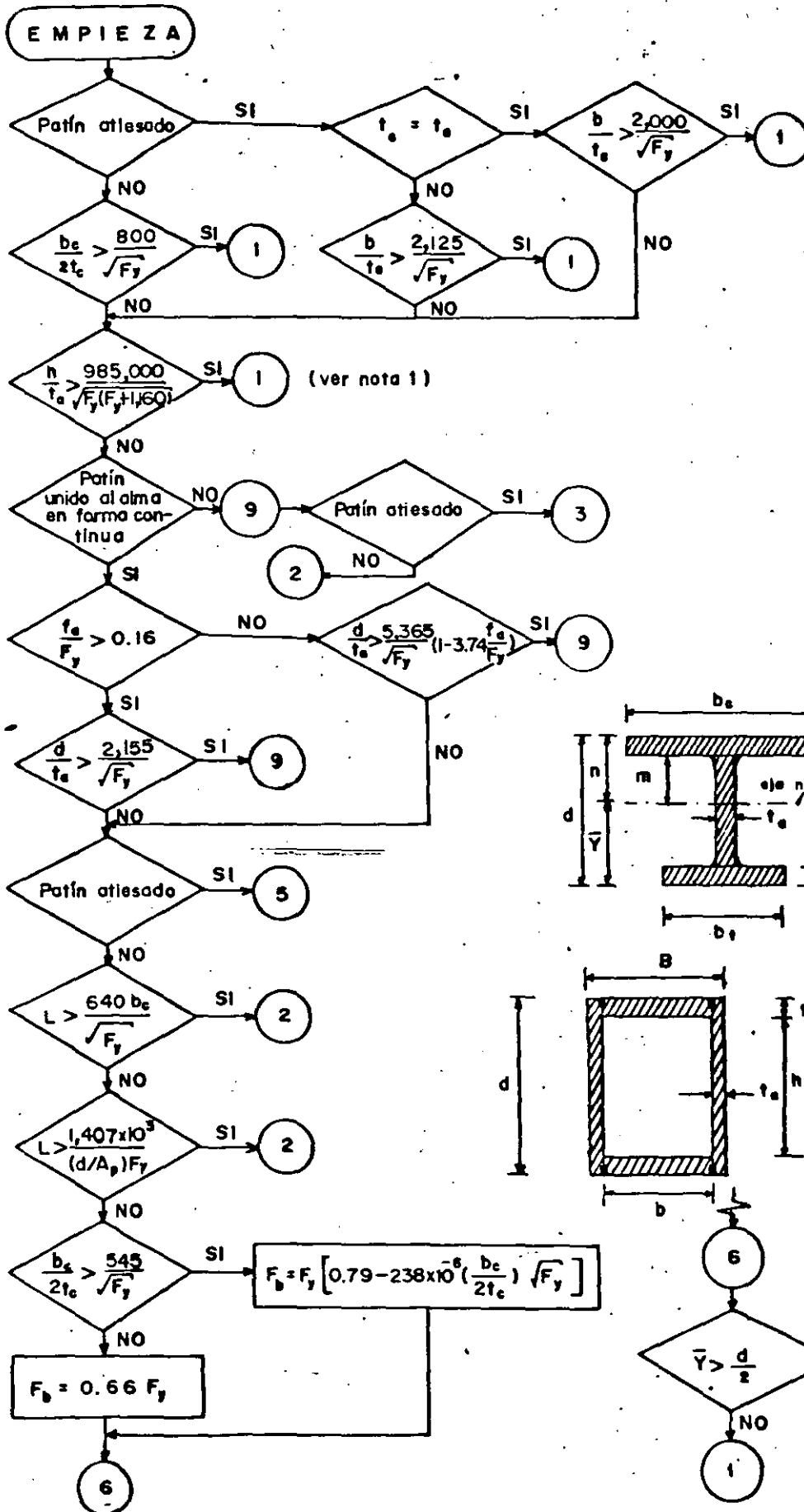
3.- El valor de  $C_b$  esta dado por :

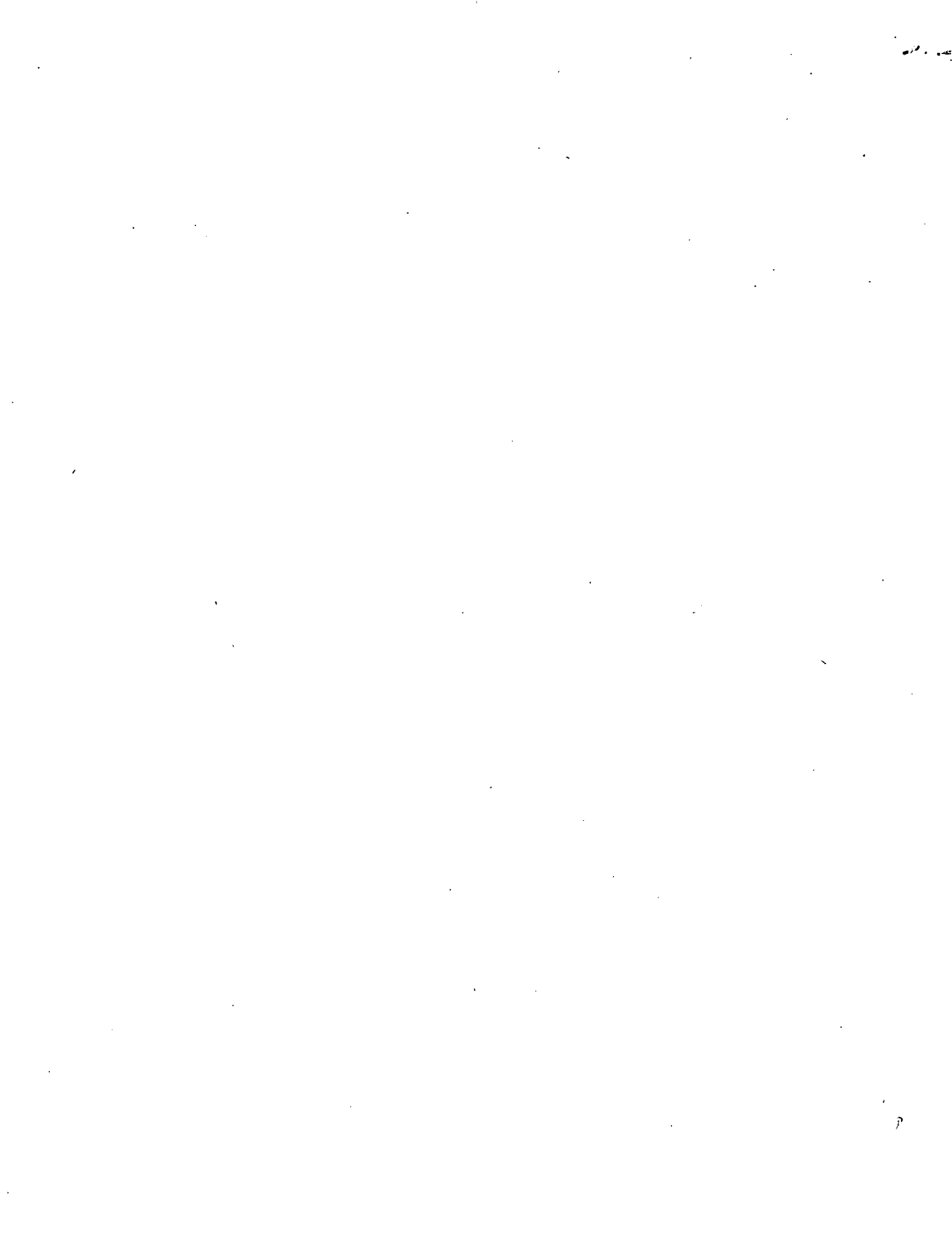
$$C_b = 1.75 + (1.05)(M_1/M_2) + (0.3)(M_1/M_2)^2 \leq 2.3$$

$M_1$  y  $M_2$  son los momentos flexionantes en los puntos de soporte lateral del tramo en estudio. El signo de la relación  $M_1/M_2$  es positiva si la viga-columna se flexiona en curvatura inversa, y negativa si se flexiona en curvatura simple. ( $M_1 \leq M_2$ ).

4.- El valor de  $C_b$  se toma igual a la unidad en vigas-columna en cantiliver o bien cuando el momento flexionante dentro de la longitud no contraventeada es mayor que en los puntos de soporte lateral.

5.- Al valuar  $F_{b_{x,y}}$  en la fórmula de Interacción  $C_b$  se toma igual a 0.85 si la estructura puede desplazarse linealmente, e igual a 1.0 si dicho desplazamiento está impedido.







**DIVISION DE EDUCACION CONTINUA  
FACULTAD DE INGENIERIA U.N.A.M.**

"DISEÑO DE ESTRUCTURAS DE ACERO"

SECCIONES COMPUESTAS

DR. PORFIRIO BALLESTEROS

NOVIEMBRE, 1984.

en los dos miembros estructurales. Ejemplos  
Típicos de secciones compuestas se muestran  
en la Fig. 2.1.

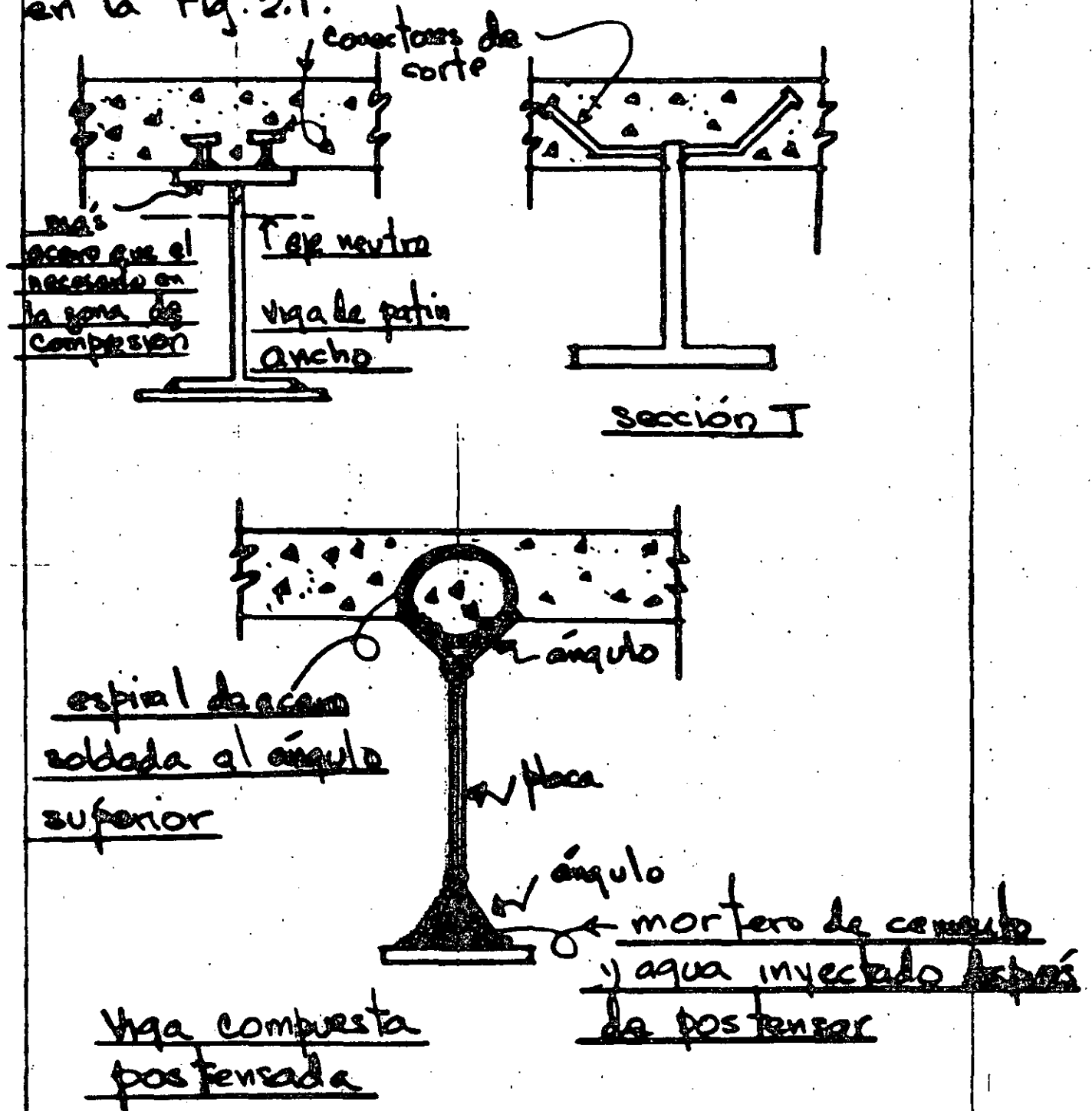


Fig. 2.1 Algunos tipos de secciones compuestas concreto-acero

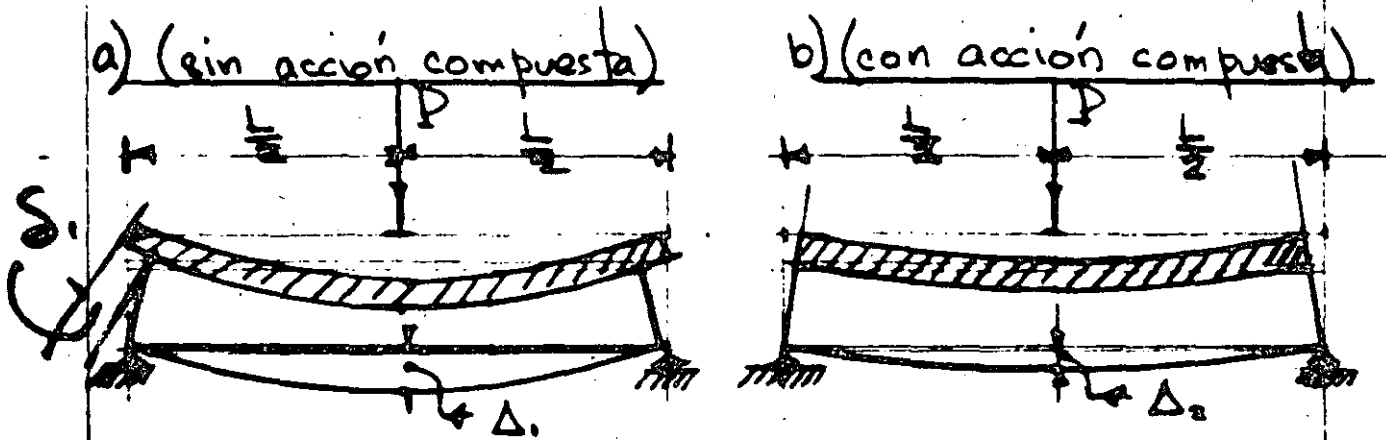


Fig. 2.2 Comparación de deflexión en vigas con y sin acción compuesta  $\Delta_1 > \Delta_2$

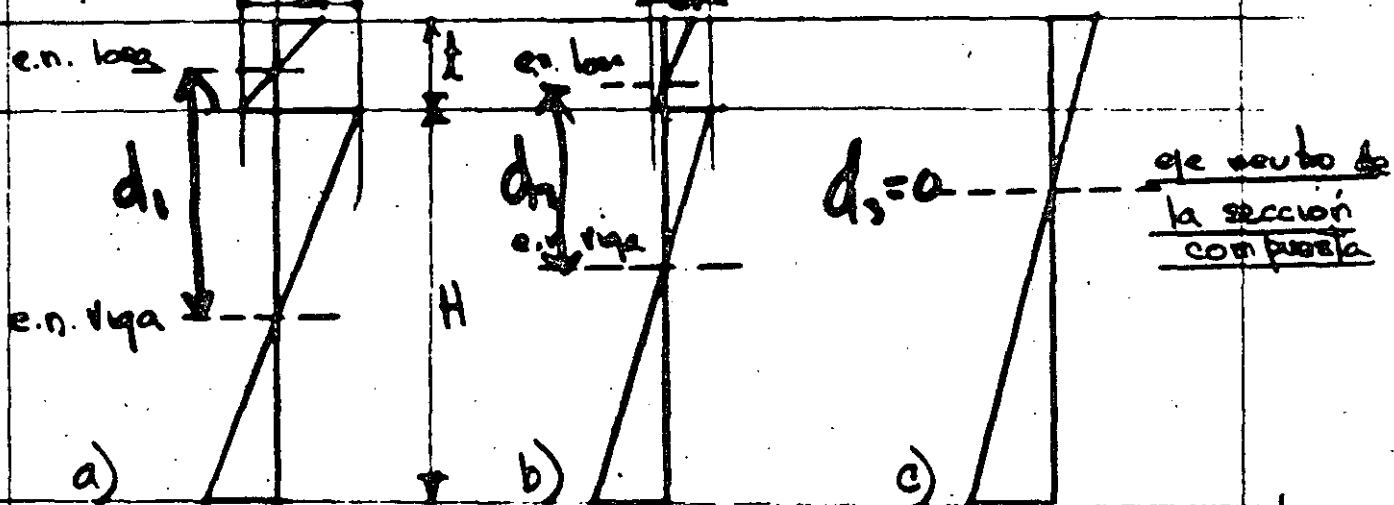
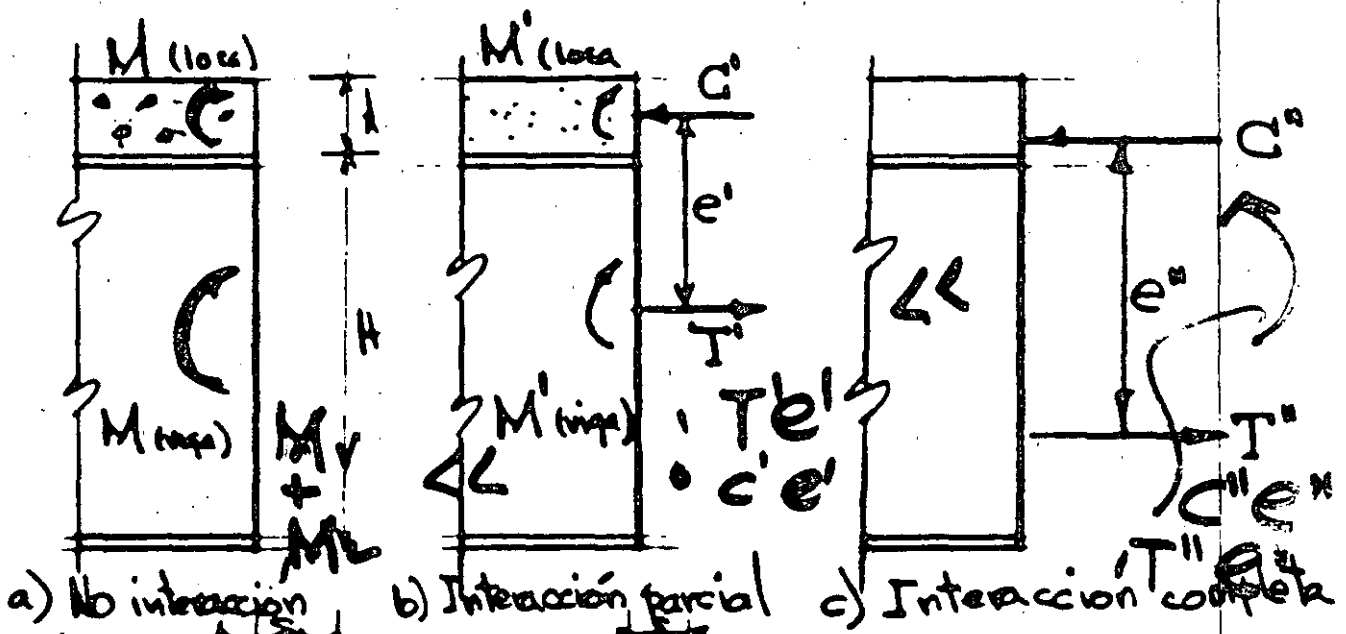


Fig. 2.3 Deformaciones unitarias en vigas compuestas

$\delta$  deformación relativa entre losa y viga cuando el sistema actúa compuesto  $\delta_1 = \delta_2 = 0$

De la Figura 2.3 a), se observa que el momento resistente es igual a

$$\sum M = \underline{M_L} + \underline{M_V} \quad (2.1)$$

Se observa que en este caso hay dos ejes neutros uno en el centro de la losa y otro en el centro de la viga y ocurre una deformación relativa losa-viga igual a  $\delta_1$ .

Considerando el siguiente caso Fig 2.3 b donde solo interacción parcial se presenta, se observa que los ejes neutros tienden a juntarse y la deformación relativa losa-viga  $\delta_2$  tiende a disminuir. Se desarrollan fuerzas parciales  $C'$  y  $T'$ . El momento resistente aumenta en las cantidades  $T'e'$  o  $C'e'$ .

Cuando se desarrolla interacción completa viga-losa,  $\underline{\delta} = 0$  y el diagrama resultante de deformación se muestra en la Fig 2.3 c. Las fuerzas  $T''$  y  $C''$  son mayores que  $T'$  y  $C'$  y su brazo de palanca  $e''$  es mayor que  $e'$ . El momento resistente es

$$\sum M = \underline{T''e''} \text{ o } \underline{C''e''} \quad (2.2)$$

### 3. Ventajas y Desventajas

Basicamente las ventajas resultantes son:

1. Reducción del peso de acero ✓
2. Menor peralte en las vigas de acero ✓
3. Aumenta la rigidez del sistema
4. Para un miembro dado se pueden lograr claros mayores.
5. Aumenta la última capacidad de carga del conjunto estructural.

La economía de acero oscila de 20 a 30%.

y la reducción de peralte origina economía en otros materiales (muros, escaleras, etc...).

Se incrementa grandemente el momento de inercia ~~del sistema~~ del sistema de piso en dirección de las vigas de acero, consecuentemente se reducen las deflexiones. La última resistencia de la sección compuesta es MUCHO MAYOR que la suma de las resistencias de la losa y la viga consideradas separadamente.

Muros y columnas compuestas se usan también en la construcción de edificios

Las desventajas o limitaciones que deben ser consideradas son las siguientes:



1. Efecto de continuidad -

2. Deflexiones a largo plazo

Actualmente (1972), solo la porción de la losa actuando en compresión se considera efectiva. En el caso de vigas continuas, la ventaja del comportamiento compuesto se reduce en el área de momentos negativos. En las columnas de edificios, no existe la posibilidad de colocar el acero suficiente para darle continuidad a la acción compuesta. En puentes si es posible hacerlo.

El problema de deformaciones a largo plazo puede ser importante si la sección compuesta está resistiendo una porción substancial de la carga muerta o si las cargas vivas son de larga duración, por lo cual es conveniente reducir el ancho efectivo o suponer una relación modular  $n$  incrementada.

4. Ancho efectivo

Con el objeto de calcular las propiedades de una sección compuesta es necesario utilizar el concepto de ancho

efectivo. Refiriéndose a la Fig. 4.1, considerando la sección compuesta bajo esfuerzos en los cuales la losa es de ancho infinito. El esfuerzo  $\sigma_x$  será máximo sobre la viga de acero y disminuirá en forma no lineal como se indica en la Fig. 4.1.

$$\int_{-b}^b \sigma_x dy$$

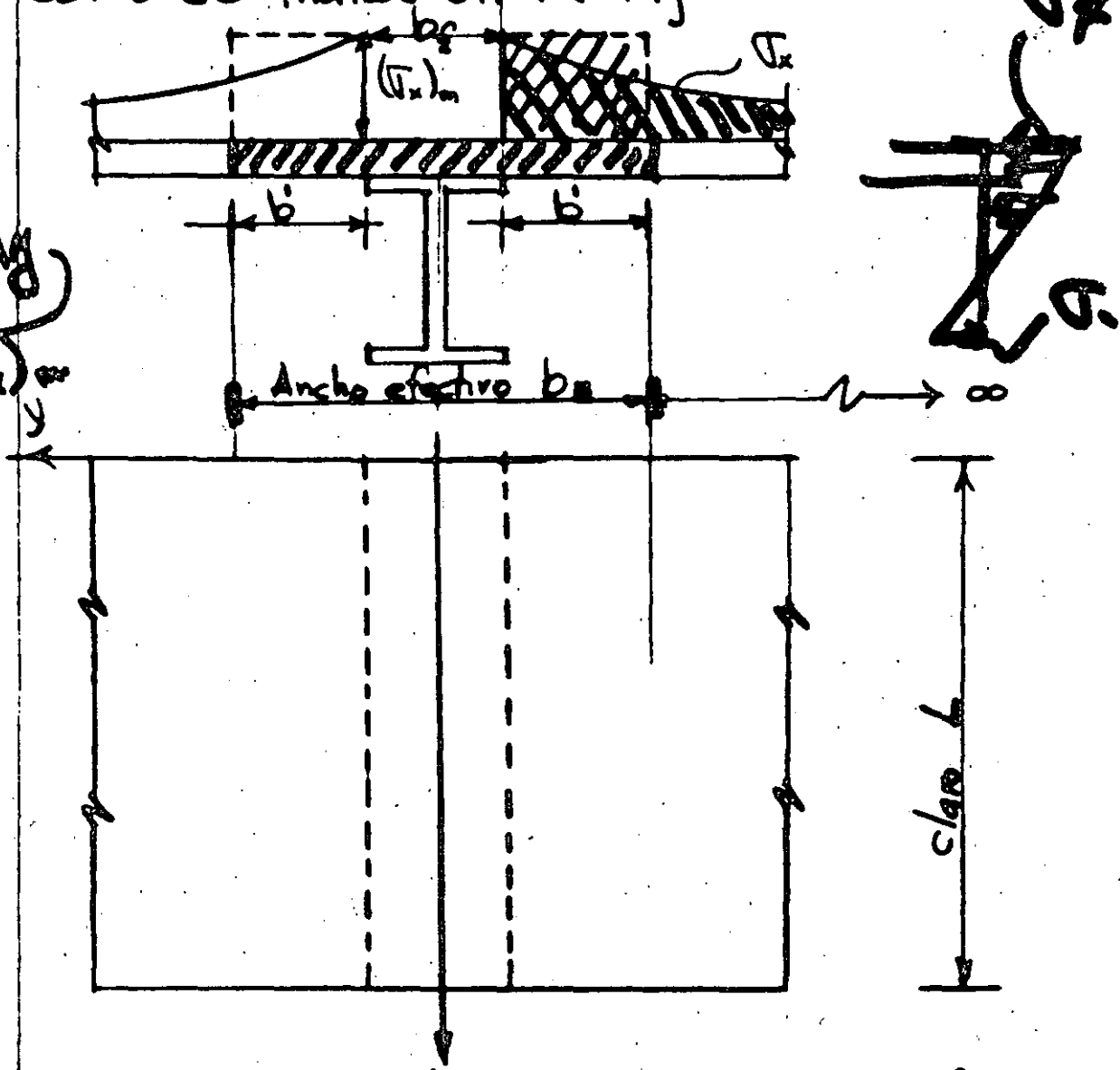


Fig. 4.1. Distribución no uniforme de esfuerzos de compresión  $\sigma_x$ , y ancho efectivo  $b_e$

El ancho efectivo de un miembro compuesto se toma como

$$b_E = b_f + 2b' \quad (4.1)$$

donde  $(2b')(\sigma_x)_{\max}$  es igual al área bajo las curvas de  $\sigma_x$ . Varios investigadores incluyendo Timoshenko<sup>12</sup> y von Kármán<sup>3</sup> han derivado expresiones para el ancho efectivo de vigas homogéneas con patines anchos; y Johnson<sup>13</sup> ha demostrado que las expresiones son también válidas para vigas en las cuales el patín y el alma son de diferentes materiales la expresión de Johnson es: Con  $0.15 \leq \nu \leq 0.2$

$$b_E = b_f + \frac{2L}{\pi(3 + 2\mu - \mu^2)} \quad (4.2) \quad \text{Donde } \nu = 0.2$$

Donde  $L$  = claro de la viga

$b_f$  = ancho del patín de la viga de acero

$\mu$  = relación de Poisson de la placa

Suponiendo  $\mu = 0.2$  para el concreto y substituyendo en (4.2) se obtiene

$$b_E = b_f + \frac{2L}{\pi[3 + 2(0.2) - (0.2)^2]} = b_f + 0.196L \quad (4.3)$$

Como simplificación para propósitos de diseño el AISI-1.11.1 ha adoptado el mismo método de calcular anchos efectivos que el ACI<sup>14</sup> hace para vigas de concreto. Refiriéndose

a la Fig. 4.2, el máximo valor de el ancho efectivo  $b_e$  permitido deberá ser el menor valor calculado por las siguientes relaciones:

a) Para vigas interiores:

$$b_e \leq \frac{L}{4} \quad (4.4a)$$

$$b_e \leq b_o \quad (4.4b)$$

$$b_e \leq b_f + 16 t_s \quad (4.4c)$$

b) Para vigas exteriores:

$$b_e \leq L/12 + b_f \quad (4.5a)$$

$$b_e \leq \frac{1}{2}(b_o + b_f) \quad (4.5b)$$

$$b_e \leq b_f + 6 t_s \quad (4.5c)$$

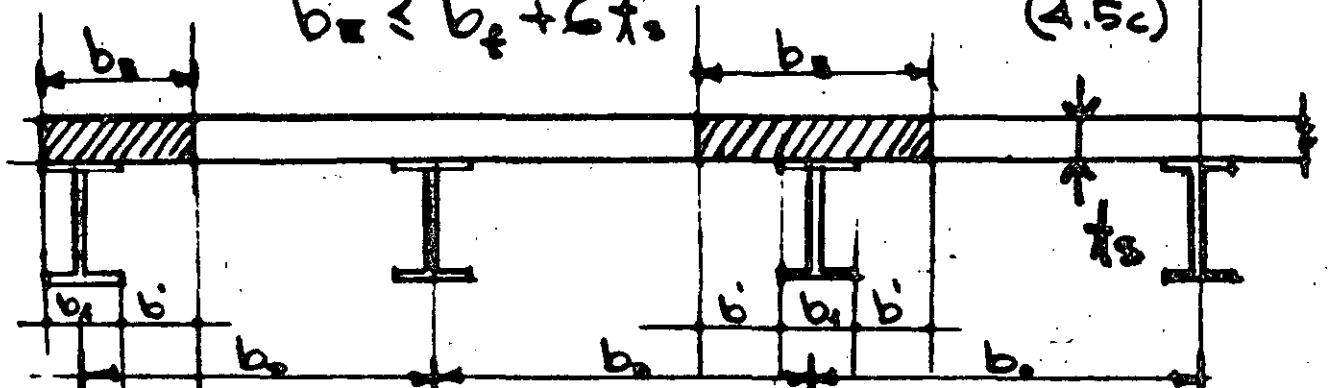


Fig. 4.2 Dimensiones que gobiernan el ancho efectivo  $b_e$  en secciones compuestas acero-concreto.

( $L = c l_{gr}$ )

Similarmnte, para el diseño de puentes la AASHTO-1969-1.7.99<sup>18</sup> recomienda lo mismo que AISI-ACI excepto Eq. 4.4c es substituida por

$$b_e \leq 12 t_s \quad (4.6)$$

y las Eq. 4.5a y c son reemplazadas por

$$b_e \leq L/12 \quad (4.7a)$$

$$b_e \leq 6 t_s \quad (4.7b)$$

### 5. Cálculo de las propiedades de la sección

Las propiedades de una sección compuesta pueden ser calculadas por el método del área transformada. En contraste con el diseño de concreto reforzado, donde el área de acero es transformada en una área de concreto equivalente, el concreto es transformado en una área equivalente de acero. Como resultado el área de concreto es reducida utilizando una losa de ancho  $b_e/n$  donde  $n$  es la relación del módulo de elasticidad del acero,  $E_s$ , al módulo de elasticidad del concreto  $E_c$ .

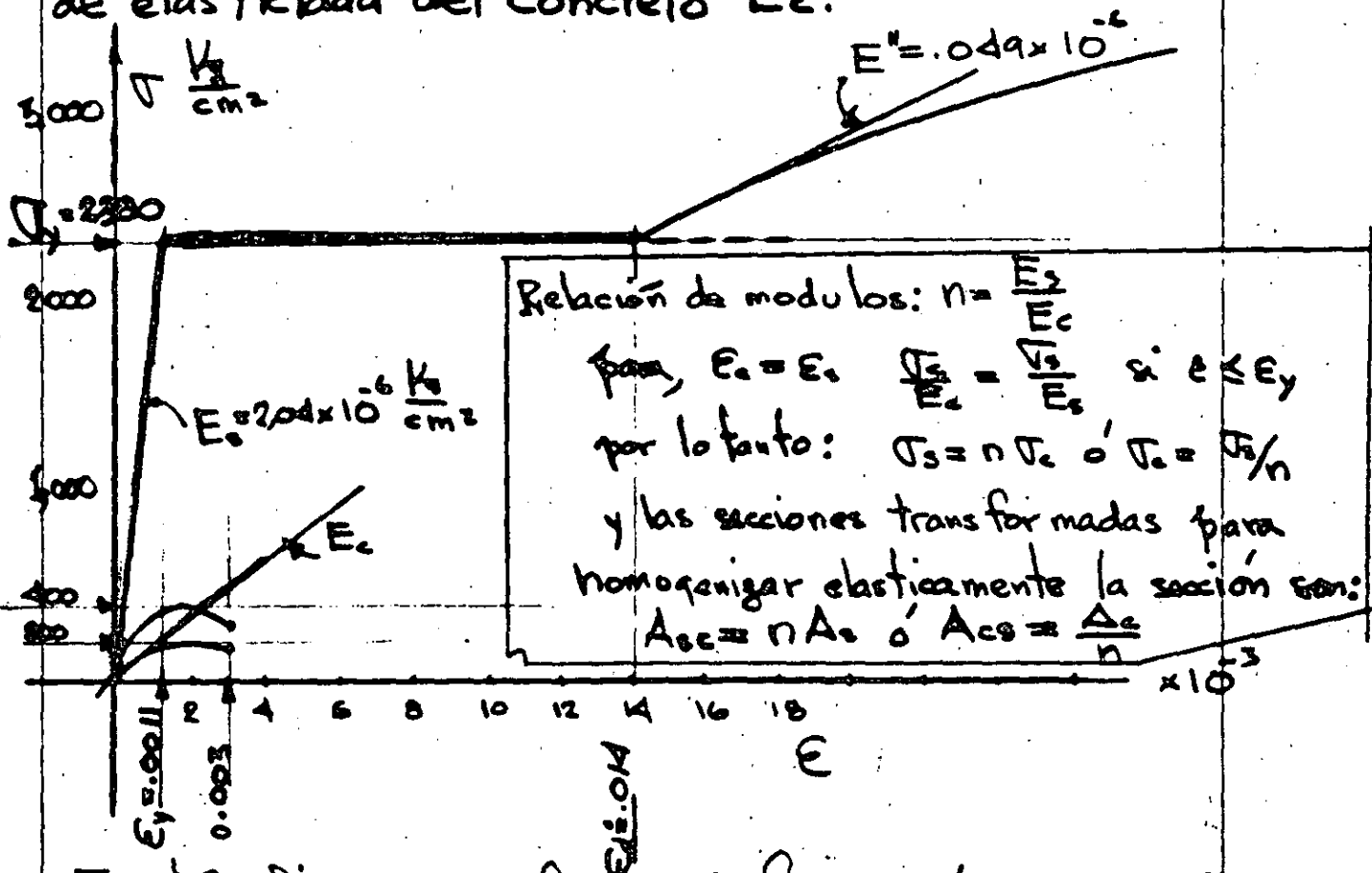


Fig. 4.2a Diagrama esfuerzo de formación acero A7 y concretos de  $f'_c = 400$  y  $300$  kg/cm<sup>2</sup>

Relación modular n. El módulo de elasticidad del concreto en  $\text{lbs/pul}^2$  puede considerarse como <sup>14</sup>

$$E_c = \gamma^{1.5} 33 \sqrt{f'_c} \quad (5.1)$$

donde  $\gamma$  es el peso volumétrico del concreto en  $\text{libras/pie}^3$  y  $f'_c$  es considerado en  $\text{libras/pul}^2$ . Para el peso ordinario del concreto de  $145 \text{ lbs/pie}^3$ , su

$1 \text{ kg/m}^3 = 16.0134 \text{ lbs/pie}^3$	
$1 \text{ kg/cm}^2 = 14.2234 \text{ lbs/pul}^2$	(5.1a)
$1 \text{ cm} = .3937 \text{ pul}$	
$1 \text{ m} = 3.28083 \text{ pies}$	

.50 valor se considera como

$$200. \quad E_c = 57,800 \sqrt{f'_c} \quad (5.2)$$

250 Ejemplo 5.1

300 Calcular la relación modular, n para un  
350 concreto de peso normal ( $145 \text{ lbs/pie}^3$  &  $2300 \text{ kg/m}^3$ )  
400 con una resistencia a la compresión  $f'_c = 3000 \text{ lbs/pul}^2$   
450  $= 211 \text{ kg/cm}^2$

Solución

De Eq. 5.1,

$$E_c = (145)^{1.5} (33) \sqrt{3000} = 57,800 \sqrt{3000}$$

$$E_c = 3,170 \frac{\text{kg}}{\text{pul}^2} = 2.23 \times 10^4 \text{ kg/cm}^2$$

lo cual da

$$n = \frac{E_s}{E_c} = \frac{29,000}{3,170} = 9.15 \approx 9$$

El mínimo valor de  $n$  permitido por el reglamento del ACI y las especificaciones de la AASHTO es 6. Para propósitos prácticos de diseño, los valores de  $n$  indicados en la tabla 5.1 pueden ser usados.

TABLA 5.1 Valores de diseño para  $n$

$f'_c$ = Resistencia a los 28 días		Relación modular $n = E_s/E_c$
lbs/pul <sup>2</sup>	kg/cm <sup>2</sup>	
3,000	211 (200)	9
3,500	246 (230)	8.5
4,000	281	8.0
4,500	316	7.5
5,000	351 (350)	7.0
6,000	422	6.5

6.22.5

6. Condiciones elásticas de la sección Transformada

Flexión pura.

Aceptando deformación plana y relación lineal es fuerza de formación de Fig. 6.1 se tiene, considerando el eje neutro coincidiendo con el eje  $x$ .

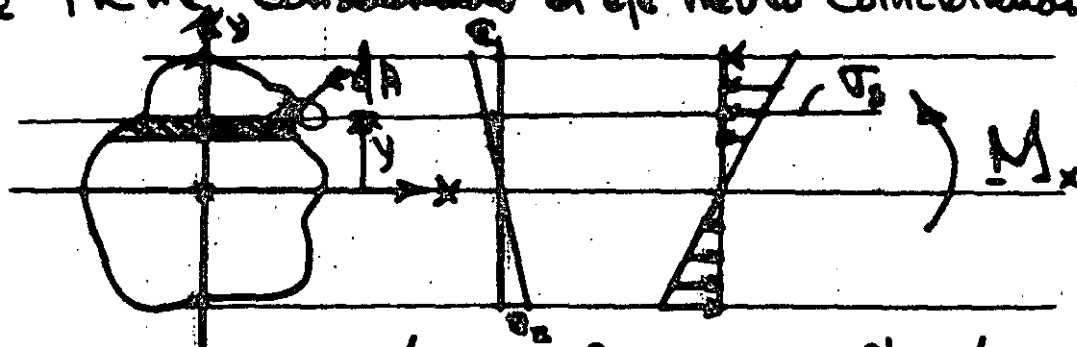


Fig. 6.1 Sección transformada en flexión pura

Ley de Hooke y de deformación plana:

$$\sigma_x = K_1 y \quad (6.1)$$

Equilibrio:

$$\text{de } \sum F_x = 0 \quad \int_A \sigma_x dA = K \int_A y dA = 0 \quad \therefore$$

$$\text{o sea } Q_x = \int_A y dA = 0 \quad (6.2)$$

(6.2) implica que el eje neutro coincide con el centroide de la sección transformada

de  $\sum M_x = 0$  se obtiene

$$M_x = \int_A \sigma_x y dA = K \int_A y^2 dA = K I_x \quad (6.3)$$

De (6.1) y (6.3) se obtiene:

$$\sigma = \frac{M_x}{I_x} y \quad (6.4)$$

Ejemplo 5.1.

Calcule las propiedades de la sección compuesta mostrada en la figura 6.2 para  $f_c' = 8000 \text{ lbs/in}^2$  y  $n = 9$

Solución

Primero, determinación del ancho efectivo:

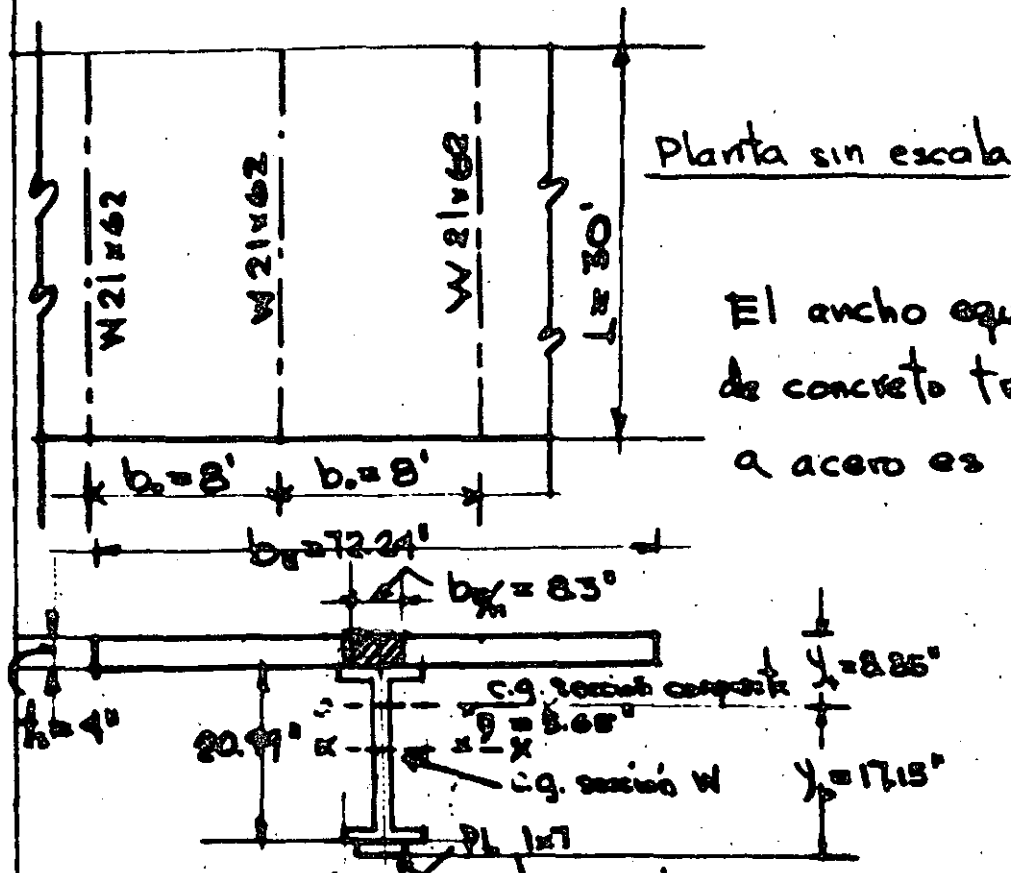
$$b_e = 0.25 L = 0.25(30 \times 12) = 90''$$

$$b_e = b_o = 8 = 12 = 96''$$

$$b_e = b_s = 16 f_s = 0.24 \times 16 = 4 = 72.24''$$

El br  
completo  
por ser  
menor





El ancho equivalente de concreto transformado a acero es  $\frac{b_o}{n} = \frac{72.24}{9} = 8.3$

Fig. 6.2 Sección compuesta ejemplo 6.1

El cálculo del centroide y momento de inercia son mostrados en la Tabla 6.1

TABLA 6.1

Elemento	Area Total o A (pul <sup>2</sup> )	Brzo de c.g. W (in)	A y pul <sup>3</sup>	A y <sup>2</sup> pul <sup>4</sup>	I <sub>o</sub>
Losla	82.12	12.495	+401.34	506.8	42.8
W21x62	18.23	0	0	0	1326.8
Cubro placa	7.00	-10.995	-76.97	846.9	
$\Sigma$	57.88		+124.37	5861.5	1369.6

$$A y^2 + I_o = I_x = 5861.5 + 1369.6 = 7231.1 \text{ pul}^4$$

$$\bar{y} = \frac{124.37}{57.88} = 5.65 \text{ in}$$

$$I = I_x - A \bar{y}^2 = 7231.1 - 57.88 (5.65)^2 = 5403 \text{ pul}^2$$

$$y_1 = 10.5 - 5.65 + 4.0 = 8.85 \text{ in}$$

$$y_2 = 10.5 + 5.65 + 1 = 17.15 \text{ in}$$

### Ejemplo 6.2 (Tarea)

Para la viga de acero WF21 x 62 con un cubre placa de 1" x 7" de la Fig. 6.2, determine

a) Los esfuerzos de servicio debidos al peso propio del concreto y de la viga suponiendo que la viga actua como obra falsa

b) Los esfuerzos de carga viva y muerta superpuestos suponiendo que después de fraguado el concreto el momento total es incrementado por 560 Kips-pie.

### 7. ULTIMA CAPACIDAD DE CARGA DE SECCIONES COMPUESTAS

La última capacidad de carga de una sección compuesta depende del esfuerzo de fluencia de la viga de acero, la resistencia de la losa de concreto y la capacidad de interacción de los conectores de corte para conectar la losa a la viga.

Las recomendaciones de última resistencia fueron aplicadas a la práctica según las recomendaciones del "ASCE-ACI Joint Committee" sobre construcción compuesta<sup>16</sup> y tuvieron ciertas modificaciones después de

investigaciones efectuadas en la Universidad de Lehigh<sup>17</sup>

La ultima resistencia en términos de la capacidad de momento último da un entendimiento más claro del comportamiento así como una medida más aproximada del factor de carga (Relación entre el momento último al momento aplicado).

El procedimiento para determinar la capacidad última de momento depende de que la posición del eje neutro quede dentro de la losa de concreto o en la viga de acero. Si el eje neutro cae dentro de la losa se dice que esta es adecuada. Si el eje neutro cae dentro de la viga de acero, la losa es considerada inadecuada, Fig. 7.1.

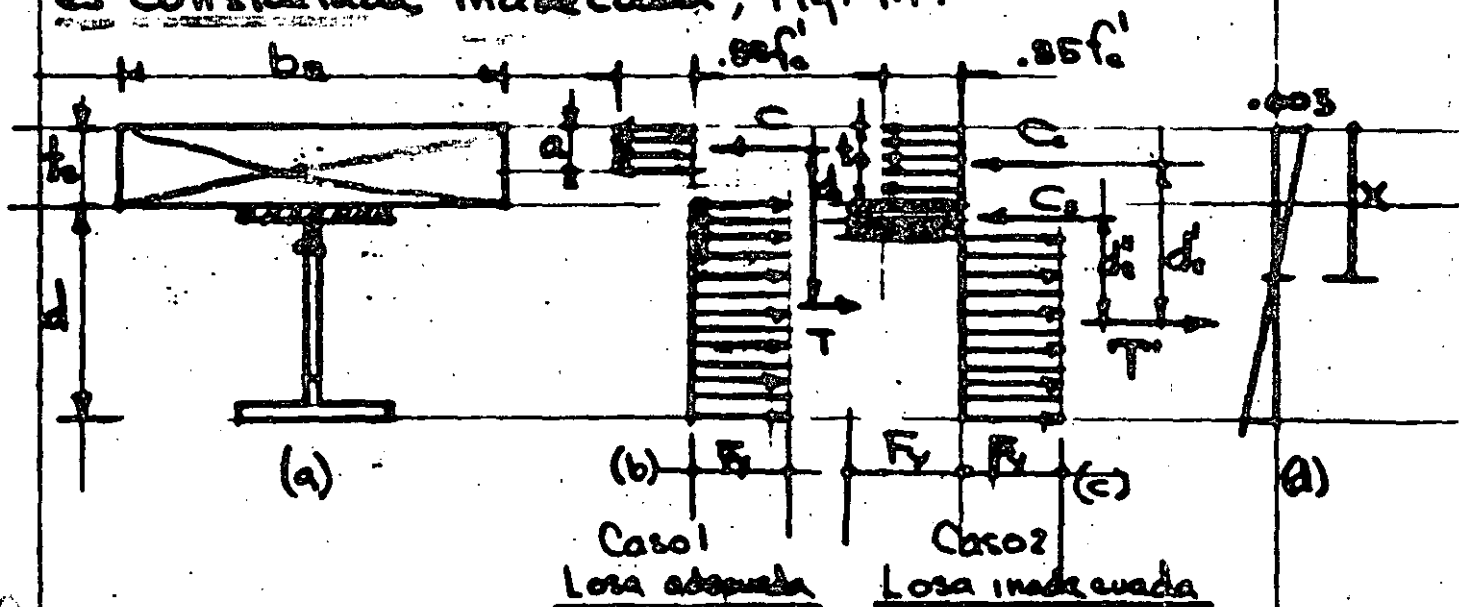


Fig. 7.1. Distribución de esfuerzos a última capacidad

Caso 1- Losa adecuada. Refiriéndose a la Fig 7.1 b y suponiendo el bloque rectangular de esfuerzos de Whitney se tiene, la última fuerza de compresión  $C$  es

$$C = 0.85 f'_c a b_e \quad (7.1)$$

y la última fuerza de tensión

$$T = A_s F_y \quad (7.2)$$

de  $T=C$  se obtiene

$$a = \frac{A_s F_y}{0.85 f'_c b_e} \quad a < t_s \quad (7.3)$$

De acuerdo con la aproximación del bloque rectangular<sup>14</sup> el eje neutro  $x = a/0.85$  para  $f'_c = 4000 \text{ lbs/pul}^2$ . La última capacidad de momento  $M_u$  es

$$M_u = C d_i = T d_i \quad (7.4)$$

Puesto que la losa es adecuada, es capaz de desarrollar una fuerza compresiva igual a la capacidad total de fluencia de la viga. Expresando  $M_u$  en términos de la fuerza en el acero da

$$M_u = A_s F_y \left( \frac{d_i}{2} + t_s - \frac{a}{2} \right) \quad (7.5)$$

Se determina  $a$  de (7.3) y si  $a \leq t_s$ ,  $M_u$  se calcula de (7.5)

Caso 2 Losa inadecuada. Si a determinada de (7.3) se excede es mayor que  $t_0$  la distribución de esfuerzos será como se muestra en Fig. 7.1c. la última fuerza compresiva en la losa será

$$C_c = 0.85 f'_c b_o t_0 \quad (7.6)$$

$C_s$  será la fuerza de compresión última del acero arriba del eje neutro como se muestra en Fig. 7.1c.

La fuerza última de tensión  $T'$  es menor que  $A_s F_y$  y es igual a

$$T' = C_c + C_s \quad (7.7)$$

$$\text{ó} \quad T' = A_s F_y - C_s \quad (7.8)$$

igualando (7.7) y (7.8) y despejando a  $C_s$  se obtiene

$$C_s = \frac{A_s F_y - C_c}{2}$$

$$\text{ó} \quad C_s = \frac{A_s F_y - 0.85 f'_c b_o t_0}{2} \quad (7.9)$$

y el momento último  $M_u$  es

$$M_u = C_c d_2'' + C_s d_2'' \quad (7.10)$$

$d_2''$  y  $d_2''$  se muestran en Fig. 7.1c

### Ejemplo 7.1

Determine la última capacidad de momento de la sección compuesta mostrada en la Fig. 7.2

Verificación si la losa es adecuada Caso 1.

$$a = \frac{A_s F_y}{.85 f'_c b_e} = \frac{10.6 (36)}{0.85 (3) 60} = 2.49'' < t_s = 4'' \quad //$$

$$C = 0.85 f'_c a b_e = .85 (3) (2.49) (60) = 381 \text{ Kips}$$

$$T = A_s F_y = 10.6 (36) = 381 \text{ Kips}$$

(Se verifica que  $T=C$ )

el brazo  $d_i = \frac{d}{2} + t - \frac{a}{2} = 7.925 + 4.0 - 1.245 = 10.68''$

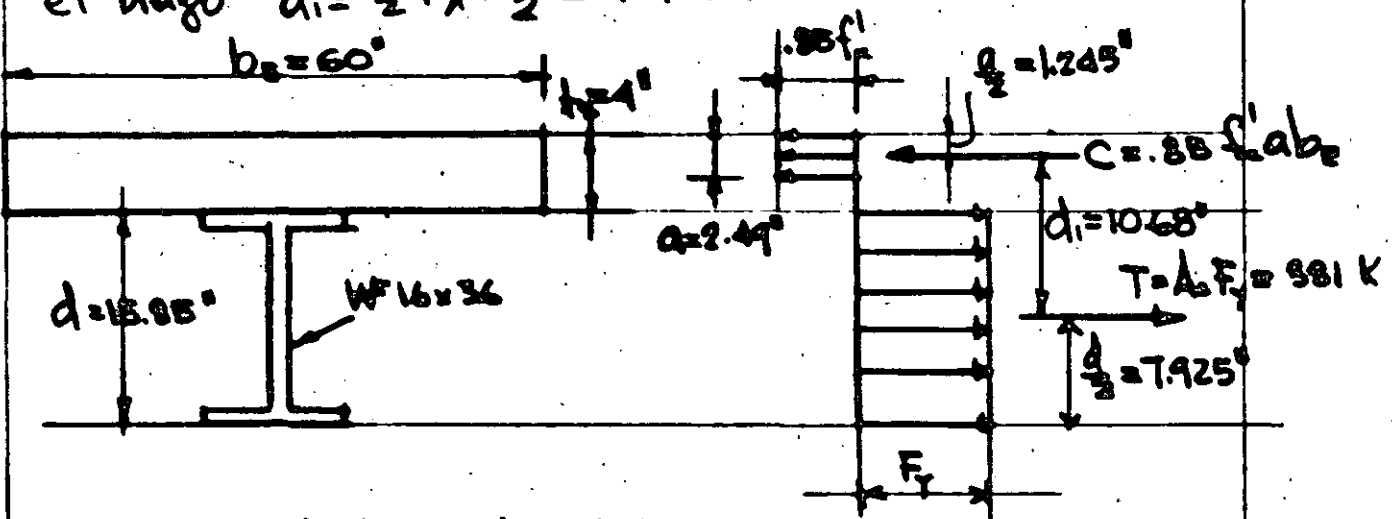


Fig. 7.2 Ejemplo 7.1

El momento último es

$$M_u = C d_i = T d_i = 381 (10.68) / 2 = 340 \text{ Kips-pie}$$

Ejemplo 7.2

Determine la última capacidad de la sección compuesta mostrada en la Fig. 7.3. Suponga acero A36,  $f'_c = 3000 \text{ lbs/pt}^2$ , y  $n = 9$ .

$f'_c$   
 $M_y$   
 $M_x$   
 $M_v$

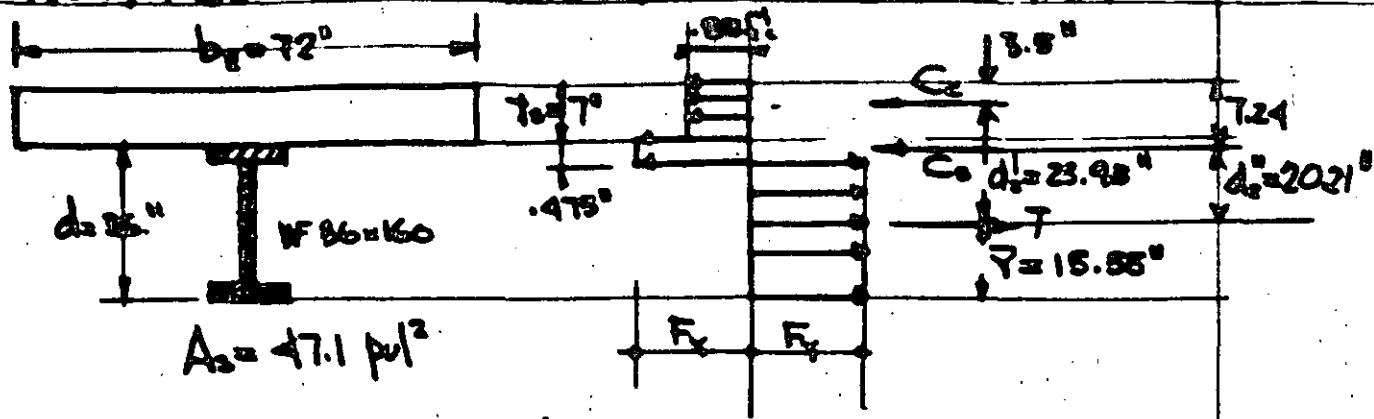


Fig. 7.3 Ejemplo 7.2

Solución: Verificación si la losa es adecuada

$$a = \frac{A_s F_y}{0.85 f_c' b_o} = \frac{(47.1)(36)}{0.85(3)(72)} = 9.22'' > \lambda_s = 7''$$

La losa es inadecuada de tomar una  $C = A_s F_y$

De ecuación 7.6,  $C_c = 0.85 f_c' b_o \lambda_s = 0.85(3)(72)(7) = 1285$  K

usando la ecuación 7.9

$$C_u = \frac{A_s F_y - 0.85 f_c' b_o \lambda_s}{2} = \frac{47.1(36) - 1285}{2} = 203 \text{ Kips}$$

Suponiendo que solo el patin de la WF 36x160 ( $b_f = 12''$ ) está en compresión  $F_y b_f d_r = C_u$  de donde

$$d_r = \frac{C_u}{F_y b_f} = \frac{203}{36(12)} = 0.475''$$

La localización del centroide de la porción de tensiones:

$$\bar{Y} = \frac{(47.1)(18) - 0.475(12)(35.76)}{47.1 - 0.475(12)} = 15.55 \text{ pulg}$$

De la Fig. 7.3 se observa que

$$M_u = C_c d_1' + C_u d_2' \\ = [1285(23.98) + 203(20.21)] / 12 = 2,910 \text{ Kips-pie}$$

**B. CONECTORES DE CORTE.**

El corte que se desarrolla entre la losa y la viga de acero durante la carga debe resistirse para que se desarrolle una sección compuesta monolítica, aunque la adherencia y la fricción sean significativamente altas nunca podrán desarrollar la interacción requerida.

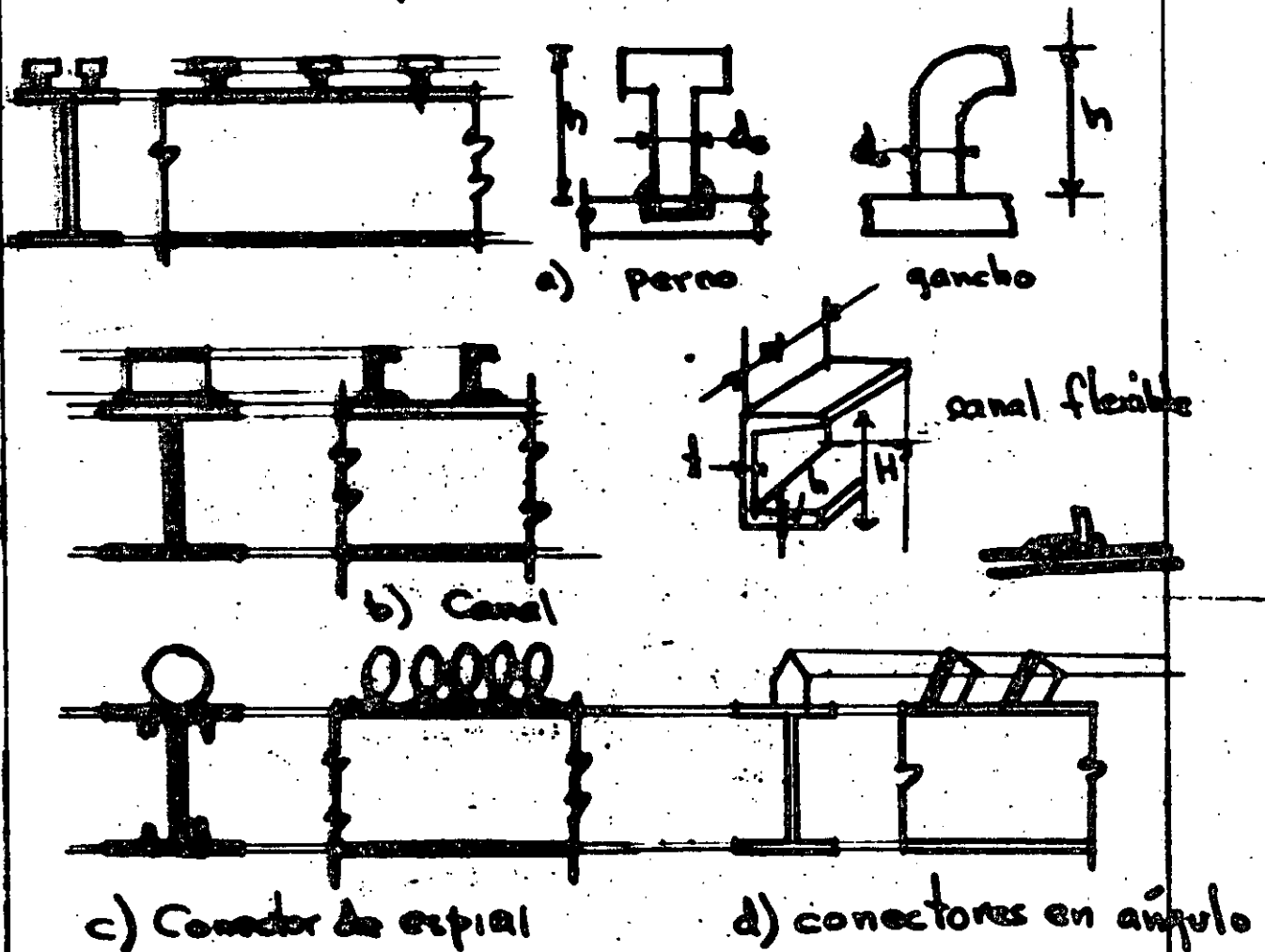


Fig. 81 Conectores de corte típicos



b ancho de la sección a la altura y de la sección transformada.

$I_g$  momento de inercia de la sección transformada respecto al eje centroidal  $g$

$\frac{dN}{dx}$  pendiente de la gráfica  $N(x)$  en la sección en consideración  $x$

$A_y$  area de la sección de  $y$  a  $y_m$

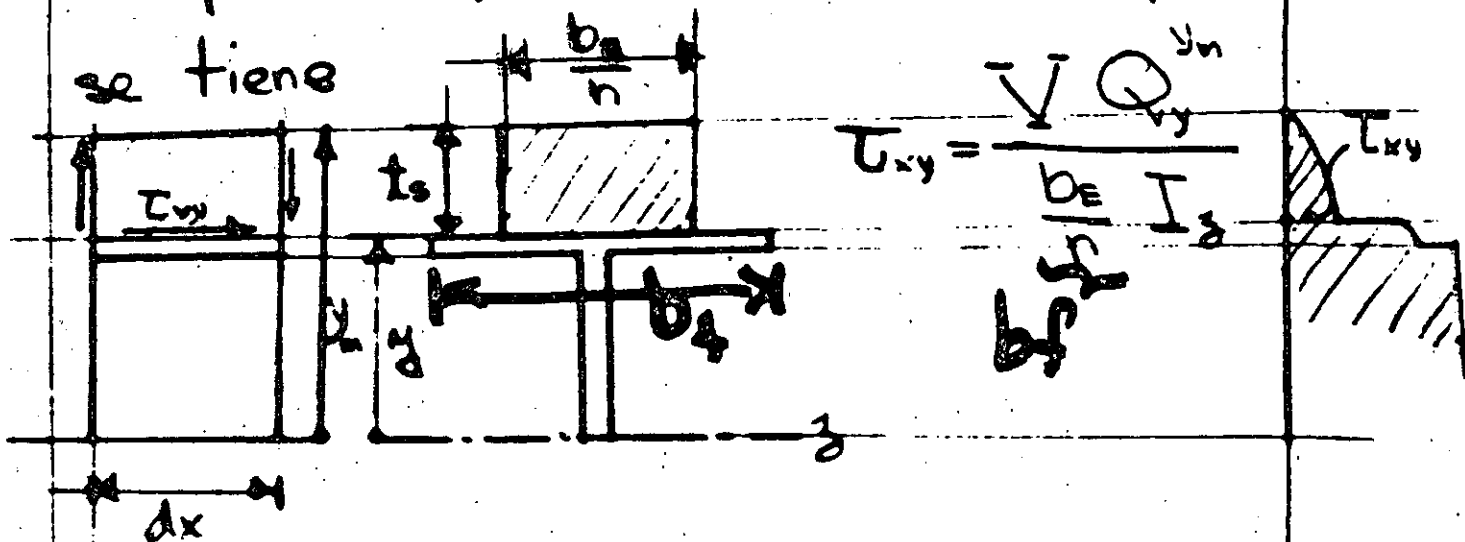
$A$  area total de la sección transformada

en el caso de flexión o  $N = \text{constante}$

$$\frac{dN}{dx} = 0 \quad \tau_{xy} = \frac{V Q_y^{y_m}}{b I_g} \quad (8.4)$$

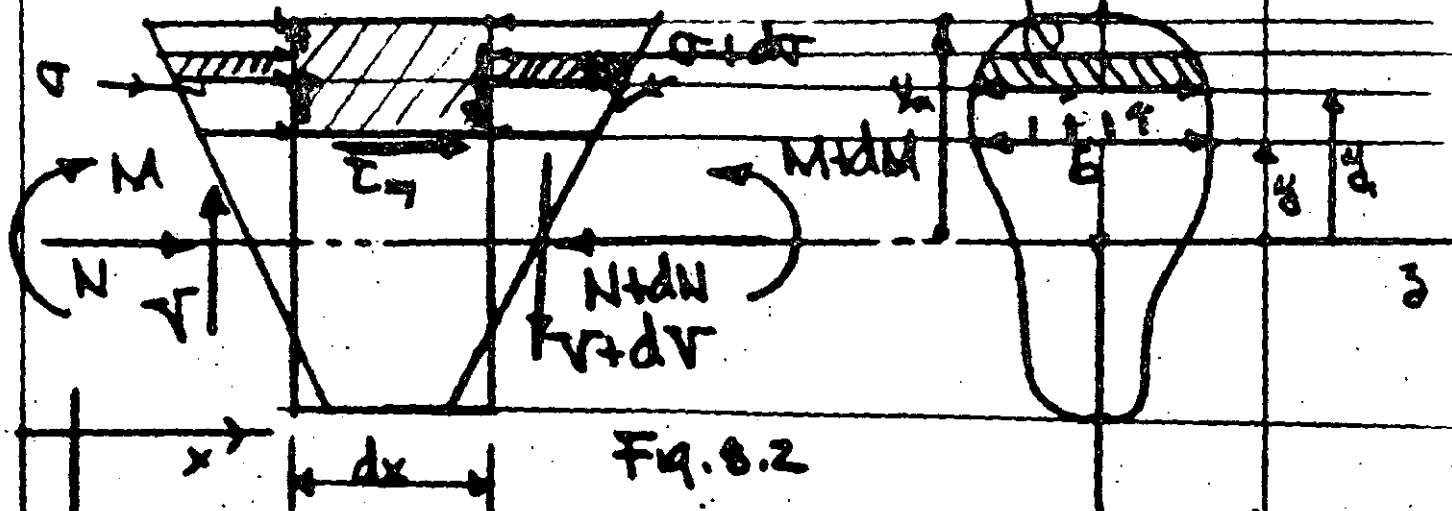
Aplicando (8.4) a la sección compuesta

se tiene



ESFUERZO CORTANTE EN CONDICIONES ELÁSTICAS

Ecua ción general del corte considerando una sección homogénea, isotrópica, deformación plana, variación lineal  $\sigma - \epsilon$ ,  
 $\int y dx$



Se tiene:  $\sigma = \frac{M}{I_z} y + \frac{N}{A}$ ,  $d\sigma = \frac{dM}{I_z} y + \frac{dN}{A}$  (8.1)

de  $\sum F_x = 0$ ,  $b \tau_{xy} dx = \int_{y_1}^{y_2} d\sigma dA$  (8.2)

Subst. (8.1) on (8.2) se obtiene

$$b \tau_{xy} = \int_{y_1}^{y_2} \left[ \frac{dM}{I_z} y + \frac{dN}{A} \right] dA = \frac{V}{I_z} \int_{y_1}^{y_2} y dA + \frac{dN}{A} \int_{y_1}^{y_2} dA$$

• sea  $\left( \tau_{xy} = \frac{V Q_y^{y_m}}{b I_z} + \frac{dN}{dx} \frac{A_y^{y_m}}{A} \right)$  (8.3)

(8.3) referida a ejes centroidales principales donde:

$V$  = cortante en la sección en consideración

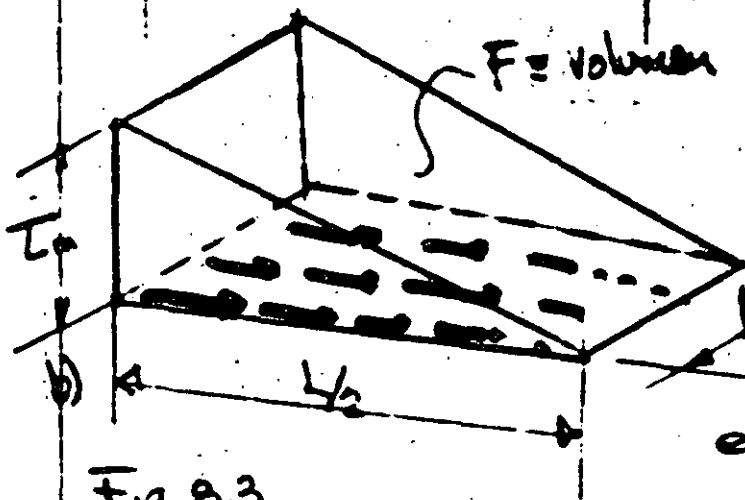
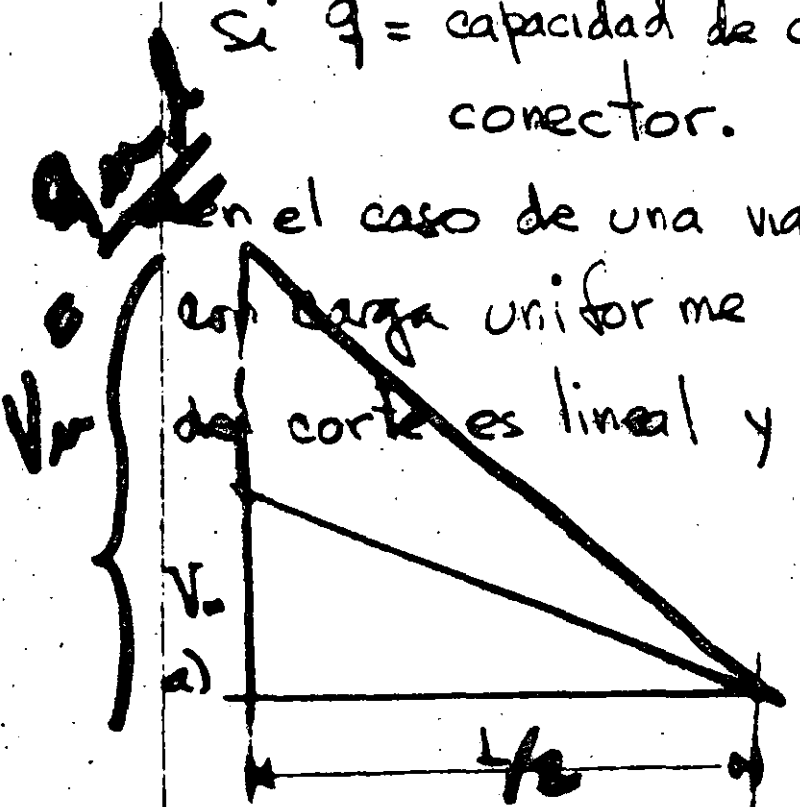
$Q_y^{y_m}$  = momento estático de área de  $y$  a  $y_m$  (transformada)

Si  $q$  = capacidad de corte permisible por conector.

En el caso de una viga libremente apoyada con carga uniforme de claro  $L$  la variación del corte es lineal y se tiene

$$V_m = \frac{qL}{2}$$

$$\tau_m = \frac{V_m Q_y}{\frac{b_E}{n} I_x} \quad (8.5)$$



La fuerza cortante total de interacción entre losa de concreto y viga metálica será

el volumen del diagrama

Fig. 8.3

de corte mostrado en Fig. 8.3 b,  $F = \frac{1}{2} \frac{b_E}{n} V_0 \frac{L}{2}$

$$F = \frac{b_E L V_0}{4n} \quad \text{y el número de}$$

conectores en el semi claro  $\frac{L}{2}$  será

$$N = \frac{F}{q} = \frac{b_E L V_0}{4nq} \quad (8.6)$$

Distribución de los conectores si la variación de corte es lineal. El problema análogo a la distribución de estribo en una viga de concreto consiste en dividir el volumen  $F$  en  $N$  volúmenes iguales.

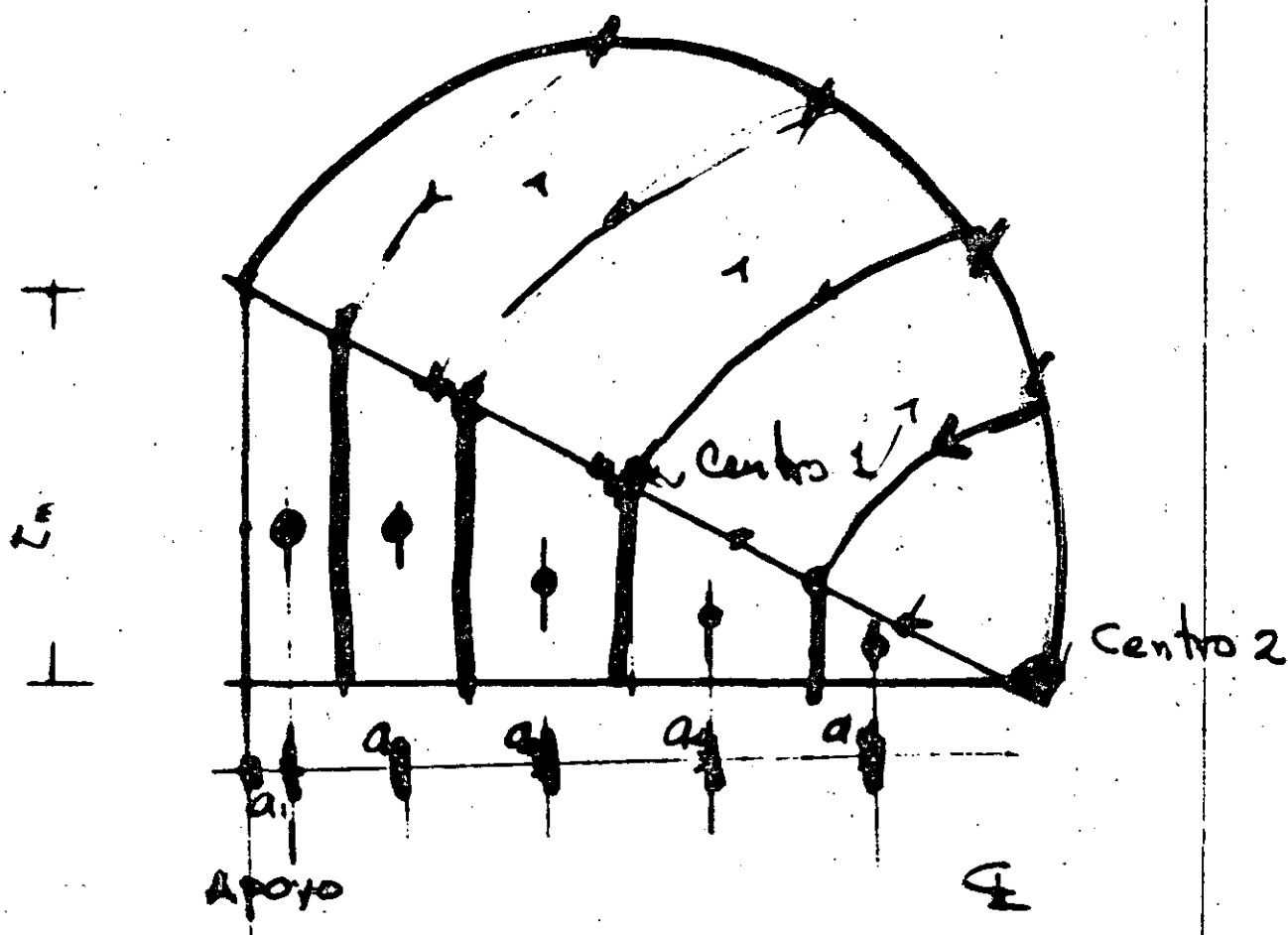


Fig. 8.4 Método gráfico para seleccionar separación entre conectores, cuando el corte varía linealmente se ilustra para  $N = 5$  conectores de corte

Condiciones de última resistencia en el cálculo de conectores de corte.

La fuerza última de compresión  $b_e$  variará linealmente y será menor o igual a

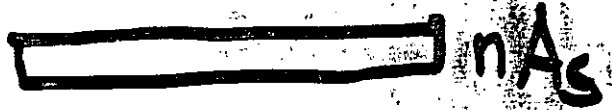
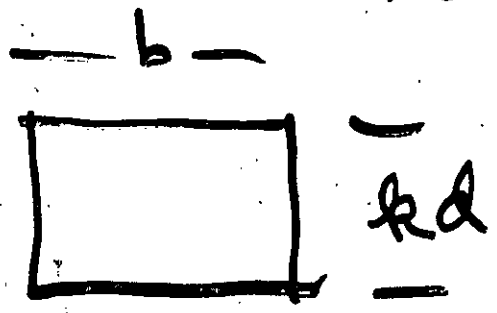
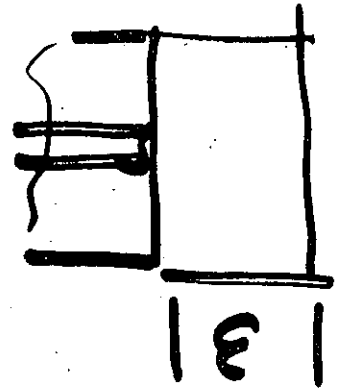
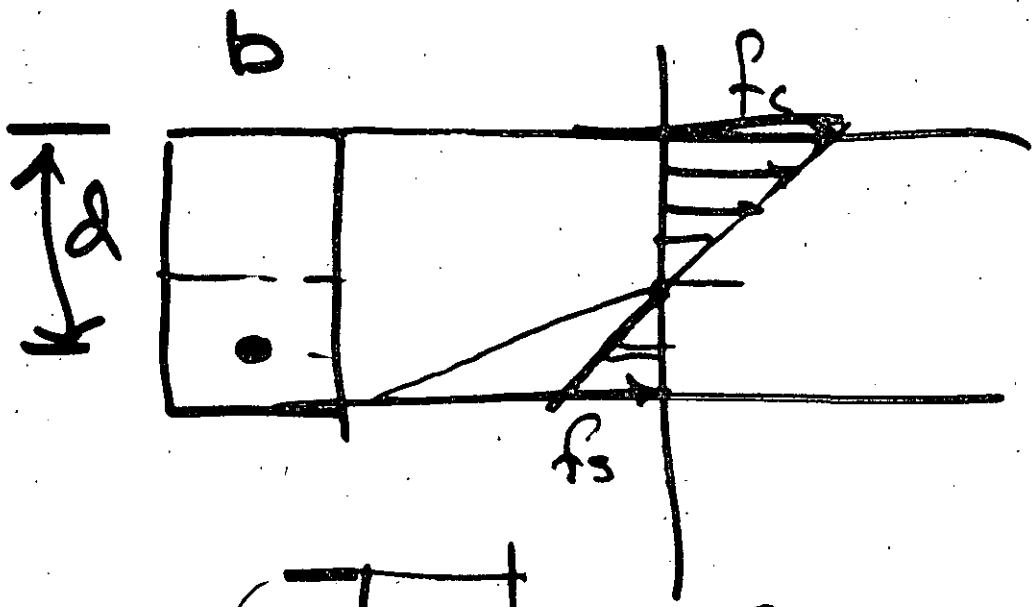
$$\text{[Diagrama de un conector de corte]} \quad C_m = 0.85 f_c' b_e t_s \quad (8.7)$$

$$\text{ó} \quad T_m = A_s f_y \quad (8.8)$$

Si un conector dado tiene una capacidad última  $(Q_{tu})$ , el número total de conectores entre los puntos de cero y máximo momento flector será

$$\left( \frac{N}{2} = \frac{C_m}{Q_{tu}} = \frac{T_m}{Q_{tu}} \right) \times \quad (8.9)$$

Es recomendable tomar el valor mayor determinado por (8.6) y (8.9) y distribuirlo linealmente, lo cual puede hacerse analíticamente o gráficamente como se indica en Fig. 8.4

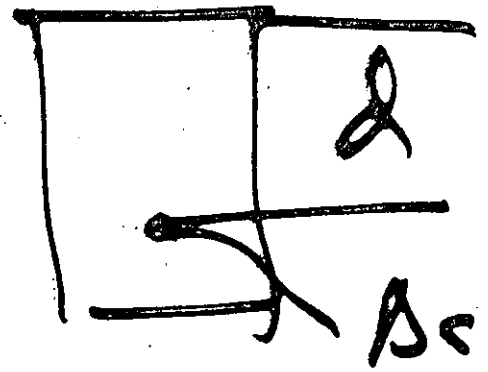
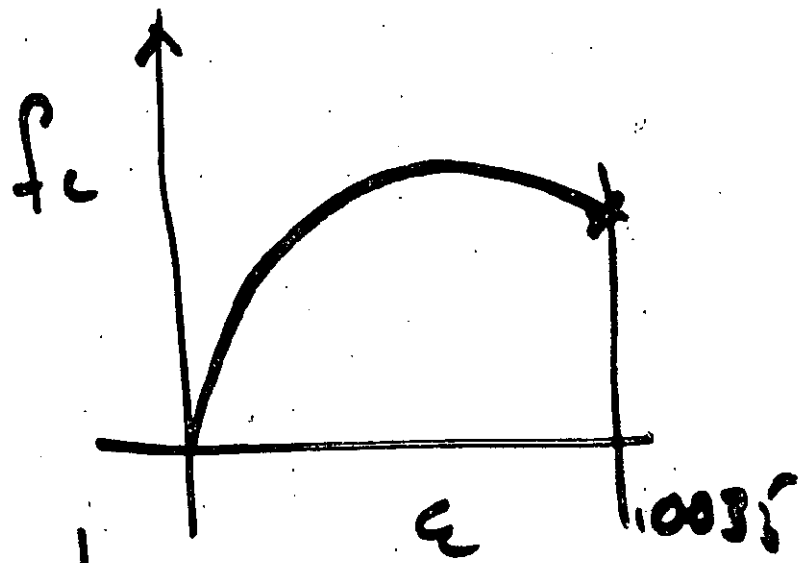
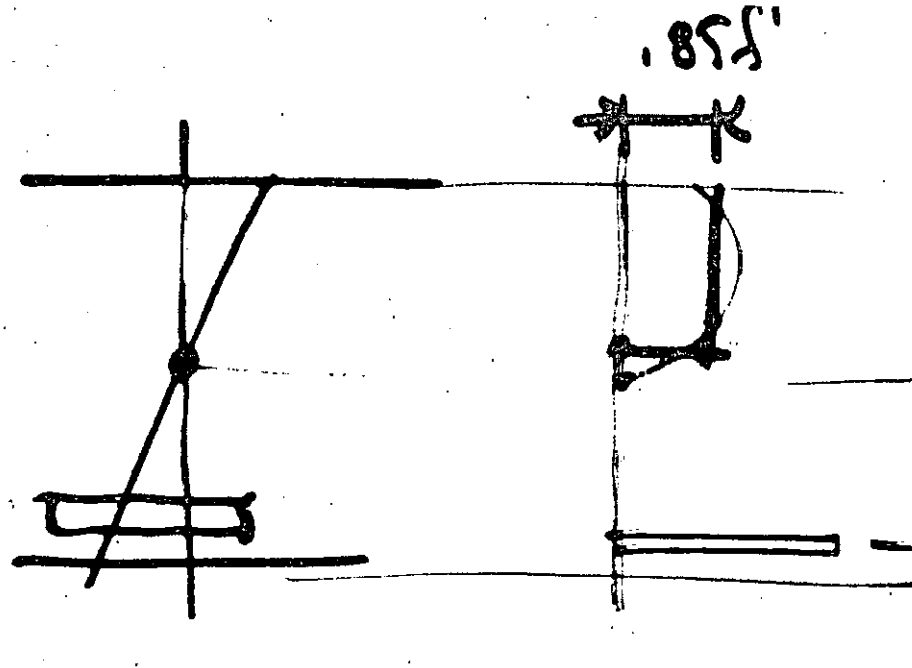


$\epsilon_c = \epsilon_s$   
 Comp & Def  
 Law de Hook

$$\frac{\Delta \epsilon_c}{\epsilon_c} = \frac{\Delta \epsilon_s}{\epsilon_s}$$

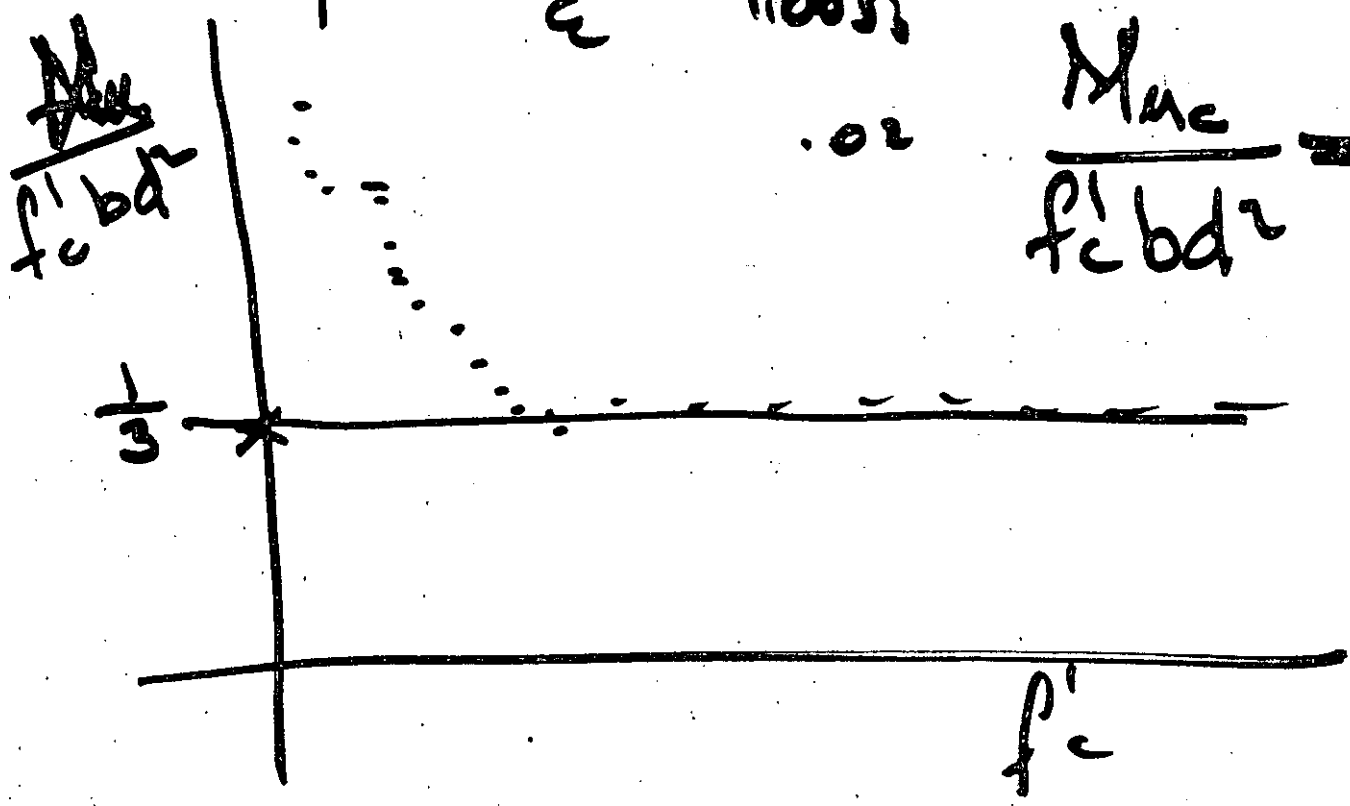
$$\Delta \epsilon_s = \frac{\epsilon_s}{\epsilon_c} \Delta \epsilon_c$$

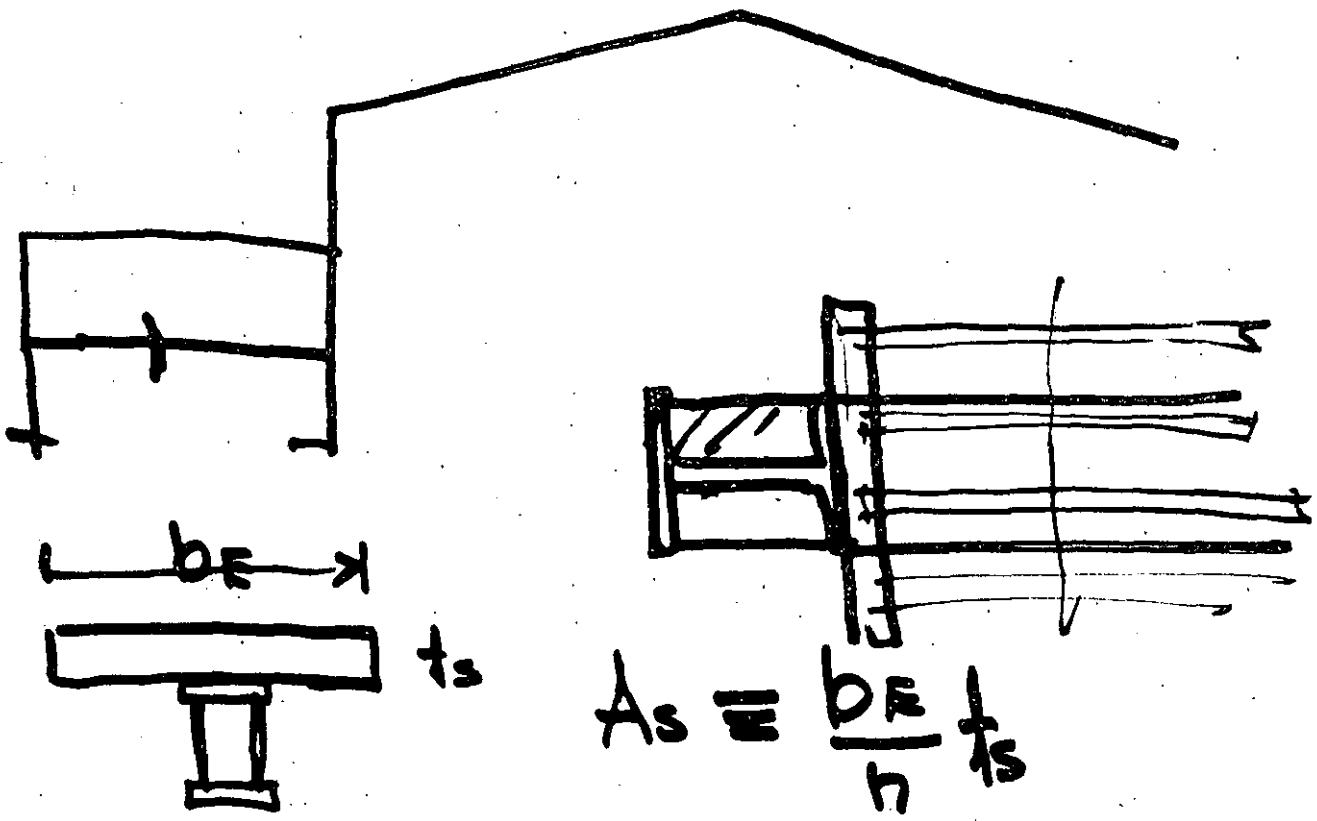
$$\Delta \epsilon_c = n \Delta \epsilon_s$$



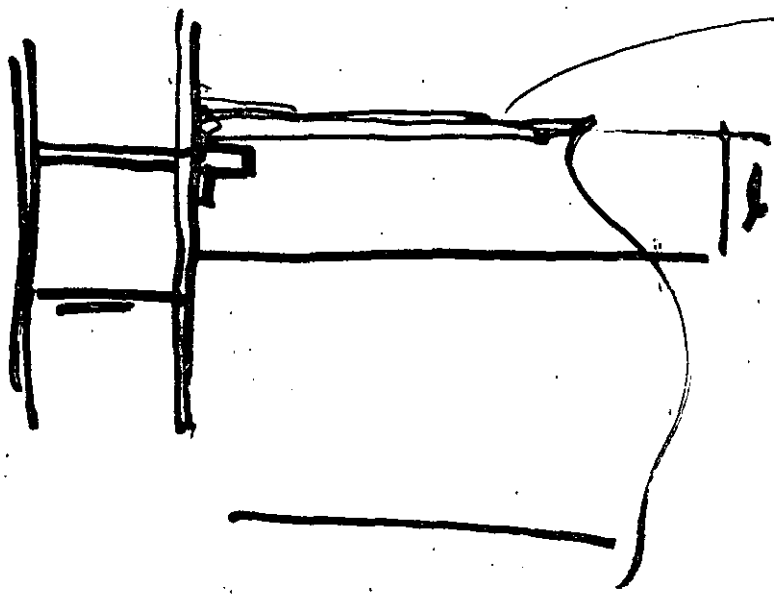
$$M_{ac} \approx (3.4) M_c$$

$$\frac{M_{ac}}{f_c b d^2} = \frac{1}{3}$$

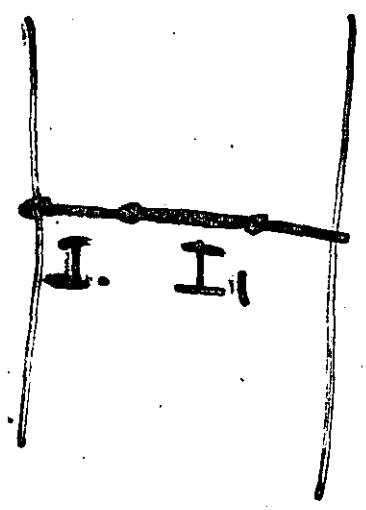




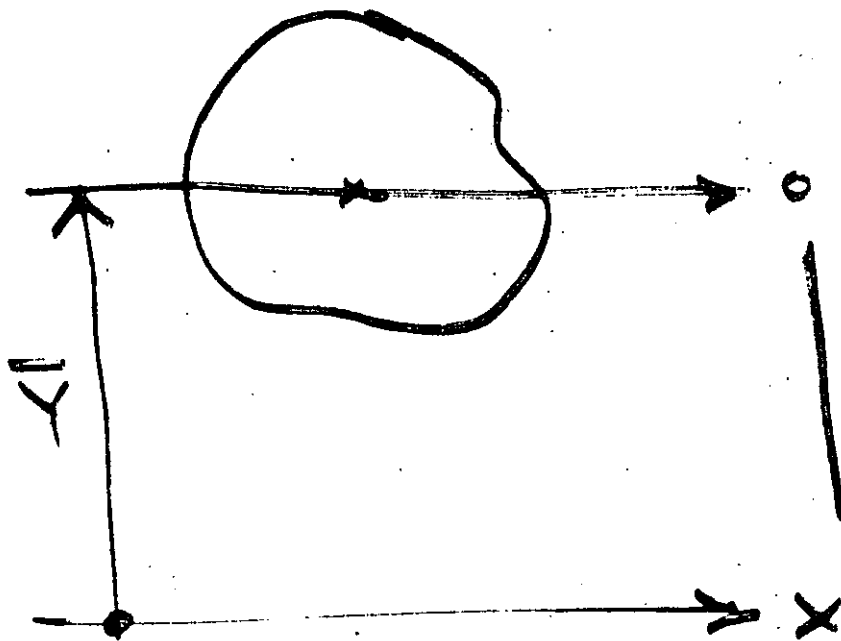
$$A_s = \frac{b d}{n} t_s$$



$\frac{L}{4}$   $\frac{L}{5}$

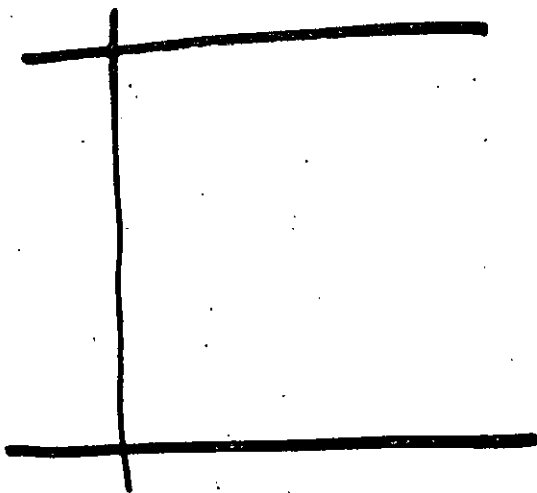






$$\underline{I_x = A \bar{y}^2 + I_{oo}}$$

$$\bar{y} = \frac{\sum A_i \bar{y}_i}{\sum A_i} = \frac{\int y dA}{\int dA} = \frac{Q_x}{A}$$





**DIVISION DE EDUCACION CONTINUA  
FACULTAD DE INGENIERIA U.N.A.M.**

DISEÑO DE ESTRUCTURAS DE ACERO

FORMULAS DE DISEÑO PARA VIGAS Y  
TRABES ARMADAS

ING. RAUL GRANADOS GRANADOS

NOV. 84

1  
FORMULAS DE DISEÑO PARA VIGAS  
Y TRABES ARMADAS.

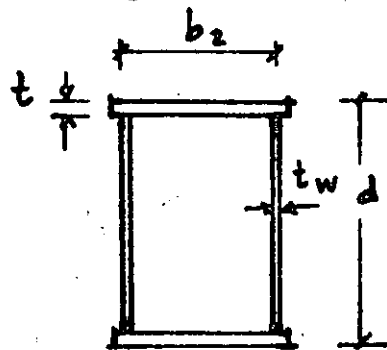
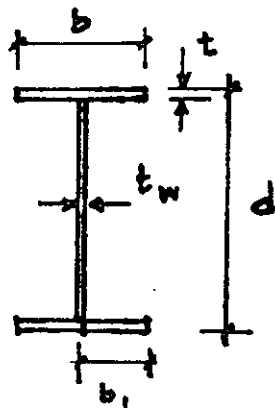
FLEXION

- A) Tensión y compresión en las fibras extremas de perfiles laminados o armados "COMPACTOS" :

$$F_b = 0.66 F_y \quad (1670 \text{ kg/cm}^2)$$

REQUISITOS PARA SECCIONES COMPACTAS :

- 1) Los patines están unidos continuamente con el alma
- 2) Se satisfacen las siguientes relaciones:



$$\frac{b_1}{t} \leq \frac{543}{\sqrt{F_y}} \quad (10.8)$$

$$\frac{d}{t_w} \leq \frac{1594}{\sqrt{F_y}} \quad (31.7)$$

$$\frac{b_2}{t} \leq \frac{5367}{\sqrt{F_y}} \quad (106.7)$$

$$3) \left(\frac{L}{b}\right) \leq \frac{637}{\sqrt{F_y}} \quad (13)$$

$$\frac{Ld}{A_f} \leq \frac{1400\ 000}{F_y} \quad (553)$$

aplicables a secciones no circulares ni tipo cajón.

$L$ : longitud no soportada lateralmente

$A_f$ : área del patín ( $bt$ )

$$4) \left(\frac{L}{b_2}\right) \leq \frac{137\ 000 + 84370 \frac{M_1}{M_2}}{F_y} \geq \frac{84370}{F_y} \quad (3),$$

$\left(\frac{L}{b_2} \leq 54 + 33 \frac{M_1}{M_2}\right)$   
 aplicable a secciones en cajón rectangulares  
 con relación  $\frac{d}{b_2} \leq 6$  y relación

$$t/t_w \leq 2$$

$M_1$  y  $M_2$  momentos menor y mayor en los extremos del tramo no soportado lateralmente.

5) La relación diámetro / espesor de pared no excederá de  $\frac{23\ 2000}{F_y}$  en secciones tubulares circulares.  $\gamma$  (92)

B) Cuanto se satisficieren los requisitos anteriores excepto que:

$$\frac{543}{\sqrt{F_y}} \leq \frac{b_1}{t} \leq \frac{796}{\sqrt{F_y}} \quad (10.8 \leq \frac{b_1}{t} \leq 15.8)$$

$$F_b = F_y \left[ 0.79 - 0.000239 \left( \frac{b_1}{t} \right) \sqrt{F_y} \right]$$

$$(F_b = F_y \left[ 0.79 - 0.012 \frac{b_1}{t} \right])$$

C) Tension y compresion en fibras extremas de secciones I o H que cumplen con los requisitos de secciones compactas, pero flexionadas alrededor del eje de menor inercia. Secciones circulares y cuadradas solidas y secciones rectangulares macizas flexionadas alrededor del eje de menor momento de inercia:

$$F_b = 0.75 F_y \quad (1890 \text{ kg/cm}^2)$$

D) Si las secciones I o H del inciso anterior satisficieren los requisitos de secciones compactas, excepto que:

$$\frac{543}{\sqrt{F_y}} \leq \frac{b_1}{t} \leq \frac{796}{\sqrt{F_y}} \quad (10.8 \leq \frac{b_1}{t} \leq 15.8)$$

$$F_b = F_y \left[ 1.075 - 0.0006 \left( \frac{b_1}{t} \right) \sqrt{F_y} \right]$$

$$(F_b = F_y \left[ 1.075 - 0.03 \frac{b_1}{t} \right])$$

E) Secciones tubulares rectangulares que satisfacen los requisitos de secciones compactas pero flexionadas alrededor del eje de menor inercia:

$$F_b = 0.66 F_y \quad (1670 \text{ kg/cm}^2)$$

F) Tensión y compresión en las fibras extremas de secciones en cajón que no satisfacen los requisitos de secciones compactas, pero sí los necesarios para evitar problemas de pandeo local:

$$F_b = 0.60 F_y \quad (1520 \text{ kg/cm}^2)$$

En estos miembros se requiere investigar la posibilidad de pandeo lateral solo si

~~MIEMBROS~~  $\frac{d}{b} > 6$

G) Para todas las demás secciones no consideradas anteriormente:

1) Tensión:  $F_b = 0.6 F_y \quad (1520 \text{ kg/cm}^2)$

2) Compresión:

a) Miembros sin problemas de pandeo local con un eje de simetría y car-

gados en el eje del  $\alpha I_m^2$  y canales flexionados alrededor del eje de mayor momento de inercia:

El valor mayor de los calculados con I y II sin exceder de  $0.6 F_y$  ( $1520 \text{ kg/lam}^2$ )

$$\text{Si } \sqrt{\frac{7150000 C_b}{F_y}} \leq \frac{L}{r_T} \leq \sqrt{\frac{35830000 C_b}{F_y}}$$

$$\left( 53 \sqrt{C_b} \leq \frac{L}{r_T} \leq 119 \sqrt{C_b} \right)$$

$$\text{(I) } \left\{ \begin{array}{l} F_b = \left[ 0.667 - \frac{F_y \left( \frac{L}{r_T} \right)^2}{109.6 \times 10^6 C_b} \right] F_y \\ \left( F_b = 1680 - \frac{\left( \frac{L}{r_T} \right)^2}{16.8 C_b} \right) \end{array} \right.$$

$$\text{Si } \frac{L}{r_T} \geq \sqrt{\frac{35830000 C_b}{F_y}} \quad (119 \sqrt{C_b})$$

$$F_b = \frac{11.95 \times 10^6 C_b}{\left( \frac{L}{r_T} \right)^2}$$

o cuando el patin de compresion es solido y aproximadamente rectangular y su area no es menor que la del patin de tension:

$$\text{(II) } \text{---} F_b = \frac{843700 C_b}{\frac{L_d}{A_f}}$$

En canales solo la <sup>6</sup> fórmula II es aplicable.

b) Miembros sin problemas de pandeo local pero no incluidos en (a)

$$F_b = 0.60 F_y \quad (1520 \text{ kg/cm}^2)$$

siempre y cuando se flexionen alrededor del eje de mayor momento de inercia y estén arriostrados lateralmente a intervalos tales que:

$$\frac{L}{b} \leq \frac{637}{\sqrt{F_y}} \quad (12.7)$$

En las expresiones I y II

$$C_b = 1.75 + 1.05 \frac{M_1}{M_2} + 0.3 \left( \frac{M_1}{M_2} \right)^2 \leq 2.3$$

$M_1$  y  $M_2$  momentos menor y mayor en los extremos de la longitud no arriostrada

$\frac{M_1}{M_2}$  se tomara positivo si el tramo se flexiona en curvatura doble y se tomara negativo en caso contrario.



7  
RELACIONES ANCHO/ESPESOR PARA EVITAR  
PROBLEMAS DE PANDEO LOCAL

$$\frac{b_1}{t} \leq \frac{796}{\sqrt{F_y}} \quad (15.8) \quad \text{secciones I}$$

$$\frac{b_2}{t} \leq \frac{1995}{\sqrt{F_y}} \quad (39.7) \quad \text{secciones caja}$$

CORTANTE

$$F_v = 0.40 F_y \quad (1010 \text{ kg/cm}^2) \quad \text{en almas sin} \\ \text{problemas de esbeltez}$$

DEFLEXIONES

$$\Delta_{max} = \frac{L}{360} \quad (\text{Flecha producida solo por} \\ \text{carga viva})$$

8

## REQUISITOS ADICIONALES PARA TRABES ARMADAS

$$A/m_2 : \quad \frac{h}{t} \leq \frac{985000}{\sqrt{F_y} (F_y + 1160)} \quad (322)$$

Esfuerzo cortante :

$$F_v = \frac{F_y}{2.89} C_v \leq 0.40 F_y \quad (\text{Sin atiesadores})$$

$$(F_v = 875 C_v \leq 1010 \text{ kg/cm}^2)$$

$$C_v = \frac{3160000 k}{F_y (h/t)^2} \quad \text{si } C_v \leq 0.8$$

$$(C_v = \frac{1249 k}{(h/t)^2}) \quad \text{" " "}$$

~~$$F_v = \frac{F_y}{2.89} C_v$$~~

$$C_v = \frac{1590}{h/t} \sqrt{\frac{k}{F_y}} \quad \text{si } C_v > 0.8$$

$$(C_v = \frac{31.6}{h/t} \sqrt{k}) \quad \text{" " "}$$

$$k = 5.34 + \frac{4}{(a/h)^2} \quad \text{si } a/h \geq 1$$

$$k = 4.00 + \frac{5.34}{(a/h)^2} \quad \text{si } a/h \leq 1$$

$$F_v = \frac{F_y}{2.89} \left[ C_v + \frac{1 - C_v}{1.15 \sqrt{1 + \left(\frac{a}{h}\right)^2}} \right] \leq 0.4 F_y \text{ CON ATIESADORES}$$

$$\left( F_v = 875 \left[ C_v + \frac{1 - C_v}{1.15 \sqrt{1 + \left(\frac{a}{h}\right)^2}} \right] \leq 1010 \text{ kg/cm}^2 \right)$$

a: separación de atiesadores

h: peralte del alma

t: espesor del alma.

## ATIESADORES

Área necesaria:

$$A_{ST} = \frac{1 - C_v}{2} \left[ \frac{a}{h} - \frac{\left(\frac{a}{h}\right)^2}{\sqrt{1 + \left(\frac{a}{h}\right)^2}} \right] \gamma D h t$$

D = 1.0 atiesadores en pares

D = 1.8 ✓ de 1 solo ángulo

D = 2.4 ✓ de 1 sola placa

$$\gamma = \frac{F_y \text{ alma}}{F_y \text{ patines}}$$

Momento de inercia  $I = \left(\frac{h}{50}\right)^4$

Esfuerzo para cálculo de los elementos de unión de los atiesadores al alma (MINIMO)

$$f_{vs} = h \sqrt{\left(\frac{F_y}{1400}\right)^3}$$

$$(f_{vs} = 2.42 h)$$

Reducción del esfuerzo en el patín de compresión por esbeltez del alma 10

$$F'_b = F_b \left[ 1.0 - 0.0005 \frac{A_a}{A_f} \left( \frac{h}{t} - \frac{6370}{\sqrt{F_y}} \right) \right]$$

$$\left( F'_b = F_b \left[ 1.0 - 0.0005 \frac{A_a}{A_f} \left( \frac{h}{t} - 127 \right) \right] \right)$$

$A_a$  : área del alma

$A_f$  : área del patín.

Combinación de esfuerzos de flexión y cortante.

Esfuerzo de tensión

$$F_b'' = \left( 0.825 - 0.375 \frac{f_v}{F_v} \right) F_y$$

$$\left( F_b'' = \left[ 2087 - 949 \frac{f_v}{F_v} \right] \right)$$

Aplastamiento del alma

Almas sujetas a cargas interiores :

$$\frac{R}{t(N+2K)} \leq 0.75 F_y \quad (1897 \text{ kg/cm}^2)$$

Almas sujetas a reacciones extremas :

$$\frac{R}{t(N+K)} \leq 0.75 F_y \quad (1897 \text{ kg/cm}^2)$$

Adicionalmente cuando <sup>11</sup> existan cargas con-  
centradas o distribuidas, no soportadas  
por atornilladores, el esfuerzo en el alma  
no excederá de:

$$\left[ 2 + \frac{4}{(a/h)^2} \right] \frac{703\,000}{(h/t)^2}$$

si el patín no  
está restringido  
~~intencionalmente~~  
contra rotación

$$\left[ 5.5 + \frac{4}{(a/h)^2} \right] \frac{703\,000}{(h/t)^2}$$

si el patín está  
restringido con-  
tra rotación



**DIVISION DE EDUCACION CONTINUA  
FACULTAD DE INGENIERIA U.N.A.M.**

DISEÑO DE ESTRUCTURAS DE ACERO

NAVES INDUSTRIALES DE ACERO

ING. JOSÉ LUIS SANCHEZ M.

NOV. 84

# Naves Industriales de Acero

## I - ESTRUCTURACION

Una nave industrial se caracteriza por llenar los requisitos necesarios para que en su interior puedan realizarse las operaciones típicas de una línea de producción industrial.

Las naves industriales frecuentemente son edificios de un solo piso con muy pocas o ninguna divisiones intermedias de modo que la estructura está localizada en las paredes perimetrales y en la cubierta que salva Jams usualmente de magnitud considerable.

La función de la cubierta es techar la superficie de la nave, es claro que la carga más importante que actúa sobre una cubierta es su peso propio y que, por lo tanto, conviene que los materiales que la integran sean lo más ligeros posibles. Se han usado tradicionalmente, láminas de asbesto, láminas metálicas, o losas precoladas de concreto ligero, apoyadas sobre estructuras de acero. Esta solución proporciona esa característica de ligereza directamente ligada a la economía de la construcción.

2

Se presentará aquí, esquemáticamente, el proyecto de una cubierta industrial del tipo mencionado.

Las dimensiones de la planta, de  $24 \times 80$  m se muestran en la fig 1.

Se proponen como elementos estructurales básicos marcos formados por armaduras de alma abierta apoyadas sobre columnas en forma de vigueta formada con tres placas soldadas.

El material de la cubierta se apoya en un sistema de largueras que tiene por fin transmitir el peso de ese material a las armaduras principales.

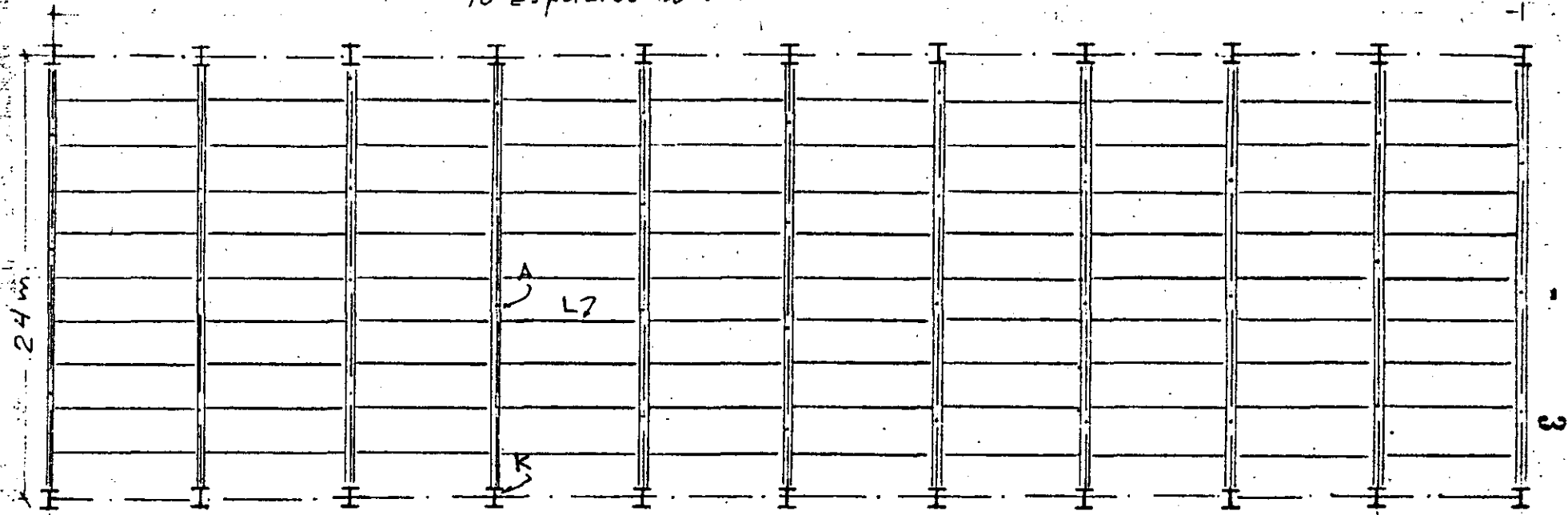
Las paredes de la nave, por razones de economía, se forman utilizando láminas de asbesta acanalada que requieren para su apoyo de otro sistema de largueros sustentado en las columnas principales (Fig. 2).

Los elementos estructurales mencionados, largueras, armaduras y columnas, constituyen un conjunto estable para soportar las fuerzas verticales que actuarán sobre la construcción; cargas muertas (peso propio de todos los elementos estructurales o no, que gravitan sobre ella) y cargas vivas (nieve, granizo, etc). Sin embargo ante la acción de fuerzas horizontales, (sismo o viento) el sistema no resulta estable.

Si las columnas y las armaduras principales se



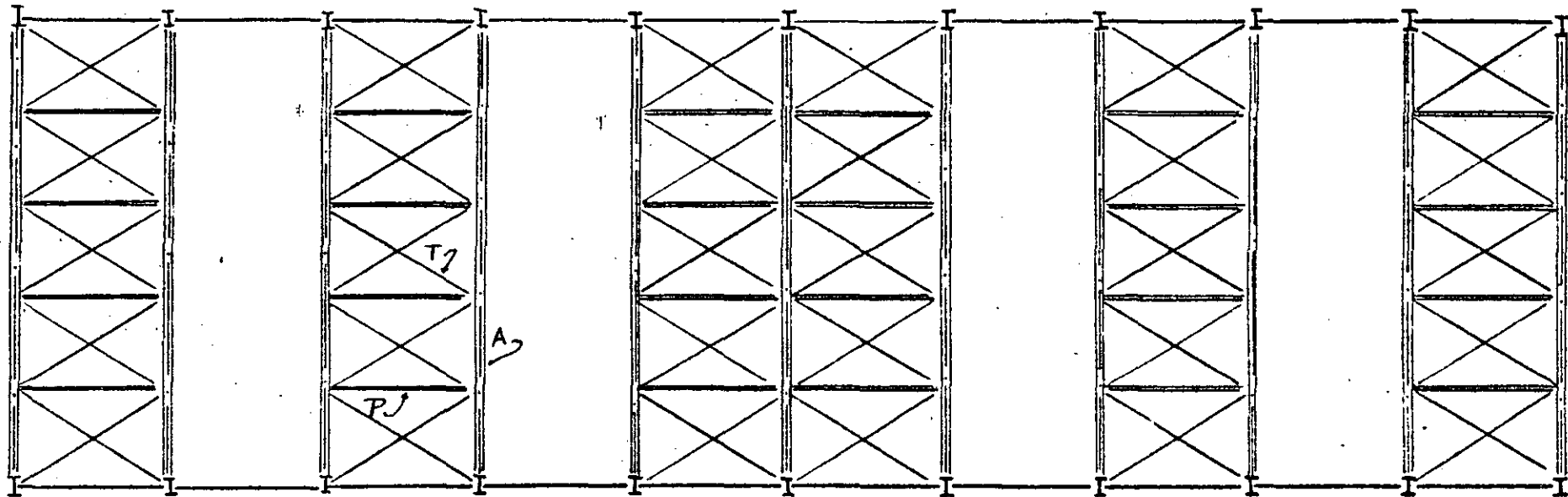
10 espacios @ 8m = 80m.



PLANTA

Distribución de columnas, armaduras y largueros.-

- A: Armaduras.
- K: Columnas.
- L: Largueros.



Distribución de contraventeo en cuerda inferior.-

- P: Puntales.
- T: Tirantes.
- A: Armaduras.

ligan rigidamente, la estructura se hace resistente en el sentido transversal ante fuerzas en esa dirección inclusive superando la base de las columnas articulada.

Sin embargo, el conjunto no tiene todavía capacidad apreciable ante fuerzas horizontales perpendiculares a su propio plano o sea en el sentido longitudinal de la nave. Cubría la posibilidad de formar marcos rígidos también en esa dirección para lograrla pero resulta en general más eficiente proporcionar en las paredes laterales, un sistema de contraventeo que transmita a la cimentación las cargas horizontales a través de fuerzas axiales en armaduras formadas por el contraventeo, las columnas y puntales longitudinales (fig 2)

Logada la estabilidad en estas dos direcciones, cualquier fuerza actuando sobre la estructura podrá descomponerse en ellas y la encontrará estable.

Una estructura además de estable debe ser económica y además funcional. El sistema estructural descrito ha demostrado ser una de las soluciones más económicas para resolver este tipo de problemas, al menos en lo que a cantidad de materiales se refiere.

Uno de los problemas de funcionamiento que debe resolverse al proyectar una nave industrial es el de su iluminación adecuada, su solución influye en la solución estructural y es por ella que en este proyecto

Los huecos se distribuyen en la forma llamada de frente de sierra en que, a través de las armaduras que funcionan como grandes ventanas orientadas al norte, se obtiene una iluminación conveniente.

Para que las fuerzas horizontales en el sentido longitudinal lleguen a los elementos que las han de transmitir a la cimentación y a las armaduras que se han dispuesto

en las paredes, es necesario utilizar algunos elementos adicia- nales que en el caso son contravientos formados por armaduras

en el nivel del patin inferior de las principales, cualquier fuerza horizontal longitudinal en la cubierta puede transmi- tirse a las paredes a través de este sistema de contraven-

tos (Fig. 3). La transmisión no sería adecuada si estos elementos lo que los hace necesarios, además

la tendencia de la cubierta a deslizar hacia abajo también es evitada con este contraviento que a veces se

coloca, también con buenos resultados en el plano del techo.

Aprovechando el efecto de diafragma de la losa del techo (capacidad de transmitir cargas en su propio plano)

este contraviento se coloca uniendo cada dos huecos, además se colocará una cruz y otra no ya que esto

basta para rigidificar toda la estructura.

## II - CARGAS

### a) Cargas muertas.

Son las que actúan en forma permanente y constante. Incluyen el peso de todas las elementos que componen la estructura, el peso de la losa del techo y la impermeabilización.

Aunque estas cargas son las que pueden valerse con mayor precisión no se conocen en detalle antes de haber diseñado la estructura, por ello tienen que estimarse a partir de un diseño preliminar o como resultado de experiencias anteriores.

En este ejemplo las cargas muertas serían:  
para el cálculo de largueros:

losa de siporex (7 cm)	53	Kg/m <sup>2</sup>	(catálogo)
impermeabilización	20	"	estimado
largueros	7	"	"
	<hr/>		
	80	Kg/m <sup>2</sup>	

para el cálculo de las armaduras añadir  
por peso de armaduras, ventanal y contraventeo

250 Kg/m (estimado)

Sobre carga útil Kg/m <sup>2</sup>	Longitudes máximas en cm.					
	Espesor de losas, cm.					
	7.5	10	12.5	15	17.5	20
50	250	350	400	475	525	550
100	225	325	375	425	475	525
150	200	300	350	400	450	525
200	175	275	325	400	450	500
250	200	275	350	400	450	500
300	200	250	325	375	425	475
350	175	250	300	350	400	450
400	175	250	275	350	375	425
450	150	225	275	325	375	400
500	150	225	275	325	375	400
550	150	225	250	300	350	375
600	125	200	250	300	325	350
<b>PESO</b> kg/m <sup>2</sup>	49	65	81	98	114	130

### LOSAS STANDARD

Existen para entrega inmediata, con un descuento especial, losas standard de las siguientes características:

Longitud cm.	Losas de techo para sobrecarga útil de			
	50 Kg/m <sup>2</sup>		100 Kg/m <sup>2</sup>	
	Espesor, cm.	Peso Propio, Kg/m <sup>2</sup>	Espesor, cm.	Peso Propio, Kg/m <sup>2</sup>
175	7.5	49	7.5	49
225	7.5	49	10	65
275	10	65	10	65

### INCOMBUSTIBILIDAD

Siporex es totalmente incombustible. Las losas de techo han sido clasificadas en: Suecia, Inglaterra, Alemania, Francia, Canadá y EE.UU., según normas oficiales, como resistentes al fuego.

### ASLAMIENTO TERMICO

El coeficiente de conductividad térmica k en las losas Siporex de peso volumétrico 0.5 es 0.1K cal/°C. hr, m para fines de cálculo.

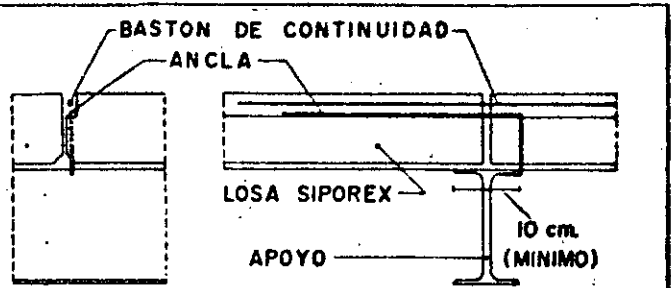


FIG. 2

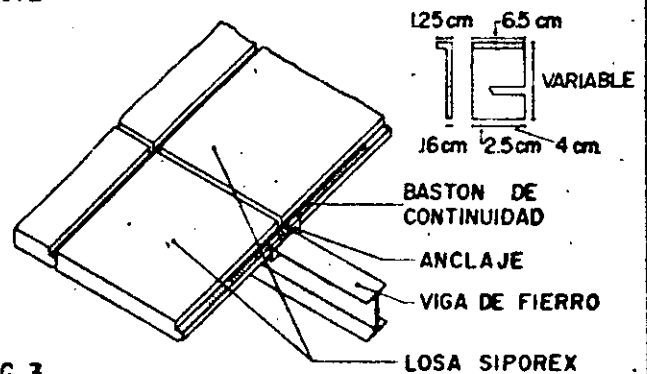


FIG. 3

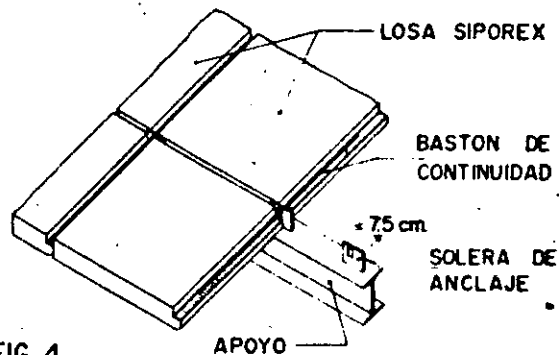


FIG. 4

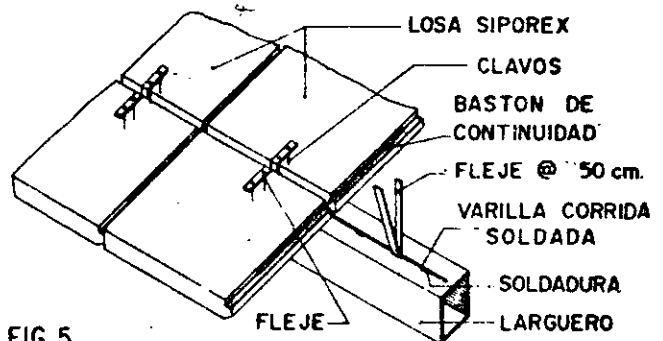


FIG. 5

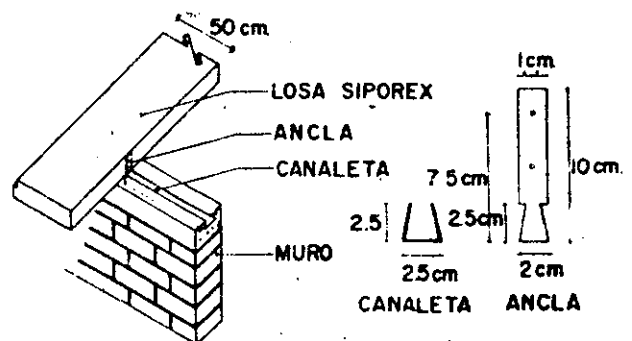


FIG. 6

Espesor de la losa en cm.	7.5	10	12.5	15	17.5	20	22.5	25
$U = \frac{K \text{ cal}}{^{\circ}\text{C. hr. m}^2}$	1.29	1.03	0.86	0.74	0.65	0.58	0.52	0.47

Los valores U para los techos, considerando la humedad del material y sin tomar en cuenta la impermeabilización son los que se muestran en la tabla anterior.

### ABSORCION DE SONIDO

Frecuencia ciclos por segundo	Materiales		
	125	500	2000
Siporex aparente	0.02	0.19	0.34
Aplanado liso	0.02	0.02	0.04
Aplanado rugoso	0.04	0.06	0.05
Concreto aparente	0.01	0.02	0.02
Vidrio	0.10	0.04	0.02

FIG. 7

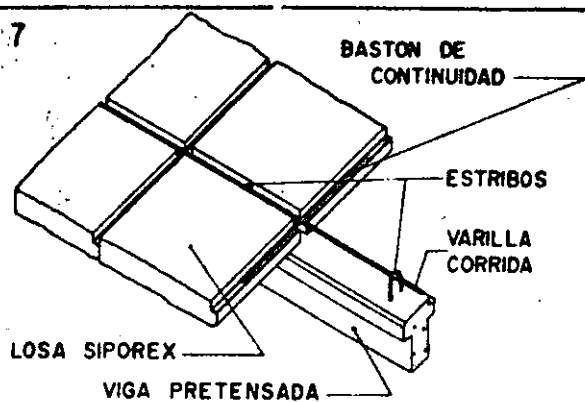


FIG. 8

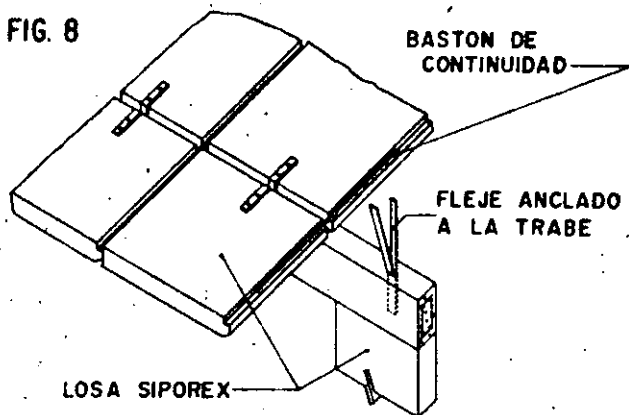


FIG. 9

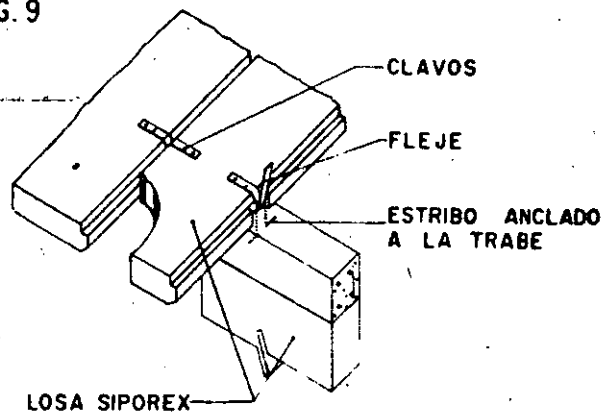
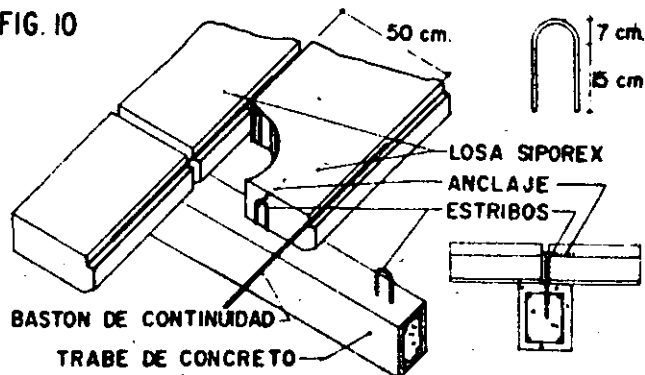


FIG. 10



### DETALLES CONSTRUCTIVOS

#### ANCLAJE

Es necesario fijar las losas Siporex a los elementos de soporte, mediante algún sistema de anclaje. En las figuras 2 al 10 se muestran algunos ejemplos.

#### BASTONES DE CONTINUIDAD

En las ranuras de las losas, precisamente a la altura de los apoyos, deberán alojarse varillas de  $\phi 6.3$  ó  $7.9$  mm. y de longitud aproximadamente igual a  $1/3$  de la longitud de la losa y como mínimo 80 cm. Estas varillas se introducen a presión en el mortero de relleno, en forma tal que queden totalmente embebidas en el mismo y a 10 ó 15 mm. de profundidad.

#### JUNTEO

Las ranuras que quedan entre losa y losa, se rellenan con mortero de cemento y arena (1:3), teniendo cuidado de mojar previamente la ranura y de que el mortero se coloque suficientemente fluido. No debe caminarse sobre las losas antes de que fragüe este mortero.

10 6.

b) Cargas vivas =

Son las que la estructura soportará normalmente durante su vida útil pero que no tienen carácter permanente.

El caso en estudio no está cubierto precisamente por el Reglamento de las Construcciones que menciona únicamente azoteas.

La carga viva más importante que pueda presentarse en esta estructura es el granizo y se estimará en  $40 \text{ Kg/m}^2$

c) Cargas accidentales =

Las constituyen las provocadas por la acción del viento y el sismo.

En cubiertas es bastante frecuente que la carga accidental que decide el diseño sea el viento, esto es debido principalmente a dos factores, la ligereza de la estructura y la amplia superficie expuesta al viento.

En este problema la primera condición no se cumple del todo luego conviene considerar ambas posibilidades.



## c) Carga de viento

11

La presión del viento es directamente proporcional al cuadrado de su velocidad, el Manual de diseño de obras civiles de la C.F.E. da recomendaciones para calcular las fuerzas de viento.

La presión se valúa con la expresión siguiente:

$$p = 0.0048 G C V_0^2$$

en ella

$G$  es un factor que tiene en cuenta la reducción de la densidad de la atmósfera con la altura  $h$  en Km. a la que se halla la construcción respecto al nivel del mar.

$$G = \frac{8 + h}{8 + 2h}$$

$V_0$  es la velocidad de diseño que debe considerarse y que varía con las condiciones particulares de cada caso.

$$V_0 = V \left( \frac{z}{10} \right)^\alpha$$

$z$  = altura de la estructura o zona de la misma que se estudia, con respecto al suelo.

$\alpha$  = factor que depende de la topografía del terreno.

$$V = K_1 K_2 V_0$$

12

8

$V_0$  = Velocidad regional del viento.

$K_1$  = factor de topografía, tiene en cuenta también las características estructurales de la construcción que hacen que la respuesta al viento sea distinta para diferentes estructuraciones.

$K_2$  = factor que considera la importancia de la estructura que se diseña.

$C$  = factor de forma de la estructura en cuestión.

En la figura 4 se muestran los coeficientes que se considerarán para el caso que se presenta en este ejemplo.

Multiplicando la presión del viento  $p$  por el área expuesta que también es definida para cada caso especial en el Manual mencionado.

Para nuestro caso al considerar el viento en el sentido longitudinal de la nave se recomienda tomar como área expuesta, además de las paredes verticales, el área vertical del primer diente más el 50% de la de todos los demás.

Deben considerarse además presiones o succiones interiores que dependen del porcentaje de aberturas que presente la nave. Cuando este es mayor del 30% del área expuesta se recomienda usar

$C = +0.8$  (presión) o  $C = -0.6$  (succión), lo que resulta más desfavorable. Cuando el porcentaje

es nulo se tomará  $\pm 0.3^{13}$  y para valores intermedios se interpolará.

Estas presiones se deben usar solamente para el diseño de elementos aislados y no para el análisis de la estabilidad de conjunto de la estructura.

La estructura que estudiamos supondremos tiene las características que siguen:

Localización: en la mesa central de la República,  
en campo abierto,  
en terreno plano,  
a 1 Km. sobre el nivel del mar.

Estructuración: tipo 1

Clase: grupo B

En esas condiciones se tiene:

$$p = 0.0048 G C V^2$$

$$G = \frac{8+h}{8+2h} = 0.9$$

$$V_0 = 140 \text{ Km/hora}$$

$$K_1 = 1.0$$

$$K_2 = 1.0$$

$$V = 1.0 \times 1.0 \times 140 = 140 \text{ Km/hora}$$

$$p = 0.0048 \times 0.9 \times 140^2 C = 84.7 C$$

Fuerza horizontal total debida al viento -

Sentido longitudinal:

Pared de barlovento:  $84.7 \times 0.75 \times 11.3 \times 24 = 17222 \text{ Kg}$

Pared de sotavento:  $84.7 \times 0.68 \times 8 \times 24 = 11058 \text{ ''}$

Techo:  $10 \times 84.7 \times 0.68 \times 24 \times 0.63 \times \sin 22^\circ = 5117 \text{ ''}$

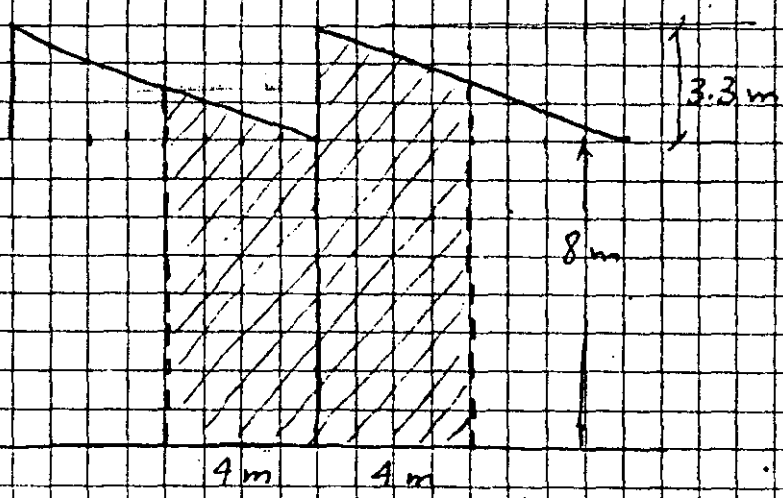
Ventanas verticales:  $84.7 \times 0.75 \times 24 \times 3.3 \times 0.5 \times 9 = 22640 \text{ ''}$

Total  $56037 \text{ Kg}$

Sentido trans versal

Consideraremos el area tributaria correspondiente a un

marco



Area =  $74 \text{ m}^2$

Empuje =  $84.7 C \times 74 = 84.7 (0.75 + 0.68) 74 = 8950 \text{ Kg}$

15

## Fuerza horizontal total debida al sismo -

De acuerdo con el Reglamento para las Construcciones en el D.F. la fuerza constante en la base de la construcción que se utilice para el diseño es igual a un coeficiente sísmico multiplicado por el peso de la construcción.

En nuestro caso el peso aproximado es de:

$$\text{En el techo} = 80 \text{ m} \times 24 \text{ m} \times 80 \text{ Kg/m}^2 = 153600 \text{ Kg}$$

$$\text{En las paredes} = 2 \times 80 \text{ m} \times 9.65 \text{ m} \times 20 \text{ Kg/m}^2 = 30880 \text{ "}$$

$$+ 2 \times 24 \text{ m} \times 11.3 \text{ m} \times 20 \text{ "} = 10850 \text{ "}$$

$$\text{Total } 195330 \text{ Kg.}$$

y el coeficiente sísmico máxima se presenta en el sentido longitudinal de la nave en que se tiene una estructura contraventada:

zona de baja compresibilidad	} Coeficiente sísmico 0.08
estructura del grupo b	
estructura del tipo 2	

El constante en la base es entonces de:

$$195330 \times 0.08 = 15626 \text{ Kg.}$$

Esta fuerza es menor a la que se presenta por viento.

Si se considera ahora un marcu en el sentido transversal se tendrá:

$$\text{Peso del techo } 24 \text{ m} \times 8 \text{ m} \times 80 \text{ Kg/m}^2 = 15360 \text{ Kg}$$

$$\text{Peso de las paredes } 2 \times 8 \text{ m} \times 9.65 \text{ m} \times 20 \text{ Kg/m}^2 = 3088 \text{ Kg}$$

El coeficiente sísmico es en este caso de 0.04 por tratarse ahora de una estructura tipo 1, la fuerza será:

$$18448 \times 0.04 = 738 \text{ Kg}$$

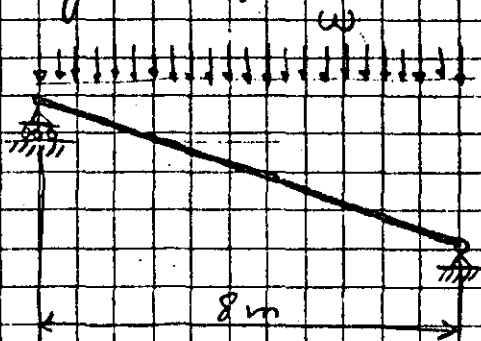
que también es bastante menor que la debida al viento.

### III ANALISIS DE LOS ELEMENTOS ESTRUCTURALES.

#### 1.- Largueros :-

Se supondrán libremente apoyados en las armaduras

Por carga vertical



w de carga muerta

$$w_{CM} = 80 \text{ Kg/m}^2 \times 2.4 \text{ m} = 192 \text{ Kg/m}$$

w de carga viva

$$w_{CV} = 40 \text{ Kg/m}^2 \times 2.4 = 86 \text{ Kg/m}$$

$$V_{CM} = 768 \text{ Kg}$$

$$V_{CV} = 384 \text{ Kg}$$

$$M_{CM} = 1536 \text{ Kg-m}$$

$$M_{CV} = 768 \text{ Kg-m}$$

Por carga vertical + viento

La fuerza sobre el techo es de succión y en el cable

mas des favorable v.l.c.:

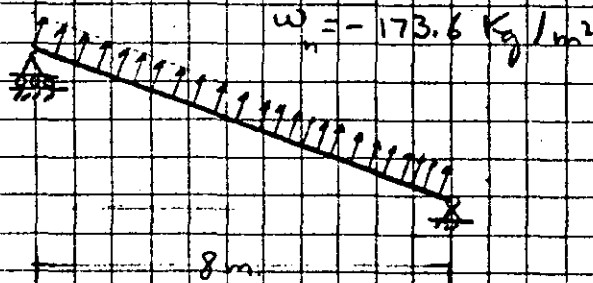
$$p_e = -1.75 \times 84.7 = -148.2 \text{ Kg/m}^2$$

a este valor debera agregarse el debido a las presiones interiores que en este caso supondremos se obtiene con un coeficiente de 0.3

$$p_i = -0.3 \times 84.7 = -25.4 \text{ Kg/m}^2$$

La carga sobre el larguero al actuar el viento sera entonces de:

$$-173.6 \text{ Kg/m}^2$$



Componente vertical:

$$w_v = -163 \text{ Kg/m}^2$$

Fga meta vertical

$$\begin{array}{r} -163 \text{ Kg/m}^2 \\ + 80 \\ \hline - 83 \end{array} \quad \text{'' (carga muerta)}$$

Se tendra entonces por carga muerta + viento:

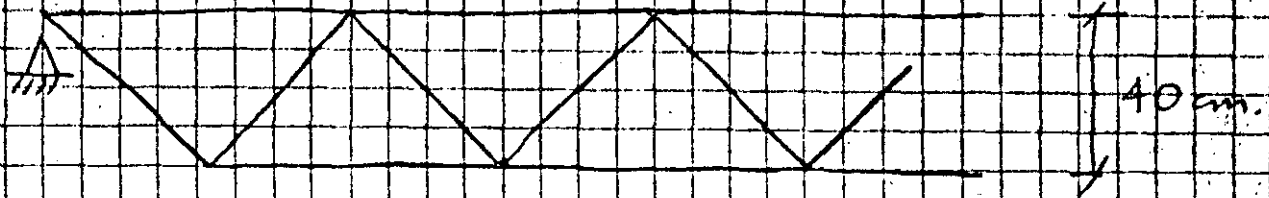
$$M_v = -1601 \text{ Kg-m}$$

$$V_v = -800 \text{ Kg}$$

La componente horizontal de la fuerza de viento produce una pequeña flexión adicional en el larguero que suele despreciarse.



## Análisis aproximado:



Carga viva + muerta:

$$\text{Fza en cada cuerda} = \frac{M}{d} = \frac{1536 + 768}{0.4} = 5760 \text{ Kg}$$

$$\text{Fza en la diagonal más desfavorable} = \frac{V}{\cos 45^\circ} = \frac{768 + 384}{0.7071} = 1629 \text{ Kg}$$

Carga muerta + viento

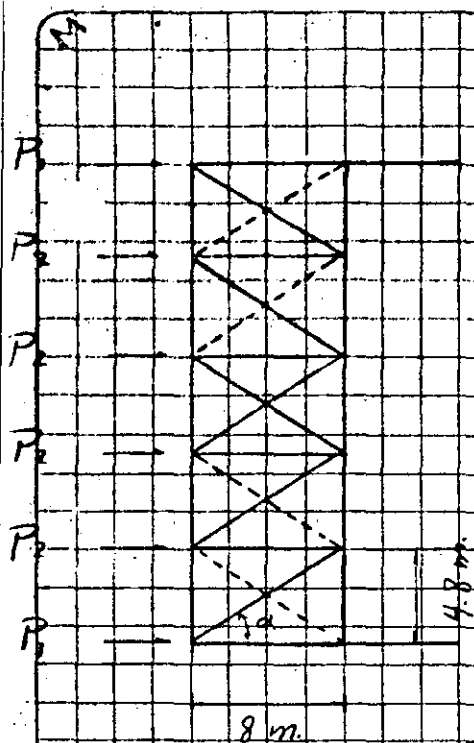
$$\text{Fza en cuerda} = 4000 \text{ Kg}$$

$$\text{Fza en diagonal} = 1131 \text{ Kg}$$

## 2. Contraventeo horizontal

Supondremos que la primera armadura horizontal soporta la reacción de la estructura de la pared y las fuerzas horizontales del primer tramo del techo.





19  
Carga P<sub>2</sub>

por la pared  $0.75 \times 84.7 \times \frac{11.3}{2} \times 4.8 = 1722 \text{ Kg}$

por el techo  $0.68 \times 84.7 \times 4.8 \times 8 \times 0.37 = 818$

por ventana vertical  $0.75 \times 84.7 \times 4.8 \times \frac{3.3}{2} = 503$

Total 3043 Kg

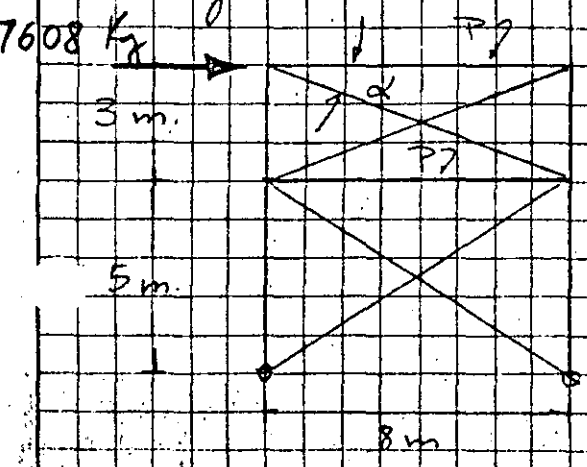
Carga P<sub>1</sub> 1522 Kg

Fza en el montante más cargado:  $\frac{2 \times 1522 + 3043 \times 4}{2} = 7608 \text{ Kg}$

Fza en la diagonal más cargada:  $\frac{7608 - 1522}{0.85} = 7076 \text{ Kg}$

3.- Contraventeo vertical

La primera cruzeta debe resistir la carga que le transmite la primera armadura del contraventeo horizontal



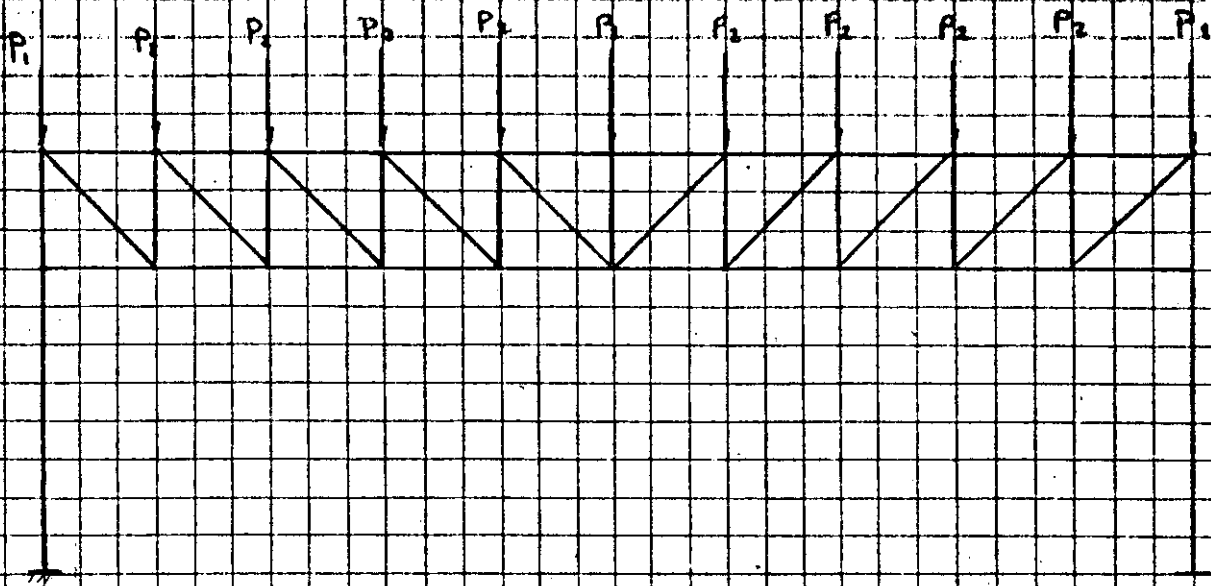
Fuerza en el puntal  $P_1 = 7608 \text{ Kg}$

Fuerza en la diagonal  $= \frac{7608}{0.85} = 8950 \text{ Kg}$

# A - Marcos Principales

20

## a) Carga vertical.



### Carga P<sub>2</sub> :

Por reacción del larguero : C.M. = 768 Kg  
C.V. = 384 kg

Por peso propio de la armadura y el vidrio

$$250 \text{ Kg/m} \times 2.4 = 600 \text{ Kg}$$

$$P_2 = 1752 \text{ Kg}$$

$$P_1 = 876 \text{ Kg}$$

## b) Carga muerta + viento longitudinal

Por reacción del larguero - 800 Kg

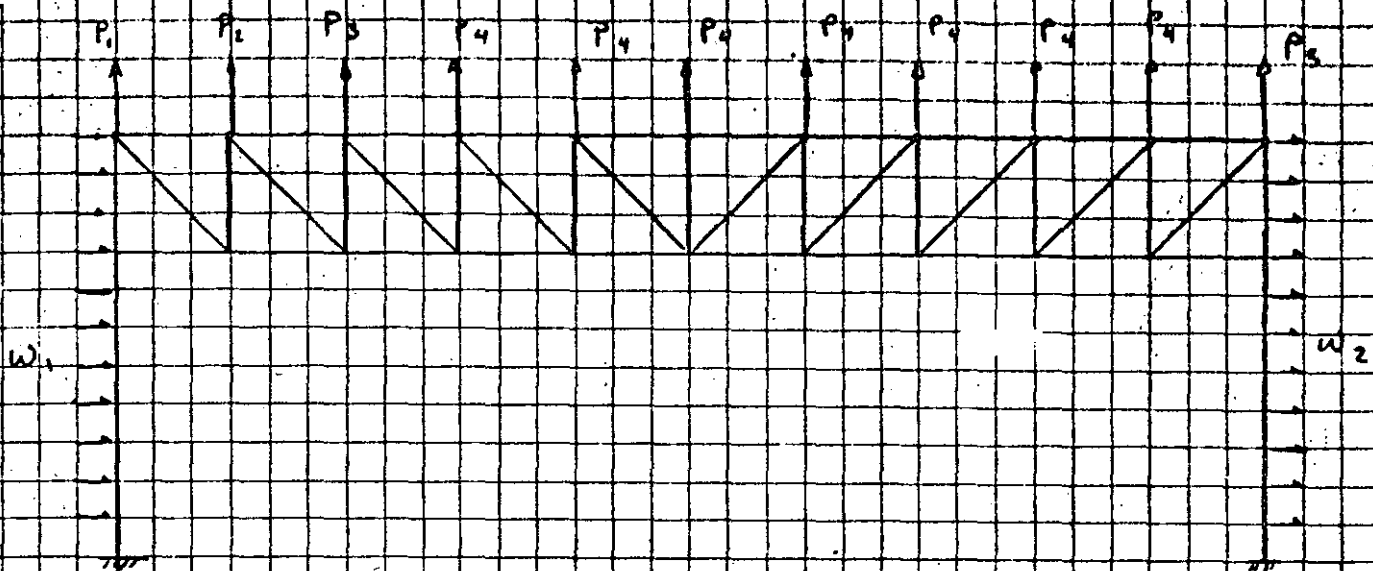
Por peso propio de armadura y vidrio + 600 Kg

$$P_2 = -200 \text{ Kg}$$

$$P_1 = -100 \text{ Kg}$$

# Carga de viento transversal

21



$$W_1 = 0.75 \times 84.7 \times 73.9 = 4694 \text{ Kg}$$

$$W_2 = 0.68 \times 84.7 \times 73.9 = 4256 \text{ "}$$

$$P_1 = 1.75 \times 84.7 \times \frac{2.4 \times 8}{2} \cos 22^\circ = 1320 \text{ Kg}$$

$$P_2 = 2640 \text{ "}$$

$$P_3 = \frac{P_2 + P_4}{2} = \frac{2640 + 1507}{2} = 2073 \text{ "}$$

$$P_4 = 1.0 \times 84.7 \times 2.4 \times 8 \times \cos 22^\circ = 1507 \text{ "}$$

# Carga de trabe carril -

22

Se supondrá como parte de la nave en estudio una trabe carril sobre la que se apoya una guisa con las características siguientes:

Capacidad en el gancho	50 Ton.
Peso del Puente	83.5 Ton.
Peso del carro	10.0 Ton.
Acercamiento máximo al eje del riel	1.8 m.

De acuerdo con las especificaciones del ALSC la carga en el gancho debe incrementarse en 25% por impacto

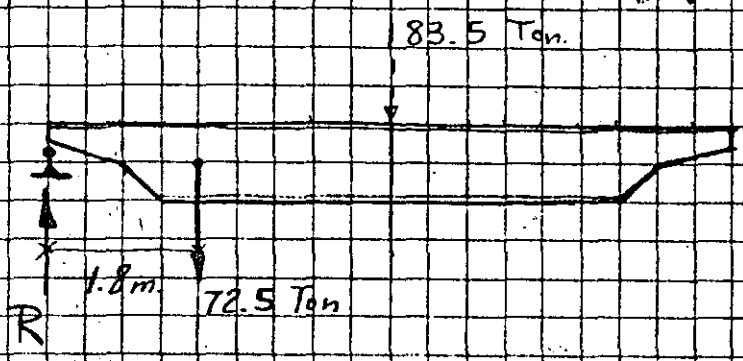
$$P_g = 50 \times 1.25 = 62.5 \text{ Ton.}$$

Además debe considerarse una fuerza horizontal aplicada en la parte superior del riel del 20% de la carga en el gancho más el peso del carro.

$$P_h = (50 + 10) \times 0.20 = 12 \text{ Ton}$$

Y una fuerza horizontal longitudinal del 10% de la reacción máxima de las ruedas

Reacciones máximas de la trabe guía sobre la armadura vertical.



$$R_{max} = \frac{83.5}{2} + \frac{72.5 \times 22.2}{24} = 109 \text{ Ton.}$$

$$R_{min} = 47 \text{ Ton.}$$

Reacción horizontal:

6 Ton. sobre cada columna

Momento debido a la excentricidad de la carga:

$$109 \times 0.25 = 27.25 \text{ T-m}$$

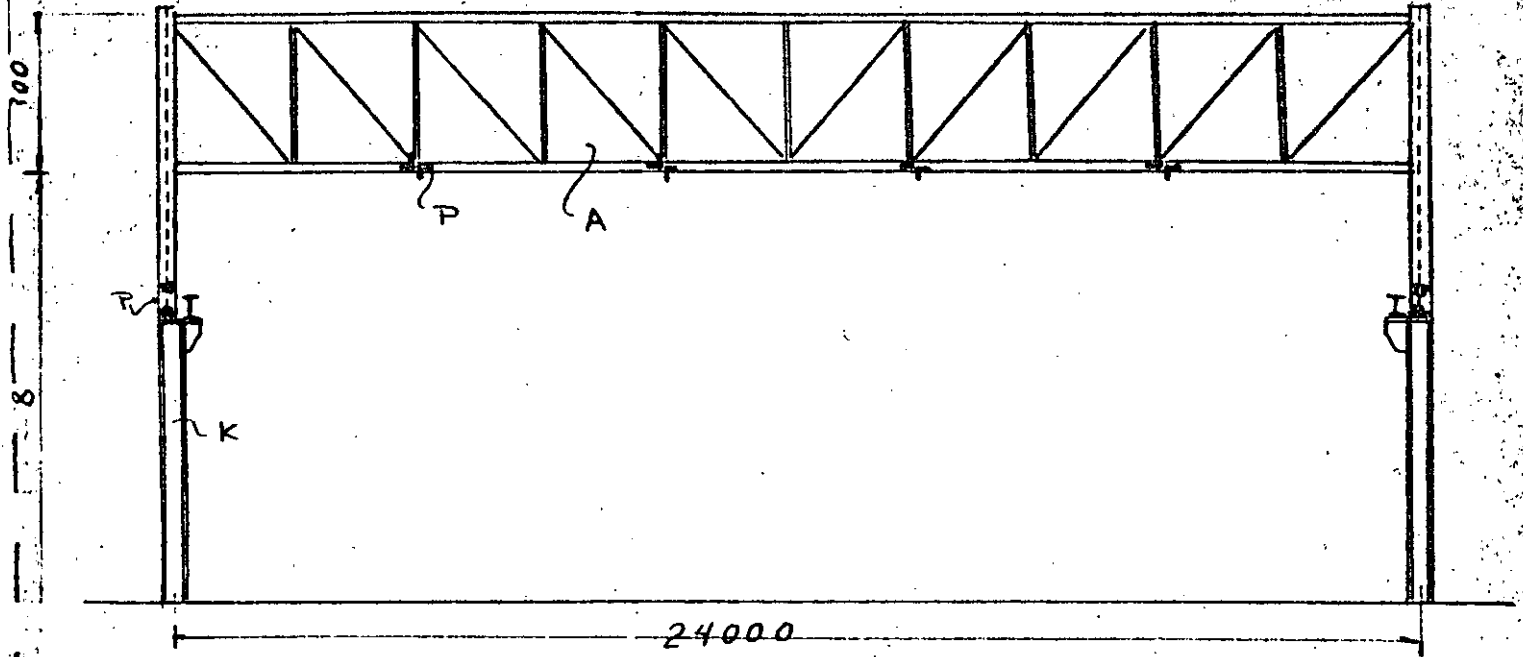
$$47 \times 0.25 = 11.75 \text{ T-m}$$

El análisis en este caso se realiza usando el programa STRESS para la solución de estructuras hiperestáticas que calcula, haciendo uso del método general de las rigideces, los elementos mecánicos y deformaciones en la estructura.

Se consideraran las siguientes condiciones de carga:

- 1.- Carga muerta
- 2.- Carga viva
- 3.- Carga de gema.
- 4.- Carga de viento transversal
- 5.- (1+2+3)
- 6.- (1+4)/1.5

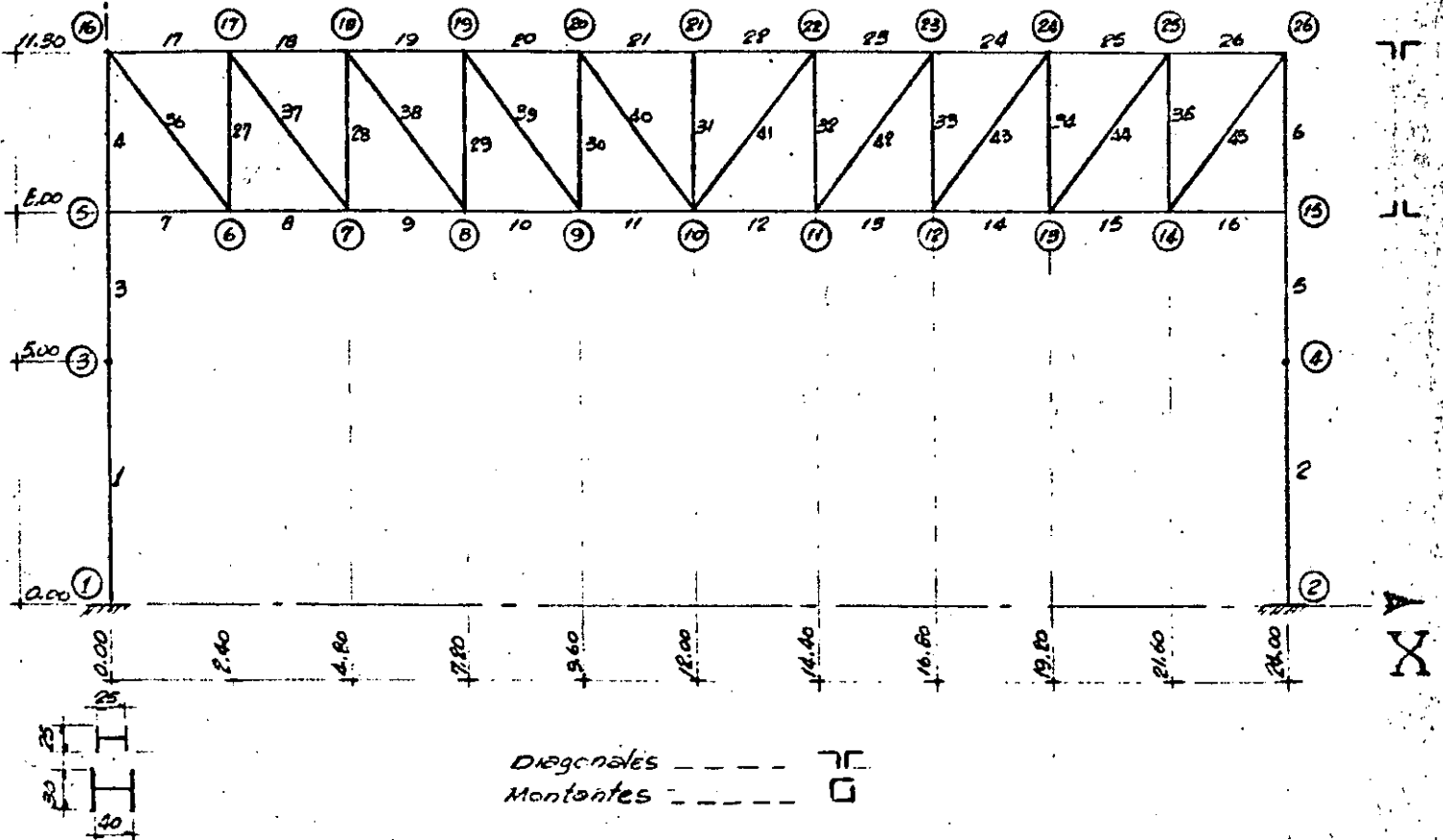
La ultima condicion se divide entre 1.5 para tener en cuenta que en este caso puede aceptarse un coeficiente de seguridad menor por ser el viento una condición variable.



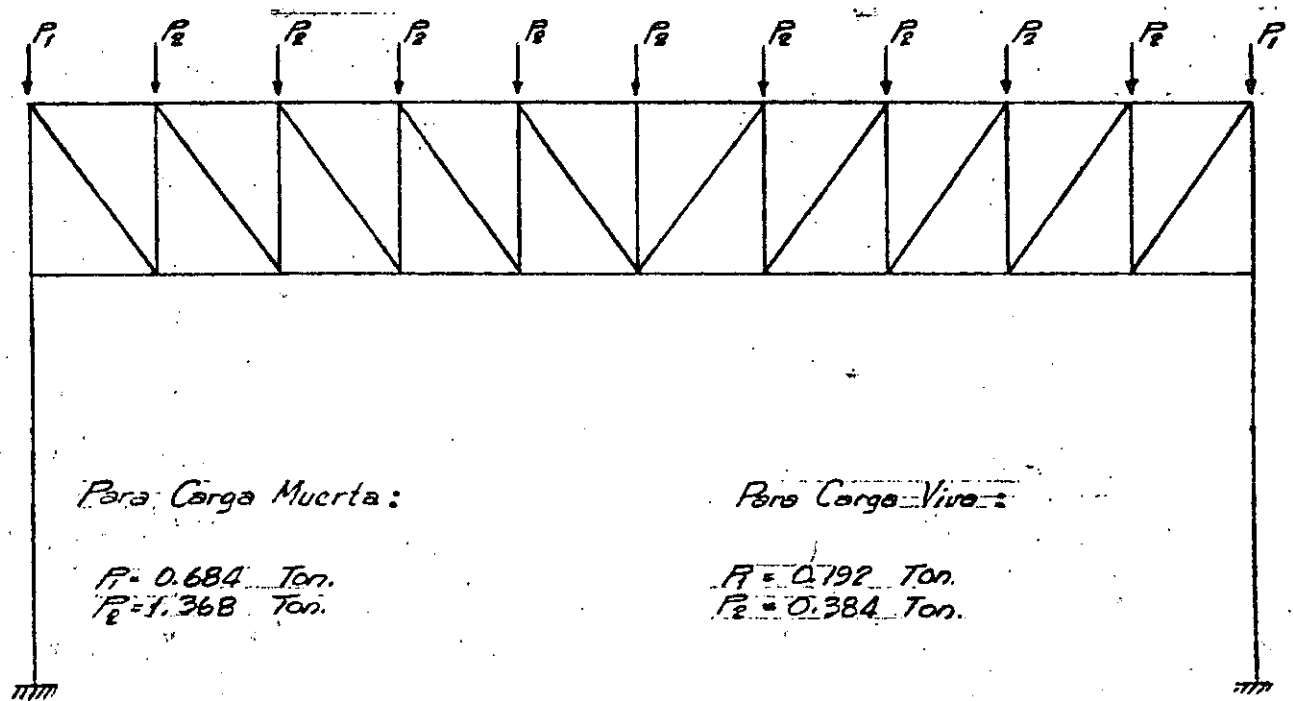
Elevación de un marco transversal tipo

# ANALISIS DEL MARCO TRANSVERSAL.

25



## CARGA VERTICAL.



Para Carga Muerta:

$$P_1 = 0.684 \text{ Ton.}$$

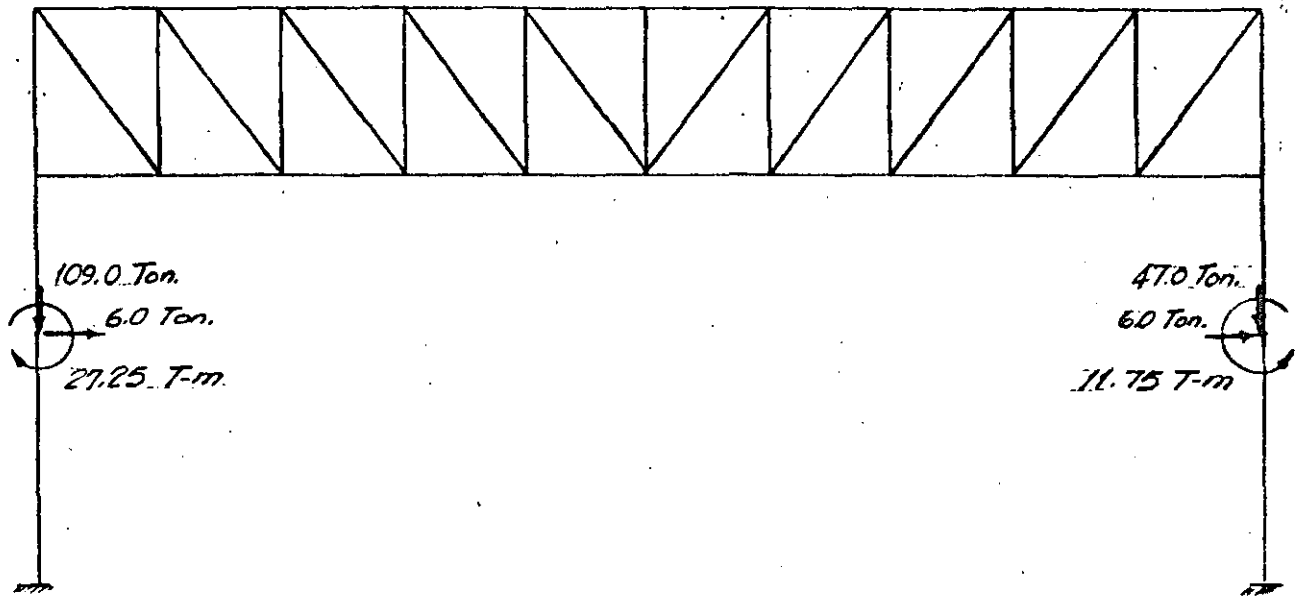
$$P_2 = 1.368 \text{ Ton.}$$

Para Carga Viva:

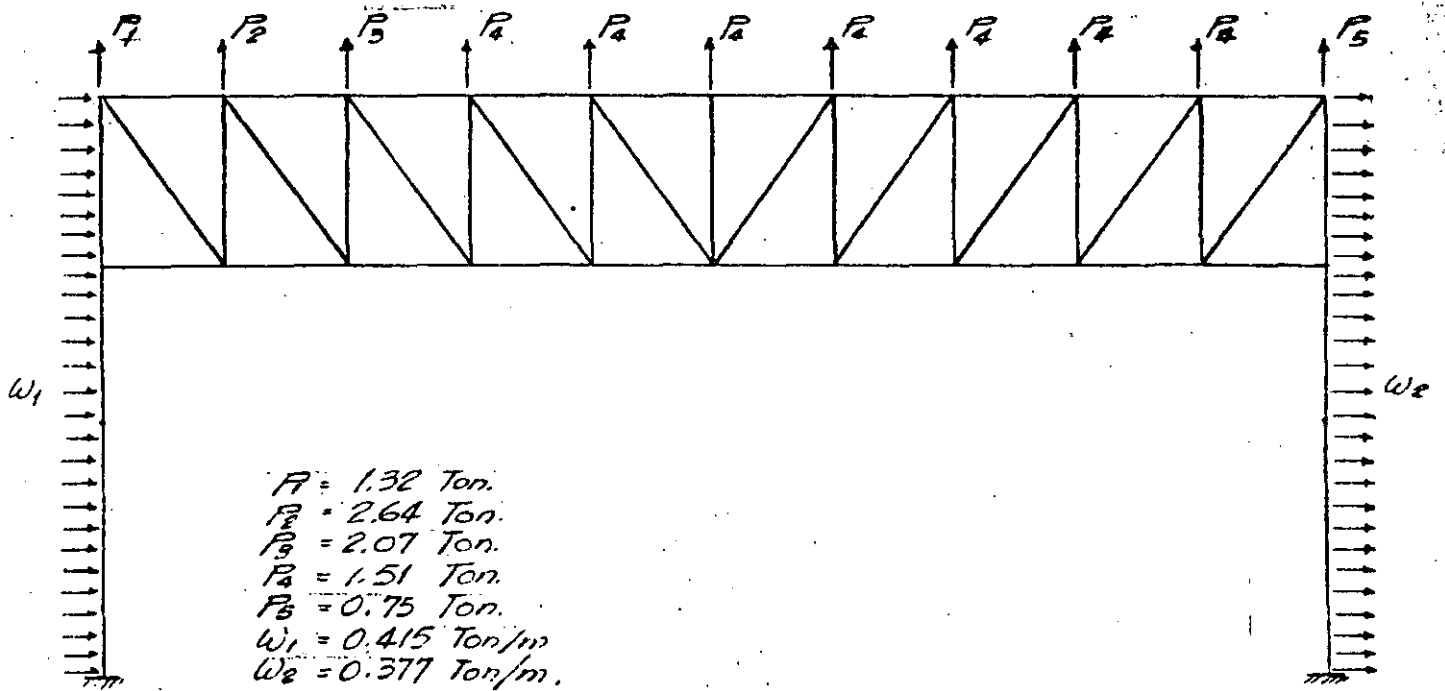
$$P_1 = 0.792 \text{ Ton.}$$

$$P_2 = 0.384 \text{ Ton.}$$

CARGA DE GRUA.-



CARGA DE VIENTO TRANSVERSAL.-





## STRUCTURE MARCO TRANSVERSAL TIPO

TYPE PLANE FRAME

NUMBER OF JOINTS 26

NUMBER OF MEMBERS 45

NUMBER OF SUPPORTS 2

NUMBER OF LOADINGS 6

JOINT COORDINATES

1	0.00	0.00	S
2	24.00	0.00	S
3	0.00	5.00	
4	24.00	5.00	
5	0.00	8.00	
6	2.40	8.00	
7	4.80	8.00	
8	7.20	8.00	
9	9.60	8.00	
10	12.00	8.00	
11	14.40	8.00	
12	16.80	8.00	
13	19.20	8.00	
14	21.60	8.00	
15	24.00	8.00	
16	0.00	11.30	
17	2.40	11.30	
18	4.80	11.30	
19	7.20	11.30	
20	9.60	11.30	
21	12.00	11.30	
22	14.40	11.30	
23	16.80	11.30	
24	19.20	11.30	
25	21.60	11.30	
26	24.00	11.30	

MEMBER PROPERTIES PRISMATIC

1 THRU	2	AX	0.017490	IZ	0.000349373
3 THRU	6	AX	0.000813	IZ	0.000062516
7 THRU	16	AX	0.002296	IZ	0.000001258
17 THRU	26	AX	0.003096	IZ	0.000003088
27 THRU	35	AX	0.001162	IZ	0.000000703
36 THRU	45	AX	0.001162	IZ	0.000000458

MEMBER INCIDENCES

1	1	3
2	2	4
3	3	5
4	5	16
5	4	15
6	15	26
7	5	6
8	6	7
9	7	8
10	8	9
11	9	10
12	10	11
13	11	12

15	13	14
16	14	15
17	16	17
18	17	18
19	18	19
20	19	20
21	20	21
22	21	22
23	22	23
24	23	24
25	24	25
26	25	26
27	6	17
28	7	18
29	8	19
30	9	20
31	10	21
32	11	22
33	12	23
34	13	24
35	14	25
36	16	6
37	17	7
38	18	8
39	19	9
40	20	10
41	10	22
42	11	23
43	12	24
44	13	25
45	14	26

CONSTANTS E 21000000.0 ALL

TABULATE ALL

LOADING I CARGA MUERTA

JOINT LOADS

16	FORCE Y	-0.684
17	FORCE Y	-1.368
18	FORCE Y	-1.368
19	FORCE Y	-1.368
20	FORCE Y	-1.368
21	FORCE Y	-1.368
22	FORCE Y	-1.368
23	FORCE Y	-1.368
24	FORCE Y	-1.368
25	FORCE Y	-1.368
26	FORCE Y	-0.684

LOADING II CARGA VIVA

JOINT LOADS

16	FORCE Y	-0.192
17	FORCE Y	-0.384
18	FORCE Y	-0.384
19	FORCE Y	-0.384
20	FORCE Y	-0.384
21	FORCE Y	-0.384

22 FORCE Y -0.384  
 23 FORCE Y -0.384  
 24 FORCE Y -0.384  
 25 FORCE Y -0.384  
 26 FORCE Y -0.192  
 LOADING III CARGA DE GRUA

JOINT LOADS

3 FORCE X 6.0  
 3 FORCE Y -109.0  
 3 MOMENT Z -27.25  
 4 FORCE X 6.0  
 4 FORCE Y -47.0  
 4 MOMENT Z 11.75

LOADING IV VIENTO TRANSVERSAL

JOINT LOADS

16 FORCE Y 1.320  
 17 FORCE Y 2.640  
 18 FORCE Y 2.073  
 19 FORCE Y 1.507  
 20 FORCE Y 1.507  
 21 FORCE Y 1.507  
 22 FORCE Y 1.507  
 23 FORCE Y 1.507  
 24 FORCE Y 1.507  
 25 FORCE Y 1.507  
 26 FORCE Y 0.7535

MEMBER LOADS

1 FORCE Y UNIFORM W -0.415  
 2 FORCE Y UNIFORM W -0.377  
 3 THRU 4 FORCE Y UNIFORM W -0.415  
 5 THRU 6 FORCE Y UNIFORM W -0.377

LOADING V AEREA MUERTA + CARGA VIVA + CARGA DE GRUA

COMBINE 1 1.0 2 1.0 3 1.0

LOADING VI CARGA MUERTA + VIENTO TRANSVERSAL

COMBINE 1 0.75 4 0.75

SOLVE .....

PROBLEM CORRECTLY SPECIFIED, EXECUTION TO PROCEED.

## STRUCTURE MARCO TRANSVERSAL TIPO

## LOADING I CARGA MUERTA

## MEMBER FORCES

MEMBER	JOINT	AXIAL FORCE	SHEAR FORCE	MOMENT
1	1	6.839	-0.233	-1.15
1	3	-6.839	0.233	-0.01
2	2	6.839	0.233	1.15
2	4	-6.839	-0.233	0.01
3	3	6.839	-0.233	0.01
3	5	-6.839	0.233	-0.71
4	5	6.788	0.170	0.63
4	16	-6.788	-0.170	-0.07
5	4	6.839	0.233	-0.01
5	15	-6.839	-0.233	0.71
6	15	6.788	-0.170	-0.63
6	26	-6.788	0.170	0.07
7	5	0.404	0.051	0.07
7	6	-0.404	-0.051	0.04
8	6	-4.018	0.002	-0.00
8	7	4.018	-0.002	0.01
9	7	-7.509	0.009	0.00
9	8	7.509	-0.009	0.01
10	8	-9.991	0.004	0.00
10	9	9.991	-0.004	0.01
11	9	-11.483	0.003	-0.00
11	10	11.483	-0.003	0.00
12	10	-11.483	-0.003	-0.00
12	11	11.483	0.003	0.00
13	11	-9.991	-0.004	-0.01
13	12	9.991	0.004	-0.00
14	12	-7.509	-0.009	-0.01
14	13	7.509	0.009	-0.00
15	13	-4.019	-0.002	-0.01
15	14	4.019	0.002	0.00
16	14	0.404	-0.051	-0.04
16	15	-0.404	0.051	-0.07
17	16	4.235	0.050	0.07
17	17	-4.235	-0.050	0.04
18	17	7.734	0.004	-0.00

31

12	0.0301	0.0019	-0.0001
13	0.0300	0.0014	-0.0003
14	0.0300	0.0008	0.0001
15	0.0299	0.0000	-0.0028
16	0.0304	0.0009	0.0014
17	0.0304	0.0017	-0.0000
18	0.0304	0.0021	0.0001
19	0.0304	0.0023	0.0000
20	0.0305	0.0024	0.0000
21	0.0305	0.0024	-0.0000
22	0.0306	0.0022	-0.0001
23	0.0307	0.0019	-0.0001
24	0.0307	0.0014	-0.0001
25	0.0308	0.0008	-0.0006
26	0.0308	0.0001	0.0010

STRUCTURE MARCO TRANSVERSAL TIPO

MEMBER FORCES FOR MEMBER 1

LOADING	JOINT	AXIAL FORCE	SHEAR FORCE	MOMENT
1	1	6.839	-0.233	-1.15
1	3	-6.839	0.233	-0.01
2	1	1.919	-0.065	-0.32
2	3	-1.919	0.065	-0.00
3	1	108.658	2.959	31.01
3	3	-108.658	-2.959	-16.21
4	1	-10.074	4.844	20.81
4	3	10.074	-2.769	-1.78
5	1	117.418	2.660	29.53
5	3	-117.418	-2.660	-16.23
6	1	-2.426	3.457	14.74
6	3	2.426	-1.901	-1.34

MEMBER FORCES FOR MEMBER 2

LOADING	JOINT	AXIAL FORCE	SHEAR FORCE	MOMENT
1	2	6.839	0.233	1.15
1	4	-6.839	-0.233	0.01
2	2	1.919	0.065	0.32
2	4	-1.919	-0.065	0.00

3	2	47.341	9.040	36.28
3	4	-47.341	-9.040	8.91
4	2	-7.260	4.105	17.72
4	4	7.260	-2.220	-1.91
5	2	56.101	9.339	37.76
5	4	-56.101	-9.339	8.92
6	2	-0.315	3.254	14.16
6	4	0.315	-1.840	-1.42

MEMBER FORCES FOR MEMBER 3

=====

LOADING	JOINT	AXIAL FORCE	SHEAR FORCE	MOMENT
1	3	6.839	-0.233	0.01
1	5	-6.839	0.233	-0.71
2	3	1.919	-0.065	0.00
2	5	-1.919	0.065	-0.20
3	3	-0.341	-3.040	-11.03
3	5	0.341	3.040	1.91
4	3	-10.074	2.769	1.78
4	5	10.074	-1.524	4.65
5	3	8.418	-3.339	-11.01
5	5	-8.418	3.339	0.99
6	3	-2.426	1.901	1.34
6	5	2.426	-0.967	2.95

MEMBER FORCES FOR MEMBER 4

=====

LOADING	JOINT	AXIAL FORCE	SHEAR FORCE	MOMENT
1	5	6.788	0.170	0.63
1	16	-6.788	-0.170	-0.07
2	5	1.905	0.047	0.17
2	16	-1.905	-0.047	-0.02
3	5	-0.306	-0.583	-1.85
3	16	0.306	0.583	-0.07
4	5	-9.925	-0.576	-4.40
4	16	9.925	2.045	-0.08
5	5	8.387	-0.364	-1.03
5	16	-8.387	0.364	-0.16
6	5	-2.352	-0.378	-2.82
6	16	2.352	1.405	-0.11

MEMBER FORCES FOR MEMBER 5

=====

LOADING	JOINT	AXIAL FORCE	SHEAR FORCE	MOMENT
1	4	6.839	0.233	-0.01
1	15	-6.839	-0.233	0.71
2	4	1.919	0.065	-0.00
2	15	-1.919	-0.065	0.20
3	4	0.341	3.040	2.83
3	15	-0.341	-3.040	6.28
4	4	-7.260	2.220	1.91
4	15	7.260	-1.089	3.04
5	4	9.101	3.339	2.82
5	15	-9.101	-3.339	7.19
6	4	-0.315	1.840	1.42
6	15	0.315	-0.992	2.82

## MEMBER FORCES FOR MEMBER 6

LOADING	JOINT	AXIAL FORCE	SHEAR FORCE	MOMENT
1	15	6.788	-0.170	-0.63
1	26	-6.788	0.170	0.07
2	15	1.905	-0.047	-0.17
2	26	-1.905	0.047	0.02
3	15	0.227	-1.913	-6.07
3	26	-0.227	1.913	-0.23
4	15	-7.282	-0.365	-2.99
4	26	7.282	1.610	-0.26
5	15	8.921	-2.132	-6.89
5	26	-8.921	2.132	-0.14
6	15	-0.370	-0.402	-2.72
6	26	0.370	1.335	-0.14

## MEMBER FORCES FOR MEMBER 7

LOADING	JOINT	AXIAL FORCE	SHEAR FORCE	MOMENT
1	5	0.404	0.051	0.07
1	6	-0.404	-0.051	0.04
2	5	0.113	0.014	0.02
2	6	-0.113	-0.014	0.01
3	5	2.455	-0.035	-0.06
3	6	-2.455	0.035	-0.02
4	5	-2.200	-0.149	-0.24
4	6	2.200	0.149	-0.10
5	5	2.973	0.030	0.03
5	6	-2.973	-0.030	0.03
6	5	-1.346	-0.073	-0.12
6	6	1.346	0.073	-0.04

## MEMBER FORCES FOR MEMBER 8

34

LOADING	JOINT	AXIAL FORCE	SHEAR FORCE	MOMENT
1	6	-4.018	0.002	-0.00
1	7	4.018	-0.002	0.01
2	6	-1.128	0.000	-0.00
2	7	1.128	-0.000	0.00
3	6	2.708	0.006	0.01
3	7	-2.708	-0.006	0.00
4	6	4.109	0.011	0.03
4	7	-4.109	-0.011	-0.00
5	6	-2.438	0.009	0.00
5	7	2.438	-0.009	0.01
6	6	0.068	0.010	0.02
6	7	-0.068	-0.010	0.00

## MEMBER FORCES FOR MEMBER 9

LOADING	JOINT	AXIAL FORCE	SHEAR FORCE	MOMENT
1	7	-7.509	0.009	0.00
1	8	7.509	-0.009	0.01
2	7	-2.107	0.002	0.00
2	8	2.107	-0.002	0.00
3	7	2.954	-0.001	-0.00
3	8	-2.954	0.001	-0.00
4	7	8.561	-0.014	-0.01
4	8	-8.561	0.014	-0.01
5	7	-6.662	0.010	0.00
5	8	6.662	-0.010	0.01
6	7	0.789	-0.003	-0.00
6	8	-0.789	0.003	-0.00

## MEMBER FORCES FOR MEMBER 10

LOADING	JOINT	AXIAL FORCE	SHEAR FORCE	MOMENT
1	8	-9.991	0.004	0.00
1	9	9.991	-0.004	0.01
2	8	-2.804	0.001	0.00
2	9	2.804	-0.001	0.00
3	8	3.204	-0.000	0.00
3	9	-3.204	0.000	-0.00
4	8	11.498	-0.004	0.00
4	9	-11.498	0.004	-0.01
5	8	-9.591	0.005	0.00



5	9	9.591	-0.005	35	0.01
6	9	1.130	-0.000		0.00
6	9	-1.130	0.000		-0.00

MEMBER FORCES FOR MEMBER 11

=====

LOADING	JOINT	AXIAL FORCE	SHEAR FORCE	MOMENT
1	9	-11.483	0.003	-0.00
1	10	11.483	-0.003	0.00
2	9	-3.223	0.000	-0.00
2	10	3.223	-0.000	0.00
3	9	3.451	-0.000	0.00
3	10	-3.451	0.000	-0.00
4	9	13.340	-0.004	0.00
4	10	-13.340	0.004	-0.01
5	9	-11.255	0.003	-0.00
5	10	11.255	-0.003	0.01
6	9	1.392	-0.000	-0.00
6	10	-1.392	0.000	-0.00

MEMBER FORCES FOR MEMBER 12

=====

LOADING	JOINT	AXIAL FORCE	SHEAR FORCE	MOMENT
1	10	-11.483	-0.003	-0.00
1	11	11.483	0.003	0.00
2	10	-3.223	-0.000	-0.00
2	11	3.223	0.000	0.00
3	10	3.948	-0.001	-0.00
3	11	-3.948	0.001	-0.00
4	10	13.739	0.002	0.00
4	11	-13.739	-0.002	-0.00
5	10	-10.759	-0.005	-0.01
5	11	10.759	0.005	0.00
6	10	1.691	-0.000	0.00
6	11	-1.691	0.000	-0.00

MEMBER FORCES FOR MEMBER 13

=====

LOADING	JOINT	AXIAL FORCE	SHEAR FORCE	MOMENT
1	11	-9.991	-0.004	-0.01
1	12	9.991	0.004	-0.00
2	11	-2.804	-0.001	-0.00
2	12	2.804	0.001	-0.00

3	11	4.195	-0.000	0.00
3	12	-4.195	0.000	-0.00
4	11	12.293	0.004	0.01
4	12	-12.293	-0.004	-0.00
5	11	-8.600	-0.005	-0.01
5	12	8.600	0.005	-0.00
6	11	1.726	0.000	0.00
6	12	-1.726	-0.000	-0.00

MEMBER FORCES FOR MEMBER 14

=====

LOADING	JOINT	AXIAL FORCE	SHEAR FORCE	MOMENT
1	12	-7.509	-0.009	-0.01
1	13	7.509	0.009	-0.00
2	12	-2.107	-0.002	-0.00
2	13	2.107	0.002	-0.00
3	12	4.446	-0.004	-0.00
3	13	-4.446	0.004	-0.00
4	12	9.761	0.007	0.01
4	13	-9.761	-0.007	0.00
5	12	-5.170	-0.017	-0.02
5	13	5.170	0.017	-0.01
6	12	1.688	-0.001	-0.00
6	13	-1.688	0.001	-0.00

MEMBER FORCES FOR MEMBER 15

=====

LOADING	JOINT	AXIAL FORCE	SHEAR FORCE	MOMENT
1	13	-4.019	-0.002	-0.01
1	14	4.019	0.002	0.00
2	13	-1.128	-0.000	-0.00
2	14	1.128	0.000	0.00
3	13	4.686	0.020	0.01
3	14	-4.686	-0.020	0.03
4	13	6.107	0.016	0.02
4	14	-6.107	-0.016	0.01
5	13	-0.460	0.016	-0.00
5	14	0.460	-0.016	0.04
6	13	1.566	0.010	0.00
6	14	-1.566	-0.010	0.01

MEMBER FORCES FOR MEMBER 16

=====

LOADING	JOINT	AXIAL FORCE	SHEAR FORCE	MOMENT
1	14	0.404	-0.051	-0.04
1	15	-0.404	0.051	-0.07
2	14	0.113	-0.014	-0.01
2	15	-0.113	0.014	-0.02
3	14	4.952	-0.114	-0.06
3	15	-4.952	0.114	-0.20
4	14	1.454	-0.022	-0.00
4	15	-1.454	0.022	-0.05
5	14	5.470	-0.179	-0.12
5	15	-5.470	0.179	-0.30
6	14	1.394	-0.055	-0.03
6	15	-1.394	0.055	-0.09

37

MEMBER FORCES FOR MEMBER 17

LOADING	JOINT	AXIAL FORCE	SHEAR FORCE	MOMENT
1	16	4.235	0.050	0.07
1	17	-4.235	-0.050	0.04
2	16	1.189	0.014	0.02
2	17	-1.189	-0.014	0.01
3	16	0.329	0.033	0.06
3	17	-0.329	-0.033	0.01
4	16	-4.241	0.014	0.05
4	17	4.241	-0.014	-0.02
5	16	5.754	0.099	0.16
5	17	-5.754	-0.099	0.07
6	16	-0.004	0.049	0.09
6	17	0.004	-0.049	0.01

MEMBER FORCES FOR MEMBER 18

LOADING	JOINT	AXIAL FORCE	SHEAR FORCE	MOMENT
1	17	7.734	0.004	-0.00
1	18	-7.734	-0.004	0.01
2	17	2.171	0.001	-0.00
2	18	-2.171	-0.001	0.00
3	17	0.082	-0.009	-0.01
3	18	-0.082	0.009	-0.00
4	17	8.708	-0.024	-0.02
4	18	-8.708	0.024	-0.03
5	17	9.988	-0.003	-0.02
5	18	-9.988	0.003	0.01
6	17	-0.730	-0.015	-0.02
6	18	0.730	0.015	-0.01

## MEMBER FORCES FOR MEMBER 19

38

LOADING	JOINT	AXIAL FORCE	SHEAR FORCE	MOMENT
1	18	10.218	0.010	0.00
1	19	-10.218	-0.010	0.02
2	18	2.868	0.002	0.00
2	19	-2.868	-0.002	0.00
3	18	-0.166	0.001	0.00
3	19	0.166	-0.001	-0.00
4	18	-11.647	-0.005	0.00
4	19	11.647	0.005	-0.02
5	18	12.921	0.014	0.00
5	19	-12.921	-0.014	0.02
6	18	-1.071	0.003	0.00
6	19	1.071	-0.003	-0.00

## MEMBER FORCES FOR MEMBER 20

LOADING	JOINT	AXIAL FORCE	SHEAR FORCE	MOMENT
1	19	11.713	0.003	-0.00
1	20	-11.713	-0.003	0.01
2	19	3.288	0.001	-0.00
2	20	-3.288	-0.001	0.00
3	19	-0.414	-0.001	-0.00
3	20	0.414	0.001	-0.00
4	19	-13.492	-0.006	0.00
4	20	13.492	0.006	-0.02
5	19	14.587	0.002	-0.01
5	20	-14.587	-0.002	0.01
6	19	-1.334	-0.002	-0.00
6	20	1.334	0.002	-0.00

## MEMBER FORCES FOR MEMBER 21

LOADING	JOINT	AXIAL FORCE	SHEAR FORCE	MOMENT
1	20	12.210	0.004	-0.00
1	21	-12.210	-0.004	0.01
2	20	3.427	0.001	-0.00
2	21	-3.427	-0.001	0.00
3	20	-0.663	0.001	0.00
3	21	0.663	-0.001	0.00
4	20	-14.240	-0.004	0.01
4	21	14.240	0.004	-0.02
5	20	14.974	0.006	-0.00

39

5	21	-14.974	-0.006	0.02
6	20	-1.522	-0.000	0.00
6	21	1.522	0.000	-0.00

MEMBER FORCES FOR MEMBER 22

=====

LOADING	JOINT	AXIAL FORCE	SHEAR FORCE	MOMENT
1	21	12.210	-0.004	-0.01
1	22	-12.210	0.004	0.00
2	21	3.427	-0.001	-0.00
2	22	-3.427	0.001	0.00
3	21	-0.664	-0.001	-0.00
3	22	0.664	0.001	-0.00
4	21	-14.239	0.004	0.02
4	22	14.239	-0.004	-0.01
5	21	14.973	-0.006	-0.02
5	22	-14.973	0.006	0.00
6	21	-1.522	0.000	0.00
6	22	1.522	-0.000	-0.00

MEMBER FORCES FOR MEMBER 23

=====

LOADING	JOINT	AXIAL FORCE	SHEAR FORCE	MOMENT
1	22	11.713	-0.003	-0.01
1	23	-11.713	0.003	0.00
2	22	3.288	-0.001	-0.00
2	23	-3.288	0.001	0.00
3	22	-0.910	-0.002	-0.00
3	23	0.910	0.002	-0.00
4	22	-13.891	0.001	0.01
4	23	13.891	-0.001	-0.01
5	22	14.091	-0.007	-0.02
5	23	-14.091	0.007	0.00
6	22	-1.633	-0.001	0.00
6	23	1.633	0.001	-0.00

MEMBER FORCES FOR MEMBER 24

=====

LOADING	JOINT	AXIAL FORCE	SHEAR FORCE	MOYENT
1	23	10.219	-0.010	-0.02
1	24	-10.219	0.010	-0.00
2	23	2.868	-0.002	-0.00
2	24	-2.868	0.002	-0.00

3	23	-1.158	40	0.005	0.00
3	24	1.158		-0.005	0.00
4	23	-12.443		0.016	0.02
4	24	12.443		-0.016	0.00
5	23	11.928		-0.007	-0.02
5	24	-11.928		0.007	0.00
6	23	-1.668		0.004	0.00
6	24	1.668		-0.004	0.00

MEMBER FORCES FOR MEMBER 25

=====

LOADING	JOINT	AXIAL FORCE	SHEAR FORCE	MOMENT
1	24	7.734	-0.004	-0.01
1	25	-7.734	0.004	0.00
2	24	2.171	-0.001	-0.00
2	25	-2.171	0.001	0.00
3	24	-1.408	-0.029	-0.01
3	25	1.408	0.029	-0.05
4	24	-9.908	-0.018	0.00
4	25	9.908	0.018	-0.05
5	24	8.496	-0.034	-0.03
5	25	-8.496	0.034	-0.04
6	24	-1.630	-0.016	-0.00
6	25	1.630	0.016	-0.03

MEMBER FORCES FOR MEMBER 26

=====

LOADING	JOINT	AXIAL FORCE	SHEAR FORCE	MOMENT
1	25	4.235	-0.050	-0.04
1	26	-4.235	0.050	-0.07
2	25	1.189	-0.014	-0.01
2	26	-1.189	0.014	-0.02
3	25	-1.652	0.113	0.06
3	26	1.652	-0.113	0.21
4	25	-6.247	0.145	0.09
4	26	6.247	-0.145	0.24
5	25	3.772	0.048	0.00
5	26	-3.772	-0.048	0.11
6	25	-1.508	0.070	0.03
6	26	1.508	-0.070	0.12

MEMBER FORCES FOR MEMBER 27

=====

LOADING	JOINT	AXIAL FORCE	SHEAR FORCE	MOMENT
1	6	6.102	-0.017	-0.02
1	17	-6.102	0.017	-0.02
2	6	1.712	41 -0.004	-0.00
2	17	-1.712	0.004	-0.00
3	6	-0.381	0.001	0.00
3	17	0.381	-0.001	0.00
4	6	-8.780	0.025	0.04
4	17	8.780	-0.025	0.03
5	6	7.433	-0.020	-0.03
5	17	-7.433	0.020	-0.03
6	6	-2.008	0.006	0.01
6	17	2.008	-0.006	0.00

MEMBER FORCES FOR MEMBER 28

=====

LOADING	JOINT	AXIAL FORCE	SHEAR FORCE	MOMENT
1	7	4.773	-0.008	-0.01
1	18	-4.773	0.008	-0.01
2	7	1.340	-0.002	-0.00
2	18	-1.340	0.002	-0.00
3	7	-0.330	0.000	0.00
3	18	0.330	-0.000	0.00
4	7	-6.075	0.010	0.01
4	18	6.075	-0.010	0.01
5	7	5.783	-0.010	-0.01
5	18	-5.783	0.010	-0.01
6	7	-0.976	0.001	0.00
6	18	0.976	-0.001	0.00

MEMBER FORCES FOR MEMBER 29

=====

LOADING	JOINT	AXIAL FORCE	SHEAR FORCE	MOMENT
1	8	3.405	-0.006	-0.01
1	19	-3.405	0.006	-0.01
2	8	0.955	-0.001	-0.00
2	19	-0.955	0.001	-0.00
3	8	-0.342	0.000	0.00
3	19	0.342	-0.000	0.00
4	8	-4.031	0.007	0.01
4	19	4.031	-0.007	0.01
5	8	4.018	-0.007	-0.01
5	19	-4.018	0.007	-0.01
6	8	-0.469	0.000	0.00
6	19	0.469	-0.000	0.00

MEMBER FORCES FOR MEMBER 30

=====

LOADING	JOINT	AXIAL FORCE	SHEAR FORCE	MOMENT
1	9	2.045	-0.003	-0.00
1	20	-2.045	0.003	-0.00
2	9	0.574	-0.000	-0.00
2	20	-0.574	0.000	-0.00
3	9	-0.339	0.000	0.00
3	20	0.339	-0.000	0.00
4	9	-2.524	0.004	0.00
4	20	2.524	-0.004	0.00
5	9	2.279	-0.004	-0.00
5	20	-2.279	0.004	-0.00
6	9	-0.359	0.000	0.00
6	20	0.359	-0.000	0.00

MEMBER FORCES FOR MEMBER 31

=====

LOADING	JOINT	AXIAL FORCE	SHEAR FORCE	MOMENT
1	10	1.360	-0.000	-0.00
1	21	-1.360	0.000	-0.00
2	10	0.381	-0.000	-0.00
2	21	-0.381	0.000	-0.00
3	10	-0.002	0.000	0.00
3	21	0.002	-0.000	0.00
4	10	-1.498	0.000	0.00
4	21	1.498	-0.000	0.00
5	10	1.739	0.000	0.00
5	21	-1.739	-0.000	0.00
6	10	-0.103	0.000	0.00
6	21	0.103	-0.000	0.00

MEMBER FORCES FOR MEMBER 32

=====

LOADING	JOINT	AXIAL FORCE	SHEAR FORCE	MOMENT
1	11	2.045	0.003	0.00
1	22	-2.045	-0.003	0.00
2	11	0.574	0.000	0.00
2	22	-0.574	-0.000	0.00
3	11	0.337	0.001	0.00
3	22	-0.337	-0.001	0.00
4	11	-1.981	-0.003	-0.00
4	22	1.981	0.003	-0.00
5	11	2.956	0.005	0.00



5	22	-2.956	-0.005	0.00
6	11	0.047	0.000	0.00
6	22	-0.047	-0.000	0.00

## MEMBER FORCES FOR MEMBER 33

LOADING	JOINT	AXIAL FORCE	SHEAR FORCE	MOMENT
1	12	3.405	0.006	0.01
1	23	-3.405	-0.006	0.01
2	12	0.955	0.001	0.00
2	23	-0.955	-0.001	0.00
3	12	0.347	0.001	0.00
3	23	-0.347	-0.001	0.00
4	12	-3.472	-0.006	-0.01
4	23	3.472	0.006	-0.01
5	12	4.708	0.009	0.01
5	23	-4.708	-0.009	0.01
6	12	-0.050	-0.000	0.00
6	23	0.050	0.000	-0.00

## MEMBER FORCES FOR MEMBER 34

LOADING	JOINT	AXIAL FORCE	SHEAR FORCE	MOMENT
1	13	4.773	0.008	0.01
1	24	-4.773	-0.008	0.01
2	13	1.340	0.002	0.00
2	24	-1.340	-0.002	0.00
3	13	0.307	0.000	-0.00
3	24	-0.307	-0.000	0.00
4	13	-5.010	-0.008	-0.01
4	24	5.010	0.008	-0.01
5	13	6.421	0.011	0.01
5	24	-6.421	-0.011	0.02
6	13	-0.177	-0.000	-0.00
6	24	0.177	0.000	0.00

## MEMBER FORCES FOR MEMBER 35

LOADING	JOINT	AXIAL FORCE	SHEAR FORCE	MOMENT
1	14	6.102	0.017	0.02
1	25	-6.102	-0.017	0.02
2	14	1.712	0.004	0.00
2	25	-1.712	-0.004	0.00

3	14	0.475	0.004	0.01
3	25	-0.475	-0.004	0.00
4	14	-6.345	-0.016	-0.02
4	25	6.345	0.016	-0.03
5	14	8.290	0.026	0.05
5	25	-8.290	-0.026	0.03
6	14	-0.182	0.000	0.00
6	25	0.182	-0.000	-0.00

MEMBER FORCES FOR MEMBER 36

=====

LOADING	JOINT	AXIAL FORCE	SHEAR FORCE	MOMENT
1	16	-7.487	-0.003	-0.00
1	6	7.487	0.003	-0.00
2	16	-2.101	-0.000	-0.00
2	6	2.101	0.000	-0.00
3	16	0.423	0.003	0.00
3	6	-0.423	-0.003	0.00
4	16	10.668	0.013	0.02
4	6	-10.668	-0.013	0.02
5	16	-9.166	-0.000	0.00
5	6	9.166	0.000	-0.00
6	16	2.385	0.007	0.01
6	6	-2.385	-0.007	0.01

MEMBER FORCES FOR MEMBER 37

=====

LOADING	JOINT	AXIAL FORCE	SHEAR FORCE	MOMENT
1	17	-5.914	-0.003	-0.00
1	7	5.914	0.003	-0.00
2	17	-1.660	-0.001	-0.00
2	7	1.660	0.001	-0.00
3	17	-0.418	-0.000	-0.00
3	7	0.418	0.000	-0.00
4	17	7.546	0.003	0.00
4	7	-7.546	-0.003	0.00
5	17	-7.156	-0.005	-0.01
5	7	7.156	0.005	-0.00
6	17	1.224	-0.000	-0.00
6	7	-1.224	0.000	-0.00

MEMBER FORCES FOR MEMBER 38

=====

LOADING	JOINT	AXIAL FORCE	SHEAR FORCE	MOMENT
1	18	-4.205	-0.002	-0.00
1	8	4.205	0.002	-0.00
2	18	-1.180	-0.000	-0.00
2	8	1.180	0.000	-0.00
3	18	0.422	0.000	0.00
3	8	-0.422	-0.000	0.00
4	18	4.975	0.003	0.00
4	8	-4.975	-0.003	0.00
5	18	-4.963	-0.002	-0.00
5	8	4.963	0.002	-0.00
6	18	0.577	0.000	0.00
6	8	-0.577	-0.000	0.00

MEMBER FORCES FOR MEMBER 39

=====

LOADING	JOINT	AXIAL FORCE	SHEAR FORCE	MOMENT
1	19	-2.528	-0.001	-0.00
1	9	2.528	0.001	-0.00
2	19	-0.709	-0.000	-0.00
2	9	0.709	0.000	-0.00
3	19	0.419	0.000	0.00
3	9	-0.419	-0.000	0.00
4	19	3.121	0.001	0.00
4	9	-3.121	-0.001	0.00
5	19	-2.818	-0.001	-0.00
5	9	2.818	0.001	-0.00
6	19	0.444	0.000	0.00
6	9	-0.444	-0.000	0.00

MEMBER FORCES FOR MEMBER 40

=====

LOADING	JOINT	AXIAL FORCE	SHEAR FORCE	MOMENT
1	20	-0.637	-0.000	-0.00
1	10	0.637	0.000	-0.00
2	20	-0.235	-0.000	-0.00
2	10	0.235	0.000	-0.00
3	20	0.424	0.000	0.00
3	10	-0.424	-0.000	0.00
4	20	1.261	0.000	0.00
4	10	-1.261	-0.000	0.00
5	20	-0.648	-0.000	-0.00
5	10	0.648	0.000	0.00
6	20	0.318	0.000	0.00
6	10	-0.318	-0.000	0.00

## MEMBER FORCES FOR MEMBER 41

```

=====
LOADING  JOINT  AXIAL FORCE      SHEAR FORCE      MOMENT
1         10      -0.837           0.000           0.00
1         22       0.837          -0.000           0.00
2         10      -0.235           0.000           0.00
2         22       0.235          -0.000           0.00
3         10      -0.419           0.000           0.00
3         22       0.419          -0.000           0.00
4         10       0.583          -0.000           0.00
4         22      -0.583          -0.000          -0.00
5         10      -1.491           0.000           0.00
5         22       1.491          -0.000           0.00
6         10      -0.190           0.000           0.00
6         22       0.190          -0.000           0.00

```

## MEMBER FORCES FOR MEMBER 42

```

=====
LOADING  JOINT  AXIAL FORCE      SHEAR FORCE      MOMENT
1         11      -2.528           0.001           0.00
1         23       2.528          -0.001           0.00
2         11      -0.709           0.000           0.00
2         23       0.709          -0.000           0.00
3         11      -0.419           0.000           0.00
3         23       0.419          -0.000          -0.00
4         11       2.448          -0.001          -0.00
4         23      -2.448           0.001          -0.00
5         11      -3.657           0.002           0.00
5         23       3.657          -0.002           0.00
6         11      -0.059           0.000           0.00
6         23       0.059           0.000          -0.00

```

## MEMBER FORCES FOR MEMBER 43

```

=====
LOADING  JOINT  AXIAL FORCE      SHEAR FORCE      MOMENT
1         12      -4.205           0.002           0.00
1         24       4.205          -0.002           0.00
2         12      -1.180           0.000           0.00
2         24       1.180          -0.000           0.00
3         12      -0.424           0.000           0.00
3         24       0.424          -0.000           0.00
4         12       4.291          -0.002          -0.00
4         24      -4.291           0.002          -0.00
5         12      -5.811           0.004           0.00
5         24       5.811          -0.004           0.00
6         12       0.064           0.000           0.00
6         24      -0.064          -0.000           0.00

```

# IV DISEÑO DE LOS ELEMENTOS ESTRUCTURALES

## a) Largueras

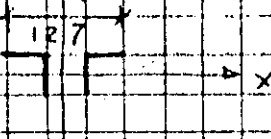
### Cuerda superior

Puede considerarse sometida a compresión pura pues el siporex que en forma continua se apoya sobre ella tiene suficiente rigidez a la flexión para salvar el claro entre nudos, por otro lado suele suponerse que el apoyo de la losa sobre la cuerda es capaz de proporcionar el arriostamiento necesario para que no se presente su pandeo lateral. En esas condiciones:

Si se usan 2 7T 51 x 51 x 5 mm.

y  $F = 5760 \text{ Kg.}$  (compresión)

pg. 14



$$r_x = 1.17$$

$$k_x = 0.9$$

$$l_x = 80 \text{ cm}$$

$$\frac{k_x l}{r} = \frac{80 \times 0.9}{1.17} = 62$$

$$F_c = 1212 \text{ Kg/cm}^2$$

$$f_a = \frac{5760}{9.2} = 626 \text{ Kg/cm}^2 < F_c$$

(E.E. pg 23)

### Cuerda inferior

La condición de carga más desfavorable se presenta al actuar el viento en que la cuerda inferior queda sometida a compresión no teniendo en este caso contraventos lateral a no ser el que pudieran proporcionar las diagonales que suele desprenderse

Usando los mismos ángulos que en la cuerda superior

$$F = \frac{4000}{1.5} = 2666 \text{ Kg}$$

$$r_y = 0.24 \times 12.7 = 3.05 \text{ cm}$$

$$l_y = 800 \text{ cm}$$

$$k_y = 0.7$$

estimado en función del tipo de coacción de la cuerda

$$\frac{k_l}{r} = \frac{0.7 \times 800}{3.05} = 184 ; F_a = 310 \text{ Kg/cm}^2$$

$$f_a = \frac{2666}{9.2} = 289.8 \text{ Kg/cm}^2 < F_a$$

Diagonales

$$2 \text{ L } 25 \times 25 \times 3 ; r = 2.5 \text{ cm} ; A = 3.04 \text{ cm}^2$$

$$F = 1629 \text{ Kg}$$

$$l = 56 \text{ m} ; \frac{k_l}{r} = 22 ; F_a = 1440 \text{ Kg/cm}^2$$

$$f_a = \frac{1629}{3.04} = 535 \text{ Kg/cm}^2 < F_a$$

Las dos ángulos de las diagonales se soldarán para unirlos.  
 Las dos ángulos que forman las cuerdas se unirán en puntos intermedios entre nudos para evitar el pandeo local de un solo ángulo de la cuerda.

### b) Marcos principales

b1) Armaduras. Su diseño es similar al de los elementos de los largueros.

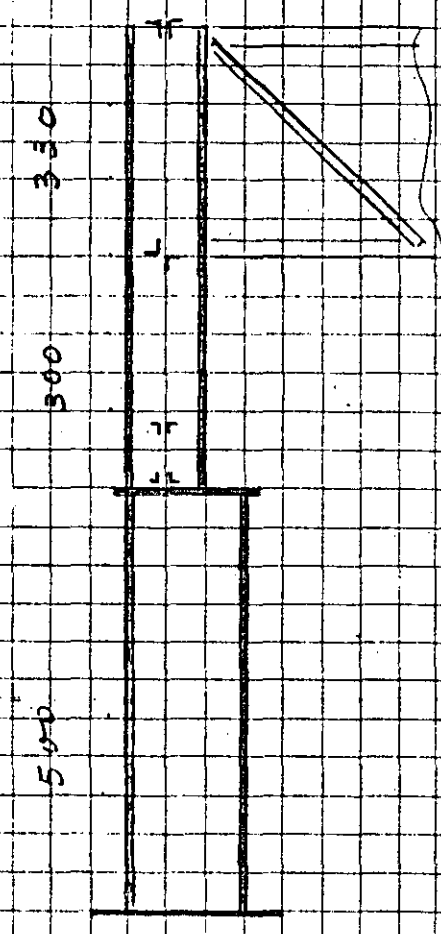
### b2) Columnas.

En su extremo inferior está empotrada en la cimentación mediante anclas unidas a la placa de base

En su extremo superior está unida a la armadura del techo cuya rigidez es mucho mayor que la de la columna y puede suponerse impide su giro, pero no el desplazamiento en el plano del marco.

En el plano perpendicular al marco la columna está anclada por puentes que forman parte de las paredes laterales

El hecho de que la columna sea de sección variable afecta al valor de la carga crítica que puede soportar la columna y por tanto su capacidad.



En la tabla que sigue se dan valores que modifican los resultados que se obtienen suponiendo la columna de sección uniforme para tener en cuenta el hecho de que la sección varía.

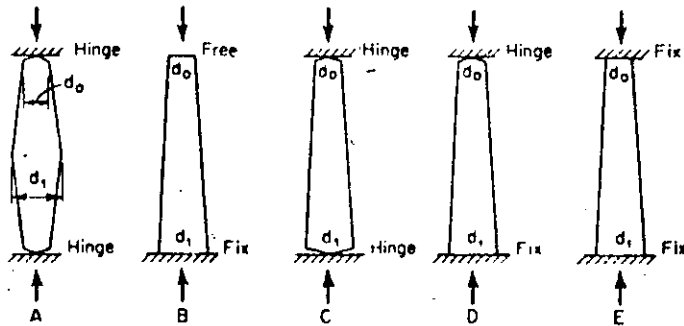


FIG. 9

Table 8. Values of  $\mu$  and  $K$  in Eqs. (7) and (8)\*

Case (Fig. 9)	K	$d_1/d_0$					
		1	2	3	4	5	6
A	1	1	2.6	4.9	7.7	11.1	14.9
B	2	1	2.6	4.9	7.7	11.1	14.9
C	1	1	2.1	3.4	4.9	6.6	8.3
D	0.7	1	2.0	3.3	4.7	6.2	7.9
E	0.5	1	2.0	3.3	4.6	6.0	7.6

\* From Ref. 3.

So long as  $A$  is constant, Eq. (7) is also valid for inelastic buckling, provided  $E$  is replaced by the tangent modulus  $E_t$ .<sup>1</sup> However, in this case the formula must be written

$$P = \frac{\pi^2 E_t A}{\left(\frac{KL}{r_0}\right)^2 \sqrt{\mu}} \quad (8)$$

Usaremos en nuestra programación esta tabla para el diseño del tramo superior de la columna.

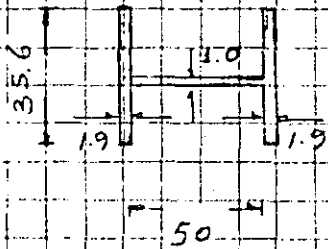
Dado que el caso que tratamos es más complejo que el que se presenta en la tabla por tenerse una gran parte de la carga concentrada donde la sección cambia, el tramo inferior se diseñará, dado que está empotrado en su base con una  $K = 2$  (E.E. pg 7) lo que probable mente es conservador.



# Diseño de la columna

51

## Trama inferior



$$Area = 18.5 \text{ cm}^2$$

$$I_x = 10119.5 \text{ cm}^3, S_x = 3748 \text{ cm}^3$$

$$I_y = 1416.5 \text{ cm}^3$$

$$r_x = 23 \text{ cm}$$

$$K_x = 2.0$$

$$\frac{K_x L_x}{r_x} = \frac{2 \times 500}{23}$$

$$r_y = 9 \text{ cm}$$

$$K_y = 1.0$$

$$\frac{K_y L_y}{r_y} = \frac{1.0 \times 500}{9} = 56$$

$$F_a = 1252 \text{ Kg/cm}^2$$

$$\frac{L d}{A_f} = \frac{500 \times 44}{35.6 \times 1.9} = 325$$

$$F_b = 1520$$

$$f_a = \frac{117418}{185} = 635 \text{ Kg/cm}^2, f_b = \frac{2953000}{3748} = 788 \text{ Kg/cm}^2$$

Tamaño  $C_m = 0.85$  (Especificaciones AISC) y aplicando

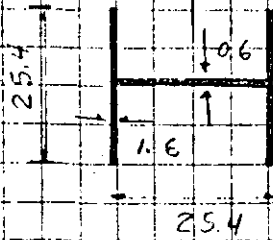
la expresión de diseño:

$$\frac{f_a}{F_a} + \frac{f_b C_m}{F_b (1 - P/P_E)} \leq 1 \quad (E E F_g 60)$$

$$\text{donde } P_E = \frac{\pi^2 E I}{(KL)^2} = \frac{2 \pi^2 10^6 \times 10119.5}{(2 \times 500)^2} = 1997509 \text{ Kg}$$

$$\frac{635}{1252} + \frac{788 \times 0.85}{1520 \left(1 - \frac{117418}{1997509}\right)} = 0.98$$

Tramo superior



$$A = 96.5 \text{ cm}^2$$

$$I_x = 13109 \text{ cm}^4 ; S_x = 916 \text{ cm}^3$$

$$I_y = 4370 \text{ cm}^4$$

$$r_x = 11.7 \text{ cm} ; l_x = 800 ; k_x = 1 \quad (\text{EE p. 7})$$

$$r_y = 6.6 \text{ cm} ; l_y = 300 ; k_y = 1$$

Tomando  $\frac{d_1}{d_2} = 2 ; u = 2$  (de la tabla)

$$\frac{1}{\sqrt{u}} \frac{K_x l_x}{r_x} = \frac{1}{\sqrt{2}} \frac{1 \times 800}{11.7} = 49 ; F_a = 1297 \text{ Kg/cm}^2 \quad (\text{EE p. 13})$$

$$\frac{K_y l_y}{r_y} = \frac{1 \times 300}{6.6} = 46$$

$$\frac{L d}{A f} = \frac{300 \times 25.4}{25.4 \times 1.6}$$

$$F_b = 1520 \text{ Kg/cm}^2$$

$$f_u = \frac{10000}{81.3} = 123$$

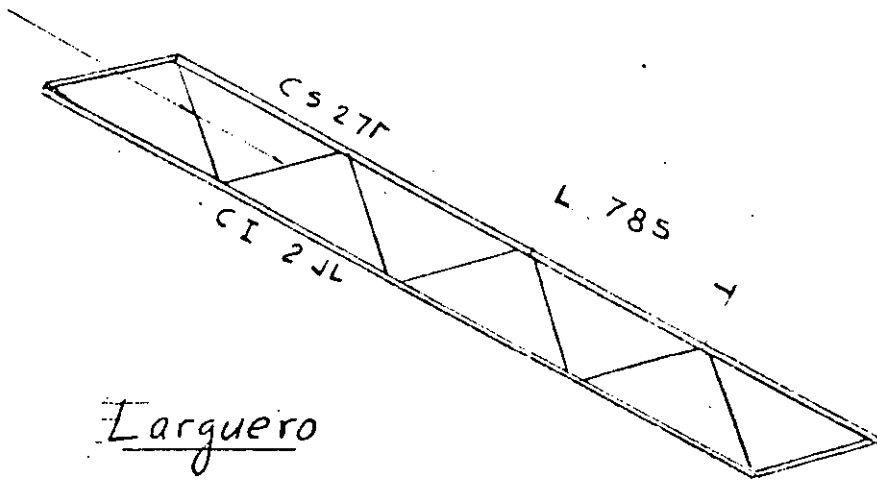
$$f_b = \frac{103000}{916} = 1204 \text{ Kg/cm}^2$$

$$\frac{123}{1297} + \frac{1204 \times 0.85}{1520} = 0.1 + 0.67 < 1.0$$

## I CONEXIONES:

Todas las conexiones son soldadas y se usarán tornillos solo para montaje.

En las figuras que se presentan a continuación se muestran una serie de conexiones típicas.



400

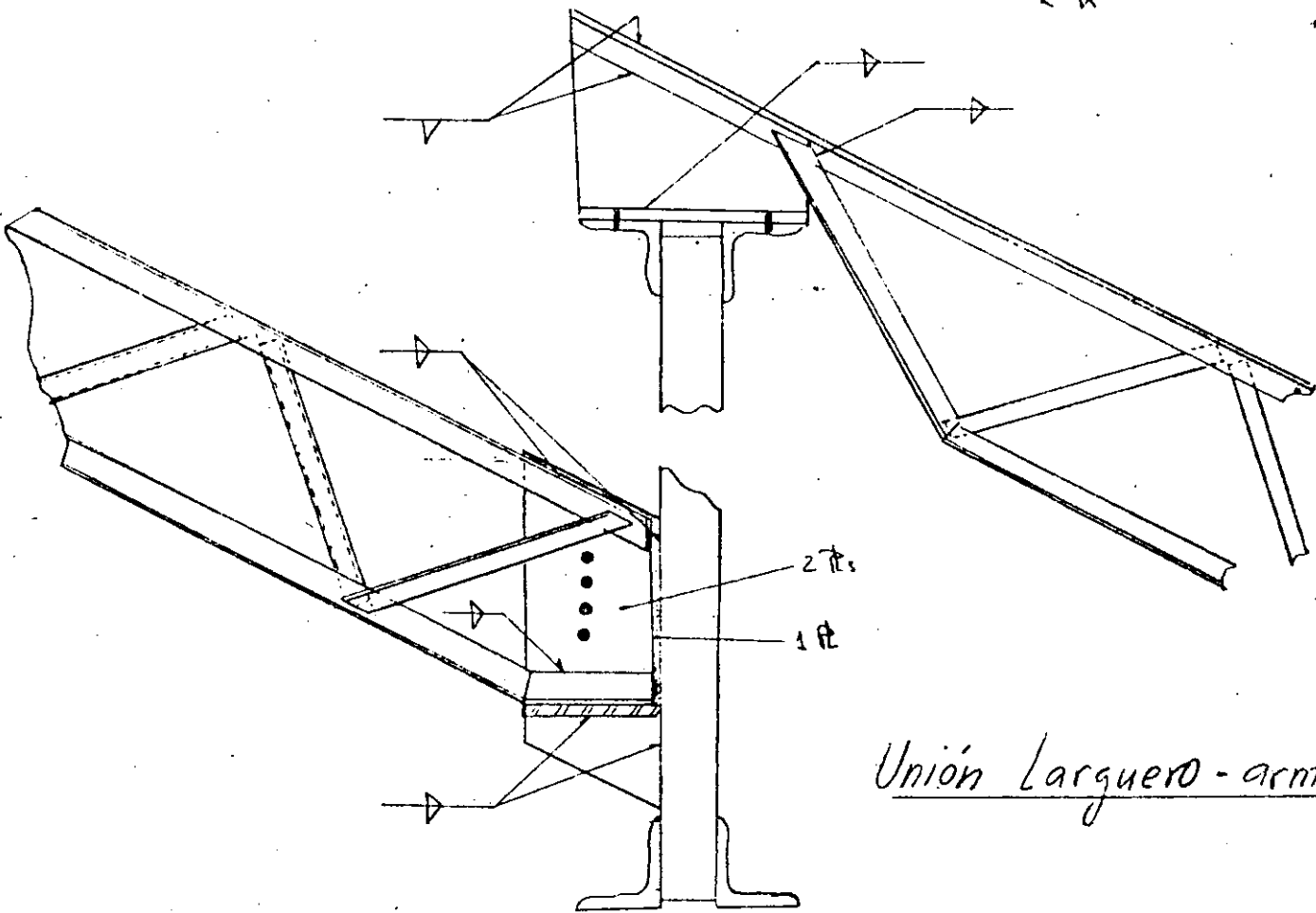
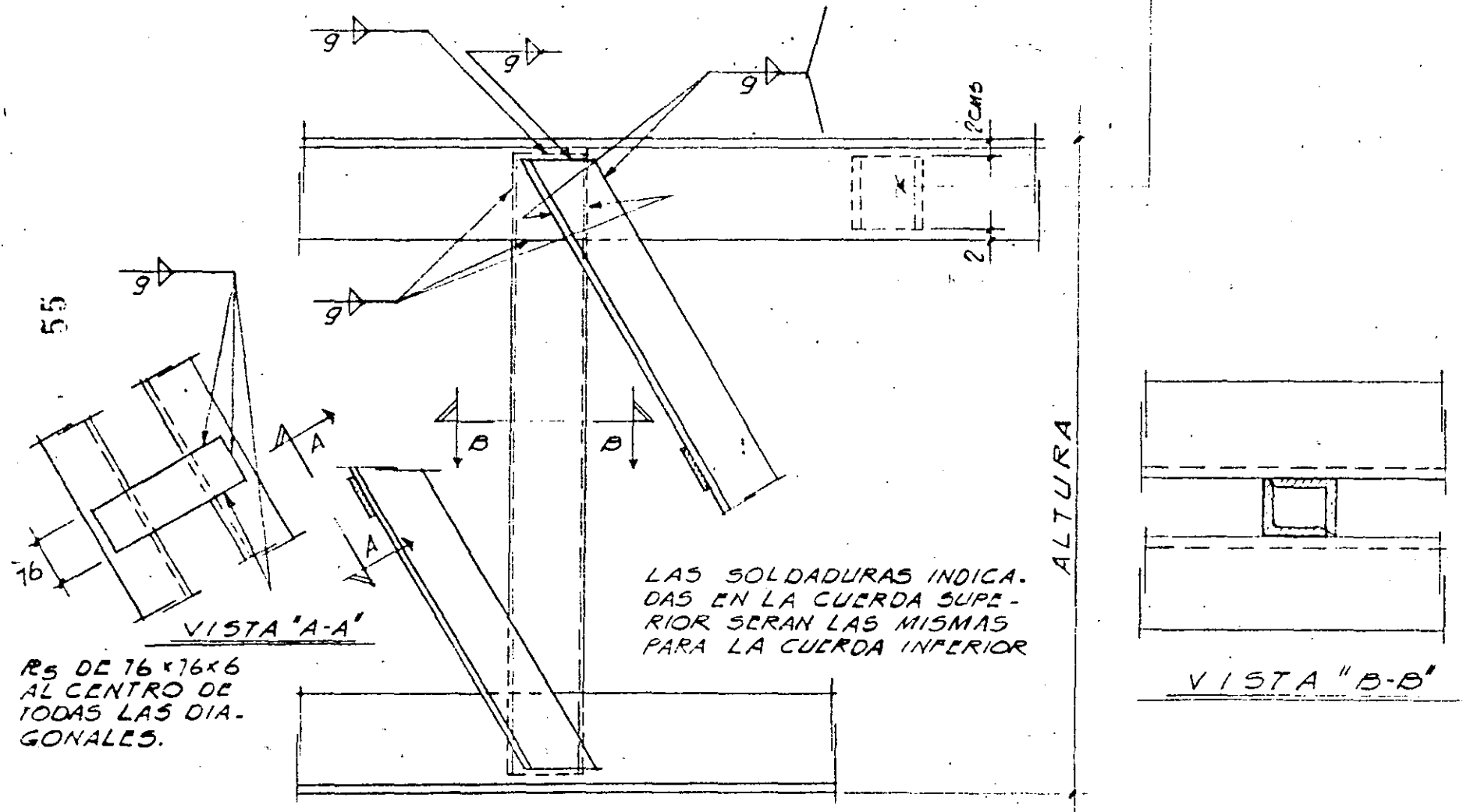


FIG. 6.

g = TAMAÑO DE SOLDADURA  
 IGUAL AL GRUESO DEL  
 ANGULO UTILIZADO EN  
 LA DIAGONAL

CAJÓN FORMADO POR  
 DOS ANGULOS  
 (AL CENTRO DE LOS TABLEROS  
 DE AMBAS CUERDAS)



55

RS DE 76x76x6  
 AL CENTRO DE  
 TODAS LAS DIA-  
 GONALES.

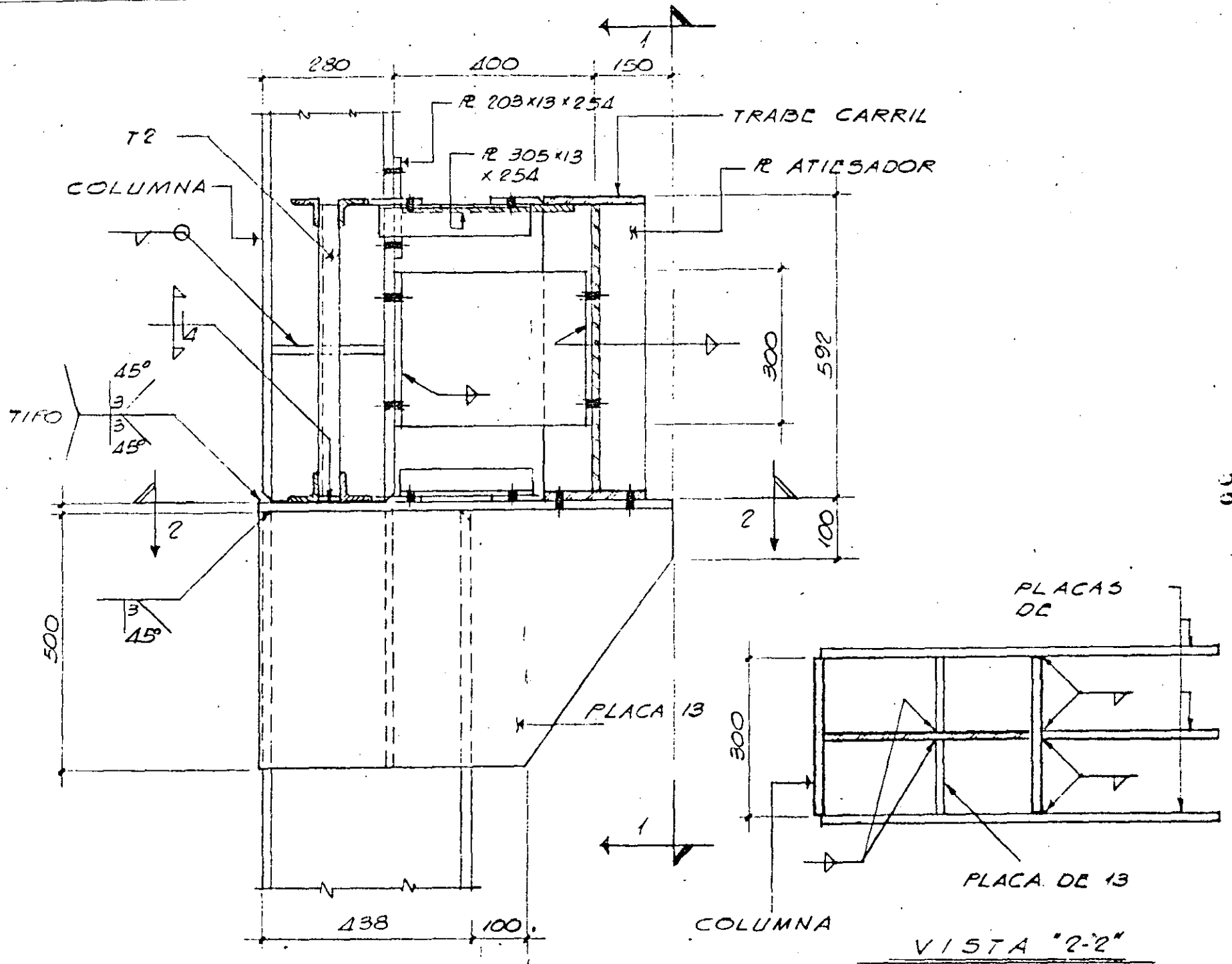
VISTA "A-A"

LAS SOLDADURAS INDICA-  
 DAS EN LA CUERDA SUPE-  
 RIOR SERAN LAS MISMAS  
 PARA LA CUERDA INFERIOR

ALTURA

VISTA "B-B"

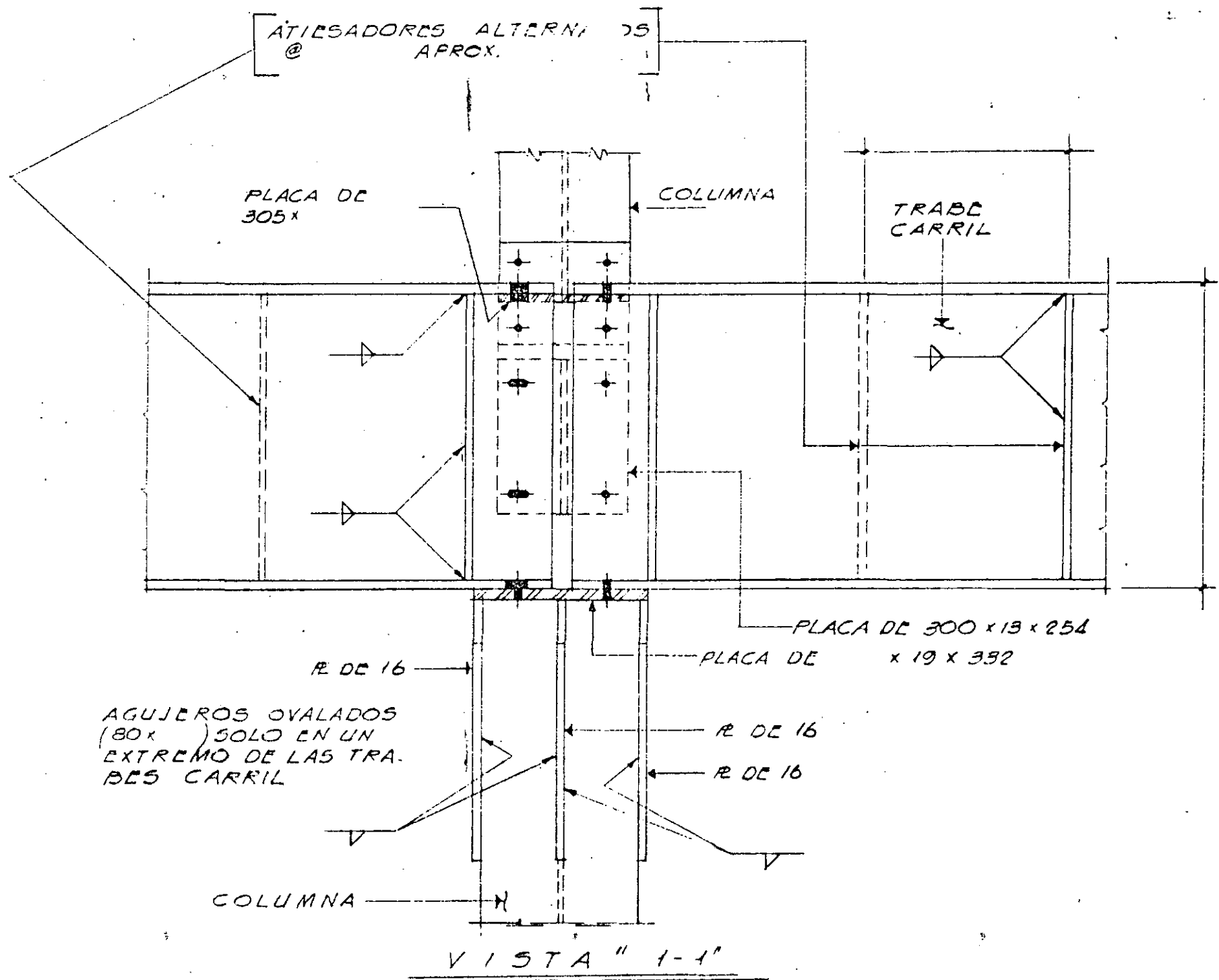
CONEXION TIPO DE MONTANTES Y  
 DIAGONALES A CUERDA SUPERIOR E  
 INFERIOR



56

CONEXIONES TIPO EN COLUMNAS

FIG. 9



57

FIG. 10



**DIVISION DE EDUCACION CONTINUA  
FACULTAD DE INGENIERIA U.N.A.M.**

DISEÑO DE ESTRUCTURAS DE ACERO

CALCULO DE LA ESTRUCTURA DEL EDIFICIO  
DESTINADO A OFICINAS, QUE SE PROYECTA  
CONSTRUIR EN LA CALLE TIBER # 66 COLONIA  
CUAUHTEMOC DE ESTA CIUDAD PROPIEDAD DE  
INMOBILIARIA RODIM. S.A. DE C.V.

DR. PORFIRIO BALLESTEROS

NOV. 84



CALCULO DE LA ESTRUCTURA DEL EDIFICIO  
 DESTINADO A OFICINAS, QUE SE PROYECTA  
 CONSTRUIR EN LA CALLE TIERER #66 COLONIA  
 CUAUHTEMOC DE ESTA CIUDAD PROPIEDAD DE  
 INMOBILIARIA RODIM, S.A. DE C.V.

## 1. GEOMETRIA.

Se indica en los planos arquitectonicos

## 2. CARGAS.

2.1 Peso propio.  $w' = 450 \text{ Kg/m}^2$

2.2 Carga viva.  $p' = 250 \text{ ''}$

Total:  $w' + p' = q' = 700 \text{ ''}$

2.3 Coeficiente sismico:  $C = 0.08$

## 3. MATERIALES

3.1 Concreto:  $f'_c \geq 250 \text{ Kg/cm}^2$

3.2 Acero de refuerzo:  $f_y \geq 4,200 \text{ Kg/cm}^2$

3.3 Acero estructural. A-36:

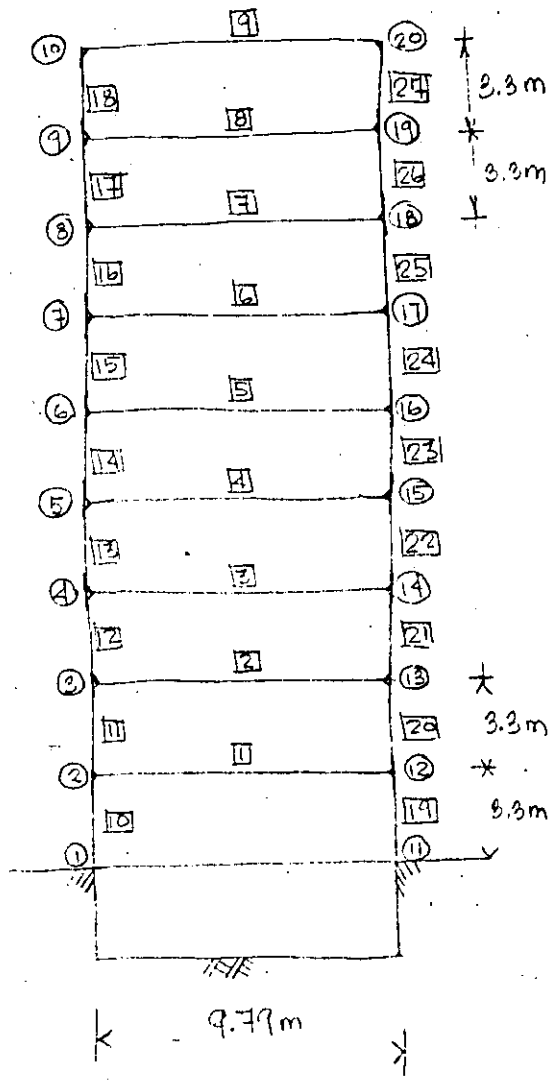
Modulo:  $E = 2.1 \times 10^6 \text{ Kg/cm}^2$

Poisson:  $\nu = 0.3$

fluencia:  $\sigma_{yp} = 2,531 \text{ Kg/cm}^2$

Deformación:  $\epsilon_{yp} = 0.001$

### 4. IDEALIZACIÓN ESTRUCTURAL (TRANSVERSAL)



claro estructural:

$$l = 10.82\text{m} - 2 \cdot (.18 + .15 + .1832)$$

$$l = 9.79\text{m}$$

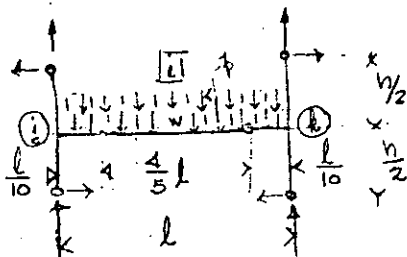
Fig.1 Corte estructural Transversal

## 4- CARGAS VERTICALES

$$W = 4.2 W' = 4.2 \times 450 = 1.89 \frac{\text{ton}}{\text{m}}$$

$$p = 4.2 p' = 4.2 \times 250 = 1.05 \text{ ''}$$

$$q = W + p = 2.94 \text{ ''}$$



## 4.1 VIGAS

$$m_{q_i}^i = \frac{1}{8} q \left( \frac{4}{5} l \right)^2 = \frac{1}{8} 2.94 \left( \frac{4}{5} \times 9.79 \right)^2$$

$$m_{q_i}^i = 22.54 \text{ Ton-m} \quad (i=1, \dots, 9) \quad (4.1)$$

$$m_{d_i}^i = q \frac{4}{5} l \cdot \frac{1}{2} \times \frac{l}{10} + q \frac{l}{10} \cdot \frac{l}{10} \times \frac{1}{2} = \frac{3}{200} q l^2$$

$$m_{d_i}^i = \frac{3 \times 2.94 \times 9.79^2}{200} =$$

$$m_{d_i}^i = 4.23 \text{ Ton-m} \quad (i=2, \dots, 20) \text{ vigas} \quad (4.2)$$

## 4.2 COLUMNAS

$$m_{d_i}^i = \frac{(4.2)}{2} = \frac{4.20}{2} = 2.11 \text{ Ton-m} \quad (4.3)$$

$$(i=10, \dots, 27)$$

## 5- CARGAS SISMICAS

Método estático

$$F_i = 0.95 C W \frac{W_i h_i}{\sum W_i h_i} \quad (5.1)$$

Donde para nuestro caso se tiene

$$W_1 = W_2 = \dots = W_i = \dots = W_9 = 550 \frac{\text{kg}}{\text{m}^2} \times \frac{9.79}{2} \text{ m} \times 4.2 \text{ m}$$

$$W_i = 11.31 \text{ Ton/piso}$$

$$W = 9 \times W_i = 9 \times 11.31 = 101.79 \text{ Ton}$$

$$\begin{aligned} \sum_1^9 W_i h_i &= W_i \sum_1^9 h_i = W_i \times 3.3 \sum_1^9 (1+2+\dots+9) \\ &= 3.3 \times 45 \times W_i \end{aligned}$$

Substituyendo los valores en (5.1) se obtiene

$$F_i = .95 \times .08 \times 9 \times 11.31 \frac{h_i}{3.3 \times 45}$$

$$F_i = .05 h_i$$

(5.2)

$$F_{2x} = F_{12x} = .05 \times 3.3 = 0.17 \text{ Ton}$$

$$F_{3x} = F_{12x} = .05 \times 3.3 \times 2 = 0.33 \text{ "}$$

$$F_{4x} = F_{14x} = .05 \times 3.3 \times 3 = 0.50 \text{ "}$$

$$F_{5x} = F_{15x} = .05 \times 3.3 \times 4 = 0.66 \text{ "}$$

$$F_{6x} = F_{16x} = .05 \times 3.3 \times 5 = 0.83 \text{ "}$$

$$F_{7x} = F_{17x} = .05 \times 3.3 \times 6 = 0.99 \text{ "}$$

$$F_{8x} = F_{18x} = .05 \times 3.3 \times 7 = 1.16 \text{ "}$$

$$F_{9x} = F_{19x} = .05 \times 3.3 \times 8 = 1.32 \text{ "}$$

$$F_{10x} = F_{20x} = .05 \times 3.3 \times 9 = 1.49 \text{ "}$$

(5.3)

### 6: CORTE SISMICO

$$V_{10} = 1.49 \text{ Ton}$$

$$V_{11} = 1.49 + 1.32 = 2.81 \text{ Ton}$$

$$V_{12} = 1.49 + 1.32 + 1.16 = 3.97 \text{ Ton}$$

$$V_{13} = 1.49 + 1.32 + 1.16 + .99 = 4.96 \text{ Ton}$$

$$V_{14} = 1.49 + 1.32 + 1.16 + .99 + .83 = 5.79 \text{ Ton}$$

$$V_{15} = 1.49 + 1.32 + 1.16 + .99 + .83 + .66 = 6.45 \text{ Ton}$$

$$V_{16} = 1.49 + 1.32 + 1.16 + .99 + .83 + .66 + .5 = 6.95 \text{ Ton}$$

$$V_{17} = 1.49 + 1.32 + 1.16 + .99 + .83 + .66 + .5 + .33 = 7.28 \text{ Ton}$$

$$V_{18} = 1.49 + 1.32 + 1.16 + .99 + .83 + .66 + .5 + .33 + .17 = 7.45 \text{ Ton}$$

$$V_{19} = 1.49 + 1.32 + 1.16 + .99 + .83 + .66 + .5 + .33 + .17 = 7.45 \text{ Ton}$$

(6.1)

## 7.- MOMENTOS SISMICOS

COLUMNAS: De (6.1) se obtiene:

$$m_{23}^{10} = 7.45 \text{ Ton} \times \frac{3.3}{2} \text{ m} = 11.92 \text{ Ton-m}$$

$$m_{23}^{11} = 7.28 \text{ Ton} \times \frac{3.3}{2} \text{ m} = 11.65 \text{ "}$$

$$m_{33}^{12} = 6.45 \text{ Ton} \times \frac{3.3}{2} \text{ m} = 11.12 \text{ "}$$

$$m_{42}^{13} = 6.45 \text{ Ton} \times \frac{3.3}{2} \text{ m} = 10.32 \text{ "}$$

$$m_{53}^{14} = 5.79 \text{ Ton} \times \frac{3.3}{2} \text{ m} = 9.26 \text{ "}$$

$$m_{62}^{15} = 4.96 \text{ Ton} \times \frac{3.3}{2} \text{ m} = 7.94 \text{ "}$$

$$m_{72}^{16} = 3.97 \text{ Ton} \times \frac{3.3}{2} \text{ m} = 6.35 \text{ "}$$

$$m_{82}^{17} = 2.81 \text{ Ton} \times \frac{3.3}{2} \text{ m} = 4.50 \text{ "}$$

$$m_{92}^{18} = 1.49 \text{ Ton} \times \frac{3.3}{2} \text{ m} = 2.38 \text{ "}$$

(7.1)

TRABES De (7.1) y equilibrio se obtiene:

$$m_{102}^9 = 2.38 \text{ Ton-m}$$

$$m_{92}^8 = 2.38 + 4.50 = 6.88 \text{ Ton-m}$$

$$m_{82}^7 = 4.50 + 6.35 = 10.85 \text{ "}$$

$$m_{72}^6 = 6.35 + 7.49 = 13.84 \text{ "}$$

$$m_{62}^5 = 7.94 + 9.26 = 17.20 \text{ "}$$

$$m_{52}^4 = 9.26 + 10.32 = 19.58 \text{ "}$$

$$m_{42}^3 = 10.32 + 11.12 = 21.44 \text{ "}$$

$$m_{32}^2 = 11.12 + 11.65 = 22.77 \text{ "}$$

$$m_{22}^1 = 11.65 + 11.92 = 23.57 \text{ "}$$

(7.2)

8.- MOMENTOS SISMICOS más CARGAS VERTICALES  
COLUMNAS De (7.1) y (4.5) se obtiene

$$\begin{aligned}
 m_{23}^{10} &= 2.11 + 11.92 = 14.03 \text{ Ton-m} \\
 m_{23}^{11} &= 2.11 + 11.65 = 13.76 \text{ " } \\
 m_{38}^{12} &= 2.11 + 11.12 = 13.23 \text{ " } \\
 m_{48}^{13} &= 2.11 + 10.32 = 12.43 \text{ " } \\
 m_{58}^{14} &= 2.11 + 9.26 = 11.37 \text{ " } \\
 m_{68}^{15} &= 2.11 + 7.94 = 10.05 \text{ " } \\
 m_{78}^{16} &= 2.11 + 6.35 = 8.46 \text{ " } \\
 m_{88}^{17} &= 2.11 + 4.50 = 6.61 \text{ " } \\
 m_{98}^{18} &= 2.11 + 2.38 = 4.49 \text{ " }
 \end{aligned}
 \tag{8.1}$$

TRABES De (7.2) y (4.2) se obtiene

$$\begin{aligned}
 m_{23}^1 &= 4.23 + 23.57 = 27.80 \text{ Ton-m} \\
 m_{33}^2 &= 4.23 + 22.77 = 27.00 \text{ " } \\
 m_{48}^3 &= 4.23 + 21.44 = 25.67 \text{ " } \\
 m_{58}^4 &= 4.23 + 19.58 = 23.81 \text{ " } \\
 m_{68}^5 &= 4.23 + 17.20 = 21.43 \text{ " } \\
 m_{78}^6 &= 4.23 + 13.84 = 18.07 \text{ " } \\
 m_{88}^7 &= 4.23 + 10.85 = 15.08 \text{ " } \\
 m_{98}^8 &= 4.23 + 6.88 = 11.11 \text{ " } \\
 m_{108}^9 &= 4.23 + 2.38 = 6.61 \text{ " }
 \end{aligned}
 \tag{8.2}$$

### 9.- DIMENSIONAMIENTO DE TRABES

#### 9.1- Tensión o compresión horizontal en Trabes en APOYOS

$$F_y/F_x = \frac{63.38}{F_x} \text{ de (9.43)}$$

$$F_1 = \frac{27.80}{0.62} = 44.84 \text{ Ton} \quad (1.41)$$

$$F_2 = \frac{27.00}{0.62} = 43.55 \text{ " } \quad (1.46)$$

$$F_3 = \frac{25.67}{0.62} = 41.40 \text{ " } \quad (1.53)$$

$$F_4 = \frac{23.81}{0.62} = 38.40 \text{ " } \quad (1.65)$$

$$F_5 = \frac{21.43}{0.62} = 34.56 \text{ " } \quad (1.83)$$

$$F_6 = \frac{18.07}{0.62} = 29.15 \text{ " } \quad (2.17)$$

$$F_7 = \frac{15.08}{0.62} = 24.32 \text{ " } \quad (2.61)$$

$$F_8 = \frac{11.11}{0.62} = 17.92 \text{ " } \quad (3.54)$$

$$F_9 = \frac{6.61}{0.62} = 10.66 \text{ " } \quad (5.95)$$

f (9.1)

#### 9.2- Sección transversal

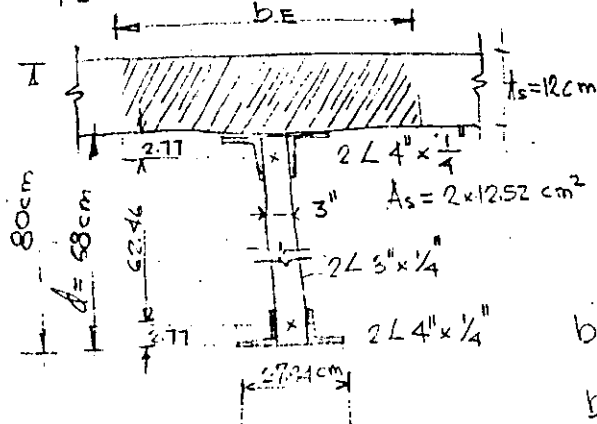


Fig. 9.1

Ancho efectivo:

claro  $l = 9.79 \text{ m}$

patrón  $b_f = 27.94 \text{ cm}$

Separación  $b_0 = 4.2 \text{ m}$

$$b_E \leq \frac{l}{4} = \frac{9.79}{4} = 2.45 \text{ m} \quad (9.2)$$

$$b_E \leq b_0 = 4.2 \text{ m}$$

$$b_E \leq b_f + 16t_s =$$

$$\leq 27.94 + 16 \times 12 = 2.20 \text{ m} //$$

Se considerará  $b_E = 200 \text{ cm}$  (9.2)

9.3-Momento último en  $\Xi$ 

Profundidad del bloque equivalente de esfuerzos

$$a = \frac{A_s f_y}{.85 f'_c b_E} = \frac{(4 \times 12.52) \times 2531}{.85 \times 250 \times 200} = 2.98 \text{ cm (9.3.1)}$$

$a < t_s$  ( $2.98 \text{ cm} < 12 \text{ cm}$ ) por lo tanto la losa es adecuada.

El momento último se expresa por

$$M_u = A_s f_y \left( \frac{d}{2} + t_s - \frac{a}{2} \right) \quad (9.3.2)$$

Substituyendo valores en (9.3.2) se obtiene

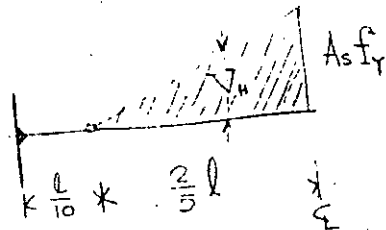
$$M_u = (4 \times 12.52) \times 2531 \left( \frac{68}{2} + 12 - \frac{2.98}{2} \right)$$

$$M_u = 5,641,752.88 \text{ Kg-cm} = 56.42 \text{ Ton-m (9.3.3)}$$

$$\text{Factor de carga } \frac{M_u}{M_d} = \frac{56.42}{22.54} = 2.50 > 1.4$$

Valor aceptable

## 9.4 Conectores



Cortante en conectores

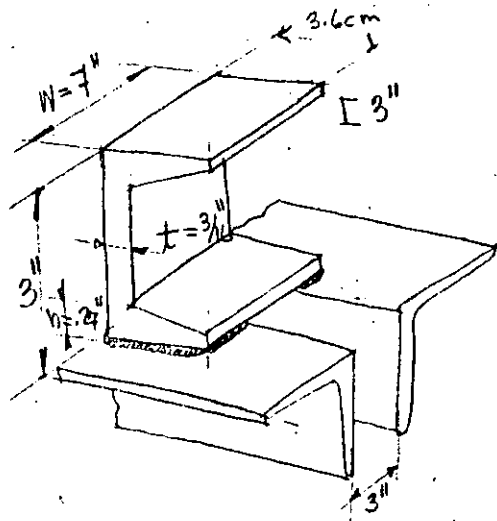
$$V_u = \frac{1}{2} A_s f_y = \frac{1}{2} (4 \times 12.52) \times 2531$$

$$V_u = 63.38 \text{ Ton} \quad (9.4.1)$$



(9)

### Capacidad de corte de un conector en cara



$$q_u = 550(h + 5t)w\sqrt{f_c'} \quad (9.4.2)$$

Subst. valores en (9.4.2)

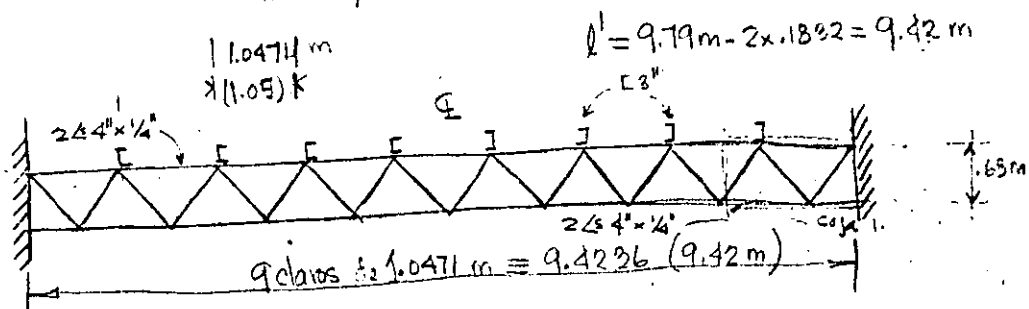
$$q_u = 550(0.27 + 5 \times \frac{3}{16}) \cdot 7 \sqrt{3.500} \quad (9.4.2)$$

$$= 82,351.00 \text{ lbs}$$

$$q_u = 37.66 \text{ Ton/con.} \quad (9.4.2)$$

Numero de conectores en  $\frac{2l}{5}$ :

$$n \geq \frac{63.38}{37.66} \geq 1.68 \text{ conectores} \equiv 2 \text{ con.}$$



Características de  $2 \times 4 \text{ inches} \times \frac{1}{4} \text{ inches}$  :  $(9.82 \text{ kg/m})$

$$A_s = 12.52 \text{ cm}^2$$

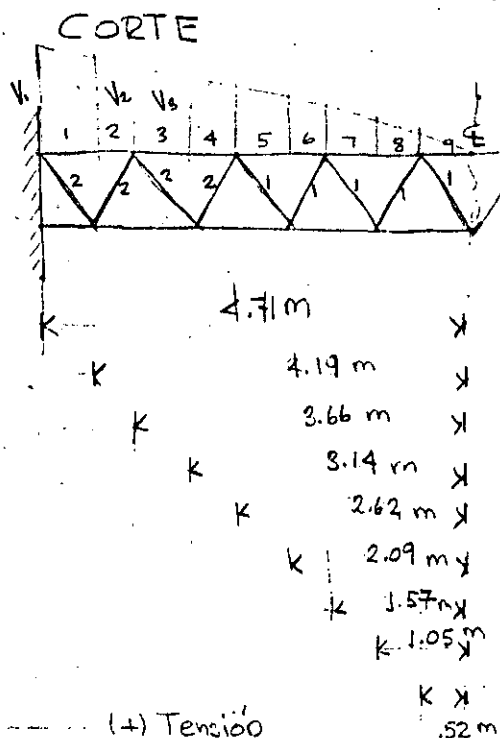
$$I_x = 124.9 \text{ cm}^4 \quad (9.4.3)$$

$$C_x = 3.18 \text{ cm}$$

$$\frac{l_u}{r_x} = \frac{104.71}{3.18} = 32.93 < 90 \text{ CORTA}$$

$$2 \times F_y = 2 \times 12.52 \times 253 = 63.38 \text{ Ton}$$

### 9.4. Tensión y compresión en diagonales



$$V_1 = 2.94 \frac{\text{Ton}}{\text{m}} \times 4.71\text{ m} = 13.85 \text{ Ton } (+)$$

$$V_2 = 2.94 \times 4.19 = 12.32 \text{ " } (-)$$

$$V_3 = 2.94 \times 3.66 = 10.76 \text{ " } (+)$$

$$V_4 = 2.94 \times 3.14 = 9.23 \text{ " } (-)$$

$$V_5 = 2.94 \times 2.62 = 7.70 \text{ " } (+)$$

$$V_6 = 2.94 \times 2.09 = 6.14 \text{ " } (-)$$

$$V_7 = 2.94 \times 1.57 = 4.62 \text{ " } (+)$$

$$V_8 = 2.94 \times 1.05 = 3.09 \text{ " } (-)$$

$$V_9 = 2.94 \times 0.52 = 1.53 \text{ " } (+)$$

(+) Tensión  
(-) compresión

$$T_1 = + \frac{13.85}{\text{Sen } 45^\circ} = + 19.59 \text{ Ton} ; \frac{19.59}{18.58} = 1.05436 \frac{\text{kg}}{\text{cm}^2}$$

$$T_2 = - \frac{12.32}{\text{Sen } 45^\circ} = - 17.42 \text{ " } ; \frac{17.42}{18.58} = 940 \text{ "}$$

$$T_3 = + \frac{10.76}{\text{Sen } 45^\circ} = + 15.22 \text{ " } ; \frac{15.22}{18.58} = 820 \text{ "}$$

$$T_4 = - \frac{9.23}{\text{Sen } 45^\circ} = - 13.05 \text{ " } ; \frac{13.05}{18.58} = 720 \text{ "}$$

$$T_5 = + \frac{7.70}{\text{Sen } 45^\circ} = + 10.89 \text{ " } ; \frac{10.89}{18.58} = 590 \text{ "}$$

$$T_6 = - \frac{6.14}{\text{Sen } 45^\circ} = - 8.68 \text{ " } ; \frac{8.68}{18.58} = 470 \text{ "}$$

$$T_7 = + \frac{4.62}{\text{Sen } 45^\circ} = + 6.53 \text{ " } ; \frac{6.53}{18.58} = 350 \text{ "}$$

$$T_8 = - \frac{3.04}{\text{Sen } 45^\circ} = - 4.30 \text{ " } ; \frac{4.30}{18.58} = 230 \text{ "}$$

$$T_9 = + \frac{1.53}{\text{Sen } 45^\circ} = + 2.16 \text{ " } ; \frac{2.16}{18.58} = 120 \text{ "}$$

$$\Delta 3'' \times \frac{5}{16}'' : 2A_1 = 11.48 \times 2 = 22.96 \text{ cm} \quad \angle 3'' \times \frac{1}{4}''$$

$$r = 2.24 \text{ cm}$$

$$l = 96.17 = \text{díl. corta}$$

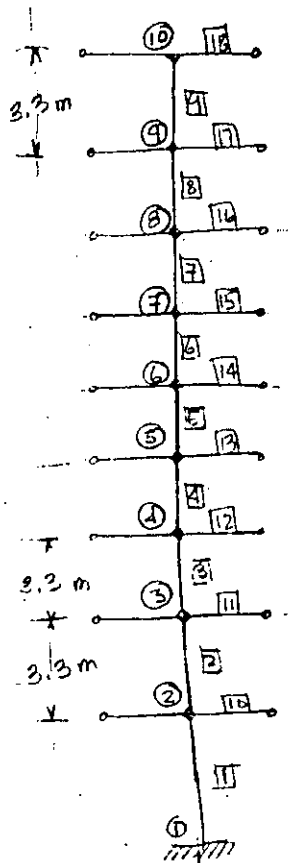
$$2A = 2 \times 9.29 = 18.58 \text{ cm}$$

$$r = 2.36 \text{ cm}$$

$$\frac{l}{r} = \frac{96.17}{2.36} = 40.75 \text{ corta}$$

### 10.- IDEALIZACIÓN ESTRUCTURAL (LONGITUDINAL)

10.1 Sismo: Se consideran los mismos valores de (5.-) Para una carga de  $75 \frac{\text{kg}}{\text{m}^2}$  (solo Estructura)



$$W_i = 4.2 \times \frac{9.79}{2} \times 75 = 1.54 \frac{\text{ton}}{\text{piso}}$$

(10.1)

$$W = 9W_i$$

$$h_1 = 3.3 \text{ m}$$

$$h_2 = 2 \times 3.3 \text{ m}$$

$$\vdots$$

$$h_9 = 9 \times 3.3 \text{ m}$$

Subst. (10.1) en (5.1) se obtiene

$$F_i = \frac{.95 \times .08 \times 9 \times 1.54}{3.3 \times 45} \cdot h_i^2$$

(10.2)

$$F_i = 0.01 h_i^2$$

los valores seran Prop. a

$$\frac{.01}{.05} = .2 \text{ de (5.3), (6.1), (7.1) y}$$

(7.2)

### 10.2 Momentos sismicos Longitudinales

Columnas:

$$M_{27}^1 = .2 \times 11.92 = 2.38 \text{ Ton-m} \quad (9.27) \quad (9.20) \text{ Ton-m}$$

$$M_{38}^2 = .2 \times 11.65 = 2.33 \text{ "}$$

$$M_{48}^3 = .2 \times 11.12 = 2.22 \text{ "}$$

$$M_{58}^4 = .2 \times 10.32 = 2.06 \text{ "}$$

$$M_{68}^5 = .2 \times 9.26 = 1.85 \text{ "}$$

$$M_{78}^6 = .2 \times 7.94 = 1.59 \text{ "}$$

$$M_{88}^7 = .2 \times 6.85 = 1.27 \text{ "}$$

$$M_{98}^8 = .2 \times 4.50 = 0.90 \text{ "}$$

$$M_{102}^9 = .2 \times 2.38 = 0.48 \text{ "}$$

(10.3)

### 10.3 Momentos sísmicos en trabes.

$$m_{23}^{10} = \frac{0.30 + 2.88}{2} = 2.36 \text{ Ton-m} \quad (9.13) \text{ Ton-m}$$

$$m_{38}^{11} = \frac{0.33 + 2.22}{2} = 2.28 \text{ "}$$

$$m_{49}^{12} = \frac{2.22 + 2.06}{2} = 2.14 \text{ "}$$

$$m_{58}^{13} = \frac{2.06 + 1.85}{2} = 1.96 \text{ "}$$

$$m_{69}^{14} = \frac{1.85 + 1.59}{2} = 1.72 \text{ "}$$

$$m_{73}^{15} = \frac{1.59 + 1.27}{2} = 1.43 \text{ "}$$

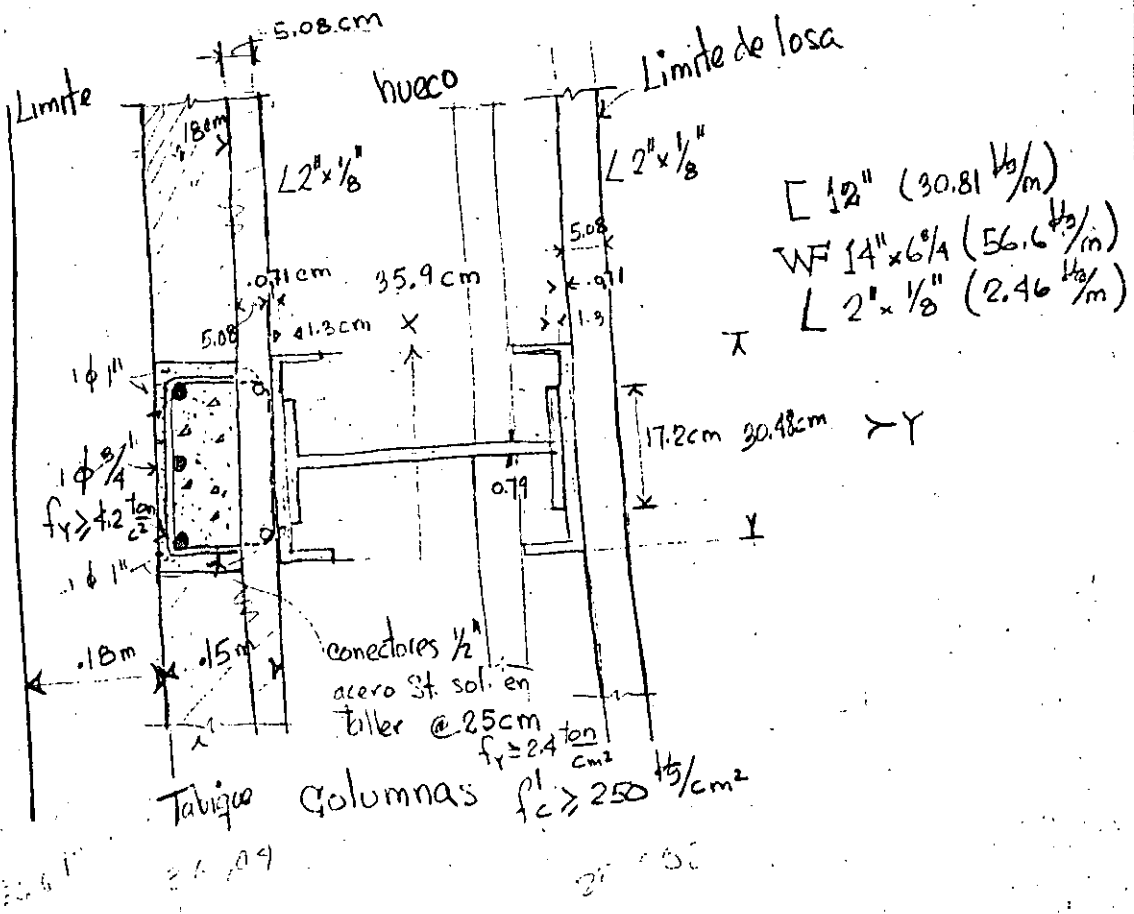
$$m_{88}^{16} = \frac{1.27 + 0.9}{2} = 1.09 \text{ "}$$

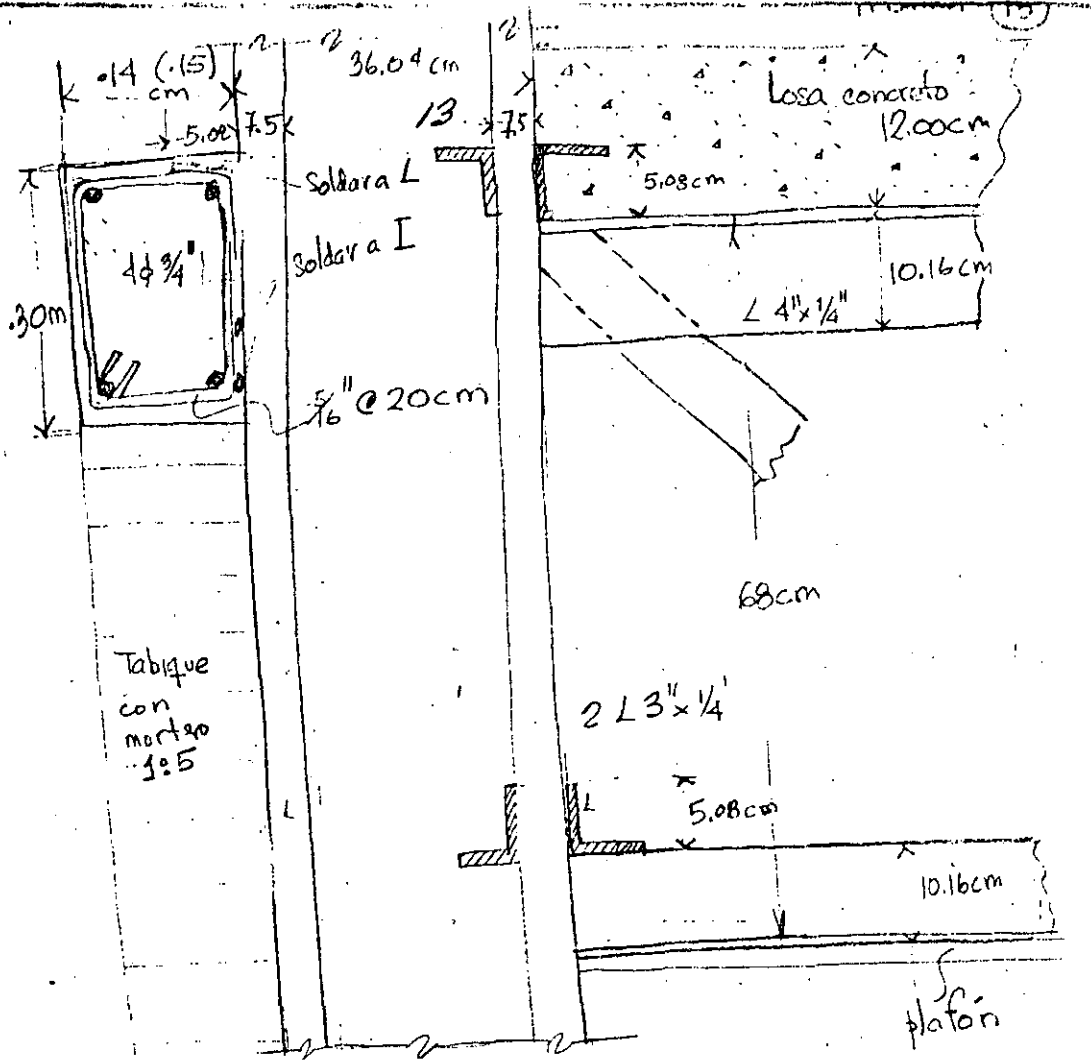
$$m_{98}^{17} = \frac{0.9 + 0.46}{2} = 0.69 \text{ "}$$

$$m_{109}^{18} = \frac{0.46}{2} = 0.24 \text{ "}$$

(10.4)

### 10.4 Sección Transversal (longitudinal)





### 10.5 Esfuerzos en Columnas

WF (IPR) 14" x 6 1/4" (56.6 kg/m)

$$\begin{aligned}
 A &= 72.06 \text{ cm}^2 & I_y &= 1023 \text{ cm}^4 \\
 d &= 35.9 \text{ cm} & S_y &= 120 \text{ cm}^3 \\
 b &= 17.2 \text{ cm} & r_y &= 3.78 \text{ cm} \\
 t_f &= 1.3 \text{ cm} \\
 t_w &= .79 \text{ cm} \\
 I_x &= 16,036 \text{ cm}^4 \\
 S_x &= 895 \text{ cm}^3 \\
 r_x &= 14.9 \text{ cm}
 \end{aligned}$$



12" (30.81 kg/m):

$$\begin{aligned}
 A &= 38.9 \text{ cm}^2 \\
 I_x &= 5,332.4 \text{ cm}^4 \\
 S_x &= 349.9 \text{ cm}^3 \\
 r_x &= 11.7 \text{ cm}
 \end{aligned}$$

$$\begin{aligned}
 I_y &= 162.7 \text{ cm}^4 \\
 S_y &= 28.6 \text{ cm}^3 \\
 r_y &= 2.05 \text{ cm} \\
 \bar{x} &= 1.78 \text{ cm}
 \end{aligned}$$

Momento de inercia de toda la sección:

$$I_x = 16,036 \text{ cm}^4 + 2 \left[ 162.7 + 38.9 \times \left( \frac{35.9}{2} + .071 - 1.78 \right)^2 \right]$$

$$I_x = 36,882.71 \text{ cm}^4$$

$$S_x = \frac{36,882.71}{\frac{35.9}{2} + .071} = 2,087.19 \text{ cm}^3$$

$$I_y = 1023 + 2 \times 5,332.4 = 11,687.80 \text{ cm}^4$$

$$S_y = \frac{11,687.80}{\frac{30.48}{2}} = 766.92 \text{ cm}^3$$

$$A = 72.06 + 2 \times 38.9 = 149.86 \text{ cm}^2$$

Columna III (10) P.B.  $N_{11} = 1.54 \frac{\text{ton}}{\text{piso}} \times 9 = 13.86 \text{ Ton}$

$$\sigma_3 = \frac{13860}{149.86} \pm \frac{238000}{766.92} = 92.49 \pm 310.33$$

$\left. \begin{array}{l} 402.82 \text{ kg/cm}^2 \\ -217.84 \text{ kg/cm}^2 \end{array} \right\} \text{Longitudinal}$

Transversal  $\parallel$  Planta baja  $N_{10} = 700 \times 4.2 \times \frac{9.79}{2} \times 9 = 129.52 \text{ Ton}$

$$\sigma_3 = \frac{129520}{149.86} \pm \frac{1403000}{2087.19} = 864.28 \pm 672.20 = 1536.48 \text{ kg/cm}^2$$

$\rightarrow 192.08 \text{ kg/cm}^2$

10.6 Esfuerzos columnas nivel 5 quitando la canal

$$I_x = 16036 \text{ cm}^4$$

col. 15

$$S_x = 895 \text{ cm}^3$$

$$N = 4 \times 700 \times 4.2 \times \frac{9.79}{2} = 57.57 \text{ Ton}$$

$$M_{63}^{15} = 10.05 \text{ ton-m}$$

$$\sigma = \frac{57570}{72.06} \pm \frac{1005000}{895} = 798.85 \pm 1122.91 = \begin{cases} 1921.76 \text{ kg/cm}^2 \\ -324.06 \text{ kg/cm}^2 \end{cases} \text{ Transversal}$$

en el sentido longitudinal

$$I_y = 1023 \text{ cm}^4$$

$$S_y = 120 \text{ cm}^3$$

$$A = 72.06 \text{ cm}^2$$

$$N = 1.54 \frac{\text{ton}}{\text{piso}} \times 5 = 7.70 \text{ Ton}$$

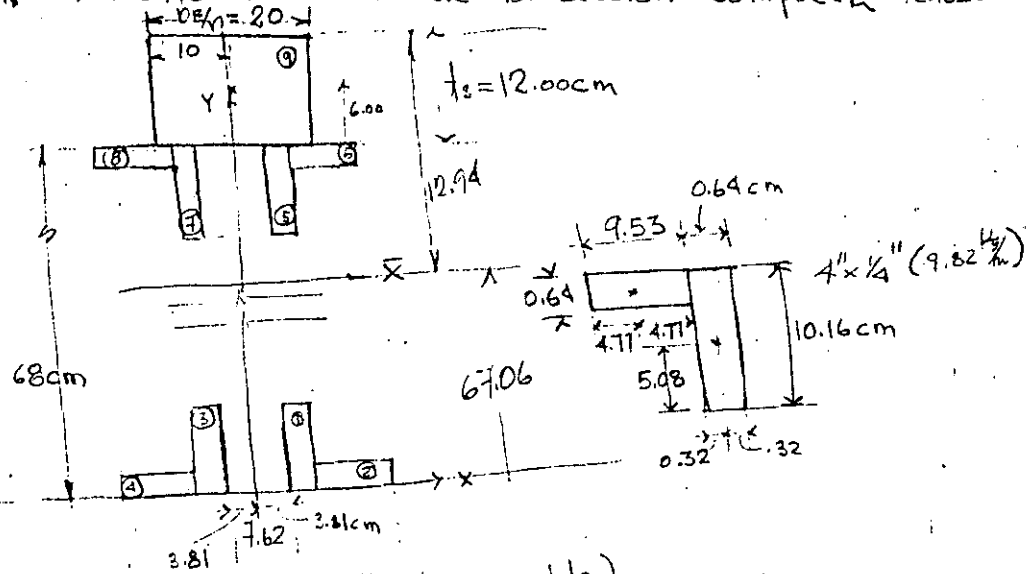
$$m = 1.59 \text{ ton-m}$$

$$\sigma = \frac{7700}{72.06} \pm \frac{159000}{120} = 106.86 \pm 1325 = \begin{cases} 1431.86 \text{ kg/cm}^2 \\ -1218.14 \text{ kg/cm}^2 \end{cases}$$

Se suprime la canal del nivel 5

hacia arriba

10.7 Momento de inercia de la sección compuesta TRABES



(Cálculo con la HP-11C programable.)

Suministro de datos

Area	$y_{oi}$	$x_{oi}$	$\Delta y_{oi}$	$\Delta x_{oi}$
1	5.08	4.13	10.16	0.64
2	0.32	9.22	0.64	9.53
3	5.08	-4.13	10.16	0.64
4	0.32	-9.22	0.64	9.53
5	62.72	4.13	10.16	0.64
6	67.68	9.22	0.64	9.53
7	62.42	-4.13	10.16	0.64
8	67.68	-9.22	0.64	9.53
9	74.00	0	12	20

Resultados Prop. Sección

$A = 290.41 \text{ cm}^2$   
 $\bar{y} = 67.06 \text{ cm}$   
 $\bar{x} = 0.00$   
 $I_y = 10,703.11 \text{ cm}^4$   
 $I_x = 1,425,042.25 \text{ cm}^4$   
 $J = 1,435,745.36 \text{ cm}^4$

$I_{xy} = \dots$   
 $I_{\bar{y}} = 10,703.11 \text{ cm}^4$   
 $I_{\bar{x}} = 119,184.07 \text{ cm}^4$   
 $I_{\bar{x}\bar{y}} = \dots$

$\phi = 0.00^\circ$   
 $I_{\bar{y}\phi} = 10,703.11 \text{ cm}^4$   
 $I_{\bar{x}\phi} = 119,184.07 \text{ cm}^4$   
 $J_\phi = 129,887.18 \text{ cm}^4$

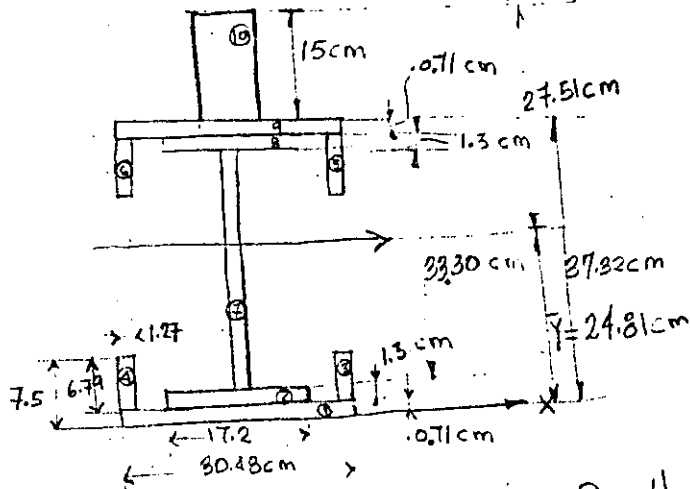
Esfuerzos en  $\sigma$  TRABES

$\sigma = \frac{M}{I_{\bar{y}\phi}} \cdot y = \frac{2254000}{119,184.07} \times 67 = -1,267.1 \text{ kg/cm}^2 \text{ (Acero)}$

$= \frac{2254000}{119,184.07} \times 13 = +245.86 \text{ kg/cm}^2$   
 $\sigma_c = 24.59 \text{ kg/cm}^2 \text{ (Concreto)}$



10.8- Sección compuesta en columnas



Datos

Area	$y_{oi}$	$x_{oi}$	$\Delta y_{oi}$	$\Delta x_{oi}$
1	0.36	0	0.71	30.48
2	1.86	0	1.30	17.2
3	4.11	14.61	6.79	1.27
4	4.11	-14.61	6.79	1.27
5	33.22	14.61	6.79	1.27
6	33.22	-14.61	6.79	1.27
7	18.66	0	33.30	0.79
8	35.96	0	1.3	17.2
9	36.97	0	0.71	30.48
10	44.82	0	15.00	3.05

Resultados Propiedades Sección

$A = 194.55 \text{ cm}^2$   
 $\bar{y} = 24.81 \text{ cm}$   
 $\bar{x} = 0.00$   
 $I_y = 11,857.44 \text{ cm}^4$   
 $I_x = 182,354.21 \text{ cm}^4$   
 $J = 194,211.65 \text{ cm}^4$   
 $I_{xy} = \text{---}$   
 $I_{\bar{y}} = 11,857.44 \text{ cm}^4$   
 $I_{\bar{x}} = 62,565.05 \text{ cm}^4$   
 $I_{xy} = \text{---}$   
 $\phi = 0.00^\circ$   
 $I_{\bar{y}\bar{y}} = 11,857.44 \text{ cm}^4$   
 $I_{\bar{x}\bar{x}} = 62,565.05 \text{ cm}^4$   
 $J_{\phi} = 74,422.49 \text{ cm}^4$

$S_x^I = \frac{62565.05}{27.51} = 2,274.27 \text{ cm}^3$   
 $S_x^{II} = \frac{62565.05}{24.81} = 2,521.77 \text{ cm}^3$

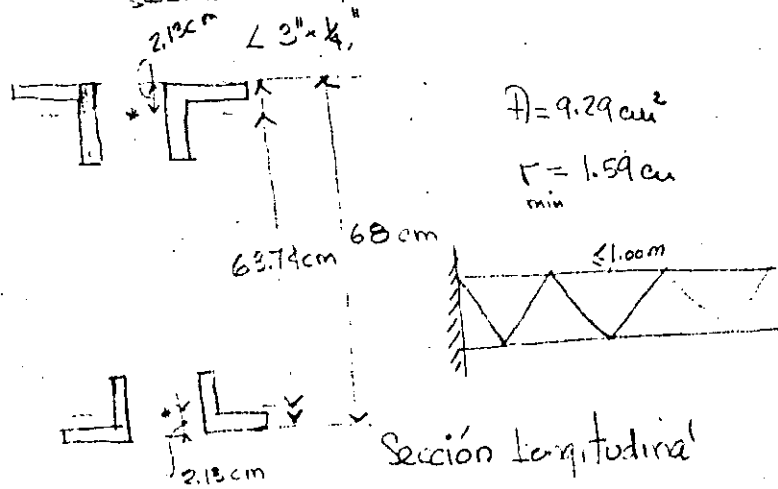
Cd III Long.  $\sigma = \frac{53640}{194.55} \pm \frac{920000}{2778.05}$   
 $= 275.71 \pm 1,182.45 =$

$S_y = \frac{11857.44}{30.48/2} = 77805 \text{ cm}^3$

$+1,458.16 \text{ Kg/cm}^2$  Est. sísmicos  
 $-906.74 \text{ Kg/cm}^2$  Longitudinales Est. + Losa Grande

Sección Longitudinal

P. Pallesco (18)



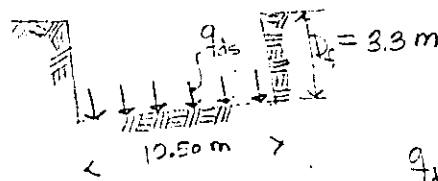
$$F_y = 2 \times 9.29 \times 253 = 47.03 \text{ Ton}$$

$$F = \frac{M}{d} = \frac{9.13}{.64} = 14.27 \text{ Ton}$$

$$\frac{F_y}{F} = \frac{47.03}{14.27} = 3.30 \text{ Aceptable}$$

## 11.- CIMENTACIÓN

11.1.- Capacidad superficial de carga a  $D_f = 3.3 \text{ m}$



La capacidad de carga superficial viene dada por

$$q_{fs} = 1.2c N_c + \gamma D_f N_q + 0.4 \gamma B N_q \quad (11.1)$$

Fig. 11.1

Donde:  $q_{fs}$  = carga de falla  
 $c$  = cohesión =  $\frac{q_u}{2} = 1.3 \text{ ton/cm}^2$   
 $\gamma$  = peso volumétrico =  $1.77 \text{ ton/cm}^3$

$B$  = ancho de cimentación =  $10.50 \text{ m}$

Para  $\phi = 0$  (ángulo de fricción)  $N_c = 5.14$   
 $N_q = 1$   
 $N_\gamma = 0$

Substituyendo valores en (11.1) se obtiene

$$q_{ds} = 1.2 \left( 1.3 \frac{\text{ton}}{\text{m}^2} \right) \times 5.14 + \left( 1.77 \frac{\text{ton}}{\text{m}^3} \right) (3.3 \text{ m}) (1) \quad \text{P. Ballastos (19)}$$

$$q_{ds} = 13.86 \frac{\text{ton}}{\text{m}^2}$$

$$q_w = \frac{13.86}{2} = 4.62 \frac{\text{ton}}{\text{m}^2} \quad (11.2)$$

Presión del peso del edificio y cargas vivas

$$p = 7 \frac{\text{ton}}{\text{m}^2} \quad (700 \text{ kg/m}^2/\text{nivel}) \quad (11.3)$$

Descarga debida a la excavación  $D_f = 3.3 \text{ m}$

$$\gamma D_f = \left( 1.77 \frac{\text{ton}}{\text{m}^3} \right) (3.3 \text{ m}) \quad (11.4)$$

$$\gamma D_f = 5.84 \frac{\text{ton}}{\text{m}^2}$$

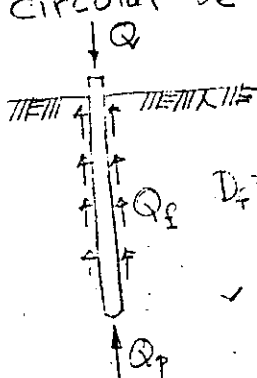
Incremento de carga en  $D_f = 3.3 \text{ m}$ , de (11.3) y (11.4)

$$\Delta p = p - \gamma D_f = 7 \frac{\text{ton}}{\text{m}^2} - 5.84 \frac{\text{ton}}{\text{m}^2}$$

$$\Delta p = 1.16 \frac{\text{ton}}{\text{m}^2} \quad (11.5)$$

(11.5) es menor que (11.2), significa que la cimentación por superficie parcialmente compensada es estable

11.2 Capacidad de carga de un pilote de fricción circular de  $d = 0.4 \text{ m}$



$$q_{dr} = 1.2c N_c + \gamma' D_f N_f + 0.6 \gamma' N_r \quad (11.6)$$

Donde:  $c$ ,  $N_c$ ,  $N_c$ ,  $N_f$  son los mismos valores de (11.1)

$$\gamma' = 0.77 \frac{\text{ton}}{\text{m}^3} \quad (\text{peso volumétrico sumergido})$$

$D_f = 20.00 \text{ m}$  Longitud del pilote

$q_{dr}$  = presión unitaria de punta.

Substituyendo valores en (11.6)

P. Ballasteros (20)

$$q_{dr} = 1.2 \left( 1.3 \frac{\text{ton}}{\text{m}^2} \right) \times 5.14 + \left( 0.77 \frac{\text{ton}}{\text{m}^3} \right) (20.00) (1)$$

$$q_{dr} = 23.42 \text{ ton/m}^2 \quad (11.7)$$

La capacidad total de punta es

$$Q_p = \frac{\pi}{4} (0.4)^2 \times 23.42$$

$$Q_p = 2.94 \text{ Ton} \quad (11.8)$$

La capacidad friccionante se expresa por

$$Q_f = \pi d D_f f = \pi (0.4) (20.00) \times 1.2 \quad (11.9)$$

$$Q_f = 30.16 \text{ Ton}$$

De (11.8) y (11.9) La capacidad total es

$$Q = Q_p + Q_f = 2.94 + 30.16$$

$$Q = 33.1 \text{ Toneladas/pilote} \quad (11.10)$$

P. Ballasteros (21)

$$N = 7457 \text{ ton}$$

$$M = 20.71$$

$$\sigma = \frac{7457000}{194.55} \pm \frac{2071000}{62565.05} \times \begin{cases} 27.51 \\ 24.81 \end{cases}$$

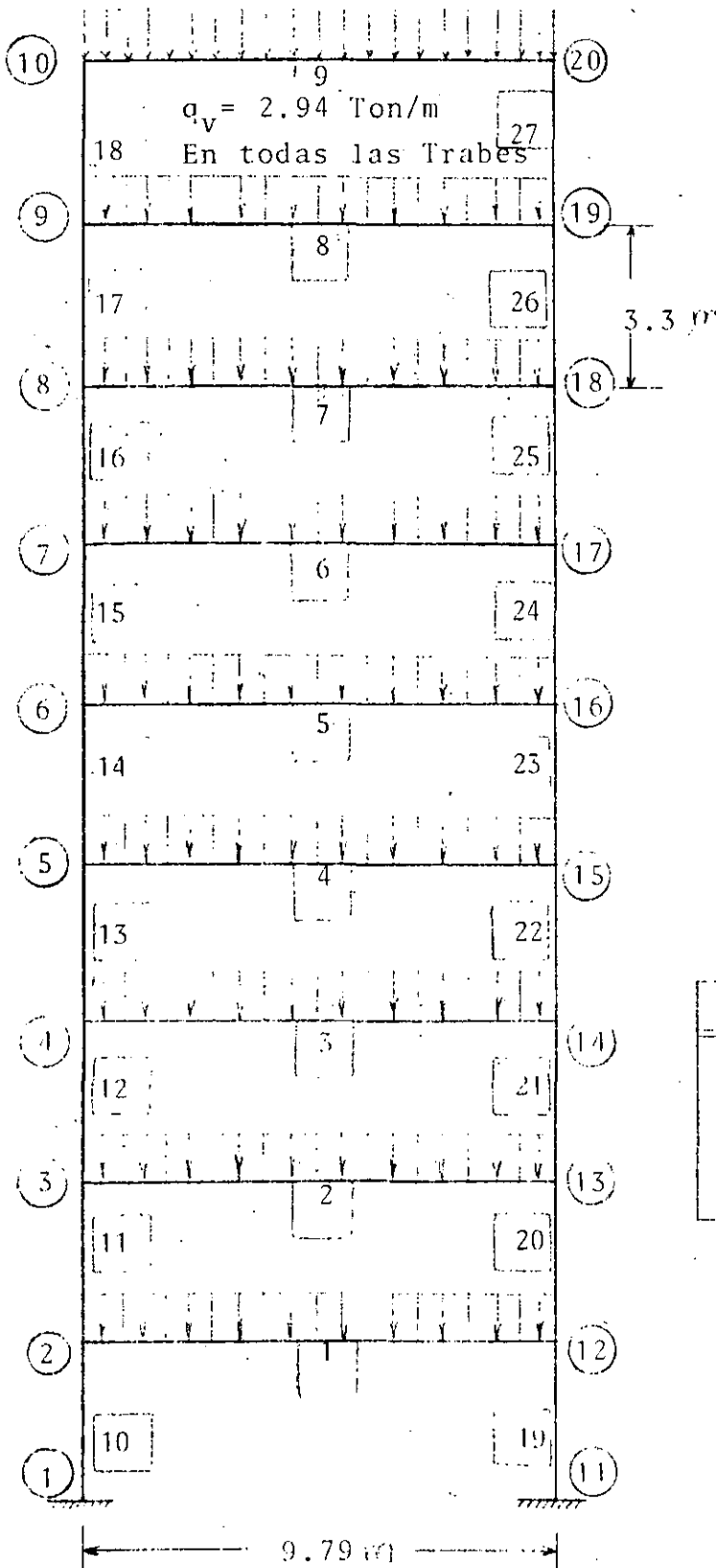
$$\sigma = \frac{N}{A} \pm \frac{M}{I} y$$

$$= \frac{2130}{200.41} \pm \frac{3330000}{119184.07} \times \begin{matrix} 12.94 \rightarrow \\ 67.02 \rightarrow \end{matrix} = \begin{matrix} 10.63 \\ 187.27 \\ (5100) \end{matrix}$$

ANALISIS DE EDIFICIO RIO TIBER GRUPO RODIN

P. BALLESTEROS DICIEMBRE 1982.

CARGA VERTICAL



○ NOBO  
□ BARRA

PROPIEDADES DE LAS SECCIONES			
Secc. uso	A (cm <sup>2</sup> )	I <sub>x</sub> (cm <sup>4</sup> )	Fac. de C.
1 Trabe	290.41	119,184.07	1.99
2 Col.	194.55	182,354.21	2.14

ESCALA : 1-150

ACOT. : Metros

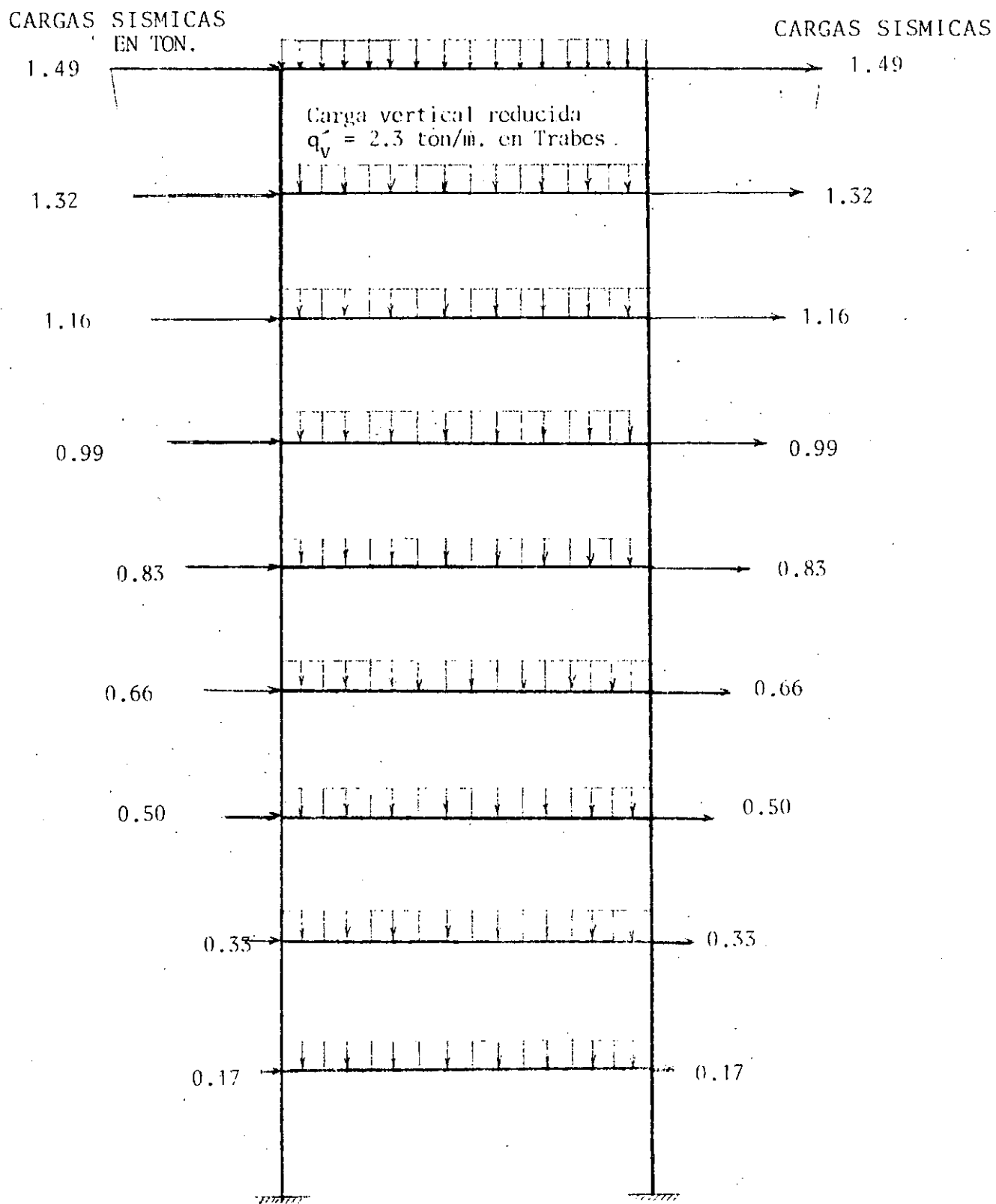
ANALISIS DE EDIFICIO RIO TIBER GRUPO RODIN:

22

II

P. BALLESTEROS DICIEMBRE 1982.

CARGA VERTICAL REDUCIDA + SISMO



\* ANALISIS DE EDIFICIO RIO TIGRE GRUPO ROSINA P. BALLESTEROS \*

1	2	3	4	5	6	7	8	9	10
11	12	13	14	15	16	17	18	19	20
21	22	23	24	25	26	27	28	29	30
31	32	33	34	35	36	37	38	39	40
41	42	43	44	45	46	47	48	49	50
51	52	53	54	55	56	57	58	59	60
61	62	63	64	65	66	67	68	69	70
71	72	73	74	75	76	77	78	79	80
81	82	83	84	85	86	87	88	89	90
91	92	93	94	95	96	97	98	99	100

- INDICES DE LOS ARCHIVOS DE ELEMENTOS Y ESTRUCTURA
- NO. DE ARCHIVO PARA ELEMENTOS
  - NO. DE ARCHIVO PARA LOS CORTANTES Y MOMENTOS
  - NO. DE ARCHIVO PARA LAS CARGAS INTERNAS
  - NO. DE ARCHIVOS PARA CUADRADOS

NO. DE ESTRUCTURAS POR ANALIZAR

NOVIEMBRE DE 1962

- NO. DE ELEMENTOS
- NO. DE TIPOLOGIAS
- NO. DE TIPOS DE MATERIAL
- NO. DE PUNTOS DE LA ESTRUCTURA
- NO. DE CUADRADOS
- NO. DE TIPOS DE SECCION
- NO. DEL PRIMER PUNTO FRONTERA
- NO. DE NUBES CON RESP. PRESCRITO
- NO. DE NUBES FRONTERA
- NO. DE CONEXIONES DE CARGA
- INDICADOR DE RESIDUOS DE ENTREPISO

22

CONSTANTES ELASTICAS DE LOS MATERIALES  
 MAT. NO. -- MODULO DE ELASTICIDAD -- COEFICIENTE DE POISSON -- PESO VOLUMETRICO  
 (TON/M\*\*2) (TON/M\*\*3)

ACIQUILINO 7.300

PARA PARAMETROS QUE DEFINEN LAS SECCIONES

TIPO	SECCION	PARAMETROS
SPECIAL		(A, IZ, EY)
RECTANGULAR		(E, H)
		(B, H, V, T)
		(B, H, V, T)
ANAL		(B, H, V, T)
REGULO		(B, H, V, T)
TRICUBAR		(D, H, V, T)
ALTA		(B, H, V, T)
CIRCULAR HUECA		(D, H)
CRUZ		(B, H, V, T, C)
TA		(B, H, V, T, C, D)
		(B, H, V, T)

• Nomenclatura • (VER FIGURAS DEL CATALOGO DE SECCIONES)

HI	ANCHURAS DE LAS SECCIONES TIPO 1, 2, 3, 4, 7, 9, 10 Y 11
BI	ANCHOS INTERIORES DE LAS SECCIONES TIPO 1, 2, 3, 4, 7, 9, 10 Y 11
HT	DIAMETRO DE LOS ANCHOS INTERIORES DE LAS SECCIONES TIPO 1, 2, 3, 4, 7, 9, 10 Y 11
HC	ALTURA DE LAS SECCIONES TIPO 1, 2, 3, 4, 7, 9, 10 Y 11
TI	ESPESOR DE LAS SECCIONES TIPO 1, 2, 3, 4, 7, 9, 10 Y 11
TT	ESPESOR DE LA TUBERIA DE LAS SECCIONES TIPO 2, 3, 4, 7, 9, 10 Y 11
FP	ESPESOR DEL PATA DE LAS SECCIONES TIPO 1, 2, 3, 4, 7, 9, 10 Y 11
ES	ESPESOR DEL PATA DE LAS SECCIONES TIPO 1, 2, 3, 4, 7, 9, 10 Y 11
CS	ANCHOS SUPERIORES DE LAS SECCIONES TIPO 1, 2, 3, 4, 7, 9, 10 Y 11
C	DISTANCIAS ENTRE LAS TUBERIAS SUPERIORES DEL ALMA Y PATIN RESPECTIVAMENTE DE LAS SECCIONES 9 Y 10
(CR)	CENTIMETROS
(M**2)	METROS A LA SEGUNDA POTENCIA
(M**4)	METROS A LA CUARTA POTENCIA
A	AREA
IZ	MOMENTO DE INERCIA RESPECTO AL EJE Z
FY	FACTOR DE FORMA PARA LA DIRECCION Y

SECCION	TIPO	BI	HI	HT	HC	TT	FP	ES	CS	C	A	IZ	FY
1	C	0.000	1.000	0.000	1.000	1.998	0.000	0.000	0.000	0.000	0.000	0.000	1.000
2	C	0.000	2.000	0.000	2.000	3.996	0.000	0.000	0.000	0.000	0.000	0.000	4.000

SECCION NO.	TIPO	BI (M)	HI (M)	HT (M)	HC (M)	TT (M)	FP (M)	ES (M)	CS (M)	C (M)	A (CM)	IZ (CM)	FY (CM)
1	C	0.000	1.000	0.000	1.000	1.998	0.000	0.000	0.000	0.000	0.000	0.000	1.000
2	C	0.000	2.000	0.000	2.000	3.996	0.000	0.000	0.000	0.000	0.000	0.000	4.000

SECCION NO.	TIPO	(M**2)	IZ (M**4)	FY
1	C	0.000	0.000	1.000
2	C	0.000	0.000	4.000

NODO NO.	ABSCISA (M)	ORDENADA (M)
1	0.000	0.000
2	0.000	1.000
3	0.000	2.000
4	0.000	3.000
5	0.000	4.000
6	0.000	5.000
7	0.000	6.000
8	0.000	7.000
9	0.000	8.000
10	0.000	9.000
11	0.000	10.000
12	0.000	11.000
13	0.000	12.000
14	0.000	13.000
15	0.000	14.000
16	0.000	15.000
17	0.000	16.000
18	0.000	17.000
19	0.000	18.000
20	0.000	19.000
21	0.000	20.000
22	0.000	21.000
23	0.000	22.000
24	0.000	23.000
25	0.000	24.000
26	0.000	25.000
27	0.000	26.000
28	0.000	27.000
29	0.000	28.000
30	0.000	29.000
31	0.000	30.000
32	0.000	31.000
33	0.000	32.000
34	0.000	33.000
35	0.000	34.000
36	0.000	35.000
37	0.000	36.000
38	0.000	37.000
39	0.000	38.000
40	0.000	39.000
41	0.000	40.000
42	0.000	41.000
43	0.000	42.000
44	0.000	43.000
45	0.000	44.000
46	0.000	45.000
47	0.000	46.000
48	0.000	47.000
49	0.000	48.000
50	0.000	49.000
51	0.000	50.000
52	0.000	51.000
53	0.000	52.000
54	0.000	53.000
55	0.000	54.000
56	0.000	55.000
57	0.000	56.000
58	0.000	57.000
59	0.000	58.000
60	0.000	59.000
61	0.000	60.000
62	0.000	61.000
63	0.000	62.000
64	0.000	63.000
65	0.000	64.000
66	0.000	65.000
67	0.000	66.000
68	0.000	67.000
69	0.000	68.000
70	0.000	69.000
71	0.000	70.000
72	0.000	71.000
73	0.000	72.000
74	0.000	73.000
75	0.000	74.000
76	0.000	75.000
77	0.000	76.000
78	0.000	77.000
79	0.000	78.000
80	0.000	79.000
81	0.000	80.000
82	0.000	81.000
83	0.000	82.000
84	0.000	83.000
85	0.000	84.000
86	0.000	85.000
87	0.000	86.000
88	0.000	87.000
89	0.000	88.000
90	0.000	89.000
91	0.000	90.000
92	0.000	91.000
93	0.000	92.000
94	0.000	93.000
95	0.000	94.000
96	0.000	95.000
97	0.000	96.000
98	0.000	97.000
99	0.000	98.000
100	0.000	99.000

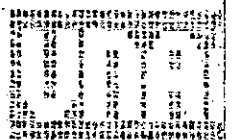
BARRA NO.	NUDO I	NUDO J	MAT. NO.	SEC. NO.	APOY. J	APOY. I	LONGITUD
1	1	2	1	1	0	0	1.000
2	2	3	1	1	0	0	1.000





\* CONDICION DE CARGA #1 : CARGA VERTICAL DE 2.94 TON/M \*

1 NO. DE CONDICION DE CARGA  
2 NO. DE CARGA EN LA BARRA  
3 NO. DE CARGA EN LA BARRA  
4 INDICADOR DE FUERZAS DE CUERPO, 1=SI; 0=NO

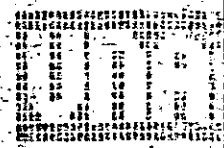


DADOS PARA EL CASO DE BARRAS CON CARGAS INTERMEDIAS DISTINTAS A PESO PROPIO  
BARRAS IND. GRAF.

26

- BARRA 1 CARGA DIST UNIFORM CONTIN(TON/M)= 2.9400
- BARRA 2 CARGA DIST UNIFORM CONTIN(TON/M)= A LA BARRA ANTERIOR
- BARRA 3 CARGA DIST UNIFORM CONTIN(TON/M)= A LA BARRA ANTERIOR
- BARRA 4 CARGA DIST UNIFORM CONTIN(TON/M)= A LA BARRA ANTERIOR
- BARRA 5 CARGA DIST UNIFORM CONTIN(TON/M)= A LA BARRA ANTERIOR
- BARRA 6 CARGA DIST UNIFORM CONTIN(TON/M)= A LA BARRA ANTERIOR
- BARRA 7 CARGA DIST UNIFORM CONTIN(TON/M)= A LA BARRA ANTERIOR
- BARRA 8 CARGA DIST UNIFORM CONTIN(TON/M)= A LA BARRA ANTERIOR
- BARRA 9 CARGA DIST UNIFORM CONTIN(TON/M)= A LA BARRA ANTERIOR
- BARRA 10 CARGA DIST UNIFORM CONTIN(TON/M)= A LA BARRA ANTERIOR
- BARRA 11 CARGA DIST UNIFORM CONTIN(TON/M)= A LA BARRA ANTERIOR
- BARRA 12 CARGA DIST UNIFORM CONTIN(TON/M)= A LA BARRA ANTERIOR

BARRA 12 CARGA DIST UNIFORM CONTIN(TON/M)=A LA BARRA ANTERIOR  
 BARRA 13 CARGA DIST UNIFORM CONTIN(TON/M)=A LA BARRA ANTERIOR  
 BARRA 14 CARGA DIST UNIFORM CONTIN(TON/M)=A LA BARRA ANTERIOR  
 BARRA 15 CARGA DIST UNIFORM CONTIN(TON/M)=A LA BARRA ANTERIOR  
 BARRA 16 CARGA DIST UNIFORM CONTIN(TON/M)=A LA BARRA ANTERIOR  
 BARRA 17 CARGA DIST UNIFORM CONTIN(TON/M)=A LA BARRA ANTERIOR  
 BARRA 18 CARGA DIST UNIFORM CONTIN(TON/M)=A LA BARRA ANTERIOR  
 BARRA 19 CARGA DIST UNIFORM CONTIN(TON/M)=A LA BARRA ANTERIOR  
 BARRA 20 CARGA DIST UNIFORM CONTIN(TON/M)=A LA BARRA ANTERIOR  
 BARRA 21 CARGA DIST UNIFORM CONTIN(TON/M)=A LA BARRA ANTERIOR  
 BARRA 22 CARGA DIST UNIFORM CONTIN(TON/M)=A LA BARRA ANTERIOR  
 BARRA 23 CARGA DIST UNIFORM CONTIN(TON/M)=A LA BARRA ANTERIOR  
 BARRA 24 CARGA DIST UNIFORM CONTIN(TON/M)=A LA BARRA ANTERIOR  
 BARRA 25 CARGA DIST UNIFORM CONTIN(TON/M)=A LA BARRA ANTERIOR  
 BARRA 26 CARGA DIST UNIFORM CONTIN(TON/M)=A LA BARRA ANTERIOR  
 BARRA 27 CARGA DIST UNIFORM CONTIN(TON/M)=A LA BARRA ANTERIOR



DESPLAZAMIENTOS NODALES DE LA ESTRUCTURA (M) 97  
 PTO. NOD. H O R I Z O N T A L V E R T I C A L G I R O S (RAD)

PTO. NOD.	H	O	R	H	O	R	I	Z	O	N	T	A	L	V	E	R	T	I	C	A	L	G	I	R	O	S	(R	A	D)
1	0	0	0	0	0	0	0	0	0	0	0	0	0	0	0	0	0	0	0	0	0	0	0	0	0	0	0	0	
2	0	0	0	0	0	0	0	0	0	0	0	0	0	0	0	0	0	0	0	0	0	0	0	0	0	0	0	0	
3	0	0	0	0	0	0	0	0	0	0	0	0	0	0	0	0	0	0	0	0	0	0	0	0	0	0	0	0	
4	0	0	0	0	0	0	0	0	0	0	0	0	0	0	0	0	0	0	0	0	0	0	0	0	0	0	0	0	
5	0	0	0	0	0	0	0	0	0	0	0	0	0	0	0	0	0	0	0	0	0	0	0	0	0	0	0	0	
6	0	0	0	0	0	0	0	0	0	0	0	0	0	0	0	0	0	0	0	0	0	0	0	0	0	0	0	0	
7	0	0	0	0	0	0	0	0	0	0	0	0	0	0	0	0	0	0	0	0	0	0	0	0	0	0	0	0	
8	0	0	0	0	0	0	0	0	0	0	0	0	0	0	0	0	0	0	0	0	0	0	0	0	0	0	0	0	
9	0	0	0	0	0	0	0	0	0	0	0	0	0	0	0	0	0	0	0	0	0	0	0	0	0	0	0	0	
10	0	0	0	0	0	0	0	0	0	0	0	0	0	0	0	0	0	0	0	0	0	0	0	0	0	0	0	0	
11	0	0	0	0	0	0	0	0	0	0	0	0	0	0	0	0	0	0	0	0	0	0	0	0	0	0	0	0	
12	0	0	0	0	0	0	0	0	0	0	0	0	0	0	0	0	0	0	0	0	0	0	0	0	0	0	0	0	
13	0	0	0	0	0	0	0	0	0	0	0	0	0	0	0	0	0	0	0	0	0	0	0	0	0	0	0	0	
14	0	0	0	0	0	0	0	0	0	0	0	0	0	0	0	0	0	0	0	0	0	0	0	0	0	0	0	0	
15	0	0	0	0	0	0	0	0	0	0	0	0	0	0	0	0	0	0	0	0	0	0	0	0	0	0	0	0	
16	0	0	0	0	0	0	0	0	0	0	0	0	0	0	0	0	0	0	0	0	0	0	0	0	0	0	0	0	
17	0	0	0	0	0	0	0	0	0	0	0	0	0	0	0	0	0	0	0	0	0	0	0	0	0	0	0	0	
18	0	0	0	0	0	0	0	0	0	0	0	0	0	0	0	0	0	0	0	0	0	0	0	0	0	0	0	0	
19	0	0	0	0	0	0	0	0	0	0	0	0	0	0	0	0	0	0	0	0	0	0	0	0	0	0	0	0	
20	0	0	0	0	0	0	0	0	0	0	0	0	0	0	0	0	0	0	0	0	0	0	0	0	0	0	0	0	
21	0	0	0	0	0	0	0	0	0	0	0	0	0	0	0	0	0	0	0	0	0	0	0	0	0	0	0	0	
22	0	0	0	0	0	0	0	0	0	0	0	0	0	0	0	0	0	0	0	0	0	0	0	0	0	0	0	0	
23	0	0	0	0	0	0	0	0	0	0	0	0	0	0	0	0	0	0	0	0	0	0	0	0	0	0	0	0	
24	0	0	0	0	0	0	0	0	0	0	0	0	0	0	0	0	0	0	0	0	0	0	0	0	0	0	0	0	
25	0	0	0	0	0	0	0	0	0	0	0	0	0	0	0	0	0	0	0	0	0	0	0	0	0	0	0	0	
26	0	0	0	0	0	0	0	0	0	0	0	0	0	0	0	0	0	0	0	0	0	0	0	0	0	0	0	0	
27	0	0	0	0	0	0	0	0	0	0	0	0	0	0	0	0	0	0	0	0	0	0	0	0	0	0	0	0	

BARRA EXT. INICIAL (TON Y TON-M) EXTREMO FINAL (TON Y TON-M) EXTREMO FINAL (TON Y TON-M)  
 NO. DE BARRA INICIAL NO. DE BARRA FINAL NO. DE BARRA INICIAL NO. DE BARRA FINAL NO. DE BARRA INICIAL NO. DE BARRA FINAL  
 1 2 12 21 2556 14 39 36 22 43363 2 72566 -14 391 50 -22 43363











ORDENADO

14.10130

-22.64295

H.25009

-14.19130

-22.64295

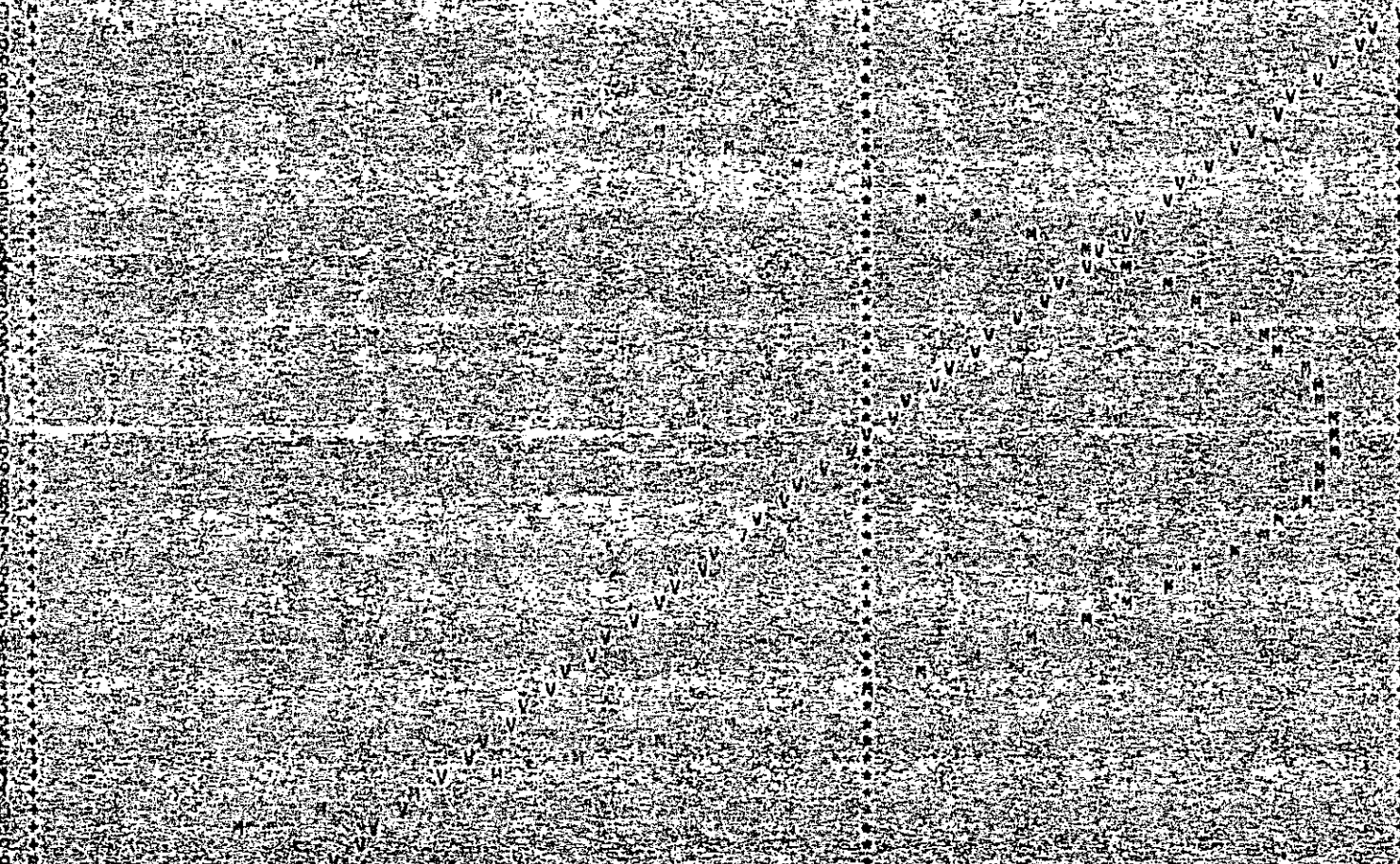
ESCALA DE LA GRAFICA = 1:20000 UNIDADES/COLUMNA

ORDENADA MENOR = 1459130

ORDENADA MAYOR = 1459130

PARA NO. PUNTO INICIAL = 7 PUNTO FINAL = 17

1  
2  
3  
4  
5  
6  
7  
8  
9  
10  
11  
12  
13  
14  
15  
16  
17  
18  
19  
20  
21  
22  
23  
24  
25  
26  
27  
28  
29  
30  
31  
32  
33  
34  
35  
36  
37  
38  
39  
40  
41  
42  
43  
44  
45  
46  
47  
48  
49  
50  
51  
52  
53  
54  
55  
56  
57  
58  
59  
60  
61  
62  
63  
64  
65  
66  
67  
68  
69  
70  
71  
72  
73  
74  
75  
76  
77  
78  
79  
80  
81  
82  
83  
84  
85  
86  
87  
88  
89  
90  
91  
92  
93  
94  
95  
96  
97  
98  
99  
100



1	44E+01	20E+00
2	38E+01	99E+00
3	32E+01	78E+00
4	27E+01	47E+00
5	21E+01	23E+00
6	15E+01	36E+00
7	09E+01	76E+00
8	04E+01	65E+00
9	70E+00	71E+00
10	21E+00	85E+00
11	06E+00	00E+00
12	00E+00	53E+00
13	01E+00	06E+00
14	01E+00	44E+00
15	01E+00	76E+00
16	01E+00	94E+00
17	01E+00	87E+00
18	03E+00	87E+00
19	03E+00	06E+00
20	03E+00	12E+00
21	03E+00	17E+00
22	03E+00	17E+00
23	03E+00	23E+00
24	03E+00	23E+00
25	03E+00	23E+00
26	03E+00	23E+00
27	03E+00	23E+00
28	03E+00	23E+00
29	03E+00	23E+00
30	03E+00	23E+00
31	03E+00	23E+00
32	03E+00	23E+00
33	03E+00	23E+00
34	03E+00	23E+00
35	03E+00	23E+00
36	03E+00	23E+00
37	03E+00	23E+00
38	03E+00	23E+00
39	03E+00	23E+00
40	03E+00	23E+00
41	03E+00	23E+00
42	03E+00	23E+00
43	03E+00	23E+00
44	03E+00	23E+00
45	03E+00	23E+00
46	03E+00	23E+00
47	03E+00	23E+00
48	03E+00	23E+00
49	03E+00	23E+00
50	03E+00	23E+00
51	03E+00	23E+00
52	03E+00	23E+00
53	03E+00	23E+00
54	03E+00	23E+00
55	03E+00	23E+00
56	03E+00	23E+00
57	03E+00	23E+00
58	03E+00	23E+00
59	03E+00	23E+00
60	03E+00	23E+00
61	03E+00	23E+00
62	03E+00	23E+00
63	03E+00	23E+00
64	03E+00	23E+00
65	03E+00	23E+00
66	03E+00	23E+00
67	03E+00	23E+00
68	03E+00	23E+00
69	03E+00	23E+00
70	03E+00	23E+00
71	03E+00	23E+00
72	03E+00	23E+00
73	03E+00	23E+00
74	03E+00	23E+00
75	03E+00	23E+00
76	03E+00	23E+00
77	03E+00	23E+00
78	03E+00	23E+00
79	03E+00	23E+00
80	03E+00	23E+00
81	03E+00	23E+00
82	03E+00	23E+00
83	03E+00	23E+00
84	03E+00	23E+00
85	03E+00	23E+00
86	03E+00	23E+00
87	03E+00	23E+00
88	03E+00	23E+00
89	03E+00	23E+00
90	03E+00	23E+00
91	03E+00	23E+00
92	03E+00	23E+00
93	03E+00	23E+00
94	03E+00	23E+00
95	03E+00	23E+00
96	03E+00	23E+00
97	03E+00	23E+00
98	03E+00	23E+00
99	03E+00	23E+00
100	03E+00	23E+00

CONTANTES EN TON Y MOMENTOS EN TON-M

ORDENADA MENOR = 1459130

ORDENADA MAYOR = 1459130

ORDENADA MAYOR = 1459130

PARA NO. PUNTO INICIAL = 7

PUNTO FINAL = 17

PUNTO FINAL = 17



14-09114 - 14-09114 - 14-09114 - 14-09114 - 14-09114





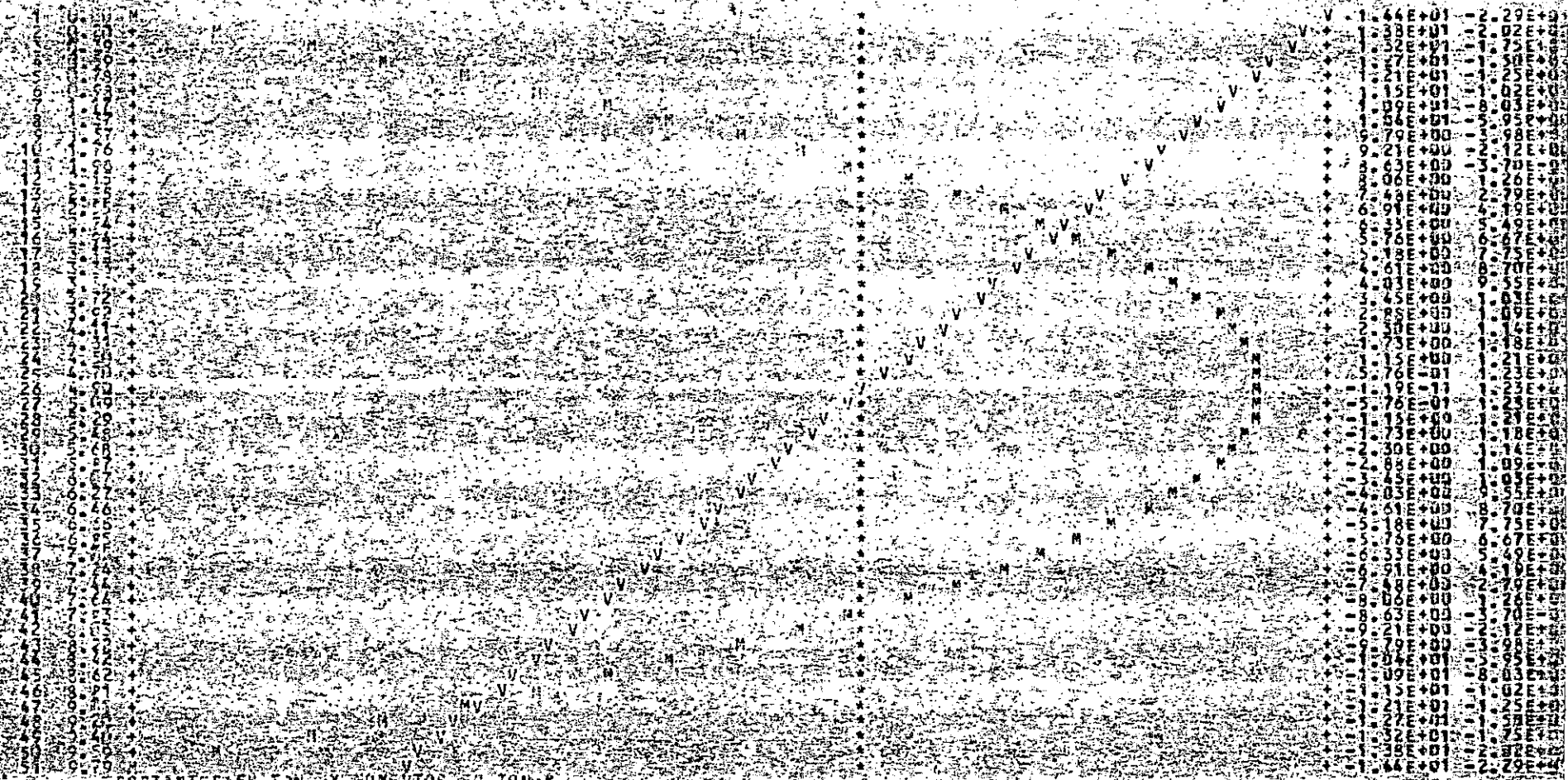


4.04702 4.04706 -22.91243 4.04706 -14.39130 -22.91243

ESCALA DE LA GRAFICA = 1.25913E+01 UNIDADES/COLUMA  
 CANTONADA MENOR = 1.25913E+01  
 CANTONADA MAYOR = 1.25913E+01

BARRA NO. 0 NURO INICIAL = 9 NURO FINAL = 19

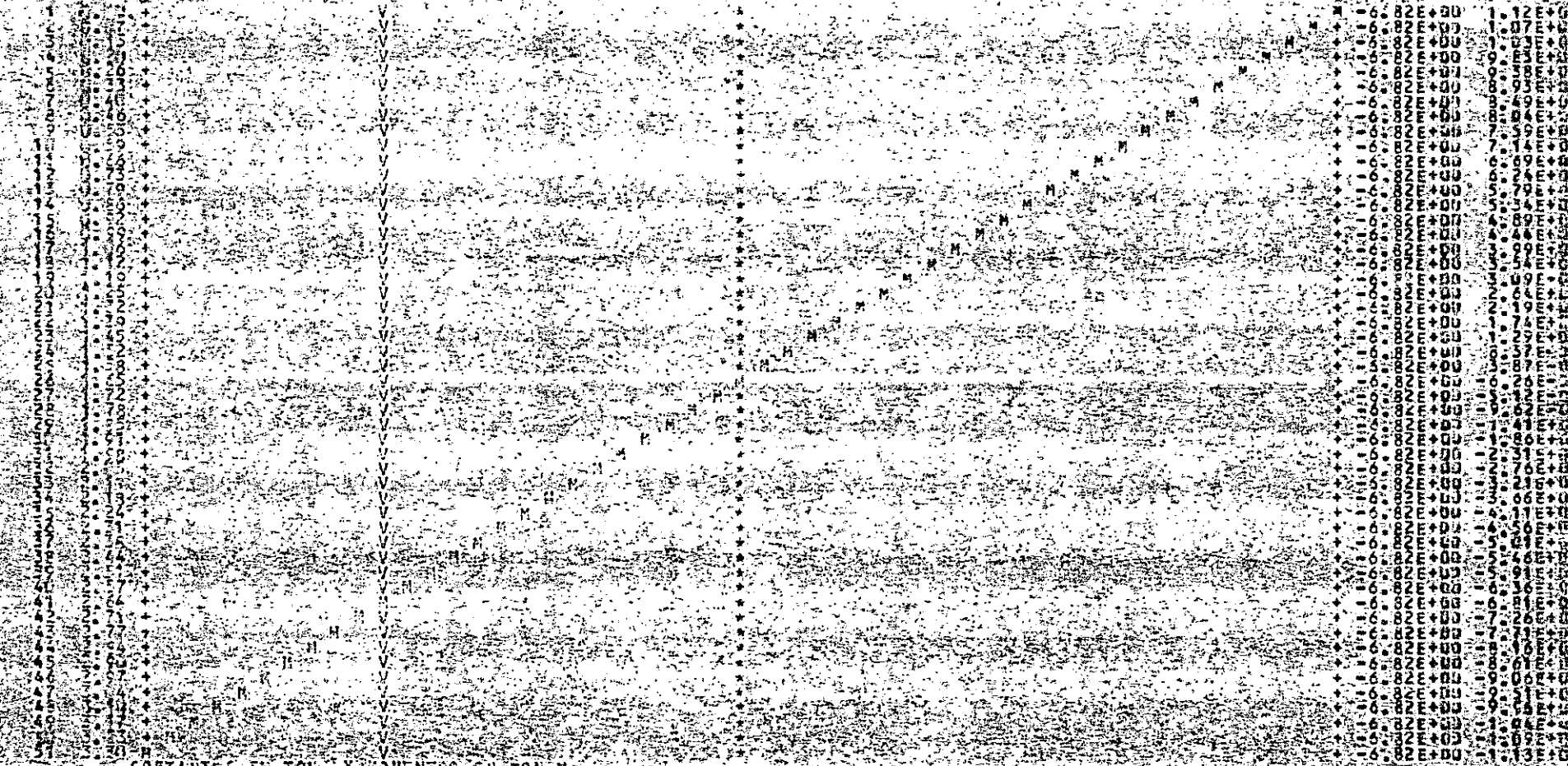
1	1	1	1
2	2	2	2
3	3	3	3
4	4	4	4
5	5	5	5
6	6	6	6
7	7	7	7
8	8	8	8
9	9	9	9
10	10	10	10
11	11	11	11
12	12	12	12
13	13	13	13
14	14	14	14
15	15	15	15
16	16	16	16
17	17	17	17
18	18	18	18
19	19	19	19



CORTANTES EN TON. Y MOMENTOS EN TON-M.

BARRA NO. INICIAL FINAL EXTREMO INICIAL (TON Y TON-M) EXTREMO FINAL (TON Y TON-M)  
 NO. DE TAMAÑO DE FLEXIONANTE NO. DE TAMAÑO DE FLEXIONANTE

ESCALA DE LA GRAFICA = 1/10000 UNIDADES/COLUMA  
ORDENADA DEL OR = -1.10000E+01  
ORDENADA DEL OR = -1.10000E+01  
BARRA NO. 10, MUDD. INICIAL = 0, MUDD. FINAL = 4



CORTANTES EN TON. Y MOMENTOS EN TON-M

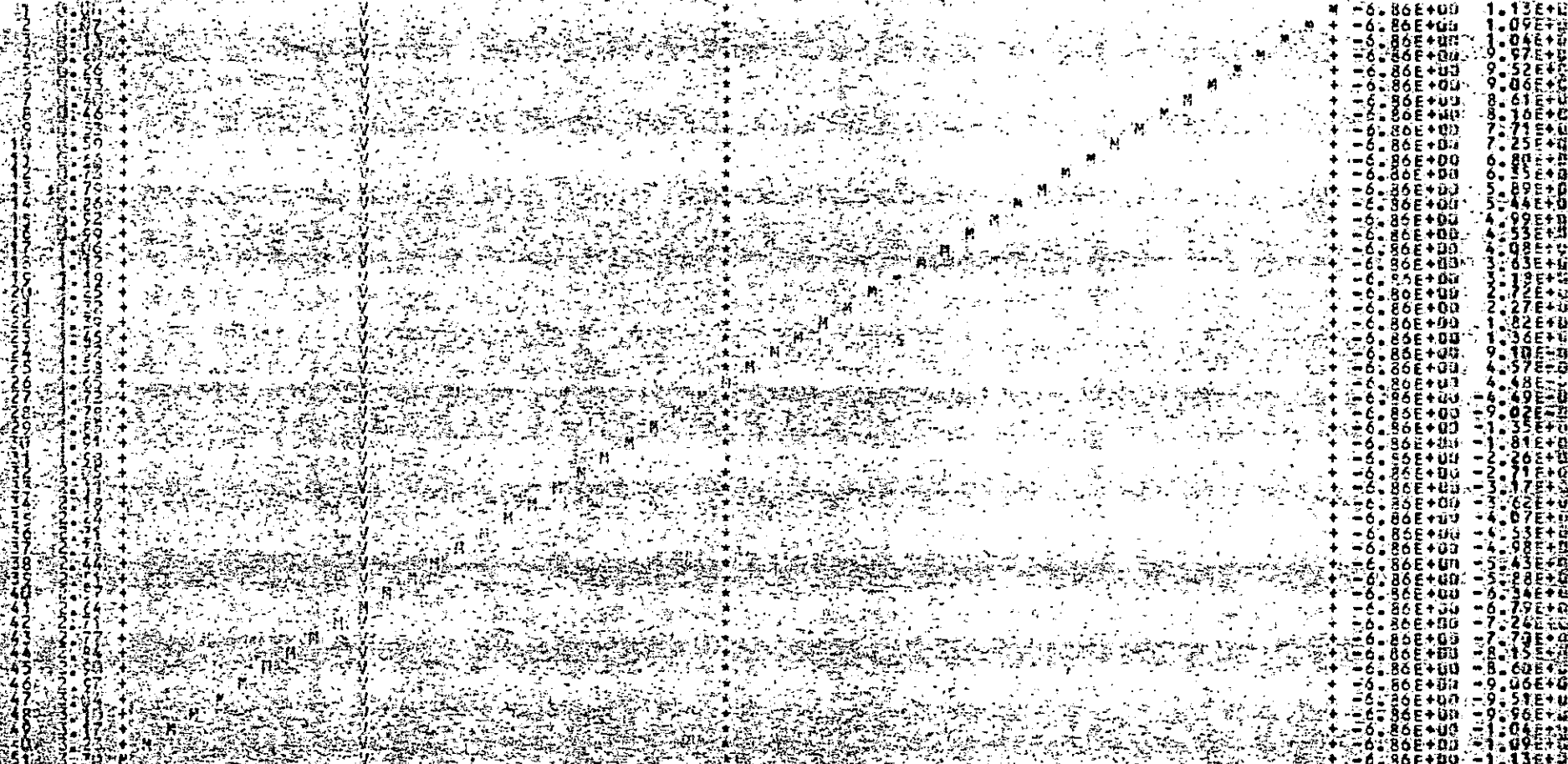
BARRA DE EXTREMO A EXTREMO INICIAL (TON Y TON-M) EXTREMO FINAL (TON Y TON-M)  
NO INICIAL FINAL MUDD. INICIAL MUDD. FINAL NO R. B. A. L. COOP. T. A. N. T. E. FLEXIONANTE

1 4 3 -86.34733 -86.36378 11.32972 -86.34733 -6.85378 -11.32976

ESCUELA DE GRAFICAS - 2.26756 - 1 UNIDADES/COLUMNA  
ORDENADA MENOR - 1.13297E+11  
ORDENADA MAYOR

BARRA NO. 13, MUDDO INICIAL= 4, MUDDO FINAL= 5

1  
2  
3  
4  
5  
6  
7  
8  
9  
10  
11  
12  
13  
14  
15  
16  
17  
18  
19  
20  
21  
22  
23  
24  
25  
26  
27  
28  
29  
30  
31  
32  
33  
34  
35  
36  
37  
38  
39  
40  
41  
42  
43  
44  
45  
46  
47  
48  
49  
50  
51  
52  
53  
54  
55  
56  
57  
58  
59  
60  
61  
62  
63  
64  
65  
66  
67  
68  
69  
70  
71  
72  
73  
74  
75  
76  
77  
78  
79  
80  
81  
82  
83  
84  
85  
86  
87  
88  
89  
90  
91  
92  
93  
94  
95  
96  
97  
98  
99  
100



CORTANTES EN TON. Y MOMENTOS EN TON-M

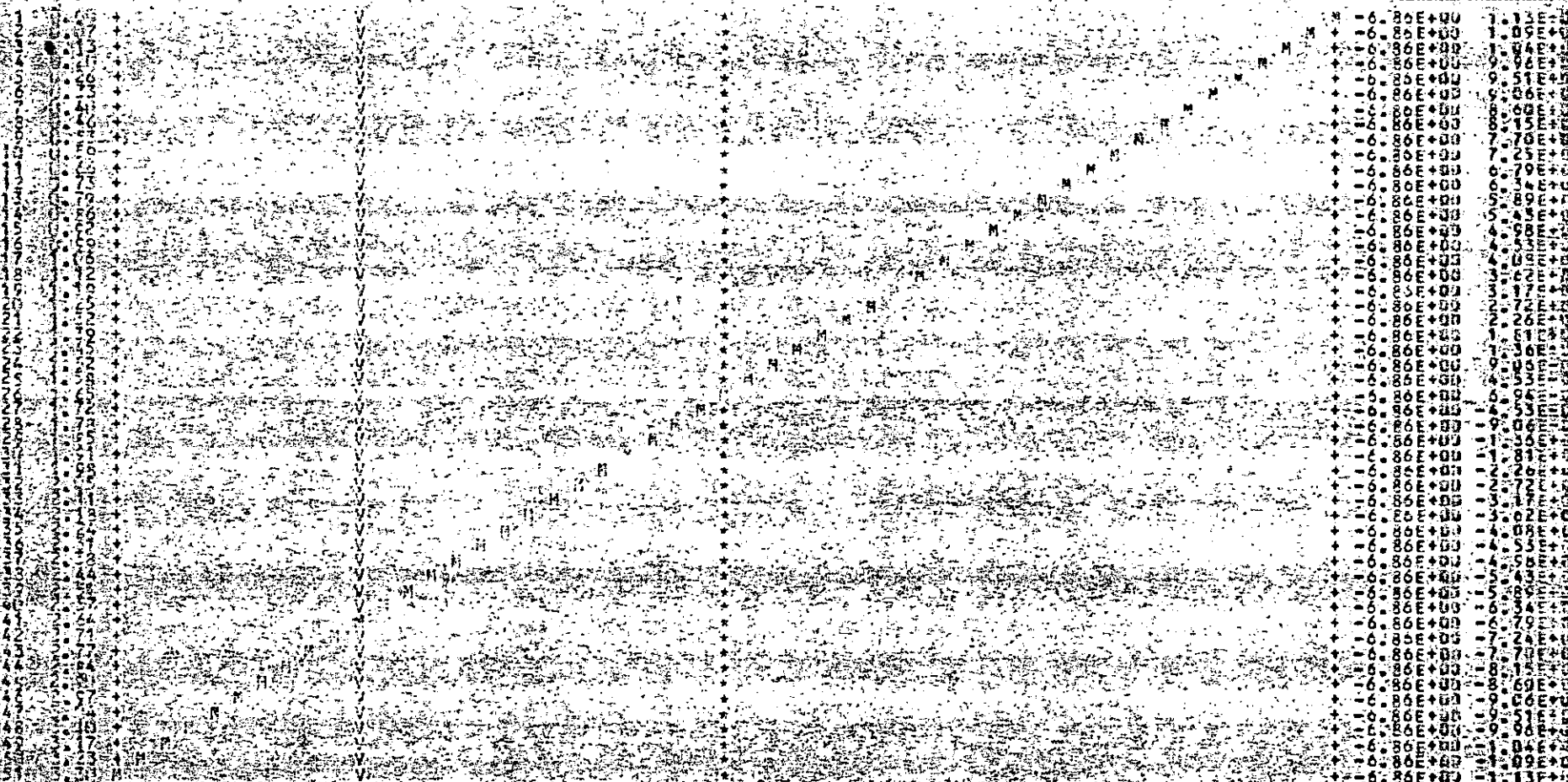
BARRA NO.	EXTREMO INICIAL (TON. Y TON-M)	EXTREMO FINAL (TON. Y TON-M)
13	4	5
INICIAL FINAL	C O R T A N T E F L E X I O N A N T E	C O R T A N T E F L E X I O N A N T E



ESCALA DE GRAFICA = 2.2657E-01 UNIDADES/COLUMA  
 ORDENADA MENOR = 1.1329E+01  
 ORDENADA MAYOR = 1.1329E+01

BARRA NO. 15, NUDO INICIAL = 5, NUDO FINAL = 6

1  
2  
3  
4  
5  
6  
7  
8  
9  
10  
11  
12  
13  
14  
15  
16  
17  
18  
19  
20  
21  
22  
23  
24  
25  
26  
27  
28  
29  
30  
31  
32  
33  
34  
35  
36  
37  
38  
39  
40  
41  
42  
43  
44  
45  
46  
47  
48  
49  
50  
51  
52  
53  
54  
55  
56  
57  
58  
59  
60  
61  
62  
63  
64  
65  
66  
67  
68  
69  
70  
71  
72  
73  
74  
75  
76  
77  
78  
79  
80  
81  
82  
83  
84  
85  
86  
87  
88  
89  
90  
91  
92  
93  
94  
95  
96  
97  
98  
99  
100



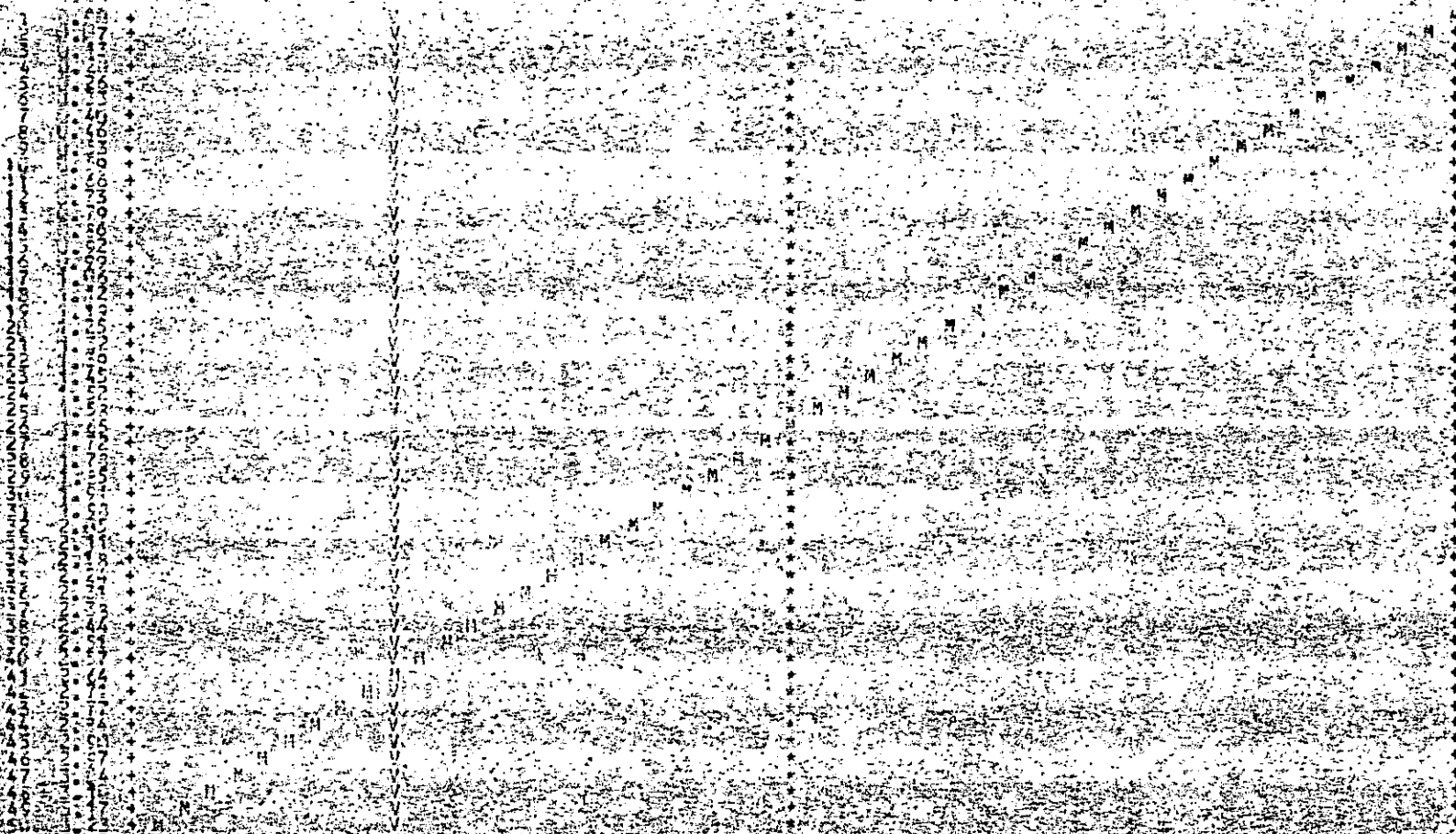
CORTANTES EN TON. Y MOMENTOS EN TON-M

BARRA EXTREMO INICIAL (TON Y TON-M) EXTREMO FINAL (TON Y TON-M)  
 NUDO INICIAL FINAL NUDO INICIAL FINAL NUDO INICIAL FINAL NUDO INICIAL FINAL  
 COEFICIENTE DE RIGIDEZ COEFICIENTE DE RIGIDEZ COEFICIENTE DE RIGIDEZ COEFICIENTE DE RIGIDEZ  
 FLEXIONANTE FLEXIONANTE FLEXIONANTE FLEXIONANTE

ESCALA DE GRAFICAS 1:26339E-01 UNIDADES/COLUMA

BARRA NO. 15. NUDO INICIAL= 6. NUDO FINAL= 7

1	2	3	4	5	6	7	8	9	10	11	12	13	14	15	16	17	18	19	20	21	22	23	24	25	26	27	28	29	30	31	32	33	34	35	36	37	38	39	40	41	42	43	44	45	46	47	48	49	50	51	52	53	54	55	56	57	58	59	60	61	62	63	64	65	66	67	68	69	70	71	72	73	74	75	76	77	78	79	80	81	82	83	84	85	86	87	88	89	90	91	92	93	94	95	96	97	98	99	100
---	---	---	---	---	---	---	---	---	----	----	----	----	----	----	----	----	----	----	----	----	----	----	----	----	----	----	----	----	----	----	----	----	----	----	----	----	----	----	----	----	----	----	----	----	----	----	----	----	----	----	----	----	----	----	----	----	----	----	----	----	----	----	----	----	----	----	----	----	----	----	----	----	----	----	----	----	----	----	----	----	----	----	----	----	----	----	----	----	----	----	----	----	----	----	----	----	----	----	-----



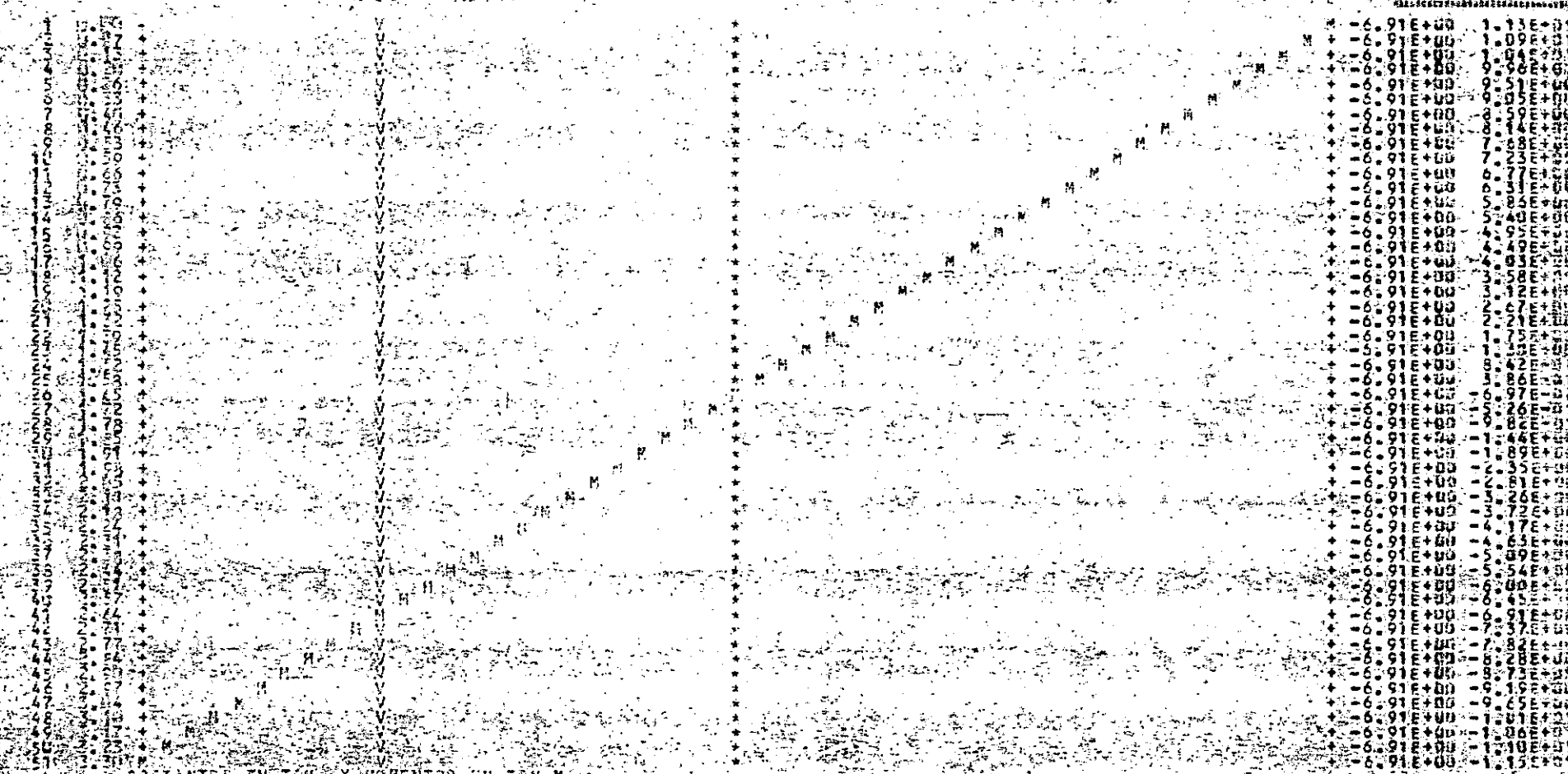
1	1.13E+00
2	1.04E+00
3	9.51E-01
4	9.00E-01
5	8.50E-01
6	7.70E-01
7	7.20E-01
8	6.70E-01
9	6.30E-01
10	5.90E-01
11	5.50E-01
12	5.10E-01
13	4.70E-01
14	4.40E-01
15	4.10E-01
16	3.80E-01
17	3.50E-01
18	3.20E-01
19	2.90E-01
20	2.60E-01
21	2.30E-01
22	2.00E-01
23	1.70E-01
24	1.40E-01
25	1.10E-01
26	8.00E-02
27	5.00E-02
28	2.00E-02
29	0.00E+00
30	0.00E+00
31	0.00E+00
32	0.00E+00
33	0.00E+00
34	0.00E+00
35	0.00E+00
36	0.00E+00
37	0.00E+00
38	0.00E+00
39	0.00E+00
40	0.00E+00
41	0.00E+00
42	0.00E+00
43	0.00E+00
44	0.00E+00
45	0.00E+00
46	0.00E+00
47	0.00E+00
48	0.00E+00
49	0.00E+00
50	0.00E+00
51	0.00E+00
52	0.00E+00
53	0.00E+00
54	0.00E+00
55	0.00E+00
56	0.00E+00
57	0.00E+00
58	0.00E+00
59	0.00E+00
60	0.00E+00
61	0.00E+00
62	0.00E+00
63	0.00E+00
64	0.00E+00
65	0.00E+00
66	0.00E+00
67	0.00E+00
68	0.00E+00
69	0.00E+00
70	0.00E+00
71	0.00E+00
72	0.00E+00
73	0.00E+00
74	0.00E+00
75	0.00E+00
76	0.00E+00
77	0.00E+00
78	0.00E+00
79	0.00E+00
80	0.00E+00
81	0.00E+00
82	0.00E+00
83	0.00E+00
84	0.00E+00
85	0.00E+00
86	0.00E+00
87	0.00E+00
88	0.00E+00
89	0.00E+00
90	0.00E+00
91	0.00E+00
92	0.00E+00
93	0.00E+00
94	0.00E+00
95	0.00E+00
96	0.00E+00
97	0.00E+00
98	0.00E+00
99	0.00E+00
100	0.00E+00

CORTANTES EN TON. Y MOMENTOS EN TON-M

BARRA NO. 15. EXTREMO INICIAL (TON. Y TON-M) 6.00000 0.00000  
 EXTREMO FINAL (TON. Y TON-M) 7.00000 0.00000  
 COEFICIENTE DE FLEXIONANTE 1.00000  
 COEFICIENTE DE FLEXIONANTE 1.00000

LA DE LA GRAFICA UNIDADES/COLUMA

CARRA NO. 16, NUDO INICIAL= 7, NUDO FINAL= 8



CORTANTES EN TON. Y MOMENTOS EN TON-M

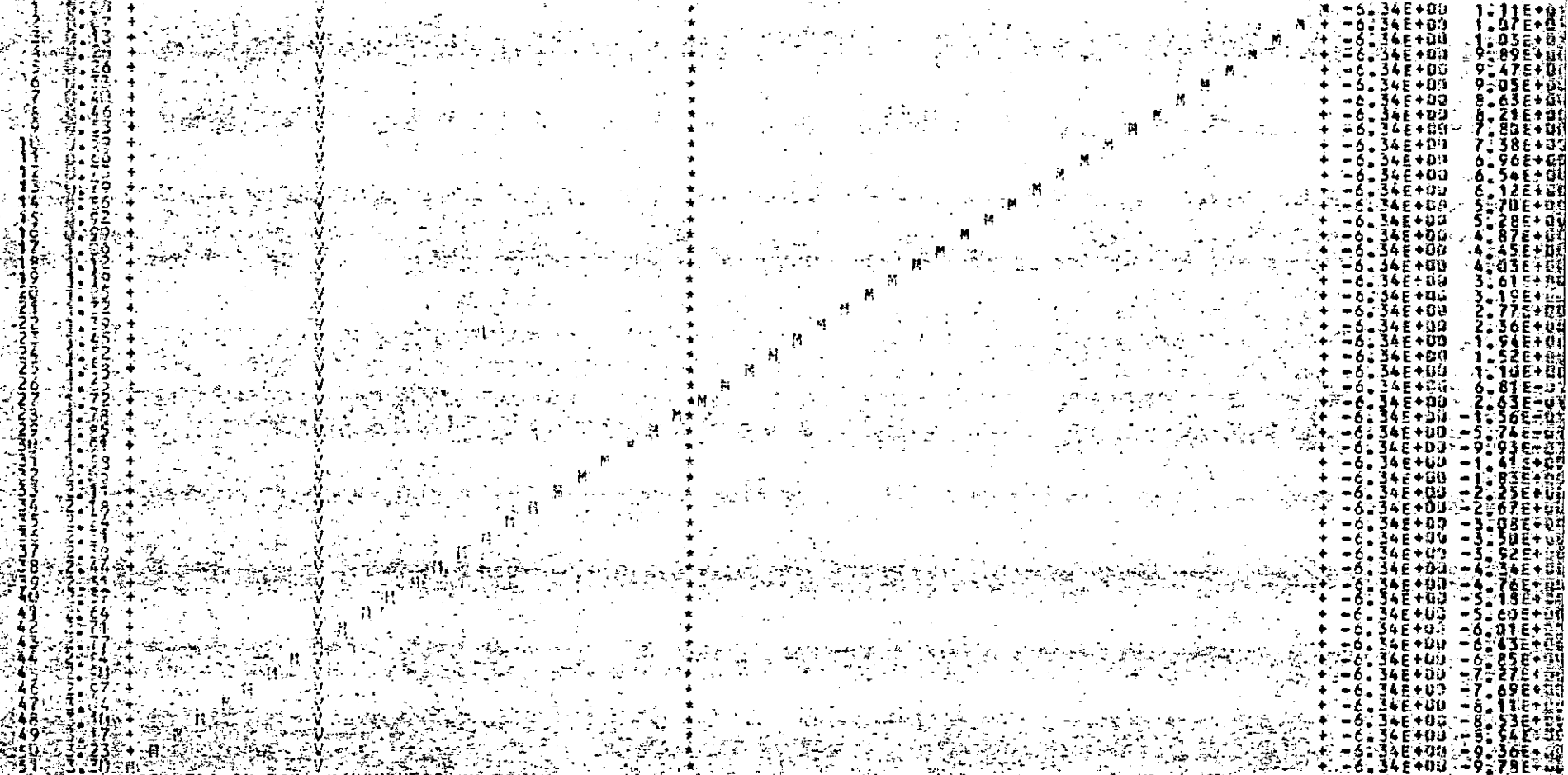
BARRA DE EXTREMO A EXTREMO EXTREMO INICIAL (TON Y TON-M) EXTREMO FINAL (TON Y TON-M)  
 NO. DE NUDO INICIAL FINAL NO. DE NUDO INICIAL FINAL NO. DE NUDO INICIAL FINAL  
 C.O.P.T. A N.C.T.E.S. FLEXIONANTE FLEXIONANTE



ESCALA DE LA GRAFICA: 1. UNIDADES/COLUMA

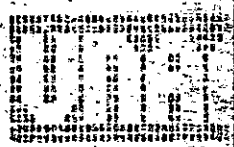
BARRA NO. 17, NUDO INICIAL = 3, NUDO FINAL = 9

NO	COORDENADA X	COORDENADA Y
1		
2		
3		
4		
5		
6		
7		
8		
9		
10		
11		
12		
13		
14		
15		
16		
17		
18		
19		
20		
21		
22		
23		
24		
25		
26		
27		
28		
29		
30		
31		
32		
33		
34		
35		
36		
37		
38		
39		
40		
41		
42		
43		
44		
45		
46		
47		
48		
49		
50		
51		
52		
53		
54		
55		
56		
57		
58		
59		
60		
61		
62		
63		
64		
65		
66		
67		
68		
69		
70		
71		
72		
73		
74		
75		
76		
77		
78		
79		
80		
81		
82		
83		
84		
85		
86		
87		
88		
89		
90		
91		
92		
93		
94		
95		
96		
97		
98		
99		
100		



CORTANTES EN TON. Y MOMENTOS EN TON-M

BARRA	EX-TREMO INICIAL (TON Y TON-M)	EX-TREMO FINAL (TON Y TON-M)
NO. INICIAL/FINAL	COORDENADA X - COORDENADA Y	COORDENADA X - COORDENADA Y



CONDICION DE CARGA DE CSECA VERTICAL REDUCCION EXISTEN.

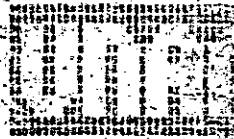
- 3. NO. DE CONEXION DE CARGA
- 4. NO. DE BARRAS CARGADAS
- 5. NO. DE NUDOS CARGADOS
- 6. INDICADOR DE FUERTAS DEL CUERPO (SI, I, NO)

DAIOS PARA EL CASO DE BARRAS CON CARGAS INTERMEDIAS DISTINTAS A PESO PROPIO  
BARRA NO INDICADA

62

- BARRA 1 CARGA DIST UNIFORM CONTIN (TON/M) = 2.000
- BARRA 2 CARGA DIST UNIFORM CONTIN (TON/M) = LA BARRA ANTERIOR
- BARRA 3 CARGA DIST UNIFORM CONTIN (TON/M) = LA BARRA ANTERIOR
- BARRA 4 CARGA DIST UNIFORM CONTIN (TON/M) = LA BARRA ANTERIOR
- BARRA 5 CARGA DIST UNIFORM CONTIN (TON/M) = LA BARRA ANTERIOR
- BARRA 6 CARGA DIST UNIFORM CONTIN (TON/M) = LA BARRA ANTERIOR
- BARRA 7 CARGA DIST UNIFORM CONTIN (TON/M) = LA BARRA ANTERIOR
- BARRA 8 CARGA DIST UNIFORM CONTIN (TON/M) = LA BARRA ANTERIOR
- BARRA 9 CARGA DIST UNIFORM CONTIN (TON/M) = LA BARRA ANTERIOR
- BARRA 10 CARGA DIST UNIFORM CONTIN (TON/M) = LA BARRA ANTERIOR
- BARRA 11 CARGA DIST UNIFORM CONTIN (TON/M) = LA BARRA ANTERIOR
- BARRA 12 CARGA DIST UNIFORM CONTIN (TON/M) = LA BARRA ANTERIOR

BARRA 12 CARGA DIST UNIFOR CONTIN(TON/M) A LA BARRA ANTERIOR  
 BARRA 13 CARGA DIST UNIFOR CONTIN(TON/M) A LA BARRA ANTERIOR  
 BARRA 14 CARGA DIST UNIFOR CONTIN(TON/M) A LA BARRA ANTERIOR  
 BARRA 15 CARGA DIST UNIFOR CONTIN(TON/M) A LA BARRA ANTERIOR  
 BARRA 16 CARGA DIST UNIFOR CONTIN(TON/M) A LA BARRA ANTERIOR  
 BARRA 17 CARGA DIST UNIFOR CONTIN(TON/M) A LA BARRA ANTERIOR  
 BARRA 18 CARGA DIST UNIFOR CONTIN(TON/M) A LA BARRA ANTERIOR  
 BARRA 19 CARGA DIST UNIFOR CONTIN(TON/M) A LA BARRA ANTERIOR  
 BARRA 20 CARGA DIST UNIFOR CONTIN(TON/M) A LA BARRA ANTERIOR  
 BARRA 21 CARGA DIST UNIFOR CONTIN(TON/M) A LA BARRA ANTERIOR  
 BARRA 22 CARGA DIST UNIFOR CONTIN(TON/M) A LA BARRA ANTERIOR  
 BARRA 23 CARGA DIST UNIFOR CONTIN(TON/M) A LA BARRA ANTERIOR  
 BARRA 24 CARGA DIST UNIFOR CONTIN(TON/M) A LA BARRA ANTERIOR  
 BARRA 25 CARGA DIST UNIFOR CONTIN(TON/M) A LA BARRA ANTERIOR  
 BARRA 26 CARGA DIST UNIFOR CONTIN(TON/M) A LA BARRA ANTERIOR  
 BARRA 27 CARGA DIST UNIFOR CONTIN(TON/M) A LA BARRA ANTERIOR



ACCIONES CONCENTRADAS EN LOS NUDOS (EN TON Y TON-M)  
 NUDO NO. FTA. HORIZONTAL FTA. VERTICAL MOMENTO

NUDO	NO.	FT. H.	FT. V.	MOM.
1	1	0.00	0.00	0.00
1	2	0.00	0.00	0.00
1	3	0.00	0.00	0.00
1	4	0.00	0.00	0.00
1	5	0.00	0.00	0.00
1	6	0.00	0.00	0.00
1	7	0.00	0.00	0.00
1	8	0.00	0.00	0.00
1	9	0.00	0.00	0.00
1	10	0.00	0.00	0.00
1	11	0.00	0.00	0.00
1	12	0.00	0.00	0.00
1	13	0.00	0.00	0.00
1	14	0.00	0.00	0.00
1	15	0.00	0.00	0.00
1	16	0.00	0.00	0.00
1	17	0.00	0.00	0.00
1	18	0.00	0.00	0.00
1	19	0.00	0.00	0.00
1	20	0.00	0.00	0.00
1	21	0.00	0.00	0.00
1	22	0.00	0.00	0.00
1	23	0.00	0.00	0.00
1	24	0.00	0.00	0.00
1	25	0.00	0.00	0.00
1	26	0.00	0.00	0.00
1	27	0.00	0.00	0.00

63

DESPLAZAMIENTOS NUDALES DE LA ESTRUCTURA (M)  
 FTO. NUDO. ROTACION EN GRADOS EN EL NUDO. ROTACION EN GRADOS EN LOS EXTREMOS (RAD)

NUDO	NO.	ROT. NUDO	ROT. EXT.
1	1	0.00	0.00
1	2	0.00	0.00
1	3	0.00	0.00
1	4	0.00	0.00
1	5	0.00	0.00
1	6	0.00	0.00
1	7	0.00	0.00
1	8	0.00	0.00
1	9	0.00	0.00
1	10	0.00	0.00
1	11	0.00	0.00
1	12	0.00	0.00
1	13	0.00	0.00
1	14	0.00	0.00
1	15	0.00	0.00
1	16	0.00	0.00
1	17	0.00	0.00
1	18	0.00	0.00
1	19	0.00	0.00
1	20	0.00	0.00
1	21	0.00	0.00
1	22	0.00	0.00
1	23	0.00	0.00
1	24	0.00	0.00
1	25	0.00	0.00
1	26	0.00	0.00
1	27	0.00	0.00





ESCALA DE LA GRAFICA = 1/1000 UNIDADES/COLUMA  
CANTONAS: 1.000000 +01  
ORDENADA: 1.000000 +01

BARRA NO. 1, NUDO INICIAL = 2, NUDO FINAL = 12

12  
11  
10  
9  
8  
7  
6  
5  
4  
3  
2  
1

1  
2  
3  
4  
5  
6  
7  
8  
9  
10  
11  
12  
13  
14  
15  
16  
17  
18  
19  
20  
21  
22  
23  
24  
25  
26  
27  
28  
29  
30  
31  
32  
33  
34  
35  
36  
37  
38  
39  
40  
41  
42  
43  
44  
45  
46  
47  
48  
49  
50  
51  
52  
53  
54  
55  
56  
57  
58  
59  
60  
61  
62  
63  
64  
65  
66  
67  
68  
69  
70  
71  
72  
73  
74  
75  
76  
77  
78  
79  
80  
81  
82  
83  
84  
85  
86  
87  
88  
89  
90  
91  
92  
93  
94  
95  
96  
97  
98  
99  
100  
101  
102  
103  
104  
105  
106  
107  
108  
109  
110  
111  
112  
113  
114  
115  
116  
117  
118  
119  
120  
121  
122  
123  
124  
125  
126  
127  
128  
129  
130  
131  
132  
133  
134  
135  
136  
137  
138  
139  
140  
141  
142  
143  
144  
145  
146  
147  
148  
149  
150  
151  
152  
153  
154  
155  
156  
157  
158  
159  
160  
161  
162  
163  
164  
165  
166  
167  
168  
169  
170  
171  
172  
173  
174  
175  
176  
177  
178  
179  
180  
181  
182  
183  
184  
185  
186  
187  
188  
189  
190  
191  
192  
193  
194  
195  
196  
197  
198  
199  
200  
201  
202  
203  
204  
205  
206  
207  
208  
209  
210  
211  
212  
213  
214  
215  
216  
217  
218  
219  
220  
221  
222  
223  
224  
225  
226  
227  
228  
229  
230  
231  
232  
233  
234  
235  
236  
237  
238  
239  
240  
241  
242  
243  
244  
245  
246  
247  
248  
249  
250  
251  
252  
253  
254  
255  
256  
257  
258  
259  
260  
261  
262  
263  
264  
265  
266  
267  
268  
269  
270  
271  
272  
273  
274  
275  
276  
277  
278  
279  
280  
281  
282  
283  
284  
285  
286  
287  
288  
289  
290  
291  
292  
293  
294  
295  
296  
297  
298  
299  
300  
301  
302  
303  
304  
305  
306  
307  
308  
309  
310  
311  
312  
313  
314  
315  
316  
317  
318  
319  
320  
321  
322  
323  
324  
325  
326  
327  
328  
329  
330  
331  
332  
333  
334  
335  
336  
337  
338  
339  
340  
341  
342  
343  
344  
345  
346  
347  
348  
349  
350  
351  
352  
353  
354  
355  
356  
357  
358  
359  
360  
361  
362  
363  
364  
365  
366  
367  
368  
369  
370  
371  
372  
373  
374  
375  
376  
377  
378  
379  
380  
381  
382  
383  
384  
385  
386  
387  
388  
389  
390  
391  
392  
393  
394  
395  
396  
397  
398  
399  
400  
401  
402  
403  
404  
405  
406  
407  
408  
409  
410  
411  
412  
413  
414  
415  
416  
417  
418  
419  
420  
421  
422  
423  
424  
425  
426  
427  
428  
429  
430  
431  
432  
433  
434  
435  
436  
437  
438  
439  
440  
441  
442  
443  
444  
445  
446  
447  
448  
449  
450  
451  
452  
453  
454  
455  
456  
457  
458  
459  
460  
461  
462  
463  
464  
465  
466  
467  
468  
469  
470  
471  
472  
473  
474  
475  
476  
477  
478  
479  
480  
481  
482  
483  
484  
485  
486  
487  
488  
489  
490  
491  
492  
493  
494  
495  
496  
497  
498  
499  
500  
501  
502  
503  
504  
505  
506  
507  
508  
509  
510  
511  
512  
513  
514  
515  
516  
517  
518  
519  
520  
521  
522  
523  
524  
525  
526  
527  
528  
529  
530  
531  
532  
533  
534  
535  
536  
537  
538  
539  
540  
541  
542  
543  
544  
545  
546  
547  
548  
549  
550  
551  
552  
553  
554  
555  
556  
557  
558  
559  
560  
561  
562  
563  
564  
565  
566  
567  
568  
569  
570  
571  
572  
573  
574  
575  
576  
577  
578  
579  
580  
581  
582  
583  
584  
585  
586  
587  
588  
589  
590  
591  
592  
593  
594  
595  
596  
597  
598  
599  
600  
601  
602  
603  
604  
605  
606  
607  
608  
609  
610  
611  
612  
613  
614  
615  
616  
617  
618  
619  
620  
621  
622  
623  
624  
625  
626  
627  
628  
629  
630  
631  
632  
633  
634  
635  
636  
637  
638  
639  
640  
641  
642  
643  
644  
645  
646  
647  
648  
649  
650  
651  
652  
653  
654  
655  
656  
657  
658  
659  
660  
661  
662  
663  
664  
665  
666  
667  
668  
669  
670  
671  
672  
673  
674  
675  
676  
677  
678  
679  
680  
681  
682  
683  
684  
685  
686  
687  
688  
689  
690  
691  
692  
693  
694  
695  
696  
697  
698  
699  
700  
701  
702  
703  
704  
705  
706  
707  
708  
709  
710  
711  
712  
713  
714  
715  
716  
717  
718  
719  
720  
721  
722  
723  
724  
725  
726  
727  
728  
729  
730  
731  
732  
733  
734  
735  
736  
737  
738  
739  
740  
741  
742  
743  
744  
745  
746  
747  
748  
749  
750  
751  
752  
753  
754  
755  
756  
757  
758  
759  
760  
761  
762  
763  
764  
765  
766  
767  
768  
769  
770  
771  
772  
773  
774  
775  
776  
777  
778  
779  
780  
781  
782  
783  
784  
785  
786  
787  
788  
789  
790  
791  
792  
793  
794  
795  
796  
797  
798  
799  
800  
801  
802  
803  
804  
805  
806  
807  
808  
809  
810  
811  
812  
813  
814  
815  
816  
817  
818  
819  
820  
821  
822  
823  
824  
825  
826  
827  
828  
829  
830  
831  
832  
833  
834  
835  
836  
837  
838  
839  
840  
841  
842  
843  
844  
845  
846  
847  
848  
849  
850  
851  
852  
853  
854  
855  
856  
857  
858  
859  
860  
861  
862  
863  
864  
865  
866  
867  
868  
869  
870  
871  
872  
873  
874  
875  
876  
877  
878  
879  
880  
881  
882  
883  
884  
885  
886  
887  
888  
889  
890  
891  
892  
893  
894  
895  
896  
897  
898  
899  
900  
901  
902  
903  
904  
905  
906  
907  
908  
909  
910  
911  
912  
913  
914  
915  
916  
917  
918  
919  
920  
921  
922  
923  
924  
925  
926  
927  
928  
929  
930  
931  
932  
933  
934  
935  
936  
937  
938  
939  
940  
941  
942  
943  
944  
945  
946  
947  
948  
949  
950  
951  
952  
953  
954  
955  
956  
957  
958  
959  
960  
961  
962  
963  
964  
965  
966  
967  
968  
969  
970  
971  
972  
973  
974  
975  
976  
977  
978  
979  
980  
981  
982  
983  
984  
985  
986  
987  
988  
989  
990  
991  
992  
993  
994  
995  
996  
997  
998  
999  
1000

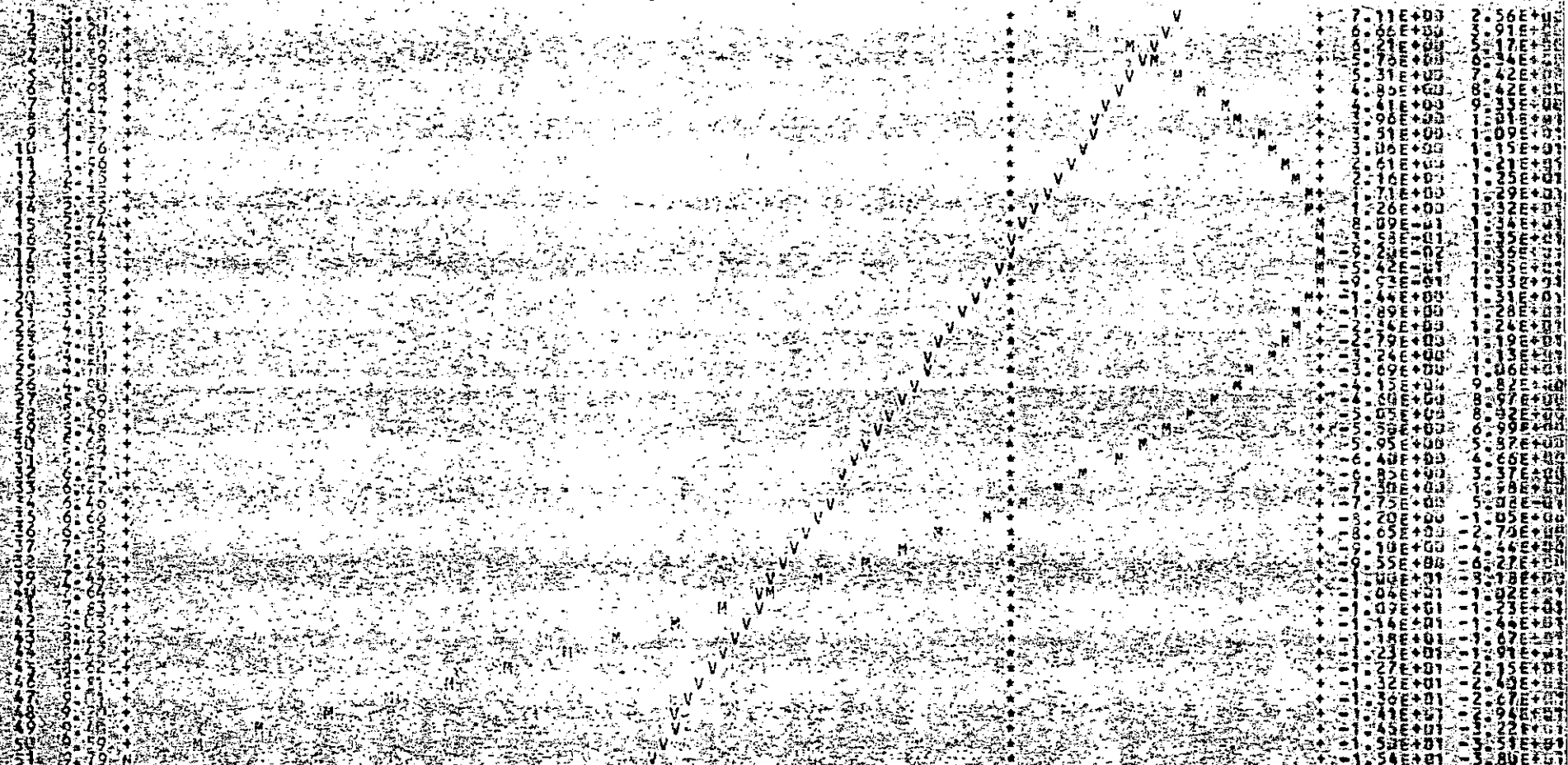
CORTANTES EN TON. Y MOMENTOS EN TON-M

BARRA: 1 2 3 4 5 6 7 8 9 10 11 12  
EXTREMO INICIAL (TON Y TON-M) : 0.000000 0.000000  
EXTREMO FINAL (TON Y TON-M) : 0.000000 0.000000  
C O R T A N T E S : F L E X I O N A N T E S

ESCALA DE GRÁFICAS      UNIDADES/COLUMA  
 DECADADA MENOR      1.00000E+01  
 DECADADA MAYOR      1.00000E+01

BARRA NO. 2, NUDO INICIAL= 7, NUDO FINAL= 13

COORDENADAS DE LOS NUDOS  
 NUDO      X      Y      Z  
 1      0.00000      0.00000      0.00000  
 2      0.00000      0.00000      0.00000  
 3      0.00000      0.00000      0.00000  
 4      0.00000      0.00000      0.00000  
 5      0.00000      0.00000      0.00000  
 6      0.00000      0.00000      0.00000  
 7      0.00000      0.00000      0.00000  
 8      0.00000      0.00000      0.00000  
 9      0.00000      0.00000      0.00000  
 10      0.00000      0.00000      0.00000  
 11      0.00000      0.00000      0.00000  
 12      0.00000      0.00000      0.00000  
 13      0.00000      0.00000      0.00000



CORTANTES EN TON. Y MOMENTOS EN TON-M

BARRA 2 A TRAVEZADO      EXTREMO INICIAL (TON Y TON-M)      EXTREMO FINAL (TON Y TON-M)  
 NUDO INICIAL/FINAL      CORTANTE Y FLEXIONANTE      CORTANTE Y FLEXIONANTE







5 6 12

7.74054

-11.32229

-11.00160

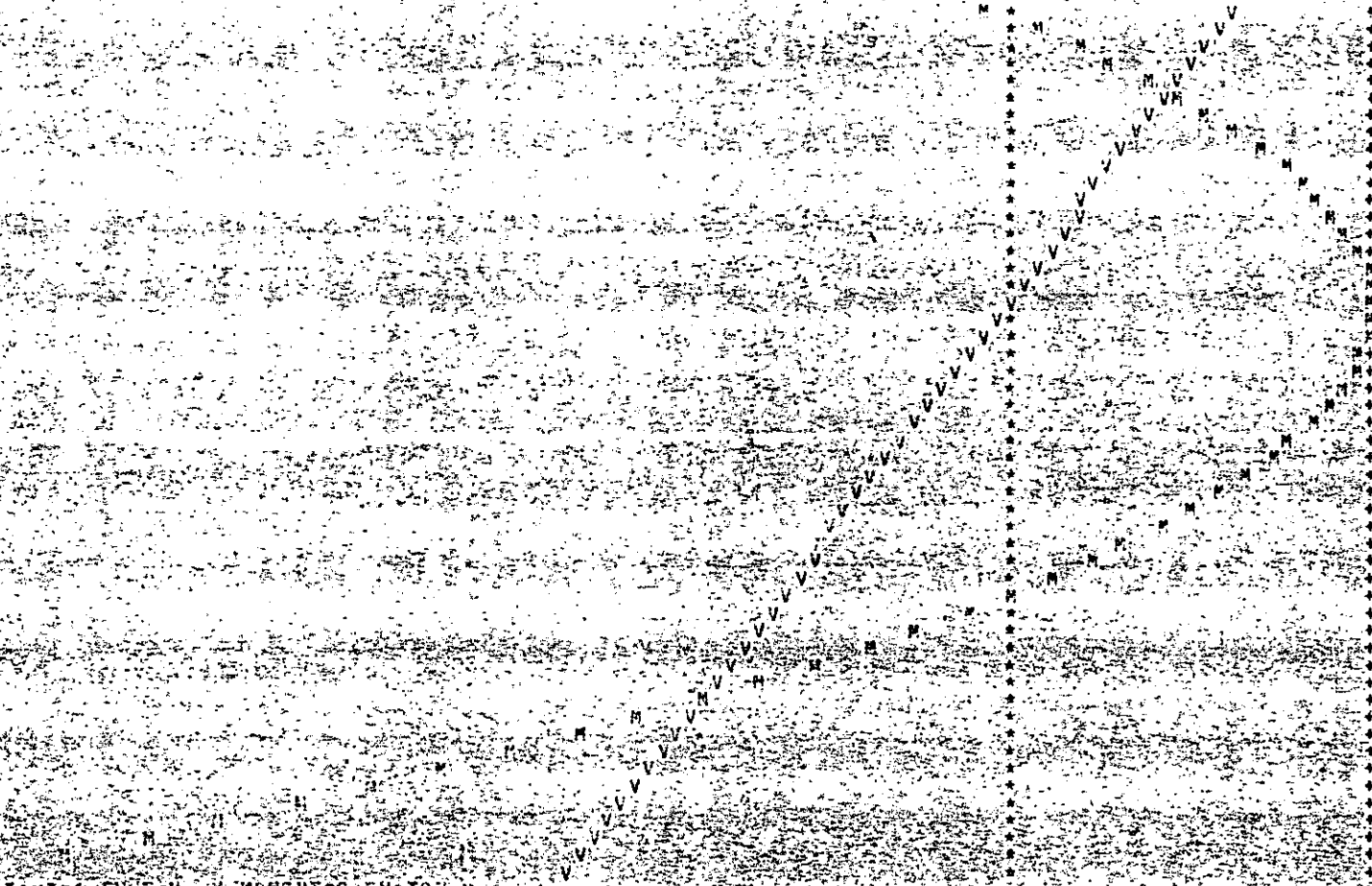
-14.77054

-34.90373

PROGRAMA DE LAS GRATICAS  
 COLUMNA DE LAS GRATICAS UNIDADES/COLUMNA  
 COLUMNA DE LAS GRATICAS UNIDADES/COLUMNA  
 COLUMNA DE LAS GRATICAS UNIDADES/COLUMNA

BARRA NO. 1 NUDO INICIAL= 6 NUDO FINAL= 15

1  
 2  
 3  
 4  
 5  
 6  
 7  
 8  
 9  
 10  
 11  
 12  
 13  
 14  
 15  
 16  
 17  
 18  
 19  
 20  
 21  
 22  
 23  
 24  
 25  
 26  
 27  
 28  
 29  
 30  
 31  
 32  
 33  
 34  
 35  
 36  
 37  
 38  
 39  
 40  
 41  
 42  
 43  
 44  
 45  
 46  
 47  
 48  
 49  
 50  
 51  
 52  
 53  
 54  
 55  
 56  
 57  
 58  
 59  
 60  
 61  
 62  
 63  
 64  
 65  
 66  
 67  
 68  
 69  
 70  
 71  
 72  
 73  
 74  
 75  
 76  
 77  
 78  
 79  
 80  
 81  
 82  
 83  
 84  
 85  
 86  
 87  
 88  
 89  
 90  
 91  
 92  
 93  
 94  
 95  
 96  
 97  
 98  
 99  
 100



7	75E+03	5	21E
8	51E+00	6	51E
9	85E+00	7	14E
10	95E+00	8	84E
11	99E+00	9	96E
12	04E+00	10	90E
13	90E+00	11	74E
14	14E+00	12	79E
15	69E+00	13	56E
16	99E+00	14	92E
17	94E+00	15	95E
18	44E+00	16	17E
19	01E+01	17	11E
20	41E+01	18	23E
21	87E+02	19	24E
22	05E+01	20	28E
23	26E+00	21	28E
24	71E+00	22	9E
25	16E+00	23	15E
26	61E+00	24	18E
27	66E+00	25	05E
28	91E+00	26	84E
29	94E+00	27	11E
30	74E+00	28	18E
31	31E+00	29	9E
32	76E+00	30	30E
33	21E+00	31	13E
34	66E+00	32	87E
35	37E+00	33	12E
36	8K+00	34	44E
37	47E+00	35	86E
38	92E+00	36	76E
39	82E+00	37	44E
40	01E+01	38	94E
41	93E+01	39	24E
42	15E+01	40	48E
43	21E+01	41	68E
44	21E+01	42	21E
45	30E+01	43	15E
46	34E+01	44	40E
47	49E+01	45	26E
48	89E+01	46	92E
49	8E+01	47	21E
50	8E+01	48	49E

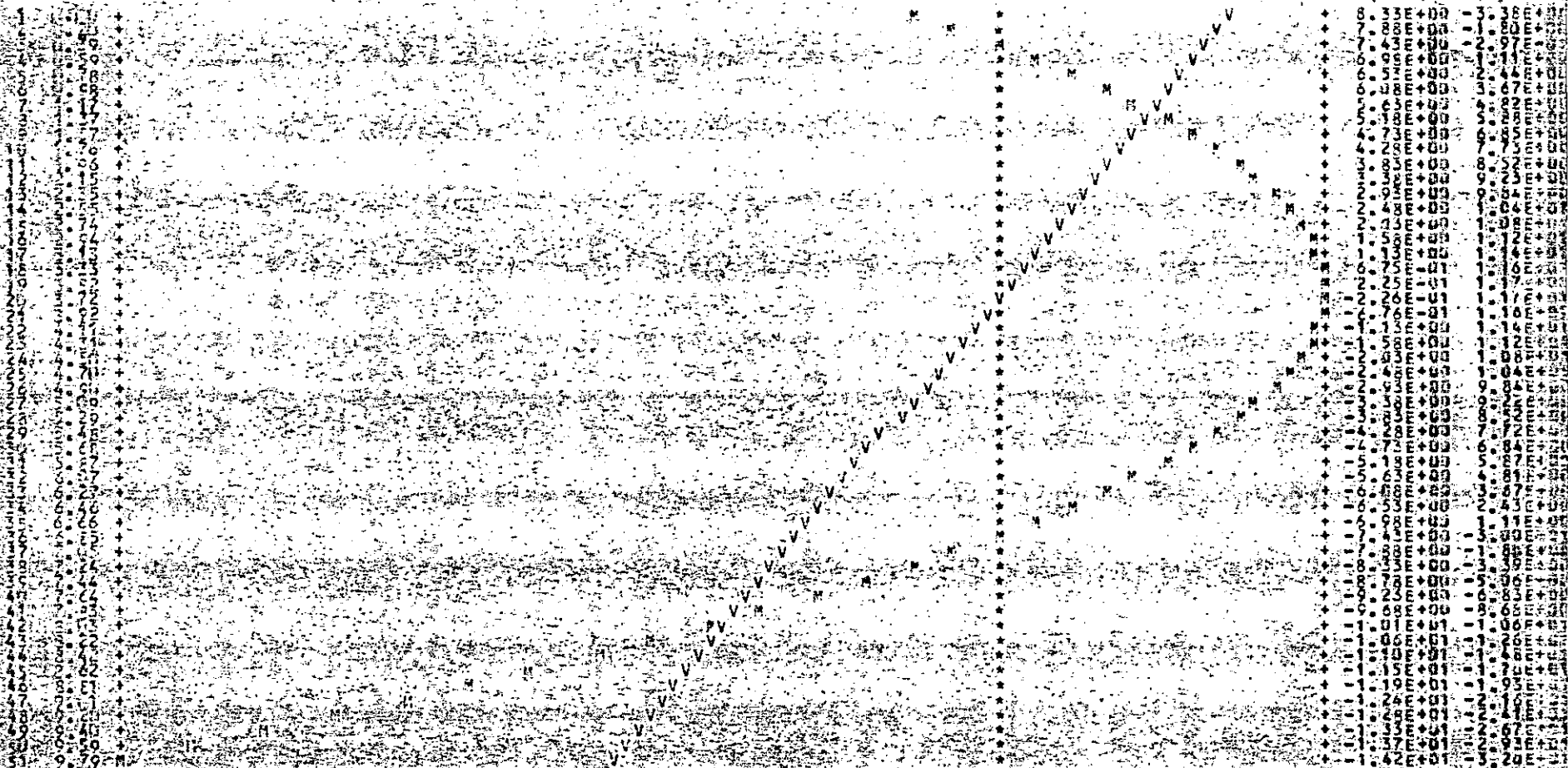
DEPTANTES EN TON. Y MOMENTOS EN TON-M

BARRA NO. 1 2 3 4 5 6 7 8 9 10 11 12 13 14 15 EXTREMO INICIAL (TON Y TON-M) EXTREMO FINAL (TON Y TON-M)  
 NO. INICIAL FINAL C O B T A B T L I FLEXIONANTE C O B T A B T L I FLEXIONANTE

ESCALA DE LA GRAFICA: 5.000000 UNIDADES/COLUMA  
 ORDENADA MENOR: 1.000000  
 ORDENADA MAYOR: 12.000000

BARRA NO. 6, NUDO INICIAL= 7, NUDO FINAL= 17

1	1
2	1
3	1
4	1
5	1
6	1
7	1
8	1
9	1
10	1
11	1
12	1
13	1
14	1
15	1
16	1
17	1



CORTANTES EN TON. Y MOMENTOS EN TON-M

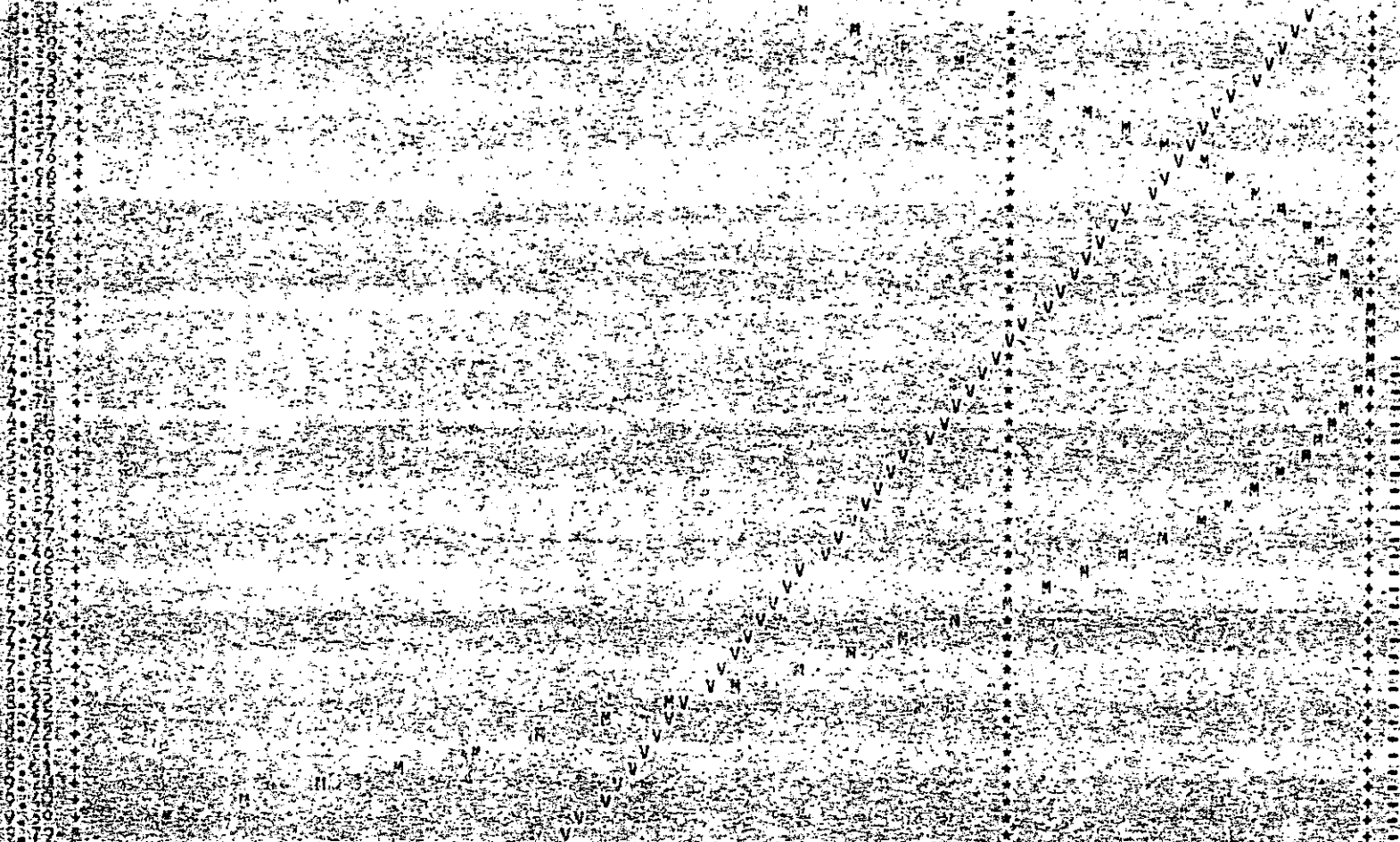
BARRA DE EXTREMOS: EXTREMO INICIAL (TON Y TON-M) EXTREMO FINAL (TON Y TON-M)  
 NO. INICIAL FINAL NO. NUDO A NUDO DE FLEXIONANTE NO. NUDO A NUDO DE FLEXIONANTE

CANTON DE LA UNIDAD GRAFICA = 06684E771 UNIDADES/COLUMNA  
 CANTON DE LA UNIDAD GRAFICA = 07025E401  
 CANTON DE LA UNIDAD GRAFICA = 07650E401

BARRA NO. 7, MUDO INICIAL = 6, MUDO FINAL = 18

1	1
2	1
3	1
4	1
5	1
6	1
7	1
8	1
9	1
10	1
11	1
12	1
13	1
14	1
15	1
16	1
17	1
18	1

1  
2  
3  
4  
5  
6  
7  
8  
9  
10  
11  
12  
13  
14  
15  
16  
17  
18  
19  
20  
21  
22  
23  
24  
25  
26  
27  
28  
29  
30  
31  
32  
33  
34  
35  
36  
37  
38  
39  
40  
41  
42  
43  
44  
45  
46  
47  
48  
49  
50  
51  
52  
53  
54  
55  
56  
57  
58  
59  
60  
61  
62  
63  
64  
65  
66  
67  
68  
69  
70  
71  
72  
73  
74  
75  
76  
77  
78  
79  
80  
81  
82  
83  
84  
85  
86  
87  
88  
89  
90  
91  
92  
93  
94  
95  
96  
97  
98  
99  
100



9.01E+00	0.68E+00
8.56E+00	0.69E+00
8.11E+00	0.70E+00
7.66E+00	0.71E+00
7.21E+00	0.72E+00
6.76E+00	0.73E+00
6.31E+00	0.74E+00
5.86E+00	0.75E+00
5.41E+00	0.76E+00
4.96E+00	0.77E+00
4.51E+00	0.78E+00
4.06E+00	0.79E+00
3.61E+00	0.80E+00
3.16E+00	0.81E+00
2.71E+00	0.82E+00
2.26E+00	0.83E+00
1.81E+00	0.84E+00
1.36E+00	0.85E+00
9.1E+00	0.86E+00
8.65E+00	0.87E+00
8.20E+00	0.88E+00
7.75E+00	0.89E+00
7.30E+00	0.90E+00
6.85E+00	0.91E+00
6.40E+00	0.92E+00
5.95E+00	0.93E+00
5.50E+00	0.94E+00
5.05E+00	0.95E+00
4.60E+00	0.96E+00
4.15E+00	0.97E+00
3.70E+00	0.98E+00
3.25E+00	0.99E+00
2.80E+00	1.00E+00
2.35E+00	1.01E+00
1.90E+00	1.02E+00
1.45E+00	1.03E+00
1.00E+00	1.04E+00
0.55E+00	1.05E+00
0.10E+00	1.06E+00
0.35E+00	1.07E+00
0.70E+00	1.08E+00
1.05E+00	1.09E+00
1.40E+00	1.10E+00
1.75E+00	1.11E+00
2.10E+00	1.12E+00
2.45E+00	1.13E+00
2.80E+00	1.14E+00
3.15E+00	1.15E+00
3.50E+00	1.16E+00
3.85E+00	1.17E+00
4.20E+00	1.18E+00
4.55E+00	1.19E+00
4.90E+00	1.20E+00
5.25E+00	1.21E+00
5.60E+00	1.22E+00
5.95E+00	1.23E+00
6.30E+00	1.24E+00
6.65E+00	1.25E+00
7.00E+00	1.26E+00
7.35E+00	1.27E+00
7.70E+00	1.28E+00
8.05E+00	1.29E+00
8.40E+00	1.30E+00
8.75E+00	1.31E+00
9.10E+00	1.32E+00
9.45E+00	1.33E+00
9.80E+00	1.34E+00
10.15E+00	1.35E+00
10.50E+00	1.36E+00
10.85E+00	1.37E+00
11.20E+00	1.38E+00
11.55E+00	1.39E+00
11.90E+00	1.40E+00
12.25E+00	1.41E+00
12.60E+00	1.42E+00
12.95E+00	1.43E+00
13.30E+00	1.44E+00
13.65E+00	1.45E+00
14.00E+00	1.46E+00
14.35E+00	1.47E+00
14.70E+00	1.48E+00
15.05E+00	1.49E+00
15.40E+00	1.50E+00
15.75E+00	1.51E+00
16.10E+00	1.52E+00
16.45E+00	1.53E+00
16.80E+00	1.54E+00
17.15E+00	1.55E+00
17.50E+00	1.56E+00
17.85E+00	1.57E+00
18.20E+00	1.58E+00
18.55E+00	1.59E+00
18.90E+00	1.60E+00
19.25E+00	1.61E+00
19.60E+00	1.62E+00
19.95E+00	1.63E+00
20.30E+00	1.64E+00
20.65E+00	1.65E+00
21.00E+00	1.66E+00
21.35E+00	1.67E+00
21.70E+00	1.68E+00
22.05E+00	1.69E+00
22.40E+00	1.70E+00
22.75E+00	1.71E+00
23.10E+00	1.72E+00
23.45E+00	1.73E+00
23.80E+00	1.74E+00
24.15E+00	1.75E+00
24.50E+00	1.76E+00
24.85E+00	1.77E+00
25.20E+00	1.78E+00
25.55E+00	1.79E+00
25.90E+00	1.80E+00
26.25E+00	1.81E+00
26.60E+00	1.82E+00
26.95E+00	1.83E+00
27.30E+00	1.84E+00
27.65E+00	1.85E+00
28.00E+00	1.86E+00
28.35E+00	1.87E+00
28.70E+00	1.88E+00
29.05E+00	1.89E+00
29.40E+00	1.90E+00
29.75E+00	1.91E+00
30.10E+00	1.92E+00
30.45E+00	1.93E+00
30.80E+00	1.94E+00
31.15E+00	1.95E+00
31.50E+00	1.96E+00
31.85E+00	1.97E+00
32.20E+00	1.98E+00
32.55E+00	1.99E+00
32.90E+00	2.00E+00

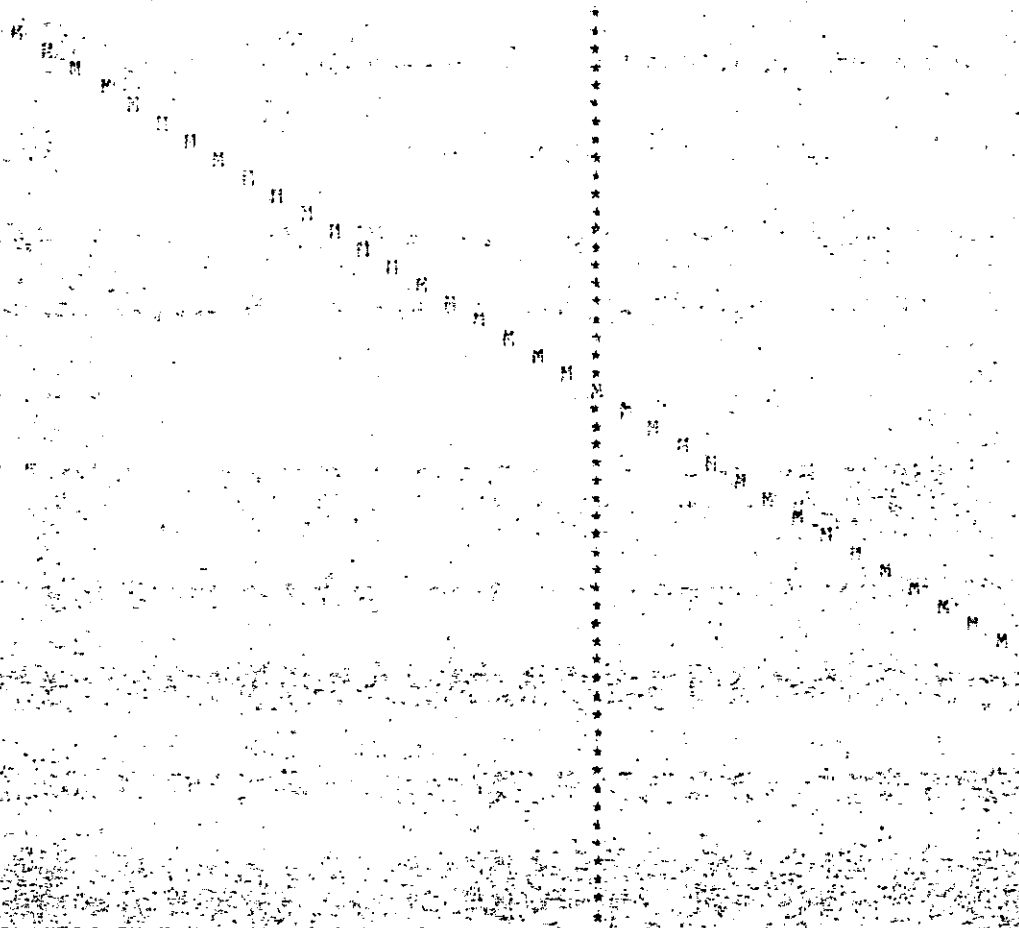
CORTANTES EN TON. Y MOMENTOS EN TON-M

ESCALA DE LA GRAFICA: UNIDADES/CLUMA  
 ORDENADA MAYOR

BARRA NO. 25, NUDO INICIAL= 17, NUDO FINAL= 17

UNIDAD  
 CLUMA

ESCALA DE LA GRAFICA: UNIDADES/CLUMA  
 ORDENADA MAYOR



9.37E+00	-1.30E+07
9.37E+00	-1.24E+07
9.37E+00	-1.18E+07
9.37E+00	-1.11E+07
9.37E+00	-1.05E+07
9.37E+00	-9.90E+06
9.37E+00	-9.28E+06
9.37E+00	-8.66E+06
9.37E+00	-8.04E+06
9.37E+00	-7.42E+06
9.37E+00	-6.80E+06
9.37E+00	-6.19E+06
9.37E+00	-5.57E+06
9.37E+00	-4.95E+06
9.37E+00	-4.33E+06
9.37E+00	-3.71E+06
9.37E+00	-3.09E+06
9.37E+00	-2.47E+06
9.37E+00	-1.85E+06
9.37E+00	-1.24E+06
9.37E+00	-6.17E+05
9.37E+00	1.44E+05
9.37E+00	6.20E+04
9.37E+00	1.24E+04
9.37E+00	1.86E+03
9.37E+00	2.48E+02
9.37E+00	3.10E+01
9.37E+00	3.71E+00
9.37E+00	4.33E-01
9.37E+00	4.95E-02
9.37E+00	5.57E-03
9.37E+00	6.19E-04
9.37E+00	6.81E-05
9.37E+00	7.43E-06
9.37E+00	8.05E-07
9.37E+00	8.66E-08
9.37E+00	9.28E-09
9.37E+00	9.90E-10
9.37E+00	1.05E-11
9.37E+00	1.11E-12
9.37E+00	1.18E-13
9.37E+00	1.24E-14
9.37E+00	1.30E-15
9.37E+00	1.36E-16
9.37E+00	1.42E-17
9.37E+00	1.49E-18
9.37E+00	1.55E-19
9.37E+00	1.61E-20
9.37E+00	1.67E-21
9.37E+00	1.73E-22
9.37E+00	1.79E-23

CONTANTES EN TON. Y MOMENTOS EN TON-M

BARRA NO. 25, NUDO INICIAL= 17, NUDO FINAL= 17  
 EXTREMO INICIAL (TON Y TON-M)  
 EXTREMO FINAL (TON Y TON-M)

GRAFICA DE LAS UNIDADES/COLUMNA

BARRA NO. 14, MUÑO INICIAL= 16, MUÑO FINAL= 17

11.00 257

CONSTANTES EN TON. Y MOMENTOS EN TON-M

11.00 257

11.00 257

11.00 257

11.00 257

11.00 257

11.00 257

11.00 257

11.00 257

11.00 257

11.00 257

11.00 257

11.00 257

11.00 257

11.00 257

11.00 257

11.00 257

BARRA DE EXTREMOS INICIAL (TON Y TON-M) EXTREMO FINAL (TON Y TON-M)
CORR. M.A.L. CORR. M.A.L.
CORR. M.A.L. CORR. M.A.L.

- 1) El intervalo de esfuerzo y la severidad de las entalladuras son las variables de esfuerzo que predominan en detalles soldados y vigas.
- 2) Otras variables tales como el esfuerzo mínimo, el esfuerzo promedio y el esfuerzo máximo no son significativas para fines de diseño.
- 3) Aceros estructurales con puntos de fluencia que varíen entre 2500 y 7000 kg/cm<sup>2</sup>, no presentan diferencias significativas para detalles soldados y fabricados del mismo modo.

Para diseñar los elementos de una estructura es necesario basarnos en normas ó especificaciones que siempre están apoyadas en la experiencia pasada y en una gran cantidad de pruebas de laboratorio. En esta forma se evita, en gran parte, que el proyectista use criterios erróneos que conduzcan a estructuras antieconómicas por -- usar factores de seguridad muy grandes, ó por el contrario, que -- buscando economías mal entendidas, se usen factores de seguridad -- tan bajos que hagan peligrar la seguridad de la estructura.

Los ejemplos que veremos están resueltos usando las especificaciones del AMERICAN INSTITUTE OF STEEL CONSTRUCTION y las normas complementarias del REGLAMENTO PARA LAS CONSTRUCCIONES DEL D. F. usando el criterio de esfuerzos permisibles.

El diseño de piezas en tensión de acuerdo con las Normas del Reglamento para las Construcciones del D. F. difiere con relación al diseño de acuerdo con las especificaciones del A I S C, en los siguientes puntos :

#### 1) Esfuerzos permisibles :

Revisión en la sección neta

A I S C

D F

$$F_T = 0.5 F_U \text{ (sección neta efectiva) } \quad F_T = 0.6 F_Y \text{ (sección neta) }$$

El criterio de falla en la sección neta establecido por el AISC -- se basa en que la fluencia del material en la zona de conexión ocasiona una deformación poco significativa respecto a la deformación total del miembro, no constituyendo este un estado límite de falla.

Por otra parte dependiendo del porcentaje de reducción del área total y de las propiedades mecánicas del acero, el miembro puede fallar -- por fractura del área neta a una carga menor que la requerida -- para la fluencia del área total. Por este motivo se toman como estados límites de falla la fluencia de la sección total ó la fractura de la sección neta.

## 2) Area neta

A I S C

D F

(Area neta efectiva)

(Area neta)

Cuando una sección no se conecta a través de todos los elementos que la forman, el A I S C define una sección neta efectiva que es igual al área neta multiplicada por un coeficiente de reducción. Este se ha determinado en base a una multitud de pruebas y estudios teóricos que han demostrado que, cuando una sección no se conecta a través de todos sus elementos de manera de lograr una transferencia uniforme de esfuerzos, la carga de falla dividida entre el área neta es generalmente menor que el esfuerzo de ruptura del acero. Esta disminución de la resistencia se debe a una concentración de esfuerzos cortantes producida por la redistribución de las fuerzas normales en la zona de conexión (Fig. 14 b).

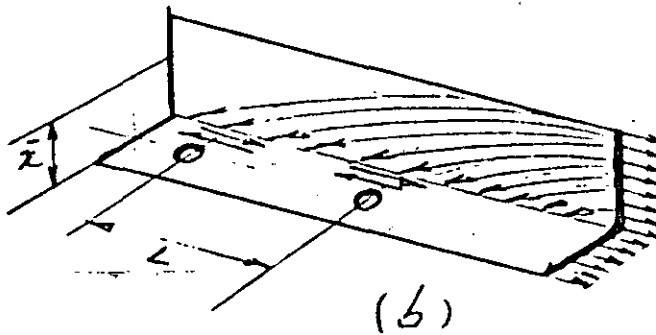


FIG 14

## 3) Relación de esbeltez

A I S C

D F

Miembros principales 240

300

Miembros secundarios 300

300



Las relaciones de esbeltez para las piezas de tensión se fijan - para que tengan una cierta rigidez para evitar movimientos laterales ó vibraciones. Estos límites no son obligatorios.

Las normas ó especificaciones que usaremos cubren los siguientes puntos :

- 1.- Materiales
- 2.- Esfuerzos permisibles
- 3.- Cargas (impacto y fatiga)
- 4.- Geometría ;  
    Esbeltez  
    Area de secciones transversales
- 5.- Conexiones
- 6.- Secciones armadas.

A continuación indicamos en que secciones de las especificaciones AISC y de las Normas de D. F. se cubren estos puntos :

	A I S C	D F
Cargas : impacto	1.3	no
Materiales	1.4	no
Esfuerzos admisibles	1.5	10.1
Cargas : fatiga	1.7	no
Esbeltez	1.8	2.
Areas netas	1.14	2.
Conexiones	1.15	5.
Secciones armadas	1.18	4. (no contempla miembros en - tensión).
Apéndice B fatiga		no





**DIVISION DE EDUCACION CONTINUA  
FACULTAD DE INGENIERIA U.N.A.M.**

DISEÑO DE ESTRUCTURAS DE ACERO

COMENTARIOS SOBRE DISEÑO  
PLASTICO EN ACERO ESTRUCTURAL

EXPOSITOR:  
DR. PORFIRIO BALLESTEROS BAROCIO

NOV. 1984

COMMENTARY ON  
PLASTIC DESIGN IN STEEL

**MANUALS: THEIR ORIGIN AND SCOPE**

*(As Developed by the Technical Procedure Committee,  
July, 1930, and Revised to March, 1935)*

---

A manual consists of an orderly presentation of facts on a particular subject, supplemented by an analysis of the limitations and applications of these facts. It contains information useful to the average engineer in his everyday work, rather than findings that may be useful only occasionally or rarely. It is not in any sense a "standard," however; nor is it so elementary or so conclusive as to provide a "rule of thumb" for non-engineers.

Furthermore, a manual, in distinction from a paper (which expresses only one person's observations or opinions), is the work of a committee or group selected to assemble and express information on a specific topic. As often as practicable the manual committee is under the general direction of one or more of the Technical Divisions, and the product evolved has been subjected to review by the Executive Committee of that Division. As a step in the process of this review, proposed manuals are often brought before the members of the Technical Divisions for comment, which may serve as the basis for improvement. When published, each manual shows the names of the committee by which it was compiled and indicates clearly the several processes through which it has passed in review, in order that its merit may be definitely understood.

---

BY A JOINT COMMITTEE OF THE  
WELDING RESEARCH COUNCIL  
AND THE  
AMERICAN SOCIETY OF CIVIL ENGINEERS

---

Copyright 1961 by the  
WELDING RESEARCH COUNCIL  
and the  
AMERICAN SOCIETY OF CIVIL ENGINEERS

---

CONTENTS

WELDING RESEARCH  
COUNCIL

Structural Steel Committee

Lehigh Project  
Subcommittee

A. Amirkian  
Lynn S. Beedle  
J. M. Crowley  
F. H. Dill  
Samuel Epstein  
Gerald F. Fox  
LaMotte Grover  
William H. Jameson  
Bruce G. Johnston  
Jonathan Jones (Deceased)  
T. C. Kavanagh  
R. L. Ketter  
Carl Kreidler  
H. W. Lawson  
Nathan M. Newmark  
Emmanuel Pisetzner  
R. M. Stuchell  
John Vasta  
T. R. Higgins, Chairman

AMERICAN SOCIETY OF  
CIVIL ENGINEERS

Engineering Mechanics Division

Committee on Plasticity  
Related to Design

Frank Baron  
John M. Biggs  
Daniel C. Drucker  
John D. Griffiths  
William J. Hall  
T. R. Higgins  
Harry N. Hill  
Eivind Hognestad  
Robert L. Janes  
Bruce G. Johnston  
William H. Munse, Jr.  
Egor P. Popov  
John B. Scalzi  
Paul S. Symonds  
Bruno Thurlimann  
George Winter  
Douglas T. Wright  
Lynn S. Beedle, Chairman

	Page
FOREWORD .....	v
1. INTRODUCTION .....	1
1.1 Structural Design .....	1
1.2 Plasticity and Design—Some Advantages and Limitations . . .	1
2. BASIC PRINCIPLES .....	4
2.1 Behavior of Material and Structural Elements .....	4
2.2 Plastic Theory .....	5
3. ANALYSIS AND DESIGN .....	8
3.1 Assumptions .....	8
3.2 Statical Method of Analysis .....	9
3.3 Mechanism Method of Analysis .....	10
3.4 Other Methods .....	13
4. GENERAL PROVISIONS .....	14
4.1 Introduction .....	14
4.2 Types of Construction .....	14
4.3 Material .....	14
4.4 Structural Ductility .....	15
4.5 Yield Stress Level .....	15
4.6 Plastic Moment .....	16
4.7 Loads .....	17
4.8 Load Factors .....	18
5. VERIFICATION OF PLASTIC THEORY .....	21
5.1 Basic Concepts .....	21
5.2 Continuous Beams .....	25
5.3 Frames .....	27
6. ADDITIONAL DESIGN CONSIDERATIONS .....	34
6.1 Shear Force .....	34
6.2 Local Buckling .....	42
6.3 Lateral Buckling .....	50
6.4 Variable Repeated Loading .....	63

	Page
<b>7. COMPRESSION MEMBERS</b> .....	73
7.1 Introduction .....	73
7.2 Reduction of the Plastic Moment Due to Axial Thrust .....	74
7.3 Moment-Carrying Capacity of Columns .....	83
7.4 Rotation Capacity .....	95
7.5 Influence of Lateral-Torsional Buckling .....	96
7.6 Frame Stability .....	97
<b>8. CONNECTIONS</b> .....	102
8.1 Introduction .....	102
8.2 Straight Corner Connections .....	103
8.3 Haunches .....	106
8.4 Tapered Haunches .....	107
8.5 Curved Haunches .....	114
8.6 Beam-to-Column Connections .....	119
8.7 Details with Regard to Welding .....	129
8.8 Details with Regard to Bolting .....	130
<b>9. DEFLECTIONS</b> .....	132
9.1 Introduction .....	132
9.2 Calculation of Deflections in the Elastic Range .....	132
9.3 Calculation of Deflections in the Plastic Range .....	133
9.4 Sample Calculation of Deflection at Ultimate Load .....	134
9.5 Step-by-Step Calculations of Deflections .....	141
9.6 Approximate Deflection at Working Load .....	144
9.7 Deflection as a Limitation .....	145
9.8 Rotation Requirements .....	146
<b>APPENDIX I. SYMBOLS</b> .....	149
<b>APPENDIX II. GLOSSARY</b> .....	154
<b>APPENDIX III. REFERENCES</b> .....	156
<b>AUTHOR INDEX</b> .....	167
<b>SUBJECT INDEX</b> .....	172

## FOREWORD

The evaluation of a considerable amount of research work has demonstrated the applicability of plastic analysis to structural design. For the type of structure to which its application is intended, plastic design results in an overall balanced design, and a more economical use of material than conventional methods. In comparison with allowable stress ("elastic") design methods, plastic design is a simpler design technique. As a consequence designers have chosen the plastic design method for more than 2,000 structures built in the United States and abroad.

This Manual documents the applicability of plastic analysis to the design of structural steel beams and frames. Theoretical considerations involved in the plastic theory and in certain secondary design problems are presented. Experimental verification is provided, and approximations in the form of design guides are suggested.

In 1959, the American Institute of Steel Construction published a report entitled "Plastic Design in Steel" which illustrates the procedures of the plastic method of design with specific reference to building construction. It supplies information to supplement clauses in a specification for plastic design. Appropriate reference is made to this valuable design aid. The recent books which should be consulted for a much fuller discussion than space permits herein are listed at the beginning of Appendix III.—References.

This Commentary is based on a series of preliminary reports prepared for the Welding Research Council and the American Society of Civil Engineers by a research group at the Fritz Engineering Laboratory, Department of Civil Engineering, Lehigh University, Bethlehem, Pa. The staff members at Fritz Laboratory included: L. S. Beedle, G. C. Driscoll, Jr., T. V. Galambos, R. L. Ketter, T. Kusuda, G. C. Lee, T. Lee, L. W. Lu, A. Ostapenko, and B. Thürlimann. The organizations that supported the research projects out of which the preliminary reports were prepared were the following: American Institute of Steel Construction, American Iron and Steel Institute, Column Research Council, the Department of the Navy (Office of Naval Research, Bureau of Ships, Bureau of Yards and Docks), and the Welding Research Council.

Although much of the experimental and theoretical work was performed at Lehigh University, the WRC-ASCE Joint Committee has broadened this Commentary by including the results of research at other institutions both in the United States and abroad. The inclusion of this information and of certain unpublished data is gratefully acknowledged.

The Joint Committee notes with sorrow the passing of one of its members, Jonathan Jones, Hon. M. ASCE. Mr. Jones' critical review of the manuscript constituted a distinct contribution to this document.

The Joint Committee recommends that this Manual be read carefully by all structural engineers.

## GENERAL PROVISIONS

## 4.1 INTRODUCTION

In this chapter there will be discussed some of the basic conditions that should be satisfied in establishing a plastic-design procedure. This includes questions regarding types of construction, materials, structural ductility (avoidance of brittle fracture), the yield-stress level to be used, the plastic moment, the loads and forces that would be considered as applied to the structure, and the load factor.

In each case the suggested provision will be given first, followed by pertinent discussion.

## 4.2 TYPES OF CONSTRUCTION

The following types of construction are suitable for plastic design:

- (a) Continuous beams.
- (b) One and two story, single and multi-span continuous type building frames.
- (c) Multi-story tier buildings with sidesway prevented by walls and/or diagonal bracing.

Plastic design is not recommended as a substitute for allowable-stress design for structures that are essentially pin-connected. It is intended for structures which depend on continuity for their ability to carry the computed ultimate load.

The necessary continuity may be achieved by welding, riveting, or bolting. The background and justification for design guides for the use of such connecting devices is discussed in Chapter 8.

## 4.3 MATERIAL

Material with the characteristics of ASTM-A7 steel for bridges and buildings should be used, with modifications, when needed, to assure weldability and ductility at lowest expected service temperature.

It is not the intent to specify any one steel, but to indicate that the important property that is required of a material is ductility at service temperature. As was shown in Ref. 3.1, many of the high-strength steels exhibit stress-strain characteristics similar to those of ASTM-A7 steel except with a higher yield-stress level. It is reasonable to expect that plastic design may be applied to structures in which such steels are used, providing they meet design guides similar to those suggested in this Manual, but appropriate to the particular material.

## 4.4 STRUCTURAL DUCTILITY

Fabrication processes should be such as to retain ductility. At plastic-hinge locations unfinished sheared edges and punched holes in tension flanges should not be permitted. Sub-punched and reamed holes for connecting devices would be satisfactory if the reaming removes the cold-worked material.

In design, triaxial states of tensile stress set up by geometrical restraints should be minimized.

This provision together with Art. 4.3 is intended to assure that brittle fracture will not prevent the formation of a plastic hinge. The assumption of ductility is an equally important aspect of elastic design and numerous design assumptions rely on it.

In plastic design the engineer should be guided by the same principles that govern the proper design of all-welded, riveted, or bolted structures designed by the allowable-stress methods, since ductility is important to both. Thus the proper material must be specified to meet the appropriate service conditions, the fabrication and workmanship must meet high standards, and design details should be such that the material is as free to deform as possible. (4.3)

With respect to fabrication, due to the severe cold working involved, punched holes and sheared edges should not be permitted in parts that might be subjected to stresses approaching the yield stress in tension at ultimate load. Punched holes would be permitted here if followed by sufficient reaming to remove the cold-worked material. In Ref. 4.2 the effect of various edge conditions on the brittle failure of steel has been studied.

## 4.5 YIELD STRESS LEVEL

For ASTM-A7 steel,

Normal stress,  $\sigma_y = 33.0$  ksi  
Shear stress,  $\tau_y = 19.0$  ksi

A yield stress level of 33.0 ksi corresponds to the minimum yield point permitted in a mill-type acceptance test of ASTM-A7 steel. Such a test differs from the test conducted in the laboratory because of a number of factors, one of the most important of which is strain rate. An extensive investigation into the yield-stress level has been conducted (4.1) using as the test specimen a complete cross section of a rolled wide-flange shape. The loading was performed in a manner that simulates "static" loading. By such a test procedure it was possible to include such effects as differences in web and flange strength, strain rate, and size, since representative cross sections from the very smallest to the largest rolled shapes were included in the program.

According to the data available at that time, this investigation showed that the most probable value of the yield-stress level is 34.1 ksi, with variations ranging from 24.6 ksi to 43.0 ksi. (According to the usual acceptance-type test, the most probable value of the yield point would be 42.6 ksi). Fig. 4.1 shows the histogram of the ratio of yield-stress level determined from a stub column test as compared with the yield-point value obtained in a mill-type acceptance test.

While 33.0 ksi is the minimum yield point permitted in acceptance tests, it turns out that it is very close to the average basic yield-stress level of this material. Thus the factor of safety includes the possibility of variation below this average value, because the design is actually based on an average, not a minimum. This situation has always existed in design, and therefore represents no departure from past practice.

4.6 PLASTIC MOMENT

$$M_p = \sigma_y Z \dots\dots\dots (4.1)$$

$\sigma_y$  = yield-stress level  
 $Z$  = plastic modulus

As pointed out in Art. 2.1, the formation of plastic hinges is of basic importance to plastic design. Fig. 2.3 shows the characteristic moment-rotation curve of a beam under bending, and the moment at "stage 5" shown in Figs. 2.2 and 2.3 is called the plastic moment. It is computed according to Eq. 4.1.

The plastic modulus  $Z$  is a geometrical function analogous to the section modulus. It is the modulus of resistance to bending of a completely yielded cross section and is calculated by taking the combined statical moment about the neutral axis of the cross-sectional areas above and below that axis.

As will be evident in Chapter 5, it is frequently observed in tests that the moment-deformation behavior is not exactly like that shown in Fig. 2.3 (see Fig. 5.4, for example). Because of strain-hardening, the resisting moment is greater than the value computed according to Eq. 4.1. However, no present simple theory can take this additional reserve in strength into account without undue complications.

For material whose characteristics are not similar to ASTM-A7 steel, but which exhibits continuous strain-hardening, it might be desirable to arrive at a

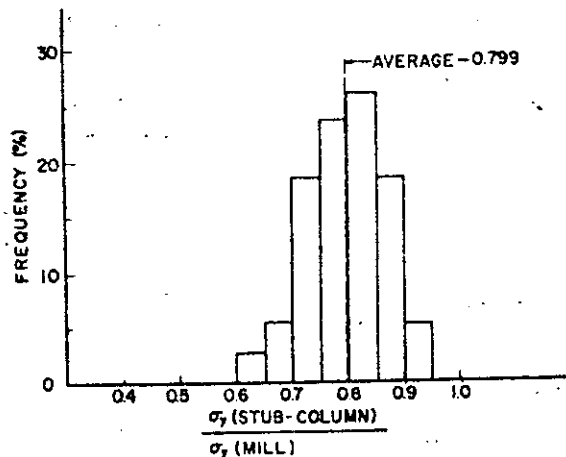


FIG. 4.1.—FREQUENCY DISTRIBUTION OF THE RATIO  $\frac{\sigma_y \text{ (Stub-Column)}}{\sigma_y \text{ (Mill)}}$

semi-empirical value for the "plastic hinge" moment. Studies would have to be made on the particular material (including bending tests and tests of indeterminate structures) to arrive at a suitable approximation for the plastic moment.

4.7 LOADS

The loads to be provided for (allowable loads) should be those that are customary for the particular type of construction. These loads are increased by a load factor to obtain an ultimate loading. Members are selected on the basis of their plastic strength to resist the most critical condition of ultimate loading.

$$P_u = F P_w \dots\dots\dots (4.2)$$

in which

- $F$  = load factor
- $P_u$  = ultimate load
- $P_w$  = allowable (working) load

A margin of safety is achieved in elastic design by the use of allowable unit stresses obtained from a unit stress level assumed to represent failure and which has been reduced by a "factor of safety." In plastic design safety is achieved by multiplying the given service loads by a "load factor" as discussed in Art. 4.8.

The use of plastic design does not involve any changes in the magnitude of the service loading  $P_w$  specified for a given structure. The difference is that, in the case of plastic design, members are selected so that the structure will just support the computed ultimate load  $P_u$ . In elastic design the members are so selected that allowable unit stresses will not be exceeded at service load  $P_w$ . (As used here  $P$  is the critical combination of given independently variable loads used as the basis for the design by either method.)

The loading conditions that would be investigated for building construction are:

1. Dead load plus live load.
2. Dead load, plus live load, plus wind or earthquake forces.

It is assumed that the live loading is static and proportional, even for the characteristic fluctuations of live load found in buildings. For unusual conditions, deflection stability would be investigated (see Art. 6.4).

In the design of structures to resist the dynamic loading resulting from blast forces, plastic-design concepts generally are used. However selection of the loading and the type of design are largely a matter of judgment and are based on studies of vulnerability, consequences of failure, and required radiation protection. In making the design it is necessary to consider the nature of the loading, increased dynamic yield strength of the material, effective load duration, distribution of mass, effective mass, and natural period of the structure, as well as other factors not commonly considered in structural design.

In designing for earthquakes most building codes provide for the application of equivalent lateral static loads to produce a desired level of earthquake resistance. In conformity with such practice, the specified loads can be multiplied by a load factor to yield design ultimate loads.

Concepts of plastic analysis are currently being considered for design to resist earthquake forces using procedures that take into account the elastic-plastic response of the structure as a function of time. Here, the variation and random nature of earthquake loading require that consideration be given to loading approximations used in the design, as well as to many of the factors noted above as of importance in designing for blast forces. Greater refinement in design procedures using these concepts must await further study.

4.8 LOAD FACTORS

Dead load plus live load	F = 1.85
Dead load plus live load plus wind or earthquake forces	F = 1.40

It should be noted that the factor of safety implicit in allowable stress design and the load factor used in plastic design are not concerned alone with the possibility of overloading. Other factors which influence the selection of an appropriate margin of safety are:

1. Approximations and uncertainties in the method of analysis.
2. Quality of workmanship.
3. Presence of residual stresses and stress concentrations.\*
4. Under-run in physical properties of material.
5. Under-run of cross-sectional dimensions of members.
6. Location and intended use of structure.

Depending on the type of structure and its intended use, the importance of any one of the foregoing factors, as compared with the others, can vary somewhat. One might arrive at a precise over-all load factor F in each case if sufficient statistical data were available to weigh properly the importance of its various constituent parts; but any resulting departure from current practice would be equally applicable to the allowable stresses specified for use in elastic designs. Since such statistical data are not available, it would seem logical to draw on the vast experience gained from allowable stress design to obtain a single average value, applicable throughout the range of building construction.

Such a value can be obtained by considering the plastic strength of simple beams in the light of the allowable stress for which these beams were proportioned, there being no necessity for requiring any greater margin of safety merely because the structure is redundant. For simple beams the load factor is equal to the ratio of the ultimate load  $P_u$  to the working load  $P_w$ ; thus F equals  $P_u/P_w$ . Since here the bending moment varies linearly with the load

$$F = \frac{P_u}{P_w} = \frac{M_p}{M_w}$$

Substituting for  $M_p$  and  $M_w$

$$F = \frac{\sigma_y Z}{\sigma_w S} = \frac{\sigma_y}{\sigma_w} f$$

in which f is the shape factor.

\*WF This factor contributes to uncertainty as to the precise stress level, the discussion in Art. 1.2, 5.1, and 5.3 shows that it may not influence the ultimate load-carrying capacity (excepting column buckling, of course).

Since adoption of its Standard Specification for Structural Steel for Buildings by the American Institute of Steel Construction in 1923, and to a limited extent even before that, the basic allowable working stress in building design in the United States has been 0.6 of the specified minimum unit yield stress of the steel furnished. Restated, the load factor against the guaranteed minimum ultimate capacity of these beams has not exceeded

$$F = \frac{30,000 \text{ psi}}{18,000 \text{ psi}} f = \frac{33,000 \text{ psi}}{20,000 \text{ psi}} f = 1.65 f \dots \dots \dots (4.3)$$

The formulation of a satisfactory load factor is therefore dependent only upon the determination of a shape factor representative of the simple beams now in service.

The variation of the shape factor for wide-flange beams and columns; and for American Standard beams is shown in Fig. 4.2. For wide-flange shapes normally used as beams listed in the "section economy" table (4.4) the shape factor varies from 1.10 to 1.18 with an average value of 1.134 and a mode (most frequently observed value) of 1.12. For wide-flange shapes normally used as columns that appear in the "column" tables of Ref. 4.4 the shape factor varies from 1.10 to 1.23 with an average value of 1.137 and a mode of 1.115. The shape-factor distribution of American Standard beams is shown in the lower portion of Fig. 4.2. The minimum is 1.14 and the maximum is 1.23, the average being 1.18.

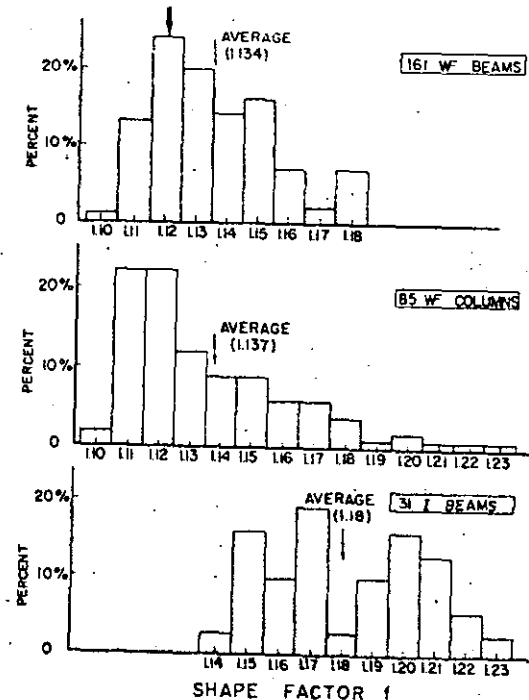


FIG. 4.2.—THE VARIATION OF SHAPE FACTOR FOR WIDE-FL/ COLUMNS AND AMERICAN STANDARD BEAMS

## GENERAL PROVISIONS

Table 4.1 shows several possible values of the load factor, depending on the choice of the shape factor. The two most reasonable values for the load factor are 1.85 and 1.88. The former would seem appropriate because it represents the shape factor that will recur most frequently in beams. The value 1.88 implies an accuracy in our knowledge of the general problem of safety that is not justified.

TABLE 4.1.—LOAD FACTOR FROM SHAPE FACTOR

Shape Factor	Factor of Safety = Yield Stress ÷ Working Stress	Load Factor
1.10—Minimum value	1.65	1.81
1.12—Mode for wide-flange beams	1.65	1.85
1.14—Average for wide-flange beams and columns	1.65	1.88
1.18—Average for American Standard I-beams	1.65	1.95
1.23—Maximum value	1.65	2.03

In the case of gravity loading in combination with wind or earthquake forces, allowable stress design specifications permit a one-third increase in computed stresses. Consistent with this allowance, the value of  $F$  for combined dead, live, and wind or earthquake loading would be  $(3/4) \times 1.85 = 1.40$ .

## Chapter 5

## VERIFICATION OF PLASTIC THEORY

In this chapter it is shown that the actual behavior of structures under test verifies the predictions of plastic theory. In Art. 5.1 it is demonstrated that structural steel exhibits the ductility assumed, and that plastic hinges will form and allow the necessary redistribution of moment. Article 5.2 presents the results of continuous-beam tests, and finally Art. 5.3 shows how tests of rigid frames verify plastic theory.

## 5.1 BASIC CONCEPTS

## Ductility of Steel

Fig. 5.1 shows the tensile stress-strain curves obtained from two coupons cut from two separate locations of an 8 W 40 beam. They are typical of the behavior of ASTM-A7 steel. The steel deforms plastically about 15 times the strain at the elastic limit and then commences to strain harden. \* Although the

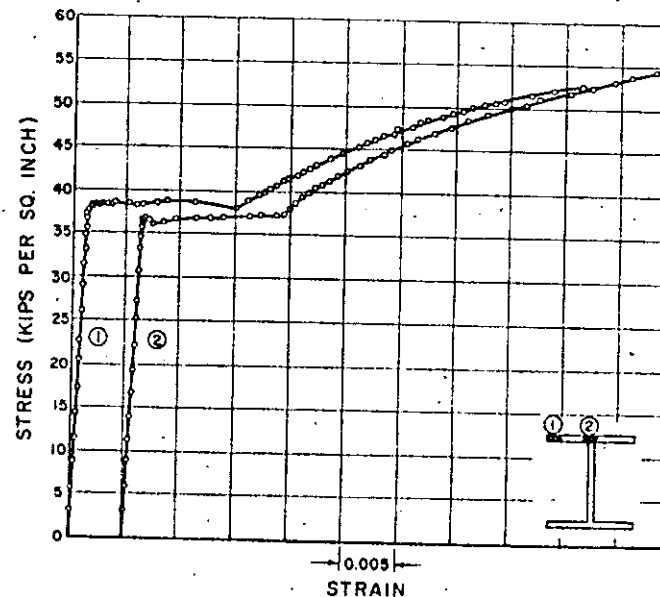


FIG. 5.1.—STRESS-STRAIN RELATIONSHIP OF TENSILE COUPONS OF ASTM-A7 STEEL(5.3)

\*ASTM-A7 requires an elongation in 2 in. of not less than 24% at failure, an elongation that is more than 200 times the maximum elastic value.



data is plotted well into the strain-hardening range, the strains shown are still considerably less than those at ultimate strength (tensile strength). The compressive and the tensile stress-strain relationships are quite similar. In fact the properties in compression are practically identical with those in tension. Fig. 5.2 shows in idealized form the stress-strain relationships for ASTM-A7 steel drawn according to average values obtained in laboratory tests.

#### The Plastic Moment and the Plastic Hinge

As a demonstration that the plastic moment is attained through plastification of a cross section, Fig. 5.3(a) shows a typical  $M-\phi$  curve obtained from a beam, a portion of which is in pure bending. (5.1) The dotted line is the idealized

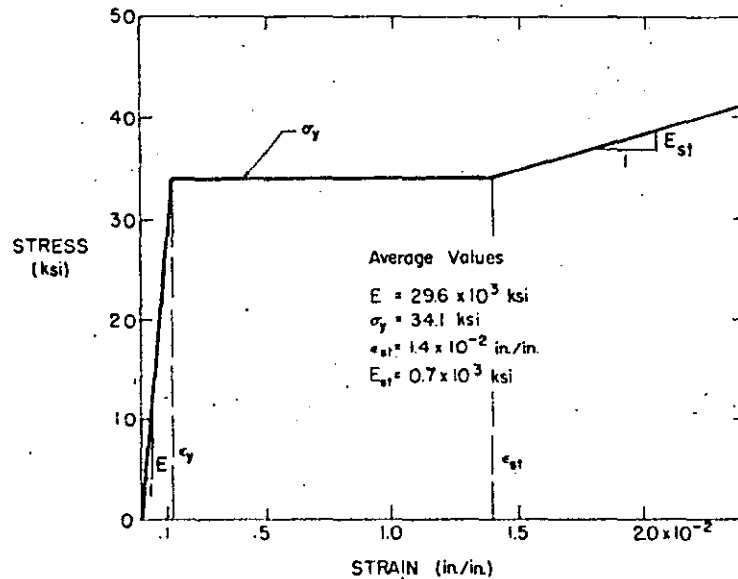


FIG. 5.2.—IDEALIZED STRESS-STRAIN RELATIONSHIP FOR ASTM-A7 STEEL

curve and the solid line through the circles shows the results of a test. The theoretical stress distributions (according to the simple plastic theory) at different stages of bending are shown in Fig. 5.3(b). Below these, in Fig. 5.3(c), are shown the corresponding stress distributions as determined from SR-4 gage measurements. It will be seen that plastification of the cross section does occur, and that the bending moment corresponding to this condition is the full plastic moment as computed from the equation  $M_p = \sigma_y Z$ .

Although there will be inevitable minor variations from the result shown in Fig. 5.3(a) the many tests conducted on rolled shapes indicate that most hot-rolled wide-flange beams will develop the strength predicted by the plastic theory and that a plastic hinge (characterized by rotation at near-constant moment) does actually form.

To be sure, a somewhat unrealistic loading condition has been taken since "pure moment" is a condition not likely to be encountered in actual structures. Usually there will be a gradient in moment, as when a single concentrated load is applied to a beam. In such a case the deformation tends to be concentrated under the load point (the point of maximum moment). Because the plast.

deformation is more localized, the strain-hardening region is reached at a lesser deflection; consequently, the beam tends to develop a moment greater

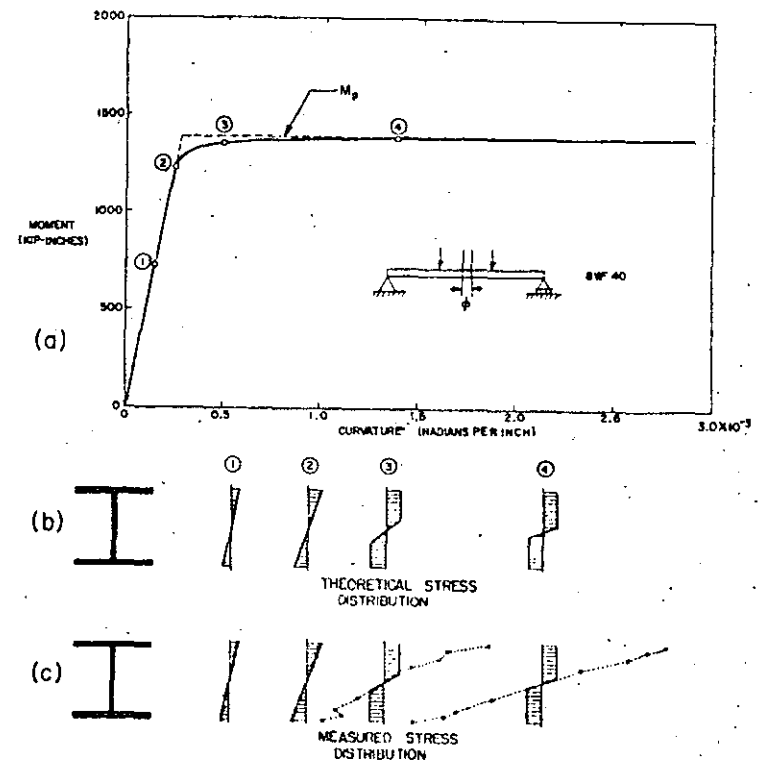


FIG. 5.3.—EXPERIMENTAL VERIFICATION OF THE MOMENT-CURVATURE RELATIONSHIP AND THEORETICAL AND COMPUTED STRESS DISTRIBUTIONS

than the plastic moment. Typical of the behavior of a beam under moment gradient is that shown in Fig. 5.4. (5.2) The theoretical load-deflection curve, with and without the inclusion of strain-hardening, is shown by dashed lines. The results of a test of such a beam are shown as a solid line: It will be noted that as a result of the strain-hardening phenomenon there is an increase in load-carrying capacity as the deformation continues beyond the yield level. The decrease in measured resistance, which occurred after a large hinge rotation at the center, resulted from local buckling of the flanges followed by lateral buckling.

Thus strain-hardening improves the moment-carrying capacity of a beam. Although it is neglected in the simple plastic theory (except for checking a beam for stability against buckling) this additional reserve strength is still present in most ordinary structures, and this contributes to an actual factor of safety that is greater than the value assumed in the simple plastic theory.

#### Redistribution of Moment

From the previous section it is seen that plastic hinge may be depended on to form at connections and at concentrated-load points. Development of

## VERIFICATION OF THEORY

the plastic moment is one of the sources of reserve strength in structural steel beyond the elastic limit. Another source is the redistribution of moment in continuous structures.

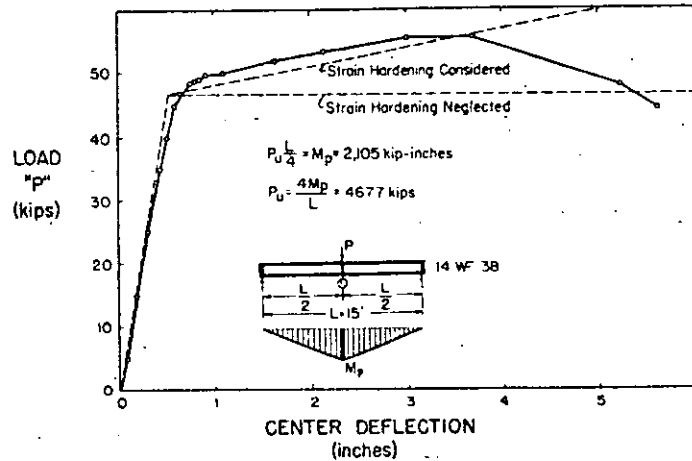


FIG. 5.4.—LOAD VERSUS CENTER DEFLECTION RELATIONSHIP OF A 14W38 BEAM

In Fig. 5.5 is shown a picture of the redistribution process—as predicted theoretically and as obtained experimentally. A test was made on a continuous beam to simulate the condition of third-point loading on a fixed-ended span; (5.3) thus experimental data was available to compare with the theoretical predictions. The fixed-ended beam and its various components are shown in four stages:

- Stage 1—at the computed elastic limit.
- Stage 2—after the plastic hinges have formed at the ends and the load has increased towards its ultimate value.
- Stage 3—when the theoretical ultimate load is first reached.
- Stage 4—after deformation has been continued through an arbitrary additional displacement.

Fig. 5.5 shows (a) the loading, (b) the deflected shape at the four stages, (c) the moment diagram, (d) the load-deflection curve, and the moment-curvature relationship near the ends (e) and at the center (f).

In the elastic range (stage 1) it will be seen that the beam behaves just as assumed by the theory, the moment at the center being one-half the moment at the fixed ends. (Figs. 5.5(c), (e), and (f)). As the moment at the ends approaches the yield moment, the curvature  $\phi$  commences to increase more rapidly; a plastic hinge begins to form (Fig. 5.5(e)). Because of this "hinge action," the additional moments due to increase in load are distributed between the ends and the center in a different ratio beyond the elastic range than before. As long as the beam is elastic the increase in moment at the center corresponding to a load increment is one-half the increase at the ends. However, after a plastic hinge forms at the ends, most of the increase of moment

occurs at the center; the moment increment at the ends is small (Figs. 5.5(e) and (f)). This is the process known as redistribution of moment.

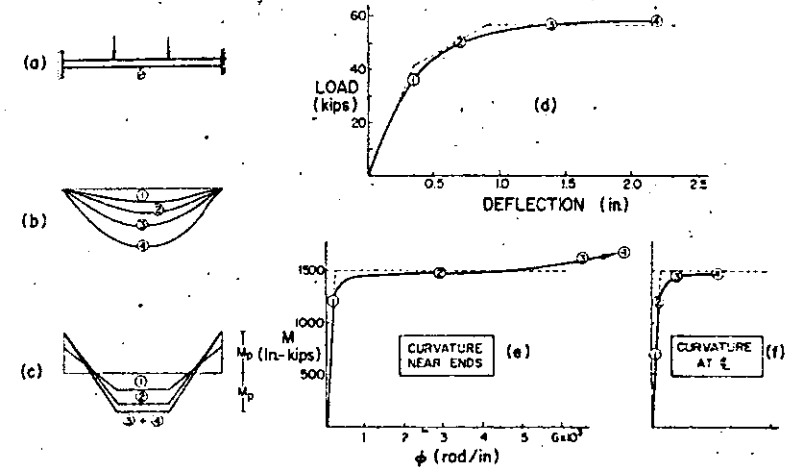


FIG. 5.5.—REDISTRIBUTION OF MOMENT AS REVEALED BY TEST ON A FIXED-ENDED BEAM

As a result of plastification at the ends, the beam actually behaves somewhat more flexibly than before (Fig. 5.5(d)). At stage 2 the elastic-moment capacity near the center is practically exhausted. It is quite evident from Fig. 5.5 that substantially all of the moment capacity has been absorbed by the time stage 3 is reached (ultimate load). Beyond this, the beam simply deforms as a mechanism with the moment diagram remaining largely unchanged, the plastic hinges at the ends and center rotating further.

Clear evidence is therefore available that redistribution of moment occurs through the formation of plastic hinges, allowing the structure to reach (and usually exceed) the theoretical ultimate load predicted by simple plastic theory.

Incidentally, Fig. 5.5(d) illustrates the gradual transition from the elastic to the inelastic range that is typical for continuous steel beams and frames. Theoretically, upon first loading the structure should remain elastic up to stage 1. However, because of the combination of unknown initial stress conditions and discontinuities, local plastic flow takes place at a lower load than that which corresponds to stage 1. But there is no effect whatever upon the ultimate load.

## 5.2 CONTINUOUS BEAMS

Fig. 5.6 shows the results of continuous-beam tests in which the members were fabricated from rolled sections. The structure and loading are shown to scale at the left. Next, the size of member (or members) is indicated. To the right is a bar graph on which is plotted the percentage of predicted ultimate strength exhibited by the test structure. A test result plotted to the "100%" line shows that the structure reached the load predicted by the simple plastic theory. The shaded portion of the bar chart represents the reserve strength beyond the elastic limit, since the end of the unshaded portion of each bar

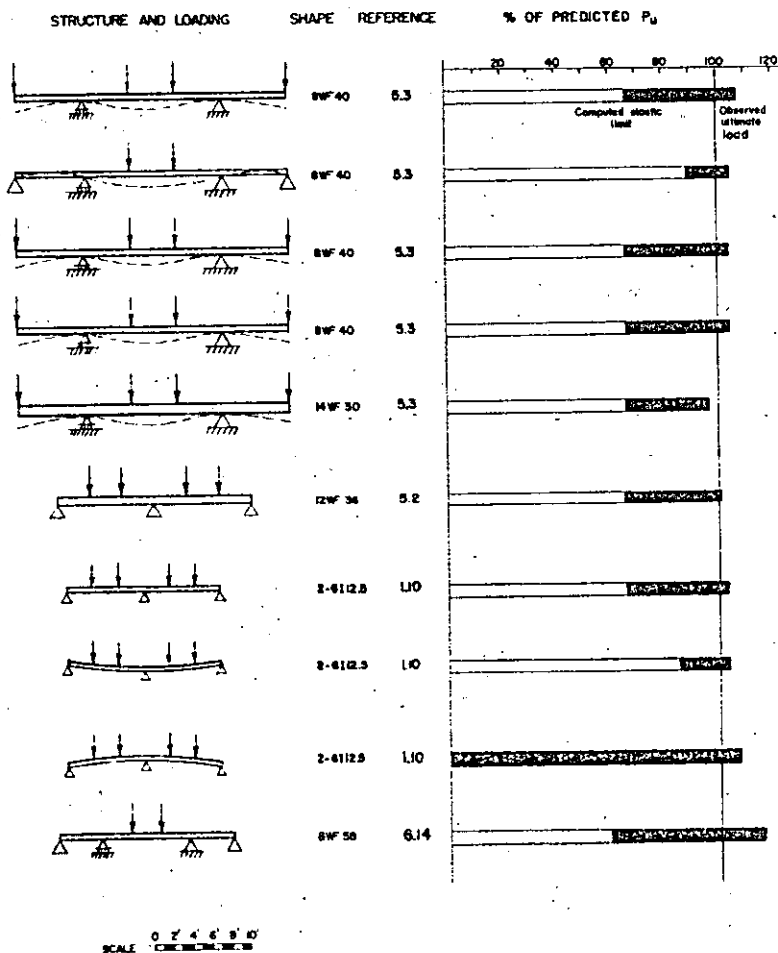


FIG. 5.6.—SUMMARY OF CONTINUOUS BEAM TEST RESULTS SHOWING CORRELATION WITH PREDICTIONS OF PLASTIC THEORY

graph is the computed elastic limit (on a non-dimensional basis) and the end of the shaded portion is the observed maximum strength.

Particularly remarkable among the continuous beam tests of Fig. 5.6 is one described in Ref. 1.10 and shown as the next to the last structure. In this experiment, prior to applying the vertical load, the center support was raised until the allowable working stress was just reached, with the result that application of the first increment of external load was, in fact, a load greater than allowed by the specifications. In spite of this, the computed ultimate load was attained. The observed ultimate load in this test was within 3% of that of the two structures shown immediately above in Fig. 5.6.

The continuous beams shown in Fig. 5.7 were tested to show that members of otherwise inadequate strength may be cover-plated to achieve the desired load-carrying capacity.

### 5.3 FRAMES

The structure shown in Fig. 5.8 is typical of some of the frames tested in the United States as part of the experimental verification of the plastic theory. The span is 40 ft and the frame was fabricated of 12 WF 36 rolled shapes. Not only has the computed ultimate load been reached at the stage shown in the photograph, but the frame has absorbed considerable additional plastic deformation while sustaining a load slightly in excess of  $P_u$ . Fig. 5.9 shows the load-deflection curve for this structure. The dashed line shows the predicted behavior based on theory and the series of open circles connected by the solid line represents the observed behavior. This result demonstrates once again that inelastic action (due to local effects) commences at a load considerably less than the predicted yield value. It also shows that the ultimate load is not affected by such initial conditions.

It is of interest to note that at ultimate load the excess of actual deflection above the computed value for this frame was no greater than that observed at the predicted yield load. This means that the methods for computing such deflections are as dependable as the elastic deflection calculations.

Figs. 5.10, 5.11, 5.12, and 5.13 show frames tested both in the United States and abroad, and represent some of the structures which have been tested to maximum load capacity prior to 1958. As before, the unshaded portion of each bar graph represents the loading range up to the computed elastic limit. The shaded portion represents the reserve strength beyond the elastic limit, the end of that part being the observed maximum load. Good agreement is observed at maximum load except for those cases in which strain-hardening accounted for an increase; it is better, in fact, than the agreement between the predicted load at first yield and the observed value. In Fig. 5.10 testing of the fourth frame was interrupted in order that the fifth test might be carried out on the same structure but with a different proportion of horizontal to vertical load.

In view of the notable agreement between plastic theory and the results of these tests, the applicability of the plastic method to structural design problems involving continuous steel beams and frames is demonstrated.

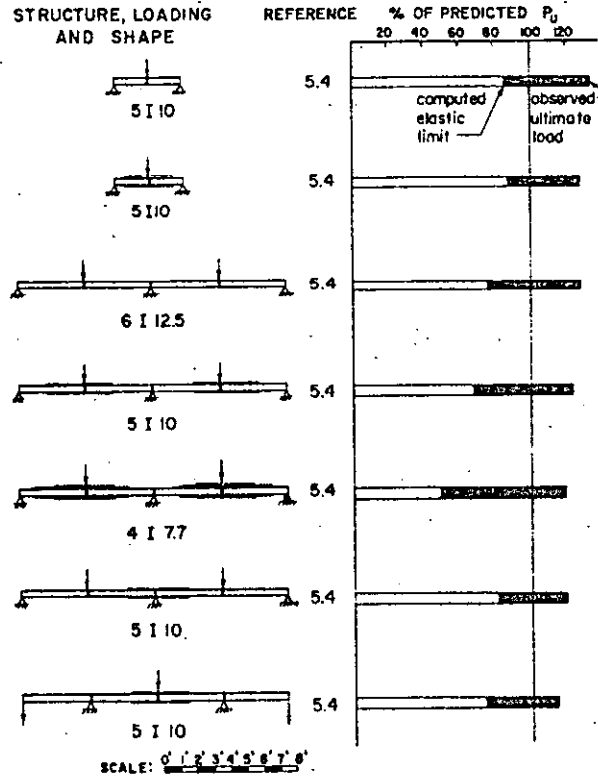


FIG. 5.7.—SUMMARY OF BEAM TEST RESULTS SHOWING CORRELATION WITH PREDICTIONS OF PLASTIC THEORY

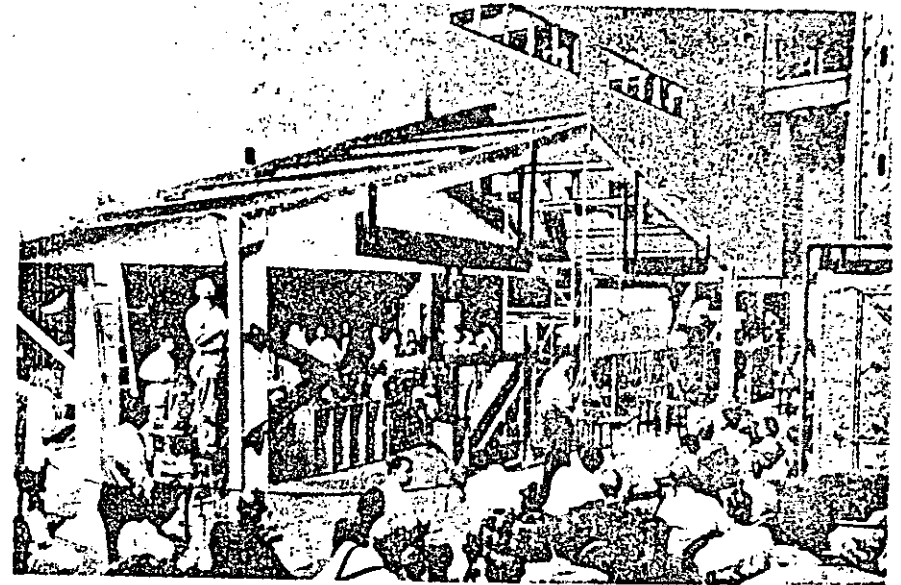


FIG. 5.8.—TEST OF A 40-FT SPAN GABLE FRAME

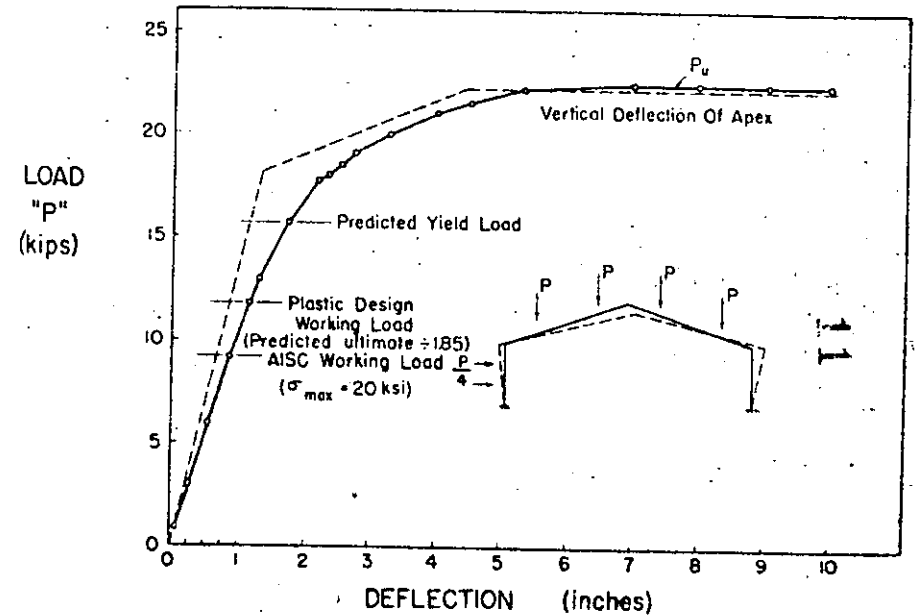


FIG. 5.9.—LOAD VERSUS CENTER DEFLECTION DIAGRAM OF TEST FRAME SHOWN IN FIG. 5.8

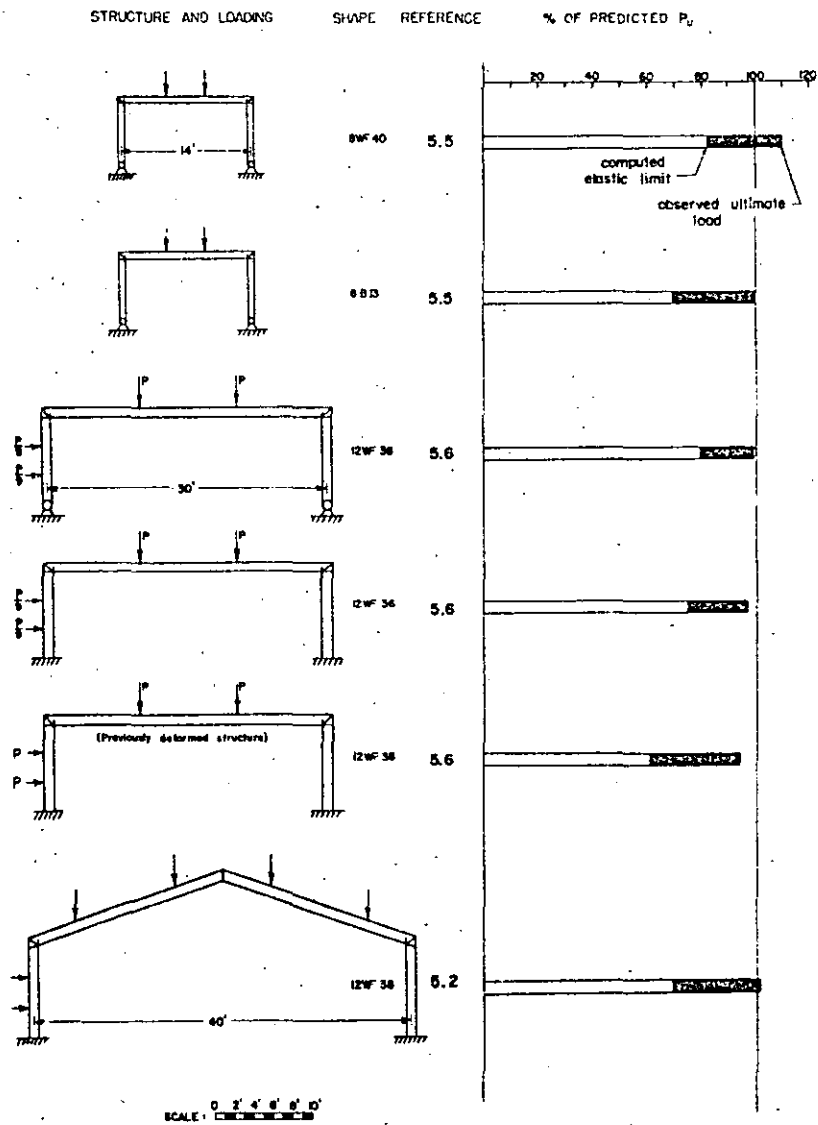


FIG. 5.10.—SUMMARY OF FRAME TEST RESULTS SHOWING CORRELATION WITH PREDICTIONS OF PLASTIC THEORY

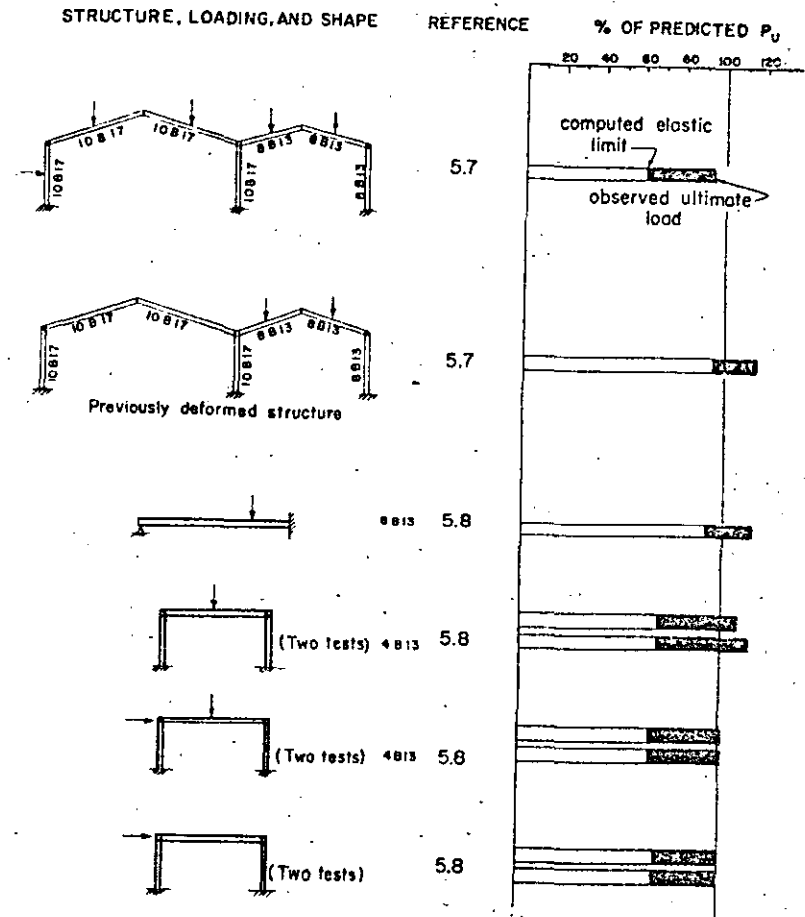


FIG. 5.11.—SUMMARY OF FRAME TEST RESULTS SHOWING CORRELATION WITH PREDICTIONS OF PLASTIC THEORY

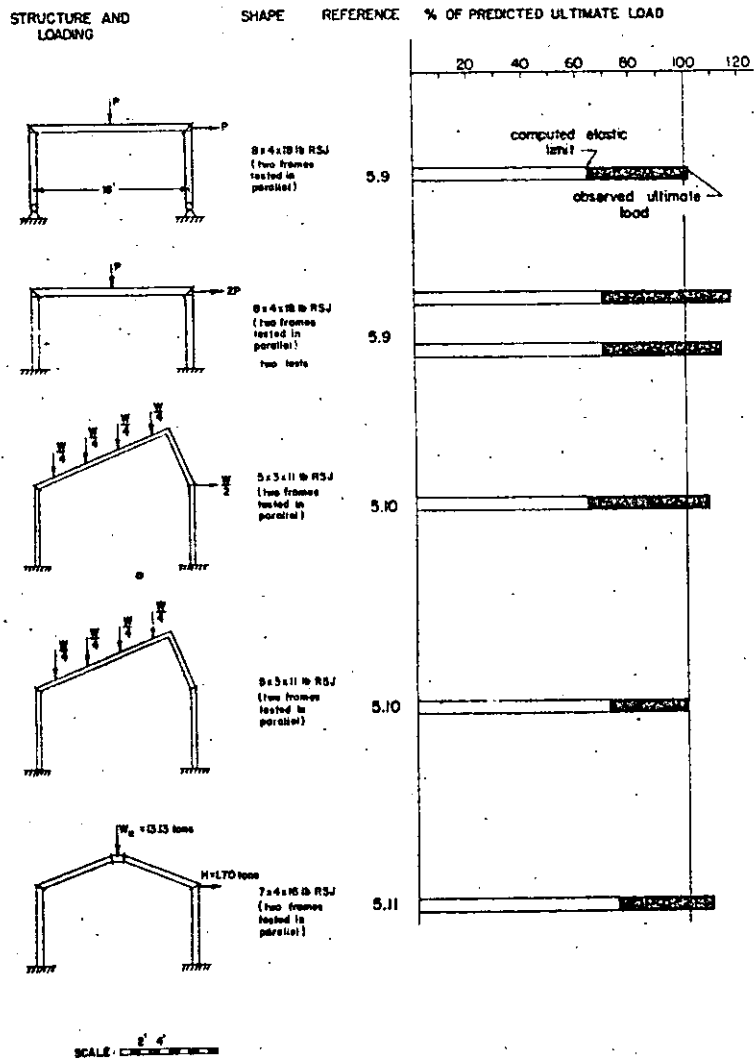


FIG. 5.12.—SUMMARY OF FRAME TEST RESULTS SHOWING CORRELATION WITH PREDICTIONS OF PLASTIC THEORY

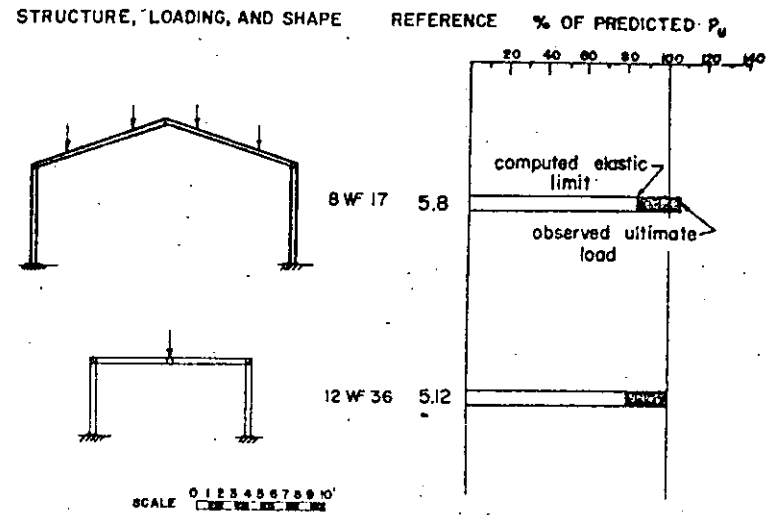


FIG. 5.13.—SUMMARY OF FRAME TEST RESULTS SHOWING CORRELATION WITH PREDICTIONS OF PLASTIC THEORY

## ADDITIONAL DESIGN CONSIDERATIONS

In the application of plastic theory to design, just as in the case of allowable-stress design, there are a number of important factors which must be evaluated. Those considered in this chapter include shear force, local buckling of flanges and webs, lateral instability, and repeated loading. The problem of column buckling is treated in Chapter 7. The background of research is described, including the important assumptions and steps of pertinent theoretical analyses. Experimental correlation is given, and approximations for design use are discussed.

## 6.1 SHEAR FORCE

## Statement of the Problem

Simple plastic theory is based on the concept of the attainment of the full plastic moment at certain sections of a structure, followed by adequate rotation at this constant moment value as the applied load increases. It must be recognized, however, that the magnitude of the moment at which large inelastic rotations occur is not constant under all circumstances. In calculating the full plastic moment  $M_p$  as  $\sigma_y Z$ , it is assumed that the member is stable and is subjected to pure bending; thus axial thrust and shear force are both ignored.

Since plastic hinges usually occur at positions where shear and axial force are present, it is of importance to be able to predict the changes in the values of the plastic moments due to these causes. In most practical cases the influence of shear force will be very small. In some special cases the combined influence of shear and axial thrust is important.

## Previous Research

The effect of transverse shear force was considered in Ref. 6.1 for the case of a beam of rectangular cross section bent about one of its axes of symmetry. An approximate solution was obtained which is valid for shear forces less than a certain limit. This solution was also extended to an I-section bent about the axis normal to the web (strong axis).

This latter solution was modified in Ref. 6.2 to determine a lower bound (which is valid over the full range of shear forces) on the value of the full plastic moment in the presence of shear forces. An upper bound on the full plastic moment when the shear force has its full plastic value was also included. In Ref. 6.3 a semi-empirical theory was proposed, which is also valid over the full range of shear forces. An upper bound on the value of the full plastic moment in the presence of shear force was presented in Ref. 6.4 for beams of rectangular and I-section. This upper bound agrees closely with the lower bound of Ref. 6.2 for large values of the shear force. Upper-bound solutions were also derived independently (6.4, 6.5) for a beam of rectangular cross section by assuming a plane-strain state and a rigid-plastic material. Ref. 6.6 demonstrated the lack of uniqueness of interaction curves for shear and

moment, explored bounds for a beam of rectangular cross section, and proposed an approximate interaction formula

$$\frac{M}{M_p} = 1 - \left(\frac{V}{V_p}\right)^4 \quad (6.1)$$

in which

$M$  = moment

$M_p$  = plastic moment =  $\sigma_y b d^2/4$

$V$  = applied shear force

$V_p$  =  $\sigma_y b d/2$

6.6 Drucker

Ref. 6.7 gives the derivation for a general expression which is valid over the full range of shear and is applicable to both rectangular and I-beams. A lower-bound solution was developed for a cantilever beam with rectangular cross section, assuming the plane stress state and allowing warping at the fixed end. (6.8) This solution was modified for wide-flange sections including an extreme case of shear failure. (3.1) Independent investigations have been made of the effect of both shear force and axial thrust on the full plastic moment. (6.9, 6.10) The theoretical results obtained in Ref. 6.10 are in fair agreement with experimental observations.

## Theoretical Analysis

In most practical situations, wide-flange or I-sections are used. However, the essentials of the problem can be shown by the simple example of a cantilever beam with rectangular cross section of depth  $d$  and width  $b$  (Fig. 6.1). The following assumptions and limitations are made for the analysis:

1. The problem is analyzed using the assumptions made in ordinary beam theory as one of plane stress.
2. Only the elastic portion can carry shearing forces.
3. The von Mises-Hencky yield criterion is adopted for the combined stress state.
4. The fixed end is allowed to warp.

As the external loading is increased, yielding will commence at the fixed end of the beam and start to penetrate into the cross section (Fig. 6.1(a)). External and internal moment and shear at section S-S in Fig. 6.1(a) are given by

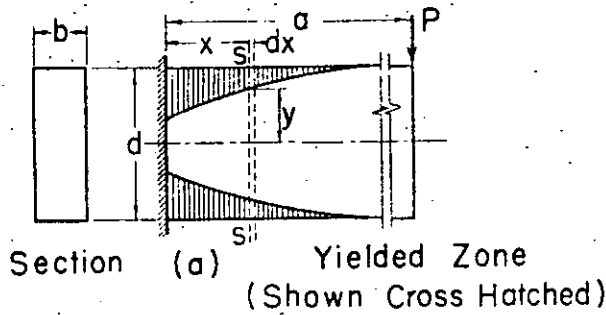
$$M = P(a-x) = M_p - \sigma_y \frac{b y^2}{3} \quad (6.2)$$

$$V = -P = \frac{dM}{dx} \quad (6.3)$$

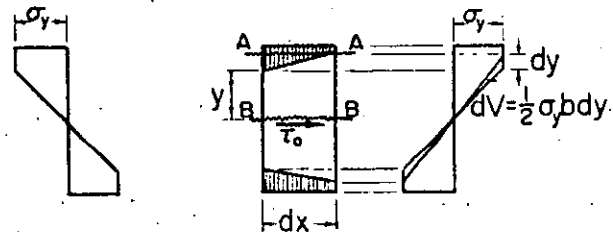
where

$$M_p = \sigma_y \frac{b d^2}{4} \text{ (full plastic moment)}$$

In order to determine the shearing stresses  $\tau$ , the horizontal equilibrium of differential element  $dx$  is considered (Fig. 6.1(b)). A beam element above a horizontal section A-A through the yielded part Fig. 6.1(b) is in horizontal equilibrium without any shearing stresses since the resultant horizontal forces on both faces are equal. Hence no shearing stresses exist in the plastic zone.



Section (a) Yielded Zone (Shown Cross Hatched)



Stress Distribution on Section S-S (b) Change of Stress Distribution in a distance dx

FIG. 6.1.—YIELDED ZONES AND STRESS DISTRIBUTION IN A CANTILEVER BEAM OF RECTANGULAR CROSS SECTION

The shearing stresses  $\tau_0$  on the neutral axis along section B-B resist the unbalanced horizontal force,

$$dV = \frac{1}{2} \sigma_y b dy \dots\dots\dots (6.4)$$

Horizontal equilibrium for the element above section B-B (the center line section) requires

$$\tau_0 b dx = dV = \frac{1}{2} \sigma_y b dy$$

or

$$\tau_0 = \left(\frac{\sigma_y}{2}\right) \left(\frac{dy}{dx}\right) \dots\dots\dots (6.5)$$

The rate of change  $dy/dx$  is obtained by differentiating Eq. 6.2 with respect to the distance along the beam,  $x$

$$\frac{dM}{dx} = V = -\frac{2}{3} \sigma_y b y \frac{dy}{dx} \dots\dots\dots (6.6)$$

which replaced in Eq. 6.5 gives

$$\tau_0 = -\frac{3V}{4by} = -\frac{3P}{4by} \dots\dots\dots (6.7)$$

It is assumed that the resistance of the section will be exhausted if this shearing stress reaches its yield value at this center line section. Using the von Mises-Hencky yield criterion for yielding under pure shear

$$\tau_{yield} = \frac{\sigma_y}{\sqrt{3}} \dots\dots\dots (6.8)$$

The limiting value for  $y$  is then given by Eq. 6.7 as

$$y = \frac{3\sqrt{3}}{4} \frac{P}{b \sigma_y} \dots\dots\dots (6.9)$$

Obviously this condition will first be reached at the fixed end  $x = 0$ ; therefore from Eq. 6.2

$$M_{ps} = P a = M_p - \sigma_y \frac{b y^2}{3}$$

Replacing  $y$  from Eq. 6.9 gives

$$\begin{aligned} M_{ps} &= M_p - \frac{9}{16} \frac{P^2}{b \sigma_y} \\ &= M_p - \frac{9}{64} P^2 a^2 \frac{4}{\sigma_y b d^2} \frac{d^2}{a^2} \end{aligned}$$

Since

$$P^2 a^2 = M_{ps}^2$$

and

$$M_p = \sigma_y \frac{b d^2}{4}$$

then

$$M_{ps} = M_p - \frac{9}{64} \frac{M_{ps}^2}{M_p} \frac{d^2}{a^2}$$

or

$$\frac{9}{64} \left(\frac{M_{ps}}{M_p}\right)^2 \frac{d^2}{a^2} + \frac{M_{ps}}{M_p} - 1 = 0 \dots\dots\dots (6.10)$$

The solution of Eq. 6.10 is given by

$$V < 18,000 w d$$

$$\frac{M_{ps}}{M_p} = \frac{8}{9} \frac{b a^2}{Z} \left( \sqrt{1 + \frac{9}{4} \frac{Z}{b a^2}} - 1 \right) \dots\dots\dots (6.11)$$

where  $Z = b d^2/4 =$  plastic modulus of rectangular cross section. Eq. 6.11 gives the desired relationship between the plastic moment  $M_{ps}$  as modified by shear and the full plastic moment  $M_p$ . It can readily be solved for the parameter  $a/d$  (length of cantilever/depth of section) for different values of the ratio  $M_{ps}/M_p$ . The result is shown in Fig. 6.2 for the curve marked "rectangle."



The rectangular cross section of Fig. 6.1(a) can be considered as the web plate of a wide-flange section. Eq. 6.11 still holds true if the appropriate plastic modulus  $Z$  of the wide-flange section is used when yielding due to

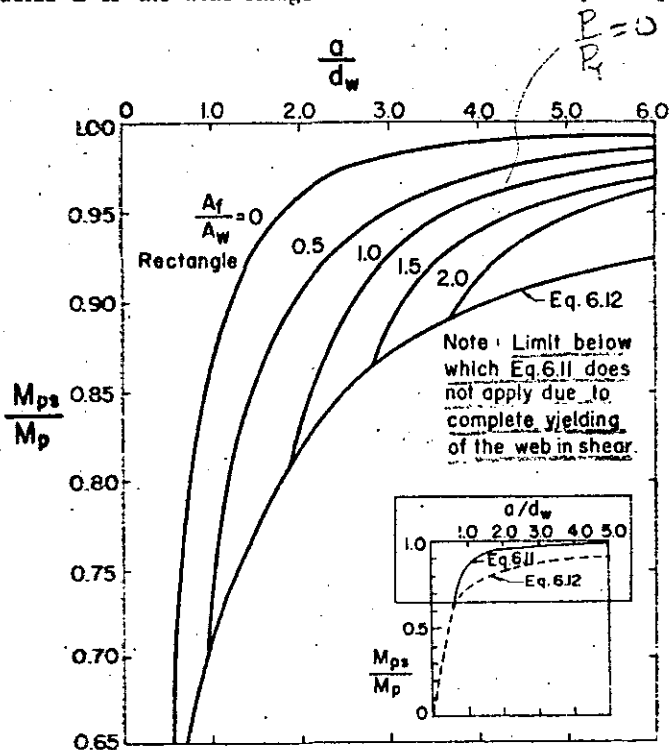


FIG. 6.2.—REDUCTION OF PLASTIC MOMENT BY SHEAR FORCE

normal stresses has penetrated into the web of the section and if the web thickness  $w$  is used instead of the breadth,  $b$ .

Fig. 6.2 shows the comparable reduction of the full plastic moment due to shear force for various ratios of the flange to web areas  $A_f/A_w$ . The case  $A_f/A_w = 0$  corresponds to a rectangle. The dimensions are given in Fig. 6.3. As indicated on the inset sketch of Fig. 6.2, only that portion of the chart for  $M_{ps}/M_p > 0.65$  is shown to the large scale.

It is emphasized that this is not a maximum-carrying-capacity solution, but rather corresponds to "first yield in shear." It would therefore be expected that members tested under this condition would display a greater strength than predicted by the theory.

For cases of high shear to moment values an extreme condition may develop where the entire moment is taken by the flanges and shear produces full yielding of the web as indicated in Fig. 6.3. Then

$$M_{ps} = M_p - \frac{1}{4} \sigma_y w d_w^2 = P a$$

$$V_y = \tau_y A_w$$

$$V_y = \frac{\sigma_y}{\sqrt{3}} d_w w = -P$$

Using these two relations the ratio  $a/d_w$  becomes

$$\frac{a}{d_w} = \frac{\sqrt{3}}{4} \frac{1}{\frac{M_{ps}}{M_p} - 1}$$

or

$$V > 18,000 w d$$

$$\frac{M_{ps}}{M_p} = \frac{1}{1 + \frac{\sqrt{3} d_w}{4 a}} \quad V > 18,000 w d \quad (6.12)$$

The limiting curve for complete yielding of the web in shear (Eq. 6.12) shown in Fig. 6.2 was computed for an average ratio of

$$\frac{d_f}{d_w} = 1.05$$

An approximation to  $V_y$  based on the condition of full yielding of the web is

$$V_y = \tau_y A_w = \left( \frac{\sigma_y}{\sqrt{3}} \right) (w d_w) \quad (6.13)$$

Since for usual wide-flange shapes

$$\frac{d_f}{d_w} \approx 1.07$$

there is obtained for the maximum allowable shear force at ultimate load

$$V_y = 18,000 w d \quad (6.14)$$

in which  $V$  is in pounds and  $w$  and  $d$  are in inches. Therefore, when the maximum shear force at ultimate load  $V$  is greater than  $18,000 w d$  (pounds), the web could be reinforced or Eq. 6.12 could be used to predict the modified plastic moment value. When  $V$  is less than  $V_y$ , Eq. 6.11 is appropriate; however it will be shown later that the implied reduction in moment capacity does not actually occur because of strain-hardening.

If, in addition to shear, an axial force is also present, a similar method of analysis may be applied. For wide-flange sections with  $A_f/A_w = 1.0$  and  $d_f/d_w = 1.05$ , the problem has been solved in Ref. 6.10. Fig. 6.4 shows the relationship of  $M_{pm}/M_p$  to  $a/d_w$  for a cantilever beam, the parameter being the magnitude of axial load  $P$ . In Fig. 6.4  $P_y$  is the axial yield load  $= \sigma_y A$ , and  $M_{pm}$  denotes the plastic-hinge moment modified to include effect of axial compression and shear force. The curve for axial force equal to zero,  $P/P_y = 0$ , is the same as that given in Fig. 6.2 for  $A_f/A_w = 1.0$ . The other curves show the combined influence of shear and axial force as functions of the ratios  $a/d_w$  and  $P/P_y$ .

In practice it is unlikely that high shear forces and high axial loads will occur in combination at points where plastic hinges are expected. If this were to occur, however, Fig. 6.4 could be used to modify a trial design that neglected this unusual combination.

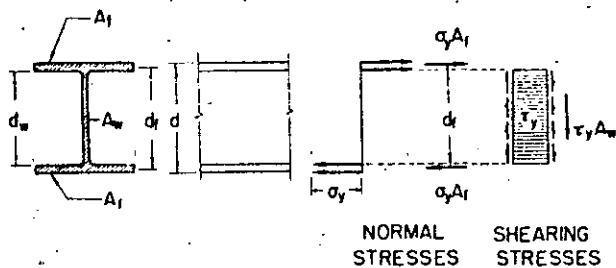


FIG. 6.3.—ASSUMED STRESS DISTRIBUTION IN A WIDE-FLANGE CROSS SECTION LOADED BY SHEAR AND MOMENT

#### Experimental Correlation

It is not easy to make a precise comparison between the theoretical predictions and experiments, since the effect of shear is quite small for wide-flange sections until the shear force  $V$  approaches the extreme value of shear failure  $V_y$  as given by Eq. 6.14. When  $V$  is in the neighborhood of  $V_y$  the load-deflection curves for beams show no appreciable horizontal portion corresponding to plastic-hinge action. Instead, it is found that the load-deflection or the moment-rotation curves continue to rise fairly steadily and to such an extent that the full plastic moment  $M_p$  is exceeded; hence no sharply defined failure condition exists.

However, the intersection of two tangents to the load-deflection or moment-rotation curves in the elastic and plastic range provides one possible criterion for evaluating experimentally the modified plastic moment of the section due to shear force. Beyond this value of moment the deflection or curvature of the beam increases more rapidly than before.

The determination of  $M_{ps}$  is shown in Fig. 6.5; the test data is taken from Ref. 6.16. Fig. 6.5 is a moment-deflection curve for a beam test in which the plastic moment was reduced by shear. An experimental value of  $M_{ps}$  is obtained by extending the elastic portion of the moment-deflection curve to an intersection with the tangent to this curve in the inelastic range. Predictions from Eqs. 6.11 and 6.14 are also indicated for comparison. The shear force  $V$  in this case is greater than 18 ksi, hence Eq. 6.14 would be used.

Fig. 6.6 shows, in tabular form, a number of tests which indicate the influence of shear on the plastic moment. The structure and loading are shown at the left. Next is indicated the size of member and the ratio  $a/d$  where  $d$  is the depth of the member and " $a$ " is the ratio  $M/V$ . For constant shear, " $a$ " is the distance from a plastic hinge to the point of inflection. Therefore " $a$ " is sometimes referred to as the length of an "equivalent cantilever beam." To the right is a bar graph on which is plotted the maximum moment corresponding to the observed maximum load and observed reduced plastic moment  $M_{ps}$  due to shear, the latter being determined as described earlier. The theoretical limit according to Eq. 6.11 or Eq. 6.12, (depending on which case is the controlling one) is shown by the dotted line. In the range where the shear force  $V$  is high and greater than 18,000  $w d$  (pounds), Eq. 6.12 is used to compute the limit predicted by the theory. Fig. 6.6 shows that the actual strength of the structure usually exceeds the full plastic moment  $M_p$  if the shear force  $V$  is less than 18,000  $w d$  (the value which assumes full web yielding,  $V_y$ ). The

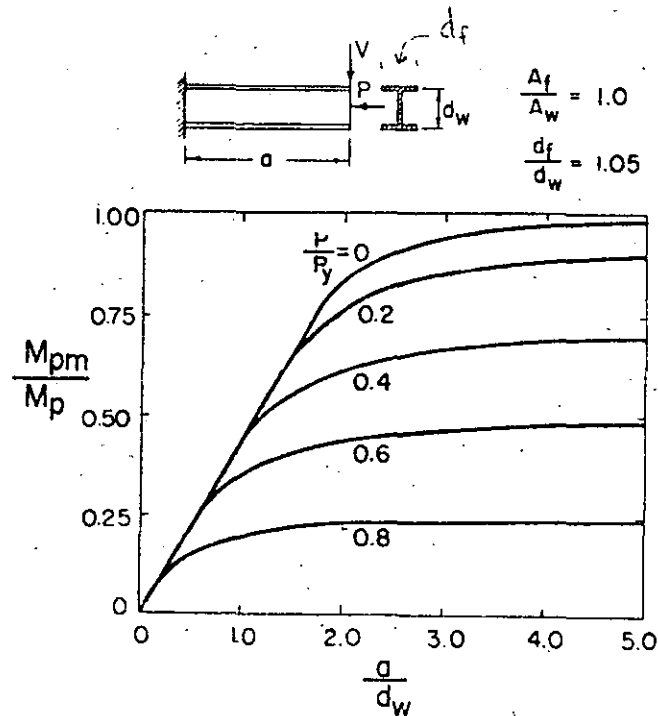


FIG. 6.4.—MOMENT CAPACITY AS MODIFIED BY THE COMBINED ACTION OF SHEAR AND THRUST ON WIDE-FLANGE CROSS SECTION

exception is Beam No. 13 which was only deficient by 4%. The influence of shear force may thus be neglected when this condition exists. Even when the shear force is greater than 18,000  $w d$ , the test results show a moment carrying capacity greater than predicted by Eq. 6.12. It is evident, however, that the latter is a reasonable limit.

While it might appear from these results that a more than ample load factor exists with regard to shear force when  $V \leq 18,000 w d$ , this fact cannot be utilized because of practical limitations. A beam with pure moment, for example, usually buckles when strain-hardening commences, and therefore cannot be counted on to support a moment greater than  $M_p$ .

The test results on the effect of both shear and axial forces<sup>(6.9)</sup> show a tendency similar to that of the bar graph in Fig. 6.6. The observed values of  $M_{pm}/M_p$  are in good agreement with the theoretical predictions in Fig. 6.4

#### Design Approximation

The effect of shear on the full plastic moment will usually be negligible for frames. High shear and moment occur in very localized zones so that strain-hardening will set in quickly and, in most cases, permit the moment to reach the full plastic value. Therefore no reduction in the plastic moment  $M_p$  is required for the effect of shear if at the ultimate load  $V$  is less than 18,000  $w d$  pounds (Eq. 6.14).

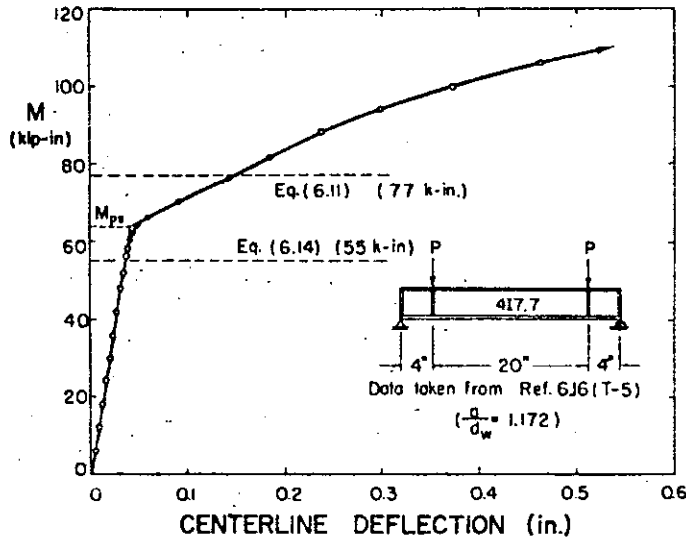


FIG. 6.5.—DETERMINATION OF THE PLASTIC MOMENT AS MODIFIED BY SHEAR,  $M_{ps}$ , USING THE TANGENT INTERSECTION METHOD

**COMBINED MOMENT AND SHEAR FORCE**

The design is satisfactory as regards shear force  $V$  if its magnitude at the ultimate load does not exceed  $18,000 wd$  ( $V$  in pounds and  $w$  and  $d$  in inches). No modification of the plastic moment is required.

**6.2 LOCAL BUCKLING**

Statement of the Problem

Rolled structural steel wide-flange shapes are so proportioned that premature local buckling will not occur for members proportioned in accordance with allowable-stress specifications. Plastic design requires that a member have capacity to sustain sufficiently large plastic hinge rotations so that such hinges may form at certain sections without the occurrence of inelastic instability and consequent loss of moment capacity. Therefore plastic design may impose more severe conditions on the local-buckling behavior of the plate elements of structural members. Local failure, both of the flange and the web, can be treated separately as plate-buckling problems making use of proper boundary conditions and restraints provided from the adjacent plate.

Previous Research

The problem of elastic and inelastic buckling below the yield stress is discussed in Ref. 6.17. Ref. 6.18 gives the first application of the deformation theory (finite stress-strain relations) to the plastic plate buckling problem. This theory was further developed (6.19) and modified (6.20). The problem of local flange buckling was discussed in an approximate manner in Ref. 6.21 and

5

$a = \frac{M}{V}$

No.	STRUCTURES (Span in inches)	SHAPE	$\frac{a}{d}$	$\frac{M_{ps}}{M_p}$ or $\frac{M_{max}}{M_p}$ 0.5 1.0	Ref.
1	4   4   4	417.7	1.0	Observed $M_{ps}$ , $M_{max}$	6.16
2	4   4   4	417.7	1.0	Eq. 6.12	6.16
3	4   4   4	417.7	1.0	Eq. 6.12	6.16
4	4   8   4	417.7	1.0	Eq. 6.12	6.16
5	4   20   4	417.7	1.0	Eq. 6.12	6.16
6	6   20   6	417.7	1.5	Eq. 6.11	6.16
7	40   40   40   40   40	12W36	2.0	Eq. 6.11	5.2
8	8   8   8	417.7	2.0	Eq. 6.11	6.16
9	8   20   8	417.7	2.0	Eq. 6.11	6.16
10	24   36   24	12W27	2.0	Eq. 6.11	6.8
11	24   24	12W27	2.0	Eq. 6.11	6.8
12	84   56   56   56   84	14W30	2.0	Eq. 6.11	6.15
13	53   36   36   36   53	8W58	2.1	Eq. 6.11	6.14
14	36   36   36	12W27	3.0	Eq. 6.11	6.8
15	84   56   56   56   84	8W40	3.4	Eq. 6.11	6.15
16	84   56   56   56   84	8W40	3.4	Eq. 6.11	6.15
17	84   56   56   56   84	8W40	3.4	Eq. 6.11	6.15
18	84   56   56   56   84	8W40	3.4	Eq. 6.11	6.15
19	48   36   48	12W27	4.0	Eq. 6.11	6.8
20	60   60	12W27	5.0	Eq. 6.11	6.8

FIG. 6.6.—SUMMARY OF TEST RESULTS FOR BEAMS UNDER COMBINED ACTION OF SHEAR AND MOMENT

possible limitations on width-thickness ratios were proposed. The flow theory (incremental stress-strain relations) has been applied to perfectly flat plates (6.22). The latter theory does not compare well with experimental results. It has been suggested that the deviations between theoretical and experimental results were due to initial imperfections (6.23). An approximate method

10

for the analysis of inelastic local buckling, considering various structural shapes, has been proposed in Ref. 6.17.

The results of further study of the stability of plates compressed beyond the yield point and even into the strain-hardening range have been presented in Ref. 6.25.

#### Theoretical Analysis

The theoretical analysis of Ref. 6.25 is based on the following assumptions:

1. The material follows an idealized stress-strain diagram (Fig. 6.7).\*
2. Yielding occurs discontinuously in slip bands such that the material is either elastic or strain-hardened.
3. The material in the elastic range is homogeneous and isotropic, while in the strain-hardening range it is homogeneous and orthotropic.
4. A linear strain variation is assumed as shown in Fig. 6.8.
5. Yielding of a compressed element starts either from both ends simultaneously or from the middle section of the element.
6. An incremental stress-strain relationship is used. However consideration is given to initial imperfections of the plate by introducing effective moduli for the strain-hardening range.
7. Interaction between plate elements is taken into account by a coefficient of restraint.

Assuming that buckling occurs without strain reversal, the equilibrium condition for a differential plate element of orthotropic material yields\*\*

$$D_x \frac{\partial^4 w}{\partial x^4} + 2H \frac{\partial^4 w}{\partial x^2 \partial y^2} + D_y \frac{\partial^4 w}{\partial y^4} = -\frac{t\sigma_x}{I} \frac{\partial^2 w}{\partial x^2} \dots \dots (6.15)$$

where

$$D_x = \frac{E_x}{1 - \nu_x \nu_y}$$

$$D_y = \frac{E_y}{1 - \nu_x \nu_y}$$

$$D_{xy} = \frac{\nu_y E_x}{1 - \nu_x \nu_y}$$

$$D_{yx} = \frac{\nu_x E_y}{1 - \nu_x \nu_y}$$

$$2H = D_{xy} + D_{yx} + 4G_t$$

and

$$G_t = \text{tangent modulus in shear.}$$

\*In order to derive a rational plate buckling equation for the inelastic range between the proportional limit and the point of strain-hardening, residual stresses must be considered. However, no general solution to the problem has been developed to date. Therefore an empirical transition curve has been proposed in Ref. 6.25.

\*\*The reader is referred to Chapter 3 of Ref. 6.49 for discussion of orthotropic material.

Table 6.1 and Figs. 6.9 and 6.10 contain solutions of various limiting cases of Eq. 6.15. Refs. 6.24 and 6.25 may be consulted for detailed derivations.

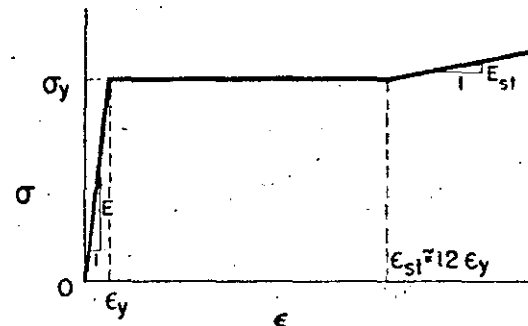


FIG. 6.7.—TYPICAL IDEALIZED STRESS-STRAIN DIAGRAM FOR ASTM A7-TYPE STRUCTURAL STEEL

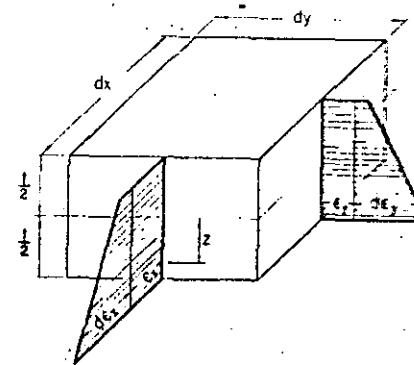


FIG. 6.8.—ASSUMED LINEAR STRAIN DISTRIBUTION (No Strain Reversal Occurs)

The effective plate moduli  $D_x$ ,  $D_y$ ,  $D_{xy}$ , and  $G_t$  were evaluated in Ref. 6.24 for ASTM A7-type steel. Their values are as follows:

$$D_x = 3,000 \text{ ksi}$$

$$D_{xy} = \nu_y D_x = \nu_x D_y = 8,100 \text{ ksi}$$

$$D_y = 32,800 \text{ ksi}$$

$$G_t = 2,400 \text{ ksi}$$

It should be kept in mind that the foregoing expressions and moduli are applicable only for ASTM-A7-type steel plates stressed to the onset of strain-hardening.

The problem of an axially loaded plate subjected also to bending in the plane of the plate is of practical importance. The web of a wide-flange beam subjected to both axial load and bending moment presents such a case. This problem has been studied in Ref. 6.25 and a diagram is presented for the allowable  $d_f/w$ -ratio of the web of a wide-flange section. As shown in Fig. 6.11, the curves are plotted for different ratios of maximum strain to yield strain,  $\epsilon_m/\epsilon_y$ . As the maximum strain of the compression flange increases, the critical  $d_f/w$ -ratio decreases. The critical value of the axial force  $P$  also decreases as the ratio of the depth to the thickness of the web increases.

TABLE 6.1.—SUMMARY OF LIMITING CASES OF THE SOLUTION OF EQ. 6.15

PLATE	BOUNDARY CONDITIONS	EXPRESSIONS FOR CRITICAL STRESSES AND FOR EFFECTIVE LENGTH
Flange Plate (Fig. 6.9)	$x=0$ Simply Supported $x=l$ Supported	$\sigma_{cr} = \left(\frac{1}{b_0}\right)^2 \left[ \frac{\pi^2}{12} D_x \left(\frac{b_0}{l}\right)^2 + G_1 \right]$
	$y=0$ Free $y=b_0$ Free	for long plate $\sigma_{cr} = \left(\frac{1}{b_0}\right)^2 G_1$
Web Plate (Fig. 6.10)	$x=0$ Simply Supported $x=l$ Supported	$\sigma_{cr} = \left(\frac{1}{d_f}\right)^2 \left[ 0.769 \sqrt{D_x D_y} - 0.270 (D_{xy} + D_{yx}) + 1.712 G_1 \right]$ $\frac{l}{d_f} = 1.46 \sqrt{\frac{D_x}{D_y}}$
	$y=0$ Fixed $y=d_f$ Free	
Web Plate (Fig. 6.10)	$x=0$ Simply Supported $x=l$ Supported	$\sigma_{cr} = \frac{\pi^2}{12} \left(\frac{y}{d_f}\right)^2 \left[ 2 \sqrt{D_x D_y} + D_{xy} + D_{yx} + G_1 \right]$ $\frac{l}{d_f} = 0.66 \sqrt{\frac{D_x}{D_y}}$
	$y=0$ Simply Supported $y=d_f$ Supported	
Web Plate (Fig. 6.10)	$x=0$ Simply Supported $x=l$ Supported	$\sigma_{cr} = \left(\frac{1}{d_f}\right)^2 \left(\frac{y}{d_f}\right)^2 \left[ 4.554 \sqrt{D_x D_y} + 1.237 (D_{xy} + D_{yx}) + 4.943 G_1 \right]$ $\frac{l}{d_f} = 0.66 \sqrt{\frac{D_x}{D_y}}$
	$y=0$ Fixed $y=d_f$ Fixed	

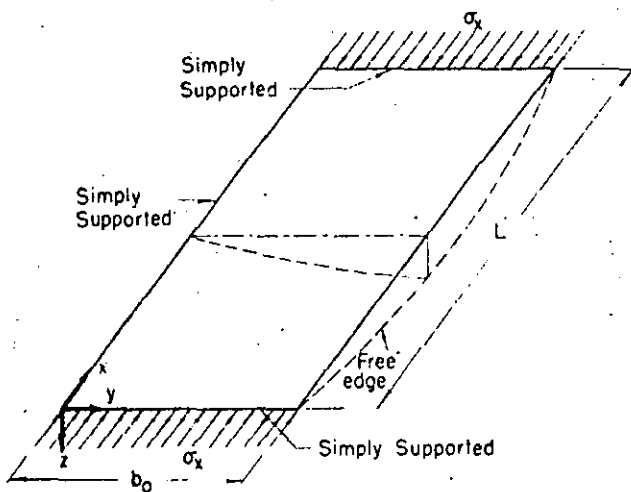


FIG. 6.9.—PLATE WITH ONE EDGE FREE SIMULATING ONE HALF OF THE FLANGE ELEMENT OF A WIDE-FLANGE SHAPE

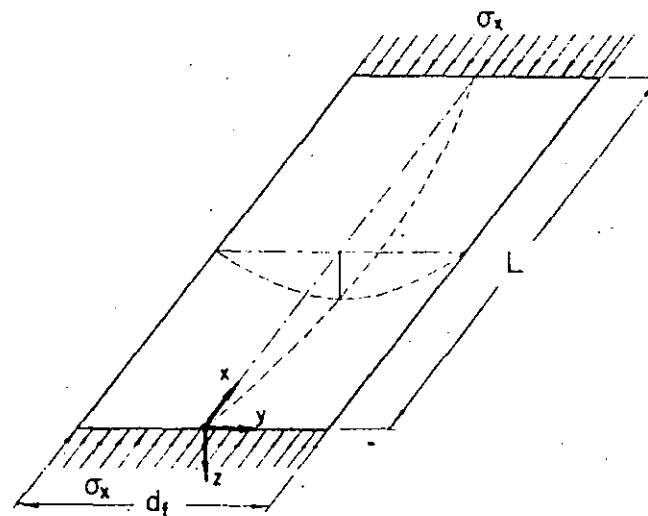


FIG. 6.10.—PLATE WITH ALL EDGES SIMPLY SUPPORTED SIMULATING THE WEB PLATE OF A WIDE-FLANGE SHAPE

#### Experimental Correlation

When tests were conducted to check the theory for local buckling of wide-flange shapes it was found that the theoretical curves gave a good description of the actual behavior of flanges and webs. Fig. 6.12 gives the experimental correlation with theory for the buckling of flange plates. Fig. 6.13 gives the same comparison for the buckling of web plates. The specimens tested in this program (6.25) included 8 W 24, 8 W 35, 10 W 21, 10 W 33, 10 W 39, and 12 W 50 shapes.

Little experimental data is available to compare with the theory in the case of bending with axial force (Fig. 6.11). Partial correlation may be found by examining the results of some corner connection tests (8.4) if one accepts the fact that the conditions of these tests were somewhat different from those on which the theory is based. This comparison is shown in non-dimensionalized form in Fig. 6.14 where the rotation of a selected length of member is plotted versus the  $d_f/w$ -ratio for  $P/P_y = 0.10$ . The curve is obtained by taking cross-curves of Fig. 6.11. Test results do not check the predictions precisely, but they do indicate a large rotation capacity. The 14 W 30 shape rotated an amount less than predicted; on the other hand, the 30 W 108 with greater  $d_f/w$ -ratio and a somewhat higher axial load ratio rotated much more than the required amount.

#### Design Approximations

For flange elements Fig. 6.12 shows that if  $b/t \leq 17$ , then a section under uniform compression can be strained to the point of strain-hardening before local buckling influences its carrying capacity.

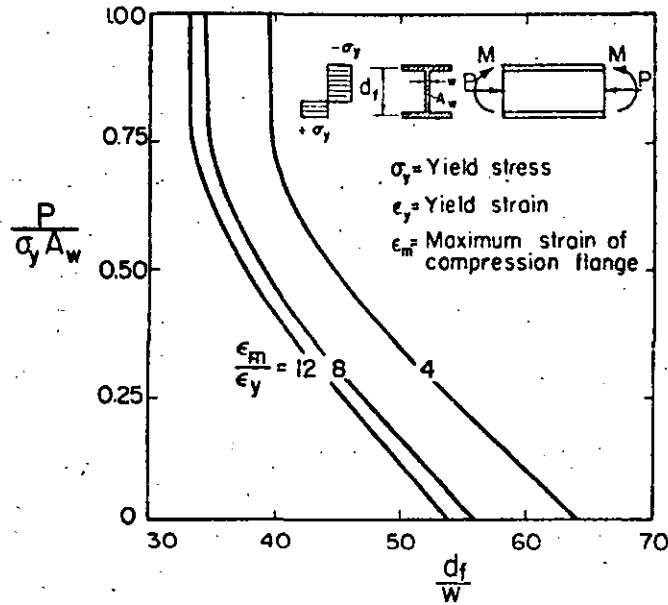


FIG. 6.11.—ALLOWABLE  $d_f/w$ -RATIO OF WEB OF FULLY PLASTIFIED WIDE-FLANGE SECTIONS

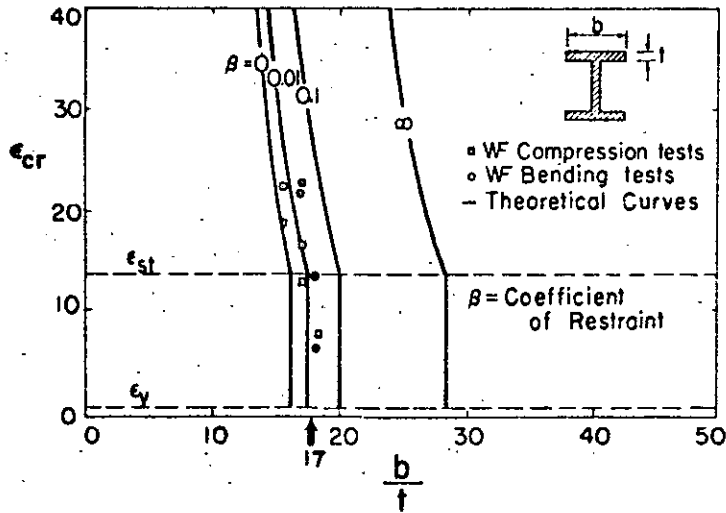


FIG. 6.12.—RESULTS OF TESTS ON WIDE-FLANGE SHAPES SHOWING CORRELATION WITH PREDICTED STRAIN AT BUCKLING OF FLANGES

Fig. 6.13 shows that the web of a shape under uniform compression would be limited to  $d_f/w < 33$  in order to reach the onset of strain-hardening. However, no such strain is needed in a plastically designed structure and it would be adequate to require only that the strain be able to reach the yield value. Thus on the basis of Fig. 6.13 the limiting value would be  $d_f/w = 41$ . Using  $d/d_f = 1.05$ , the ratio of  $d/w$  may go as high as 43 under uniform compression.

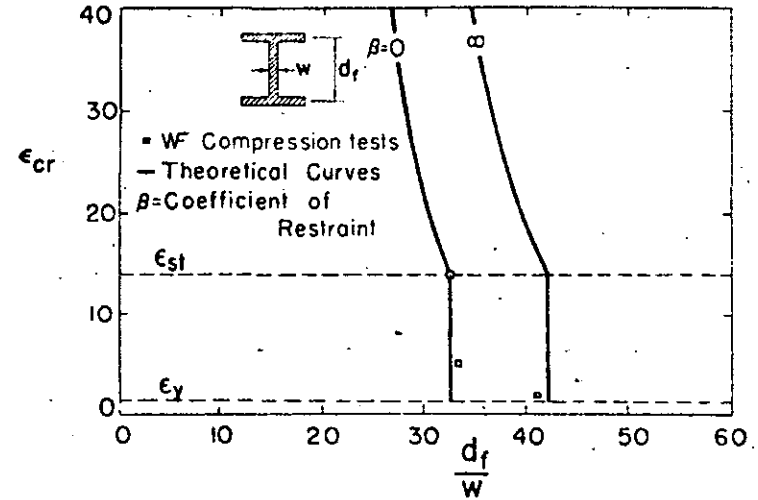


FIG. 6.13.—RESULTS OF TESTS ON WIDE-FLANGE SHAPES SHOWING STRAIN AT WHICH WEB BUCKLING OCCURRED

For combined bending and compression a design approximation may be developed that is based on the results given in Fig. 6.11. This approximation is shown as a solid line in Fig. 6.15 and is to be compared with the theoretical solution shown by the dashed line. This latter solution assumes the following

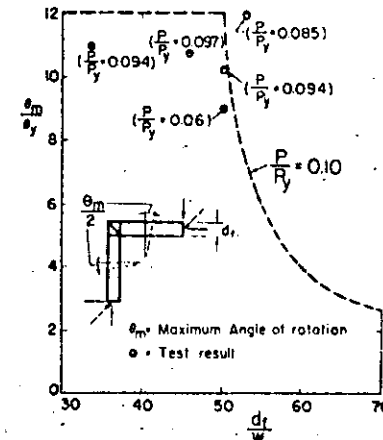


FIG. 6.14.—RESULTS OF TESTS ON WIDE-FLANGE SHAPES IN WHICH BOTH AXIAL FORCE AND BENDING WERE PRESENT, (The dotted line shows the predicted web buckling curve for  $P/P_y = 0.10$ .)

relationships:  $A/A_w = 2$ ,  $d/d_f = 1.05$ , and  $\epsilon_{max}/\epsilon_y = 4.0$ . The design approximation, shown by the solid line, is

$$\frac{d}{w} = 70 - 100 \frac{P}{P_y}, \quad \left( \frac{P}{P_y} \leq 0.27 \right) \dots \dots \dots (6.16)$$

From Eq. 6.16, for  $P/P_y = 0$ , the upper limit of  $d/w$  would be 70.

In summary, for use in plastic design involving shapes of ASTM-A7-type steel ( $\sigma_y = 33$  ksi), the following values are suggested to assure that premature local buckling will not occur:

**LOCAL BUCKLING OF STRUCTURAL SHAPES**

For I-sections, wide-flange beams or welded H-shapes of ASTM A7-type steel

(1) Flanges — Compression due to bending, and/or axial force

$$\frac{b}{t} \leq 17$$

(2) Web — Uniform compression

$$\frac{d}{w} \leq 43$$

(3) Web — Bending and compression

$$\frac{d}{w} = 70 - 100 \frac{P}{P_y} \quad \left( \frac{P}{P_y} \leq 0.27 \right)$$

$$\frac{d}{w} = 43 \quad \left( \frac{P}{P_y} > 0.27 \right)$$

where  $b$  and  $t$  are the width and thickness of the flange respectively,  $d$  denotes the section depth, and  $w$  is the web thickness.

For other outstanding flanges and plate stiffeners intended to be stable in the plastic region.

(4)  $\frac{b'}{t} = 8.5$

where  $b'$  is the width of outstanding plate element.

For rolled shapes, a small upward variation of the  $b/t$  ratio to include, for example, the 14W30 ( $b/t = 17.58$ ) would be reasonable. This section performed adequately under test.

In practice, if a selected section cannot meet the above requirements, a different section may be used or stiffeners could be added to prevent local buckling. It is fortunate that nearly all rolled wide flange and I-shapes are satisfactory with regard to local instability.

**6.3 LATERAL BUCKLING**

**Statement of the Problem**

In order to realize the necessary inelastic rotations at plastic-hinge locations the members must have sufficient lateral support so that lateral-torsional buckling will not reduce the plastic resisting moment at these sections while the hinge rotate. When a member buckles laterally it undergoes lateral

9

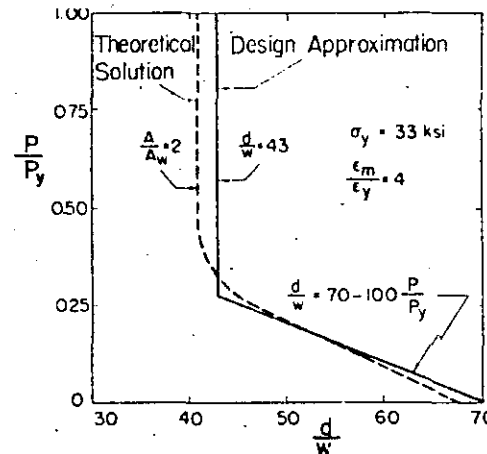


FIG. 6.15.—LIMITING SLENDERNESS RATIOS FOR THE WEB PLATE OF WIDE-FLANGE SHAPES UNDER COMBINED BENDING AND AXIAL COMPRESSION.

bending and twisting. Elastic regions of the beam resist this buckling through lateral bending stiffness  $I_y$  and torsional resistance. The latter consists of two parts:\*

- a) Resistance associated with St. Venant torsion; and
- b) Resistance associated with warping torsion (or cross bending).

A member with an adequate combination of these properties will have effective resistance to lateral-torsional buckling. (6.26)

The types of lateral support available in actual structures vary greatly. For most structures, however, the points of applied loading also constitute points of lateral support.

**Previous Research**

Although many studies of the lateral-torsional buckling of elastic members have been published, there are few solutions available in the inelastic range. It has been suggested (6.17) that the effects of inelastic behavior may be allowed for by determining the most critically stressed section and using a tangent-modulus reduction factor ( $\tau = E_t/E = G_t/G$ ) in the elastic solutions. This practice offers a simple and expedient means of approximating inelastic effects and is generally considered to be conservative. However, recent investigations (6.29) indicate that in some cases it may be on the unsafe side. Ref. 6.30 refers to these and other approximations in connection with design applications. In Ref. 7.15 it is shown that test results for laterally unsupported wide-flange shapes agree very well with the concept that the ratio between the elastic critical buckling stress and the actual critical buckling stress is the same in the inelastic range for beams and columns.

This problem has been studied in detail by considering the effect of yielding (idealized stress-strain curve) on the lateral flexural rigidity and initial

\* See, for example, Ref. 6.26 for a discussion of St. Venant torsion and warping torsion.

22

torsional rigidity of a rectangular cross section. (6.31) This solution corresponds to the reduced modulus solution of an axially loaded column. Ref. 6.32 pointed this out and deduced an equivalent formula on the basis of a tangent modulus load, assuming no unloading of the cross section.

These results for pure bending were extended to the case of I-beams in Ref. 6.33. The conclusions, however, were modified by other practical considerations. Eventually from this work limiting critical lengths of I-beams were presented as a basis for design. (1.1) The fundamental concept behind this work is a tacit reliance on the post-buckling strength of a member to provide the necessary moment resistance over a large range of its deformation.

The solution of the various cases on a systematic basis was reported in Ref. 6.28. This reference also presented a design procedure for determining the spacing of lateral supports such that the members would not buckle laterally before the required plastic hinges had formed. Although a simplifying approximation has been made for practical use, the method still possesses three inadequacies:

- 1) Under conditions of loading where the moment diagram has a small gradient, the procedure gives results which are too conservative when compared with test results.
- 2) The method of design is an iterative procedure because of the restraining influence of adjacent segments on the segment being braced.
- 3) One of the necessary parameters is the amount of plastic hinge rotation required to obtain a complete re-distribution of moments corresponding to the ultimate load. Unless an assumption is made of a single given amount of rotation, this would have to be computed analytically and would therefore complicate the design procedure.

#### Theoretical Analysis

Assuming, as in the solution to local instability problems that the process of yielding of structural steel is non-homogeneous, (6.27) the actual material will be in either the elastic or the strain-hardened state. Since the material in each of these regions behaves in a linear homogeneous manner characterized by its appropriate moduli, it is reasonable to assume that the problem can be reduced, in a somewhat simplified manner, to the consideration of a member with an abrupt change in stiffness. (6.25) In the case of a completely strain-hardened member the resistance to buckling depends almost entirely on warping torsion instead of on a combination of St. Venant torsion and lateral bending strength as in the fully elastic case. For a member with partial strain-hardening, the effects of St. Venant torsion, moment gradient and end restraint are then considered as modifications of the basic solution.

The basic assumptions for the theoretical analysis (6.28) are as follows:

- 1) The material in a member deformed beyond the elastic limit either is at a strain less than the yield strain or has reached the strain-hardening range.
- 2) The distribution of the elastic and strain-hardening zones depends on the magnitude and location of the over-all inelastic deformation. Strain-hardening is assumed to start at the end of the member at the point of maximum moment and to spread from that point.
- 3) It is assumed that the member is initially straight and that no lateral or torsional deflection takes place before buckling. This approach leads mathematically to an eigenvalue problem. The lowest point of bifurcation

of equilibrium is obtained by considering no strain reversal. At this point of buckling, therefore, the linear incremental stress-strain relations can be used. The two different zones are characterized by the incremental elastic and strain-hardening moduli, respectively.\*

- 4) A solution can be obtained by solving the normal linear differential equations for both regions and matching the boundary conditions between them.
- 5) The cross section is restricted to an open, doubly symmetrical, thin-walled shape.
- 6) The cross section is idealized so that the whole section will be considered as either elastic or strain-hardened under flexure. The condition of having a non-homogeneous material over the cross section is difficult to handle analytically since the differential equations of equilibrium would have variable coefficients. As shown in Ref. 6.28 this assumption of an idealized cross section gives conservative results.

When the loading is restricted to the case of loading in one principal plane at the boundary only, with zero axial force and zero applied forces along the beam, the basic equations can be re-written in the following form:

$$E C_w \frac{d^4 \beta}{dz^4} - G K \frac{d^2 \beta}{dz^2} + M_\xi \frac{d^2 u}{dz^2} = 0 \quad \dots \dots \dots (6.17a)$$

$$E I_x \frac{d^4 v}{dz^4} = 0 \quad \dots \dots \dots (6.17b)$$

$$M_\xi \frac{d^2 \beta}{dz^2} + 2 \frac{dM_\xi}{dz} \frac{d\beta}{dz} + E I_y \frac{d^4 u}{dz^4} = 0 \quad \dots \dots \dots (6.17c)$$

in which

- $E C_w$  = warping rigidity
- $G K$  = St. Venant torsional rigidity
- $E I_x$  = bending rigidity of the beam about strong axis
- $E I_y$  = bending rigidity of the beam about weak axis
- $\beta$  = angle of twist about shear center
- $u$  = displacement of shear center in weak direction
- $v$  = displacement of shear center in strong direction
- $z$  = axis along the beam,  $0 \leq z \leq L$
- $M_\xi$  = applied bending moment along the beam about the strong axis
- $L$  = length of beam

The problem solved in Ref. 6.28 was a single-span beam with load applied in the maximum principal plane of bending. Both simply supported and fixed-end conditions were considered. The simple supports, however, were assumed

\* Another possible solution would be to analyze for the ultimate strength of the member; this solution, however, has not been obtained up to the present.



to be able to resist twisting. Part of the beam was considered elastic and part strain-hardened as shown in Fig. 6.16. For the strain-hardened portion (length  $\alpha L$ ) Eqs. 6.17 were modified by introducing the strain-hardening modulus in lieu of the elastic values. The continuity conditions were introduced at the juncture of the elastic and strain-hardened portions. The effect of moment gradient is shown in Fig. 6.17 and the effect of St. Venant torsion is shown in Fig. 6.18. The differential equations mentioned above were solved by a numerical procedure based on finite differences using the appropriate boundary conditions. The computations for determining the eigenvalue for various

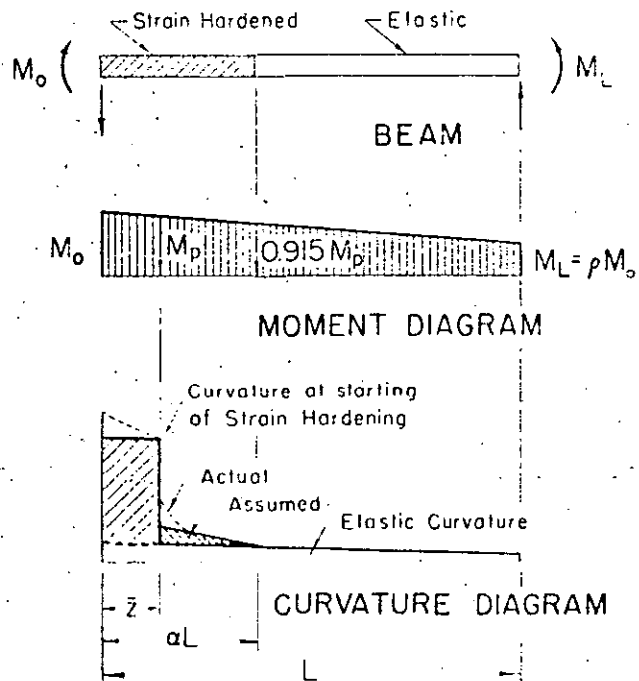


FIG. 6.16.—MOMENT-CURVATURE DIAGRAM FOR A PARTIALLY YIELDED BEAM UNDER MOMENT GRADIENT

conditions of restraint, loading, and extent of strain-hardening were carried out on a digital computer.

Four series of results were obtained as follows:

- 1) Member simply supported at each end;
- 2) Member fixed at each end;
- 3) Member fixed at end  $z = 0$ , simple at end  $z = L$ ;
- 4) Member simply supported at end  $z = 0$ , fixed at end  $z = L$ .

The basic critical buckling length for simply supported beams under uniform plastic moment is determined from the expression  $A = L_{cr} \sqrt{\frac{Z}{d I_y}}$  where  $A$ , the eigenvalue, equals 11.28 and  $Z$  is the plastic modulus of the cross section.

For a wide-flange beam it has been shown (6.28) that  $\sqrt{d I_y/Z} \approx 1.60 r_y$ , therefore  $L_{cr}/r_y = 18$ . This length is then corrected for the effects of moment gradient and extent of yielding over the unbraced length of the member. Correction factors are also determined for the St. Venant torsional resistance of the member and the effect of end fixity. These correction factors can be expressed in terms of  $\rho$ , the ratio of the smaller to the larger end moments. (Figs. 6.17 and 6.18). Finally the critical buckling length can be expressed as

$$\frac{L_{cr}}{r_y} = 18 \nu_\rho \nu_\alpha \nu_s \nu_\gamma \sqrt{\frac{M_p}{M_o}} \dots \dots \dots (6.18)$$

in which

- $\nu_\rho$  = correction factor for moment gradient
- $\nu_\alpha$  = correction factor for partial yielding ( $\alpha L$ )
- $\nu_s$  = correction factor for St. Venant torsion.
- $\nu_\gamma$  = correction factor for end fixity
- $M_p/M_o$  = ratio of plastic moment to actual moment at  $z = 0$

Experimental Correlation

Two specimens provided with fixed-end conditions by boxing in the end sections of the members were tested under constant moment. (6.28) The "fixed-end" condition was one in which the beam could rotate freely in the loading

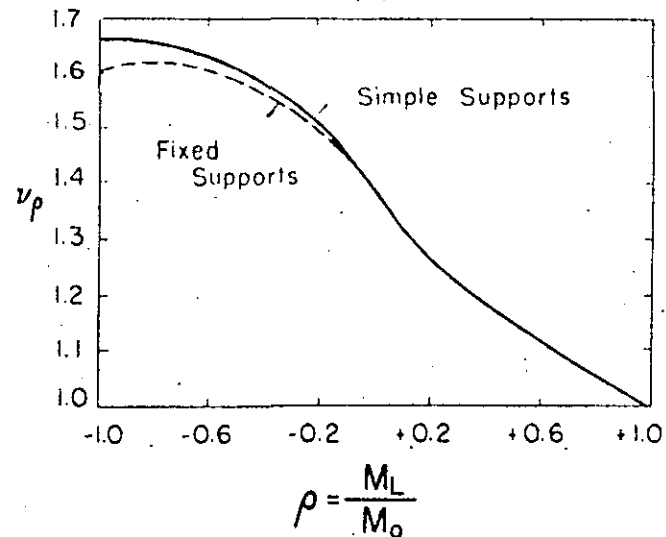


FIG. 6.17.—EFFECT OF MOMENT GRADIENT AS COMPARED TO UNIFORM MOMENT FOR LATERAL-TORSIONAL BUCKLING FOR BEAMS SIMPLY SUPPORTED OR FIXED-ENDED (WARPING TORSION ONLY)

plane (strong direction) but rotation was prevented in the weak direction and twisting was prevented with respect to the longitudinal axis of the beam. These conditions, however, were not realized in the actual test as evidenced by movement of the loading points and twisting of the end supports. Therefore, the values of  $\nu_\alpha$  obtained from the test results were considerably lower than values predicted by the theoretical analysis for the fixed-end beam.

Further tests were conducted (6.34) in order to find the effect of moment ratio  $\rho$  on the critical buckling length of the simply supported beam. Four specimens were tested with moment ratios of 0.40, 0.71, 0.90 and 0.98 respectively. Fig. 6.19 shows a typical curve of moment vs. lateral rotation for

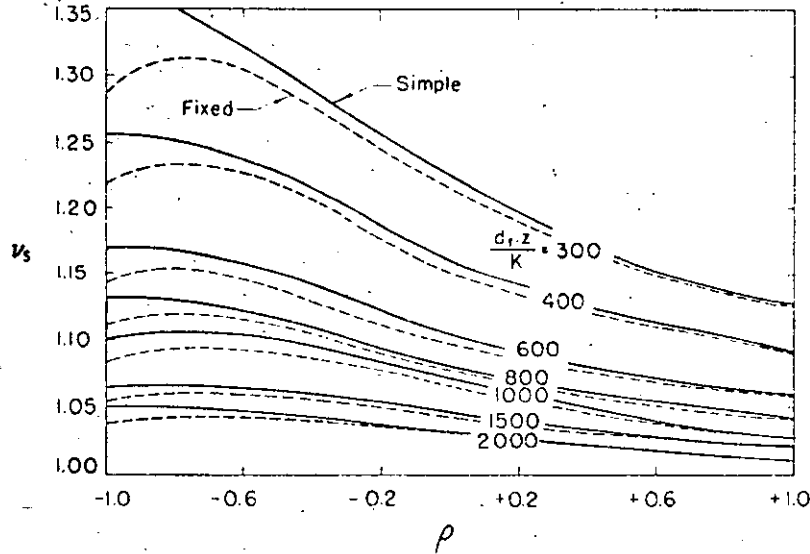


FIG. 6.18.—EFFECT OF ST. VENANT TORSION ( $d_f Z/K$ ) ON THE CRITICAL BUCKLING LENGTH FOR BEAMS SIMPLY SUPPORTED OR FIXED-ENDED

$\rho = 0.71$ , together with the relation of the moment and rotation about the strong axis. The inelastic angle change  $H_B$ , between load points, is computed from  $H_B = \theta_m - \theta_p$  where  $\theta_m$  is the total rotation about the strong axis between load points at the maximum test load and  $\theta_p$  is the total rotation when the maximum moment first reached  $M_p$ . The term  $H_B$  is also the portion of the hinge angle that occurs in the critical segment between load points. The ratio  $H_B/(L\phi_p)$  is used to express rotation on a nondimensional basis (where  $L$  is the distance between load points and  $\phi_p = M_p/(EI)$  is the elastic part of the curvature at the plastic moment). Fig. 6.19 indicates that the test beam buckled laterally soon after the plastic moment was reached but that buckling did not prevent the plastic hinge from rotating at substantially constant moment. The observed values of  $H_B/(L\phi_p)$  are shown in Fig. 6.20 at the corresponding moment ratios and slenderness ratios,  $L/r_y$ , of the sections tested. The solid line corresponds to a value of  $H_B/(L\phi_p) = 3$ . These tests indicate that the design approximations outlined below and plotted in Fig. 6.20 give conservative results.

Design Approximation

The critical buckling length  $L_{cr}/r_y$  is given by Eq. 6.18 as mentioned previously and these correction factors can be obtained by a trial and error procedure using tables and figures given in Ref. 6.28. For instance, the correction factor  $\nu_\alpha$  for the effect of partial strain-hardening of the member depends upon the moment ratio  $\rho$  and the yielded length  $\alpha L$ . The value of  $\alpha$  depends also on the moment ratio  $\rho$  and the angle of rotation of the beam at hinge points.

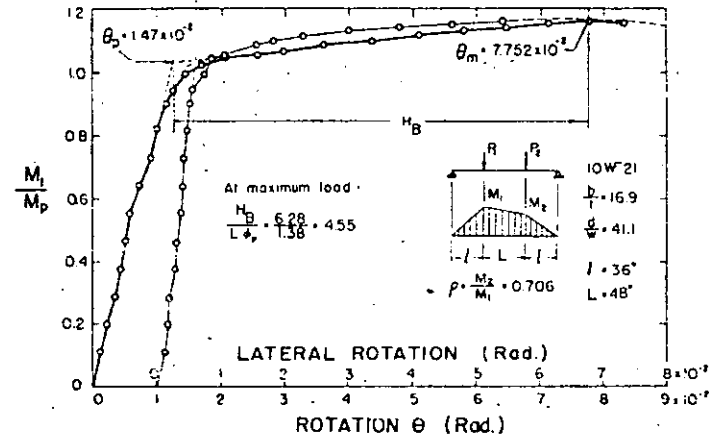


FIG. 6.19.—MOMENT VERSUS ROTATION CURVES OF A LATERAL BUCKLING TEST UNDER MOMENT GRADIENT

It may be too tedious to compute the critical length between two adjoining points using many figures and tables. Therefore, the following approximations are made for each correction factor:

- 1)  $\nu_\rho = 1.34 - 0.34\rho$ , which approximates the curves in Fig. 6.17.
- 2)  $\nu_\alpha$  is assumed to be related to  $\alpha$  only.
- 3)  $\alpha$  is obtained from the moment ratio  $\rho$  and angle of rotation  $H/L\phi_p$ .
- 4) Then  $\nu_\alpha$  can be expressed in terms of  $\rho$  with a parameter of rotation angle. A reasonable value of  $H_B/L\phi_p = 3$  is chosen on the basis of practical considerations.
- 5)  $\nu_s = 1.08 - 0.04\rho$ , which approximates the curve labeled  $d_f Z/K = 800$  in Fig. 6.18 and is based on the following values for wide-flange beams:

$$\sqrt{\frac{d}{Z}} / r_y \approx 1.60, \frac{A_f}{A_w} \approx 1.0, \frac{d_f}{d_w} \approx 1.05$$

where  $A_f$  is the area of one flange,  $A_w$  denotes web area,  $d_f$  is the flange distance and  $d_w$  represents the web depth.

- 6)  $\sqrt{M_p/M_0} \approx 1.0$ .

From these approximations the correction factors (except that due to end restraint) are simplified, and the final relationship between the critical length and moment ratio can be expressed as a straight line,

$$\frac{L_{cr}}{r_y} = (48 - 30\rho) \nu_\gamma \dots \dots \dots (6.19)$$

25

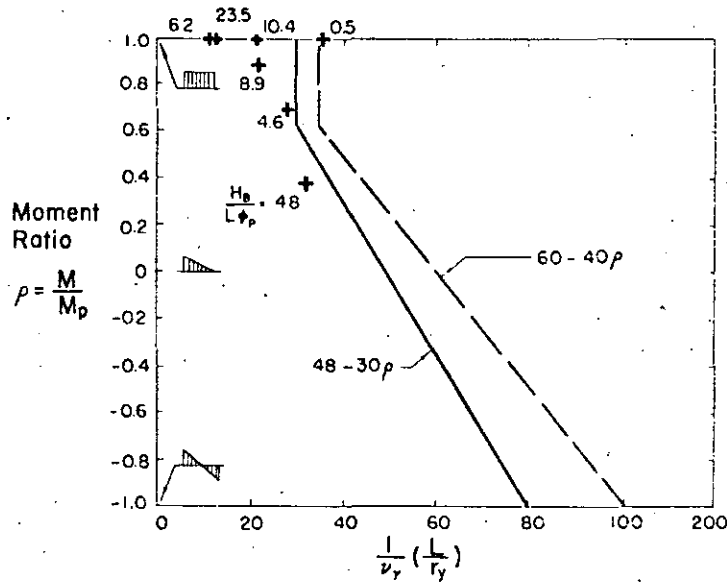


FIG. 6.20.—CRITICAL SLENDERNESS RATIO AS A FUNCTION OF THE MOMENT RATIO FOR LATERAL BUCKLING OF BEAMS

The value of  $L_{cr}/r_y$  need not be less than 30, since the theory is known to be overly conservative when  $\rho > 0.6$ .

7) The correction factor  $\nu_y$  for end restraint depends on the stiffness of the adjacent segments as shown in Fig. 6.21 where  $k_l$  is the larger stiffness and  $k_s$  the smaller stiffness of adjacent segments respectively. (6.34) A support with  $k_s = 0$  provides no major axis bending resistance but does provide resistance to twisting. The stiffness factor  $k$  is approximated by

$$k = \frac{3 E I_A}{L_A} \left[ 1 - \frac{L_A}{L_{Acr}} \right]^2 \dots \dots \dots (6.20)$$

where  $L_A$  is the actual length and  $I_A$  denotes the moment of inertia of the adjacent segment. The term  $L_{Acr}$  is given by Eq. 6.19 (with  $\nu_y = 1.0$ ) for the adjacent segment next to a plastic hinge. If the adjacent span is not next to a plastic hinge then  $L_{Acr}$  is given by

$$\left. \begin{aligned} \frac{L_{Acr}}{r_{yA}} &= \sqrt{|\rho|} \left[ 1.34 - 0.34 \rho_A \right] \text{ for } 0 \leq |\rho| \leq 0.9 \\ \frac{L_{Acr}}{r_{yA}} &= 151 - 38 \rho_A - 1,100 (\rho - 0.9) \text{ for } 0.9 < |\rho| < 1.0 \end{aligned} \right\} (6.21)$$

in which

$\rho$  = moment ratio in segment being investigated

$\rho_A$  = moment ratio in adjacent segment.

13

A value for  $\nu_y$  is obtained by entering Fig. 6.21 with  $k_s/k_l$  and  $k_l L/(3 E I)$ , where  $L$  is the actual length and  $I$  is the moment of inertia of segment under investigation.

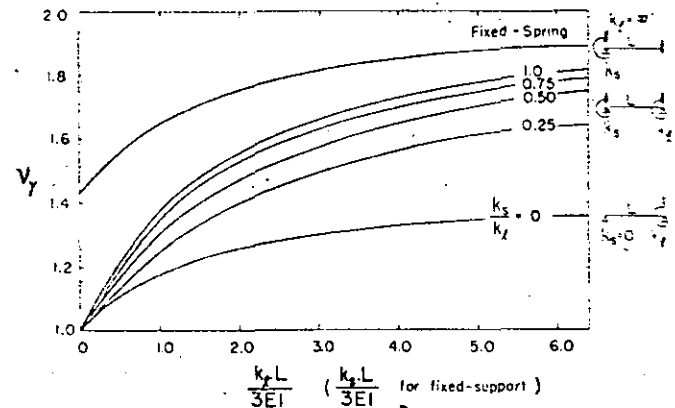


FIG. 6.21.—RESTRAINT FACTOR FOR CONTINUOUS BEAMS SHOWING INFLUENCE OF ADJACENT SPAN ON THE CRITICAL SPAN

Design Approximation for Equal E I/L

For a continuous beam with constant  $E I$  and equal unbraced segment lengths, the ratio

$$\frac{k_s}{k_l} = \frac{1 - \left( \frac{L}{L_{scr}} \right)^2}{1 - \left( \frac{L}{L_{fcr}} \right)^2} \leq 1.0 \dots \dots \dots (6.22)$$

and the value

$$\frac{k_l L}{3 E I} = 1 - \left( \frac{L}{L_{fcr}} \right)^2 \leq 1.0 \dots \dots \dots (6.23)$$

Then  $\nu_y$  is found from Fig. 6.21 as before.

Since the value of  $k_l L/(3 E I)$  is less than 1.0, as can be shown with the aid of Fig. 6.21, the variation of  $\nu_y$  versus  $k_s/k_l$  for  $0 < k_s L/(3 E I) < 1.0$  is nearly a straight-line function and is approximated (6.34) by the expression

$$\nu_y = 1.0 + 0.2 \frac{k_l L}{3 E I} \left( 0.9 + \frac{k_s}{k_l} \right) \dots \dots \dots (6.24)$$

Simplified Design Procedure

Recognizing that the effect of end restraint, extent of yielding, St. Venant torsion, moment gradient, required hinge rotation, and axial force are inter-related and that the exact value of one of these parameters cannot be determined without knowledge of the others, a practical design approach would be to assign a representative value to the restraint factor  $\nu_y$  in lieu of the consideration of the separate effects. From Fig. 6.21 it may be seen that an average value of  $\nu_y$  is 1.25 for the continuous beam with constant  $E I$  and equal unbraced segment lengths. An equation developed on this basis is as follows

20

$$L_{cr} = \left(60 - 40 \frac{M}{M_p}\right) r_y, \text{ but not less than } 35 r_y \dots \dots (6.25)$$

Eq. 6.25 is shown in Fig. 6.20 as a dashed line. When  $M/M_p = 1.0$ ,  $\nu_y = 1.17$  and when  $M/M_p = -1.0$ ,  $\nu_y = 1.28$ . Such a variation is reasonable because the correction factor  $\nu_y$  for the moment ratio  $M/M_p$  increases with that ratio.

Thus, an approximate value has been established for the effect of all of the correction factors required by the theoretical analysis. In the event the designer would like to use unbraced lengths greater than those indicated by this expression he may use the method based on the theoretical analysis by taking into account each parameter individually and performing the necessary iteration if he feels that the slightly increased allowable unbraced length which might result would be justified by the additional design time involved.

**LATERAL BRACING**

The spacing of bracing in the region of plastic hinges where rotation would be required may be determined from the following simplified formula

$$\left. \begin{aligned} \frac{L}{r_y} &\leq 60 - 40 \frac{M}{M_p} \text{ for } \frac{M}{M_p} < 0.625 \\ \frac{L}{r_y} &\leq 35 \text{ for } \frac{M}{M_p} > 0.625 \end{aligned} \right\} \dots \dots (6.25)$$

in which  $L$  = distance between bracing points

$r_y$  = radius of gyration in the weak direction

$\frac{M}{M_p}$  = end-moment ratio

To obtain somewhat greater unbraced lengths, the procedures outlined above can be used.

The spacing of bracing in the non-yielded portions of the structure may be determined by methods used in allowable-stress design.

**Illustrative Examples**

The design procedure is essentially a trial-and-error method if the unbraced length is determined by the consideration of lateral-torsional buckling only. However, in practical design the unbraced length may be fixed by other structural considerations and then must be examined for lateral-torsional buckling. The general procedure for investigating a given unbraced length is:

- 1) From the moment diagram find moment ratios for this segment and its adjacent unbraced segments.
- 2) Find  $L_{cr}/r_y$  for each segment from Eq. 6.19 or Eq. 6.21.
- 3) Compute stiffnesses of the adjacent segments from Eq. 6.20.
- 4) Compute the ratio  $k_s/k_\ell$  and the value  $k_\ell L/(3 EI)$ .
- 5) Find  $\nu_y$  from Fig. 6.21.
- 6) The actual length of the segment being investigated should be less than  $\nu_y L_{cr}$ .

Since the spacing of purlins and girts is usually uniform, the particular unbraced length that must be investigated in a design will be the one with the

largest moment ratio at a hinge point where rotation would be required. Ordinarily this means that the bracing spacing would be checked in the region of formation of the first plastic hinge. (The sequence of hinge formation is discussed in Chapter 9). Of course, if all segments meet the requirement that would be stipulated for a first plastic hinge location, then no further consideration of hinge sequence would be needed.

**Example I: Continuous Beam (Fig. 6.22).**

The example will first be worked without any regard to sequence of hinge formation. The problem will then be solved again on the basis that the first hinge forms at the ends.

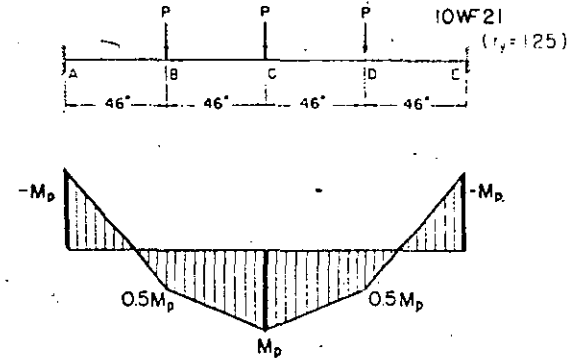


FIG. 6.22.—ILLUSTRATIVE EXAMPLE I OF LATERAL BRACING

- 1) Considering only the effect of moment ratio, the critical span is either BC or CD. The moment ratios are  $\rho_{AB} = \rho_{DE} = -0.5$  and  $\rho_{BC} = \rho_{CD} = 0.5$
- 2) All spans are next to a plastic hinge, therefore the critical length of each span considered as a simple beam,  $\nu_y = 1.0$ , is given by Eq. 6.19 as

$$\frac{L_{BCcr}}{r_y} = \frac{L_{DEcr}}{r_y} = 63, \text{ then } L_{BCcr} = L_{DEcr} = 78.75 \text{ in.}$$

$$\frac{L_{BCcr}}{r_y} = \frac{L_{CDcr}}{r_y} = 33, \text{ then } L_{BCcr} = L_{CDcr} = 41.25 \text{ in.}$$

- 3) Since the beam is symmetrical about point C, then  $k_{CD} = 0$ , which means that there is no restraint on span BC due to span CD. From Eq. 6.20,

$$k_{AB} = \frac{3 EI}{L_{AB}} \left[ 1 - \left( \frac{L_{AB}}{L_{BCcr}} \right)^2 \right] = \frac{3 EI}{L_{AB}} \left[ 1 - \left( \frac{46}{78.75} \right)^2 \right] = \frac{3 EI}{L_{AB}} 0.66, \text{ } k_{CD} = 0$$

$$4) \frac{k_s}{k_\ell} = \frac{k_{CD}}{k_{AB}} = 0$$

$$\frac{k_\ell L}{3 EI} = \frac{k_{AB} L_{BC}}{3 EI} = 0.66$$

- 5) From Fig. 6.21,  $\nu_y = 1.13$   
 6)  $L_{BCcr} = 1.13 \times 41.25 \text{ in.} = 46.6 \text{ in.} > 46 \text{ in.}$  (OK)

Approaching the problem with the added information that the first hinges form at ends A and E, the critical span is AB (and DE, by symmetry). Then

$$k_{BC} = \frac{3EI}{L_{BC}} \left[ 1 - \left( \frac{L_{BC}}{L_{BCcr}} \right)^2 \right] = \frac{3EI}{L_{BC}} \left[ 1 - \left( \frac{46}{41.25} \right)^2 \right]$$

Since the resulting value is negative,  $k_{BC} = 0$ . For the special case of a fixed-end (Fig. 6.21),  $\nu_y = 1.43$ . Then

$$(L_{AB})_{cr} = 1.43 \times 78.75 \text{ in.} = 112.5 \text{ in.} > 46 \text{ in.}$$
 (OK)

Thus, the chosen length is satisfactory. In fact, this was evident in step 2 where it was found that  $(L_{AB})_{cr} = 78.75 \text{ in.}$  with  $\nu_y = 1.0$ .

If the approximation of Eq. 6.25 had been used,

$$L_{cr} = [60 - 40(-0.50)] 1.25 = 100 \text{ in.}$$
 (OK)

**Example II: Corner of rectangular frame (Fig. 6.23).**  
 The critical segment is BC.

- 1) Moment ratios:

$$\rho_{AB} = -0.05 \text{ (elastic-plastic)}$$

$$\rho_{BC} = +0.75 \text{ (plastic-elastic)}$$

$$\rho_{CD} = +0.67 \text{ (elastic)}$$

- 2)  $\frac{(L_{AB})_{cr}}{r_y} = 48 - 30(-0.05) = 49.5$ ,  $(L_{AB})_{cr} = 78.6 \text{ in.}$

$$\frac{(L_{BC})_{cr}}{r_y} = 30 \text{ for } \rho > 0.6, (L_{BC})_{cr} = 46 \text{ in.}$$

$$\frac{(L_{CD})_{cr}}{r_y} = \frac{107}{\sqrt{0.75}} (1.34 - 0.34 \times 0.67) = 137, L_{CD} = 208 \text{ in.}$$

3)  $k_{AB} = \frac{3EI}{L_{AB}} \left[ 1 - \left( \frac{60}{75} \right)^2 \right] = \frac{3EI}{L} \times 0.36 = k_s$

$$k_{CD} = \frac{3EI}{L_{CD}} \left[ 1 - \left( \frac{60}{208} \right)^2 \right] = \frac{3EI}{L} \times 0.92 = k_f$$

4)  $\frac{k_s}{k_f} = 0.39$

- 5) Using Eq. 6.24,

$$\nu_y = 1.0 + 0.2(0.92)(0.9 + 0.39) = 1.24$$

6)  $(L_{BC})_{cr} = (1.24)(46) = 57 \text{ in.} < 60 \text{ in.}$  (call OK)

Note: By Eq. 6.25,  $\frac{(L_{BC})_{cr}}{r_y} = 35$ ,

$$(L_{BC})_{cr} = (35)(1.52) = 53.2 \text{ in.}$$

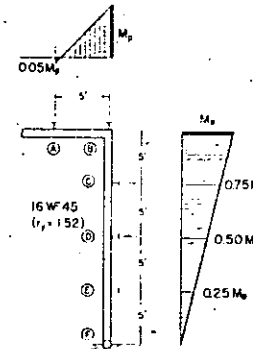


FIG. 6.23.—ILLUSTRATIVE EXAMPLE II OF LATERAL BRACING

#### 6.4 VARIABLE REPEATED LOADING

##### Statement of the Problem

In the previous discussions it has been assumed that the structures under consideration were subjected to all of the applied loads acting simultaneously. It has been further assumed that the applied loads increase in their magnitude until the limit load is reached. During this process none of the applied loads are permitted to change their directions and the ratio of load magnitudes to each other remains fixed. Such loading is termed proportional loading.

In practice the separate loads on a structure may not satisfy the condition of proportionality. Instead, the separate loads may change in magnitude independently from each other. These non-proportional loads are called "variable repeated loads" in the literature. Although these loads act generally in a random manner it is convenient to assume a cyclic pattern in discussing the problem.

Two modes of failure that may result from repeated loading are considered in the following:

##### a) Fatigue and Alternating Plasticity

Fatigue is failure of the material by fracture as a result of repeated loading on the structure. In particular, failure will occur at a relatively low number of cycles when the repeated loading is such that yielding of the material occurs alternately in tension and compression at a given cross section. This phenomenon is known as "alternating plasticity." During each cycle of load application plastic flow will take place and eventually will lead to fracture.

Fatigue within the normally elastic range is of little concern in usual building frames.

##### b) Deflection Stability

This type of failure is characterized by an increase in deflection during each cycle of loading, the increments of deflection being in the same direction.

This mode of failure is termed "incremental collapse." The problem is to determine the limits on the loads for which these increments cease after a few cycles of load application and the deflection "stabilizes." When a structure reaches this state of stabilized deflection it is said to have "shaken down" and the corresponding set of loads is referred to as the "stabilizing load" or the "shakedown load." The structure henceforth responds to the load in a purely elastic manner.

Previous Investigations

Ref. 6.35 was the first to recognize that under variable repeated loads, a structure may fail due to a lack of deflection stability. Further extensive studies in this field were reported in Refs. 6.36, 6.37, and 6.38. In recent years, the results of other analyses and experiments have been published in Refs. 6.39 to 6.46. Experimental investigations of portal frames(6.47) and rectangular model frames, (6.40) have been conducted.

Theoretical Analysis

a) Alternating Plasticity

A condition of alternating plasticity is illustrated by the example of a cantilever beam with a concentrated load acting at the free end (Fig. 6.24). The load P is assumed at first as being applied in a downward direction and the resulting moment-curvature relationship at the built-in section is shown from (o) to (a) in Fig. 6.24. If instead, the load were applied in the opposite direction, the corresponding M-φ curve would be that shown in Fig. 6.24 from (o) to (c). If at point (a) the load P is gradually released and finally applied in the opposite direction, the M-φ relationship is linear for a range of moment, designated as ΔM<sub>y</sub>. The magnitude of ΔM<sub>y</sub> is less than or at most equal to 2M<sub>y</sub>, the precise value being a function of the residual stress and the Bauschinger effect. At point (b), yielding starts in the opposite direction. Finally a point (d) corresponding to -P<sub>max</sub> is reached. To complete the cycle, as loads are released and then reversed, the resulting behavior would be as shown by the dashed line d-e-f-a.

Failure due to alternating plasticity will not occur when ranges of moment values exist for which a section behaves elastically regardless of its previous loading history. As a first approximation the Bauschinger effect may be ignored and this range of moment (ΔM<sub>y</sub> in Fig. 6.24) may be taken as

$$\Delta M_y = 2 M_y = 2 \frac{M_p}{f} \dots \dots \dots (6.26)$$

The necessary condition for eliminating the possibility of alternating plasticity is:

$$(M_i)_{max} - (M_i)_{min} \leq 2 \frac{M_p}{f} \dots \dots \dots (6.27)$$

where M<sub>i</sub> denotes the elastic moment values at any section "i" being investigated. Procedures for calculating the limit for alternating plasticity in the case of indeterminate structures may be found in Ref. 1.6.

b) Deflection Stability

As noted previously, under repeated application of a certain sequence of loads an increment of plastic deformation in the same sense may occur during each cycle. The maximum load for which these increments cease after a few cycles is called the stabilizing (or shakedown) load. In Fig. 6.25 is plotted

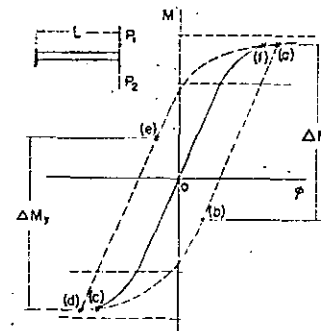


FIG. 6.24.—MOMENT-CURVATURE RELATIONSHIP AT THE BUILT-IN END OF A CANTILEVER BEAM UNDER ALTERNATING PLASTICITY

diagrammatically the number of loading cycles versus the deflection under the load at the end of each cycle. When P is equal to or less than a certain critical value P<sub>S</sub>, a set of residual moments will be set up in the structure after a few cycles during which the deflection approaches a limit value. All further repetitions of load are carried elastically. If P is greater than P<sub>S</sub>, the deflection does not stabilize but continues to grow for each cycle of load application. A description of this phenomenon may be found in the several references that pertain to this article.

It is possible to determine mathematically the maximum load P<sub>S</sub> for which the deflection of the structure will finally stabilize. The condition to be fulfilled is that at points of maximum moment the absolute value of the sum of the residual moment M<sub>r</sub> and the elastic moment M produced by the loads does not exceed the full plastic moment value M<sub>p</sub>. In general terms:

$$|(M_i)_r + (M_i)_{max}| = M_p \dots \dots \dots (6.28)$$

Eq. 6.28 may be applied to the problem shown in Fig. 6.26(a) a continuous beam of two equal spans, the supports of which can take upward and downward reactions. Suppose the load P is first applied at B. An elastic analysis would produce the moment diagram shown in Fig. 6.26(b) with M<sub>B</sub> = (13/64) P L. As a second phase of the loading, two equal loads applied at B and D would give the elastic moment diagram shown in Fig. 6.26(c). Due to any inelastic deformation that may occur under load, the only possible shape of the residual moment diagram is that shown in Fig. 6.26(d).

Applying Eq. 6.28, and defining the residual moment diagram positive as shown in Fig. 6.26(d), the conditions to be satisfied are as follows:

$$\text{At section B: } \left| \frac{13}{64} P L + (M_r)_B \right| = M_p \dots \dots \dots (6.29)$$

$$\text{At section C: } \left| -\frac{12}{64} P L + (M_r)_C \right| = M_p \dots \dots \dots (6.30)$$

29

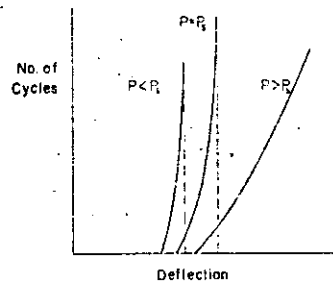


FIG. 6.25.—DIAGRAMMATIC REPRESENTATION OF DEFLECTION STABILITY (SHAKEDOWN)

However, the residual moments can have only a linear variation across the span with the maximum value at C (Fig. 6.26(d)) so that

$$(M_r)_B = \frac{1}{2} (M_r)_C \quad (6.31)$$

Expressions for the stabilizing load  $P_s$  are obtained from Eqs. 6.29, 6.30 and 6.31. Thus,

$$\frac{13}{64} P_s L + \frac{1}{2} (M_r)_C = M_p$$

and

$$\frac{12}{64} P_s L - (M_r)_C = M_p$$

From these two conditions the stabilizing load  $P_s$  and the residual moment  $(M_r)_C$  are determined. Hence

$$P_s = \frac{96}{19} \frac{M_p}{L} = 5.06 \frac{M_p}{L} \quad (6.32)$$

and

$$(M_r)_C = -\frac{1}{19} M_p \quad (6.33)$$

The results of this calculation are shown in Fig. 6.27. The elastic moment diagram due to  $P_s$  acting at B is shown in Fig. 6.27(a). The moment diagram with loads at B and D is shown in Fig. 6.27(b). Fig. 6.27(c) is the residual moment diagram after stabilization at load  $P_s$ . Combining Fig. 6.27(c), in turn, with Figs. 6.27(a) and 6.27(b), one obtains the final moment diagram for  $P_s$  acting at B only (Fig. 6.27(d)) and at B and D simultaneously (Fig. 6.27(e)). It is evident that Eq. 6.28 is satisfied.

According to the simple plastic theory,

$$P_u = \frac{5}{L} M_p \quad (6.34)$$

17

Thus, from Eqs. 6.32 and 6.34

$$P_s/P_u = 84.4\% \quad (6.35)$$

Eq. 6.35 indicates that the stabilizing load is theoretically about 16% lower than the ultimate load  $P_u$  in this example.

As a check on alternating plasticity, the following condition must be satisfied

$$(M_i)_{\max} - (M_i)_{\min} \leq 2 \frac{M_p}{L} = 2 M_y$$

In the previous example at section B

$$(M_B)_{\max} = \frac{13}{64} \left( \frac{96}{19} M_p \right) = \frac{39}{38} M_p$$

$$(M_B)_{\min} = -\frac{3}{64} \left( \frac{96}{19} M_p \right) = -\frac{9}{38} M_p$$

$$(M_B)_{\max} - (M_B)_{\min} = \frac{48}{38} M_p < 2 M_y$$

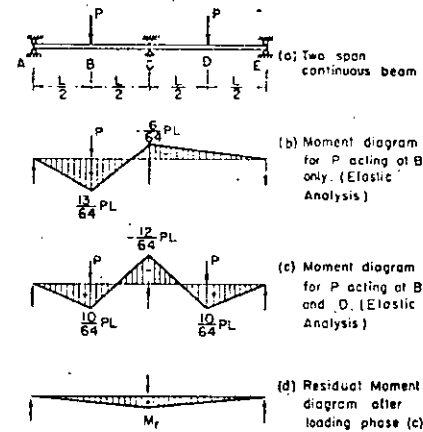


FIG. 6.26.—TWO-SPAN CONTINUOUS BEAM UNDER VARIABLE REPEATED LOADING (DEFLECTION STABILITY)

Actually, the increase in deflection for a load  $P < P_s$  will cease as strain-hardening sets in. A discussion of the effect of strain-hardening can be found either in Ref. 6.43 or 5.48.

Experimental Correlation

Experimental studies have been performed using continuous beams and rectangular frames. An investigation of two-span continuous beams was reported

30

In Ref. 6.48. Later, tests of the same structure were made using loads applied at the center of each span (6.45) and using off-center loads to simulate the worst possible condition. (6.46)

Deflection stability has been investigated (6.40) by testing small scale rectangular portal frames with symmetrical vertical load and horizontal load. Test results indicated that the observed stabilizing loads were about 10% higher than those given by theory. Experiments on a series of frames subjected to variable repeated loading have been made (6.47) investigating both alternating plasticity and deflection stability phenomena. Test results show

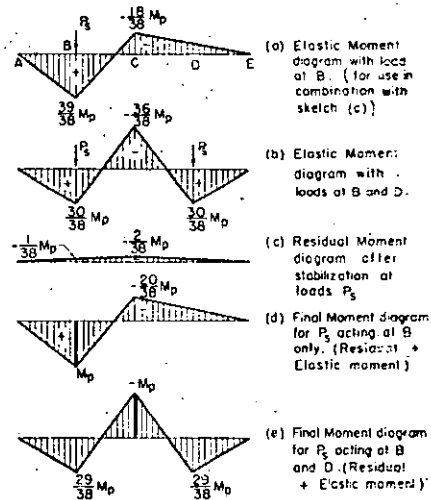


FIG. 6.27.—TWO-SPAN CONTINUOUS BEAM OF FIG. 6.26 UNDER STABILIZING LOAD  $P_s$

that the theoretical analysis (based on no strain-hardening) gives conservative predictions and that strain-hardening may increase the stabilizing load. (6.43, 6.46)

All results indicated that the experimental values were higher than those given by theory. Tables 6.2, (6.45) 6.3, (6.46) 6.4, (6.47) and 6.5 (6.40) contain a summary of each of the previous important observations. In these tables is indicated the loading sequences used in a given cyclic load test. The terms  $\alpha$  and  $\beta$  denote the proportion of a particular load applied during one phase of a cyclic loading sequence.

#### Relationship to Design

Practically every recent investigator of the subject has concluded that the problem of variable repeated loading may be disregarded for building frames

TABLE 6.2.—TEST RESULTS OF DEFLECTION STABILITY OF TWO-SPAN CONTINUOUS BEAMS

LOADING CONDITION	$\alpha$	THEORETICAL RELATIONSHIP $\frac{P_s}{P_u}$ (%)	OBSERVED RELATIONSHIP	$P_s$ (Obs) $P_s$ (Theo)
CYCLIC LOADING (DEFLECTION STABILITY)	0	84.2	85.7	102
	1/4	87.6	86.7	99
	1/2	91.5	96.2	105
	3/4	91.6	95.6	100
PROPORTIONAL LOADING		$\frac{P_{max}}{P_u} = 100$	$\frac{P_{max}}{P_u} = 100$	

$P_s$  = Stabilizing Load  
 $P_u$  = Theoretical failure load by simple plastic theory  
 $P_{max}$  = Observed plastic failure load

TABLE 6.3.—TEST RESULTS OF DEFLECTION STABILITY OF TWO-SPAN CONTINUOUS BEAMS

LOADING CONDITION	P (Theo.) (kips)	P (Obs.) (kips)	$\frac{P (Obs.)}{P (Theo.)}$ (%)
PROPORTIONAL LOADING			
TWO LOADS	$P_u = 16.81$	$P_{max} = 17.08$	101.6
SINGLE LOAD	$P_u = 16.81$	$P_{max} = 17.68$	105.2
CYCLIC LOADING (DEFLECTION STABILITY)	$P_s = 13.72$	$P_s = 14.8$	$\frac{P_s}{P_u} = 88$



TABLE 6.4.—TEST RESULTS OF RIGID FRAMES UNDER VARIABLE REPEATED LOADING

LOADING CONDITION	STRUCTURES	$P_u$ or $P_s$ (theo) kips	$P_u$ or $P_s$ (obs) kips	$P/P_{theo}$ (%)	$P_u$ (theo) kips	$P_u/P_s$ (%)
ALTERNATING PLASTICITY		5.6B	6.00	106	5.76	100
DEFLECTION STABILITY		5.81	6.80	117	7.76	87.7

TABLE 6.5.—TEST RESULTS OF RIGID FRAMES UNDER VARIABLE REPEATED LOADING

LOADING CONDITION	STRUCTURES*	$P_u$ (theo) lbs	$P_s$ (obs) lbs	$P/P_{theo}$ (%)	$P_{max}/P_{theo}$ (%)
Proportional Loading		92.5	101	109.2	109.2
	(2 Tests)	92.4	101	109.2	109.2
Cyclic Loading		87.9	93.5	106.5	101.0
	(3 Tests)	87.2	95.5	109.5	103.0
	Loading sequence a=1, b=1 a=0, b=0 a=0, b=1 a=0, b=0	88.9	93.0	104.9	101.5
		78.0	89.5	114.9	96.6
(2 Tests)	79.3	90.5	114.1	97.9	
Loading sequence a=1, b=1 a=0, b=0 a=1, b=1 a=0, b=0					

\*AB members were 1/4" sq sections

designed for the usual conditions of static loading. The probability of failure by a single overload appears to be much greater than the probability of failure by alternating plasticity or by loss of deflection stability.

Of particular significance is the fact that the ratio of live load to dead load must be very large before the load-carrying capacity is reduced because of load repetitions. In nearly all of the tests described in this section, extreme examples were chosen in which all of the load was considered to be live load. It is unusual to find such extreme load variations in building structures. The live load is seldom more than two-thirds of the total load and usually it is of the order of one-third of the total.

It must be remembered that the load factor  $F$  does not provide for possible overloads alone. It also accounts for such additional factors as variation in material properties, dimensions, workmanship, fabrication, methods of analysis, etc. Therefore, variation in live load alone could not properly be assumed to account for the full value of the factor of safety.

The fact has been emphasized<sup>(6.43)</sup> that failure due to increase of deflection is a gradual process so that ample warning of danger is available. This implies that a lower load factor is acceptable for  $P_s$  than that provided for  $P_u$ .

Finally, the results of the most recent tests using rolled shapes have shown that the observed stabilizing load was always greater than the theoretically predicted value. Since the theoretical values of  $P_s$  are seldom more than 20% below  $P_u$ , the practicality of this problem loses much of its significance. Although account could be taken of variable repeated loading by using a higher load factor, such a procedure is neither reasonable nor necessary for ordinary building frames.

#### VARIABLE REPEATED LOADING

Deflection stability need not be investigated in the design of statically loaded building frames.

Chapter 7  
COMPRESSION MEMBERS

33

7.1 INTRODUCTION

Simple plastic theory assumes that a member subjected to bending moments will sustain a certain limiting bending moment value (the "plastic moment"  $M_p$ ) that is dependent only on the geometrical properties of the cross section and the yield stress of the steel. When this maximum moment is approached, curvature increases indefinitely and a hinge type of action occurs. The presence of axial force tends to alter this situation. In the following the various effects of axial force on the behavior of members in a rigid frame will be described.

As loads are applied to a rigid frame, the individual members which comprise the structure are subjected to various combinations of axial thrust, end moments, and end restraints. In many cases in plastically designed structures, the stiffnesses of the end restraints do not influence the behavior of the column because of the formation of plastic hinges.

For an individual member which is subjected to bending moments and an axial force, and which is sufficiently braced in the lateral direction, or a member which is bent about its weak axis, the mode of failure will be that of excessive bending in the plane of the applied moments.

If a member bent about the strong axis has insufficient lateral bracing, and if a large difference exists between the bending stiffnesses about each of the principal axes of the cross section, the member may bend out of the plane of the applied moments and twist at the same time. This type of failure is called "lateral-torsional buckling."

An additional type of failure, which is basically different from those described previously, involves the structure as a whole, and may occur when sidesway of the structure is not prevented. This condition is characterized by a shift of the total structural deformation pattern from one that is symmetrical to one that is anti-symmetrical and is accompanied by an over-all lateral displacement of the frame. This situation will occur in a symmetrical structure that is symmetrically loaded when, at a critical magnitude of the loading, the total resistance of the structure to lateral movement becomes zero. The possibility of this "sidesway" or "frame" type of instability places a restriction on the ranges of applicability of the individual member-strength solutions.

A further situation may develop when the structure in question deforms horizontally from the first load application. For these cases the horizontal displacement of the column top with respect to the base may alter the carrying capacity of the individual member. This type of action would be similar in nature to that limiting the maximum carrying capacity of beam-columns. As in that case, there would be reached a certain loading for which the structure would continue to deform in the direction of initial movement ("excessive bending").

As pointed out in previous sections of this Manual (Art. 6.3), the problem of rotation capacity may also influence the design. It may be necessary in certain situations to insure a relatively large rotation at near-maximum loads.

In the following articles, the effects of axial force will be discussed, and methods will be outlined for their consideration in the design of one story and two-story rigid frames.

7.2 REDUCTION OF THE PLASTIC MOMENT DUE TO AXIAL THRUST

Statement of the Problem

If a member is subjected to the combined action of bending moment and axial force, the available plastic moment capacity is reduced from the full value of  $M_p$  to a lesser value that will be designated as  $M_{pc}$ . However, the design procedure may be easily modified to take this reduction into account since it has been demonstrated that the all-important "plastic hinge" characteristic is still retained at this lower moment. Because this is a property of the cross section, the value of  $M_{pc}$  as considered in this article is independent of the external loading and the slenderness ratio, and it is immaterial whether the axial force is in compression or tension. Even though instability effects are excluded, the methods developed here give a good approximation of the actual behavior of very short compression members and of certain other columns of practical proportions, as will be shown in Art. 7.3.

Previous Research

Ref. 7.1 is the first published work on the influence of axial thrust on the moment capacity of a short column. Methods of determining  $M_{pc}$  are given in Refs. 7.2 to 7.5, 3.1 and 1.6.

Theoretical Analysis

As an illustration of the influence of axial thrust on the plastic moment value, consider the rectangular section shown in Fig. 7.1. Assuming, for example, that the thrust is maintained constant and that the moment is progressively increased, the moment-curvature relationship will be that shown non-dimensionally in Fig. 7.1. (The moment is non-dimensionalized by dividing it by  $M_p$ , and the curvature is non-dimensionalized by dividing it by  $\phi_y$ , the curvature at the inception of yielding.) It is assumed here that the axial force is in compression. For purposes of comparison, the curve for no axial force is shown as a dashed line in Fig. 7.1. Yielding starts first in the outer fiber of the compression side of the member (stress diagram A in Fig. 7.1). Only after a portion of this side has yielded, will the tension side begin to yield (stress diagram B).

As was the case when axial force was not present, the hinge condition corresponds to that situation in which the cross section is fully yielded. (Stress diagram D in Fig. 7.1, or as redrawn in Fig. 7.2.) However, there will no longer be equal areas yielded in tension and compression as in the case of bending without axial load. Thus the neutral axis no longer coincides with the centroidal axis. Hinge rotations for the computation of the virtual work performed by the mechanism may still be assumed about the centroid of the section; the error for the structures considered in this Manual is negligible. For very deep built-up sections, however, the effect of the shift of the neutral axis may not be neglected. (7.6)

The value of  $M_{pc}$  for any cross section can be obtained from the equations of equilibrium of the internal and external forces; that is,

$$P = \int_A \sigma \, dA \quad \dots \dots \dots (7.1a)$$

$$M = \int_A \sigma \, y \, dA \quad \dots \dots \dots (7.1b)$$

In Eq. 7.1  $\sigma$  is the stress at a given fiber,  $y$  is the distance of that fiber from the centroidal axis,  $dA$  is the differential area element, and the integration is performed over the entire cross section. Eq. 7.1a results in the following expression for the rectangular section (see Fig. 7.2)

$$P = \frac{\sigma_y b}{2} \quad \dots \dots \dots (7.2)$$

Eq. 7.1b gives

$$M_{pc} = \frac{\sigma_y b}{4} (d^2 - 4 y_0^2) \quad \dots \dots \dots (7.3)$$

Substituting Eq. 7.2 into Eq. 7.3, and noting that  $\sigma_y b d = \sigma_y A = P_y$  and that

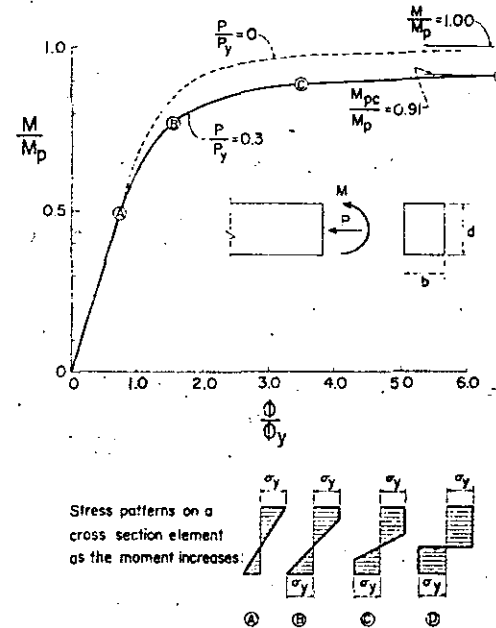


FIG. 7.1.—MOMENT-CURVATURE RELATIONSHIP FOR RECTANGULAR SECTION.

for no axial force present  $M_{pc} = M_p = \sigma_y b d^2/4$ , the non-dimensional expression for the reduced plastic moment for a rectangular section is

$$\frac{M_{pc}}{M_p} = 1 - \left(\frac{P}{P_y}\right)^2 \quad \dots \dots \dots (7.4)$$

By a similar process the values of  $M_{pc}$  can be computed for any section. Equations follow for wide-flange sections subjected to bending about the strong and weak axes. The nomenclature is shown on the inset in Fig. 7.3.

Strong Axis Bending of Wide-Flange Sections:

Neutral axis in web:

$$\frac{M_{pc}}{M_p} = 1.00 - \frac{A^2 (P/P_y)^2}{4 w Z_x} \quad [0 < P/P_y < w (d-2t)/A] \quad (7.5)$$

Neutral axis in flange:

$$\frac{M_{pc}}{M_p} = \frac{A \left(1 - \frac{P}{P_y}\right) \left[ d - \frac{A \left(1 - \frac{P}{P_y}\right)}{2b} \right]}{2 Z_x} \quad [w (d-2t) / A < P/P_y < 1.00] \quad (7.6)$$

Weak Axis Bending of Wide-Flange Sections:

Neutral axis in web:

$$\frac{M_{pc}}{M_p} = 1.00 - \frac{A^2 (P/P_y)^2}{4 d Z_y} \quad [0 < P/P_y < w d/A] \quad (7.7)$$

Neutral axis in flange:

$$\frac{M_{pc}}{M_p} = \frac{A^2}{8 t Z_y} \left[ \frac{4 b t}{A} - \left(1 - \frac{P}{P_y}\right) \right] \left[ 1 - \frac{P}{P_y} \right] \quad [w d/A < P/P_y < 1.00] \quad (7.8)$$

In the above expressions  $Z_x$  is the plastic modulus about the x-axis (strong axis) and  $Z_y$  is the plastic modulus about the y-axis (weak axis).

Although Eqs. 7.5 to 7.8 are given in a form suitable for determining  $M_{pc}$  for a given wide-flange section, they do not readily indicate the influence of cross-sectional shape. Equations for strong axis bending which reflect this influence are given in Ref. 3.1 in terms of the ratios  $A_f/A_w$ .<sup>\*</sup> These equations contain the simplifications that for wide-flange shapes  $d/d_w$  and  $d_f/d_w$  are about the same for all shapes used as columns and are approximately equal to 1.10 and 1.05, respectively.

<sup>\*</sup> In Ref. 3.1  $A_f$  = area of two flanges.

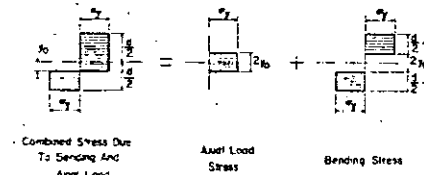


FIG. 7.2.—STRESS PATTERN AT  $M = M_{pc}$ .

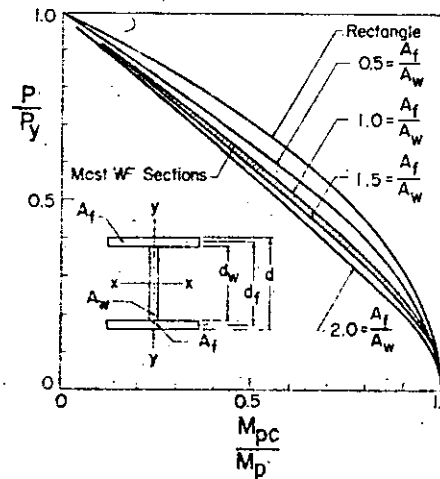


FIG. 7.3.—INTERACTION CURVE FOR STRONG-AXIS BENDING OF WIDE-FLANGE SECTION (MOMENTS ABOUT X-X ONLY, I = C)

The non-dimensional plot of these equations for various  $A_f/A_w$  ratios is shown in Fig. 7.3. The corresponding equations for weak axis bending of wide-flange shapes are:

Neutral axis in web:

$$\frac{M_{pc}}{M_p} = 1.00 - \left(\frac{w}{b}\right)\left(\frac{d_w}{d}\right) \left[ \frac{1 + (2 A_f/A_w)^2}{2 A_f/A_w + w/b} \right] \left(\frac{P}{P_y}\right)^2$$

$$\left[ 0 < P/P_y < (d/d_w) \left( \frac{1}{1 + \frac{2 A_f}{A_w}} \right) \right] \dots (7.9)$$

Neutral axis in flange:

$$\frac{M_{pc}}{M_p} = \left(1 - \frac{P}{P_y}\right) \left[ \frac{\left(1 + \frac{2 A_f}{A_w}\right)^2}{\left(\frac{2 A_f}{A_w}\right)\left(\frac{2 A_f}{A_w} + \frac{w}{b}\right)} \right] \times \left[ \frac{2}{1 + \frac{2 A_f}{A_w}} - \left(1 - \frac{P}{P_y}\right) \right]$$

$$\left[ \left(\frac{d}{d_w}\right) \left( \frac{1}{1 + \frac{2 A_f}{A_w}} \right) < \frac{P}{P_y} < 1.00 \right] \dots (7.10)$$

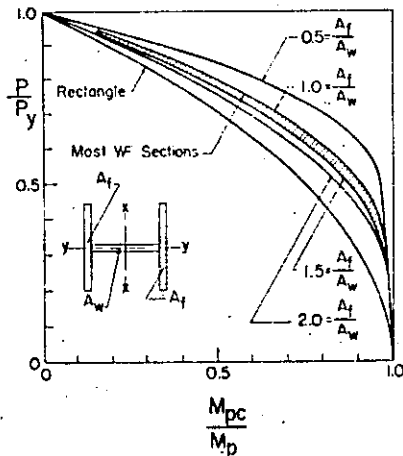


FIG. 7.3.—INTERACTION CURVE FOR WEAK-AXIS BENDING OF WIDE-FLANGE

Assuming such typical values as  $w/b = 0.04$  and  $d/d_w = 1.10$ , the curves shown in Fig. 7.4 are obtained for weak-axis bending.

From Figs. 7.3 and 7.4 it is evident that the range of the equations for most wide-flange sections falls in a very narrow band. This fact simplifies the problem of formulating design rules (see subsequent section on design recommendations).

The behavior of wide-flange columns subjected to biaxial bending (that is, where the applied bending moment is not about one of the principal axes) is discussed in Ref. 7.7.

Experimental Correlation

Fig. 7.5 shows the correlation between a set of experimental data and theory. (5.2) Each of the three tests was carried out on 12 WF 36 members which were so short that instability was no problem ( $L/r_x = 7.0$ ). Furthermore, flexure about the weak axis was prevented by the arrangement of the

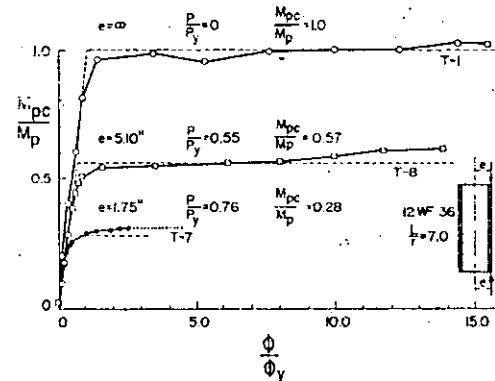


FIG. 7.5.—TESTS OF ECCENTRICALLY LOADED SHORT COLUMNS.

knife edges at the column ends. This permitted rotation in the strong direction only. The results are plotted as nondimensional moment-versus-curvature curves to indicate the influence of axial force on the reduction of the plastic hinge moment. For member T-1 the axial load was zero (pure bending). Members T-7 and T-8 were loaded by an eccentric force. As would be expected, the hinge moment for T-7 and T-8 does not reach the full value of  $M_p$ . The hinge condition, however, was realized in all cases (see Fig. 7.5) and the experimentally determined value of  $M_{pc}$  was close to that predicted by Eqs. 7.5 and 7.6 (represented by horizontal dashed lines in Fig. 7.5).

To afford a clearer indication of the correlation between this set of test data and predictions, Fig. 7.8 gives the experimentally determined initial yield and ultimate strength values plotted on an interaction diagram similar to that described earlier.\* Included in this comparison is the result of a pure

\*The interaction diagram for the theoretical ultimate strength was constructed using Eqs. 7.5 and 7.6; the initial yield curve represents the elastic limit computed from the equation  $\sigma_y = (P/A) + (M/S)$ .

axial load test (T-6) of the same cross section. Due to the presence of residual stress, the elastic interaction curve slightly overestimates initial yielding. The ultimate-load curve, on the other hand, slightly underestimates the capacity; this is because of strain-hardening.

Results of a series of tests (7.4) on short 3 in. standard British I-Beams are shown in Fig. 7.7; excellent agreement with the theory is indicated. A constant moment was first applied to the member and axial force was subsequently increased until the member had fully plastified.

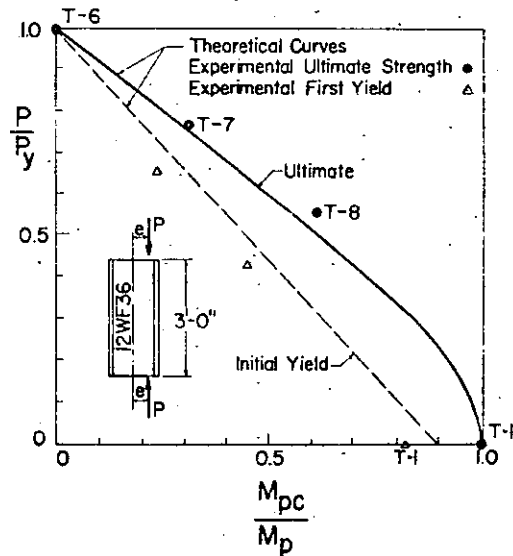


FIG. 7.6.—TESTS OF ECCENTRICALLY LOADED SHORT COLUMNS.

The experimental evidence shows that for mild steel the reduction in moment capacity due to the presence of axial force can be closely predicted by the theories outlined.

Design Recommendations

To account for the influence of axial force in design, any of the appropriate equations or curves of this section could be used. However, since the curves for wide-flange shapes fall within a relatively narrow band (see Figs. 7.3 and 7.4), it is possible to obtain simple approximate expressions for these cross sections.

For strong-axis bending the influence of axial force may be neglected if P is less than 15% of  $P_y$ , where  $P_y = \sigma_y A$ . If the axial force is larger, the

interaction between moment and force may be expressed as:

$$\frac{M_{pc}}{M_p} = 1.18 \left[ 1 - \frac{P}{P_y} \right] \dots (7.11)$$

The corresponding equation for weak-axis bending is:

$$\frac{M_{pc}}{M_p} = 1.19 \left[ 1 - \left( \frac{P}{P_y} \right)^2 \right] \dots (7.12)$$

Eq. 7.12 need only be used when P is more than 40% of  $P_y$ . These approximations yield an error of less than 5% (Figs. 7.8 and 7.9).

One way of using these interaction equations is to find a trial section based on bending considerations alone and then to adjust this section by successive corrections until the conditions of the interaction equations are fulfilled.

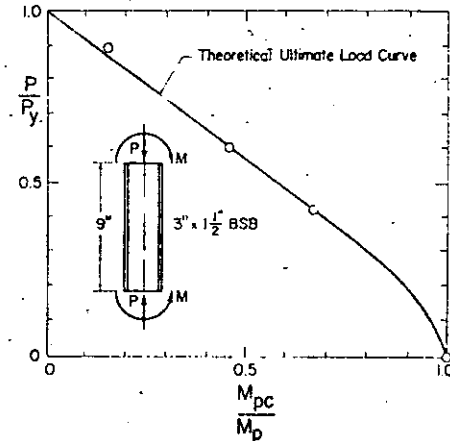


FIG. 7.7.—SHORT COLUMNS LOADED IN BENDING AND COMPRESSION.

Thus a design guide may be formulated in order to account for the influence of axial thrust. It must be kept in mind that instability effects are neglected, and so these equations apply in the strictest sense only to short columns. Calculations including the effects of instability have shown that the strong axis interaction equation (Eq. 7.11) is also valid for columns subjected to certain loading conditions (see Art. 7.3).

In summary, the following equations are suitable for determining the reduction of plastic moment due to axial force:

**REDUCTION OF PLASTIC MOMENT CAPACITY****Strong Axis Bending, Wide-Flange Sections:**For  $0 < P < 0.15 P_y$ , use  $M_{pc} = M_p$ For  $0.15 P_y < P < P_y$ ,  $M_{pc} = 1.18 \left( 1 - \frac{P}{P_y} \right) M_p$ **Weak Axis Bending, Wide-Flange Sections:**For  $0 < P < 0.4 P_y$ , use  $M_{pc} = M_p$ For  $0.4 P_y < P < P_y$ ,  $M_{pc} = 1.19 \left[ 1 - \left( \frac{P}{P_y} \right)^2 \right] M_p$ **Rectangular Section:**

$$M_{pc} = \left[ 1 - \left( \frac{P}{P_y} \right)^2 \right] M_p$$

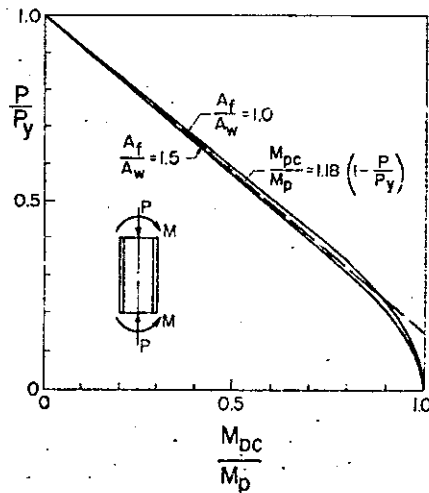


FIG. 7.8.—APPROXIMATE INTERACTION EQUATION FOR WIDE-FLANGE SECTION (STRONG AXIS BENDING, SHORT COLUMN).

**7.3 MOMENT-CARRYING CAPACITY OF COLUMNS****Statement of the Problem**

Although the solutions that were obtained in the preceding section represent a basic characteristic of the cross section and are adequate for short columns, they do not always correspond to the loading that a longer column can sustain.

As an illustration of the problem, consider the eccentrically loaded column of Fig. 7.10. As the load is increased beyond initial yielding at midlength, plastification progresses along and across the column, thereby reducing its resistance to further loading. Fig. 7.11 shows a typical load-versus-center-deflection curve for an eccentrically loaded column. The portion of the curve

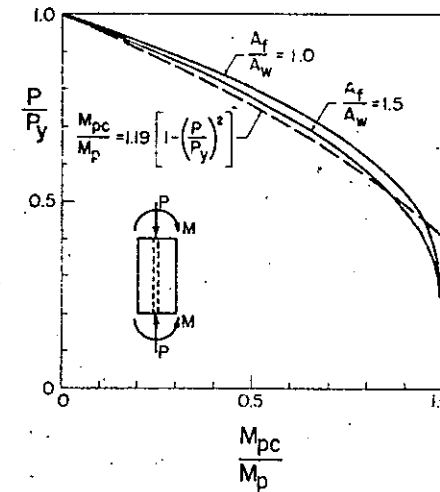


FIG. 7.9.—APPROXIMATE INTERACTION EQUATION FOR WIDE-FLANGE SECTION (WEAK AXIS BENDING, SHORT COLUMN).

from O to A represents the column behavior when the stresses are still elastic. The portion A - B represents the range of partial yielding. Finally, when the P-versus- $y_d$  curve reaches point B, a further increase in load becomes impossible because the internal stiffness of the column is just enough to resist P and the moment  $P(e+y_d)$ . It is with the determination of this maximum value of P that this section is concerned. It is evident that this type of failure occurs by virtue of excessive bending in the plane of the applied moments.

A column will not fail in the manner just discussed if the cross section under consideration has markedly different values of bending stiffness in the

two principal directions (a characteristic of wide-flange sections). If the member is subjected to bending about the stronger of the two axes, and if no torsional restraint at its ends or intermediate lateral restraint is provided, the column will twist and bend out of the plane of loading; in general its strength will be reduced. This phenomenon is known as "lateral-torsional buckling" and is the subject of Art. 7.5.

If lateral-torsional buckling is prevented, the eccentrically loaded column (or the column with end bending moments plus an axial thrust) can "fail" only after a certain amount of yielding has taken place. The problem is therefore not one of stress but one of stability. The point of indifferent equilibrium occurs when the internal stiffness is just enough to resist the external moments. Thus for certain columns the condition of full plasticity (defined by stress diagram D in Fig. 7.1) will not be reached.

#### Previous Research

An extensive résumé of the early work on eccentrically loaded columns is contained in sections 9 through 12 of Ref. 6.17.

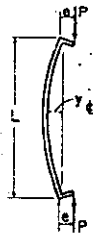


FIG. 7.10.—ECCENTRICALLY LOADED COLUMN.

Recent work has extended the investigations of the early researchers in this field. Solutions to the problem of eccentrically loaded, end-restrained rectangular columns were presented in Refs. 1.1 and 7.8. Other investigations have been made of the problem of hinged-end, as-rolled, wide-flange steel columns bent about their major axes. (7.9, 7.10, 7.11)

Parallel to the efforts of the determination of the strength of eccentrically loaded columns by rational means, attempts to define empirical interaction equations for predicting column strength have been made. Among these, the most recent and most extensive work is reported in Ref. 6.29 which proposes the interaction equation

$$\frac{P}{P_{cr}} + \frac{M_{equ}}{M_p \left(1 - \frac{P}{P_e}\right)} \leq 1.00 \quad (7.13)$$

in which

$P$  = axial load on the column

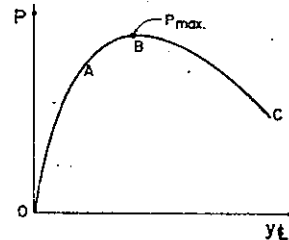


FIG. 7.11.—LOAD-DEFLECTION CURVE FOR ECCENTRICALLY LOADED COLUMN.

$P_{cr}$  = maximum axial force the column can carry if no bending moment is present; this value includes the influence of the effective length

$M_{equ}$  = equivalent end bending moment which may be expressed as follows:

$$M_{equ} = \sqrt{0.3(M_1^2 + M_2^2) + 0.4 M_1 M_2} \quad (7.14)$$

$M_1$  = larger of the two end moments

$M_2$  = smaller of the two end moments (the sign of  $M_2$  is negative in Eq. 7.14 if it causes a curvature opposite to that caused by  $M_1$ )

$P_e$  = the elastic ("Euler") buckling load of the column in the plane of the moments

$M_p$  = full plastic moment of the cross section

In case the maximum moment occurs at the end of the column, the following equation holds for the interaction between P and M:

$$\frac{P}{P_y} + \frac{0.85 M_1}{M_p} = 1.00 \quad (7.15)$$

In design, both Eqs. 7.13 and 7.15 must be checked. Whichever equation furnishes the smaller values of M or P is governing.\*

It has been shown that Eqs. 7.13 and 7.15 are conservative if compared with results of column tests. (6.29)

Besides the theoretical work on this topic, many experiments have been conducted, notably those reported in Refs. 7.5, 7.8, 7.9, 7.12, 7.13, 7.14, and 6.29. It is impossible herein to do full justice to the immense effort that has been put forth in solving the various aspects of the eccentrically loaded column problem. Therefore, only a few have been mentioned; a more complete review of work done before 1950 has been listed in Ref. 6.17 and the most recent research has been summarized by the Column Research Council in Ref. 7.15.

#### Theoretical Analysis

From the many available solutions, one has been selected which represents most nearly the conditions that exist in a plastically designed rigid frame of the type considered in this Manual (that is, one-story or two-story frames). The results of Ref. 7.10 have been chosen, because they represent a so-called "exact" solution (for including the influence of residual stress on column strength) and are directly applicable to columns fabricated from as-rolled wide-flange shapes which are subjected to bending about their strong axes.

In the development of the theory, the following assumptions are made:

- The mode of failure will be that of excessive bending in the plane of the moments; furthermore, this plane is taken to be the strong plane of the section.
- Lateral-torsional buckling is prevented.
- The material is mild, structural grade steel such as ASTM-A7 or A373, which is assumed to possess the idealized stress-strain curve of Fig. 2.1.
- Members are originally straight, free from accidental end eccentricities, and are of uniform cross section along their length.

\* Eq. 7.15 is a rearrangement of Eq. 7.11.



- e) Plane sections before bending remain plane after bending.  
 f) The end slope of the deflected column is small.  
 g) The behavior of the column in the frame is the same as that of an isolated member loaded with axial force and end bending moments.

Interaction curves for strong-axis bending of a rolled wide-flange section are developed in Ref. 7.10 by an iterative procedure. The influence of residual stresses due to cooling after rolling is included in these calculations, thus giving solutions for as-delivered columns. The particular residual stress pattern which is used (see Fig. 7.12) is typical of commonly used wide-flange column sections. (7.9, 7.16, 4.1) A maximum compressive residual stress of  $0.3 \sigma_y$  is assumed in the calculations.

Interaction curves for wide-flange sections are shown in Figs. 7.13 and 7.14 for two loading conditions. These curves have been computed numerically for the 8 W 31 shape; however, they represent a good approximation for any other wide-flange section. The 8 W 31 section has been chosen because of its low shape factor ( $f = 1.10$  as compared to the average value of 1.14). Hence the curves are conservative for other sections in the ratio of their shape factor to 1.10. The interaction curves show a non-dimensional plot of the relationship between the axial force (abscissa) and end bending moment

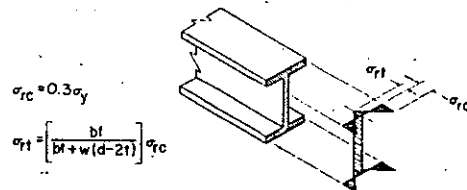


FIG. 7.12.—ASSUMED COOLING RESIDUAL STRESS PATTERN.

(ordinate) for constant values of the slenderness ratio in the direction of bending.

Fig. 7.13 gives the curves for a loading condition in which two equal end moments cause the column to bend in single curvature; Fig. 7.14 shows the curves for the case where only one end moment is applied (moment ratios of 1.0 and 0, respectively).

A complete description of the calculations necessary to obtain these interaction curves is given in Ref. 7.10. Only a brief outline of the procedure is given here to show how one point on a curve is obtained. For a given section an axial force, length and end bending moment value are assumed. The end slope corresponding to this loading is computed by a numerical integration process; that is, curvatures obtained from the moment-curvature diagram of Fig. 7.15 are integrated to give the deflected shape and thus the end slope of the column. This process is repeated for several values of the end moment (length and axial force remaining constant) until an end moment versus end rotation curve can be constructed. The maximum point on this curve corresponds to the highest end moment which this column can support, thus giving one point on the interaction curves of Figs. 7.13 or 7.14.

The curves of Figs. 7.13 and 7.14 have been computed for steel with a yield stress of 33 ksi. If it is desired to use these curves for steel with a different

yield stress level, an approximate result can be obtained if the actual slenderness ratio of the column is multiplied by the factor  $\sqrt{\sigma_y/33}$  where  $\sigma_y$  is the yield stress of the particular steel (expressed in ksi).

#### Experimental Correlation

Figs. 7.16 through 7.20 show the experimental correlation of various tests with the interaction curves of Figs. 7.13 and 7.14.

Fig. 7.16 correlates the theory with tests performed on hat-shaped sections. (7.12) This cross section conforms most nearly to the assumptions made in the derivation of the interaction curves (namely, that lateral buckling cannot take place since bending is about the weak axis, and yet the action of a

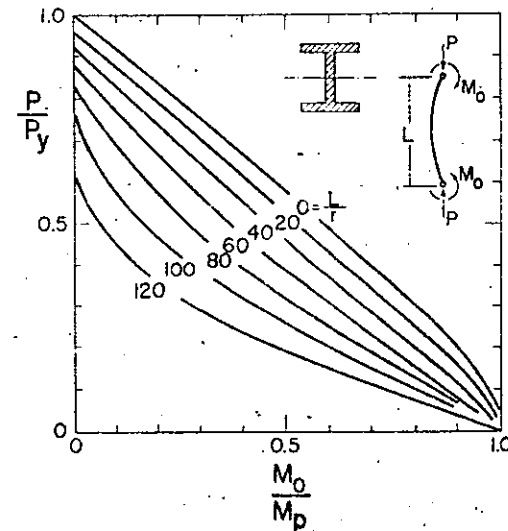


FIG. 7.13.—INTERACTION CURVES FOR STRONG AXIS BENDING OF WIDE-FLANGE SECTIONS.

wide-flange shape bent about its strong axis is simulated). The correlation shown in Fig. 7.16 is good.\* In this figure as well as in the following figures, the continuous line refers to the theoretical curves for the given eccentricities; the points represented by circles, squares, or triangles are the experimental points. These have been corrected to include the influence of specimen yield stress other than 33 ksi. In Fig. 7.16 the experimental points fall slightly above the theoretical curves; this is as would be expected since the shape factors of

\*These tests also give good correlation with the interaction equation (Eq. 7.13) as shown in Fig. 6 of Ref. 7.12.

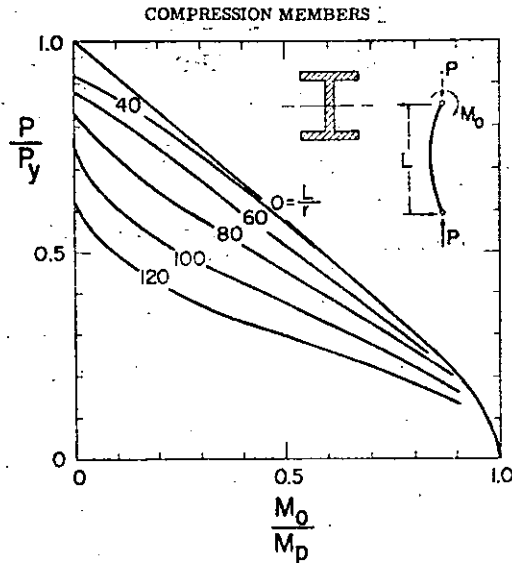


FIG. 7.14.—INTERACTION CURVES FOR STRONG-AXIS BENDING OF WIDE-FLANGE SECTIONS.

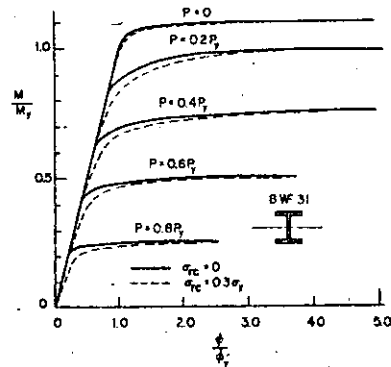


FIG. 7.15.—MOMENT-THRUST-CURVATURE RELATIONSHIPS FOR AN 8WF 31 SECTION, INCLUDING THE INFLUENCE OF RESIDUAL STRESS.

(the hat sections are slightly above those of wide-flange sections, and the residual stress is somewhat below that assumed in the theory outlined here ( $f = 1.17, 1.18, \text{ and } 1.25$  for the three sections that were tested;  $\sigma_{rc}(\text{max.}) = 0.23 \sigma_y$  by measurement as compared to  $0.3 \sigma_y$  of the theory).

The correlation with tests reported in Ref. 7.13 is shown in Fig. 7.17. The test setup was such that the columns were essentially pin ended with respect to bending in the strong direction, and fixed ended in the weak direction. This

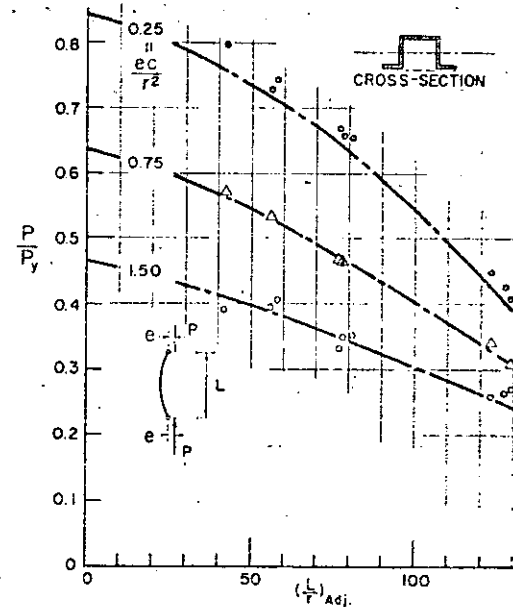


FIG. 7.16.—COMPARISON OF COLUMN TEST RESULTS WITH THEORY.

was done by the use of knife edges placed perpendicular to the web. The test columns usually failed by lateral-torsional buckling. It is interesting to note, however, that except for the tests which fall close to the region where failure would have been due to "Euler buckling" in the weak direction (see dotted curve) the correlation with the theory which neglects lateral-torsional behavior is reasonably good. In constructing the dotted Euler buckling curve the effective column length with respect to the  $y$ -axis was taken as  $0.6$  times the column length; this effective length was determined experimentally.

The test results published in Ref. 6.29 are compared with theoretical predictions in Fig. 7.18. The D1E profiles, of which the test columns were made, are geometrically similar to American wide-flange profiles. The end conditions of the columns were essentially pin ended in both principal directions, since the end fixtures consisted of almost frictionless, hydraulically-seated steel hemispheres. For such end conditions the lowest possible restraint is offered to lateral-torsional buckling. As shown in Fig. 7.18, most of the test points agree rather well with the theory which neglects this type of buckling, even though failure was by lateral-torsional instability. Comparison was made only for the loading case where moment was applied at one end of the column.

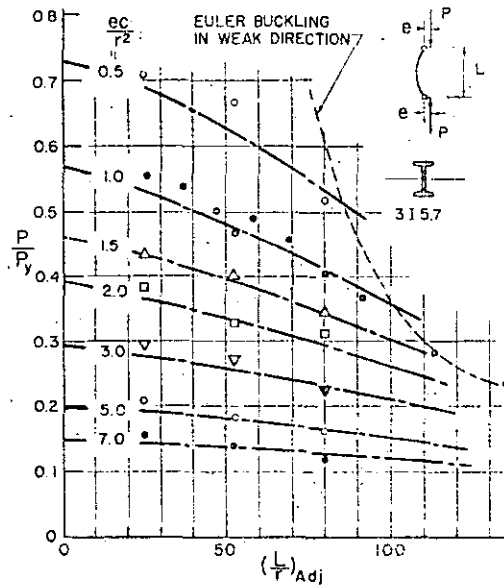


FIG. 7.17.—COMPARISON OF COLUMN TEST RESULTS WITH THEORY.

Fig. 7.19 shows the results of experiments reported in Ref. 7.14. The end conditions here were the same as for the tests in Ref. 7.13. The theoretical correlation is quite good.

Tests performed at Lehigh University also confirm the theoretical prediction. The test results are compared with theoretical curves in Fig. 7.20. The loading condition, slenderness ratio, and the column size are indicated in this figure. Intermediate lateral braces were provided to prevent lateral-torsional buckling (except for tests T-13, T-23, and T-20). The location of these braces

was determined in accordance with Eq. 6.25. These braces were adequate for the prevention of lateral-torsional buckling. Good correlation is seen to exist between theory and experiment in Fig. 7.20, except for test T-13, which was considerably stronger than predicted. This was a relatively short column with a low axial force, and therefore its strength should reflect the influence of strain-hardening.

The foregoing comparisons of theory with experimental results show that the interaction curves of Figs. 7.13 and 7.14 can be used to predict column behavior quite accurately, provided lateral-torsional buckling is prevented. The

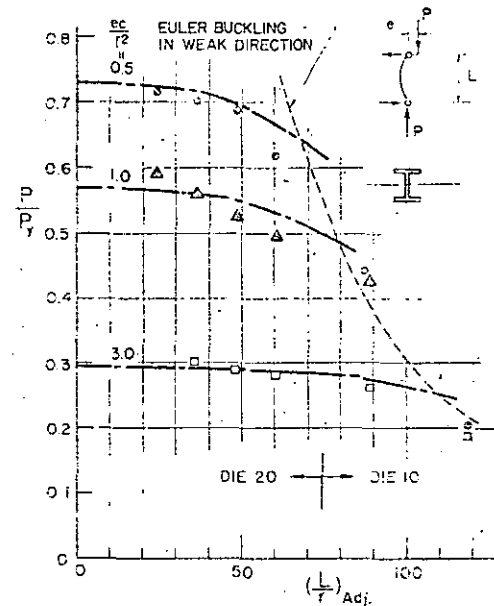


FIG. 7.18.—COMPARISON OF COLUMN TEST RESULTS WITH THEORY.

specimens used for the experiments in all but one of the test programs were rolled wide-flange shapes, probably containing a similar residual stress pattern to that present in the 8 W 31 shape used in deriving these curves. The hat sections of Ref. 7.12 had quite a different residual stress pattern (see Fig. 3 of Ref. 7.12). However, correlation seems to be equally good for these tests also.

### Design Recommendations

The interaction curves shown for two loading cases for the strong axis bending of wide-flange shapes in Figs. 7.13 and 7.14 can be used directly in design. As a convenience in interpolating, the interaction curves have been reduced to approximate design equations by means of curve fitting. (7.10) In order to arrive at simple approximate equations, their application is limited to  $0 < P/P_y < 0.6$  and to  $0 < L/r < 120$ . These limits place all practical problems in plastic design well within the scope of the equations, at least for buildings one or two stories in height.

In order to apply the following design rules, the column must be adequately braced in the direction perpendicular to the applied moments so as to

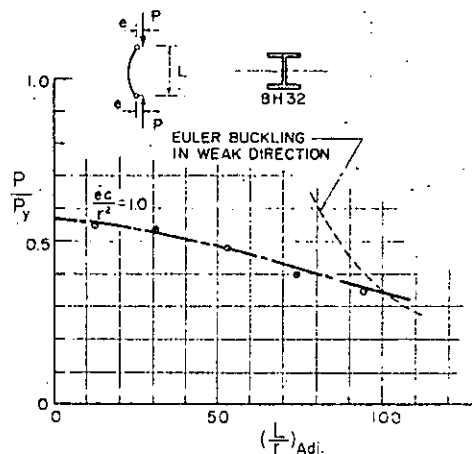


FIG. 7.19.—COMPARISON OF COLUMN TEST RESULTS WITH THEORY.

prevent lateral-torsional buckling. The ends are assumed torsionally restrained by the beams which frame into them. The ensuing discussion assumes that the moments produce bending about the strong axis, as is generally the case. For weak-axis bending the use of the suggested approximate formulas would usually lead to conservative designs. In this case lateral-torsional buckling would not be a problem. The above defined limits of axial force and slenderness ratio are appropriate, provided the whole frame is restrained from becoming unstable by means of sway-bracing, by the lateral support of an adjoining structure of known stability, or by lateral stiffness furnished by the walls, floor slabs, and the roof.

The foregoing solutions of the case where the moment ratio is +1 (Fig. 7.13) and 0 (Fig. 7.14)\* may be extended to cover all cases of column loading in the following manner:

A column which is bent into double curvature (into an S-shape) by equal end moments (moment ratio equal to -1), can be thought of as two columns of

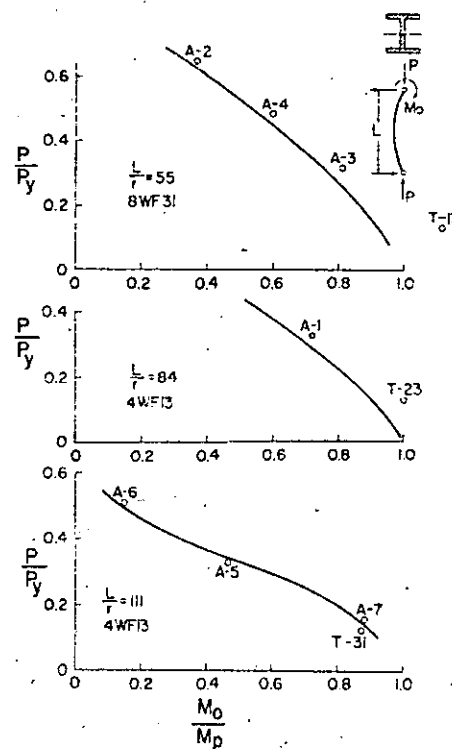


FIG. 7.20.—COMPARISON OF COLUMN TEST RESULTS WITH THEORY.

the type shown on the inset of Fig. 7.14, where the inflection point at the center provides the moment-free pin joint. Thus, if the slenderness ratio of the column is 80, the corresponding slenderness of the effective column is only 40. In Fig. 7.14 it may be observed that for slenderness ratios ranging from 0 to 40 and for  $0 < P < 0.6 P_y$  the curves are almost identical to the curve

\*Moment ratio is defined as the ratio of the smaller of the two end moments to the larger one. It is positive when each moment causes the same curvature (single curvature) and negative when each moment causes opposite curvatures to the other.

for full plasticity ( $L/r = 0$ ). Thus, in the case of loading producing double curvature, the equation for a zero-length member may be used (Eq. 7.11) without causing an appreciable error. Under certain conditions however, this column may "unwind" from its antisymmetrical deflection configuration and fail by concentric buckling. This occurs when the axial force equals the critical buckling load for the corresponding axially loaded column. The strength of the column against this type of failure is reduced due to yielding at the ends where the moment is applied, and thus "unwinding" (7.17) will occur before the "Euler" buckling load is reached. To safeguard against this type of failure, the application of Eq. 7.11 is limited to  $0 < P/P_y < 0.6$  and  $0 < L/r < 100$ .

For columns with a moment ratio from -1.0 to 0, the equations for the more severe case could be used (that is, for a moment ratio of 0). Similarly, the equation for a moment ratio of +1.0 could be used if the ratio ranges from 0 to +1.0.

In summary, the following guides are listed for the design of steel wide-flange columns bent about the major axis in frames where sidesway is prevented:

#### WIDE-FLANGE COLUMNS, STRONG-AXIS BENDING

##### Range of Application:

The slenderness ratio with respect to the axis of bending must be equal to or less than 120 and the axial force must be equal to or less than  $0.6 P_y$ . The column must be adequately supported laterally, and sidesway must be prevented by external means.

##### Column Equations:

1. Ratio of end moments of -1.0\* (Fig. 7.14)

$$\frac{M_o}{M_p} = 1.18 \left( 1 - \frac{P}{P_y} \right) \cdot \frac{M_o}{M_p} < 1.0 \quad (7.16)$$

2. Ratio of end moments varying from -1 to 0 (Fig. 7.14)

$$\frac{M_o}{M_p} = B - G \left( \frac{P}{P_y} \right) \cdot \frac{M_o}{M_p} < 1.0 \quad (7.17)$$

$$\text{where } B = 1.13 + \frac{(L/r)}{3,080} + \frac{(L/r)^2}{185,000}$$

$$G = 1.11 + \frac{(L/r)}{190} - \frac{(L/r)^2}{9,000} + \frac{(L/r)^3}{720,000}$$

3. Ratio of end moments varying from 0 to +1.0 (Fig. 7.13)

$$\frac{M_o}{M_p} = 1.00 - K \left( \frac{P}{P_y} \right) - J \left( \frac{P}{P_y} \right)^2 \quad (7.18)$$

$$\text{where } K = 0.420 + \frac{(L/r)}{70} - \frac{(L/r)^2}{29,000} + \frac{(L/r)^3}{1,160,000}$$

$$J = 0.770 - \frac{(L/r)}{60} + \frac{(L/r)^2}{8,700} - \frac{(L/r)^3}{606,000}$$

\*For Eq. 7.16 only the limits of  $P$  and  $L/r$  should lie between  $0 < P < 0.6 P_y$  and  $0 < L/r < 100$ .

In Eqs. 7.16 and 7.17 the quantity  $M_o$  should be taken as the larger of the two end moments. Values of  $B$ ,  $G$ ,  $K$ , and  $J$  are tabulated for slenderness ratios of 0 to 120 in Ref. 1.3.

#### 7.4 ROTATION CAPACITY

If a frame is to fail by the formation of a mechanism, the column ends may be required to undergo a certain amount of inelastic rotation; at the same time the axial load and end moments must be maintained on this column. This is especially true of a column which contains the first plastic hinge, since this hinge must continue to rotate until the last plastic hinge of the frame is developed. The problem is thus to determine whether a column end can undergo the needed rotation and still support the loads for which it was designed.

The rotation requirement of a particular hinge in order to form a mechanism under a given loading condition can be determined for any given column by an elastic-plastic method. (7.18) This method will be discussed further in Chapter 9.

The theory outlined in Art. 7.3 permits the calculation of the end moment versus end slope curve up to the point of maximum moment. Information from a study (7.19) will permit the construction of the full end moment versus end slope curves for any rolled wide-flange section. A theoretical evaluation of the rotation capacity problem will therefore be available.

An evaluation of the performance of columns in tests shows that adequate rotation capacity will be exhibited for the usual one-story or two-story structure, provided that lateral-torsional buckling of the columns is prevented.

The following facts may be deduced about rotation capacity from tests:

- 1) In all of the experiments on full-scale frames, described in Art. 5.3, the maximum loads which were sustained were at least equal to the theoretical loads computed on the basis of the simple plastic theory. It is evident therefore, that the ends of these columns exhibited the rotation capacity required to form a mechanism. As is shown in Art. 5.3, the loading and dimensions of these frames were of practical proportions.
- 2) Observations of the rotational behavior of as-rolled wide-flange columns subjected to bending moments about the strong axis were made in Ref. 7.20. The tests were performed on 8 W 31 and 4 W 13 columns, which ranged in slenderness ratio from 27 to 111. Most of the columns were subjected to a constant axial load of  $0.12 P_y$  and to a number of different end moment conditions. No lateral bracing was provided between the supports for any of the tests; the prevalent mode of failure was therefore lateral-torsional buckling. Many of the tested columns exhibited a rotation capacity of at least twice the rotation at the elastic limit, the best performance corresponding to the case of unequal end moments. In some instances the moment versus end rotation curve was still rising when the test was discontinued.
- 3) The results from one of the current series of tests at Lehigh University are shown in Fig. 7.21. Also shown are the data pertaining to this test. The curve shows the moment-rotation relationship at the end as the applied moment was increased from zero to its maximum value while the axial load was held constant. The slenderness ratio in the direction of bending was 55, and the member was braced laterally according to the rules of Art.

6.3 (Eq. 6.25). The total rotation was over four times the hypothetical elastic rotation at the maximum moment when the load began to drop off. The rotation capacity of this column appears satisfactory. Further tests on laterally restrained columns have shown that rotation capacity increases as the axial load and slenderness ratio decrease.

From the discussion above, the following conclusions may be drawn about rotation capacity: For one-story and two-story rigid frames the column ends can be expected to supply the required rotation, provided lateral-torsional buckling is prevented (see recommendations in Art. 7.5). For the very infrequent cases when the axial force is high ( $P > 0.3 P_y$ ), when the column is very slender ( $L/r > 100$ ), or when the equal or nearly equal end moments cause single curvature deformation, it would be appropriate to check the sequence of hinge formation. In many cases such columns would contain "last" hinges. If it were found that this was not the case, one could specify a larger column in order to force the hinge to occur elsewhere first.

#### 7.5 THE INFLUENCE OF LATERAL-TORSIONAL BUCKLING

If a column has sufficiently different bending stiffnesses in its two principal directions and if the external bending moments are applied in the stronger direction, the column may not reach the strength implied in Art. 7.3 unless adequate lateral bracing is provided. It will usually fail by lateral-torsional buckling before excessive bending in the plane of the moments is reached.

This type of buckling has been observed by investigators who have conducted eccentrically loaded column tests on wide-flange sections where the eccentricity caused bending about the strong axis. (6.29, 7.13, 7.20, 7.21)

For columns of intermediate slenderness ratio, which usually occur in one-story or two-story rigid frames, lateral-torsional buckling does not take place until parts of the column have yielded. Although theoretical solutions\* for elastic lateral-torsional buckling are available for a wide range of loading and end conditions, a complete solution to the inelastic problem is still lacking. An inelastic solution has been obtained for a column bent by equal end moments which cause single curvature deformation. (7.23) Good correlation of this theory with test results was observed. Further research is being directed towards the solution of other loading cases.

Lateral-torsional buckling of a column which is located in a plastically designed structure may tend to exaggerate the following two effects:

- 1) The maximum strength predicted by the theory of Art. 7.3 may not be fully realized.
- 2) The rotation capacity may be impaired.

The greatest reduction in strength is associated with columns deflected in single curvature by equal end moments if the ends of the columns are completely unrestrained in the weak direction. (7.23) Tests of columns under equal end moments causing single curvature but in which almost full re-

\* For a summary of these see Chapters 3 and 4 of Ref. 6.17 and Ref. 7.15; a most comprehensive treatment of the problem is given in Ref. 7.22.

straint about the weak axis was achieved, (7.13) show that in almost all instances it is possible to reach the strength predicted by the theory of Art. 7.3 (see Figs. 7.17 and 7.19). The exception is where the axial load is close to the "Euler" buckling load. For other loading cases such as the one shown in Fig. 7.18, the reduction of strength due to lateral-torsional buckling becomes even less.\*

It may thus be concluded that for the type of columns which occur in the structures considered in this Manual (that is, columns for which the axial force is relatively low), the column theory of Art. 7.3 will give a satisfactory prediction of column strength provided that considerable restrains of the column ends in the weak direction is present. Commonly used base-plate and anchor-bolt arrangements, and the necessary transverse beams between adjacent frames at the column top will in general insure this.

The second possible effect of lateral-torsional buckling is to influence the rotation capacity. Since Ref. 7.20 shows that the rotation capacity may be reduced if the member fails by lateral instability, it is recommended that lateral-torsional buckling be prevented by suitable intermediate bracing in regions of plastic bending. Until future research discloses a perhaps more liberal procedure, it is suggested that the spacing of the bracing points be in accordance with the recommendations made in Art. 6.3 (Eq. 6.25). In case loading produces symmetrical single curvature, the minimum bracing distance of  $35r_y$  should be used throughout the column length. Fig. 7.21 shows the results of a test in which the lateral support spacing was in accordance with Eq. 6.25. The lateral support was adequate to prevent lateral-torsional buckling failure.

#### 7.6 FRAME STABILITY

In Art. 7.3 a method was presented by which the strength of individual columns subjected to an axial force and to bending moments in one of its principal planes can be predicted if no lateral-torsional buckling occurs. As was pointed out in Art. 7.1, the maximum load which the structure as a whole can carry may be less than the load computed on the basis of the strength of its individual members if sidesway is not prevented. In this case the possibility exists that the frame as a whole becomes unstable before the plastic mechanism is formed. If this occurs the structure is said to have failed by

\*frame instability.

Frame instability may manifest itself by one of the following two phenomena:

- 1) If a frame is subjected to a combination of horizontal and vertical forces, it deforms laterally from the first load application. The change in geometry may alter the carrying capacity of the individual column, since the column top is no longer over the column base and hence additional bending moments are introduced by the vertical loads. The whole structure becomes unstable in this deformed position much like the eccentrically loaded beam-column of Art. 7.3. A load-deformation

\* If a calculation of the reduction in strength is desired, the methods of Ref. 7.20 may be used. An approximation of this strength may also be obtained by using the interaction equation (Eq. 7.13), where  $M_p$  is replaced by the critical lateral buckling moment and  $P_y$  is the weak axis buckling load.

curve is shown for this type of instability in Fig. 7.22. At a certain critical loading, the structure continues to deform without an increase of load.

- 2) If a symmetrical structure is loaded by symmetrical vertical forces (Fig. 7.22), it is possible that the frame may pass from a symmetrical, stable deflection configuration to an unsymmetrical, unstable configuration. At this instant the total resistance to an over-all lateral movement becomes zero. The load-deflection curve is characterized by a shift from a situation where  $P$  can increase as the deformations increase to one where large deflections develop without an increase in load. This behavior is analogous to that of a centrally loaded column, in which bifurcation of equilibrium is possible at a certain critical load.

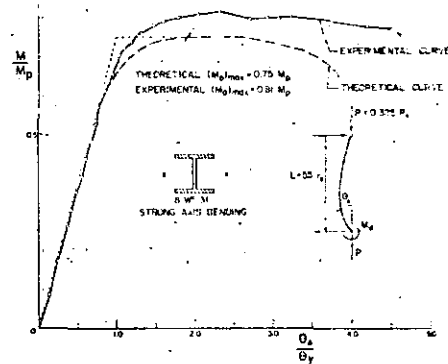


FIG. 7.21.—MOMENT VERSUS END-ROTATION TEST RESULTS.

The first of these phenomena is under study. (7.24) These theoretical and experimental studies are attempting to establish limits of loading and frame geometry in which frame instability will not be a problem. They will have particular application to multi-story frames. This type of instability has never been observed in any of the previous full-scale frame tests. In practical structures additional stiffness is available due to the walls, floor slabs and the roof. None of the aforementioned full-scale frame tests received the benefit of this additional stiffening. Nevertheless, they performed in a satisfactory manner.

The second of these effects has been under extensive investigation for structures where the forces may be assumed to act in the column only, that

is, when primary bending effects can be neglected (Fig. 7.22). A summary of this work can be found in Chapters 6 and 7 of Ref. 6.17 and in Refs. 7.15 and 7.25. In such cases the "effective" length of the column is said to be increased beyond the actual length. Theoretically, it is possible for the effective length to vary from  $K L = L/2$  to  $K L = \infty$ . Usually the restraint offered by the effect of walls, roofs, and floor slabs is sufficient to prevent frame instability, the forces necessary to prevent it being relatively small. (7.26) The most serious instability condition results when the column bases are actually pin ended. It should be pointed out that partial base fixity, affording

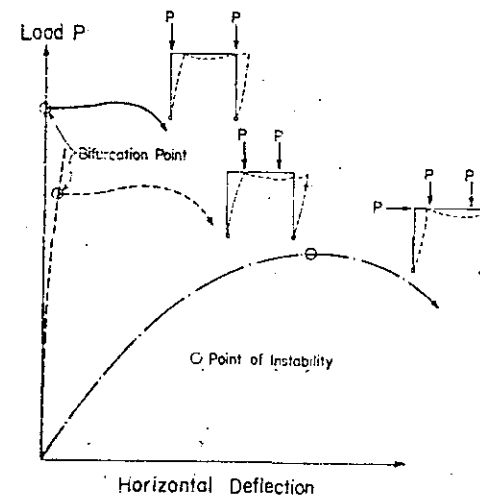


FIG. 7.22.—TYPES OF FRAME INSTABILITY.

even a small amount of resistance to rotation, can reduce the effective length considerably. (7.27)

The loading condition for which the foregoing discussion holds (that is, only axial loads in the columns and little or no bending) is seldom met in practice. Rigid frames are primarily designed to support loads by bending action rather than by compression. It has been shown (as discussed on p. 225, Ref. 6.17) that for a symmetric, single-story, single-bay rigid frame, which is loaded in the beam by two equal, vertical forces at equal distances from the column, the resulting critical load is only slightly smaller than the critical load obtained by placing all the loads on the columns, despite the presence of bending.

At the present time (1961) there is no method by which inelastic frame instability can be predicted precisely. The problem is being studied analytically and

experimentally at several institutions, and it can be expected that some better methods will be forthcoming. Experiments are currently being conducted on steel rigid frame models at Lehigh University to determine the range of the axial force and the slenderness ratio for which frame instability need not be considered.

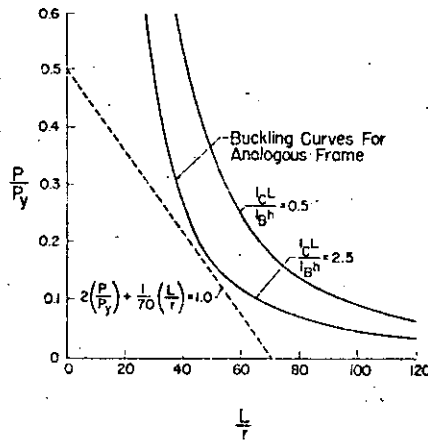
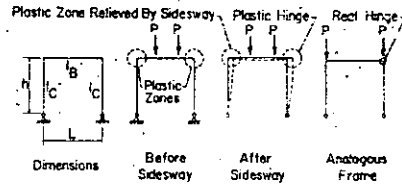


FIG. 7.23.—APPROXIMATE SOLUTION OF FRAME STABILITY IN PLASTIC DESIGN.

Approximate calculations show that frame instability for plastically designed structures will not occur if the slenderness ratio and the axial load ratio of the columns are held within the following limits:

$$2 \left( \frac{P}{P_y} \right) + \left( \frac{1}{70} \right) \left( \frac{L}{r} \right) < 1.00 \dots \dots \dots (7.19)$$

Justification for this rule may be found by considering the single-story, single-bay frame shown in Fig. 7.23. Just before sidesway takes place, par-

tially plastified zones may develop at both knees of the frame. At sidesway the "windward" knee unloads (that is, it becomes elastic again) and the "leeward" knee becomes more plastified due to a corresponding increase in rotation. The curves in Fig. 7.23 show a safe solution of this problem wherein this plastic hinge is replaced by a "real" hinge (resisting moment neglected) and the loads are moved to the top of the columns. The straight line of Eq. 7.19 is seen to be safe when compared to the curves for the analogous frame for the ratio of  $I_C L / b^3 h < 2.5$ . Partial base fixity would increase the resistance of the frame considerably as shown recently by experiments on frame models at Lehigh University, where partial base fixity was accomplished by rigidly attaching a beam between the ends of the columns.

47



8.1 INTRODUCTION

Connections play a key role in assuring that a structure can reach the computed ultimate load. Since connections frequently are located at points of maximum shear and moment, the details must assure the performance that is assumed in design. The principal requirements for connections are:

1. Sufficient strength.
2. Adequate rotation capacity.
3. Overall stiffness for maintaining the location of all structural units relative to each other.
4. Economical fabrication.

The various types of connections which will be discussed and which are typical of those that might be encountered in steel framed structures are designated

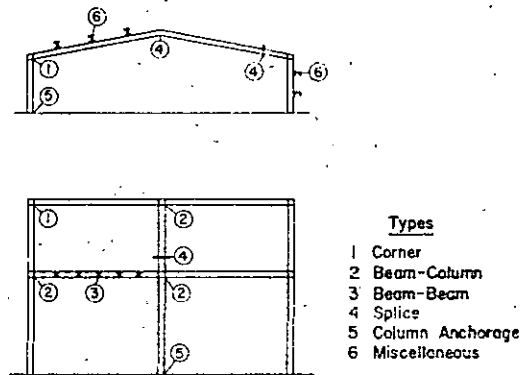


FIG. 8.1.—TYPES OF CONNECTIONS

In Fig. 8.1. These include corner connections (straight and haunched), beam-to-column connections, beam-to-beam connections, splices, column anchorages, and miscellaneous connections (purlins, girts, and bracing).

Primary attention is given herein to corner connections and beam-to-column connections. Methods of analysis are based on assumptions of stress distribution at ultimate load which satisfy equilibrium but do not violate the plasticity condition. Solutions thus constitute lower bounds to connection capacity. The same principles would be applicable, however, for the analysis of other connection types.

8.2 STRAIGHT CORNER CONNECTIONS

Straight corner connections are formed by directly joining two rolled sections. Straight corner connections in which the rolled sections are joined at right angles (as at 1 in Fig. 8.1) are sometimes called square corner connections. Studies of the theory, design, and behavior of square corner connections may be found in Refs. 8.1 to 8.6. The basic principles of the theory of connections will be illustrated by considering an unreinforced square corner connection. It is more critical than a connection in which the members do not join at right angles. Fig. 8.2(a) shows the moment diagram for a typical rectangular frame loaded with a uniformly distributed load. A typical unreinforced

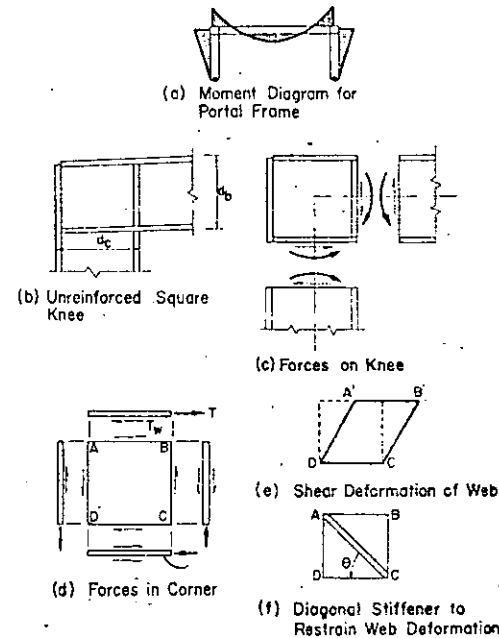


FIG. 8.2.—STRAIGHT CORNER CONNECTIONS

corner connection is sketched in Fig. 8.2(b). The moment, thrust, and shear acting on the connection are depicted in Fig. 8.2(c).

In arriving at a simple analysis of the forces in a knee it is assumed that normal stresses caused by bending moment and thrust are all carried in the flanges and that shear stresses are all carried by the web. In Fig. 8.2(d), the action of the applied forces on the parts of the corner and of the parts on each other are represented by arrows. The tensile force in the outer flange of the

beam is carried into the web in shear along line AB. In a like manner, the tensile force in the outer flange of the column is carried through the endplate into the web as a shear along line AD. In each case, the tensile stress in the flange is assumed to be linearly reduced from  $\sigma_y$  at the edge of the corner (B or D) to zero at the external corner (A).

The prolongation of the inner flange of the beam carries two external forces: the shear of the column and the normal force due to bending and thrust in the beam. The resultant of these two forces is carried into the corner as a shear along line DC. A similar pair of force components exerted on the vertical stiffener causes shear along line BC of the web.

In considering the effect of the forces on the equilibrium and behavior of the corner connection, it is rather obvious that an unsatisfactory condition would exist if there were insufficient material to carry the forces without buckling or general yielding. Assuming that the horizontal rolled section continues through the knee, its flanges AD and CD of Fig. 8.2(d) are sufficient to resist any forces carried in the members outside the knee and are selected to preclude local flange buckling. The end plate AD should have the same area as the flange of the column. The vertical stiffener BC must have sufficient area to carry the column compression flange force into the beam web. In all cases the welds must be sufficient to transmit the required shear or normal force. Study of the square web panel reveals that the shear forces would tend to deform the panel as shown in Fig. 8.2(e).

Consideration of the equilibrium of the horizontal forces on the portion of the outer flange between A and B in Fig. 8.2(d) will give an expression for the web thickness required to resist shear. According to the approximation stated earlier the force in the flange is given by

$$T \approx \frac{M_p}{d_b}$$

in which

$d_b$  = depth of beam

The maximum web shear resisting force between A and B must not exceed

$$T_w = \tau_y w d_c$$

in which

$w$  = thickness of web

$d_c$  = depth of column

Equating the shear and flange forces gives the required web thickness  $w_r$ :

$$w_r = \frac{M_p}{\tau_y d_b d_c}$$

According to the Mises yield criterion for yielding under pure shear the limiting shear yield stress  $\tau_y$  equals  $\sigma_y/\sqrt{3}$ . Using this criterion, the required web thickness becomes

$$w_r = \frac{\sqrt{3} M_p}{\sigma_y d_b d_c} \dots \dots \dots (8.1)$$

This resulting expression for  $w_r$  is similar to that obtained in Ref. 8.1. It has been shown that the use of more exact analysis does not alter the results of calculations substantially.(8.1)

For most wide-flange sections the web thickness will be less than  $w_r$ , in which case reinforcement is required. This may take the form of a doubler plate which increases the total thickness of the web to the required amount. However, it is nearly always more practical to provide a symmetrical pair of diagonal stiffeners. Diagonal stiffeners act somewhat like the diagonals of a truss panel in preventing shear deformation. Fig. 8.2(f) shows diagonal stiffeners between corners A and C of the web. The diagonal stiffeners are able to resist part of the normal stresses in the flanges.

By considering equilibrium of the forces on the top flange, the required area of the diagonal stiffeners may be obtained. The flange force  $T$  must be resisted by the web shear  $T_w$  and the horizontal component of the diagonal stiffener force  $T_s$ . The magnitude of the latter component is given by

$$T_s = \sigma_y A_s \cos \theta$$

in which

$A_s$  = area of a symmetrical pair of diagonal stiffeners

$\theta$  = angle of diagonal stiffeners with the horizontal ( $\tan \theta = d_b/d_c$ )

Noting that  $T$  must equal  $T_w + T_s$  the stiffener area is found as

$$A_s = \frac{1}{\cos \theta} \left[ \frac{M_p}{\sigma_y d_b} - \frac{w d_c}{\sqrt{3}} \right] \dots \dots \dots (8.2)$$

The actual performance of straight corner connections has been studied in several tests. In Fig. 8.3 are shown the results of tests on four straight connections, A, K, L, and M made from 8B13 members.(8.1) The moment-rotation curves of the connections are compared with the moment-rotation curve for an 8D13 beam as shown by the heavy line. Of major interest are strength, stiffness, and rotation capacity. Each connection reached a maximum moment greater than that of an 8B13 beam. The rotation of each of the knees was great enough to be considered adequate to allow a structure to form a mechanism. The initial stiffness of the knees was approximately the same as that of the rolled beam, but larger rotations occurred in the knees at a lower moment because of residual stresses. However the larger rotations were not severe enough to impair the practical effectiveness of the connections.

Results of five additional tests on straight corner connections are given in Fig. 8.4. These tests were performed on knees joining several sizes of wide-flange beams.(8.4) The shaded zone at  $M_h/M_y = M_p$  is so marked to depict the range of spread in shape factor of the five wide flange shapes that were tested. These tests confirm that these knees also satisfied the requirements for use in plastic design.

## STRAIGHT CORNER CONNECTIONS

## Web Thickness Required:

$$w_r = \frac{\sqrt{3} M_p}{\sigma_y d_b d_c} \dots \dots \dots (8.1)$$

## Web Stiffening:

If the web of a connection is deficient in thickness, it may be reinforced by doubler plates to meet the requirements of Eq. 8.1 or by diagonal stiffeners welded to the flanges and to the web. The area of a symmetrical pair of diagonal stiffeners should be

$$A_s = \frac{1}{\cos \theta} \left[ \frac{M_p}{\sigma_y d_b} - \frac{w d_c}{\sqrt{3}} \right] \dots \dots \dots (8.2)$$

In which

$$\theta = \tan^{-1} (d_b/d_c)$$

## 8.3 HAUNCHES

Haunches of either the tapered or the curved type are sometimes used to achieve a pleasing appearance. Their use in elastic design makes it possible to adapt the section of the haunch to follow more closely the shape of the moment diagram, furnishing approximately the resisting moment required at a number of given sections with resulting economies of material. Similarly, in plastic design the use of haunches also makes possible a reduction in size of the main member, which may mean the difference between using a built-up member and using a more economical rolled shape. Although the haunch will permit a reduction in main member size, it will be costly to fabricate and thus may offset some of the savings that will be realized by using the smaller main member.

Tests of haunched connections designed by methods intended primarily for elastic structures revealed that the connections exhibited good strength, but that some lacked sufficient rotation capacity. The lack of rotation capacity was attributed to premature lateral buckling. (8.1) Recently developed methods of analysis confirmed by tests show that plastic hinges can function properly in the haunch if adequate provision is made to prevent such buckling. (8.7)

The effect of haunches on the analysis of a frame is to increase the number of sections at which plastic hinges may form. However, the methods of analysis are unchanged. Fig. 8.5 gives the results of a mechanism analysis of a portal frame with haunches. The correct solution depends on the loading and geometry of the structure. For the given geometry and loading the correct solution would be Mechanism 4 (Fig. 8.5(e)) and the resulting moment diagram (Fig. 8.5(g)) shows that the plasticity condition is not violated. The required plastic hinge moment  $M_p$  of the main members is smaller as a result of using the haunches. At the same time, it is necessary that the haunch be able to carry a moment  $M_h$  which is greater than this  $M_p$ -value. From the final moment diagram (Fig. 8.5(g)) the moment, thrust, and shear at any cross section of the frame may be determined for purposes of design.

## 8.4 TAPERED HAUNCHES

A sketch of a typical tapered haunch is given in Fig. 8.6. The forces to be considered in the design of the haunch are the moment, thrust, and shear at Section 1 where the rolled section is joined to the haunch. These would be determined from an analysis of the complete structure (Fig. 8.5).

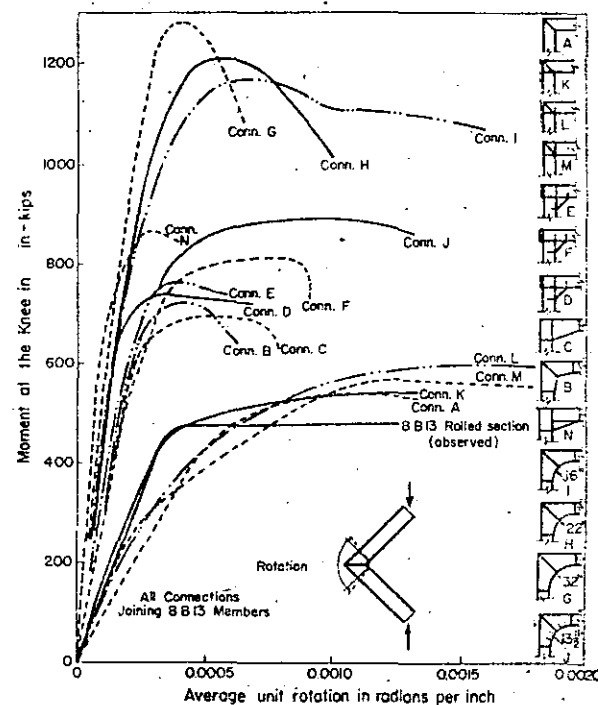


FIG. 8.3.—MOMENT-ROTATION CURVES OF CONNECTIONS

Three main problems must be considered in the design of tapered haunches. These are: (1) resistance to bending in the tapered portion of the haunch, (2) resistance to local and lateral buckling, and (3) shear stresses in the web and flange forces in and around the corner panel BDFE (Fig. 8.6).

In analyzing the tapered portion of the haunch for resistance to bending, cross sections perpendicular to the layout line of the structure may be considered. The web thickness and flange width of the haunch are usually made

equal to those of the adjoining rolled section. This insures that the web is able to carry at least as much shear and axial force as the web of the rolled section. Changes in the resistance to bending moment of the haunch may be controlled, therefore, by the thickness of the flanges and by the depth of the haunch. The outer flange is usually parallel to the layout line and the inner flange makes an angle of taper  $\beta$  with the layout line, thus defining the depth of the haunch at any point. At any distance  $x$  along the haunch, the moment of resistance of the cross section perpendicular to the layout line must equal or exceed the applied moment at that section determined from the plastic analysis.

The plastic moment of resistance of any cross section is given by (8.7)

$$M_{px} = \sigma_y Z_x \dots \dots \dots (8.3)$$

where  $Z_x$  is the plastic modulus at the particular section. It has been shown that if the plastic moment of resistance is adequate at the rolled section (sec-

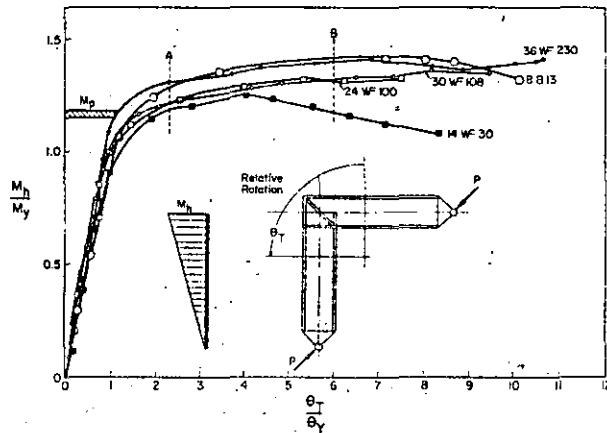


FIG. 8.4.—MOMENT-ROTATION CURVES FOR SIZE-EFFECT SERIES OF CONNECTIONS

tion 1, Fig. 8.6) and at the re-entrant corner (section 2, Fig. 8.6), there will be no necessity of checking at other sections along the haunch. (8.7)

In proportioning tapered haunches, it is desirable that the flanges have the same size as the nominal dimensions of the adjoining rolled section. In this case, the flange area presented on a cross section perpendicular to the layout line would be different for a sloping flange at angle  $\beta$  than for a flange parallel to the layout line. The effective cross section would be unsymmetrical with respect to its major axis with resulting complexities in the calculation of the plastic modulus  $Z$ .

In Ref. 8.7, a somewhat simplified analysis is suggested to reduce the complexities of computations. As shown in Fig. 8.6, the stress in the sloping compression flange is assumed to act in the direction of the flange. To calculate the moment in the desired direction, the component of flange force parallel to

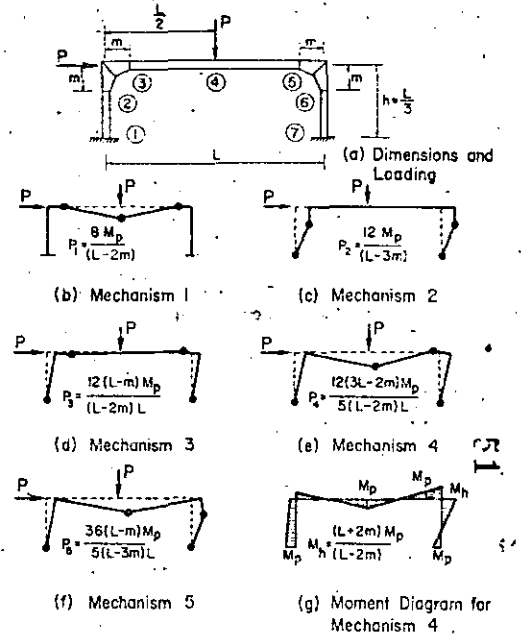


FIG. 8.5.—ILLUSTRATIVE EXAMPLE—ANALYSIS OF PORTAL FRAME WITH HAUNCHES ( $h = L/3$ )

the layout line must be obtained by multiplying the flange force by  $\cos \beta$ . By increasing the area of the sloping flange, the components of flange force in each flange may be made equal, thus providing effective symmetry to the cross section. The necessary area of the sloping flange is

$$A_c = \frac{A_t}{\cos \beta} \dots \dots \dots (8.4)$$

in which

$A_c$  = area of sloping (compression) flange plate

Hence

$$A_s = 2 A_c \sin \left( 22.5^\circ - \frac{\gamma}{4} \right) \dots \dots \dots (8.16)$$

Eq. 8.18 will tend to control the design of diagonal stiffeners for most curved haunches rather than Eq. 8.12. In the case of steeper gables (large  $\gamma$ ), it is possible that Eq. 8.12 may require larger stiffeners.

Results of tests of curved connections (8.8) are given in Fig. 8.3. Test 49 was made on a specimen which had the maximum unsupported flange length recommended by Eq. 8.8 and it performed very well. Test 48 was performed

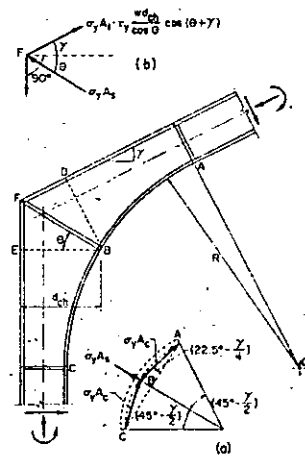


FIG. 8.10.—DIAGONAL STIFFENER FORCES IN A GABLED CURVED HAUNCH

on a specimen with a greater unsupported compression flange length, but with the flange thickness increased to reduce strains. This specimen also performed satisfactorily, but had somewhat less rotation capacity. Results of some earlier tests shown in Fig. 8.3 give an opportunity to observe the effect of radius of curvature on rotation capacity. Connection H with  $R = 5.5 b$  had somewhat less capacity. Connection G with  $R = 8 b$  had the least rotation capacity, and might be considered inadequate. Connection J, of a slightly different design, had  $R = 3.4 b$ , and exhibited very good rotation capacity.

CURVED HAUNCHES

Required Plastic Modulus

The plastic modulus furnished at any point in the haunch must be adequate to resist the applied moment at that point. For typical values of  $R$  and moment gradient, the central angle  $\beta$  to the section controlling the thickness of the flange is about  $12^\circ$ . If the web of the haunch is no thinner than the web of the beam, the thickness of flange required to provide an adequate plastic modulus is given by

$$t_f = \frac{d_x - \sqrt{d_x^2 \left( \frac{b}{b-w} \right) - \frac{4 M_x}{\sigma_y (b-w)}}}{2} \dots \dots (8.13)$$

Lateral Buckling

The critical unbraced length of a curved compression flange strained to the point of strain-hardening without premature lateral buckling is conservatively estimated as

$$L_{cr} = (R \sigma)_{cr} = 4.8 b \dots \dots \dots (8.8)$$

The critical unbraced length of a compression flange may be increased by increasing the thickness of the flanges.

Cross Bending

The effect of cross bending on connection behavior will be negligible if

$$\frac{b^2}{2 R t} \leq 1 \dots \dots \dots (8.16)$$

Diagonal Web Stiffeners

To reinforce the web against buckling due to radial compression in the curved inner flange, a symmetrical pair of diagonal stiffeners may be provided having a total area

$$A_s = 2 A_c \sin \left( 22.5^\circ - \frac{\gamma}{4} \right) \dots \dots \dots (8.18)$$

For steep gabled haunches the diagonal stiffener thickness should also be checked by means of Eq. 8.12.

8.6 BEAM-TO-COLUMN CONNECTIONS

Fig. 8.11 shows three common types of beam-to-column connections used on planar structures. The function of the "Top" and "Interior" connections is to transmit moment from one beam to another, the column carrying any unbalanced moment. The "Side" connection transmits beam moment to the upper and lower columns. The design problem is to provide sufficient stiffening material so that the connection will transmit the moment. Some columns are

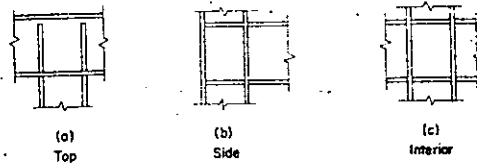


FIG. 8.11.—TYPES OF BEAM-TO-COLUMN CONNECTIONS

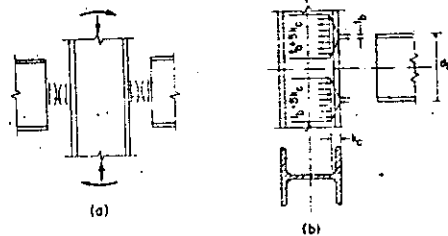


FIG. 8.12.—FORCES ON BEAM-TO-COLUMN CONNECTIONS

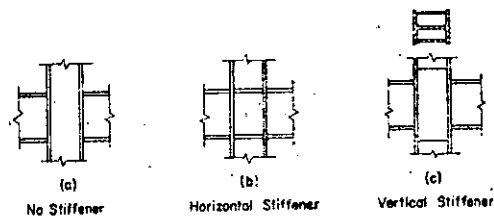


FIG. 8.13.—STIFFENING OF BEAM-TO-COLUMN CONNECTIONS

sturdy enough to carry full-moment beam connections without stiffening. Other columns require stiffening of their webs or flanges to aid in carrying the concentrated forces from the flanges of the connected beams.

Studies on the design and the behavior of full moment interior beam-to-column connections are reported in Refs. 8.9 and 8.10.

In treating problems relating to beam-to-column connections, the case of connections without stiffening will be examined as to the adequacy or inadequacy of the connections, and then some methods of providing necessary stiffening will be presented.

#### Columns Without Stiffeners

In Fig. 8.12(a) are shown schematically the moments and forces on a typical interior beam-to-column connection. In Fig. 8.12(b), the effect of a beam moment on a column is shown as a couple composed of the two flange forces, the beam web forces being of secondary importance. Significant effects of the beam flange forces can occur in two regions in the column. The first region is the column web where yielding may be accompanied by buckling due to the beam compression flange force or by fracture due to the beam tension flange force. The second region is the column flange where bending may contribute to the fracture of welds connecting the beam flange to the column flange.

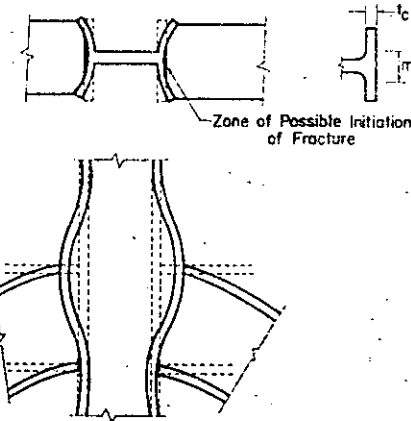


FIG. 8.14.—COLUMN FLANGE BENDING IN TENSION REGION

The tensile force in the beam flange tends to pull the outstanding column flanges as shown in Fig. 8.14. At the toes of the column flanges, flexibility allows the beam and column flanges to deform together. However, at the middle of the column flange where it is restrained by the column web, deformation is restricted and fracture is most likely to start there.

A column without stiffeners must be able to maintain static equilibrium both in regions of web yielding and flange bending. Stresses in the column caused by a concentrated beam flange force will spread out as they penetrate into the column. Because of this, the intensity of stress decreases with deeper penetration. If the spread of stresses is insufficient to reduce their intensity to the yield level at the depth of the base of the column flange fillet ( $k$ -depth), the web will not be able to provide sufficient reactive resistance to the beam flange force. This effect is most serious in the region stressed by the beam compression flange. Rational analysis of the spread of stress in a wide-flange section is difficult and is usually replaced by a linear assumption based on test results. Ref. 8.10 gives the results of several tests and recommends that the stress in the column be assumed to be distributed on a 2.5:1 slope from the point of contact to the column "k-line." As shown in Fig. 8.12(b), this assumption implies that the force of a beam flange is resisted by a length of column web equal to  $(t_b + 5 k_c)$  at the column "k-line," where  $t_b$  is the beam flange thickness and  $k_c$  is the column fillet depth. For equilibrium, the resistance of the effective area of the web must equal or exceed the applied concentrated force of the beam tension or compression flange.

$$\text{Column web resistance} = \sigma_y w_c (t_b + 5 k_c) \dots \dots \dots (8.19)$$

$$\text{Beam flange force} = \sigma_y A_f \dots \dots \dots (8.20)$$

which gives

$$\sigma_y w_c (t_b + 5 k_c) \geq \sigma_y A_f \dots \dots \dots (8.21)$$

in which

$w_c$  = column web thickness

$A_f$  = area of one flange of beam

If the column web resistance is insufficient to carry the beam flange forces, stiffeners must be provided.

Static equilibrium in cases where the column flange thickness is small involves the consideration of bending in the column flange due to the beam tension or compression flange forces. The analysis is further complicated by the fact that the flange bending occurs in two directions, both longitudinal and transverse to the axis of the member as can be visualized from Fig. 8.14. To solve the problem it is necessary to make assumptions regarding the distribution of the beam flange force on the column flange, the extent of the zone of bending in the column flange, and the effect of the central portion where the column flange joins the column web. It may be assumed that the fully yielded beam flange puts a line load on the column flange. For the beam,

$$\text{Beam flange force} = \sigma_y A_f \dots \dots \dots (8.22)$$

The thick center portion of the column flange between the ends of the fillets may be assumed to resist the beam flange force with an axial force as if it were rigid. Thus

$$\text{Column flange direct resistance} = \sigma_y t_b m \dots \dots \dots (8.23)$$

in which

$m$  = distance between fillet extremities of flange of column

The remaining portion of the column flange resistance is due to bending of the projecting portion of the flange, and is affected by the projecting width of flange, thickness of flange, length of line load, length of the zone affected by bending, and strength of the material. In general, the action can be looked on as a case of plate bending, with the flange thickness being the most important geometric property. The force of resistance to the beam flange line load may be expressed by:

$$\text{Column flange bending resistance} = c_1 \sigma_y t_c^2 \dots \dots \dots (8.24)$$

in which

$c_1$  is a coefficient depending on the width of column and beam flanges, extent of two-way bending, distance between column flange fillets, and boundary conditions.

To develop the full yield strength of the beam flange, the column flange resistance must be at least equal to it:

$$\sigma_y A_f = \sigma_y t_b m + c_1 \sigma_y t_c^2 \dots \dots \dots (8.25)$$

If the column flange resistance is found to be deficient, the column flange is too thin, and stiffening is required. This effect is most serious in the region stressed by the beam tension flange.

In Ref. 8.10, Eq. 8.25 is evaluated by means of "yield line theory,"\* assuming a plate bending mechanism which extends for a length of column flange equal to  $12 t_c$ . Additional assumptions of the relative dimensions of beams and columns are made in such a way as to assure the most conservative result. From this combination of assumptions, the column flange thickness to resist a given beam flange area is obtained as follows

$$t_c \geq 0.4 \sqrt{A_f} \dots \dots \dots (8.26)$$

Results of tests showed that connections proportioned according to Eq. 8.26 carried the plastic moment of the beam satisfactorily. Fig. 8.15 shows the results of tests on connections designed to meet the appropriate design criteria. The "A" tests are those without stiffeners which satisfied both Eqs. 8.21 and 8.26.

#### Columns With Stiffeners

If the column web thickness satisfies Eq. 8.21, column stiffeners are not needed adjacent to the beam compression flange. If the column flange thickness satisfies Eq. 8.26, column stiffeners are not needed adjacent to the beam tension flange. If the column proportions fail to satisfy either of these equations, however, stiffeners should be provided. Two types of stiffeners are shown in Fig. 8.13, the horizontal stiffener and the vertical stiffener. Both types of

\* Yield line theory is an upper bound plastic analysis of bending of plates in which plastic hinges are assumed to form along lines in a plate to form a mechanism.

stiffener may be proportioned by considering the additional amount of resisting force required to achieve equilibrium. The stiffeners should also be proportioned to maintain stability under their full load.

Horizontal stiffeners should preferably be furnished in symmetrical pairs opposite both beam flanges. They should be welded to the column flange and web by either groove or fillet welds. Vertical stiffeners should also be furnished in symmetrical pairs and should be deep enough to allow the beam flange force to be dispersed in the stiffener in the same manner in which it is assumed to be dispersed in the web in Eq. 8.19.

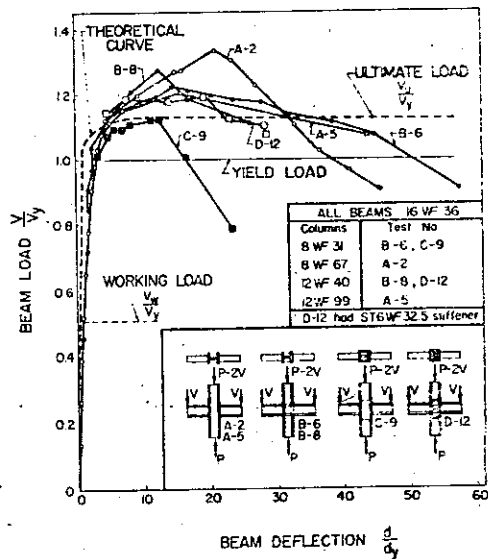


FIG. 8.15.—RESULTS OF TWO-WAY CONNECTION TESTS

Results of tests on connections using both types of stiffening are given in Ref. 8.10. Some of them are shown in Fig. 8.15. These tests and tests without stiffening were used to help establish semi-empirical methods of deciding the need for stiffeners and the proportioning of stiffeners to resist thrusts of beam flanges. If the moments applied by the beams to the columns were unsymmetrical, the same methods would be appropriate.

Critical Parts of Connections

The preceding analyses have shown that the use of stiffeners may depend either on compression in the column web (Eq. 8.21) or on tension normal to the column flange (Eq. 8.26) resulting from the end moments of the beams. For most of the rolled column sections normally only one type of failure need be checked, depending on the proportions of the column. The sections controlled by each type of failure may be tabulated, thus simplifying design.

Eq. 8.21 states that a connection will be on the verge of needing stiffeners in the compression region if

$$A_f = w_c(t_b + 5 k_c) \dots \dots \dots (8.27)$$

From Eqs. 8.26 and 8.27 this connection will or will not need stiffeners in the tension region according to whether

$$t_c \leq 0.4 \sqrt{w_c(t_b + 5 k_c)} \dots \dots \dots (8.28)$$

that is

$$\frac{t_c}{\sqrt{k_c w_c}} \leq 0.4 \sqrt{5 + \frac{t_b}{k_c}} \dots \dots \dots (8.29)$$

For all practical combinations of rolled beams and columns that might be used in this type of connection,

$$0.2 < t_b/k_c < 0.8 \dots \dots \dots (8.30)$$

By taking  $t_b/k_c = 0.2$ , it is seen that this connection will need stiffeners in the tension region if

$$\frac{t_c}{\sqrt{k_c w_c}} < 0.91 \dots \dots \dots (8.31)$$

By taking  $t_b/k_c = 0.8$ , it is seen that the connection will not need stiffeners in the tension region if

$$\frac{t_c}{\sqrt{k_c w_c}} > 0.96 \dots \dots \dots (8.32)$$

Fig. 8.16 shows a plot of the values of  $t_c/\sqrt{k_c w_c}$  for all wide-flange columns in the 8 in., 10 in., 12 in., and 14 in. series. It can be seen that in most cases the column need only be checked for compression. For values of  $t_c/\sqrt{k_c w_c}$  between 0.91 and 0.96 the need for column stiffening will depend on the beam, and both tension and compression should be checked.

Shear Stiffening

When the moments in the two beams at an interior connection differ by a large amount, they may cause large shears in the column web, tending to deform the web in the same manner as in a corner connection (Fig. 8.2(e)). With such an unbalance of moments, the shear in the web should be checked, and if necessary, diagonal stiffeners or a doubler plate should be added. (1.2) In Fig. 8.17(a) the shears and moments acting on a typical connection are shown. Fig. 8.17(b) is a free body diagram of the forces acting on the column web just below the top flange stiffener. The forces are V, the horizontal shear present



In the column above the connection and two tensile flange forces  $T_1$  and  $T_2$ . The flange forces are obtained approximately by dividing the moment in the respective beams by the beam depths. The net result of these forces must be resisted by a shear stress  $\tau$  acting on an area of column web equal to  $w_c d_c$ . Thus

$$\tau w_c d_c = \frac{M_2}{d_b} - \frac{M_1}{d_b} - v \dots (8.33)$$

Assuming that  $\tau_y = \sigma_y/\sqrt{3}$ , the required web thickness to resist shear is

$$w_c = \frac{\sqrt{3}}{\sigma_y d_c} \left( \frac{M_2}{d_b} - \frac{M_1}{d_b} - v \right) \dots (8.34)$$

when the directions of moments and shears are as shown in Fig. 8.17(b). If the actual web thickness of the column is less than that in Eq. 8.34, diagonal

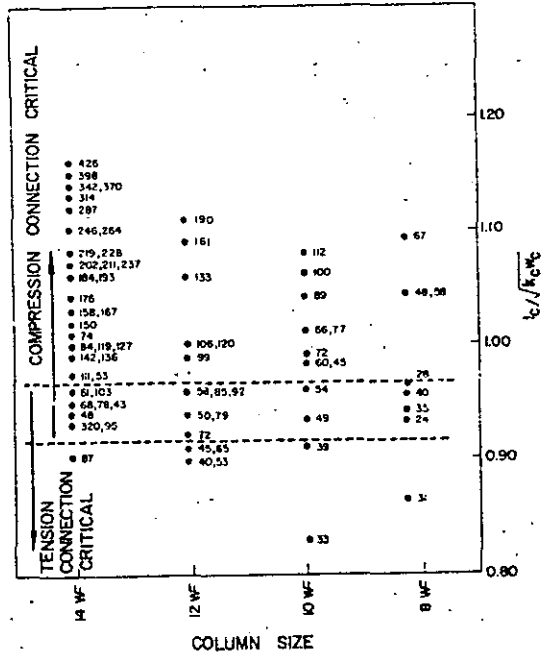


FIG. 8.18.—CRITICAL PARTS OF CONNECTIONS

stiffeners similar to those in Fig. 8.2(f) or web doubler plates could be used to carry the excess shearing force. The special case of a "one-sided" beam-to-column connection is obtained when  $M_1$  equals zero.

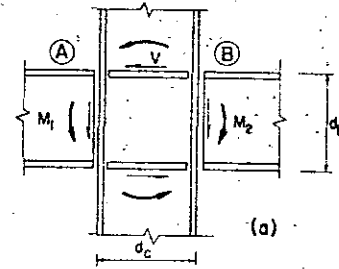


FIG. 8.17a.—SHEAR AND MOMENT ON CONNECTION WITH UNEQUAL MOMENTS ON BEAMS



FIG. 8.17b.—FREE BODY DIAGRAM OF FORCES ACTING ON TOP STIFFENER AND COLUMN WEB

Four-Way Beam-to-Column Connections:

Frequently additional beams must be framed into a single joint on a column forming a four-way beam-to-column connection. Two beams may be framed into a column web either by direct welding or by plate plus seat type of connections. When connections such as these are used, the question has been raised as to whether the triaxial stresses in the column web might cause premature failure, or on the other hand, whether a beneficial effect might be obtained through the partial stiffening action of the beams framing into the column web. A limited number of tests have been made on four-way connections. In the specimens tested, there was no adverse effect of triaxial stresses indicated. (8.10)

Sketches of the four-way connections tested are shown in Fig. 8.18. The direct-welded type, shown in Fig. 8.18(a) had a column web thickness meeting the requirement of Eq. 8.21 and hence the column web required no reinforcement to prevent crippling due to the forces applied to the column flanges by the

beams. The addition of two more identical beams, welded directly to the column web, appeared to stiffen the web. In the second type of connection (Fig. 8.18(b)), the horizontal plates which served as top plate and seat plate for the beams framing into the column web also served as stiffeners for the column. Because the beams framing into the web were not as deep as those welded to the column flanges, the bottom stiffener was 4 in. away from its ideal location opposite the lower flange of the deeper beam. However, the connection per-

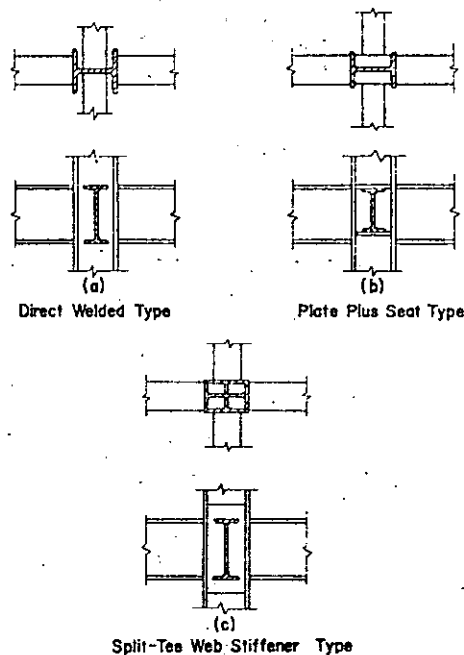


FIG. 8.18.—TYPES OF FOUR-WAY INTERIOR BEAM-TO-COLUMN CONNECTIONS

formed satisfactorily. The connection in Fig. 8.18(c) used split-tee sections for stiffeners in the same way that vertical plates had been used in two-way connections. The stems of the tees served to support both the stiffeners and the column web. The flanges of the split tees served as suitable surfaces to which beams could be directly welded to complete the connection. The performance of this connection was also satisfactory. The four-way connection

tests of Ref. 8.10 were performed with considerable axial load in the columns in order that the results could reflect the influence of this practical loading situation. All of these tests were performed under a symmetrical moment condition. Some special problems still remain to be solved when unequal moments are introduced.

For the design of four-way connections Ref. 8.10 recommends that the connection of the beams to the column flange be designed exactly as in a two-way connection as if the beams framing to the column web were not present. Test specimens of four-way connections designed on this assumption performed better than comparable two-way connections.

#### BEAM-TO-COLUMN CONNECTIONS (Beams Joined to Column Flanges)

##### Unstiffened Columns

Column stiffeners are not needed adjacent to the beam compression flanges if

$$w_c \geq \frac{-A_f}{t_b + 5k_c} \dots \dots \dots (8.21)$$

Column stiffeners are not needed adjacent to the beam tension flanges if

$$t_c \geq 0.4 \sqrt{A_f} \dots \dots \dots (8.26)$$

##### Column Stiffeners

Column stiffeners at points of bearing of beam flanges should be proportioned to carry the excess of beam flange force over that which the column web and flange are able to carry. (Stiffeners should also be proportioned so as not to buckle.)

##### Shear Stiffening in Column

When unbalanced moments or external forces cause shear stresses in excess of the column web capacity, stiffening should be provided for the column. Such stiffening may take the form of diagonal stiffeners or web doubler plates.

#### 8.7 DETAILS WITH REGARD TO WELDING

In butt welds, the forces are carried in compression or tension, and are limited by the tensile or compressive resistance of the base metal or weld metal depending on which is least. Since weld metal is stronger than the base metal normally used in any joint, the strength of butt welds should be calculated on the basis of  $\sigma_y$ , the yield strength of the base metal.

A nominal shear stress of 22.4 ksi was selected for fillet welds. The basis for the 22.4 ksi stress was a load factor of 1.65 applied to a working stress of 13.6 ksi as presently (1961) permitted by the AWS code for building construction. (8.11) Thus the calculated shear stress at maximum load exceeded the

working stress by the same ratio that a normal stress of 33 ksi exceeds a working stress of 20 ksi. Use of these stresses at ultimate load results in weld sizes for a simple beam which are usually the same as those which have proven satisfactory for years in allowable stress design.

The results of the tests in connections described in Refs. 8.4, 8.6, and 8.8 verified that the welds designed using these assumptions were adequate in that no weld failure occurred.

#### WELD STRESSES

Butt welds may be assumed capable of developing on their minimum throat section the tensile yield stress of the base metal.

Fillet welds may be assumed to be capable of developing at least the shearing yield stress of the weld metal on their minimum throat section. A safe design value may be obtained by multiplying the value presently used in allowable stress design by the ratio  $\sigma_v/\sigma_w$ , where  $\sigma_w$  is the allowable tensile stress of the material being used.

#### 8.8 DETAILS WITH REGARD TO BOLTING

Bolted joints in plastic design will probably have their greatest application as field joints for erection of structures.

It could be argued that judicious selection of the locations of such joints will place them at points of low moment so that the joints will remain elastic. The design of these joints then could be handled by conventional elastic methods. However, it sometimes becomes advantageous to make field connections at points of high moment. It is thus advisable to have available methods for proportioning bolted joints to develop the full plastic moment of the connected members.

Two possible approaches available for full capacity connections are (1) to keep all parts of the joint "elastic" at maximum moment, and (2) to design parts of the joints so that fasteners and plates may yield at maximum moment along with the main members. Recent studies have emphasized the latter approach.

A limited amount of research has been performed on bolted joints designed to develop the full plastic moment of beams. Refs. 8.12 and 8.13 give the results of tests of connections using ASTM A-325 high tensile bolts. The connections in Ref. 8.12 included both beam splices and beam-to-column connections and for each case there were examples with the bolts in shear and in tension. The connections in Ref. 8.13 were butt-type connections with the bolts in tension. The results of the test programs show that it is possible to design and fabricate high tensile bolted joints which will develop the full bending strength of a member. Fig. 8.19 gives the general layout of joints which performed satisfactorily as reported in Refs. 8.12 and 8.13.

Methods of analysis and design are not discussed in detail in Ref. 8.12. Methods are discussed in Ref. 8.13, but the author suggests that better procedures based on the same fundamentals can be developed.

The essential features of any analysis of a full-moment bolted connection are the assumptions as to the load capacity of each individual bolt, the manner in which the compressive components of force are to be carried, the location of the neutral axis, and the strength of any detail material (fittings) used in forming the joint. It seems reasonable to conclude that precise solutions for the ultimate strength of joints are not necessary provided that the solutions constitute lower bounds.

An example of the assumptions that might be made in designing a high strength bolted joint is given in Ref. 8.13 as exemplified by Fig. 8.19(a), 8.19(c), and 8.19(f). The number and location of bolts in a joint were first assumed. For the bolts in tension, an "ultimate" load capacity was taken in this reference as 1.3 times the proof load of the bolts. The shear resistance provided by each bolt at ultimate load due to friction was taken at one-fourth its initial tension. All structural steel parts of the joint were assumed to be stressed to yield point. To analyze the trial design, a compression area was computed sufficient to resist the combined reaction of all the "working" bolts, that is, those on the

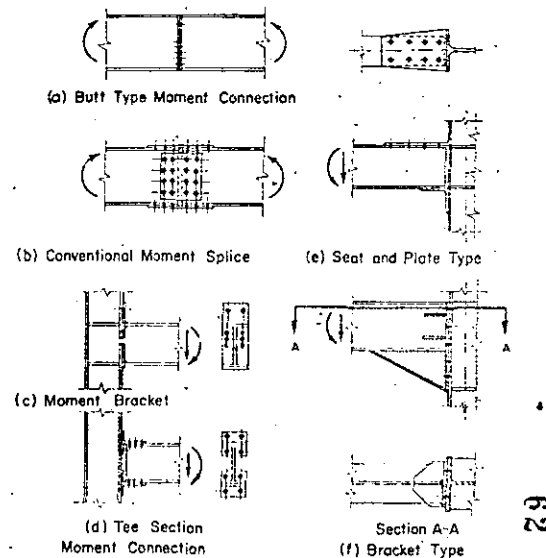


FIG. 8.19.—TYPES OF PLASTIC MOMENT CARRYING HIGH TENSILE BOLTED CONNECTIONS

tension side of the neutral axis (axis of rotation). The bending moment produced by the couple made up of the bolt tension forces and the compression force, had to equal or exceed the applied bending moment.

Ref. 8.13 notes that plastically designed joints with high tensile bolts in tension require a smaller number of bolts and less fitting material than conventional moment splices which use the bolts only in shear.

Although accurate procedures leading to the most economical safe design are not yet available, the results of research show that safe bolted joints can be designed to develop the plastic moment of the members with reasonable economy.

8.1 INTRODUCTION

Connections play a key role in assuring that a structure can reach the computed ultimate load. Since connections frequently are located at points of maximum shear and moment, the details must assure the performance that is assumed in design. The principal requirements for connections are:

1. Sufficient strength.
2. Adequate rotation capacity.
3. Overall stiffness for maintaining the location of all structural units relative to each other.
4. Economical fabrication.

The various types of connections which will be discussed and which are typical of those that might be encountered in steel framed structures are designated

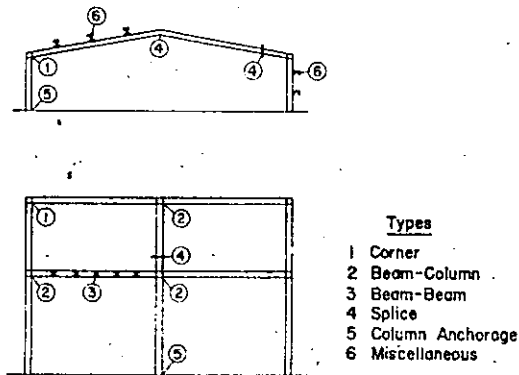


FIG. 8.1.—TYPES OF CONNECTIONS.

in Fig. 8.1. These include corner connections (straight and haunched), beam-to-column connections, beam-to-beam connections, splices, column anchorages, and miscellaneous connections (purlins, girts, and bracing).

Primary attention is given herein to corner connections and beam-to-column connections. Methods of analysis are based on assumptions of stress distribution at ultimate load which satisfy equilibrium but do not violate the plasticity condition. Solutions thus constitute lower bounds to connection capacity. The same principles would be applicable, however, for the analysis of other connection types.

8.2 STRAIGHT CORNER CONNECTIONS

Straight corner connections are formed by directly joining two rolled sections. Straight corner connections in which the rolled sections are joined at right angles (as at 1 in Fig. 8.1) are sometimes called square corner connections. Studies of the theory, design, and behavior of square corner connections may be found in Refs. 8.1 to 8.6. The basic principles of the theory of connections will be illustrated by considering an unreinforced square corner connection. It is more critical than a connection in which the members do not join at right angles. Fig. 8.2(a) shows the moment diagram for a typical rectangular frame loaded with a uniformly distributed load. A typical unreinforced

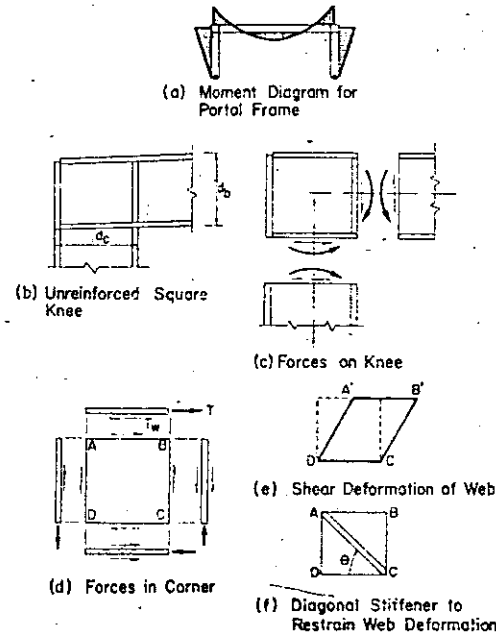


FIG. 8.2.—STRAIGHT CORNER CONNECTIONS

corner connection is sketched in Fig. 8.2(b). The moment, thrust, and shear acting on the connection are depicted in Fig. 8.2(c).

In arriving at a simple analysis of the forces in a knee it is assumed that normal stresses caused by bending moment and thrust are all carried in the flanges and that shear stresses are all carried by the web. In Fig. 8.2(d), the action of the applied forces on the parts of the corner and of the parts on each other are represented by arrows. The tensile force in the outer flange of the

beam is carried into the web in shear along line AB. In a like manner, the tensile force in the outer flange of the column is carried through the endplate into the web as a shear along line AD. In each case, the tensile stress in the flange is assumed to be linearly reduced from  $\sigma_y$  at the edge of the corner (B or D) to zero at the external corner (A).

The prolongation of the inner flange of the beam carries two external forces: the shear of the column and the normal force due to bending and thrust in the beam. The resultant of these two forces is carried into the corner as a shear along line DC. A similar pair of force components exerted on the vertical stiffener causes shear along line BC of the web.

In considering the effect of the forces on the equilibrium and behavior of the corner connection, it is rather obvious that an unsatisfactory condition would exist if there were insufficient material to carry the forces without buckling or general yielding. Assuming that the horizontal rolled section continues through the knee, its flanges AB and CD of Fig. 8.2(d) are sufficient to resist any forces carried in the members outside the knee and are selected to preclude local flange buckling. The end plate AD should have the same area as the flange of the column. The vertical stiffener BC must have sufficient area to carry the column compression flange force into the beam web. In all cases the welds must be sufficient to transmit the required shear or normal force. Study of the square web panel reveals that the shear forces would tend to deform the panel as shown in Fig. 8.2(e).

Consideration of the equilibrium of the horizontal forces on the portion of the outer flange between A and B in Fig. 8.2(d) will give an expression for the web thickness required to resist shear. According to the approximation stated earlier the force in the flange is given by

$$T \approx \frac{M_p}{d_b}$$

in which

$d_b$  = depth of beam

The maximum web shear resisting force between A and B must not exceed

$$T_w = \tau_y w d_c$$

in which

$w$  = thickness of web

$d_c$  = depth of column

Equating the shear and flange forces gives the required web thickness  $w_r$ :

$$w_r = \frac{M_p}{\tau_y d_b d_c}$$

According to the Mises yield criterion for yielding under pure shear the limiting shear yield stress  $\tau_y$  equals  $\sigma_y/\sqrt{3}$ . Using this criterion, the required web thickness becomes

$$w_r = \frac{\sqrt{3} M_p}{\sigma_y d_b d_c} \quad (8.1)$$

This resulting expression for  $w_r$  is similar to that obtained in Ref. 8.1. It has been shown that the use of more exact analysis does not alter the results of calculations substantially.(8.1)

For most wide-flange sections the web thickness will be less than  $w_r$ , in which case reinforcement is required. This may take the form of a doubler plate which increases the total thickness of the web to the required amount. However, it is nearly always more practical to provide a symmetrical pair of diagonal stiffeners. Diagonal stiffeners act somewhat like the diagonals of a truss panel in preventing shear deformation. Fig. 8.2(f) shows diagonal stiffeners between corners A and C of the web. The diagonal stiffeners are able to resist part of the normal stresses in the flanges.

By considering equilibrium of the forces on the top flange, the required area of the diagonal stiffeners may be obtained. The flange force  $T$  must be resisted by the web shear  $T_w$  and the horizontal component of the diagonal stiffener force  $T_s$ . The magnitude of the latter component is given by

$$T_s = \sigma_y A_s \cos \theta$$

in which

$A_s$  = area of a symmetrical pair of diagonal stiffeners

$\theta$  = angle of diagonal stiffeners with the horizontal ( $\tan \theta = d_b/d_c$ )

Noting that  $T$  must equal  $T_w + T_s$  the stiffener area is found as

$$A_s = \frac{1}{\cos \theta} \left[ \frac{M_p}{\sigma_y d_b} - \frac{w d_c}{\sqrt{3}} \right] \quad (8.2)$$

The actual performance of straight corner connections has been studied in several tests. In Fig. 8.3 are shown the results of tests on four straight connections, A, K, L, and M made from 8B13 members.(8.1) The moment-rotation curves of the connections are compared with the moment-rotation curve for an 8B13 beam as shown by the heavy line. Of major interest are strength, stiffness, and rotation capacity. Each connection reached a maximum moment greater than that of an 8B13 beam. The rotation of each of the knees was great enough to be considered adequate to allow a structure to form a mechanism. The initial stiffness of the knees was approximately the same as that of the rolled beam, but larger rotations occurred in the knees at a lower moment because of residual stresses. However the larger rotations were not severe enough to impair the practical effectiveness of the connections.

Results of five additional tests on straight corner connections are given in Fig. 8.4. These tests were performed on knees joining several sizes of wide-flange beams.(8.4) The shaded zone at  $M_H/M_y = M_p$  is so marked to depict the range of spread in shape factor of the five wide flange shapes that were tested. These tests confirm that these knees also satisfied the requirements for use in plastic design.

## STRAIGHT CORNER CONNECTIONS

Web Thickness Required:

$$w_r = \frac{\sqrt{3} M_p}{\sigma_y d_b d_c} \dots \dots \dots (8.1)$$

Web Stiffening:

If the web of a connection is deficient in thickness, it may be reinforced by doubler plates to meet the requirements of Eq. 8.1 or by diagonal stiffeners welded to the flanges and to the web. The area of a symmetrical pair of diagonal stiffeners should be

$$A_s = \frac{1}{\cos \theta} \left[ \frac{M_p}{\sigma_y d_b} - \frac{w d_c}{\sqrt{3}} \right] \dots \dots \dots (8.2)$$

In which

$$\theta = \tan^{-1} (d_b/d_c)$$

## 8.3 HAUNCHES

Haunches of either the tapered or the curved type are sometimes used to achieve a pleasing appearance. Their use in elastic design makes it possible to adapt the section of the haunch to follow more closely the shape of the moment diagram, furnishing approximately the resisting moment required at a number of given sections with resulting economies of material. Similarly in plastic design the use of haunches also makes possible a reduction in size of the main member, which may mean the difference between using a built-up member and using a more economical rolled shape. Although the haunch will permit a reduction in main member size, it will be costly to fabricate and thus may offset some of the savings that will be realized by using the smaller main member.

Tests of haunched connections designed by methods intended primarily for elastic structures revealed that the connections exhibited good strength, but that some lacked sufficient rotation capacity. The lack of rotation capacity was attributed to premature lateral buckling. (8.1) Recently developed methods of analysis confirmed by tests show that plastic hinges can function properly in the haunch if adequate provision is made to prevent such buckling. (8.7)

The effect of haunches on the analysis of a frame is to increase the number of sections at which plastic hinges may form. However, the methods of analysis are unchanged. Fig. 8.5 gives the results of a mechanism analysis of a portal frame with haunches. The correct solution depends on the loading and geometry of the structure. For the given geometry and loading the correct solution would be Mechanism 4 (Fig. 8.5(e)) and the resulting moment diagram (Fig. 8.5(g)) shows that the plasticity condition is not violated. The required plastic hinge moment  $M_p$  of the main members is smaller as a result of using the haunches. At the same time, it is necessary that the haunch be able to carry a moment  $M_h$  which is greater than this  $M_p$ -value. From the final moment diagram (Fig. 8.5(g)) the moment, thrust, and shear at any cross section of the frame may be determined for purposes of design.

## 8.4 TAPERED HAUNCHES

A sketch of a typical tapered haunch is given in Fig. 8.6. The forces to be considered in the design of the haunch are the moment, thrust, and shear at Section 1 where the rolled section is joined to the haunch. These would be determined from an analysis of the complete structure (Fig. 8.5).

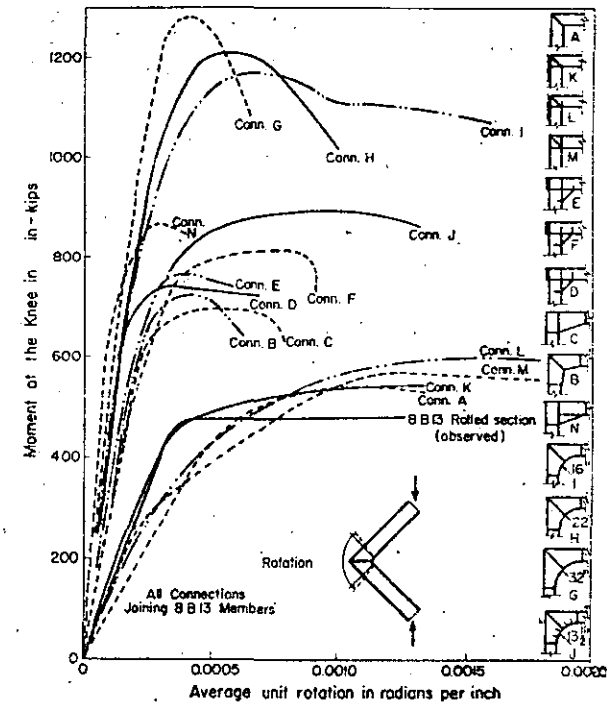


FIG. 8.3.—MOMENT-ROTATION CURVES OF CONNECTIONS

Three main problems must be considered in the design of tapered haunches. These are: (1) resistance to bending in the tapered portion of the haunch, (2) resistance to local and lateral buckling, and (3) shear stresses in the web and flange forces in and around the corner panel BDFE (Fig. 8.6).

In analyzing the tapered portion of the haunch for resistance to bending, cross sections perpendicular to the layout line of the structure may be considered. The web thickness and flange width of the haunch are usually made

equal to those of the adjoining rolled section. This insures that the web is able to carry at least as much shear and axial force as the web of the rolled section. Changes in the resistance to bending moment of the haunch may be controlled, therefore, by the thickness of the flanges and by the depth of the haunch. The outer flange is usually parallel to the layout line and the inner flange makes an angle of taper  $\beta$  with the layout line, thus defining the depth of the haunch at any point. At any distance  $x$  along the haunch, the moment of resistance of the cross section perpendicular to the layout line must equal or exceed the applied moment at that section determined from the plastic analysis.

The plastic moment of resistance of any cross section is given by (8.7)

$$M_{px} = \sigma_y Z_x \dots \dots \dots (8.3)$$

where  $Z_x$  is the plastic modulus at the particular section. It has been shown that if the plastic moment of resistance is adequate at the rolled section (sec-

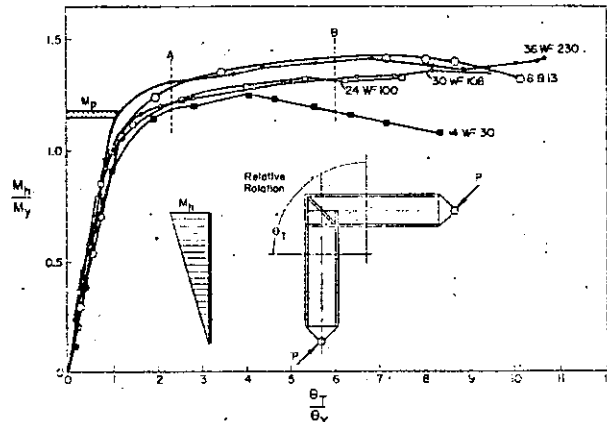


FIG. 8.4.—MOMENT-ROTATION CURVES FOR SIZE-EFFECT SERIES OF CONNECTIONS

tion 1, Fig. 8.6) and at the re-entrant corner (section 2, Fig. 8.6), there will be no necessity of checking at other sections along the haunch. (8.7)

In proportioning tapered haunches, it is desirable that the flanges have the same size as the nominal dimensions of the adjoining rolled section. In this case, the flange area presented on a cross section perpendicular to the layout line would be different for a sloping flange at angle  $\beta$  than for a flange parallel to the layout line. The effective cross section would be unsymmetrical with respect to its major axis with resulting complexities in the calculation of the plastic modulus  $Z$ .

In Ref. 8.7, a somewhat simplified analysis is suggested to reduce the complexities of computations. As shown in Fig. 8.6, the stress in the sloping compression flange is assumed to act in the direction of the flange. To calculate the moment in the desired direction, the component of flange force parallel to

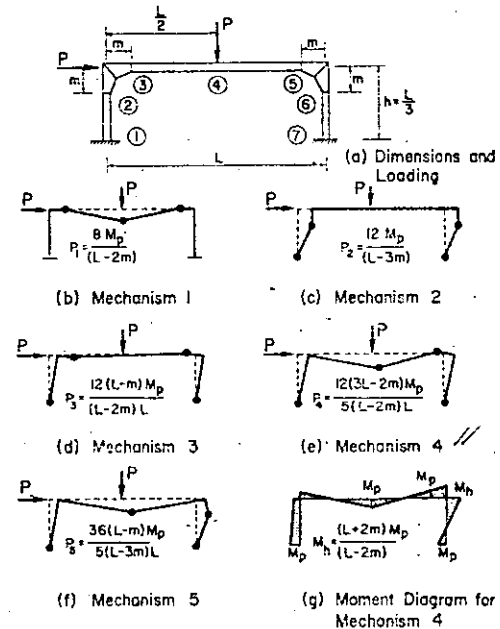


FIG. 8.5.—ILLUSTRATIVE EXAMPLE—ANALYSIS OF PORTAL FRAME WITH HAUNCHES ( $h = L/3$ )

the layout line must be obtained by multiplying the flange force by  $\cos \beta$ . By increasing the area of the sloping flange, the components of flange force in each flange may be made equal, thus providing effective symmetry to the cross section. The necessary area of the sloping flange is

$$A_c = \frac{A_t}{\cos \beta} \dots \dots \dots (8.4)$$

in which

$A_c$  = area of sloping (compression) flange plate

66

$A_t$  = area of straight (tension) flange plate  
 $\beta$  = angle between sloping flange and layout line  
 The plastic modulus at any section will be

$$Z_x = b t_f (d_x - t_f) + \frac{w}{4} (d_x - 2 t_f)^2 \dots \dots \dots (8.5)$$

in which

- $b$  = width of flange
- $d_x$  = depth of haunch at any section  $x$
- $w$  = web thickness
- $t_f$  = thickness of the straight (tension) flange plate

In cases where the angle  $\beta$  is less than  $20^\circ$ , the required increase in area suggested in Eq. 8.4 would not exceed 6%. Most practical design procedures would neglect such a difference. For all practical purposes, both

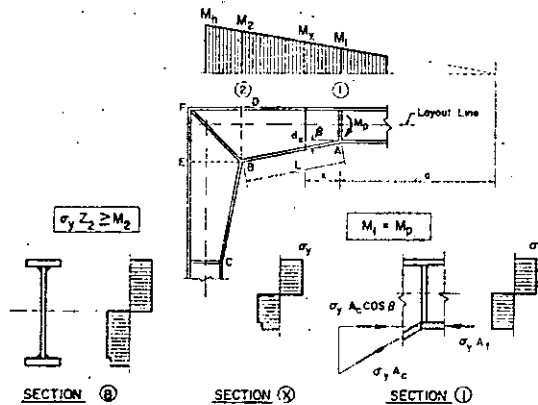


FIG. 8.6.—FORCES ON TAPERED HAUNCH

flanges should probably be made equal and still use the assumption that the cross section is symmetrical and that its centroid is at mid-depth.

The resistance to local buckling of the flanges of tapered haunches may be assured by adhering to the recommendations of Chapter 6.

Lateral buckling of tapered haunches depends on the slenderness of the compression flange and on the extent to which the flange is yielded and strain hardened. It is assumed that positive lateral support of the inner flange will be provided at points A, B, and C (Fig. 8.6). Since the web provides restraint against buckling of the flange about its weak axis, the flange must buckle in its strong direction between points of support.

A conservative approximate expression for the critical buckling length of the compression flange has been obtained (8.7) by using the tangent modulus.

5

buckling concept (6.25, 6.17). It is assumed that the compression flange is uniformly stressed to  $\sigma_y$ , that the strain in the flange just reaches  $\epsilon_{st}$ , and that the flange buckles as a pin-ended column between points of lateral bracing. These assumptions result in a critical slenderness of:

$$\left(\frac{L_{cr}}{r_x}\right)^2 = \pi^2 \frac{E_{st}}{\sigma_y} \dots \dots \dots (8.6)$$

which when solved for  $L_{cr}$  gives:

$$L_{cr} = b \pi \sqrt{\frac{E_{st}}{12 \sigma_y}} \dots \dots \dots (8.7)$$

in which

- $L_{cr}$  = critical length for lateral buckling of compression flange
- $b$  = width of flange
- $r_x$  = radius of gyration of flange =  $b/\sqrt{12}$
- $E_{st}$  = strain-hardening modulus of steel
- $\sigma_y$  = yield stress of steel assumed in the design

By substituting the material properties,  $E_{st}$  (assumed to be 900 ksi at initial strain-hardening) and  $\sigma_y$  (assumed to be 33 ksi) the following critical length is obtained for fully strain-hardened compression flanges of ASTM-A 7 type steel:

$$L_{cr} = 4.8 b \dots \dots \dots (8.8)$$

This expression neglects any restraint to buckling offered by adjacent portions of the flange or by the web.

Frequently it will be found that  $L_{cr}$  given by Eq. 8.8 will be less than the value obtained from the original haunch layout. In such a case, additional points of lateral support could be provided. Also the flange thickness or the depth of the haunch at Section 2 (Fig. 8.6) could be increased. Ref. 8.7 suggests methods for accomplishing such modifications.

The shear stresses in the web and flange forces around the corner panel BDFE (Fig. 8.6) are of the same character as those shown in Fig. 8.2(d) for a square corner, and would result in deformation similar to that in Fig. 8.2(c) when the forces exceed the shear strength of the panel. The problem may be examined in more general form with the aid of the sketch of a haunched knee of a gable bent shown in Fig. 8.7. In this knee, the forces on the panel BDFE are to be determined. For the most severe loading, the cross sections BD and BE will be fully yielded and the total area of the flanges at these sections will be stressed to  $\sigma_y$ . At the re-entrant corner B, the inner flanges will have an unbalanced component of force in the direction of BF in the absence of a web stiffener. This unbalanced component of flange force would have to be carried by the web. The web could be fully yielded due to bending stresses at point B, so it is advisable to neglect the carrying capacity of the web and furnish a symmetrical pair of diagonal stiffeners along FB.

At the outer corner F, the situation is slightly different because part of the flange force could be carried by shear in the web along lines EF and DF thus reducing the components of flange force to be carried by the diagonal stiffeners at F. For this reason, the selection of diagonal stiffeners will usually be governed by equilibrium at the re-entrant corner B.

67



$$\sum F_x = \sigma_y A_1 \cos \theta - \tau_y \frac{w d_{ch}}{\cos \theta} \cos(\theta + \gamma) \cos \theta - \tau_y (\sigma_y A_2 \cos \theta) = 0 \quad (8.11)$$

The maximum possible forces in the two flanges and in the diagonal stiffener at corner B are shown in Fig. 8.7(a). The required area of the diagonal stiffener may be determined from an equation of equilibrium of horizontal components of these forces as follows:

$$\sum F_x = \sigma_y A_B \cos \theta - \sigma_y A_{c1} \cos(\beta_1 + \gamma) + \sigma_y A_{c2} \sin \beta_2 = 0 \dots (8.9)$$

then

$$A_B = \frac{A_{c1} \cos(\beta_1 + \gamma) - A_{c2} \sin \beta_2}{\cos \theta} \dots (8.10)$$

- in which
- $A_B$  = area of a symmetrical diagonal stiffener
- $A_{c1}$  = area of a symmetrical part of diagonal stiffener
- $A_{c2}$  = area of inner flange of rafter haunch
- $A_{c2}$  = area of inner flange of column haunch
- $\gamma$  = angle of inclination of rafter
- $\theta$  = angle of slope of diagonal stiffener
- $\beta_1$  = angle of taper of rafter haunch
- $\beta_2$  = angle of taper of column haunch

In Fig. 8.7(b) the maximum possible forces at the outer corner F are shown. Equilibrium of horizontal components gives

$$\sigma_y A_{11} \cos \gamma - \tau_y \frac{w d_{ch}}{\cos \theta} \cos(\theta + \gamma) \cos \gamma - \sigma_y A_{11} \cos \theta = 0 \dots (8.11)$$

Substituting  $\tau_y = \sigma_y / \sqrt{3}$  and solving for the required stiffener area gives

$$A_B = \left[ \frac{A_{11}}{\cos \theta} - \frac{w d_{ch} \cos(\theta + \gamma)}{\sqrt{3} \cos^2 \theta} \right] \cos \gamma \dots (8.12)$$

- in which
- $A_{11}$  = area of outer flange of beam haunch
- $w$  = web thickness of haunch
- $d_{ch}$  = depth of column haunch at section EB (Fig. 8.7)

If Eq. 8.12 should result in a zero or negative value for  $A_B$ , the implication is that the shear capacity of the web is adequate to transmit the outer flange force, and that diagonal stiffeners are needed only to transmit the unbalance of the inner flange force. Since in any case the web will carry some force, Eq. 8.10 based on equilibrium at the inner corner will control for ordinary haunch proportions rather than Eq. 8.12.

Transverse stiffeners at the junctions of the tapered and prismatic sections (points A and C) may be designed to carry the unbalance of the flange forces due to the sudden change in direction. Since the angles  $\beta_1$  and  $\beta_2$  are generally quite small, the size of the stiffeners usually will be governed by minimum size requirements.

A series of tests of haunched corner connections has given experimental results agreeing very well with the concepts just outlined. (8.8) Moment-

rotation curves for these tests are shown in Fig. 8.8. Specimens 44 and 45 were made with the critical length of compression flange as given by Eq. 8.8. Specimen 44 was not braced against twisting at the inner corner while specimen 45 was braced. Specimen 45 performed satisfactorily while specimen 44 buckled before it reached the computed ultimate load although it exhibited considerable post buckling strength. Specimens 46 and 47 had compression-flange lengths

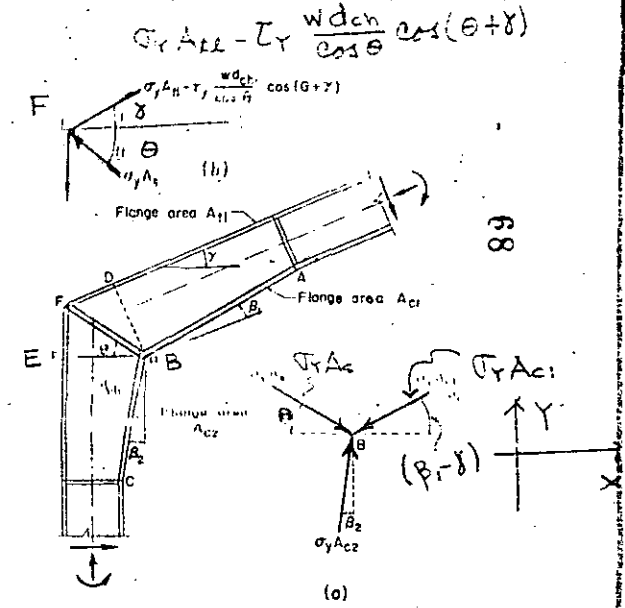


FIG. 8.7.—DIAGONAL STIFFENER FORCES IN A GABLED TAPERED HAUNCH

greater than that given by Eq. 8.8, but were modified by increasing the haunch depth and by increasing the flange thicknesses respectively. These specimens also performed satisfactorily in that they met the requirements stated earlier.

The results of these tests indicate that safe and adequate connections may be made by meeting the requirements derived by the theory. In summary, the following suggestions are made with regard to proportioning of tapered haunched connections:

**TAPERED HAUNCHES**

Fig. 8.7

**Required Plastic Modulus:**

The plastic modulus should be checked for resistance to the applied moment at the deep end and the shallow end of each haunch.

**Local Buckling:**

The recommendations of Chapter 6 should be followed to assure that premature local buckling of flanges will not occur.

**Lateral Buckling:**

The critical unbraced length of a compression flange which may be strained to the point of strain-hardening throughout its entire length without premature lateral buckling is conservatively estimated as:

$$L_{CR} = 4.8 b \quad (8.8)$$

The critical unbraced length of a compression flange may be increased substantially by increasing the angle of taper  $\beta$  or by increasing the thickness of the flanges.

**Diagonal Web Stiffeners:**

To resist an unbalance of inner flange forces and reinforce the web against undue shear deformation, a symmetrical pair of diagonal stiffeners may be provided having a total area:

$$A_B = \frac{A_{c1} \cos(\beta_1 + \gamma) - A_{c2} \sin \beta_2}{\cos \theta} \quad (8.10)$$

Diagonal stiffeners should be welded to the web and to both flanges.

**Transverse Stiffeners:**

Transverse stiffeners at the junctions of the tapered haunch and prismatic section serve to carry the unbalance of the inner flange force due to the sudden change in direction. Minimum size requirements will usually govern the thickness.

**8.5 CURVED HAUNCHES**

In Fig. 8.9 are shown the layout and the applied forces for a typical curved haunch. The haunch must be designed to withstand the plastic hinge moment of the rolled section at its connection to the haunch and any larger moment which develops in the haunched portion as a result of the moment gradient.

As with tapered haunches, the three main problems to be considered in the design of curved haunches are: (1) resistance to bending in the haunch, (2) resistance to local and lateral buckling, and (3) shear stresses in the corner panel BDFE (Fig. 8.10).

The plastic moment of resistance at any cross section  $x$  of the haunch perpendicular to the layout line is (Fig. 8.9)

$$M_{px} = \sigma_y Z_x \quad (8.3)$$

As in tapered haunches, increasing the thickness of the curved flange would compensate for the reduction in effective section due to the inclination  $\beta$  of the flange and would make the section effectively symmetrical about its half depth. The theoretically required thickness is given by (8.7).

$$t_c = t_f / \cos \beta \quad (8.4a)$$

in which

$t_c$  = thickness of the compression flange plate

$\beta$  = central angle between point of tangency and given section of knee

For all practical cases, the controlling angle  $\beta$  will be small (approximately  $12^\circ$ ) and symmetry can be assumed without increasing the compression flange thickness. Assuming symmetry, the section modulus at any section  $x$  is

$$Z_x = b t_f (d_x - t_f) + \frac{w}{4} (d_x - 2 t_f)^2 \quad (8.5)$$

in which

$d_x$  = depth of haunch at any section ( $x$ )

$$= d + R (1 - \cos \beta)$$

$R$  = radius of curvature of inner flange

$$x = R \sin \beta$$

Eq. 8.5 may be substituted into Eq. 8.3 for  $M_{px}$  and the result equated to  $M_x$ , the applied moment which must be resisted. Solving for the thickness of the tension flange gives

$$t_t = \frac{d_x - \sqrt{d_x^2 \left( \frac{b}{b-w} \right) - \frac{4 M_x}{\sigma_y (b-w)}}}{2} \quad (8.13)$$

At some station along the haunch defined by a controlling value of the angle  $\beta$ , the values of  $d_x$  and  $M_x$  will require a maximum flange thickness. For values of the radius of flange curvature and distance to the inflection point that would be encountered ordinarily in practice, the controlling angle  $\beta$  has been found to be about  $12^\circ$  (8.7).

The resistance to local buckling of the flanges of curved haunches may be assured by following the recommendations of Chapter 6.

Lateral stability of curved haunches dependent upon the resistance to buckling of the compression flange perpendicular to the plane of the web. Ref. 8.7 contains an approximate solution obtained by analyzing the problem as the buckling of a curved beam simply supported at the points of tangency and at the diagonal stiffener. To simplify the analysis the curved flange is conservatively assumed to have a uniform stress distribution over its whole area and length. The tangent modulus equation for the buckling of fully strain-hardened steel plates gives the following expression for the critical arc length of flange: (8.7.8.25)

stiffener may be proportioned by considering the additional amount of resisting force required to achieve equilibrium. The stiffeners should also be proportioned to maintain stability under their full load.

Horizontal stiffeners should preferably be furnished in symmetrical pairs opposite both beam flanges. They should be welded to the column flange and web by either groove or fillet welds. Vertical stiffeners should also be furnished in symmetrical pairs and should be deep enough to allow the beam flange force to be dispersed in the stiffener in the same manner in which it is assumed to be dispersed in the web in Eq. 8.19.

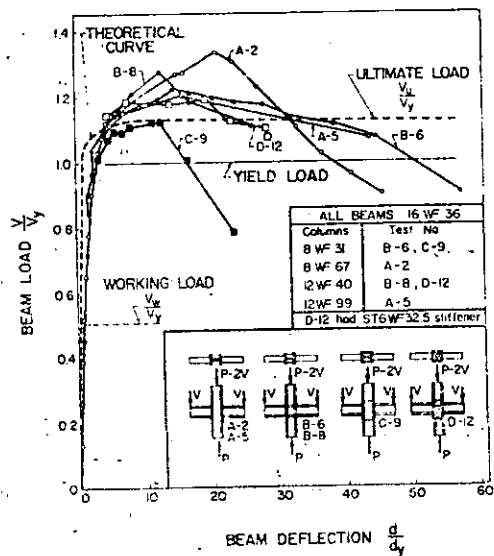


FIG. 8.15.—RESULTS OF TWO-WAY CONNECTION TESTS

Results of tests on connections using both types of stiffening are given in Ref. 8.10. Some of them are shown in Fig. 8.15. These tests and tests without stiffening were used to help establish semi-empirical methods of deciding the need for stiffeners and the proportioning of stiffeners to resist thrusts of beam flanges. If the moments applied by the beams to the columns were unsymmetrical, the same methods would be appropriate.

Critical Parts of Connections

The preceding analyses have shown that the use of stiffeners may depend either on compression in the column web (Eq. 8.21) or on tension normal to the column flange (Eq. 8.26) resulting from the end moments of the beams. For most of the rolled column sections normally only one type of failure need be checked, depending on the proportions of the column. The sections controlled by each type of failure may be tabulated, thus simplifying design.

Eq. 8.21 states that a connection will be on the verge of needing stiffeners in the compression region if

$$A_f = w_c(t_b + 5 k_c) \dots \dots \dots (8.27)$$

From Eqs. 8.26 and 8.27 this connection will or will not need stiffeners in the tension region according to whether

$$t_c \lesssim 0.4 \sqrt{w_c(t_b + 5 k_c)} \dots \dots \dots (8.28)$$

that is

$$\frac{t_c}{\sqrt{k_c w_c}} \lesssim 0.4 \sqrt{5 + \frac{t_b}{k_c}} \dots \dots \dots (8.29)$$

For all practical combinations of rolled beams and columns that might be used in this type of connection,

$$0.2 < t_b/k_c < 0.6 \dots \dots \dots (8.30)$$

By taking  $t_b/k_c = 0.2$ , it is seen that this connection will need stiffeners in the tension region if

$$\frac{t_c}{\sqrt{k_c w_c}} < 0.91 \dots \dots \dots (8.31)$$

By taking  $t_b/k_c = 0.8$ , it is seen that the connection will not need stiffeners in the tension region if

$$\frac{t_c}{\sqrt{k_c w_c}} > 0.96 \dots \dots \dots (8.32)$$

Fig. 8.16 shows a plot of the values of  $t_c/\sqrt{k_c w_c}$  for all wide-flange columns in the 8 in., 10 in., 12 in., and 14 in. series. It can be seen that in most cases the column need only be checked for compression. For values of  $t_c/\sqrt{k_c w_c}$  between 0.91 and 0.96 the need for column stiffening will depend on the beam, and both tension and compression should be checked.

Shear Stiffening

When the moments in the two beams at an interior connection differ by a large amount, they may cause large shears in the column web, tending to deform the web in the same manner as in a corner connection (Fig. 3.2(e)). With such an unbalance of moments, the shear in the web should be checked, and if necessary, diagonal stiffeners or a doubler plate should be added. (1,2) In Fig. 8.17(a) the shears and moments acting on a typical connection are shown. Fig. 8.17(b) is a free body diagram of the forces acting on the column web just below the top flange stiffener. The forces are V, the horizontal shear present

In the column above the connection and two tensile flange forces  $T_1$  and  $T_2$ . The flange forces are obtained approximately by dividing the moment in the respective beams by the beam depths. The net result of these forces must be resisted by a shear stress  $\tau$  acting on an area of column web equal to  $w_c d_c$ . Thus

$$\tau w_c d_c = \frac{M_2}{d_b} - \frac{M_1}{d_b} - v \quad \dots \dots \dots (8.33)$$

Assuming that  $\tau_y = \sigma_y/\sqrt{3}$ , the required web thickness to resist shear is

$$w_c = \frac{\sqrt{3}}{\sigma_y d_c} \left( \frac{M_2}{d_b} - \frac{M_1}{d_b} - v \right) \quad \dots \dots \dots (8.34)$$

when the directions of moments and shears are as shown in Fig. 8.17(b). If the actual web thickness of the column is less than that in Eq. 8.34, diagonal

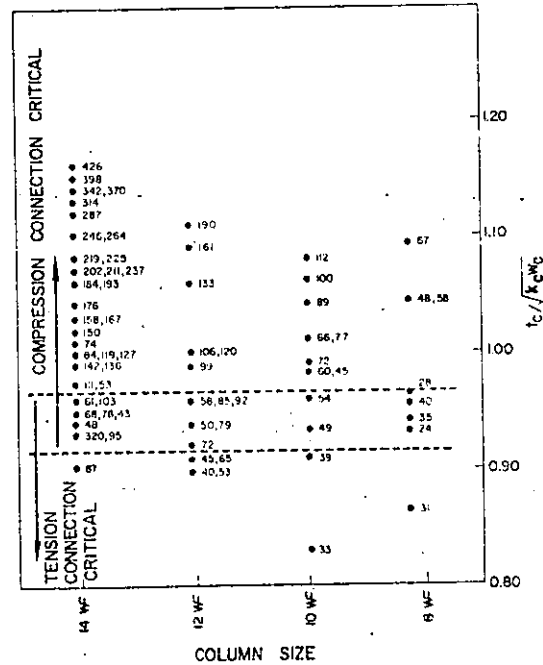


FIG. 8.16.—CRITICAL PARTS OF CONNECTIONS

stiffeners similar to those in Fig. 8.2(f) or web doubler plates could be used to carry the excess shearing force. The special case of a "one-sided" beam-to-column connection is obtained when  $M_1$  equals zero.

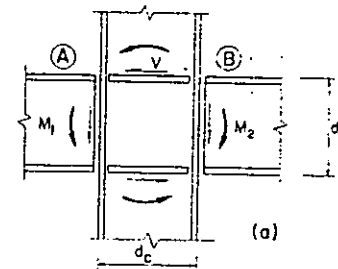


FIG. 8.17a.—SHEAR AND MOMENT ON CONNECTION WITH UNEQUAL MOMENTS ON BEAMS

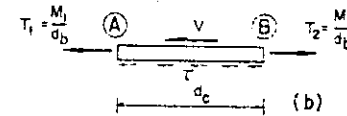


FIG. 8.17b.—FREE BODY DIAGRAM OF FORCES ACTING ON TOP STIFFENER AND COLUMN WEB

Four-Way Beam-to-Column Connections

Frequently additional beams must be framed into a single joint on a column forming a four-way beam-to-column connection. Two beams may be framed into a column web either by direct welding or by plate plus seat type of connections. When connections such as these are used, the question has been raised as to whether the triaxial stresses in the column web might cause premature failure, or on the other hand, whether a beneficial effect might be obtained through the partial stiffening action of the beams framing into the column web. A limited number of tests have been made on four-way connections. In the specimens tested, there was no adverse effect of triaxial stresses indicated. (8.10)

Sketches of the four-way connections tested are shown in Fig. 8.18. The direct-welded type, shown in Fig. 8.18(a) had a column web thickness meeting the requirement of Eq. 8.21 and hence the column web required no reinforcement to prevent crippling due to the forces applied to the column flanges by the

13

75

## 9.6 APPROXIMATE DEFLECTION AT WORKING LOAD

It has been suggested (9.8) that an upper bound for the deflection at working load may be obtained by dividing the calculated deflection at ultimate load by the load factor.\* Calculations were made to compare this type of estimate with calculated and measured deflections at working load. Bar graphs showing these comparisons for five structures are given in Fig. 9.7. Each deflection is plotted as a percentage of the calculated deflection  $\delta_u$  at ultimate load. Thus, the deflection estimated at working load is always 54% of  $\delta_u$  when the load factor is 1.85. The deflection calculated from an elastic analysis at the plastic design working load and an observed deflection at working load from a test are shown where available. For a further comparison, a bar showing 1/360 of the span is plotted to the same scale as the deflections.\*\*

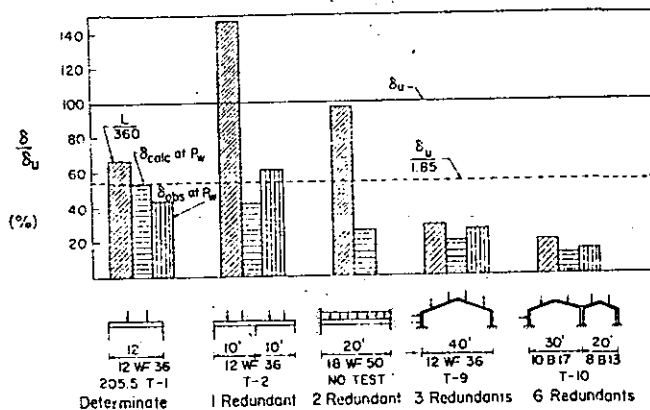


FIG. 9.7.—COMPARISON OF DEFLECTIONS AT WORKING AND ULTIMATE LOADS WITH ESTIMATED WORKING LOAD DEFLECTION.

The bar graphs show that the estimate of deflections made by dividing  $\delta_u$  by the load factor is more and more in error as the number of statically indeterminate reactions increases. Whereas the approximate estimate is very good for one redundant, the estimate is four times the actual deflection at working load for the structure with six redundants. This estimate would imply excessive deflection whereas the actual deflection here was well below  $L/360$ . Unfortunately, no simple rule can be established for estimating how much in error the original calculation might be. Much depends on the order of formation of the plastic hinges. In any structure in which all plastic hinges form simultaneously, the estimate will equal the true deflection.

\* The intersection of the dot-dash line 0-4 in Fig. 9.6 with the horizontal line indicating the magnitude of  $P_w/P_u$  is a graphical representation of this upper bound for deflection at working load of a single span gabled frame.

\*\*  $L/360$  is not suggested as an appropriate deflection limitation: it is shown merely because it is probably of the same order of magnitude as any practical deflection limitation.

The approximate procedure suggested is satisfactory whenever the estimated deflection calculated from this procedure does not exceed the prescribed deflection limitation. Otherwise it is necessary to resort to more accurate (and complicated) methods of calculation.

## 9.7 DEFLECTIONS AS A LIMITATION

One of the most important questions about deflections in plastic design is whether or not they will constitute an undue design limitation. The answer to this question on the basis of available test results and calculations is: no.

Admittedly, on the basis of the few tests and calculations for examples shown, it cannot be stated that all possible combinations have been studied. Variations in load and span do change the relationships. However, it is believed on the basis of the studies which have been made that the statements

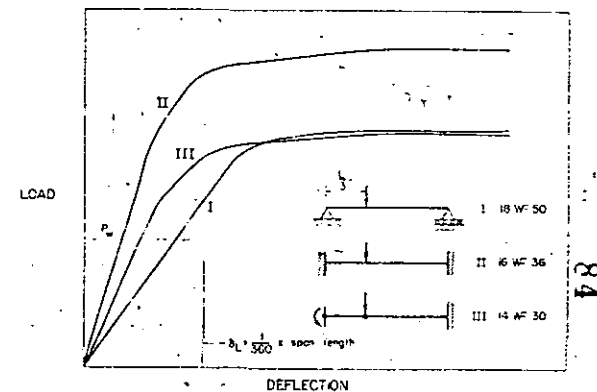


FIG. 9.8.—LOAD-DEFLECTION RELATIONSHIP FOR THREE DIFFERENT BEAM DESIGNS FOR SUPPORTING THE SAME LOAD.

made here apply to typical cases and also to cases within the range of practical extremes.

Consider the case shown in Fig. 9.8 (1.2). The problem is to design a beam to carry a given load on a given span. First, picture the beam being designed as simply-supported, this being the standard with which the safety factor is compared in plastic design. The rolled section required would be an 18 WF 50 and the load-deflection curve would be as shown by curve I in Fig. 9.8. A horizontal mark on the graph indicates the value of the working load, and a vertical mark indicates the deflection which is equivalent to  $L/360$  of the span.

Next consider a fixed-ended beam designed to carry the same load on the same span according to elastic design. Because of the negative moment at the fixed ends, only a 16 WF 36 would be required. The load-deflection curve would be as given by curve II in Fig. 9.8. It is seen that the deflection at working load is considerably less than that of the simply-supported beam. The elastically

designed beam with fixed ends would support a much greater ultimate load than that of the simple beam. This indicates that, although both beams are designed for the same working load and both are "safe," the built-in beam has an excess margin of safety against ultimate load.

The third case in Fig. 9.8 indicates an even more economical solution by plastic design. Here only a 14 W 30 is required. The load-deflection curve shows that the load capacity is equal to that of the simple beam. Though the deflection at working load for case III is greater than case II, it is considerably less than case I and would be acceptable.

### 9.8 ROTATION REQUIREMENTS

In addition to the problem of deflections in plastic design the rotations at plastic hinges must also be considered. For example, in the beam of Fig. 9.5, it is the inelastic rotation at the left support which allows redistribution of moments to the load point and right support of the member, thereby making possible the increase in load from points A to D. Similarly, in any continuous structure, some rotation must take place at the first plastic hinges to form, except in the case where all hinges form simultaneously. The measure of this required rotation is referred to as the hinge angle. It is of interest to determine the hinge angle that would be required in structures in order to formulate certain secondary design guides which depend upon this function.

The hinge angle may be calculated as part of the deflection calculations described in Art. 9.4. The results of numerous hinge angle calculations are presented in Ref. 9.3. Some of these results have been used in the determination of the required lateral bracing for bending members given in Art. 6.3.

In some cases, the calculated hinge angle required to form a mechanism may be quite large, implying a limitation on the design. However, practical considerations suggest that almost as good load carrying capacity may exist with a much lower hinge angle requirement. In Fig. 9.9 is plotted the theoretical load versus hinge rotation  $H$  at the first plastic hinge of a two-span portal frame. Seven labelled points on the curve indicate the formation of seven plastic hinges in reaching the mechanism state. Point (7) is the hinge angle that would be calculated in a rotation capacity study. Note, however, that at the formation of the next-to-last plastic hinge, point (6), the load is 98.2% of the maximum load. In order to attain this load, the required rotation is only  $0.54 M_p L / (E I)$ , or about one-third of the amount calculated for a full mechanism ( $1.52 M_p L / (E I)$ ). Assurance of reaching 98% of a predicted load, along with a reasonable load factor or safety factor is generally accepted as good engineering practice. Thus, it is seen that the problem of large required rotation in highly redundant structures is not as serious as might first be suspected.

Experimental verification that a structure may behave quite satisfactorily even though it may not meet the full rotation requirement is given in Ref. 5.7. A test was performed on the two-span frame of Fig. 9.9. Although the frame did not quite attain the computed ultimate on the basis of a 40 ksi coupon stress, it reached 97.4% of this value, or well in excess of an ultimate load based upon a 33 ksi yield point (Fig. 9.10). Observations indicated that six of the seven plastic hinges were formed before lateral buckling occurred due to the instability of a lateral support which was made very flexible for test purposes. There is every reason to believe that with adequate lateral support the seventh plastic hinge would have formed, and an even greater load would have been

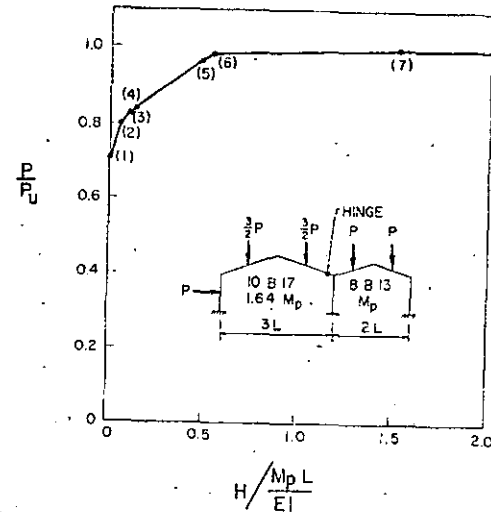


FIG. 9.9.—HINGE ANGLE REQUIRED FOR A TWO-SPAN PORTAL FRAME.

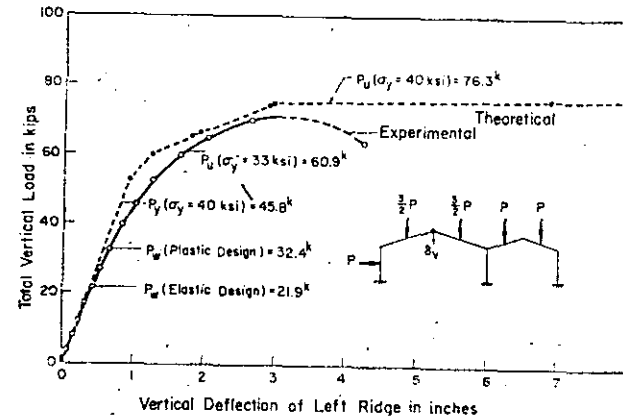


FIG. 9.10.—EXPERIMENTAL LOAD-DEFLECTION CURVE OF TWO-SPAN PORTAL FRAME.

reached due to strain-hardening. For highly indeterminate multispan frames, large hinge angles may be required for the full development of a mechanism. However, for these same frames the load at the formation of the next-to-last hinge is almost as great as the maximum load, while the rotation at that instant is substantially less, as in the case shown in Fig. 9.9. Hence a lower limit for rotation capacity requirement, suitable for general design purposes, need not be related to the large theoretical rotations associated with highly redundant frames.

## APPENDIX I.—SYMBOLS

A	= area of cross section;
$A_c$	= area of sloping (compression) flange plate in tapered or curved haunch;
$A_{c1}$	= area of inner flange of rafter haunch (Fig. 8.7);
$A_{c2}$	= area of inner flange of column haunch (Fig. 8.7);
$A_f$	= area of one flange of wide-flange shape, $A_f = b t$ ;
$A_s$	= area of symmetrical pair of diagonal stiffeners;
$A_t$	= area of straight (tension) flange plate in tapered haunch;
$A_{t1}$	= area of outer flange of beam haunch (Fig. 8.7);
$A_w$	= area of web, $A_w = w d$ ;
a	= distance from end of cantilever to critical section of beam;
B	= beam-column interaction equation coefficient;
b	= flange width; = breadth of rectangular cross section;
b'	= width of outstanding plate element;
$b_0$	= width of plate simulating flange element of wide-flange shape;
$C_w$	= warping constant;
c	= distance from centroid to extreme fiber;
$D_x$	= $E_x / (1 - \nu_x \nu_y)$ ;
$D_y$	= $E_y / (1 - \nu_x \nu_y)$ ;
$D_{xy}$	= $\nu_y D_x$ ;
$D_{yx}$	= $\nu_x D_y$ ;
d	= depth of section (subscripts b and c denote beam and column);
$d_{ch}$	= depth of column haunch (Fig. 8.7);
$d_f$	= distance between centers of two flanges;
$d_w$	= web depth of wide-flange shape, $d_w = d - 2 t$ ;
$d_x$	= depth of haunch at section x (Figs. 8.6 and 8.9);
E	= Young's modulus of elasticity;
$E_{st}$	= strain-hardening modulus;
$E_t$	= tangent modulus;
$E_x$	= tangent modulus in x-direction;
$E_y$	= tangent modulus in y-direction;
e	= eccentricity;
F	= load factor of safety;

R6

## SYMBOLS

$f$	= shape factor, $f = M_p/M_y = Z/S$ ;
$G$	= modulus of elasticity in shear; = beam-column interaction equation coefficient;
$G_{st}$	= modulus of elasticity in shear at onset of strain-hardening;
$G_t$	= tangent modulus in shear;
$H$	= horizontal reaction or load; = hinge angle required at a plastic hinge;
$H_B$	= portion of hinge angle that occurs in the critical (buckling) segment of member;
$h$	= story height;
$I$	= moment of inertia (subscripts $x$ and $y$ denote axes, subscripts $b$ and $c$ denote beam and column);
$J$	= beam-column interaction equation coefficient;
$K$	= torsion constant; = beam-column interaction equation coefficient; = effective column length coefficient;
$k$	= distance from flange face to end of fillet (subscript $c$ denotes column fillet); = stiffness factor of a beam (subscripts $l$ and $s$ refer to adjacent segments and denote larger and smaller stiffness factors);
$L$	= span length parameter; = actual column length; = distance between points of lateral support;
$L_A$	= length of adjacent segment between points of lateral support;
$L_{cr}$	= critical unsupported length for lateral buckling;
$L_{Acr}$	= critical length (based on simple span) of adjacent segment;
$L_{lcr}$	= critical length (based on simple span) of adjacent segment (subscript $l$ denotes longer critical length);
$L_{scr}$	= critical length (based on simple span) of adjacent segment (subscript $s$ denotes shorter critical length);
$l$	= length of segment (slope-deflection equations);
$M$	= bending moment;
$M_{equ}$	= equivalent moment for beam-column;
$M_h$	= moment at the haunch point;
$M_i$	= elastic moment at section "i";
$M_L$	= bending moment about strong axis at $Z = L$ ;
$M_{max}$	= maximum moment;
$M_0$	= column end moment (a useful end moment); = bending moment about strong axis at $Z = 0$ ;

## SYMBOLS

$M_p$	= plastic moment;
$M_{pc}$	= plastic hinge moment modified to include the effect of axial compression;
$M_{pm}$	= plastic hinge moment modified to include the effect of axial compression and shear force;
$M_{ps}$	= plastic hinge moment modified to include the effect of shear force;
$M_{px}$	= plastic moment of resistance at section "x" of a haunch;
$M_r$	= residual moment;
$M_w$	= moment at working (service) loads;
$M_x$	= moment at section "x" of haunch;
$M_y$	= moment at which yielding first occurs in flexure;
$\Delta M_y$	= range of moments in which $M-\phi$ curve is linear;
$M_1$	= larger of two end moments on a beam-column;
$M_2$	= smaller of two end moments on a beam-column;
$m$	= moments in a structure in equilibrium with a unit load; = distance between fillet extremities of flange of column;
$P$	= concentrated or axial load;
$P_a$	= maximum load for alternating plasticity;
$P_{cr}$	= critical load on axially loaded column;
$P_e$	= Euler buckling load;
$P_{max}$	= maximum load;
$P_s$	= stabilizing ("shakedown") load;
$P_t$	= tangent modulus load;
$P_u$	= ultimate load (theoretical);
$P_w$	= working (service) load;
$P_y$	= load on beam when yield stress level is reached in flexure; = axial load corresponding to yield stress level, $P_y = A \sigma_y$ ;
$R$	= radius of curved haunch;
$r$	= radius of gyration (subscripts denote flexural axes);
$r_x$	= radius of gyration of compression flange of haunch in strong direction;
$S$	= section modulus, $S = I/c$ ;
$s$	= distance along member;
$T$	= force;
$T_B$	= horizontal component of diagonal stiffener force;
$T_w$	= web shear force;



$t$	= flange thickness (subscripts c and t denote compression (or column) and tension flange);
$V$	= shear force; = vertical reaction;
$V_p$	= $\frac{1}{2} \sigma_y b d$ for rectangular section;
$V_Y$	= maximum allowable shear force at ultimate load;
$u, v, w$	= displacements in x, y, and z directions, respectively;
$W$	= total distributed load (subscripts u, w, and y denote ultimate, working, and yield loads, respectively);
$W_E$	= external work due to virtual displacement;
$W_i$	= internal work due to virtual displacement;
$w$	= distributed load per unit of length; = web thickness (subscript c denotes column web);
$w_r$	= required web thickness;
$x$	= longitudinal coordinate;
$y$	= transverse coordinate;
$y_c$	= center line deflection;
$y_o$	= distance between centroid and neutral axis;
$Z$	= plastic modulus (subscripts denote flexural axes, $Z = \frac{M_p}{\sigma_y}$ );
$Z_x$	= plastic modulus at section "x" of a haunch;
$z$	= lateral coordinate; = distance along beam;
$\alpha$	= central angle of curved flange between points of lateral support; = proportion of a given length in strain-hardened state; = non-dimensional parameter locating the position of a plastic hinge; = non-dimensional load parameter used in cyclic loading studies;
$\beta$	= angle between two non-parallel flanges (Fig. 8.6 and 8.9); = coefficient of restraint; = angle of twist about shear center; = second non-dimensional load parameter used in cyclic loading studies;
$\beta_1$	= angle of taper of rafter haunch (Fig. 8.7);
$\beta_2$	= angle of taper of column haunch (Fig. 8.7);
$\gamma$	= shearing strain; = angle of inclination of rafter (Fig. 8.7);
$\Delta$	= virtual displacement; = deflection of a joint due to translation;
$\delta$	= deflection (subscripts u, w, and y denote deflection at ultimate, working, and yield load, respectively);
$\epsilon$	= strain (subscripts denote direction);

$\epsilon_{cr}$	= critical strain at which local buckling occurs;
$\epsilon_{st}$	= strain at onset of strain-hardening;
$\epsilon_y$	= strain corresponding to theoretical onset of plastic yielding;
$\theta$	= measured angle change, rotation; = mechanism angle; = angle of slope of diagonal stiffener;
$\theta_m$	= angle of rotation at maximum load;
$\theta_A$	= rotation of joint A due to transverse loads assuming simply supported ends of member;
$\theta_y$	= elastic limit rotation (theoretical);
$\nu$	= Poisson's ratio;
$\nu_s$	= correction factor for St. Venant torsion;
$\nu_c$	= correction factor for extent of yielding;
$\nu_y$	= correction factor for end fixity;
$\nu_p$	= correction factor for moment gradient;
$\nu_x$	= coefficient of dilation for stress increment in x-direction;
$\nu_y$	= coefficient of dilation for stress increment in y-direction;
$\rho$	= ratio of smaller end moment to larger end moment for a segment ( $-1 \leq \rho \leq 1$ );
$\rho_A$	= ratio of end moments for adjacent segment;
$\sigma$	= normal stress;
$\sigma_{cr}$	= critical buckling stress;
$\sigma_r$	= residual stress (subscripts rc and rt denote compression and tension);
$\sigma_w$	= allowable (working) stress;
$\sigma_y$	= yield-stress level;
$\tau$	= shear stress;
$\tau_o$	= shear stress on neutral axis;
$\tau_y$	= shear yield stress;
$\phi$	= rotation per unit length or average unit rotation, curvature;
$\phi_p$	= $M_p/(EI)$ ; and
$\phi_y$	= curvature corresponding to first yield in flexure.

APPENDIX II.—GLOSSARY

Allowable stress design—A design method which defines the limit of structural usefulness as the load at which a calculated stress equal to the yield point of the material is first attained at any point (usually disregarding local stress raisers).

Factor of safety—As used in elastic (allowable stress) design, it is a factor by which the yield stress is divided to determine a working or allowable stress for the most highly stressed fiber.

Hinge angle—The angle of rotation through which a yielded segment of a beam must sustain its plastic moment value.

Load factor—In plastic design, a factor by which the working load is multiplied to determine the ultimate load. This choice of terms serves to emphasize the reliance upon load-carrying capacity of the structure rather than upon stress.

Mechanism—An articulated system able to deform without a finite increase in load. It is used in the special sense that the linkage may include real hinges and/or plastic hinges.

Moment ratio—The ratio of the numerically smaller end moment to the moment at the opposite end of a segment. End moments causing single curvature correspond to a positive moment ratio while double curvature gives a negative moment ratio.

Plastic design—A design method for continuous steel beams and frames which defines the limit of structural usefulness as the "ultimate load." (The term, "plastic" comes from the fact that the ultimate load is computed from a knowledge of the strength of steel in the plastic range).

Plastic hinge—A yielded zone which forms in a structural member when the plastic moment is applied. The beam rotates as if hinged, except that it is restrained by the moment  $M_p$ .

Plastic modulus—The modulus of resistance to bending of a completely yielded cross section. It is the combined statical moment about the neutral axis of the cross-sectional areas above and below that axis.

Plastic moment—The resisting moment of a fully-yielded cross section.

Plastification—Gradual penetration of yield stress from the outer fiber towards the centroid of a section under increasing moment. Plastification is complete when the plastic moment,  $M_p$ , is attained.

Proportional loading—All loads increase in a constant ratio, one to the other.

Redistribution of moment—A process which results in the successive formation of plastic hinges until the ultimate load is reached. As a result of the formation of plastic hinges, less highly-stressed portions of a structure may carry increased moments.

Rotation capacity—The angular rotation which a given cross-sectional shape can sustain at the plastic moment value without prior local failure.

Shape factor—The ratio  $M_p/M_y$ , or  $Z/S$ , for a cross section.

Ultimate load or plastic limit load—The load attained when a sufficient number of yield zones have formed to permit the structure to deform plastically without further increase in load. It is the largest load a structure will support, when perfect plasticity is assumed and when such factors as instability, strain-hardening and fracture are neglected.

Yield moment—In a member subjected to bending, the moment at which an outer fiber first attains the yield stress level.

Yield stress level—The average stress during yielding in the plastic range. It is the stress determined in a tension test when the strain reaches 0.005 in/in.

68



**DIVISION DE EDUCACION CONTINUA  
FACULTAD DE INGENIERIA U.N.A.M.**

DISEÑO DE ESTRUCTURAS DE ACERO

FLEXION BIAXIAL

DR. PORFIRIO BALLESTEROS BAROCIO

Nº OV. 1984

## DESPUES DEL LIMITE ELASTICO

por

Porfirio Ballesteros\*

---

SUMARIO

Acceptando las hipótesis de deformación plana de secciones, diagrama idealizado esfuerzo-deformación, e isotropía. Se determina la ecuación general del esfuerzo normal a una sección transversal de un elemento estructural, en condiciones semi-plásticas, concluyéndose como casos particulares, las condiciones plásticas y elásticas. Se estudian diferentes posiciones de los ejes coordenados con el propósito de simplificar las operaciones numéricas. Se estudian condiciones de última capacidad de carga de columnas cortas a flexo-compresión no simétrica, y vigas bajo flexión bi-axial y se determinan diversos gráficos de interacción bi-axial para el diseño de secciones de acero estructural indicadas en los manuales de México y Estados Unidos.

Y se presenta el programa general para una sección cualquiera en lenguaje computacional FORTRAN-IV.

## NOTACION

$A_e$  Área elástica

$A_p$  Área plástica

$d$  longitud del eje neutro a través de la sección

---

\* Profesor de la División de Estudios Superiores de la Facultad de Ingeniería de la UNAM.

- $e_x, e_y$  excentricidades de la carga normal con respecto a los ejes coordenados.
- $x_c$  abscisa al origen del eje neutro
- $y_c$  ordenada al origen del eje neutro
- $n = \frac{A_p}{A_p + A_e}$  grado de plastificación
- $y_0$  distancia del eje neutro a la traza de plastificación.
- $I_x, I_y, I_{xy}$  momentos y productos de inercia del área elástica
- $M$  momento flector resultante en la sección
- $M_x, M_y$  componentes de  $M$  respecto a los ejes coordenados
- $M_u$  valor límite o último de  $M$
- $N$  carga excéntrica
- $N_u$  valor límite o último de  $N$
- $Q_x, Q_y$  momentos estáticos del área elástica respecto a los ejes coordenados
- $q_x, q_y$  momentos estáticos del área plástica respecto a los ejes coordenados
- $\sigma_x$  esfuerzo en un punto  $(x, y)$  paralelo al eje  $z$
- $\sigma_c$  esfuerzo de cedencia del material
- $a, b, c.$  constantes

## I N T R O D U C C I O N

Aceptando las hipótesis de deformación plana<sup>1</sup>, relación entre esfuerzo y deformación idealizada, Fig. 1 y un material iso-

<sup>1</sup> Navier, "Résumé des leçons sur l'application de la mécanique" 3d ed., Paris 1864, edited by Saint-Venant.

trópico y homogéneo. Para deformaciones menores que la deformación unitaria de fluencia  $\epsilon_y$ , regirá la Ley de Hooke, y para deformaciones mayores a la de fluencia, el esfuerzo para cualquier deformación será igual al esfuerzo de fluencia o cedencia  $\sigma_y$ .

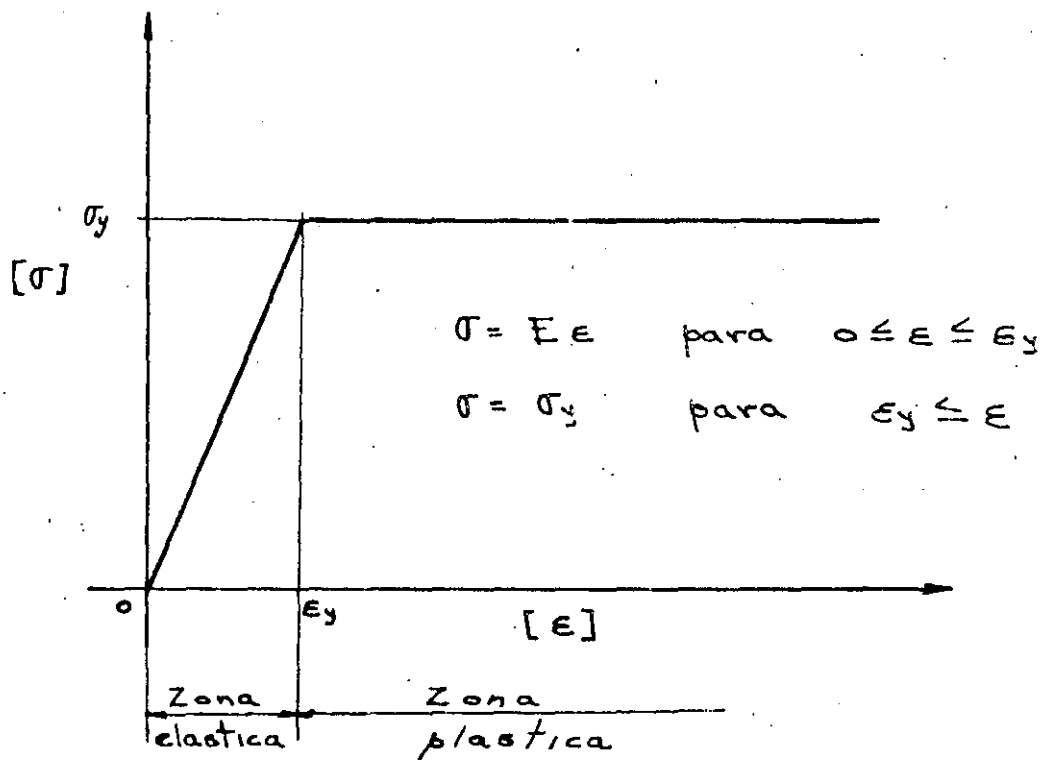


Fig. 1 Diagrama esfuerzo-deformación idealizado.

Considerando una sección intermedia cualquiera  $m-n$  del elemento estructural en equilibrio mostrado en la Fig. 2. Estudiaremos los esfuerzos reactivos de la porción A, debidos a la componente normal de la acción de la porción B.

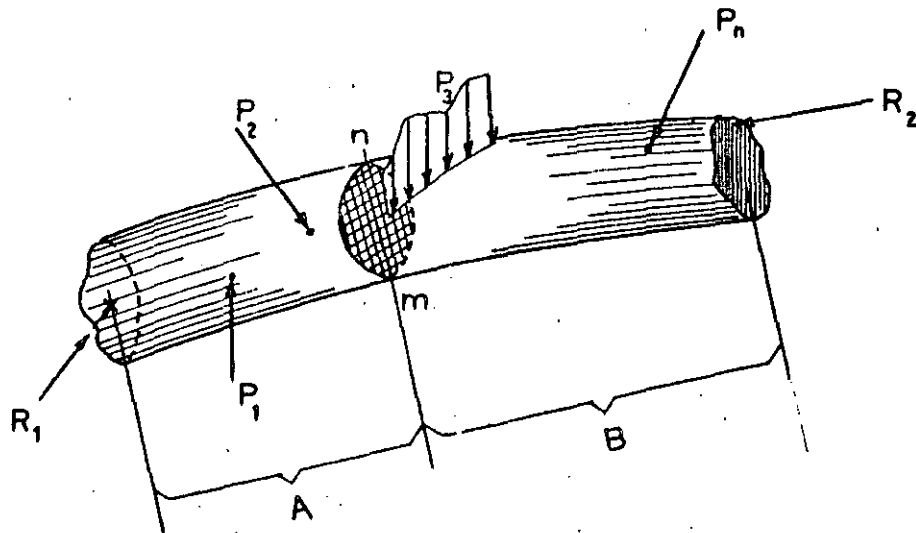


Fig. 2 Elemento estructural en equilibrio.

#### ECUACION GENERAL DE ESFUERZOS DE FLEXION.

En la Fig. 3 la sección  $m-n$  se encuentra contenida en el plano  $(x,y)$ .  $N$  es la componente normal de la acción de la porción B sobre la porción A, y  $e_x, e_y$  sus excentricidades referi-

das a un sistema coordenado cualquiera. Las áreas (1, 2, 3) y (4, 5, 6) se encuentran plastificadas es decir a esfuerzos mayores que el de cedencia del material, y el área (1, 3, 4, 6) se encuentra bajo la acción de esfuerzos menores al de cedencia y rige la Ley de Hooke. El eje (7-8) es el eje neutro, recta de deformaciones y esfuerzos nulos. Las rectas (1-3) y (6-4) son paralelas al eje neutro, se encuentran a la misma distancia de éste y se denominarán trazas de plastificación.

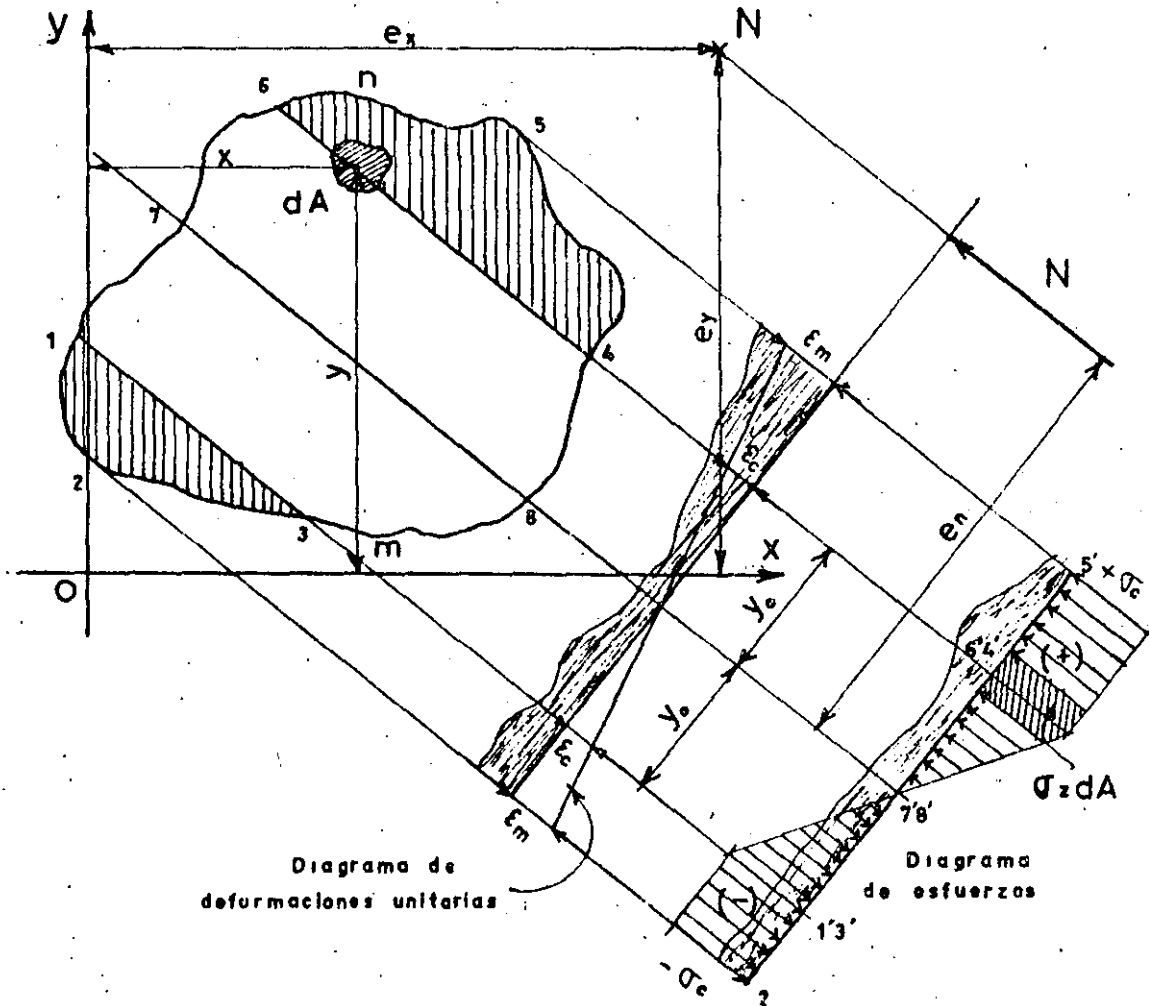


Fig. 3 Distribución de esfuerzos a flexo-compresión en condiciones elasto-plásticas.



Según Navier la superficie  $m-n$  permanecerá plana después de la deformación. Por lo tanto la ecuación de la deformación  $z(x,y)$  será la ecuación general del plano referida al sistema coordenado  $(x,y,z)$ , y aceptando la proporcionalidad entre es - fuerzo y deformación tendremos como ecuación del esfuerzo en la región (1, 3, 8, 4, 6, 7), zona elástica:

$$\sigma_z = \sigma_e = Kz = ax + by + c. \quad (1)$$

Y en las regiones (1, 2, 3) y (6, 4, 5) zona plástica, será:

$$\sigma_z = \sigma_p = \pm \sigma_c. \quad (2)$$

De las condiciones de estática se tiene:

$$\left. \begin{aligned} \int_A \sigma_z dA &= N \\ \int_A \sigma_z y dA &= M_x = Ne_y \\ \int_A \sigma_z x dA &= M_y = Ne_x \end{aligned} \right\} \quad (3)$$

Substituyendo (1) y (2) en (3) se obtiene:

$$\left. \begin{aligned} \int_{A_0} (ax+by+c) dA + \int_{A_p} \sigma_c dA &= N \\ \int_{A_0} (ax+by+c)y dA + \int_{A_p} \sigma_c y dA &= M_x \\ \int_{A_0} (ax+by+c)x dA + \int_{A_p} \sigma_c x dA &= M_y \end{aligned} \right\} \quad (4)$$

utilizando la notación expuesta previamente (4) se transforma

a:

$$\left. \begin{aligned} \begin{bmatrix} Q_y & Q_x & A_0 \\ I_{xy} & I_x & Q_x \\ I_y & I_{xy} & Q_y \end{bmatrix} \begin{pmatrix} a \\ b \\ c \end{pmatrix} &= \begin{bmatrix} N - \sigma_c A_p \\ M_x - \sigma_c q_x \\ M_y - \sigma_c q_y \end{bmatrix} \end{aligned} \right\} \quad (5)$$

(5) es un sistema de 3 ecuaciones simultáneas con 3 incógnitas,

a, b y c. Definiendo a:

$$\left. \begin{aligned} \Delta = \begin{bmatrix} Q_y & Q_x & A_0 \\ I_{xy} & I_x & Q_x \\ I_y & I_{xy} & Q_y \end{bmatrix}, \quad \Delta_a = \begin{bmatrix} (N - \sigma_c A_p) & Q_x & A_0 \\ (M_x - \sigma_c q_x) & I_x & Q_x \\ (M_y - \sigma_c q_y) & I_{xy} & Q_y \end{bmatrix} \\ \Delta_b = \begin{bmatrix} Q_y (N - \sigma_c A_p) & A_0 \\ I_{xy} (M_x - \sigma_c q_x) & Q_x \\ I_y (M_y - \sigma_c q_y) & Q_y \end{bmatrix}, \quad \Delta_c = \begin{bmatrix} Q_y & Q_x & (N - \sigma_c A_p) \\ I_{xy} & I_x & (M_x - \sigma_c q_x) \\ I_y & I_{xy} & (M_y - \sigma_c q_y) \end{bmatrix} \end{aligned} \right\} \quad (6)$$

1 Para ser consistentes con el signo de  $\sigma_z$  definido por ecuación (2), y poder sacar a  $\sigma_c$  fuera del signo integral es necesario establecer para  $q_x$ ,  $q_y$  y  $A_p$  la convención de: Areas plásticas, en tensión negativas, y en compresión positivas.

la solución del sistema (5) viene dada por

$$a = \frac{\Delta_a}{\Delta} \quad , \quad b = \frac{\Delta_b}{\Delta} \quad , \quad c = \frac{\Delta_c}{\Delta} \quad (7)$$

substituyendo (7) en (1) se obtiene

$$\sigma_x = \frac{1}{\Delta} (\Delta_a x + \Delta_b y + \Delta_c) \quad (8)$$

La ecuación (8) es la expresión general para determinar el esfuerzo normal en el área elástica.

La ecuación del eje neutro se obtiene de (8) para  $\sigma_x = 0$ .

$$\Delta_a x + \Delta_b y + \Delta_c = 0 \quad (9)$$

La abscisa y ordenada al origen del sistema coordenado del eje neutro se obtienen de (9) para  $y = 0$  y  $x = 0$

$$x_c = -\frac{\Delta_c}{\Delta_a} \quad , \quad y_c = -\frac{\Delta_c}{\Delta_b} \quad (10)$$

## CASOS ELASTICOS

Los esfuerzos en la sección serán menores que el de cedencia y se tiene que

$$A_p = 0, \quad n = \gamma, \quad A = A_0, \quad q_x = q_y = 0$$

Ejes centroidales.— Por definición de centroide de una sección es un punto tal que los momentos estáticos son nulos y en este caso tendremos que  $Q_x = Q_y = 0$ ,  $I_x \neq 0$ ,  $I_y \neq 0$ ,  $I_{xy} \neq 0$ ,  $M_x \neq 0$ ,  $M_y \neq 0$  y los determinantes (6) se reducen a

$$\left. \begin{aligned} \Delta &= A (I_{xy}^2 - I_x I_y) \\ \Delta_a &= A (I_{xy} M_x - I_x M_y) \\ \Delta_b &= A (I_{xy} M_y - I_y M_x) \\ \Delta_c &= N (I_{xy}^2 - I_x I_y) \end{aligned} \right\} \quad (11)$$

y las ecuaciones (8) (9) y (10) se transforman a

$$\sigma_z = \frac{I_{xy} M_x - I_x M_y}{I_{xy}^2 - I_x I_y} x + \frac{I_{xy} M_y - I_y M_x}{I_{xy}^2 - I_x I_y} y + \frac{N}{A} \quad (12)$$

$$(I_{xy} M_x - I_x M_y) x + (I_{xy} M_y - I_y M_x) y + \frac{N}{A} (I_{xy}^2 - I_x I_y) = 0 \quad (13)$$

$$x_c = - \frac{I_{xy}^2 - I_x I_y}{I_{xy} M_x - I_x M_y} \times \frac{N}{A}, \quad y_c = - \frac{I_{xy}^2 - I_x I_y}{I_{xy} M_y - I_y M_x} \times \frac{N}{A} \quad (14)$$

Ejes centroidales principales..- Corresponden a girar los ejes centroidales a un ángulo  $\alpha$  tal que el producto de inercia se anule, por lo tanto los determinantes (11) se reducen nuevamente a

$$\left. \begin{aligned} \Delta &= -I_x I_y A \\ \Delta_a &= -I_x A M_y \\ \Delta_b &= -I_y A M_x \\ \Delta_c &= -I_x I_y N \end{aligned} \right\} \quad (15)$$

y las ecuaciones (8) (9) y (10) se transforman a

$$\sigma_x = \frac{M_y}{I_y} x + \frac{M_x}{I_x} y + \frac{N}{A} \quad (16)$$

$$\frac{e_x}{I_y} x + \frac{e_y}{I_x} y + \frac{l}{A} = 0 \quad (17)$$

---

La forma de efectuar el giro por medio del círculo de Mohr viene expuesto en la mayoría de los textos de Estática y Resistencia de Materiales.

$$x_c = -\frac{I_y}{e_x A} = -\frac{r_y^2}{e_x}, \quad y_c = -\frac{I_x}{e_y A} = -\frac{r_x^2}{e_y} \quad (18)$$

donde  $r_x^2 = \frac{I_x}{A}$ ,  $r_y^2 = \frac{I_y}{A}$

Ecuaciones de esfuerzos y posición del eje neutro en ejes centroidales y centroidales principales son derivadas en la mayoría de los textos de Resistencia de Materiales no las omitimos por su importancia.

Ejes con origen de coordenadas en la fuerza N.— En este caso se

tiene que  $M_x = M_y = 0$ ,  $Q_x \neq 0$ ,  $Q_y \neq 0$

$I_x \neq 0$ ,  $I_y \neq 0$ ,  $I_{xy} \neq 0$  y los determinantes (8) se reducen a

$$\left. \begin{aligned} \Delta &= Q_y (I_x Q_y - I_{xy} Q_x) - Q_x (I_{xy} Q_y - I_y Q_x) + A (I_{xy}^2 - I_x I_y) \\ \Delta_a &= N (I_x Q_y - I_{xy} Q_x) \\ \Delta_b &= N (I_{xy} Q_y - I_y Q_x) \\ \Delta_c &= N (I_{xy}^2 - I_x I_y) \end{aligned} \right\} \quad (19)$$

y las ecuaciones (8) (9) y (10) se transforman a

$$\sigma_x = \frac{1}{\Delta} (\Delta_a x + \Delta_b y + \Delta_c) \quad (20)$$

$$(I_x Q_y - I_{xy} Q_x)x + (I_{xy} Q_y - I_y Q_x)y + (I_{xy}^2 - I_x I_y) = 0 \quad (21)$$

$$x_c = -\frac{I_{xy}^2 - I_x I_y}{I_x Q_y - I_{xy} Q_x}, \quad y_c = -\frac{I_{xy}^2 - I_x I_y}{I_{xy} Q_y - I_y Q_x} \quad (22)$$

### CASOS ELASTICO-PLASTICOS Y PLASTICOS

Cierta zona de la sección empezará a plastificarse y en esa área los esfuerzos serán igual al de cedencia  $\sigma_c$ .

#### Ejes centroidales principales respecto al área elástica.-

En este caso se tiene que  $Q_x = Q_y = I_{xy} = 0$  y el resto de los parámetros será diferente de cero y los determinantes (11) se reducen a

$$\left. \begin{aligned} \Delta &= - I_x I_y A_e \\ \Delta_a &= - I_x A_e (M_y - \sigma_c q_y) \\ \Delta_b &= - I_y A_e (M_x - \sigma_c q_x) \\ \Delta_c &= - I_x I_y (N - \sigma_c A_p) \end{aligned} \right\} \quad (23)$$

y las ecuaciones (8) (9) y (10) se transforman a

$$\sigma_c = \frac{M_x - \sigma_c q_x}{I_x} y + \frac{M_y - \sigma_c q_y}{I_y} x + \frac{N - \sigma_c A_p}{A_c} \quad (24)$$

$$\frac{M_y - \sigma_c q_y}{I_y} x + \frac{M_x - \sigma_c q_x}{I_x} y + \frac{N - \sigma_c A_p}{A_c} = 0 \quad (25)$$

$$x_c = -\frac{I_y}{A_c} \frac{N - \sigma_c A_p}{M_y - \sigma_c q_y}, \quad y_c = -\frac{I_x}{A_c} \frac{N - \sigma_c A_p}{M_x - \sigma_c q_x} \quad (26)$$

Ejemplo.- Considerando una sección rectangular Fig. 4 a flexión simple en una dirección, la ecuación (24) se reduce a

$$\sigma_c = \frac{M_x - \sigma_c q_x}{I_x} y - \frac{\sigma_c A_p}{A_c} \quad (27)$$



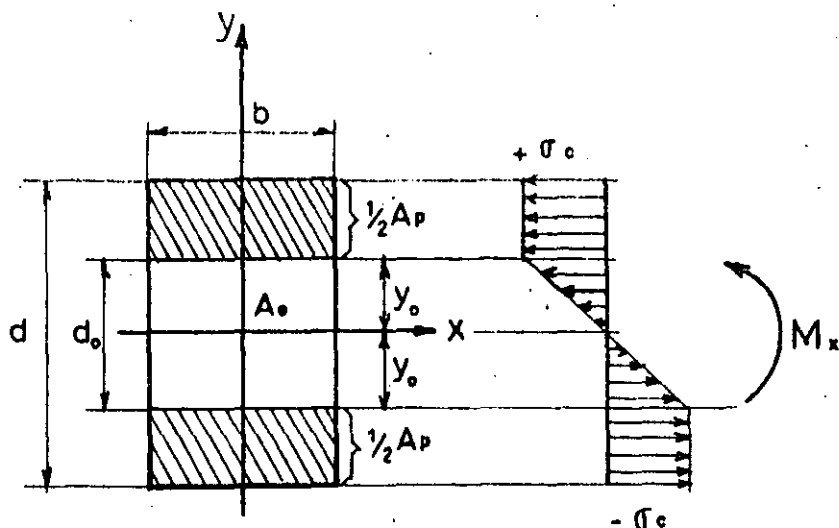


Fig. 4 Sección rectangular a flexo-compresión.

donde:  $I_x = \frac{1}{12} b d^3$  ,  $q_x = \int_{A_p} y dA = \frac{b}{4} (d^2 - d_0^2)$

$A_p = \int_{A_p} dA = 0$  Substituyendo estos valores en (27) para  $(\bar{\sigma}_x)_{y=\frac{d_0}{2}} = \bar{\sigma}_c$

y despejando a  $M_y = M$  se obtiene

$$M = \frac{bd^2}{6} \bar{\sigma}_c + \left( \frac{bd^2}{4} - \frac{bd_0^2}{4} \right) \bar{\sigma}_c = \bar{\sigma}_c S_0 + \bar{\sigma}_c (Z - Z_0) \tag{28}$$

(28) es la expresión conocida para el momento flector de secciones rectangulares en estado elástico plástico.

Ejes en los cuales el eje de las x coincide con el eje neutro.-

---

\* Por la convención de que áreas plásticas en tensión son negativas, y en compresión positivas.

Considerando la sección mostrada en la Fig. 5, y tomando el eje neutro como el eje de las x, y el eje y en cualquier posición conveniente. En este caso la distribución de esfuerzos (1) y

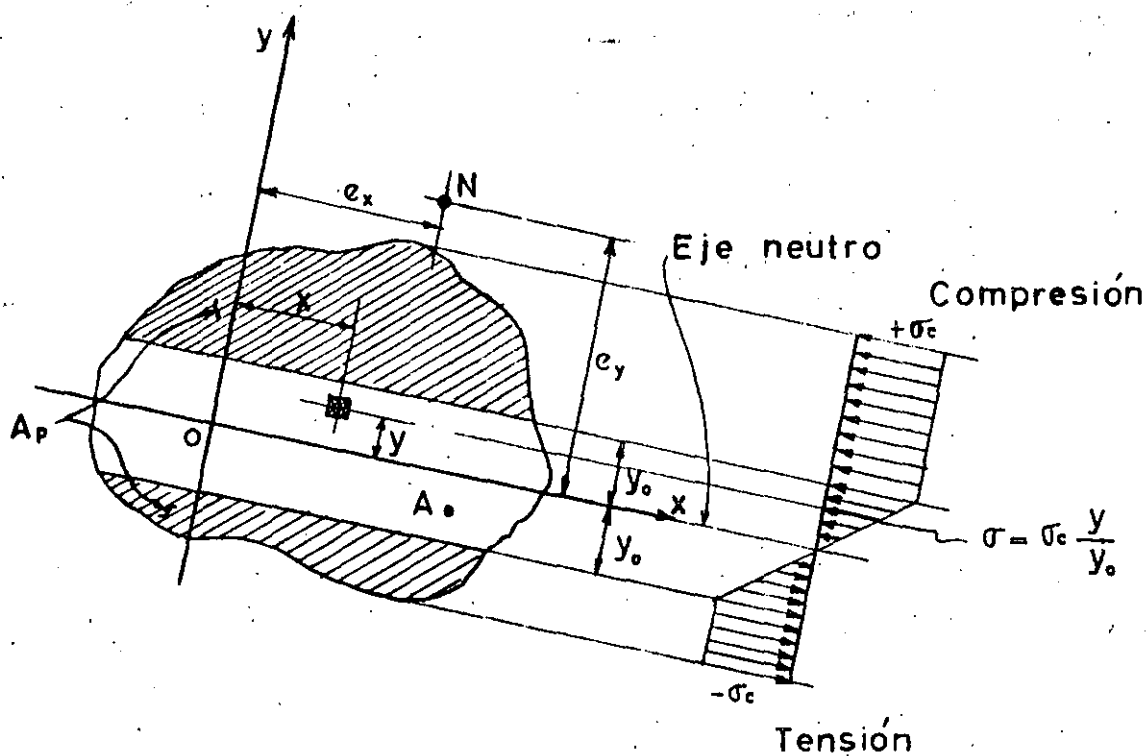


Fig. 5 Eje neutro coincidiendo con el eje x, en Flexo-compresión

(2) se reducen a

$$\left. \begin{aligned} \sigma_z &= \frac{\sigma_c}{y_0} y & \text{para} & \quad -y_0 \leq y \leq y_0 \\ \sigma_z &= \sigma_c & \text{para} & \quad y \geq y_0 \\ \sigma_z &= -\sigma_c & \text{para} & \quad y \leq -y_0 \end{aligned} \right\} \quad (29)$$

donde  $\bar{\sigma}_c$  es el esfuerzo de cedencia y  $y_0$  la distancia del eje neutro a la traza de plasticidad. Las condiciones de equilibrio (3) y (4) se reducen a

$$\left. \begin{aligned} N &= \int_{A_e} \sigma_z dA + \int_{A_p} \sigma_z dA & (a) \\ Ne_y &= \int_{A_e} \sigma_z y dA + \int_{A_p} \sigma_z y dA & (b) \\ Ne_x &= \int_{A_e} \sigma_z x dA + \int_{A_p} \sigma_z x dA & (c) \end{aligned} \right\} \quad (30)$$

donde  $N$  es la carga excéntrica,  $e_x$  y  $e_y$  las distancias de  $N$  a los ejes coordenados,  $A_e$  y  $A_p$  denota respectivamente las áreas elásticas y plásticas.

Substituyendo (29) en (30) y despejando a  $e_x$  y  $e_y$  se llega a

$$e_x = \frac{I_{xy} + y_0 q_y}{Q_x + y_0 A_p} \quad (31)$$

$$e_y = \frac{I_x + y_0 q_x}{Q_x + y_0 A_p}$$

donde

$$\left. \begin{aligned}
 A_p &= \int_{A_p} dA \\
 q_x &= \int_{A_p} y dA \\
 q_y &= \int_{A_p} x dA \\
 Q_x &= \int_{A_o} y dA \\
 I_x &= \int_{A_o} y^2 dA \\
 I_{xy} &= \int_{A_o} xy dA
 \end{aligned} \right\} (32)$$

El valor de la carga excéntrica definido por (30a), puede convenientemente expresarse en la forma

$$N = \sigma_c \left( \frac{Q_x}{y_o} + A_p \right) \quad (33)$$

Para la convención de signo adoptada,  $N$  es una carga de compresión si es positiva.

Para el caso plástico, (31) llega a

$$\left. \begin{aligned} e_x &= \lim_{y_c \rightarrow 0} \left( \frac{I_{xy} + y_c q_y}{Q_x + y_c A_p} \right) = \frac{q_y}{A_p} \\ e_y &= \lim_{y_c \rightarrow 0} \left( \frac{I_x + y_c q_x}{Q_x + y_c A_p} \right) = \frac{q_x}{A_p} \end{aligned} \right\} \quad (34)$$

y la carga  $N$  dada por (33) tiende a la última capacidad de carga de la sección  $N_u$  y es definida por

$$N_u = \lim_{y_c \rightarrow 0} \left[ \bar{\sigma}_c \left( \frac{Q_x}{y_c} + A_p \right) \right] = \bar{\sigma}_c A_p \quad (35)$$

Flexión pura.- En el caso de Flexión pura Fig. 6, de nuevo considerando como eje neutro el eje de las  $x$ , y el eje  $y$  en cualquier posición conveniente las condiciones de equilibrio son

$$\left. \begin{aligned} 0 &= \int_{A_0} \sigma_z dA + \int_{A_p} \sigma_z dA = \bar{\sigma}_c \left( \frac{Q_x}{y_c} + A_p \right). \\ M_x &= \int_{A_0} \sigma_z y dA + \int_{A_p} \sigma_z y dA = \bar{\sigma}_c \left( \frac{I_x}{y_c} + q_x \right). \\ M_y &= \int_{A_0} \sigma_z x dA + \int_{A_p} \sigma_z x dA = \bar{\sigma}_c \left( \frac{I_{xy}}{y_c} + q_y \right). \end{aligned} \right\} \quad (36)$$

donde  $M_x$  y  $M_y$  son las componentes de  $M$  respecto a los ejes coordenados.

El momento flector es dado por

$$M = \sqrt{M_x^2 + M_y^2} = \sigma_c \sqrt{\left(\frac{I_x + q_x}{y_c}\right)^2 + \left(\frac{I_{xy} + q_y}{y_c}\right)^2} \quad (37)$$

El ángulo de inclinación de M es dado por

$$\tan. \theta = \frac{M_y}{M_x} = \frac{I_{xy} + y_c q_y}{I_x + y_c q_x} \quad (38)$$

Consistente con el signo de  $\sigma_c$ , definido por (29),  $\theta$  es positivo cuando se mide en dirección de las manecillas del reloj, con respecto al eje x, y M,  $M_x$  y  $M_y$  son positivos en la dirección indicada en la Fig. 6.

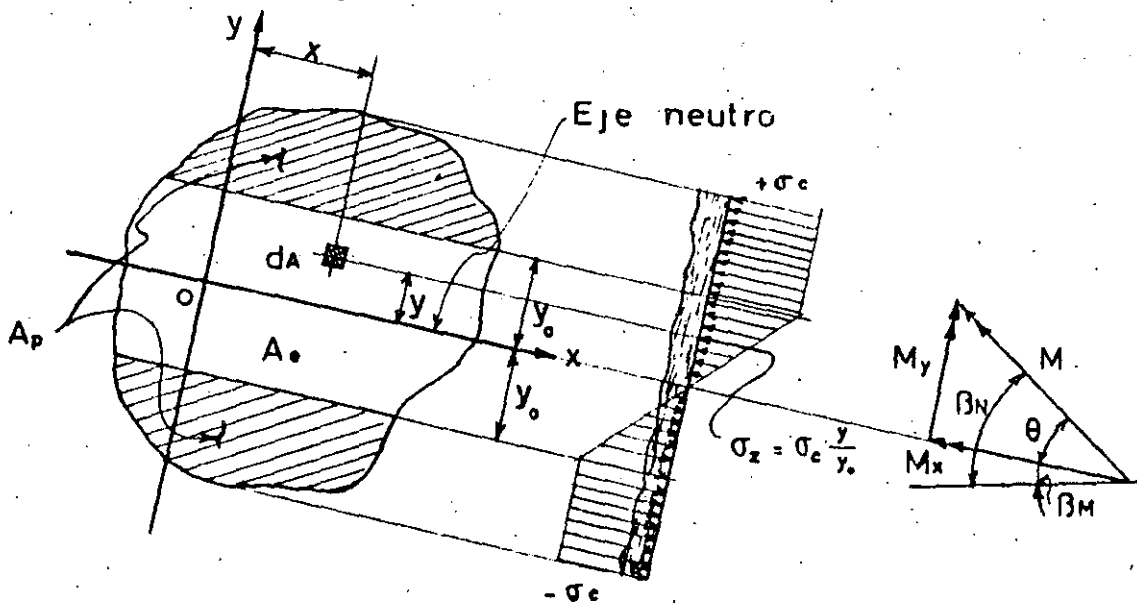


Fig. 6 Eje neutro coincidiendo con eje x, en Flexión bi-axial.

Para la sección totalmente plastificada  $M$  tiende a  $M_u$  y (37) y (38) se transforman en

$$M_u = \lim_{y_c \rightarrow 0} \left[ \sigma_c \sqrt{\left(\frac{I_x}{y_c} + q_x\right)^2 + \left(\frac{I_{xy}}{y_c} + q_y\right)^2} \right] = \sigma_c \sqrt{q_x^2 + q_y^2} \quad (39)$$

$$\theta = \tan^{-1} \left[ \lim_{y_c \rightarrow 0} \left( \frac{I_{xy} + y_c q_y}{I_x + y_c q_x} \right) \right] = \tan^{-1} \frac{q_y}{q_x} \quad (40)$$

(39) y (40) nos definen el momento último o límite de una sección cualquiera bajo la acción de flexión bi-axial.

#### C O N C L U S I O N E S

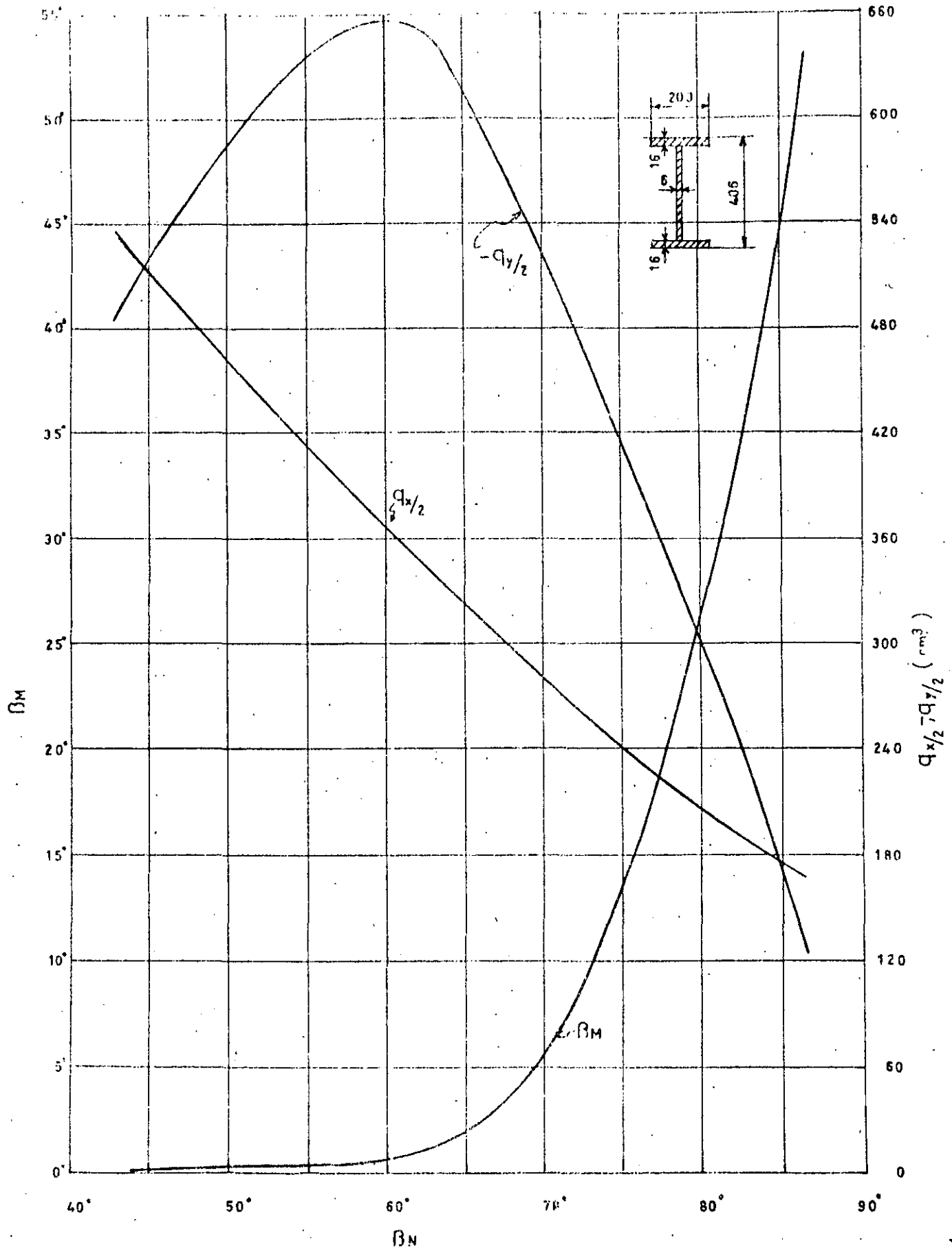
Utilizando las fórmulas (34), (35), (39) y (40), provenientes de las condiciones de equilibrio, cuando el eje neutro coincide con el eje de las  $x$ . Se han preparado gráficos de diseño límite para columnas y vigas bajo las condiciones de Flexo-compresión y flexión bi-axial. Es importante mencionar que en el caso de columnas tendremos el valor último  $N_u$  de la carga normal de la columna corta. En ambos casos se deberá trabajar el ele -

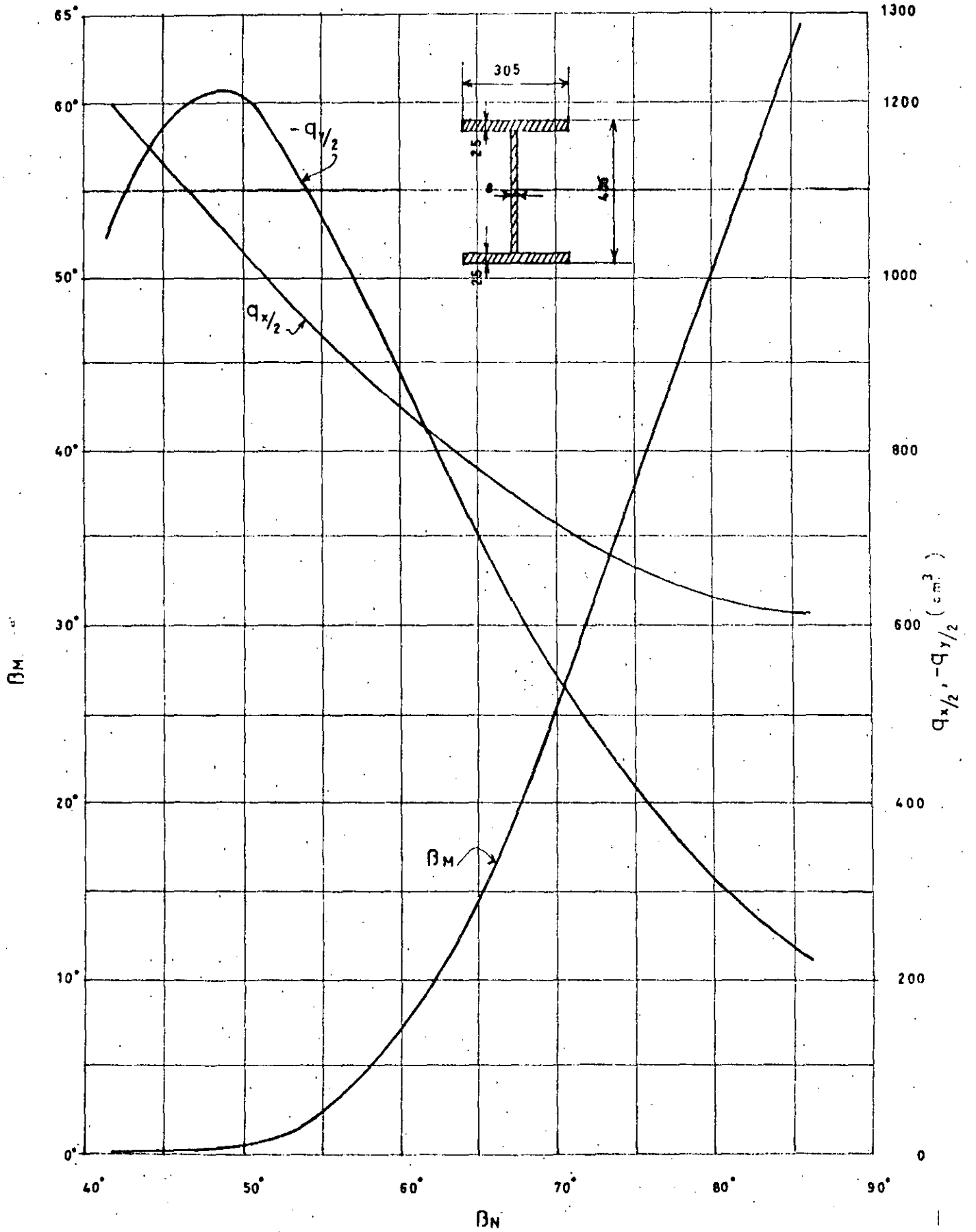
mento estructural con el factor de carga apropiado dependiendo este de la relación de carga muerta a carga viva, y la reducción adecuada por esbeltez.

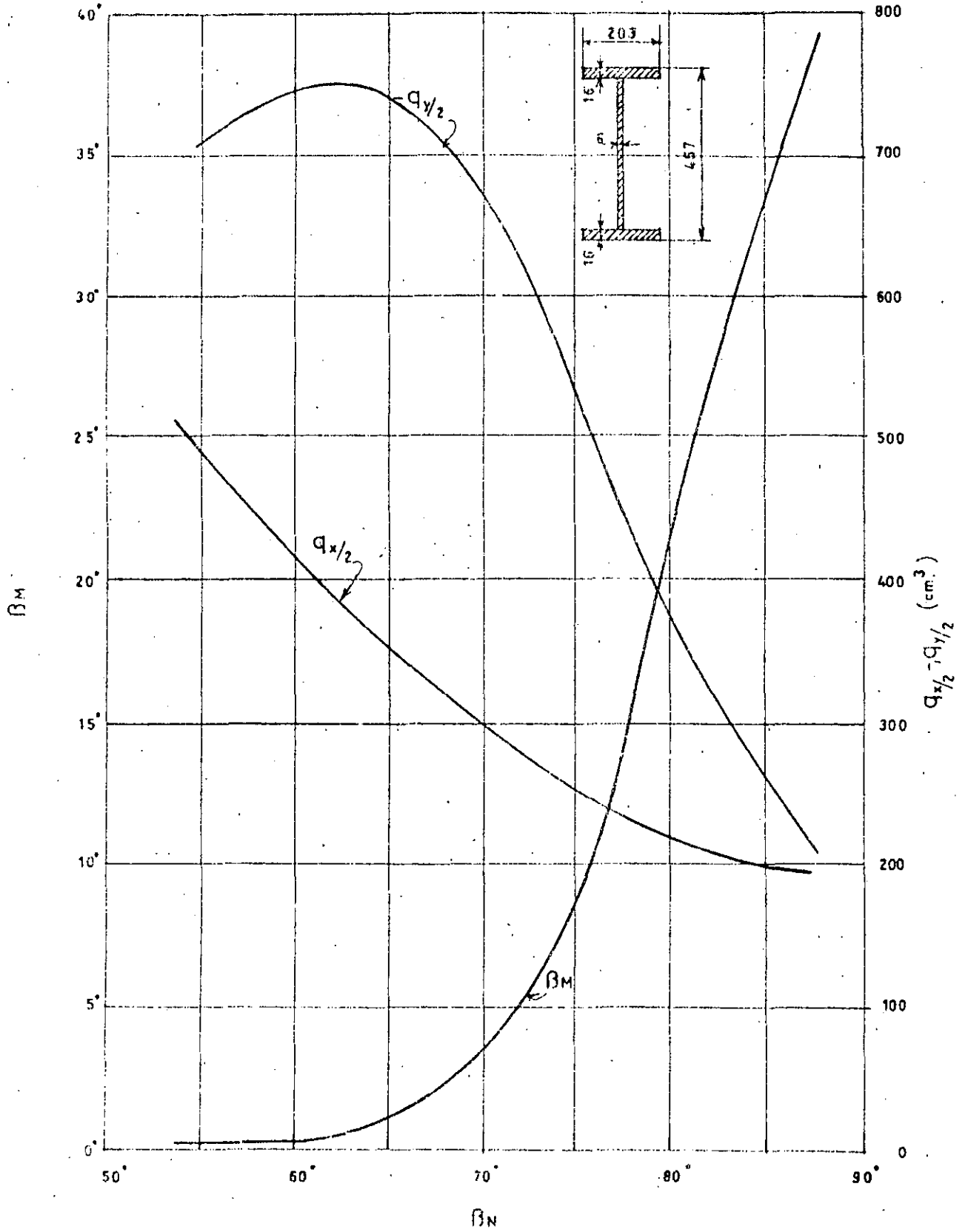
## R E F E R E N C I A S

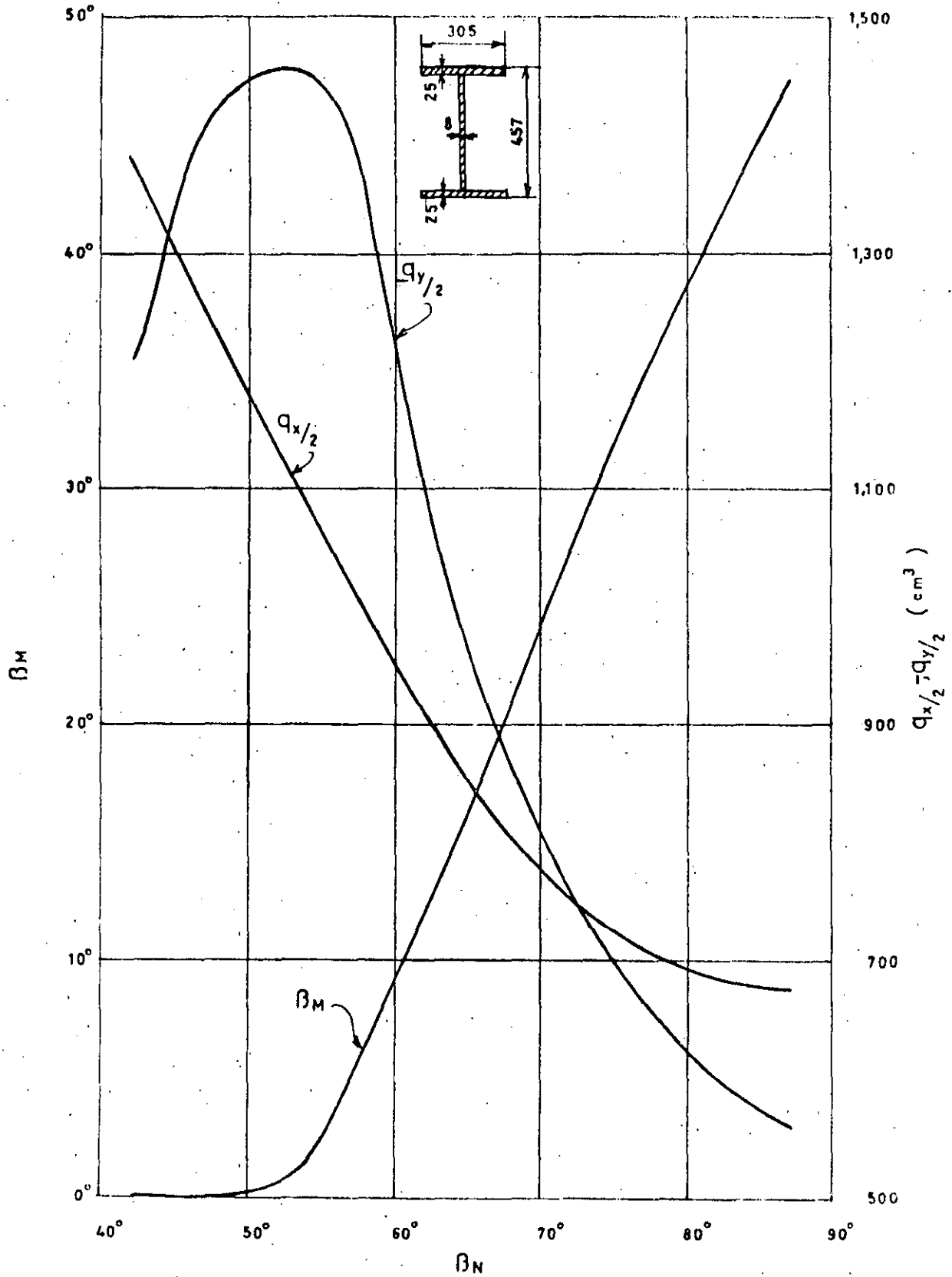
1. Aghababian, M. S. and Popov, E. P. "Unsymmetrical Bending of Rectangular Beams Beyond the Elastic Limit". Proceedings of the First National Congress of Applied Mechanics, 1951.
2. Beedle, L. S. Thurlimann, B. and Ketter, R. L., "Plastic Design in Structural Steel" Fritz Engineering Laboratory Report No. 205. 32. Lehigh University, Bethlehem Pennsylvania, 1955, p. 9. 1.
3. P. Ballesteros, S. L. Lee. "Ultimate Strength of Short Struts" Journal Structural Division, Proceedings of the ASCE, paper 1358, September, 1957.
4. P. Ballesteros, J. E. Arriaga. "Economía de Acero debido al Diseño Plástico". Primer Symposium Panamericano de Estructuras, Instituto Politécnico Nacional, 1961, México, D. F.

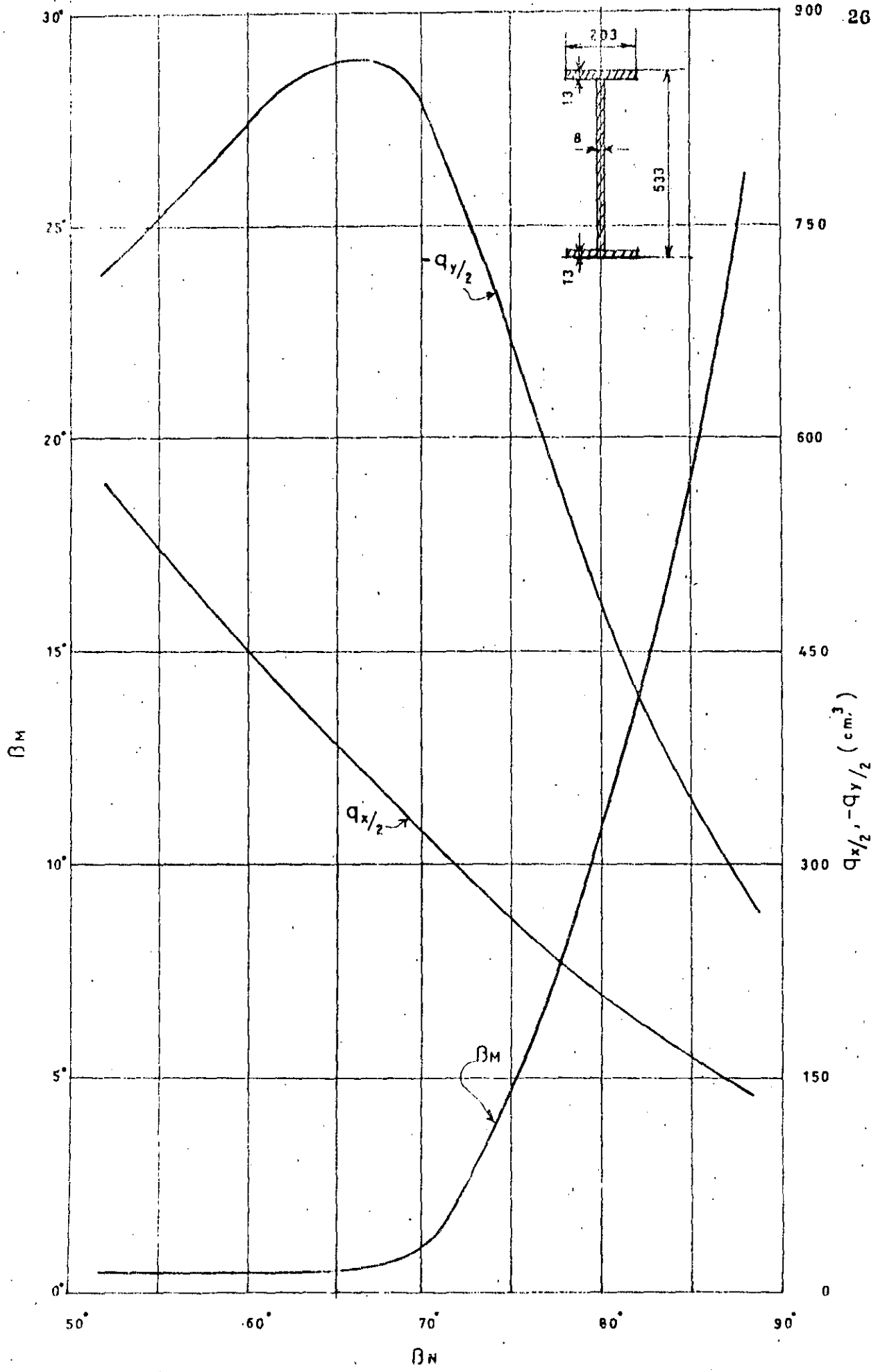


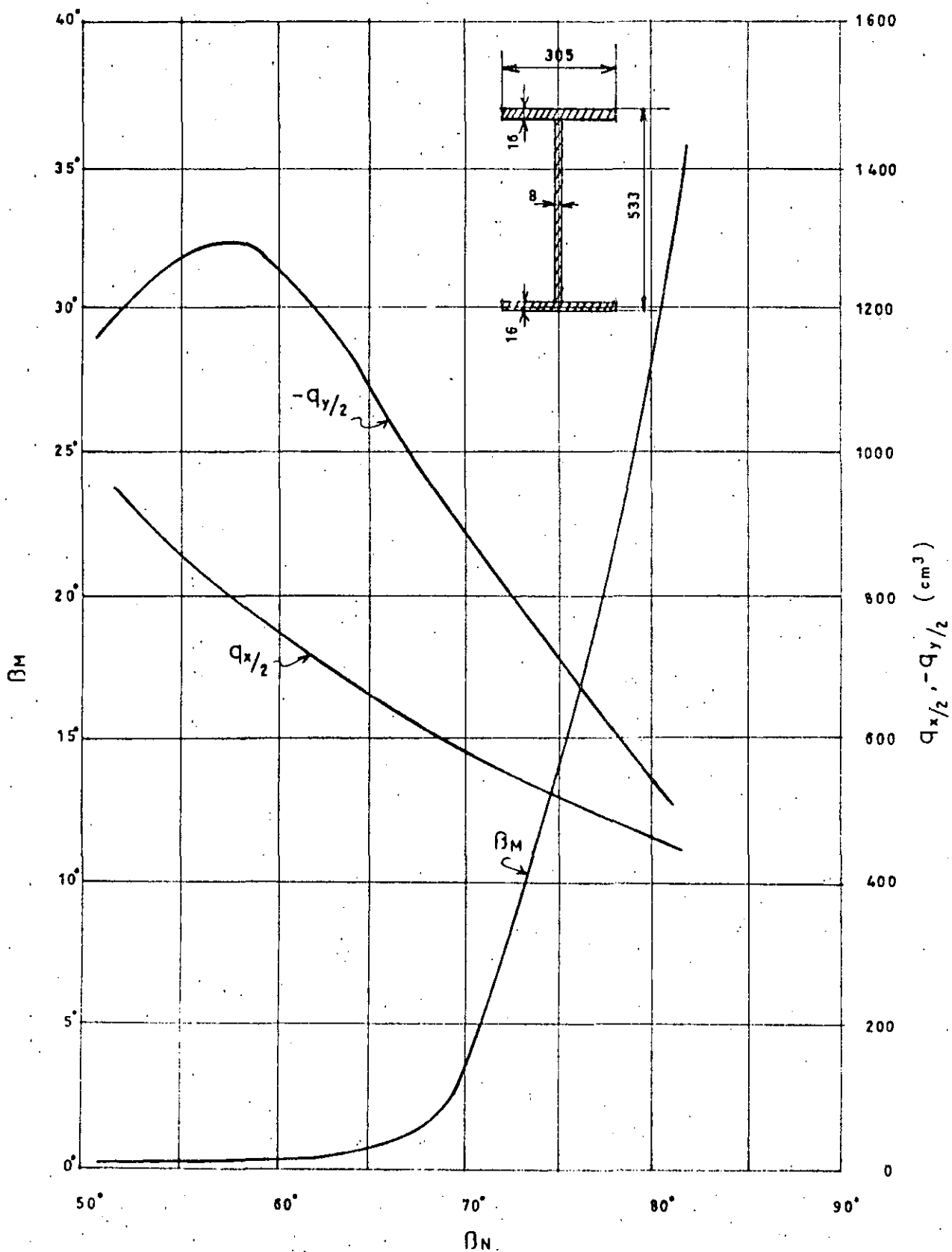


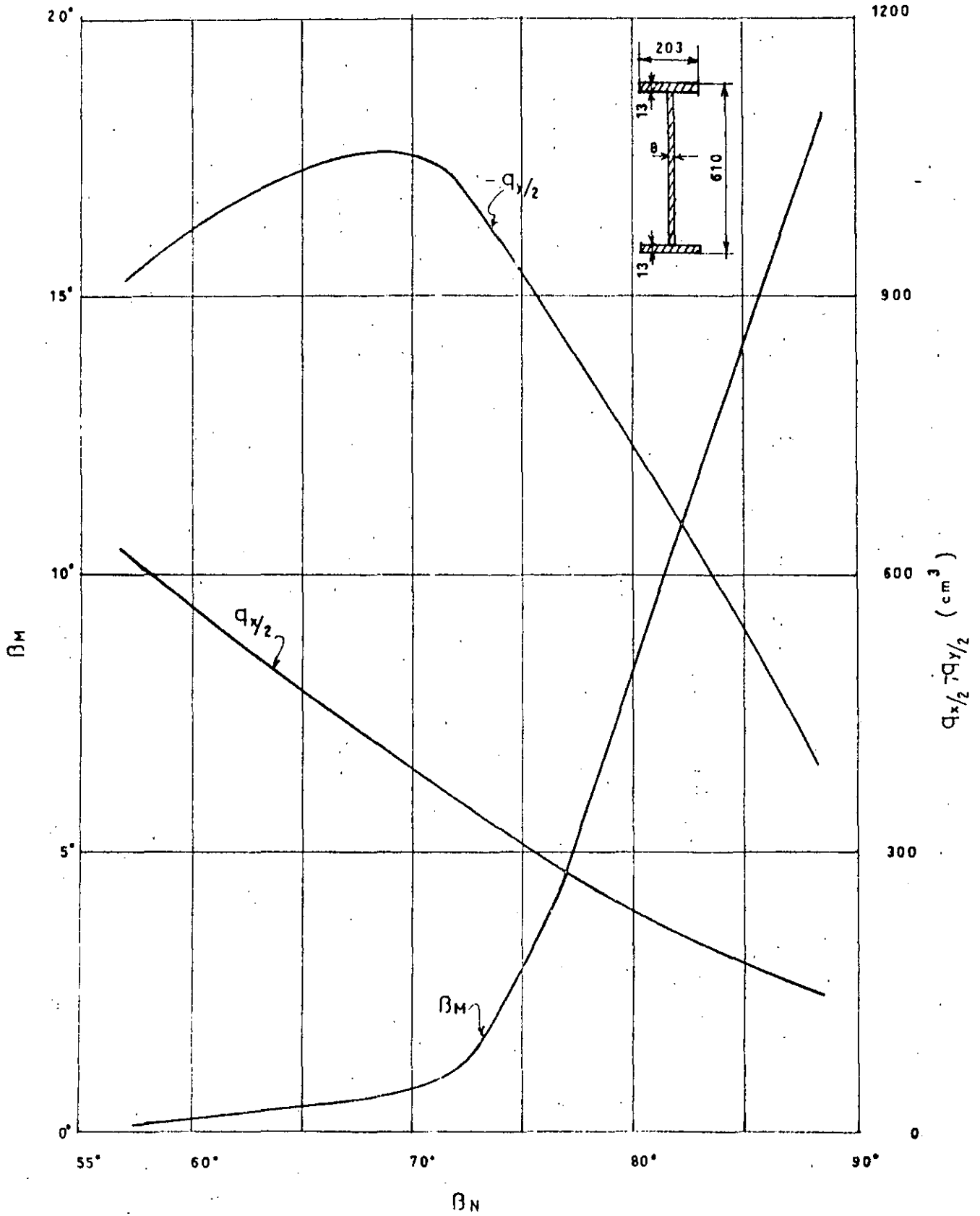


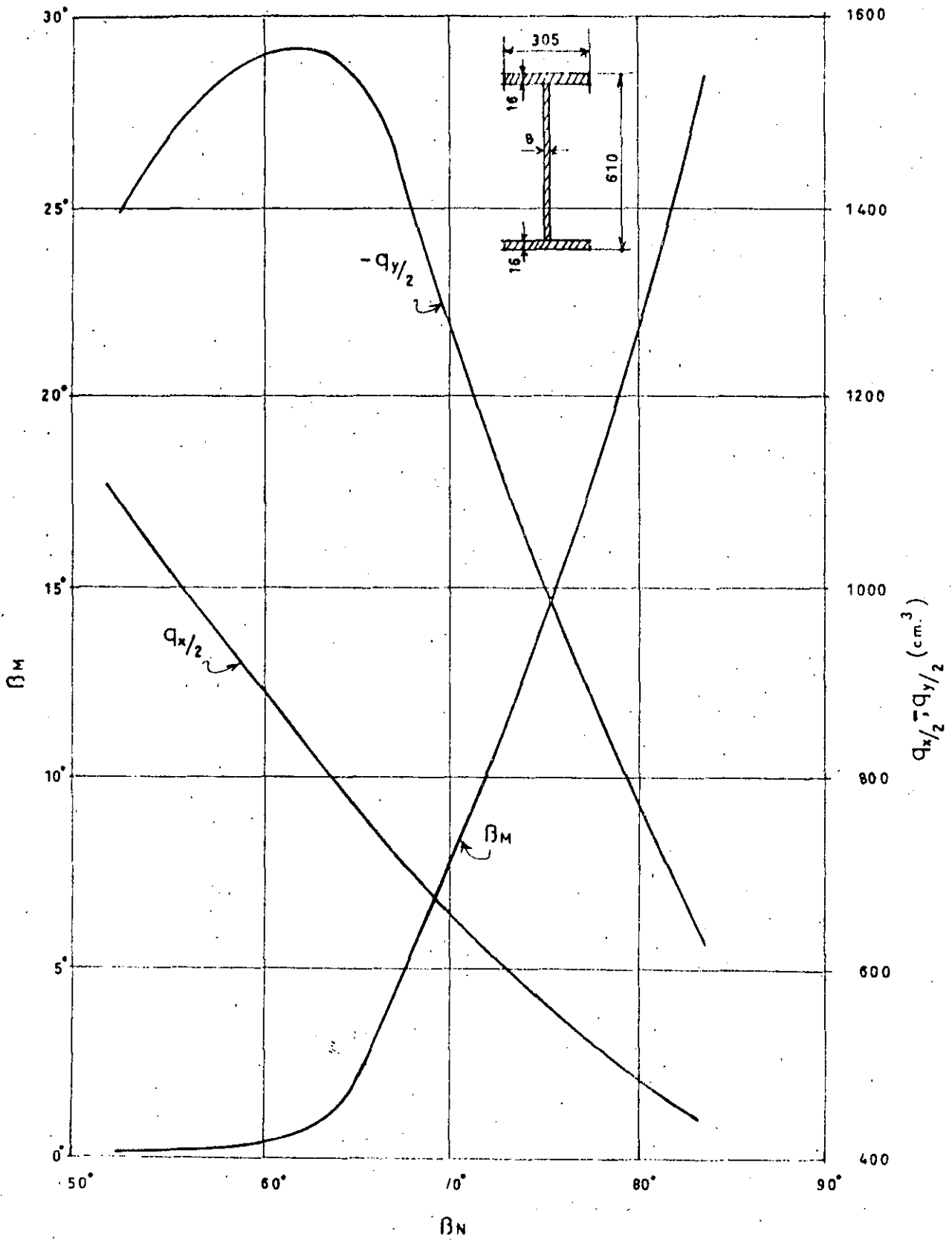




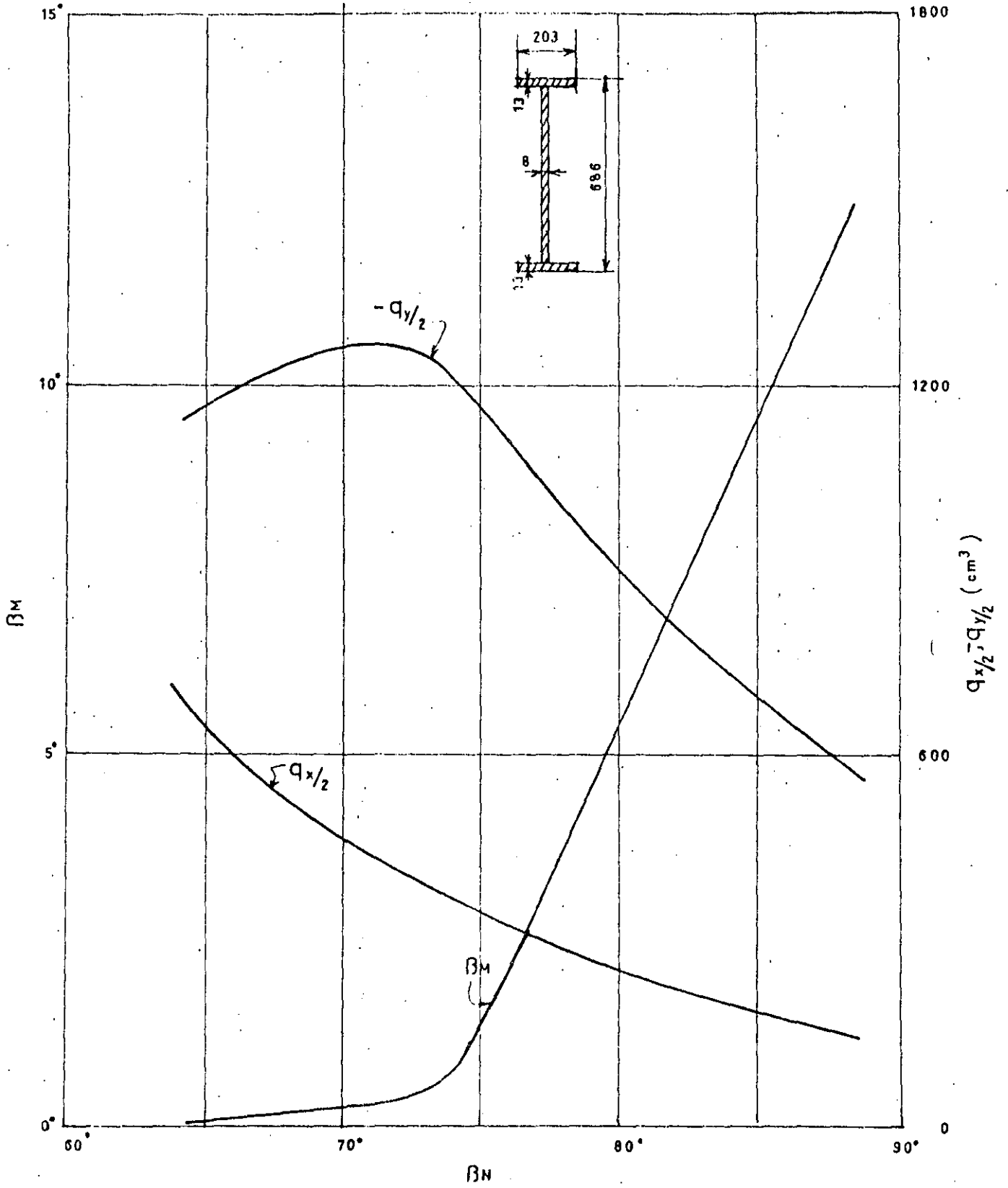


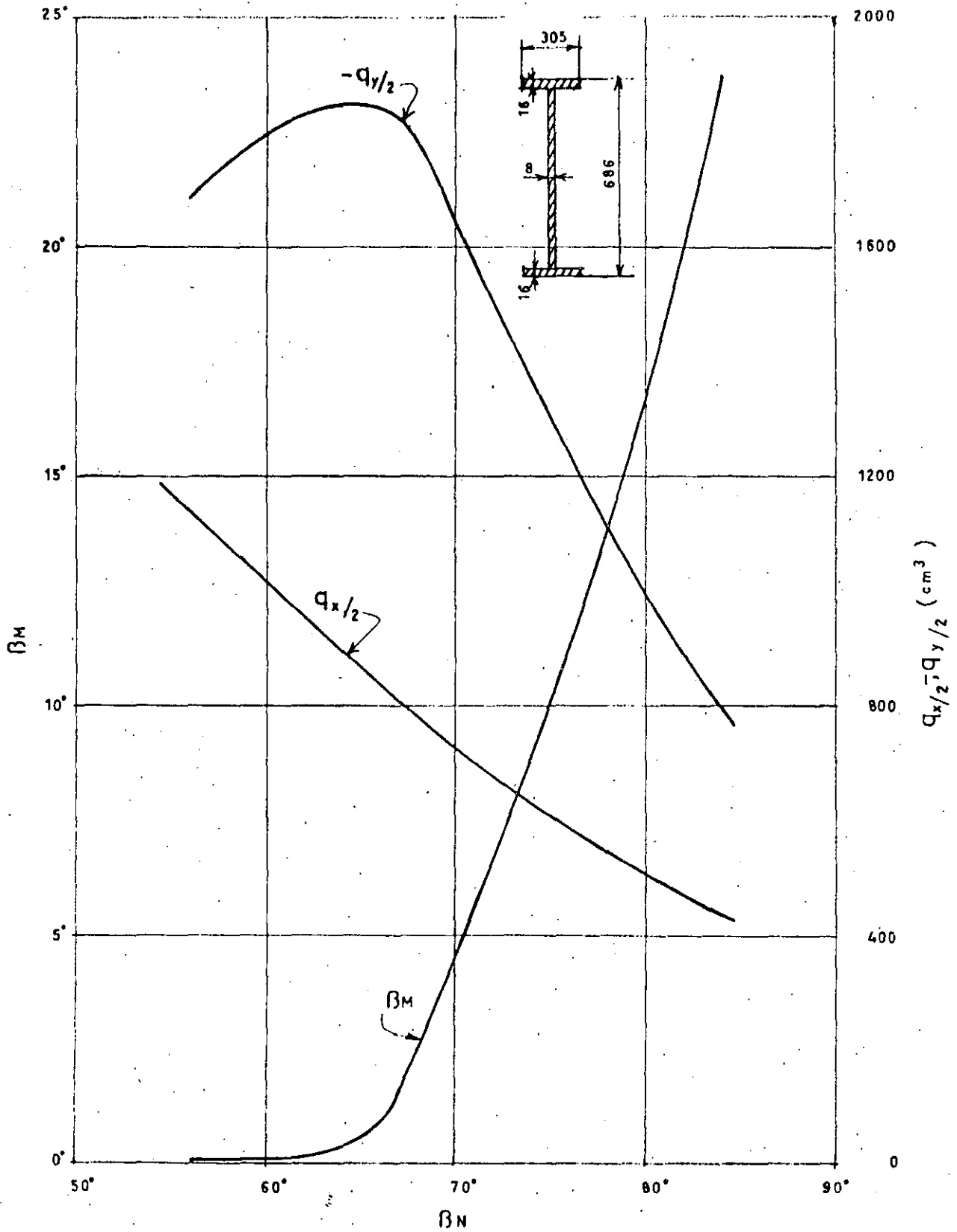


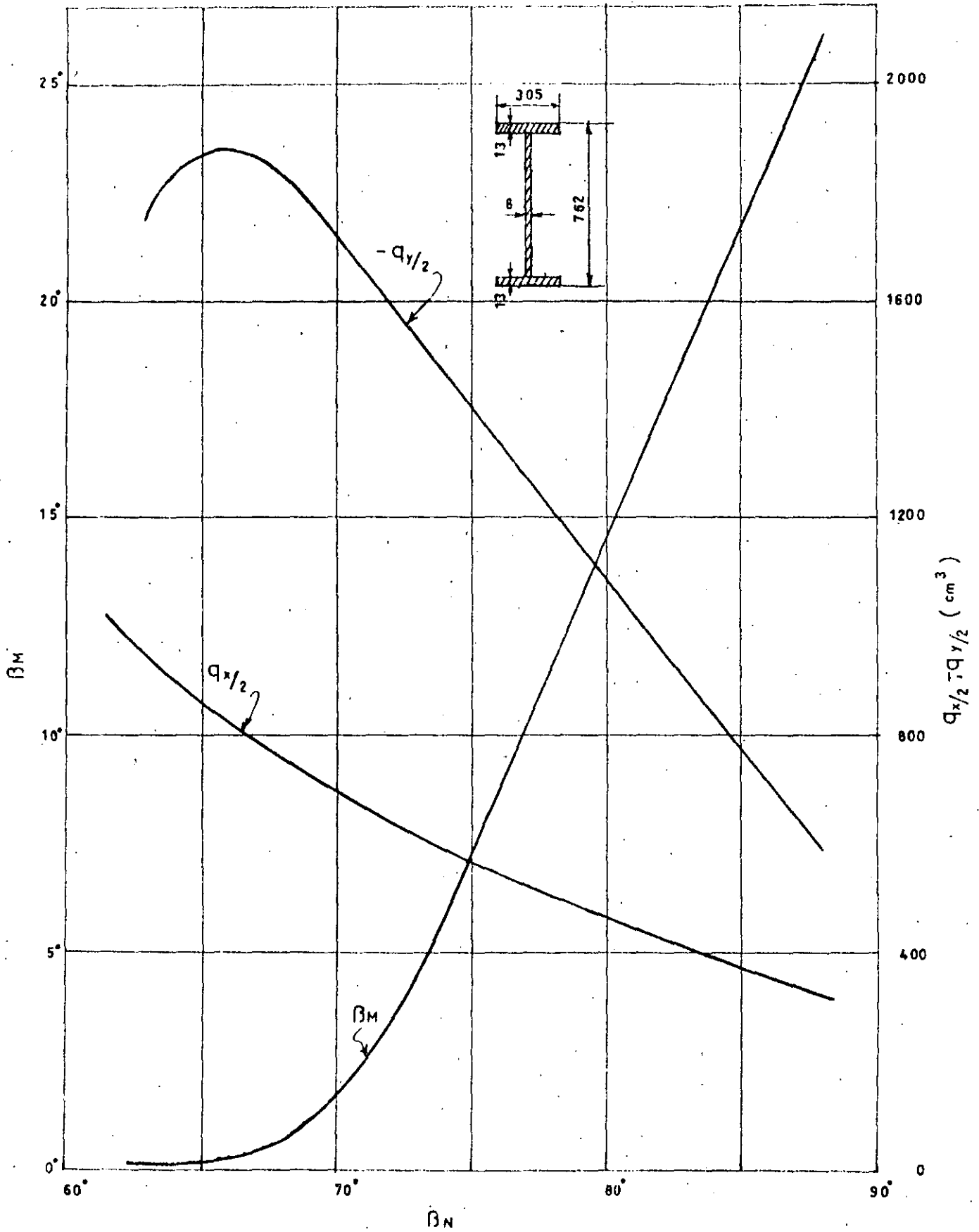


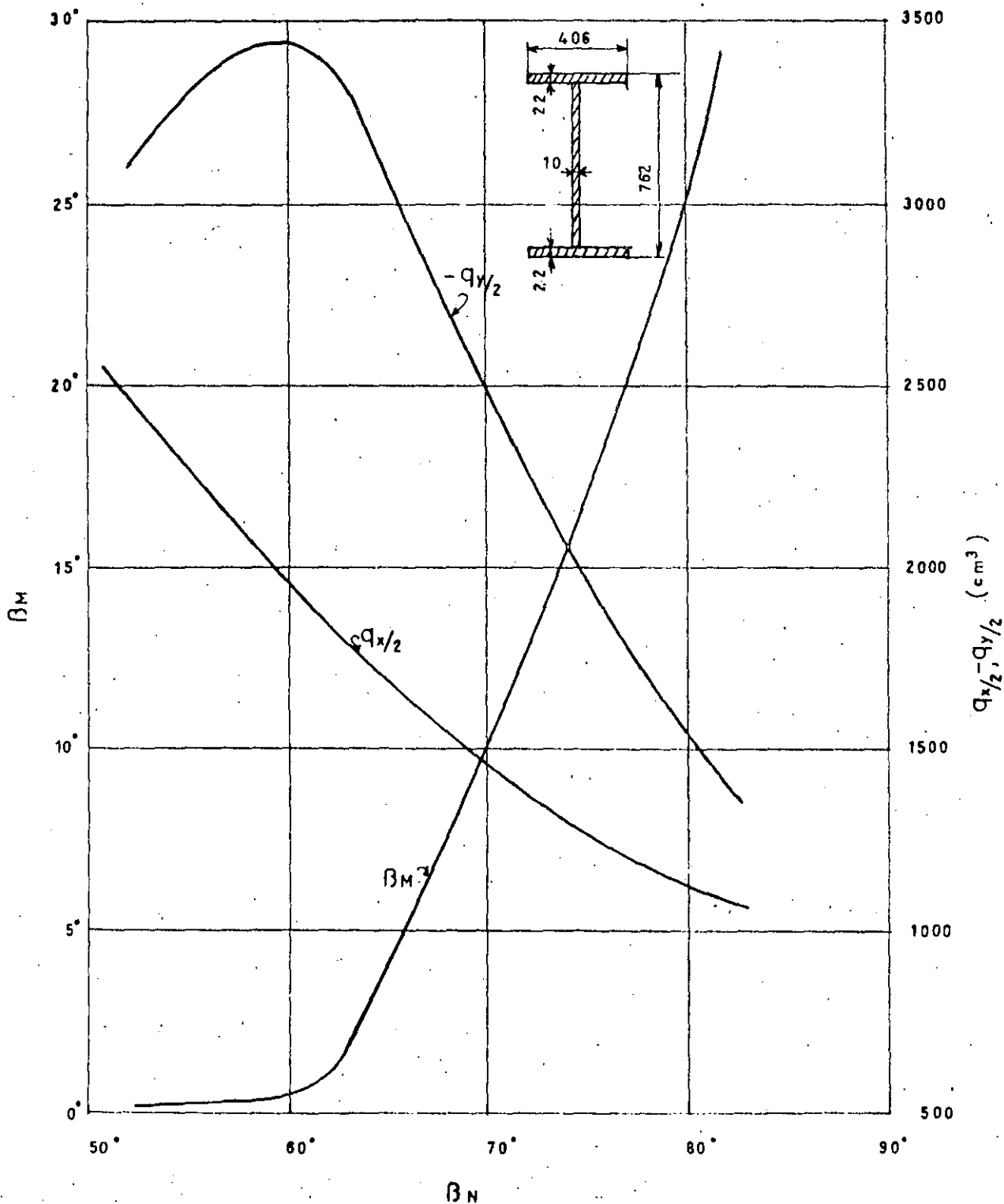


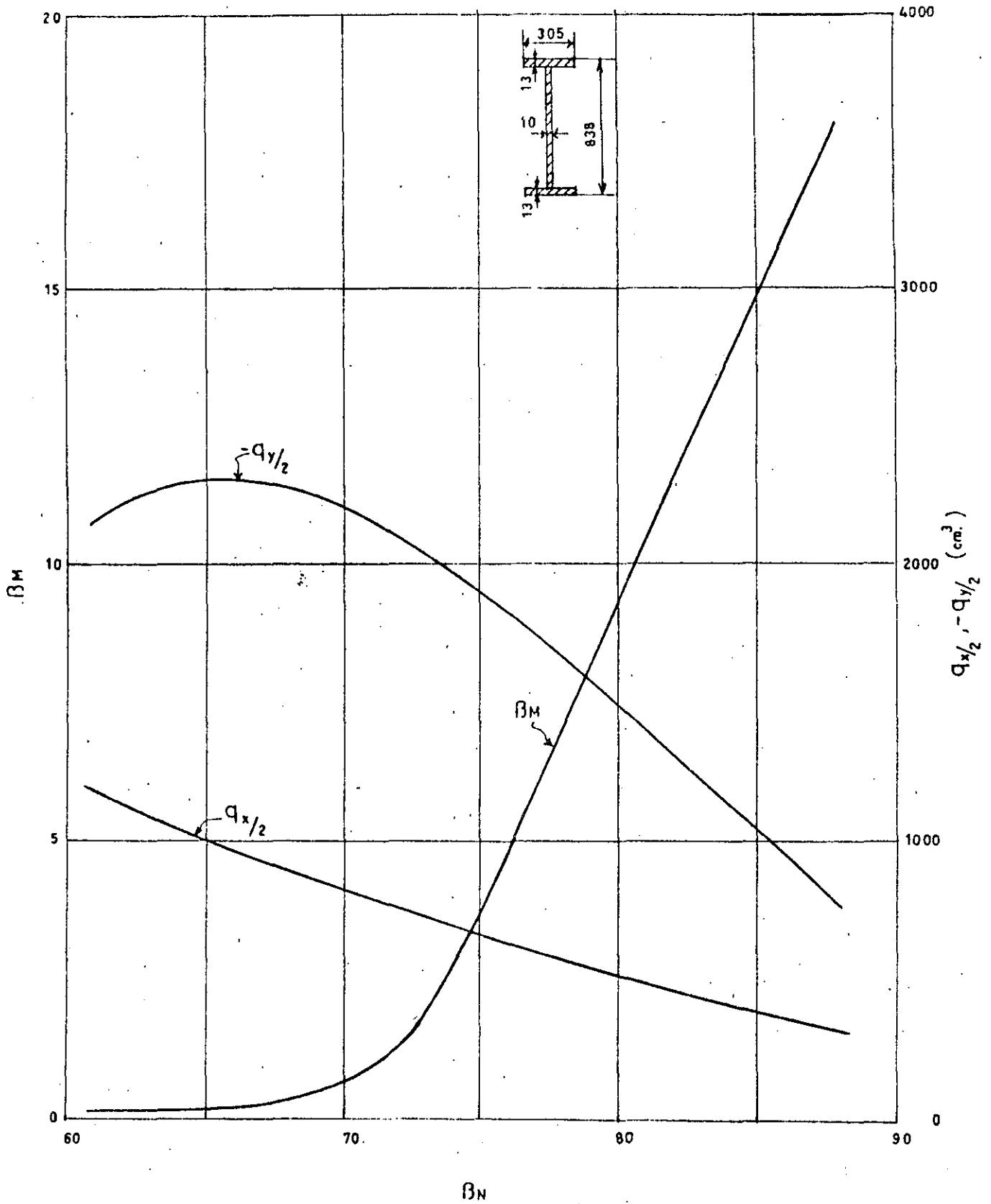


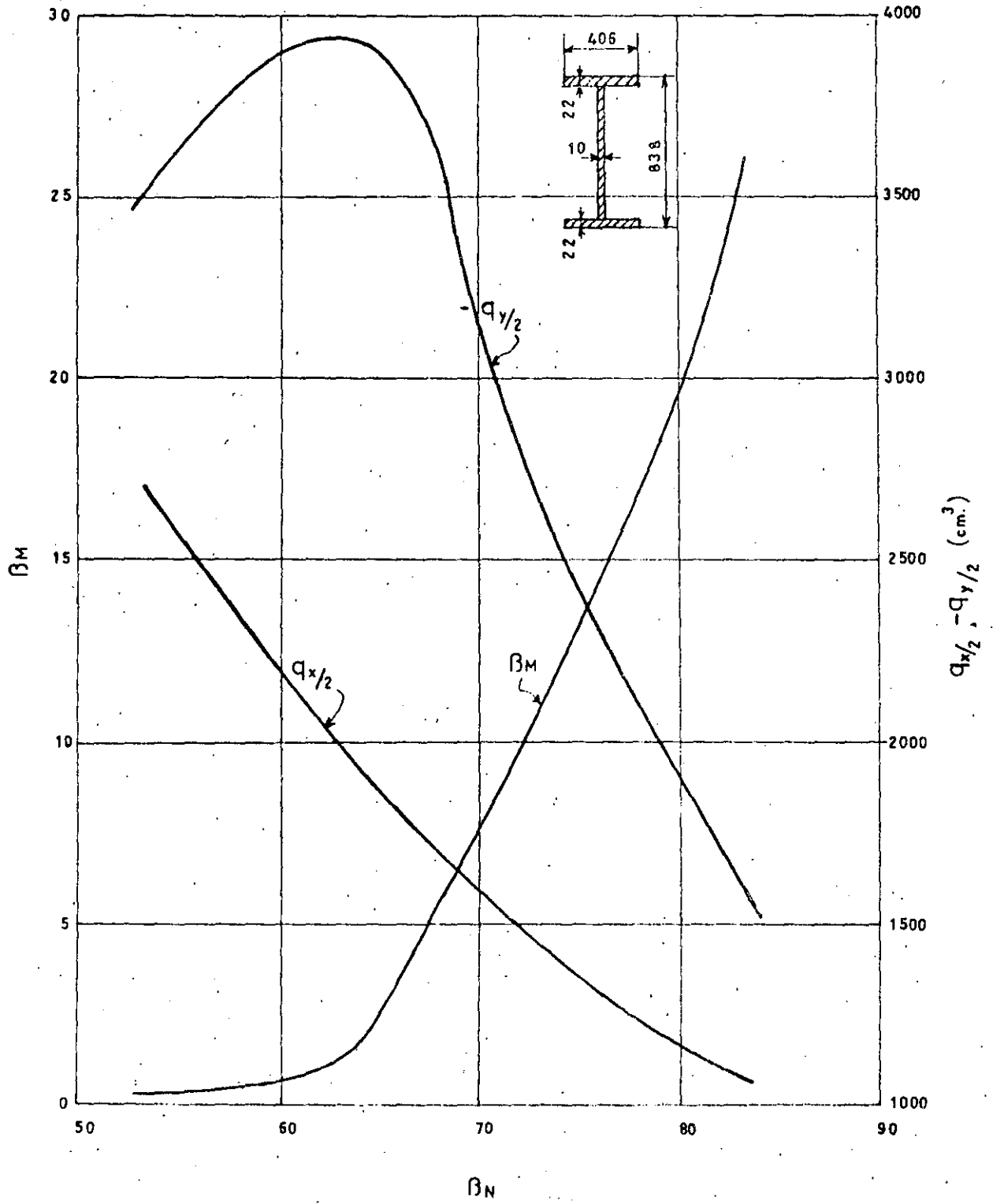


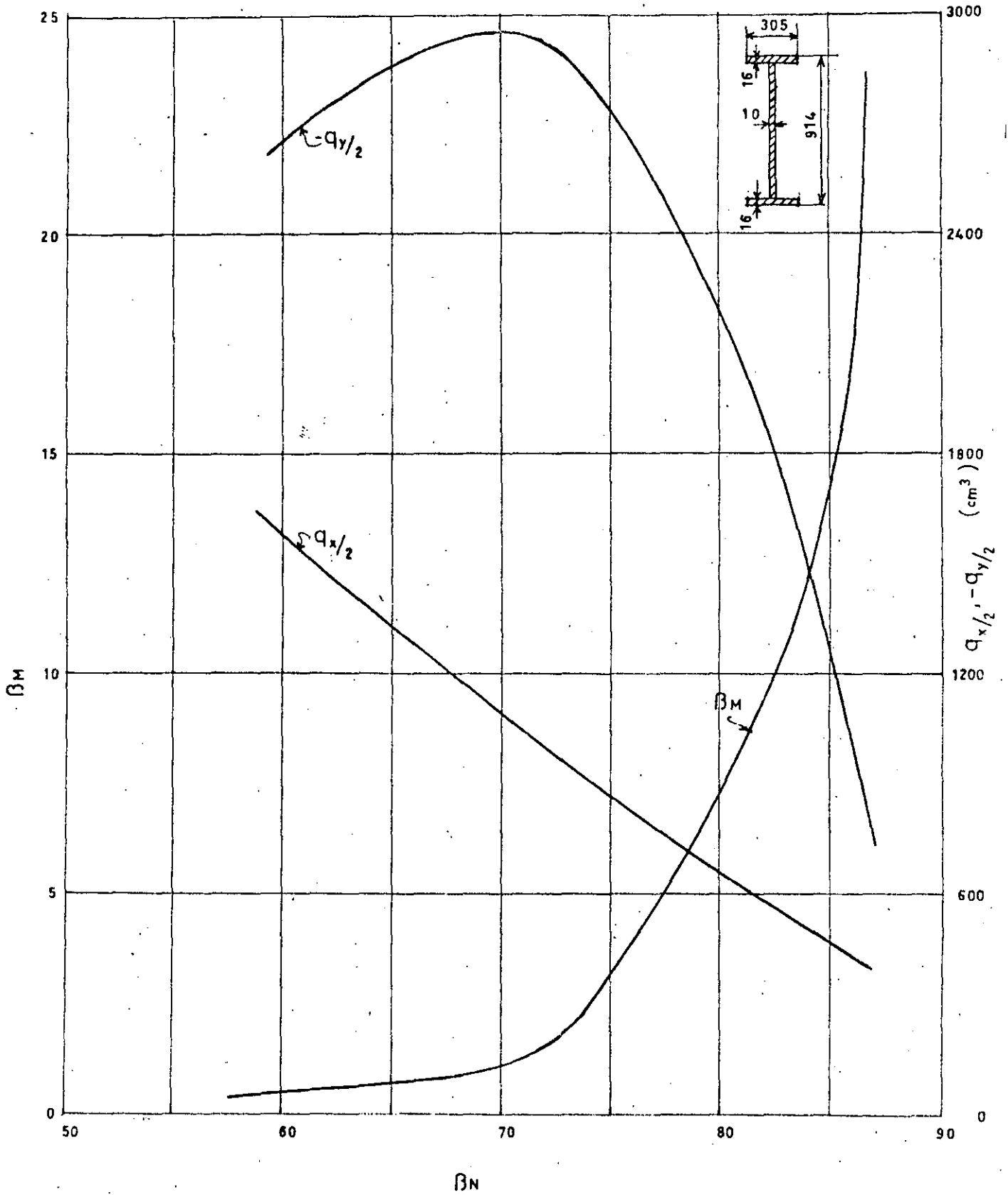


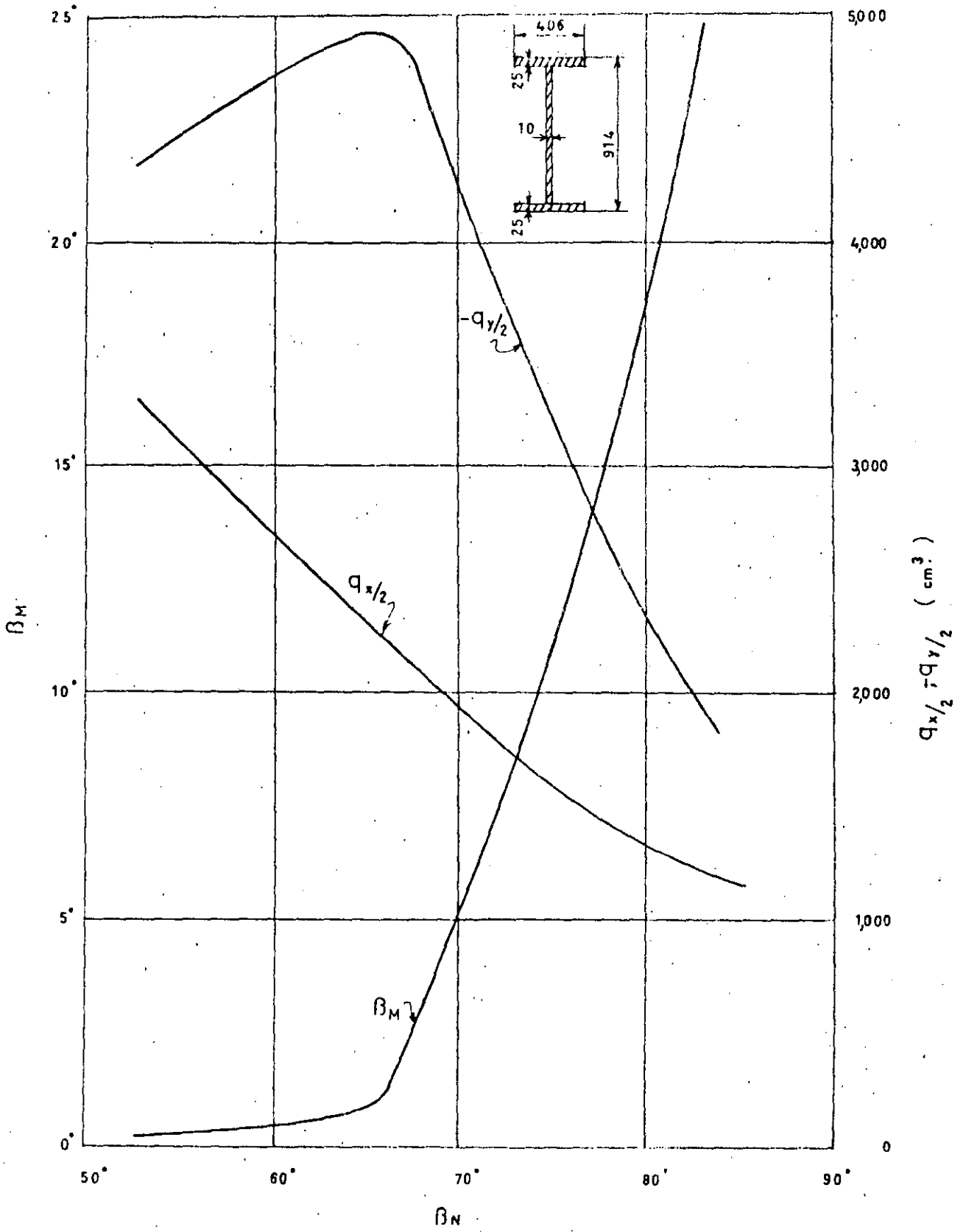




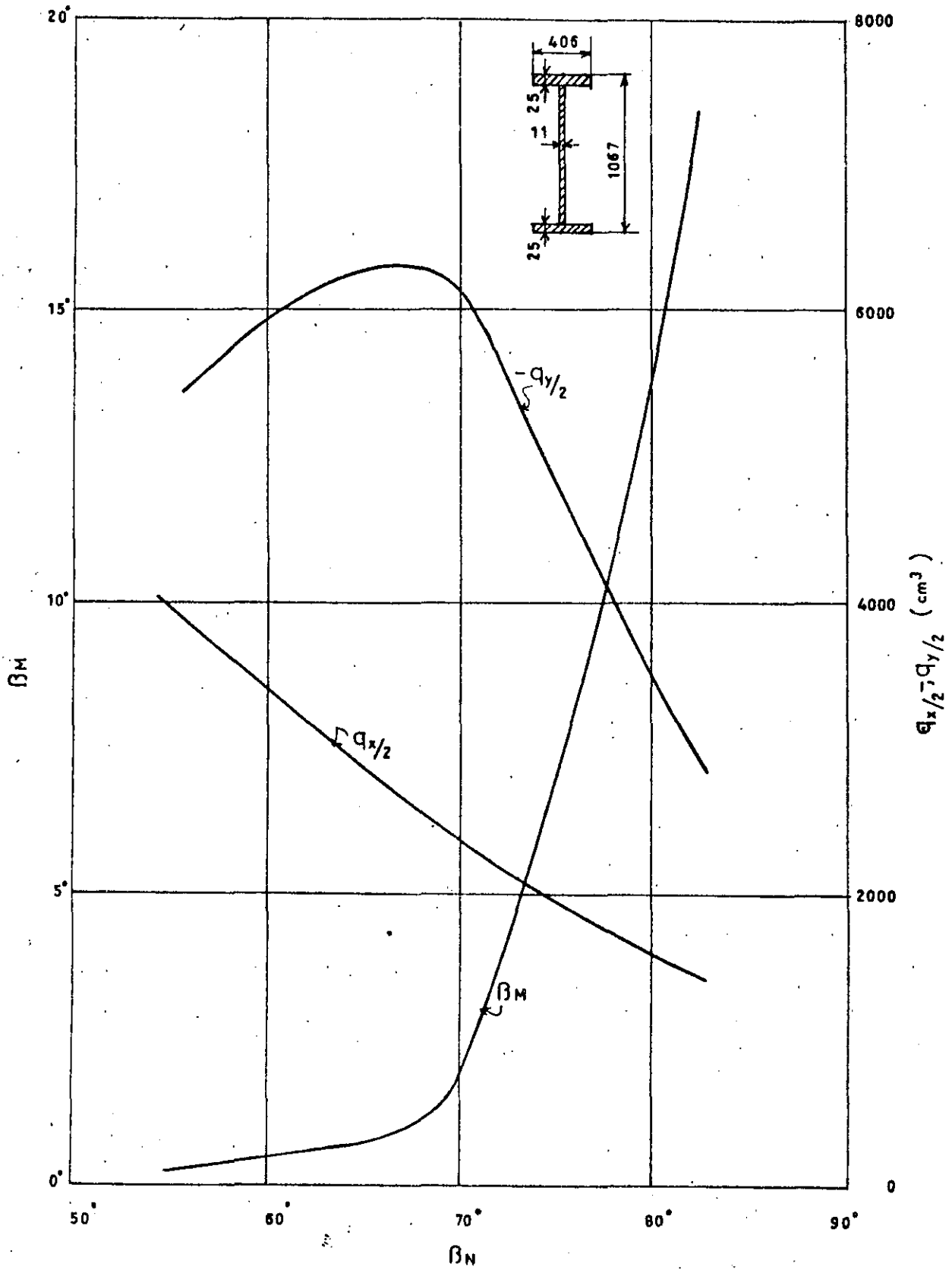


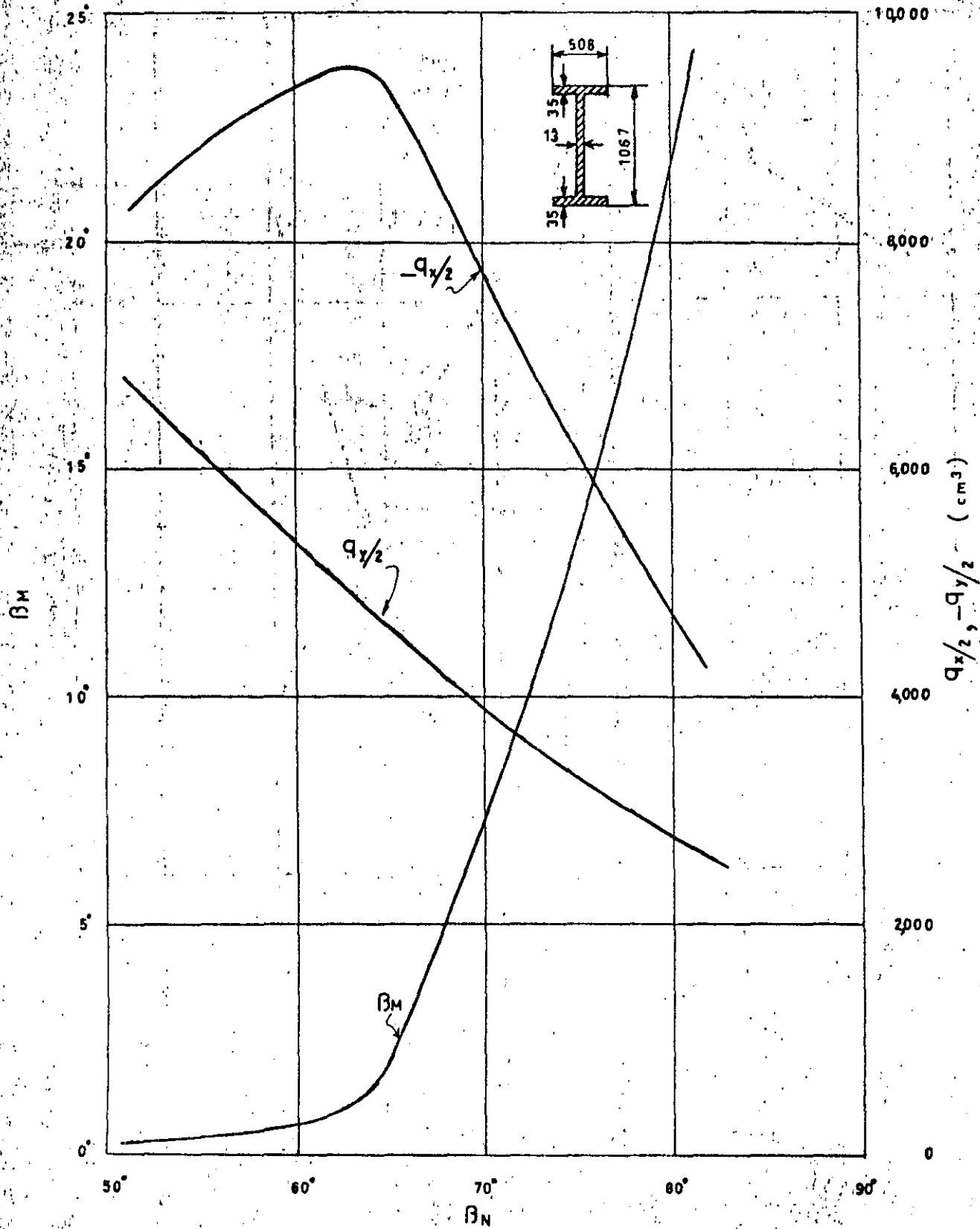


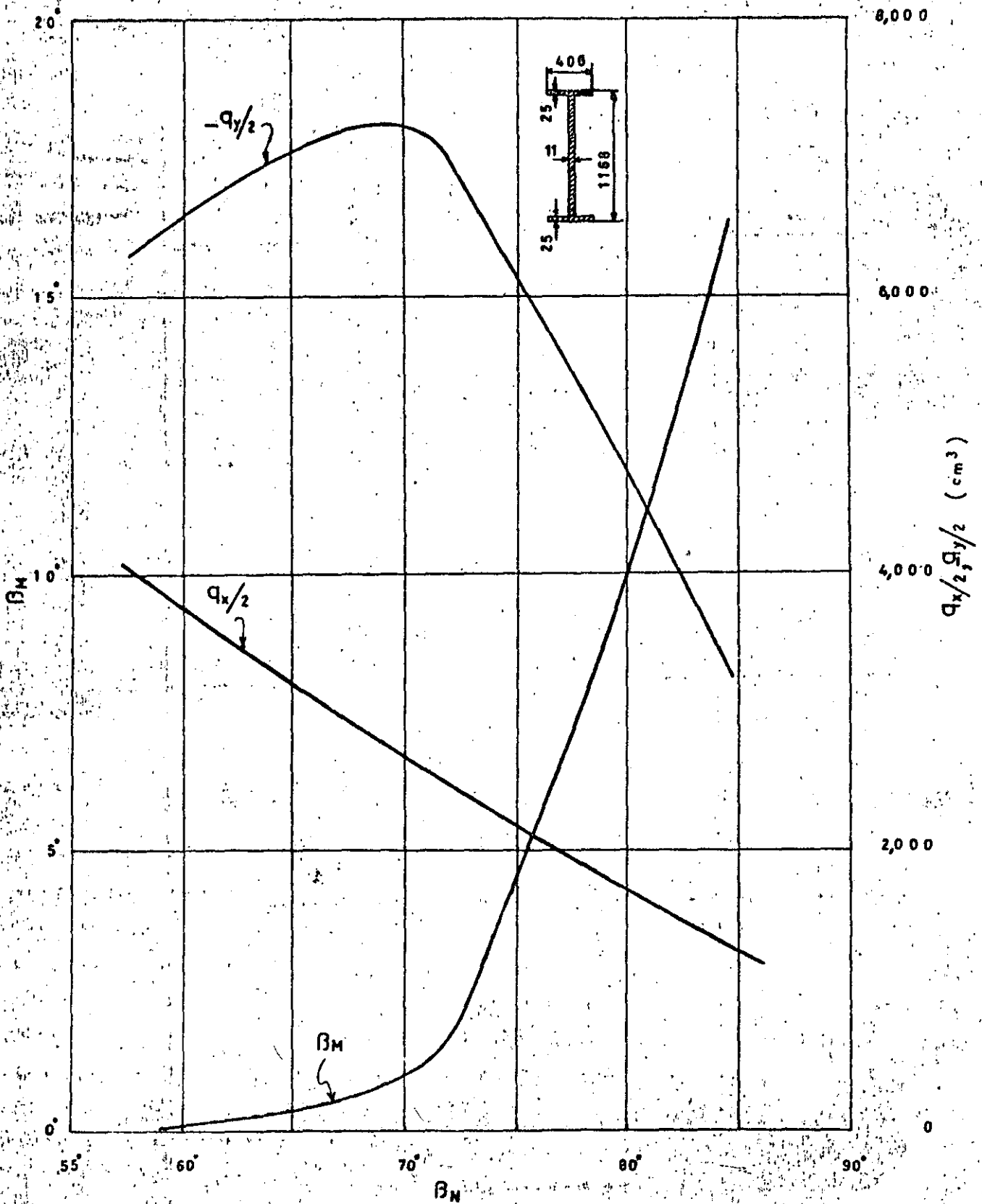


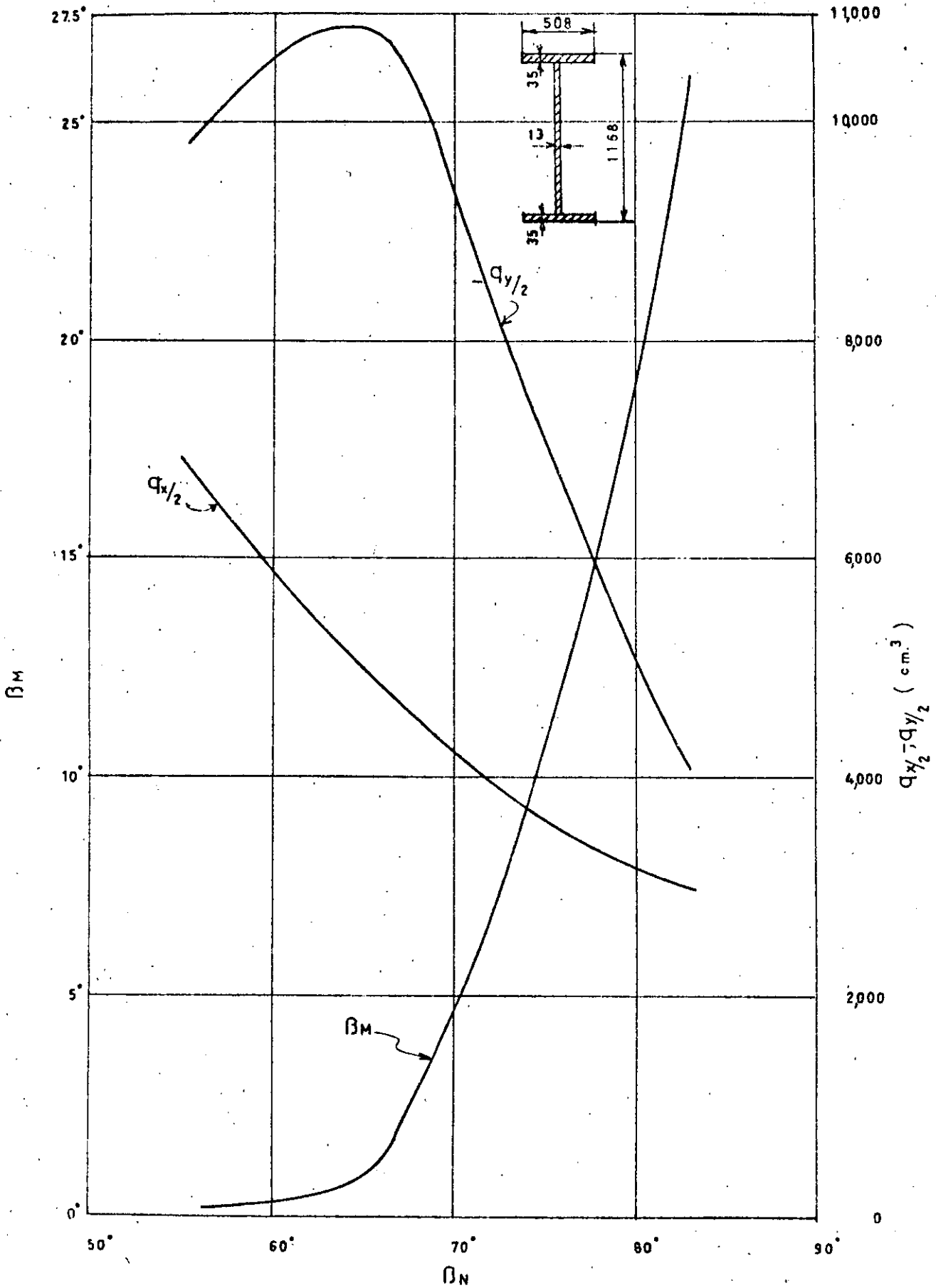


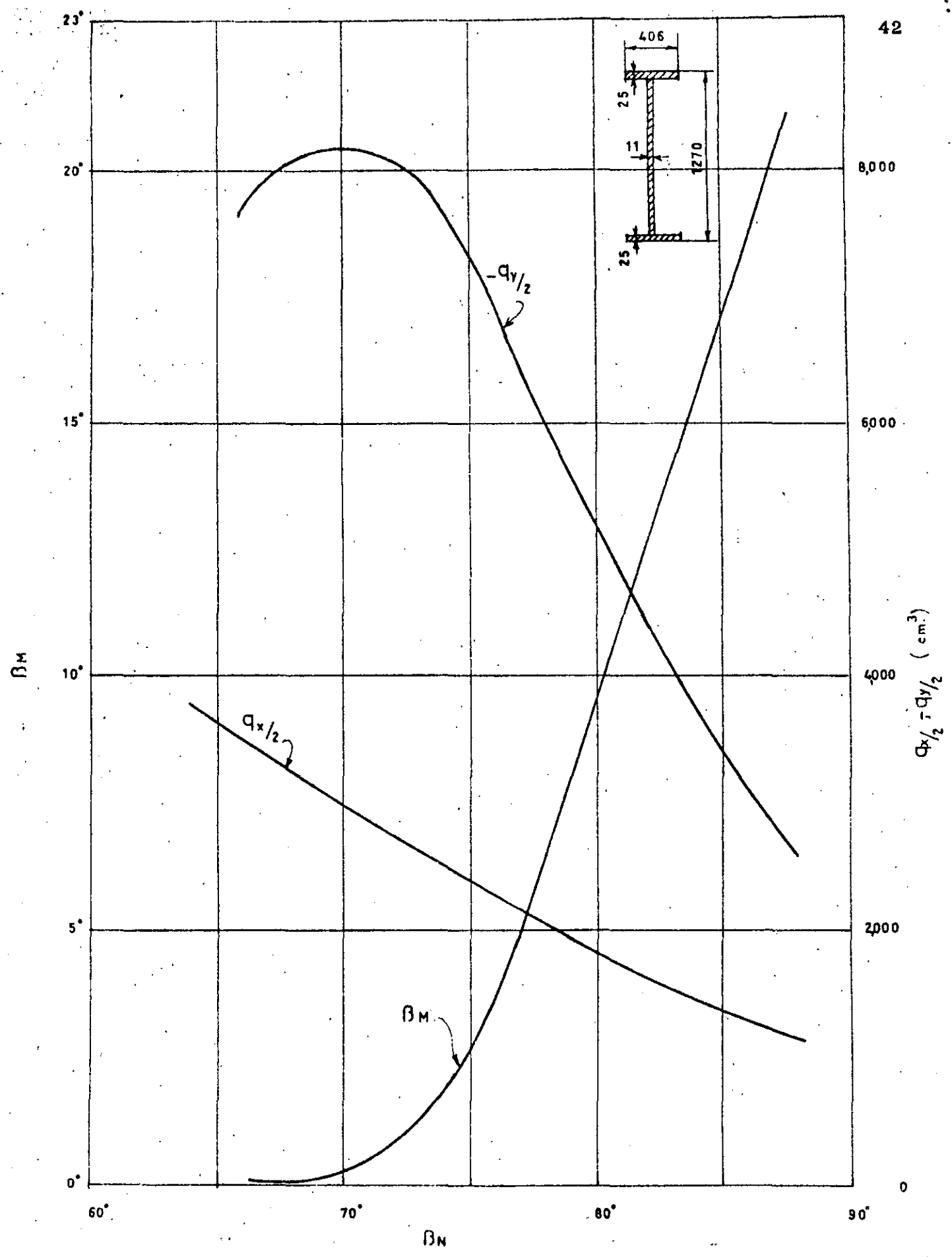


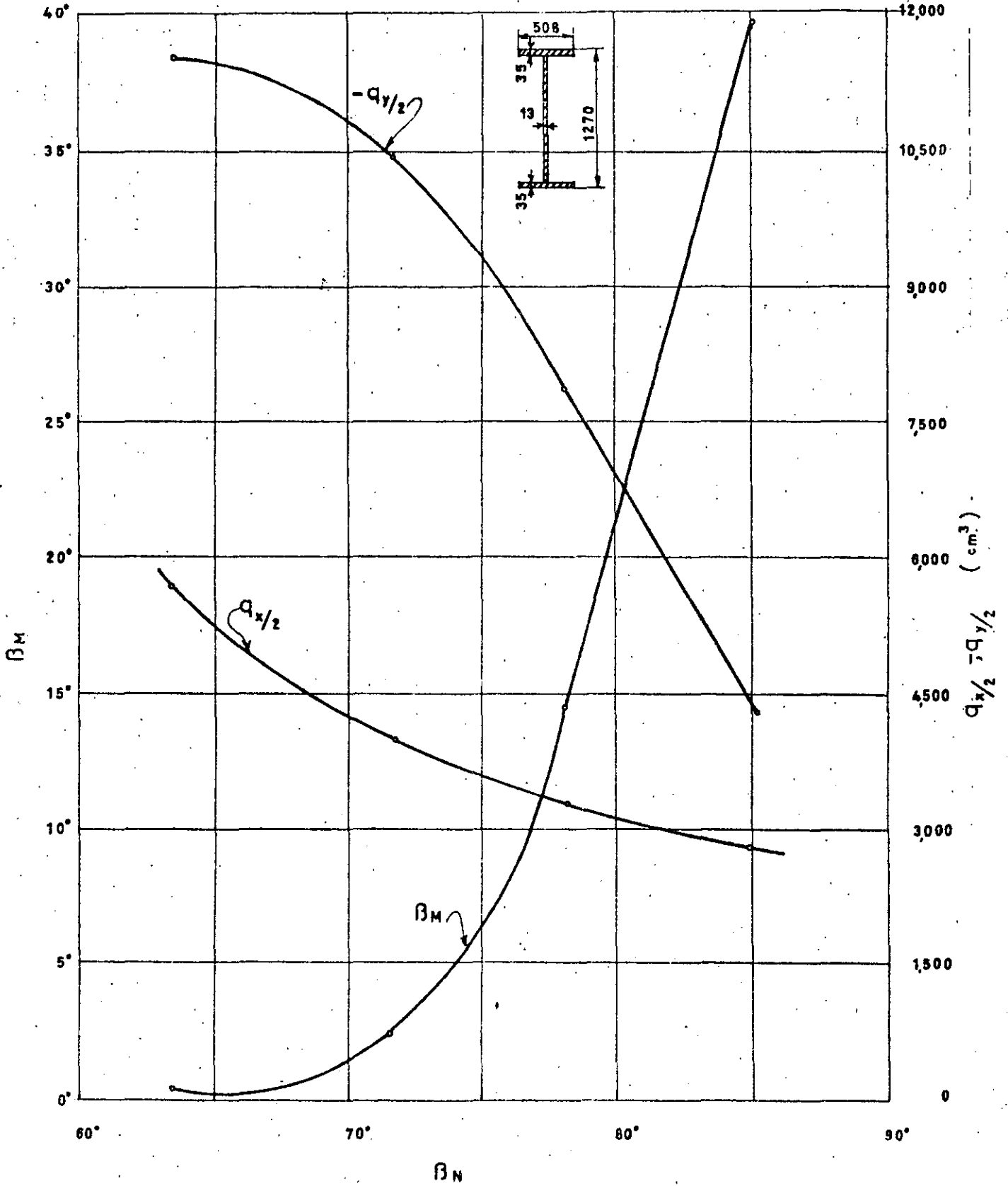


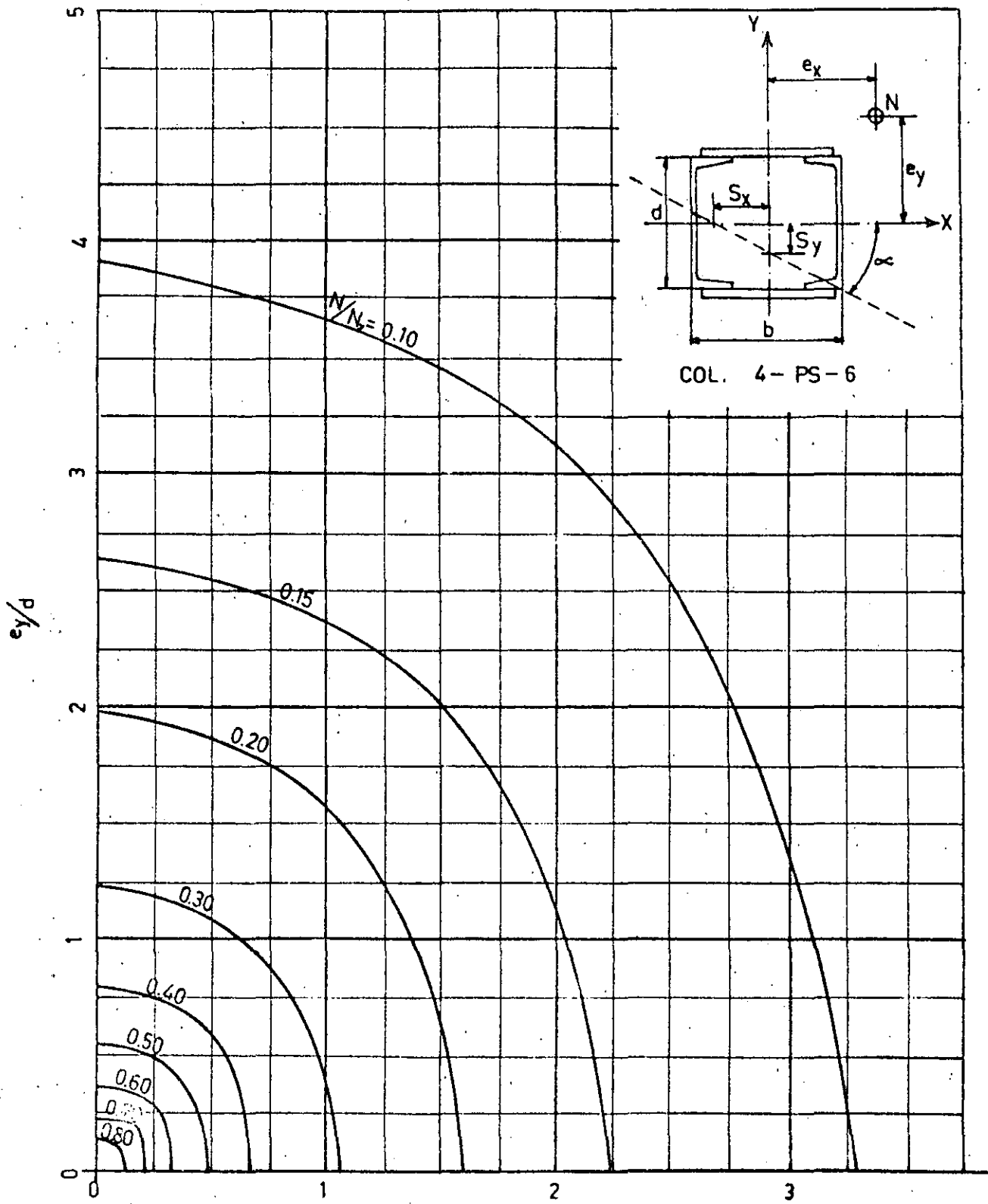








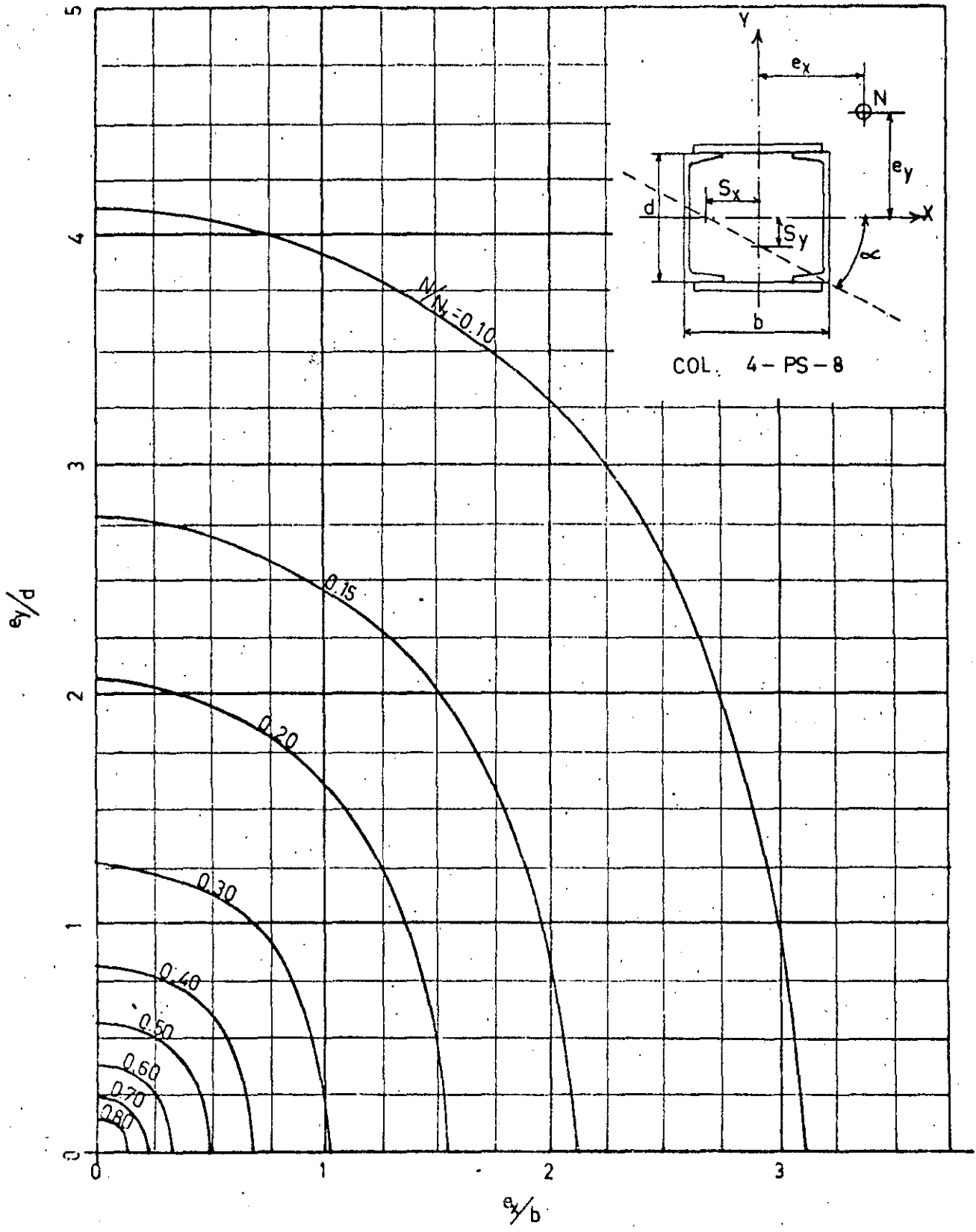




COL. 4-PS-6

DIAGRAMA

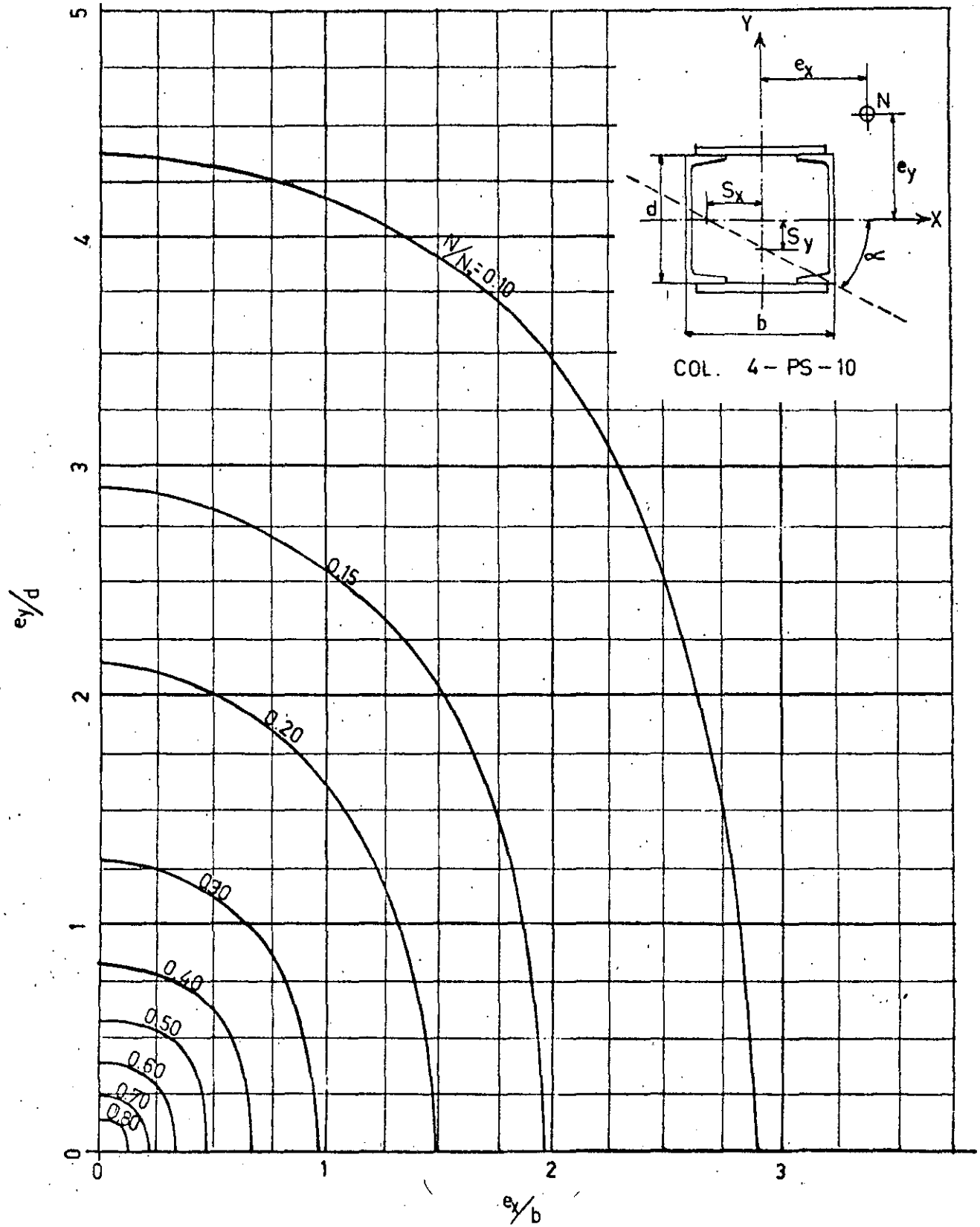
$N/N_y$



DIAGRAMA

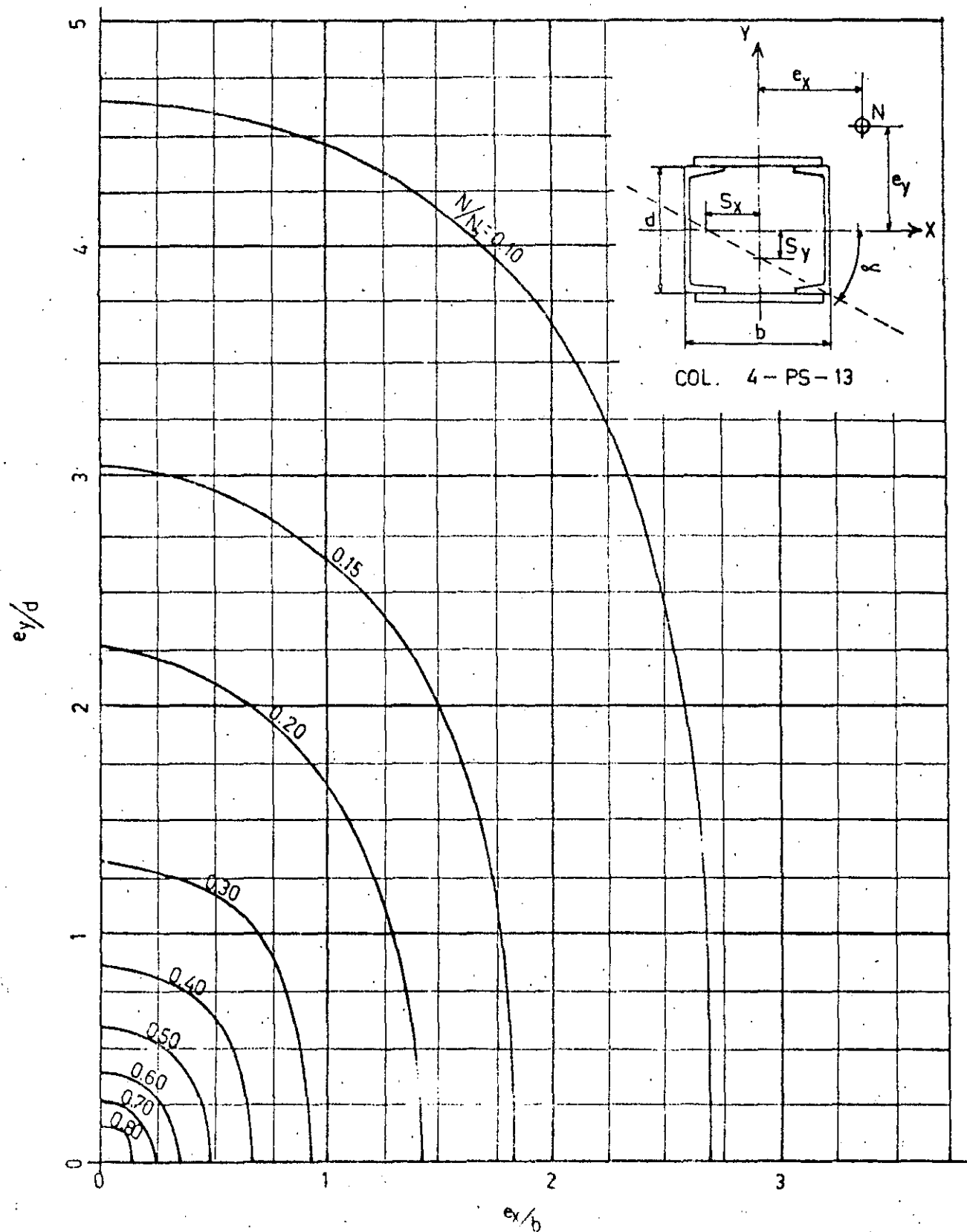
$N/N_y$





DIAGRAMA

$N/Ny$



DIAGRAMA

$N/N_y$

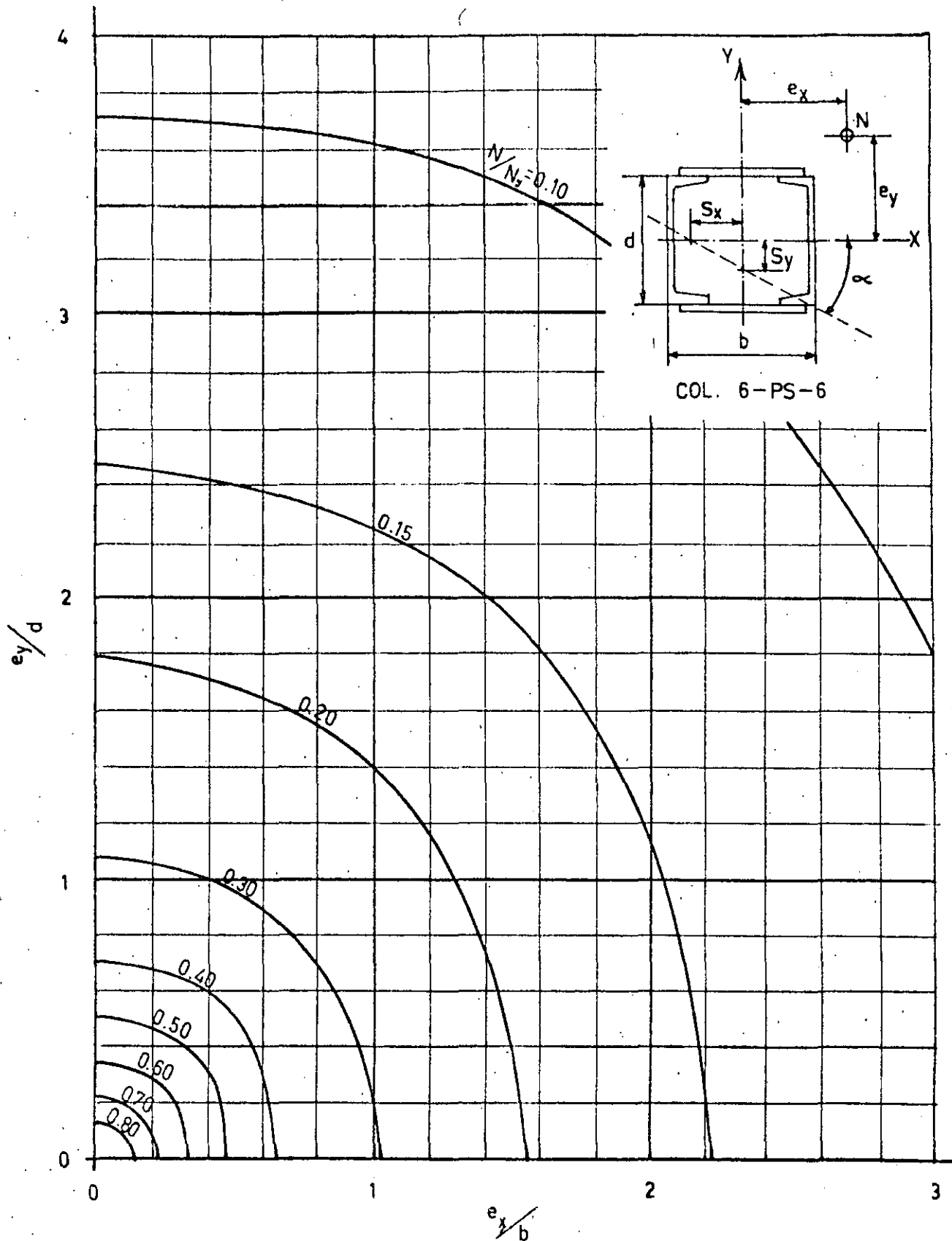


DIAGRAMA  $N/N_y$

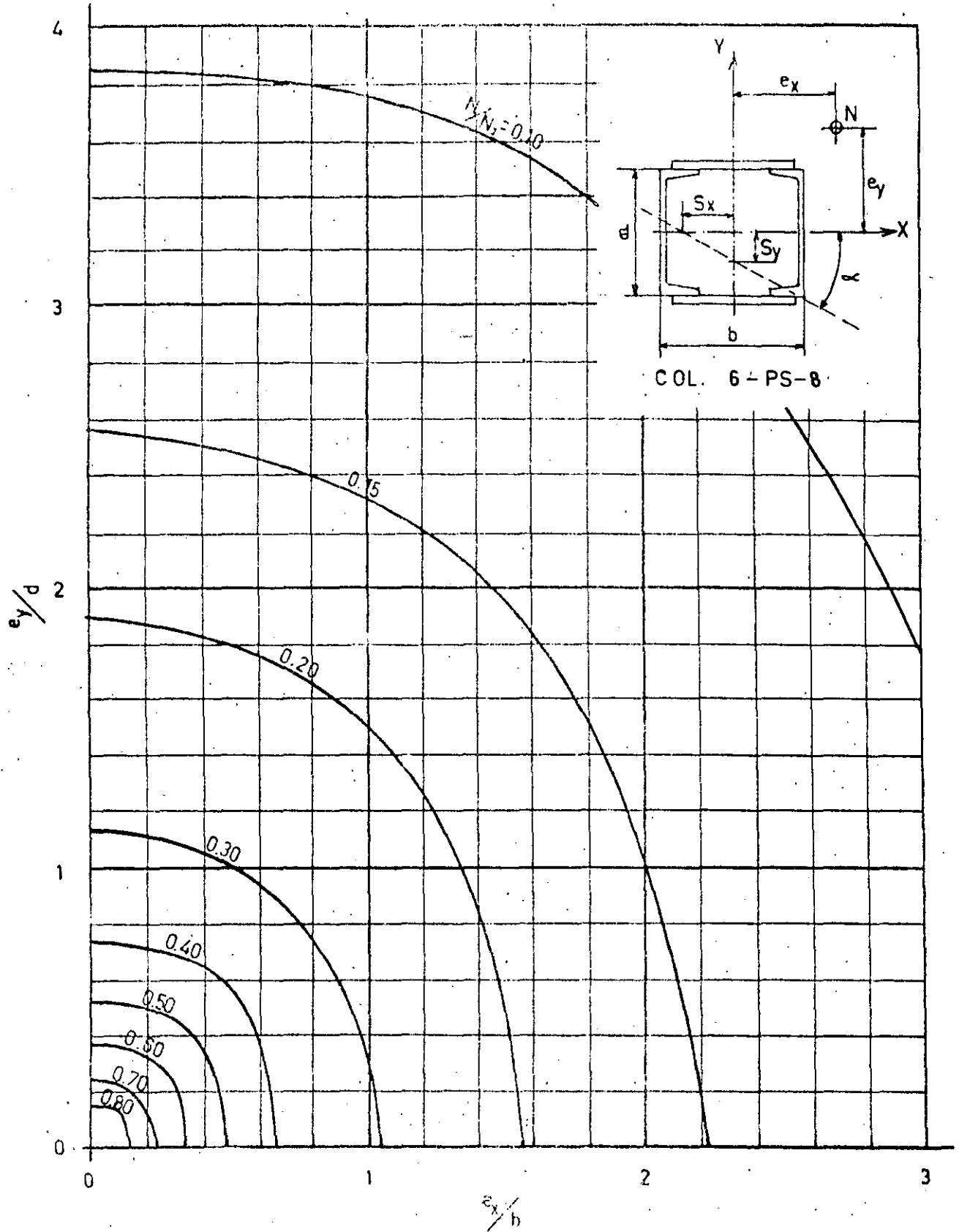
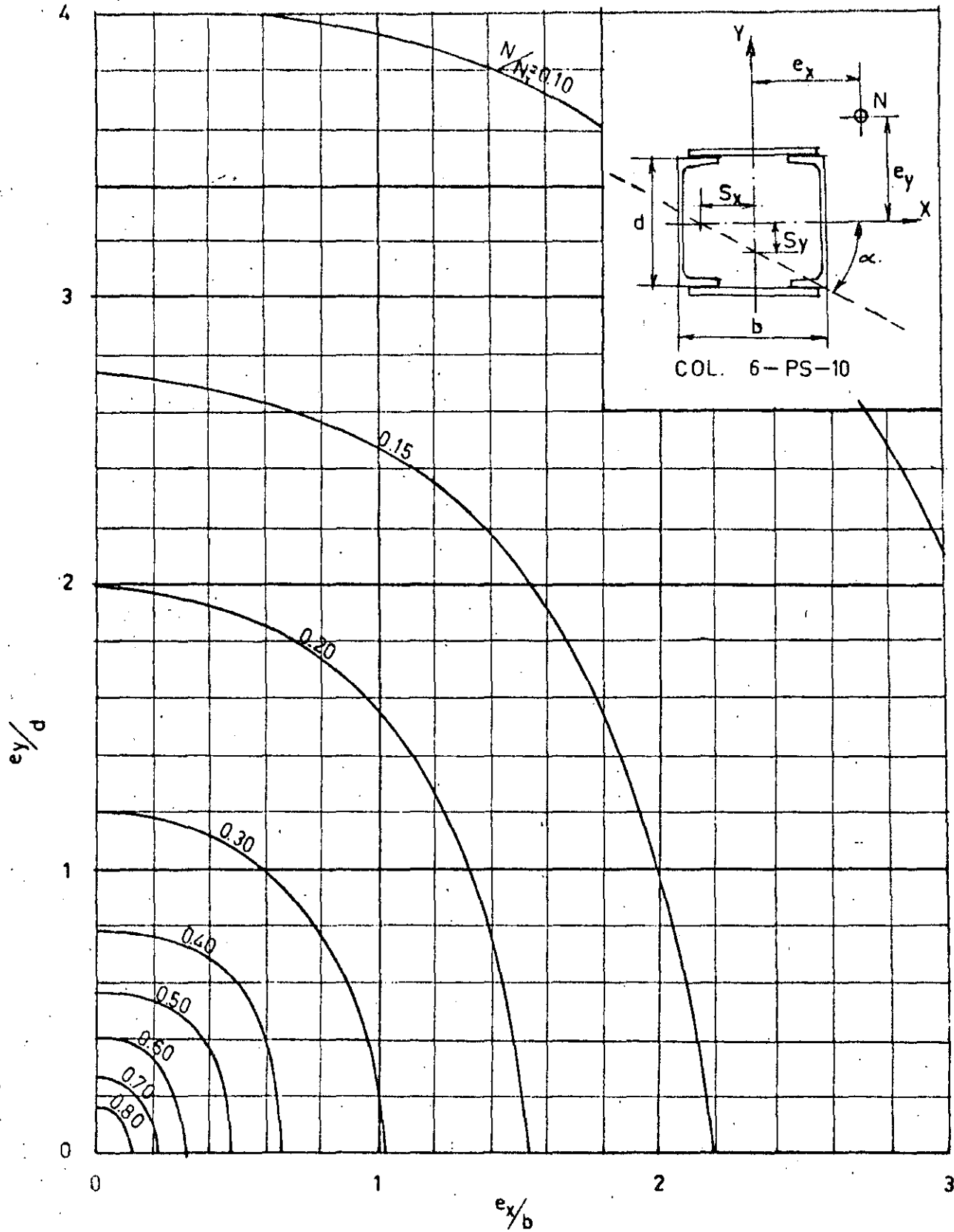
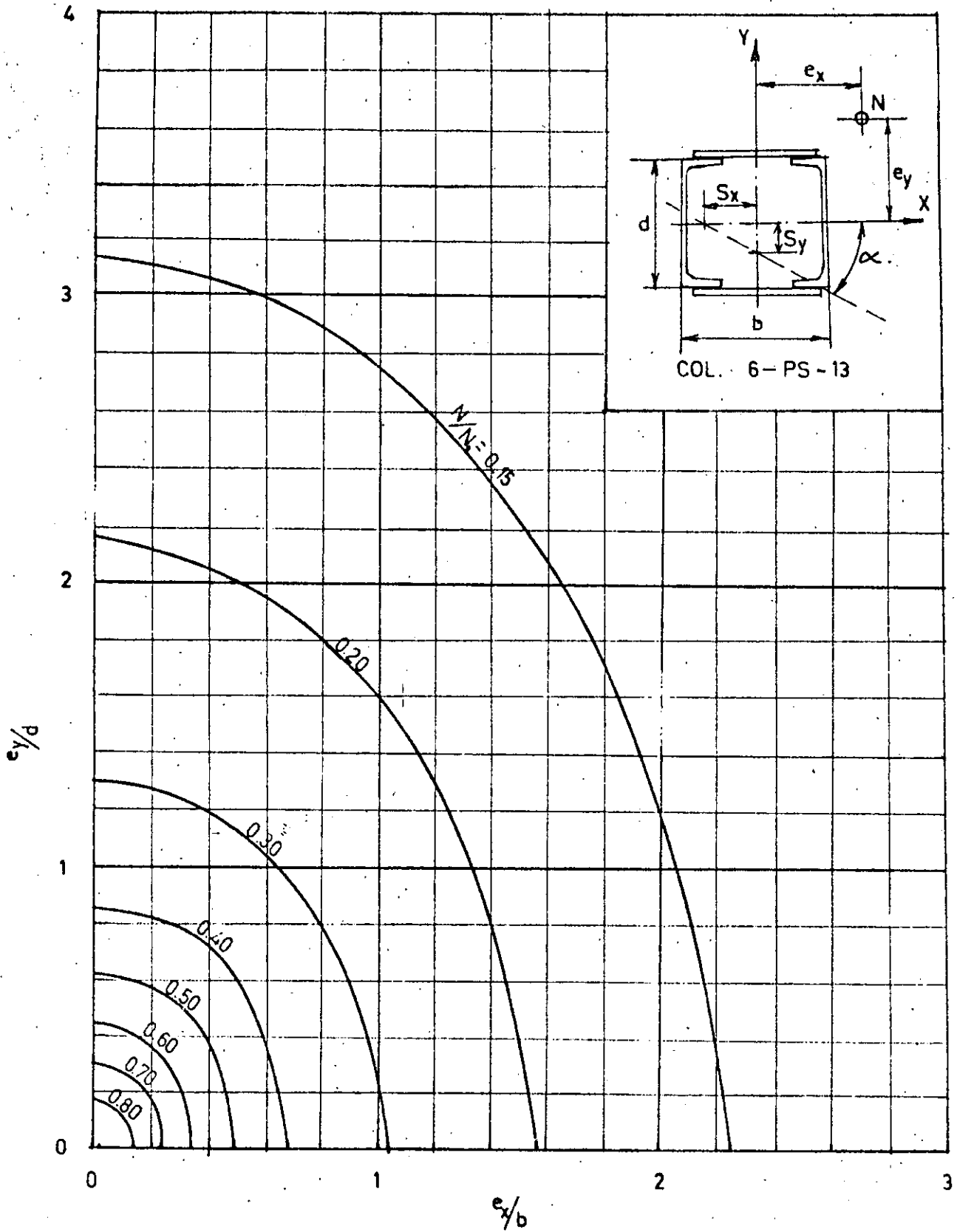


DIAGRAMA  $N/N_y$



D I A G R A M A

$N/N_y$



D I A G R A M A

$N/N_y$

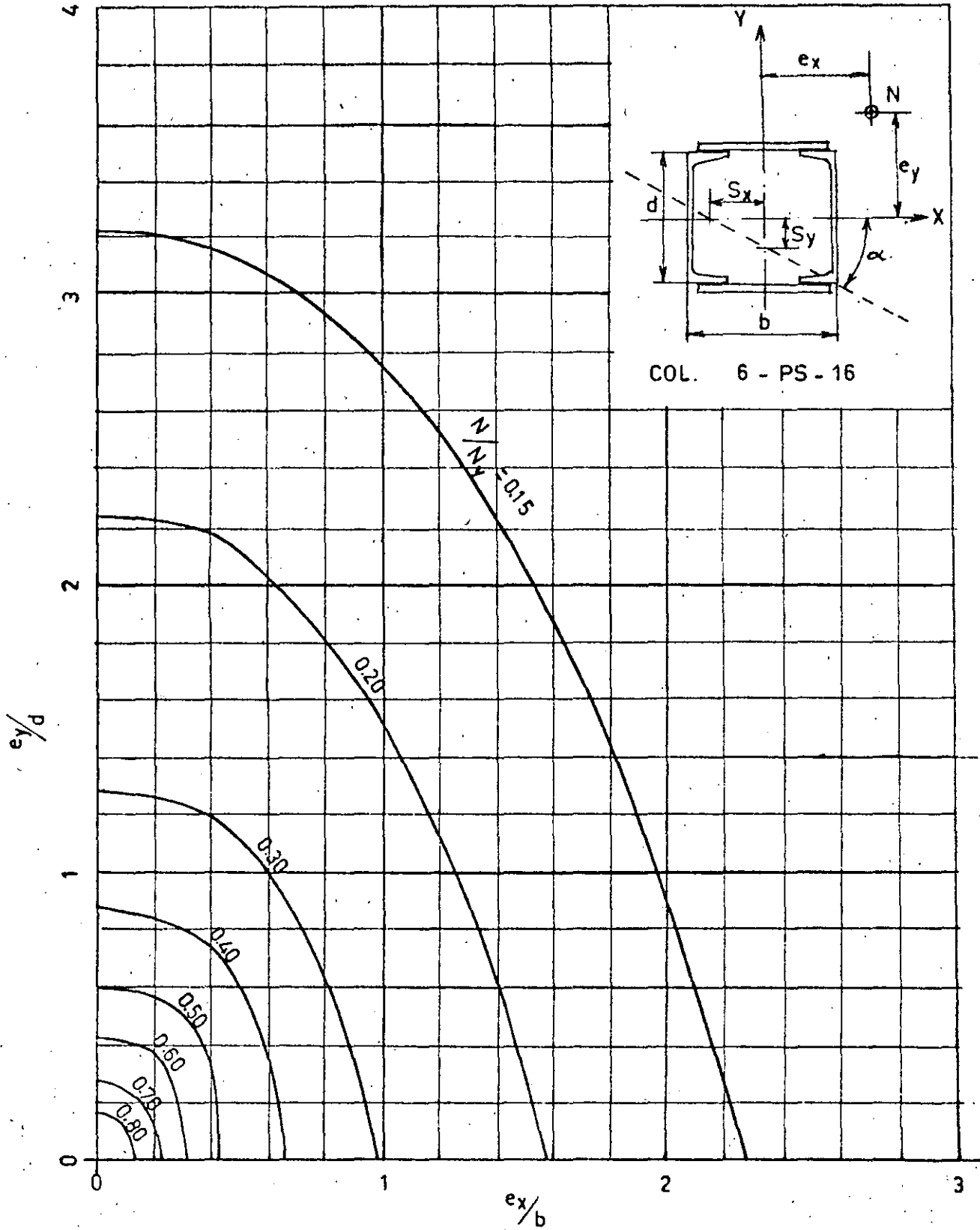
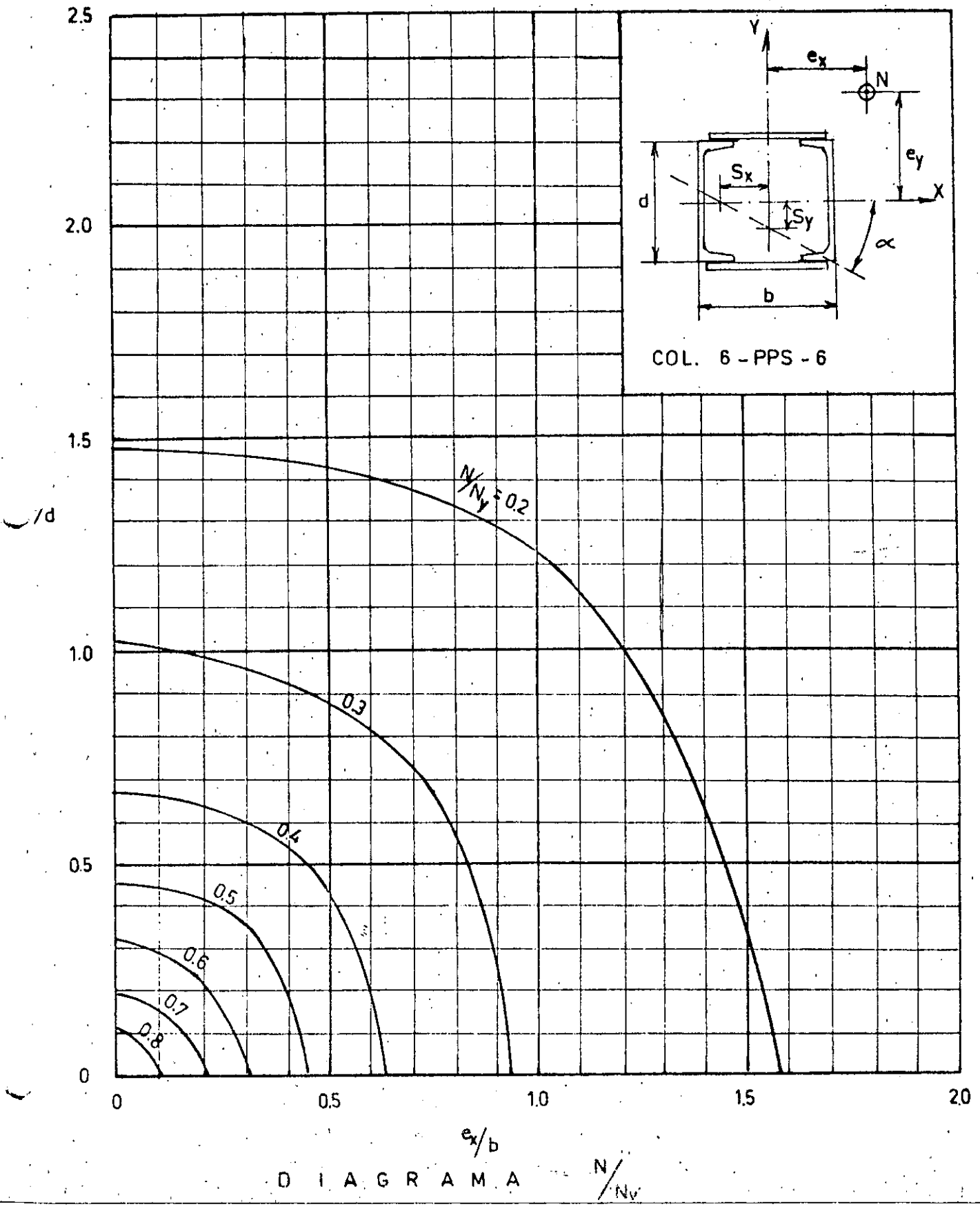
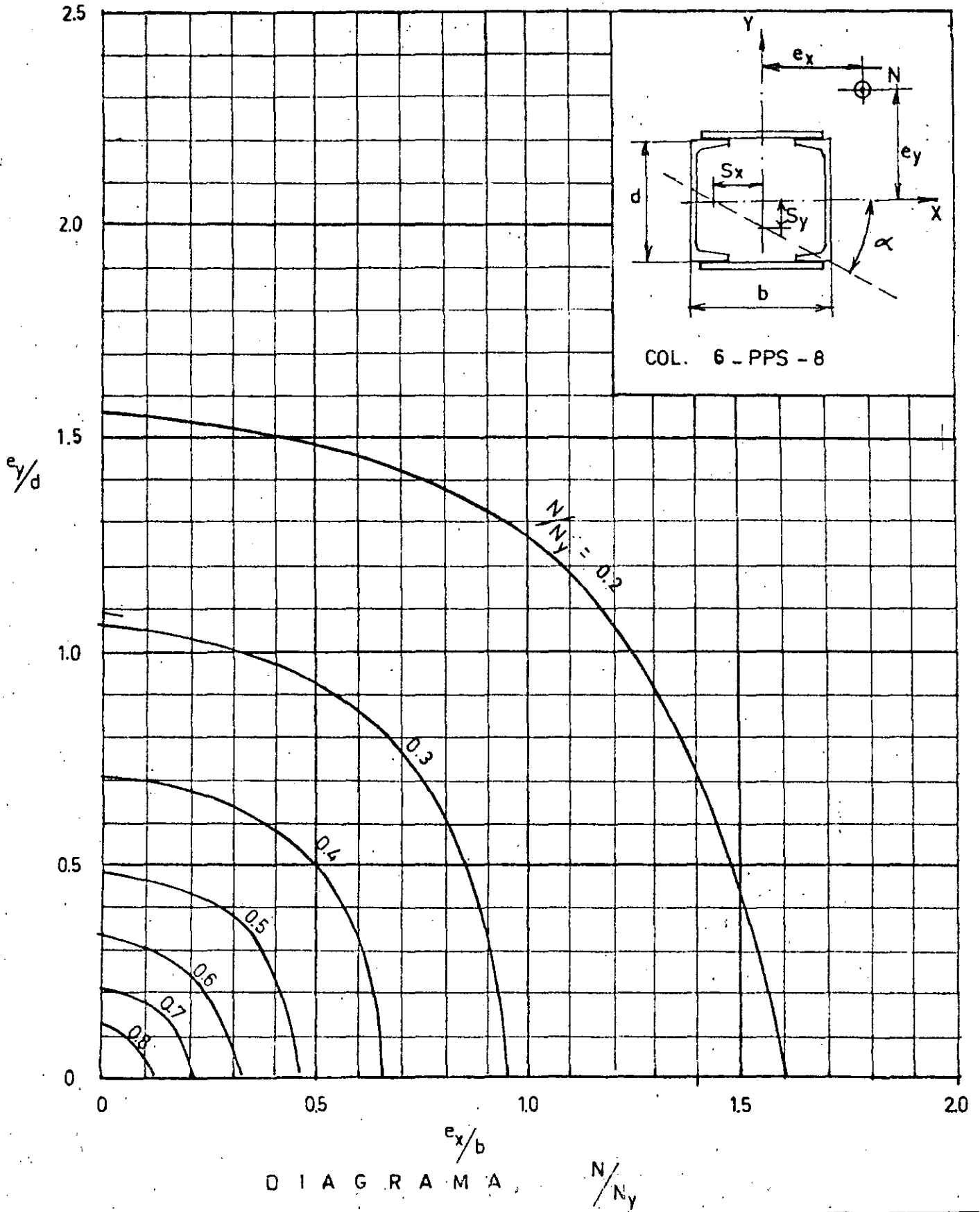


DIAGRAMA  $N/N_y$



D I A G R A M A  $N/N_v$





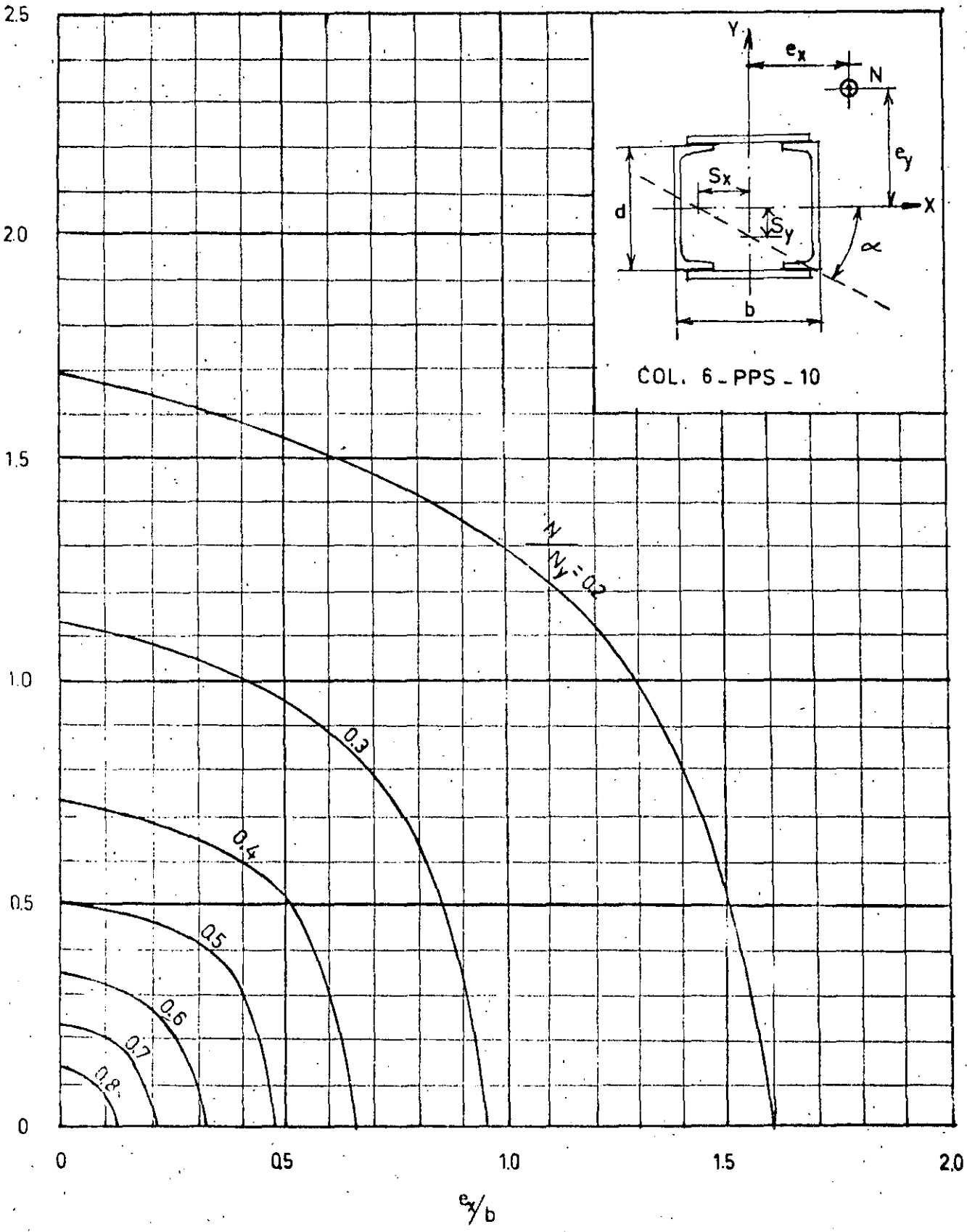
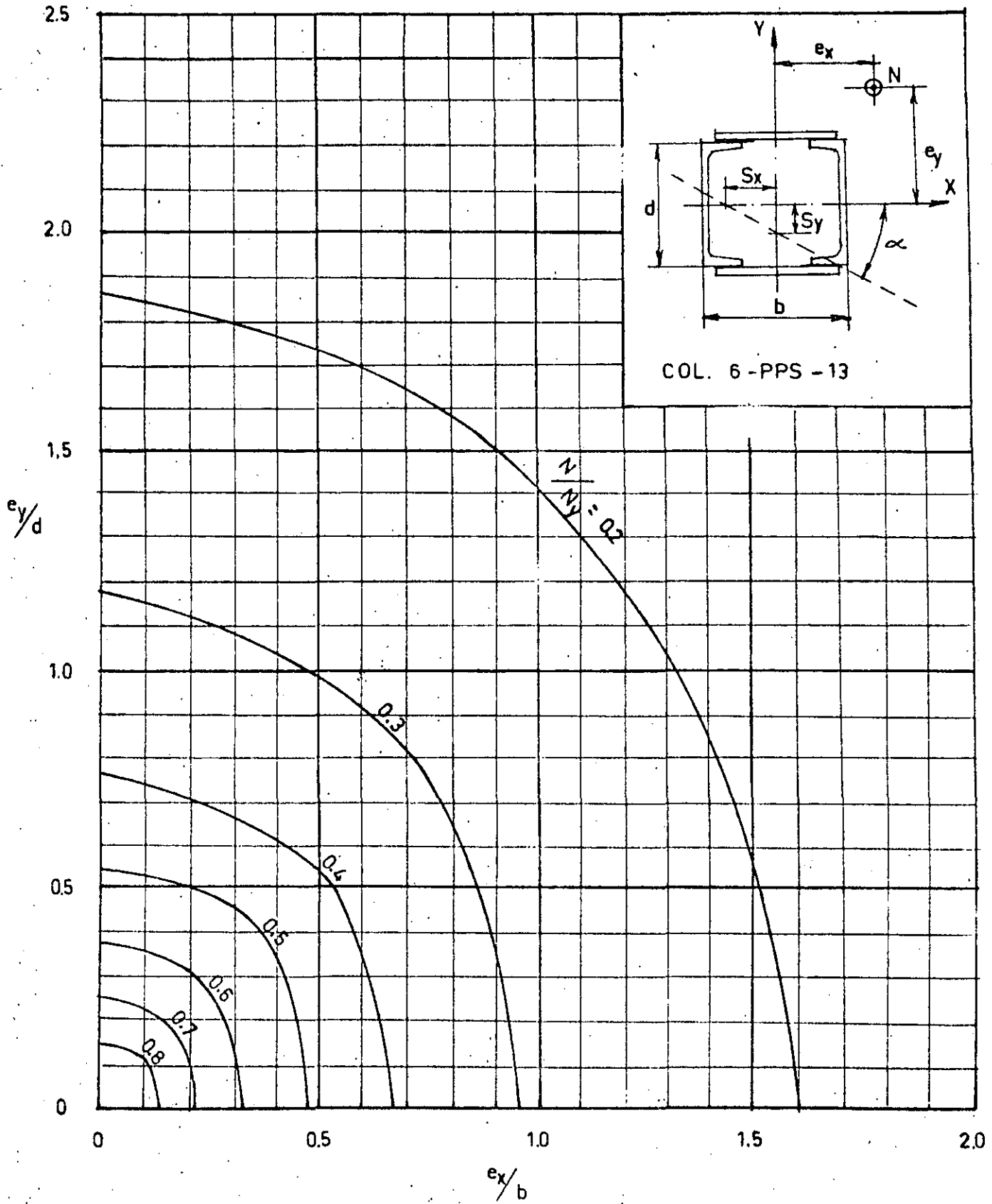
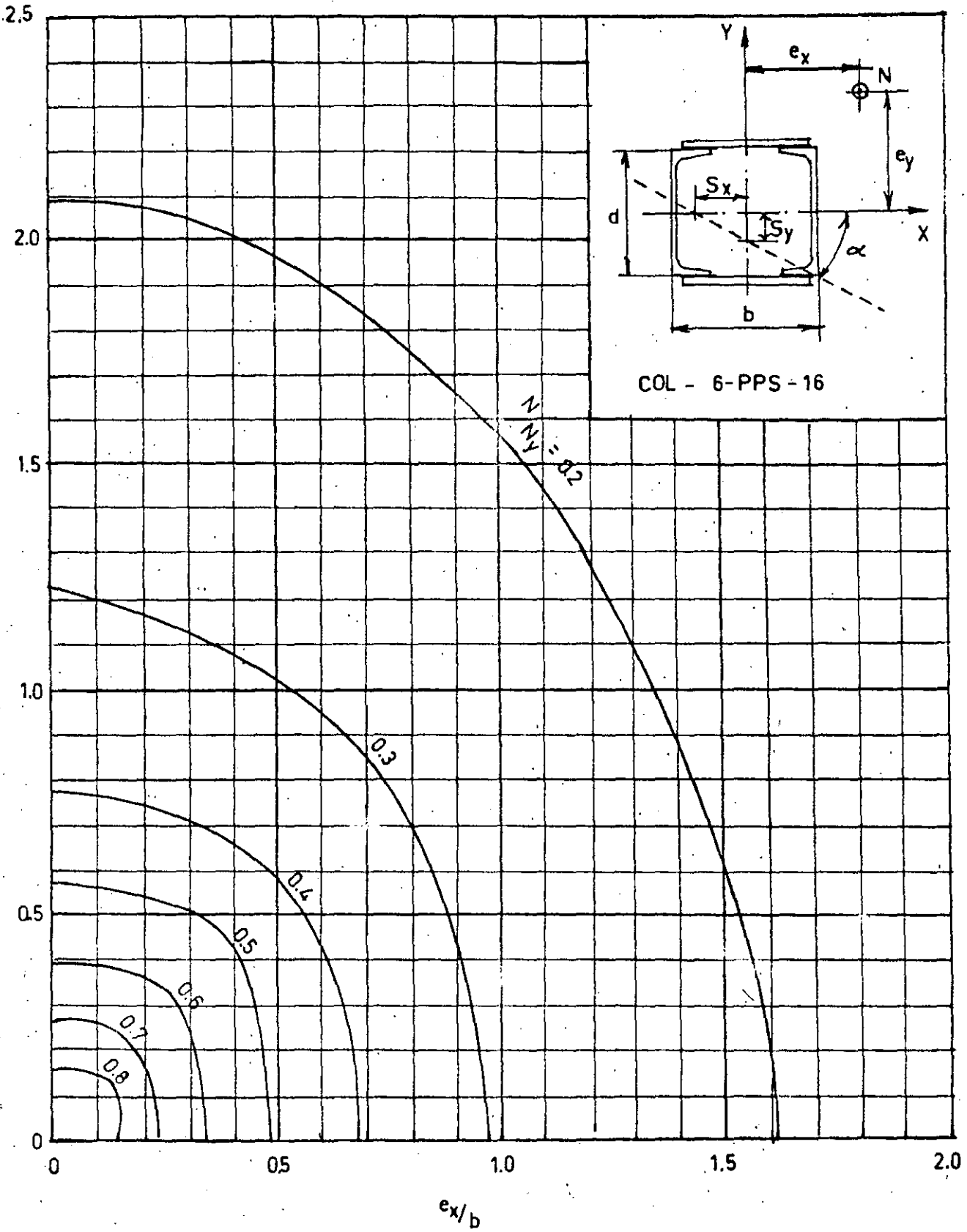


DIAGRAMA  $N/N_u$



COL. 6-PPS-13



COL - 6-PPS - 16

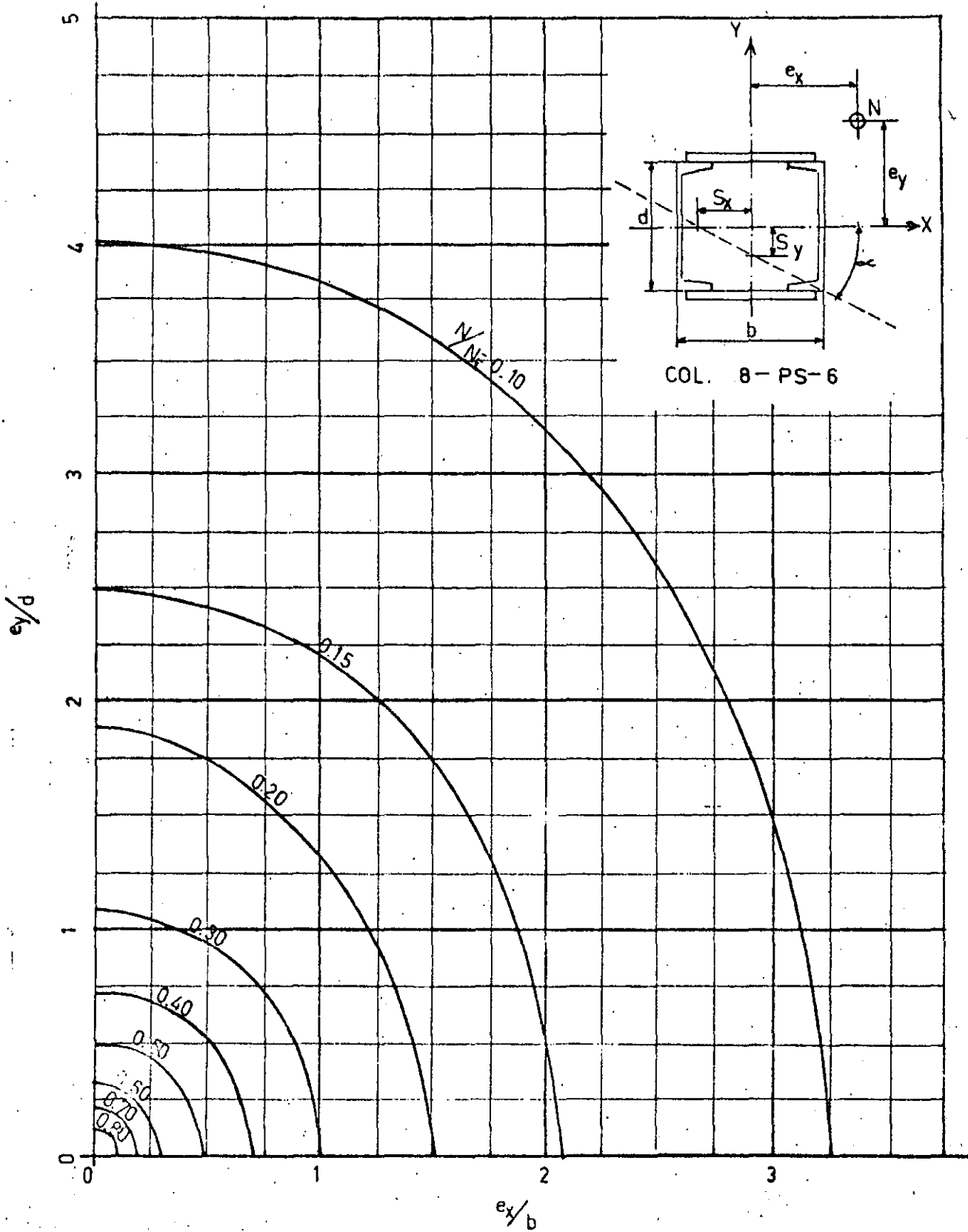
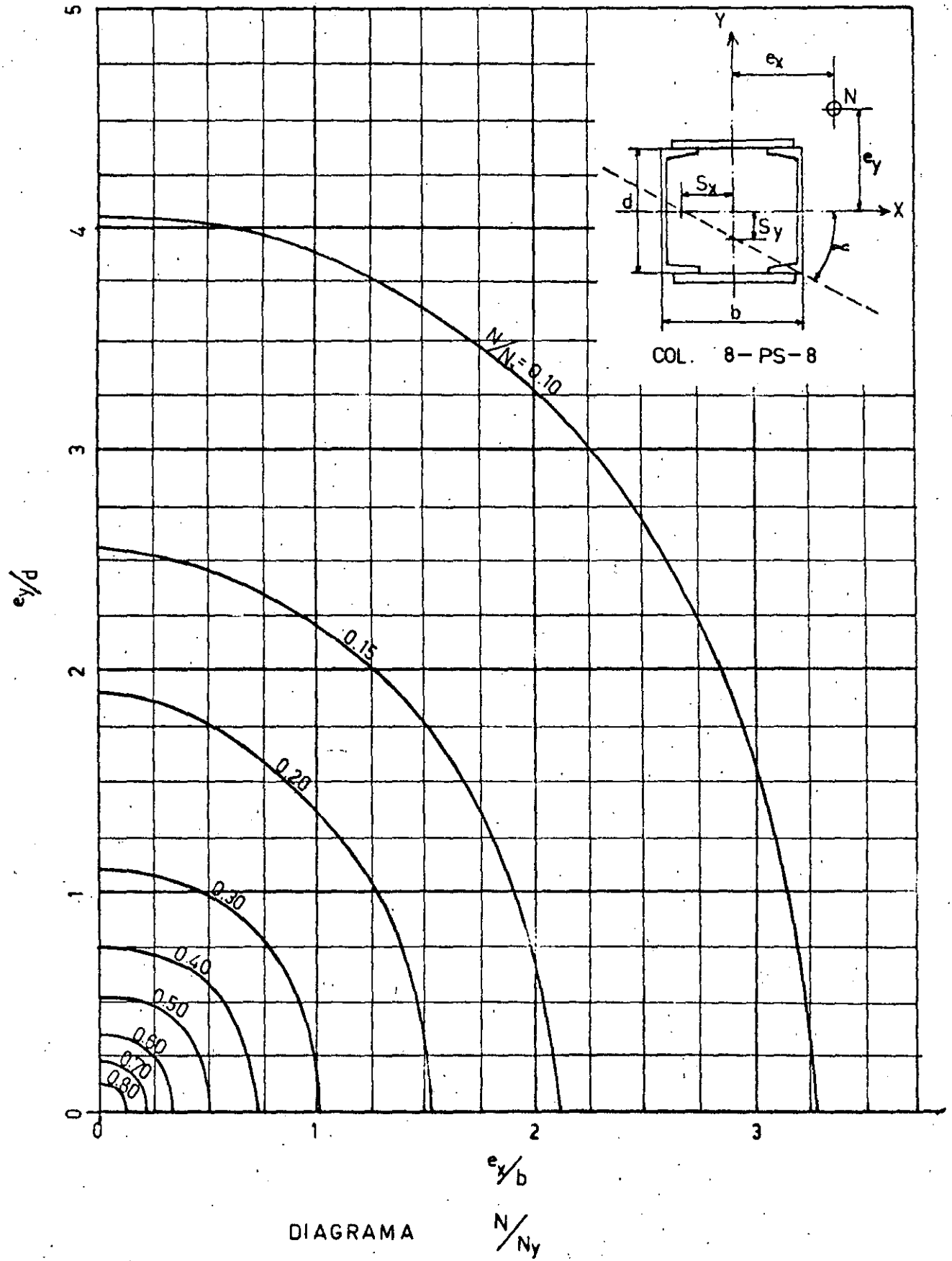
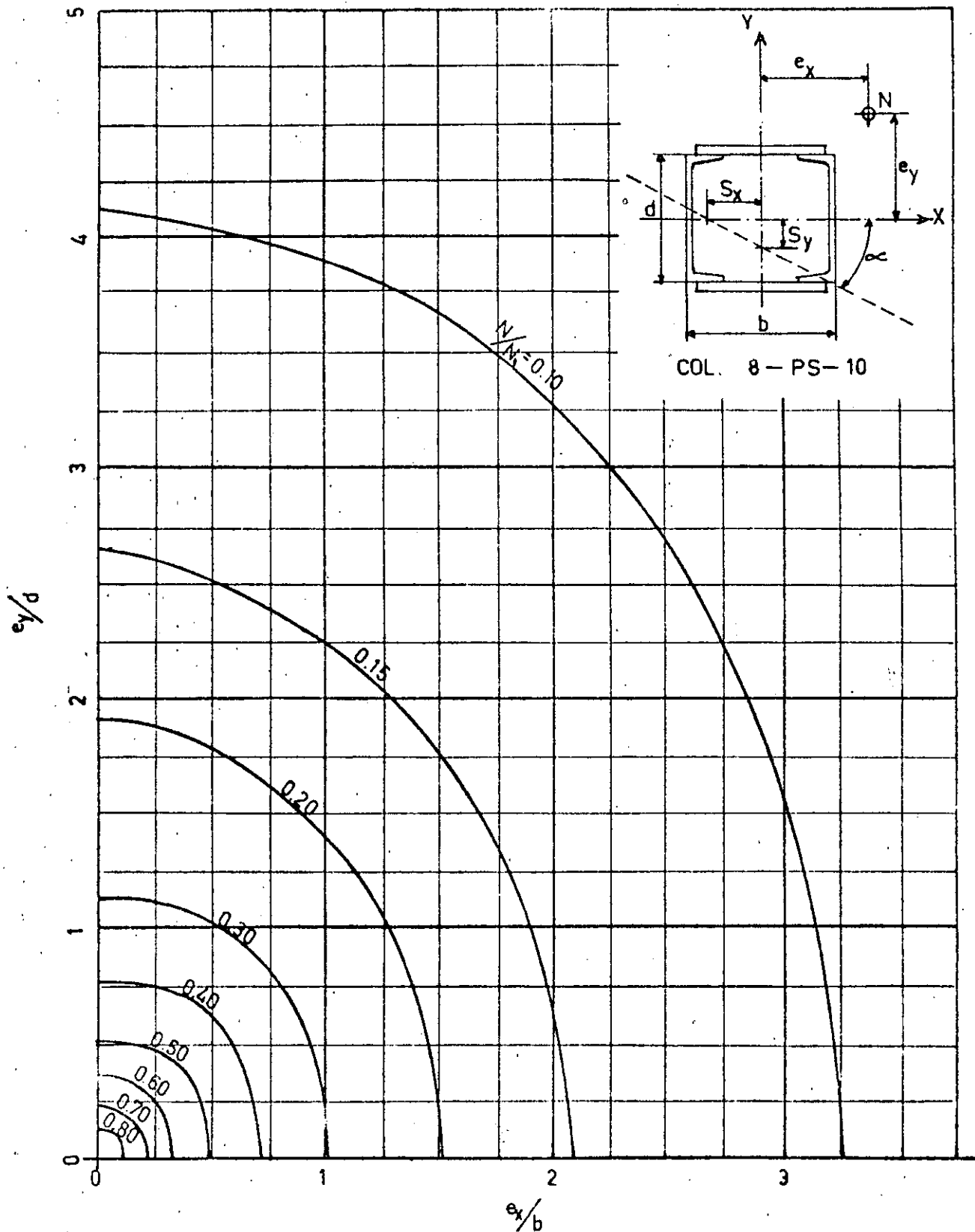


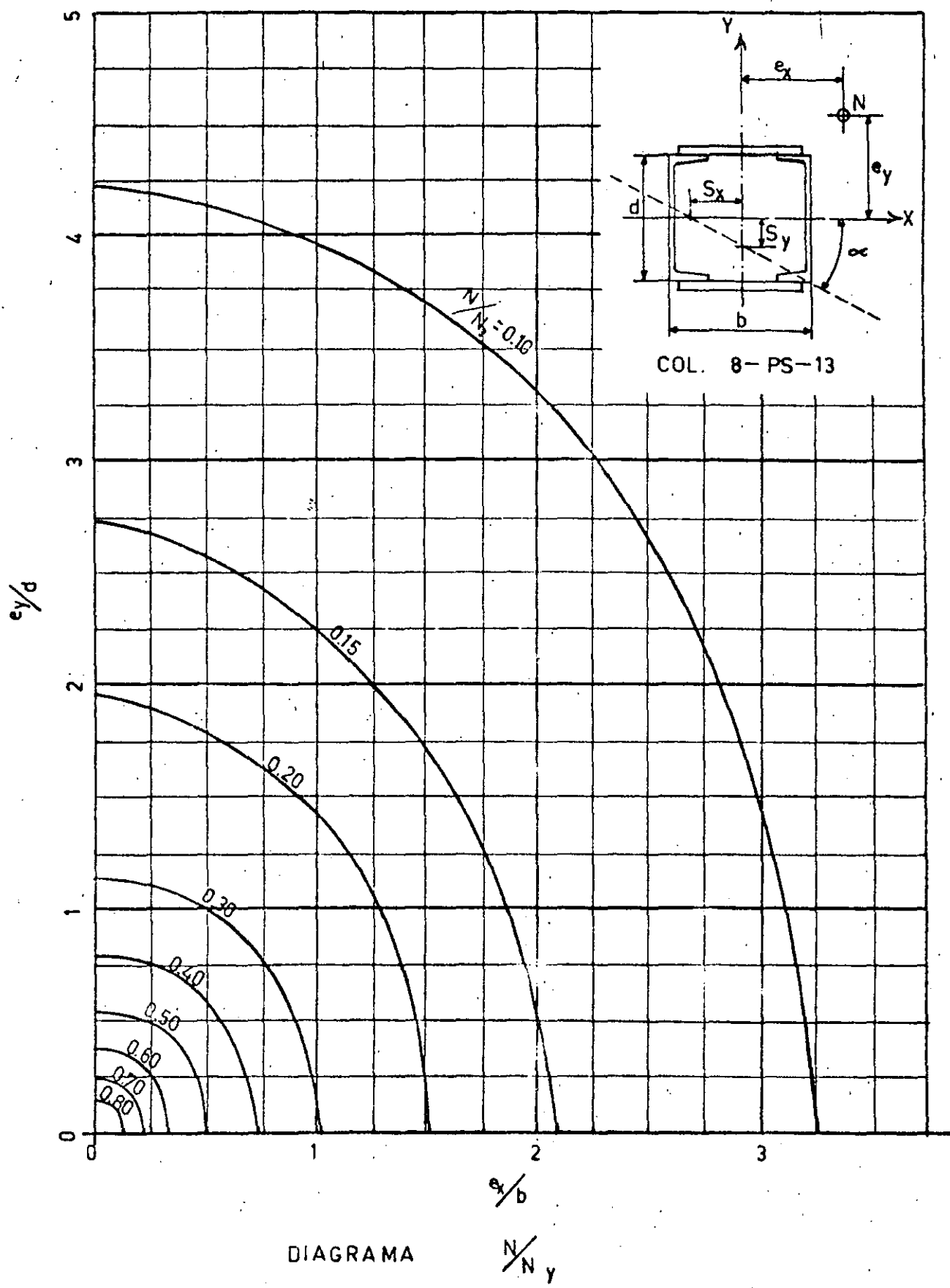
DIAGRAMA  $\frac{N}{N_y}$



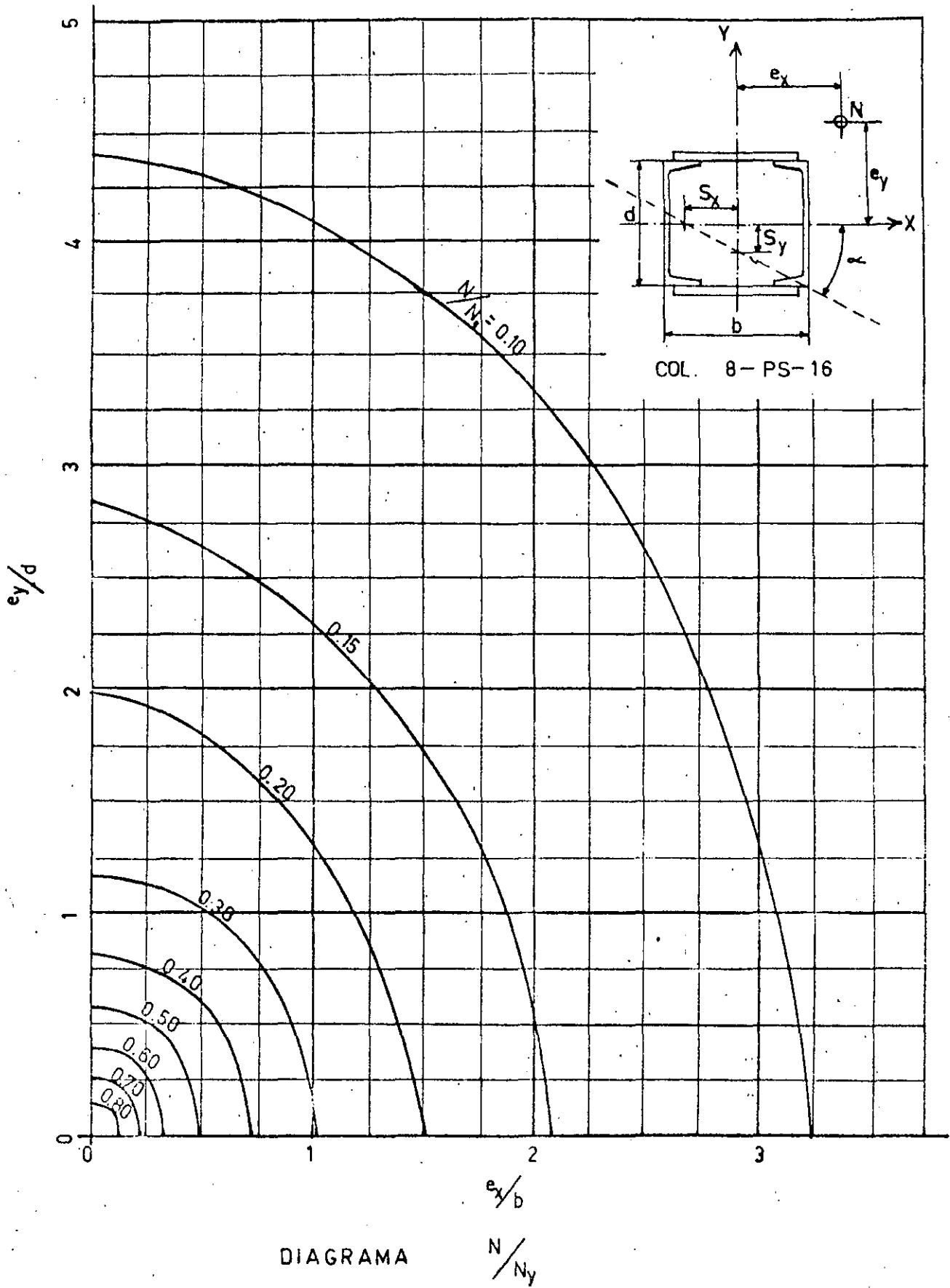


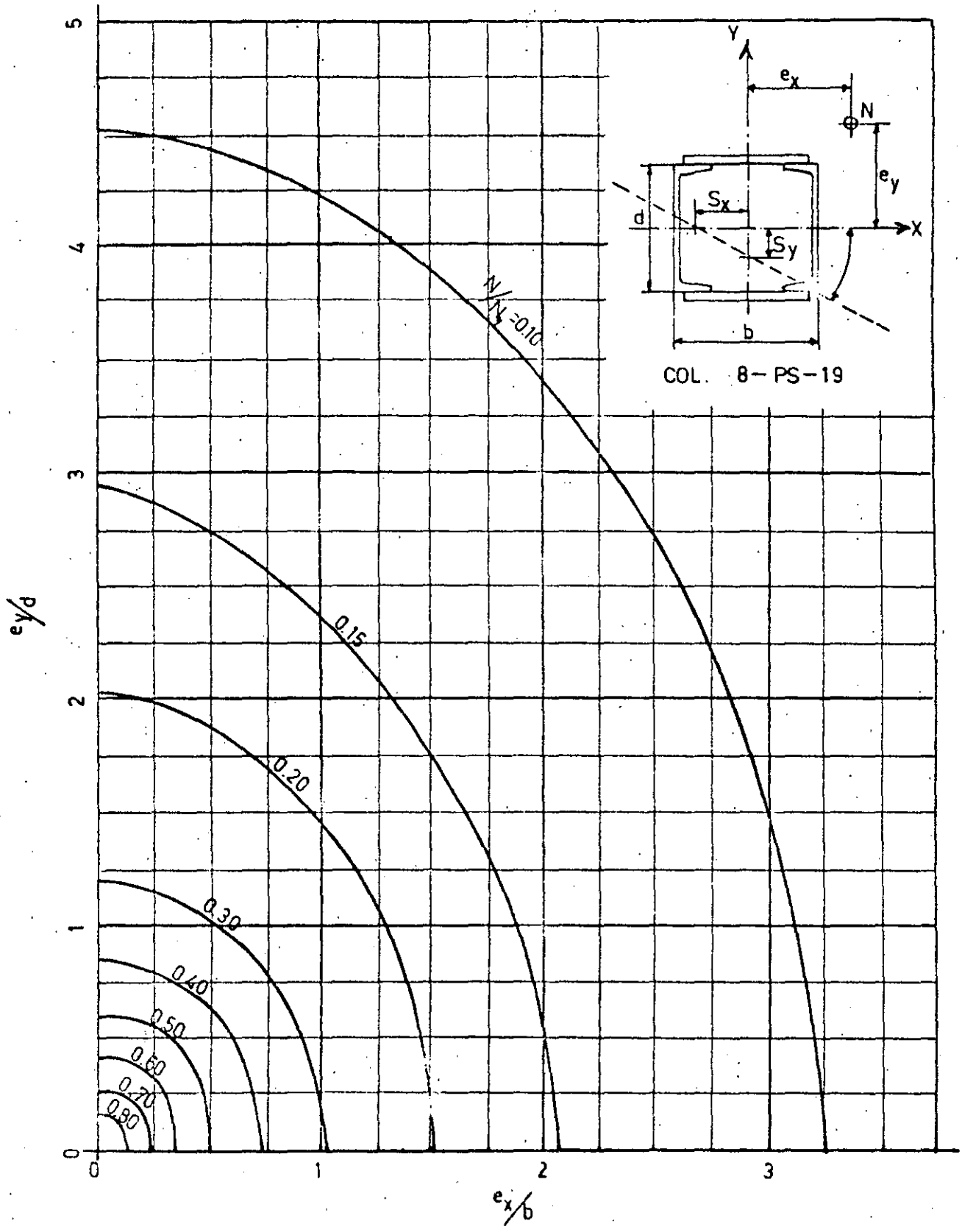
DIAGRAMA

$N/N_y$



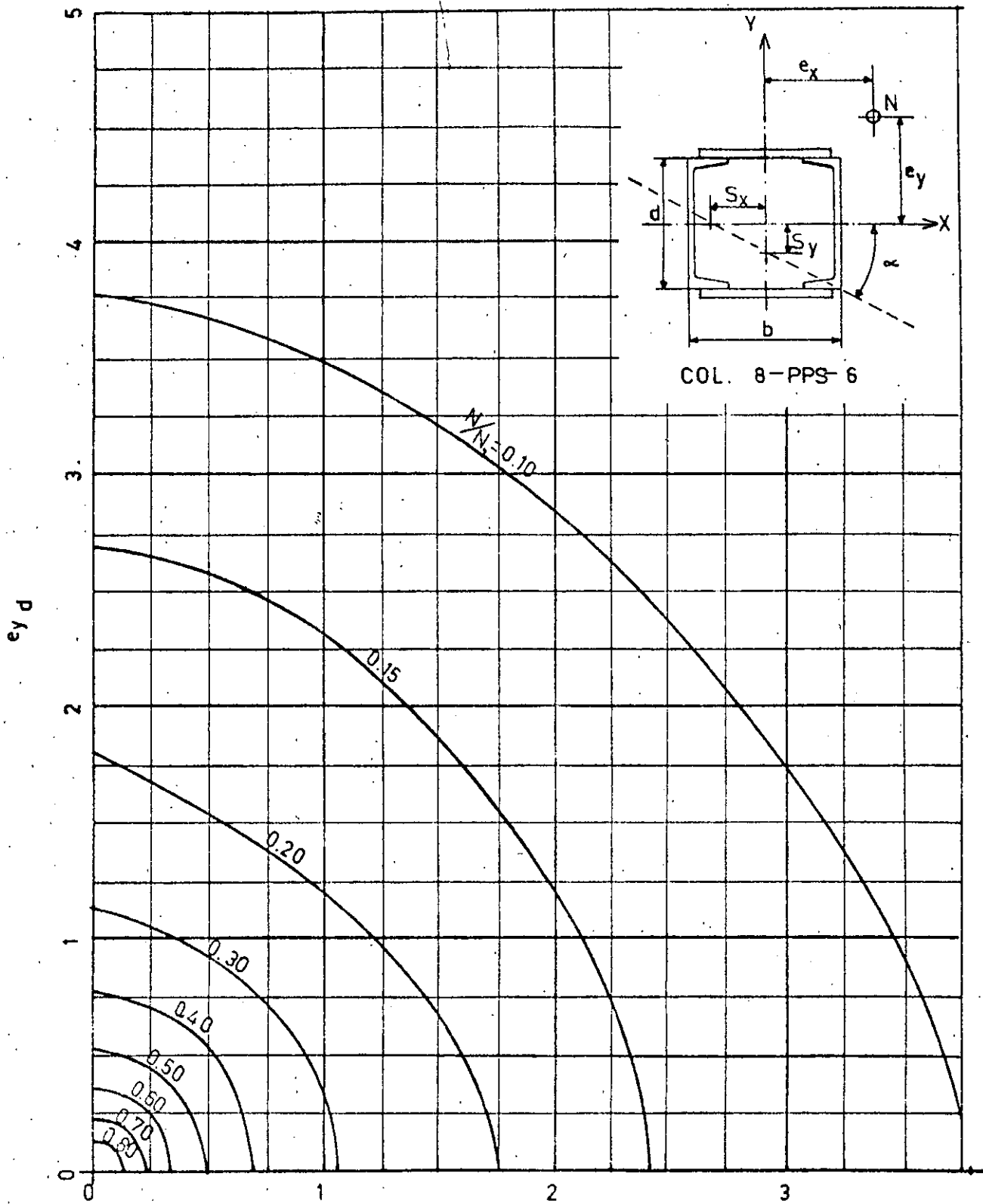






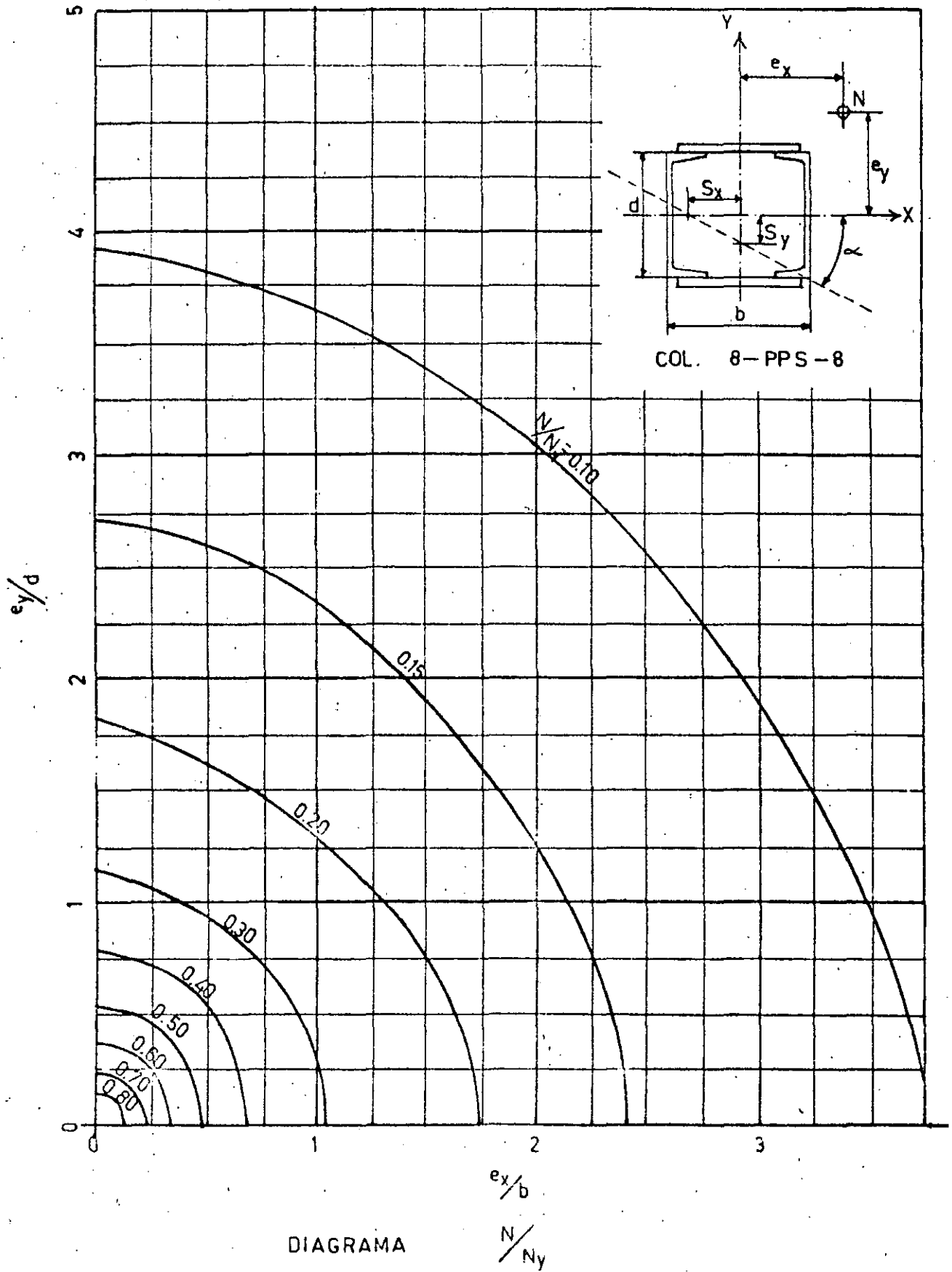
DIAGRAMA

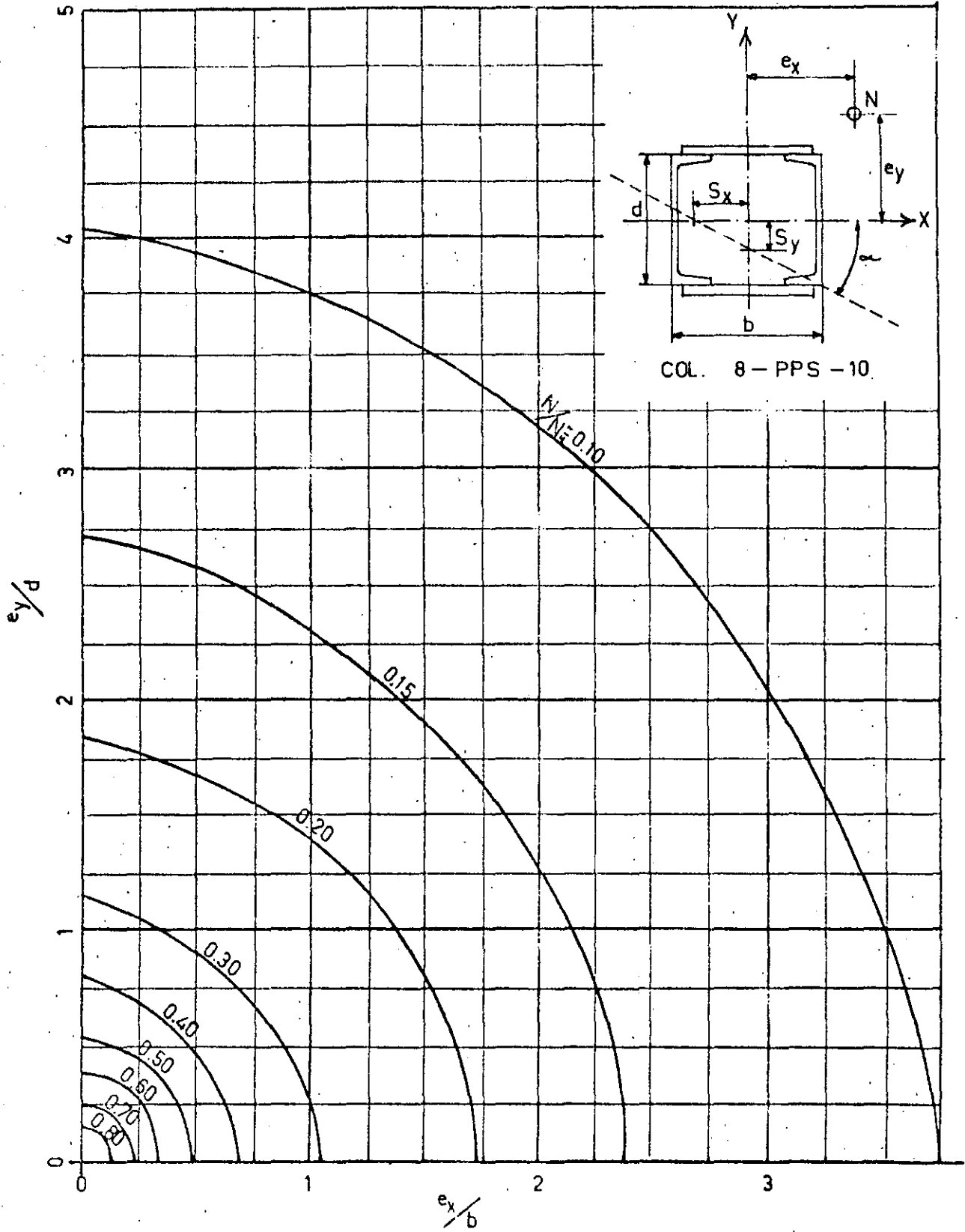
$N/N_y$



DIAGRAMA

$\frac{N}{N_y}$

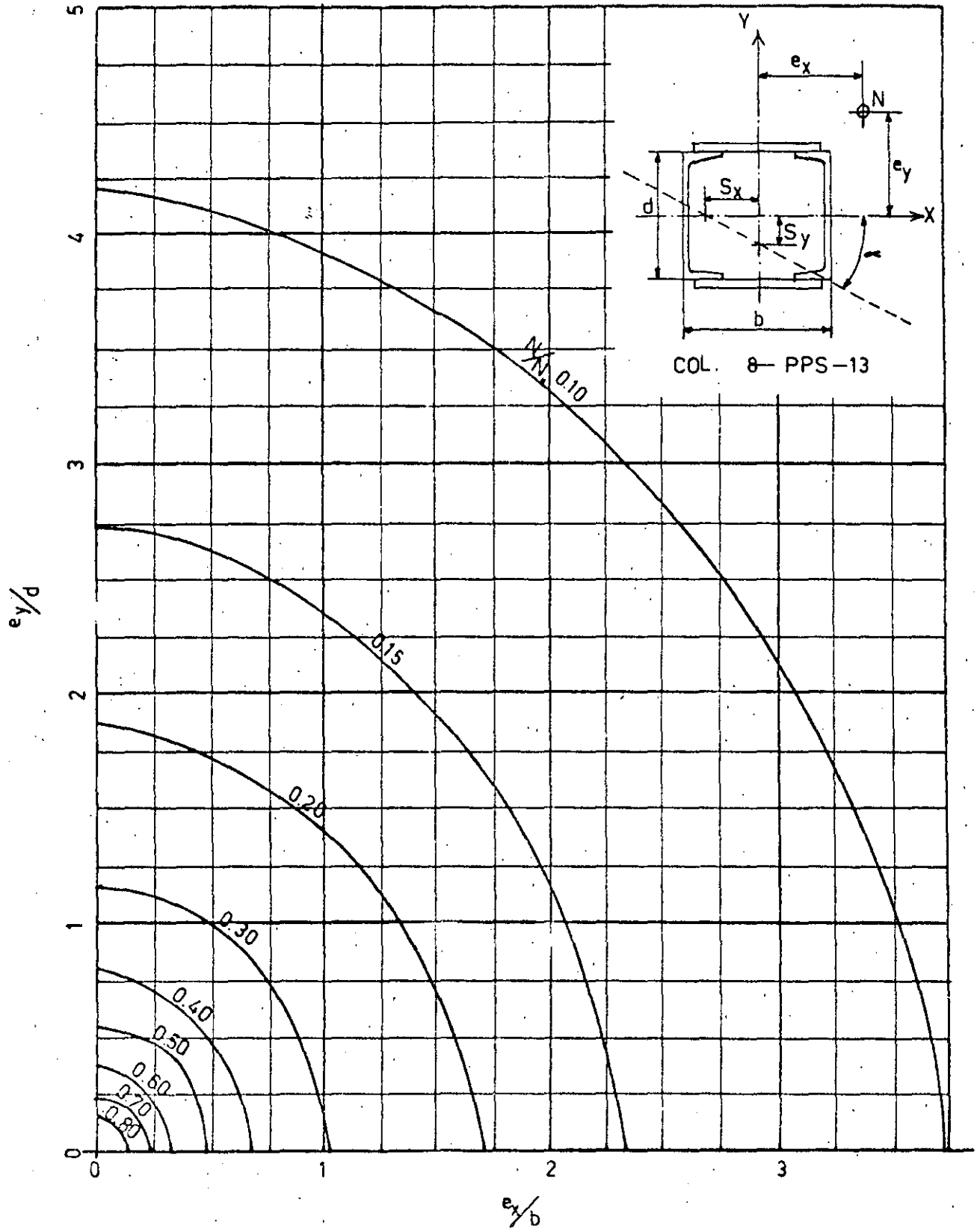




COL. 8 - PPS - 10

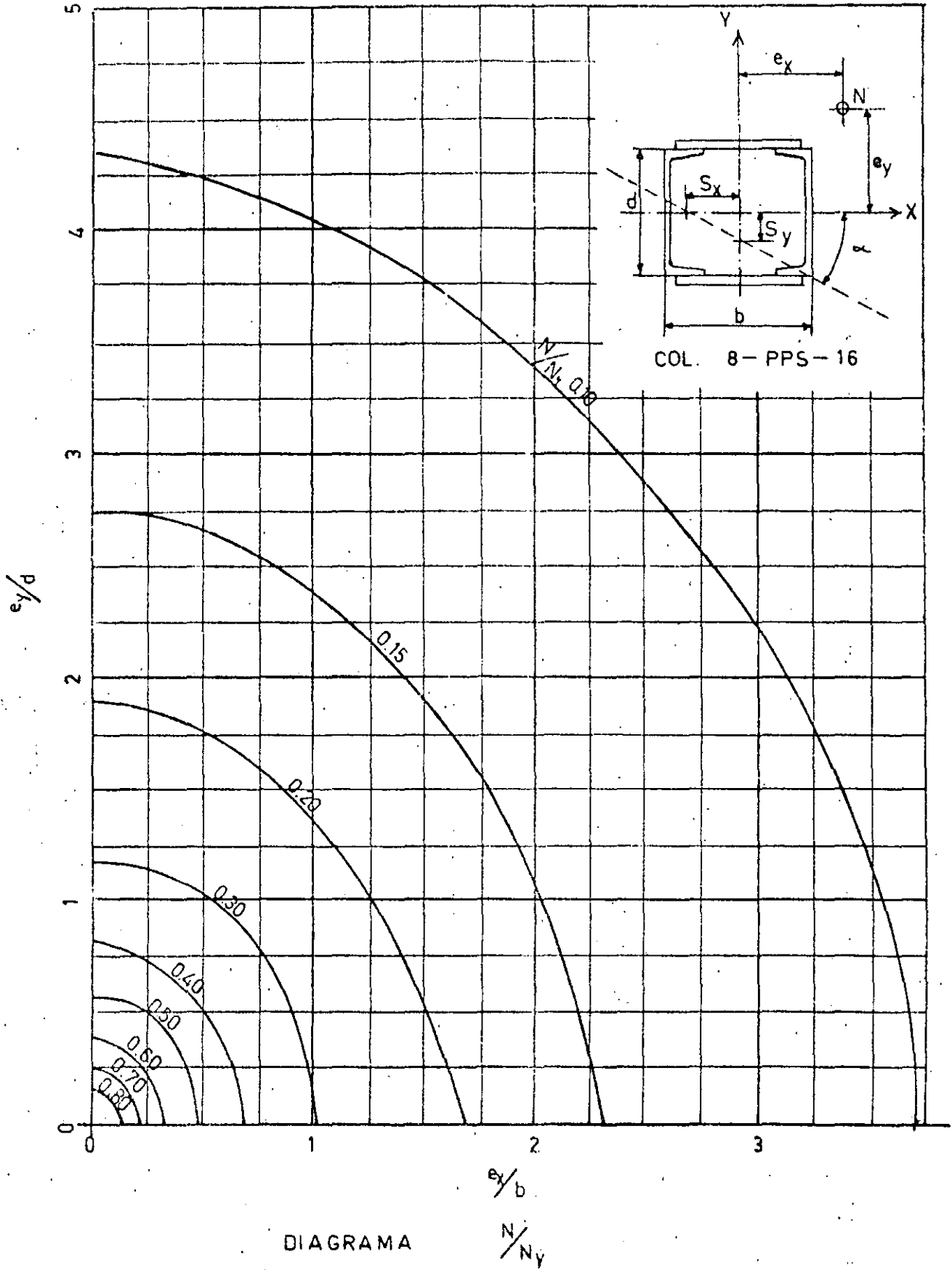
DIAGRAMA

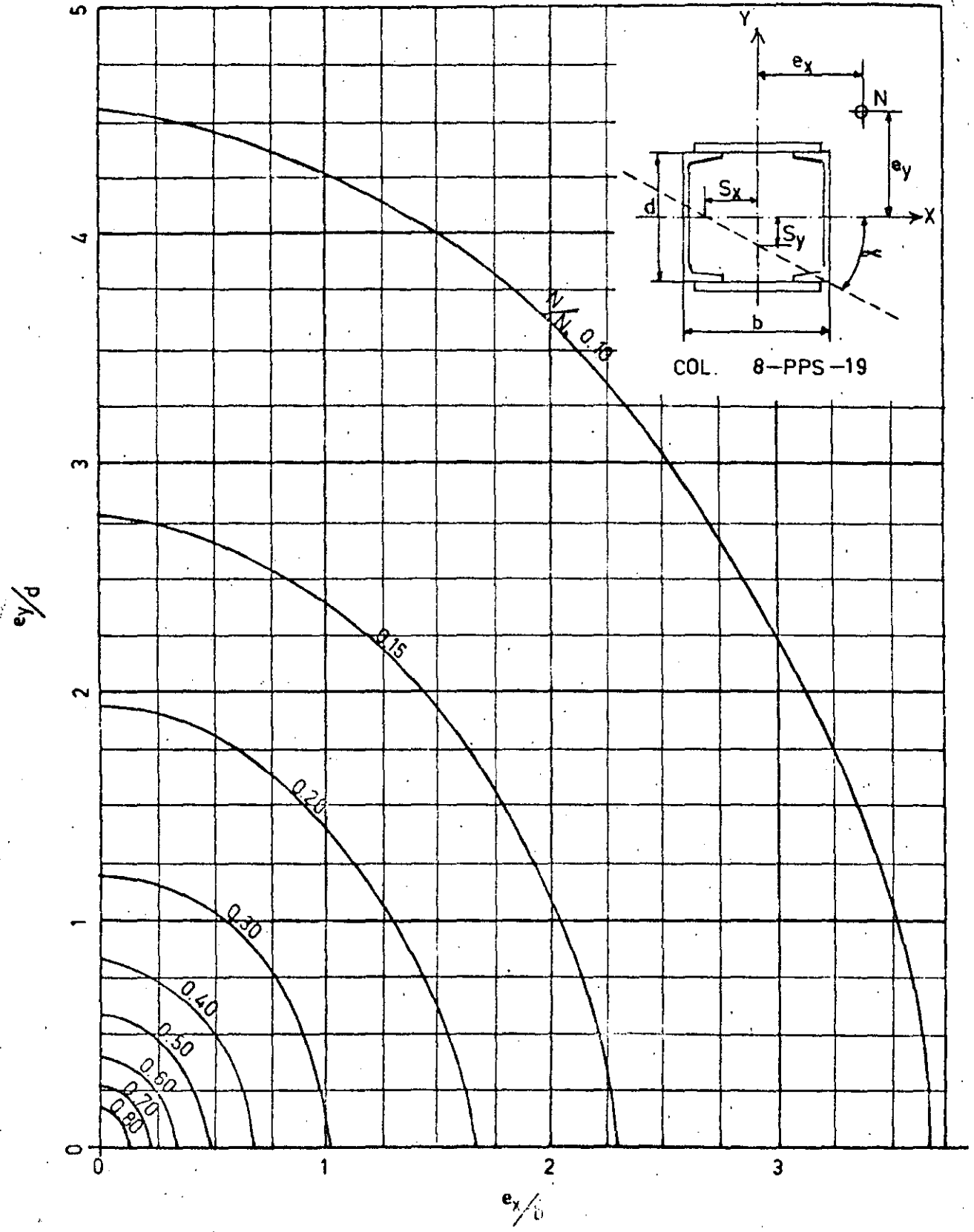
$N/N_y$



DIAGRAMA

$N/N_y$

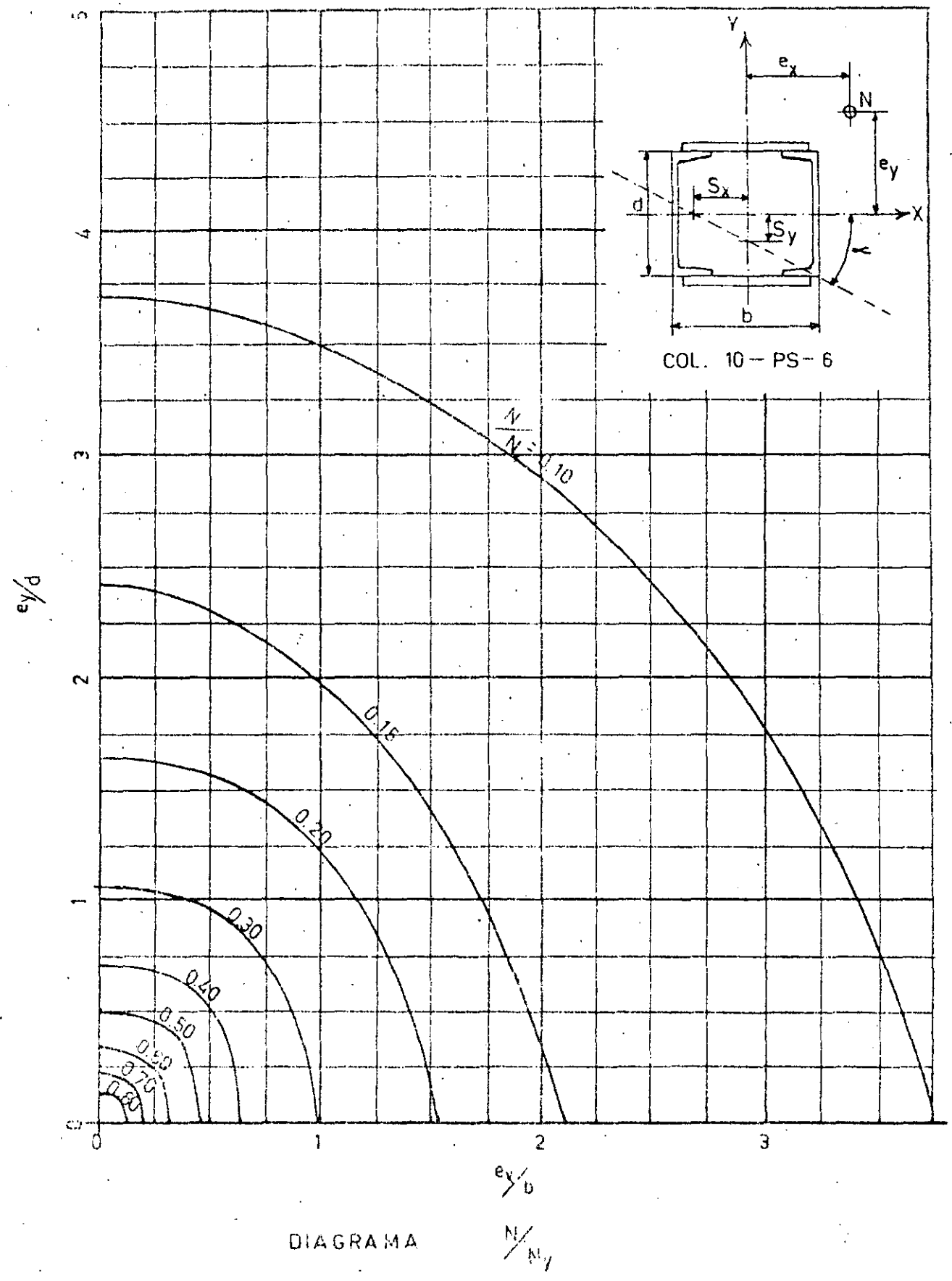


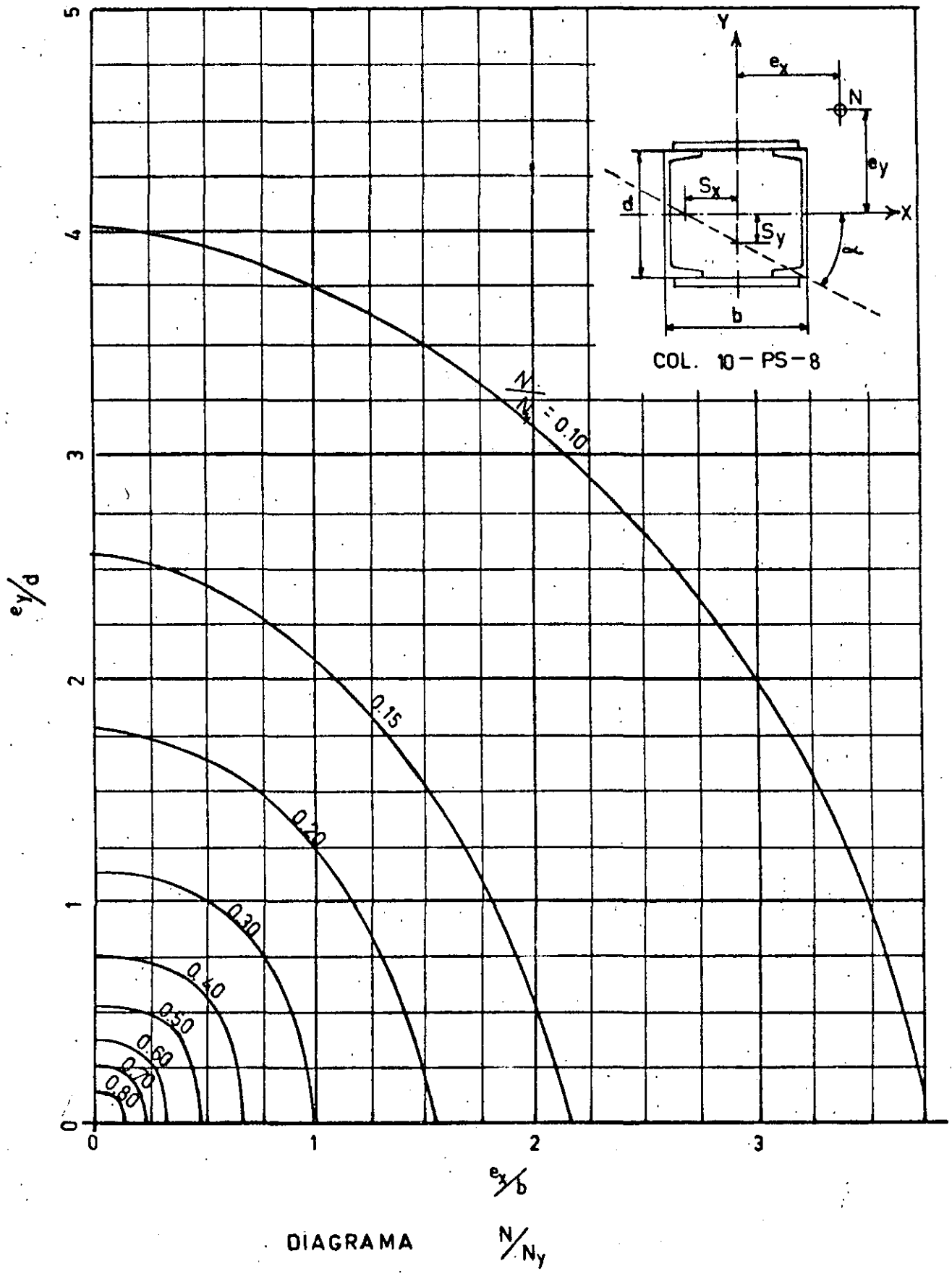


DIAGRAMA

$N/N_y$

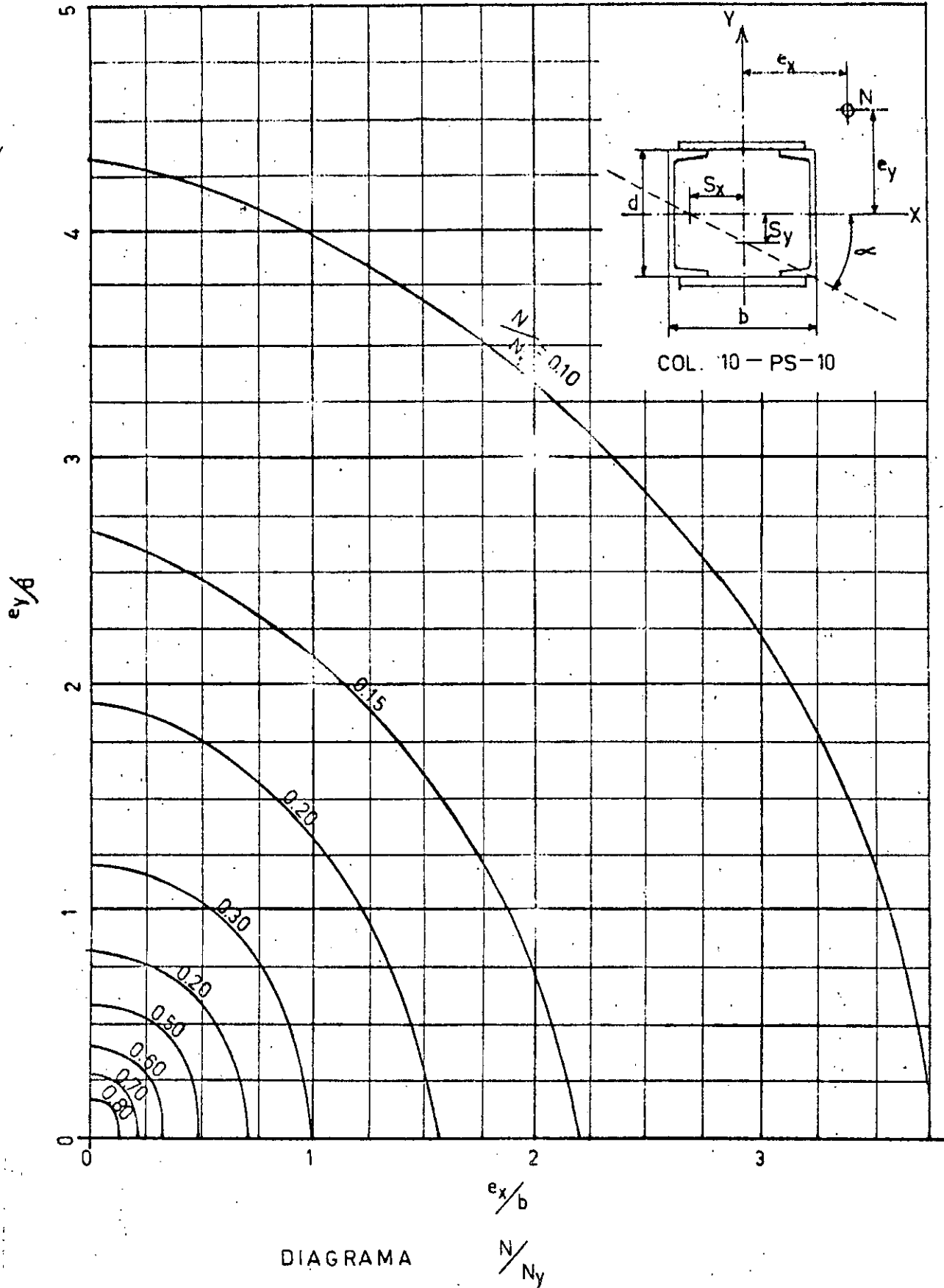


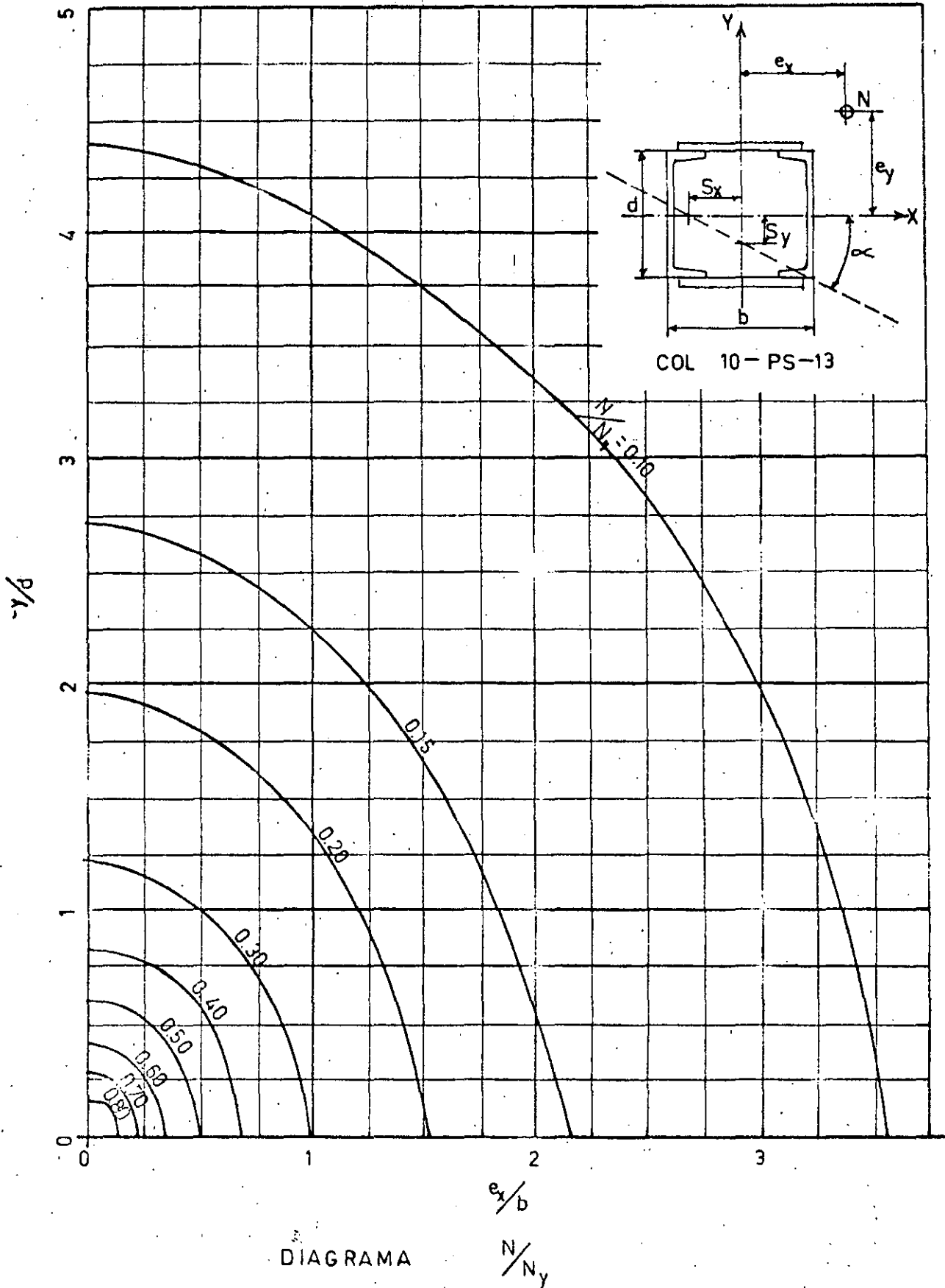




DIAGRAMA

$N/N_y$





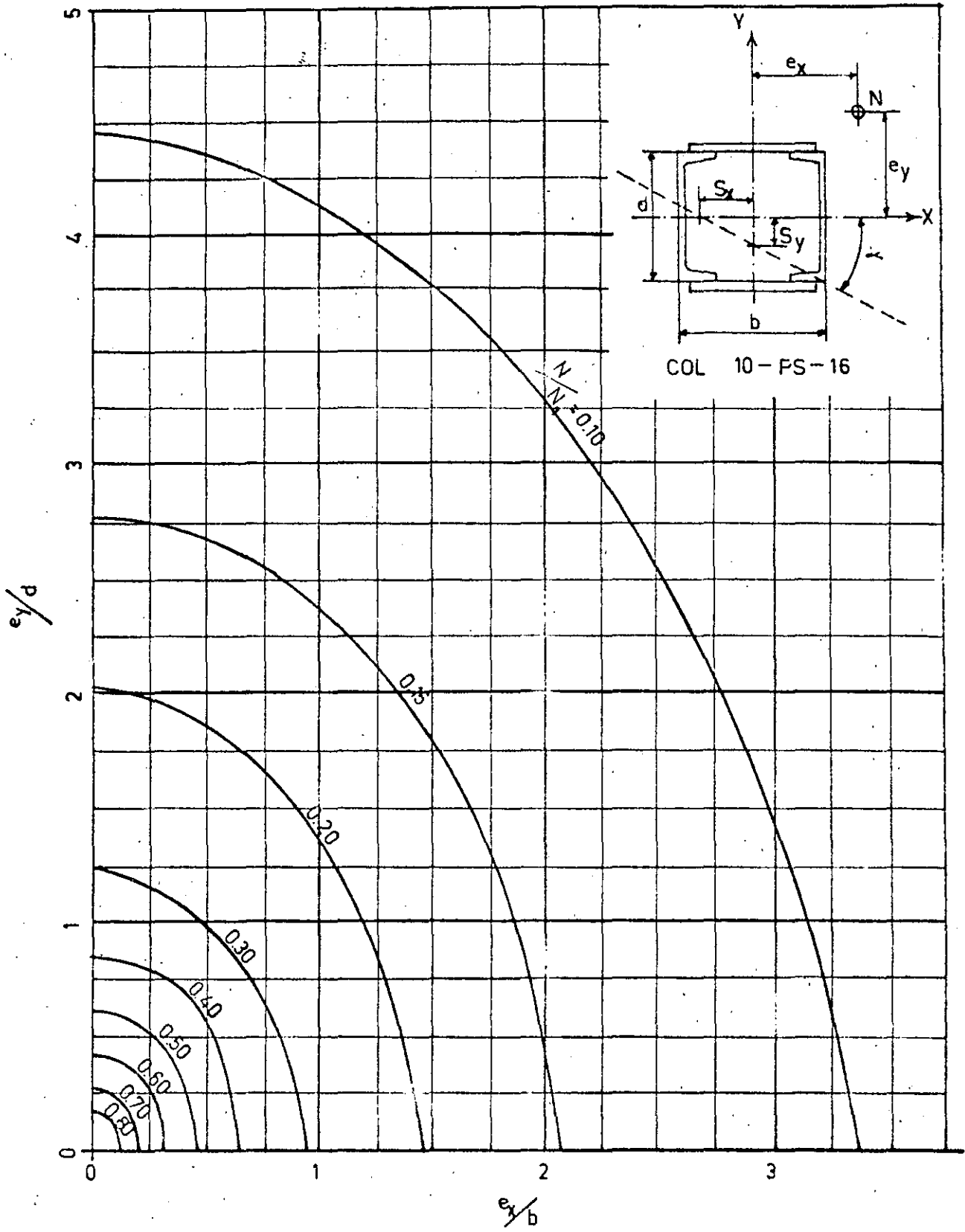
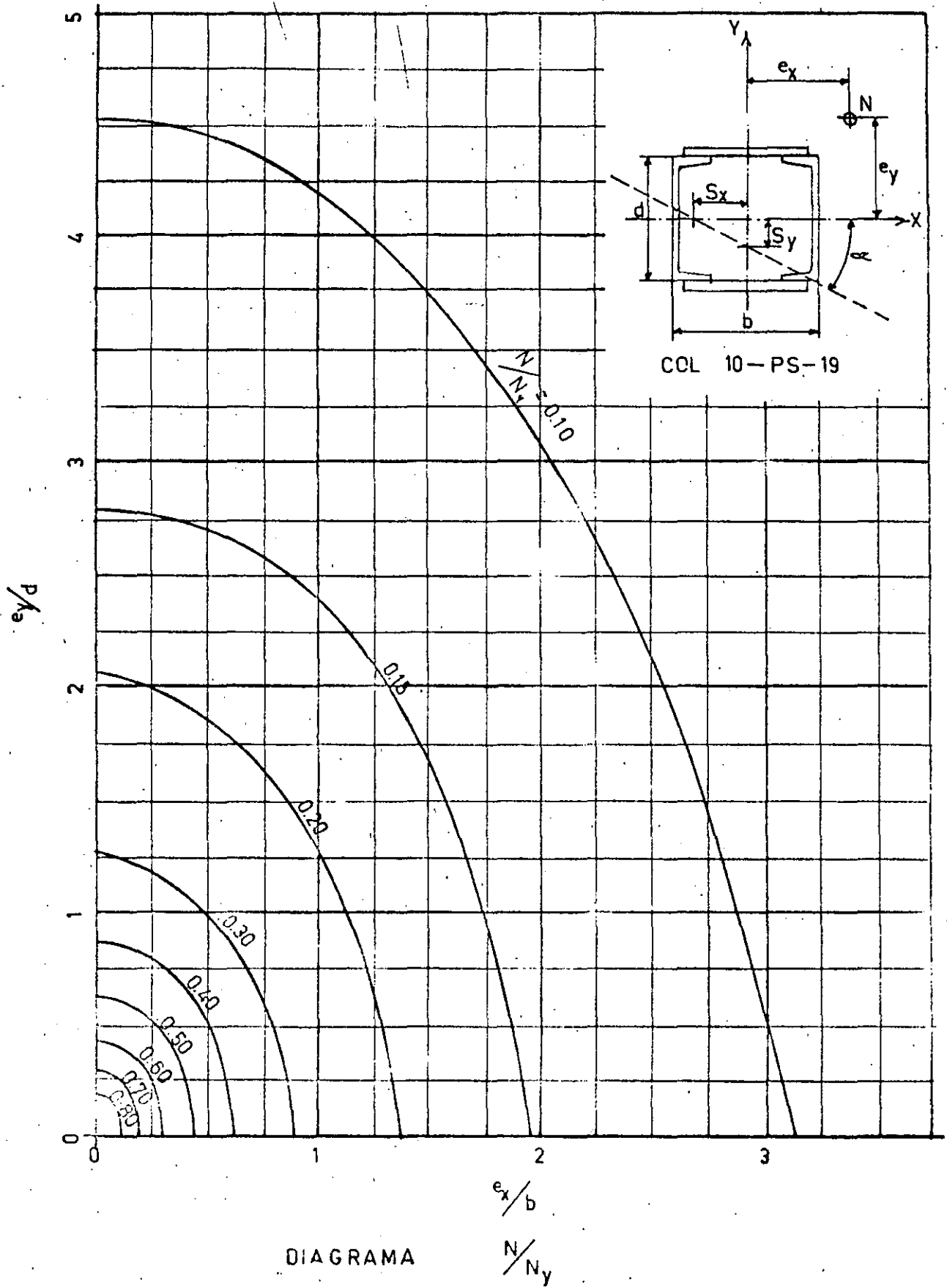
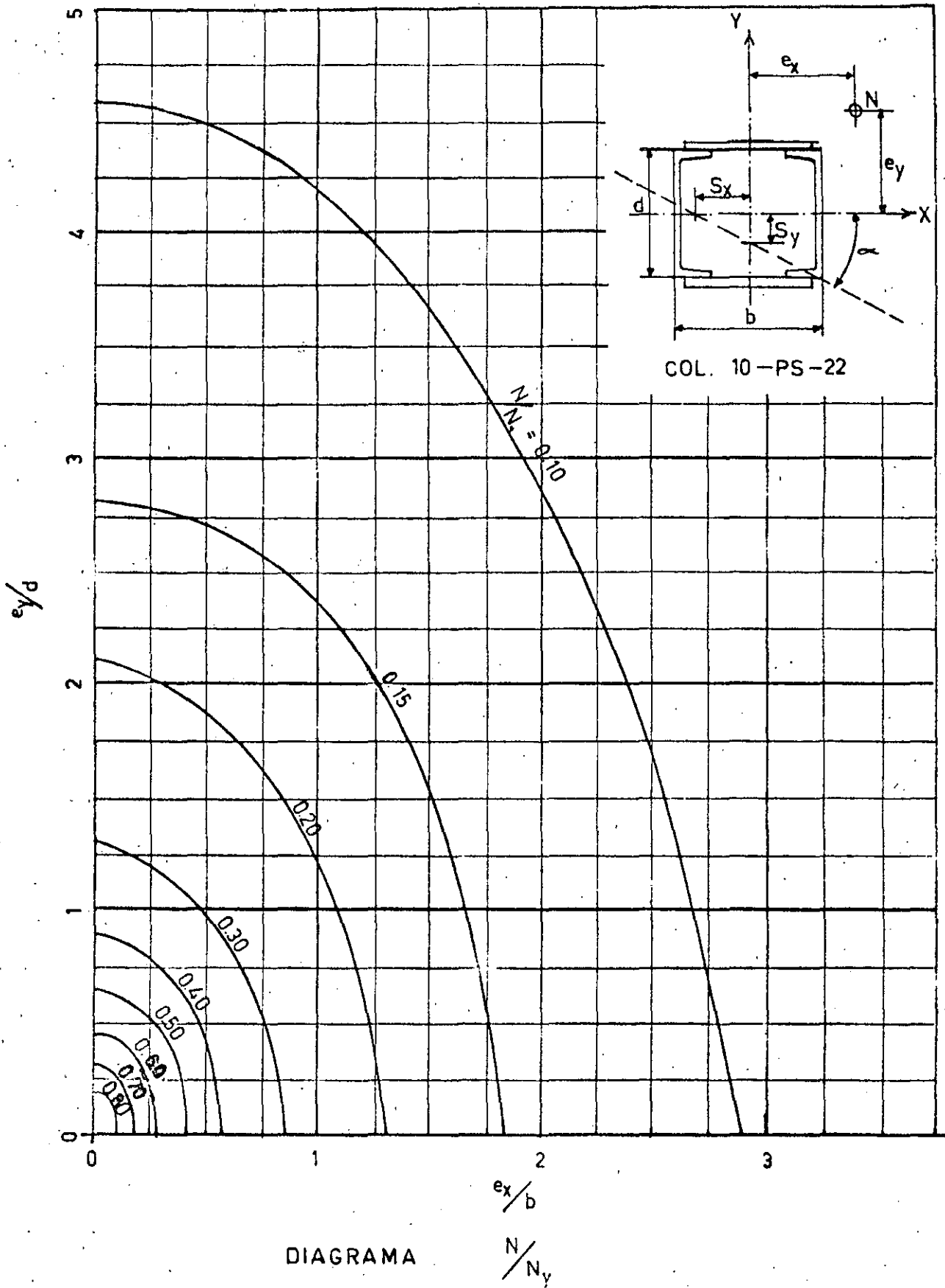
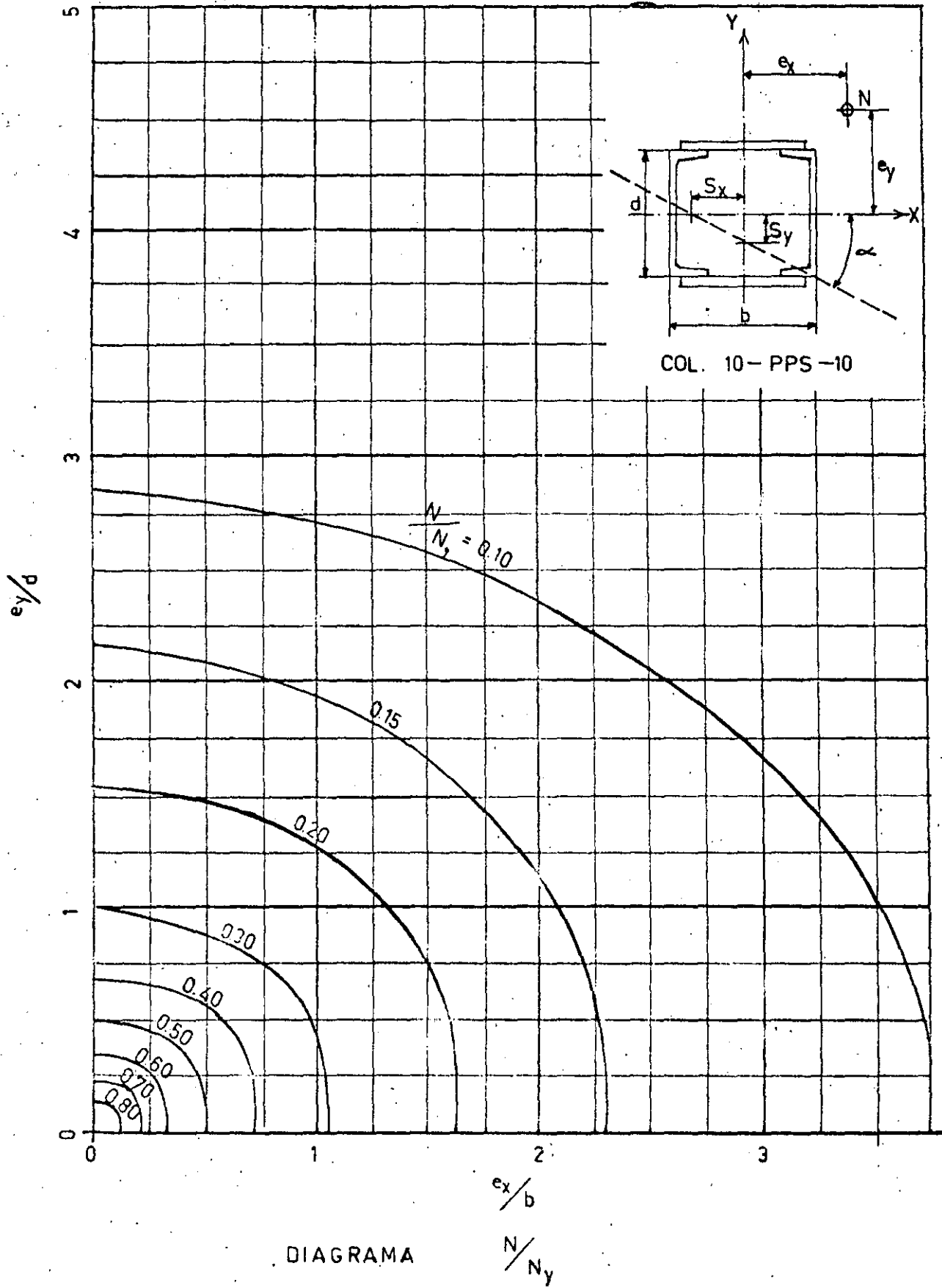


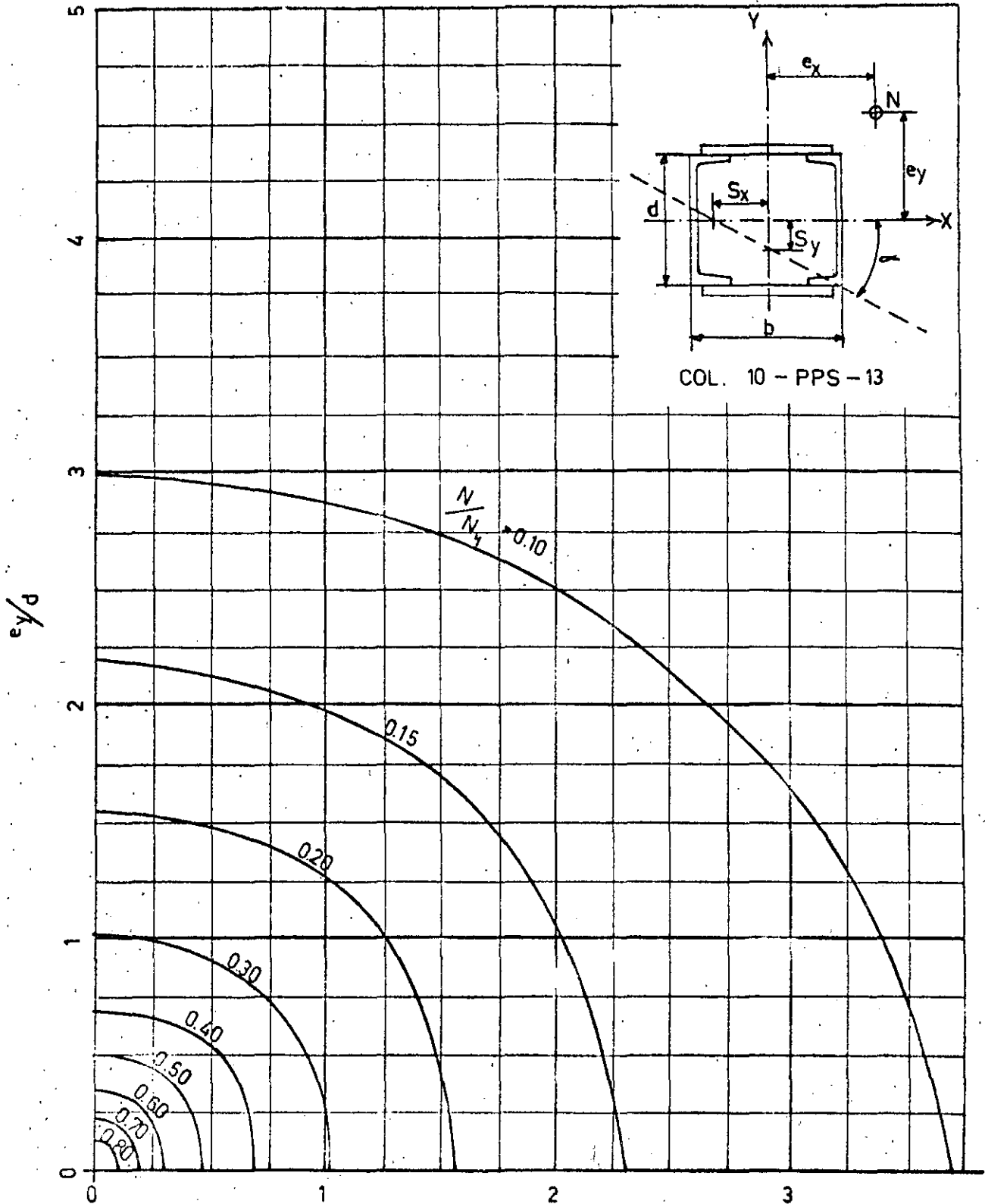
DIAGRAMA  $N/N_y$





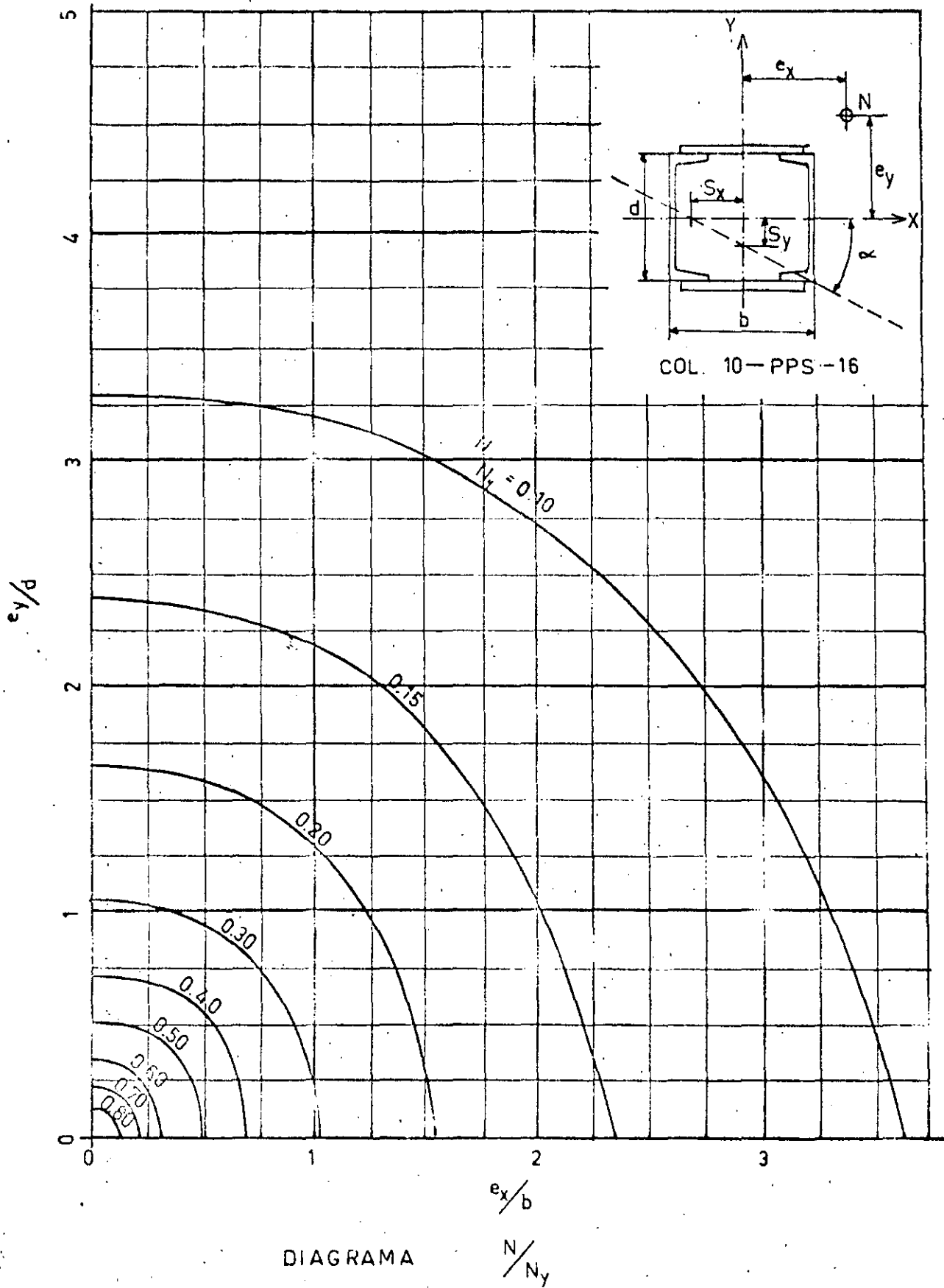


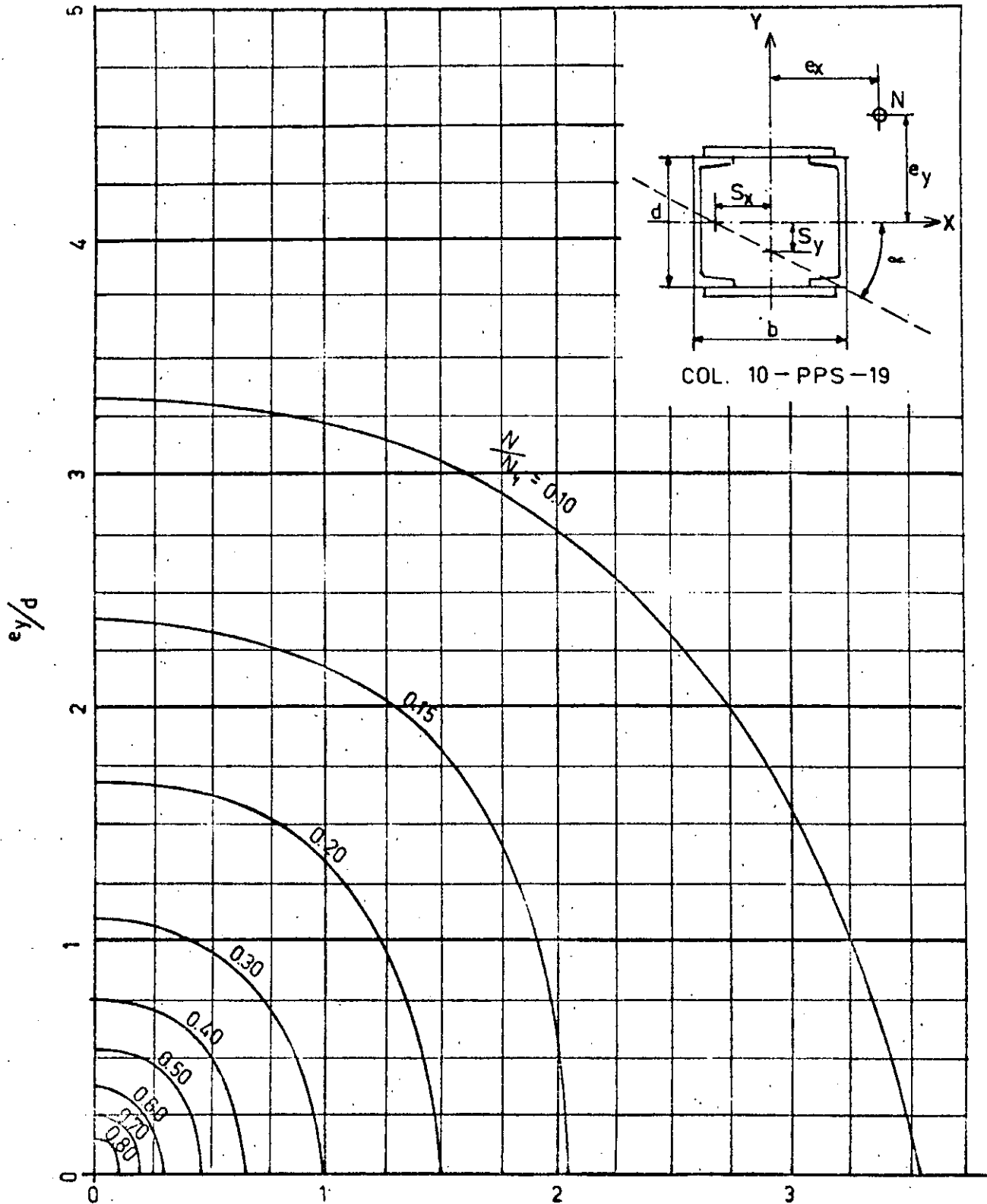




DIAGRAMA

$\frac{e_x}{b}$   
 $\frac{N}{N_y}$

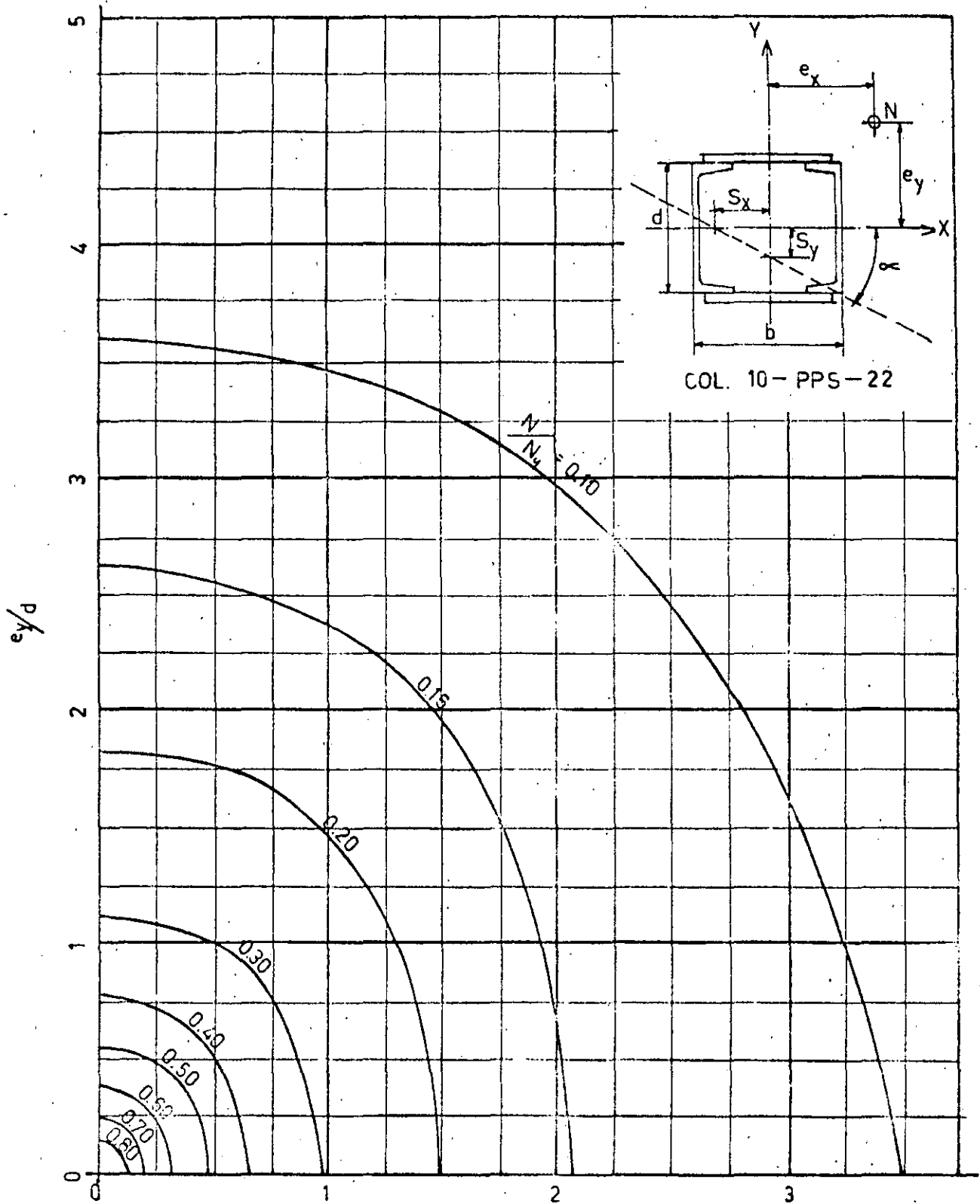




COL. 10 - PPS - 19

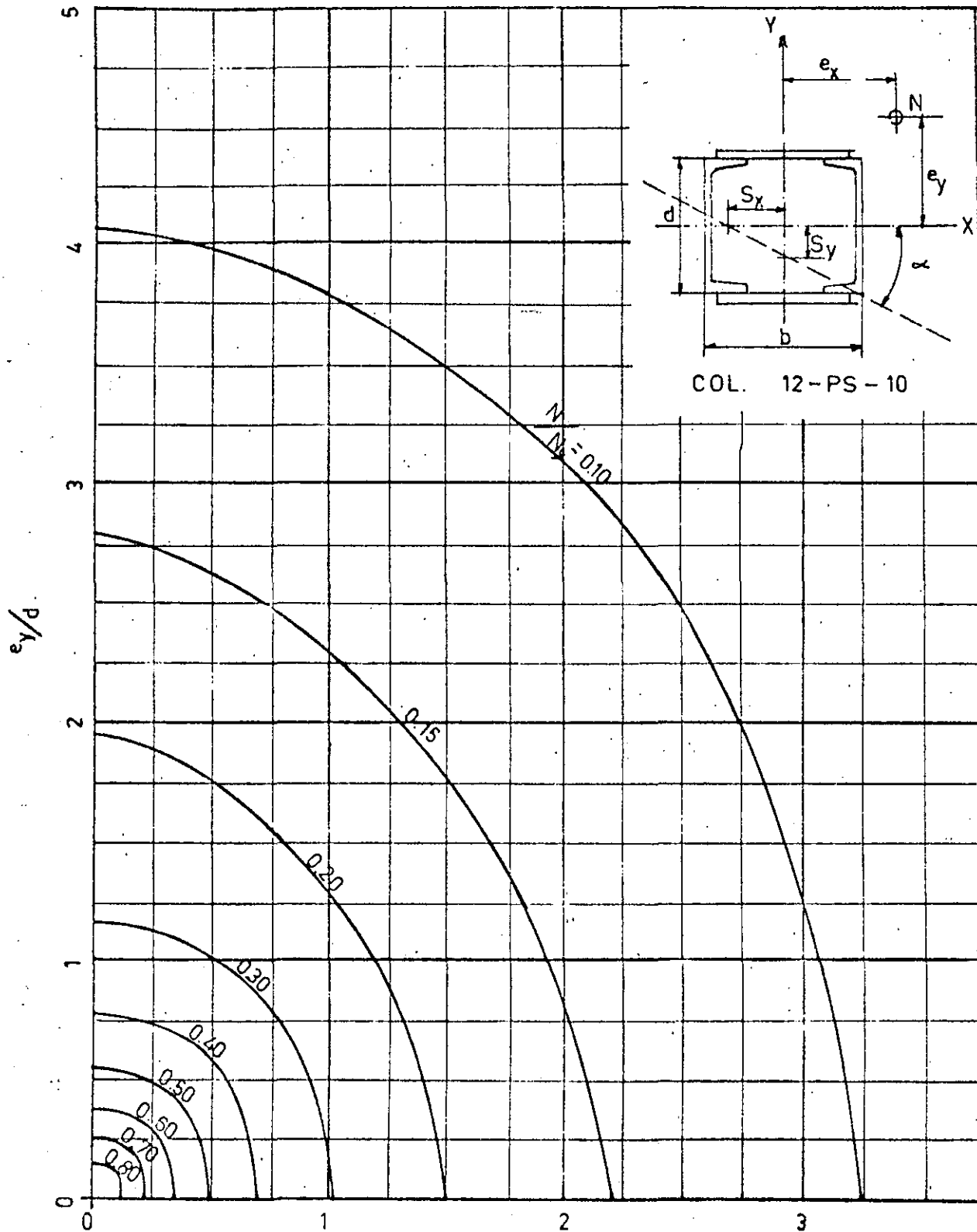
DIAGRAMA

$e_x/b$   
 $N/N_y$



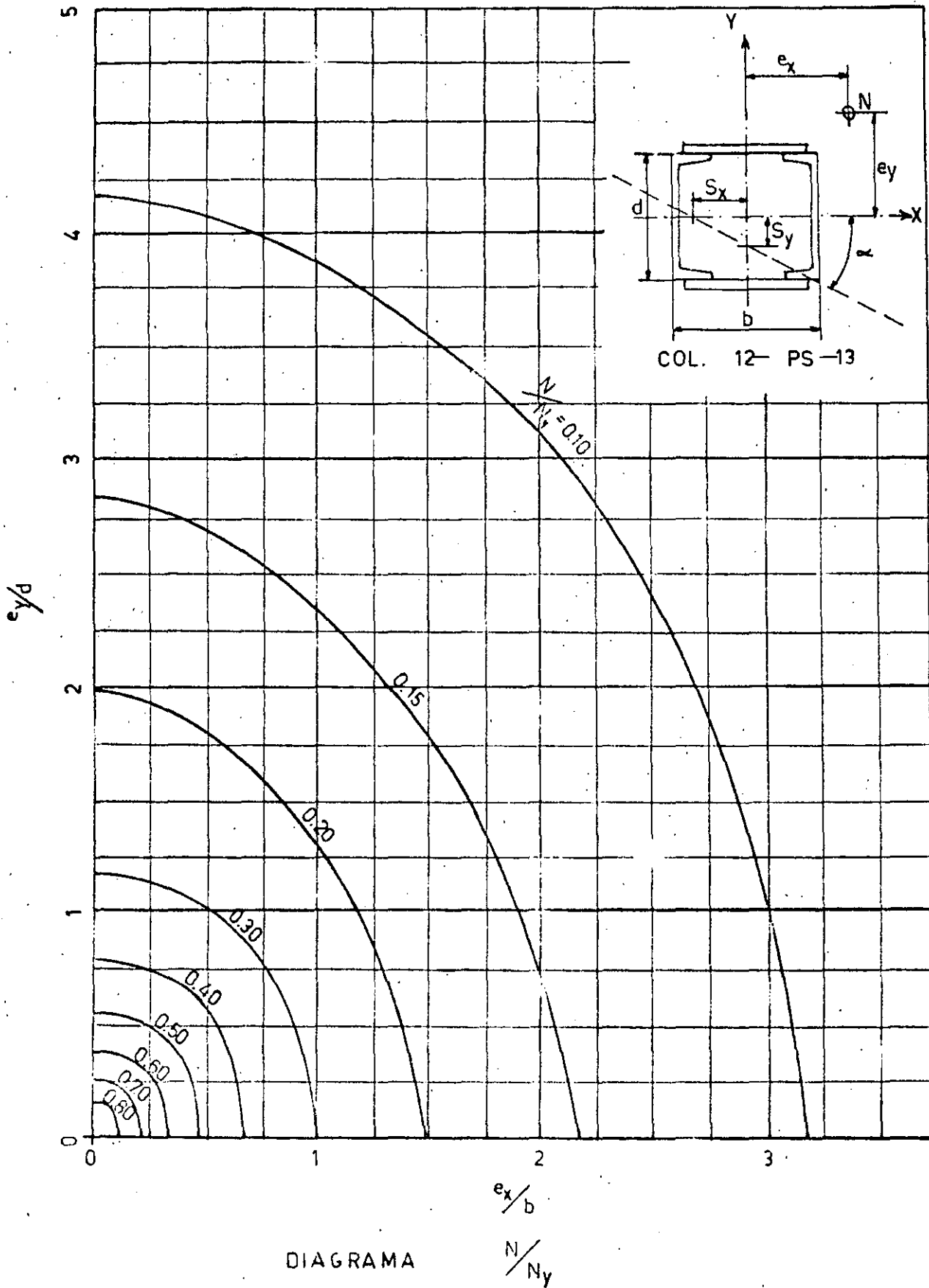
DIAGRAMA

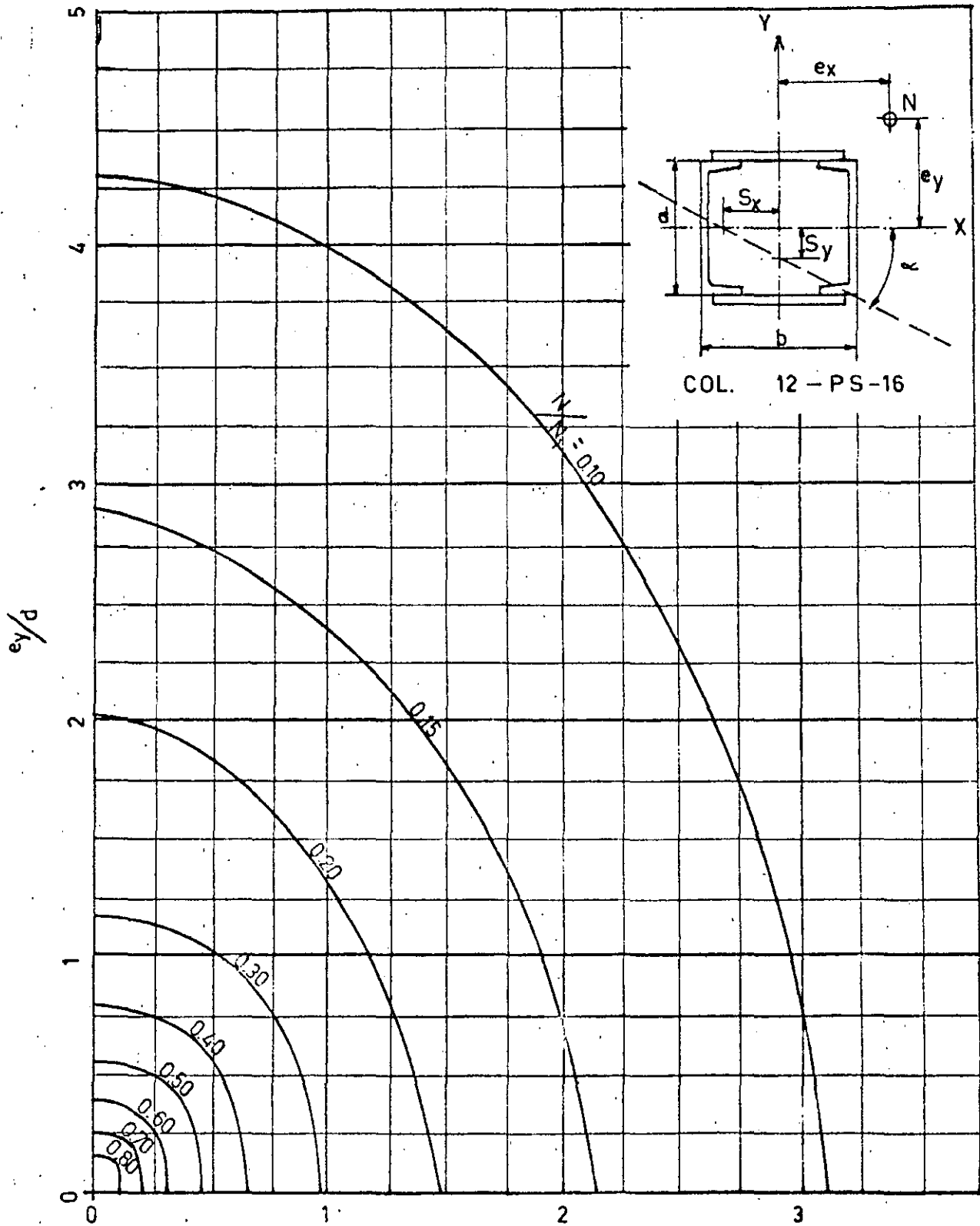
$N/N_y$



DIAGRAMA

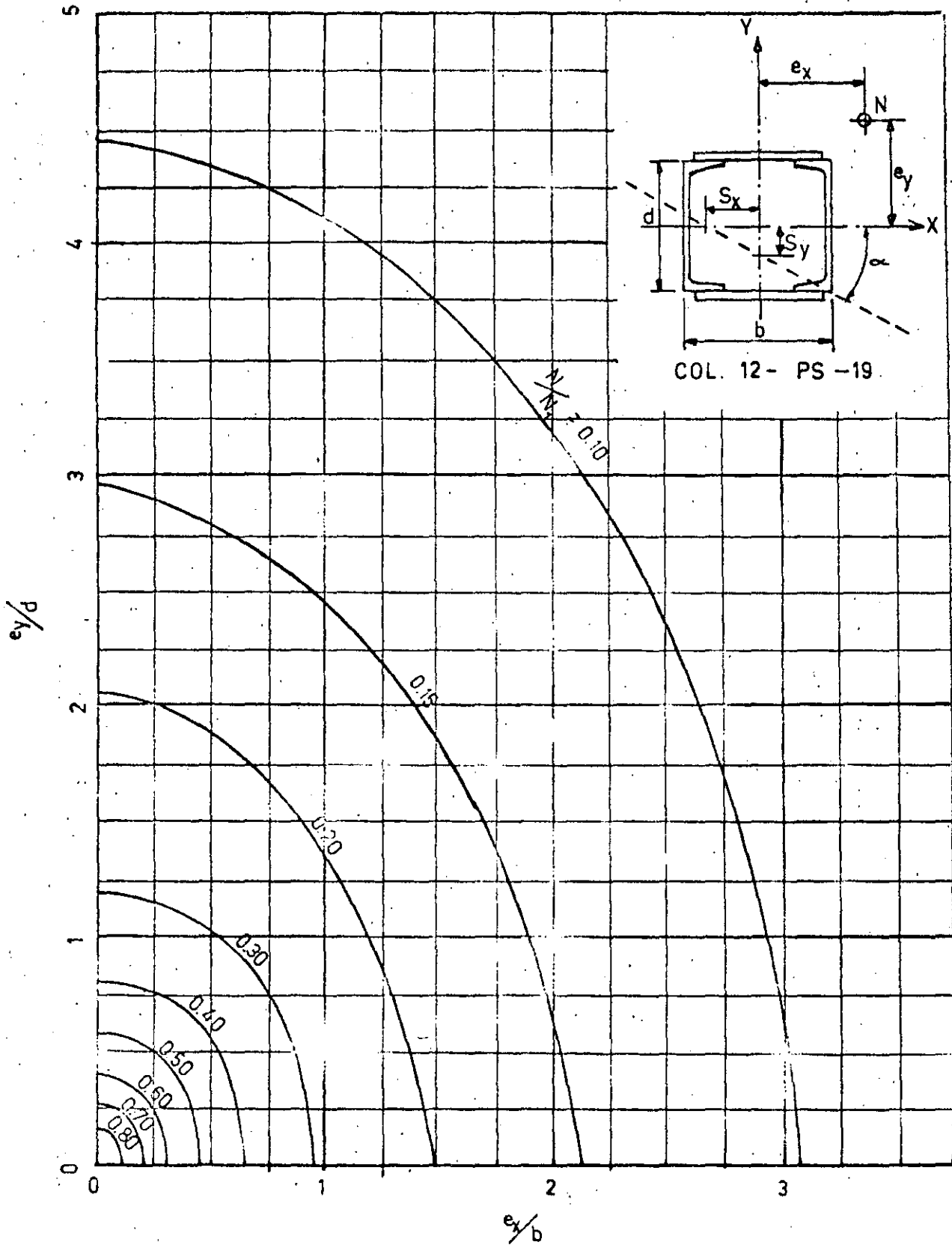
$e_x/b$   
 $N/N_y$





DIAGRAMA

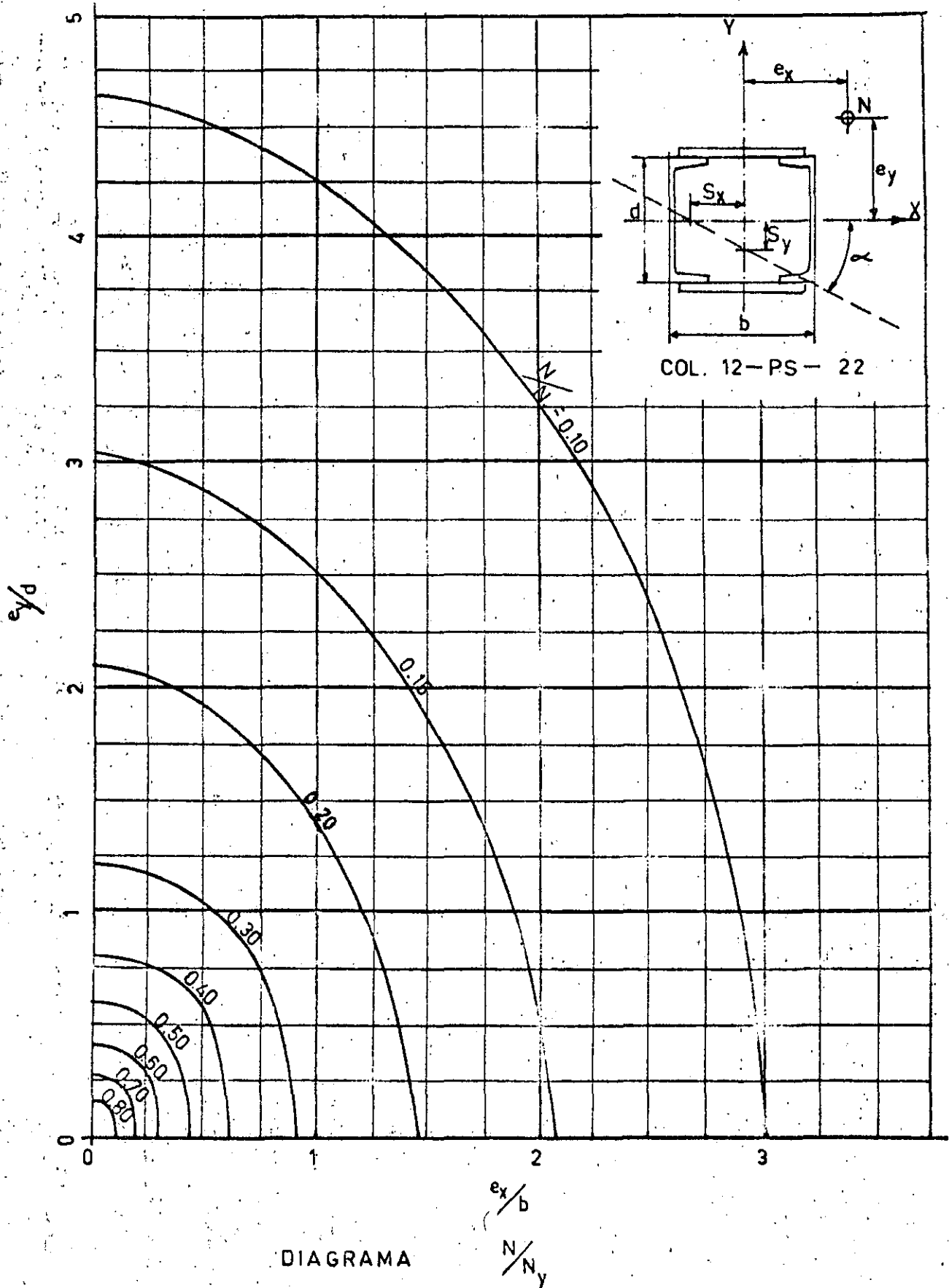
$e_x/b$   
 $N/N_y$

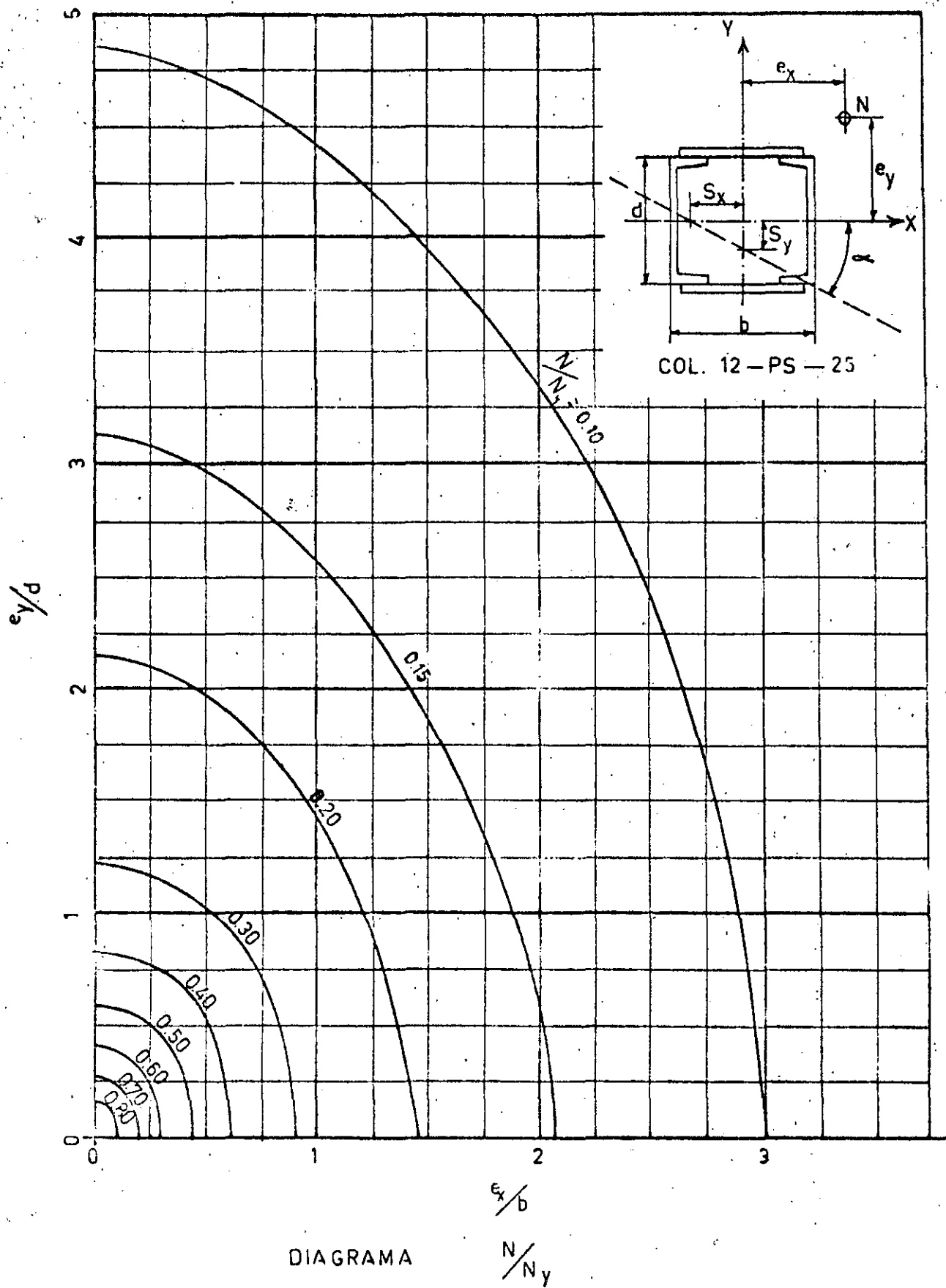


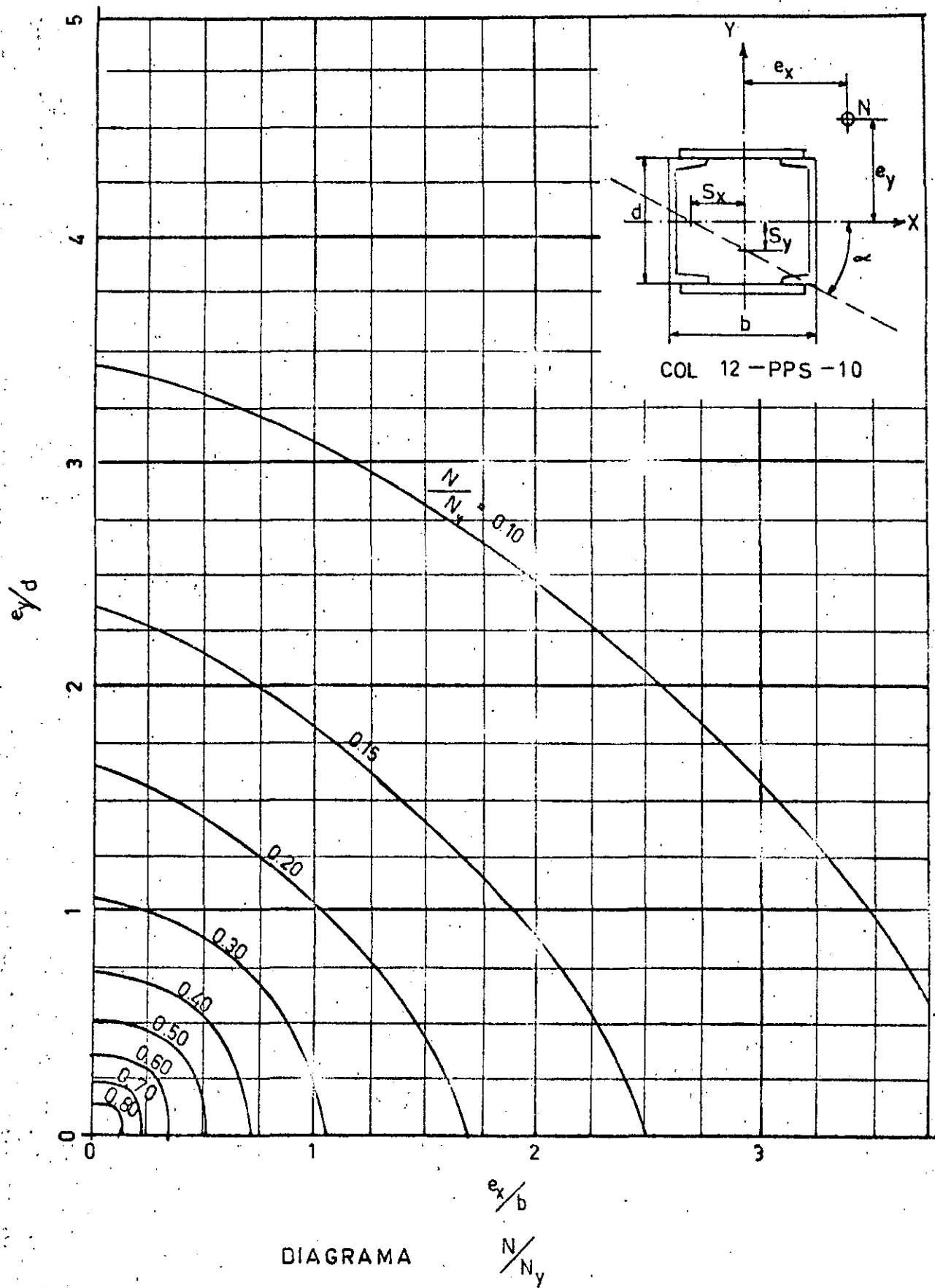
DIAGRAMA

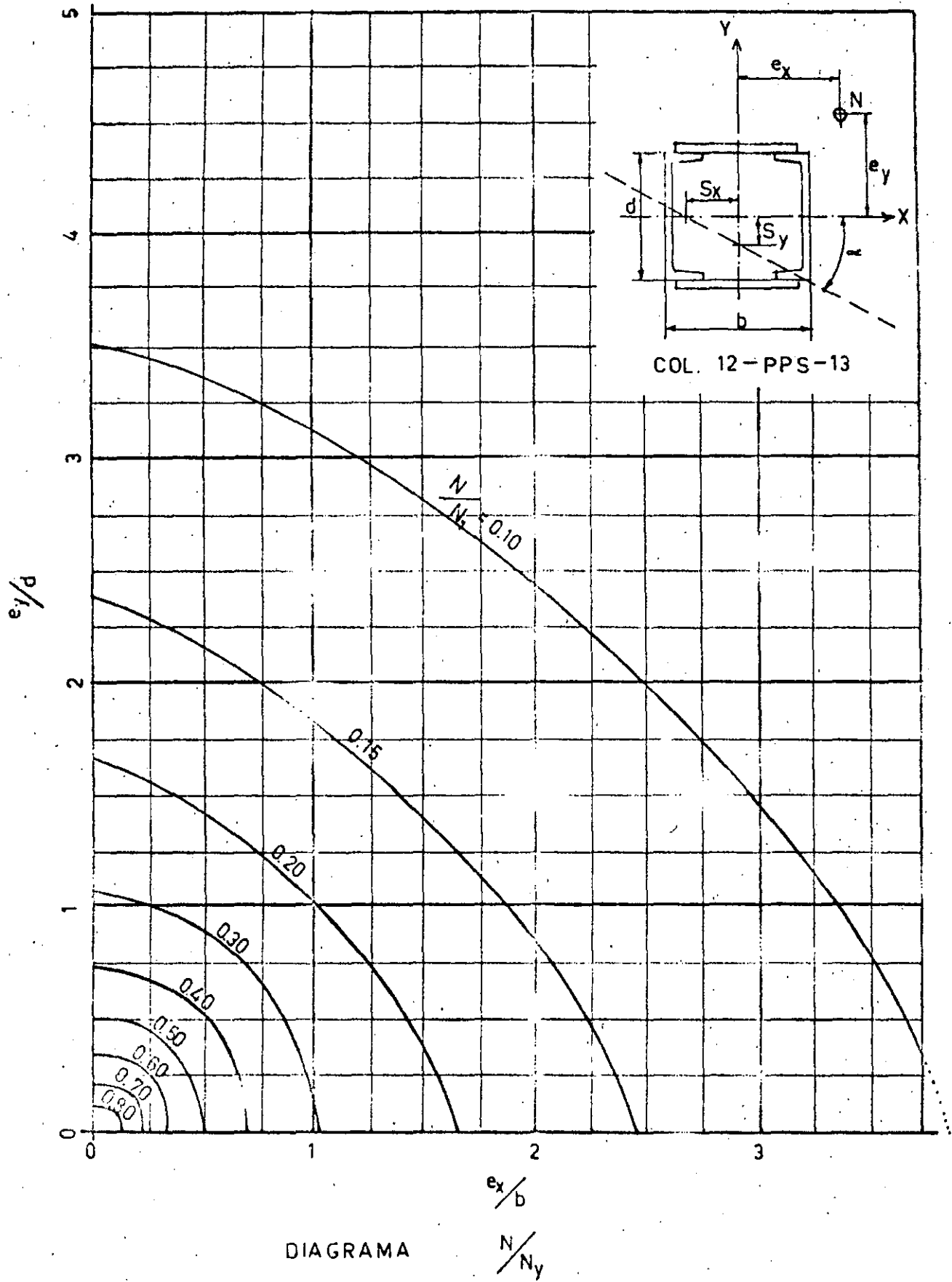
$\frac{N}{N_y}$

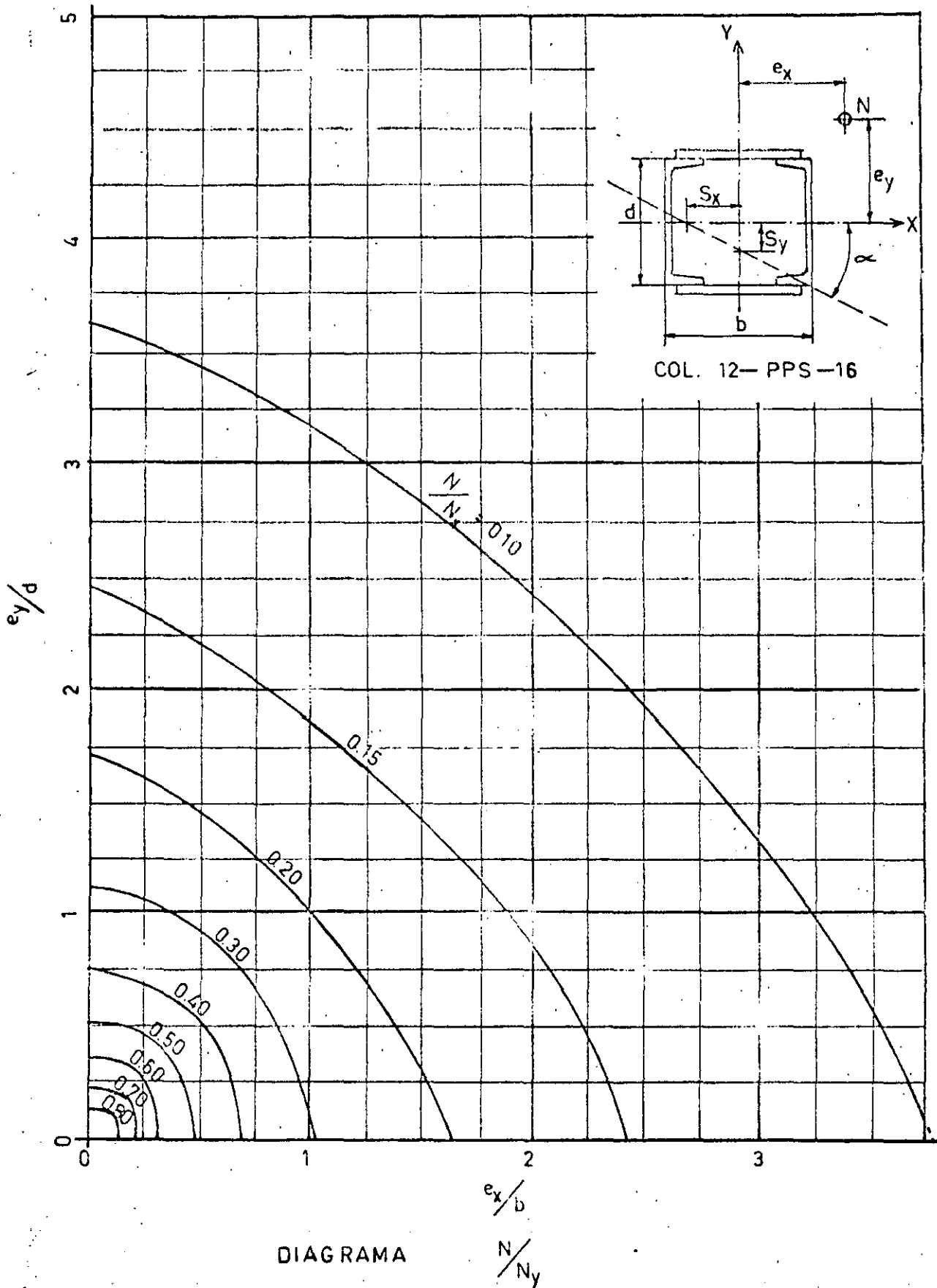


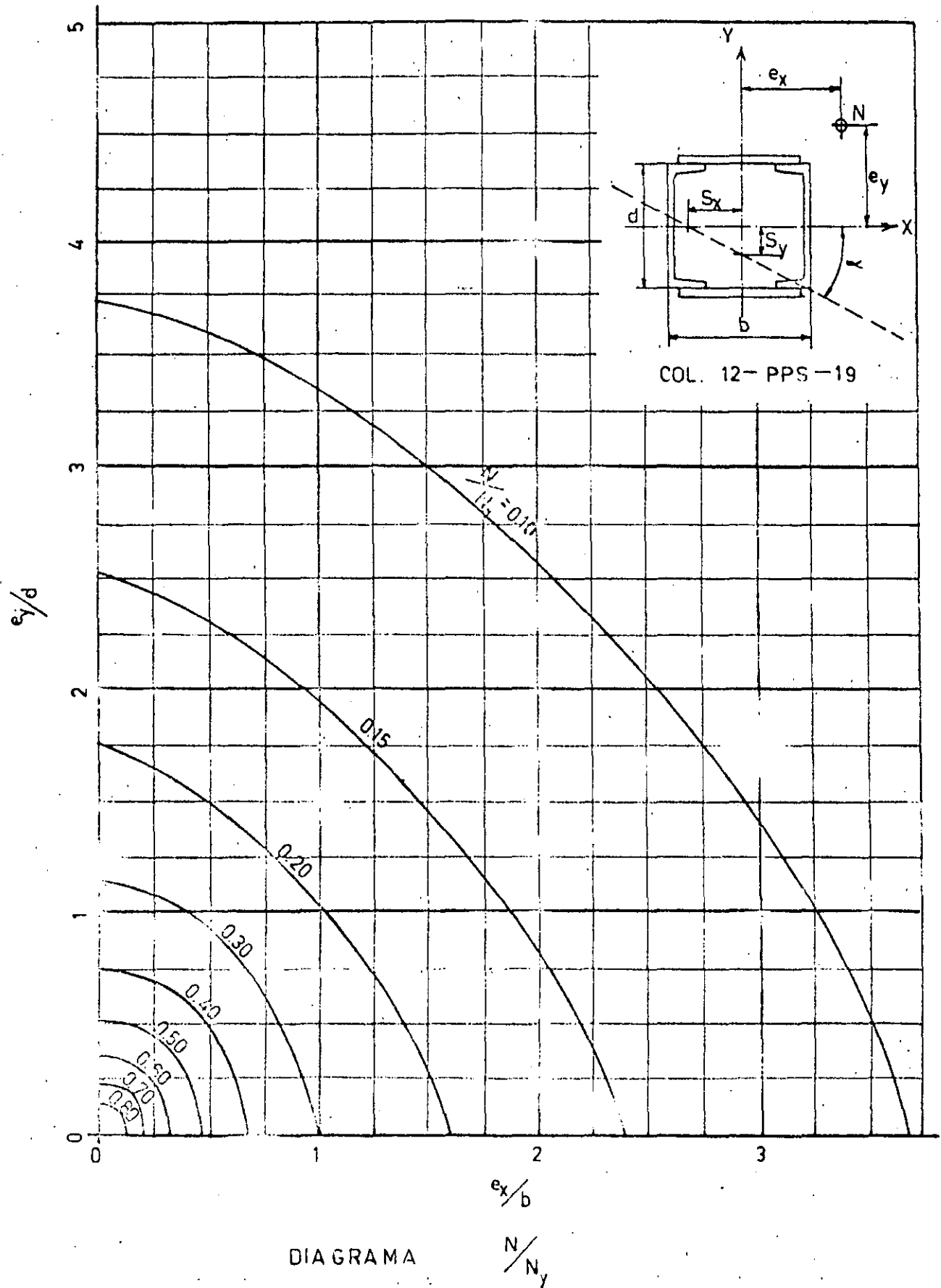


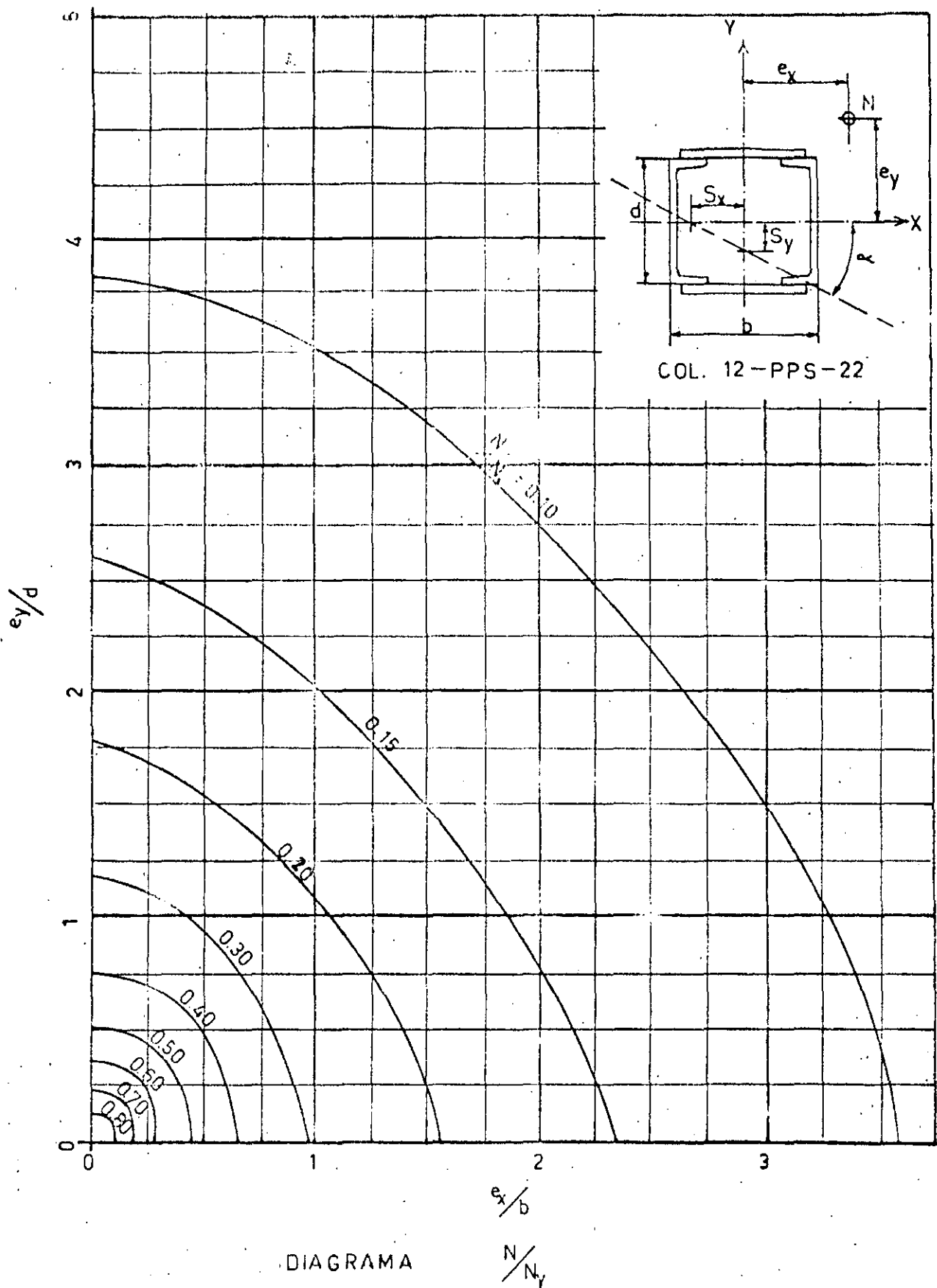


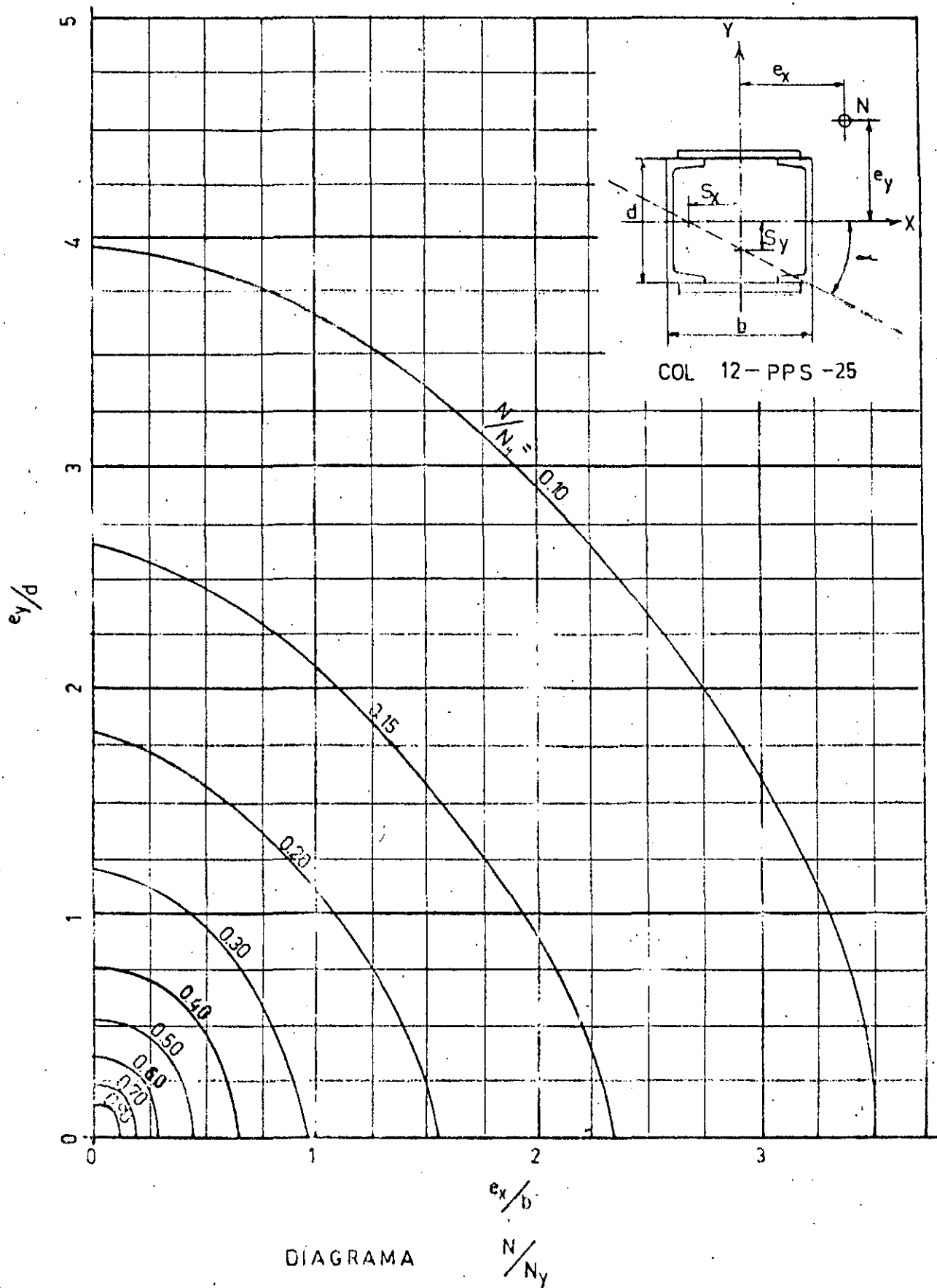
















---

Journal of the  
**STRUCTURAL DIVISION**  
Proceedings of the American Society of Civil Engineers

---

**ULTIMATE STRENGTH OF SHORT STRUTS**

S. L. Lee<sup>1</sup>, A.M. ASCE and P. Ballesteros<sup>2</sup>, J.M. ASCE  
(Proc. Paper 1358)

---

**ABSTRACT**

The determination of the ultimate strength of short struts of any cross section subjected to the action of eccentric loads or pure non-symmetrical bending is treated in this paper. The analysis is based upon an idealized stress-strain relationship assuming constant stress for strain beyond the yield point.

It is well known that an analytical approach to these problems results in unwieldy equations even in the simpler cases and for the more general cases, a solution is well nigh impossible. An approximate solution is presented in this paper. Under any loading condition, the position of the neutral axis is first assumed and successive approximations are obtained by translational and rotational corrections. The expressions for the correction increments, derived from the equilibrium conditions, are simple and two or three cycles usually suffice to arrive at a satisfactory solution.

Numerical examples dealing with several different cross sections are given to illustrate the procedure. Application of this method to the elasto-plastic case is also demonstrated.

**INTRODUCTION**

The determination of the ultimate strength of short struts subjected to eccentric loads or pure nonsymmetrical bending entails, even in the simpler

---

<sup>1</sup>NOTE. Discussion open until February 1, 1958. Paper included in the copyrighted Journal of the Structural Division of the American Society of Civil Engineers, Vol. 83, No. 5, September, 1957.  
<sup>2</sup>Asst. Prof., Civ. Eng. Dept., Northwestern Technological Inst., Northwestern Univ., Evanston, Ill.  
<sup>3</sup>Graduate Student, Civ. Eng. Dept., Northwestern Technological Inst., Northwestern Univ., Evanston, Ill.



cases, (1, 2) unwieldy analytical expressions and, for more general cases, an analytical solution becomes extremely complex if at all possible. An approximate solution is discussed in this paper applicable not only to the plastic case but also to the elastoplastic case. The following assumptions form the basis of the analysis: (1) Plane sections remain plane after bending. (2) The material remains elastic up to the yield point after which it deforms plastically sustaining constant stress. The stress-strain relationships in tension, compression and bending are identical.

The general equations will be derived for the elastoplastic case of which the plastic case is the upper limit.

### Eccentric Loads

Consider the section shown in Fig. 1a and take the neutral axis as the x-axis of the rectangular coordinates, the y-axis assuming any convenient position. The stress distribution curve shown in Fig. 1b may be expressed as follows:

$$\begin{aligned} \sigma &= \frac{N}{A} \left( 1 + \frac{e_x x}{r^2} + \frac{e_y y}{r^2} \right) & | -y_0 \leq y \leq y_0 \\ \sigma &= \sigma_y & | y \geq y_0 \\ \sigma &= -\sigma_y & | y \leq -y_0 \end{aligned} \quad (1)$$

where  $\sigma_y$  is the yield stress and  $y_0$  the distance from the neutral axis to the fiber which just reaches yield point. The equilibrium conditions require that

$$N = \int_{A_e} \sigma dA + \int_{A_p} \sigma dA \quad (2a, b, c)$$

$$N e_x = \int_{A_e} \sigma y dA + \int_{A_p} \sigma y dA$$

$$N e_y = \int_{A_e} \sigma x dA + \int_{A_p} \sigma x dA$$

where  $N$  is the eccentric load,  $e_x$  and  $e_y$  the distances of  $N$  from the coordinate axes while  $A_e$  and  $A_p$  denote respectively the elastic and plastic areas. Substituting (1) in (2) and solving for  $e_x$  and  $e_y$  lead to

$$e_x = \frac{\int_{A_e} \sigma y dA + \int_{A_p} \sigma y dA}{N} \quad (3a, b)$$

where



$$\begin{aligned} Q_x &= \int A_p \sigma_x y \, dA \\ Q_y &= \int A_p \sigma_x x \, dA \end{aligned} \quad (4)$$

$$\begin{aligned} I_x &= \int A_p y^2 \, dA \\ I_y &= \int A_p x^2 \, dA \end{aligned}$$

The signs of  $A_p$ ,  $Q_x$ , and  $Q_y$  given by (4) must be consistent with the sign of  $\sigma$  defined by (1), i.e., plastic areas are positive if in compression and negative if in tension. The value of the eccentric load, given by (2a), may be conveniently expressed in the form

$$N = C_y \left( \frac{Q_x}{y_0} + A_p \right) \quad (5)$$

For the sign convention adopted,  $N$  is a compressive load if positive. For the plastic case, (3) becomes

$$\begin{aligned} C_y \left( \frac{Q_x}{y_0} + A_p \right) &= \frac{A_p \sigma}{A_p} \\ C_y \left( \frac{Q_x}{y_0} + A_p \right) &= \frac{Q_x}{y_0} \end{aligned} \quad (6a, b)$$

and the ultimate load is given by

$$N_u = \frac{A_p \sigma_u}{y_0} \left( \frac{Q_x}{y_0} + A_p \right) = \sigma_u A_p \quad (7)$$

For a given eccentricity and a fixed value of  $y_0$ , zero in the plastic case, the position of the neutral axis must be so located that (3) or (6) is satisfied. This position may be defined by the angle of inclination of the neutral axis with respect to any fixed axis and the perpendicular distance between the eccentric load and the neutral axis,  $ey$ . The determination of this position may best be done by first assuming any reasonable position and then improve it by means of translational and rotational corrections.

Let  $N$ , in Fig. 2, be the given position of the eccentric load, and  $ox$  the assumed position of the neutral axis. Also let the position of  $o'x'$ , which is parallel to  $ox$ , be such that (3b) is satisfied, i.e.

$$N = \frac{A_p \sigma_u}{y_0} \left( \frac{Q_x}{y_0} + A_p \right) = \frac{A_p \sigma_u}{y_0} \left( \frac{Q_x}{y_0} + A_p \right) \quad (8)$$

where  $A_e$  and  $A_p$  are the elastic and plastic areas associated with  $o'x'$ . Since the distance between  $ox$  and  $o'x'$ ,  $\delta$ , is small, (8) may be approximated



where  $A_c$  and  $A_p$  are the areas associated with  $\sigma_x$ . Solving (9) for  $\delta$  leads to

$$\delta = \frac{I_x - e_y Q_x - y_0 (I_y - e_x Q_y)}{e_y A_c} \quad (10)$$

where  $\delta$  is the translational correction increment, positive when measured toward the positive direction of the  $y$ -axis. All the quantities in (10) are those associated with  $\sigma_x$ .  $A_c$  is the absolute value of the elastic area.

Corresponding to  $\sigma'_x$  and any conveniently chosen vertical axis  $\sigma'_y$ , (3) yields  $e'_x$  and  $e'_y$  which define the position of  $N'$ , the resultant of the forces acting on the section with the neutral axis located at  $\sigma'_x$ . From Fig. 2 it is evident that the position of the neutral axis  $\sigma'_x$  may be further improved by rotating it through an angle  $\alpha$  to position  $\sigma''_x$ . The rotational correction increment is

$$\alpha = \frac{e'_y Q'_x - e'_x Q'_y}{I'_x - e'_y Q'_x} \quad (11)$$

and the direction is obvious. The choice of the center of rotation depends upon the geometry of the section and is best shown by the numerical example.

The translational and rotational corrections are repeated until the computed position of  $N$  defined by (3) coincides with the given position of  $N$ . The value of  $N$  is then computed by (5).

The same procedure may be employed in the plastic case for which the translational correction increment is derived by setting  $y_0 = 0$  in (10). Thus

$$\delta = \frac{I_x - e_y Q_x}{e_y A_c} \quad (12)$$

where  $b$  is the total length of the neutral axis intercepted within the section as shown in Fig. 3. When the neutral axis is located, the ultimate load is then determined by (7).

### Pure Bending

In the case of a section subjected to the action of a bending moment  $M$  (Fig. 4), taking the neutral axis as the  $x$ -axis with the  $y$ -axis assuming any convenient position, the equilibrium conditions are

$$\begin{aligned} \sum F_x &= 0 & \sum F_y &= 0 & \sum M_x &= 0 \\ \int \sigma_x dA &= 0 & \int \sigma_y dA &= 0 & \int \sigma_y y dA &= 0 \end{aligned} \quad (13a)$$



where  $M_x$  and  $M_y$  are the components of  $M$  about the coordinate axes. The bending moment is given by

$$M = \sqrt{M_x^2 + M_y^2} = \sigma \sqrt{\left(\frac{I_x}{I_y} - 1\right) M_x^2 + M_y^2} \quad (14)$$

The angle of inclination of  $M$  with respect to the  $x$ -axis is given by the relationship

$$\tan \theta = \frac{M_y}{M_x}$$

which, giving regards to (13b,c), leads to

$$\theta = \tan^{-1} \left( \frac{E \alpha_1 \alpha_2 \delta + M_y}{E \alpha_1 \alpha_2 \delta + M_x} \right) \quad (15)$$

Consistent with the sign of  $\sigma$  defined by (1),  $\theta$  is positive when measured clockwise from the  $x$ -axis and  $M_x$ ,  $M_y$ , and  $M$  are positive as indicated by the double arrows in Fig. 4, adopting the right-hand screw rule.

Let  $o'x'$  (Fig. 5) be the assumed position of the neutral axis and  $o'y'$  which is parallel and at a distance of  $\delta$  to  $o'y$ , be so located that (13a) is satisfied, i.e.,

$$\int_{A_1} (y - \delta) dA_1 - \int_{A_2} y dA_2 = 0 \quad (16)$$

As previously done, approximating (16) by

$$\frac{E}{I_y} \int_{A_1} (y - \delta) dA_1 - \sigma \int_{A_2} y dA_2 = 0 \quad (17)$$

and solving for  $\delta$  lead to

$$\delta = \frac{E \alpha_1 \alpha_2 \delta + M_y}{\alpha_2} \quad (18)$$

where  $\delta$  is the translational correction increment, positive when measured toward the positive direction of the  $y$ -axis.

Corresponding to  $o'x'$  and any conveniently assumed position of  $o'y'$ , (15) yields  $\theta$  which defines the direction of the resultant moment acting on the section. Unless the correct position of the neutral axis is assumed the computed value of  $\theta$  is different from the given value of  $\theta$ . The difference between these two values indicates the approximate magnitude of the rotational correction. The direction is obvious.

As in the case of eccentric load, the translational and rotational corrections may be repeated until the resultant moment acting on the section coincides with the given moment. For sections such as angles and I-sections, convergence is relatively slow. An alternate method, the better one in this case, is to plot the angles of inclination of the neutral axes versus the angles



of inclination of the corresponding resultant moments acting on the section and determine the correct position of the neutral axis by interpolation from the curve. The value of  $M$  is then computed by (14).

The same procedure may be employed in the plastic case for which (14), (15) and (18) become, upon substitution of  $y_0 = 0$ , respectively

$$M_p = \int_{-c}^c \left[ \sigma_y \left( \frac{x}{b} + q \right) + \left( \frac{x}{b} + q \right) \right] = \sigma_y / b \int_{-c}^c (x + qb) dx \quad (19)$$

$$\theta = -\tan^{-1} \left[ \lim_{y \rightarrow 0} \left( \frac{2 + 2\sigma_y b_0 q_0}{2x + qb} \right) \right] = -\tan^{-1} \frac{2q}{b} \quad (20)$$

$$\delta = \lim_{y \rightarrow 0} \left( \frac{Q_y + y_0 A_p}{I_c} \right) = \frac{A_p}{2b} \quad (21)$$

where  $\theta$  is positive when measured clockwise from the  $x$ -axis,  $\delta$  is positive when measured toward the positive direction of the  $y$ -axis and  $b$  is as defined in Fig. 3.

### Numerical Examples

#### Example 1

Consider the rectangular section shown in Fig. 6a subjected to the action of an eccentric load  $N$  located as shown. The problem is to determine the ultimate value of  $N$  which the section can sustain in terms of the yield stress  $\sigma_y$  of the material. The neutral axis is first assumed to be at a distance of 5.6 in. from  $N$  with an angle of inclination of  $34^\circ$ . The corresponding values of  $A_p$  and  $q_x$  are computed in Table 1a, and  $b$  is 4.8 in. Area I is  $\triangle ACE$ , area II  $\triangle ABD$ , area III  $\triangle DFH$  and area IV  $\triangle EGH$ . Substituting these values and  $e_y = 5.6$  in. in (12) yields  $\delta = -0.21$  in. which indicates that the neutral axis should be translated further away from  $N$  to the position shown in Fig. 6b.

Next the values of  $A_p$ ,  $q_x$  and  $q_y$  corresponding to the translated position of the neutral axis are calculated in Table 1b, and (6a,b) yield  $e_x'' = 1.78$  in. and  $e_y'' = 5.73$  in. which define the position of the resultant force  $N'$  acting on the section. The  $y$ -axis in this case is taken through the center of gravity of area II. With respect to the coordinate axes, the position of  $N$  is defined by  $e_x = -3.28$  in. and  $e_y = 5.81$  in. It should be observed that by this translational correction the value of  $e_y$  is improved considerably. Substituting  $e_x$ ,  $e_x''$  and  $e_y''$  in (11) yields  $\alpha = 14.7^\circ$  which indicates that the neutral axis should be rotated to the position shown in Fig. 6c. The center of rotation, point  $O$  in Fig. 6b, is located midway between points  $A$  and  $B$ . The choice of this point is rather arbitrary, but (12) indicates that if the numerator ( $e_y A_p = q_x$ ) is kept close to zero, the subsequent translational correction may be avoided. In this particular case, observe that the values of  $e_y$  and  $q_x$  for trials (a) and (b) remain fairly constant, hence the numerator of (12) can be kept very small if  $A_p$  is kept fairly constant. This can be done by making  $\triangle A'AO$  approximately equal to area  $B'BO$ .

The values of  $A_p$ ,  $q_x$  and  $q_y$  corresponding to the rotated position of the neutral axis are computed in Table 1c. (12) yields  $\delta = 0$  and (6a,b) yield  $e_x'' = 1.86$  in. and  $e_y'' = 5.57$  in. which are reasonably close to the values of  $e_x$  and  $e_y$  shown in Fig. 6c. (7) yields the ultimate load  $N_u/\sigma_y = 3.89$  in<sup>2</sup>.

A glance at Fig. 6c shows that, in the case of eccentric load, the location of the neutral axis should be such that the centers of gravity of the two cross sectional areas divided by the axis and the position of the eccentric load should lie on the same straight line. From consideration of equilibrium, this point is evident.

### Example 2

Consider the section shown in Fig. 7 subjected to an eccentric load  $N$  located as shown. Fig. 7a shows the assumed position of the neutral axis so located that the observation just mentioned is visually satisfied. Table 2a shows that, although the computed value of  $e_y$  differs considerably from the given value, the translational correction is only  $-0.06$  in. The translated position of the neutral axis is shown in Fig. 7b. With the  $y$ -axis passing through the given position of  $N$ , the calculation shown in Table 2b yields  $\theta = 0.9^\circ$  and the neutral axis is next rotated  $0.9^\circ$  about point  $O$  to the position shown in Fig. 7c. The values of  $e_x$  and  $e_y$  corresponding to the rotated axes are determined in Table 2c and can be seen to agree fairly well with the values shown in Fig. 7c. As before, (7) gives the ultimate load  $N_u/O_y = 1.22 \text{ in}^2$ .

### Example 3

To illustrate the procedure for the determination of the ultimate strength of a section under nonsymmetrical bending, consider the section shown in Fig. 8. The applied moment  $M$  is inclined at an angle of  $20^\circ$  from the major axis. (21) indicates that if  $A_p$  is kept zero, no translational correction is needed in the solution. The double symmetry of the section suggests readily that  $A_p$  will remain zero if the neutral axis passes through the centroid of the section, an observation which again is obvious from the view point of equilibrium. As mentioned previously, convergence of the successive approximations in this type of sections is comparatively slow, hence the alternate method will be employed. While three trials are sufficient to obtain a solution, four positions of the neutral axis are assumed for the purpose of illustration as shown respectively in Fig. 8a, b, c and d and the corresponding values of  $q_x$  and  $q_y$  are calculated in Table 3a, b, c and d. (20) yields the values of  $\theta$ , the angles of inclination of the resultant moments acting on the section with respect to the neutral axes. The angles of inclination of these moments with respect to the major axes. The angles of inclination of these moments with respect to the major axis of the section,  $\beta_M$ , are next computed and plotted in Fig. 9 against the angles of inclination of the neutral axis,  $\beta_N$ . The intersection of this curve with the horizontal line  $\beta_M = 20^\circ$  gives the correct position of the neutral axis,  $\beta_N = 77^\circ 30'$ . The corresponding values of  $q_x$  and  $q_y$  are then substituted in (19) giving the ultimate moment  $M_u/O_y = 20.2 \text{ in}^3$ . It is of interest to note, in Fig. 9, that  $\beta_M$  is practically zero for  $\beta_N < 60^\circ$ .

It may be observed from this example that in the determination of the ultimate strength of a section subjected to pure bending, the neutral axis should be so located that the two cross sectional areas divided by the neutral axis should be equal and their centers of gravity should lie on a straight line perpendicular to the vector representing the applied moment. These two observations may be drawn directly from the conditions of equilibrium.

4. The fillets in the angle and the wide-flange section treated in Example 3 are disregarded for simplicity, the error incurred being negligible.



### Example 4

To demonstrate the application of the above procedure to the elastoplastic case, consider the section shown in Fig. 10a. The problem is to determine the value of the applied moment  $M$ , shown in Fig. 10b, such that  $y_0 = 0.5''$ . As a first trial, take  $Z = 2.23$  and  $\beta_N = 60^\circ$ . The corresponding values of  $A_p$ ,  $A_e$  and  $Q_x$  are computed in Table 4a<sub>1</sub>, and substituting them in (18) leads to  $\theta = 0.061''$ . The translated position of the neutral axis is defined by  $Z = 2.14$  and  $\beta_N = 60^\circ$  and the corresponding sectional properties are calculated in Table 4a<sub>2</sub>. (14) yields the value of  $M$  and (15) yields  $\theta = -30.7^\circ$  corresponding to which  $\beta_M = 29.3^\circ$ . It has been observed that the convergence of the successive approximations in this type of sections is relatively slow. Therefore, while the difference between the computed value of  $\beta_M$  and the given one is  $6.7^\circ$ , a partial rotational correction, say  $3.5^\circ$ , may speed up the convergence. Furthermore, in the case under consideration,  $Q_x = 0$  and (18) indicates that the translational correction may be avoided by keeping  $A_p$  close to zero. This can be accomplished by keeping the sum of areas I and II equal to that of areas III and IV, which is an easy task since the thickness of the angle is constant. With these observations in mind, the position of the neutral axis is next rotated to that defined by  $Z = 2.23$  and  $\beta_N = 63.5^\circ$  and the corresponding geometric properties of the cross section are computed in Table 4c. Again (15) yields  $\theta = -26.7^\circ$  for which  $\beta_M = 36.8^\circ$  and  $M$  is determined by (14). This trial shows that the partial translational correction overshoots the correct position of the neutral axis by a small amount and a reversed partial correction in the next trial, say  $0.4^\circ$ , should yield a solution. To illustrate the alternate approach to this problem, however, a position of the neutral axis between those of trials (a) and (c) will be assumed. The calculation in Table 4b yields the corresponding values of  $\beta_M$  and  $M$ . The values of  $\beta_M$ ,  $Z$  and  $M/\sigma_y$  are then plotted against  $\beta_N$  in Fig. 10c. The intersection of the  $\beta_M = \beta_N$  curve with the line  $\beta_M = 36^\circ$  leads to the desired solution:  $\beta_N = 63.09^\circ$ ,  $Z = 2.265$  in. and  $M/\sigma_y = 5.43$  in<sup>3</sup>.

### CONCLUSION

Although the method of analysis presented in this paper is approximate by nature, careful execution of the solution with the aid of large scale figures yields reasonably accurate results for practical purposes. The equations employed are not involved, entailing only simple numerical calculation. Keeping the observations made in the numerical examples in mind, three trials should suffice to lead to a solution.

In the case of pure bending, it is comparatively easy to prepare graphs for the ultimate strength of commonly used sections with a few values of  $\beta_M$ . In the case of eccentric load, however, two parameters are involved and the work becomes more laborious. The ultimate strength under any loading condition may be obtained by interpolation from these graphs.

### NOTATIONS

- $A_e$  absolute value of elastic area
- $A_p$  plastic area, defined by (4)
- $b$  length of neutral axis, defined in Fig. 3

- $e_x, e_y$  eccentricity of normal load with respect to the coordinate axes, defined by (3) or (6)
- $I_x, I_y$  moment and product of inertia of the elastic area, defined by (4)
- $M$  bending moment, defined by (14)
- $M_x, M_y$  components of  $M$  about the coordinate axes, defined by (13b, c)
- $M_u$  ultimate value of  $M$ , defined by (19)
- $N$  eccentric load, defined by (5)
- $N_u$  ultimate value of  $N$ , defined by (7)
- $Q_x, Q_y$  static moment of the plastic area with respect to the coordinate axes, defined by (4)
- $Q_x$  static moment of the elastic area, defined by (4)
- $z_0$  distance from neutral axis to fiber which just reaches yield point
- $Z$  distance defined in Fig. 10a
- $\alpha$  rotational correction increment, defined by (11)
- $\beta_M$  angle of inclination of  $M$  with respect to the horizontal axis
- $\beta_N$  angle of inclination of neutral axis with respect to the horizontal axis
- $\delta$  translational correction increment, defined by (10), (12), (18) or (21)
- $\theta$  angle of inclination of  $M$  with respect to neutral axis
- $\sigma$  normal stress, defined by (1)
- $\sigma_y$  yield stress of material

## BIBLIOGRAPHY

1. Aghababian, M. S. and Popov, E. P., "Unsymmetrical Bending of Rectangular Beams Beyond the Elastic Limit," Proceedings of the First National Congress of Applied Mechanics, 1951.
2. Beedle, L. S., Thurlimann, B. and Ketter, R. L., "Plastic Design in Structural Steel," Fritz Engineering Laboratory Report No. 205.32, Lehigh University, Bethlehem, Pennsylvania, 1955, p. 9.1.



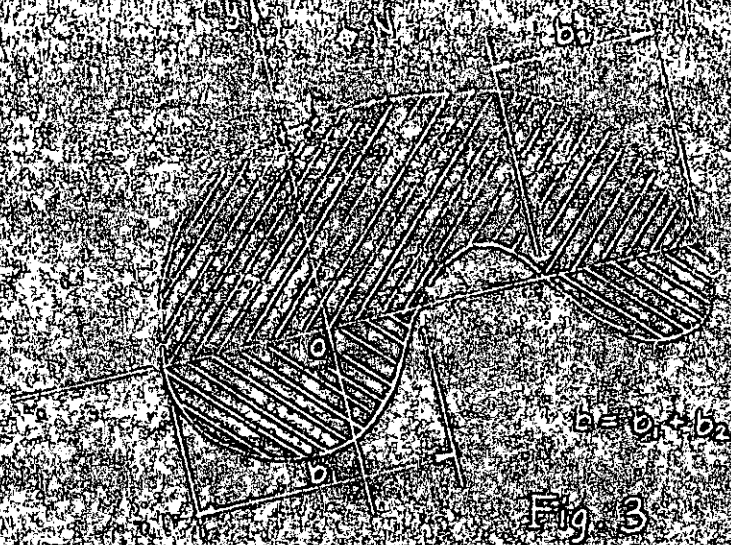


Fig. 3

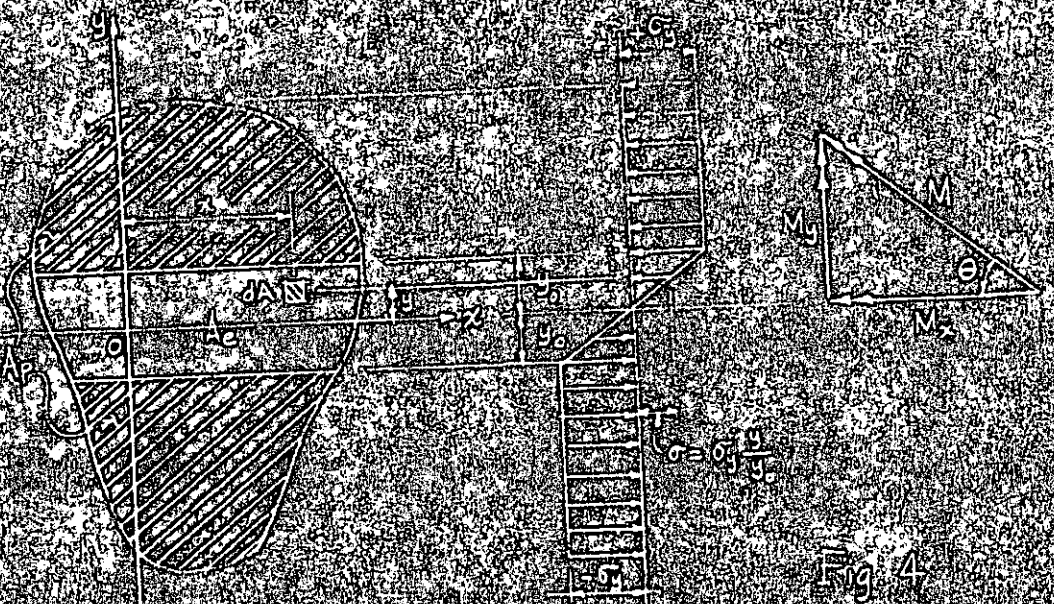


Fig. 4

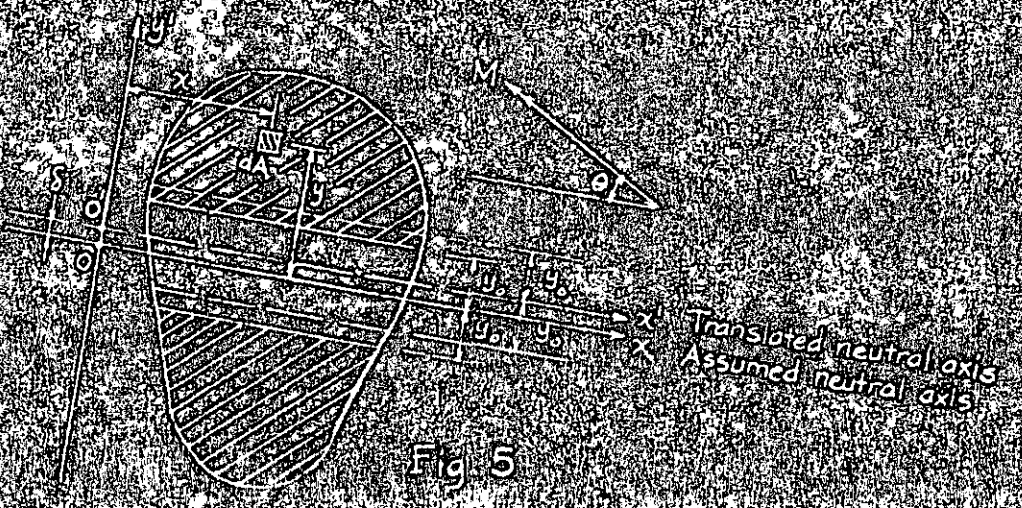


Fig. 5

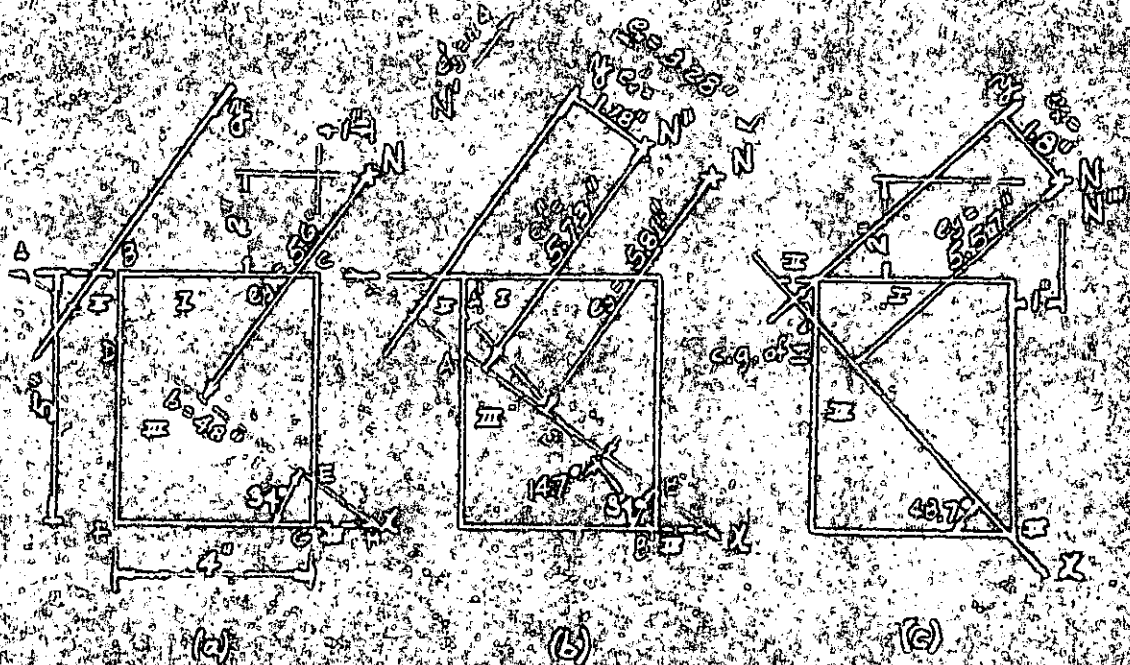


Fig. 6

Trial	Area No.	$A_p$ (in <sup>2</sup> )	$\bar{x}$ (in)	$\bar{y}$ (in)	$\sum x$ (in)	$\sum y$ (in)	$\sum$ (in)	$e_x$ (in)	$e_y$ (in)	$\alpha$
a	I	12.40	1.10	13.63						
	II	-1.45	0.40	-0.53						
	III	-9.60	-0.97	9.30						
	IV	0.60	-0.25	-0.15						
	$\Sigma$	1.95		22.20			-0.21		11.4	
b	I	13.35	1.20	10.61	2.51	15.00				
	II	-1.16	0.45	-0.33	0	0				
	III	-8.19	-0.40	7.96	3.90	-3.90				
	IV	0.32	-0.16	-0.06	6.50	2.06				
	$\Sigma$	4.02		23.09	7.16		6.73	5.73	12.7°	
c	I	12.20	1.16	14.15	2.87	35.29				
	II	-0.255	0.10	-0.02	0	0				
	III	-0.04	-0.14	7.55	3.48	-21.95				
	IV	-0.019	0.06	-0.02	6.95	0.124				
	$\Sigma$	3.89		26.67	7.22	0	1.86	5.57	0	

Eq. (7)  $N_p/\bar{y} = A_p = 3.89 \text{ in}^2$

Table 1



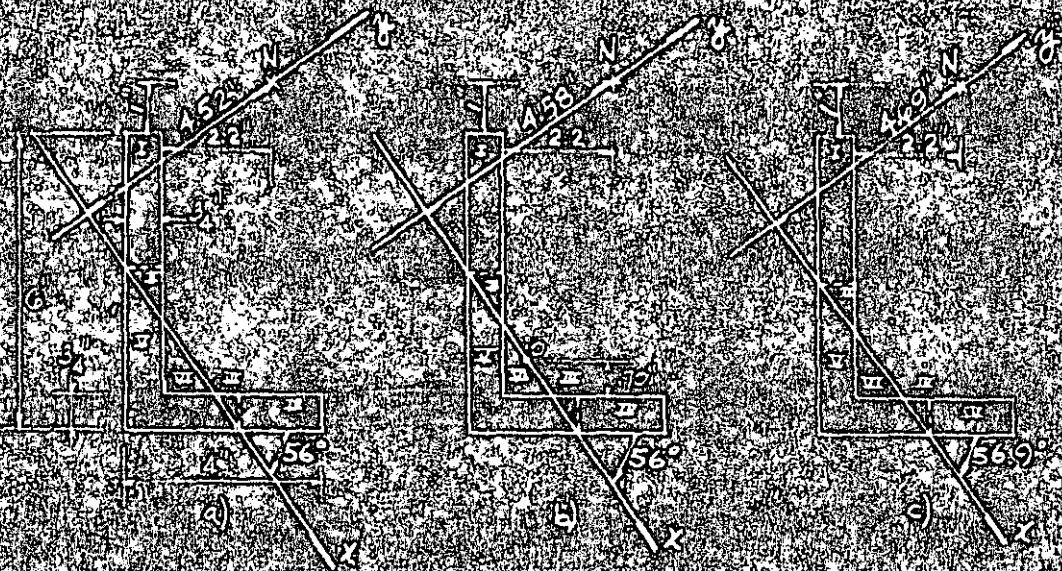


Fig. 7 - L6-4-3/2

Eq. (2) (6a) (6b) (4)

Trial	Area No.	$A_p$ (m)	$h$ (m)	$A_p h$ (m)	$x$ (m)	$x^2$ (m)	$S$ (m)	$e$ (m)	$e_1$ (m)	$e_2$ (m)
a	I	2.02	1.07	2.16						
	II	.39	.20	.08						
	III	.19	.14	.09						
	IV	1.29	.91	1.17						
	V	-3.74	-.61	2.28						
	VI	.74	-.23	-.21						
	$\Sigma$	.89		5.51				0.06		6.21
b	I	2.11	1.10	2.32	.52	.12				
	II	.39	.21	.08	2.05	.81				
	III	.19	.14	.03	4.82	.89				
	IV	1.36	.96	1.30	5.52	7.49				
	V	-3.16	-.60	2.08	3.61	12.50				
	VI	.60	-.22	-.13	3.76	2.28				
	$\Sigma$	1.19		5.68		.09		0.75	4.75	0.9
c	I	2.18	1.15	2.52	.48	1.05				
	II	.37	.20	.08	2.01	.75				
	III	.18	.16	.03	4.72	.87				
	IV	1.31	.91	1.19	5.48	7.20				
	V	-3.42	-.60	2.05	3.53	12.06				
	VI	.60	-.25	-.15	3.62	2.16				
	$\Sigma$	1.22		5.72		.03		-.074	4.69	0

Table 2

Eq. (3)  $N_b / o_j = A_p = 1.22 \text{ m}^2$



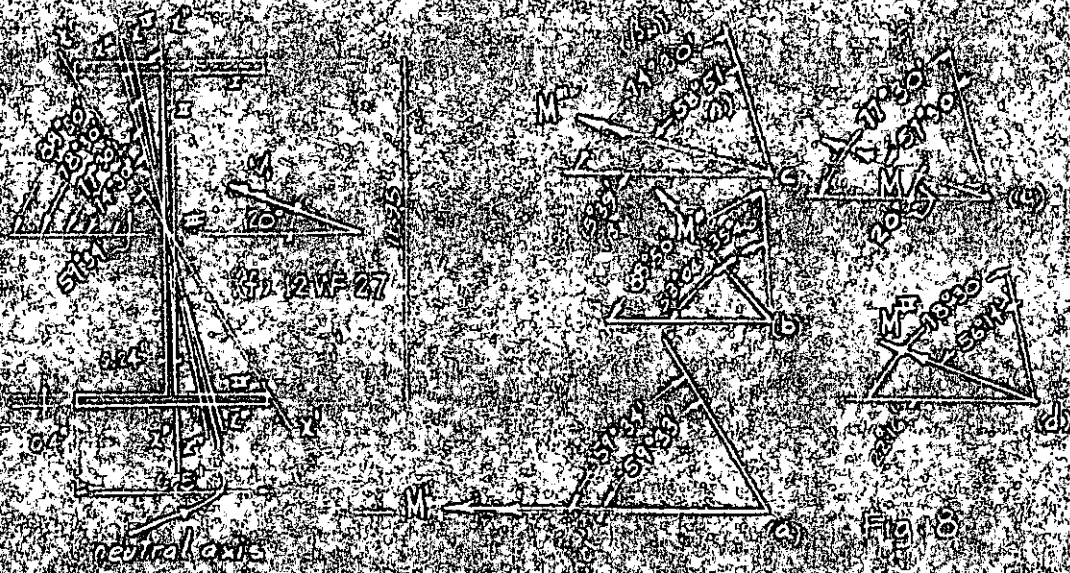
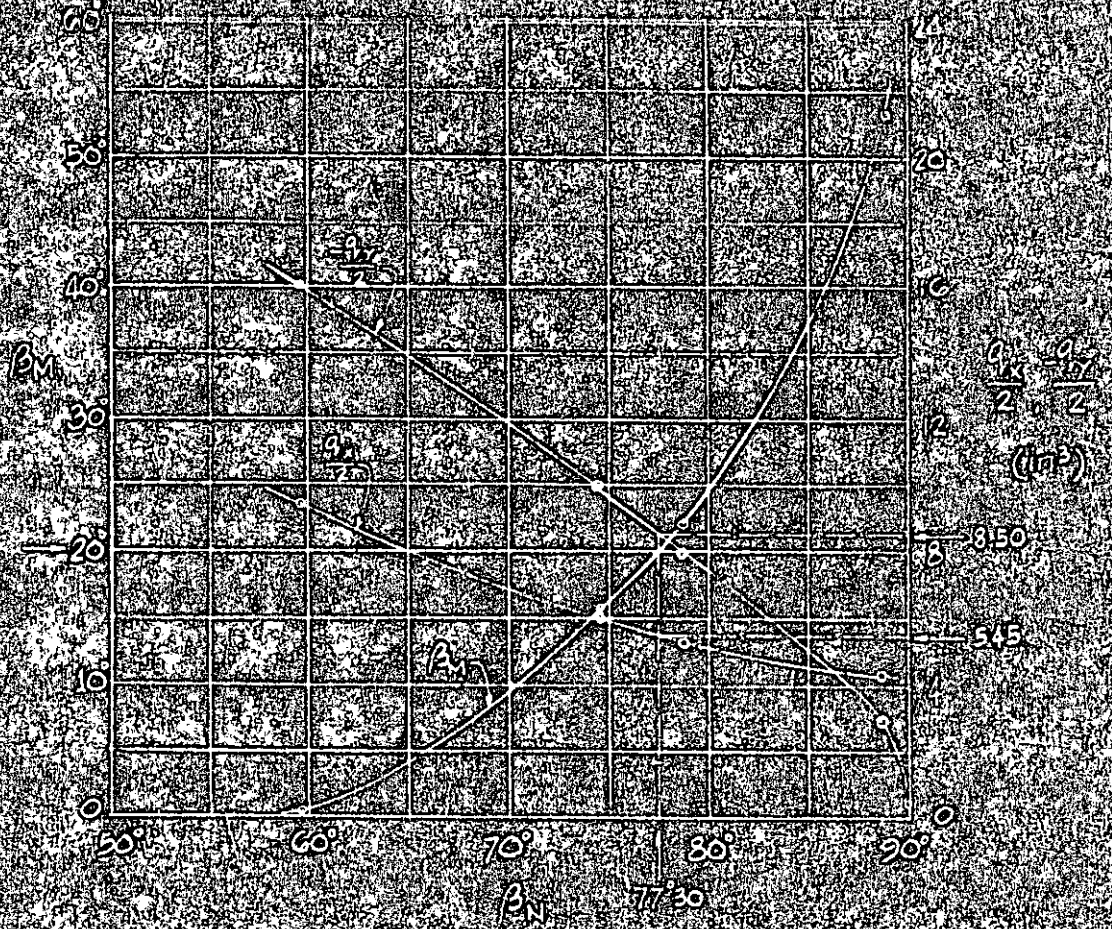


Fig 8

Trial	Area No.	$\sum P$ (lb)	$\sum Q$ (lb)	$\sum R$ (lb)	$\sum S$ (lb)	$\sum T$ (lb)	$\theta$
a	I	2.60	2.91	7.54	-4.95	-12.66	
	II	1.29	1.45	1.67	-2.45	-0.16	
	III	.076	.03	.01	-.001	0	
	$\sum \Sigma$			9.62	-7.41	-12.66	
							55.33
b	I	1.96	1.65	2.24	-5.72	-7.76	
	II	1.24	.09	.12	-1.90	-2.52	
	III	1.24	1.55	1.93	5.31	7.21	
	$\sum \Sigma$			4.29	-2.31	-3.07	
							35.46
c	I	1.95	2.35	4.53	-5.31	-10.35	
	II	1.21	.30	.97	-2.90	-3.52	
	III	.12	.09	.01	-.15	-.02	
	IV	.63	.73	.45	-6.20	3.92	
	$\sum \Sigma$			6.02	-3.49	-9.97	
						58.51	
d	I	1.76	2.18	3.84	-5.21	-9.54	
	II	1.18	.53	.68	-2.30	-3.29	
	III	.30	.09	.03	-.19	-.06	
	IV	.61	.97	.77	-6.10	4.93	
	$\sum \Sigma$			5.32	-13.80	-7.96	
						56.14	

Table 3





For  $\beta_M = 20^\circ$      $\beta_N = 77.5^\circ$   
 $q_u = 1090 \text{ in}^2$   
 $q_v = 170 \text{ in}^2$

By Eq (19)     $M_{1/6} = \sqrt{(q_u) - (q_v)} = 29.2 \text{ in}^2$

Fig 9



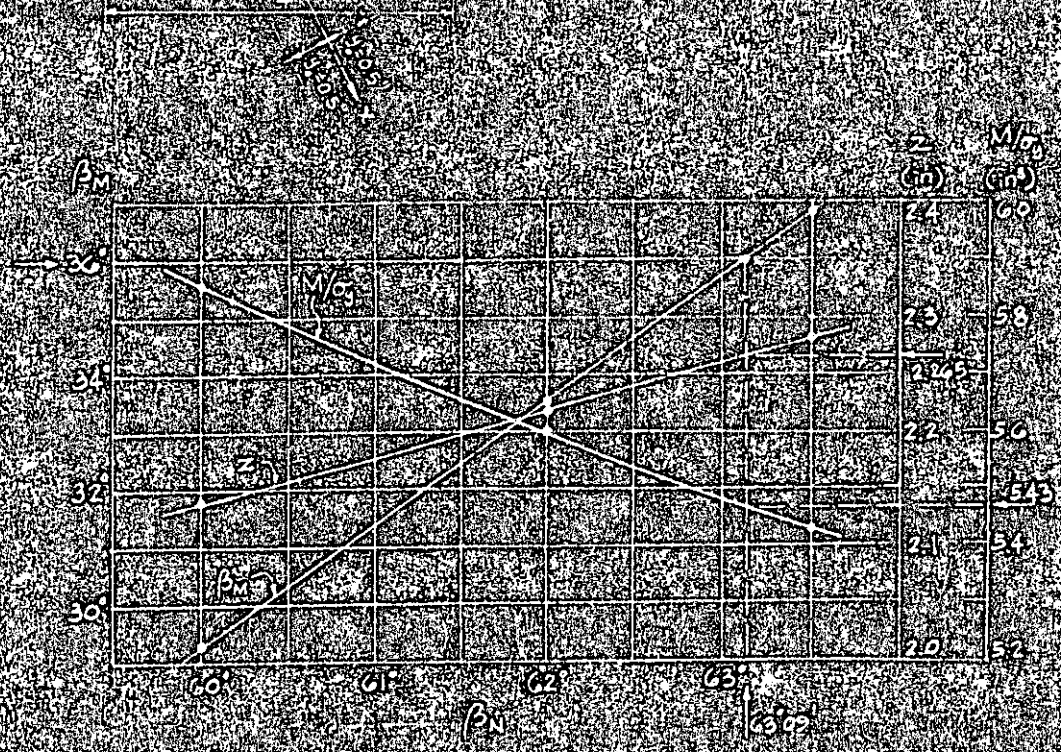
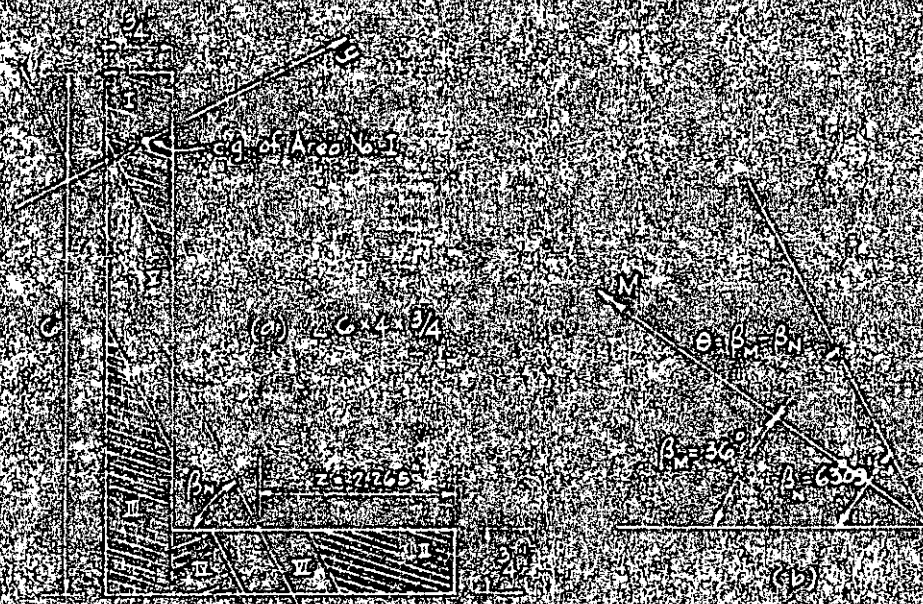


FIG. 10 (c)



E<sub>1</sub> (15)  
(or 16) (14)

Tral	Z (in)	α	A <sub>1</sub> (in <sup>2</sup> )	z (in)	A <sub>2</sub> (in <sup>2</sup> )	Z (in)	Q <sub>1</sub> (in <sup>3</sup> )	A <sub>C</sub> (in <sup>2</sup> )	Z <sub>C</sub> (in)	Q <sub>2</sub> (in <sup>3</sup> )	A <sub>22</sub> (in <sup>2</sup> )	Q <sub>3</sub> (in <sup>3</sup> )	β <sub>1</sub>	β <sub>2</sub>	Y <sub>16</sub> (in)		
a	223	60°	1.33								I						
			0.07								II						
			1.65									III					
			0.52									IV					
										1.50		0	V				
										0.90		0	VI				
										2.36		0	Σ	(0.001)			
d	214	60°	1.37	0.94	1.19	0	0				I						
			0.02	1.09	1.10	5.52	5.63					II					
			1.73	1.10	1.90	5.36	5.81					III					
			0.55	0.82	0.45	4.49	2.47					IV					
										1.50	125	212	0	V			
										0.86	0.72	0.42	0	VI	30.7°	29.3	5.80
										0.01	4.65	2.05	2.36	1.97	1.70	0	Σ
b	222	60°	1.15	0.88	1.01	0	0				I						
			1.10	1.0	1.28	5.52	6.07					II					
			1.75	1.05	1.84	3.46	6.06					III					
			0.49	0.78	0.38	4.58	2.24					IV					
										1.67	1.35	2.59	0	V			
										0.84	0.70	0.30	0	VI	28.5°	33.5	5.60
										0.01	4.51	2.23	2.44	2.05	2.23	0	Σ
c	228	63.5°	1.05	0.84	0.88	0	0				I						
			1.5	1.9	1.37	5.55	6.38					II					
			1.75	1.04	1.82	3.53	6.21					III					
			0.45	0.79	0.10	4.66	2.10					IV					
										1.09	1.1	2.20	0	V			
										0.81	0.70	0.34	0	VI	28.7°	30.3	5.43
										0	4.43	1.93	2.50	2.11	2.26	0	Σ

Table 4



**DIVISION DE EDUCACION CONTINUA  
FACULTAD DE INGENIERIA U.N.A.M.**

DISEÑO DE ESTRUCTURAS DE ACERO

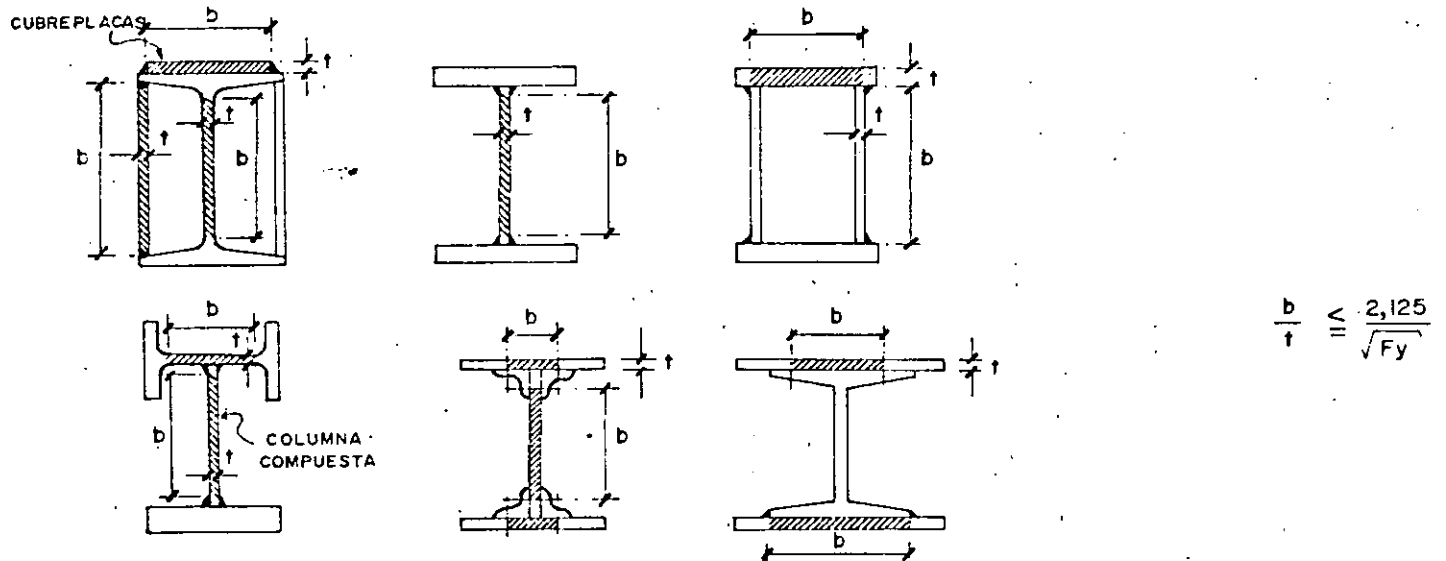
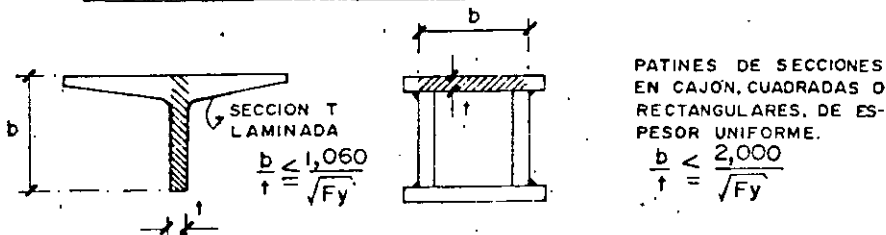
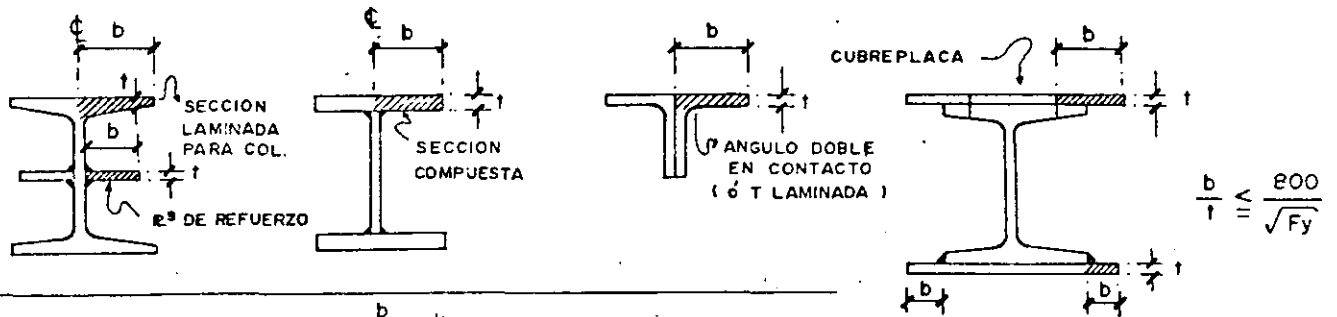
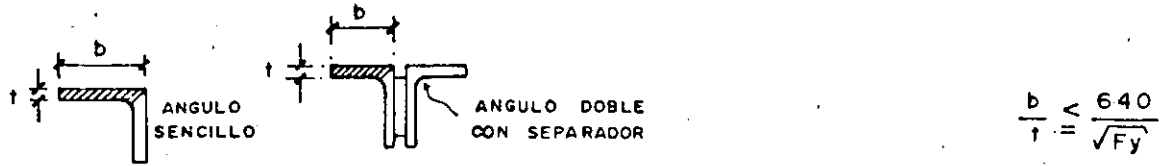
ANEXOS

NOV. 84

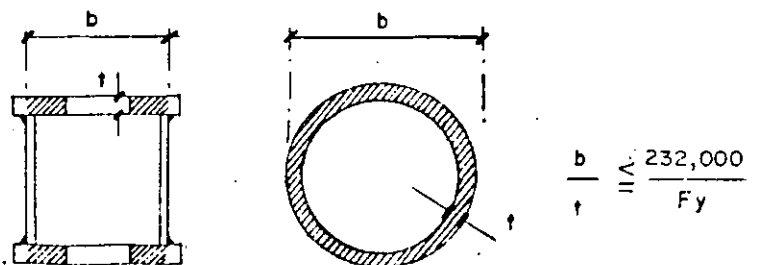
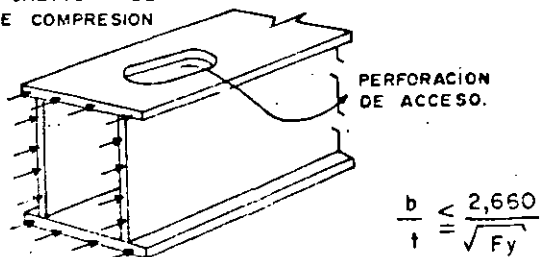
# RELACIONES ANCHO-ESPESOR MAXIMAS

PARA ELEMENTOS DE MIEMBROS SUJETOS A COMPRESION DIRECTA O COMPRESION UNIFORME DEBIDA A FLEXION

( AISC, 1980, 8ª edición )

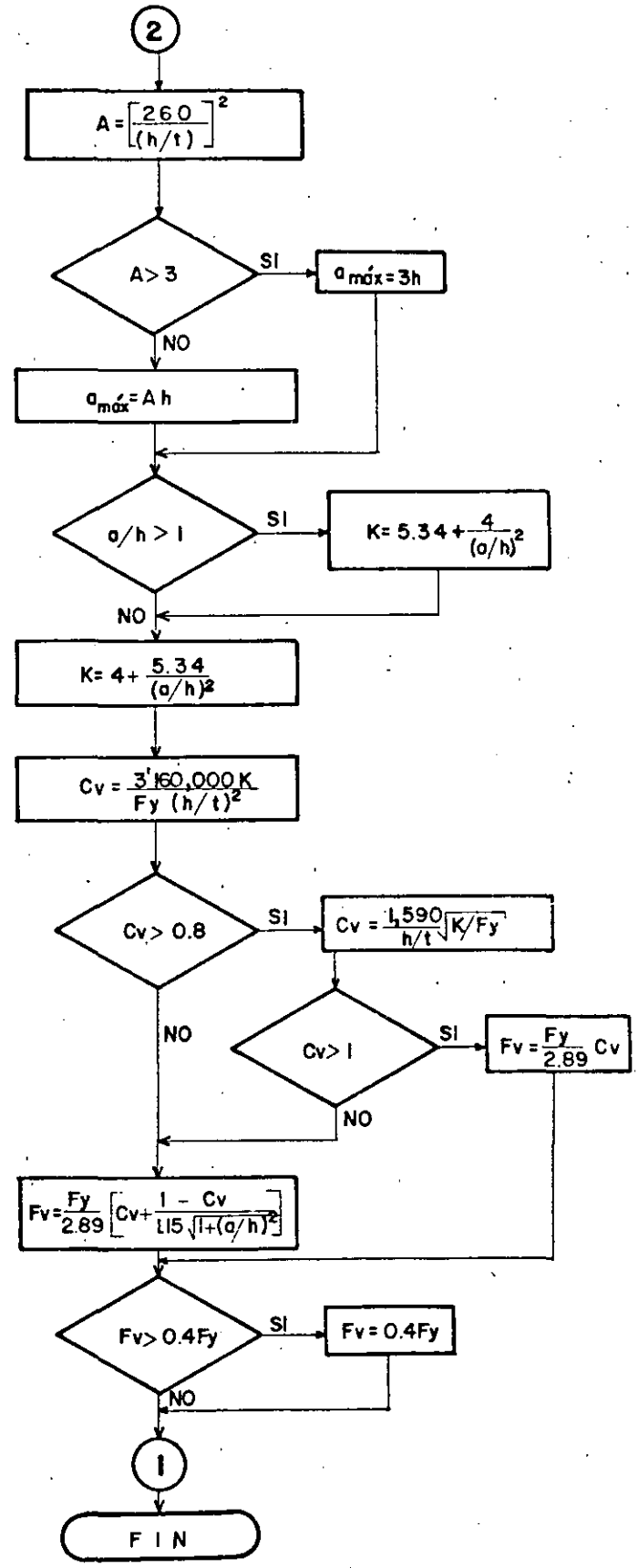
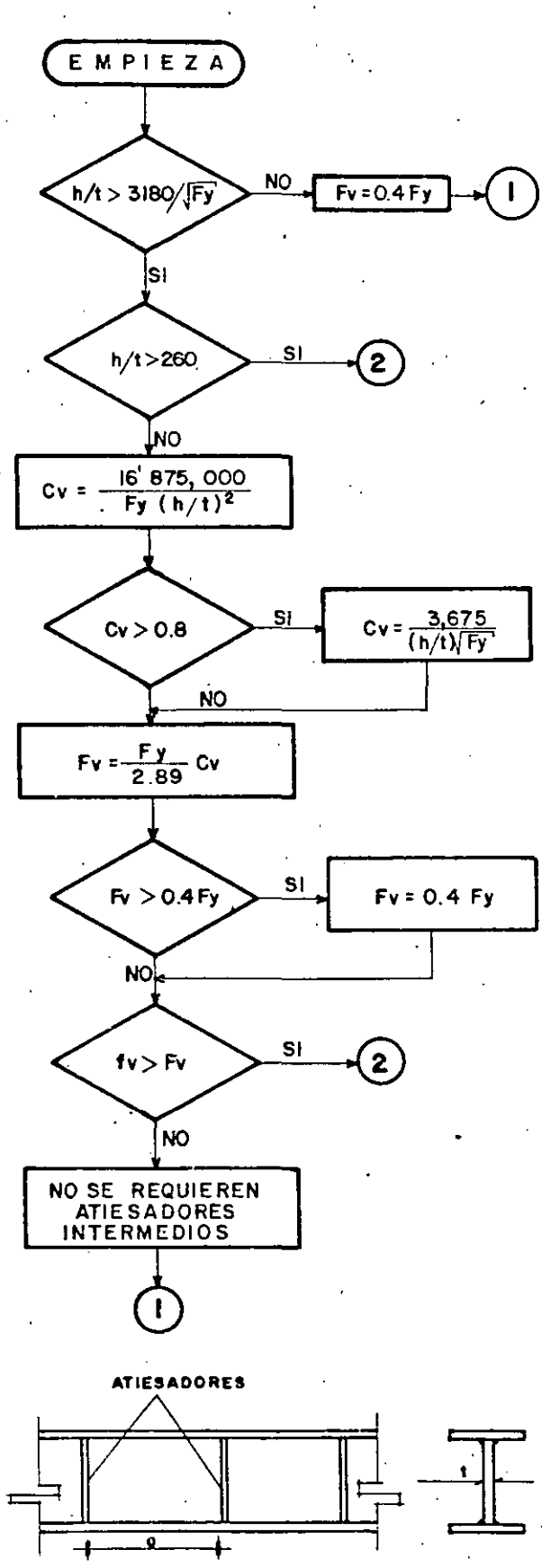


UTILICÉSE LA SECCION NETA MINIMA PARA CALCULAR EL ESFUERZO DE COMPRESION



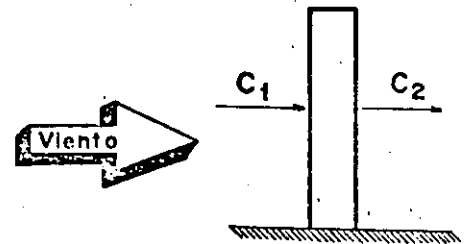
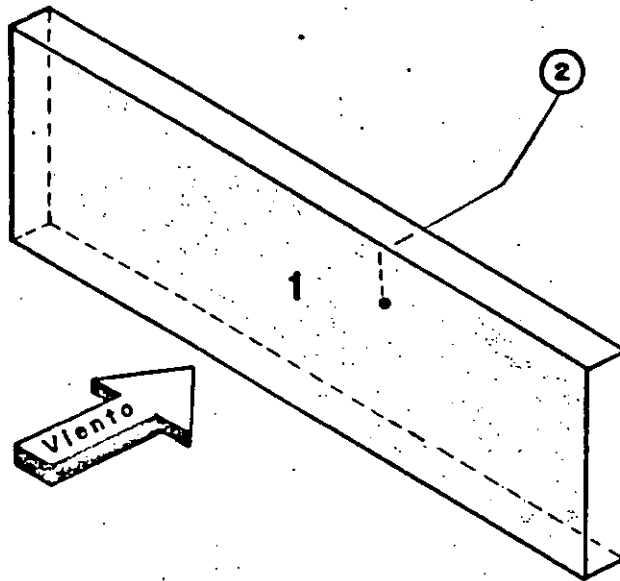
NOTA: Si se excede la relación  $b/t$  en una o más placas del perfil, el diseño se hará de conformidad con el Apéndice C de las citadas especificaciones.

CALCULO DEL ESFUERZO CORTANTE PERMISIBLE,  $F_v$ , EN VIGAS O EN TRABES ARMADAS



\* EN SECCIONES LAMINADAS SE PUEDE TOMAR COMO LA PARTE RECTA DEL ALMA.

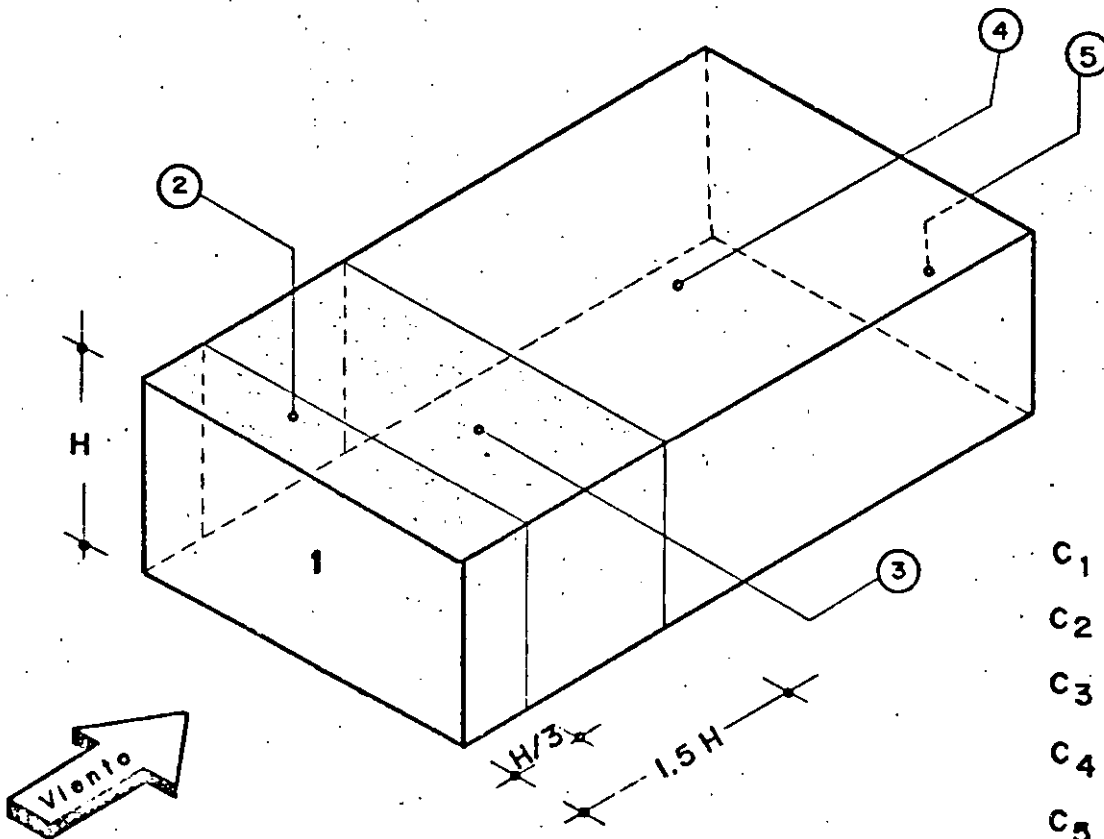
I.- ESTABILIDAD DE BARDAS AISLADAS



$C_1 = 0.75$

$C_2 = -0.68$

II.- EDIFICIOS CON PLANTA Y ELEVACION RECTANGULARES



$C_1 = 0.75$

$C_2 = -1.75$

$C_3 = -1.0$

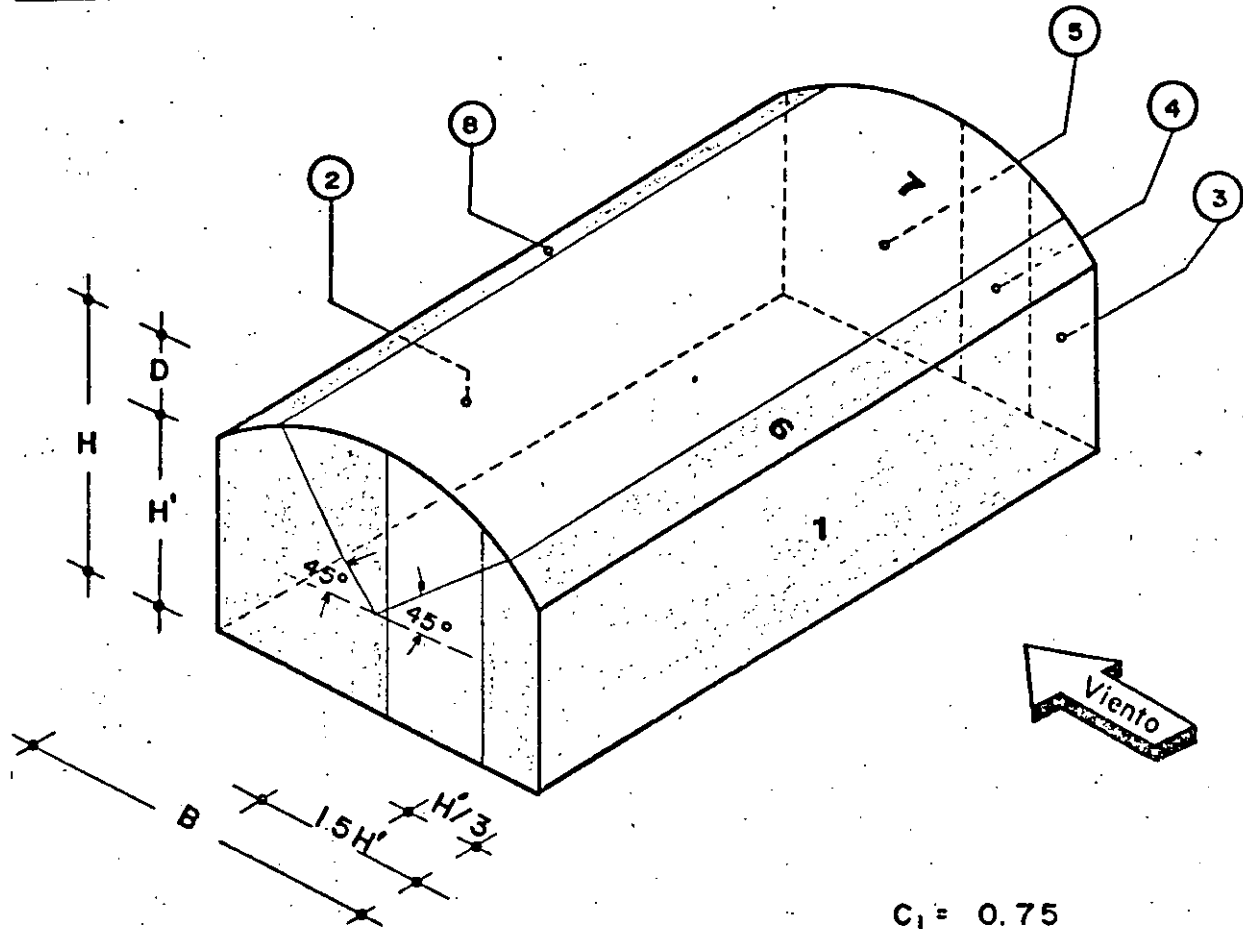
$C_4 = -0.40$

$C_5 = -0.68$

NOTAS :

a) Coeficientes estipulados por el Reglamento D.D.F - 76 para cálculo de presiones externas.

III.- CUBIERTAS DE ARCO CIRCULAR.



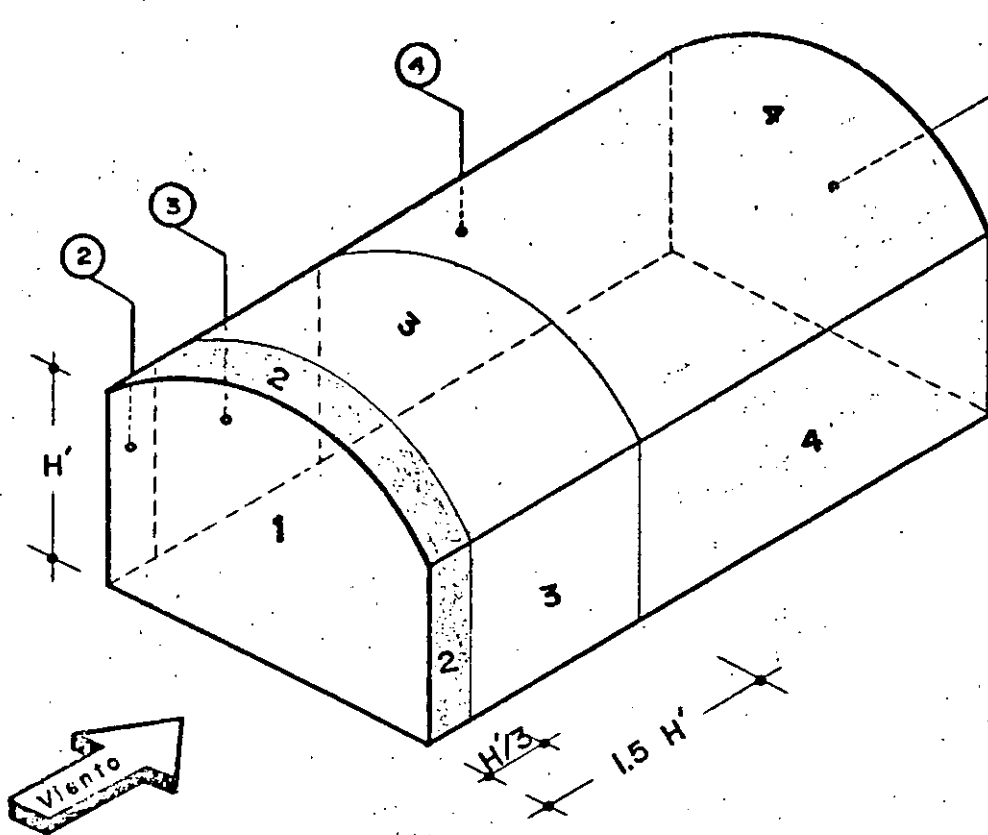
- $C_1 = 0.75$
- $C_2 = -0.68$
- $C_3 = -1.75$
- $C_4 = -1.00$
- $C_5 = -0.40$

Coeficiente	$D / H \leq 0.3$	$D / H = 1.0$
$C_6$	$4(D / B) - 1.75$	$1.4 (D / B)$
$C_7$	$-0.5 (D / B) - 1.0$	$-(D / B) - 0.7$
$C_8$	$- 0.55$	$- 0.55$

NOTAS : a) Coeficientes estipulados por el Reglamento D.D.F - 76, para cálculo de presiones externas.

b) Para  $0.3 < D / H < 1.0$ , Interpólese linealmente.

### IV - CUBIERTA DE ARCO CIRCULAR



Sin muro (sotavento)

$$C_1 = 0.75$$

$$C_2 = -1.75$$

$$C_3 = -1.0$$

$$C_4 = -0.40$$

Presión Interior  $C = 0.6$

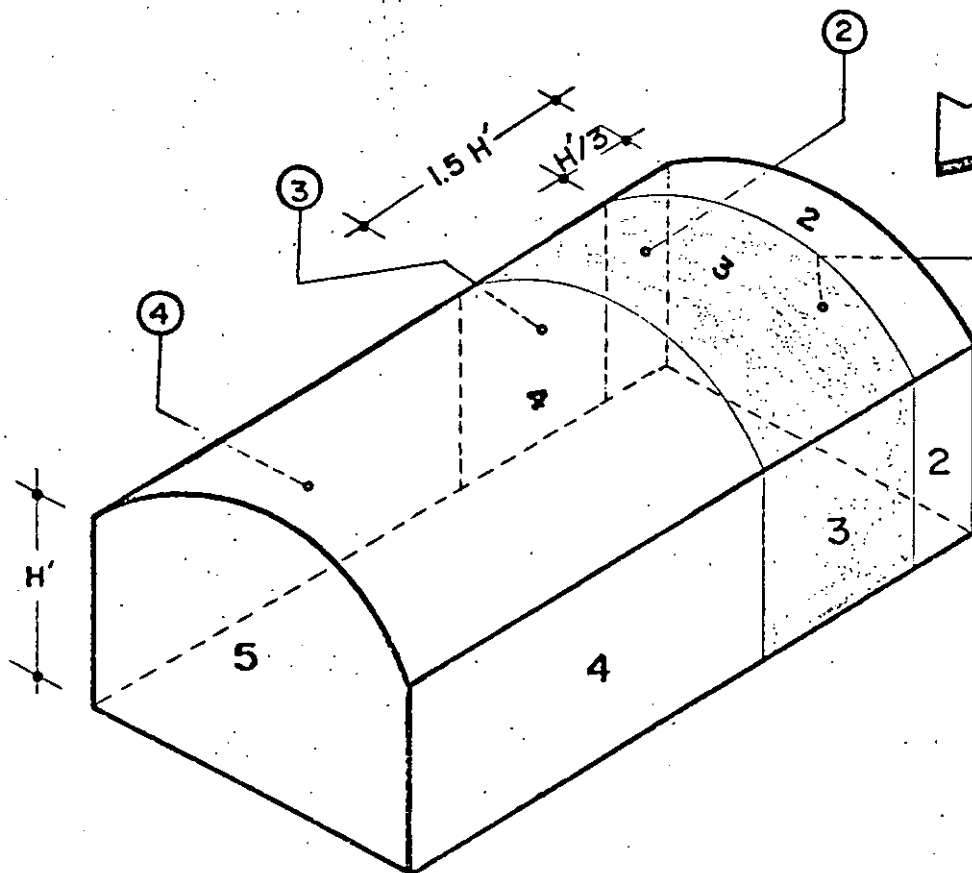
Presión Total :

$$\bar{C}_1 = 0.75 + 0.6 = 1.35$$

$$\bar{C}_2 = -1.75 + 0.6 = -1.15$$

$$\bar{C}_3 = -1.0 + 0.6 = -0.40$$

$$\bar{C}_4 = -0.40 + 0.6 = 0.20$$



Sin muro (barlovento)

$$C_2 = -1.75$$

$$C_3 = -1.00$$

$$C_4 = -0.40$$

$$C_5 = -0.68$$

Presión interior  $C = 0.8$

Presión Total :

$$\bar{C}_2 = -1.75 - 0.8 = -2.55$$

$$\bar{C}_3 = -1.00 - 0.8 = -1.80$$

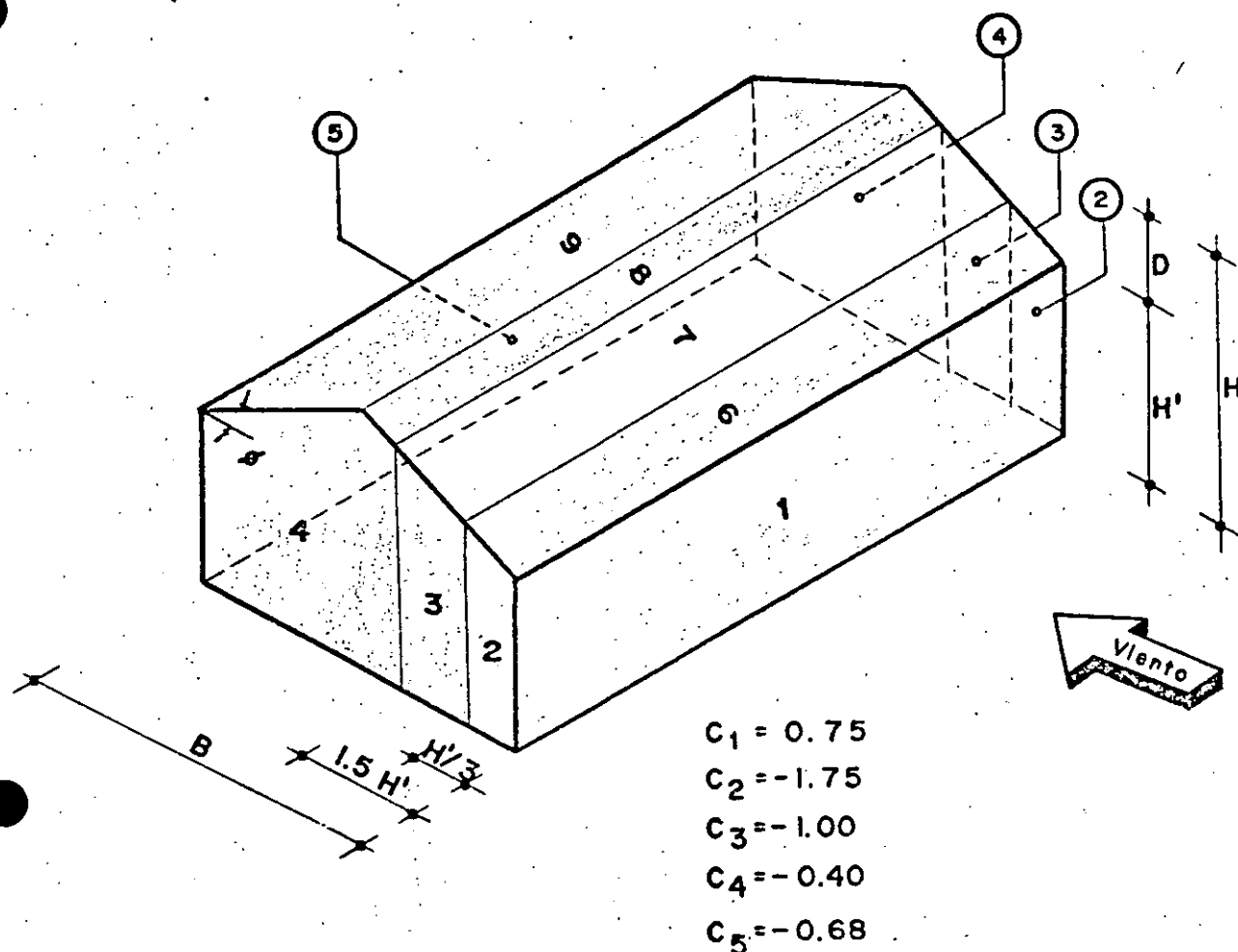
$$\bar{C}_4 = -0.40 - 0.8 = -1.20$$

$$\bar{C}_5 = -0.68 - 0.8 = -1.48$$

**NOTAS :**

- a) Coeficientes estipulados por el Reglamento D. D. F. - 76 para cálculo de presiones externas

V<sub>d</sub> CUBIERTA DE DOS AGUAS



Inclinación	C <sub>6</sub>	C <sub>7</sub>	C <sub>8</sub>	C <sub>9</sub>
Menor de 65°:				
Si D/H ≤ 0.3	-1.75 + 0.0385ϕ	-1.0 + 0.027ϕ	-0.4 + 0.018ϕ	-0.68
D/H = 1.0	0.5 Tan ϕ < 0.75	0.4 Tan ϕ < 0.75	0.25 Tan ϕ < 0.75	-0.68
Mayor de 65°	0.75	0.75	0.75	-0.68

Tan ϕ = 2D / B

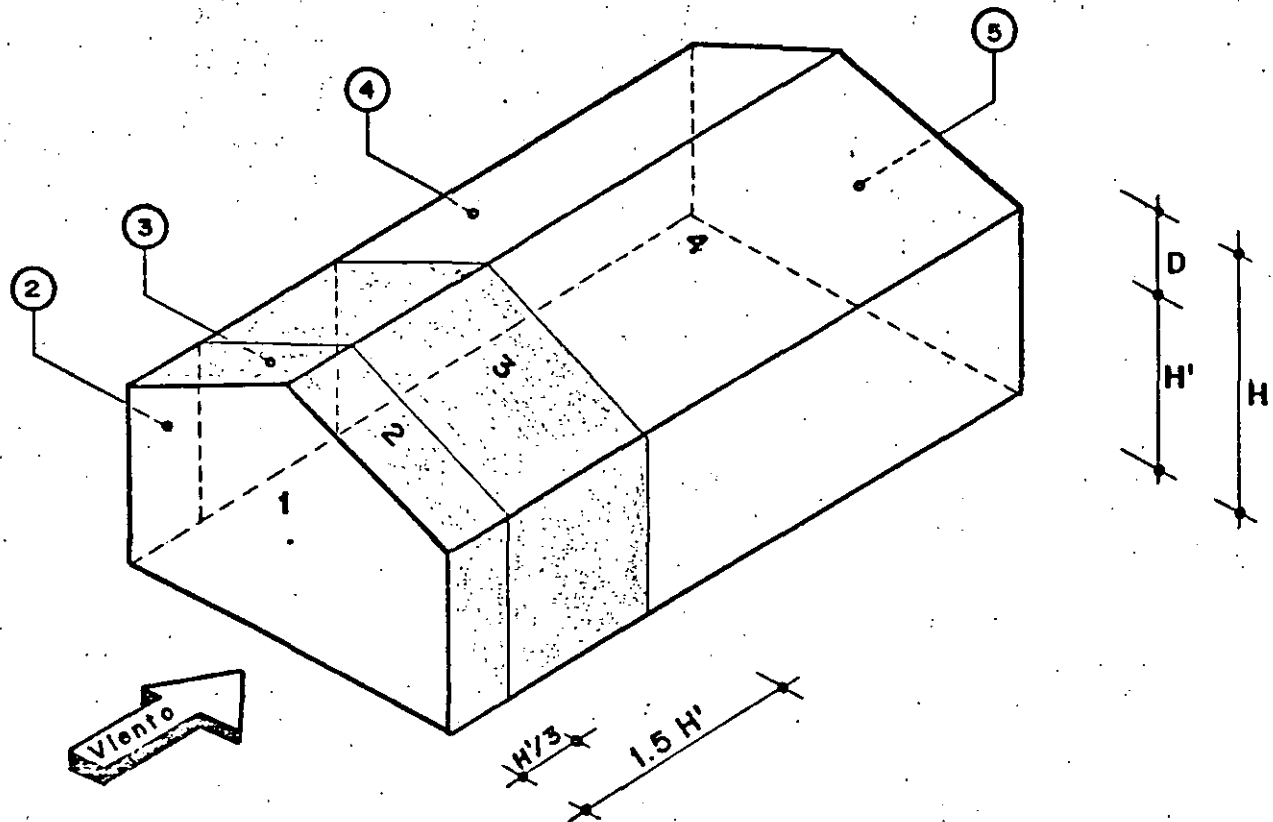
NOTAS : a) Coeficientes estipulados por el Reglamento D. D. F. - 76 para cálculo de presiones externas

b) Si el coeficiente de empuje calculado en cualquier zona resulta menor de 0.4, en valor absoluto, se tomará C = ± 0.4 (el más desfavorable)

c) Para 0.3 < D/H < 1.0, Interpólese linealmente.



## V<sub>b</sub>- CUBIERTA DE DOS AGUAS



$$C_1 = 0.75$$

$$C_2 = -1.75$$

$$C_3 = -1.0$$

$$C_4 = -0.40$$

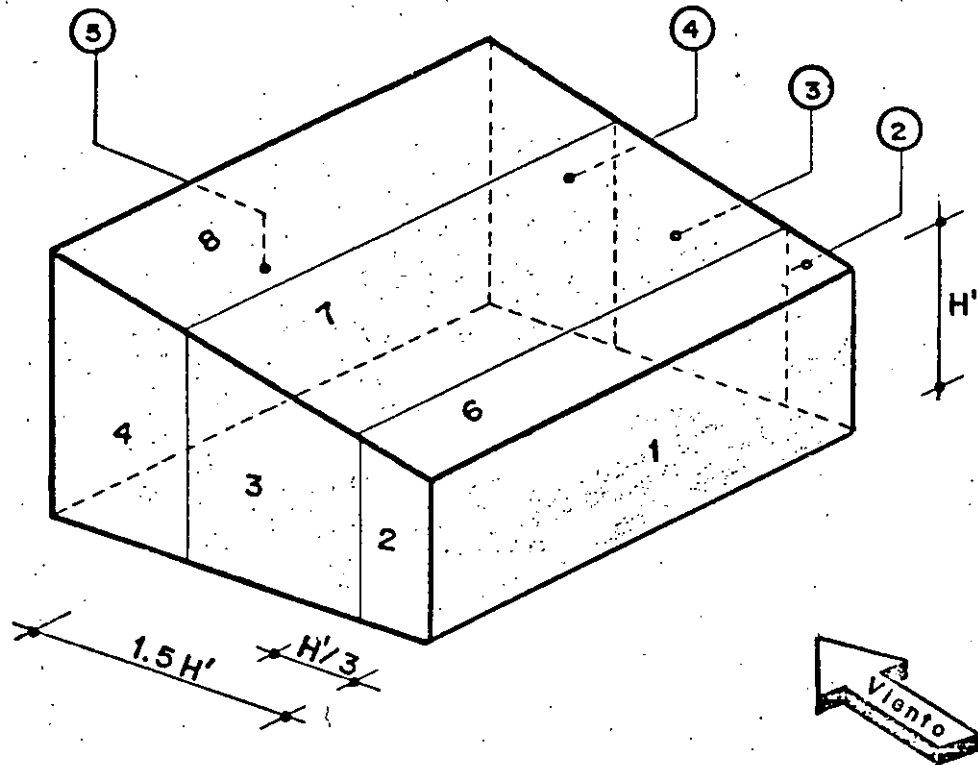
$$C_B = -0.68$$

### NOTAS :

a).- Coeficientes estipulados por el Reglamento D.D.F. - 76,  
para cálculo de presiones externas.

VI a) CUBIERTA DE UN AGUA.

( Orientada hacia barlovento )



$$C_1 = 0.75$$

$$C_2 = -1.75$$

$$C_3 = -1.0$$

$$C_4 = -0.40$$

$$C_5 = -0.68$$

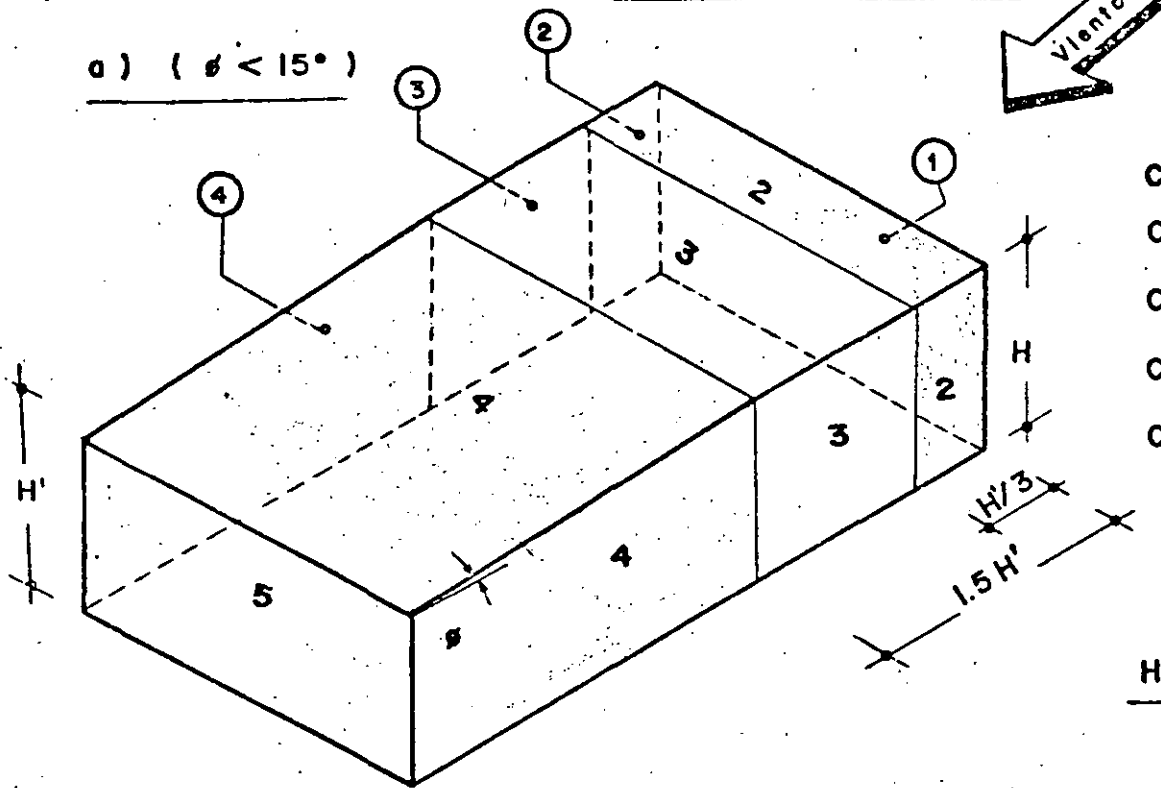
**NOTAS :**

a) Coeficientes estipulados por el Reglamento D.D.F. - 76, para cálculo de presiones externas

b) Para  $C_6$ ,  $C_7$  y  $C_8$ , ver cubiertas de dos aguas.

VI b - CUBIERTA DE UN AGUA (orientada hacia sotavento)

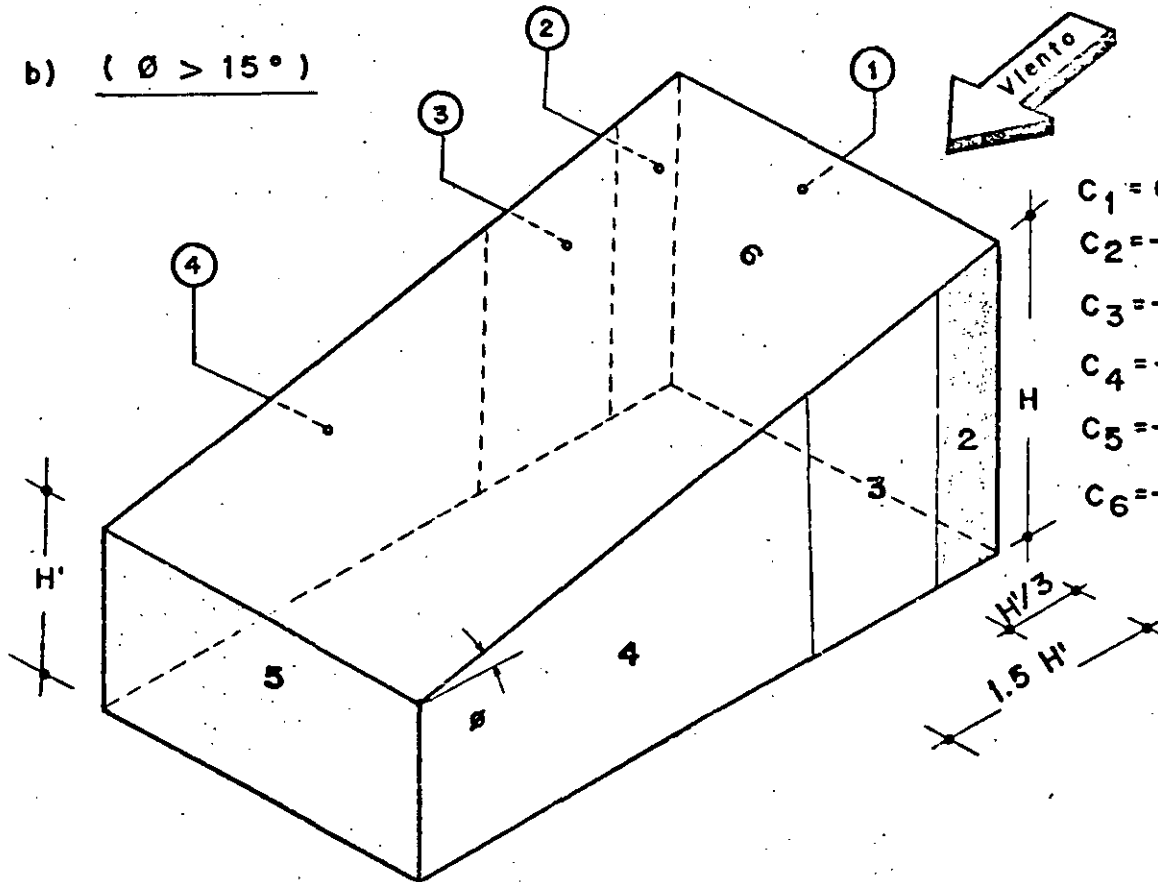
a) ( $\theta < 15^\circ$ )



- $C_1 = 0.75$
- $C_2 = -1.75$
- $C_3 = -1.00$
- $C_4 = -0.40$
- $C_5 = -0.68$

$H > H'$

b) ( $\theta > 15^\circ$ )

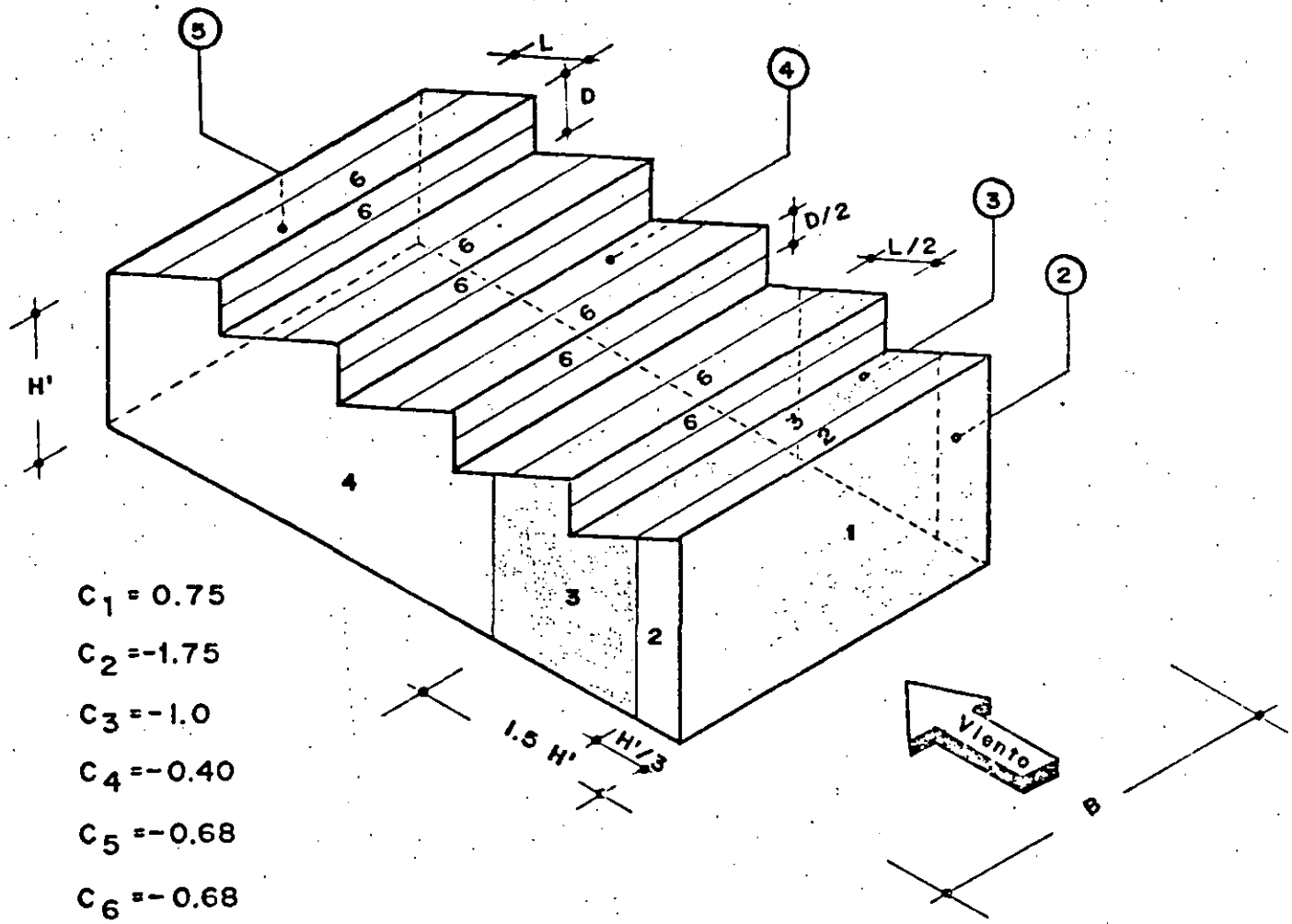


- $C_1 = 0.75$
- $C_2 = -1.75$
- $C_3 = -1.0$
- $C_4 = -0.40$
- $C_5 = -0.68$
- $C_6 = -0.68$

NOTAS : a):- Coeficientes estipulados por el Reglamento D.D.F. - 76, para cálculo de presiones externas

b):- Para viento paralelo a las generatrices, ver techo de dos aguas.

VII a - CUBIERTA EN FORMA DE DIENTES DE SIERRA

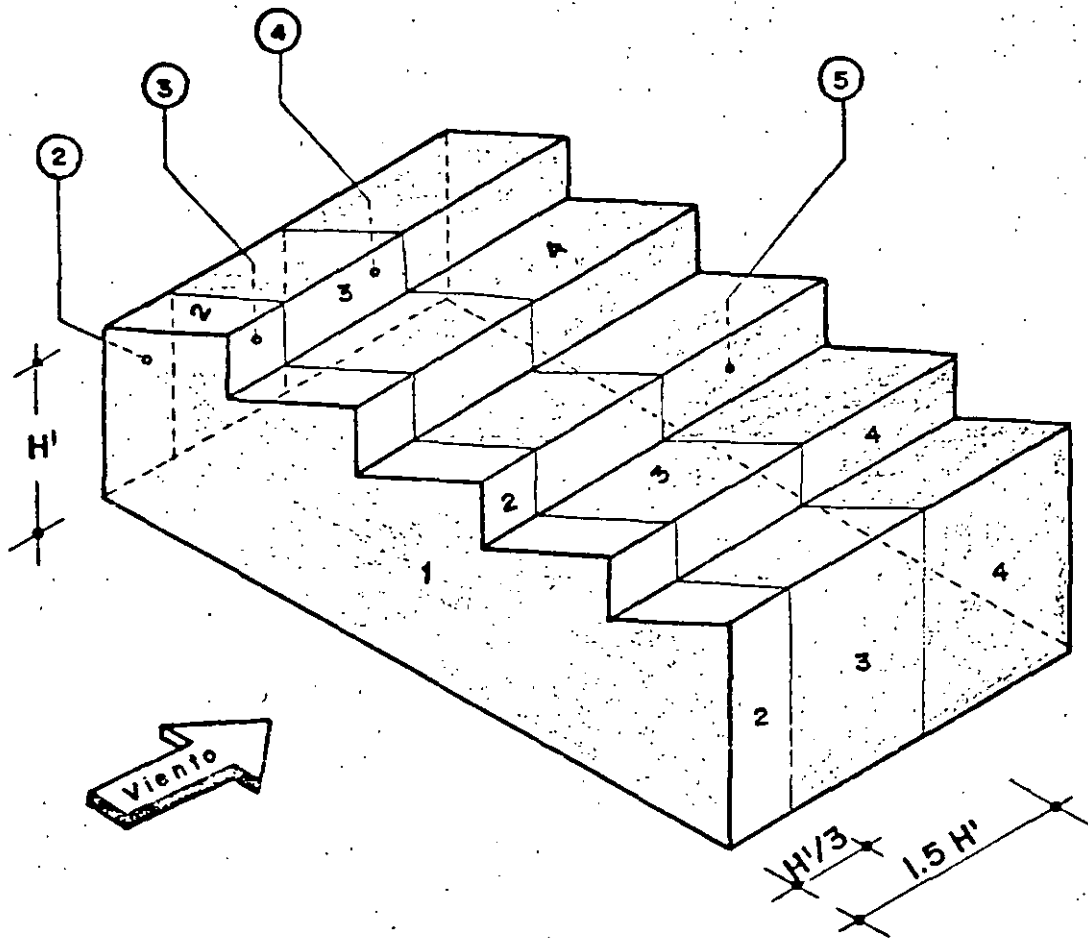


- $C_1 = 0.75$
- $C_2 = -1.75$
- $C_3 = -1.0$
- $C_4 = -0.40$
- $C_5 = -0.68$
- $C_6 = -0.68$

**NOTAS :**

- a):- Coeficientes estipulados por el Reglamento D.D.F. - 76, para cálculo de presiones externas.
- b):- Si  $\phi$  es menor de  $15^\circ$ , en el techo del primer diente - apareceran (2), (3) (y (4) si  $H'$  es pequeña); si  $\phi$  es mayor de  $15^\circ$ , en todo el techo del primer diente se tomara  $C = - 0.68$ .

VII b.- CUBIERTA EN FORMA DE DIENTES DE SIERRA



$$C_1 = 0.75$$

$$C_2 = -1.75$$

$$C_3 = -1.0$$

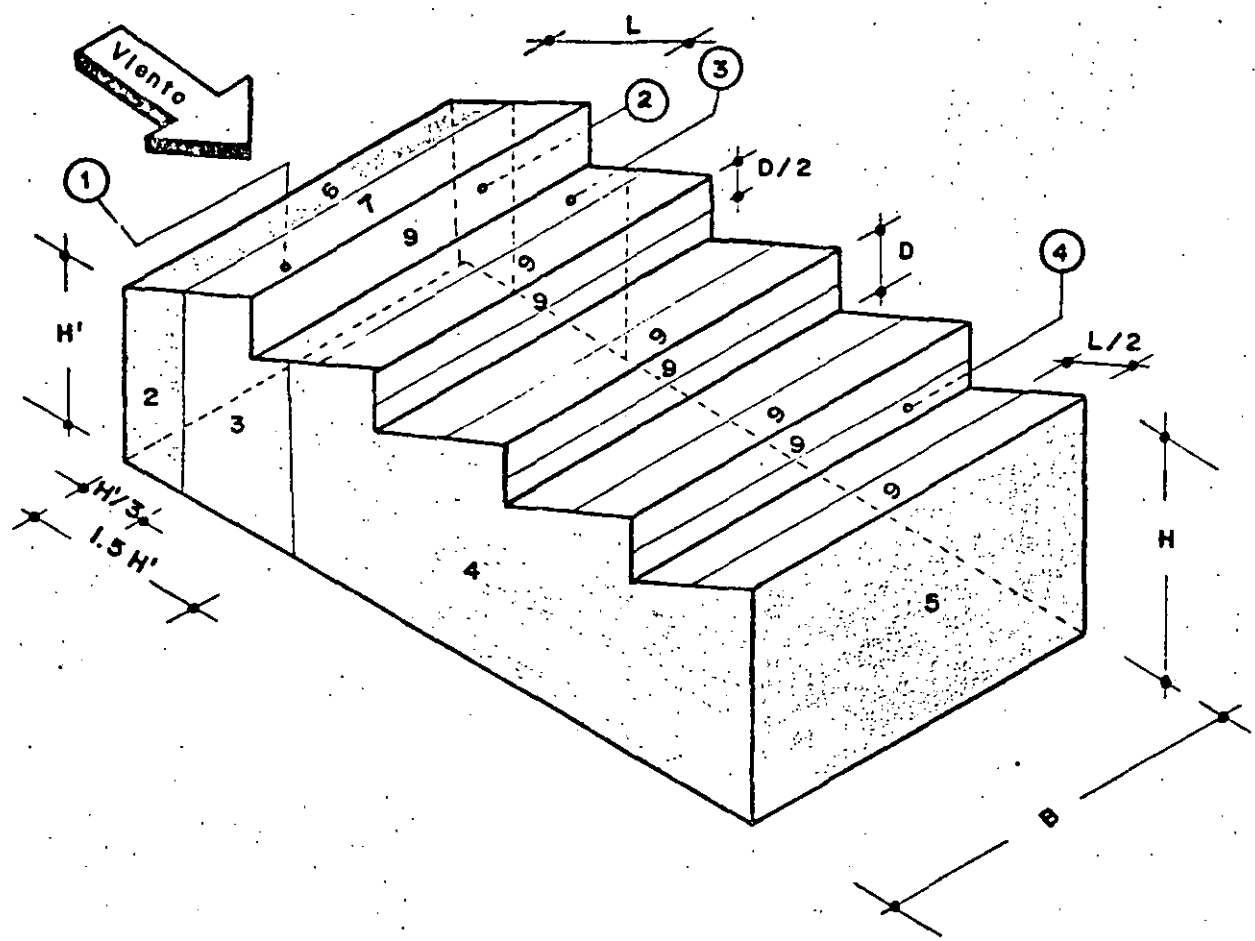
$$C_4 = -0.40$$

$$C_5 = -0.68$$

NOTAS :

a).- Coeficientes estipulados por el Reglamento D.D.F. - 76, para cálculo de presiones externas.

VIIc.- CUBIERTA EN FORMA DE DIENTES DE SIERRA



$C_1 = 0.75$

$C_2 = -1.75$

$C_3 = -1.0$

$C_4 = -0.40$

$C_5 = -0.68$

$C_6$  } Ver cubiertas de dos aguas.

$C_7$  }  $C_7$  y  $C_8$  aparecerán ( $C_8$  no está dibujada)

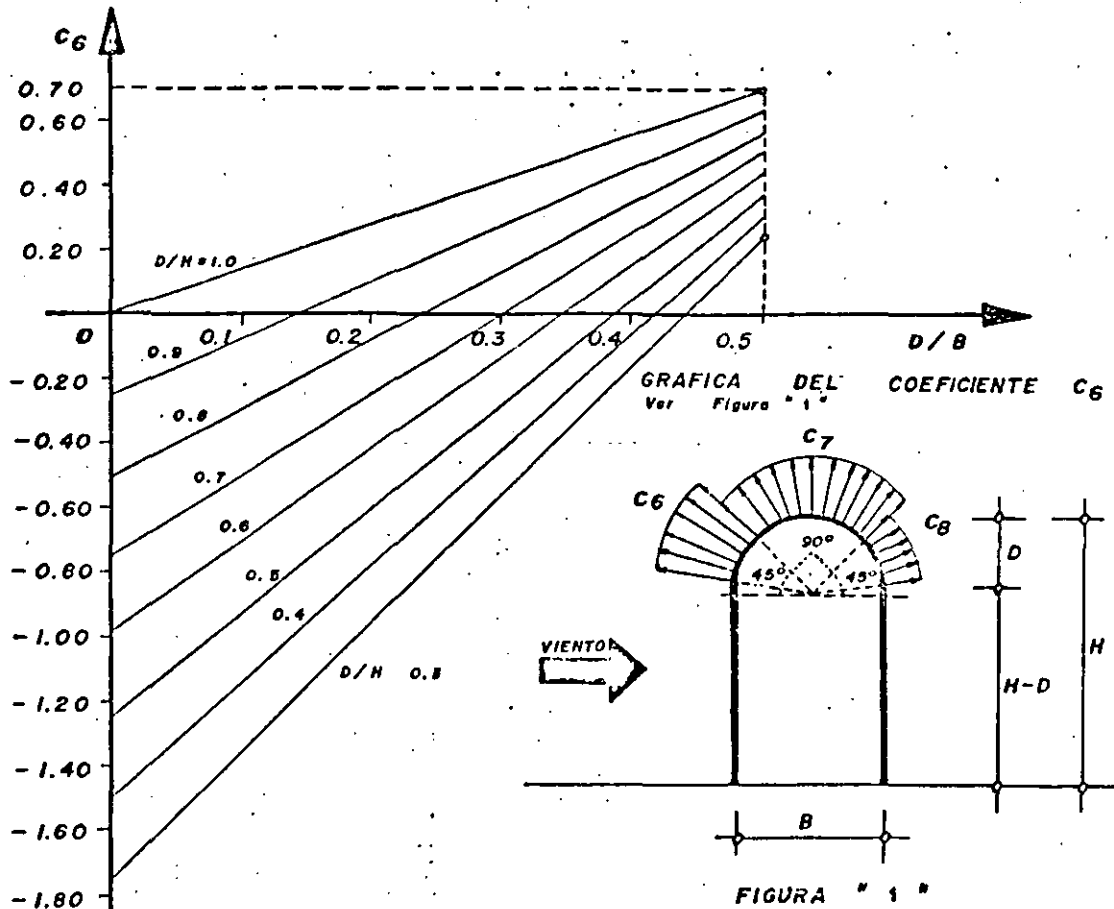
$C_8$  } dependiendo de si  $L > 1.5 H'$

$C_9 = -0.68$

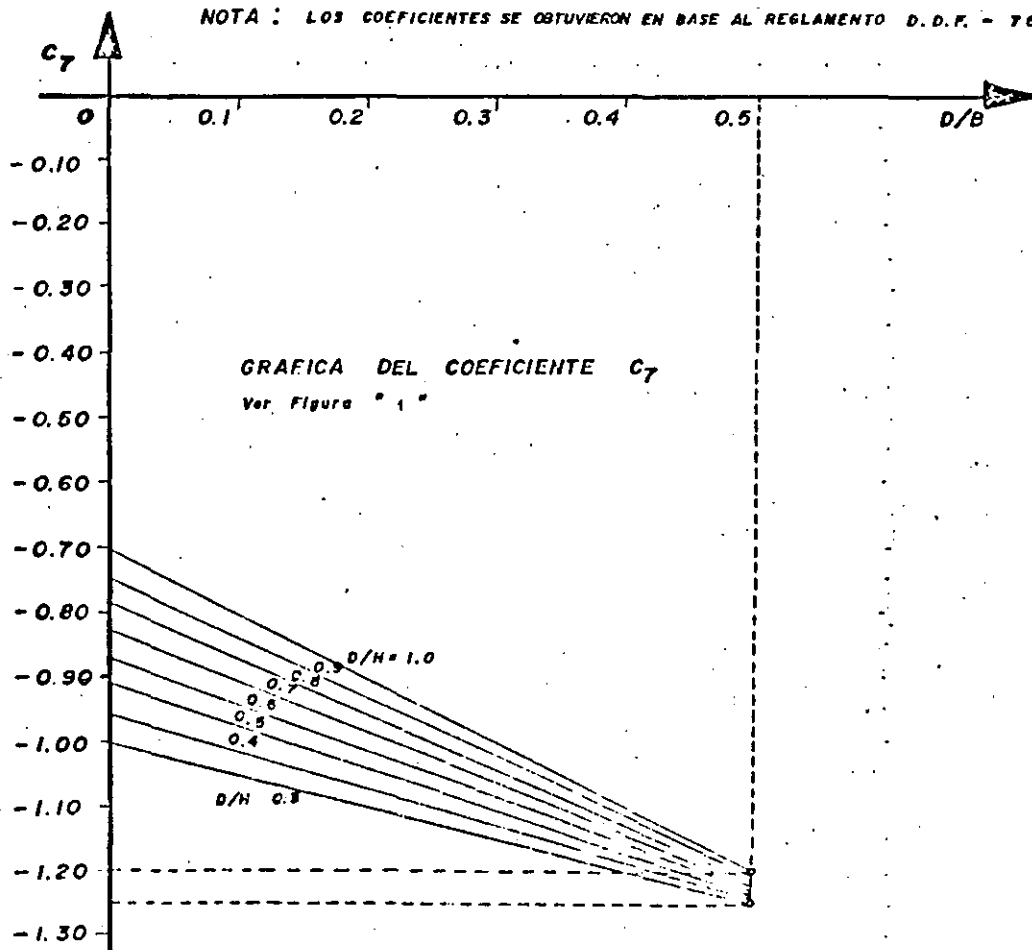
**NOTAS :**

a): Coeficientes estipulados por el Reglamento D.D.F. - 76, para cálculo de presiones externas.

GRAFICAS DE COEFICIENTES DE EMPUJE DE VIENTO, EN TECHOS DE -  
CUBIERTA DE ARCO CIRCULAR.



NOTA : LOS COEFICIENTES SE OBTUVIERON EN BASE AL REGLAMENTO D. D. F. - 76



$C_8 = -0.55$

GRAFICAS DE COEFICIENTES DE EMPUJE DE VIENTO EN EL TECHO, EN ZONA DE BARLOVENTO, PARA CUBIERTAS DE UNA O DOS AGUAS.

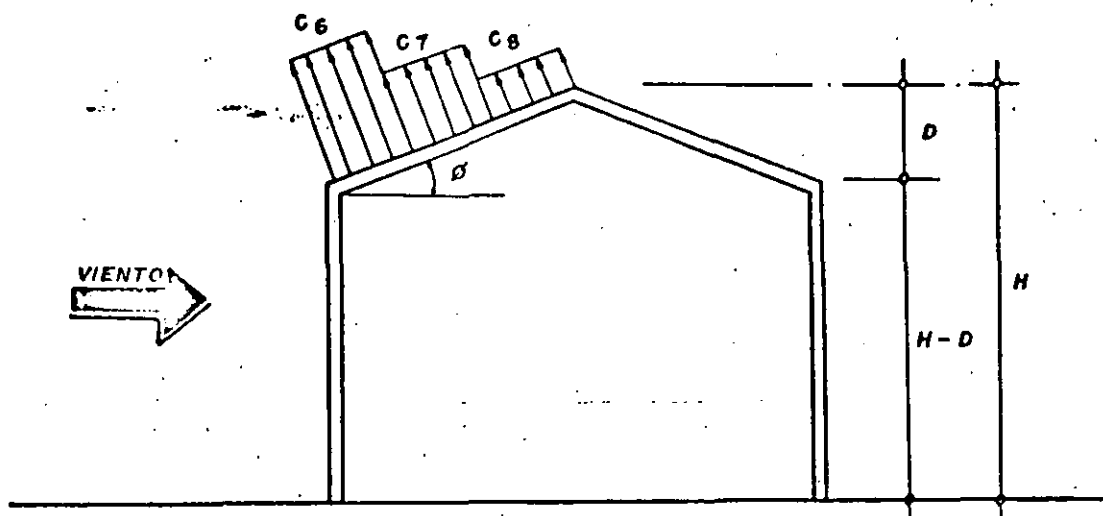
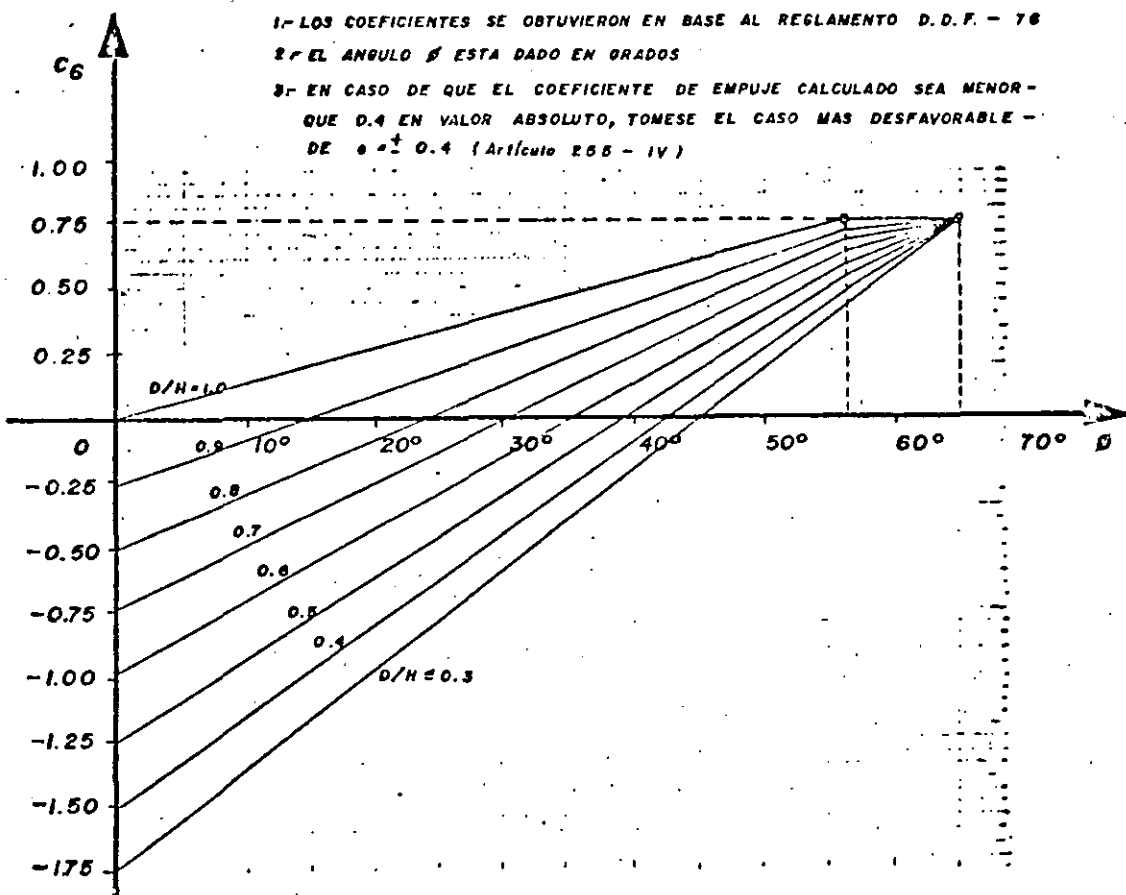


Figura "A"

$p = 0.0055 C_v^2$

NOTAS :

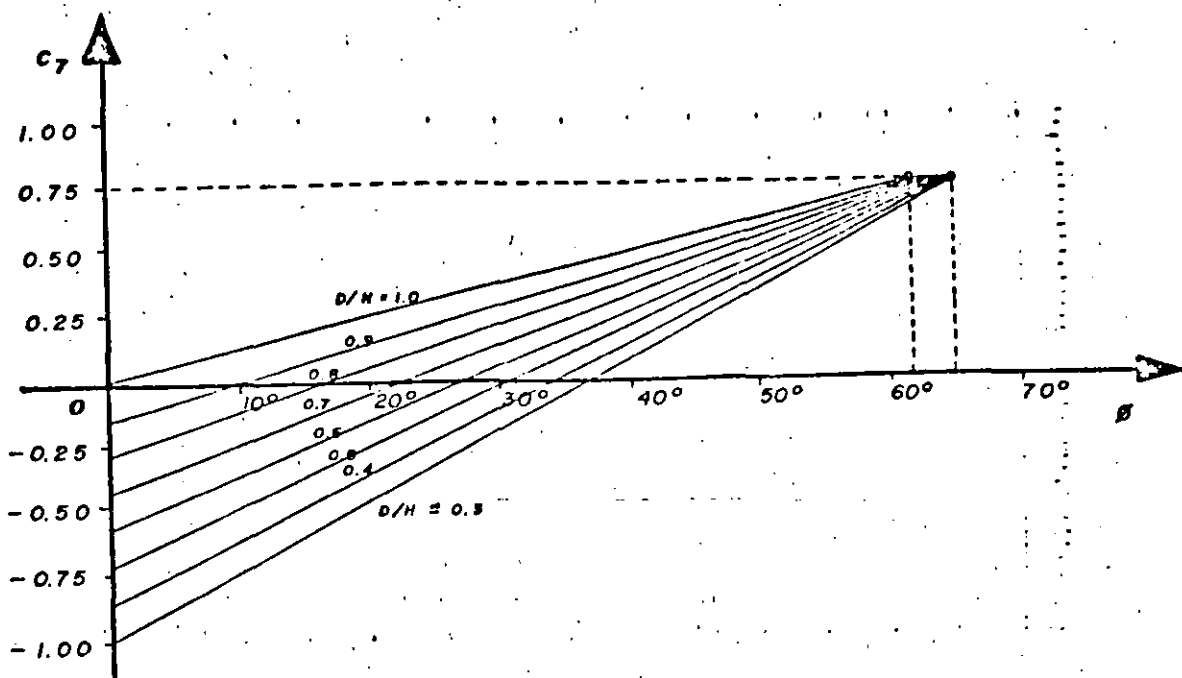
- 1- LOS COEFICIENTES SE OBTUVIERON EN BASE AL REGLAMENTO D.D.F. - 76
- 2- EL ANGULO  $\beta$  ESTA DADO EN GRADOS
- 3- EN CASO DE QUE EL COEFICIENTE DE EMPUJE CALCULADO SEA MENOR QUE 0.4 EN VALOR ABSOLUTO, TOMESE EL CASO MAS DESFAVORABLE DE  $\pm 0.4$  (Artículo 255 - IV)



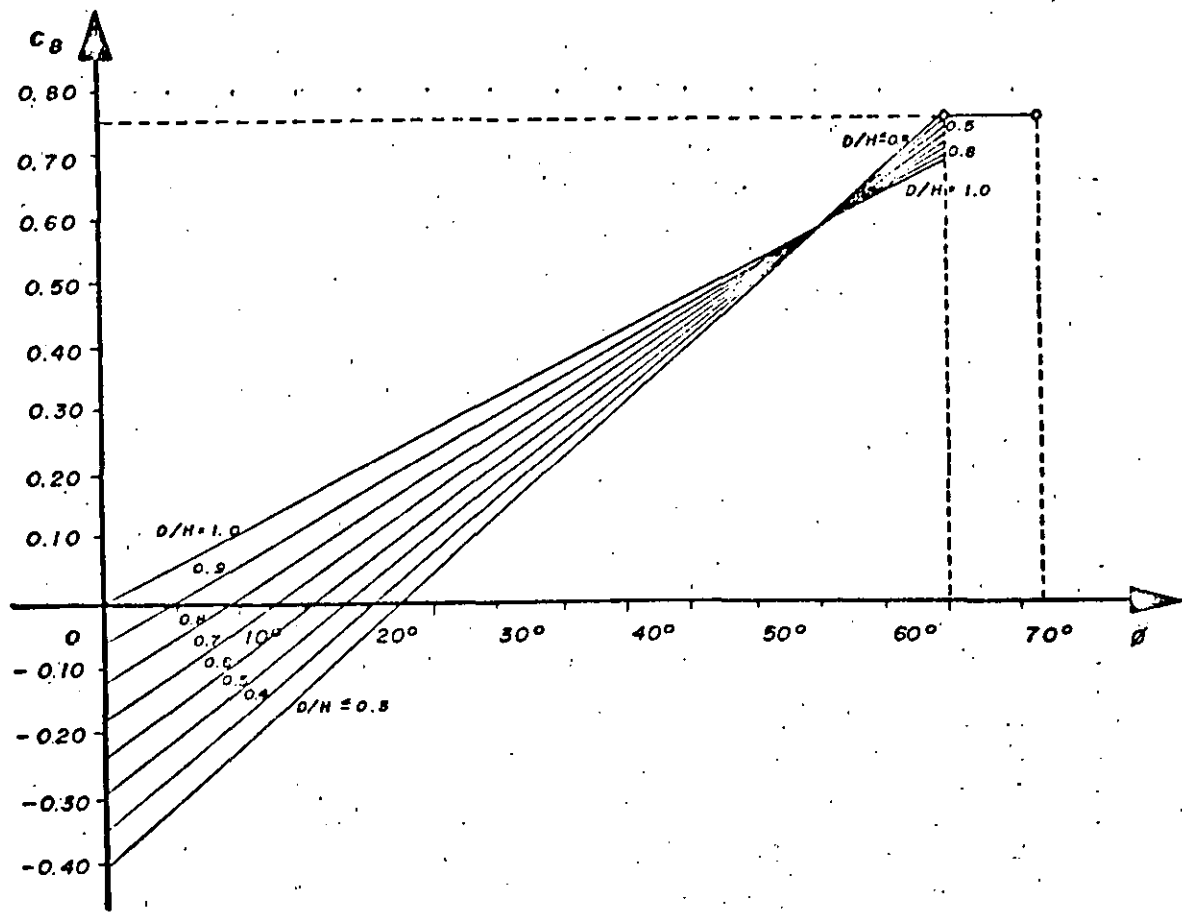
GRAFICA DEL COEFICIENTE  $C_6$

VER. Figura "A"





GRAFICA DEL COEFICIENTE  $C_7$   
Ver Figura "A"



GRAFICA DEL COEFICIENTE  $C_8$   
Ver Figura "A"



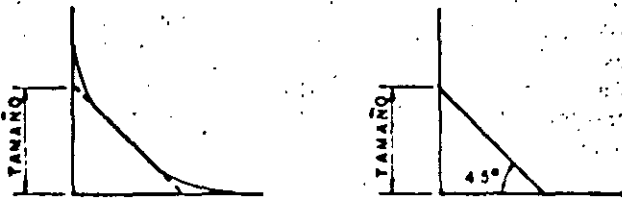
**DIVISION DE EDUCACION CONTINUA  
FACULTAD DE INGENIERIA U.N.A.M.**

DISEÑO DE ESTRUCTURAS DE ACERO

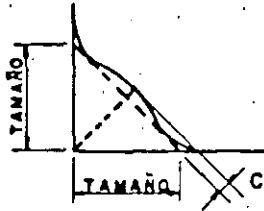
MONTAJE EDIFICIO RIO TIBER

*Ing. Manuel Lins Luján  
Dr. Porfirio Ballesteros  
Ing. Peña Ballestros*

NOVIEMBRE, 1984

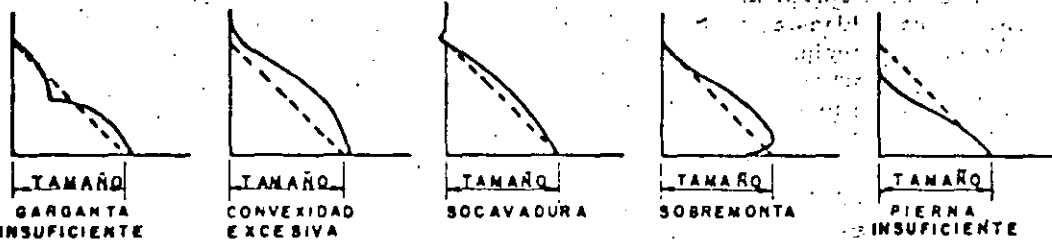


PERFILES DESEABLES DE SOLDADURA DE FILETE

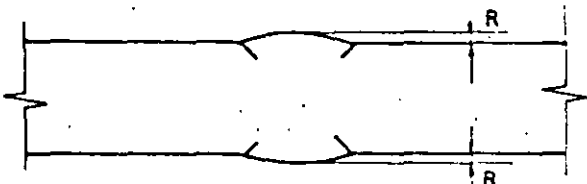


C = CONVEXIDAD  
NO DEBERA EXCEDER  
EL VALOR ESPECIFICADO

PERFIL ACEPTABLE DE SOLDADURA DE FILETE



PERFILES DEFECTUOSOS DE SOLDADURA DE FILETE



R = REFUERZO  
NO DEBERA EXCEDER  
EL VALOR ESPECIFICADO

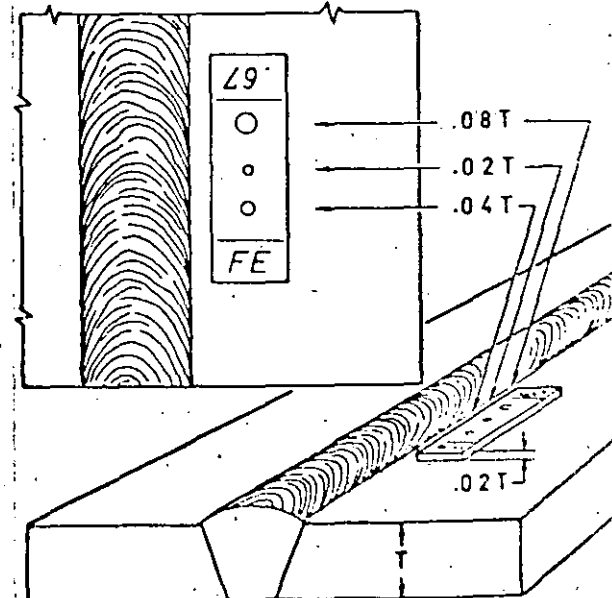
PERFIL ACEPTABLE DE SOLDADURA A TOPE



PERFILES DEFECTUOSOS DE SOLDADURA A TOPE

PERFILES DE SOLDADURA

ILUSTRANDO PERFILES ACEPTABLES  
Y DEFECTUOSOS DE SOLDADURA



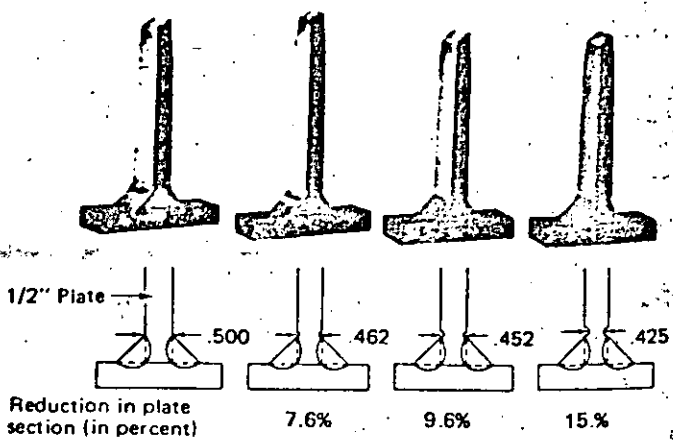


Fig. 11-5. Samples were deliberately prepared to show the effect of undercut. All samples were pulled in tension under a static load. In all cases, failure occurred in the plate and not in the weld.

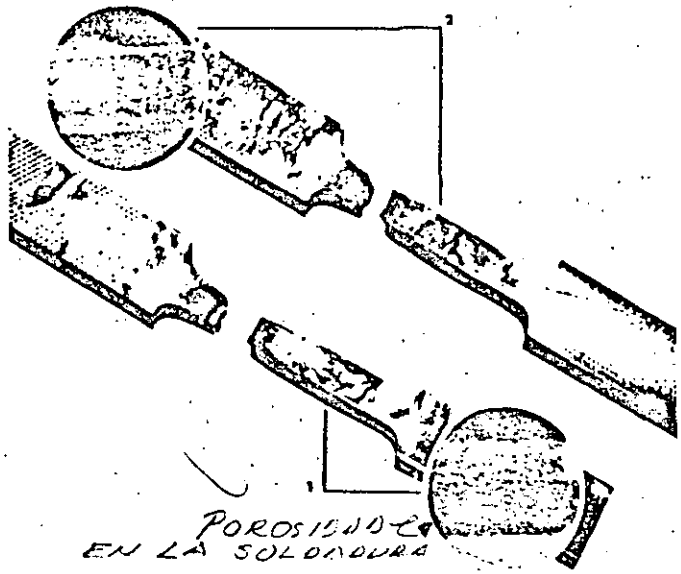
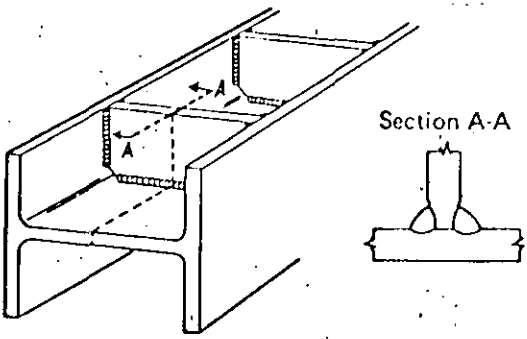


Fig. 11-3. Weld 1 has considerable porosity, as shown by the radiograph (inset). Weld 2 has no porosity. When the specimens were pulled, both broke in the plate at approximately 60,100 psi. In each instance, the weld was stronger than the plate, despite the porosity in the one weld.

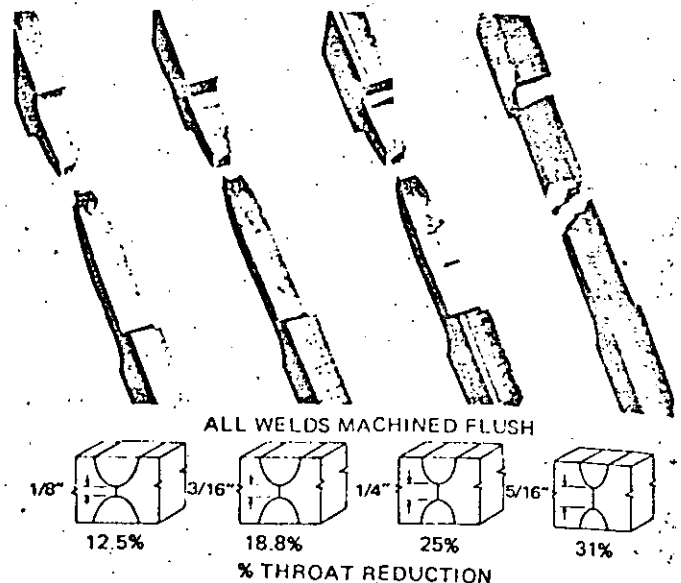
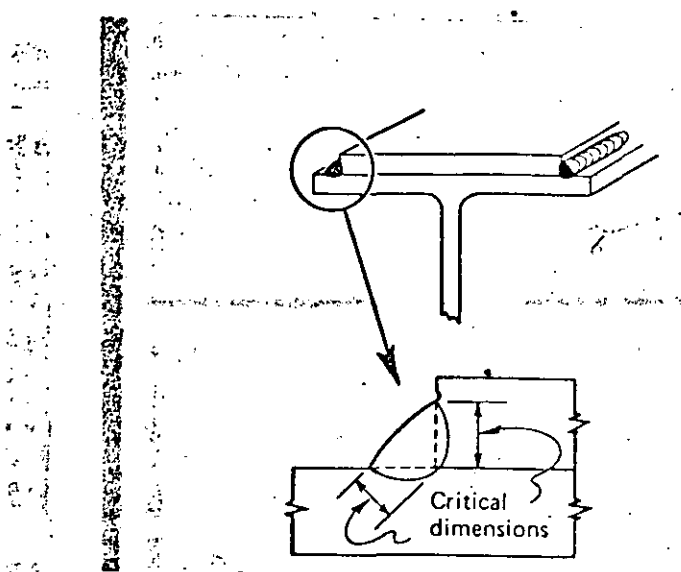
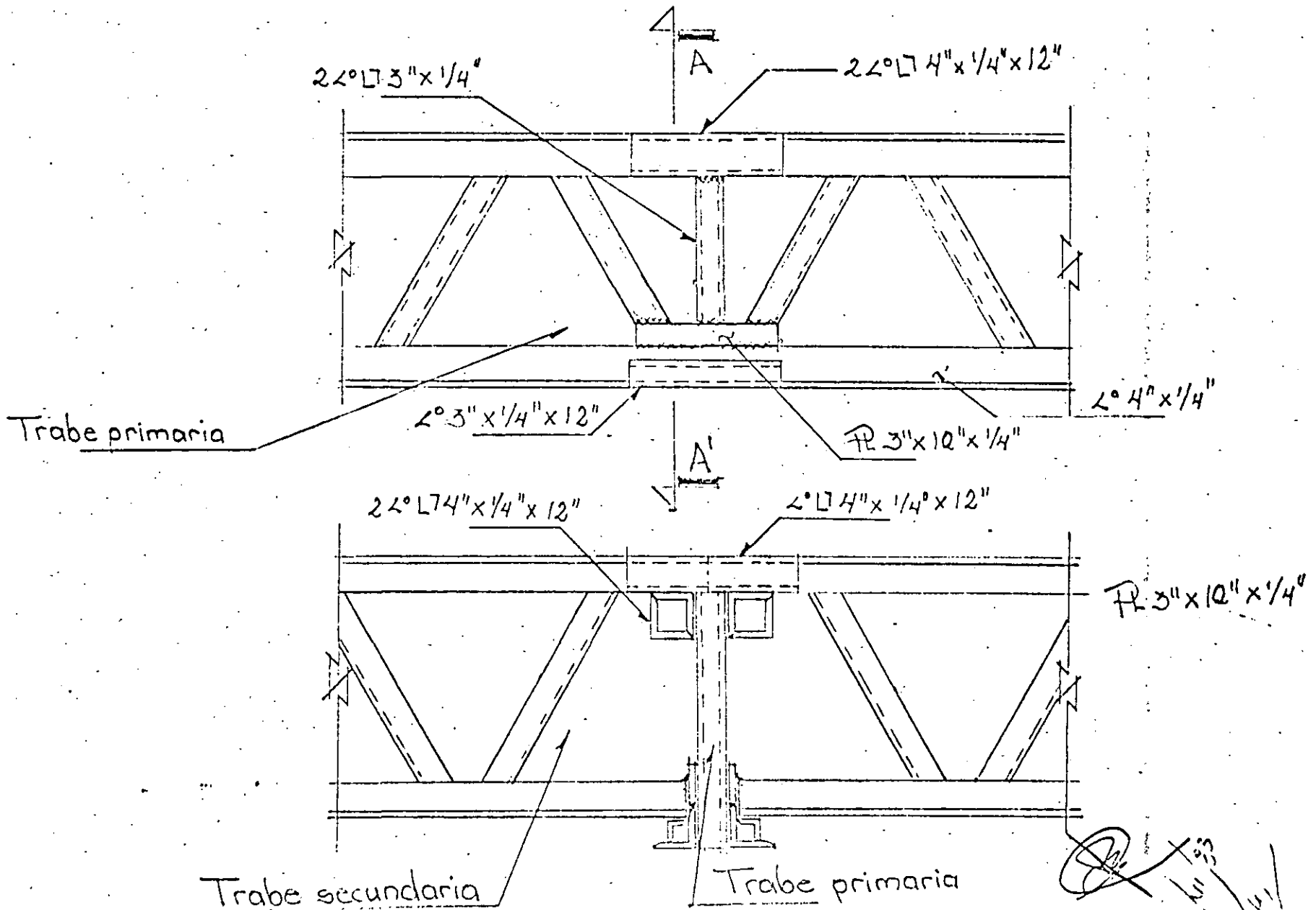


Fig. 11-4. Weld samples made with progressive degrees of lack of fusion. All welds were machined flush before tensile testing. Weld failure finally occurred when the unpenetrated throat dimension reached 31% of the total joint throat. All specimens were made with 1-in. plate, A-36 steel, and E7018 electrode.

Refuerzos para conexión de trabe secundaria con trabe primaria

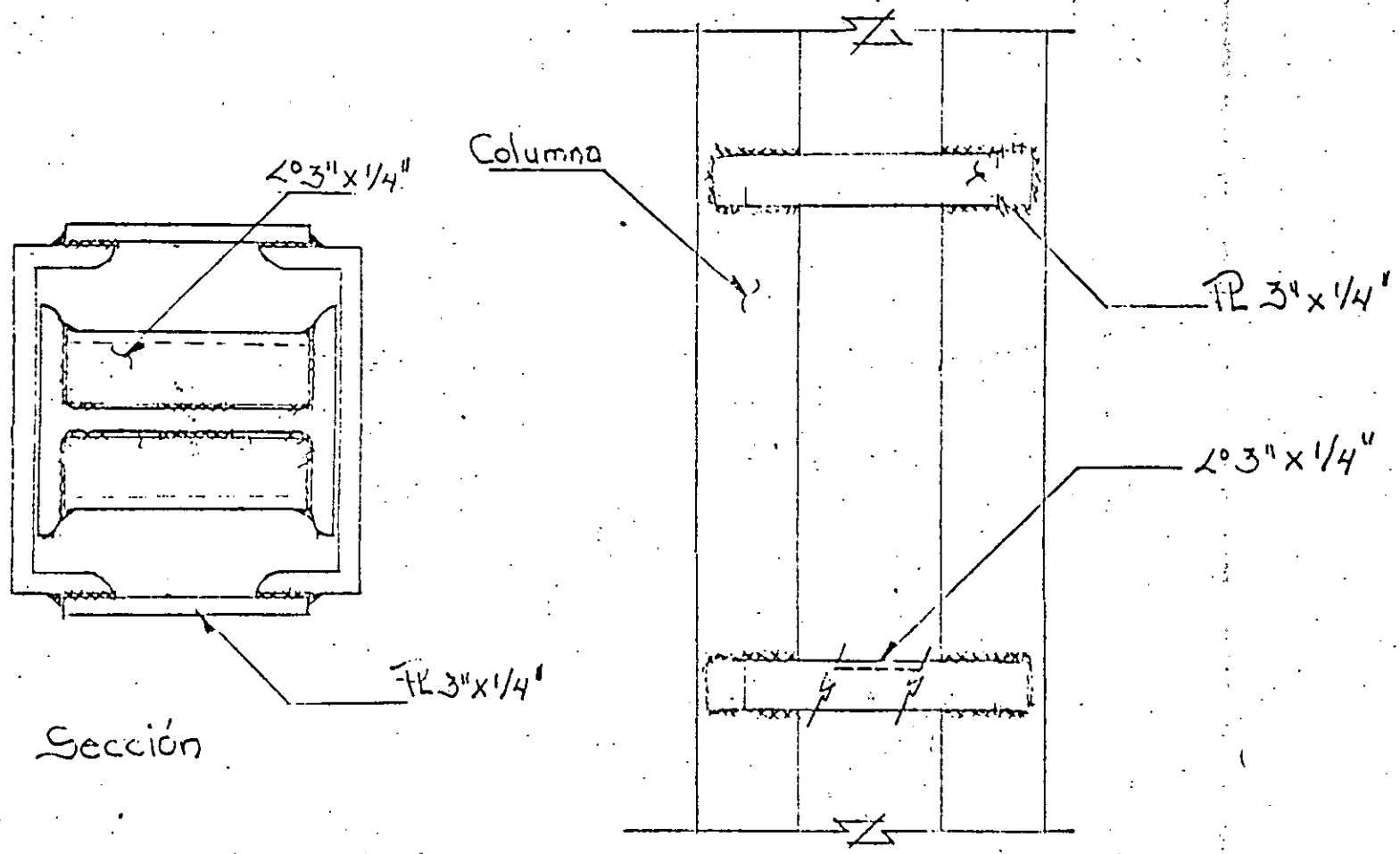
H-4-2-3



CORTE A-A'  $\angle 3" \times 1/4" \times 12"$

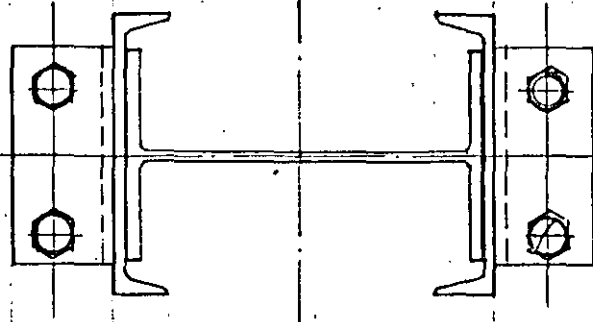
*[Handwritten signature and date]*  
30/11/55

# Refuerzo de continuidad para la conexión columna - trabe (con patines)

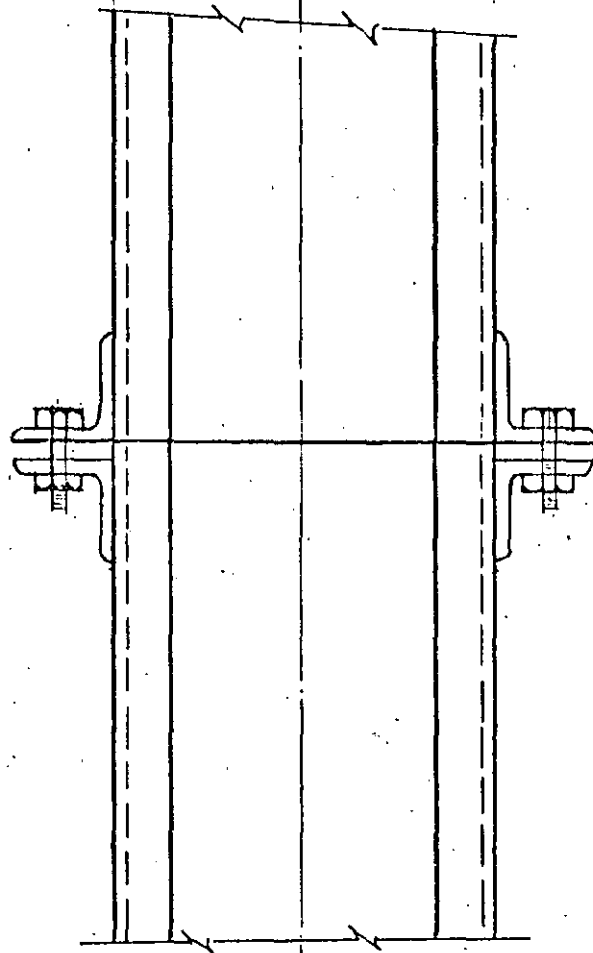


Nota: Estos detalles de conexión fueron propuestos por Capen Ingeniería, S.A. y autorizados por el calculista ~~X~~ Ballesteros

22/11/23



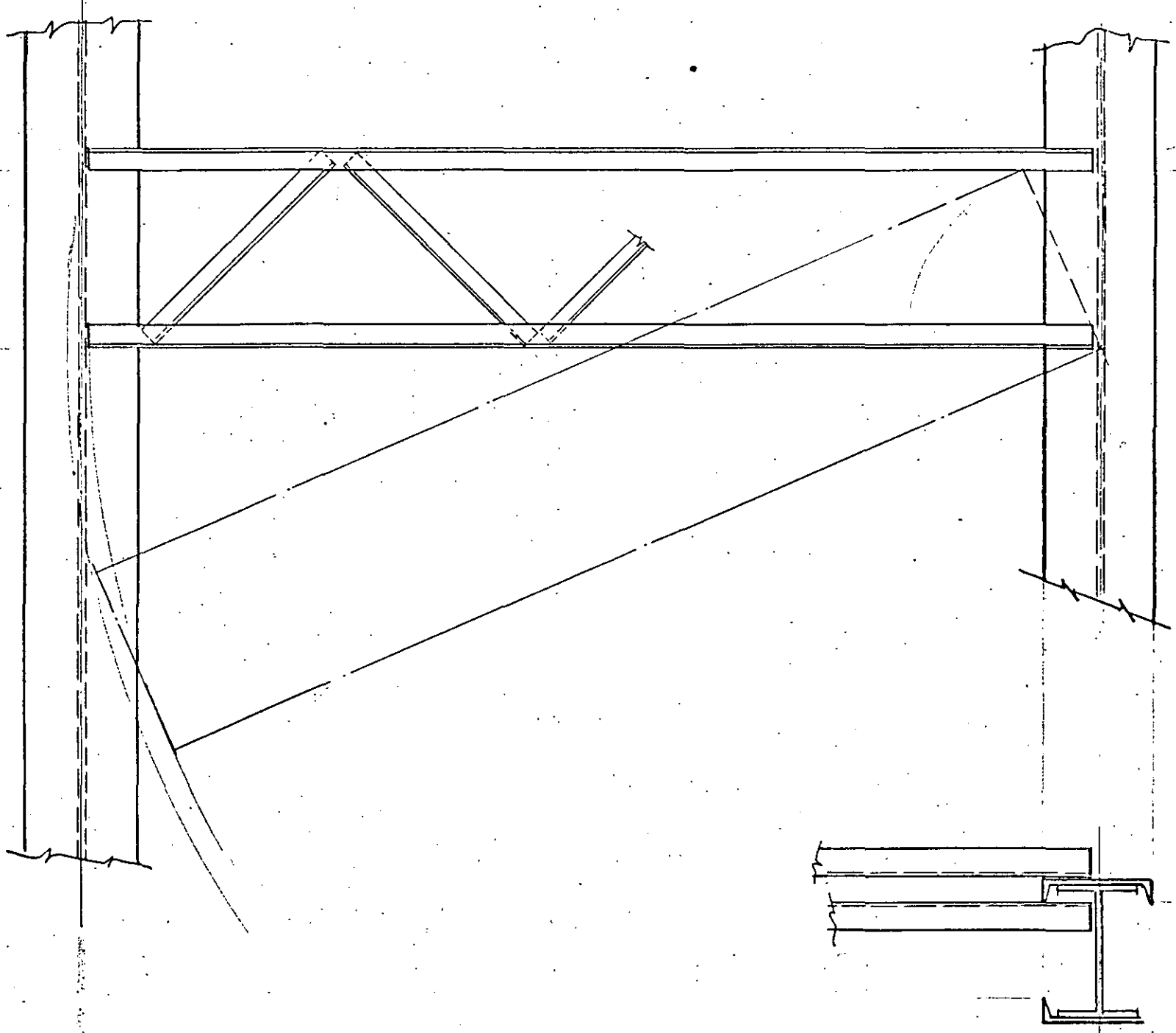
CONEXION PROVISIONAL PARA  
MONTAJE

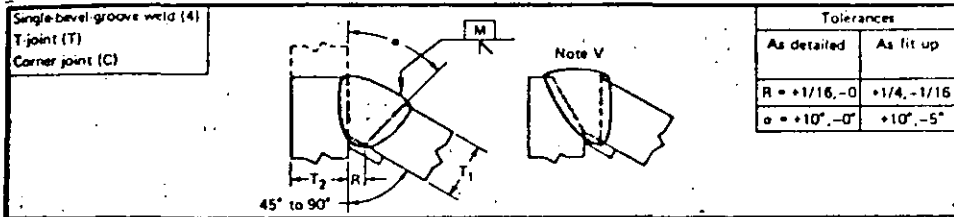






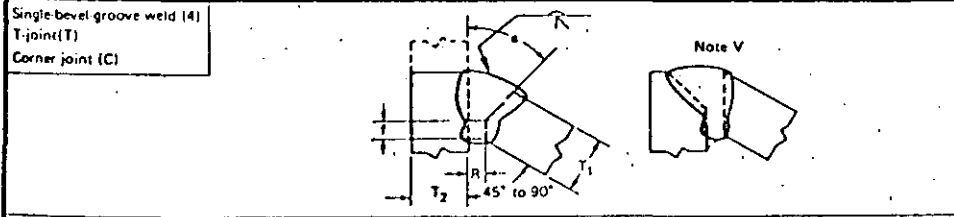
6



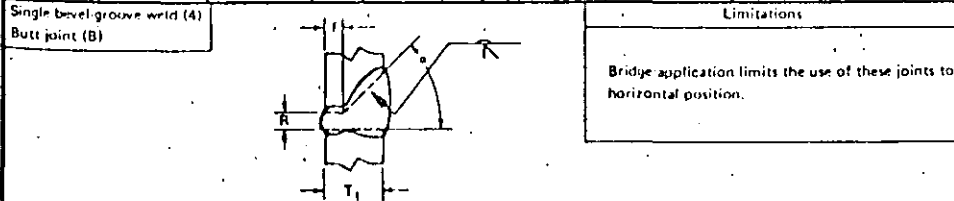


Tolerances	
As detailed	As fit up
R = +1/16, -0	+1/4, -1/16
α = +10°, -0°	+10°, -5°

Welding process	Joint designation	Base metal thickness (U = unlimited)		Groove preparation		Permitted welding positions	Gas shielding for (FCAW)	Notes
		T <sub>1</sub>	T <sub>2</sub>	Root opening	Groove angle			
SMAW	TC-U4d	U	U	R = 1/4	α = 45°	All	-	J,V
				R = 3/8	α = 30°			
GMAW FCAW	TC-U4d GF	U	U	R = 3/16	α = 30°	All	Required	A,J,V
				R = 3/8	α = 30°			
				R = 1/4	α = 45°	All	Not req.	
SAW	TC-U4b-S	U	U	R = 3/8	α = 30°	Flat	-	J,V
				R = 1/4	α = 45°			



Welding process	Joint designation	Base metal thickness (U = unlimited)		Root opening Root face Groove angle	Tolerances		Permitted welding positions	Gas shielding for (FCAW)	Notes
		T <sub>1</sub>	T <sub>2</sub>		As detailed	As fit up			
		SMAW	TC-U4b		U	U			
GMAW FCAW	TC-U4b GF	U	U	R = 0 f = 1/8 max α = 45°	+1/16, -0 +10°, -0°	+1/4, -0 ±1/16 +10°, -5°	All	Not required	A,C J,V
SAW	TC-L4b-S	3/4 max	U	R = 0 f = 1/8 max α = 60°	±0 +0, -1/8 +10°, -0°	+1/4, -0 ±1/16 +10°, -5°	Flat	-	J,V, Y



Welding process	Joint designation	Base metal thickness (U = unlimited)		Root opening Root face Groove angle	Tolerances		Permitted welding positions	Gas shielding for (FCAW)	Notes
		T <sub>1</sub>	T <sub>2</sub>		As detailed	As fit up			
		SMAW	B-U4		U	-			
GMAW FCAW	B-U4 GF	U	-	R = 0 to 1/8 f = 0 to 1/8 α = 45°	+1/16, -0 +10°, -0°	not limited +10°, -5°	All	Not required	A,C

See Notes on page preceding Prepared Weld Joint Tables

### SUBMERGED ARC-WELDING PROCEDURES - Multiple Electrodes

**FILLET WELDS** may be made in the flat or horizontal position (4.15.2)

Neither depth or max width of fusion shall exceed width at surface (4.11.7) May be waived if testing shows this to be free from cracking.

**GROOVE WELDS** shall be made in the flat position (4.15.1) single or multiple electrodes may be used in making root passes of groove welds.

When **SURFACE WIDTH** in a groove on which a layer of weld metal is to be deposited exceeds:

Use multiple electrodes which are displaced laterally... or a split layer technique with two electrodes in tandem. Use a split layer technique with two electrodes in tandem.

Single electrode. One electrode connected to one power source.  
 Parallel electrode. Two electrodes connected to same power source, usually a single feeder, current is the total for two electrodes.  
 Welding may be performed with one or more single electrodes, one or more parallel electrodes, or a combination of single and parallel electrodes. (4.11.1)

Max size of electrode is 1/4" (4.11.3)  
 Thickness of layers is not limited (4.15.2)  
 Does not necessarily apply to A514 steel (4.11.2)

### SUBMERGED ARC-WELDING PROCEDURES - Single Electrodes

**FILLET WELDS** may be made in the flat or horizontal position (4.14.1)

Neither depth or max width of fusion shall exceed width at surface (4.11.2) May be waived if testing shows this to be free from cracking.

**GROOVE WELDS** shall be made in the flat position. 1/4" max thickness of all layers except root and face pass.

When **SURFACE WIDTH** in a groove on which a layer of weld metal is to be deposited exceeds:

Use a split layer technique, no limit on current. Split layer technique shall be used if root opening is 1/2" or greater, no limit on current.

Max size of electrode is 1/4" (4.11.3)  
 Does not necessarily apply to A514 steel (4.11.2)

### GAS METAL-ARC & FLUX-CORED ARC WELDING - Single Electrode

#### MAXIMUM SIZE ELECTRODE AND THICKNESS OF PASS (4.18)

Split layer shall be used if width of the layer exceeds 5/8 inch. 1/4" Max. thickness of all weld layers except root and surface layers. Multiple pass, split layer shall be used if root opening is 1/2 inch or greater.

Roots of complete penetration groove welds without backing must be gouged.

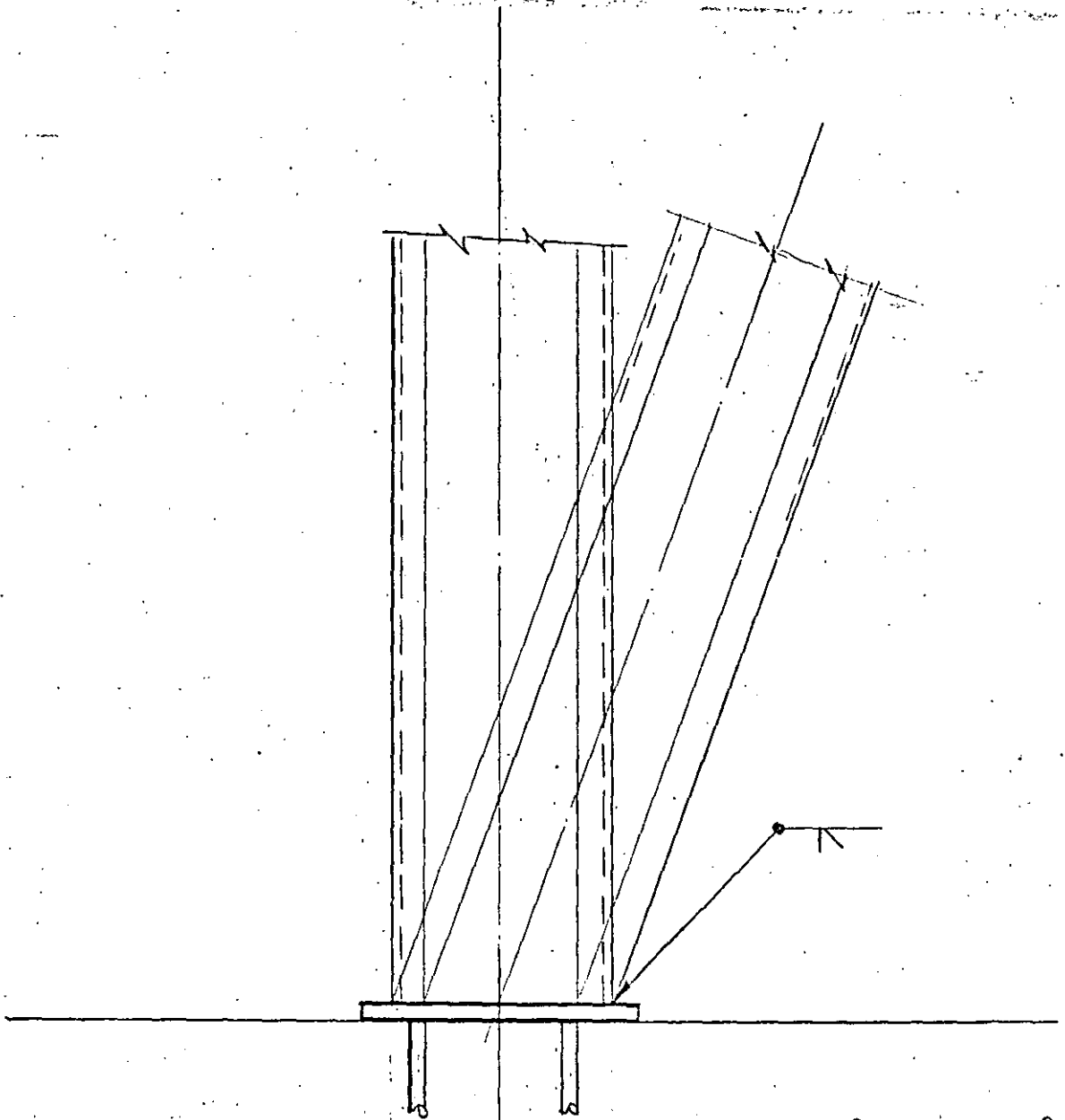
### MANUAL SHIELDED METAL-ARC WELDING (4.10)

#### MAXIMUM SIZE ELECTRODE AND THICKNESS OF PASS

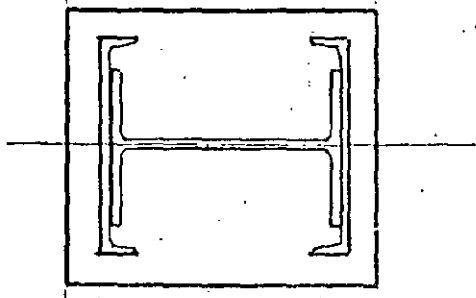
No backing 3/16" Max.

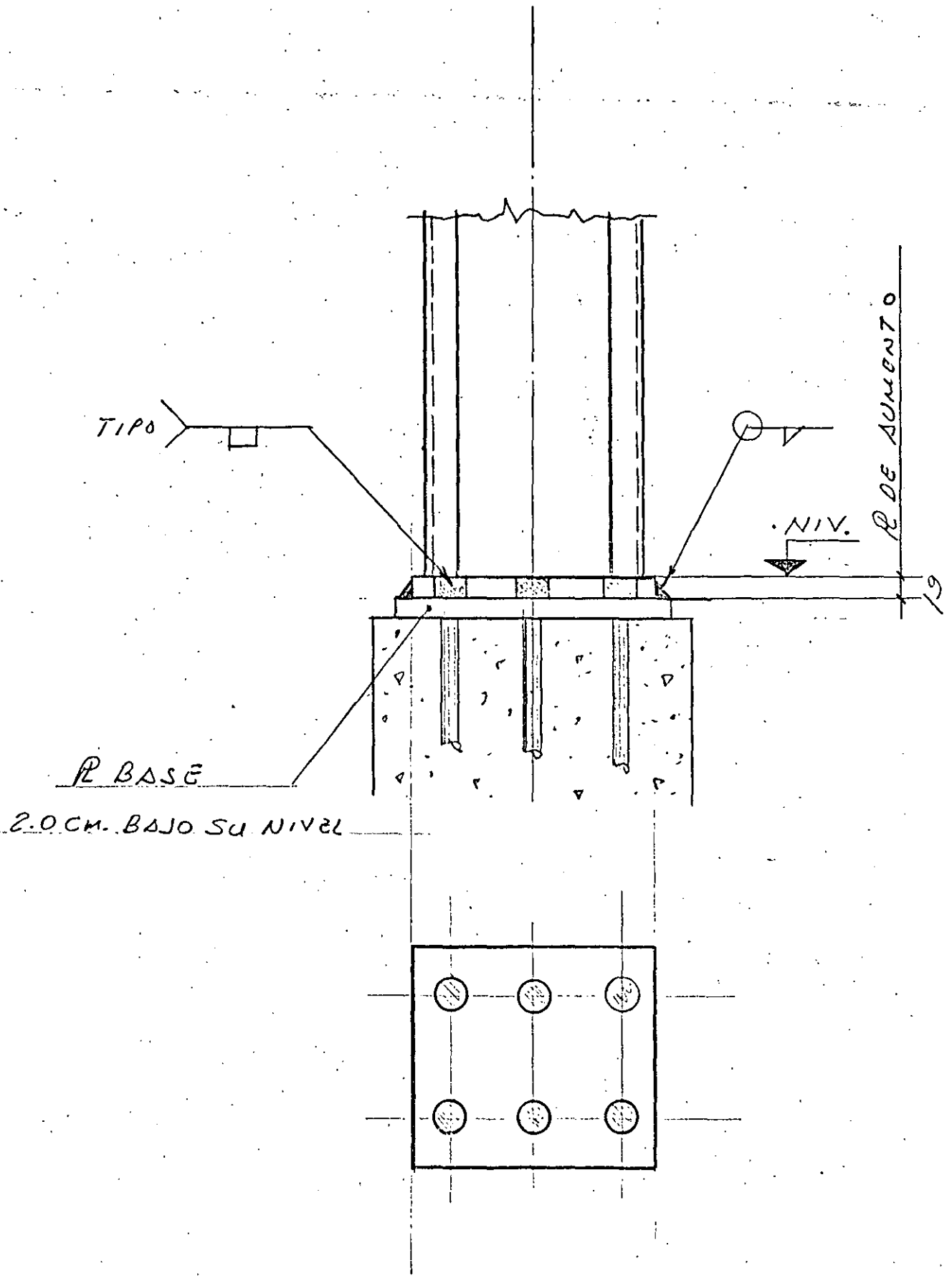
\*If EXX 14, 15, 16 or 18 electrode is used.

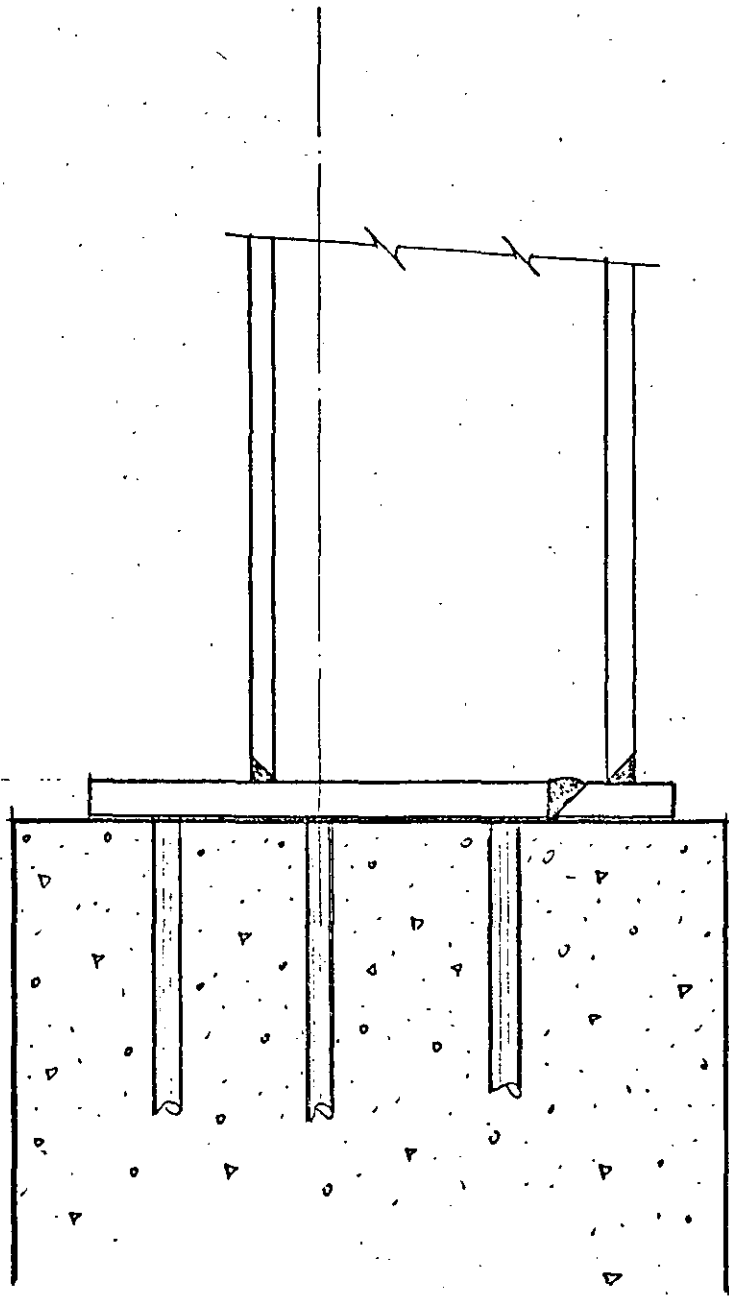
Fig. 11-40. AWS procedures for welding prequalified joints.



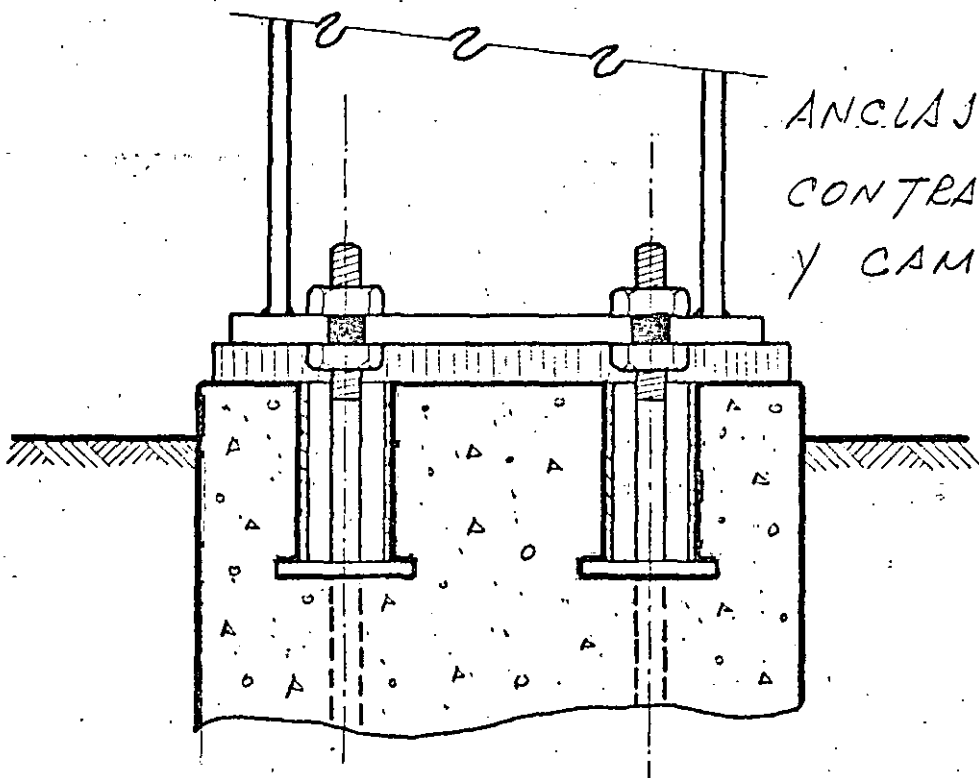
DESPLOME POR  
SOLDADURA



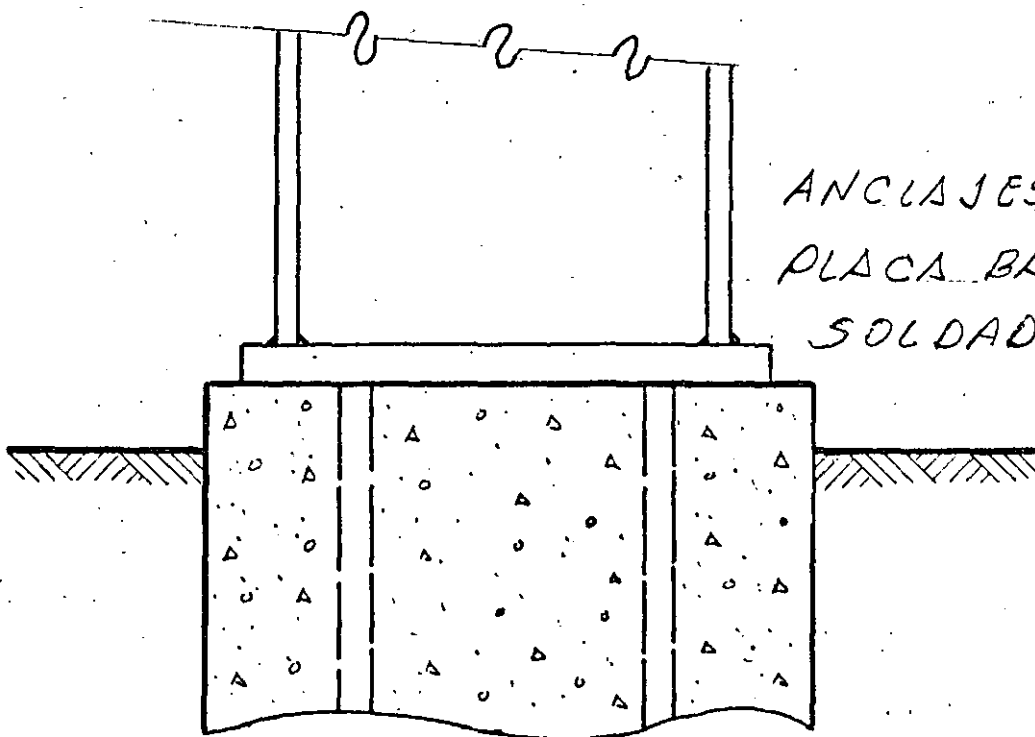




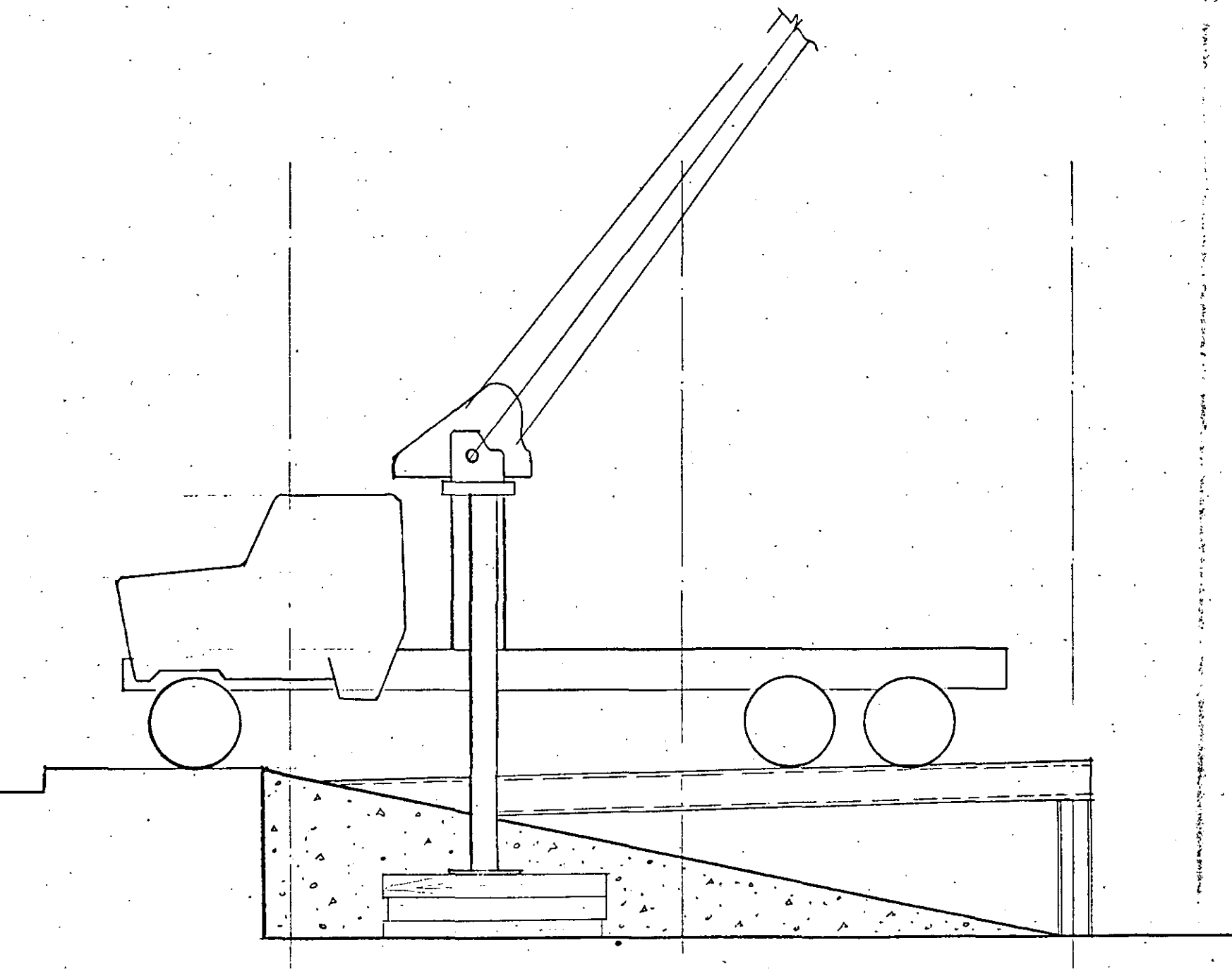
ERROR POR ALINEAMIENTO



ANCLAJES CON  
CONTRATUERCAS  
Y CAMISAS



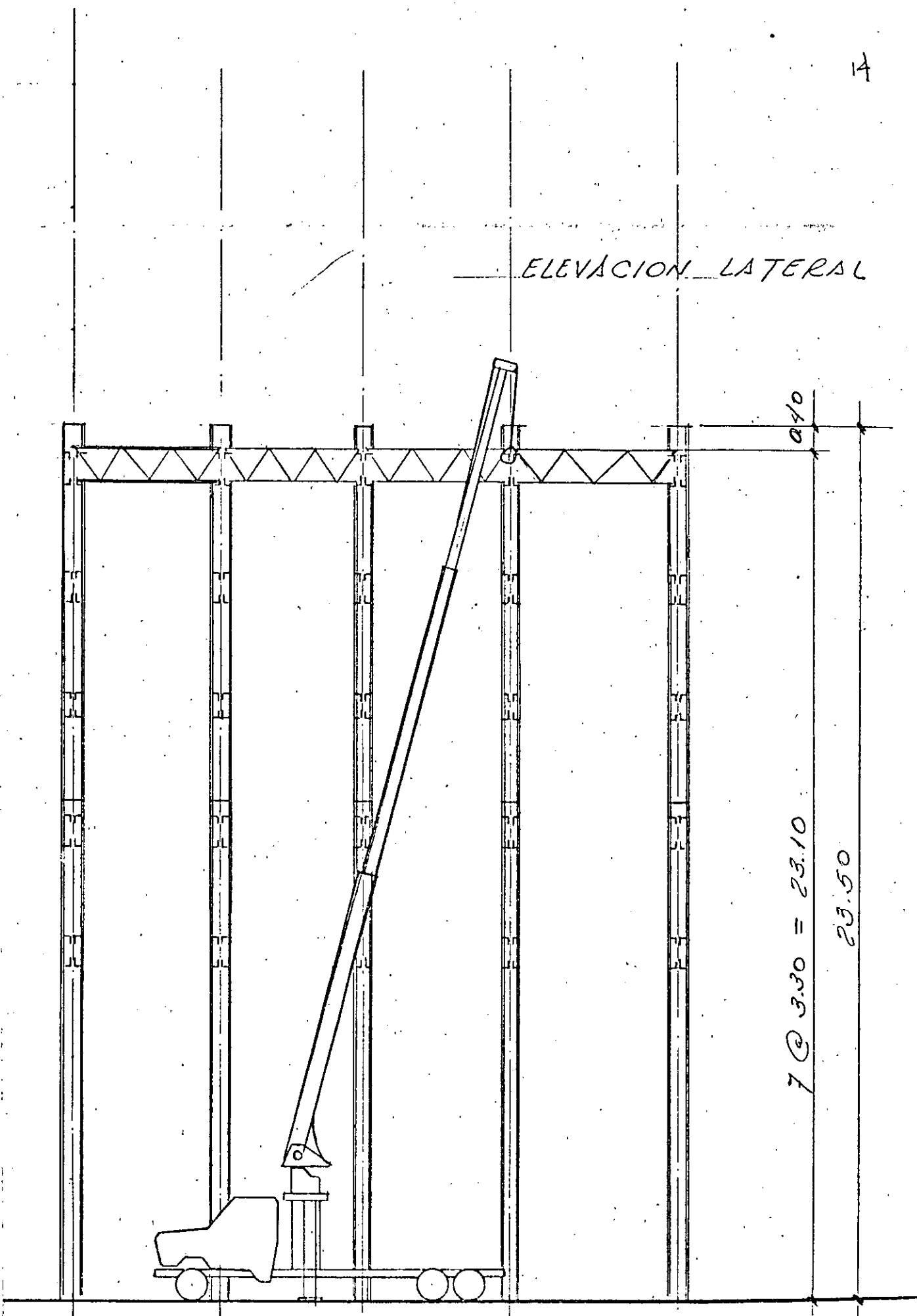
ANCLAJES CON  
PLACA BASE  
SOLDADA



MONTAJE EN ZONA DE RAMPA



ELEVACION LATERAL



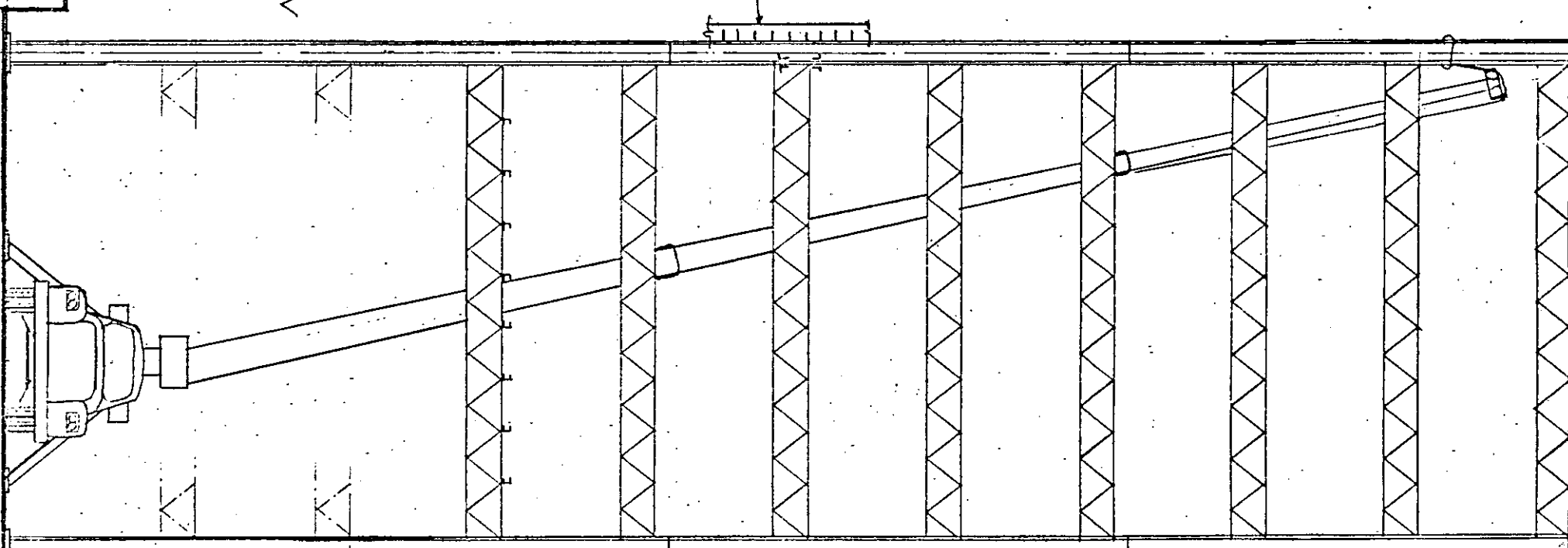
7 @ 3.30 = 23.10

23.50

0.40

ELEVACION  
FRONTAL

MURO



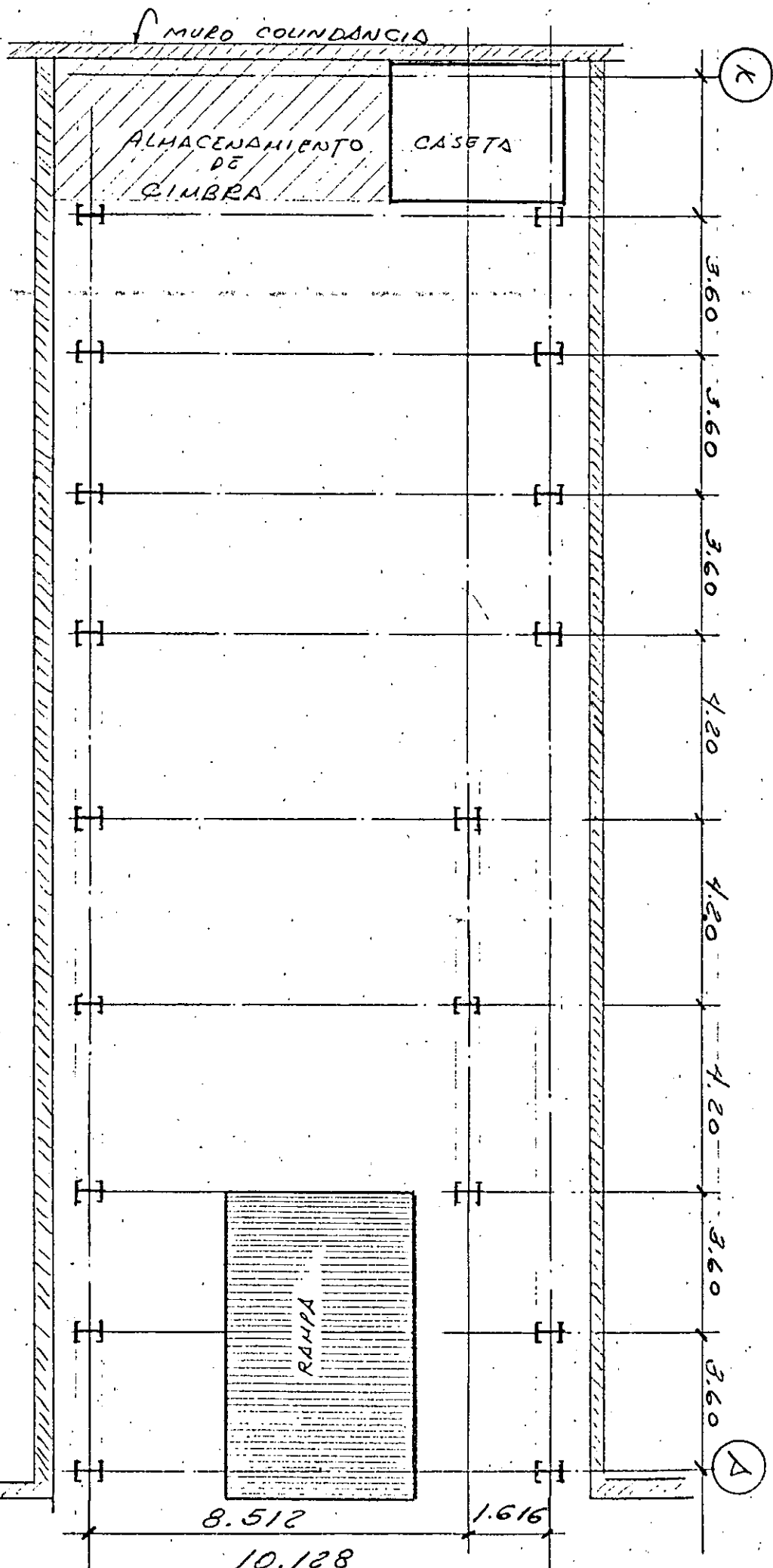
3.30

3.30

6.60

26.40

33.00



PLANTA



**DIVISION DE EDUCACION CONTINUA  
FACULTAD DE INGENIERIA U.N.A.M.**

DISEÑO DE ESTRUCTURAS DE ACERO

JUNTAS SOLDADAS

DR. PORFIRIO BALLESTEROS

NOVIEMBRE, 1984.

## Welding

### 5.1. INTRODUCTION AND HISTORICAL DEVELOPMENT

The process of welding denotes the joining of metal pieces by heating to a plastic or fluid state, with or without pressure. In its simplest form, "welding" has been known and used for several thousand years. Historians have speculated that the early Egyptians may have first used pressure-welding about 5500 B.C. in making copper pipes from sheets by overlapping the edges and hammering. Winterton<sup>1</sup> has reported that Egyptian art objects dating about 3000 B.C. have been found on which gold foil has been hammered and fused onto the base copper. This type of welding, called *forge welding*, was man's first process to join pieces of metal together. A well known early example of forge welding is the Damascus sword which was made by forging layers of iron with different properties. Interestingly, forge welding was sufficiently well developed and important enough to the early Romans that they named one of their gods, Vulcan (the god of fire and metalworking) to represent that art. In recent times, the word vulcanizing has been used in reference to treating rubber, with sulfur but originally was used to mean "to harden." Today, forge welding is practically a forgotten art in which the village blacksmith was the last major practitioner. Welding, as we know it today is much more complex and highly refined and the remainder of this section will trace some of the important events which have contributed to the art. Specific welding processes are discussed in Sec. 5.2.

Very little progress in welding technology had been made until 1877, prior to which time most of the then known processes such as forge welding and brazing had been used for at least 3,000 years. The origin of resistance welding began around 1877 when Professor Elihu Thompson began a set of experiments<sup>2,3</sup> reversing the polarity of transformer coils. He received his first patent<sup>4</sup> in 1885 and the first resistance butt welding machine was demonstrated at the American Institute Fair<sup>2</sup> in 1887. In



Welding of space trusses—Upjohn Company Office Building Courtesy Whitehead and Kales Company, Detroit.

1889 Coffin<sup>2</sup> was issued a patent for flash-butt welding which became one of the important butt welding processes.

Zerner, in 1885 introduced the carbon-arc welding process, making use of two carbon electrodes and N. G. Slavynoff<sup>3</sup> in Russia was the first to use the metal-arc process using uncoated, bare electrodes in 1888. Coffin, working independently also investigated the metal-arc process and was issued a U.S. Patent in 1892. In 1889, A. P. Strohmeyer<sup>2</sup> introduced the concept of coated metal electrodes to eliminate many of the problems associated with the use of bare electrodes.

Thomas Fletcher<sup>1</sup> in 1887 used a blowpipe burning hydrogen and oxygen and showed that he could successfully cut or melt metal. In 1901-03 Fouche and Picard developed torches which could be used with acetylene and thus the era of oxyacetylene welding and cutting began.

The period between 1903 and 1918 saw the use of welding primarily as a method of repair, the greatest impetus occurring during World War I (1914-18). Welding techniques proved to be especially adapted to repairing ships which had been damaged. Winterton<sup>6,7</sup> reported that in 1917 there were 103 interned enemy ships alone in the United States which were damaged and the number of persons employed in welding operations rose from 8,000 to 33,000 during the period 1914-18.

After 1919, the use of welding as a construction and fabrication tech-

nique began to develop with copper-tungsten alloy electrodes being first used for spot welding techniques<sup>6</sup> in 1920. The period 1930-50 saw many improvements<sup>7,8</sup> in the development of welding machines. The submerged-arc welding process in which the arc is buried under a powdered flux was first used commercially in 1934 and patented in 1935.

Today there are over 50 different welding processes which can be used to join various metals and their alloys. Those of particular interest to the structural engineer are discussed in Sec. 5.2.

## 5.2. BASIC PROCESSES

As defined by the *Welding Handbook*,<sup>9</sup> "Welding is the process of joining two or more pieces of material, often metallic, by a localized coalescence or union across an interface." Most welding processes involve heating the material to be welded, or at least involve energy input to the material. The heat generation may be categorized according to its source; as electrical, chemical, optical, mechanical, and solid state. Heat is used to melt the base metal and filler material in order that flow of material will occur, i.e., that fusion will take place. In addition, heat is used to increase ductility so that plastic flow can occur even if melting does not take place; further, heating helps to remove contaminating films on the material.

The most common welding processes, particularly for welding structural steel, use electrical energy as the heat source; the most often used is the electric arc. The arc consists of a relatively large current discharge between electrode and base material sustained through a thermally ionized gaseous column, called a plasma.<sup>9</sup> In arc welding, fusion occurs by the flow of material across the arc, without pressure being applied.

Other processes, not ordinarily used for steel structures, involve other energy sources, and some of those processes involve the application of pressure, either in the absence or presence of flow of molten material. Bonding may also occur by diffusion, wherein atomic particles intermix across the interface and melting of the base material does not occur.

There are many welding processes which have special uses for particular metals and for various thicknesses. This section emphasizes those processes which are used in the welding of carbon and low-alloy steel for buildings and bridges. However, in order to present an idea of the broad spectrum of processes, a number of them are listed according to the sources of energy for generating heat and/or inducing the bonding process:

### (a) Electrical energy

1. Arc welding—fusion process; heat from electric arc.

2. Resistance welding—pressure process; heat from resistance to the flow of current.
3. Induction welding—fusion combined with pressure; heat by electromagnetic induction.
4. Electroslag welding—fusion process where molten slag provides heat; electric current is conducted through the slag without an arc.

### (b) Chemical energy

1. Oxyacetylene gas welding—fusion process; heat from acetylene burning in the presence of oxygen.
2. Thermit welding—fusion process; heat from chemical reaction between a metal oxide and aluminum.

### (c) Optical energy

1. Laser-beam welding—fusion process; heat from application of a concentrated coherent light striking the surfaces to be joined.
2. Electron-beam welding—fusion process; heat from conversion of kinetic energy of high velocity electrons bombarding the surfaces to be joined.

### (d) Mechanical energy

1. Friction welding—pressure process without melting of base material; heat generated from friction between a stationary and rotating member subject to high normal force on the interface to be joined.
2. Ultrasonic welding—pressure process without melting of base material; heat generated by high-frequency vibrating energy.
3. Explosion welding—pressure process without melting of base material; heat generated by high velocity impact on the interface resulting from a controlled detonation.

### (e) Solid-State Bonding

One might call this category natural welding, wherein pressure is applied and the temperature is raised but no melting occurs. After a period of time diffusion occurs by atoms moving across the original joint interface and intermixing to create a solid state bond. Good clean surface preparation is important in this process.

For design of steel structures, arc welding is the category of processes which are of particular interest. For some situations involving light-gage steel, resistance welding may also be important.

**Shielded Metal-Arc Welding.** This is the most usual type of welding sometimes called the manual stick electrode method. Heating is accomplished by means of an electric arc between a coated electrode and the materials being joined. The welding circuit is shown in Fig. 5.2.1a.

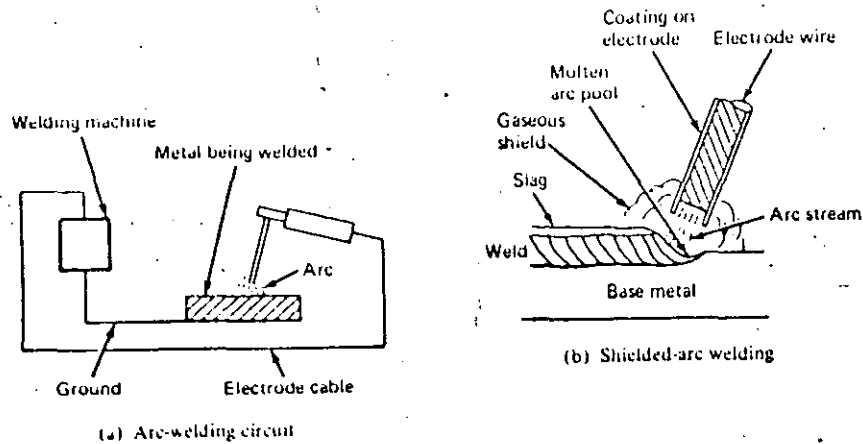


Fig. 5.2.1. Shielded metal-arc welding.

The coated electrode is consumed as the metal is transferred from the electrode to the base material during the welding process. The electrode wire becomes filler material and the coating is converted partly into a shielding gas, partly into slag, and some part is absorbed by the weld metal. There is a wide variety of coating materials producing different proportions of gas and slag.

The transfer of metal from electrode to the work being welded is induced by molecular attraction and surface tension, without application of pressure. The shielding of the arc prevents atmospheric contamination of the molten metal in the arc stream and in the arc pool. It prevents nitrogen and oxygen from being picked up and forming nitrides and oxides which may cause embrittlement.

The electrode coating may perform the following functions:

- Produces a gaseous shield, as described above.
- Introduces other materials, such as deoxidizers, to refine the grain structure of the weld metal.
- Produces a blanket of slag over the molten pool and the solidified weld to protect it from oxygen and nitrogen in the air, and also retards cooling.

The electrode material is specified under ASTM A233, (AWS A5.1) for carbon steel welding and ASTM A316 (AWS A5.5) for low alloy steel welding. The strength and designations are referred to in Chapter 2. The designations are E60XX for 60 ksi tensile strength, E70XX for 70 ksi tensile strength, etc. Table 5.12.1 indicates which coated electrodes should be used with each particular structural steel.

For welding high-carbon or low-alloy steels, low hydrogen electrodes with special precautions are recommended, and required by AISC-1.5.3

for use on A242, A441, A572, and A588 steels. The low-hydrogen electrode is a rod with a carbonate of soda, or "lime," coating. The use of this electrode requires a different technique from the conventional electrode in that it requires a short arc and provides globular-type, rather than a spray-type transfer of metal from the electrode to the work. However, it is required by AISC because the as-welded mechanical properties have been found to be superior to properties obtained using other types of electrode coatings.

The process is the principal one used for manual welding of steel structures.

**Gas-Shielded Arc Welding.** In gas-shielded arc-welding, fusion occurs under a shield of protective gas (inert or reactive) by the heat of an electric arc between a metal electrode (consumable or nonconsumable) and the piece being welded. Essentially two major processes may be considered; those with a nonconsumable electrode and those using a continuously fed consumable electrode.

**Gas Tungsten-Arc Welding (TIG).** The gas tungsten-arc welding process uses a nonconsumable tungsten electrode which is contained in a holder with a sheath through which the shielding gas passes, as shown in Fig. 5.2.2. This method, commonly called TIG (tungsten inert gas), uses an

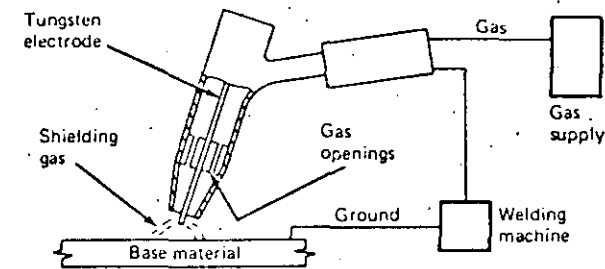


Fig. 5.2.2. Gas tungsten-arc welding.

inert gas, such as argon or helium, for the protection shield. Rarely, if ever, is this method used for welding structural steel, though it is common for welding aluminum and magnesium which are beginning to receive wider structural usage.

**Gas Metal-Arc Welding.** In this process the electrode is a continuous wire that is fed from a coil through the electrode holder. The shielding, as in the TIG method, is entirely from an externally supplied gas or gas mixture.

Originally, this method was used only with inert gas shielding, hence, the name MIG (metal-inert gas) has been used. Reactive gases alone are generally not practical; the exception is CO<sub>2</sub> (carbon dioxide). The use of CO<sub>2</sub> has become extensively used for welding of steels, either alone or in a mixture with inert gases.

Argon as a shielding gas works for welding virtually all metals; however, it is not recommended for steels because of its expense and the fact that other shielding gases and gas mixtures are acceptable. For welding carbon and some low-alloy steels either (1) 75 percent argon and 25 percent CO<sub>2</sub>, or (2) 100 percent CO<sub>2</sub> is recommended.<sup>9</sup> For low alloy steels where toughness is important, it is recommended<sup>9</sup> to use a mixture of 60-70 percent helium, 25-30 percent argon, and 4-5 percent CO<sub>2</sub>.

The shielding gas serves the following functions in addition to protecting the molten metal from the atmosphere:

- (a) Controls the arc and metal-transfer characteristics.
- (b) Affects penetration, width of fusion, and shape of the weld region.
- (c) Affects the speed of welding.
- (d) Controls undercutting.

By mixing an inert gas with a reactive gas the arc may be made more stable and the spatter during metal transfer may be reduced. The use of CO<sub>2</sub> alone for welding steel is the least expensive procedure, because of its lower cost for shielding gas, higher welding speed, better joint penetration, and sound deposits with good mechanical properties. The only disadvantage is that it gives harsh and excessive spatter.

The electrode material for welding carbon steels is an uncoated mild steel, deoxidized carbon manganese steel, designated A559 (AWS A5.18) as described in Chapter 2. For welding low-alloy steel a deoxidized low-alloy material is necessary.

The gas metal-arc welding method using CO<sub>2</sub> shielding is good for the lower carbon and low-alloy steels usually used in buildings and bridges.

**Submerged-Arc Welding.** In this fusion-arc welding process the arc is not visible because it is covered by a blanket of granular, fusible material, as shown in Fig. 5.2.3. The bare metal electrode is consumable in that it

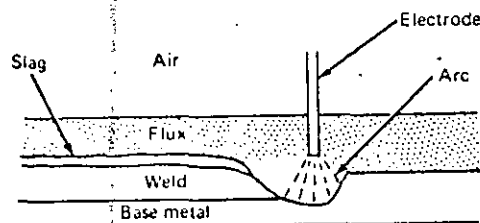


Fig. 5.2.3. Submerged-arc process.

is deposited as filler material. The end of the electrode is kept continuously shielded by the molten flux over which is deposited a layer of unfused flux in its granular condition.

The flux, which is the special feature of this method, provides a cover which allows the weld to be made without spatter, sparks, or smoke. The granular flux is laid usually automatically along the seam ahead of the advancing electrode. It protects the weld pool against the atmosphere, serves to clean the weld metal, and modifies the chemical composition of the weld metal.

Welds made by the submerged-arc process are found to have uniformly high quality; exhibiting good ductility, high impact strength, high density and good corrosion resistance. Mechanical properties of the weld are consistently as good as the base material.

The bare-rod electrodes are of mild steel designated E6XX or E7XX according to ASTM A558 (AWS A5.17), indicating a minimum tensile strength of 60 or 70 ksi, respectively. Fluxes are also classified under A558 (AWS A5.17) and designated by a prefix F followed by a two-digit number indicating tensile strength and impact strength requirements for the resulting welds. The combination of flux and electrode is usually designated together, such as F7X-E6XX, where the last three digits classify the electrode.

The submerged arc method is commonly used to weld steel in shop fabrication operations using automatic or semiautomatic equipment.

**Flux-Cored Arc Welding.** This is a gas metal-arc process using flux cored filler, and may be with or without external gas shielding. For welding of steel usually a CO<sub>2</sub> shielding gas is used. Instead of a coating on the electrode, which is not feasible for a continuously fed electrode wire; the coating material, or flux, is contained in the core of the electrode.

The electrodes are specified as a mild steel type E60T or E70T under AWS A5.20, and for tensile strengths greater than 70 ksi may be referred to as Grades E80T, E90, E100T, and E110T for tensile strength of 80, 90, 100 and 110 ksi, respectively.

**Stud Welding.** The most commonly used process of welding a metal stud to a base material is known as arc stud welding, an essentially automatic process but similar in characteristics to manual shielded arc welding. The stud serves as the electrode and an electric arc is created from the end of the stud to the plate. The stud is contained in a gun which controls the timing during the process. Shielding is accomplished by placing a ceramic ferrule around the end of the stud in the gun. The gun is placed in position and the arc is created, during which time the ceramic ferrule contains



the molten metal. After a short instant of time, the gun drives the stud into the molten pool and the weld is completed leaving a small fillet around the stud. Full penetration across the shank of the stud is obtained and the weld is completed usually in less than one second.

**Oxyacetylene Welding.** This early method wherein heat is generated from the combustion of a mixture of oxygen and acetylene has now been essentially replaced by electric arc welding. However the oxyacetylene torch is widely used for cutting steel, as well as for heating to camber and flame-straighten steel.

For most fabrication of steel buildings or bridges, either shielded metal-arc welding using coated electrodes is used for manual operation, or the submerged arc process with bare electrodes and granular flux is used for automatic and semiautomatic operations.

**5.3. WELDABILITY OF STRUCTURAL STEEL**

Most of the ASTM-specification construction steels can be welded without special precautions or special procedures. Chapter 2 discusses the three basic categories of structural steels:

- (a) Carbon steels .....(Sec. 2.2)
- (b) High-strength low-alloy steels .....(Sec. 2.3)
- (c) Heat-treated low-alloy steels .....(Sec. 2.4)

The discussion in Chapter 2 also includes the steels contained in the various commonly used electrodes. Section 5.12 discusses the need to select the proper electrode to join a particular grade of steel and a summary of the "matching" electrodes and the base steel is given in Table 5.12.1.

The *weldability* of a steel is a measure of the ease of producing a crack-free and sound structural joint. Some of the readily available structural steels are more suited to welding than others, and are discussed in Chapter 2. Welding procedures should be based on a steel's chemistry instead of the published maximum alloy content since most mill runs are usually below the maximum alloy limits set by its specification. Table 5.3.1 shows the ideal chemical analysis of the carbon steels. Most mild steels fall well within this range, while higher-strength steels may exceed the ideal analysis shown in Table 5.3.1.

When a mill produces a run of steel it maintains a complete record of its chemical content which follows all sections made from the particular ingot. If the designer is concerned about the chemistry of a particular grade of steel, he may request a Mill Test Report. Any variation in

TABLE 5.3.1  
Preferred Analysis of Carbon Steel<sup>10</sup>  
for Good Weldability

Element	Normal Range, percent	Percent Requiring Special Care
Carbon	0.06-0.25	0.35
Manganese	0.35-0.80	1.40
Silicon	0.10 max	0.30
Sulfur	0.035 max	0.050
Phosphorus	0.030 max	0.040

chemical content above the ideal values may be evaluated and special welding procedures be set up to insure a properly welded joint.

It should be noted, however, that most structural welding situations do not require the caution implied by the previous paragraph.

**5.4. TYPES OF JOINTS**

The types of joints used in structural connections depend on many design considerations, including the size and shape of the members coming into the joint, the type of loading, the amount of joint area available for welding, and the relative costs for various types of welds. There are five basic types of welded connections although many variations and combinations are found in practice. The five basic types are the butt, lap, tee, corner, and edge joints, as shown in Fig. 5.4.1.

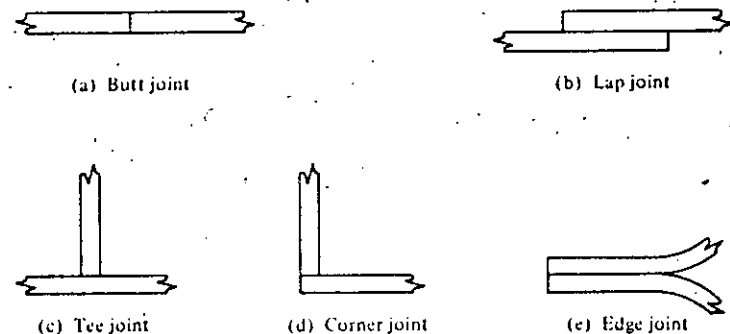


Fig. 5.4.1. Basic types of welded joints.

**Butt Joints.** The butt joint is used mainly to join the ends of flat plates of the same or nearly the same thicknesses. The principal advantage of this type of joint is to eliminate the eccentricity developed in single lap joints as shown in Fig. 5.4.1b. When used in conjunction with full penetration welds, butt joints minimize the size of a connection and are usually more

esthetically pleasing than built-up joints. Their principal disadvantage lies in the fact that the edges to be connected must usually be specially prepared (beveled, or ground flat) and very carefully aligned prior to welding. Little adjustment is possible and the pieces must be carefully detailed and fabricated. As a result, most butt joints are made in the shop where the welding process can be accurately controlled.

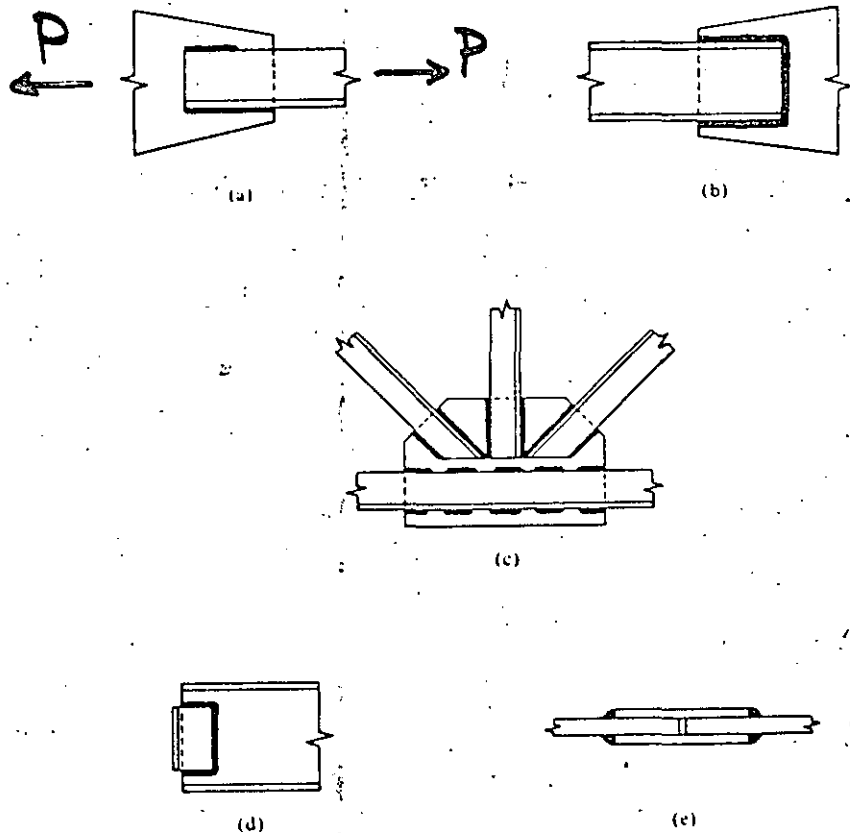


Fig. 5.4.2. Examples of lap joints.

**Lap Joints.** The lap joint is the most common type of joint and is used in a large variety of connections. Figure 5.4.2 shows a few common applications of the lap joint. There are two principal advantages to using lap joints:

1. *Ease of fitting.* Pieces being joined do not require the preciseness in fabricating as do the other types of joints. The pieces can be slightly shifted to accommodate minor errors in fabrication or to make adjustments in length.

2. *Ease of joining.* The edges of the pieces being joined do not need special preparation and are usually sheared or flame cut. Lap joints are especially adapted to accepting fillet welds and are therefore equally well suited to shop or field welding. The pieces being joined are in most cases simply clamped together without the use of special jigs. Occasionally the pieces are positioned by a small number of erection bolts which may either be left in place or removed after the welding is completed.

A further advantage of the lap joint is the ease in which plates of different thicknesses can be joined, such as in the double lap joint in Fig. 5.4.2e. The reader should especially note the truss connection shown in Fig. 5.4.2c and consider the difficulty in making such a connection by any other type of joint.

**Tee Joints.** This type of joint is used to fabricate built up sections such as tees, H-shapes, plate girders, bearing stiffeners, hangers, brackets, and in general, pieces framing in at right angles as shown in Fig. 5.4.2c. This type of joint is especially useful in that it permits sections to be built up of flat plates which can be joined by either fillet or groove welds.

**Corner Joints.** Corner joints are used principally to form built-up rectangular box sections such as used for columns and for beams required to resist high torsional forces.

**Edge Joints.** Edge joints are generally not structural but are most frequently used to keep two or more plates in a given plane or to maintain initial alignment.

As the reader can infer from the previous discussions, the variations and combinations of the five basic types of welds are virtually infinite. Since there is usually more than one way to connect one structural member to another, the designer is left with the decision for selecting the best joint (or combination of joints) in each given situation.

## 5.5. TYPES OF WELDS

The four basic types of welds are the groove, fillet, slot, and plug welds as shown in Fig. 5.5.1. Each basic type of weld has specific advantages which determines the extent of its usage. The four basic types of welds and their variations constitute virtually all of the structural welds found in common practice. Broadly speaking, the usage of the basic welds are: groove welds, 15 percent; fillet welds, 80 percent; the remaining 5 percent are made up of the slot, plug, and other special welds.

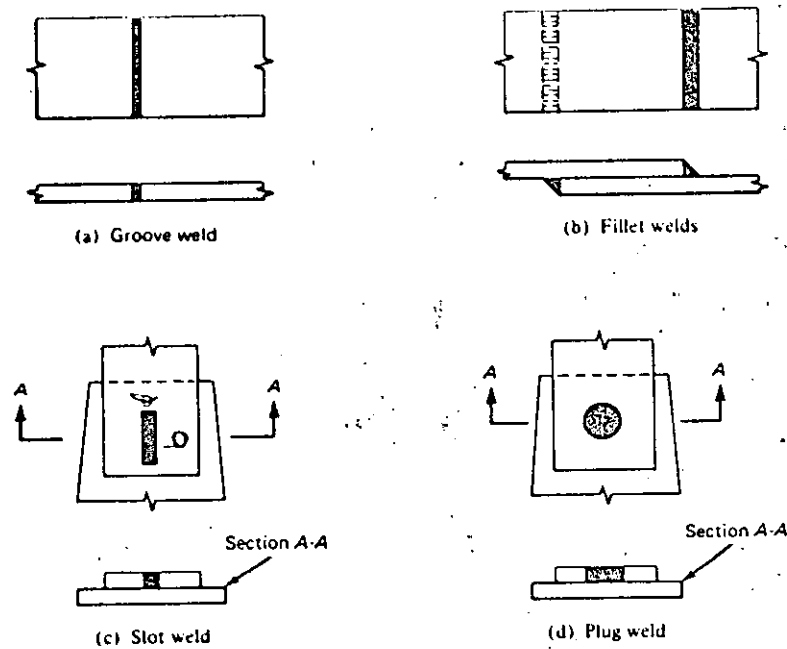


Fig. 5.5.1. Basic types of welds.

**Groove Welds.** The principal use of groove welds is to connect structural members which are aligned in the same plane. Since groove welds must transmit the entire load at a particular joint they usually must have at least as good structural properties as the members which they connect; in which case they may be referred to as full penetration welds. There are many variations of groove welds and each is classified according to its particular shape. Each type of groove weld requires a specific edge preparation and is named accordingly.

Figure 5.5.2 shows the common types of groove welds and indicates the end preparations required for each. The selection of the proper groove weld is dependent on the cost of the edge preparations and the cost of making the weld. The final selection as to which type of groove weld to use must also consider the facilities of the fabricator making the welds, his ability to provide the required edge preparations and whether or not the welding can be done on both sides. Groove welds may also be used in connections as shown in Fig. 5.5.3.

**Fillet Welds.** Fillet welds owing to their overall economy, ease of fabricating, and adaptability are the most widely used of all the basic welds. Fillet welds offer great flexibility to the designer since they are adaptable

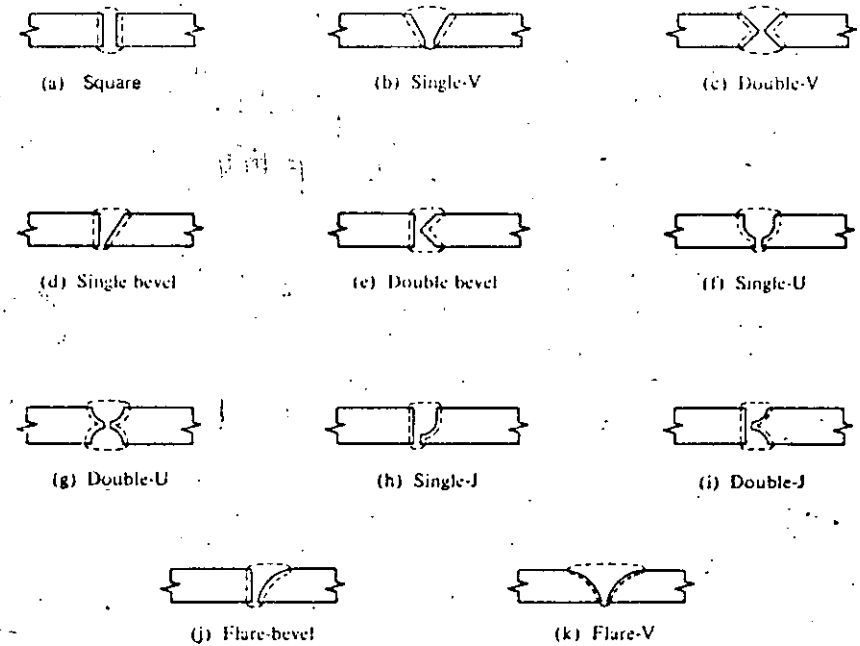


Fig. 5.5.2. Variations of groove welds.



Fig. 5.5.3. Uses of groove welds in tee joints.

to a large variety of connections, a few of which were shown in Fig. 5.5.4. They generally require less precision in the "fitting up" since the plates being joined can be moved about more than groove welds that may require specific gaps or critical alignment. This is particularly advantageous to welding in the field or in realigning members or connections that were fabricated within accepted tolerances but which may not fit as accurately as desired. In addition, the edges of pieces being joined seldom need special preparation such as beveling or squaring since the edge conditions resulting from the usual flame cutting or from shear cutting procedures are generally adequate.

**Slot and Plug Welds.** Slot and plug welds may be used exclusively in a connection as shown in Figs. 5.5.1c and d, or they may be used in combi-

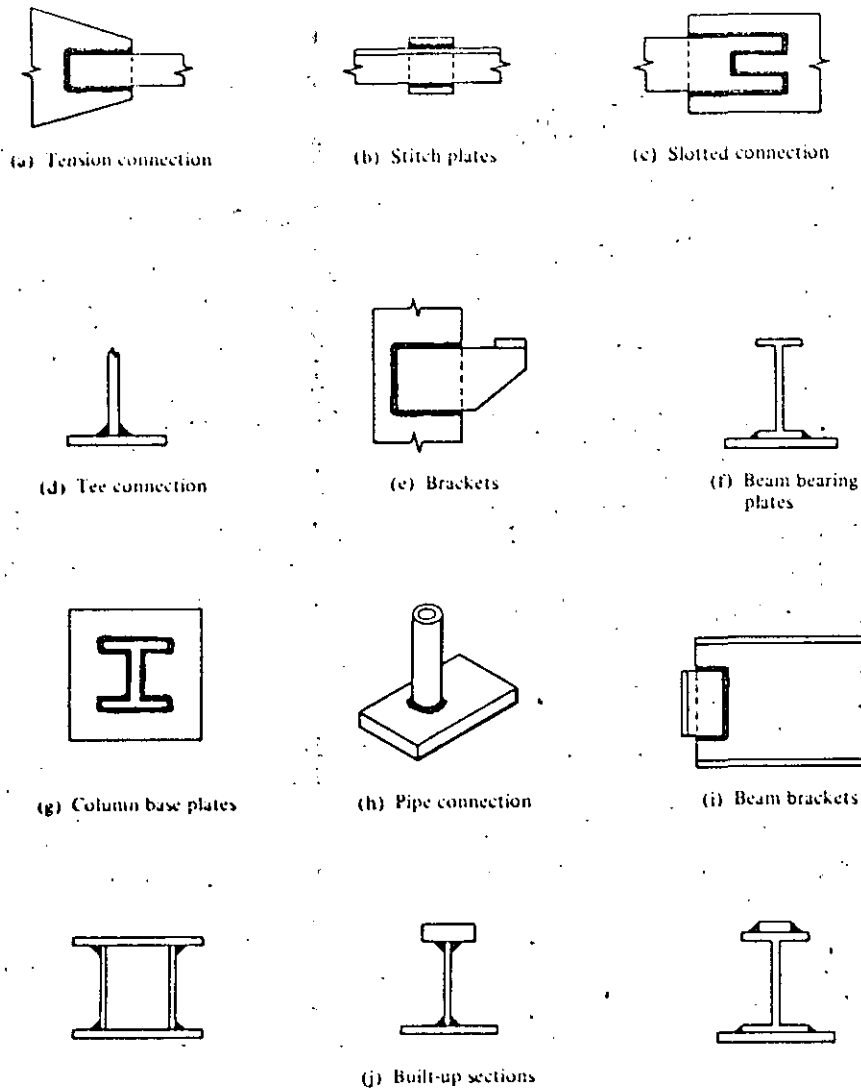


Fig. 5.5.4. Typical uses of fillet welds.

nation with fillet welds as shown in Fig. 5.5.5. A principal use for plug or slot welds is to transmit shear in a lap joint when the size of the connection limits the length available for fillet or other edge welds. Slot and plug welds are also useful in preventing overlapping parts from buckling.

### 5.6. WELDING SYMBOLS

Before a connection or joint is welded, the designer must in some way be able to instruct the steel detailer and the fabricator as to the type

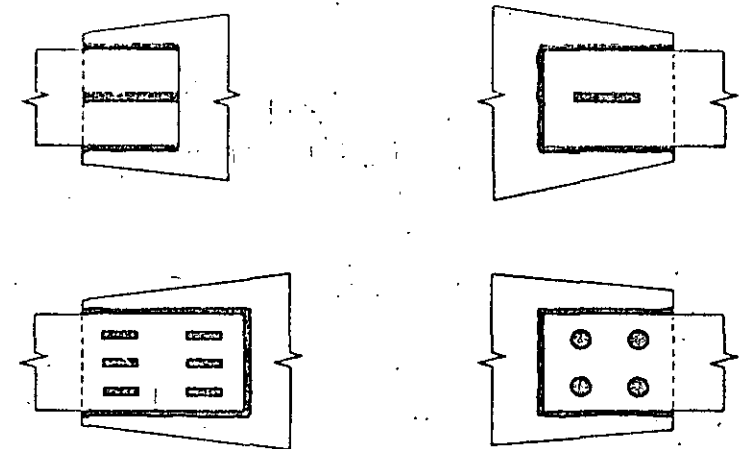


Fig. 5.5.5. Slot and plug welds in combination with fillet welds.

and size of weld required. The basic types of welds and some of their variations are discussed in Sec. 5.5. If individual and detailed instructions were needed each time a connection was made, the task of providing directions for making the joint would indeed be formidable.

The need for a simple and yet accurate method for communicating between the designer and fabricator gave rise to a type of shorthand symbols which characterize the type and size of weld. As a result, the American Welding Society welding symbols, shown in Fig. 5.6.1, indicate the shape of the weld and its size, as well as any special instructions.

Most of the commonly made connections do not require special instructions and are typically specified as shown in Fig. 5.6.2. For a more detailed use of welding symbols the reader is referred to the AISC Manual, various publications of the American Welding Society, and to special publications.<sup>11</sup>

The reader may feel that the number of symbols is burdensome. However, the system of designating welds is broken down into a few basic types which are built up to give a complete set of instructions. Whenever a particular connection is used in many parts of a structure, it may only be necessary to show a typical detail as shown in Fig. 5.6.3a. Whenever special connections are used, they should be detailed sufficiently to leave no doubt as to the designer's intentions, as shown in Fig. 5.6.3b.

In Fig. 5.6.3b the designer specified that the plug weld be made in the shop and ground flush while the double bevel weld connecting the gusset plate to the column be made in the field. Since the designer did not specify where the fillet welds attaching the angle to the gusset plate were to be made, the steel fabricator would be free to make the decision. However, in this particular detail, it would be better to make the fillet welds in the shop since the plug weld might be over stressed during the field erection process. In general, the fabricator will make as many welds in the

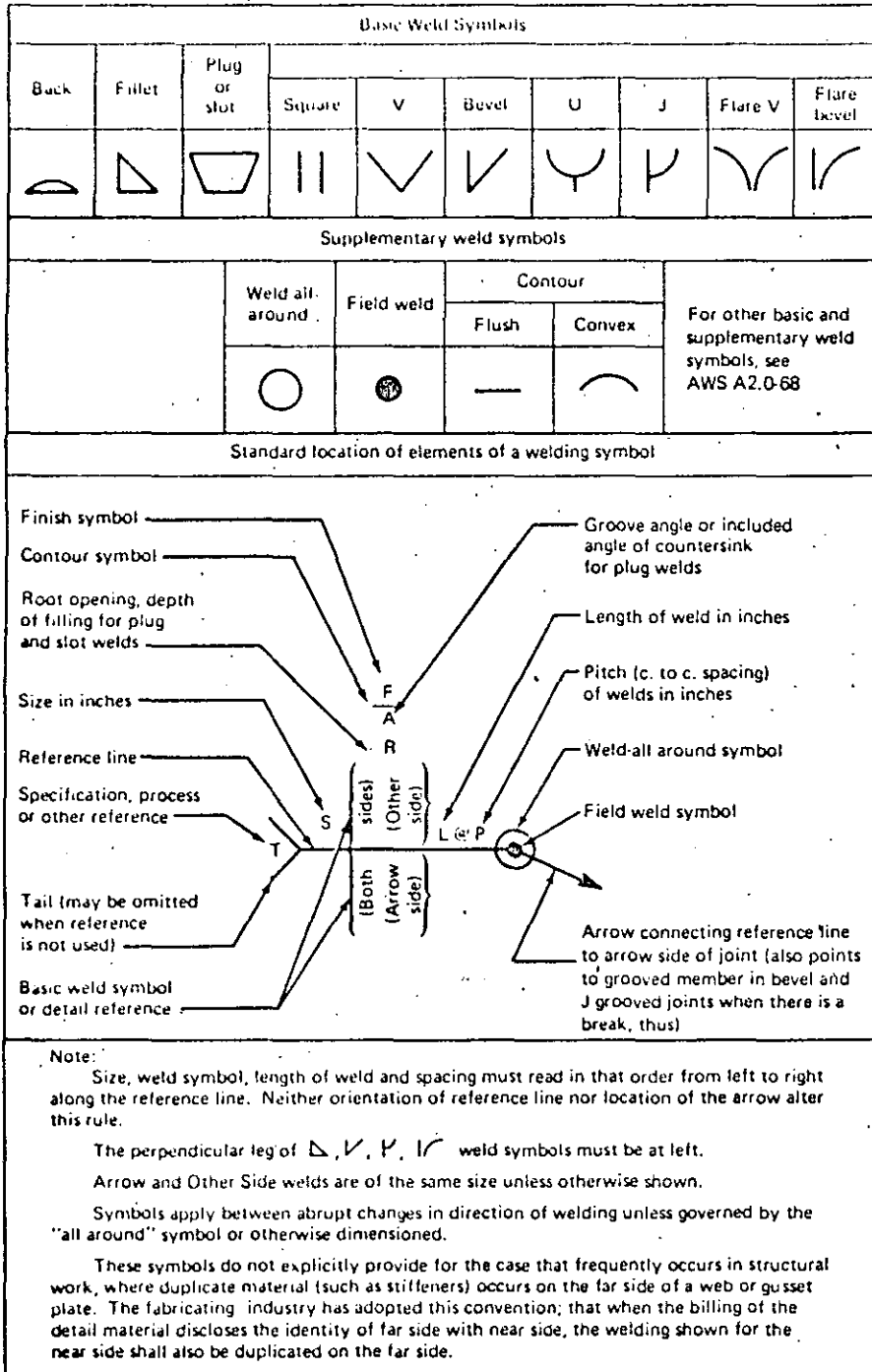


Fig. 5.6.1. Standard welding symbols (from AISC Manual).

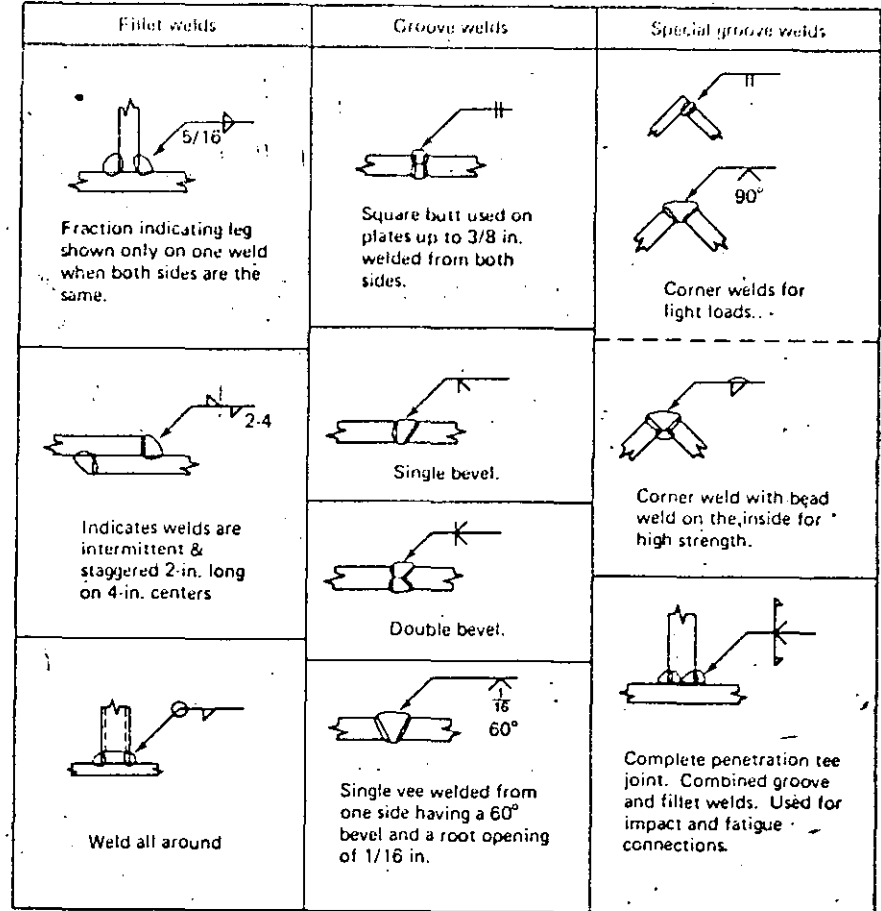


Fig. 5.6.2. Common uses of welding symbols.

shop as he can, due to economic considerations. Therefore, it is most critical that the designer specify those welds he wants to be *field welded*.

### 5.7. FACTORS AFFECTING THE QUALITY OF WELDED CONNECTIONS

Providing a satisfactory welded connection requires the combination of many individual skills, beginning with the actual design of the weld and ending with the welding operation. A well designed weld does not insure a strong connection unless it is properly made in the shop or field. It is therefore necessary that the structural engineer be aware of the factors that affect the quality of a weld and design his connections accordingly.

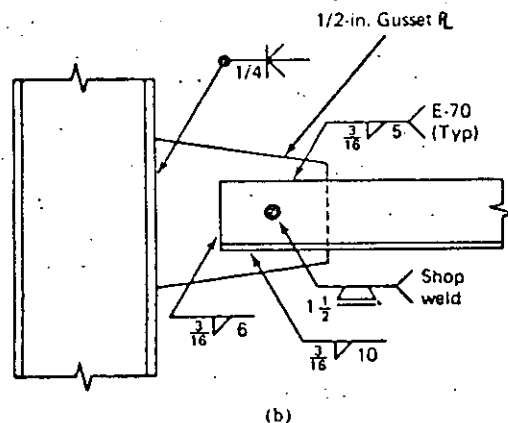
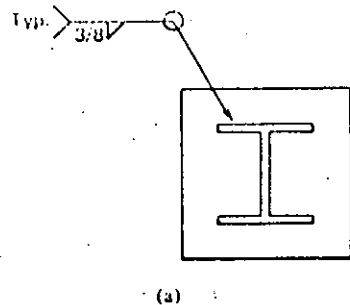


Fig. 5.6.3. Typical welding details.

**Proper Electrodes, Welding Apparatus, and Procedures.** After the proper electrode is specified to match the steel in the pieces being joined as indicated in Sec. 5.12 the diameter of the welding electrode must be selected. The particular size of the electrode selected is based on the size of the weld to be made and on the output of the welding apparatus. It is important that the welding apparatus be capable of providing sufficient current for the size of electrode being used. Since most welding machines have controls for reducing the current output, electrodes smaller than the maximum capability can easily be accommodated and should be used.

Since the depositing of weld metal in metal-arc welding is by the electromagnetic field and not by gravity, the welder is not limited to flat or horizontal welding positions. The four basic welding positions are shown in Fig. 5.7.1. The designer should avoid whenever possible the overhead position as shown in Fig. 5.7.1d, since it is the most difficult to make and control. Joints welded in the shop are usually positioned in the

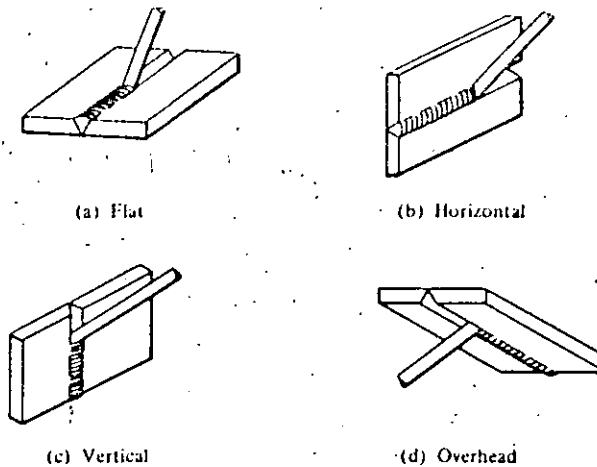


Fig. 5.7.1. Basic welding positions.

flat or horizontal positions but welds made in the field may assume any welding position depending on the orientation of the connection. The designer should therefore use precaution in specifying field welds.

**Proper Edge Preparation.** Typical edge preparations provided for groove welds are shown in Fig. 5.7.2. The root opening *R* is the separation of the

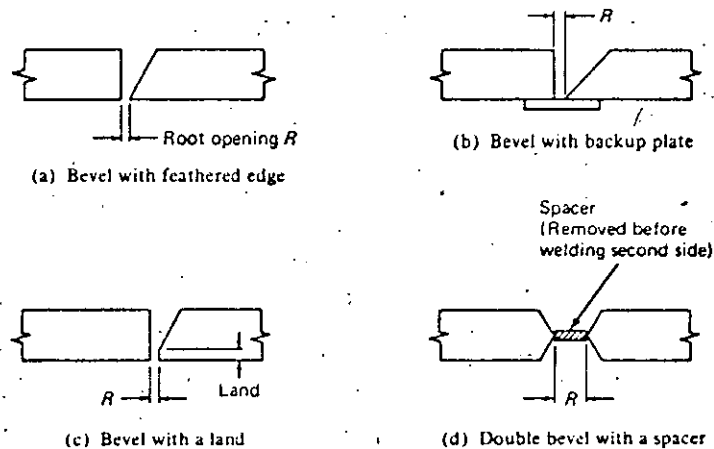


Fig. 5.7.2. Typical edge preparations for groove welds.

pieces being joined and is provided for electrode accessibility to the base of a joint. The smaller the root opening the greater must be the angle of the bevel. The feathered edge as shown in Fig. 5.7.2a is subject to burn-through unless a backup plate is provided as shown in Fig. 5.7.2b.

Backup strips are commonly used when the welding is to be done from one side only. The problem of burn-through is lessened if the bevel is provided a land as shown in Fig. 5.7.2c. The welder should *not* provide a backup plate when a land is provided since there would be a good possibility that a gas pocket would be formed preventing a full penetration weld. Occasionally a spacer, as shown in Fig. 5.7.2d, is provided to prevent burn-through but is gouged out before the second side is welded.

**Control of Distortion.** Another factor affecting weld quality is shrinkage. If a single bead is put down in a continuous manner on a plate, it will cause the plate to distort as shown in Fig. 5.7.3. Such distortions may



Fig. 5.7.3. Distortion of plate.

easily take place unless care is exercised in both the design of the joint and the welding procedure. Figure 5.7.4 shows the result of using unsym-

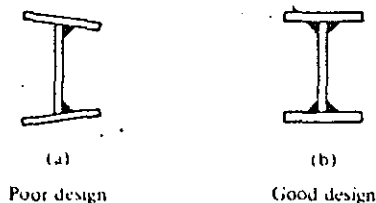


Fig. 5.7.4. Effect of weld placement.

metrical welds as compared to symmetrical welds. Although there are many techniques available for minimizing distortion, the most common one is that of staggering intermittent welds as shown in Fig. 5.7.5a, and then returning to fill in the spaces as shown in Fig. 5.7.5b, a typical sequence being shown. For many structures, such as plate girders, short segments of weld (though not usually regular intermittent welds) may be used at strategic locations to give enough strength to hold all pieces in place; then, the continuous lines of weld are placed.

To minimize shrinkage and to insure adequate ductility, the American Welding Society has established recommendations for minimum preheat and interpass temperatures which are summarized in Table 5.7.1 (see p. 184) from AISC-1.23.6.

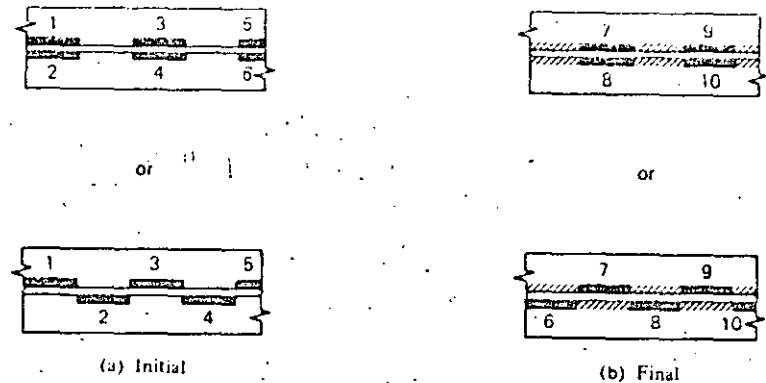


Fig. 5.7.5. Sequences for intermittent welds.

The following summarizes ways of minimizing distortion:

1. Reduce the shrinkage forces by
  - (a) Using minimum weld metal; for grooves use no greater root opening than necessary; do not overweld.
  - (b) Using as few passes as possible.
  - (c) Using proper edge preparation and fit-up.
  - (d) Using intermittent weld, at least for preliminary connection.
  - (e) Using backstepping; depositing weld segments toward the previously completed weld; i.e., depositing in the direction opposite to the progress of welding the joint.
2. Allow for the shrinkage to occur by
  - (a) Tipping the plates so after shrinkage occurs they will be correctly aligned.
  - (b) Using prebending of pieces.
3. Balance shrinkage forces by
  - (a) Using symmetry in welding; fillets on each side of a piece contribute counteracting effects.
  - (b) Using scattered weld segments.
  - (c) Using peening; stretching the metal by a series of blows.
  - (d) Using of clamps, jigs, etc; this forces weld metal to stretch as it cools.

## 5.8. POSSIBLE DEFECTS IN WELDS

Unless good welding techniques and procedures are used, a number of possible defects may result relating to discontinuities within the weld. Some of the more common defects are: incomplete fusion, inadequate

TABLE 5.7.1  
(AISC Table 1.23.6)  
Minimum Preheat and Interpass Temperature, °F<sup>1</sup>

Thickness of Thickest Part at Point of Welding (inches)	Welding Process				ASTM A514
	Shielded Metal-Arc Welding with Low Hydrogen Electrodes	Shielded Metal-Arc Welding with Low Hydrogen Electrodes; Submerged Arc Welding; Gas Metal-Arc Welding, or Flux Cored Arc Welding	Shielded Metal-Arc Welding with Low Hydrogen Electrodes; Submerged Arc Welding with Carbon or Alloy Steel Wire; Neutral Flux, Gas Metal-Arc Welding, or Flux Cored Arc Welding	Submerged Arc Welding with Carbon Steel Wire, Alloy Flux	
To 1/4 in.	None 2,3	None 2	70	50	50
Over 1/4 to 1 1/2 in.	150	70 <sup>4</sup>	150	125	200
Over 1 1/2 to 2 1/2 in.	225	150 <sup>4</sup>	225	175	300
Over 2 1/2 in.	300	225	300	225	400

<sup>1</sup>Welding shall not be done when the ambient temperature is lower than 0°F. When the base metal is below the temperature listed for the welding process, being used and the thickness of material being welded, it shall be preheated except as otherwise provided in such manner that the surface of the part on which weld metal is being deposited are at or above the specified minimum temperature for a distance equal to the thickness of the part being welded, but not less than 3 in., both laterally and in advance of the welding. Preheat and interpass temperatures must be sufficient to prevent crack formation. Temperature above the minimum shown may be required for highly restrained weld. For A514 steel the maximum preheat and interpass temperature shall not exceed 400°F for thicknesses up to 1 1/2 in., inclusive, and 450°F for greater thicknesses.

<sup>2</sup>When base metal temperature is below 32°F, preheat base metal to at least 70°F and maintain this minimum temperature during welding.

<sup>3</sup>This provision also applies to A36 steel in thicknesses up to 1 in.

<sup>4</sup>Minimum preheat for A36 steel in thicknesses up to 2 in. shall be 50°F.

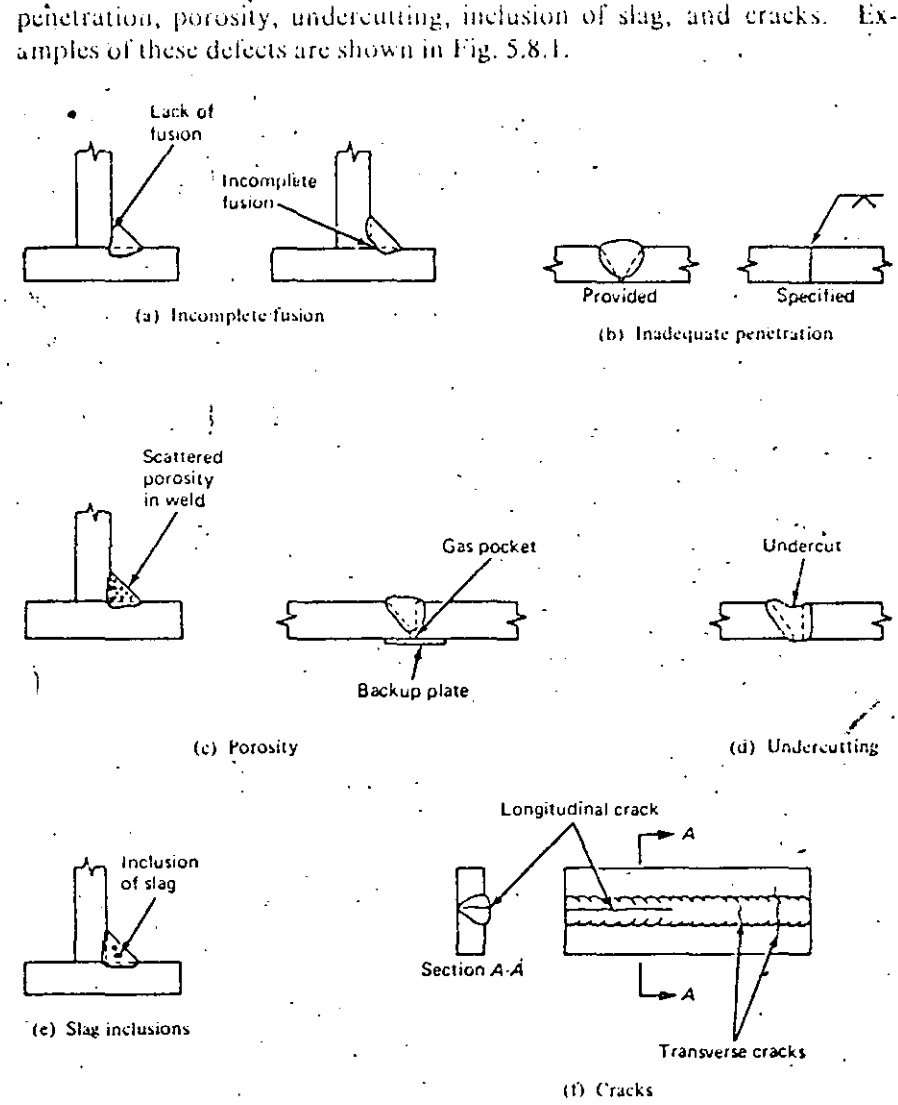


Fig. 5.8.1. Possible weld defects.

**Incomplete fusion.** Incomplete fusion may occur if the surfaces to be joined have not been properly cleaned and are coated with mill scale, slag, oxides or other foreign materials. Another cause of this type of defect is the use of welding equipment of insufficient current, so that base metal does not reach melting point. Too rapid a rate of welding will also have the same effect.



**Inadequate Penetration.** Inadequate penetration means the weld extends a shallower distance through the depth of the groove than specified, as shown in Fig. 5.8.1, where complete penetration was specified: Partial penetration may be adequate penetration for some situations.

This type of defect, relating primarily to groove welds, occurs as a result of insufficient groove angles, excessively large electrodes, insufficient welding current, excessive welding rates or insufficient gaps at the root of the welds. Using backup plates is a useful means to prevent this defect.

**Porosity.** Porosity occurs when voids or a number of small gas pockets are trapped during the cooling process. This type of defect results from using excessively high current or too long an arc length. Porosity may occur uniformly dispersed through the weld, or it may be a large pocket concentrated at the root of a fillet weld or at the root adjacent to a backup plate in a groove weld. The latter is caused by poor welding procedures and careless use of backup plates.

**Undercutting.** The use of excessive current or an excessively long arc may burn or dig away a portion of the base metal reducing the thickness of the joint at the edge of the weld. This type of defect is easily detected by visual inspection and can be corrected by depositing additional weld material.

**Slag Inclusion.** Slag is formed during the welding process as a result of chemical reactions of the melted electrode coating and consists of metal oxides and other compounds. Having a lower density than the molten weld metal, the slag normally floats to the surface, where upon cooling, it is easily removed by the welder. However, too rapid a cooling of the joint may trap the slag before it can rise to the surface. Overhead welds as shown in Fig. 5.7.1d are especially subject to slag inclusions and must be carefully inspected. When several passes are necessary to obtain the desired weld size, the welder must remove slag between each pass. Failure to properly do so is a common cause of slag inclusion.

**Cracks.** Cracks are breaks in the weld metal, either longitudinal or transverse to the line of weld which result from internal stress. Cracks may also extend from the weld metal into the base metal or may be entirely in the base metal in the vicinity of the weld. Cracks are perhaps the most harmful of weld defects; however, tiny cracks called *microfissures* may not have any detrimental effect.

Some cracks form as the weld begins to solidify, generally caused by brittle constituents, either brittle states of iron or alloying elements, form-

ing along the grain boundaries. More uniform heating and slower cooling will prevent the "hot" cracks from forming.

Cracks may also form at room temperature parallel to but under the weld in the base material. These cracks arise in low-alloy steels from the combined effects of hydrogen, a brittle martensite microstructure, and restraint to shrinkage and distortion. Use of low-hydrogen electrodes along with proper preheating and postheating will minimize such "cold" cracking.

## 5.9. INSPECTION AND CONTROL

The enormous success and growth in recent years in the area of structural welding of buildings and bridges could not have occurred without some means of inspection and control. The welding industry has led in the development of guidelines which, if followed, virtually insure a sound weld. The inspection and control procedure should begin before the first arc is struck, continue throughout the welding procedure, and if necessary, a pretest of the joint should be made to assure its satisfactory performance. Since such close supervision is not possible on every weld made, the following suggestions will serve as a guideline to achieve good structural welds:

- (a) Establish good welding procedures.
- (b) Use only prequalified welders.
- (c) Use qualified inspectors and have them present.
- (d) Use special inspection techniques when necessary.

Good welding procedures can be developed from recommendations from the AWS, AISC, and the manufacturers of welding supplies and equipment. The procedure to be followed will depend on the chemical and physical properties of the materials, the types and sizes of weld, and the particular equipment used.

All welders should be required to have passed an American Welding Society Qualification Test before being permitted to make a structural connection. Although this is usually considered adequate, it doesn't prove the ability of the welder to make welds at the actual job site, particularly if the welds are unusual or difficult and were not specified in the Qualification Test. Happily, most welding contractors exercise their own control over their welders in such situations.

The use of qualified welding inspectors at a jobsite generally has the effect of causing welders to perform their best work, feeling that the inspector is able to recognize the quality of their welds. The welding inspector should be a competent welder himself and be able to recognize the possible defects discussed in Sec. 5.8. Any poor or suspicious welds should be cut out and replaced.

The simplest and least expensive method of inspection is *visual* but is dependent on the competence of the observer. A welding gage such as shown in Fig. 5.9.1a offers a rapid means of checking the size of fillet welds.

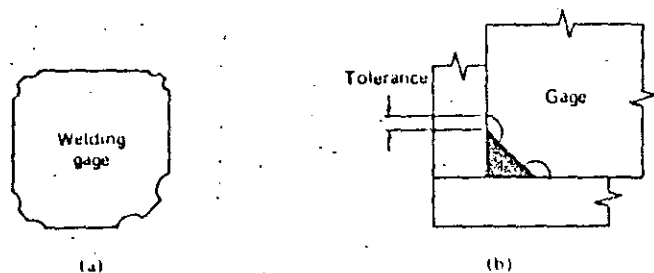


Fig. 5.9.1. Checking size of fillet welds.

For more important structures and for welds whose failure could be catastrophic, more rigid inspection techniques should be used. Some of the useful ones are the ultrasonic, radiographic, and magnetic particle methods. The *ultrasonic* method<sup>12</sup> passes ultrahigh-frequency sound waves through the weldment. Defects in a particular weld will reflect the sound waves while a weld without defects will not impede passage of the waves. *Radiographic* methods include the use of both X-rays and gamma rays. In this method the radiating source is placed on one side of the weld and a photographic plate on the other. This method is expensive and requires special precautions be taken due to the hazards of radiation. However, the method is reliable and furnishes a permanent record. The *magnetic particle* testing method uses iron powder which is spread around the welded area and polarized by passing an electric current through the weld. Small local poles will be formed at the edges of any defects, and this may be interpreted by an experienced observer.

## 5.10. ECONOMICS OF WELDED MEMBERS AND CONNECTIONS

There are many factors which must be examined when considering the overall economy in welded connections. Some of the factors such as the amount of electrode material used can easily be computed while other factors may be intangible such as the value to be placed on esthetics. The actual economy of welded connections must be viewed from a broad aspect and include the overall design of the structural system.

Welded connections are usually neater in appearance, providing a less cluttered effect in contrast to bolted or riveted connections. Figure 5.10.1 shows a comparison between a section of a riveted or bolted plate girder and a section of a welded plate girder. Besides the neater appearance of

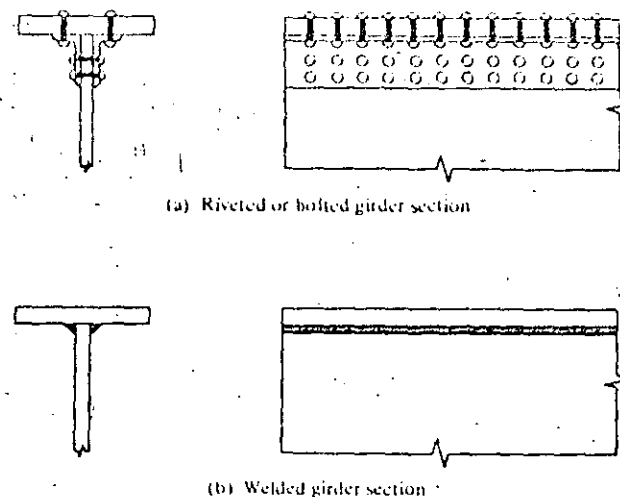


Fig. 5.10.1. Comparison between plate girders.

the welded joint, welded connections offer the designer more freedom to be innovative in his entire design concept. The designer is not bound to standard sections but may build up any cross section he feels to be most advantageous. Similarly, he can use the best configuration to transmit the loads from one member to another.

Welded connections generally eliminate the need for holes in members except possibly for erection purposes. Therefore, the problem of determining the minimum net section in tension members as discussed in Chapter 3 need not be considered. Since it is usually the holes at the ends that govern the design of a bolted or riveted tension member, a welded connection will generally result in a member with a smaller cross section.

Welded connections can sometime reduce field construction costs by the fact that members may be shifted slightly to accommodate minor errors in fabricating or erection. Also, members may be easily shortened by cutting and rejoining by suitable welding as well as lengthened by splicing a piece of the same cross section.

In addition, there are several direct factors which influence the cost of welding. Generally, welding that is performed in the shop is less expensive than field welding. Some of the reasons for this are availability in the shop of automatic welding machines, a more pleasant and less hostile environment (the weather), and the availability of special jigs for holding the pieces to be welded in a more favorable position. Also, work to be done can be scheduled for a continuous operation whereas field welding must often wait for cranes and special erection equipment. Other operations such as the proper preheating of pieces to be welded can be difficult if not impossible to perform in the field. Other factors which influence

TABLE 5.10.1  
Relative Cost Factors for Welded Joints<sup>1)</sup>  
(Based on a Cost Factor at 1.00 for a 1/4 in. Fillet Weld)

Type Size (1/16 in.)	Fillet 45°		Fillet 60°-30°		Single V 60°		Single V 90°		Single Bevel 45°		Single Bevel 60°		Double V 60°		Double Bevel 45°		Double Bevel 60°		Square Groove		Plug Welds (per 100 holes 1 in. deep)	
	Diagram	Factor	Diagram	Factor	Diagram	Factor	Diagram	Factor	Diagram	Factor	Diagram	Factor	Diagram	Factor	Diagram	Factor	Diagram	Factor	Diagram	Factor	Diagram	Factor
1/16		0.55		0.65		1.35		1.75		1.30		1.35		1.20		1.75		2.00		0.55		25.20
1/8		0.70		0.80		1.80		2.70		1.80		1.95		1.45		2.50		2.20		0.60		39.50
3/16		0.85		0.95		2.50		3.60		2.50		2.70		1.85		3.45		2.90		0.80		57.50
1/4		1.00		1.25		3.45		4.95		3.15		3.45		2.40		3.90		3.70		1.00		78.80
5/16		1.20		1.75		3.80		5.10		3.50		3.90		2.90		4.70		4.30		1.20		104.00
3/8		2.00		3.30		5.55		8.00		5.05		5.55		4.70		7.55		6.45		1.50		132.00
7/16		2.60		4.20		7.85		11.50		7.10		7.90		5.45		10.10		8.20		4.80		165.00
1/2		3.80		6.30		10.20		15.30		9.10		10.22		7.05		12.95		9.65		5.55		
5/8		5.30		8.90		12.80		20.15		11.50		12.95		9.15		13.25		10.00				
3/4		7.10		12.00		15.70		25.60		14.15		15.95		11.15		16.45		11.80				
1		9.15		15.50		19.00		30.20		16.90		19.10		13.15		19.85		14.10				
1 1/8		11.50		19.50		22.50		35.70		20.15		22.75		15.70		24.00		16.70				
1 1/4		14.10		24.00		26.40		42.85		23.60		26.75		18.30		28.10		19.60				
1 1/2		17.00		29.10		30.90		49.80		27.30		31.20		20.80		32.50		22.60				
1 3/4		20.00		34.50		35.40		59.00		31.20		35.60		23.40		36.90		25.40				
2					40.00		45.00	69.20		35.50		40.40		26.20		41.15		28.20				
2 1/4					45.00			79.00		40.00		45.50		29.00		46.40		31.10				
2 1/2																						
2 3/4																						
3																						

Notes: Factors apply to all weld processes. A single weld position is assumed for entire weld.

welding costs are:

1. Cost of preparing the edges to be welded.
2. The amount of weld material required.
3. The ratio of the actual arc time to overall welding time.
4. The amount of handling required.
5. General overhead costs.

The factors listed above are generally unknown to the designer since the fabricator is usually not selected until after the design has been completed. However the designer must still make decisions—should he specify short large fillet welds or long small fillet welds? Should he specify large fillet welds or groove welds? If he decides to use groove welds he must then select the proper and most economical type.

In most instances the designer is not as concerned with the specific costs of each type of weld as he is with *relative* cost of the various types and sizes. As aid to the designer, Donnelly<sup>13</sup> developed relative cost factors relating the cost of fillet and groove welds of common sizes to the cost of a single-pass 1/4 in. fillet weld. This work is reproduced in Table 5.10.1. The cost of a specific weld can be determined by Eq. 5.10.1 once the designer can obtain the local costs.

$$\text{Cost of Weld} = (\text{Length of Weld}) \times (\text{Factor from Table 5.10.1}) \times (\text{Local Cost}) \quad (5.10.1)$$

Currently (1971), welded connections are used for the vast majority of shop connections and a sizable though not a majority of field connections.

### 5.11. SIZE AND LENGTH LIMITATIONS FOR FILLET WELDS

Since all types of welding involve the heating of the metal pieces, prevention of too rapid a rate of cooling is of fundamental importance to achieving a good weld. It is therefore imperative to consider the effect of the plate thickness on rate of cooling. Consider the two extreme thicknesses of plates in Fig. 5.11.1, each of which has received a bead of fillet weld. Most of the heat energy given off during the welding process is absorbed by plates being joined. The thicker plate shown in Fig. 5.11.1a dissipates the heat vertically as well as horizontally whereas the thinner plate is essentially limited to a horizontal dissipation. In other words, the thicker the plate, the faster heat is removed from the welding area, thereby lowering the temperature in the region of the weld. Since a minimum temperature is required to cause the base metal to become molten, it is therefore necessary to provide as a minimum, a weld of sufficient size (and heat content) to prevent the plate from removing the heat at a faster rate than it is being supplied. Unless a proper temperature is maintained in the area being welded a lack of fusion will result.

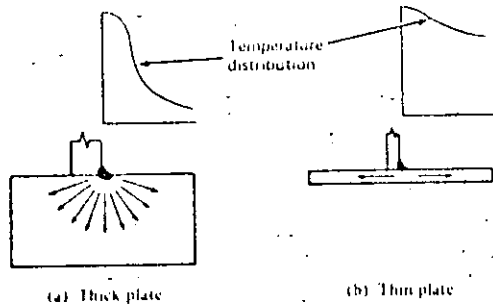


Fig. 5.11.1. Effect of thickness on cooling rate.

**Minimum Fillet Weld Size.** Recognizing the effect of plate thickness in the cooling rate, *minimum* fillet weld sizes have been established to insure fusion and to minimize distortion. Table 5.11.1 shows the minimum sizes of fillet welds depending on the plate thicknesses.

TABLE 5.11.1  
(AISC-Table 1.17.5)  
Minimum Fillet Weld Sizes

Material Thickness of Thicker Part Joined, inches	Minimum Size of Fillet Weld, inches
To 1/4 inclusive	1/8
Over 1/4 to 1/2	3/16
Over 1/2 to 3/4	1/4
Over 3/4 to 1 1/2	5/16
Over 1 1/2 to 2 1/4	3/8
Over 2 1/4 to 6	1/2
Over 6	5/8

According to the AISC-1.17.5, the above fillet weld sizes are governed by the thicker of the two pieces being joined, except that the weld size need not exceed the thickness of the thinner piece joined unless a larger size is required by calculated stress.

**Maximum Fillet Weld Size Along Edges.** The *maximum* size of fillet welds used along the edges of pieces being joined is limited by the thickness of the thinner piece. The maximum permitted by AISC-1.17.6 is, as shown in Fig. 5.11.2.

1. Along edges of material less than 1/4 in. thick, the maximum size may be equal to the thickness of the material.
2. Along edges of material 1/4 in. or more in thickness, the maximum size shall be 1/16 in. less than the thickness of the material, unless the weld is especially designated on the drawings to be built out to obtain full throat thickness.

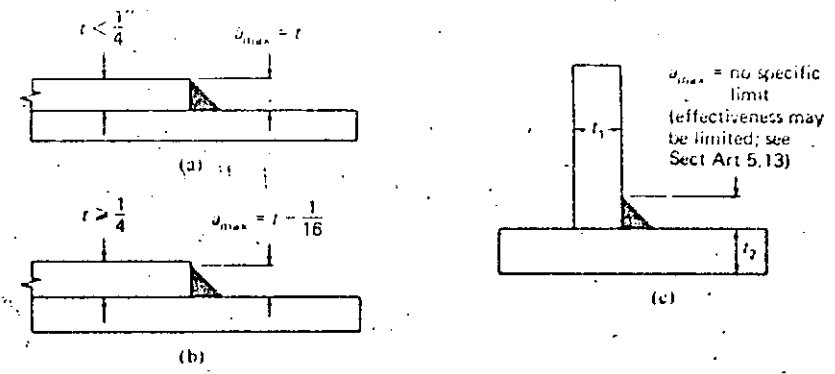


Fig. 5.11.2. Maximum weld size.

**Minimum Effective Length of Fillet Welds.** When placing a fillet weld, the welder builds up the weld to its full dimension as near the beginning of the weld as he can. However, there is always a slight tapering off in the region where the weld is started and where it ends. AISC-1.17.7 therefore limits the minimum effective length of fillet welds to four times their nominal size. If this criterion is not met, the size of the weld shall be considered to be one-fourth of the effective length.

AISC-1.17.10 also recommends the use of end returns, whenever practicable as shown in Fig. 5.11.3. For other limitations the reader is referred to the AISC Specification.

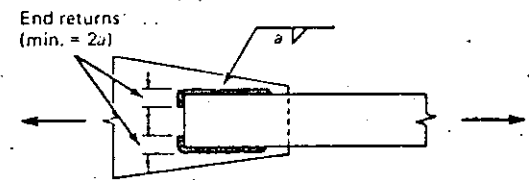


Fig. 5.11.3. Use of end returns.

**5.12. ALLOWABLE STRESSES**

Since welds must transmit the entire load from one member to another, welds must be sized accordingly and be formed from the correct electrode material.

While distribution of stresses in fillet welds is discussed in Sec. 5.14, it is noted here that fillet welds are assumed for design purposes to transmit loads through *shear stress* on the effective area no matter how the fillets are oriented on the structural connection. Groove welds transmit loads exactly as the pieces they join.

The required electrode material for groove welds depends on the base

TABLE 5.12.1  
(AISC-Table I.17.2)  
Electrodes for Use with Various Steels

Base Metal <sup>3</sup>	Welding Process			
	Shielded Metal-Arc	Submerged-Arc	Gas Metal-Arc	Flux Cored-Arc
ASTM A36, A53 Gr. B, A375, A500, A501, A529, and A570 Gr. D and E	AWS A5.1 or A5.5, E60XX or E70XX <sup>5</sup>	AWS A5.17 F6X or F7X-EXXX	AWS A5.18 E70S-X or E70U-1	AWS 5.20 E60T-X or E70T-X (except EXXX-2 and EXX-3)
ASTM A242, A441, A572 Grades 42 thru 60 and A588 <sup>4</sup>	AWS A5.1 or A5.5, E70XX <sup>5</sup>	AWS A5.17 F7X-EXXX	AWS A5.18 E70S-X or E70U-1	AWS 5.20 E70T-X (except E70T-2 and E70T-3)
ASTM A572 Grade 65	AWS A5.5 E80XX <sup>5</sup>	Grade F80	Grade E80S	Grade E80T
ASTM A514 over 2 1/2" thick	AWS A5.5 E100XX <sup>5</sup>	Grade F100	Grade E100S	Grade E100T
ASTM A514 2 1/2" thick and under	AWS A5.5 E110XX <sup>5</sup>	Grade F110	Grade E110S	Grade E110T

Use of the same type filler metal having next higher mechanical properties is permitted.

<sup>1</sup>When welds are to be stress relieved the deposited weld metal shall not exceed 0.05 percent vanadium.

<sup>2</sup>See Article 422 of AWS D1.0-69 for electrode and electrode gas metal requirements.

<sup>3</sup>On joints involving base metals of different yield strengths, filler metals applicable to lower yield strength may be used.

<sup>4</sup>For architectural exposed bare unpainted applications, the deposited weld metal shall have similar atmospheric corrosion resistance and coloring characteristics as the base metal used. The steel manufacturer's recommendation shall be followed.

<sup>5</sup>Low hydrogen classifications.

metal in the members and is given in Table 5.12.1 for various welding processes. When the electrodes specified in Table 5.12.1 are used, the allowable tension, compression, and shear stresses on complete penetration groove welds are the same as for the base metal, as summarized in Table 5.12.2.

TABLE 5.12.2  
(from AISC Table I.5.3)  
Allowable Stresses in Groove Welds

Kind of Stress	Permissible Stress
Tension and compression parallel to axis of any complete-penetration groove weld	Same as for base metal
Tension normal to effective throat of complete-penetration groove weld	Same as allowable tensile stress for base metal
Compression normal to effective throat of complete or partial-penetration groove weld	Same as allowable compressive stress for base metal
Shear on effective throat of complete- and partial-penetration groove welds	Same as allowable shear stress for base metal

The allowable stresses for (1) shear on the effective area of fillet welds, (2) the tensile stress normal to the axis on the effective area of a partial penetration groove weld; and (3) the shear stress on the effective area of a plug or slot weld are shown in Table 5.12.3 and are equal to 0.3 times the electrode tensile strength.

The allowable stresses on fillet welds (Table 5.12.3) have been significantly increased in the 1969 AISC Specification over those previously used. For the E60 and E70 electrodes, the only ones included in 1963 AISC Specification, the increase is about 33 percent. Recent tests<sup>14</sup> and reevaluation of earlier tests have resulted in this increase. Reference 14 states "in recognition of improvements in the art of welding that have taken place in the past 40 years, the more liberal working stress provision — 0.3 times the electrode tensile strength — appears fully justified."

The effective areas are discussed in Sec. 5.13 and the limitations on the maximum and minimum size of fillet welds are discussed in Sec. 5.11.

### 5.13. ESTABLISHING EFFECTIVE AREAS OF WELDS

The allowable stresses on the various types of welds summarized in Sec. 5.12 are dependent upon their *effective areas*. The effective areas of groove or fillet welds are considered to be the product of the *effective throat* dimension  $t_e$ , times the length of the weld.

The effective throat dimension is based on the nominal size and the shape of the weld. The nominal throat dimension may be thought of as the minimum width of the expected failure plane. The following discus-

TABLE 5.12.3  
Allowable Stresses in Fillet Welds and Plug or Slot Welds  
(from AISC-1.5.3)

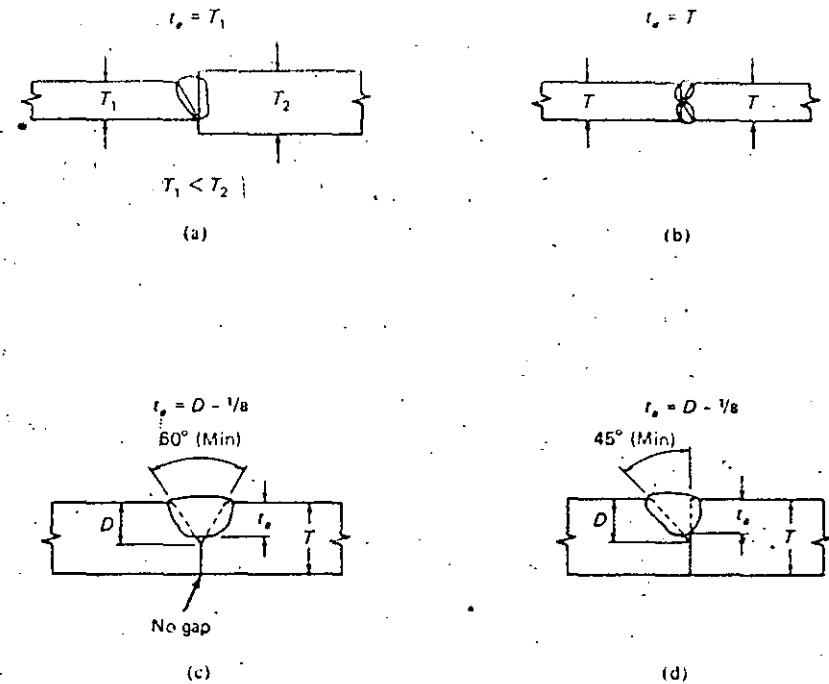
Kind of Stress	Permissible Stress	Required Electrode <sup>2</sup>	"Matching" Base Metal <sup>2</sup>
Shear stress on effective throat of fillet weld regardless of direction of application of load; tension normal to the axis on the effective throat of a partial-penetration groove weld; and shear stress on effective area of a plug or slot weld. The given stresses shall also apply to such welds made with the specified electrode on steel having a yield stress greater than that of the "matching" base metal. The permissible stress, regardless of electrode classification used, shall not exceed that given in the table for the weaker "matching" base metal being joined.	18.0 ksi	AWS A5.1, E60XX electrodes AWS A5.17, F6X-FXXX flux-electrode combination AWS A5.20, E60F-X electrodes	A500 Grade A A570 Grade D
	21.0 ksi	AWS A5.1 or A5.5, E70XX electrodes AWS A5.17, F7X-EXXX flux-electrode combination AWS A5.18, E70S-X or E70U-1 electrodes AWS A5.20, E70T-X electrodes	A36 A53 Grade B A242 A375 A441 A500 Grade B A501 A529 A570 Grade E A572 Grades 42 to 60 A588
	24.0 ksi	AWS A5.5, E80XX electrodes Grade 80 Submerged Arc, Gas Metal-Arc or Flux Cored Arc Weld Metal	A572 Grade 65
	27.0 ksi	AWS A5.5, E90XX electrodes Grade 90 Submerged Arc, Gas Metal-Arc or Flux Cored Arc Weld Metal	A514 over 2 1/2 in. thick
	30.0 ksi	AWS A5.5, E100XX electrodes Grade 100 Submerged Arc, Gas Metal-Arc or Flux Cored Arc Weld Metal	A514 over 2 1/2 in. thick
33.0 ksi	AWS A5.5, E110XX electrodes Grade 110 Submerged Arc, Gas Metal-Arc or Flux Cored Arc Weld Metal	A514 2 1/2 in. and less in thickness	

<sup>1</sup>Fillet welds and partial penetration groove welds joining the component elements of built-up members, such as flange-to-web connections, may be designed without regard to the tension or compression stress in these elements parallel to the axis of the welds.

<sup>2</sup>Only low-hydrogen electrodes shall be used on A242, A441, A514, A572 and A588.

sion will consider the effective throat dimensions for each of the basic types of welds.

**Groove welds.** The effective throat dimension of a full penetration groove weld is the thickness of the thinner part joined as shown in Figs. 5.13.1a and b. The effective throat dimension of single and double partial-penetration groove welds is the depth of the groove except in the case of a bevel joint made by the manual shielded metal-arc process. In the latter case, the effective throat dimension shall be taken (AISC-1.14.7) as the



Note: welds (c) & (d) made by manual shielded metal-arc process

Fig. 5.13.1. Effective throat dimensions for groove welds (AISC-1.14.7).

depth of the groove less 1/8 in. but cannot be less than  $\sqrt{t_1/6}$  where  $t_1$  is the thickness of the thinner piece being joined, as shown in Figs. 5.13.1c and d.

**Fillet Welds.** The effective throat dimension of fillet welds is the shortest distance from the root to the face of the weld, as shown in Fig. 5.13.2. Assuming the fillet weld to have equal legs of nominal size  $a$ , the effective throat,  $t_e$ , is  $0.707a$ . If the fillet weld is designed to be unsymmetrical (a rare situation) with unequal legs, as shown in Fig. 5.13.2b, the value of  $t_e$

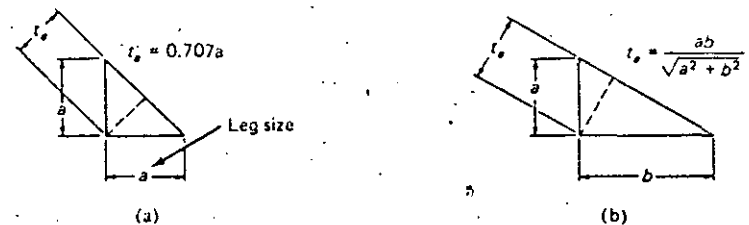


Fig. 5.13.2. Effective throat dimensions for fillet welds (except by submerged-arc process).

must be computed from the diagrammatic shape of the weld. The effective throat dimensions for fillet welds made by the submerged arc process are modified by AISC-1.14.7 as follows:

- (a) For fillet welds with the leg size equal to or less than  $\frac{3}{8}$  in., the effective throat dimension shall be taken as equal to the leg size  $a$ .
- (b) For fillet welds larger than  $\frac{3}{8}$  in., the effective throat dimension shall be taken as the theoretical throat dimension plus 0.11 in. (i.e.,  $0.707a + 0.11$ ).

Tables 5.13.1 and 5.13.2 summarize the effective throat dimensions and the allowable shear resistance  $R_w$  of fillet welds in kips per inch of weld.

TABLE 5.13.1  
Allowable Resistance of Fillet Welds, kips/in.  
(Metal Shielded-Arc Process)

Allowable Shear in Fillet Welds, $R_w$ , Kips per Inch of Weld							
Nominal Size, in.	Effective Throat (AISC-1.14.7)	Minimum Tensile Strength of Weld, ksi					
		60	70	80	90	100	110
$\frac{1}{8}$	0.088	1.59	1.86	2.12	2.39	2.69	2.92
$\frac{1}{16}$	0.132	2.38	2.78	3.18	3.58	3.97	4.37
$\frac{3}{16}$	0.177	3.18	3.71	4.24	4.77	5.30	5.83
$\frac{1}{4}$	0.221	3.98	4.64	5.30	5.96	6.63	7.30
$\frac{5}{16}$	0.265	4.77	5.57	6.36	7.16	7.95	8.75
$\frac{3}{8}$	0.309	5.57	6.49	7.42	8.35	9.28	10.21
$\frac{7}{16}$	0.353	6.36	7.42	8.48	9.54	10.60	11.66
$\frac{1}{2}$	0.398	7.16	8.35	9.54	10.74	11.93	13.12
$\frac{9}{16}$	0.442	7.95	9.28	10.61	11.93	13.26	14.58
$\frac{5}{8}$	0.486	8.75	10.21	11.67	13.12	14.58	16.04
$\frac{3}{4}$	0.530	9.54	11.13	12.72	14.31	15.91	17.50

TABLE 5.13.2  
Allowable Resistance of Fillet Welds, kips/in.  
(Submerged-Arc Process)

Allowable Shear in Fillet Welds, $R_w$ , Kips per Inch of Weld							
Nominal Size, in.	Effective Throat (AISC-1.14.7)	Minimum Tensile Strength of Weld, ksi					
		60	70	80	90	100	110
$\frac{1}{8}$	0.125	2.25	2.62	3.00	3.37	3.75	4.12
$\frac{1}{16}$	0.187	3.37	3.94	4.50	5.06	5.62	6.19
$\frac{3}{16}$	0.250	4.50	5.25	6.00	6.75	7.50	8.25
$\frac{1}{4}$	0.312	5.62	6.56	7.50	8.44	9.37	10.31
$\frac{5}{16}$	0.375	6.75	7.87	9.00	10.12	11.25	12.37
$\frac{3}{8}$	0.419	7.55	8.80	10.06	11.32	12.58	13.84
$\frac{7}{16}$	0.463	8.34	9.73	11.12	12.51	13.90	15.30
$\frac{1}{2}$	0.508	9.14	10.66	12.18	13.71	15.23	16.75
$\frac{9}{16}$	0.552	9.93	11.59	13.25	14.90	16.56	18.21
$\frac{5}{8}$	0.596	10.73	12.52	14.31	16.09	17.88	19.67
$\frac{3}{4}$	0.640	11.52	13.44	15.36	17.28	19.21	21.13

**Plug and Slot Welds.** The effective shearing area of plug or slot welds is their nominal area in the shearing plane. The resistance of plug or slot welds is the product of the nominal cross section times the allowable stress as discussed in Sec. 5.12.

#### EXAMPLE 5.13.1

Using AISC specs, determine the effective throat dimension of a  $\frac{7}{16}$ -in. fillet weld produced by (a) shielded metal-arc process and (b) submerged-arc process.

#### Solution

$$(a) t_e = 0.707a = 0.707(0.4375) = 0.309 \text{ in.}$$

$$(b) t_e = 0.707a + 0.11 = 0.707(0.4375) + 0.11 = 0.419 \text{ in.}$$

#### EXAMPLE 5.13.2

Using AISC specs, determine the allowable shear resistance of a  $\frac{3}{8}$ -in. fillet weld produced by (a) shielded metal-arc process, and (b) submerged-arc process. Assume minimum tensile strength of 70 ksi.

#### Solution

$$(a) t_e = 0.707(0.375) = 0.265 \text{ in.}$$

$$R_w = 0.265(70) = 0.265(21) = 5.57 \text{ kips/in.}$$

$$(b) t_e = 0.375 \text{ in.}$$

$$R_w = 0.375(21.0) = 7.87 \text{ kips/in.}$$

The solution to Examples 5.13.1 and 5.13.2 may be checked by referring to Tables 5.13.1 and 5.13.2.

#### EXAMPLE 5.13.3

Determine the allowable capacity of a  $\frac{3}{4}$  in. diam. plug weld using E70 electrode material. Use AISC specs.

#### Solution

Assuming the weld diameter satisfies the limitations of AISC-1.17.12 relating to the dimension of the piece in which the plug weld is made,

$$\begin{aligned} \text{Capacity} &= 0.3f_u(\pi D^2/4) \\ &= 21(\pi)(0.75)^2/4 = 9.28 \text{ kips} \end{aligned}$$

**Maximum Effective Fillet Weld Size.** In Sec. 5.11 the limitations on maximum and minimum fillet weld size and length relating to practical design considerations were given. Those requirements relate to the size of weld that is actually placed. Regarding strength, however, no fillet weld or welds of whatever size may be permitted in design to carry a greater load than permitted on the adjacent base material.

Consider the two lines of fillet weld transmitting the shear  $V$  across

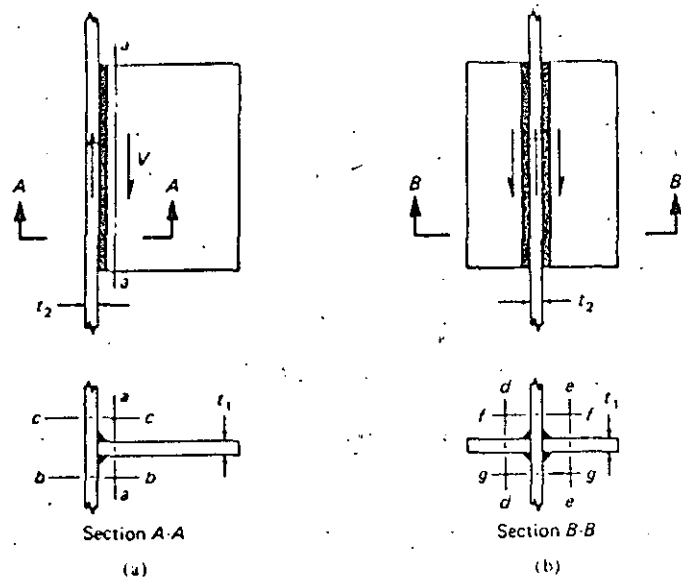


Fig. 5.13.3. Critical sections for possible overstressing of base material.

section *a-a* of Fig. 5.13.3a. Equating the capacity per inch of the weld to capacity per inch in shear (see AISC-1.5.1.2) on the plate gives.

$$\overbrace{2a(0.707)(0.3f_u)}^{\text{weld}} = \overbrace{0.4F_y t_1}^{\text{plate}} \quad (5.13.1)$$

$$a_{\text{max eff}} = \frac{0.4F_y t_1}{2(0.707)(0.3f_u)} = 0.945 \frac{F_y t_1}{f_u} \quad (5.13.2)$$

where  $t_1$  = thickness of base material

$f_u$  = tensile strength of electrode material (70 for E70 electrodes)

$F_y$  = yield stress of base material

Sections *b-b* and *c-c* will not be critical since two lines of weld transfer load across two sections; maximum effective weld size for the transfer across *b-b* and *c-c* is

$$a(0.707)(0.3f_u) = 0.4F_y t_2 \quad (5.13.3)$$

$$a_{\text{max eff}} = 1.89 \frac{F_y t_2}{f_u} \quad (5.13.4)$$

Considering the four fillets of Fig. 5.13.3b, sections *d-d* and *e-e* are the same as section *a-a* and Eq. 5.13.2 applies. On sections *f-f* and *g-g* four fillets are transferring load across two sections:

$$4a(0.707)(0.3f_u) = 2(0.4F_y) t_2$$

and the result is again, Eq. 5.13.2.

EXAMPLE 5.13.4

Determine the capacity per inch of weld,  $R_w$ , to be used in design of the flange to web connection in Fig. 5.13.4. The plates are A36 steel and E70 electrodes are to be used with (a) the shielded metal-arc process, and (b) the submerged-arc process.

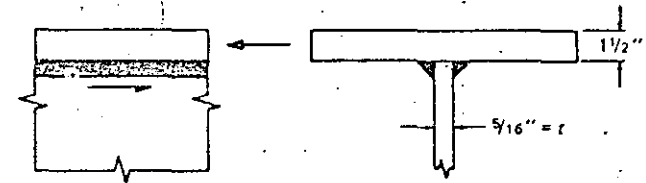


Fig. 5.13.4. Example 5.13.4.

Solution

Minimum weld size =  $a_{\text{min}} = 1/16$  (AISC-1.17.5)

(a) Shielded metal-arc process. Equation 5.13.2 applies

$$a_{\text{max eff}} = 0.945 \frac{F_y t_1}{f_u} = 0.945 \frac{36(t)}{70} = 0.485t$$

$$= 0.485(0.3125) = 0.152 \text{ in.}$$

$$R_w = 2(0.152)(0.707)21 = 4.51 \text{ kips/in. for 2 fillets}$$

Even though a  $1/16$ -in. fillet must be placed, its strength in design may not exceed the strength assuming  $a = 0.152$  in.

(b) Submerged arc process. Here the throat dimension may equal the leg size. Equating weld strength to plate strength gives

$$2(a)(21) = 0.4(36)t$$

$$a_{\text{max eff}} = 0.342t = 0.342(1/8) = 0.107 \text{ in.}$$

$$R_w = 2(0.107)21 = 4.51 \text{ kips/in.}$$

Again, the same result is obtained as in (a) since 4.51 kips/in. is the allowable capacity of the web plate, and is well below the actual weld capacity.

5.14. STRESS DISTRIBUTION IN FILLET WELDS

The procedure for designing welded connections uses as criteria of safety nominal stresses in the welds. Just as for bolted and riveted connections, nominal stresses for welds assumed the weld is elastic and the plates making up the joint are rigid. If a welded joint is subjected to pure shear, compression, or tension, the stresses in the welds are assumed to be uniform over the length of the welds. If a weld is subjected to pure moment or pure torsion, the stresses are assumed to vary linearly depend-



ing on location of the neutral axis. If two or more of the previous design conditions exist simultaneously the stresses are assumed to be their vector sum.

However, the actual stress distribution in a welded connection is complex even in the simplest joint. It must be recognized that the welds and the pieces being joined must deform together, otherwise a separation will occur. In addition, the true stresses are altered by the existence of residual stresses due to the cooling of the welds, warping stresses arising from poor weld procedures, and stress relieving in the pieces being joined. A detailed and quantitative study of the actual stresses in welded connection is beyond the scope of this text. However, in order for the reader to obtain an appreciation for the complexity of the problem, a few common types of joints will be shown.

Figure 5.14.1 shows the typical shear distribution in longitudinal fillet welds

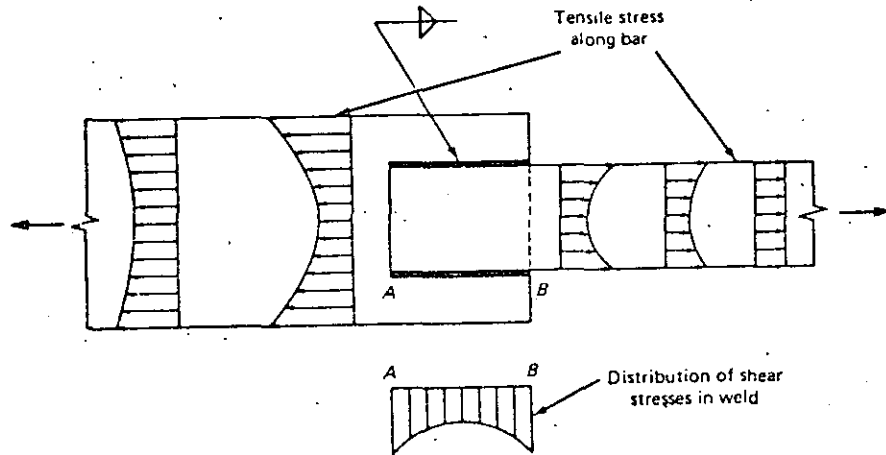


Fig. 5.14.1. Typical stress distribution in a lap joint with longitudinal fillet welds.

welds. The actual magnitude of the variation from points *A* to *B* will depend upon length of the weld as well as the ratio of widths of the two plates being joined. Figure 5.14.2 shows the typical shear distribution for transverse fillet welds. Again the magnitude of the shear distribution will depend upon the relative width of the plates and length of the weld.

The stress distributions in fillet welds used to connect tee-joints is somewhat more complex as indicated in Fig. 5.14.3. Due to the tendency of the fillet to rotate about point *C*, the maximum tensile stress in the *y*-direction,  $f_y$ , is approximately 4 times the nominal or average stress  $f_{y, avg}$ .

If an exact analysis were required each time a connection was designed, very few welded connections would be made. In order to eliminate the need for such an exact analysis, a factor of safety is used to

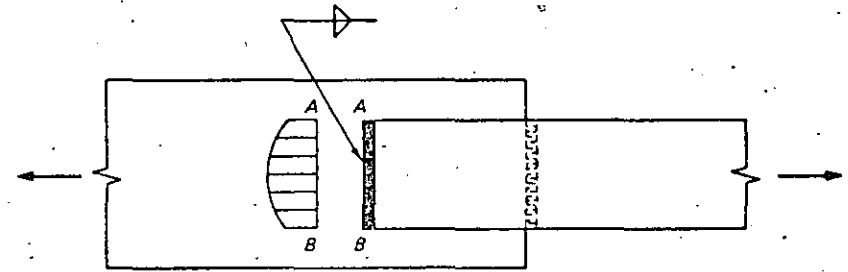


Fig. 5.14.2. Typical stress distribution in a lap joint with transverse fillet welds.

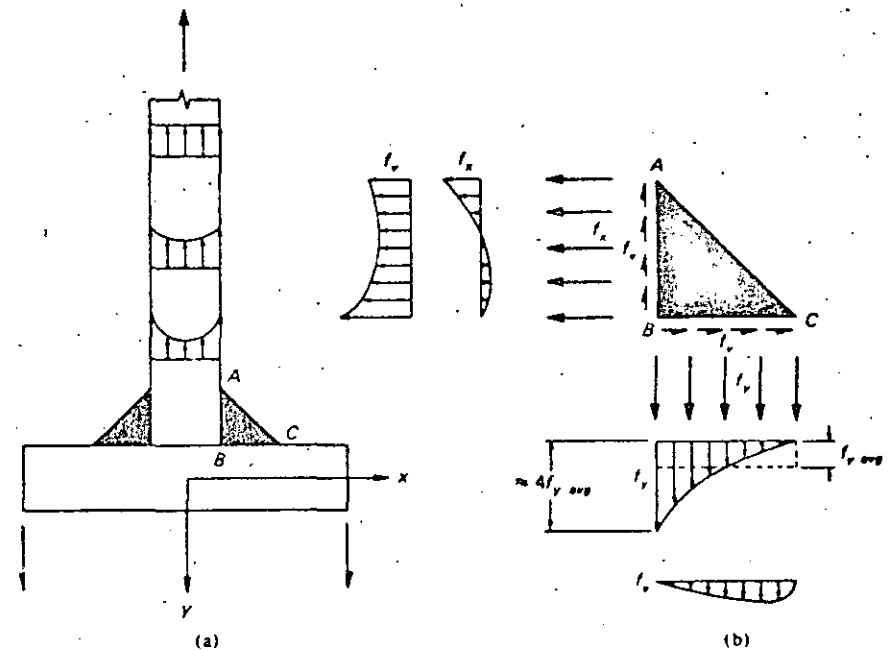


Fig. 5.14.3. Typical stress distribution in a tee joint with fillet welds (shear transverse to fillet).

arrive at the allowable nominal stresses based on the manner of computing nominal stress and the desired relationship between service load and ultimate strength. By this logic, the designer is able to make a reasonable analysis on the basis of nominal stresses and select appropriately sized welds with confidence. The fact that the welds will deform plastically after yielding and thus redistribute unusually high stresses is analogous to the assumptions made for rows of bolts as discussed in Sec. 4.5.

It would serve little purpose to develop an "exact" analysis for welded joints, since in most engineering design problems the loading is

virtually never known to that degree of precision. However, the above discussion should serve to alert the reader to the true distribution of the stresses and should temper his approach to the design of welded connections.

### 5.15. WELDS CONNECTING MEMBERS UNDER DIRECT AXIAL STRESS

In the design of welds connecting members in pure tension or compression, the principal task is to insure that the welds are at least as strong as the members they connect and that the connection does not introduce significant eccentricity of loading.

**Groove Welds.** In the case of full-penetration groove welds as shown in Fig. 5.5.2, the full strength of the cross section is insured by selecting the proper electrode corresponding to the base material (the material in the members) as indicated in Table 5.12.1.

#### EXAMPLE 5.15.1

Select the required thickness of the plates (A572 Grade 55) and the proper electrode material assuming a bevel weld and the submerged-arc process for the member in Fig. 5.15.1.

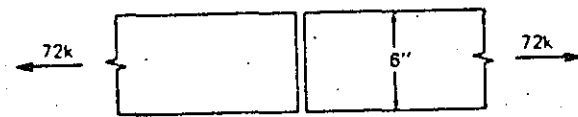


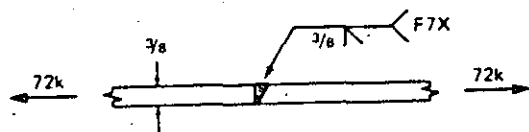
Fig. 5.15.1. Example 5.15.1.

#### Solution

Since there are no holes to consider, the net section is 6 in. times the required thickness,  $t_{reqd}$ . The allowable tensile stress  $F_t$  in the member is  $0.6F_y$ , or 33 ksi. The required thickness is, therefore,

$$t_{reqd} = \frac{T}{6F_t} = \frac{72}{6(33)} = 0.364 \text{ in.}, \text{ use } R_5 \frac{3}{8} \times 6$$

From Table 5.12.1, use F7X-EXXX flux electrode combination and a full-penetration bevel weld.



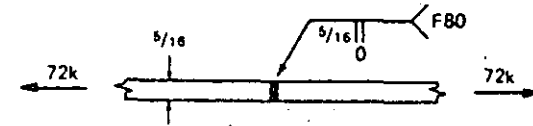
#### EXAMPLE 5.15.2

Repeat Example 5.15.1 using A572 Grade 65 plates and a square-groove weld with a zero root opening.

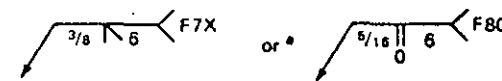
#### Solution

$$t_{reqd} = \frac{72}{6(0.6)F_y} = \frac{72}{6(0.6)65} = 0.308 \text{ in.}, \text{ use } R_5 \frac{5}{16} \times 6$$

From Table 5.12.1, use Grade 80 submerged-arc process.



*Note:* In Examples 5.15.1 and 5.15.2 it was not necessary to include the length of the welds as shown below since they are to be made the full width of the plates unless otherwise specified.



#### EXAMPLE 5.15.3

Determine the capacity of the tee connection shown below and detail the proper double-bevel weld, assuming a shielded metal-arc process. Assume the flange of the tee does not control design.

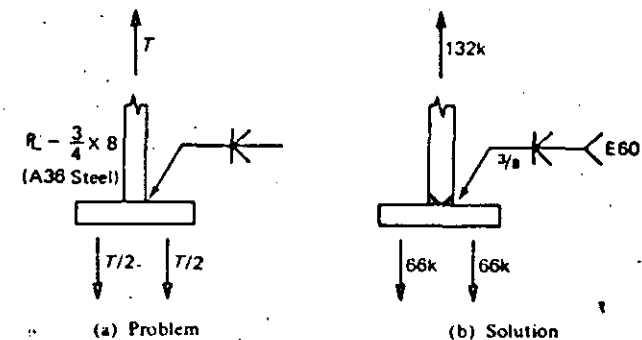


Fig. 5.15.2. Example 5.15.3.

#### Solution

The allowable tensile force is

$$T = 8(0.75)22 = 132 \text{ kips}$$

From Table 5.12.1, use E60 electrodes.

*Note:* On the basis of strength only, a single  $\frac{3}{8}$ -in. bevel could have been used instead of the double-bevel weld specified. However, welding the stem of the tee from one side only may cause excessive warping and introduces eccentricity into the connection.

**Fillet Welds.** The design procedure for fillet welds is based on the nominal shear stress of the fillet weld on the effective area as discussed in Sec. 5.13. The selection of the size of the fillet weld is based on the thickness of the pieces being joined and the available length over which the fillet welds can be made. Other factors such as the type of welding equipment used, whether the welds are to be made in the field or in the shop, and the size of other welds being made will also influence the size of fillet specified. Large fillet welds require larger diameter electrodes which in turn require larger and bulkier welding equipment, not necessarily convenient for field use. The most economical size of fillet weld made in the field is about  $\frac{3}{16}$  in. Also, if a certain size of fillet weld is used in adjacent areas to the particular joint in question, it is advisable to use the same size since then the same electrodes and welding equipment could be used and the welder would not have to alter his procedure to accommodate a larger or smaller weld. In addition, inspection of the welds is further simplified.

#### EXAMPLE 5.15.4

Determine the size and length of the fillet weld for the lap joint shown below assuming the submerged-arc process and the plates are A36 steel.

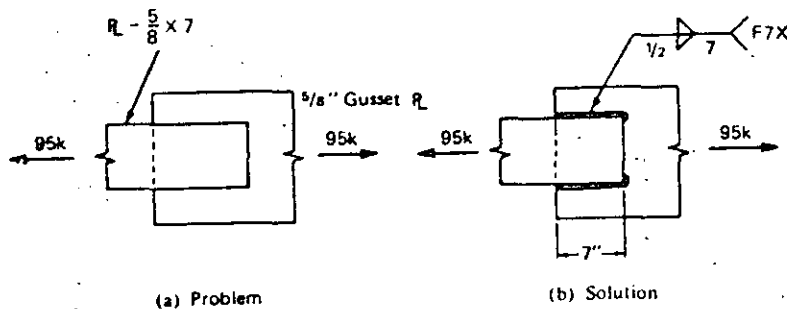


Fig. 5.15.3. Example 5.15.4.

#### Solution

Referring to Sec. 5.11,

$$\text{Maximum size} = \frac{5}{8} - \frac{1}{16} = \frac{9}{16}$$

$$\text{Minimum size} = \frac{3}{16}$$

Assuming that the connection is to be shop-welded, use  $\frac{1}{2}$  in. fillet.

From AISC-1.14.7, since the nominal size of fillet weld is over  $\frac{3}{16}$  in., the effective throat dimension is equal to the theoretical throat plus 0.11 in.

$$\text{Effective throat} = 0.707(0.50) + 0.11 = 0.4635 \text{ in.}$$

From Table 5.12.3 use F7X-EXXX flux electrode combination.

From Table 5.12.3, the capacity of  $\frac{1}{2}$ -in. fillet weld per inch of length is

$$R_w = (\text{Effective throat})(\text{allowable stress}) \\ = 0.4635(21.0) = 9.73 \text{ kips/in.}$$

Length of weld,  $L_w$ , required is

$$L_w = \frac{95}{9.73} = 9.76 \text{ in., use } \frac{1}{2}\text{-in. fillet, 7 in. on each side.}$$

Fillet length is extended to satisfy AISC-1.17.7 (par. 2).

#### EXAMPLE 5.15.5

Rework Example 5.15.4 using  $\frac{1}{4}$ -in. fillet welds.

#### Solution

Since the nominal size is less than  $\frac{3}{16}$  the full leg dimension may be used as the effective throat dimension for submerged-arc welding.

$$R_w = 0.250(21.0) = 5.25 \text{ kips/in.}$$

$$\text{Reqd } L_w = \frac{95}{5.25} = 18.1 \text{ in., say 19 in.}$$

Two possible solutions are shown in Fig. 5.15.4, both of which provide 19 in. of  $\frac{1}{4}$ -in. fillet welds.

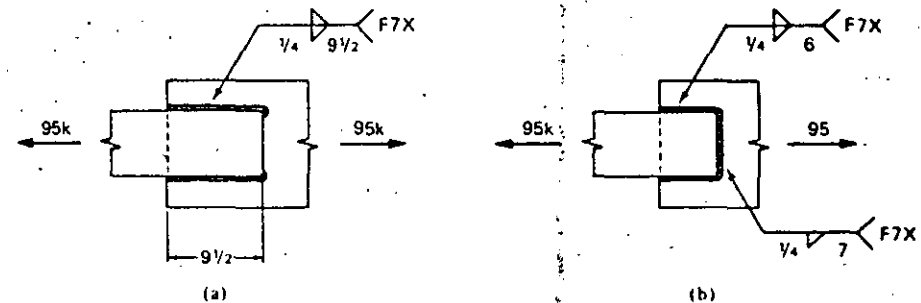


Fig. 5.15.4. Solutions to Example 5.15.5.

The solution in Fig. 5.15.4b is preferred since it is more compact and reduces the overall size of the connection.

In a great number of cases, members subjected to direct axial stress are themselves unsymmetrical and cause eccentricities in welded connections. Consider the angle tension member shown in Fig. 5.15.5 welded as indicated. The force  $T$ , applied at some distance from the connection will act along the centroid of the member as shown. The force  $T$  will be resisted by the forces  $F_1$ ,  $F_2$ , and  $F_3$  developed by the weld lines. The forces  $F_1$  and  $F_3$  are assumed to act at the top and bottom edges, respectively, of the angle shown. The force  $F_2$  will act at the centroid of the weld which is located at  $d/2$ . Taking moments about some point  $A$

located on the bottom edge of the member and considering clockwise moments positive,

$$\Sigma M_A = -F_1 d - F_2 d/2 + T y = 0 \quad (5.15.1)$$

or

$$F_1 = \frac{T y}{d} - \frac{F_2}{2} \quad (5.15.2)$$

The force  $F_2$  is equal to the resistance of the weld per inch times the length of the weld:

$$F_2 = R_w L_w \quad (5.15.3)$$

Considering horizontal force equilibrium gives

$$\Sigma F_H = T - F_1 - F_2 - F_3 = 0 \quad (5.15.4)$$

Solving Eqs. 5.15.1 and 5.15.4 simultaneously gives

$$F_3 = T \left( 1 - \frac{y}{d} \right) - \frac{R_w}{2} \quad (5.15.5)$$

Designing the connection shown in Fig. 5.15.5 to eliminate eccentricity caused by the unsymmetrical weld is called *balancing the welds*. The procedure for balancing the welds may be summarized as follows:

1. After deciding on the proper weld size and electrode, compute the force resisted by the end welds  $F_2$  (if any) on the basis of Eq. 5.15.3.
2. Compute  $F_1$  on the basis of Eq. 5.15.2.
3. Compute  $F_3$  on the basis of Eq. 5.15.5, or

$$F_3 = T - F_1 - F_2 \quad (5.15.6)$$

4. Compute the lengths,  $L_{w1}$  and  $L_{w3}$ , on the basis of

$$L_{w1} = \frac{F_1}{R_w} \quad (5.15.7a)$$

and

$$L_{w3} = \frac{F_3}{R_w} \quad (5.15.7b)$$

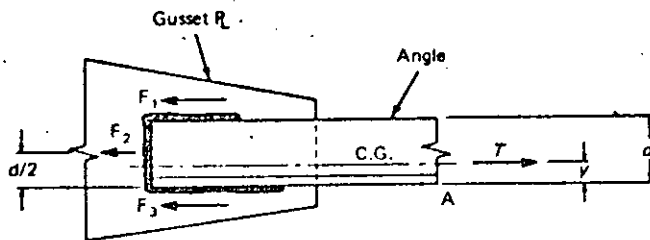


Fig. 5.15.5.

It is noted that approximately balanced welds are desirable; however, unless the member is subject to repeated variations in stress, balanced connections for "single angle, double angle, and similar type members is not required" by AISC-1.15.3.

EXAMPLE 5.15.6.

Design the fillet welds to develop the full strength of the angle shown in Fig. 5.15.6 minimizing the effect of eccentricity. Assume the gusset plate does not govern and the shielded metal-arc process is used.

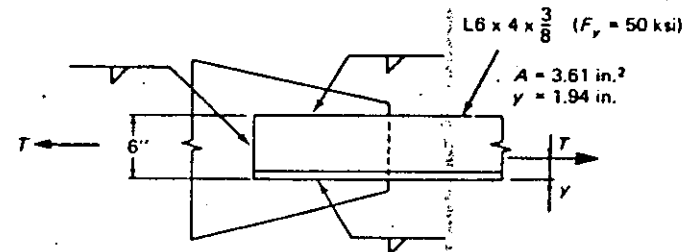


Fig. 5.15.6. Example 5.15.6.

Solution

Using the forces as in Fig. 5.15.7,

$$T = 0.6 F_y A = 0.6(50)3.61 = 108.3 \text{ kips}$$

Minimum size fillet weld =  $\frac{3}{16}$  in. (Table 5.11.1)

Maximum size fillet weld =  $\frac{5}{16}$  in. (Fig. 5.11.2)

Use  $\frac{3}{16}$  in. fillet weld with E70 electrodes.

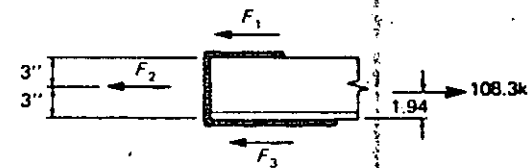


Fig. 5.15.7.

From Eq. 5.15.3,

$$F_2 = R_w L_w = \frac{3}{16}(0.707)(21.0)6 = 2.79(6) = 16.7 \text{ kips}$$

From Eq. 5.15.2,

$$F_1 = \frac{T y}{d} - \frac{F_2}{2} = \frac{108.3(1.94)}{6} - \frac{16.7}{2} = 26.6 \text{ kips}$$



From Eq. 5.15.6

$$F_3 = T - F_1 - F_2 = 108.3 - 26.6 - 16.7 = 65.0 \text{ kips}$$

From Eqs. 5.15.7a and 5.15.7b,

$$L_{w1} = \frac{F_1}{R_w} = \frac{26.6}{2.79} = 9.54 \text{ in., say 10 in.}$$

and

$$L_{w3} = \frac{F_3}{R_w} = \frac{65.0}{2.79} = 23.3 \text{ in., say 24 in.}$$

Use welds as summarized in Fig. 5.15.8, though for better economy larger welds would be preferred to reduce connection length.

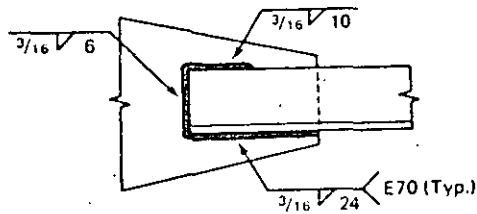


Fig. 5.15.8. Solution for Example 5.15.6.

#### EXAMPLE 5.15.7.

Rework Example 5.15.6 if the weld at the end of the angle is omitted, and submerged-arc process is used instead of the shielded metal-arc process.

**Solution**

Again, try  $\frac{3}{16}$ -in. weld on the  $F_y = 50$  ksi base material. Using the forces in Fig. 5.15.9,

$$F_1 = \frac{T_y}{d} - \frac{F_2}{2} = \frac{108.3(1.94)}{6} - 0 = 35.0 \text{ kips}$$

$$F_3 = T - F_1 - F_2 = 108.3 - 35.0 - 0 = 73.3 \text{ kips}$$

$$R_w = (\frac{3}{16})(21) = 3.94 \text{ kips/in.}$$

$$L_{w1} = \frac{35.0}{3.94} = 8.9 \text{ in., say 9 in.}$$

$$L_{w3} = \frac{73.3}{3.94} = 18.65 \text{ in., say 19 in.}$$

The length of  $L_{w3}$  requires an excessively large joint which probably is uneconomical. Therefore it is advisable to use a larger size fillet weld.

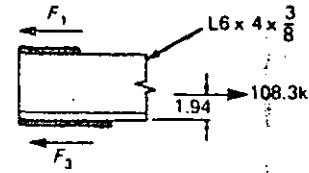


Fig. 5.15.9.

Try a  $\frac{3}{16}$ -in. weld.

Effective throat dimension =  $\frac{3}{16}$  (submerged arc process)

The forces  $F_1$  and  $F_3$  are independent of the weld size and the new required lengths are

$$L_{w1} = \frac{35.0}{\frac{3}{16}(21.0)} = 5.33 \text{ in., say } 5\frac{1}{2} \text{ in.}$$

$$L_{w3} = \frac{73.3}{\frac{3}{16}(21.0)} = 11.17 \text{ in., say } 11\frac{1}{2} \text{ in.}$$

Use welds as summarized in Fig. 5.15.10.

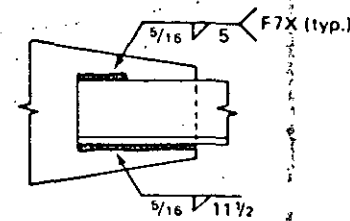


Fig. 5.15.10. Solution for Example 5.15.7.

**Slot and Plug Welds.** Slot and plug welds depend upon their shear strength in the shearing plane between the plates being joined. As indicated in Sec. 5.7, their principal use is in lap joints. Plug welds are also occasionally used to fill up holes in connections, such as beam to column angles where temporary erection bolts had been placed to align the members prior to welding. This latter usage is generally not considered to be structural although in certain cases, the designer may consider the strength of the plug weld in designing the rest of the welds in a given connection. As a rule, plug and slot welds will be designed to work together with other welds, usually fillet welds, in lap joints as shown in Fig. 5.5.5.

#### EXAMPLE 5.15.8.

Assuming A36 steel determine the value of  $T$  permitted by AISC on the connection in Fig. 5.15.11.



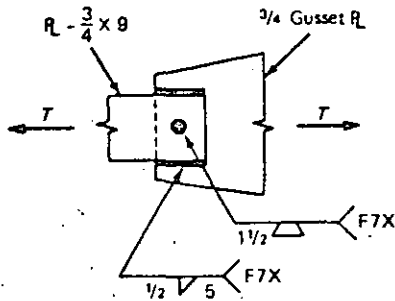


Fig. 5.15.11. Example 5.15.8.

**Solution**

The resistance per inch supplied by the 1/2-in. fillet welds,  $R_w$ , is

$$R_w = [0.5(0.707) + 0.11](21) = 9.73 \text{ kips/in.}$$

The total resistance provided by the fillet welds  
 $= 10(9.73) = 97.3 \text{ kips}$

The resistance provided by the 1 1/2 plug weld  
 $= \frac{\pi(1.5)^2}{4} (21.0) = 37.1 \text{ kips}$

The value of  $T$  is equal to

$$T = 97.3 + 37.1 = 134.4 \text{ kips}$$

Check capacity of plate:

$$T = 9(0.75)22 = 148.5 \text{ kips} > 134.4 \text{ k} \quad \text{OK, } T = 134.4 \text{ kips}$$

**EXAMPLE 5.15.9.**

Compute the allowable capacity of the connection shown in Fig. 5.15.12 according to AISC, assuming A572 Grade 50 steel.

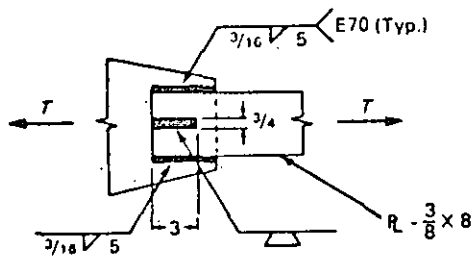


Fig. 5.15.12. Example 5.15.9.

**Solution**

From Table 5.13.1, a 3/16 in. E70 fillet weld provides 2.78 k/in.  $[(3/16)(0.707)(21)]$ . The total resistance provided by the fillet welds

$$= 2(5)2.78 = 27.8 \text{ kips}$$

The resistance provided by the slot weld

$$= 3/4 (3)(21) = 47.3 \text{ kips}$$

The value of  $T$  is given by

$$T = 27.8 + 47.0 = 74.8 \text{ kips}$$

Check capacity of plate:

$$T = 8(3/8)30 = 90 \text{ kips} > 74.8 \text{ k}; \quad \text{thus } T = 74.8 \text{ kips.}$$

**EXAMPLE 5.15.10.**

Design an end connection to develop the full tensile value of an C8 x 13.75 in a lap length of 5 inches. The channel of A572 Grade 50 steel is connected to a 3/8-in. plate and fillet welds are limited to 3/8 in. and are to be made by the shielded metal-arc process. Use AISC specifications.

**Solution**

Channel capacity =  $P = F_t A = 0.6(50)4.02 = 120.5 \text{ kips}$

(a) Fillet weld. Use E70 electrodes.

Minimum  $a = 3/16 \text{ in. (AISC-1.17.5)}$

Maximum  $a = 0.303 - 3/16 = 0.24$ , say  $1/4 \text{ in. (AISC-1.17.6)}$

While 1/4-in. weld must be used on one end along the channel web, 3/8-in. weld could be used along the flanges. It is better not to mix the fillet sizes, so try 3/8 in. all around.

$$R_w = 3/8(0.707)(21) = 3.71 \text{ kips/in.}$$

$$\text{Reqd } L_w = \frac{P}{R_w} = \frac{120.5}{3.71} = 32.5 \text{ in.}$$

Since the length all around is only 26 in.; additional capacity from fillet welds in a large slot, slot welds, or plug welds, is necessary.

(b) Slot Weld. Try a slot weld in accordance with AISC-1.17.12.

$$\begin{aligned} \text{Min width of slot} &= \left( t + \frac{5}{16} \right) [\text{rounded to next odd } 1/16 \text{ in.}] \\ &= 0.303 + 0.3125 = 0.6155 \\ &[\text{rounded to } 1/8 \text{ in.}] \end{aligned}$$





$$\text{Max width of slot} = 2\frac{1}{4}a = 2\frac{1}{4}\left(\frac{1}{4}\right) = 0.56 = \frac{9}{16} \text{ in.}$$

$$\text{Load to be carried by slot} = 120.5 - (26 - 0.56)3.71 = 26.0 \text{ kips}$$

Try  $\frac{9}{16}$  in. width of slot:

$$\text{Length reqd} = \frac{26.0}{\left(\frac{9}{16}\right)(21)} = 2.2 \text{ in.}$$

$$\text{Max length of slot} = 10a = 10\left(\frac{1}{4}\right) = 2.25 \text{ in.}$$

Use a slot weld  $\frac{9}{16} \times 2\frac{1}{4}$ . The final design is shown in Fig. 5.15.13.

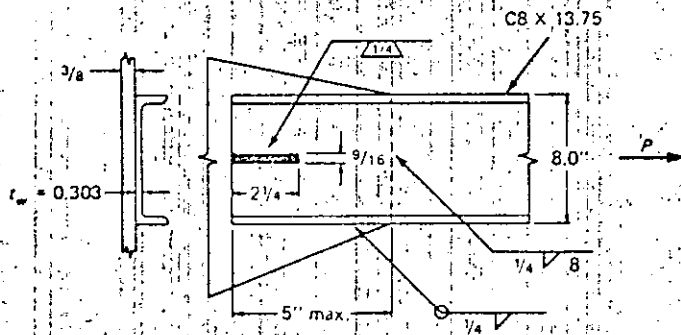


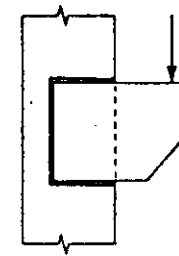
Fig. 5.15.13 Solution for Example 5.15.10.

## 5.16. ECCENTRIC WELDED CONNECTIONS.

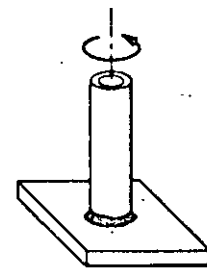
The versatility and ease of welding make welded connections desirable for a wide variety of usages. In actual practice, welded connections often use a group of welds rather than a single weld, the result being that the welds may be subjected to more than one type of loading. Examples of various types of loading are shown in Fig. 5.16.1. As in the case of eccentric bolted connections (Sec. 4.7), the exact elastic analysis of the stresses in eccentric welded connections is impractical. In addition to the complex stress distribution discussed in Sec. 5.14, the great variety of possible combinations of loading and grouping of welds makes it necessary to evaluate the adequacy of a connection on the basis of nominal stresses.

The general procedure for investigating the nominal stress in weld groups is based on the general assumptions discussed in Sec. 5.14 and the principles of mechanics. The procedure, in brief, consists of the following steps:

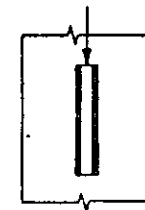
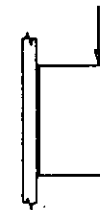
1. Establish the *effective* throat dimension  $t$ , and draw the effective cross section of the weld group.
2. Establish a coordinate system and determine the centroid of the weld group.



(a) Shear and torsion



(b) Pure torsion



(c) Shear and bending

Fig. 5.16.1. Types of eccentric loading.

3. Determine the forces acting on the weld group.
4. Compute the individual stresses in the welds at critical points resulting from direct shear, torsion, and moment.
5. Combine the individual stresses vectorially.

The general procedure outlined above is illustrated in the examples that follow.

**Eccentric Shear (Shear and Torsion).** In order to expand the general procedure for combined shear and torsion, consider the connection shown in Fig. 5.16.2a. The effective cross section and the applied force system are shown in Fig. 5.16.2b. In developing the procedure the following notation will be used:

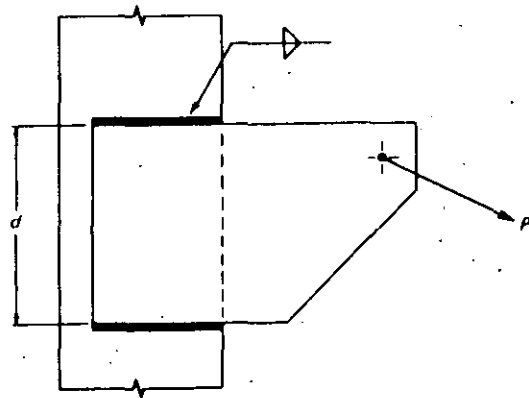
$$f' = \frac{P}{A} = \text{stress due to direct shear} \quad (5.16.1)$$

$$f'' = \frac{Tr}{I_p} = \text{stress due to torsional moment} \quad (5.16.2)$$

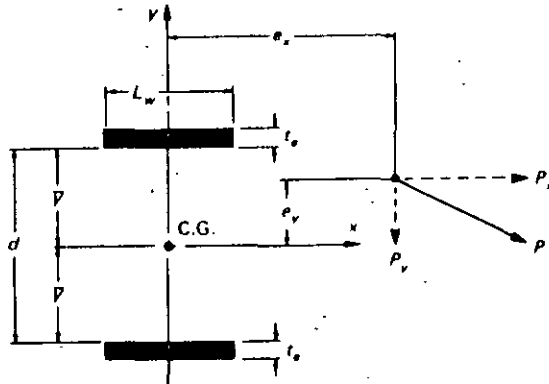
where  $r$  = radial distance from the centroid to point of stress  
 $I_p$  = polar moment of inertia

For computing nominal stresses the *locations* of the lines of weld are defined by edges along which the fillets are placed, rather than to the center





(a) Connection



(b) Effective cross section

Fig. 5.16.2. Eccentric bracket connection.

of the effective throat. This makes little difference, since the throat dimension is usually small. As discussed for eccentrically loaded bolted connections it is convenient to use a cartesian coordinate system and compute  $x$  and  $y$  components of the forces on welds.

For the general case shown in Fig. 5.16.2, the components of stress due to direct shear and torsion are

$$f'_x = \frac{P_x}{A} \tag{5.16.3a}$$

$$f'_y = \frac{P_y}{A} \tag{5.16.3b}$$

$$f''_x = \frac{T_y}{I_p} = \frac{(P_x e_y + P_y e_x) y}{I_p} \tag{5.16.4a}$$

$$f''_y = \frac{T_x}{I_p} = \frac{(P_x e_y + P_y e_x) x}{I_p} \tag{5.16.4b}$$

$$\text{where } I_p = I_x + I_y = \Sigma I_{xx} + \Sigma A \bar{y}^2 + \Sigma I_{yy} + \Sigma A \bar{x}^2 \tag{5.16.5}$$

In Eq. 5.16.5,  $\bar{x}$  and  $\bar{y}$  refer to distances from the center of gravity of the weld group to the center of gravity of the individual weld segments.  $I_{xx}$  and  $I_{yy}$  refer to the moments of inertia of the individual segments with respect to their own centroidal axes.

Thus, for the situation of Fig. 5.16.2, Eq. 5.16.5 becomes

$$\begin{aligned} I_p &= 2 \left[ \frac{L_w (t_w)^3}{12} \right] + 2 [L_w (t_w) (\bar{y})^2] + 2 \left[ \frac{t_w (L_w)^3}{12} \right] \\ &= \frac{t_w}{6} [L_w (t_w)^2 + 12 L_w (\bar{y})^2 + L_w^3] \end{aligned} \tag{5.16.6}$$

For practical situations, the first term of Eq. 5.16.6 is neglected because, with  $t_w$  small, the term is not significant compared to the other terms. Hence

$$I_p \approx \frac{t_w}{6} [12 L_w (\bar{y})^2 + L_w^3] \tag{5.16.7}$$

Then, after evaluating the torsional components in accordance with Eqs. 5.16.4, the  $x$  and  $y$  components of the resultant stress are

$$f_x = f'_x + f''_x \tag{5.16.8a}$$

$$f_y = f'_y + f''_y \tag{5.16.8b}$$

and the resultant stress  $f_r$  is

$$\begin{aligned} f_r &= \sqrt{(f_x)^2 + (f_y)^2} \\ &= \sqrt{(f'_x + f''_x)^2 + (f'_y + f''_y)^2} \end{aligned} \tag{5.16.9}$$

The resultant stress  $f_r$  is considered to be a nominal shear stress on the effective throat area of fillet welds. AISC-1.5.3 gives the allowable values as discussed in Sec. 5.12. The safe capacity  $R_w$  of a fillet weld per inch of weld is

$$R_w = (t_w) (\text{allowable unit stress})$$

or

$$\frac{R_w}{t_w} = \text{allowable unit stress}$$

For satisfactory safety, it is required from analysis that

$$f_r \leq \frac{R_w}{t_w} \tag{5.16.10}$$



For investigating stresses in weld groups, such as in Fig. 5.16.2,  $I_p$  may be computed as illustrated in obtaining Eq. 5.16.7. Note that the throat dimension  $t_e$  may be factored out of Eq. 5.16.7; this may always be done. Following through the computation of stress components and obtaining  $f_s$ , one will find that  $t_e$  appears as a denominator multiplier in the resultant stress  $f_s$ . By multiplying  $f_s$  by  $t_e$ , a resultant load per inch is obtained which may be compared with allowable  $R_w$  to establish whether or not safety is adequate. In other words, one may frequently desire to use Eq. 5.16.10 in the form

$$f_s t_e \leq R_w \quad (5.16.11)$$

When designing welds, the throat dimension  $t_e$  is frequently unknown and is to be solved for. In such cases it is usually convenient to compute  $I_p$  assuming  $t_e = 1$ ; thus one may think of having computed  $f_s t_e$ , the actual load per inch on the weld group. Thus, for design, it is required that

$$t_e \geq \frac{f_s}{\text{allowable stress}} \quad (5.16.12)$$

where  $f_s$  is in *ksi units*. Or Eq. 5.16.12 may be written

$$t_e \geq \frac{f_s(1)}{R_w} \quad (5.16.13)$$

where  $f_s(1) = f_s t_e$  with  $t_e = 1$ , and is in *kips per inch units*.

Treating the welds making up the effective cross section in Fig. 5.16.2 as line welds (i.e., as in deriving Eq. 5.16.7 with  $t_e = 1$ ) and using the general terms  $b$  and  $d$ , as shown in Fig. 5.16.3, Eq. 5.16.7 becomes

$$I_p = \frac{1}{6} \left[ 12b \left( \frac{d}{2} \right)^2 + b^3 \right] = \frac{b}{6} [3d^2 + b^2] \quad (5.16.14)$$

Table 5.16.1 gives  $I_p$  values treated as properties of lines for other common weld configurations.

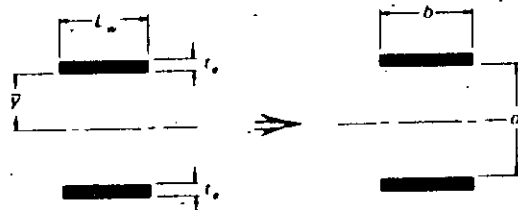


Fig. 5.16.3.

TABLE 5.16.1  
Properties of Welds Treated as Lines

Section $b = \text{width}; d = \text{depth}$	Section Modulus $I_x/\bar{y}$	Polar Moment of Inertia, $I_p$ about Center of Gravity
1.	$S = \frac{d^2}{6}$	$I_p = \frac{d^3}{12}$
2.	$S = \frac{d^2}{3}$	$I_p = \frac{d(3b^2 + d^2)}{6}$
3.	$S = bd$	$I_p = \frac{b(3d^2 + b^2)}{6}$
4.	$\bar{y} = \frac{d^2}{2(b+d)}$ $\bar{x} = \frac{b^2}{2(b-d)}$	$S = \frac{4bd + d^2}{6}$ $I_p = \frac{(b+d)^4 - 6b^2d^2}{12(b+d)}$
5.	$\bar{x} = \frac{b^2}{2b+d}$	$S = bd + \frac{d^2}{6}$ $I_p = \frac{8b^3 + 6bd^2 + d^3}{12} - \frac{b^4}{2b+d}$
6.	$\bar{y} = \frac{d^2}{b+2d}$	$S = \frac{2bd + d^2}{3}$ $I_p = \frac{b^3 + 6b^2d + 8d^3}{12} - \frac{d^4}{2d+b}$
7.	$S = bd + \frac{d^2}{3}$	$I_p = \frac{(b+d)^3}{6}$
8.	$\bar{y} = \frac{d^2}{b+2d}$	$S = \frac{2bd + d^2}{3}$ $I_p = \frac{b^3 + 6bd^2}{12} - \frac{d^4}{b+2d}$
9.	$S = bd + \frac{d^2}{3}$	$I_p = \frac{b^3 + 3b^2d + d^3}{6}$
10.	$S = \pi r^2$	$I_p = 2\pi r^3$



EXAMPLE 5.16.1

Compute the size of fillet weld required using E70 electrodes for the connection shown in Fig. 5.16.4. Assume that the plate does not govern or control weld size.

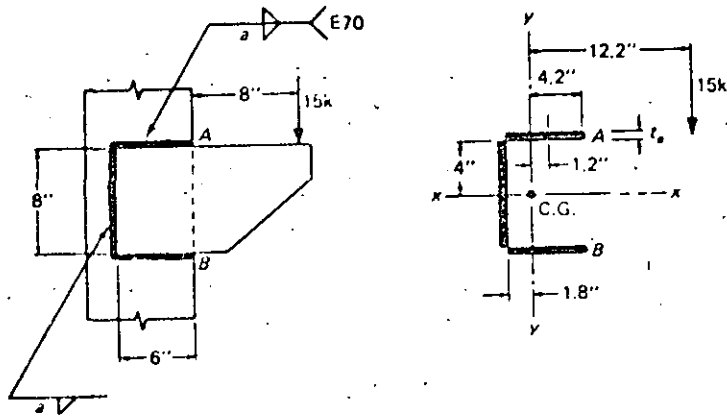


Fig. 5.16.4. Example 5.16.1.

Solution

The highest stress on the weld group will occur at point A or B. The solution will be illustrated by carrying  $t_w$  as a factor throughout the computation.

Locate the centroid of the entire configuration by taking moments about the edge of the vertical weld:

$$\bar{x} = \frac{2t_w(6)(3)}{2(6t_w) + 8t_w} = 1.8 \text{ in.}$$

$$I_p = t_w \left\{ \frac{(8)^3}{12} + 2[6(4)^2] + 2 \left[ \frac{(6)^3}{12} + 2[6(1.2)^2] + 8(1.8)^2 \right] \right\}$$

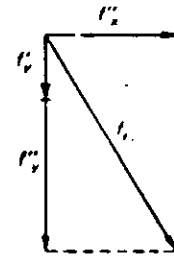
$$= t_w(313.9) \text{ in.}^4$$

The bracketed multiplier of  $t_w$  in the  $I_p$  expression is the property of lines as found in Table 5.16.1.

$$A = t_w[2(6) + 8] = t_w(20.0) \text{ sq in.}$$

$$f_y' = \frac{P_y}{A} = \frac{15}{t_w(20)} = \frac{0.75}{t_w} \text{ ksi}$$

$$f_y'' = \frac{T_y}{I_p} = \frac{15(12.2)4}{t_w(313.9)} = \frac{2.34}{t_w} \text{ ksi}$$



$$f_y'' = \frac{T_y}{I_p} = \frac{15(12.2)4}{t_w(313.9)} = \frac{2.34}{t_w} \text{ ksi}$$

The resultant stress  $f_r$  is

$$f_r = \sqrt{\frac{(2.34)^2 + (2.45 + 0.75)^2}{t_w^2}} = \frac{3.97}{t_w} \text{ ksi}$$

It will be apparent from the calculation that one may easily obtain the same numerical result by assuming  $t_w = 1$ .

Using Eq. 5.16.12, which is merely setting  $f_r$  equal to its maximum allowable value,

$$\text{Reqd } t_w = \frac{f_r}{\text{allowable stress}} = \frac{3.97}{21} = 0.189 \text{ in.}$$

$$\text{Reqd } a = \frac{t_w}{0.707} = \frac{0.189}{0.707} = 0.267 \text{ in., say } \frac{1}{4} \text{ in.}$$

Use  $\frac{1}{4}$ -in. E70 fillet welds.

For the general solution of welds under eccentric loading as in Fig. 5.16.4, the AISC Manual has tables, "Eccentric Loads on Weld Groups," using the terms as defined in Fig. 5.16.5. As given by the AISC Manual,

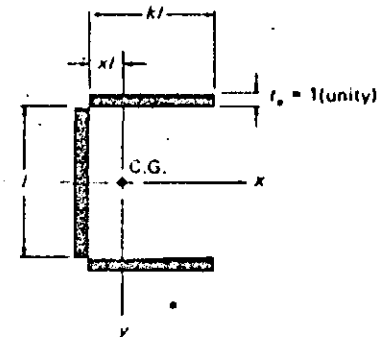


Fig. 5.16.5. Terminology for AISC Manual, "Eccentric Loads on Weld Groups."





$$I_p = \frac{L^3}{12} - \frac{k^2 l^4 (1+k)^2}{L} \quad (5.16.15)$$

$$\bar{x} = xl = \frac{(kl)^2}{L} \quad (5.16.16)$$

where  $l$  = length of vertical weld  
 $kl$  = length of horizontal weld  
 $L = l + 2ki$  = total length of weld

**EXAMPLE 5.16.2**

Recheck  $I_p$  in Example 5.16.1 using the AISC method.

*Solution*

Using Eq. 5.16.15,

$$kl = 6 \text{ in.}; \quad l = 8 \text{ in.}; \quad k = \frac{6}{8} = 0.75$$

$$L = 8 + 2(6) = 20 \text{ in.}$$

$$I_p = \frac{(20)^3}{12} - \frac{(0.75)^2 (8)^4 (1 + 0.75)^2}{20} = 667 - 352 = 315 \text{ in.}^2$$

This agrees within slide-rule error to the previously computed value of 313.9 in.<sup>2</sup>

**Shear and Bending.** Combined shear and bending stresses are computed by vectorially adding the *nominal* shear and bending stresses. The procedure is illustrated by considering the bracket shown in Fig. 5.16.6a and the effective cross section of the weld group shown in Fig. 5.16.6b. Figure 5.16.7 shows the variation of the shear and bending stresses. The reader should note that the actual maximum shear and bending stresses occur at different locations. However, in simplifying the computations, the shear stresses are assumed to be nominally distributed as shown in Fig. 5.16.7c.

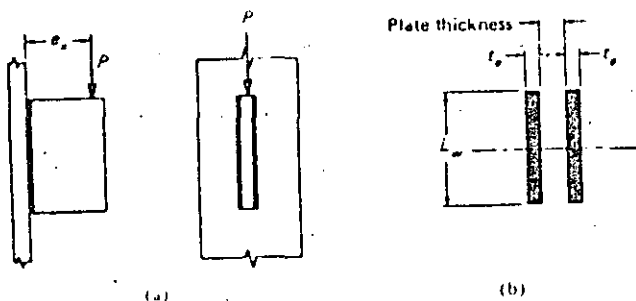


Fig. 5.16.6.

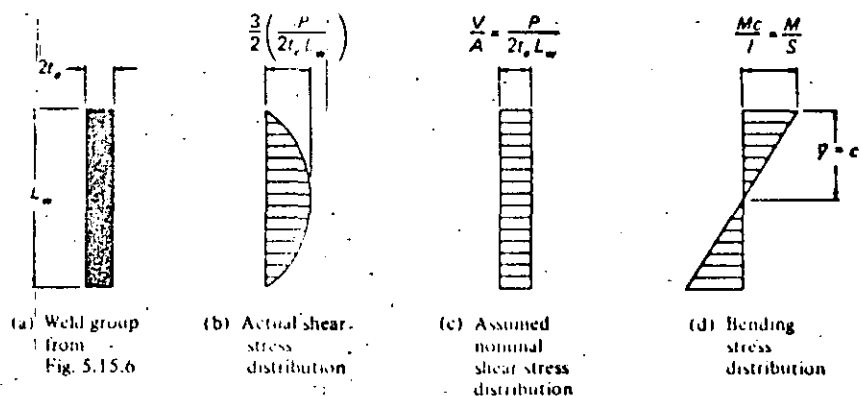


Fig. 5.16.7.

The nominal shear stress is then added *vectorially* to the maximum bending stress.

For this particular case the assumed vertical shear stress from Eq. 5.16.3b is

$$f'_y = \frac{P_y}{A} = \frac{P}{2t_w L_w}$$

and the horizontal stress due to bending is

$$f'_x = \frac{Mc}{I} = \frac{(Pe_s)(L_w/2)}{\left[ \frac{2t_w(L_w)^3}{12} \right]} = \frac{3Pe_s}{t_w(L_w)^2}$$

The stress resultant is

$$f_r = \sqrt{(f'_y)^2 + (f'_x)^2}$$

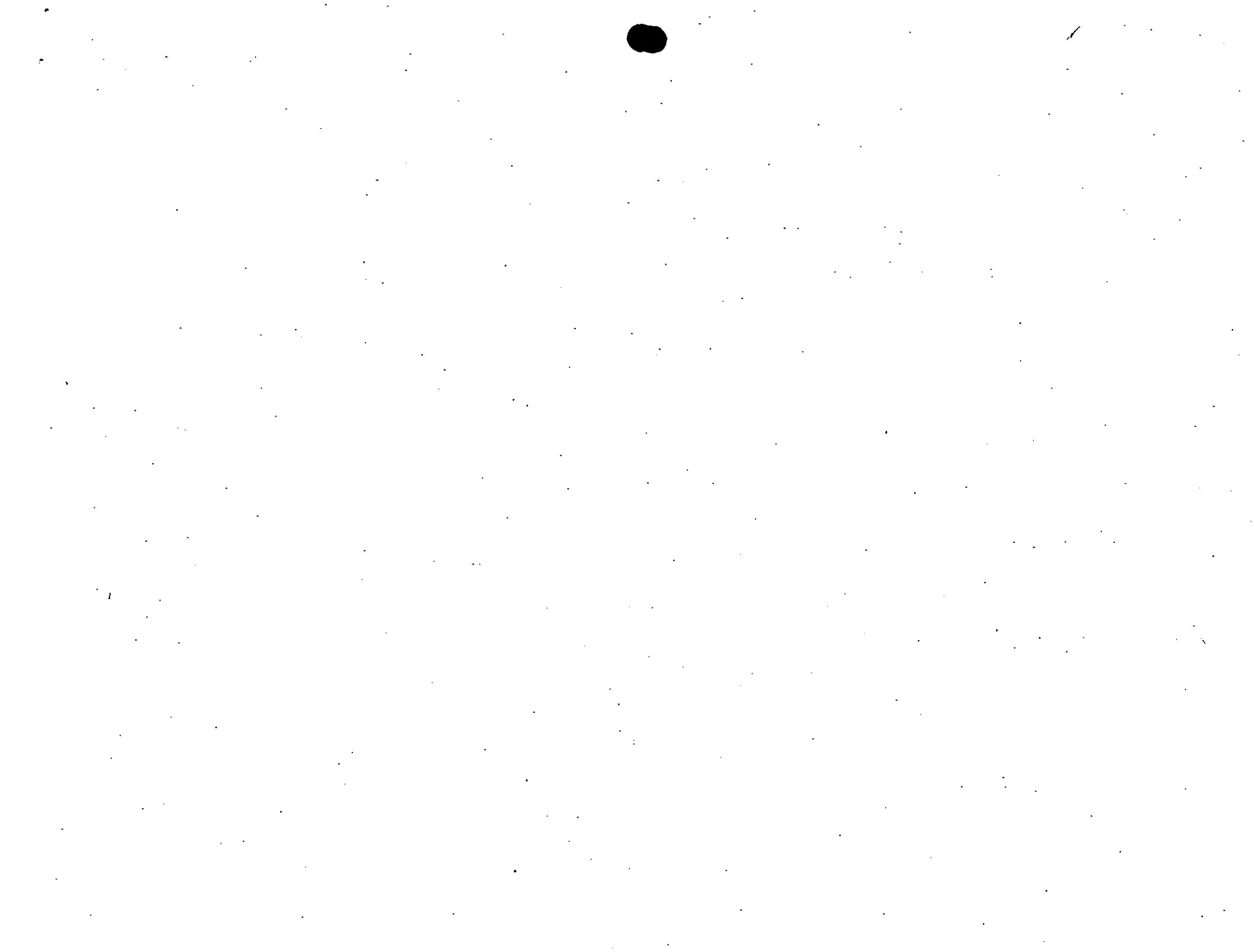
For the flexural stress component,  $I$  equals either  $I_x$  or  $I_y$ , whichever is the axis for bending. The  $I$  values may be computed as the properties of line configurations in a manner similar to that used for  $I_p$ . For some commonly used configurations,  $S = I/\bar{y}$  expressions are given in Table 5.16.1.

**EXAMPLE 5.16.3**

Compute the size of E70 fillet weld required for the connection shown in Fig. 5.16.8a using shielded metal-arc process. Assume that the column and bracket does not control.

*Solution*

$$f'_y = \frac{P}{A} = \frac{10}{2(10)} = 0.50 \text{ ksi}$$



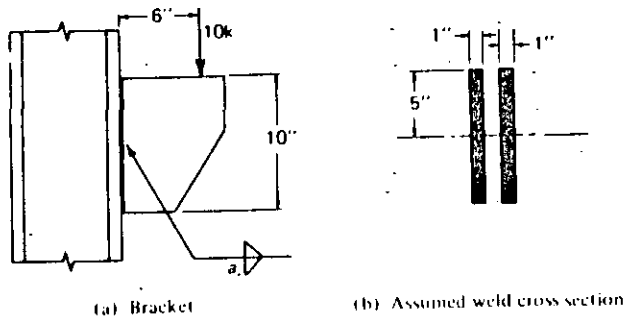


Fig. 5.16.8. Example 5.16.3.

$$I_x = \frac{(1)(10)^3}{12} = 83.33 \text{ in.}^4$$

$$f'_v = \frac{Mc}{I} = \frac{10(6)5}{83.3} = 3.60 \text{ ksi}$$

$$f_r = \sqrt{(0.5)^2 + (3.6)^2} = 3.64 \text{ ksi for 1-in. effective throat.}$$

$$\text{Reqd } t_e = \frac{f_r}{\text{allowable stress}} = \frac{3.64}{21} = 0.173 \text{ in.}$$

$$\text{Reqd } a = \frac{0.173}{0.707} = 0.244 \text{ in.}$$

Use 1/4-in. E70 fillet welds.

**Design for Lines of Weld Under Moment.** Even when there are moderate returns at the top of lines of fillet weld, an estimate of the length required may be obtained by using the same approach as used for determining the number of bolts in a line in Sec. 4.7. In Fig. 4.7.8,  $R/p$  has units of kips per inch and corresponds to  $f_r$  when  $t_e$  is unity for welds.

For pure moment on one line of weld,

$$f_r = \frac{M}{S} = \left[ \frac{1}{6} L_w^2 \right] \text{ kips/in.} \quad (5.16.17)$$

Since the maximum value of  $f_r$  is  $R_w$ ,

$$R_w = \frac{6M}{L_w^2}$$

or

$$\text{Reqd } L_w = \sqrt{\frac{6M}{R_w}} \quad (5.16.18)$$

Equation 5.16.18 for welds corresponds to Eq. 4.7.22 for bolts. Since it is correct only for pure moment,  $R_w$  should be taken as a reduced value to account for direct shear.

**EXAMPLE 5.16.4**

Determine the length  $L$  required to carry the load in Fig. 5.16.9, using 1/16-in. E70 fillet weld.

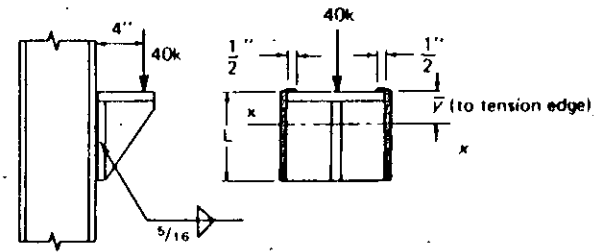


Fig. 5.16.9. Example 5.16.4.

**Solution**

Estimate  $L$  required by using Eq. 5.16.18:

$$R_w = \frac{5}{16} (0.707) 21 = 4.65 \text{ kips/in.}$$

$$M = 40(4) = 160 \text{ in.-kips per 2 weld lines}$$

$$\text{Reqd } L \approx \sqrt{\frac{6M}{R_w}} = \sqrt{\frac{6(160/2)}{4.0}} = 11 \text{ in.}$$

where a reduced value of  $R_w$  has been used to account for the direct shear effect. The return will add additional strength; try  $L = 10$  in.

Investigate configuration using weld properties as lines computed from basic principles,

$$\bar{y} = \frac{2(10)5}{2(10 + 0.5)} = \frac{100}{21} = 4.76 \text{ in.}$$

Direct shear:

$$f'_v = \frac{40}{20} = 2.00 \text{ kips/in.}$$

Since little direct shear is carried by the returns, they are neglected above.

$$\begin{aligned} I_x &= \frac{2L^3}{12} + 2L(5.0 - 4.76)^2 + 2(0.5)(4.76)^2 \\ &= \frac{(10)^3}{6} + 20(0.24)^2 + (4.76)^2 = 190.6 \text{ in.}^2 \end{aligned}$$



$$S = \frac{I}{\bar{y}} = \frac{190.6}{4.76} = 40.0 \text{ in.}^2$$

Flexure:

$$f_x'' = \frac{M}{S} = \frac{160}{40} = 4.0 \text{ kips/in.}$$

Resultant:

$$f_r = \sqrt{(2.00)^2 + (4.00)^2} = 4.48 \text{ kips/in.} < 4.65 \quad \text{OK}$$

Use  $L = 10 \text{ in.}$

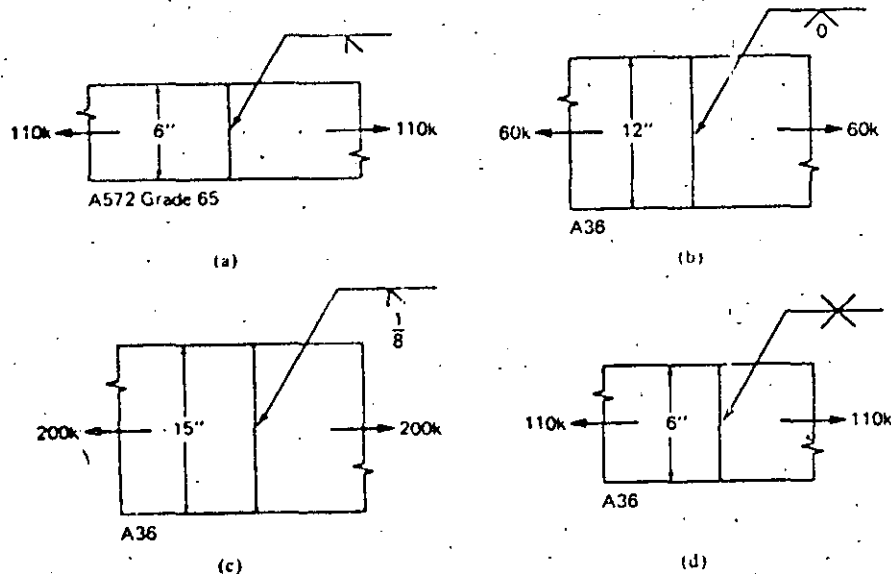
Additional treatment of eccentric loads on welds is to be found in Chapter 13 on connections.

**PROBLEMS**

All problems are to be done according to the latest AISC specifications, unless otherwise indicated.

5.1. Determine the proper plate thickness and indicate which ones, if any, of the following joints made by the submerged arc process are acceptable according to AISC-1.17.2. Refer to AISC Manual, "Welded Joints."

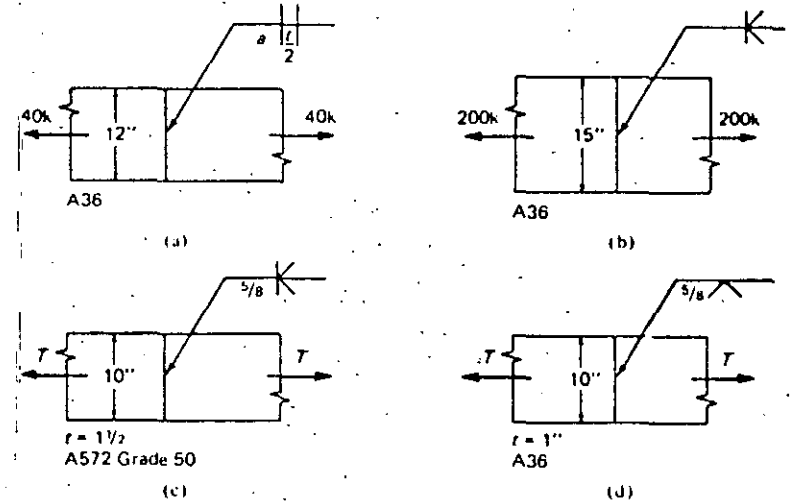
- (a) Single bevel groove, butt joint, welded from one side.
- (b) Single-V groove, butt joint, welded one side with no root opening.
- (c) Single bevel groove, butt joint, welded from one side with a backup plate.
- (d) Double-V groove; butt joint.



Prob. 5.1.

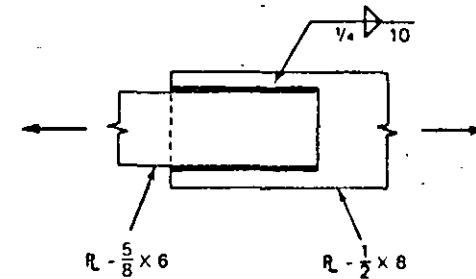
- 5.2. Determine either the plate thickness and weld material, or the capacity  $T$  of the joint for the given conditions; assuming shielded metal-arc process:
  - (a) Square groove, butt joint.
  - (b) Double-bevel groove, butt joint.
  - (c) Double-bevel groove, butt joint, welded from both sides, partial penetration.
  - (d) Single-V groove, butt joint, welded from one side, partial penetration.

For cases (a) and (b), is there a maximum thickness for which the type of weld may be used? Show cross section for welds in all four cases. (Refer to AISC Manual, "Welded Joints.")



Prob. 5.2.

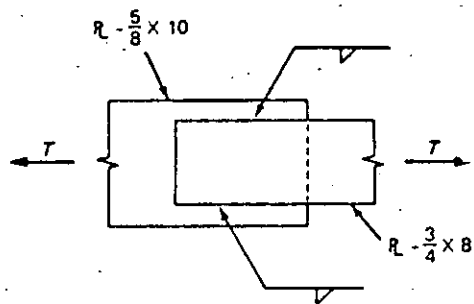
- 5.3. Determine the capacity of the connection shown, using the submerged-arc process: (a) use A36 steel, (b) use A572 Grade 55. Assume appropriate electrode material is to be used.



Prob. 5.3.

- 5.4. Determine the fillet welds required to develop the capacity of the connection shown. Specify the proper electrode for using the submerged-arc process: (a) use A572 Grade 42 steel, (b) use steel with  $F_y = 100 \text{ ks}$ .

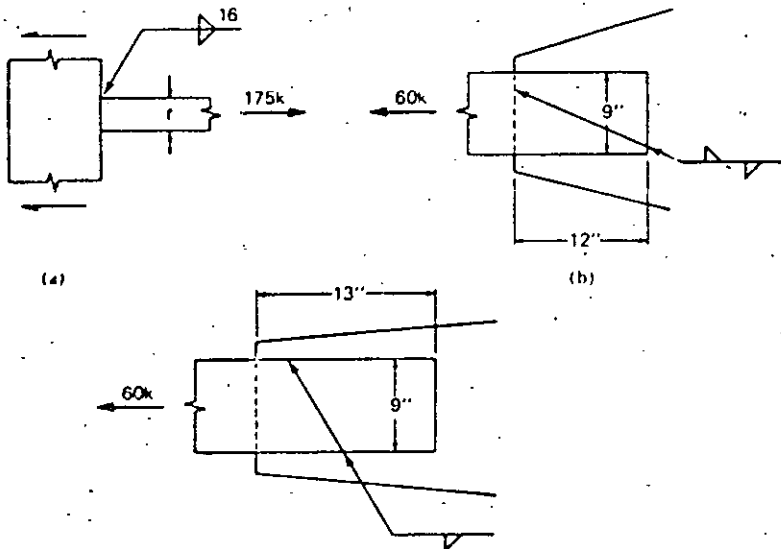




Prob. 5.4.

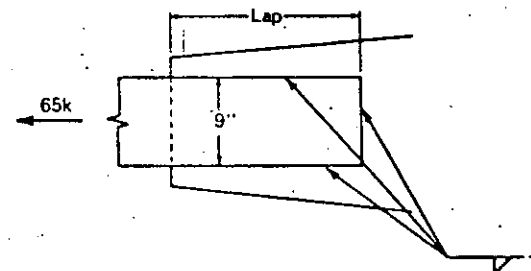
5.5. Determine the plate thickness and weld size to be specified for the joints shown. State type of weld material to be used for shielded metal-arc process.

- (a) Fillet welded tee joint; A36 steel.
- (b) Fillet welded lap joint; compare A36 steel with A572 Grade 50.
- (c) Fillet welded lap joint; compare A36 and A572 Grade 50; what lap distance will give the best joint?



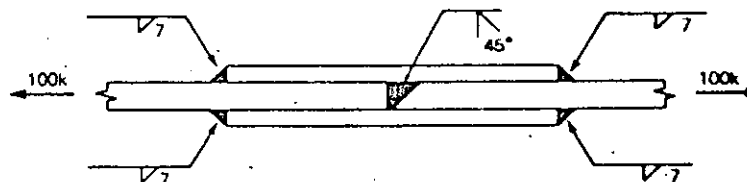
Prob. 5.5.

5.6. Determine the length of lap, weld size, and plate thickness of the 9-in. wide plate, to obtain the most efficient joint. Use A572 Grade 50 steel, and the shielded metal-arc process.



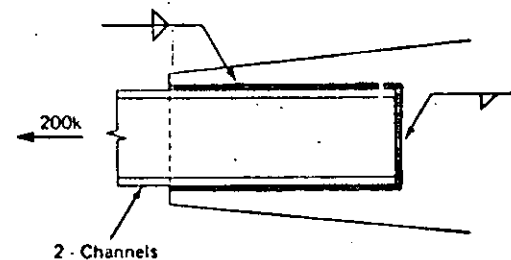
Prob. 5.6.

5.7. Design the reinforced lap joint shown, assuming the plates are 7-in. wide. Use A36 steel and the shielded metal-arc process. (Refer to AISC Manual, "Welded Joints"-BTC p. 4).



Prob. 5.7.

5.8. Select a pair of channels and design the welds assuming the shielded metal-arc process: (a) use A36 steel, and (b) use A572 Grade 60 steel.



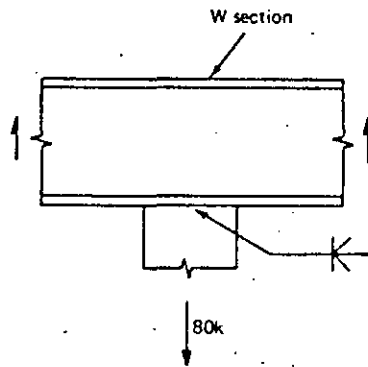
Prob. 5.8.

5.9. Design the plate framing into the W section and the welds, assuming shielded metal-arc process is to be used.

- (a) Use A572 Grade 42 steel.
- (b) Use A572 Grade 65 steel.
- (c) Use A572 Grade 42 steel, with fillet welds instead of groove weld.
- (d) Use A572 Grade 65 steel, with fillet welds instead of groove weld.

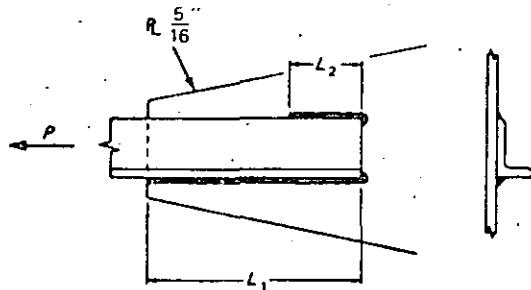






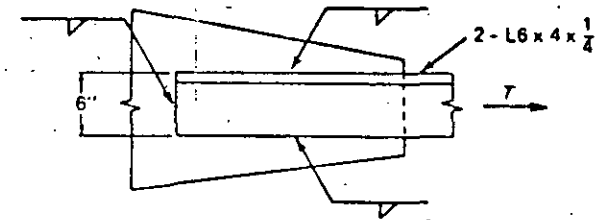
Prob. 5.9.

- 5.10. A  $5 \times 3\frac{1}{2} \times \frac{3}{8}$  angle of A572 Grade 50 steel is connected by its long leg to a  $\frac{3}{8}$ -in. gusset plate. Develop the full tensile capacity of the angle and use a balanced fillet welded connection even though AISC specs permit neglecting eccentricity in static load cases. The shielded metal-arc process is to be used. Use the following arrangements for the design:
- $\frac{3}{16}$ -in. weld on toe and back, with none on end.
  - $\frac{1}{4}$ -in. weld on toe and  $\frac{3}{8}$ -in. weld on back, and none on end.



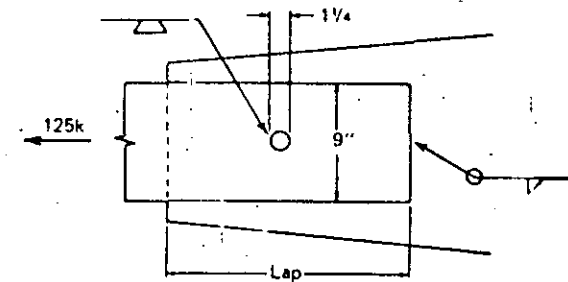
Prob. 5.10.

- 5.11. Design a balanced connection for two  $7 \times 4 \times \frac{1}{2}$  angles connected by their long legs to a  $\frac{3}{8}$ -in. gusset plate. A572 Grade 60 steel is used and welding is by the shielded metal-arc process. Detail the joint to balance the loads and still give the shortest possible overlap.
- 5.12. Design the welds indicated to develop the full strength of the angles and minimize eccentricity. Use the submerged-arc welding process.
- Use A36 steel.
  - Use A572 Grade 50 steel.
  - Use A572 Grade 65 steel.
  - Use A36 steel, but omit weld on the end of angles.
  - Use A572 Grade 65 steel, but omit weld on the ends of angles.



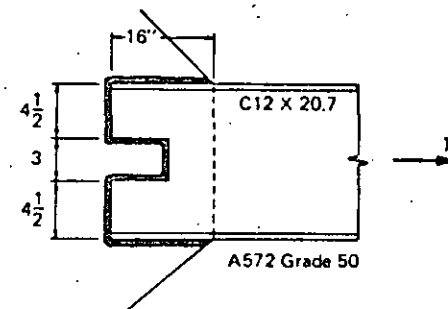
Prob. 5.12.

- 5.13. Assume the joint of Prob. 5.6 must be redesigned to carry 125 kips, and there exists a possibility of some accidental bending which cannot be computed. Thus, to insure a tighter joint a  $1\frac{1}{4}$ -in. diam. plug weld is to be used. Determine the thickness of the smaller plate, the amount of lap, and the weld size for the best joint. Use A572 Grade 50 steel, and assume shielded metal-arc welding process is to be used.



Prob. 5.13.

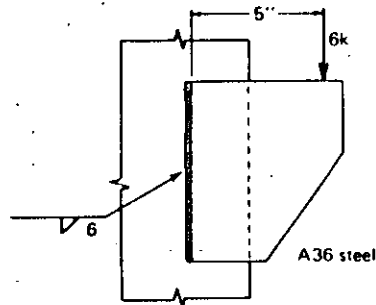
- 5.14. Determine the minimum length of slot in order to develop the full strength of a C12 x 20.7 welded to a  $\frac{3}{8}$ -in. plate. Use the same size fillet weld over the entire length, and assume it is to be placed by the shielded metal-arc process.



Prob. 5.14.

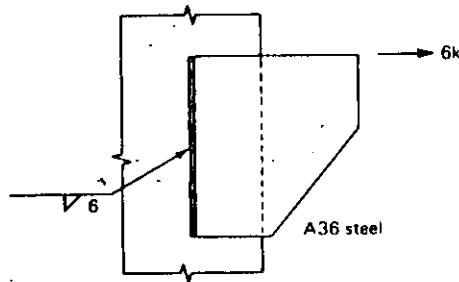


- 5.15. For the joint shown, what is the shear per inch of weld,  $R_w$ , at the most highly stressed point? (In computing the polar moment of inertia, let the width of the effective section be unity, then  $I_p = L^3/12$ , as given in Table 5.16.1.)



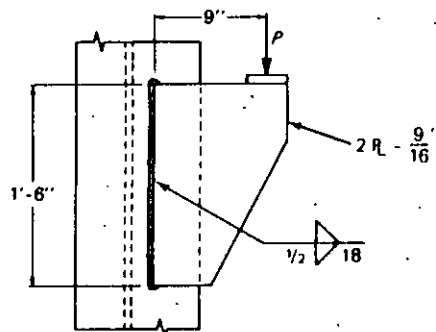
Prob. 5.15.

- 5.16. What is the weld size required for the bracket shown if the shielded metal-arc process is used?



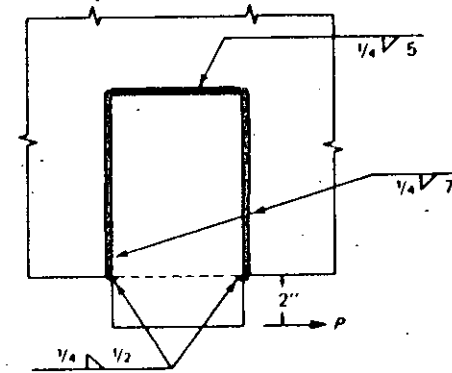
Prob. 5.16.

- 5.17. For the bracket shown, find the safe capacity  $P$  based on the weld. Neglect any returns at ends and assume the shielded metal-arc process is to be used.



Prob. 5.17.

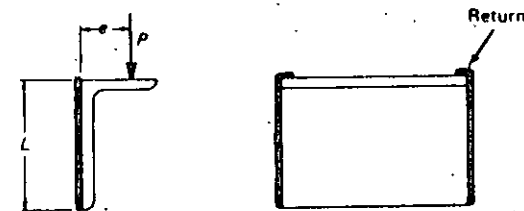
- 5.18. Ignoring the effect of returns at the lower end of the connection, and allowing a resultant stress of 2.4 kips per inch of fillet weld, what is the maximum allowable load  $P$  for the given connection?



Probs. 5.18 and 5.19.

- 5.19. Recompute the capacity for the connection of Prob. 5.18, using  $1/8$ -in. fillet weld on the sides and  $1/4$  on the end. Neglect the returns. Assume shielded metal-arc process is to be used and the plates are of A572 Grade 50 steel.
- 5.20. Derive the general expression for the required weld size on the seat-angle (E70 electrodes with shielded metal-arc process) in terms of  $P$ ,  $L$ , and  $e$ , using the following assumptions:
- Ignoring the returns at the top.
  - Considering an average return of  $L/12$ .
  - Using a return equal to twice the weld size.

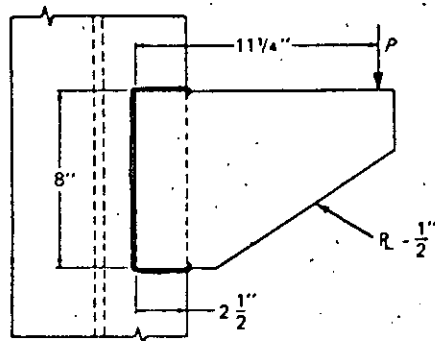
If  $e = 2\frac{1}{8}$  in. and  $L = 6$  in., determine using assumption (a) the weld size needed to carry a load  $P = 38.3$  kips. For the weld size selected, check the capacity which may be carried using all three assumptions.



Prob. 5.20.

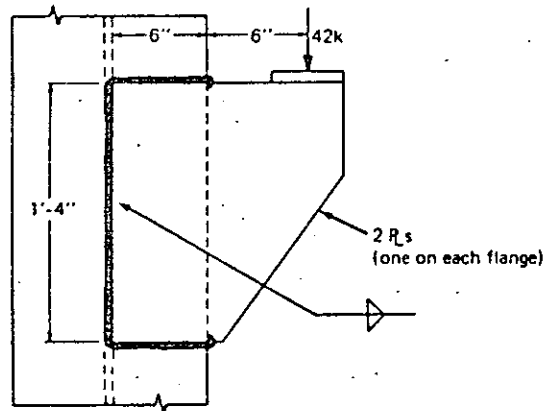
- 5.21. Determine the capacity  $P$  for the bracket shown. The weld size is  $1/8$  in. and E70 electrodes are used with shielded metal-arc process. Compare answer with AISC Manual tables.





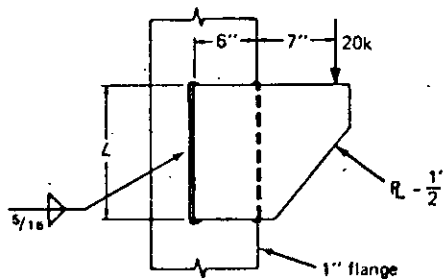
Prob. 5.21.

- 5.22. For the welded bracket shown, find the theoretical weld size required for strength if material is A36 steel and E70 electrode material is used with shielded metal-arc process. Neglect end returns at the upper and lower right-hand corners.



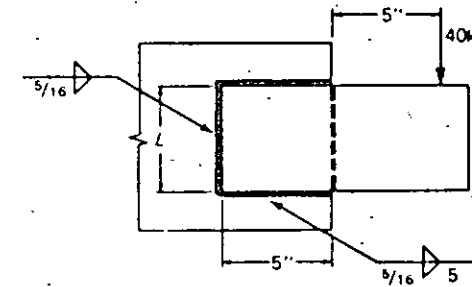
Prob. 5.22.

- 5.23. Determine the length  $L$  required when using  $5/16$ -in. fillet weld on A36 steel with shielded metal-arc welding.



Prob. 5.23.

- 5.24. Using basic principles, determine the length  $L$  required to safely carry the 40-kip load using  $5/16$ -in. weld. Assume steel is A572 Grade 50 and shielded metal-arc process is to be used for welding.

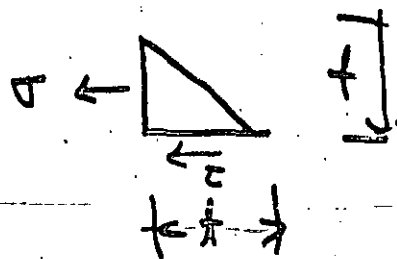
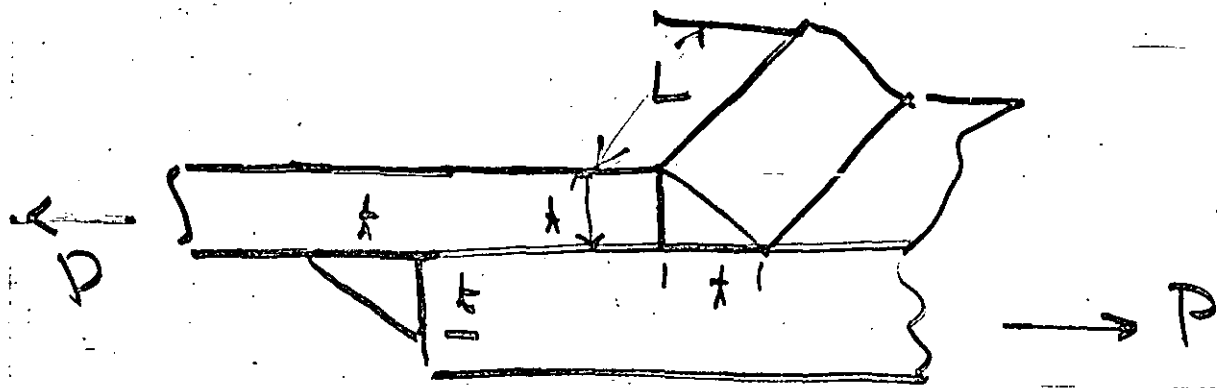


Prob. 5.24.

## SELECTED REFERENCES

1. K. Winterton, "A Brief History of Welding Technology," *Welding and Metal Fabrication*, November 1962.
2. "100 Years of Metalworking-Welding, Brazing and Joining," *The Iron Age*, June 1955.
3. H. Carpmael, *Electric Welding and Welding Appliances*, D. Van Nostrand Company, London, 1920.
4. P. M. Hall, "77 Years of Resistance Welding," *Welding Engineer*, February 1954; March 1954; April 1954.
5. G. Herden, *Schweiss und Schneid-Technik*, Carl Marhold Verlag, Halle, East Germany, 1960.
6. K. Winterton, "A Brief History of Welding Technology," *Welding and Metal Fabrication*, December 1962.
7. J. H. Davies, *Modern Methods of Welding*, D. Van Nostrand Company, New York, 1922.
8. E. Viall, *Electric Welding*, McGraw-Hill Book Company, New York, 1921.
9. *Welding Handbook*, 6th ed., Vol. 2, *Welding Processes; Gas, Arc, and Resistance*, American Welding Society, New York, 1969.
10. Omer W. Blodgett, *Design of Welded Structures*, James F. Lincoln Arc Welding Foundation, 1966.
11. *Welding Handbook*, 6th ed., Vol. 1, *Fundamental of Welding*, American Welding Society, New York, 1968.
12. "Weld Defects Sound Off," *The Iron Age*, Mar. 27, 1969.
13. J. A. Donnelly, "Determining the Cost of Welded Joints," *Engineering Journal*, AISC, Vol. 5, No. 4 (October 1968), pp. 146-147.
14. T. R. Higgins and F. R. Preece, "Proposed Working Stresses for Fillet Welds in Building Construction," *Engineering Journal*, AISC, Vol. 6, No. 1 (January 1969), pp. 16-20.



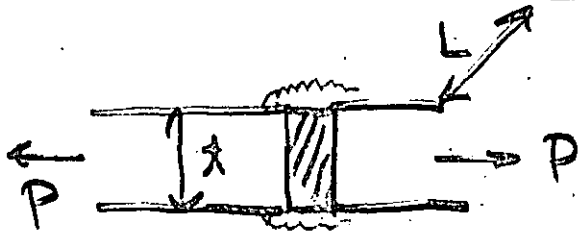


$$\frac{1}{2}(\text{Area de Tension}) = Lt$$

$$\frac{1}{2}(\text{" " " corte}) = Lt$$

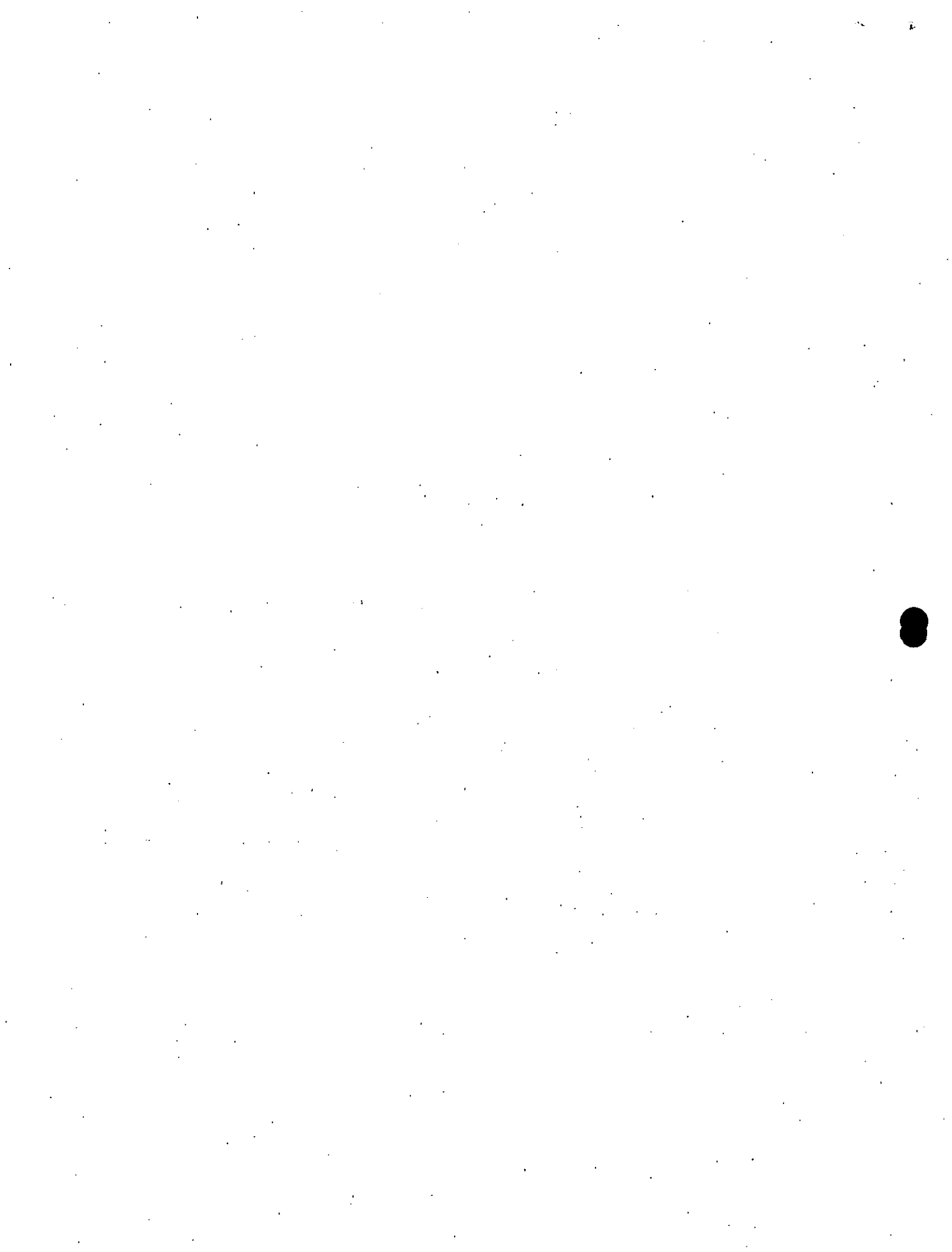
$$P = \sigma = \frac{P}{2Lt} \leq \text{admissible coef.}$$

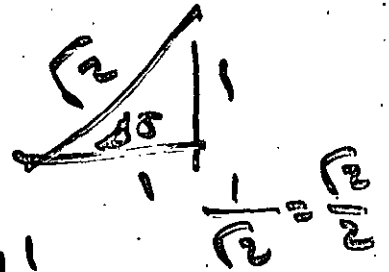
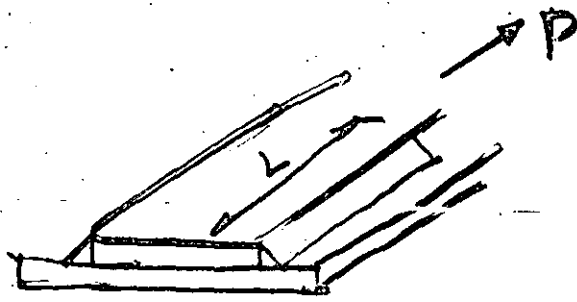
$$\tau = \frac{P}{2Lt} \leq \text{admissible T}$$



$$\sigma = \frac{P}{Lt} \leq \text{admissible tens}$$







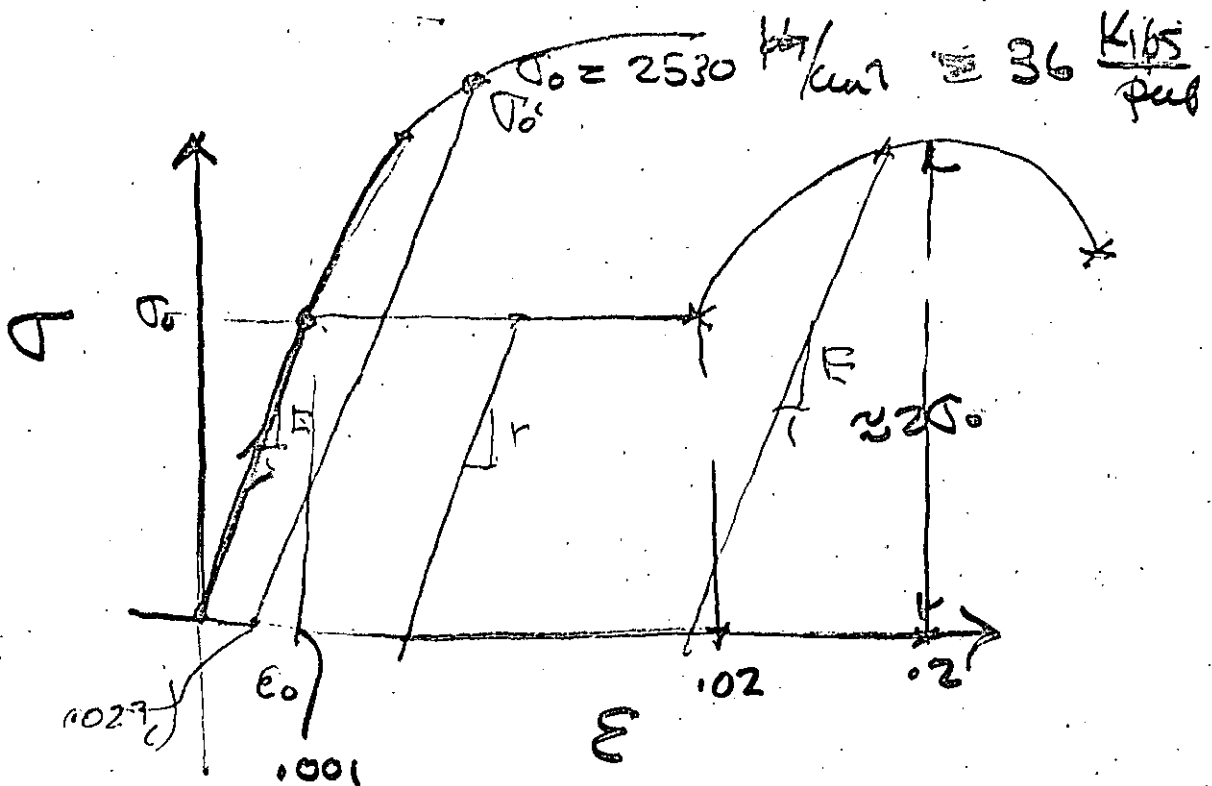
$L, t'$

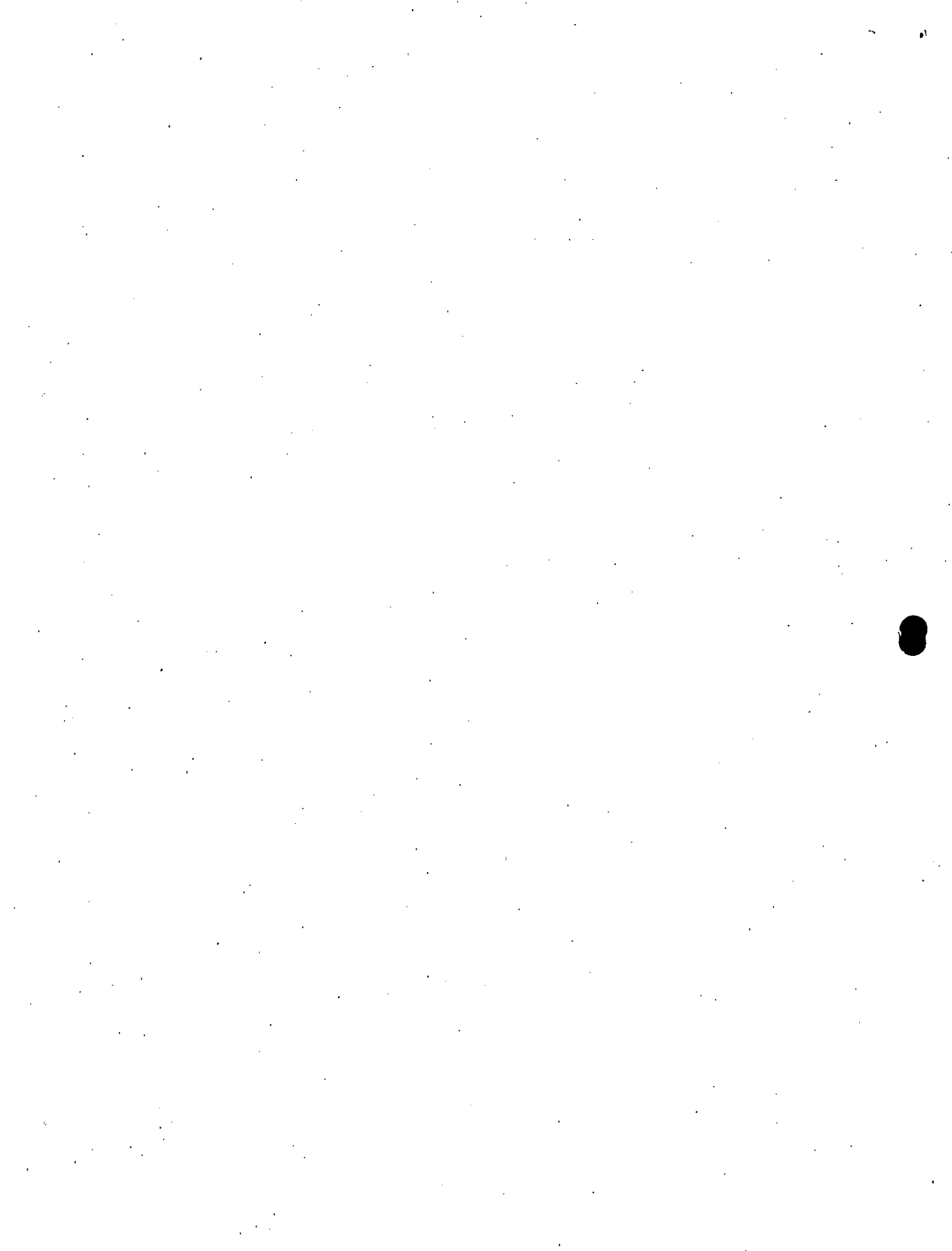
( $\tau$ ) est. de corte  
admissible en la  
soldadura  $\frac{\text{kg}}{\text{cm}^2}$   
 $\frac{\text{lbs}}{\text{pul}^2}$



$$\tau = \frac{P}{\frac{t'}{\text{en } 45^\circ} \times L \times 2} = \frac{\sqrt{2} P}{2 t' L}$$

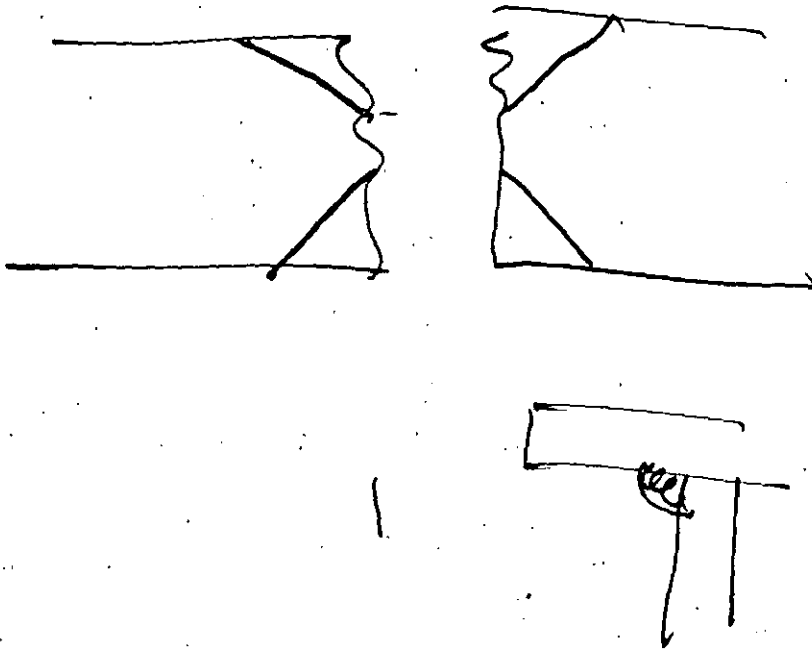
$\tau, P, t', L.$





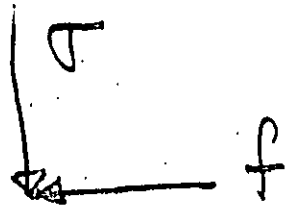
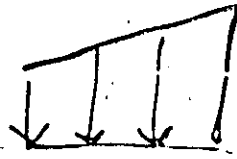
$$\frac{P}{\frac{\pi}{4} d^2} = \tau \leq \text{admissible}$$

$$\frac{P}{bd} = \tau \leq \quad "$$

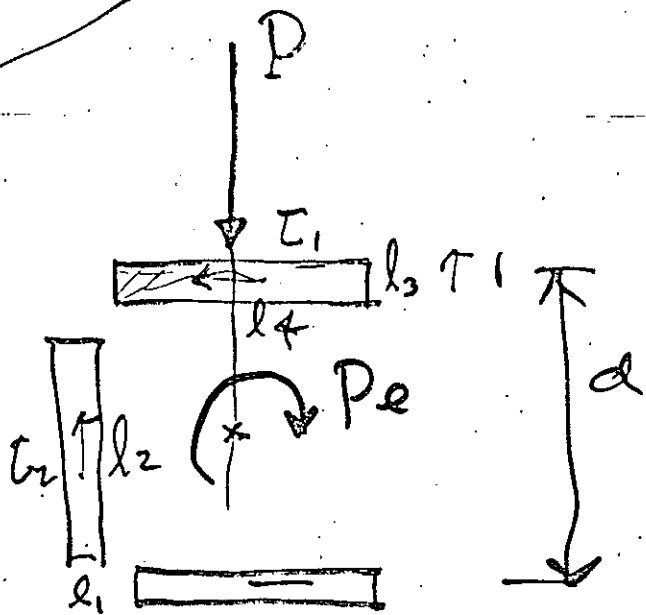
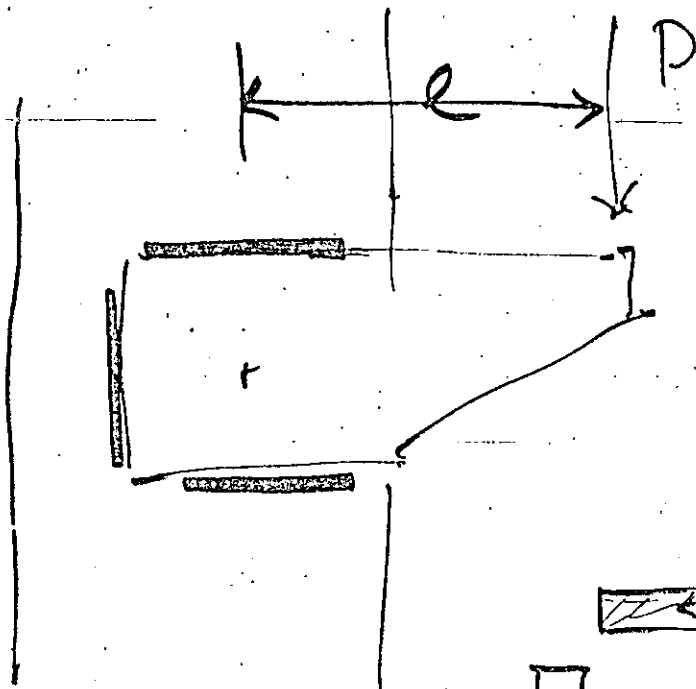




$M \leq N$



$$\tau \leq f$$



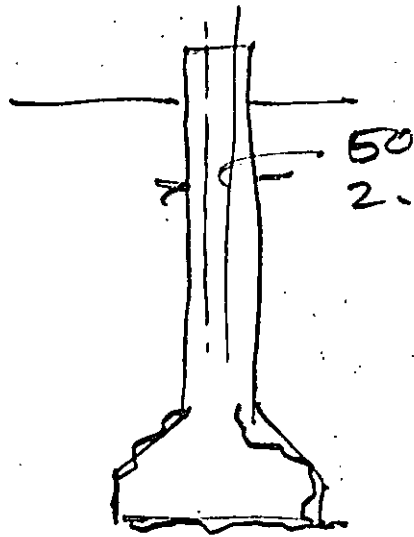
$$\tau_1 = \frac{P}{A}$$

$$\tau_1 = \frac{P}{l_1 l_2} \leq \underline{adn}$$

$$(\tau_2 + l_3 l_4) d = Pe$$

$$\tau_2 = \frac{Pe}{l_3 l_4 d} \leq \underline{\underline{adn}}$$



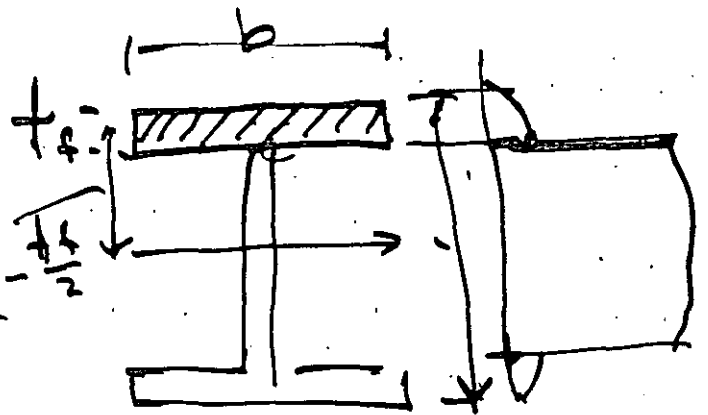
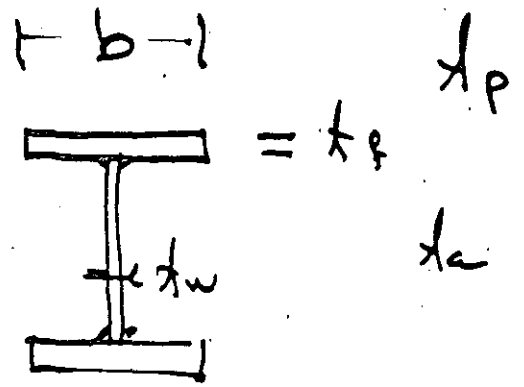
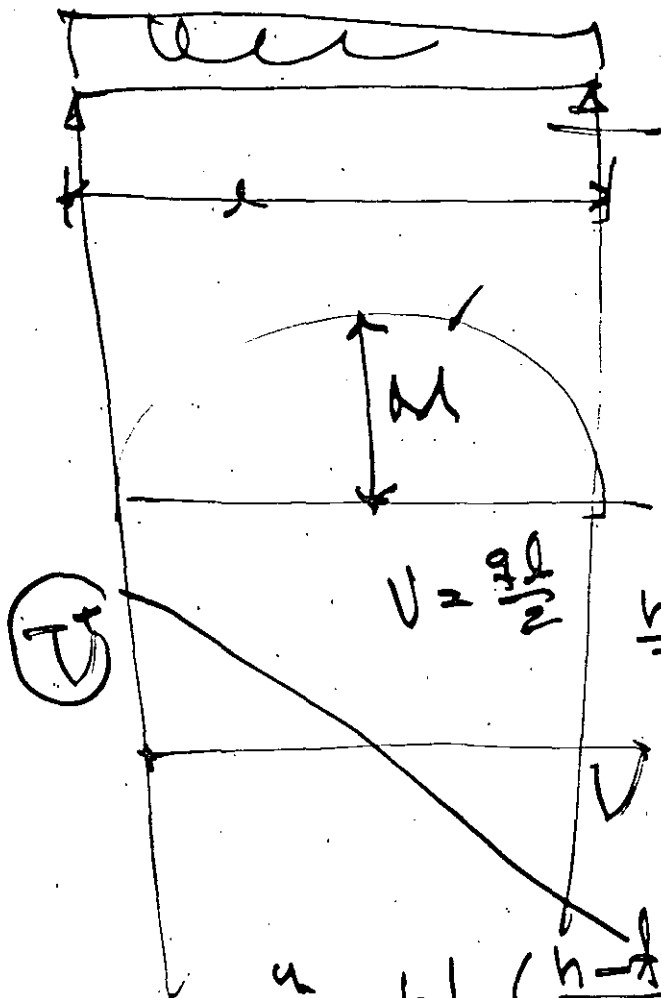


	Acero:	1.10' (\$/lb)	_____	✓
	Solda:	$(\times \frac{H+4A}{1000}) \times (\$/lb)$	_____	✓
M	Pinta	←	_____	✓
	M.O. Horas	$\frac{H+4A}{?}$	_____	✓
	Equipo (Fab)		_____	✓
	Armon	(%) (7.0)	_____	
	Transp.	(3%)	_____	
M.L.	{Montaje		_____	
	(M.D. + U.T.)	(18%)	_____	C.D.
		(60%)	_____	



10/13/18





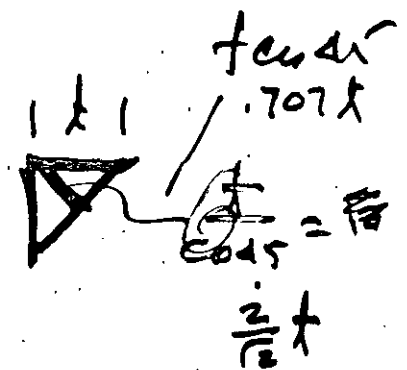
$$Q_y = b t_f \left( \frac{h - t_f}{2} \right)$$

$$v = \frac{Q_y}{I_z}$$

$$b = t_w$$

$$I_z =$$

$$v = \frac{\Delta Q_y}{b I_z}$$

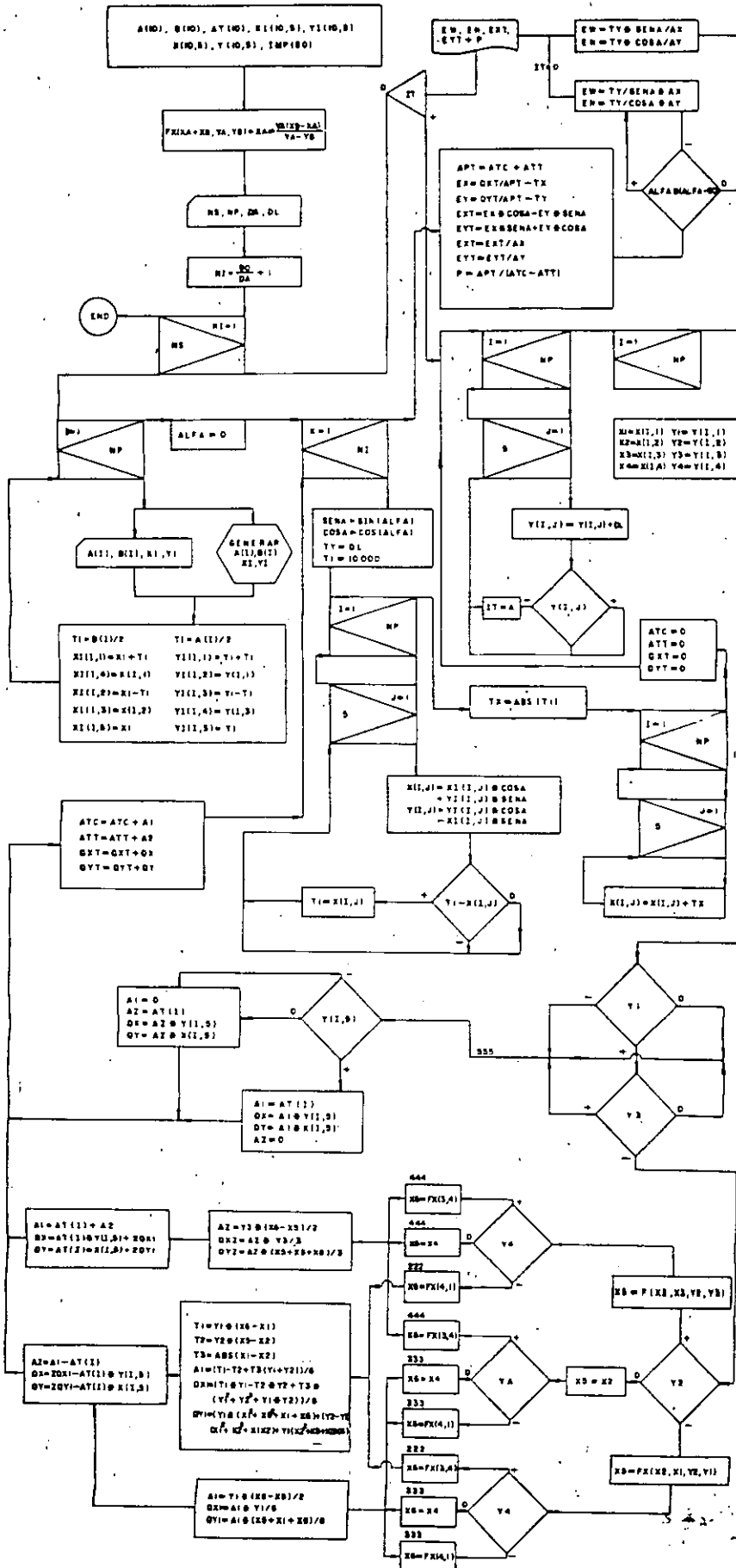


$$2 \left\{ \left( \frac{v}{2} \right) \frac{h}{2} \times .707 (t) \right\} = F_T$$

$$v = \left( t t_w \frac{h}{2} \right)^{\frac{1}{2}}$$

$$\tau_s = \frac{h}{2} (.707 t) \times 2$$

$$= \leq adu$$



DIRECTORIO DE ALUMNOS DEL CURSO "DISEÑO DE ESTRUCTURAS DE ACERO" IMPARTIDO EN ESTA DIVISION DEL 26 AL 30 DE NOVIEMBRE DEL PRESENTE AÑO.

- 1.- ALONSO TORRES RAMIRO  
AZUCAR, S.A. DE C.V.  
SUBGERENTE DE PROYECTOS  
AV. MORELOS No. 104  
COL. JUAREZ  
06600 MEXICO, D.F.  
592-33-00  
COLINA DE LA QUEBRADA No. 173  
COL. BULEVARES  
560-55-10
- 2.- ARAIZA RODRIGUEZ JOSE LUIS  
SECRETARIA DE COMUNICACIONES Y TRANSP.  
AUXILIAR DE RESIDENTE DE CONSERVACION  
ABUNDIO MARTINEZ No. 12-4  
IXMIQUILPAN, HGO.
- 3.- AREAN MARTINEZ JOSE A.  
S. C. T.
- 4.- AYALA MUÑIZ ROBERTO  
GEOSISTEMAS, S.A.  
INGENIERO DE PROYECTOS  
ANICETO ORTEGA No. 1310  
COL. DEL VALLE  
534-37-20 ext. 25  
ROLANDO GARROS No. 197-1  
COL. AMPLIACION CIVIL  
DELEGACION VENUSTIANO CARRANZA  
15740 MEXICO, D.F.
- 5.- BARRERA PAREDES JESUS ALFONSO  
UNIVERSIDAD DE SONORA  
MAESTRO  
BOULEVARD LUIS ENCINAS Y CALLE ROSALES  
COL. CENTRO  
2-10-46 ext. 153  
AVENIDA DOCE No. 196  
COL. APOLO  
HERMOSILLO, SON.  
510-06
- 6.- BORBON FRANCO JORGE Z.
- 7.- CARBAJAL GRANADOS JOSE LUIS  
OBRAS PUBLICAS DEL EDO. GUERRERO  
JEFE DEPTO. DE CALCULO  
PALACIO DE GOBERNACION 4o. PISO  
CHILPANCINGO, GRO.  
249-02  
PARTENON No. 16  
COL. LOS CEDROS  
DELEGACION COYOACAN  
671-13-93
- 8.- CASTILLO VAZQUEZ JAIME  
UNIVERSIDAD IBEROAMERICANA  
CENTRO LAS TORRES No. 395  
COL. PRADO CHURUBUSCO  
PARIS No. 81  
DELEGACION GUSTAVO A. MADERO  
07330 MEXICO, D.F.
- 9.- CIENFUEGOS ALVARADO CARLOS  
ESIA, IPN PLANTEL TECAMACHALCO  
PROFESOR MATERIA ESTRUCTURAS  
FUENTE DE LEONES No. 28  
COL. TECAMACHALCO  
56500 EDO. DE MEXICO  
599-72-31  
ALEJANRIA No. 29  
COL. CLAVERIA  
DELEGACION AZCAPOTZALCO  
02080 MEXICO, D.F.  
527-67-88

10.- CRISTO PARRA EDUARDO  
HYLSA, S.A.  
ING. DISEÑO CIVIL AVANZADO  
AV. LOS ANGELES Y AV. MONICA

MONTERREY

11.- CUENCA DIAZ JUAN  
UNIVERSIDAD AUTONOMA DEL EDO. MEXICO  
PROFESOR TIEMPO COMPLETO  
INSTITUTO LITERARIO No. 100  
COL. CENTRO  
TOLUCA, EDO. DE MEXICO

M. MATAMOROS No. 702  
TOLUCA, EDO. DE MEXICO  
496-70

12.- CHACON GARCIA FCO. DE JESUS  
CHACON Y ASOCIADOS  
GERENTE GENERAL  
ESCORIAL No. 30 ALTOS 5  
DELEGACION COYOACAN  
04800 MEXICO, D.F.  
594-75-30

UNIVERSIDAD No. 520-2  
COL. NARVARTE  
DELEGACION BENITO JUAREZ  
03020 MEXICO, D.F.  
594-75-30

13.- DURAZO ORTIZ ARMANDO  
ESC. ING. UNIVERSIDAD DE SONORA  
BOULEVARD LUIS ENCINAS Y CALLE ROSALES  
COL. CENTRO  
HERMOSILLO, SON.  
2-10-46 ext. 153

NO REELECCION No. 23 OTE  
COL. CENTRO  
HERMOSILLO, SON.

14.- FLORES MENDOZA JOSE  
DEPTO. DISTRITO FEDERAL  
JEFE DE OFICINA  
SAN ANTONIO ABAD No. 231-7o. PISO  
COL. OBRERA  
DELEGACION CUAUHTEMOC  
06800 MEXICO, D.F.  
588-37-66

GRAL. IGNACIO ZARAGOZA MZANA. 3  
LOTE 9 C-1  
COL. VILLA DE LAS MANZANAS  
DELEGACION COACALCO  
55700 EDO. DE MEXICO  
781-78-44

15.- FUENTES NAVA JAVIER  
COMISION FEDERAL DE ELECTRICIDAD

16.- GARCIA CUEVAS TOMAS  
SECRETARIA AGRICULTURA RECURSOS HIDRAULICOS  
PROYECTISTA  
CERRADA JUAN SANCHEZ AZCONA No. 1723  
COL. DEL VALLE  
DELEGACION BENITO JUAREZ  
524-73-07

CALLE 65 No. 42  
COL. STA. CRUZ MEYEHUALCO  
DELEGACION IZTAPALAPA  
691-01-39

17.- GARICA HERNANDEZ ANDRES B.  
S. C. T.  
JEFE DE PROYECTOS  
FERNANDO No. 247  
COL. ALAMOS  
DELEGACION BENITO JUAREZ  
590-93-52

2a. CDA. DE ALBERTO SALINAS MZA. 3  
LOTE 23  
COL. AVIACION CIVIL  
DELEGACION VENUSTIANO CARRANZA  
558-52-16

18.- GONZALEZ ZEPEDA ROGELIO  
DIREC. GRAL. OBRAS MARITIMAS  
CALCULISTA - PROVIDENCIA No. 607  
COL. DEL VALLE 523-28-15

FELIPE DE LA GARZA No. 163  
COL. JUAN ESCUTIA  
DELEGACION IZTAPALAPA 09100 MEX. D.

- 27.- LOZANO GONZALEZ JOSE PABLO  
S. C. T.  
PROYECTISTA  
FERNANDO No. 242  
COL. ALAMOS  
DELEGACION BENITO JUAREZ  
590-93-52
- MONTEALBAN No. 71  
COL. NARVARTE  
DELEGACION BENITO JUAREZ  
03020 MEXICO, D.F.  
519-42-43
- 28.- MARTINEZ BREMONT MARIO A.  
CIA. LUZ Y FZA. DEL CENTRO  
TECNICO C.-20B  
TLALOC No. 90-2o. PISO  
COL. TLAXPANA  
DELEGACION MIGUEL HIDALGO  
592-37-18
- REPUBLICAS No. 105-206  
COL. PORTALES  
DELEGACION BENITO JUAREZ  
03300 MEXICO, D.F.  
672-42-57
- 29.- MARTINEZ GARCIA JOSE CARLOS  
DIREC. GRAL. OBRAS MARITIMAS S.C.T.  
INGENIERO ESPECIALIZADO  
CALLE PROVIDENCIA No. 807  
COL. DEL VALLE  
DELEGACION BENITO JUAREZ  
523-28-15
- NIEBLA No. 166  
COL. SAN PEDRO XALPA  
DELEGACION AZCAPOTZALCO  
02710 MEXICO, D.F.  
352-22-80
- 30.- MENCHACA MENCHACA RAUL  
UNIVERSIDAD AUTONOMA AGUASCALIENTES  
JEFE DEPTO. CONSTRUC. ESTRUCTURAS  
JARDIN DEL ESTUDIANTE No. 1  
AGUASCALIENTES, AGS.  
70505-ext. 159
- LOPEZ VELARDE No. 216-3  
AGUASCALIENTES, AGS.
- 31.- MENDOZA MONROY RAUL  
CIA. LUZ Y FZA. DEL CENTRO  
INGENIERO CL20 ALTA  
TLALOC No. 90-2o. PISO  
COL. TLAXPANA  
DELEGACION MIGUEL HIDALGO  
592-37-18
- AV. ANDROMEDA No. 18  
COL. JARDINES DE SATELITE  
NAUCALPAN DE JUAREZ, EDO. DE MEXICO
- 32.- NARVAEZ RANGEL ALFREDO  
CIA. DE LUZ Y FZA. DEL CENTRO  
INGENIERO CL-20 ALTA  
TLALOCA No. 90-2o. PISO  
COL. TLAXPANA  
DELEGACION MIGUEL HIDALGO  
592-37-18
- JOSE MA. ROA BARCENAS No. 134-3  
COL. OBRERA  
DELEGACION CUAUHTEMOC  
06000 MEXICO, D.F.  
578-57-19
- 33.- QUINTANA PACHECO JESUS  
UNIVERSIDAD DE SONORA  
MAESTRO  
BOULEVARD LUIS ENCINAS Y CALLE ROSALES  
COL. CENTRO  
HERMOSILLO, SON.  
2-10-46
- LEOPOLDO RAMOS No. 331  
COL. BALDERRAMA  
HERMOSILLO, SON.  
4-36-95

- 42.- SANTIAGO BRAVO GABRIEL  
D. G. C. O. H. D. D. F.  
INGENIERO RESIDENTE  
AV. PROLONG. CANAL MIRAMONTES S/N  
COL. EJIDOS DE HUIPULCO  
DELEGACION TLALPAN
- FLORICULTURA No. 291  
COL. 20 DE NOVIEMBRE  
DELEGACION VENUSTIANO CARRANZA  
15300 MEXICO, D.F.  
789-96-08
- 43.- SERRANO SALDAÑA MIGUEL  
S. C. T.  
JEFE DE PROYECTOS  
AV. FERNANDO No. 247  
COL. ALAMOS  
DELEGACION BENITO JUAREZ  
593-93-52
- CALLE 25 No. 116  
57210 MEXICO, D.F.
- 44.- SILVA MORALES ROBERTO  
SUPERVISORES TECNICOS CONSTRUCCIONES  
SUPERVISOR ESTRUCTURAL Y CIVIL  
PONIENTE 5 - 125 - 11  
ORIZABA, VER.
- 37 PONIENTE No. 514  
PUEBLA, PUE.  
40-14-01
- 45.- SOTO GODINEZ ANDRES  
S. A. R. H.  
PROYECTISTA  
CERRADA JUAN SANCHEZ AZCONA No. 1733  
COL. DEL VALLE  
DELEGACION BENITO JUAREZ  
524-73-07
- ANDALUCIA No. 42-10  
COL. ALAMOS  
DELEGACION BENITO JUAREZ
- 46.- TADDEI ZAVALA EDMUNDO  
UNIVERSIDAD SONORA  
MAESTRO DE MEDIO TIEMPO  
BOULEVARD LUIS ENCINAS Y CALLE ROSALES  
210-46 ext. 153
- AGUSTIN MELGAR No. 16  
COL. LA HUERTA  
HERMOSILLO, SON.  
4-05-50
- 47.- TAPIA ZALETÁ FRANCISCO  
CIA. LUZ Y FZA. DEL CENTRO, S.A.  
INGENIERO TECNICO  
MELCHOR OCAMPO No. 171  
COL. TLAXPANA  
DELEGACION MIGUEL HIDALGO  
592-37-18
- MINA No. 210-A-204  
COL. GUERRERO  
DELEGACION CUAUHEMOC
- 48.- TOLEDANO GONZALEZ EDUARDO SAUL  
DIREC. GRAL. OBRAS MARITIMAS  
INGENIERO CIVIL  
PROVIDENCIA No. 807-2o. PISO  
COL. DEL VALLE  
523-28-15
- 4o. ANDADOR RIO SAN JAVIER No. 76-A  
COL. JORGE NEGRETE  
DELEGACION GUSTAVO A. MADERO  
07680 MEXICO, D.F.
- 49.- TOVAR ROJAS ROBERTO  
CONSORCIO MINERO BENITO JUAREZ  
ENCARGADO PROYECTOS CIVILES  
TAPEIXTLES; MANZANILLO, COLIMA
- PARICUTIN No. 166-E  
COL. VELLAVISTA  
MANZANILLO, COL.-

50.- VALLEJO GONZALEZ JUAN DANIEL  
CIA. DE LUZ Y FZA. DEL CENTRO  
ING. PROYECTISTA  
TLALOC No. 90-2o. PISO  
COL. TLAXPANA  
DELEGACION MIGUEL HIDALGO  
592-37-18

VALLE DE MEXICO, No. 30  
COL. VISTA DEL VALLE  
NAUCALPAN DE JUAREZ, EDO. DE MEXICO  
52390  
592-37-18

51.- VILLALOBOS LOPEZ JULIO  
DIREC. GRAL. OBRAS MARITIMAS  
INGENIERO CALCULISTA  
PROVIDENCIA No. 807  
COL. DEL VALLE  
523-28-15

MUITLE No. 59  
COL. VICTORIA DE LAS DEMOGRACIAS  
DELEGACION ATZCAPOTZALCO  
02810 MEXICO, D.F.

52.- VIÑAS RODRIGUEZ JAIME  
AEROPUERTOS Y SERV. AUXILIARES  
SUPERVISOR OBRAS  
AV. 602 No.161  
COL. SAN JUAN DE ARAGON  
571-07-21

ATZCAPOTZALCO No. 247  
FRAC. LA FLORIDA  
ECATEPEC DE MORELOS  
571-07-21